

Suresh Chandra Satapathy
K. Srujan Raju
Jyotsna Kumar Mandal
Vikrant Bhateja *Editors*

Proceedings of the Second International Conference on Computer and Communication Technologies

IC3T 2015, Volume 2

Advances in Intelligent Systems and Computing

Volume 380

Series editor

Janusz Kacprzyk, Polish Academy of Sciences, Warsaw, Poland
e-mail: kacprzyk@ibspan.waw.pl

About this Series

The series “Advances in Intelligent Systems and Computing” contains publications on theory, applications, and design methods of Intelligent Systems and Intelligent Computing. Virtually all disciplines such as engineering, natural sciences, computer and information science, ICT, economics, business, e-commerce, environment, healthcare, life science are covered. The list of topics spans all the areas of modern intelligent systems and computing.

The publications within “Advances in Intelligent Systems and Computing” are primarily textbooks and proceedings of important conferences, symposia and congresses. They cover significant recent developments in the field, both of a foundational and applicable character. An important characteristic feature of the series is the short publication time and world-wide distribution. This permits a rapid and broad dissemination of research results.

Advisory Board

Chairman

Nikhil R. Pal, Indian Statistical Institute, Kolkata, India
e-mail: nikhil@isical.ac.in

Members

Rafael Bello, Universidad Central “Marta Abreu” de Las Villas, Santa Clara, Cuba
e-mail: rbellop@uclv.edu.cu

Emilio S. Corchado, University of Salamanca, Salamanca, Spain
e-mail: escorchedo@usal.es

Hani Hagras, University of Essex, Colchester, UK
e-mail: hani@essex.ac.uk

László T. Kóczy, Széchenyi István University, Győr, Hungary
e-mail: koczy@sze.hu

Vladik Kreinovich, University of Texas at El Paso, El Paso, USA
e-mail: vladik@utep.edu

Chin-Teng Lin, National Chiao Tung University, Hsinchu, Taiwan
e-mail: ctlin@mail.nctu.edu.tw

Jie Lu, University of Technology, Sydney, Australia
e-mail: Jie.Lu@uts.edu.au

Patricia Melin, Tijuana Institute of Technology, Tijuana, Mexico
e-mail: epmelin@hafsamx.org

Nadia Nedjah, State University of Rio de Janeiro, Rio de Janeiro, Brazil
e-mail: nadia@eng.uerj.br

Ngoc Thanh Nguyen, Wroclaw University of Technology, Wroclaw, Poland
e-mail: Ngoc-Thanh.Nguyen@pwr.edu.pl

Jun Wang, The Chinese University of Hong Kong, Shatin, Hong Kong
e-mail: jwang@mae.cuhk.edu.hk

More information about this series at <http://www.springer.com/series/11156>

Suresh Chandra Satapathy · K. Srujan Raju
Jyotsna Kumar Mandal · Vikrant Bhateja
Editors

Proceedings of the Second International Conference on Computer and Communication Technologies

IC3T 2015, Volume 2



Springer

Editors

Suresh Chandra Satapathy
Department of Computer Science
and Engineering
Anil Neerukonda Institute of Technology
and Sciences
Visakhapatnam
India

K. Srujan Raju
Department of Computer Science
and Engineering
CMR Technical Campus
Hyderabad
India

Jyotsna Kumar Mandal
Department of Computer Science
and Engineering
Kalyani University
Nadia, West Bengal
India

Vikrant Bhateja
Department of Electronics and
Communication Engineering
Shri Ramswaroop Memorial Group
of Professional Colleges
Lucknow, Uttar Pradesh
India

ISSN 2194-5357

ISSN 2194-5365 (electronic)

Advances in Intelligent Systems and Computing

ISBN 978-81-322-2522-5

ISBN 978-81-322-2523-2 (eBook)

DOI 10.1007/978-81-322-2523-2

Library of Congress Control Number: 2015944452

Springer New Delhi Heidelberg New York Dordrecht London
© Springer India 2016

This work is subject to copyright. All rights are reserved by the Publisher, whether the whole or part of the material is concerned, specifically the rights of translation, reprinting, reuse of illustrations, recitation, broadcasting, reproduction on microfilms or in any other physical way, and transmission or information storage and retrieval, electronic adaptation, computer software, or by similar or dissimilar methodology now known or hereafter developed.

The use of general descriptive names, registered names, trademarks, service marks, etc. in this publication does not imply, even in the absence of a specific statement, that such names are exempt from the relevant protective laws and regulations and therefore free for general use.

The publisher, the authors and the editors are safe to assume that the advice and information in this book are believed to be true and accurate at the date of publication. Neither the publisher nor the authors or the editors give a warranty, express or implied, with respect to the material contained herein or for any errors or omissions that may have been made.

Printed on acid-free paper

Springer (India) Pvt. Ltd. is part of Springer Science+Business Media (www.springer.com)

Preface

This volume contains 80 papers presented at the 2nd International Conference on Computer & Communication Technologies held during 24–26 July 2015 at Hyderabad, hosted by CMR Technical Campus in association with Division-V (Education and Research) CSI. It proved to be a great platform for researchers from across the world to report, deliberate, and review the latest progress in the cutting-edge research pertaining to intelligent computing and its applications to various engineering fields. The response to IC3T 2015 was overwhelming. It received a good number of submissions from different areas relating to intelligent computing and its applications in main tracks and three special sessions and after a rigorous peer-review process with the help of our program committee members and external reviewers, we finally accepted quality papers with an acceptance ratio of 0.35. We received submissions from seven overseas countries.

Dr. Vipin Tyagi, Jaypee University of Engineering & Technology, Guna, MP, conducted a Special Session on “Cyber Security and Digital Forensics,” Dr. K. Ashoka Reddy Principal, Kakatiya Institute of Technology & Science, Warangal, and Prof. Tara Sai Kumar, CMR Technical Campus, Hyderabad, conducted a Special Session on “Applications for Fuzzy Systems in Engineering” and Dr. Suma V. Dean, Research and Industry Incubation Centre (Recognized by Ministry of Science and Technology, Government of India), Dayananda Sagar Institutions, Bangalore, conducted a Special Session on “Software Engineering and Applications.”

We take this opportunity to thank all keynote speakers and special session chairs for their excellent support to make IC3T 2015 a grand success.

The quality of a referred volume depends mainly on the expertise and dedication of the reviewers. We are indebted to the program committee members and external reviewers who not only produced excellent reviews but also did them in short time frames. We would also like to thank CSI Hyderabad, CMR Group of Institutions, DRDO and JNTUH for coming forward to support us to organize this mega convention.

We express our heartfelt thanks to Mr. Ch. Gopal Reddy, Chairman of CMR Technical Campus, Smt. C. Vasanthalatha, Secretary of CMR Technical Campus,

and Dr. A. Raji Reddy Director of CMR Technical Campus, faculty and administrative staff for their continuous support during the course of the convention.

We would also like to thank the authors and participants of this convention, who have considered the convention above all hardships. Finally, we would like to thank all the volunteers who spent tireless efforts in meeting the deadlines and arranging every detail to make sure that the convention runs smoothly. All the efforts are worth and would please us all, if the readers of this proceedings and participants of this convention found the papers and event inspiring and enjoyable. We place our sincere thanks to the press, print, and electronic media for their excellent coverage of this convention.

July 2015

Suresh Chandra Satapathy
K. Srujan Raju
Jyotsna Kumar Mandal
Vikrant Bhateja

Team IC3T 2015

Chief Patrons

Sri. C. Gopal Reddy, Chairman
Smt. C. Vasanthalatha Reddy, Secretary
Dr. A. Raji Reddy, Director

Advisory Committee

Dr. A. Govardhan, SIT, JNTUH
Dr. V. Kamakshi Prasad, HOD-CSE, JNTUCEH
Prof. S.K. Udgata, HCU
Dr. Vasumathi, JNTUH
Dr. B. Padmaja Rani, JNTUH
Dr. O.B.V. Ramanaiah, JNTUH
Dr. B.N. Bhandari, JNTUH
Dr. Amit Acharya, JNTUH
Dr. D. Rajya Lakshmi, JNTUV
Dr. C. Srinivasa Kumar, VITSH(VU)
Dr. V. Kamaskshi Prasad, JNTUH
Dr. M.B.R. Murthy, CMRCET
Dr. M.V. Krishna Rao, CMRIT
Dr. M. Janga Reddy, CMRIT
Dr. L. Pratap Reddy, JNTUH
Dr. T. Anil Kumar, SRIITH
Dr. K. Srinivas Rao, CMRCET
Dr. Sahu Chatrapati, JNTUM
Dr. Vaka Murali Mohan, BRC

Program Chairs

Dr. A. Govardhan
Prof. G. Srikanth
Dr. K. Srujan Raju
Dr. Suresh Chandra Satapathy

Conveners

Prof. Dimlo. U. Fernandes
Mrs. K. Neeraja
Prof. T. Sai Kumar

Organizing Committee

Dr. K. Srujan Raju
Prof. G. Srikanth
Mr. N. Bhaskar
Mr. V. Naresh Kumar
Mr. A. Bharath Kumar, ECE
Mrs. B. Ragini Reddy, ECE
Mr. S. Venkatesh, ECE
Mrs. P. Satyavathi, CSE
Mr. N. Bhaskar, CSE
Prof. T. Sai Kumar
Prof. Dimlo. U. Fernandes
Mr. Md. Rafeeq
Mr. B. Ravinder
Mrs. J. Srividya, CSE
Mrs. Ch. Sudha Rani, ECE
Mrs. K. Mohana Lakshmi, ECE
Mr. J. Narasimha Rao, CSE
Mrs. B. Rama Devi, ECE, KITS

Program Committee

Ms. V. Swapna
Mr. Narasimha Rao

Mrs. Suvarna Gothane
Mrs. J. Srividya
Mr. K. Murali
Mr. Ch. Sudha Mani

Finance Committee

Prof. G. Srikanth
Mr. D. Venkateshwarlu

Publicity Committee

Dr. K. Srujan Raju
Mr. M. Ajay Kumar
Mr. P. Nagaraju
Mr. Anirban Paul

Exhibition Committee

Prof. T. Sai Kumar
Mrs. D. Anuradha
Mrs. A. Anusha
Mr. Ameen Uddin Md.

Transport Committee

Mr. R. Nagaraju
Mr. U. Yedukondalu
Mr. A. Bharath Kumar
Mr. V. Pradeep kumar

Hospitality Committee

Prof. K. Neeraja
Ms. Ch. Swapna

Mrs. K. Kiranmai
Mr. Md. Abdul Naqi

Sponsorship Committee

Mr K. Bharath
Mr. P. Kranthi Rathan
Mr. E. Uma Shankar
Mr. Ch. Narendra

Marketing & PR Committee

Mr. Md. Shabeer
Mr. S. Satyanarayan Reddy
Mr. A. Vamshidhar Reddy
Mr S. Madhu
Mr. S. Venkatesh
Mr. G. Kranthi Kiran

Registrations Committee

Mrs. P. Satyavathi
Mrs. K. Mohana Lakshmi
Mrs. K. Shrisha
Mrs. K. Jeji

Cultural Committee

Mrs. Shriya Kumari
Mrs. B. Ragini
Ms. B. Karuna Sree
Mr. M. Mahesh Babu

Web Portal Committee

Dr. K. Srujan Raju, CMRTC
Mr. T. Santhosh Kumar, CSI-Hyderabad Chapter
Mr. Chandra Mohan

International Advisory Committee/Technical Committee

Mr. Gautham Mahapatra, Sr. Scientist, DRDO, India.
Dr. A. Damodaram, Director, Academic & Planning, JNTUH
Dr. A. Govardhan, Director, SIT-JNTUH, India
Dr. Kun-Lin Hsieh, NTU, Taiwan
Dr. Ahamad J. Rusumdar, KIT, Germany
Dr. V.R. Chirumamilla, EUT, The Netherlands
Dr. Halis Altun, MU, Turkey
Dr. Vakka Murali Mohan, BRC, India
Dr. K .Ashoka Reddy, KITSW, India
Dr. Md. Zafar Ali Khan, IITH, India
Dr. S.K. Udagata, UOH, India
Mr. Anirban Pal, Tech Mahindra, India

External Reviewers Board

Ankur Singh Bist, KIET, Ghaziabad, India
Dac-Nhuong Le, VNU University, Hanoi, Vietnam
Sumit Ashok Khandelwal, MIT Academy of Engineering, Pune, India
Srinivas Sethi, Indira Gandhi Institute of Technology, India
Kavita Choudhary, ITM University, Gurgaon, India
Ashwini B. Abhale, D.Y. Patil College of Engineering, Akurdi, India
Sadhana J. Kamatkar, University of Mumbai, Mumbai, India
Musheer Ahmad, Jamia Millia Islamia, New Delhi, India
Mridu Sahu, NIT, Raipur, Chhattisgarh, India
Ranjan Tripathi, SRM-GPC, Lucknow (Uttar Pradesh), India
Steven Lawrence Fernandes, Sahyadri College of Engineering & Management, Mangalore, India
G. Rosline Nesa Kumari, Saveetha School of Engineering, Saveetha University Chennai, India
Arshad Mohd. Khan, Innovative Technologies, Hyderabad, India
Nikhil Bhargava, CSI ADM, Ericsson, India
Chirag Arora, KIET, Ghaziabad, India

H.V. Jayashree, PESIT, Bangalore, India
Ravi Tomar, University of Petroleum and Energy Studies, Dehradun, India
Sourav Samanta, University Institute of Technology, BU, India
Srinivas Aluvala, SR Engineering College, Warangal, India
Ritesh Maurya, ABVIITM, Gwalior, India
Abdul Wahid Ansari, University of Delhi, New Delhi, India
Gaikwad Bharatratna Pralhadrao, LPP Institute, Vivekanand College Campus, Aurangabad
A.N. Nagamani, PESIT, Bangalore, India
Balasaheb Deokate, Vidya Pratisthan's College of Engineering, Baramati, India
Satya Narayan Tazi, Government Engineering College, Ajmer, India
Sherin Zafar, Jamia Millia Islamia, New Delhi, India
Dileep Kumar Yadav, MRCE, Faridabad, India
Gustavo Fernandez, Austrian Institute of Technology, Vienna, Austria
Banani Saha, University of Calcutta, Kolkatta, India
Jagdish Chandra Patni, University of Petroleum and Energy Studies, Dehradun, India
Sayant Chakraborty, NIT, Durgapur, India
Kamble Vaibhav Venkatrao, Dr. Babasaheb Ambedkar Marathwada University, Aurangabad, Maharashtra, India
Tushar V. Ratanpara, C.U. Shah University, Gujarat
Hem Kumar Gopal, Government College for Women, Mandya, India
Rupayan Das, University of Engineering & Management (UEM), Jaipur, Rajasthan
Maheswari Senthilkumar, Sambhram Institute of Technology, Bangalore, India
Hemprasad Y. Patil, LGNSCE, University of Pune, India
Angshuman Khan, University of Engineering & Management, Jaipur, India
Kamal Kant Sharma, Chandigarh University, Gharuan, Mohali, India
Sk. Md. Obaidullah, Aliah University, Kolkata, West Bengal, India
Nilanjan Dey, Bengal College of Engineering and Technology, Durgapur, India
Andhe Dharani, Mother Teresa Women's University, India
Sandip Das, University of Engineering and Management, Jaipur
Chayan Halder, West Bengal State University, Barasat, Kolkata, India
Vipin Khattri, SRMU, Lucknow-Deva Road, Uttar Pradesh
Alak Majumder, NIT, Arunachal Pradesh, India
Amartya Mukherjee, Bengal College of Engineering and Technology, Durgapur, India
Suvojit Acharjee, NIT, Agartala, India
Aarti Singh, MMICCTBM, M.M. University, Mullana, India
Ramesh Sunder Nayak, Canara Engineering College, Benjanapadavu, Mangalore, India
P.K. Gupta, Jaypee University of Engineering and Technology, Raghogarh, India
Shilpa Bahl, KIIT, Gurgaon, India
Sudhir Kumar Sharma, Ansal Institute of Technology, GGS Indraprastha University, Gurgaon, India
Bikesh Kumar Singh, NIT, Raipur, Chhattisgarh, India

Inderpreet Kaur, Chandigarh University, Gharuan, Mohali
Subuhi Khan, AMU, Aligarh, India
Shabana Urooj, GBU, Greater Noida, India
Mukul Misra, SRMU, Lucknow-Deva Road, Uttar Pradesh
Paras Jain, Jaypee University of Engineering and Technology, Raghogarh, India
Suresh Limkar, AISSMS IOIT, Pune, India
Pritee Parwekar, ANITS, Vishakhapatnam, India
Sri. N. Madhava Raja, St. Joseph's College of Engineering, Chennai, Tamil Nadu, India
S. Ratan Kumar, ANITS, Visakhapatnam
S. Sridevi Sathya Priya, Karunya University, Coimbatore, Tamilnadu, India
Nishant Shrivastava, Jaypee University of Engineering and Technology, Raghogarh, India
Rajinikanth Venkatesan, St. Joseph's College of Engineering, Chennai, India
Sireesha Rodda, GITAM University, Visakhapatnam, Andhra Pradesh, India
Tanmoy Halder, University of Kalyani, West Bengal, India
Garima Singh, Jaypee University of Information Technology, Waknaghat, Solan, Himachal Pradesh, India
A. Rajireddy, CMR Technical Campus, Hyderabad
Somnath Mukhopadhyay, University of Kalyani, West Bengal, India
Abhinav Krishna, SRMGPC, Lucknow (Uttar Pradesh), India
Himanshi Patel, SRMGPC, Lucknow (Uttar Pradesh), India
Arindam Sarkar, University of Kalyani, West Bengal, India
Y.V. Srinivasa Murthy, NIT, Surathkal, India
Uttam Mondal, College of Engineering & Management, Kolaghat, India
Akanksha Sahu, SRMGPC, Lucknow (Uttar Pradesh), India
Tara Sai Kumar, CMR Technical Campus, Hyderabad
B.N. Biswal, BEC, Bhubaneswar
And many more.....

Contents

Human Gait Recognition Using Gait Flow Image and Extension Neural Network	1
Parul Arora, Smriti Srivastava and Shivank	
Improved Topology Preserving Maps for Wireless Sensor Networks Through D-VCS	11
Dhanya Gopan, P. Divya and Maneesha Vinodini Ramesh	
Real-Time Processing and Analysis for Activity Classification to Enhance Wearable Wireless ECG	21
Shereena Shaji, Maneesha Vinodini Ramesh and Vrindha N. Menon	
Adaptive Video Quality Throttling Based on Network Bandwidth for Virtual Classroom Systems	37
Jobina Mary Varghese, Balaji Hariharan, G. Uma and Ram Kumar	
Efficiency–Fairness Trade-Off Approaches for Resource Allocation in Cooperative Wireless Network	47
Manisha A. Upadhyay and D.K. Kothari	
An Enhanced Security Pattern for Wireless Sensor Network	61
Venu Madhav Kuthadi, Rajalakshmi Selvaraj and Tshilidzi Marwala	
Honey Pot: A Major Technique for Intrusion Detection	73
Rajalakshmi Selvaraj, Venu Madhav Kuthadi and Tshilidzi Marwala	
Computational Intelligence-Based Parametrization on Force-Field Modeling for Silicon Cluster Using ASBO.	83
S.N. Gondakar, S.T. Vasan and Manoj Kumar Singh	

Natural Language-Based Self-learning Feedback Analysis System	99
Pratik K. Agrawal, Abrar S. Alvi and G.R. Bamnote	
Adaptive Filter Design for Extraction of Fetus ECG Signal	109
Ranjit Singh, Amandeep Singh and Jaspreet Kaur	
Improving Query Processing Performance Using Optimization Techniques for Object-Oriented DBMS	119
Sheetal Dhande and G.R. Bamnote	
Linear and Non-linear Buckling Testing on Aluminium Structures	129
Snigdha Sharma, Shilpi Ghosh, Ankesh Yadav and Shabana Urooj	
A Performance Analysis of OpenStack Open-Source Solution for IaaS Cloud Computing.	141
Vo Nhan Van, Le Minh Chi, Nguyen Quoc Long, Gia Nhu Nguyen and Dac-Nhuong Le	
The Application of Sub-Pattern Approach in 2D Shape Recognition and Retrieval	151
Muzameel Ahmed and V.N. Manjunath Aradhya	
A Data-Driven Approach for Option Pricing Algorithm	163
Dipti Ranjan Mohanty and Susanta Kumar Mishra	
Moderator Intuitionistic Fuzzy Sets and Application in Medical Diagnosis	171
Bhagawati Prasad Joshi and Pushpendra Singh Kharayat	
An Empirical Comparative Study of Novel Clustering Algorithms for Class Imbalance Learning	181
Ch. N. Santhosh Kumar, K. Nageswara Rao and A. Govardhan	
Augmenting Women's Safety-in-Numbers in Railway Carriages with Wireless Sensor Networks	193
Anusha Rahul, Vishnu Narayanan, Alin Devassy and Anand Ramachandran	
Analysis of Student Feedback by Ranking the Polarities	203
Thenmozhi Banan, Shangamitra Sekar, Judith Nita Mohan, Prathima Shanthakumar and Saravanakumar Kandasamy	
Seizure Onset Detection by Analyzing Long-Duration EEG Signals	215
Garima Chandel, Omar Farooq, Yusuf U. Khan and Mayank Chawla	

Enhancing the Performance of MapReduce Default Scheduler by Detecting Prolonged TaskTrackers in Heterogeneous Environments	225
Nenavath Srinivas Naik, Atul Negi and V.N. Sastry	
Prototype of a Coconut Harvesting Robot with Visual Feedback	235
Alexander J. Cyriac and V. Vidya	
Suppression of Impulse Noise in Digital Images Using Hermite Interpolation	241
Saumya Satpathy, Figlu Mohanty and Prasant Kumar Pattnaik	
Wireless Personal Area Network and PSO-Based Home Security System	251
Anita Gehlot, Rajesh Singh, Piyush Kuchhal, M.S. Yadav, Mahesh Kr. Sharma, Sushabhan Choudhury and Bhupendra Singh	
A Framework for Ranking Reviews Using Ranked Voting Method	263
Rakesh Kumar, Aditi Sharan and Chandra Shekhar Yadav	
Multi-level Thresholding Segmentation Approach Based on Spider Monkey Optimization Algorithm	273
Swaraj Singh Pal, Sandeep Kumar, Manish Kashyap, Yogesh Choudhary and Mahua Bhattacharya	
Dynamic Multiuser Scheduling with Interference Mitigation in SC-FDMA-Based Communication Systems	289
P. Kiran and M.G. Jibukumar	
Design of Proportional-Integral-Derivative Controller Using Stochastic Particle Swarm Optimization Technique for Single-Area AGC Including SMES and RFB Units	299
K. Jagatheesan, B. Anand, Nilanjan Dey and M.A. Ebrahim	
An Enhanced Microstrip Antenna Using Metamaterial at 2.4 GHz	311
Sunita, Gaurav Bharadwaj and Nirma Kumawat	
Adaptive MAC for Bursty Traffic in Wireless Sensor Networks.	319
Akansha Verma, M.P. Singh, Prabhat Kumar and J.P. Singh	
Secured Authentication and Signature Routing Protocol for WMN (SASR)	327
Geetanjali Rathee, Hemraj Saini and Satya Prakash Ghrera	

A Minimal Subset of Features Using Correlation Feature Selection Model for Intrusion Detection System	337
Shilpa Bahl and Sudhir Kumar Sharma	
Analysis of Single-Layered Multiple Aperture Shield for Better Shield Effectiveness	347
N.S. Sai Srinivas, VVSSS. Chakravarthy and T. Sudheer Kumar	
MRI Classification of Parkinson's Disease Using SVM and Texture Features	357
S. Pazhanirajan and P. Dhanalakshmi	
Variational Mode Feature-Based Hyperspectral Image Classification	365
Nikitha Nechikkat, V. Sowmya and K.P. Soman	
Implementation of Fuzzy-Based Robotic Path Planning	375
Divya Davis and P. Supriya	
Texture Segmentation by a New Variant of Local Binary Pattern	385
Mosiganti Joseph Prakash and J.M. Kezia	
Integrating Writing Direction and Handwriting Letter Recognition in Touch-Enabled Devices	393
Akshay Jayakumar, Ganga S. Babu, Raghu Raman and Prema Nedungadi	
A New Approach for Single Text Document Summarization	401
Chandra Shekhar Yadav, Aditi Sharan, Rakesh Kumar and Payal Biswas	
Analysis, Classification, and Estimation of Pattern for Land of Aurangabad Region Using High-Resolution Satellite Image	413
Amol D. Vibhute, Rajesh K. Dhumal, Ajay D. Nagne, Yogesh D. Rajendra, K.V. Kale and S.C. Mehrotra	
A Novel Fuzzy Min-Max Neural Network and Genetic Algorithm-Based Intrusion Detection System	429
Chandrashekhar Azad and Vijay Kumar Jha	
Real-Time Fault Tolerance Task Scheduling Algorithm with Minimum Energy Consumption	441
Arvind Kumar and Bashir Alam	

Completely Separable Reversible Data Hiding with Increased Embedding Capacity Using Residue Number System.	449
Geethu Mohan and O.K. Sikha	
A Metric for Ranking the Classifiers for Evaluation of Intrusion Detection System	459
Preeti Aggarwal and Sudhir Kumar Sharma	
Analysis of Different Neural Network Architectures in Face Recognition System	469
E.V. Sudhanva, V.N. Manjunath Aradhy and C. Naveena	
A Novel Approach for Diagnosis of Noisy Component in Rolling Bearing Using Improved Empirical Mode Decomposition	479
Rahul Dubey and Dheeraj Agrawal	
A Novel Solution of Dijkstra's Algorithm for Shortest Path Routing with Polygonal Obstacles in Wireless Networks Using Fuzzy Mathematics	489
Dhruba Ghosh, Sunil Kumar and Paurush Bhulania	
Asymmetric Coplanar Waveguide-Fed Monopole Antenna with SRR in the Ground Plane.	499
S. Nikhila, Poorna Mohandas, P. Durga and Sreedevi K. Menon	
Image Processing of Natural Calamity Images Using Healthy Bacteria Foraging Optimization Algorithm	505
P. Lakshmi Devi and S. Varadarajan	
Necessitate Green Environment for Sustainable Computing.	515
Bhubaneswari Bisoyi and Biswajit Das	
Determinantal Approach to Hermite-Sheffer Polynomials	525
Subuhi Khan and Mumtaz Riyasat	
Intelligent Traffic Monitoring System.	535
Satya Priya Biswas, Paromita Roy, Nivedita Patra, Amartya Mukherjee and Nilanjan Dey	
Analysis of Mining, Visual Analytics Tools and Techniques in Space and Time.	547
K. Nandhini and I. Elizabeth Shanthi	

Dimensionality Reduced Recursive Filter Features for Hyperspectral Image Classification	557
S. Lekshmi Kiran, V. Sowmya and K.P. Soman	
Customized Web User Interface for Hadoop Distributed File System	567
T. Lakshmi Siva Rama Krishna, T. Ragunathan and Sudheer Kumar Battula	
Reinforcing Web Accessibility for Enhanced Browsers and Functionalities According to W3C Guidelines	577
Nehal Joshi and Manisha Tijare	
Feature and Search Space Reduction for Label-Dependent Multi-label Classification	591
Prema Nedungadi and H. Haripriya	
Link Expiration-Based Routing in Wireless Ad Hoc Networks	601
Shweta R. Malwe, B. Thrilok Chand and G.P. Biswas	
Analysis of Dual Beam Pentagonal Patch Antenna	611
R. Anand, Jesmi Alphonsa Jose, Anju M. Kaimal and Sreedevi Menon	
Combination of CDLEP and Gabor Features for CBIR	621
L. Koteswara Rao, D. Venkata Rao and Pinapatruni Rohini	
Scheduling Real-Time Transactions Using Deferred Preemptive Technique	631
Sohel A. Bhura and A.S. Alvi	
An Intelligent Packet Filtering Based on Bi-layer Particle Swarm Optimization with Reduced Search Space	639
B. Selva Rani and S. Vairamuthu	
Storage Optimization of Cloud Using Disjunctive Property of π	649
Umar Ahmad, Vipul Nayyar and Bashir Alam	
Co-training with Clustering for the Semi-supervised Classification of Remote Sensing Images	659
Prem Shankar Singh Aydav and Sonjharia Minz	

Contents	xxi
An Integrated Secure Architecture for IPv4/IPv6 Address Translation Between IPv4 and IPv6 Networks	669
J. Amutha, S. Albert Rabara and R. Meenakshi Sundaram	
Logistic Regression Learning Model for Handling Concept Drift with Unbalanced Data in Credit Card Fraud Detection System	681
Pallavi Kulkarni and Roshani Ade	
Music Revolution Through Genetic Evolution Theory	691
Hemant Kumbhar, Suresh Limkar and Raj Kulkarni	
Low-Cost Supply Chain Management and Value Chain Management with Real-Time Advance Inexpensive Network Computing	699
K. Rajasekhar and Niraj Upadhyaya	
Opinion Classification Based on Product Reviews from an Indian E-Commerce Website	711
Debaditya Barman, Anil Tudu and Nirmalya Chowdhury	
Mitigation of Fog and Rain Effects in Free-Space Optical Transmission Using Combined Diversity	725
Dhaval Shah and Dilipkumar Kothari	
Technology Involved in Bridging Physical, Cyber, and Hyper World	735
Suresh Limkar and Rakesh Kumar Jha	
Cloud Load Balancing and Resource Allocation	745
Himanshu Mathur, Satya Narayan Tazi and R.K. Bayal	
A Novel Methodology to Filter Out Unwanted Messages from OSN User's Wall Using Trust Value Calculation	755
Renushree Bodkhe, Tushar Ghorpade and Vimla Jethani	
Resource Prioritization Technique in Computational Grid Environment	765
Sukalyan Goswami and Ajanta Das	
Fuzzy-Based M-AODV Routing Protocol in MANETs	773
Vivek Sharma, Bashir Alam and M.N. Doja	

Cuckoo Search in Test Case Generation and Conforming Optimality Using Firefly Algorithm	781
Kavita Choudhary, Yogita Gigras, Shilpa and Payal Rani	
Time Domain Analysis of EEG to Classify Imagined Speech	793
Sadaf Iqbal, P.P. Muhammed Shanir, Yusuf Uzzaman Khan and Omar Farooq	
Accurate Frequency Estimation Method Based on Basis Approach and Empirical Wavelet Transform	801
Lakshmi Prakash, Neethu Mohan, S. Sachin Kumar and K.P. Soman	
Hybrid Recommender System with Conceptualization and Temporal Preferences	811
M. Venu Gopalachari and P. Sammula	
An Approach to Detect Intruder in Energy-Aware Routing for Wireless Mesh Networks	821
P.H. Annappa, Udaya Kumar K. Shenoy and S.P. Shiva Prakash	
Author Index	831

About the Editors

Dr. Suresh Chandra Satapathy is currently working as Professor and Head, Department of Computer Science and Engineering, Anil Neerukonda Institute of Technology and Sciences (ANITS), Vishakhapatnam, Andhra Pradesh, India. He obtained his Ph.D. in Computer Science Engineering from JNTUH, Hyderabad and Master degree in Computer Science and Engineering from National Institute of Technology (NIT), Rourkela, Odisha. He has more than 27 years of teaching and research experience. His research interests include machine learning, data mining, swarm intelligence studies, and their applications to engineering. He has more than 98 publications to his credit in various reputed international journals and conference proceedings. He has edited many volumes from Springer AISC and LNCS in past and he is also the editorial board member in few international journals. He is a senior member of IEEE and Life Member of Computer society of India. Currently, he is the National Chairman of Division-V (Education and Research) of Computer Society of India.

Dr. K. Srujan Raju is the Professor and Head, Department of Computer Science and Engineering, CMR Technical Campus. Professor Srujan earned his Ph.D. in the field of Network Security and his current research include computer networks, information security, data mining, image processing, intrusion detection, and cognitive radio networks. He has published several papers in referred international conferences and peer reviewed journals and also he was on the editorial board of CSI 2014 Springer AISC series 337 and 338 volumes. In addition to this, he has served as reviewer for many indexed journals. Professor Raju is also awarded with Significant Contributor, Active Member Awards by Computer Society of India (CSI) and currently he is the Hon. Secretary of CSI Hyderabad Chapter.

Dr. Jyotsna Kumar Mandal has M.Sc. in Physics from Jadavpur University in 1986, M.Tech. in Computer Science from University of Calcutta. He was awarded Ph.D. in Computer Science and Engineering by Jadavpur University in 2000. Presently, he is working as Professor of Computer Science and Engineering and former Dean, Faculty of Engineering, Technology and Management, Kalyani University, Kalyani, Nadia, West Bengal for two consecutive terms. He started his

career as lecturer at NERIST, Arunachal Pradesh in September, 1988. He has teaching and research experience of 28 years. His areas of research include coding theory, data and network security, remote sensing and GIS-based applications, data compression, error correction, visual cryptography, steganography, security in MANET, wireless networks, and unify computing. He has produced 11 Ph.D. degrees, three submitted (2015) and eight are ongoing. He has supervised three M.Phil. and 30 M.Tech. theses. He is life member of Computer Society of India since 1992, CRSI since 2009, ACM since 2012, IEEE since 2013, and Fellow member of IETE since 2012, Executive member of CSI Kolkata Chapter. He has delivered invited lectures and acted as program chair of many international conferences and also edited nine volumes of proceedings from Springer AISC series, CSI 2012 from McGraw-Hill, CIMTA 2013 from Procedia Technology, Elsevier. He is reviewer of various international journals and conferences. He has over 355 articles and five books published to his credit.

Prof. Vikrant Bhateja is Associate Professor, Department of Electronics and Communication Engineering, Shri. Ramswaroop Memorial Group of Professional Colleges (SRMGPC), Lucknow and also the Head (Academics & Quality Control) in the same college. His areas of research include digital image and video processing, computer vision, medical imaging, machine learning, pattern analysis and recognition, neural networks, soft computing and bio-inspired computing techniques. He has more than 90 quality publications in various international journals and conference proceedings. Professor Vikrant has been on TPC and chaired various sessions from the above domain in international conferences of IEEE and Springer. He has been the track chair and served in the core-technical/editorial teams for international conferences: FICTA 2014, CSI 2014 and INDIA 2015 under Springer-ASIC Series and INDIACom-2015, ICACCI-2015 under IEEE. He is associate editor in International Journal of Convergence Computing (IJConvC) and also serving in the editorial board of International Journal of Image Mining (IJIM) under Inderscience Publishers. At present he is guest editor for two special issues floated in International Journal of Rough Sets and Data Analysis (IJRSDA) and International Journal of System Dynamics Applications (IJSDA) under IGI Global publication.

Human Gait Recognition Using Gait Flow Image and Extension Neural Network

Parul Arora, Smriti Srivastava and Shivank

Abstract This paper represents a new technique to recognize human gait using gait flow image (GFI) and extension neural network (ENN). GFI is a gait period-based technique, based on optical flow. ENN combines the extension theory and neural networks. So a novel ENN-based gait recognition method is proposed, which outperforms all existing methods. All the study is done on, CASIA-A database, which includes 20 persons. The results derived using ENN are compared with support vector machines (SVM) and nearest neighbor (NN) classifiers. ENN proved to have 98 % accuracy and lesser iterations as compared to other traditional methods.

Keywords Gait flow image · Extension neural network · Optical flow · Support vector machine · Nearest neighbor

1 Introduction

Human identification has become a challenging area from the pattern recognition point of view. Many biometric modalities such as face, finger print, iris, etc., have been used for human identification. The limitation of these modalities is that they use some specific devices to obtain features and their intrusive nature. Unlike the modalities mentioned above, gait, a behavioral modality, is a right choice to identify human based on their non-intrusive characteristics. To obtain gait patterns of a

P. Arora (✉) · S. Srivastava · Shivank
Netaji Subhas Institute of Technology, New Delhi, India
e-mail: parul.narula@gmail.com

S. Srivastava
e-mail: smriti.nsit@gmail.com

Shivank
e-mail: shivanksinghal92@gmail.com

subject, a single camera is enough [1]. Gait recognition can easily identify people at a distance by their walk manner.

Two different approaches have been adopted to recognize gait: model-based and model-free. Model-based techniques [2, 3] work on structural model of the human body. Model-free methods do not require any structure model; it works on information stored in binary silhouettes [4–6].

There are many ways to represent a gait based on gait period [7]. Out of them, one newly developed technique is a gait flow image (GFI) [8]. A GFI more directly focuses on the dynamic components, where the optical flow lengths observed on the silhouette contour are averaged over the gait period. Optical flow is a method to determine the information through the relative motion of the gait sequences. GFI is more informative and adaptive compared to other gait representations [8]. The proposed method demonstrates its performance on a gait benchmark CASIA-A dataset [9]. Moreover, in this paper, a novel technique to recognize gait using extension neural network (ENN) is proposed [10]. The proposed method [10] adapts to a new pattern as well as adjusts the boundaries of classified features. In this paper, ENN, support vector machine (SVM), and nearest neighbor (NN) are used to classify data obtained from GFI images. The experimental results show the outperformance of the proposed ENN over SVM and NN.

2 Human Silhouette Extraction

CASIA-A database directly provides gait silhouette images. For preprocessing, first region of interest (ROI) is extracted from the gait silhouettes. Next, normalization and centralization are performed on ROI to make testing easier for all subjects. Resultant size of the image after preprocessing is 128×88 . Figure 1 shows unprocessed image on left side and final image after preprocessing on the right side.

2.1 Finding Gait Period

Gait period is defined as the total number of frames in one gait cycle. The gait period can be calculated by white pixels in the silhouette image. Since the lower

Fig. 1 Original unprocessed image and final processed image

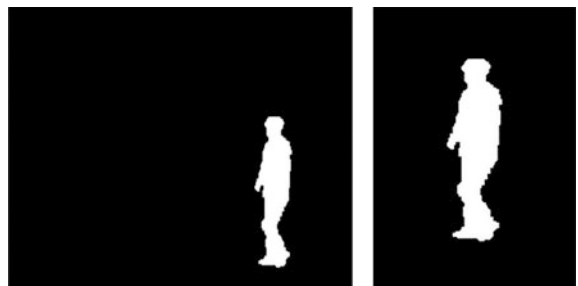
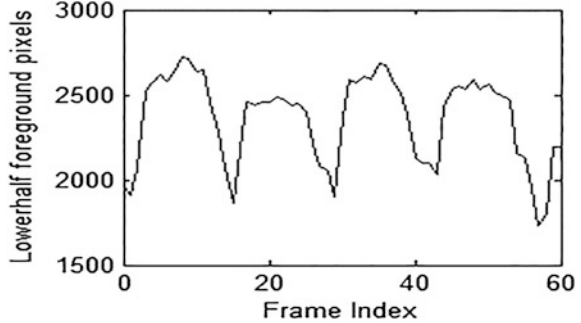


Fig. 2 Variations of foreground pixels over time



part of the body is more dynamic than the upper part, we use lower half of the silhouette image in order to find the gait period. When both legs are far apart, the number of pixels would be more as compared to when legs overlap each other. Thus, by counting the number of pixels in every frame, we get a periodic waveform, which is used to calculate gait period as shown in Fig. 2.

3 Gait Flow Image

Gait flow image captures the dynamic details from the gait patterns. For GFIs, initially the optical flow is calculated from the key frames of each gait cycle. Optical flow is estimated from two consecutive frames. For optical flow field calculation, we used Horn and Schunck's approach [11] (see Eq. (1)).

Optical flow field has two parts: one is horizontal field $uF_{t,i}$ and another vertical field $vF_{t,i}$. Horn and Schunck's optical flow method requires regularization constant to be set at 0.5, and we repeat the computation for five iterations.

$$(uF_{t,i}(m, n), vF_{t,i}(m, n)) = \text{OpticalFlow}(I_{t,i}(m, n), I_{t+1,i}(m, n)) \quad (1)$$

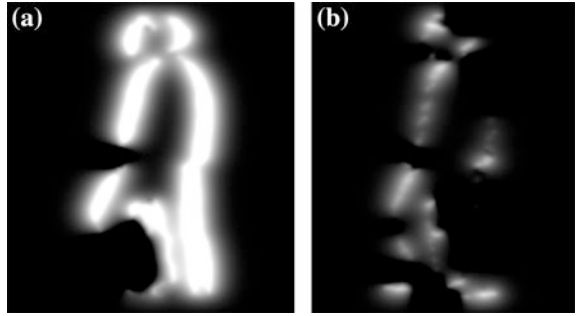
where $I_{t,i}(m, n)$ is the silhouette image at time t , i represents the particular gait cycle.

In order to calculate the vertical optical flow field $vF_{t,i}(m, n)$ and horizontal optical flow field $uF_{t,i}(m, n)$, a function `OpticalFlow` is created, where m and n are the coordinates of an image.

Figure 3 shows the horizontal and vertical components after the optical flow calculation. By combining these components, magnitude of resultant image is derived using Eq. (2).

$$\begin{aligned} \text{Mag}F_{t,i}(m, n) &= \|(uF_{t,i}(m, n), vF_{t,i}(m, n))\| \\ &= \sqrt{(uF_{t,i}(m, n))^2 + (vF_{t,i}(m, n))^2} \end{aligned} \quad (2)$$

Fig. 3 Optical flow images of human silhouette
a horizontal component u **b** vertical component v



Then we convert this resultant image into binary flow image ($\text{BF}_{t,i}$) depicted in Eq. (3). Binary flow image actually reveals the subject's movement. The black portion represents the motion. The white portion represents the static information.

$$\text{BF}_{t,i}(m, n) = \begin{cases} 0 & \text{if } \text{Mag}F_{t,i}(m, n) \geq 1 \\ 1 & \text{otherwise} \end{cases} \quad (3)$$

where $\text{BF}_{t,i}(m, n)$ represents the binary flow image at time t in cycle i . During a single gait cycle i , N number of actual silhouette images generates $N - 1$ binary flow images. By taking average of the binary flow images, GFI is generated using Eq. (4).

$$\text{GFI}_i(m, n) = \frac{\sum_{t=1}^{N-1} \text{BF}_{t,i}(m, n)}{N - 1} \quad (4)$$

where N represents the gait period. Figure 4 shows an example of GFI.

Fig. 4 GFI of a person for one gait cycle



The number of GFI depends on two important factors: Total number of frames in a sequence and its associated gait period. Due to variation in walking frequencies, the number of GFIs in the whole sequence may differ. For one gait cycle, we are getting one GFI, so to increase the samples of GFI; we shifted our sequence by some frames and then calculated its gait period and GFI. In this way, we can have multiple numbers of samples, according to our requirement.

4 Extension Neural Network

In gait recognition, the developed features are spread over a range. Therefore, ENN is most suitable classifier for this application.

4.1 Architecture of ENN

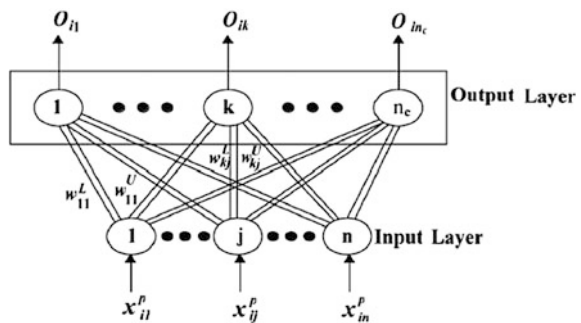
The ENN model with input node and output node is shown graphically in Fig. 5. The input nodes convert the input features into a pattern image by using a set of weights, which are the parameters of ENN. Two types of weights are used between input nodes and output nodes. Each one represents lower and upper limit of weights. The w_{kj}^L and w_{kj}^U are the weights used between input and output nodes, respectively. The output node further enhances this process. One active node at a time helps classify or recognize the input pattern.

The proposed ENN is divided into two phases—Training phase and the testing phase, which are described below.

4.2 Training Phase of ENN

The ENN adapts supervised method of learning; by tuning the weights, ENN achieves good clustering performance. Let training set is defined as $\{X_1, A_1\}$,

Fig. 5 Architecture of extension neural network (ENN)



$\{X_2, A_2\} \dots \{X_Q, A_Q\}$, where Q is the training patterns, X_i is an input vector, and A_i is the corresponding output of the neural network. The i th input vector is $X_i^s = \{x_{i1}^s, x_{i2}^s, \dots, x_{in}^s\}$, where n represents the total number of features and s is the i th pattern. To check the clustering performance, total error rate E_Q is defined in the terms of total error numbers (N_m) and total training patterns (Q), shown below:

$$E_Q = \frac{N_m}{Q} \quad (5)$$

The training phase can be described in the form of an algorithm, given below:

Step 1 The feature range of training data actually decides the lower and upper limits of connection value between input and output nodes, described as follows:

$$w_{kj}^L = \min_{i \in Q} \left\{ x_{ij}^k \right\}, \quad w_{kj}^U = \max_{i \in Q} \left\{ x_{ij}^k \right\} \quad (6)$$

For $k = 1, 2, \dots, n_c; j = 1, 2, \dots, n$

Step 2 Then, calculate cluster center of every cluster, only at initial level.

$$Z_k = \{z_{k1}, z_{k2}, \dots, z_{kn}\} \quad (7)$$

$$z_{kj} = \frac{(w_{kj}^L + w_{kj}^U)}{2} \quad (8)$$

Step 3 Observe i th training pattern and its class name s .

$$X_i^s = \{x_{i1}^s, x_{i2}^s, \dots, x_{in}^s\}, s \in n_c$$

Step 4 Extension distance (ED), a parameter, is used to estimate the distance between the training pattern X_i^s and the k th class.

$$ED_{ik} = \sum_{j=1}^n \left[\frac{|x_{ij}^s - z_{kj}| - (w_{kj}^U - w_{kj}^L)/2}{|(w_{kj}^U - w_{kj}^L)/2|} + 1 \right], k = 1, 2, \dots, n_c \quad (9)$$

Step 5 Find out the value of k^* , which satisfies $ED_{ik^*} = \min\{ED_{ik}\}$. If $k^* = s$, move to Step 7 else jump to Step 6.

Step 6 Accordingly tune the weights of s th and the k^* th class as follows:

(a) Update the centers of s th and the k^* th class:

$$\begin{aligned} z_{Sj}^{\text{new}} &= z_{Sj}^{\text{old}} + \eta(x_{ij}^s - z_{Sj}^{\text{old}}), \\ z_{k^*j}^{\text{new}} &= z_{k^*j}^{\text{old}} + \eta(x_{ij}^s - z_{k^*j}^{\text{old}}) \end{aligned} \quad (10)$$

(b) Update the weights of p th and the k^* th clusters:

$$\begin{cases} w_{Sj}^{L(\text{new})} = w_{Sj}^{L(\text{old})} + \eta(x_{ij}^S - z_{Sj}^{\text{old}}) \\ w_{Sj}^{U(\text{new})} = w_{Sj}^{U(\text{old})} + \eta(x_{ij}^S - z_{Sj}^{\text{old}}) \end{cases} \quad (11)$$

$$\begin{cases} w_{k^*j}^{L(\text{new})} = w_{k^*j}^{L(\text{old})} + \eta(x_{ij}^S - z_{k^*j}^{\text{old}}) \\ w_{k^*j}^{U(\text{new})} = w_{k^*j}^{U(\text{old})} + \eta(x_{ij}^S - z_{k^*j}^{\text{old}}) \end{cases} \quad (12)$$

where η parameter is the learning rate. The training is done to tune the weights of p th and k^* th clusters only. Therefore, ENN speeds up the process and adapt itself for a new environment

- Step 7 To train for all patterns, repeat the steps from number 3 to 6. This ends a training epoch.
 Step 8 Then stop the process, if process converges, otherwise return to Step 3.

4.3 Testing Phase of ENN

Step 1 Fix the calculated weight array of the ENN.

Step 2 Read any pattern, which is to be tested

$$X_t = \{x_{t1}, x_{t2}, \dots, x_{tn}\} \quad (13)$$

- Step 3 Then, by the same distance measure extension distance (ED), estimate the distance between the tested pattern and every class by Eq. (9).
 Step 4 Find out k^* , which satisfy $ED_{ik^*} = \min\{ED_{ik}\}$, and read output node, which indicates the class of the tested pattern.
 Step 5 Stop after classifying all tested patterns, else go to Step 2.

5 Experimental Results

In order to prove the good performance and advantages of ENN in gait recognition, we compared proposed ENN classifier with NN and SVM. NN classifier, being very simple, uses the normalized Euclidean distance measure to evaluate the similarity between GFI probe sequence and GFI gallery sequence [8]. SVM is a supervised learning classification method based on structural risk minimization, which is the expectation of the test error for the trained machine [12].

Table 1 Comparison of different classifiers

	ENN	SVM	NN
Accuracy (CCR)	98 %	96.5 %	94.7 %
Iterations	3	35	N/A

5.1 Dataset

All the study is done on CASIA-A dataset [9] provided by CASIA academy. This database consists of 20 persons, and for each person, we calculated 5 GFI images for training and 5 GFI images for testing, only for the lateral view (90°). Each GFI image is of size 128×88 , so if we concatenate all pixels in a single row, we get 11264 features.

In training phase of ENN, the total number of training patterns Q is (20 persons \times 5 samples) 100, a number of features n are 11,264, and a number of classes are 20. For ENN, the learning rate is chosen as $\eta = 0.01$. Table 1 compares the performance based on the correct classification rate (CCR) of the proposed ENN-based recognition system with SVM and NN classifier. The CCR is calculated as follows:

$$\text{CCR} = \frac{N_c}{N} \times 100(\%) \quad (14)$$

where N_c is the total number of samples, which is correctly recognized. N represents the total number of gait samples. Table 1 shows that ENN method gives a higher score as compared to other classifiers and takes less iteration to run the code.

To compare the effectiveness of the proposed approach, we have compared our results with the already developed features [13, 14] in Table 2. Results are also shown through confusion matrix illustrated in Table 3.

Table 2 Comparison of different recognition methods

Dataset	Recognition accuracy (%)		
Casia-A	Wang [13]	Chen [14]	GFI +ENN
	88.75	92.5	98

Table 3 Confusion matrix for our proposed methodology

Test Train	P1	P2	P3	P4	P5	P6	P7	P8	P9	P10	P11	P12	P13	P14	P15	P16	P17	P18	P19	P20
P1	5																			
P2		5																		
P3			5																	
P4				4						1										
P5					5															
P6						5														
P7							5													
P8								5												
P9									5											
P10										4										
P11											5									
P12												5								
P13													5							
P14														5						
P15															5					
P16																5				
P17																	5			
P18																		5		
P19																			5	
P20																				5

6 Conclusions

This work presents a new gait recognition method based on ENN. The proposed method is applied on GFI, which represents the dynamic components of a gait sequence. Compared with other recognition methods like SVM and NN, ENN adapts new environment and takes less iteration to train the system. It is proved to have high accuracy (98 %), which is comparable with the performance of SVM; but by taking less iterations, it has also proved to have less computation.

References

1. Yu, C.C., Cheng, C.H., Fan, K.C.: A gait classification system using optical flow features. *J. Inf. Sci. Eng.* **30**(1), 179–193 (2014)
2. Yam, C., Nixon, M.S., Carter, J.N.: Automated person recognition by walking and running via model-based approaches. *Pattern Recogn.* **37**(5), 1057–1072 (2004)
3. Wang, L., Ning, H., Tan, T., Hu, W.: Fusion of static and dynamic body biometrics for gait recognition. *IEEE Trans. Circuits Syst. Video Technol.* **14**(2), 149–158 (2004)
4. Kale, A., Sundaresan, A., Rajagopalan, A.N., Cuntoor, N.P., Roy-Chowdhury, A.K., Kruger, V., Chellappa, R.: Identification of humans using gait. *IEEE Trans. Image Process.* **13**(9), 1163–1173 (2004)
5. Sarkar, S., Phillips, P.J., Liu, Z., Vega, I.R., Grother, P., Bowyer, K.W.: The humanoid gait challenge problem: Data sets, performance, and analysis. *IEEE Trans. Pattern Anal. Mach. Intell.* **27**(2), 162–177 (2005)
6. Arora, P., Hanmandlu, M., Srivastava, S.: Gait based authentication using gait information image features. *Pattern Recognition Letters* (2015)

7. Arora, P., Srivastava, S.: Gait recognition using gait Gaussian image. In: IEEE Second International Conference on Signal Processing and Integrated Networks (SPIN), pp. 915–918. IEEE press (2015)
8. Lam, T.H., Cheung, K.H., Liu, J.N.: Gait flow image: A silhouette-based gait representation for human identification. *Pattern Recogn.* **44**(4), 973–987 (2011)
9. Wang, L., Tan, T., Ning, H., Hu, W.: Silhouette analysis based gait recognition for human identification. *IEEE Trans. Pattern Anal. Mach. Intell. (PAMI)* **25**(12), 1505–1518 (2003)
10. Wang, M.H., Hung, C.P.: Extension neural network and its applications. *Neural Netw.* **16**(5), 779–784 (2003)
11. Horn, B.K., Schunck, B.G.: Determining optical flow. In: Technical Symposium East, pp. 319–331. International Society for Optics and Photonics (1981)
12. Vapnik, V.N.: Estimation of dependences based on empirical data, vol. 41. Springer, New York (1982)
13. Wang, L., Tan, T., Hu, W., Ning, H.: Automatic gait recognition based on statistical shape analysis. *IEEE Trans. Image Process.* **12**(9), 1120–1131 (2003)
14. Chen, S., Gao, Y.: An invariant appearance model for gait recognition. In: IEEE International Conference on Multimedia and Expo, pp. 1375–1378. IEEE press (2007)

Improved Topology Preserving Maps for Wireless Sensor Networks Through D-VCS

Dhanya Gopan, P. Divya and Maneesha Vinodini Ramesh

Abstract Network management is crucial to implement large wireless sensor network. The network may contain hundreds to thousands of node. Furthermore, it is imperative to know the connectivity and location of the nodes to envision the framework of the network. Compared to GPS and other localization techniques, the virtual coordinate (VC) system is an affordable and efficient solution. In previous studies, the hop count from all anchor nodes was used to define the VC of a node, but the studies do not address the chance of having the same virtual coordinates. This paper introduces a distance-based virtual coordinate system (D-VCS) that uses physical distance along the shortest path from all anchor nodes to obtain distinctive virtual coordinates (VC). In the current study, we tested and analyzed the proposed D-VCS and compared it with the hop-based VCS mentioned in a previous study. We introduced a metric for connectivity error which quantitatively analyzed the precision of the introduced system. After completing the study, we observed that the TPM obtained from D-VCS shows lesser error compared to hop-based VCS. Furthermore, there was a mean deviation in connectivity error of approximately 23 % between both systems.

Keywords Wireless sensor network • Virtual coordinate and connectivity

D. Gopan (✉) · P. Divya · M.V. Ramesh
Amrita Center for Wireless Networks and Applications,
Amrita Vishwa Vidyapeetham, 690525 Kerala, India
e-mail: dhanyagopan29@gmail.com

P. Divya
e-mail: divyap@am.amrita.edu

M.V. Ramesh
e-mail: maneesham@am.amrita.edu

1 Introduction

Wireless sensor network (WSN) applications are spread over a wide range of domains such as environmental monitoring, health monitoring, military, inventory tracking, and disaster detection systems. These networks containing thousand to millions of nodes provide distributed monitoring by their properties such as collaboration, adaptation, and self organization. However, the distributed nodes may not have knowledge on their coordinates, relative distance from the neighbors, whole structure of the network, and physical voids in the network. This knowledge is significant for developing network awareness among the nodes for efficient data transfer.

A large sensor network with nodes having knowledge about their location is not a realistic solution due to the huge cost involved in integrating GPS, inaccessibility of GPS signal in environment, such as indoor or under dense foliage, and the complexity and errors of other localization techniques. In this scenario, one of the major requirements is to develop virtual coordinates (VCs) for each node. This has been achieved through a VCS [1]. VCS is capable of preserving the node's connectivity in the network. However, this VCS method lacks in generating distinctive virtual coordinates for all nodes in the network. Hence, network awareness cannot be completely achieved through a hop-based VCS alone.

Topology preserving maps (TPM) [1] preserve the neighborhood information of a network that does not have exact physical coordinates but provides a distorted map of the original topology. TPM gives the ability to visualize the structural characteristics of such networks. It maintains the internal and external outlines of the network and provides an alternative for physical maps for many applications such as tracking [2], routing, mapping, and boundary detection. TPM will also make network design and network management processes easy for large sensor networks.

The paper [1] introduces a technique for obtaining a topology preserving map of the network through a virtual coordinate system (VCS) which uses hop count to generate VC. We propose a distance-based VCS to improve the accuracy of the map obtained using hop-based VCS. This will provide more accurate TPM of the network by providing distinctive VC for every node. This will be helpful for better and efficient WSN routing, boundary detection, backbone identification of the network, and network management.

Section 2 discusses the related work. Section 3 details the distance-based VCS generation technique. Section 4 discusses the simulation and the performance evaluation of the proposed methodology. The conclusion and the future work are described in Sect. 5.

2 Related Work

Large-scale application includes a high density of nodes deployed in areas. This brings its own challenges which include scalability, fault tolerance, density, operating environment, transmission media, and sensor network topology [3]. On the

other hand, it also brings real-time challenges due to the varying dynamic environment or physical damages of devices. Network awareness means achieving knowledge about the entire network, density of the network, physical layout, and physical voids. Network awareness among nodes helps maintain sensor network services without any delay due to node failures. Also, knowledge of structural characteristics is vital for the management of large topology complex networks.

The self awareness among nodes will improve network quality of services and resources utilization. In [4], the authors introduced a self-management solution to detect fires in an area using a Voronoi diagram to identify nodes and angstrom index to prioritize the messages. When the risk of fire was high, data was disseminated at a high data rate or else reduced. This method was for a specific application. Thus, there is a need to bring a self awareness technique that can be applied to all scenarios.

In the research papers [1, 5], the authors proposed a scheme to generate virtual coordinates which represent minimum hop count from anchor nodes. Through singular value decomposition transformation, they generated the topology preserving map. The authors observed that the performance of address-based routing improved as the network awareness develops in the node. However, in these studies, the authors have not considered reducing the probability of having the same virtual coordinate for some nodes in scenarios where density of nodes is high or nodes have a high range.

Geographic routing [6] which scales well is best for resource constraint large sensor networks. For this, nodes should know the location of all the other nodes. Node localization cost, deployment, use of GPS, and failing due to physical voids are the limitations of geographic routing. In order to overcome these limitations, virtual coordinate systems are introduced to generate virtual coordinates which can be used as an alternative to geographic coordinates. In [7], the authors performed a conformal mapping to prevent failure of greedy forwarding at intermediate nodes.

Mal et al. [8] come up with a VCS where they used connectivity information in the setup phase to generate virtual region. In order to route packets in regions that have the same virtual coordinates, the authors used neighbor table for route which needed regular updating. Therefore, there is need to develop a VCS that accounts for nodes that have distinctive virtual coordinates.

Virtual coordinates are obtained with reference to anchors nodes selected in VCS. Thus, anchor placement in the network plays a major role. Extreme node search (ENS) [9] uses a directional transformation to identify how many anchors should be placed and its position in the network. A solitary anchor node is placed at the center in the spanning path virtual coordinate system (SPVCS) [10] which showed better performance for small networks. In the Virtual Coordinate assignment protocol (VCap) [11], the farthest three nodes in the network were chosen as anchor nodes to generate virtual topology.

Most of the work done in achieving network awareness will be helpful in achieving fault tolerance, efficient resource utilization, and efficient and cost-effective replacements for geographic routing for large-scale sensor networks. Our work focuses on achieving network awareness by enhancing the topology

preserving map considering different network topologies, voids, connectivity and reducing the probability for having nodes with the same virtual coordinates.

3 Design of Distance-Based Virtual Coordinate System

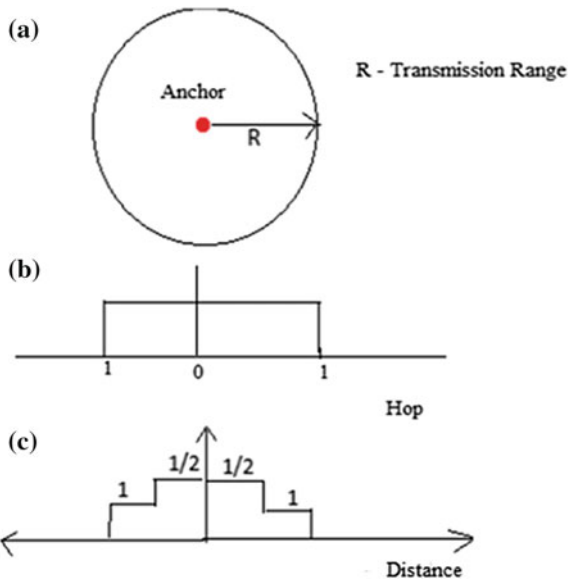
Among different virtual coordinate systems, a major study has been done on hop-based VCSs where every node has virtual coordinates which represents the minimum hop distance from anchor nodes in the network. So in this system, nodes within the transmission range of an anchor node will have same virtual coordinates. The resulting TPM obtained through this system does not portray the actual physical topology of the network. Hence, it is necessary to introduce a technique which is able to reveal those hidden structural characteristics by reducing the chance to have nodes with the same virtual coordinates. Thus, we introduce a novel distance-based virtual coordinate system (D-VCS) to capture the structural characteristics of a network in a better way compared to hop-based VCS. Here, instead of minimum hop distance from anchor nodes, the physical distance between the nodes along the shortest path to all anchor nodes is used to generate the virtual coordinates.

Consider an anchor node as shown in Fig. 1a, having a transmission range ' R ' in VCS. All the nodes that lie inside the circle of radius R will have the same minimum hop distance from this particular anchor node, i.e., a hop count of one for all nodes within the range R as depicted in Fig. 1b. However, in the case of the proposed distance-based VCS, instead of hop count, the physical distance between the node and the anchor estimated using any localization method such as RSSI is used to calculate the VC. So every nodes within the transmission range will have a distinctive position based on the distance, i.e., each node inside the range of the anchor will have different coordinates which is shown as multiple levels in Fig. 1c. Even if the density of the network becomes high or if the range of the nodes is high, the probability of having nodes with the same virtual coordinates can reduce through this approach. The proposed D-VCS to generate accurate topology preserving maps also consists of three main phases as in the existing hop-based VCS: virtual coordination (VC) generation, topology coordinate (TC) generation, and topology preserving map (TPM) generation. The main difference of the proposed algorithm with the existing hop-based VCS is in the virtual coordination (VC) generation phase, wherein we determine the actual distance between nodes rather than the hop count.

3.1 Virtual Coordinate Generation

In hop-based VCS, the minimum hop distance from all anchor nodes is represented as the virtual coordinates of every node in the network. However, in the proposed distance-based VCS, the virtual coordinate is characterized by the summation of

Fig. 1 Limitation of hop-based VCS

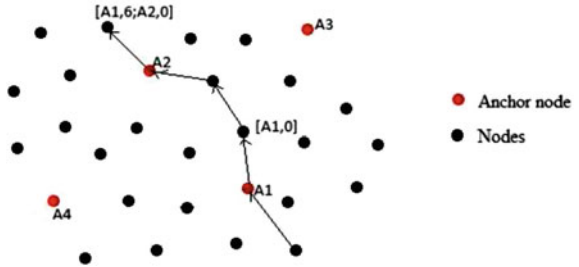


distance between nodes along the shortest path to all anchor nodes. If a network consists of N nodes in which M nodes are chosen as anchor nodes, i th node is represented by the vector;

$$P(i) = [d_{iA1}, d_{iA2}, \dots, d_{iAM}] \quad (1)$$

where $d_{iA1}, d_{iA2}, \dots, d_{iAM}$ are the distance from i th node to all M anchor nodes, respectively. In the VC generation phase, all the nodes will generate its VC through the initial setup phase which uses random routing. When a packet is received by an anchor node for the first time, it will attach its ID and a distance value field and forwards it to the random neighbor node. A node will store the node ID when it receives the message from a node for the initial time, and it will calculate the distance from the sender. The node will then add this calculated value with the distance value in the message received. Figure 2 shows an example network showing VC generation. When the packet is sent by the anchor A_1 , it will append its ID A_1 and a distance value field with value zero. When this packet is received by a node, it calculates the distance from the sender and adds it with the distance value from the packet. If the distance between the nodes is 2 units, on receiving the packet from A_1 , it calculates the distance as 2 and adds this with 0, received as the distance value from the node. So the node will have 2 as the shortest distance from anchor A_1 . Eventually all the nodes will generate VC when sufficient packets are flowed through the network.

Fig. 2 An example showing VC generation



3.2 Topology Preserving Map Generation

In the topology coordinate generation phase, a node will generate its topology coordinates using singular value decomposition (SVD) on the VC matrix of the network. The length of VC vector of all nodes in the network will be M if there are M anchor nodes in the network. There is a matrix which contains VCs of all nodes in the network, P of order $N \times M$. In order to procure the significant information about the topology from the dataset P , we apply SVD on P

$$P = U \cdot S \cdot V^T \quad (2)$$

where U , S , and V are $N \times N$, $N \times M$, and $M \times M$ matrices, respectively. Then $U \cdot S$ gives coordinates for P under the new basis V .

$$P_{\text{svd}} = U \cdot S \quad (3)$$

$$[x, y] = [P_{\text{svd}2}, P_{\text{svd}3}] \quad (4)$$

where P_{svd} is an $N \times M$ matrix which contains the information about the original network. The most significant information lies in the first component and it decreases for higher components. The second and third components contain the two-dimensional x and y coordinates, and thus, they are used to generate topology preserving maps.

4 Simulation and Results

The realization of the proposed D-VCS was done on Matlab 7.8.0, R2009a. In order to qualitatively analyze the accuracy of the maps obtained, we considered different network topologies such as random network with void, rectangular network, and rectangular network with void. In each network, we tried to vary the size of the network, density of the network, number of anchor nodes, anchor placement, and

transmission range and analyzed the effect on the topology preserving map obtained. Furthermore, in order to quantitatively analyze the efficiency of the TPM obtained using the proposed distance-based VCS, we introduced a metric known as connectivity error.

4.1 Effect of Transmission Range

It is observed that when the range of the nodes were high in such a way that nodes had one hop connectivity with most of the nodes in the network, the hop-based VCS failed to map the network. When the transmission ranges of the nodes were low, both hop- and distance-based VCS showed similar maps. In Fig. 3, the first map is the original rectangular network with void including 106 nodes, 5 anchor nodes placed on boundaries, and one on the center, with all nodes having a range of 200 units. The second map is the TPM based on hop-based VCS, and the third map shows the TPM based on D-VCS. It can be seen that the hop-based VCS failed to obtain TPM compared to the D-VCS. Since the nodes had a high range, all the nodes were in one hop connectivity with the anchor nodes; thus, every node had the same virtual coordinates. When the transmission range was small of 10 units, both hop-based and distance-based VCS showed similar maps which can be seen in Fig. 4.

4.2 Effect of Number of Anchor Nodes

When the number of anchor node in the network increases, the probability of having identical virtual coordinates decreases because each node will have distinct

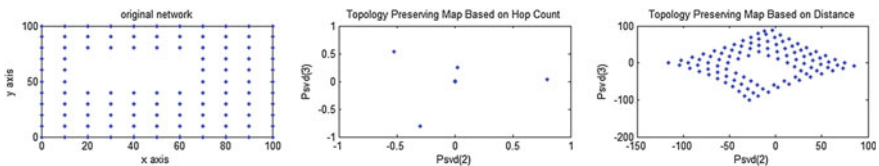


Fig. 3 Rectangular network with void; 106 nodes, transmission range 200, 5 anchor nodes

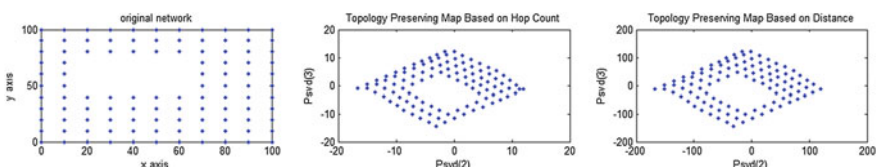


Fig. 4 Rectangular network with void; 106 nodes, transmission range 10, 5 anchor nodes

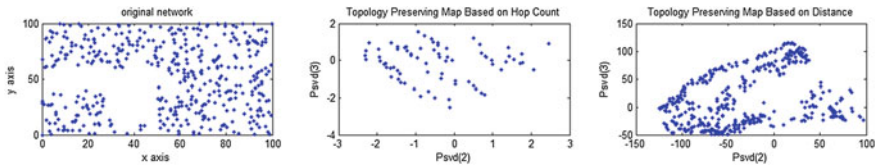


Fig. 5 Random network with void; 500 nodes, transmission range 50, 10 anchor nodes

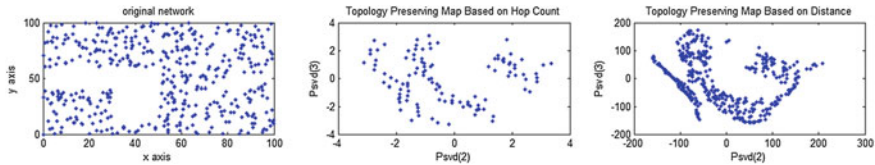


Fig. 6 Random Network with void; 500 nodes, transmission range 50, 20 anchor nodes

distance between all the anchor nodes, and thus, accuracy of the map increases. In case of random network with void of size 500 nodes, the network with 20 anchor nodes had better topology preserving map than the network with 10 anchor nodes. Figure 5 shows the random network with 10 anchor nodes and Fig. 6 with 20 anchor nodes.

4.3 Effect of Anchor Placement in the Network

It is observed that proper anchor placement on the network played a major role on the accuracy of the maps. In case of the rectangular network, when the anchors were placed on the boundaries, and one on the center of the network, more accurate TPM was obtained as shown in Fig. 7, than compared to same network with same number of anchors placed randomly as shown in Fig. 8. It can be observed that networks with anchors placed far apart obtained a better map than networks with randomly placed anchors.

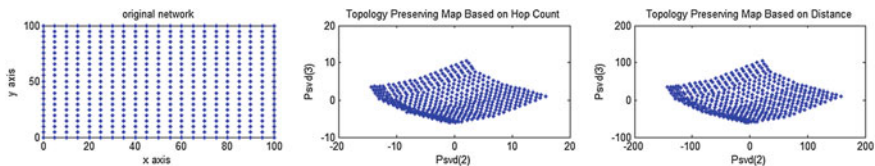


Fig. 7 Rectangular Network; 441 nodes, transmission range 10, 5 anchors placed on boundaries of the network

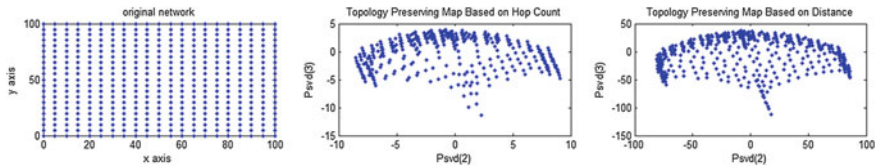


Fig. 8 Rectangular network; 441 nodes, transmission range 10, 5 anchors randomly placed

Table 1 Connectivity error for different network topologies for both distance- and hop-based VCS

Network topology	Transmission range	Connectivity error of hop-based VCS (%)	Connectivity error for distance-based VCS (%)
Random	40	61.75	48.10
Random	80	38.87	15.72
Rectangular	20	67.71	38.16
Rectangular	60	96.01	20.12
Rectangular	80	34.70	29.88
Rectangular with void	20	50.23	30.16
Rectangular with void	80	59.32	58.22

4.4 Connectivity Error

Connectivity error represents the error in total connectivity that each node has in the original network with the total connectivity and each node has in the TPM. It is observed that the TPM obtained from D-VCS shows lesser error compared to hop-based VCS which can be seen in Table 1. Furthermore, there was a mean deviation in connectivity error of approximately 23 % between both systems.

5 Conclusion

We performed an enhancement of the existing hop-based VCS by introducing distance-based VCS where the virtual coordinates of each node were characterized by the summation of the physical distance between nodes along the shortest path to all anchor nodes. It was observed that the distance-based VCS generated better topology preserving maps for different network topologies. In the case of high transmission range, distance-based VCS showed better TPM while hop-based VCS failed as a result of having the same virtual coordinates for nodes. The number of anchors and its placement in the network also affected the TPM generation. The connectivity error

metric was less for distance-based TPM than the hop-based TPM. In the future, the improved TPM can be used for better routing and network awareness in WSNs.

Acknowledgments We would like to express our sincere gratitude to our beloved Chancellor Sri Mata Amritanandamayi Devi (AMMA) for the immeasurable motivation and guidance to do this research. We would also like to express our sincere gratitude to Dr. Anura P. Jayasumana, Professor, Colorado State University, USA for the time he dedicated to help us in our research and the seamless guidance and support. This project is partly funded by a grant from Information Technology Research Agency (ITRA), Department of Electronics and Information Technology (DeitY), Govt. of India.

References

1. Dhanapala, D.C., Jayasumana, A.P.: Topology preserving maps from virtual coordinates for wireless sensor networks. In: IEEE 35th Conference on Local Computer Networks, pp. 136–143. Oct 2010
2. Jiang, Y., Dhanapala, D., Jayasumana, A.: Tracking and prediction of mobility without physical distance measurements in sensor networks. In: IEEE International Conference on Communications, pp. 1845–1850. June 2013
3. Akyildiz, I.F., Su, W., Sankarasubramaniam, Y., Cayirci, E.: A survey on sensor networks. *Comm. Mag.* **40**(8), 102–114 (2002)
4. Ruiz, L.B., Braga, T.R.M., Silva, F.A., Assunção, H.P., Nogueira, J.M.S., Loureiro, A.A.F.: On the design of a self-managed wireless sensor network. In: IEEE Communication Magazine (2005)
5. Dhanapala, D., Jayasumana, A.: Clueless nodes to network-cognizant smart nodes: achieving network awareness in wireless sensor networks. In: Consumer Communications and Networking Conference (CCNC), pp. 174–179. IEEE, Jan 2012, 4
6. Karp, B., Kung, H.T.: GPSR: greedy perimeter stateless routing for wireless networks. In: Proceedings of MobiCom2000
7. Sun, S., Yu, J., Zhu, L., Wu, D., Cao, Y.: Construction of generalized ricci flow based virtual coordinates for wireless sensor network. *IEEE Sens. J.* **12**(6), (2012)
8. Ma, Z., Jia, W., Wang, G.: Routing with virtual region coordinates in wireless sensor networks. In: IEEE 10th International Conference on Trust, Security and Privacy in Computing and Communications, pp. 1657–1661. Nov 2011
9. Dhanapala, D., Jayasumana, A.: Anchor selection and topology preserving maps in WSNs 2014; a directional virtual coordinate based approach. In: IEEE 36th Conference on Local Computer Networks, pp. 571–579. Oct 2011
10. Liu, K., Abu-Ghazaleh, N.: Stateless and guaranteed geometric routing on virtual coordinate systems. In: 5th IEEE International Conference on Mobile Ad Hoc and Sensor Systems, pp. 340–346. MASS, Sept 2008
11. Caruso, A., Chessa, S., De, S., Urpi, A.: GPS free coordinate assignment and routing in wireless sensor networks. In: 24th Annual Joint Conference of the IEEE Computer and Communications Societies INFOCOM 2005, vol. 1, pp. 150–160. Proceedings IEEE, March 2005

Real-Time Processing and Analysis for Activity Classification to Enhance Wearable Wireless ECG

Shereena Shaji, Maneesha Vinodini Ramesh and Vrindha N. Menon

Abstract Health care facilities in rural India are in a state of utter indigence. Over three-fifths of those who live in rural areas have to travel more than five km to reach a hospital and health care services are becoming out of reach for economically challenged communities in India. Since rural communities experience about 22.9 % of deaths due to heart disease [1], there is a need to improve remote ECG monitoring devices to cater to the needs of rural India. The existing wearable ECG devices experience several issues in accurately detecting the type of heart disease someone has due to the presence of motion artifacts. Hence, even though wearable devices are finding their place in today's health care systems, the above-mentioned issues discourage a doctor in depending upon it. So to enhance the existing wearable ECG device, we designed a context aware system to collect the body movement activity (BMA). In this paper, an innovative BMA classifier has been designed to classify the physical activities of user from the real-time data received from a context aware device. The test results of the BMA classifier integrated with the complete system show that the algorithm developed in this work is capable of classifying the user activity such as walking, jogging, sitting, standing, climbing upstairs, coming downstairs, and lying down, with an accuracy of 96.66 %.

Keywords Body movement activity (BMA) · BMA classifier · Motion artifacts · Context aware

S. Shaji (✉) · M.V. Ramesh · V.N. Menon
Amrita Center for Wireless Networks and Applications,
Amrita Vishwa Vidyapeetham, Amritapuri, Kollam, India
e-mail: shereenashaji12@gmail.com

M.V. Ramesh
e-mail: maneesha@am.amrita.edu

V.N. Menon
e-mail: vrindanmenon@am.amrita.edu

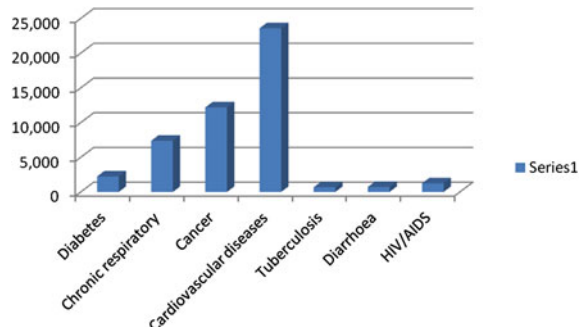
1 Introduction

Health care in rural India is 1.5 times more expensive than urban areas [2]. Every year, approximately 20 million people are forced to live below the poverty line due to expensive health care costs. Wearable health care devices can be used to deliver low cost and efficient health care services.

A comparison of mortality rates for major diseases is shown in Fig. 1. According to the world health organization, heart-related disorders will kill almost 20 million people by 2015 [4]. However, there are no existing low cost systems that would help us identify the reason for the abnormalities in heart functions. As cardiovascular diseases are one of the most common diseases in rural India, it is crucial to integrate preventive measures or provide early warnings about such diseases. This necessitates continuous monitoring of the patients ECG devices to provide appropriate medical advice in real time to patients in rural villages.

With the development of wireless sensor networks and embedded system technologies, miniaturized wearable health monitoring equipment has become practically realistic. This can help in remotely monitoring a patient's health status. Since cardiac diseases are one of the major concerns in rural India, system for detecting cardiac diseases is highly necessary. One of the methods for detecting cardiac diseases is achieved through ECG signal analysis. ECG is used to monitor the heart's rhythm and generates a waveform by picking up electrical impulses from the polarization and depolarization of cardiac tissue. This waveform is widely adapted to diagnose and assess major health risks and chronic cardiac disease. This project deals with improving the quality of the data received from a remote wearable ECG device attached to the body of the patient, which can aid the doctor in diagnosing the patient properly. Accurate interpretation of the electrocardiogram requires high-quality signals that are free from distortion and artifacts. Motion and noise artifacts arising from a biological origin will affect the degradation of ECG signal quality. Artifacts cause significant problems as it affects the display information during surgery, and it also makes early detection and warning of imminent heart-related diseases difficult. Another problem faced is the inaccurate information recorded in automated systems which have become a source of false alarms.

Fig. 1 Mortality from major communicable and non-communicable diseases, 2030 [3]



Therefore, to improve the quality of the ECG, the physical movement of the patient should also be compared, classified, and monitored simultaneously.

The motion artifact in the ECG is related to the body movement activity (BMA). BMA can be collected effectively using an accelerometer. Accelerometer signals can be used as reference signals to identify the type of movement which can be further used to filter out motion artifacts. It is one of the best methods to identify patient activity and is proportional to external forces and hence can reflect the intensity and frequency of human movement. This paper focuses on the design of a context aware system, integrated with an efficient BMA classifier algorithm to detect patient movement and to classify them in real time. In future, these results can be used to remove motion artifacts in ECG signals.

Section 2 describes the related work. Section 3 proposes the design of a context aware system. Section 4 discuss about the feature extraction of accelerometer data. Section 5 describes the implementation and testing of the system, and Sect. 6 gives the conclusion.

2 Related Work

The challenges with existing schemes are small amplitude, narrow width, and varying wave shape which makes artifacts difficult to detect, especially in the presence of electrical noise. Due to pulse variation caused by BMA, there are chances for misinterpretation of ECG data (disease like arrhythmia). The existing systems have many issues like high power consumption, less memory availability, and high computational cost. This paper discusses about the design of real-time cardiac monitoring without restricting patient activity.

Kalisz et al. conducted a detailed analysis of activity recognition using an available accelerometer database [5]. Data from 29 users performing daily activities like walking, jogging, climbing stairs, sitting, and standing were collected to implement the system. The aggregated data were controlled using a mobile phone application. The paper only shows the simulation result related to the available database. The limitation of this system is the activity recognition results are generated off-line and are not reported back to the mobile phone and the user.

Pawar et al. proposed a technique to identify the motion artifacts and classify the specific type of activities from the ECG signal [6]. Two different types of unrelated BMA were used to find motion artifacts. A particular class of BMA was classified by applying Eigen decomposition in the corresponding ECG data. The system accurately tested stair climbing; however, there was confusion when testing walking, climbing down stairs, and movement of the left, right, or both arms. The proposed method here used accelerometer data with computationally less intensive statistical classifiers to detect the motion-induced artifacts (MIA). The cost of power for computations when the device is in a continuous monitoring mode has to be kept at a minimum.

Sharma et al. conducted a detailed analysis of frequency-based classification of activities such as rest, walk, and run, using data from an accelerometer [7]. The paper highlighted the classification of user activities based on frequency components seen in the accelerometer readings in a wireless sensor network. The data collection was done in the order of REST-WALK-RUN, and the classifier was developed only for these activities. The main limitation was that the system was tested placing the sensor unit only on the chest. The system was tested only using single-hop communication not multi-hop communication.

Figo et al. conducted a detailed analysis of context recognition from accelerometer data by using preprocessing techniques [8]. The approaches used the main signal processing techniques such as time domain, frequency domain, and discrete representation domains. Each domain had its own specific method to abstract raw signal data, and early classification and some data compression techniques made it possible to use it in context recognition. Frequency-domain techniques were better at the computational cost than FFT method or wavelet.

3 Design of Context Aware System

An existing wearable ECG device that can be worn as a belt around the patient's waist was used to perform our research and enhance the accuracy and effectiveness of the ECG system. The wearable ECG device was enhanced so that the device would capable to collect the ECG and accelerometer data of the patient and send it via Bluetooth to the patient's smart phone.

Using the BMA classifier algorithm and artifact detection method, an initial level filtering of ECG data was performed in real time to remove the artifacts. Based on the clean data and using the cellular network, the warnings were sent to doctors for diagnosis and future analysis. As the first phase, we designed a context aware system to classify BMA.

The objective of the proposed system was to collect real-time ECG data along with the accelerometer data congruent to body movements. The system classified the real-time accelerometer data as different activities related to body movements occurred. These results were then sued to identify the motion artifacts in the ECG data. The overall architecture of this system is shown in Fig. 2. The major modules of the systems were a wearable device, a mobile phone integrated with an accelerometer, and a data acquisition and processing unit. The details are given below.

3.1 Wearable Device

The device consists of a wearable sensor unit which was used to gather real-time data from users. The heart of the wearable unit is ADS1292, a single-chip analog front end for ECG from Texas Instruments, and an MSP430 micro-controller and to

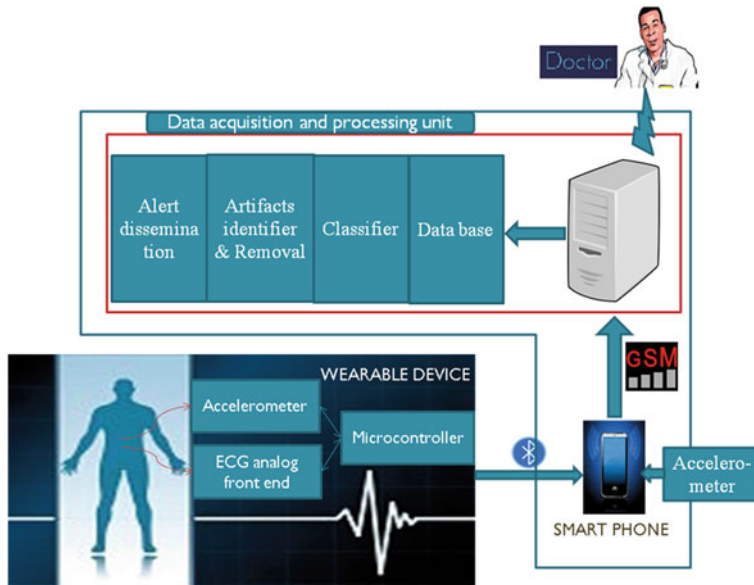


Fig. 2 Overall system architecture

monitor the connection between skin and electrode, which has the ability to monitor physical activities in low power mode. Bluetooth 2.0 connectivity was used to transmit data to a smart phone or to a compatible wireless device.

The data from the wearable device was sent via Bluetooth to the patient's smart phone. An android application was implemented on the smart phone which used the Bluetooth serial port profile (SPP) to connect with the wearable ECG device. The smart phone used a GSM network to send the data received from the wearable device to the remote data server (RMD).

3.2 Data Acquisition and Processing Unit

The data acquisition and processing unit consisted of a database, classifier, artifact identifier, alert dissemination, etc. The data acquisition unit received the data and stored them in the database. A BMA classifier algorithm ran on the back-end server to classify the user's activities. The classifier combined different processing techniques in an optimal way to classify the BMA accurately. The results were shown in the visualization unit. Further extension of the system was provided by simultaneously analyzing the accelerometer data and then using it to predict and filter out the motion artifact present in the ECG data.

4 Feature Extraction from Accelerometer Data

4.1 Orientation of Accelerometer

In this system, a tripl- axis accelerometer ADXL345 with a measurement range of ± 2 g was used to monitor activity. The placement of the accelerometer is shown in Fig. 3. When the person was standing (ideal case), the x -axis output was 0 g, the y -axis output was 1 g, and z -axis output was 0 g. An initial level classification was done for the basic activities like sitting, standing, and lying down from the orientation of the accelerometer. Also, major changes in the data were observed in the y -axis during dynamic body movements.

4.2 Preprocessing Techniques

There were both time- and frequency-domain-based preprocessing techniques. Time-domain preprocessing techniques were mean, average, root-mean square value, min/max, range, and variance. The frequency-domain approach included a fourier frequency transform (FFT) and dominant frequency. Simple mathematical and statistical methods were used to extract basic information from accelerometer data. Using these methods for preprocessing helped to select key signal characteristics. The details of various preprocessing techniques are given below:

- (1) Min/Max: Returns smallest and largest magnitude. This classifier was used for the study of short-duration body movements.
- (2) Range: Provided the difference between the largest and smallest values. This information was used to find out the dynamicity in the data, which could help in discriminating similar activities like walking, running, and jogging.



Fig. 3 Orientation of accelerometer in a wearable device

- (3) Mode: Retrieves the value that occurs most often. This was relevant only if the data is repetitive.
- (4) Median: Provided the middle value in the list of numbers. It was used to identify different inclination angles while walking, as well as to distinguish between types of postures with threshold-based techniques.
- (5) Mean: Provided the average value. It required low computational cost and is done with minimal memory requirements. It was used to process accelerometer data with random spikes and noise.
- (6) RMS: It gave a statistical measure of the magnitude of a varying quantity. It was used to distinguish walking patterns.
- (7) Variance: Defined as the average of the squared differences from the mean. This classifier was used to identify the signal stability.
- (8) Dominant frequency: Used to find the maximum frequency component in the signal.

Frequency-domain techniques were extensively used to capture the repetitive nature of accelerometer signal. Frequency-domain techniques seemed to provide both fairly good accuracy and consistency.

5 Feature Extraction from Accelerometer Data

5.1 BMA Classifier Implementation

A classifier was designed to classify seven activities such as lying down, walking, jogging, standing, sitting, climbing upstairs, and coming downstairs. The accuracy of the classifier was tested in two stages. An initial framework of the classifier was designed using an existing database. The database included data collected from 29 users performing daily activities such as walking, jogging, climbing stairs, sitting, and standing. Based on the test observation, various thresholds and decisions were set to increase the efficiency of the classifier. The second test was conducted on real data collected from 5 users (both male and female) ranging in ages (20–25). The accelerometer was placed on the hand, pocket, and belt positions. A total of 105 samples of accelerometer data for the duration of 30 s were collected at 100 samples/s while the user was performing daily activities such as jogging, walking, standing, climbing upstairs, coming downstairs, lying down, and sitting. As the wearable device, accelerometer was under test stage, a smart phone-based accelerometer, kept in the same orientation, was used as a substitute to test the classifier. The accelerometer was oriented in a way that the x -axis gave the horizontal movements, the y -axis value represented the up and down movements, and the value of the z -axis represented the forward body movement. This is shown in Fig. 4.

The flow chart of the proposed BMA classifier algorithm is shown in Fig. 5. A threshold based approach was used here for the classification of user activity. The classifier checked whether input is jogging or standing. If the activity was not

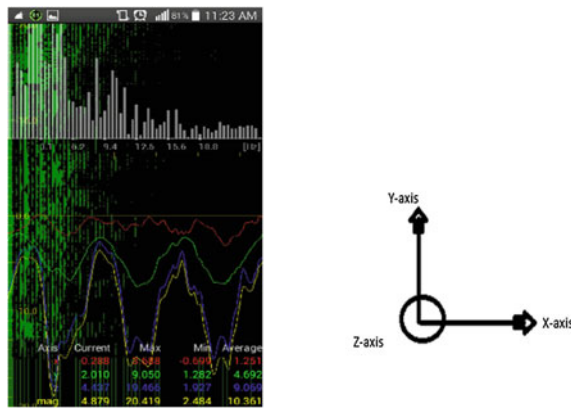


Fig. 4 Jogging activity occurs in y-axis

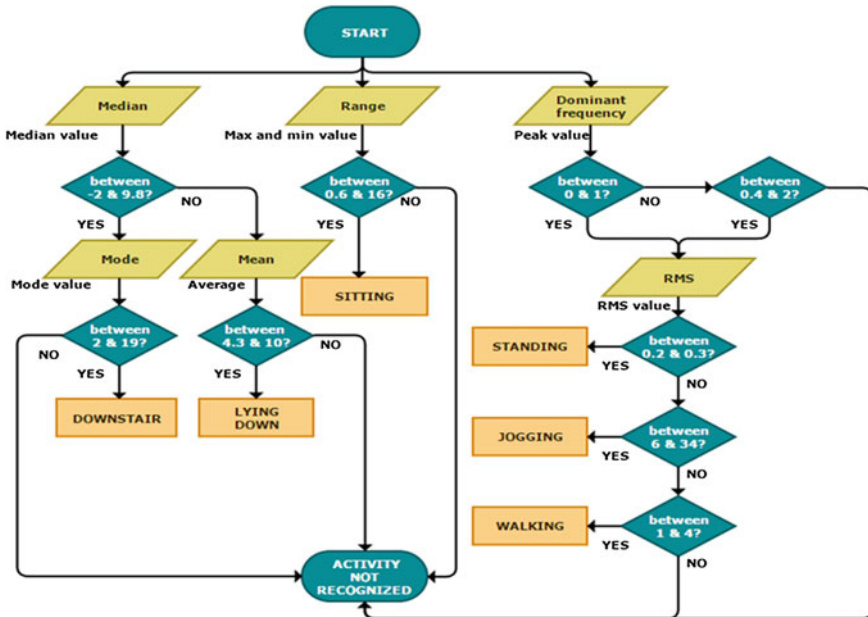


Fig. 5 Flowchart of BMA algorithm running in the MATLAB

jogging or standing, it would go to the start stage. Otherwise, it would go to the RMS classifier algorithm. If the output of the RMS classifier is not jogging/standing, it check the activity is walking. The range classifier takes the input signal and checked the activity is sitting. If the activity was not sitting, then it

was going to the end stage. The RMS and Median classifier collected the signal from input. The median classifier checked if the activity was climbing downstairs or not. If the activity was climbing downstairs, input goes to the mode classifier. If the output was not downstairs, it goes to the mean classifier checked it was lying-down activity; otherwise, the graph is ending. The collected data was fed into the data acquisition and processing unit that contains the BMA classifier algorithm running on MATLAB. Different classifiers are implemented in the MATLAB. Based on the multiple classifiers, the real-time data from a mobile phone is classified. The results of the above tests are given below.

5.2 Testing and Results

When the patient was engaging in activities like walking or jogging, there was a random nature shown in the x -axis (red), y -axis (green), and z -axis (blue) (Figs. 6 and 8). In the case of jogging, there was a relatively high acceleration in the y -axis. Frequency-domain techniques were extensively used to capture the periodic nature of the accelerometer's signal. It was used to detect the repetitive nature of a specific activity such as walking or running. The two movements were distinguished with a dominant frequency classifier, RMS, and mean classifier. The magnitude of the x -, y -, and z -axis values were used to distinguish between lying down and standing because there was no periodic pattern. In this experiment, the activity of walking was classified as moving with an average speed of 4.5 km/h. Jogging was classified as moving with an average speed of 5 km/h. All the experiments were done with the help of the triple-axial accelerometer at different positions. In the case of jogging and walking, there is a periodic nature shown in Figs. 7 and 8. In the case of standing and lying, more similarities existed. This is shown in Figs. 10 and 11. With the help of g-force, the orientation of accelerometer can be measured. In the case of sitting, the gap among x -, z -, and y -axis data is large, but with standing, the gap is less and is shown in Figs. 11 and 12. The plot of the accelerometer data for different activities is shown in Figs. 6, 7, 8, 9, 10, 11, 12, 13 and 14.

The above results show that in the case of standing and jogging dominant, frequency showed 100 % accuracy while variance and RMS showed 86.66 %.

Fig. 6 Walking

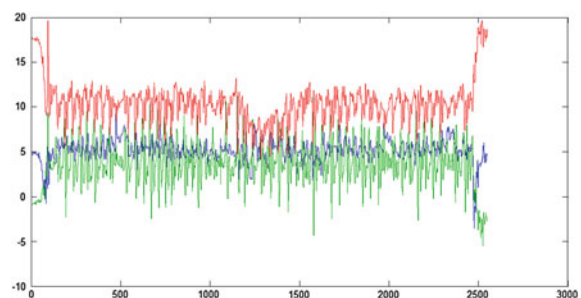


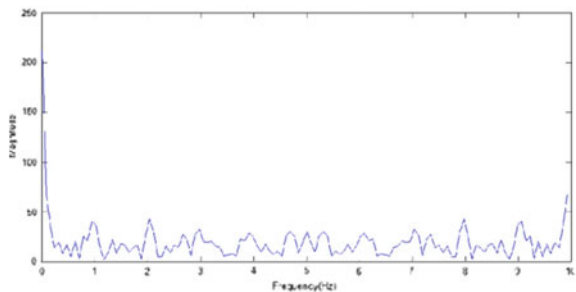
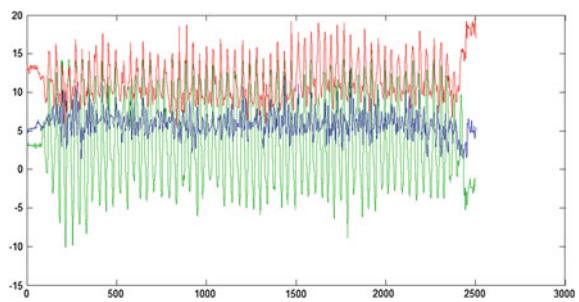
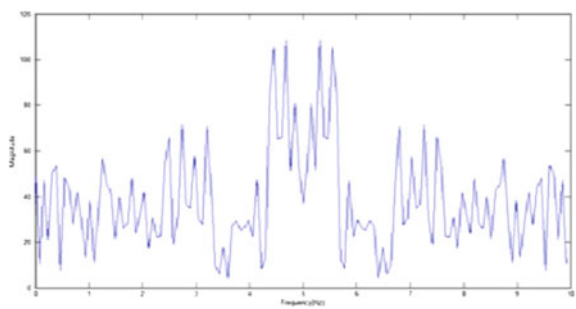
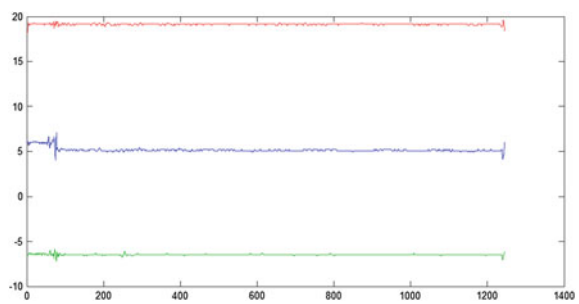
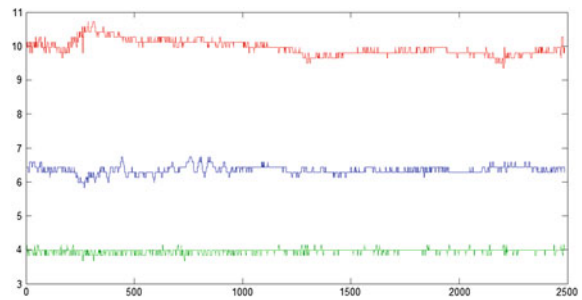
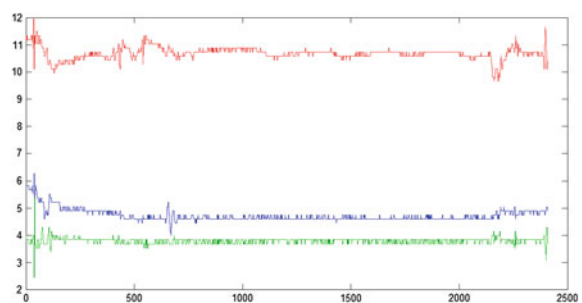
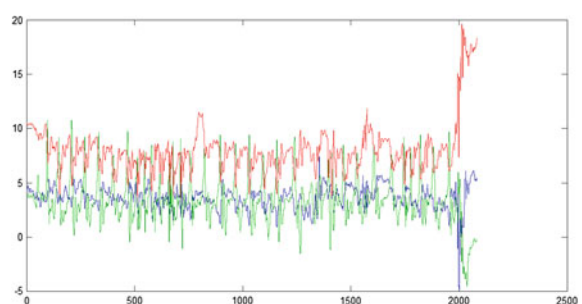
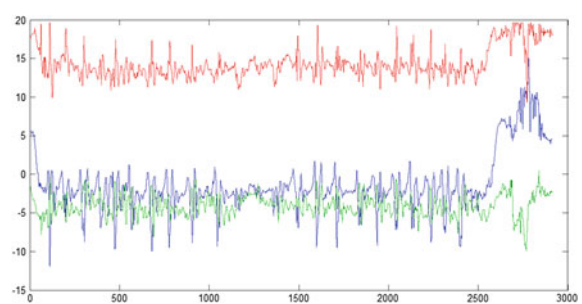
Fig. 7 Walking (FFT)**Fig. 8** Jogging**Fig. 9** Jogging (FFT)**Fig. 10** Lying down

Fig. 11 Standing**Fig. 12** Sitting**Fig. 13** Upstairs**Fig. 14** Downstairs

In the case of walking, RMS showed 93.33 % accuracy and for downstairs, median showed 100 % accuracy. In the case of sitting, range gave 93.33 % accuracy. Finally, in the lying-down activity, RMS technique showed 100 % accuracy. In the case of climbing upstairs, 86.6 % accuracy was obtained using the dominant frequency technique. The performance of the developed classifier was analyzed by using confusion matrices Tables 1, 2, 3, 4, 5, 6, 7, 8, 9, 10 and 11.

The proposed BMA classifier algorithm showed that in the case of standing and jogging, the dominant frequency showed 100 % accuracy, and the RMS and mean showed 93.33 % accuracy. In the case of walking, RMS showed 93.33 % accuracy, and for downstairs, the median showed 100 % accuracy. In the case of sitting, the range classifier showed 93.33 % accuracy. Finally, while lying down, the mean and median showed 100 % accuracy. In the case of climbing upstairs, the dominant frequency showed 86.6 % accuracy. The above result showed that the overall accuracy of the classifier was 96.66 %.

Table 1 Lying-down activity

X	Y	Z
-0.3521	0.2375	9.8889
-0.4295	-0.4997	9.9159
1.4263	0.483	9.9766
1.1668	1.0559	9.9877
0.5994	0.7897	9.9877

Table 2 Dominant frequency classifier

	ST	JO	WA	SI	UP	DW	LY
ST	15	0	0	0	0	0	0
JO	0	15	0	0	0	0	0
WA	0	1	9	0	5	0	0
SI	11	0	0	3	0	0	0
UP	0	1	0	0	12	2	0
DW	0	2	1	0	8	4	0
LY	12	0	0	0	0	0	3

Table 3 Minimum classifier

	ST	JO	WA	SI	UP	DW	LY
ST	7	0	0	3	0	5	0
JO	0	13	1	0	0	1	0
WA	0	5	9	0	1	0	0
SI	11	0	0	1	0	0	0
UP	0	5	7	0	2	0	0
DW	0	4	7	0	2	1	0
LY	1	0	0	0	1	0	13

Table 4 Maximum classifier

	ST	JO	WA	SI	UP	DW	LY
ST	10	0	0	1	1	0	0
JO	0	4	0	0	0	0	0
WA	0	11	3	0	1	0	0
SI	14	0	0	0	0	0	0
UP	0	10	2	0	1	1	0
DW	0	10	3	0	0	0	0
LY	0	1	0	0	0	0	12

Table 5 Mean classifier

	ST	JO	WA	SI	UP	DW	LY
ST	13	1	0	0	0	0	0
JO	2	13	0	0	0	0	0
WA	0	14	1	0	0	0	0
SI	11	1	0	1	0	0	0
UP	5	7	1	0	2	0	0
DW	6	4	0	0	1	0	0
LY	0	0	0	0	0	0	15

Table 6 Average mean classifier

	ST	JO	WA	SI	UP	DW	LY
ST	12	0	0	0	0	0	2
JO	2	10	1	0	1	0	0
WA	6	6	2	0	0	0	1
SI	14	1	0	0	0	0	0
UP	7	5	0	0	2	0	1
DW	8	6	0	0	0	1	0
LY	1	11	0	0	1	0	1

Table 7 Mode classifier

	ST	JO	WA	SI	UP	DW	LY
ST	0	0	1	0	0	13	0
JO	0	2	0	0	0	3	0
WA	1	1	1	0	0	5	1
SI	0	1	1	0	0	13	0
UP	0	4	1	0	0	11	0
DW	1	1	1	0	0	12	0
LY	0	0	6	0	1	0	7

Table 8 Median classifier

	ST	JO	WA	SI	UP	DW	LY
ST	7	1	0	0	0	5	0
JO	0	4	1	0	0	4	0
WA	0	5	2	0	0	3	1
SI	2	0	0	0	0	12	0
UP	0	3	0	0	1	11	0
DW	1	0	0	0	0	14	0
LY	0	0	0	0	0	0	15

Table 9 RMS classifier

	ST	JO	WA	SI	UP	DW	LY
ST	13	0	1	0	0	0	0
JO	0	13	0	0	0	0	0
WA	0	0	14	0	0	0	0
SI	12	0	0	0	0	0	1
UP	0	0	14	0	1	0	0
DW	0	3	8	0	3	0	0
LY	12	0	2	0	0	0	0

Table 10 Variance classifier

	ST	JO	WA	SI	UP	DW	LY
ST	5	0	0	10	0	0	0
JO	0	11	0	0	0	1	0
WA	0	13	1	0	0	0	0
SI	0	0	1	14	0	0	0
UP	0	13	0	0	1	1	0
DW	0	12	0	0	1	0	0
LY	2	0	4	0	8	0	1

Table 11 Proposed BMA classifier

	ST	JO	WA	SI	UP	DW	LY
ST	15	0	0	0	0	0	0
JO	0	15	0	0	0	0	0
WA	0	0	14	0	1	0	0
SI	0	0	0	14	0	1	0
UP	0	1	1	0	13	0	0
DW	0	0	0	0	0	15	0
LY	0	0	0	0	0	0	15

6 Conclusion and Future Work

In this paper, we presented the study of various preprocessing techniques for classifying BMA and developed an initial framework of a classifier algorithm for classifying patient BMA. Both time- and frequency-domain-based preprocessing techniques were used to improve the accuracy of the classifier. The results showed that the developed classifier was capable of classifying user activity with an accuracy of 96.66 %. The frequency-domain technique, which classified the data more accurately, was used as the base of the developed classifier algorithm. Based on the analysis, the hip was found to be the best place to put a triple-axis accelerometer to detect activities. The future goal of this study is to enhance the efficiency of the classifier and to incorporate real-time dynamic filtering to deliver an artifact-free ECG signal for diagnostic purposes.

Acknowledgments We would like to express our sincere gratitude to our beloved Chancellor Sri. Mata Amritanandamayi Devi (AMMA) for the immeasurable motivation and guidance to carry out this research.

References

1. Rural areas providers healthcare informatics. <http://articles.economictimes.indiatimes.com>
2. Rural areas providers' healthcare informatics. <http://articles.economictimes.indiatimes.com>
3. Data mining approach to detect heart diseases. <http://www.academia.edu>
4. Healthcare in India. <http://www.tenet.res.in>
5. Kwapisz, J.R., Weiss, G.M., A. Moore, S.: Activity recognition using cell phone accelerometers. In: Proceedings of the Fourth International Workshop on Knowledge Discovery from Sensor Data
6. Pawar, T., Chaudhuri, S., Duttagupta, S.: Body movement activity recognition for ambulatory cardiac monitoring. In: IEEE Transactions on Biomedical Engineering
7. Sharma, A., Purwar, A., Lee, Y.-D., Lee, Y.-S., Chung, W.-Y.: Frequency based classification of activities using accelerometer data. In: IEEE International Conference on Multisensor Fusion and Integration for Intelligent Systems. MFI, Aug 2008
8. Figo, D., Diniz, P., Ferreira, D. Cardoso, J.: Preprocessing techniques for context recognition from accelerometer data. Pers. Ubiquitous Comput. **14**(7), 645–662 (2010). <http://dx.doi.org>

Adaptive Video Quality Throttling Based on Network Bandwidth for Virtual Classroom Systems

Jobina Mary Varghese, Balaji Hariharan, G. Uma and Ram Kumar

Abstract Current e-Learning solutions enable viewing and interaction with participants who are geographically distant. However, these systems often are prone to delay, jitter, and packet loss owing to network fluctuation. The dynamic nature of bandwidth congestion requires us to dynamically adapt the quality of video streaming. In this paper, we attempt to alter the quality of streaming on the fly, by monitoring packet loss due to network congestion. To achieve this, we setup a simplistic classroom architecture consisting of one local and two remote classrooms with the camera feeds of the participants displayed in each other's location. The camera feeds are flagged in accordance to their predetermined priority level, and the flagging is altered in accordance to the dynamic interactions in the classroom. In the advent of network congestion, the packet loss of the recipient is monitored, and the capture resolutions of all the other feeds are altered dynamically, to make allowance for the prominent streams to remain unaffected. The effectiveness of the system is measured using participant feedback. Results indicate that the participants do not feel any perceivable change in the quality of the multimedia content presented to them.

Keywords Virtual class room • Remote class room • Resolution • Video streaming

J.M. Varghese (✉) · B. Hariharan · G. Uma · R. Kumar
Amrita Center for Wireless Networks and Applications,
Amrita Vishwa Vidyapeetham, Amritapuri, Kollam, India
e-mail: Jobz1991@gmail.com

B. Hariharan
e-mail: balajih@am.amrita.edu

G. Uma
e-mail: umag@am.amrita.edu

R. Kumar
e-mail: ramkumar@am.amrita.edu

1 Introduction

In today's internet popular applications such as Skype, WebEx, Google hangout, etc. carries video and audio data. The importance of video and audio data is increasing in a rapid way since it conveys information in a meaningful manner. Virtual class room is another application where the student and professor are at different location and they interact with each other through internet with the help of audio and video data. So the students in the remote location will get the same experiences as if they are in the same class room and there will be a full interactivity between the students and teachers. However, in all the above systems, reliability is a serious issue since it is not controlled by a single person. The network speed variations and isochronous nature of audio and video invite more congestion in bandwidth resulting in the unavailability of information, packet loss, drop in video quality, and poor end-user experience.

Increase for internet on demand has led to need for high-quality video and audio streaming services [1]. But for live streaming, it is difficult to get high-quality audio and video frames simultaneously. Delivering the video and audio contents on time becomes difficult in a fixed network bandwidth along with the existing congestion.

The performance of a system will degrade under the presence of too many packets. The number of packet sent is directly proportional to the number of packets delivered [2]. However, when the amount of traffic increases beyond a limit, the routers are no longer able to cope up with it and they began to drop the packets. At the time of high-traffic congestion, the performance will be reduced resulting in no packet delivery. During the streaming of a multimedia traffic, delay is an important factor. A slight delay in the transmission of a video packet before its play out time will result in the loss of video packet and continuity in playing. Less-quality video sequences and fluctuating quality of video sequences are quite infuriating to the end users. The reliable delivery of video stream from the main class room to the remote class room during the time of congestion is a serious problem for virtual class room scenario, since the transmission happens through internet. In order to rectify the negative impact of congestion, a control video quality adjustment is necessary.

The proposed system can be considered as one of the most optimum solutions to deliver the video contents during real-time video streaming with high-bandwidth congestion. This can be made possible by adjusting the quality of the video for a certain extent by changing the resolution. The system will throttle the video quality which would alleviate all the above problems and ensure a reliable delivery of video in the virtual class scenario.

The rest of the paper has been structured as follows. Section 2 provides the related work. Section 3 details the system architecture. In Sect. 4, we present the software implementation and the result obtained. Finally, we present our conclusion in Sect. 5. Future work is discussed in Sect. 6.

2 Related Work

Ritikesh et al. [3] proposes an approach to improve the quality of the multimedia content by assuming different utilities. They found a frame scheduling algorithm, so that it is possible to allocate bandwidth to the video streams based on the utility function. The impact of frame rate and quantization step size on the quality of video is too high. They calculated the utility metric associated with packets of video frames as the ratio of frame quality to that of the product of resolution and deadline of that frame. Utility of different frames was calculated by giving more size-based priority for the frames having similar utility. The smaller the size, the higher the priority is. Since the video scheduling is based on utility, the chances of dropping the video frames at base layers get minimized. This will help using the bandwidth effectively by reducing the jitter.

Zhang et al. [4] explains about a method to adjust the quality of Skype calls during the time of high network congestion. Under normal condition, the call can be done in a smooth manner without any difficulty. At the same time, under high congestion to get the continuity in video calls, they have used a rate control mechanism and a back-off scheme to adjust the video quality. Basic quality adjustment in Skype can be done by means of transmission control protocol (TCP) and user datagram protocol (UDP). The sender will adjust the UDP sending rate by analyzing the TCP connection report from receiver about the current network condition.

The paper of Reddyvari et al. [5] provides a method to enhance the end-user experience by means of a video scheduling policy. This will ultimately help solving the troubles related with scalable H.264 video scheduling. H.264 will improve the video quality by utilizing the video scalabilities like temporal video scalability, quality video scalability, and space-based scalability. Temporal scalability adjusts the GOP size by the creation or deletion of video layers. In quality video scalability, different quantization parameters are given to different video layers.

Khanna et al. [6] explains a method to provide good end-user experience by the proper allocation of resources. The quality of service and performance of both unicast and multicast video transmission can be improved by critical resource allocation. Results proved that performance of this scheme is far better when compared to other schemes. The video quality perception has been improved by variable frame rate, highest frame rate, and a model parameter.

Ehsan and Shyam [7] deal with a scheme to enhance the end-user experience during the time of video transmission by considering the frame priority. The central controller will look the traffic queue, and resource allocation is done based on the bandwidth request. Congestion in network always leads to drop in video packets. To avoid this, the central controller will provide different service classes to the video streams based on a minimum bandwidth. I-frame plays a great role to provide better quality than the other frames like I, P, and B. It has got an essential role in decoding the video. Higher amount of bit rate is provided for the most valuable I-frame. The loss of I-frame is solved by assigning a greater bandwidth before the

sharing of bandwidth between other frames. We can protect the bandwidth by giving the bandwidth to the other video frames except the I-frame used bands. The main disadvantage of this method is that the system will stop working whenever a node which would not support priority comes into the network and also the cost factor. Our proposed system is a solution for this which is independent of the priority.

3 System Model

This work proposes an optimal solution of multimedia content transmission in a virtual class room environment under high-bandwidth congestion. In response to network condition, the resolution of the video stream is adjusted so as to ensure graceful quality and to maintain a smooth continuous play out. Consider a simplistic virtual class room environment of three class rooms, consisting of a main class room (C1) and two remote class rooms (C2 and C3) as in Fig. 1. The main class room transfers the audio and video data at a given rate through internet. Remote class room-1 (C2) can accommodate the incoming data since it has got the same bandwidth and data rate as that of the main class room. Remote class room-2 (C3) does not have enough resources to accommodate the incoming audio and video which would result in bandwidth congestion. So the students in the remote class room-2 will have a poor end-user experience. During the congestion period, the remote class room-2 will experience loss in packets, and some amount of time delay which would finally produce video streams of poor quality. Under these circumstances, the proposed system will provide an optimum solution by measuring the presence of congestion. The network is adapted by adjusting the existing video quality to a much lower level by change in resolution. Later the video will stream in the original quality whenever the network has come back with enough resources.

Fig. 1 Overall system architecture

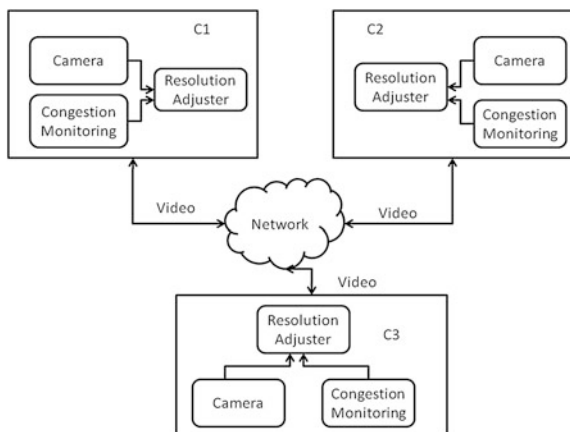
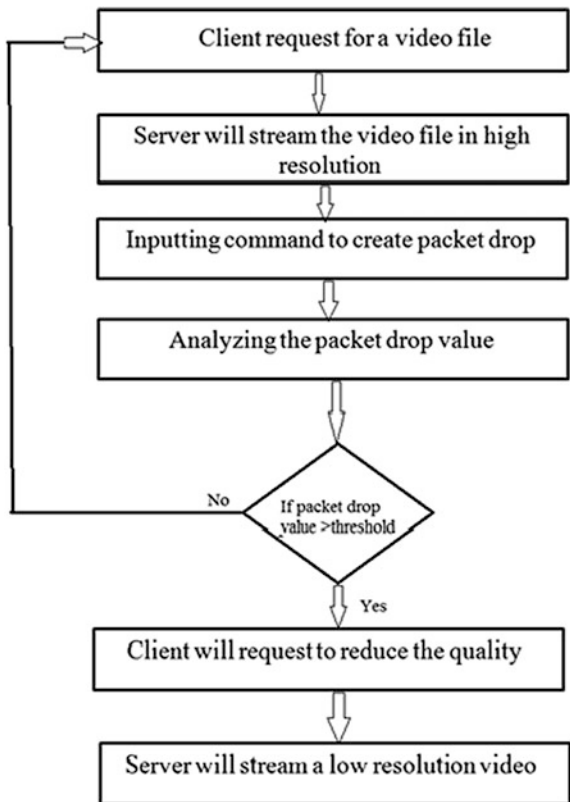


Fig. 2 Flow chart of the system



In our system model, we consider one camera attached machine (server) and a display machine (client). The server will capture the video of the main class room where the professor is standing. This raw video data will be encoded using fast forward moving picture expert group (FFmpeg) [8] which is a solution to stream audio and video data. Under normal condition, this streamed video will be forwarded to the client in high resolution. The client will respond by a congestion report to the server if there is a discontinuity in video delivery due to congestion. The congestion report carries the information to reduce the quality as shown in Fig. 2, and socket programming is used for this exchange of information. Then the server will do the reduction in quality by streaming the video data in low resolution. The experimentation is done with an assumption that the decoding errors are occurring only because of congestion even though interference may also lead to errors in network. The packet drop is introduced manually using iptables for creating the network congestion and peak signal to noise ratio (PSNR) is taken into account for evaluating the quality of video in the model.

4 Software Implementation and Results

The software implementation of the system consists of three major steps. The steps are given as follows:

Step 1: Creation of random packet drop. This can be performed by an iptable command. Iptables is an application program at the user level. It will organize the table given by kernel of Linux [9]. Using iptable commands, we can randomly create packet drop, or we can delay the incoming packets. The command for producing a random packet drop of 10 % is as follows:

```
Iptables -A INPUT -m statistic -mode random -probability 0.1 -j DROP [10]
```

- Step 2: Monitoring the congestion. A threshold value is taken to switch between the high resolution and the low resolution. For the analysis purpose, the threshold value of packet drop is taken as 25 %. Result shows that without changing the resolution up to the limit of 25 % packet drop, it is able to render the video without discontinuity. Beyond 25 % the effect of congestion is too high. That is why the threshold value of packet drop is selected as 25 %. The value of the packet drop will be continuously monitored. Whenever the packet drop is above the threshold value, we will stream the video in a low resolution. If the packet drop is less than the threshold value, then the video content is streamed in high resolution.
- Step 3: Streaming the video in high and low resolution using FFmpeg. FFmpeg is an open source tool that produces libraries and programs for handling multimedia data. Based on the report that gets from the receiver side, the sender can take measurements to adjust the resolution.

Scenario 1: Without introducing any packet drop The test is conducted by not introducing any packet drop using iptable, i.e., the packet loss is 0 %. Then the client will request for a video file, and the server will stream a high-resolution video towards the client as shown in Figs. 3 and 4.

Scenario 2: With the introduction of packet drop In the second scenario, the test is conducted by introducing random packet drop using iptables. The packet drop value is analyzed and compared with the threshold value. If it is less than the threshold value, then the server will stream at high resolution toward the client as shown in Figs. 5 and 6.

In Figs. 7 and 8, a packet drop of 40 % which is greater than the threshold value is shown. In this condition, the client will request the server to reduce the resolution, and the server will stream in low resolution.

If we send a video of 40 % packet drop without reducing the resolution, then the video which is delivering at the client side will be of poor quality as shown in Fig. 9. In this time, the video would be blocky causing irritation to the end users.

Fig. 3 Packet drop is 0 %

```

--- 192.168.1.67 ping statistics ---
10 packets transmitted, 10 received, 0% packet loss, time 8998ms

PING 192.168.1.67 (192.168.1.67) 56(84) bytes of data.
64 bytes from 192.168.1.67: icmp_seq=1 ttl=64 time=0.018 ms
64 bytes from 192.168.1.67: icmp_seq=2 ttl=64 time=0.050 ms
64 bytes from 192.168.1.67: icmp_seq=3 ttl=64 time=0.049 ms
64 bytes from 192.168.1.67: icmp_seq=4 ttl=64 time=0.052 ms
64 bytes from 192.168.1.67: icmp_seq=5 ttl=64 time=0.062 ms
64 bytes from 192.168.1.67: icmp_seq=6 ttl=64 time=0.052 ms
64 bytes from 192.168.1.67: icmp_seq=7 ttl=64 time=0.052 ms
64 bytes from 192.168.1.67: icmp_seq=8 ttl=64 time=0.054 ms
64 bytes from 192.168.1.67: icmp_seq=9 ttl=64 time=0.051 ms
64 bytes from 192.168.1.67: icmp_seq=10 ttl=64 time=0.060 ms

--- 192.168.1.67 ping statistics ---
10 packets transmitted, 10 received, 0% packet loss, time 8998ms
rtt min/avg/max/mdev = 0.018/0.050/0.062/0.011 ms

packet delay amount in % = 0
sending 0
■ 32.83 M-V: 2.679 fd= 0 aq= 0KB vq= 0KB sq= 0B f=0/0

```

Fig. 4 Video frame streaming at high resolution**Fig. 5** Packet drop is 10 %

```

--- 192.168.1.67 ping statistics ---
10 packets transmitted, 9 received, 10% packet loss, time 8996ms

PING 192.168.1.67 (192.168.1.67) 56(84) bytes of data.
64 bytes from 192.168.1.67: icmp_seq=1 ttl=64 time=0.041 ms
64 bytes from 192.168.1.67: icmp_seq=2 ttl=64 time=0.049 ms
64 bytes from 192.168.1.67: icmp_seq=3 ttl=64 time=0.053 ms
64 bytes from 192.168.1.67: icmp_seq=4 ttl=64 time=0.050 ms
64 bytes from 192.168.1.67: icmp_seq=5 ttl=64 time=0.104 ms
64 bytes from 192.168.1.67: icmp_seq=6 ttl=64 time=0.055 ms
64 bytes from 192.168.1.67: icmp_seq=7 ttl=64 time=0.059 ms
64 bytes from 192.168.1.67: icmp_seq=8 ttl=64 time=0.061 ms
64 bytes from 192.168.1.67: icmp_seq=10 ttl=64 time=0.065 ms

--- 192.168.1.67 ping statistics ---
10 packets transmitted, 9 received, 10% packet loss, time 8996ms
rtt min/avg/max/mdev = 0.041/0.059/0.104/0.019 ms

packet delay amount in % = 10
sending 0
■ 10.47 M-V: 0.153 fd= 9 aq= 0KB vq= 0KB sq= 0B f=1/1

```

Fig. 6 Video streaming at high resolution during 10 % packet drop



Fig. 7 40 % packet drop

```
--- 192.168.1.67 ping statistics ---
10 packets transmitted, 6 received, 40% packet loss, time 8998ms
rtt min/avg/max/mdev = 0.044/0.056/0.066/0.010 ms
rnode/receive.ppt
packet delay amount in N = 40
sending I
[mp4v4 @ 0xb0d0333e60] ac-tex damaged at 7 5     0KB sq=    0B f=3/3
[mp4v4 @ 0xb0d0333e60] Error at MB1 122
[mp4v4 @ 0xb0d0333e60] concealing 154 DC, 154 AC, 154 MV errors in I frame
[mp4v4 @ 0xb0d0333e60] 1. marker bit missing in 3. esc=    0B f=3/3
[mp4v4 @ 0xb0d0333e60] Error at MB1 305
[mp4v4 @ 0xb0d0333e60] concealing 161 DC, 161 AC, 161 MV errors in P frame
[mp4v4 @ 0xb0d0333e60] concealing 161 DC, 161 AC, 161 MV errors in P frame
[mp4v4 @ 0xb0d041460] slice end not reached but screenspace end (2133 left 79033C, score= -4563)
[mp4v4 @ 0xb0d041460] concealing 88 DC, 88 AC, 88 MV errors in P frame
[mp4v4 @ 0xb0d041460] ac-tex damaged at 8 14     0KB sq=    0B f=3/3
[mp4v4 @ 0xb0d0333e60] Error at MB1 123
[mp4v4 @ 0xb0d0333e60] concealing 88 DC, 88 AC, 88 MV errors in I frame
[mp4v4 @ 0xb0d041460] 1. marker bit missing in 3. esc=    0B f=3/3
[mp4v4 @ 0xb0d041460] Error at MB1 199
[mp4v4 @ 0xb0d041460] concealing 88 DC, 88 AC, 88 MV errors in P frame
[mp4v4 @ 0xb0d041460] slice end not reached but screenspace end (14 left 700C60, score= -4601)
[mp4v4 @ 0xb0d041460] concealing 88 DC, 88 AC, 88 MV errors in P frame
[mp4v4 @ 0xb0d041460] Error at MB1 329
[mp4v4 @ 0xb0d0323ae0] concealer does not match F_code
[mp4v4 @ 0xb0d0323ae0] concealer 66 DC, 66 AC, 66 MV errors in P frame
[mp4v4 @ 0xb0d041460] ac-tex damaged at 8 14     0KB sq=    0B f=3/3
[mp4v4 @ 0xb0d041460] Error at MB1 328
[mp4v4 @ 0xb0d041460] concealing 88 DC, 88 AC, 88 MV errors in I frame
```

Fig. 8 Video streaming at lower resolution during 40 % packet drop



Fig. 9 Normal condition, video frame streaming at poor quality



5 Conclusion

A novel solution is proposed to improve the end-user experience for a virtual class room environment during congestion periods. Our system model will deliver video contents to the end users for a virtual class room system without any discontinuity. The method adopted for our model is quality optimization which is based on the resolution adjustment considering the availability of bandwidth. Results indicate that the students in the main class room and remote class room will never face any noticeable change in the quality of video even in the time of congestion. A PSNR value of greater than 37 db, representing a high-quality video, is obtained in our experiment where the resolution change is done during the time of congestion.

6 Future Work

The proposed system does not consider multiple displays and multiple camera inputs. It would be better to implement a system which can handle multiple displays and multiple camera inputs and to reduce the quality of the video streams depending up on the priority. The high-priority videos could be asking a query by a remote student, professor's lecture video, etc. An approach to stream the high-priority video in high resolution and reducing the resolution of the rest of the video streams can be considered as an effective way for streaming under high-bandwidth congestion.

Acknowledgments We would like to express our sincere gratitude to our beloved Chancellor Sri. Mata Amritanandamayi Devi (AMMA) for the immeasurable motivation and guidance for doing this work.

References

1. Krishnapriya, S., Hariharan, B., Kumar, S.: Resolution scaled quality adaptation for ensuring video availability in real-time systems. In: 9th International Conference on Embedded System High Performance Computing and Communication, pp. 873–878. IEEE (2012)
2. Tanenbaum, A.S.: Computer networks, 4th edn (2003)
3. Ritikesh, K., Jagannatham, A.K.: Utility based video scheduling for quality maximization in 4G WIMAX wireless networks. In: Proceedings of the First International Conference on Wireless Technologies for Humanitarian Relief (2011)
4. Zhang, X., Xu, Y., Hu, H., Liu, Y., Guo, Z., Wang, Y.: Profiling Skype video calls: rate control and video quality. In: Proceedings INFOCOM, pp. 621–629. IEEE (2012)
5. Reddyvari, V.R., Jagannatham, A.K.: Quality optimal policy for H.264 scalable video scheduling in broadband multimedia wireless networks. In: International Conference on Signal Processing and Communications (SPCOM), pp. 1–5, (2012)
6. Jagannatham, A.K., Khanna, N.: Optimal frame rate allocation and quantizer selection for unicast and multicast wireless Scalable video communication. IETE J. Res. (2011)
7. Ehsan, H., Shyam, P.: A quality driven cross layer solution for mpeg video streaming over wimax networks. IEEE Trans. Multimed. **2**, 1140–1148 (2009)
8. FFmpeg. <https://ffmpeg.org/ffmpeg.html>
9. Iptables. <http://en.wikipedia.org/wiki/Iptables>
10. Packetdrop. <http://stackoverflow.com>

Efficiency–Fairness Trade-Off Approaches for Resource Allocation in Cooperative Wireless Network

Manisha A. Upadhyay and D.K. Kothari

Abstract Optimum resource allocation problem of cooperative wireless communication is discussed in this paper. Looking at the variety in services offered in wireless network and time-varying nature of the channel, it is need of the time to go for dynamic resource allocation which not only improves the performance but also enhances reliability, coverage, and user satisfaction in cooperative network. Efficiency and fairness are two different perspectives of resource allocation which are very difficult to achieve at the same time. We have presented three approaches for performing trade-off between efficiency and fairness in systematic manner. First approach is based on converting the data rate achieved by the user in terms of utility and then maximizes the total utility of all the users. It is shown that a properly design utility function is able to result any desired trade-off. Second approach is based on putting the restrictions of minimum resources that must be assigned to the user and maximum resources that can be given to the user. The resources that assign to any user vary between this limit. The minimum and maximum are determined by the parameters A ($0 < A \leq 1$) and B (>1). In the third approach, $E\text{-}F$ function is presented which is able to provide trade-off based upon the values of E ($1 < E \leq 2$) and F ($0 \leq F \leq 1$). In all the three cases, the total resources available for distribution are kept constant. Fairness is measured by Jain's fairness Index, and loss of efficiency is measured in terms of price of fairness.

Keywords Efficiency–Fairness trade-off · Cooperative communication · Amplify and forward · Resource allocation · Utility

M.A. Upadhyay (✉) · D.K. Kothari
Institute of Technology, Nirma University, Ahmedabad, India
e-mail: manisha.upadhyay@nirmauni.ac.in

D.K. Kothari
e-mail: dilip.kothari@nirmauni.ac.in

1 Introduction

Cooperative communication has shown its potential in fighting against fading in wireless networks by exploiting broadcasting as inherent characteristics of wireless communication [1]. Wireless nodes help each other to relay the data received by them to provide diversity combining at the destination without using multiple antennas in the hand-held devices. Properly designed cooperative diversity protocol results in improved data rates, battery power saving, and higher reliability [2]. The helper or the relay may be another similar node, or it may be installed by the service provider to enhance diversity combining in the network [3].

Duplication of transmission by the relay/s puts forward the problems like increased interference, wastage of power, and need of more spectra. The solution of these problems lies in dynamic optimum resource allocation to the each node in the network. Looking at the variety of applications provided by wireless service providers in data network, the requirement of resources depends on type, delay tolerance, and error tolerance of the application, which makes the resource allocation problem more difficult.

Two characteristics of a resource allocation scheme are efficiency and fairness. It is very difficult to achieve both of them simultaneously. If the goal of resource allocation is to maximize total data rate of the network, then more resources would be given to the sources with good channel condition, and the sources with poor channel do not get adequate resources. With limited resources, it is also difficult to cater different user demands fully. Equal allocation of the resources would not be fair to either of service provider and user. Therefore, it is utmost necessary to make trade-off between efficiency and fairness in systematic way so that users are satisfied and the resources are utilized optimally. In this paper, we have considered delay tolerant data services and three approaches for performing efficiency–fairness trade-off are presented: (i) Utility function-based approach (ii) Resource Constraint-based approach (iii) $E\text{-}F$ function-based approach.

2 Related Work

Different objective functions and strategies for resource allocation for cooperative communication have been presented in [4–12]. Performance improvement with optimal power allocation has been depicted in [4, 5]. Quality of service provisioning for FDMA/TDMA-based relay network using optimal resources is presented in [6]. Optimum power allocation results in improved performance of Decode and Forward (DF) cooperative network in [7]. Saving in resources for achieving given target with optimum resource allocation is depicted in [8]. Resource allocation to ensure fairness to all the users is addressed in [9] but the loss of efficiency to ensure the fairness is not included. If power and bandwidth are optimized jointly, its performance is better compared to optimizing power alone.

In [10], joint optimization of power and bandwidth allocation has been presented. It has demonstrated efficient and fair allocation of resources separately. Efficiency–fairness trade-off for relay selection is presented in [11]. In our previous work [14], we modified the total data-rate maximizing technique ensuring certain minimum resource allocation to each user in the network for Amplify–Forward and Decode–Forward cooperative networks. The concept of utility-based resource allocation to achieve desired quality of service in wireless network has been depicted [12, 13]. We have considered utility-based resource allocation and presented four utility functions which can very easily allocate resources to achieve desired efficiency and fairness trade-off in multi-user AF cooperative network in our previous work in [15]. In [16], we have evolved a generic utility function to perform efficiency–fairness trade-off for achieving different quality of service parameters in centralized cooperative data network.

In this paper, we have presented three approaches to perform efficiency–fairness trade-off in Amplify and forward protocol-based cooperative network: (i) Utility function-based approach, (ii) Resource Constraint-based approach, (iii) E – F function-based approach. Utility-based approach is already presented in our earlier work [14, 15, 16]. It is included here briefly for sake of comparison with the remaining two approaches. We have presented system model in Sect. 3, followed by discussion on utility function-based approach in Sect. 4, resource constraint-based approach in Sect. 5, and E – F function-based approach in Sect. 6. In Sect. 7, performance matrices to measure fairness and loss of efficiency are depicted. Simulation results and discussion are presented in Sect. 8, followed by conclusion in Sect. 9.

3 System Model

A network consisting of $i = \{1, 2, \dots, N\}$ sources, single relay, and single destination is considered. The resources are available in common pool with destination. One relay is assumed to be installed by the service provider to help many sources. We assume that destination has channel state information among the source–relay (S – R), the source–destination (S – D), and the relay–destination (R – D) channels. Based upon the instantaneous channel state information, the destination allocates bandwidth to sources to transmit their information and relay to retransmit it. The destination also instructs each source and relay to control their radiated power dynamically. In this way, power and bandwidth—both the resources, are assigned to the nodes optimally.

In the basic amplify and forward (AF) relaying scheme, the relay forwards a scaled version of the received signal to the destination, regardless of the source–relay (S – R) link quality. Let h_{sr} be the channel gain for source–relay link, h_{rd} be the channel gain for relay–destination link, and h_{sd} be the channel gain of source–destination link, P_s and P_r are the source and relay power, respectively, and W_s and

W_r are bandwidths allocated to the source and relay, respectively, No is the additive White gaussian noise (AWGN).

The source transmits the symbol blocks to both the relay and the destination. At the destination, the received signal to noise ratio (SNR) due to the direct path can be given as

$$\text{SNR}_{\text{sd}} = \frac{h_{\text{sd}}P_s}{W_sN_o} \quad (1)$$

The source is able to achieve maximum data rate of the direct path only can be given as

$$R_{\text{sd}} = W_s \log \left(1 + \frac{h_{\text{sd}}P_s}{W_sN_o} \right) \quad (2)$$

The relay also receives the signal transmitted by the source. In case of Amplify AB and Forward, a relay retransmits it by amplifying it. At the destination, the received SNR due to the retransmitted signal by the relay can be given as

$$\text{SNR}_{\text{rd}} = \frac{h_{\text{rd}}P_r}{W_rN_o} \quad (3)$$

The destination combines direct signal from the source and retransmitted signal from the relay using maximal ratio combining. After combining, the SNR of AF technique can be given as

$$\text{SNR}_{\text{srd}}^{\text{AF}} = \frac{h_{\text{sd}}P_s}{W_sN_o} + \frac{\frac{h_{\text{sr}}P_s}{W_sN_o} \cdot \frac{h_{\text{rd}}P_r}{W_rN_o}}{\frac{h_{\text{sr}}P_s}{W_sN_o} + \frac{h_{\text{rd}}P_r}{W_rN_o} + 1} \quad (4)$$

As a result of cooperation, the data rate achieved can be given as

$$R_{\text{srd}}^{\text{AF}} = W \log \left(1 + \frac{h_{\text{sd}}P_s}{WN_o} + \frac{\frac{h_{\text{sr}}P_s}{WN_o} \cdot \frac{h_{\text{rd}}P_r}{WN_o}}{\frac{h_{\text{sr}}P_s}{WN_o} + \frac{h_{\text{rd}}P_r}{WN_o} + 1} \right) \quad (5)$$

where $W = W_s = W_r$

In the next section, the utility function-based resource allocation technique is presented.

4 Utility Function-Based Approach

The degree of satisfaction of user for a given amount of resource can be represented as utility. Utility function-based resource allocation in wireless network is presented in [12, 13]. Here, utility as a function of data rate is considered, which in turn, depends on allocated power and bandwidth.

$$U = f(R_{\text{sr}}^{\text{AF}})$$

In our previous work [14], we considered various utilities as a function of data rate for real-time fixed data rate, elastic traffic, and best effort type of users. In [15], a family of utility functions capable of achieving efficiency–fairness trade-off has been presented. A generic utility function to achieve desired degree of efficiency and fairness has been presented in [16]. Next, we present the optimization problem for resource allocation. Total power available for allocation to all the sources is $P_{s,\max}$, and a relay has maximum power $P_{r,\max}$, for cooperating with i users in the network. Total bandwidth available for allocation is W_{\max} . Relay uses the same bandwidth as the bandwidth assigns to that source to retransmit the information of that user. The optimization problem determines resource allocations to maximize the sum of utility of all the users in the network. The resource allocation problem can be formulated as follows:

$$\begin{aligned} \max_{\{W, P_s, P_r\}} \quad & \sum_i U(R_{\text{sr}}^{\text{AF}}) \text{ subject to } \sum_i P_{si} \leq P_{s,\max}, \quad P_{si} > 0, \\ & \sum_i P_{ri} \leq P_{r,\max}, \quad P_{ri} > 0, \quad \sum_i W_i \leq W_{\max}, \quad W_i > 0, \end{aligned} \quad (6)$$

In the above stated optimization problem, the total resources are upper bounded by $P_{s,\max}$, $P_{r,\max}$, and W_{\max} . There is no restriction on the amount of minimum or maximum amount of resource to be allocated to each user. In the next section, the approach of resource allocation with the restriction of minimum and maximum resource to each user has been depicted.

5 Resource Constraint-Based Approach

In order to achieve efficiency–fairness trade-off, another approach is to put restriction on minimum and maximum resources which can be assigned to any user. In multi-user wireless network, each user faces different channels. Equal resources assign to them would not result in equal data rate. The efficiency perspective is to assign more resources to the user with good channel condition to maximize sum data rate of the network. But this perspective is very much “unfair” to the user with bad channel condition. As a trade-off, we present the technique to assign certain minimum resource to each user so that even the worst channel user would not be

deprived of resources completely. Remaining resources are then assigned to the users to maximize sum data rate of the network. The partition of resources for fairness and efficiency is depicted by (A, B) parameters, where $0 \leq A \leq 1$ is fairness parameter, and $B \geq 1$ is efficiency parameter.

Consider multiple units of resource R to be distributed among N users. The equal share given to each of them would be R/N . Minimum and maximum resource assigned to any user is $A * R/N$ and $B * R/N$, respectively. If $A = B = 1$, all users would be assigned with equal share R/N . When $A < 1$, small portion of R/N is ensured to the each user and then remaining part of the resource is distributed among all the users to achieve efficiency. Now, the resource allocation problem with (A, B) parameter can be formulated as follows:

$$\begin{aligned} \max_{\{W, P_s, P_r\}} \quad & \sum_i (R_{srd}^{\text{AF}}) \quad \text{subject to} \quad \sum_i P_{si} \leq P_{s,\text{max}}, \quad P_{si} \geq A * P_s^{\text{eq}}, \quad P_{si} \leq B * P_s^{\text{eq}}, \\ & \sum_i P_{ri} \leq P_{r,\text{max}}, \quad P_{ri} \geq A * P_r^{\text{eq}}, \quad P_{ri} \leq B * P_r^{\text{eq}}; \quad \sum_i W_i \leq W_{\text{max}}, \quad W_i \geq A * W^{\text{eq}}; \quad W_i \leq B * W^{\text{eq}} \end{aligned} \quad (7)$$

where P_s^{eq} , P_r^{eq} , and W^{eq} are equal allocation of power to all the sources, equal allocation of relay power to each source, and equal allocation of bandwidth to each user and $0 \leq A \leq 1$, $B \geq 1$. The constraints show that the source power, relay power, and bandwidth are upper bounded by $P_{s,\text{max}}$, $P_{r,\text{max}}$, and W_{max} . Each user must be assigned with minimum $A * (.)^{\text{eq}}$ resource, i.e., A times the equal allocation and remaining resources are to distribute among all users such that maximum resource given to any user is $B * (.)^{\text{eq}}$, i.e., B times the equal allocation, where $(.)^{\text{eq}}$ is the equal share of the resource source power, relay power, and bandwidth. By selecting appropriate value of A and B , desired degree of efficiency and fairness can be achieved.

6 E-F Function-Based Approach

In this section, a function reflecting efficiency and fairness as its components is employed to optimize resource allocation. The function is as stated below.

$$\varphi_{EF}^R = \text{sign}(1 - F) \left\{ \sum_{i=1}^N \left(\frac{R_i}{\sum_{j=1}^N R_j} \right)^{1-F} \right\}^{\frac{1}{F}} \left(\sum_{i=1}^N R_i \right)^E \quad (8)$$

where R_i is the data rate achieved by user i with the assigned resource. $i = \{1, 2, \dots, N\}$ set of users, F is fairness function, E determines efficiency, and φ_{EF}^R is the function which performs efficiency-fairness trade-off depending upon the values of E and F . This function is proved to satisfy axioms of fairness [16]. The value of F determines the type and degree of fairness. Different values of F result in max-min fairness, proportional fairness, α -fairness, etc. [18] Here, the value of

$F \in (0, 1)$ which gives α -fairness. Accordingly, the value of $E \in (1, 2)$. The optimization problem is formed as shown below.

$$\begin{aligned} & \max_{\{W, P_s, P_r\}} \sum_i \varphi_{EF}^R \\ & \text{subject to } \sum_i P_{si} \leq P_{s,\max}, \quad P_{si} > 0, \quad \sum_i P_{ri} \leq P_{r,\max}, \quad P_{ri} > 0, \quad \sum_i W_i \leq W_{\max}, \quad W_i > 0, \end{aligned} \quad (9)$$

The source power, relay power, and bandwidth are allocated to maximize the E - F function with appropriate weight to fairness and efficiency.

7 Performance Metrics

To measure the fairness, a well-known Jain's fairness index is considered as a performance criterion. In order to achieve desired fairness, efficiency has to be sacrificed. To quantify the loss of efficiency, price of fairness parameter is employed.

7.1 Fairness Index (Jain's Fairness Index)

Fairness index is defined as

$$F(x) = \frac{\left(\sum_{i=1}^n x_i\right)^2}{n * \sum_{i=1}^n x_i^2} \quad (10)$$

It rates the fairness of a set of values where there are n users and x_i is the throughput for the i th connection. The result ranges from $1/n$ (worst case) to 1 (best case), and it is maximum when all users receive the same allocation. Properties of fairness function can be found in [17, 18].

7.2 Price of Fairness (PoF)

The reduction in data rate for achieving fairness is defined as Price of Fairness [18].

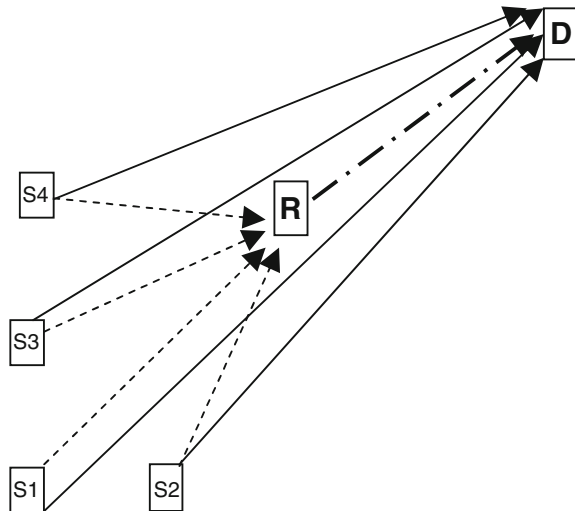
$$\text{PoF} = (R_{\text{eff}} - R_{\text{fair}})/R_{\text{fair}} \quad (11)$$

where R_{eff} is sum total data rate with efficient allocation and R_{fair} is the sum total data rate with fair allocation. Although efficiency and fairness seem to be difficult to obtain at the same time, our approaches presented here can achieve reasonable fairness with nominal loss in efficiency.

8 Simulation Results and Discussion

A multi-user network is considered here in which there are 4 sources communicating with a common destination with the help of a relay is shown in Fig 1. The channel has been modelled as Path loss channel model with exponent three. The relay is assumed to be capable of handling full-duplex communication. Channels assigned to sources are assumed to be orthogonal so that all the sources can simultaneously communicate without causing interference for each other. The destination is assumed to have channel state information of each pair of nodes in the network, based on which, the destination determines the channel to be assigned to each user, the power to be radiated by each source, and power used by the relay to help each source in order to achieve the desired goal of optimization. Channel bandwidth, source power, and relay power under consideration for allocation are normalized to 1 so that the allocation indicates the percentage of the total resource assigned to a particular node to satisfy various criteria of efficiency and fairness. The central controller at destination determines the amount of resource to be used by each node and informs all through reverse control channel at regular interval. We consider the distances between the nodes such that path loss is minimum for user 4 and gradually increased for user 3, 2, and 1. User 1 faces the worst channel.

Fig. 1 System model of multi-user cooperative network



8.1 Utility Function-Based Approach

Efficiency–fairness trade-off with the help of designing suitable utility function is depicted in our previous work [14, 15]. We have considered the following utility functions for showing the degree of trade-off:

1. $U = \sum_{i=1}^N R_i$	2. $U = \sum_{i=1}^N \log R_i$
3. $U = \sum_{i=1}^N 1 - \exp^{-R_i}$	4. $U = \sum_{i=1}^N R_i^{0.1} - 1/0.1$
5. $U = \sum_{i=1}^N R_i^{(1-0.3)} / (1 - 0.3)$	6. $U = \sum_{i=1}^N R_i^{(1-0.7)} / (1 - 0.7)$

The first utility function is to maximize the sum total data rate of the system. This is the most efficient function. It will allocate the resources to the user with good channel condition. Sum total of the system is maximized, but the individual user with bad channel condition suffers a lot. Subsequent utility function (2)–(6) provides trade-off between efficient and fair allocation as shown in Fig. 2 and Table 1. Fairness index varies between 0 and 1, 1 indicating complete fairness. Price of fairness compares total data rate achieved in function 2–5 with the data rate achieved in utility function (1).

Table 1 shows that fairness index in order of more than 0.9 can be achieved by utility functions 2, 4, and 6 with the price of fairness 0.247, 0.241, and 0.0227, respectively. Utility function 3 shows very little price of fairness with fairness in the

Fig. 2 Utility-based approach

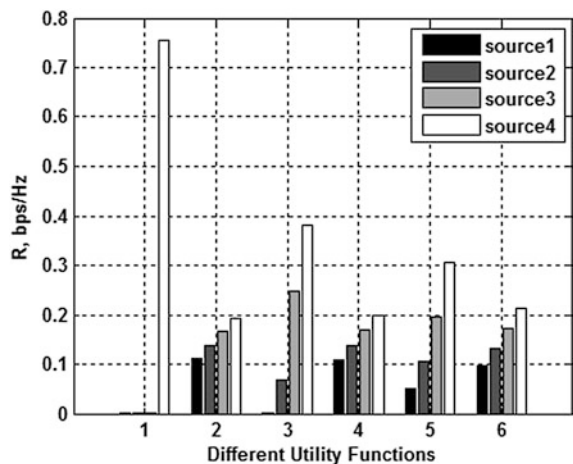


Table 1 Efficiency-fairness trade-off offered by utility functions

	Utility function	Total data rate	Fairness index	Price of fairness
1	$\sum_{i=1}^N R_i$	0.757	0.251	0
2	$\sum_{i=1}^N \log R_i$	0.607	0.962	0.247
3	$\sum_{i=1}^N 1 - \exp^{-R_i}$	0.698	0.577	0.085
4	$\sum_{i=1}^N R_i^{0.1} - 1/0.1$	0.610	0.953	0.241
5	$\sum_{i=1}^N R_i^{(1-0.3)} / (1 - 0.3)$	0.657	0.744	0.152
6	$\sum_{i=1}^N R_i^{(1-0.7)} / (1 - 0.7)$	0.617	0.929	0.227

range of 0.5. Utility function 5 shows reasonable fairness of 0.744 with price of fairness 0.152. The coefficients 0.1, 0.3, and 0.7 shown in utility functions 4–6 can be further changed to fine-tune efficiency fairness trade-off up to the desired level.

8.2 Resource Constraint-Based Approach

Each user is assigned that minimum A times its equal share and maximum B times its equal share.

Equal share of source power, relay power, and bandwidth to four users would be 0.25 part of each resource. In case $A = 0.5$ and $B = 1.5$, minimum resource to be given to the user must be $0.5 \times 0.25 = 0.125$ and maximum resource to be given to each user cannot be more than $1.5 \times 0.25 = 0.375$. In this way, parameter A ensures minimum resource to be assigned to the user, whereas B puts restriction on maximum resource drained by any one user. Fig. 3 shows that when $B = 2.1$ and $A = 0.2$, only $0.2 \times 0.25 = 0.05$ portion is assigned to each user and then remaining resources are assigned in order to obtain efficiency. When $A = 1$, irrespective of B , each user is assigned with equal share of the resource so the user can achieve the data rate as per their channel condition.

Figure 4 shows fairness index and price of fairness as a function of fairness parameter A and efficiency parameter B . When A is small, small B leads to high fairness index. As B increases, more emphasis is given to efficiency so fairness reduces. When $A = 1$, irrespective of B , fairness index remains same. Price of fairness is the measure to indicate loss of efficiency incurred for achieving fairness. As fairness increases, price of fairness also goes up.

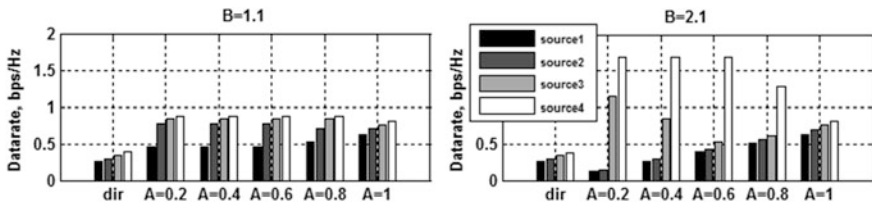


Fig. 3 Comparison of data rate achieved by each user in two cases **a** $B = 1.1$ **b** $B = 2.1$

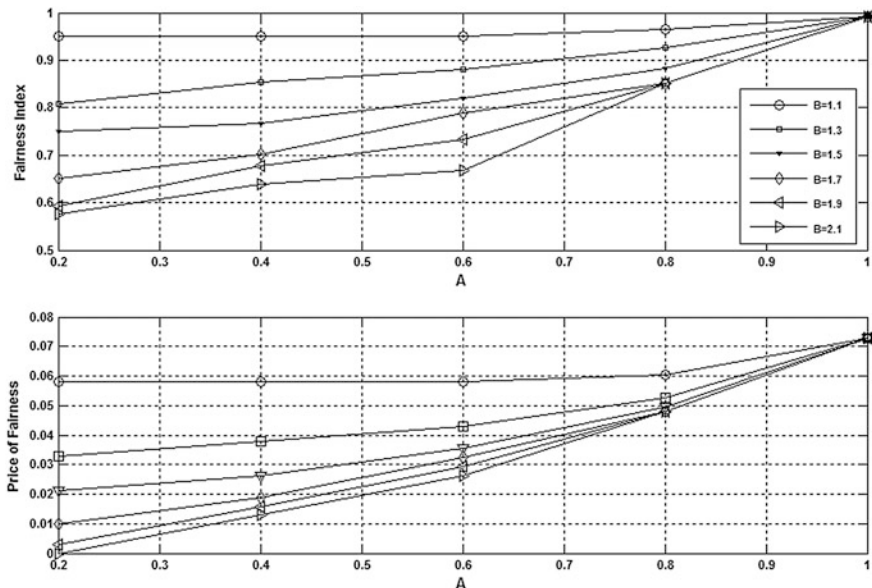


Fig. 4 Fairness index and price of fairness for resource constraint-based approach

8.3 E-F Function-Based Approach

In this approach, as per (8), smaller value of F leads to more fairness of resources to each user. As F varies from 0.1 to 0.9, fairness reduces. Efficiency parameter E is varied from 1 to 2 for getting higher efficiency. Figure 5 exhibits total data rate of the network as a function of fairness function F for different values of Efficiency parameter E . Figure 6 shows the fairness index as a function of fairness and efficiency parameters.

Fig. 5 Smaller value of F results in loss of efficiency

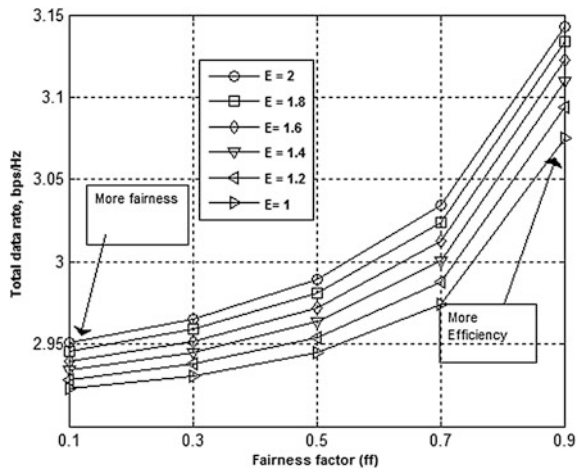
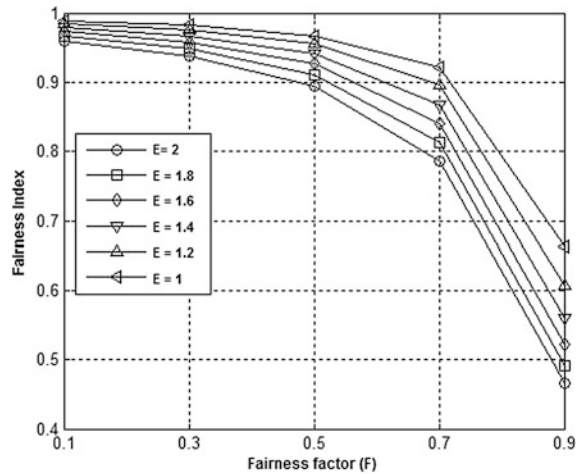


Fig. 6 Larger value of E leads to more efficiency



9 Conclusion

Three approaches for performing efficiency-fairness trade-off in cooperative wireless communication network have been presented in this paper. Utility function-based approach is able to give fairness index as high as more than 0.95 with price of fairness more than 0.24. Properly designed utility function would be able to give desired fairness with reasonable loss of efficiency. In second approach, it has been apparent that for smaller value of A , larger B gives more efficiency and for A approaches to 1, the allocation would be fair complete with significant price of fairness. The E - F function-based approach gives fair allocation for smaller value of F leads to fairness index approaching near to 1, while larger value of E gives higher

sum total data rate (i.e., more efficiency). In all these approaches, we have kept the restriction on the total available resources. Therefore, it can be concluded that even with the limited resources availability, it is possible to achieve desired fairness and efficiency. To cater different users differently, it is also possible to assign resources with priority with the help of these techniques. However, we leave the objective of priority-based allocation using these approaches for future work.

References

1. Laneman, J.N., Tse, D.N.C., Wornell, G.W.: Cooperative diversity in wireless networks: efficient protocols and outage behaviour. *IEEE Trans. Info. Theory* **50**, 3062–3080 (2004)
2. Le, L., Hossain, E.: Multihop cellular networks: potential gains, research challenges, and a resource allocation framework. *IEEE Comm. Mag.* **45**, 66–73 (2007)
3. Peter Hong, Y.-W., Huang, W.-J., Jay Kuo, C.-C.: Cooperative Communication and Networking, Springer, doi [10.1007/978-1-4419-7194-4](https://doi.org/10.1007/978-1-4419-7194-4), (2010)
4. Deng, X., Haimovich, A.M.: Power allocation for cooperative relaying in wireless networks. *IEEE Comm. Letters* **9**, 994–996 (2005)
5. Zhao, Y., Adve, R.S., Lim, T.J.: Improving amplify-and-forward relay networks: optimal power allocation versus selection. *IEEE Trans. Wireless Commun.* **6**(8), 3114–3123 (2007)
6. Xie, L., Zhang, X.: TDMA and FDMA based resource allocations for quality of service provisioning over wireless relay networks. In: Proceedings of the IEEE Wireless Communication Networking Conference, Hong Kong, pp. 3153–3157, (2007)
7. Luo, J., Blum, R.S., Cimini, L.J., Greenstein, L.J., Haimovich, A.M.: Decode-and-forward cooperative diversity with power allocation in wireless networks. *IEEE Trans. Wirel. Commun.* **6**(3), 793–799 (2007)
8. Gong, X., Vorobyov, S.A., Tellambura, C.: Joint bandwidth and power allocation with admission control in wireless multi-user networks with and without relaying. *IEEE Trans. Signal Process.* **59**(4) (2011)
9. Abrar, M., Gui, X., Punchihewa, A.: Radio resource Allocation in multi-user cooperative relaying networks with resource block pairing and fairness constraints. *Int. J. Wirel. Inform. Netw.* Springer, **20**(4) (2013)
10. Chen, Bin, Li, Youming, Yaohui, Wu, Liu, Xiaoqing, Zou, Ting: Power-Minimizing Resource Allocation in Multiuser Cooperative Relay Communications. *J. Commun. Netw. Sci. Res.* **5**, 48–52 (2013)
11. Chen, Wei, et al. Fair and efficient resource allocation for cooperative diversity in ad-hoc wireless networks. In Proceedings of the IEEE WCNC, Hong Kong, pp. 4096–4101, (2007)
12. Xiao, M., Shroff, N.B., Chong, E.K.P.: A utility-based power-control scheme in wireless cellular systems. *IEEE/ACM Trans. Netw.* **11**(2) (2003)
13. Cao, Y., Li, V.O.K.: Utility-Oriented Adaptive QoS and Bandwidth Allocation in Wireless Networks. In Proceedings of the IEEE ICC (2002)
14. Upadhyay, M.A., Kothari, D.K.: Optimal resource allocation techniques for Cooperative AF and DF wireless networks, In proc. of IEEE Int. Conf on Signal Processing & Integrated network – SPIN2014 (2014)
15. Manisha A. Upadhyay, D.K.Kothari, : Resource allocation techniques for cooperative AF wireless networks—efficiency fairness trade-offs. In the Proceedings of the IEEE TENCON, Bangkok (2014)
16. Upadhyay, M.A., Kothari, D.K.: Generic utility function based resource allocation for efficiency-fairness trade-off in cooperative wireless network, (Under Review IET-Communication)

17. Jain, R.; Chiu, D.M.; Hawe, W.: A quantitative measure of fairness and discrimination for resource allocation in shared computer systems. *ACM Trans. Comput. Syst.* (1984)
18. Joe-Wong, C., Lan, T., Chiang, M.: Multi-resource allocation: fairness-efficiency trade-offs in a unifying framework. In *Proceedings of the INFOCOM*, pp. 1206–1214 (2012)

An Enhanced Security Pattern for Wireless Sensor Network

Venu Madhav Kuthadi, Rajalakshmi Selvaraj and Tshilidzi Marwala

Abstract Numerous schemes for data aggregation are done by encryption for privacy of data, and thus, homomorphism has been reviewed and designed on the wireless sensor network (WSN) to improve security. WSN is an emerging and challenging technology in the area of the research because of its vital scope with low power energy associated with it. Several application sensors collect information or data from different sensed nodes and will be aggregated to a host computer or a base station. Data aggregation happens in a network between intermediate nodes which causes to reduce energy consumption on these nodes to make efficient network performance. The algorithm used in existing aggregation system does not provide sufficient security functionality and is more vulnerable to several attacks. Furthermore, some compromised nodes also inject false data which leads to a falsify data aggregation which is forwarded to base station. The enlargement of WSNs is thrombosed due the limited energy constraints. The main focus of this paper is done mainly on enhancing energy in WSN by working on the enhancement of some routing protocol. This paper also explains on eliminating of data vulnerability, security aggregation, and false data injecting attack by presenting different robust surveys and protocols. In this paper, initial discussions are done on WSN with a detailed overview of sensor, and reviews are made on providing security of wireless sensor network. The proposed novel idea is used in aggregating data during exchanging of messages and to preserve its data privacy and also to overcome problem in network construction (NC) and its security. The NC is done by

V.M. Kuthadi (✉)

Department of AIS, University of Johannesburg, Johannesburg, South Africa
e-mail: vkuthadi@uj.ac.za

R. Selvaraj

Department of Computer Science, BIUST, Gaborone, Botswana
e-mail: selvarajr@biust.ac.bw

T. Marwala

Faculty of Engineering and the Built Environment, University of Johannesburg,
Johannesburg, South Africa
e-mail: tmarwala@uj.ac.za

clustering its topology, and assigning heads to each cluster with huge communication range, also security pattern generation is created for protecting the data information.

Keywords Wireless sensor network • Data aggregation • False data injecting attack • Pattern generation

1 Introduction

Usually, the wireless sensor networks (WSNs) are made up of low power and less expensive sensing devices with fixed memory, computation, and communicating resources. This Wireless sensor networks offer minimum cost solutions for issues over the military and civilian application including tracking target of battleground, health care and environment, traffic regulation and wildfire detection monitoring. Because of the low intensity cost of WSN, it contains a common resources and hardware [1]. The benefit of the recent technology has made the production of mass inexpensive for sensor nodes that keep the particular benefit of sensing, despite their tiny size communication and processing abilities. A wireless sensor network contains distributed sensor nodes that are interconnected without wires [2]. WSN is a set of nodes where every node has their own attributes like processor, receiver, transmitter, and sensors, and this type of sensors basically will have low-cost mechanism to perform sensing task. The WSN [3] mostly gets operated in uncontrolled and public area for monitoring particular events, and therefore, network security is still a major problem [4]. WSN is able to collect the accurate and reliable data in different and harmful areas and help making a secure way in defense system, industrial control, traffic management, environment observation, smart home, medical care, military affairs, etc. The sensor nodes that have cheap and limited resources totally depend on battery power for supplying of electricity [5]. There are several clustering benefits presented which reduce the size of routing table and stores at a particular node. The cluster heads are also capable to extend the life of battery for the specific node and network. Cluster head performs data aggregation in cluster and decrements redundant packet number [6]. The sensors networks are commonly prepared for data processing and capabilities of communication.

The measurement parameter is the sensing circuit from the surroundings of nodes in WSN which transforms it into electric signal [7]. A Wireless sensor network which is unstructured contains a huge collection of sensor nodes which are organized automatically [9] in the form of ad hoc network to communicate with each nodes. Secondly, a structured WSN implements the sensor nodes in planned manner. This paper considers the crippling attack which is against entire sensor network routing protocol. The attention of proposed approach is to work on routing protocol and has been designed securely and more effectively for fixing proper

routing of sensor network [8, 9]. The proposed work of this paper deals with security goals and models for threats and also for routing security in WSNs. The proposed technique also contains security analysis in detail for each foremost protocol of routing and algorithm for topology maintenance and for conservation of energy in Wireless Sensor Networks, and finally, it prevents attacks over WSNs routing protocols.

2 Related Work

This paper work has been gone through several studies and papers in the domain of sensor network. In those theses, the authors have presented software and hardware aspects for the sensor network. Cam et al. [10] have proposed the pattern codes for protocol of ESPDA that represents the feature of actual data which perform the aggregation of data. The sensor firstly generates and transmits the codes of pattern for CH instead of transmitting the sensing data. The pattern code mapping is refreshed for the security intervals in the periodically range of sensor reading. Then, the CH defines the different codes of pattern and makes only one request for one sensor node in every different code of pattern for transmitting the actual data in the base station. Additionally, for making the enhanced bandwidth and energy, this idea improves the security for the cause of the CH that does not require the decryption of actual sensed data aggregation [11] which presented a safe data aggregation, and it only considers the integrity of message and confidence of message which is the most important. Particularly, the transmission of aggregated data from higher cluster head is having more confidence compare with the particular sensor data. However, they are proposing security mechanism over the aggregation that assures the confidentiality of message by security level increment such that the base station purposes an aggregated data. Chan et al. [12] have proposed Aggregate-Commit-Prove ideas for safe aggregation of data, in which the base station data aggregation correctness requests the tiny pieces of sensor data.

Nazirbabar et al. [13] have proposed the clustering of energy-balanced WSN which presents an algorithm for the formation of cluster in energy balance, intra-cluster, inter-cluster, and CH selection communication which are proposed to extend the WSN lifetime. Zhou et al. [14] have proposed the control of topology and location of the irregularity model of radio. The simulation result shows that the irregularity of radio having a huge effect on the layer routing than the MAC. It is showing that the irregularity of the radio tends to error a larger localization for maintaining the connectivity communication in topology. Kung et al. [15] have proposed the concept of multihop-LEACH and energy-LEACH that known as LEACH-M. Energy-LEACH improves the CH technique. The multihop-LEACH improves the mode of communication between the multihop and single hop within sink. Chen et al. [16] have proposed the unequal clustering for sensor network in multihop. The simulated result presenting the mechanism of unequal clustering

balances the consumption of energy which is suitable over the each sensor node to achieve the actual improvement for the life time of sensor network.

Cao et al. [17] have proposed a new idea of the protocol uCast supporting an enhanced content for the energy distribution in network. The uCast is supporting a huge number session of the multicast, particularly, when the session of destination number is small. Hi le et al. [18] have proposed a new idea for the enhanced protocol of energy that is known as Route Maintenance on the basis of threshold of the energy and delay of the node lifetime and the efficient overall network. In the literature survey, we found some specific issues over the wireless sensor network; those problems are considered in our proposed technique and try to overcome on it. However, the specific problems are mentioned below:

- The attacker illegally gets multiple identities on one node. By this, the attacker mostly affects the routing mechanism.
- The attacker uses tunneling mechanism to establish himself between them by confusing the routing protocol.
- Attacker places himself in a network with high-capability resources.

3 Proposed Mechanisms

3.1 Overview

There are several routing protocols of the sensor network that is simple, and because of the simplicity sometimes, it is more susceptible for attacking on the protocol of the general ad hoc. Most of the attack of network layer over sensor networks belongs to Acknowledgement spoofing, HELLO flood attacks, Selective forwarding, Sinkhole attacks, Spoofed, altered, or replayed routing information, Sybil attacks, or Wormholes. In our proposed work, we are implementing a novel idea, which will identify the attack is either intruder or compromised node attack. Figure 1 shows the proposed architecture that improves the data confidentiality and security of the accessing services. There is some novel idea proposed to define the accuracy of this research paper like network construction (NC), security pattern generation, source authentication, data integrity and freshness, and data confidentiality. These techniques are providing an efficient way of approach to solve this problem over the wireless sensor network. The NC is creating and maintaining the secure network, and security pattern generation makes a secure way to access the network via secure pattern. The other techniques like data confidentiality that contains the security of information and keeping confidential on the network.

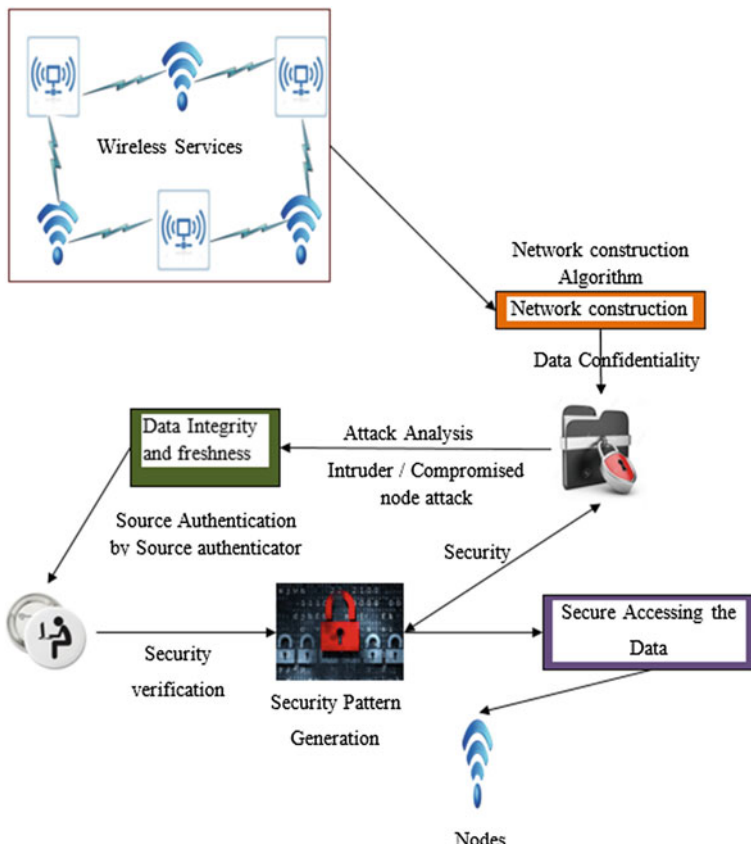


Fig. 1 Proposed WSN architecture

3.2 *Data Confidentiality*

In WSN, confidentiality of the data assures the security of the sensitive data never being disclosed for the unauthorized access or parties, and this is the major problem in the task of the decisive software application. The sensor node should not have to release any access to the neighbor sensor node. Thus, the several sensor nodes, software application transmitting the sensitive data, such as secret key, and consequently, it is too much important to create the safe sensor node channel. The information over the public sensor, like as public keys and detection of sensor, must have to encrypt the several extent for protecting the attack of traffic analysis. However, the information of routing must be confidential in some cases as the affected node could be able to use the information for degrading the performance of network. The quality-based method proposed for keeping the secure sensitive data by encryption of the data using a secret key will be used for maintaining the confidence.

3.3 Freshness and Data Integrity

Although the data confidentiality mechanism guarantees, the intended parties can only get the data without encryption and it does not prevent the data alteration. The data integrity guarantees that the transferred message is not corrupted. A, attacker node can corrupt the system and stop to make function properly on the network. Because of an unreliable channel of communication, data alteration is possible without any intruder. For preventing the data integrity, the cyclic or authentication codes are used. Although data confidentiality guarantees that only intended parties obtain the un-encrypted plain data, it does not protect data from being altered. Data integrity guarantees that the message being transferred is never corrupted. A malicious node may just corrupt messages to prevent network from functioning properly. In fact, due to unreliable communication channels, data may be altered without the presence of an intruder. Thus, message authentication codes or cyclic codes are used to prevent data integrity.

Data aggregation results in alterations of data; therefore, it is not possible to have end-to-end integrity check when data aggregation is employed. Moreover, if a data aggregator is compromised, then it may corrupt sensor data during data aggregation, and the base station has no way of checking the integrity of this aggregated sensor data. Providing data integrity is not enough for wireless communication because compromised sensor nodes are able to listen to transmitted messages and replay them later on to disrupt the data aggregation results. Data freshness protects data aggregation schemes against replay attacks by ensuring that the transmitted data is recent.

3.4 Source Authentication

From WSN that utilizes wireless medium, the sensor nodes required a mechanism for authentication to identify the spoofed packets or maliciously injected. The authentication of the Source enables sensor node to assure the identification of the peer node to communicate. Furthermore, a node of compromised data is behind numerous fake identities which make the integrity of corrupted data. If there are two nodes communicating, then the authentication process could be provided by the symmetric key. The secret key shared between the sender and receiver is computing the MAC for the transmitted data.

3.5 Network Construction

In our proposed privacy scheme, choosing a topology is based on the tree for performing the intermediate aggregation. This is because of the topology-based clustering which gets affected by the range of communication among the CH and it is affected by the huge amount of the message for NC.

3.6 Security Pattern Generation (SPG)

The nodes in WSNs are receiving the security pattern through CH. Cluster head is containing threshold value. The value of intervals is for the defined data, which is based on the value of threshold for every parameters of the environment. The value of threshold and the interval variation depends on the requirement of the users and defined for the precision over the environment where the network is implemented. An algorithm that is computing the critical values for every interval generates a lookup table by using the security pattern, where the number is broadcast and generated through CH Randomly. In wireless sensor network, the SPG algorithm is being executed by every WSN. Before transmitting real data, sensor nodes send a code in pattern format to CH.

3.7 Algorithm

3.7.1 Network Construction (NC)

```

Command NC (Meg_Type, msg_Type, Message msg)
{
01. If (A = Sink node)
{
02. Overflow (BS_ID, init_Level);
exit;
}
03. Wait for receiving the HELLO message;
04. If (Nodes receiving message through sensor nodes)
{
05. If (msg_Type = HELLO)
{
06. Set rec_Level, rec_HopCnt, parent_ID from message;
07. NetInfo_curEntry++;
08. If(1 + rec_HopCnt < cur_HopCnt) cur_HopCnt = 1 + rec_HopCnt;
09. else
break;
10. If (leaf node ≠ TOS_LOC_ADD)
11. Overflow (cur_NodeID, cur_Level);
}
12. If(msg_Type = JOIN)
{
13. If (Parent_Node ≤ Max_Child_Node)
14. Net_Info_Parent = parent_ID;
15. else

```

```

RESET (send message) to Node
}
}
16. End

```

3.7.2 Algorithm: Security Pattern Generation (SPG)

Input: Sensed Data Type, Environment parameters, threshold levels (interval), and Data Accuracy

Output: Security Pattern codes (**SPC**)

Start

1. Declare arrays with 100 interval, visit [100] [100]

2. Variables SPC = starting point = null value

3. **if** (new seed)

then

4. **for** i = 1 to n

5. threshold[i-1] ‘-’ threshold [i] = interval [i]

6. **endfor**

7. Critical value assignment for every created interval

8. Form the visit table for critical value by updating the every Sensed. Data interval and critical value

9. **endif**

10. **while** ('D'(sensed data) is available)

11. Get actual sensed data from environment.

12. Round off the value Data Accuracy.

13. Find the critical value for every current Sensed Data by using lookup Table

14. SPC = Append value (critical value) + SPC

15. Repeat 13 &14 step until all timestamp parameters are done.

16. Send final Sensor ID, timestamp, SPC to cluster-head.

17. **endwhile**

End

4 Results and Discussion

Some of the experiments are conducted, and data are extracted, which were done on the Windows 7, Intel Pentium(R), CPU G2020 and Processor speed 2.90 GHz. The proposed novel technique for wireless sensor network is made to make WSN more secure and are constructed with Security Pattern Generation (SPG). These techniques help increasing the reliability of WSN, where attackers can be easily identified and prevented from accessing of services. The data confidentiality is been higher and secured by SPG.

4.1 Attack Identification

In Table 1, we have presented the result of our experiment that shows the detection of attack when compared with the several existing systems and our proposed system. The accurate detection of attack is completely satisfied by the proposed work.

4.2 Data Confidentiality

Figure 2 presents the confidentiality of the data that is high and secure. The data security and confidentiality are much intended in the wireless sensor network. Our proposed work focuses on the security of the data and confidentiality of the data.

Table 1 Attack identification accuracy in existing and proposed works

Techniques	Attack				
	Sinkhole attack	Wormholes attack	HELLO flood	Sybil attacks	Spoofing
ESPDA protocol	✓	✓	•	•	✓
Data aggregation	•	✓	✓	✓	✓
Aggregate commit prove	✓	✓	•	✓	✓
Energy-balanced cluster	✓	✓	•	✓	•
Network construction	✓	✓	✓	✓	✓

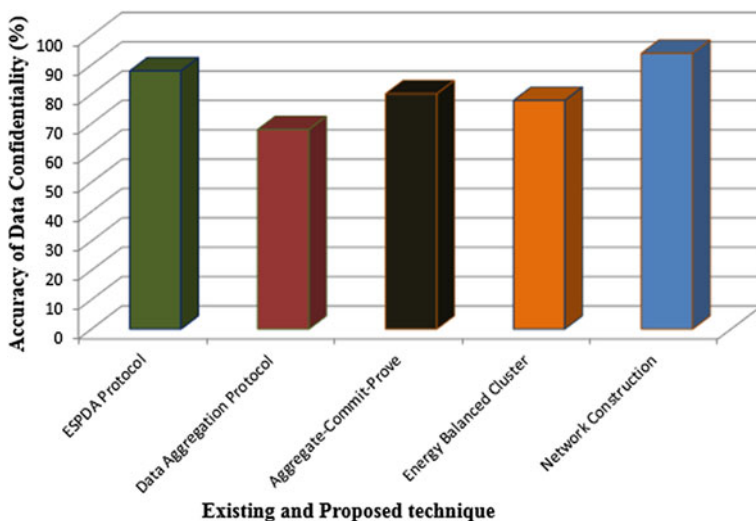


Fig. 2 The accuracy of data confidentiality in existing and proposed works

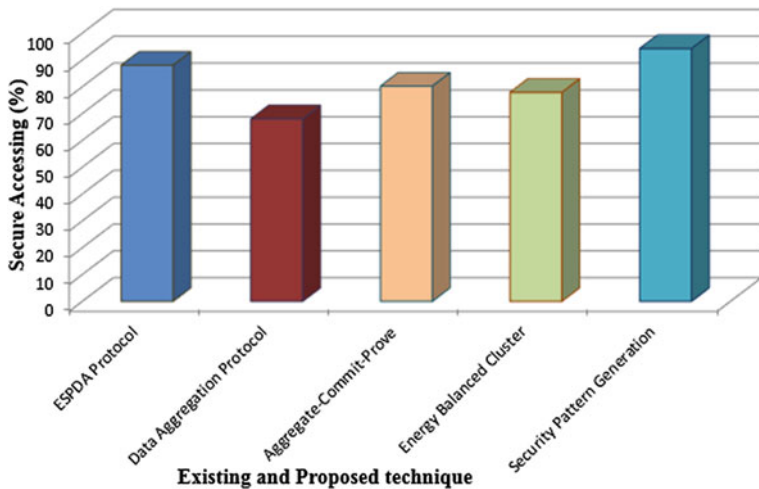


Fig. 3 Secure accessing between existing and proposed systems

4.3 Secure Accessing

Our proposed research work experimental results are shown in Fig. 3. The secure accessing is high when compared to the several existing techniques. Here, secure accessing in the network is mostly demanded issue over the network.

5 Conclusion

In this paper, a novel and enhanced method has been proposed for the purpose of WSN security, and this proposed technique is known as SPG and NC. In Wireless sensor network, NC is constructing a secure path and maintaining very well over the network. This NC is mainly based on the topology that helps communicating within the cluster head, and a huge amount of message is transmitted in the network very securely. The SPG is performing a very crucial role in the security over network by generating the secure verification key. This SPG work is based on the threshold value, where it is computing the critical value for each and every interval for creating the security pattern table. Beyond of these methods, in the phase of constructing network, the data confidentiality process is being executed for securing the users content and keeping it confidential on the network, as well as protecting from the malicious node also. These proposed techniques are more efficient in compare to the any other existing techniques. These techniques have provided a better solution for the network security-related issues. In future, we may plan to reduce the size of data and increase the network life time over the wireless network.

References

1. Sanli, H.O., Ozdemir, S., Cam, H.: SRDA: Secure reference based data aggregation protocol for wireless sensor networks. In: 60th IEEE Vehicular Technology Conference, USA, pp. 4650–4654 (2004)
2. Stefanos, A.N., Dionisis, K., Dimitrios, D.V., Christos, D.: Energy efficient routing in wireless sensor networks through balanced clustering. *Algorithms* **6**, 29–42 (2013)
3. Kuthadi, V.M., Rajendra, C., Selvaraj, R.: A study of security challenges in wireless sensor networks. *JATIT* **20**(1), 39–44 (2010)
4. Abhishek, P., Tripathi, R.C.: A Survey on Wireless Sensor Networks Security. *Int. J. Comput. Appl.* **3**(2), 43–49 (2010)
5. Yao, L., Cui, X., Wang, M.: An energy-balanced clustering routing algorithm for wireless sensor network. In: WRI World Congress on Computer Science and Information Engineering, Los Angeles, CA, pp 316–320 (2009)
6. Vaibhav, V.D., Bhagat, A.R.: Energy distributed clustering for improving lifetime of wireless sensor network. *Int. J. Emerg. Sci. Eng.* **1**(7), 62–65 (2013)
7. Gupta, G., Younis, M.: Performance evaluation of load-balanced clustering of wireless sensor networks. In: 10th International Conference on Telecommunications, USA, pp. 1577–1853 (2003)
8. Chris, K., David, W.: Secure routing in wireless sensor networks. *Ad Hoc Netw.* **1**, 293–315 (2003)
9. Kuthadi, V.M., Selvaraj, R., Marwala, T.: An efficient web services framework for secure data collection in wireless sensor network. *British J. Sci.* **12**(1), 18–31 (2015)
10. Cam, H., Ozdemir, S., Nair,P., and Muthuavinashiappan, D.: ESPDA: energy-efficient and secure pattern-based data aggregation for wireless sensor networks. In: 2nd IEEE Conference on Sensors, Toronto, Canada (2003)
11. Suat, O., Yang, X.: Secure data aggregation in wireless sensor networks. *Comput. Netw.* **53** (12), 2022–2037 (2009)
12. Chan, H., Perrig, A., Przydatek, B., Song, B.: SIA: Secure Information Aggregation in Sensor Networks. *J. Compu. Secur.* **15**(1), 69–102 (2007)
13. Nazir, B., Hasbullah, H.: Energy balanced clustering in wireless sensor network. In: International Symposium in Information Technology, Kuala Lumpur, pp. 569–574 (2010)
14. Zhou, G., He, T., Krishnamurthy, S., Stankovic, J.A.: Models and solutions for radio irregularity in wireless sensor Networks. *ACM Trans. Sens. Netw.* **2**(2), 221–262 (2006)
15. Kung, H., Hua, J., Chen, C.: Drought forecast model and framework using wireless sensor networks. *J. Inform. Sci. Eng.* **22**, 751–769 (2006)
16. Chen, G., Li, C., Ye, M., Wu, J.: An unequal cluster- based routing strategy in wireless sensor networks. *J. wirel. Netw.* **15**(2), 193–207 (2009)
17. Cao, Q., He, T., Abdelzaher, T.: uCast: Unified Connectionless Multicast for Energy Efficient Content Distribution in Sensor Networks. *IEEE Trans. Parallel Distrib. Syst.* **18**(2), 240–250 (2007)
18. Hu, L., Li, Y., Chen, Q., Liu, J.: A new energy-aware routing protocol for wireless sensor networks. In: International Conference on Wireless Communications, Net-working and Mobile Computing, Shanghai, pp. 2444–2447 (2007)

Honey Pot: A Major Technique for Intrusion Detection

Rajalakshmi Selvaraj, Venu Madhav Kuthadi and Tshilidzi Marwala

Abstract Generally, Intrusion detection system (IDS) is installed in industrial environment for protecting network that works based on signature, where they are not capable of detecting most unidentified attacks. The detection of undefined attack and intrusion is not more helpful to identify the several kinds of attack, where intrusion-based attack has become a challenging task to detect intruder on network. A skilled attacker can obtain a sensible information and data from the system after knowing the weakness. Distributed denial of service (DDoS) is a major threat over the security and most enlarging thread in recent days. There are so many types of Denial of Service (DoS) such as Teardrop, Smurf, Ping of Death, and Clone attack. The aim of the cyber defense system is to detect the main cause of the several counter attacks on the enterprise network. On the way to fix these issues, we are proposing a novel idea that relies on honey pot technique and packet data analysis which are trained by the sample of malware after using the Intrusion detection technique in both ways separately as Network and Anomaly intrusion detection system. Some approaches are not being easily implemented in the network of real enterprises, because of practicability training system which is trained by the sample of malware or deep analysis of packet inspection or depends on the host-based technique that requires a big capacity for storage over the enterprise. The honey pots are one of the most successful techniques to collect the sample of malware for

R. Selvaraj (✉) · T. Marwala
Faculty of Engineering and the Built Environment, University of Johannesburg,
Johannesburg, South Africa
e-mail: selvarajr@biust.ac.bw

T. Marwala
e-mail: tmarwala@uj.ac.za

R. Selvaraj
Department of Computer Science, BIUST, Gaborone, Botswana

V.M. Kuthadi
Department of AIS, University of Johannesburg, Johannesburg, South Africa
e-mail: vkuthadi@uj.ac.za

the purpose of analysis and identification of attacks. Honey pot is a novel technology which consists of massive energy and possibilities in the field of security. It helps reading the behavior of the attack and attacker information.

Keywords Honey pot • IDS • Packet analysis • Intruder

1 Introduction

The computer system security is one of the most important areas of consideration in Information Technology (IT). There is a quick progress in this field because everyone wants to keep the information secure, and no one wants to leak their information to the Attacker by the intrusion and compromised data [1]. Recently, the internet has become a popular way to communicate with computers all over the world. When the constant Communication has been creating some new possibility, it also brings the several chances for the malicious-affected users. The significance of the security over network is growing, the IDS is one of the methods to identify the malicious behavior over the network [1, 2]. The numbers of internet users are increasing continuously per day. The internet traffic is getting high every day by the user crowd, so the internet security is mostly required in the recent days in the area of computing system. Honey pot system is developed for detecting and analyzing the malicious attack which tries to access the network. Honey pot is a machine that looks like a real database, server, and Operating System (OS) for the attackers. A Honey pot system attracts the attacker and it gives an invitation for attack. The goal of the honey pot is to secure the existence system from the attackers and gain the information of the attackers by creating a log case for their harmful activity by the specific IP address [3]. The attackers perform their work professionally in the automated and well-organized environment after controlling over the zombie machine for which network of the enterprise is preferable. As the infected systems are most dangerous in the cyber-attack, decontaminant of them is one of the main aims for Active Cyber Defense (ACD); thus, the initially step is inevitably analyzed. The effect of the Scalable and practical system is with the ability of standing growth and efficient identification of the malwares for detecting the infected machines [4]. The main aim of the honey pot is to identify the attacker and let them to access the network and store the information of the intrusion like IP address, TCP address, etc., and then divert their path to the fake database instead of accessing the real database. Nowadays, the intrusion detection is the big issue for the research behavior [5]. Honey pots are one of the strong agents to identify the attacker and capture the intruder information based on intelligence and black-hat behaviors. Some distinct services like IDS and firewall are signature-based services, and a lot of work has been done in the field of the signature-based detection. Therefore, the

honey pots are the one of the most interesting techniques for controlling the attack on the internet. It easily collects the information about the attacker. When compared to other technique, honey pot is reducing the risk of attack [6]. Once attacker reaches to the firewall system, then they will easily collect all the valuable data from the system and nothing will be remaining to save from them [7]. With the additional approach of Booby traps it is possible to prevent the weakness of the system and attracts the intruders to the system. This system starts interaction with the attacker and collects all the information of attackers. This latest technique is known as Honey pot [8]. The proposed method discussed about the intrusion aspects, origin, and cause and also included the information in detail for the packet sources. We are providing the several detection methods, tools, and systems for intrusion classification. We are not only focusing on the analysis and classification of IP traffic but also trying to focus on the several updated methods, tools, analysis, and systems.

2 Related Work

Jeremy et al. [9] have proposed a design of the high interaction over the honey pot to present a result with discussion. They have presented two types of honey pot host, the First class stops accessing the unauthorized users and reinstallation, and second class allows the reinstallation. The author of the [10], aimed to secure the information of the system from the attacker or unauthorized access against the DoS. This is gained by controlling the traffic of attack and mechanism of pushback. Vinu Das [10] proposed the honey pot on the basis of the distribution detection of attack from different sources of attack by using the traditional system of honey pot [11] and distributed consumption for enhancing the overall protection of system area. The system identifies the attacking behavior by the database feature invasion, which could be compatible with the snorting feature of library, and detecting the recent invasion features by real-time up-gradation. Divya et al. [12] developed IDS which contains hybrid honey pot with GA (genetic algorithm), where the high interaction of the attacker has been established with the unknown attackers. Yun Yang et al. [13] proposed an IDS with C4.5 DT (Decision Tree) algorithm. In this technique, intrusion creation rule gains the information over the attacker in ratio. The authors' experimental result produces that the IDS C4.5 algorithm is effective and feasible and the rate of accuracy is high. Jiqiang et al. [14] have proposed a note on the black-hat community services that make a harmful access in the system for stealing the secret information, where the honey pot system attracts the attacker and gain their information and store them. The honey pot is the most valuable for creating a new signature for detecting the intruders.

Rameshbabu et al. have proposed the Egress filtering technique to filter the [15] outbound traffic of network. Here, the author proposed an example related to the DoS attacks which can provide the details of intruders and prevent to access the attacks as well as provide the description of the filtering execution. Siva et al. [16] have proposed the techniques of utilizing the port hopping that communicates with

the parties of application over port. But here no pre-calculation procedure has been done which makes it easier to trace randomly.

3 Proposed Work

3.1 Overview

Honey pots are largely used in the security field for defecting, preventing, and detecting the breaches that abandoned the security measure, and make more efficient and accurate measurement for security purpose. The methods of honey pot consumption directly implement the role of honey pot in security system. Basically, honey pot is a mechanism of collecting and learning the information. Its main aim is not only to catch the black-hat community attacker and put charges over them but also the aim of it is to attract the attackers and hacker and collect information about them. This information will be helpful for the future study and attacking ideas. We are proposing a novel idea in our project called virtual honey pot, which will identify and catch the intrusion on the network shown in Fig. 1.

3.2 Intrusion Detection

3.2.1 Network-Based Intrusion Detection System

Network-based Intrusion Detection System (NIDS) observes the crowd flows over another host. Observing area in the network-based region can either enlarge or minimize the particular area with the related effort. Network-based intrusion detection system has a capability to stand against the crowd over network to maintain the effect. With the increasing traffic, the network-based IDS has to clear the traffic and observe in the manner of time.

3.2.2 Anomaly-Based Intrusion Detection System

Anomaly-based Intrusion Detection System (AIDS) observes the activity, transaction, outgoing traffic, and behavior to detect the intrusion by anomaly detection. It checks the behavior of users on the notion that is different from the normal behavior identified as an attacker. The administrator of the system sets the limitation of the normal behavior. AIDS is prone for the false positive. AIDS is causing the heavy process on the network system. We have two factors: first one is False Positive: Anomalies are signed as an intrusive when that is not an intrusive, and other one is False Negative: Anomalies are not signed as an intrusive when that is an intrusive.

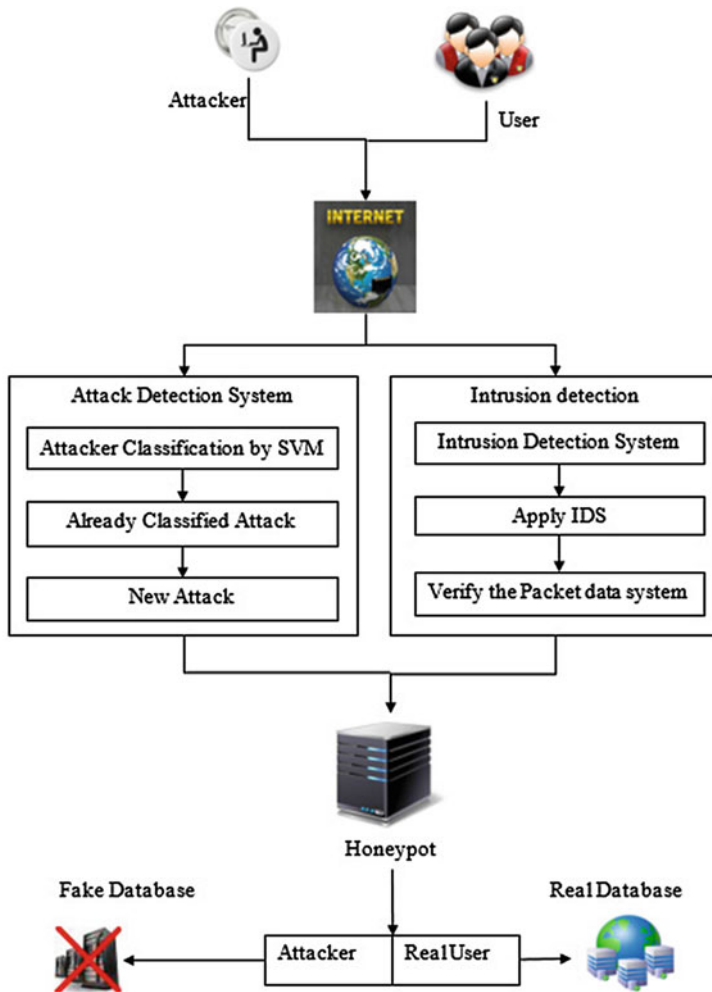


Fig. 1 Proposed honey pot architecture

3.2.3 Honey Pot

The honey pots are intended to imitate the systems to detect intrusion which has a tendency to break the intruder limit in accessing the overall network. When it is successful, then the attacker will not know that they are monitored and tricked. Most of the honey pot systems are installed inside the firewall so they can do better control over full network; however, it is possible to implement outside the firewalls. The firewall system within honey pot works in an opposite way: the honey pots are allowing the incoming attackers instead of blocking them and divert their path from

the real database to false database and restrict the function which attackers try to access.

3.2.4 Packets Analysis

These functions present an analysis for capturing the packet and exploring the information. This information consists of TCP, IP, ICMP, and UDP header. Then, the packet divides between two (source and destination) IP address and stores the records in each 4 s. It is functionally applied in every connection and defines the attack and normal behavior.

3.2.5 Support Machine Vector (SVM)

Support Vector Machines (SVM) is a classifier which was designed to classify the binary format. The application for classification will solve the problem based on the multi-class. SVM supports the decision tree which combines the decision tree and SVM that enhance a way to solve out the problem of multi-class. This technique is most effective and can decrease the timing of testing and training processes and increase the system efficiency. Some distinct way to create the binary trees will divide the set of data into the various subsets from the root to leaf till all subset merged into the one class. The creation of the binary tree function is having a huge power for the classification. For the construction of multi-class IDS, this research work implements a novel approach based on the DT.

3.3 Algorithm

3.3.1 Intrusion Detection System

IDS takes the packet as input from the network and also monitors the time slot of incoming flow. While monitoring the time slot and packet, IDS detects the malicious time slot and checks for the suspicious flow and extracts the malicious flow from the traffic, and it processes and generates the new filtering rule. Signatures are built from the filtering rule for intrusion detection.

$$\text{IDS } (P, T) = \{\text{FR, SGN, L2}\}$$

Where,

T = time slot,

FR = Filtering Rule.

SGN = Signature Created.

L2 = Log Report.

3.3.2 Honey Pot

The captured packets are used as an input in the honey pot and precede the packet to attain the information for every particular system from the origin of packet. Honey pot precedes the packet analysis and generated reply to engage the client system from host.

$$HP(P) = CLD + L1.$$

Where, client

P = {ICMP,TCP,UDP} = Set of packet entering to the system.

CLD = {cIP,PType,Preply} = client details.

cIP = client IP.

PType = packet type.

Preply = Reply packet.

L1 = Log Report

3.3.3 Packet Analysis

Algorithm

1: Begin to receive packets

 For every packet p

 if (Received_protocol == Transmission Control Protocol)

 Infer features of Transmission Control Protocol extract

 else

 if (Received_protocol == User Datagram Protocol)

 Infer features of User Datagram Protocol

 else

 if (Received_protocol == Internet Control Message Protocol)

 Infer features of Internet Control Message Protocol

2: After collecting the features wait for two seconds

3: Split the data into records based on the connection between two Internet Protocol addresses.

4: For all connection

 Apply DT rules

5: Output of Log

6: End

4 Results and Discussion

In order to measure the performance of our proposed approach, a sequence of experiments on extracted dataset were conducted based on the following configuration. Our proposed method was implemented in Windows 7, Intel Pentium(R), CPU G2020, and Processor speed 2.90 GHz.

Table 1 presents the identification of the intrusion over several existing techniques with honey pot, and the result shows that the honey pot detection rate is high among them. There are total 12 features used, and in all features, the overall intrusion detection rate is high for the honey pot.

The intrusion detection shown in Fig. 2 is high in the honey pot techniques. When compared to existing techniques, the honey pot is most effective and efficient.

In Fig. 3, the result of the experiment presents the difference between Honey pot and some existing technique which is producing the irrelevant information to the

Table 1 Classifier and accuracy beyond intrusion

Features used	Classifier	Accuracy	Normal		DoS	
			True	False	True	False
			Positive	Positive	Positive	Positive
12	OneR	82.625	0.895	1.001	0.811	0.213
12	C4.5	91.795	0.937	0.106	0.876	0.118
12	Naive bayes	81.443	0.854	0.059	0.806	0.105
12	Honey pot	97.953	0.999	0.003	0.979	0.001

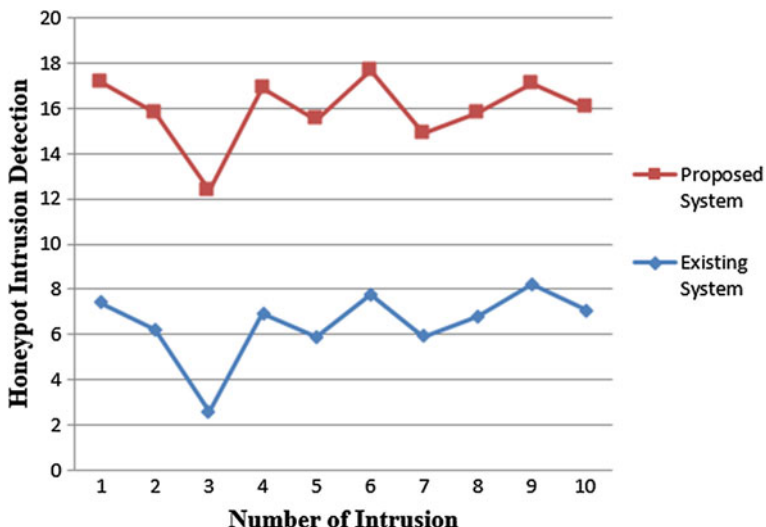


Fig. 2 Honey pot intrusion detection

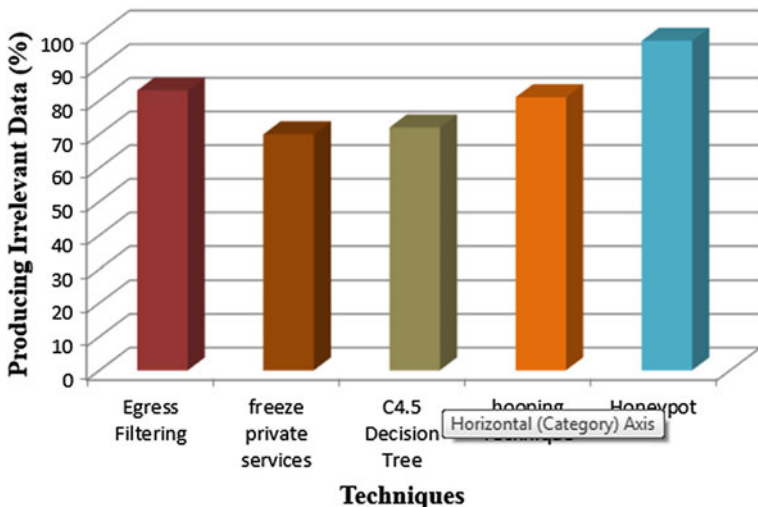


Fig. 3 Producing irrelevant information to attacker

intruders or attackers. The honey pot is producing the more irrelevant information to intruders or attackers, and it is one of the best techniques to gain the information about them.

5 Conclusion

In our proposed work, we have proposed a novel technique with the honey pot and IDS. These techniques are a major part for the defensive operations. These methods are very efficient for the security purposes on the network and prevent the stealing of data from the attackers or intruders. The proposed technique has main goal to confuse the intruders and collect their information in the system and show them a wrong path or send them to an irrelevant data. These techniques will help to identify the next move of the attackers with the novel ideas and technology. The attackers belong to the black-hat community, and they tends to steal the data from any system with a new techniques, so the obtaining information like IP address, TCP Address, etc., will surely help to know their further moves. By knowing attackers next move, honey pot will secure the users' information and prevent the intruder access on the network or system. The Honey pot system is playing a crucial role in detecting the attackers and showing them a fake database.

References

1. Shyamasundar, L.B.: An auto configured hybrid honeypot for improving security in computer systems. *Int. J. Comput. Sci. Inform. Technol.* **6**(1), 84–88 (2015)
2. Parimala, H.C., Kavitha, B.: Achieving higher network security by preventing DDoS attack using honeypot. *Int. J. Comput. Netw. Secur.* **6**(1), 40–45 (2014)
3. Suruchi, N., Sandeep, K.: Advanced honeypot system for analysing network security. *Int. J. Curr. Res. Acad. Rev.* **2**(4), 65–70 (2014)
4. Fatih, H., Abdulkadir, P., Erkam, U., Bakir, Emre., Necati, S.: An automated bot detection system through honeypots for large-scale. In: 6th International Conference on Cyber Conflict, Estonia, pp. 255–272 (2014)
5. Meghana, S., Vidya, D.: Intrusion detection technique using data mining approach: survey. *Int. J. Innov. Res. Comput. Commun. Eng.* **2**(11), 6352–6359 (2014)
6. Brijendra, P., Ramakrishna, C., Rakesh, S., Sanjeev, K.: Implementation of port density based dynamic clustering algorithm on honey net data. *Int. J. Adv. Comput. Eng. Netw.* **2**(6), 76–82 (2014)
7. Dasen, R., Juan., W., and Qiren, Y.: An intrusion detection algorithm based on decision tree technology. In: Asia-Pacific Conference on Information Processing, Shenzhen, pp. 333–335 (2009)
8. McHugh, J., Christie, A., Allen, J.: Defending yourself: the role of intrusion detection system. *IEEE* **17**(5), 42–51 (2000)
9. Jeremy, B., Jean-Francois, L., Christian, T.: Security and results of a large-scale high-interaction honeypot. *J. Comput.* **4**(5), 395–404 (2009)
10. Das, V.: Honeypot scheme for distributed denial-of-service attack. In: International Conference on Advanced Computer Control, India, pp. 497–501 (2009)
11. Kuthadi, V.M., Rajendra, C., Selvaraj, R.: A study of security challenges in wireless sensor networks. *JATIT* **20**(1), 39–44 (2010)
12. Divya, A.C.: GHIDS: A Hybrid Honeypot System Using Genetic Algorithm. *Int. J. Comput. Technol. Appl.* **3**(1), 187–191 (2012)
13. Yun, Y., Hongli, Y.: Design of distributed honeypot system based on intrusion tracking. In: 3rd International Conference on Communication Software and Networks, China, pp. 196–198 (2011)
14. Jiqiang, Z., Keqi, W.: Design and implementation of dynamic virtual network. In: International Conference on Electronic and Mechanical Engineering and Information Technology, Harbin, China, pp. 2131–2134 (2011)
15. Selvaraj, R., Kuthadi, V.M., Marwala, T.: An effective ODAIDS-HPs approach for preventing, detecting and responding to DDoS attacks. *Brit. J. Appl. Sci. Technol.* **5**(5), 500–509 (2015)
16. Siva, T., Phalgun, K.E.S.: Controlling various network based ADoS attacks in cloud computing environment: by using port hopping technique. *Int. J. Eng. Trends Technol.* **4**(5), 2099–2104 (2013)

Computational Intelligence-Based Parametrization on Force-Field Modeling for Silicon Cluster Using ASBO

S.N. Gondakar, S.T. Vasan and Manoj Kumar Singh

Abstract A new parametrization of the small-size silicon cluster is proposed in this paper to improve the quality of predicted energy value by potential energy function in force-field modeling. ASBO-based concept has applied to evolve the parameters under different circumstances and cluster structure. The performance of new parameters is compared with the other well-established parameters in stillinger-weber energy function and its variants. Under known and unknown environment, effects of higher dimension in energy predicting capability are also analyzed. A significant improvement is observed in predicting the small cluster energy value with a proposed solution compared to values obtained with existing parameters. PSO with dynamic weight (DWPSO) is also applied to analyze the comparative capability of ASBO in solution exploration and convergence characteristics, and there is a remarkable improvement observed with ASBO-based solution.

Keywords Nanotechnology · Molecular force field · Potential energy function · Interatomic interaction · Computational intelligence · ASBO · PSO

S.N. Gondakar
Department of Physics, VTU, Belgaum 590018, Karnataka, India
e-mail: shreenivas100@gmail.com

S.T. Vasan
Department of Engineering Physics, Rural Engineering College, Hulkoti, India
e-mail: drvasanrec@gmail.com

M.K. Singh (✉)
Manuro Tech Research Pvt. Ltd, Bangalore 560097, India
e-mail: mksingh@manuroresearch.com

1 Introduction

Nanotechnology has made tremendous progress at least at the research level in recent years, and it can be defined as the engineering of functional systems at the molecular scale. But there are certain fundamental physical limitations because of its operational scale where macroscopic world physics does not apply. In result, along with implementation complexity, proper interpretation and analysis are also fundamental issues which have to handle in a very careful manner under nanotechnology environment. Instead of analytical approximation, numerical simulations are used for better interpretation of experimental results. In this contest involvement of computational intelligence-based concepts like evolutionary computation, swarm intelligence, artificial neural network, and other machine learning paradigm can play important role in development of the optimal results as well as in the development of nanotechnology-based applications for the future. There are numbers of examples and possibilities like in scanning probe microscopy, analysis, and modeling of biological systems, drugs design, the detail analysis of material modeling and their characteristics, simulation environment in nanoscience, and optimal design of nanodevices are few of them. Computational nanotechnology from an application perspective has been discussed in [1]. Artificial morphogenesis-based concept has presented in [2] for the creation of physical objects with a complex structure from the nanoscale up to the macro scale.

Molecular modeling is helpful to extract the relevant information about properties and processes on the molecular level. It is possible to describe electronic interactions completely with the Schrodinger equation, but complexity enhanced very much for large systems. It might be appropriate in some instances to use the classical model description to simplify the analysis of electronic interactions. Force fields utilize the parameterizable functions to define the electron interactions rather than explicit consideration of electrons as quantum mechanical methods do. Force-field methods are capable of predicting number of important properties like structures as well as vibrational frequencies and properties depending on those frequencies, elastic constants, point defect, dislocation, shear, fracture, phase transition, melting temperature, electrical properties such as dipole moments or infrared spectral intensities are few of them. In the past number of research, work has been defined to model the force field with two- and three-atom interactions like Stillinger [3] has defined in solid and liquid form of silicon. Various extensions of SW potential have also been defined in past [4–7]. Different computational intelligence-based techniques have applied in force-field modeling and their parameters fitting [8–11].

There are huge possibilities in nanotechnology for utilizing small atomic clusters as a fundamental building block element in well controlled and optimal design environment of nanostructures [12–14]. Clusters provide the facility for molecules to take shape of solids. Therefore, change in characteristics from molecules to bulk materials can be understood in detail by having the microscopic analysis of clusters. Properties available in molecules and solids may be very different in comparison to

clusters where the size of clusters decides the associated properties quality. For these reasons, in nanoelectronics where the material has to deliver defined electronic, optical, and other physical properties, the investigations of atomic clusters of semiconductor elements are important. In Semiconductor material, silicon is a well-known element and has its own importance because of its numerous applications.

Computational intelligence has huge modeling references from natural system. Apart from others, social interaction-based computational modeling, especially swarm intelligence, has shown huge success in many applications. Detail discussion about ASBO and PSO has presented in [15] and in [16].

2 Molecular Force Field

The concept of model potentials, generally speaking, is based on the Born-Oppenheimer approximation. If it is assumed that there is no external force, then (1) expressed the total energy of a system of N interacting particles.

$$E_N = \phi_1 + \phi_2 + \phi_3 + \phi_4 + \cdots \phi_n + \cdots \quad (1)$$

where ϕ_n represents the sum of n -body interaction energies. On the other hand, (2) represents the total energy of a system of N non-interacting particles.

$$E'_N = \phi_1 \quad (2)$$

The difference between these two total energies ($E_N - E'_N$) gives the total interaction energy of a system of N interacting particles as in (3) as a function of their positions.

$$\begin{aligned} \Phi &= E_N - E'_N = \phi_2 + \phi_3 + \phi_4 + \cdots + \phi_n + \cdots \\ \Phi &= \phi(r_1, r_2, r_3, \dots, r_N) \\ \Phi &= \sum_{i < j} U_2(r_i, r_j) + \sum_{i < j < k} U_3(r_i, r_j, r_k) + \cdots + \sum_{i < j, \dots, < n} U_n(r_i, r_j, \dots, r_n) + \cdots \end{aligned} \quad (3)$$

where U_2 , U_3 , and U_n , represent two-, three-, and n -body interactions, respectively. The quantity Φ is measurable, which describes the total configuration energy (or potential energy) of the system. In this so-called many-body expansion of Φ , because of faster convergence, effect of higher moments is negligible hence can be neglected for final force-field modeling. In the early development of force-field calculations, the sum of two-body interactions was taken to estimate the total potential energy Φ like, in Lennard-Jones-type functions. Many properties and process can be understand by Lennard-Jones systems; however, in number of different situations because of neglecting many-body interactions, this first-order

approximation is not suitable and produces results inconsistent with many experiments, particularly in the case of systems containing atoms other than those with closed-shell structures. Hence, in addition to two-body interactions, three-body interactions are also necessary to be considered in the calculation of potential energies.

2.1 The SW Potential

With the SW potential [3], the total energy is obtained as a combination of two-body and three-body interactions as given in (4)–(8), and it is treated as reference interatomic potential because of its success in different situation and simplicity.

$$\Phi_{\text{sw}} = \phi_2 + \phi_3 = \sum_{i < j} U_{ij} + \sum_{i < j < k} W_{ijk} \quad (4)$$

$$U_{ij} = \varepsilon f_2(r_{ij}/\sigma), \quad W_{ijk} = \varepsilon f_3(r_i/\sigma, r_j/\sigma, r_k/\sigma) \quad (5)$$

$$f_2(r) = \begin{cases} A(\text{Br}^{-p} - r^{-q})e^{(r-a)^{-1}}, & r < a \\ 0, & r \geq a \end{cases} \quad (6)$$

$$f_3(r_i, r_j, r_k) = h(r_{ij}, r_{ik}, \theta_{jik}) + h(r_{ji}, r_{jk}, \theta_{ijk}) + h(r_{ki}, r_{kj}, \theta_{ikj}) \quad (7)$$

$$h(r_{ij}, r_{ik}, \theta_{jik}) = \lambda e^{\left[\gamma(r_{ij}-a)^{-1} + \gamma(r_{ik}-a)^{-1}\right]} \times \left(\cos \theta_{jik} + \frac{1}{3}\right)^2 \quad (8)$$

2.2 Gong Potential [4]

This potential energy function is a modified form of the SW potential. Modification has given in three-body interaction factor as defined in (9).

$$\Phi_{\text{Gp}} = \Phi_{\text{sw}} \text{ with } h'_{\text{gn}}(r_{ij}, r_{ik}, \theta_{jik})$$

where

$$h'_{\text{gn}}(r_{ij}, r_{ik}, \theta_{jik}) = \lambda e^{\left[\gamma(r_{ij}-a)^{-1} + \gamma(r_{ik}-a)^{-1}\right]} \times \lambda_1 \left[z_1 + (z_0 + \cos \theta_{jik})^2\right] \left(\cos \theta_{jik} + \frac{1}{3}\right)^2 \quad (9)$$

2.3 Globus Potential [5]

This is a modified version of SW potential. Modification has given in two-body interaction by providing a parameter ‘ c ’ in exponential term and in three-body interaction factors, by providing an additive factor α as given in (10) and (11).

$$\Phi_{\text{Gp}} = \Phi_{\text{sw}} \text{ with } f_2'(r) \quad \text{and} \quad h'_{\text{gl}}(r_{ij}, r_{ik}, \theta_{jik})$$

where

$$f_2(r) = \begin{cases} A(\text{Br}^{-p} - r^{-q})e^{c/(r-a)^{-1}}, & r < a \\ 0, & r \geq a \end{cases} \quad (10)$$

$$h'_{\text{gl}}(r_{ij}, r_{ik}, \theta_{jik}) = \alpha + \lambda e^{[\gamma(r_{ij}-a)^{-1} + \gamma(r_{ik}-a)^{-1}]} \times \left(\cos \theta_{jik} + \frac{1}{3} \right)^2 \quad (11)$$

3 Parametrization Using ASBO

There are six unknown parameters ($A, B, p, q, \lambda, \gamma$) in SW potential function, which have to be estimated to fit the energy function in target clusters, nine parameters in Gong potential function ($A, B, p, q, \lambda, \gamma, \lambda 1, z0, z1$) and eight parameters ($A, B, p, q, \lambda, \gamma, c, \alpha$) in Globus potential function. These energy functions are very sensitive to the parameter values, landscape created by these parameters is very complex, and high-order nonlinearity exists. Hence, to achieve the optimal solution, a heuristic search method seems to be the better choice. We have applied an efficient new heuristic method called adaptive social behavior optimization (ASBO) to achieve our objectives.

3.1 Adaptive Social Behavior Optimization (ASBO)

There are a number of examples available in natural systems where evolution takes place in different forms and shapes. Survival is a fundamental reason of evolution and formation of social structure is the key reason to increase the chances of survival. At present, human social structure can be considered as one of the best and successful social formations where the numbers of stimulating and driving factors are available. Based on influences, directly or indirectly available in the social life of human, ASBO is a heuristic and a stochastic search method which is simple and self-adaptive to deliver the global solution [15]. It is true that in comparison with genetic evolution, effect of social interactions is much faster and more effective.

There are three macro-social influencing operators available in ASBO which affects the individual maximally, namely: inspiration from leader, inspired by neighbors and self inspiration. Level of influence must be adaptive and time dependent; hence, adaptive characteristics of these influences have defined by self-adaptive mutation strategy. Two populations exist all time in progress; among them, one belongs to solution population, which represents the phenotype coding of solution and other population is influencing level population with three parameters, each corresponding to depth of influence by leader, neighbors, and self best. With respect to the problem, using the fitness function, a fitness value for each and every member is defined. An individual in the population having the maximum fitness value is treated as a leader at the present time population. A group of three individuals in the population having next nearest higher fitness value is treated as logical neighbors for an individual. Change by each influence is additive in nature, hence the total change in existing value because of influence and new value is defined for every member of the population using (12) and (13).

$$\Delta x_{i+1} = \sum_{k=1}^3 (C_k R_k [F_k - X_i]) \quad (12)$$

where C_k are adaptive depth of influence ≥ 0 , and F_k are the influencing factors; $R_k \in U[0, 1]$

$$X_{i+1} = X_i + \Delta x_i \quad (13)$$

3.2 Steps to Adapt the New Set of Influence Depth

- (i) A population of N trial solution initialized. Each solution taken as a pair of real-valued vector (p_j, σ_j) , for all $j \in \{1, 2, 3\}$, with three dimensions corresponding to the number of progress variables. The initial components of each p_i , for all $i \in \{1, 2, \dots, N\}$ were selected in accordance with a uniform distribution ranging over a presumed solution space. The values of σ_i , for all, the so-called strategy parameters were initially set to some small value (less than 1).
- (ii) One new depth level p'_i, σ'_i generated from each old individual p_i, σ_i by (14) and (15)

$$p'_i(j) = p_i(j) + \sigma_i(j) \times N(0, 1) \quad (14)$$

$$\begin{aligned} \sigma'_i(j) &= \sigma_i(j) \times e^{[\tau' N(0, 1) + \tau N_j(0, 1)]} \\ \forall j \in \{1, 2, 3\}, \text{ and } \tau &= \left(\sqrt{2\sqrt{n}} \right)^{-1}, \quad \tau' = (\sqrt{2n})^{-1} \end{aligned} \quad (15)$$

where $p_i(j)$, $p'_i(j)$, $\sigma_i(j)$, $\sigma'_i(j)$ denote the ‘ j th’ component of the vectors X_i , X'_i , σ_i , σ'_i respectively, and $N(0, 1)$ is a random number from Gaussian distribution. $N_j(0, 1)$ is a new random number sampled for each new value of ‘ j ’ using Gaussian distribution, and ‘ n ’ is the number of parameters which have to be evolved.

There is a cascade structure of two phases under which the whole processes are completed to get the global solution. (i) A PF number of different populations having same population size (PZ) are initialized through uniform distribution in solution range, and ASBO evolution steps are applied independently up to fixed, say Pth, number of iterations for each population. With evolution of all PF populations, obtained fitness values at the end and all influence depth constants are stored for each and every member from their evolved population. This phase assures to have good diversity in their search process and localize the region of the solution in a faster manner. (ii) A new population of size PZ is created by selecting members from all final population of the first phase, which are having higher fitness value along with their existed depth of influence to form the second-stage population. Over this newly generated population, ASBO evolution steps are applied to get the final solution. This second phase will explore the solution in the environment of the multisocial culture to get the optimal solution.

3.3 Simulation Environment and Result Analysis

Because of its importance in technological development, silicon is one of the most intensely studied elements in the periodic table. Numerous synthesis and processing methods have been developed to enable its use in microelectronic devices. The small cluster of silicon is very different from bulk crystal lattice; hence, we have developed the parameter estimation with silicon cluster having atoms 3–5. There are a number of clusters having different structure and their energy values, as shown in Table 1.

We have applied DWPSO and ASBO under different environments. In DWPSO, inertia weight value is dynamic with iteration rather than fixed, and it decreases from 1.2 to 0.1 with iterations. This will give a large jump at the beginning of the search and smaller as it moves toward a solution. A constriction factor (0.72) is also applied to keep the change bounded.

First, we have given a comparative environment for both methods, maintaining balance in terms of population size and number of iterations. Total 10 different trials have given with population size equal to 100 for both algorithms while the number of allowed iterations for PSO has given equal to 3000 while for ASBO, it is 100 in the first stage and 2000 in second stage so that overall there are effectively 3000 iterations available. Solution search space has defined in a range of $[-10, 100]$ for all parameters. Clusters, C1, C2, C3, and C4 as shown in Table 1, have taken to estimate the parameters for SW, Gong, and Globus potential functions. The

Table 1 Silicon cluster structure and associated bond length with energy value

Cluster	Structure	Bond	Bond length (Å)	Binding energy (eV)
C1		1–2	2.37	-4.836
C2		1–2	2.47	-4.914
C3		1–2	2.433	-8.197
		2–3	2.815	
C4		1–2	2.384	-11.611
C5		1–2	2.581	-7.26
C6		1–2	2.342	-7.177
		2–3	2.498	
		3–4	2.487	

Table 2 *Rmse* performance of ASBO and PSO using SW function in 10 trials

Performance	ASBO		PSO	
	($\epsilon = 1, \sigma = 1$)	($\epsilon = 2.16826, \sigma = 2.0951$)	($\epsilon = 1, \sigma = 1$)	($\epsilon = 2.16826, \sigma = 2.0951$)
Mean	0.4326	0.5516	1.0784	1.2515
Std. dev.	0.0117	0.0532	0.1486	0.3616
Beast	0.4272	0.4660	0.9209	0.6454
Worst	0.4547	0.6398	1.1912	1.5650

objective function is defined as the root-mean square error (*rmse*) for these clusters with respect to their expected binding energy. Clusters C5 and C6 have taken to validate the estimated parameters. In all potential function parameters, ϵ and σ are energy and distance scaling factors, respectively, which set the cohesive energy and lattice constant of the cubic diamond silicon. We have done the estimation of parameters for two different set values of ϵ and σ and performances for SW and Gong function have estimated by ASBO and PSO to minimize the *rmse* value. Obtained performances for 10 independent trials have shown in Table 2 and in Table 3.

There are several points which are noticeable: (i) Gong function delivered the lesser *rmse* compared to SW function in both ASBO and PSO. This is because nine parameters are available in Gong function in comparison to SW function where only six parameters are available. (ii) ASBO has delivered always lower *rmse*

Table 3 *Rmse* performance of ASBO and PSO using Gong function in 10 trials

Performance	ASBO		PSO	
	($\epsilon = 1, \sigma = 1$)	($\epsilon = 2.16826, \sigma = 2.0951$)	($\epsilon = 1, \sigma = 1$)	($\epsilon = 2.16826, \sigma = 2.0951$)
Mean	0.1715	0.0640	1.1912	1.7380
Std. Dev.	0.1537	0.0378	2.1050	0.7595
Beast	0.0588	0.0129	1.1911	1.1909
Worst	0.5279	0.0855	1.1912	3.1346

Table 4 Energy prediction performance by ASBO using SW function in 10 trials

Performance	ASBO ($\epsilon = 1, \sigma = 1$)					
Cluster	C1	C2	C3	C4	C5	C6)
Target binding energy	-4.8360	-4.9140	-8.1970	-11.6110	-7.2600	-7.1770
Predicted mean energy	-4.0470	-5.1308	-8.0802	-11.8667	-6.5678	-6.4522
Std. dev. of pred. energy	0.0196	0.0076	0.0095	0.0085	0.0603	0.2325
Best predicted energy	-4.0688	-5.1247	-8.0912	-11.8587	-6.6362	-6.7128
Worst predicted energy	-4.0115	-5.1463	-8.0595	-11.8836	-6.4586	-6.0405

compared to PSO. (iii) for $\sigma = \epsilon = 1$, ASBO performances are best with SW function for predicting the more accurate energy value in C5 and C6 clusters, whereas with Gong function, it could not converge at all even though there is lesser *rmse* observed in known environment with Gogn function compared to SW function. This indicates that, the large number of parameters can learn the target in a better manner, but it loses the generalize capability. DWPSO has delivered its best with Gong function at $\epsilon = 2.16826, \sigma = 2.0951$. Estimated parameters and correspondingly predicted energy values have also presented in Tables 2, 3, 4, 5 and 6.

We have applied Globus function also using ASBO and DWPSO for 10 independent trials, and obtained *rmse* has shown in Table 7. ASBO again outperformed DWPSO, and predicted energy value for all clusters by ASBO has shown in Table 8.

Best estimated parameters by ASBO and DWPSO along with original estimated parameters by past research have shown in Table 9. ASBO has delivered best with SW function with ($\epsilon = 1, \sigma = 1$), and DWPSO has delivered best with Gong function with ($\epsilon = 2.16826, \sigma = 2.0951$). ASBO has delivered the best performance in comparison to all others with significant differences. Comparative analysis between these functions and corresponding estimated parameters in delivering minimum *rmse* value has shown in Table 10.

Table 5 Energy prediction performance by ASBO using Gong function in 10 trials

Performance	ASBO ($\epsilon = 2.16826, \sigma = 2.0951$)					
Cluster	(C1)	C2	C3	C4	C5	C6)
Target binding energy	-4.8360	-4.9140	-8.1970	-11.6110	-7.2600	-7.1770
Predicted mean energy	-4.7165	-4.9304	-8.2011	-11.6521	×	×
Std. dev. of pred. energy	0.0711	0.0111	0.0103	0.0236	-	-
Best predicted energy	-4.8117	-4.9162	-8.1998	-11.6189	-	-
Worst predicted energy	-4.5602	-4.9529	-8.2110	-11.6982	-	-

Table 6 Energy prediction performance by PSO using Gong function in 10 trials

Performance	PSO ($\epsilon = 2.16826, \sigma = 2.0951$)					
Cluster	(C1)	C2	C3	C4	C5	C6)
Target binding energy	-4.8360	-4.9140	-8.1970	-11.6110	-7.2600	-7.1770
Predicted mean energy	-4.8468	-5.8988	-5.5097	-11.9255	-7.7781	-6.2678
Std. dev. of pred. energy	0.2579	1.8159	1.5818	0.8093	5.3098	2.8087
Best predicted energy	-4.5561	-6.8332	-6.8321	-11.3903	-5.2038	-3.7497
Worst predicted energy	-4.9394	-2.4562	-2.7265	-13.4346	-13.6638	-9.1111

Table 7 *Rmse* performance of ASBO and DWPSO using globus function

Performance	ASBO	DWPSO
Mean	0.0366	2.0408
Std. dev.	0.0491	0.7257
Beast	0.0004	0.4003
Worst	0.1362	2.3899

Table 8 Energy prediction performance by ASBO using globus function

Performance			ASBO			
Cluster	(C1)	C2	C3	C4	C5	C6
Target binding energy	-4.8360	-4.9140	-8.1970	-11.6110	-7.2600	-7.1770
Predicted mean energy	-4.8988	-4.9154	-8.1598	-11.6112	-10.5240	-5.7515
Std. dev. of pred. energy	0.0836	0.0050	0.0512	0.0024	0.3213	0.0574
Best predicted energy	-4.8367	-4.9141	-8.1965	-11.6110	-10.2338	-5.7292
Worst predicted energy	-5.0647	-4.9265	-8.0498	-11.6167	-11.1531	-5.6560

Table 9 Parameters' value for different energy functions

Parameter	ASBO	PSO	SW [3]	Gong [4]	Globus [5]	VBWM [6]	Lpizza [7]
A	06.2651	01.1149	Av*	Av*	40.83	Av*	19.0
B	31.8004	20.4730	Bv*	Bv*	784.12	Bv*	0.65
p	04.6122	100.00	4	4	9.94	4	3.5
q	00.0190	0.0	0	0	-0.8	0	0.5
λ	99.9707	0.0	21	21	77.23	31.5	31
γ	31.6350	100.00	1.2	1.2	3.91	1.2	1.1
ϵ	1.0	2.16826	2.16826	2.16826	1.0	1.6483	1.0419
σ	1.0	2.0951	2.0951	2.0951	1.0	2.0951	2.128
λ_1	-	100.00	-	25	-	-	-
Z0	-	0.0	-	-0.5	-	-	-
Z1	-	0.0	-	0.45	-	-	-
C	-	-	-	-	6.31	-	-
α	-	-	-	-	16.88	-	-

$$\text{Av}^* = 7.049556277, \text{Bv}^* = 0.6022245584$$

Table 10 Rmse value with all silicon clusters for different energy functions

Parameter	ASBO	PSO	SW [3]	Gong [4]	Globus [5]	VBWM [6]	Lpizza [7]
rmse	0.5	2.9	118.3	2072.6	82.2	145.9	77.6

Convergence characteristics for ASBO and PSO two different sets of ($\epsilon = 1$, $\sigma = 1$) and ($\epsilon = 2.16826$, $\sigma = 2.0951$) with two SW and Gong potential functions have shown in Figs. 1, 2 and 3, while for Globus function, it is available in Fig. 4. It can observe that with all plot, DWPSO converges prematurely and even a large number of further iterations could not improve any more. This shows basically the tendency of DWPSO to trap in local minima, and if the landscape is very irregular, there is no way to come out from there. ASBO in first phase not only evolves some good candidates of the solution, but also generates good diversity, and in a second phase of evolution, they explore the solution space in a more efficient manner. In result,

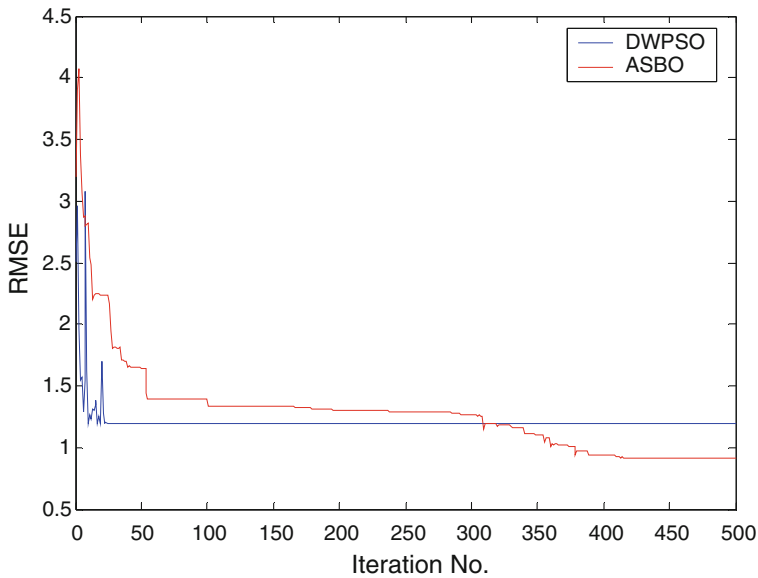


Fig. 1 Convergence characteristics for $rmse$ in SW function with ($\epsilon = , \sigma = 1$) using ASBO and DWPSO in first 500 iterations

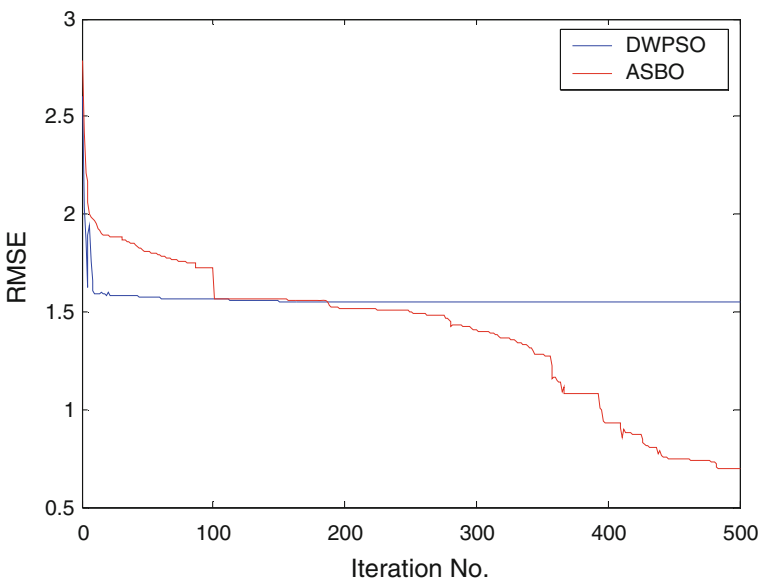


Fig. 2 Convergence characteristics for $rmse$ in SW function with ($\epsilon = 2.16826, \sigma = 2.0951$) using ASBO and DWPSO in first 500 iterations

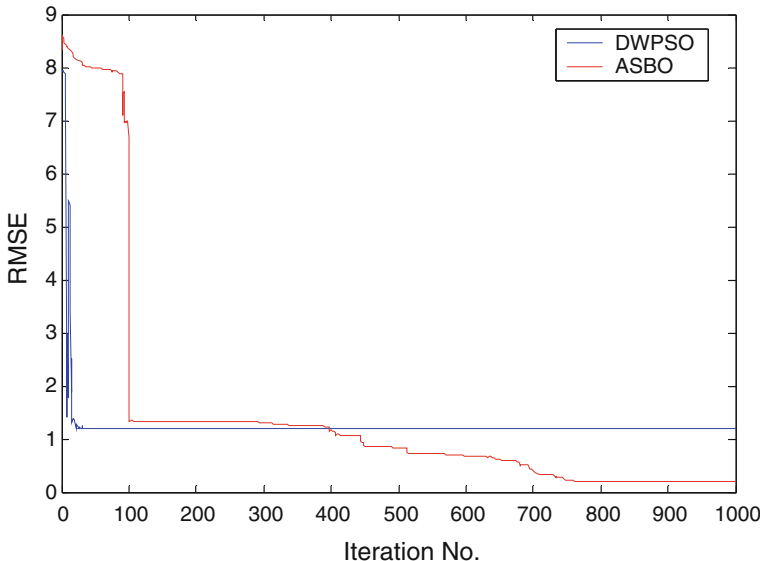


Fig. 3 Convergence characteristics for $rmse$ in Gong function with ($\epsilon = 1$, $\sigma = 1$) using ASBO and DWPSO in first 1000 iterations

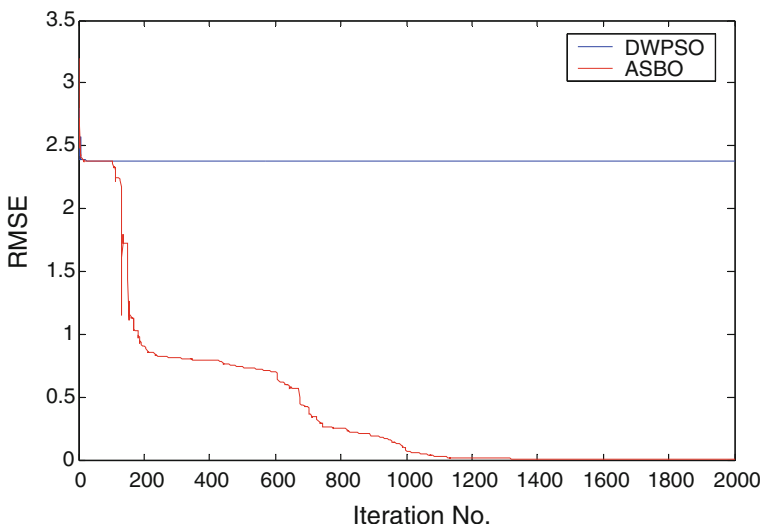


Fig. 4 Convergence characteristics for $rmse$ in Globus function with ($\epsilon = , \sigma = 1$) using ASBO and DWPSO in first 2000 iterations

the fundamental requirement of the good heuristic search method, maintaining balance between exploration and exploitation takes place in an optimal manner.

4 Conclusion

Our goal was to enhance the ability of the potential energy function based on SW potential function to have a better predicting capability of energy by fitting optimal parameters in the potential function. To explore the optimal parameters over very irregular landscape defined by potential function, human social structure-based optimization method, ASBO has applied. It is observed with the experimental analysis that, an extension of SW function, Gong function which has more parameters comparatively, is performed well in known domain, but performed poorly in unknown environment. In this research, there is further reduction in SW function parameters, which is defined by nullifying the effect of scaling parameters which cause a significant improvement in generalization capability of energy prediction. ASBO has shown outstanding performances in the exploration of solution in comparison to DWPSO and other available original parameters.

Acknowledgments This research has completed in Manuro Tech Research Pvt. Ltd., Bangalore, India. The Authors express their thanks to Mrs. Reeta Kumari (Director) for her valuable suggestion to accomplish this research.

References

1. Srivastava, D., Atluri, S.N.: Computational nanotechnology: a current perspective. *CMES* **3** (5), 531–538 (2002)
2. MacLennan, B.J.: Morphogenesis as a model for nano communication. *Elsevier Nano Commun. Netw.* **1**, 199–208 (2010)
3. Stillinger, W.: Computer simulation of local order in condensed phase of silicon. *Phys. Rev.* **31**(8) (1985)
4. Gong, X.G., Zheng, Q.Q., He, Y.-Z.: Structural properties of silicon clusters: an empirical potential study. *J. Phys. Condens. Matter* **7** (1995)
5. Globus, A., Menon, M., Ricks, E., Srivastava, D.: Evolving molecular force field parameters for Si and Ge. *NSTI Nanotechnol. Conf. Trade Show* (2003)
6. Vink, R., Barkema, W.M.: Fitting the Stillinger-Weber potential to amorphous silicon. *Elsevier J. Non-Cryst. Solids* **282**(2–3), 248–255 (2001)
7. Pizzagalli, L.: A new parametrization of the Stillinger-Weber potential for an improved description of defects and plasticity of silicon. *J. Phys. Condens. Matter* **25**(5) (2013)
8. Mostaghim, S.: Molecular force field parametrization using multi-objective evolutionary algorithms. *IEEE, CEC.* **1** (2004)
9. Slepoy, A., Peters, M.D., Thompson, A.P.: Searching for globally optimal functional forms for interatomic potentials using genetic programming with parallel tempering. *J. Comput. Chem.* **28**(15), 2465–2471 (2007)
10. Larsson, H.R., Hartke, B.: Fitting reactive force fields using genetic algorithms. *Comput. Method Mater. Sci.* **13**(1) (2013)
11. Pukrittayakamee, A., Malshe, M.: Simultaneous fitting of a potential energy surface and its corresponding force filed using feed forward neural network. *J. Chem. Phys.* **130**, 134101 (2009)
12. Hiura, H., Miyazaki, T., Kanayama, T.: *Phys. Rev. Lett.* **86**, 1733 (2001)
13. Katircioglu, S., Erkoc, S.: *Physica E* **9**, 314 (2001)

14. Baturin, V.S.: Structural and electronic properties of small silicon clusters. *J. Phys. Conf. Series* **510** (2014)
15. Singh, M.K.: A new optimization method based on adaptive social behavior: ASBO. Springer AISC **174**, 823–831 (2012)
16. Clerc, M., Kennedy, J.: The particle swarm-explosion, stability, and convergence in a multidimensional complex space. *IEEE Trans. Evol. Comput.* **6**(1) (2002)

Natural Language-Based Self-learning Feedback Analysis System

Pratik K. Agrawal, Abrar S. Alvi and G.R. Bamnote

Abstract Internet has gained a wide popularity in recent years. The people's interaction and sharing of their views about a particular subject and providing feedback to them have increased rapidly. The feedbacks are mainly in the form of numeric rating and free text words. The numeric rating can be easily processed but to process free text words is an important task. In this paper, different approaches are reviewed and based on that a self-learning feedback analysis system is proposed, which analyzes the feedback and provides an accurate result that helps in decision making.

Keywords Semantic • Artificial intelligence • Sentiment analysis • Ontology

1 Introduction

Online Communication has gained much popularity due to the current advance in Internet technologies. The People are free to share their feedback about the particular products or as well as the students are also sharing their feedback about the institute in which they study. Online blogs and Forums provide a platform to people to share their feedback or views globally by just clicking a button. People carefully view and summarize this feedback before taking any important discussion. The People's way of thinking and taking the discussion has been gradually becoming efficient day by day with the use of modern technology.

P.K. Agrawal (✉) · A.S. Alvi · G.R. Bamnote

Department of Computer Science & Engineering, Prof Ram Meghe Institute of Technology & Research, Badnera Amravati, India
e-mail: pratik.agrawal@gmail.com

A.S. Alvi
e-mail: abrar_alvi@rediffmail.com

G.R. Bamnote
e-mail: grbamnote@rediffmail.com

© Springer India 2016

S.C. Satapathy et al. (eds.), *Proceedings of the Second International Conference on Computer and Communication Technologies, Advances in Intelligent Systems and Computing* 380, DOI 10.1007/978-81-322-2523-2_9

The People's feedbacks are in the form of structured as well as unstructured form. The structured feedback deals with numerical data, and unstructured feedback includes free text words. Online blogs, forums, and Guest discussion have opened up the new way of providing the unstructured form of feedback. When come up to the point of analysis, the numerical data can be easily processed as it includes number only but to process free text words is a major challenge nowadays.

The paper outlines as follows: various approaches for dealing with the analysis of free text words are reviewed in Sect. 2 of the literature review. Section 3 proposed a new methodology for analysis of textual feedback. The overall outcomes are represented in the conclusion.

2 Related Work

Zha et al. proposed a product aspect ranking framework to identify the important aspects of products from numerous consumer reviews. The framework contains three main components, i.e., product aspect identification, aspect sentiment classification, and aspect ranking. The algorithm simultaneously explores aspect frequency and the influence of opinions given to each aspect over the overall opinions. The product aspects are finally ranked according to their importance scores [1].

Zhiyuan Chen, Arjun Mukherjee, and Bing Liu developed an automatic aspect extraction framework which has the ability to learn knowledge automatically from a vast number of review sample and uses the learned knowledge in finding various coherent aspects [2].

Zhu et al. solved the problem of multi-aspect content-based rating inference. They address the problem of aspect-based segmentation in which they categories the reviews into multiple single-aspect textual parts and processing the single aspects based on the reviews and at last combining the result. They have also focused on the aspect augmentation approach in which they created a feature vector for each aspect and based on the reviews calculated the aspect-based rating inference [3].

Xu Xueke et al.'s center of attention for online customer reviews was to improve aspect-level opinion mining. They stated the Joint Aspect/Sentiment (JAS) model for jointly extracting aspects and aspect-dependent sentiment lexicons [4].

Xiuzhen Zhang, Lishan Cui, and Yan Wang identify the "all good reputation" problem which is mainly popular in various E-commerces for the reputation management systems. The high reputation scores for sellers cannot effectively rank sellers and therefore cannot influence potential customers to select genuine sellers to transact with. The author proposed CommTrust an efficient algorithm to calculate dimension trust scores and weights via retrieving aspect from feedback comments and clustering them [5].

Desheng Dash Wu, Lijuan Zheng, and David L. Olson proposed sentiment ontology for online opinion posts in stock markets. The sentiment ontology approach is a combination of opinion analysis and machine learning. The machine

learning approach like support vector machine takes the static data that formulates the rule and based on that simplifies the conditional modeling [6].

Danushka Bollegala et al. identify the problem that different words are used in different domains for expressing the same polarity. Every domain requires opinion dataset for polarity identification and creating different datasets for each domain is quite tedious and expensive process. For this, they proposed a machine learning classifier approach that is trained with all the opinion words from the entire domain so that the classifier can easily process the sentiment words as well as it works on the cross-domain sentiment classification [7].

3 Proposed Work

The proposed system aims to develop natural language-based self-learning textual feedback analysis system for textual feedback data which is capable of evaluating the textual feedback. Proposed architecture for this research work is as shown in Fig. 1.

The proposed system is divided into six modules. They are as follows:

- Feedback data collection form
- Preprocessing
- Ontology generation
- Semantic analysis
- Artificial intelligence analysis
- Sentiment analysis.

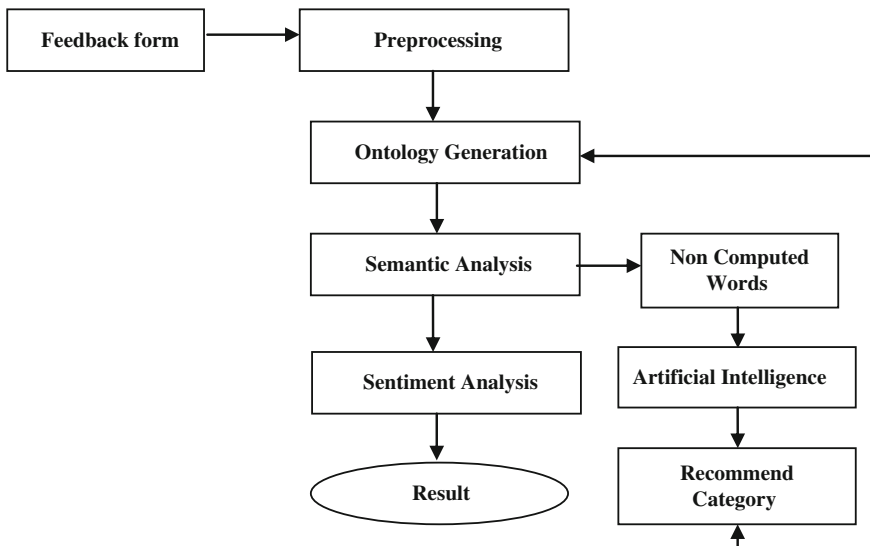


Fig. 1 Self-learning feedback analysis system architecture

3.1 Feedback Data Collection Form

The feedbacks are collected from the people by using the two standard approaches: quantitative feedback and qualitative feedback. The Feedback Form is designed in Fig. 2. The quantitative feedback deals with the questionnaires and in the form of radio button those are not able to provide depth knowledge about the people opinions but requires less time for collection. The qualitative feedback collects the feedback from the people in the form of blogs, surveys, and face-to-face interviews that are able to provide depth knowledge about the people opinions but requires more time for collection. The proposed method makes uses of these both quantitative and qualitative approaches to create an interactive form that will be able to take the accurate opinions from the people within the time limit as well as the spam opinions that are given by unethical sources will be filtered out in order to get the genuine opinions from the people.

The Feedback data collection form consists of questionnaires from the quantitative approach about the particular entity of the organization. The form asks for suggestions if the user has selected the parameter very bad, bad, neutral, and good in order to retrieve valuable opinions from the user about the particular entity. The form consists of questionnaires on all the major entity that is related to organization as well as it provides the user with the free space to write their opinions about any other entities. The form is design in order to get quick and accurate feedback from the users.

3.2 Preprocessing

The preprocessing or part of speech tagging is important step in analysis of unstructured text data. This step tags the word with the part of speech tags from the English dictionary that the tagging helps identify the important words irrespective of their position in the sentences. The identified important words along with their tags are used for further processing. There are various pos tagger available for English like Stanford, Sharp NLP, and Ri Wordnet that works well depending on the input provided. The Proposed work focuses on the designing and development of the pos tagger that works in all conditions and provides with the better tagging performance. Comparing the Stanford, Sharp NLP, and Ri WorldNet pos tagger and

Fig. 2 Feedback form

Feedback Form for College
1) Opinion about Canteen?
<input type="radio"/> Very Bad <input type="radio"/> Bad <input type="radio"/> Neutral <input type="radio"/> Good <input type="radio"/> Excellent
Suggestion for Improvement:
2) Opinions for improvement in any other entities of the college?

combining the features of that tagger, a new hybrid tagger is to design so that it works under all scenarios.

3.3 Ontology Generation

The feedback or opinions are always given to the particular entity of the organization or the features of the products in the E-commerce world. The structure of the organization plays a great role in identifying and mapping the feedback or opinions. The entities or features are differentiated based on their properties and value that they pose. Every time the users cannot mention the entity name, their properties, and values of that entity. Ontology structure helps in arranging the organization entity in the binary tree structure form. Consider the example of the Bank Ontology in Fig. 3, the various entities of the bank like employee, service, security, etc. that are related directly or indirectly are mapped in the structure. These entities can be further classified based upon their properties and values. In this way, a generalized and efficient structure can be formed.

3.4 Semantic Analysis

The semantic analysis consists of identifying the features or entity from the sentences about which the user has provided the opinions and mapping that reference entity with the ontology structure of the organization. The semantic analysis makes use of the machine learning approach. The machine learning approach is provided with the inputs in the learning phase, and based on that learning data, the machine learning trained the system. There are various machine learning approaches that are

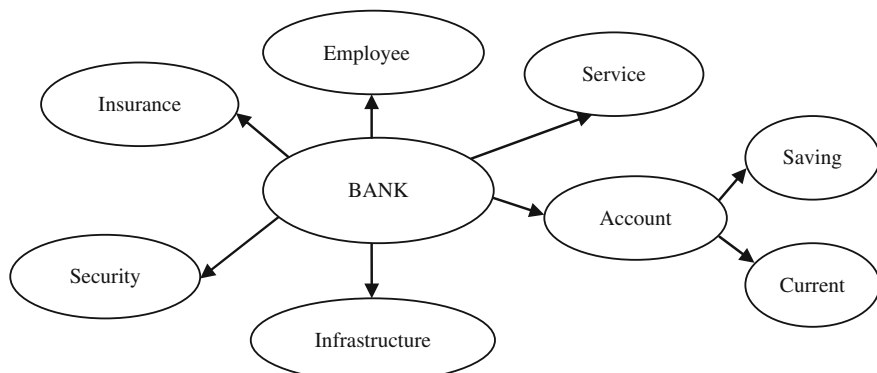


Fig. 3 Bank (organization) ontology structure

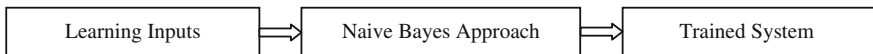


Fig. 4 Learning phase of semantic analysis

available, and based on the literature reviews, the naive base machine learning algorithms perform well in this system. The learning phase is illustrated in Fig. 4.

- The tagged words (NP, NN) from the preprocessed stage are compared with the properties values and facts of the entity in the semantic analysis module.
- If the matching of the words goes above the certain threshold value, then the words are mapped with the structure of the organization and consider for sentiment analysis processing in the next step.
- And the words that are not matched or that are non-computed go to the artificial intelligence modules for further processing.
- In this way, semantic analysis computes the analysis of the features of the entity.

3.5 Artificial Intelligence Module

The Artificial intelligence module takes the non-computed words that are not matched in the ontology structure for processing in the Semantic analysis module as shown in Fig. 5. The module evaluates the properties and facts of the non-computed words with the help of the knowledge database available in the form of WordNet and online query. The Artificial Intelligence Module is design in Fig. 6. The properties and facts of the non-computed words that are identified are then matched with the predefined structure ontology, and if the matching goes above the set threshold values, then the recommendation is passed to the evaluator for adding the new entity to the structure.

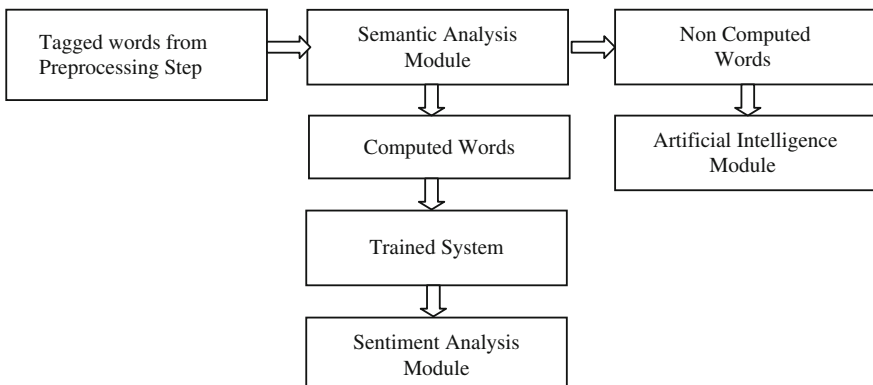


Fig. 5 Semantic analysis module

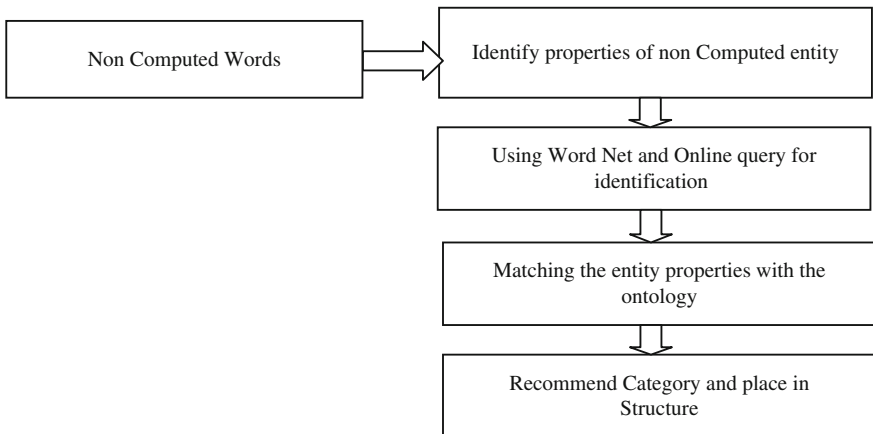


Fig. 6 Artificial intelligence module

3.6 Sentiment Analysis

The sentiment analysis module takes the words that are tagged with Adjective, Adverb, and Verb tags from the preprocessing step. The opinions expressed about the entity are evaluated from these words so analyses of these tag words are important. According to Literature Review, Sentiment analysis is domain dependent because the words have different meanings in different domains. Consider the examples of domain of book in that “2 states book is excellent” in that excellent expresses the positive opinions about the book whereas consider the domain of food in that “Cheese Pizza is delicious” the word delicious is expressing the positive polarity so different words are used for expressing the same polarity in different domains. The Sentiment Analysis Module is illustrated in Fig. 7. The proposed work aims at developing the sentiment module that will work efficiently on various domains [8].

The Proposed methodology for sentiment analysis module is as follows:

- Extracting the tagged words like Adjective, Adverb, and Verb from the Preprocessing Module.
- Defining the Rule-based Approach for executing the conjunction, polarity changing on the verb and adverb terms, non-negative terms, etc.
- Creating the datasets for the positive, negative, and neutral words from all the domains.
- Considering the non-computed words and matching those words with the word, net dictionary or online query identifying their base polarity and adding them to the datasets.
- Calculating the Polarity of the computed words and extracting suggestions given by the user.

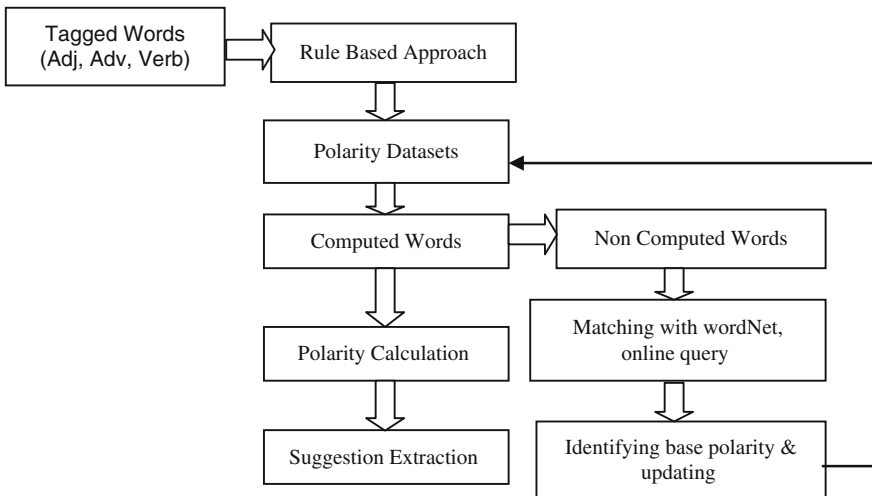


Fig. 7 Sentiment analysis module

4 Conclusion

Feedback analysis is an important task for very organization because it helps them in finding the problems related to their products as well as with the employees of the organization. In this paper, Natural language-based self-learning feedback analysis system is proposed, which analyzes the textual feedback and helps in decision making. The future work is to implement the proposed system and evaluate it on different datasets for precision and recall.

References

1. Zha, Z.-J., Yu, J., Tang, J., Wang, M., Chua, T.-S.: Product aspect ranking and its applications. *IEEE Trans. Knowl. Data Eng.* **26**(5), 136 (2014)
2. Chen, Z., Mukherjee, A., Liu, B.: Aspect extraction with automated prior knowledge learning in ACL (2014)
3. Zhu, J., Zhang, C., Ma, M.Y.: Multi-aspect rating inference with aspect-based segmentation. *IEEE Trans. Affect. Comput.* **3**(4), 469–481 (2012)
4. Xueke, X., Xueqi, C., Songbo, T., Yue, L., Huawei, S.: Aspect-level opinion mining of online customer reviews. In: Proceedings of the Management and Visualization of User and Network Data China Communications March (2013)
5. Zhang, X., Cui, L., Wang, Y.: CommTrust computing multi-dimensional trust by mining E-commerce feedback comments. *IEEE Trans. Knowl. Data Eng.* **26**(7) 2014
6. Wu, D.D., Zheng, L., Olson, D.L.: A decision support approach for online stock forum sentiment analysis. *IEEE Trans. Syst. Man Cybern. Syst.* **44**(8), 1077–1087 (2014)

7. Bollegala, D., Weir, D., Carroll, J.: Cross-domain sentiment classification using sentiment sensitive thesaurus. *IEEE Trans. Knowl. Data Eng.* **25**(8), 1719–1731 (2013)
8. Liu, C.-L., Hsaio, W.-H., Lee, C.-H., Lu, G.-C., Jou, E.: Movie rating and review summarization in mobile environment. *IEEE Trans. Syst. Man Cybern. Part C Appl. Rev.* **42**(3), 397–407 (2012)

Adaptive Filter Design for Extraction of Fetus ECG Signal

Ranjit Singh, Amandeep Singh and Jaspreet Kaur

Abstract The fetal ECG is a useful tool in the assessment of condition of fetus heart before and during labor time and also contains more information than sonography. Early detection of fetal heart defect helps the selection of appropriate treatment before and during pregnancy. FECG signal obtained by non-invasive method is affected from the background noise and MECG interference as FECG signal is weak relative to MECG signal and competing noise. This interference produced by MECG signal and other artifacts can be canceled by application of adaptive filters using LMS and RLS algorithms. In this paper, we have purposed an adaptive filter algorithm which has shown better results than standard LMS algorithm for the detection of Fetus ECG Signal.

Keywords FECG · MECG · RLS · LMS

1 Introduction

There are many diseases which are found to be by birth. The heart defects are the most common causing problems during pregnancy period. These defects can be so minor that it does not affect the baby significant up to many years after the birth and can be so dangerous that it may lead to death of new born within few hours.

R. Singh (✉)

Department of Physics, S.L.I.E.T., Longowal, Sangrur, India
e-mail: ranjit_longowal@yahoo.co.in

A. Singh

Department of Electronics and Communication, G.N.D.U., Amritsar, India
e-mail: amandeep.singh.sodha@gmail.com

J. Kaur

Department of Electronics and Communication, G.N.D.U., Regional Campus,
Fattu Dhinga, Amritsar, India
e-mail: gill_jas8@hotmail.com

Approximately 1 % of new born babies take birth with heart defects. The FECG can provide more reliable information than the sonography about the condition of heart of fetus. The distance between R-R peaks of ECG signal gives important information about the cardiac condition of fetus. The FECG signal is used to know the well being of fetus and also can be used to detect the multiple pregnancy (twin, thrice, etc.). The FECG signal can be recorded by application of abdominal electrode, but this recorded signal is contaminated by MECG signal and power line interference. It is also affected by the respiration process of mother, contraction of uterus, and movement of fetus. The FECG signal is relatively weak than MECG signal as its power is approximately 10 % of MECG signal so it is dominated by MECG signal. Also both signals may contain overlapping band of frequencies; hence, it is almost impossible to extract the FECG signal from the recorded signal by use of conventional filters. So we require suitable technique for the extraction of FECG. There are various methods and techniques for this purpose. These methods include the blind source separation (BSS) [1], Auto- & Cross-correlation techniques [2], singular value decomposition (SVD) [3] or SVD with independent component analysis (ICA), [4] matching pursuits [5, 6], wavelet transformation [7], Bayesian filtering [8], non-linear projections [9], third-order cumulate [10], and adaptive filters [11–15] with algorithms least-mean square (LMS) and recursive least square (RLS) that are most commonly used. By comparing these techniques, the adaptive filter is best suitable for FECG extraction due to its simplicity, can be realized in real time, and gives the fruitful results. In 1975, WIDROW firstly developed this application by use of LMS and still most efficient technique for its simplicity and widespread use. But the classical LMS suffers from the slow rate of convergence and still corrupted with noise. In this paper, learning from its limitations, we purposed an adaptive filter algorithm which shows better experimental results over classical LMS and RLS.

2 Data Collection

The FECG signal can be recorded by two methods: First is invasive method in which ECG electrode is positioned on scalp of fetus. In this method, there is a possible threat of permanent rapturing of membrane and can be only possible during the labor time. Second is non-invasive method in which ECG signal can be recorded by using chest and abdominal electrode, respectively, for the maternal and fetus composite ECG signals. In non-invasive method, help of a cardiologist, digital storage CRO is required for recording of ECG signal, and also permission of patient should be granted. It also suffers from lack of standard fetal signal for comparison. So for the experimental purpose, the other method is to synthesize the maternal and fetal ECG signal in MATLAB assuming mother heartbeat rate 89 beats per minute at sampling rate 2700 Hz with peak voltage 3.5 mV and fetus heartbeat rate 120 beats per minute at 1725 Hz sampling rate having peak voltage 0.25 mV.

These signals have been synthesized by using ‘ecg’ function in MATLAB as

$$x1 = 3.5 * \text{ecg}(2700) \quad (1)$$

$$x2 = 0.25 * \text{ecg}(1725) \quad (2)$$

First signal corresponds to mother ECG, and second is corresponding to fetus ECG. After generation, these signals have been smoothed using Sgolay Filter as

$$y1 = \text{sgolayfilt}(\text{kron}(\text{ones}(1, 13), x1), 0, 21) \quad (3)$$

$$y2 = \text{sgolayfilt}(\text{kron}(\text{ones}(1, 20), x2), 0, 17) \quad (4)$$

where for any two variables ‘r’ and ‘s’

$$\text{kron}(r, s) = [r(1, 1) * s \ r(1, 2) * s \ r(1, 3) * s \ r(2, 1) * s \ r(2, 2) * s \ r(2, 3) * s]$$

Signals which are to be processed are

$$\text{mhb} = y1(n) \quad (5)$$

$$\text{fhb} = y2(n) \quad (6)$$

where n is number of iterations, forming a combined signal as

$$d = \text{mhb} + \text{fhb} \quad (7)$$

The fetal ECG signal is dominated by maternal ECG signal due to its high relative strength. The maternal signal propagates through the chest cavity to abdomen. Hence, abdomen electrode contains both maternal and fetal composite signals.

The main goal of Adaptive filter is to extract the fetal signal from the composite signal for this purpose the maternal signal can act as reference noise source. So in

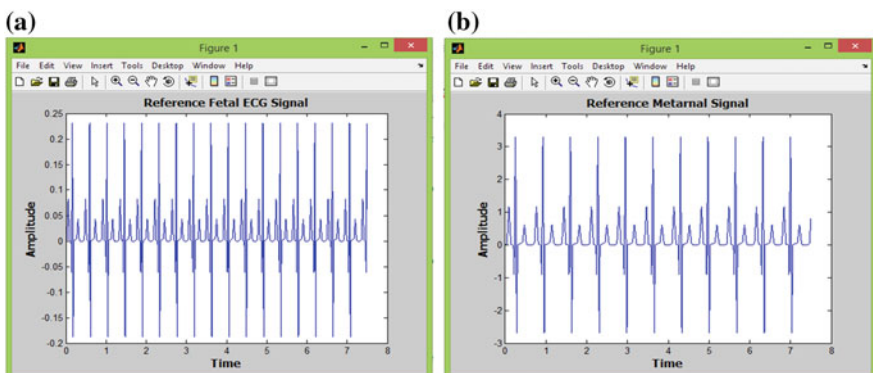
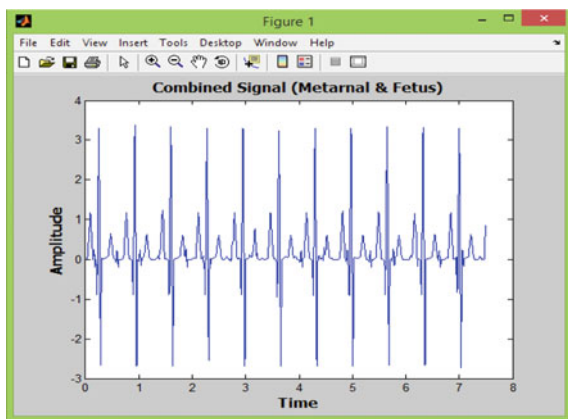


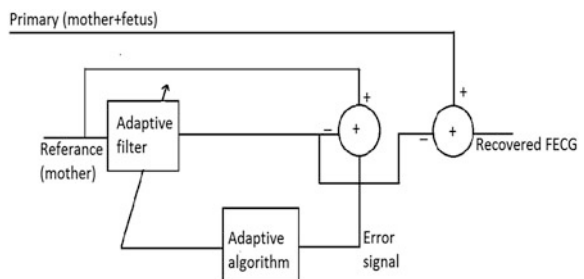
Fig. 1 **a** Reference FECG signal. **b** Reference maternal signal

Fig. 2 Combined signal

first step, we mix the maternal and fetal ECG signals to get composite signal. Maternal ECG signal will act as reference noise source. Figure 1a shows the FECG generated signal and similarly MECG signal is shown in Fig. 1b while composite abdominal signal is shown in Fig. 2, which is dominated by maternal heart beat propagates from chest cavity to the abdomen of the pregnant woman.

3 Data Analysis

The basic noise canceling situation is illustrated in Fig. 3 (on next page); a signal (d_n) is transmitted over a channel to a sensor that receives the signal plus uncorrelated noise (r_n). The combined signal forms the “primary input” to noise canceller. A second sensor receives noise which is uncorrelated with signal but correlated with noise contained in composite signal. This sensor provides “reference input” to the noise canceller, i.e., maternal signal. The noise is filtered to produce an output which is close replica of the noise contaminated in the composite signal. This output is subtracted from the primary input to produce system output.

Fig. 3 Adaptive noise canceling principle

The reference input is processed by an adaptive filter that automatically adjusts its own transfer function through our purposed algorithm that responds to an error signal in such a way that filter can operate under changing conditions and can readjust itself continuously to minimize the error signal. The transfer function of the adaptive filter depends upon the error signal and mu (μ) and reconstructs the maternal signal which is close replica of original maternal signal in less numbers of iterations. After a few basic processes, the filter (Base on LMS algorithm) was subjected to learning process as

$$n1 = (x1(i + (N - 1) : -1 : i))' \quad (8)$$

$$y(i) = n1' * w \quad (9)$$

$$e(\text{if}) = \text{mhb}(i) - y(i) \quad (10)$$

$$w = w + ((2 * \text{mu} * e(i)) * n1) \quad (11)$$

where two parameters ‘ w ’and ‘ $x1$ ’ are calculated as

$$w = \text{zeros}(N, 1) \quad (12)$$

$$x1 = [\text{zeros}(1, N - 1)x] \quad (13)$$

An additional parameter mu has been defined with a constant value as

$$\text{mu} = 0.0009$$

which is used for adaptation of filter while optimization of error results.

The main difference between the purposed algorithm and standard LMS is in calculation of error signal which is generated by subtracting the reconstructed maternal signal from the reference maternal signal. The recovered fetus signal is obtained by subtracting reconstructed maternal signal from the combined signal.

4 Simulation Results

The purposed algorithm has been implemented in MATLAB. It is clear from the fetus error signal that except very starting period, we recover the almost exact fetus signal. The reconstructed maternal signal, error in the recovered maternal signal, recovered fetal signal, and error in the recovered fetal signal are shown in Figs. 4, 5, 6 and 7 respectively. The parameter mu should be kept at the value of 0.0210 for the best results. This value is obtained by performing the experiment repeatedly. It should be noted that the comparison of the reconstructed signal and the reference signal has been done using MATLAB, and the error signal has also been generated using the same along with calculating the accuracy (Extent up to which the

Fig. 4 Reconstructed maternal signal

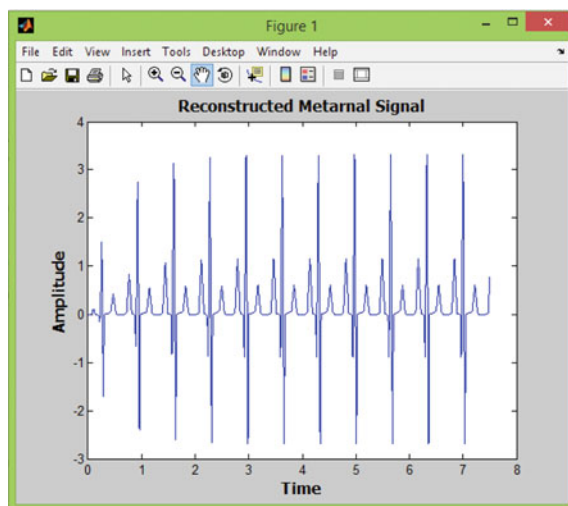
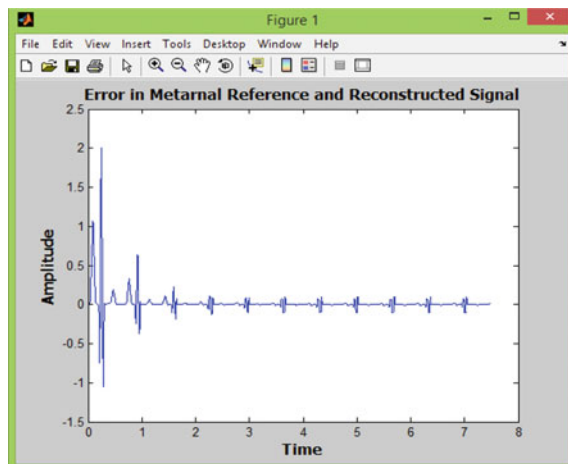


Fig. 5 Error in recovered maternal signal



reference and reconstructed signals are same, and error is approaching zero). Due to minimum error in the recovered signal, it is easy to correctly diagnosis for a pathologist which results saving of valuable lives (Figs. 8 and 9).

5 Challenges

The most significant challenge faced during the work was capturing the images obtained by the ECG machine. It is very typical task to locate the electrode at exact position; moreover, for obtaining the reference fetal signal, electrode should be

Fig. 6 Reconstructed fetal signal

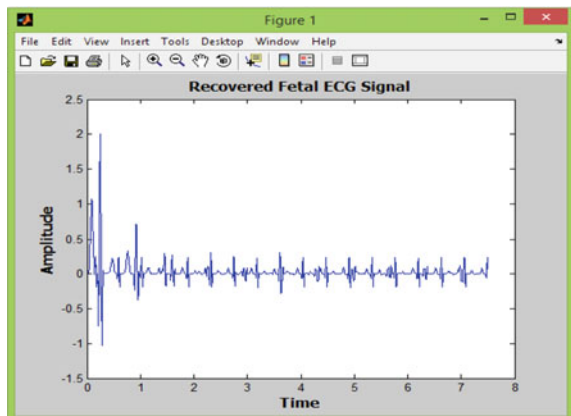


Fig. 7 Error in recovered fetal signal

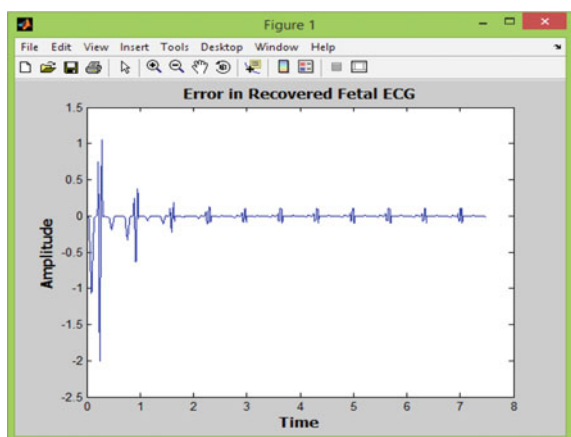
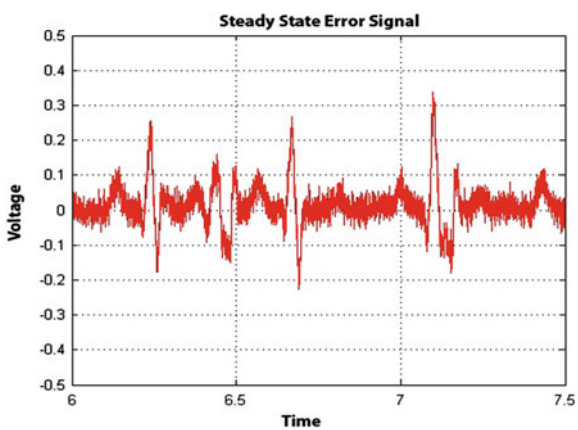


Fig. 8 Error signal by using standard LMS
(MATLAB-DSP toolbox demo)



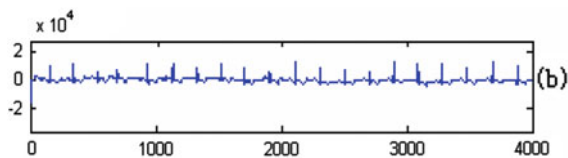


Fig. 9 Error signal using RLS algorithm (Extraction of fetal ECG-Yanjun Zeng et al.)

Table 1. Values of performance metrics

S. no.	Parameter of performance	Value of parameter
1	L2RAT	0.9991
2	MAXERR	0.2239
3	MSE	2.0883 e-04
4	PSNR	84.9329

touched with scalp of fetus which may lead to permanent rapture of membrane. It is also only possible in labor time so it is decided to generate the ECG signals in the MATLAB with parameters given in the literature (Table 1).

6 Conclusion and Future Work

In this paper, we have proposed and implemented a new algorithm to extract the FECG from the composite signal obtained from the abdominal electrode. At a glance, results show that

1. A simplified algorithm is developed and implemented.
2. Low-mean square error (MSE).
3. Higher peak signal to noise ratio (PSNR).
4. Better performance than standard LMS algorithm.

After verification of the result in different environment conditions, it should be implemented in real-time applications and can be tried as to make hybrid model with GA or PSO optimization techniques.

References

1. De Lathauwer, L., et al.: Fetal electrocardiogram extraction by blind source separation. *IEEE Trans. Biomed. Eng.* **47**(5), 567–572 (2000)
2. Van Bemmel, J.H.: Detection of weak electro-cardiograms by autocorrelation and cross correlation envelopes. *IEEE Trans. Biomed. Eng.* **15**, 17–23 (1968)

3. Callaerts, D., De Moor, B., Vandwalle, J., Sansen, W.: Comparison of SVD methods to extract the fetal ECG from coetaneous electrode signals. *Med. Biol. Eng. Comput.* **28**, 217–224 (1990)
4. Rizk, M.S., et al.: Virtues and Vices of Source Separation Using Linear Independent Component Analysis for Blind Source Separation of Nonlinearly Coupled and Synchronized Fetal and Mother ECGs. *IEEE EMBS*, USA (2001)
5. Akay, M., Mulder, E.: Examining fetal heart-rate variability using matching pursuits. *IEEE Eng. Med. Biol. Mag.* **15**(5), 64–67 (1996)
6. Zgallai, W.: Non-invasive fetal heartbeat detection using bispectral contour matching. In: International Conference on Electronics, Biomedical Engineering and its Application, pp. 7–8. Dubai (2012)
7. Agante, P.M., de Sá, J.P.M.: ECG noise filtering using wavelets with soft thresholding methods. In: Proceedings of the Computers in Cardiology'99, pp. 535–542 (1999)
8. Sameni, R.: Extraction of Fetal Cardiac Signals. PhD Thesis Sharif University of Technology, Tehran, Iran
9. Schreiber, T., Kaplan, D.: Signal separation by nonlinear projections, The fetal electrocardiogram. *Phys. Rev. E* **53**, R4326 (1996)
10. Zgallai, W., et al.: Third-order cumulant signature matching technique for non-invasive fetal heart beat identification. *IEEE ICASSP* **5**, 3781–3784. Germany (1997)
11. Widrow, B., et al.: Adaptive noise cancellation: principles and applications. *Proc. IEEE* **63** (12), 1692–1716 (1975)
12. Kholdi, E., et al.: A new GA-Based adaptive filter for fetal ECG extraction, Word academy of science engineering and technology **54**, 2011. In: Prasanth, K., et al. (ed.) *Fetal ECG Extraction Using Adaptive Filters*, vol. 2, issue 4 April (2013)
13. Larks, S.D.: Present status of fetal electrocardiography. *IEEE Trans. Bio-med. Electron.* **9**(3), 176–180 (1962)
14. Drumright, T.: *Adaptive Filtering*. Spring, USA (1998)
15. Zgallai, W.: Embedded volterra for prediction of electromyographic signals during labor. In: The 16th IEEE International Conference DSP, Greece (2009)

Improving Query Processing Performance Using Optimization Techniques for Object-Oriented DBMS

Sheetal Dhande and G.R. Bamnote

Abstract This work is based on strategies of query optimization of object-oriented database and subsequent techniques for implementing those strategies. First, an extension of direct navigation method optimization, this proposed methodology can handle multiple attributes of objects through direct navigation method and second is an extension of cache-based optimization for complex queries. Proposed algorithms work on complex queries which involved number of objects and attributes. The experimental result shows that proposed algorithms are capable of handling multiple attributes and gives more optimized result.

Keywords Query optimization • Object-oriented database management system (OODBMS) • ODMG

1 Introduction

Major research work in the field of query optimization concerns relational databases. Although methods developed for relational systems have possible for object DBMSs, here we present state of art of optimization for object database. Query processing is usually subdivided into sequence of consecutive steps and one of such sequence is as follows [1].

Representation: Standard query language defined the query is transformed into some inner form.

S. Dhande (✉)

Department of Computer Engineering, Sipna College of Engineering,
University of Amravati, Amravati, Maharashtra, India
e-mail: sheetaldhandedandge@gmail.com

G.R. Bamnote

Department of Computer Science and Engineering, PRMIT&R, SSGBAU,
Amravati, Maharashtra, India
e-mail: grbamnote@rediffmail.com

Standardization: Inner form of query gets transformed to some homogeneous, concrete form and that is many times considered as a starting point of query optimization. In relational database most used form is conjunctive normal form (CNF), in this selective predicate is conjunction of conditions, and disjunctive normal form (DNF), in which a selective predicate is diverse of conditions.

Simplification: Unnecessary, repetitive calculations are eliminated.

Amelioration: Sequence of operation (access plan) of query will change of resulting form of query only for most optimized plan in terms of cost of query and cheapest plan will be chosen for further execution. An approach to amelioration is cost-based optimization based on algebraic manipulations.

Execution: The query is evaluated according to the generated access plan. In modern architecture phases of query processing comprised parsing and validating and optimization [2].

Query Parser: Check whether a query is syntactically and semantically correct, and transform it into some inner form.

Query Optimization: The optimizer invoked with internal representation of query as input so that a query plan or execution plan may be devised for retrieving the information that is required. Optimizer should generate a set of plans rich enough to contain the optimal plan but small enough to keep the optimization effort acceptable.

2 Literature Survey

The intend of query optimization is to find the best query evaluation plan that reduces input/output operations, increases performance and network time and effort, total resource usage, a mixture of the above, or some other performance measure.

Query optimization in Stack-Based Query Language (SBQL) Subieta [2] and his team have worked on mostly query optimization methodologies in object-oriented database through the project like ODRA. They have worked on Stack-Based Approach (SBA) for object-oriented database, as a formal methodology of building object query languages, which is exceptionally well prepared for query optimization.

Pieciukiewicz et al. [3] have worked on recursive query giving out for optimal result processing of query in SBQL.

Bleja and Subieta [4] have developed (and implemented) the methods based on rewriting parting out self-determining subqueries, rules based on the distributivity property, removing dead associate queries, query modification for processing stateless functions and views, by their work in, “Query Optimization by Rewriting Compound Weakly Dependent Subqueries”.

Kozankiewicz et al. [5] also worked on Distributed Query Optimization in the Stack-Based Approach.

Cybula and Subieta [6, 7] have developed methods based on query caching—storing results of queries in order to reclaim them by their work, ‘Query Optimization through Cached Queries for Object-Oriented Query Language SBQL’ and ‘Query Optimization by Result caching in the Stack-Based Approach’.

Plodezien and Subieta [8] also have been worked on Optimization methods in object Query Language. They gave concept of direct navigation through offset address of object.

Dhande and Bamnote [9–11] have been working on cache query management, indexing on object-oriented queries and direct navigation method for optimized the Object-oriented database management system (OODBMS) queries. Our major work is based on these three methods of optimization,

First, the proposed scheme extends the existing direct navigation through offset address for multiple attributes. Second, we extend [10] the cache-based query optimization for identifying various building blocks of cached results useful for retrieving and answering other queries and combining many cached queries while producing a result of one extensive query (Figs. 1, 2 and 3).

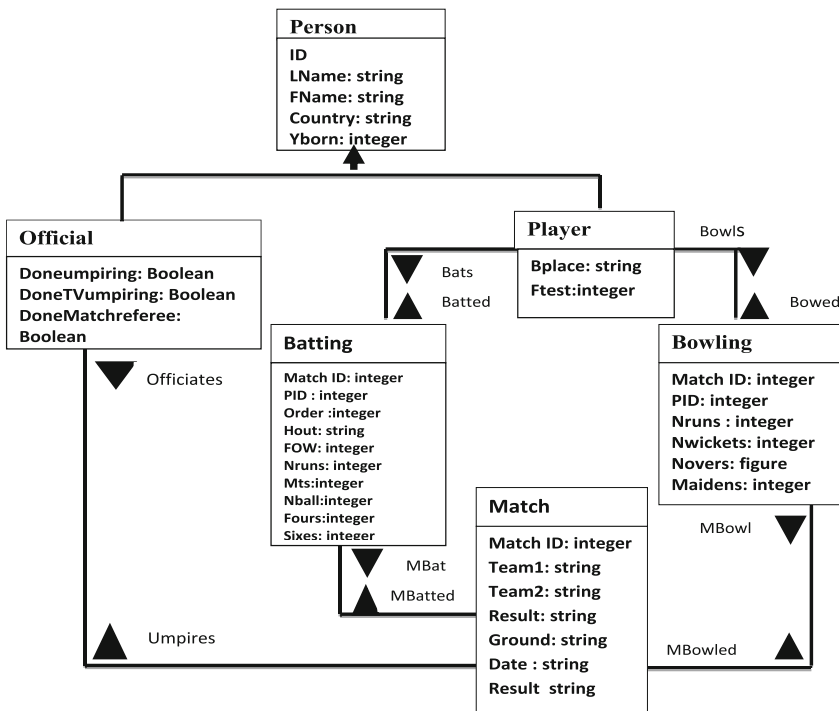


Fig. 1 Class diagram for Cricket database, used to test different strategies of optimization

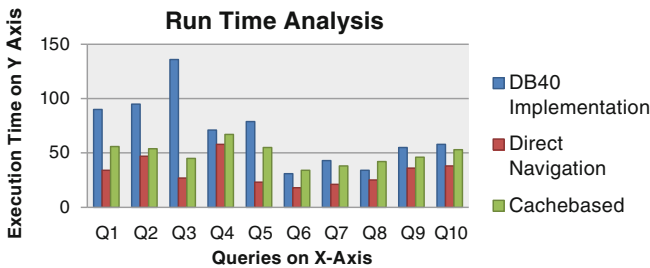


Fig. 2 This histogram shows runtime analysis of queries (Q1, Q2, Q3, Q4, Q5, Q6, Q7, Q8, Q9, Q10) for DB40 and our approach of direct navigation, cache-based implementation

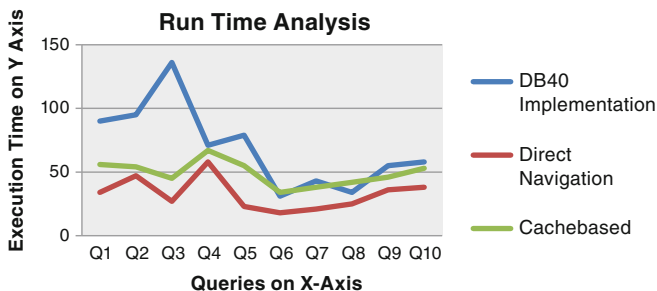


Fig. 3 This graph shows runtime analysis of queries (Q1, Q2, Q3, Q4, Q5, Q6, Q7, Q8, Q9, Q10) for DB40 and our approach of direct navigation, cache-based implementation

3 Query Optimization Through Direct Navigation for Multiple Attributes

The method extends to cover more general cases such as handling several attributes by adding more columns in result set stack. Here we proposed method of direct navigation for multiple attribute (each of those columns would contain the identifiers of different entities) by which direct navigation on many diverse object attributes is possible.

For example, The Query

“Retrieve the number of runs that Ponting has scored in the matches.”

OQL form:

```

Select B.NRuns
From Players p, Batting b
Where P.id= B.id and P.Lname = "pointing"

```

SBQL FORM: Batting . NRuns ,

Can be rewritten in the form

```
Batting dnav (offset_of_NRuns)
```

And the query

```
(NRuns where Player.Lname= " ponting").batted .players.id
.bats.batting.id
```

To the form of

```
(((( NRuns where P.Lname= " ponting") ( dnav ( offset-
of_batted) (dnav(offset_of_id)).Player
dnav(offset_of_bats)).batting (dnav(offset_of_id)) )
```

where the offset_of_batted, offset_of_id (player id), offset_of_bats, offset_of_id (batting id) are the offsets of appropriate attribute in objects Person, Batting, Player, respectively.

Code has created multiple columns/iterators to save id of identifier, which handles the conditions in where clause; here we are implemented for two conditions player name and playerid, respectively.

The main advantage of this methodology is that it is useful for answering complex queries. This methodology is implemented using direct navigation and the experimental results are discussed in the next section.

4 Cached-Based Query Optimization

Dhande [11, 12] extends method to cover more general cases, when the semantically equivalent query (written in the same or a different way) is submitted by the same or other user, after parsing, type checking, and normalization of the query, optimizer sends the query to the server side query cache manager. Query cache manager searches for the query in the query cache registry and if found there will return the unique identification number (UIN) of the corresponding result to the client, thus avoiding the recompilation of previously stored result. Using this UIN, query interpreter (on the client system) can fetch the stored result of the query directly from the server. If the query is not found in query cache registry, query cache manager will send a message to an optimizer (on the client side database system) signifying that a query is not cached and hence its result needs to be calculated. Optimizer then does not rewrite the query.

For example “Find maximum score of Dhoni and MatchId of all matches in database in which Dhoni batted”.

```
Batting where PID IN( (player where Lname= "Dhoni").playerID).matchID,Max( Nruns)
```

In this query, we find subquery.

```
Qsub1: ( player where Lname= "Dhoni").playerID group as P  
and  
Qsub2: max( Bats.Batting.Nruns) group as q
```

And transform whole query to following form.

```
( ( ( player where Lname= "Dhoni").playerID) group as P  
) .((Batting where PID IN .P ). matched , batted.player.q  
)
```

We decompose query by identifying subqueries, if subquery is matched and proposed as cached query uniquely identified by its reference id (reference id, which we created to identify cache result stored in cache to identify query).

```
Batting where PID IN  
($cache(reference_id#1).matchID, (batted  
player($cache(reference_id#2))  
public static final Comparator<Player> LnameComparator =  
new Comparator<Player>() {  
    @Override  
    public int compare(Player o1, Player o2) {  
        return o1.lname.compareTo(o2.lname); } };
```

5 Experimental Results

Research study has been done with SBA to object query and programming language. Syntax and semantics of SBQL have perceived, thus it allows precise reasoning concerning aspect of query optimization method.

The proposed method is implemented by coding the algorithm in SBQL4 J. This is an extension to java language based on stack-based architecture. It provides capabilities similar to Microsoft LINQ for Java language. It also allows processing

Java objects with queries. It is hundred percent compatible with current Java Virtual Machines, and can be safely used in any Java project (compatible with Java 6) [13, 14].

Sample queries used for result assessment are the following; first five are complex queries, consideration for complex queries is based on clauses and contains many conditions.

- Q1: Retrieve the number of runs that Ponting has scored in the matches.
- Q2: Find matchIds of all Matches in the database in which Tendulkar batted.
- Q3: Find all ground names where the umpire Buckner has officiated.
- Q4: Find Player whose name start with ‘sin’.
- Q5: Find the Maximum Score of Tendulkar.
- Q6: Print all the objects *Player*.
- Q7: Find all the information about objects *Players* from India.
- Q8: Find details of all matches played in Australia.
- Q9: Enlist collective information about Indian *Player* born after 1980?
- Q10: List *Matches* played in which India or Australia was *Team1*.

The experimental results Figs 2, 3 show that the proposed method provides good result through direct navigation in case of complex queries. The Execution time is less as compared to standard object-oriented database. To make comparison we use here as standard DB40, an open source object Database

The experimental results show that our approach provides more optimized result for same queries.

Table 1 shows the execution time required for sample queries in DB40 (An open source object database management system). Execution time required sample queries without optimization technique through execution of SBSQL and Execution

Table 1 Execution time required sample queries in Java plug-in, opensource object database DB40, and three proposed approaches, i.e. Direct navigation, cached-based approach, and index-based approach

Query	Sample size	Execution time by standard ODBMS DB40 (in ms)	Execution time by SBSQL for Java (in ms)	Execution time by our approach, direct navigation (in ms)	Execution time by our approach, cache-based optimization (in ms)
Q1	400	90	2655	34	56
Q2	400	95	2962	47	54
Q3	400	136	2988	27	45
Q4	400	71	2772	58	67
Q5	400	79	2069	23	55
Q6	400	31	1099	18	34
Q7	400	43	1594	21	38
Q8	400	34	1569	25	42
Q9	400	55	1764	36	46
Q10	400	58	1866	38	53

time required sample queries proposed approach i.e., direct navigation, Cache based, and proves that the proposed scheme can produce more optimal result in terms of execution time.

6 Conclusion

The main aim of this work was to analyze traditional and new methods for improving performance of query processing in object DBMS. The novelty of this approach is that it makes use of universal object data model (i.e SBA). The proposed technique extends direct navigation method for multiple attributes, an extension of cache based optimization. The proposed methods are based on SBQL syntactical definition. Algorithms suggested for proposed technique are implemented using Java and SBQL4J plug-in for java.

Static analysis is effective tool of static query optimization, which enables to gather all information that determines whether a given transformation can be applied on a query. Optimization methods can be applied by rewriting, like direct navigation and indexing. The main objective of this research work is to study, investigate and suggest query optimization methods to Object Database. It can be concluded that using the proposed techniques for query optimization, will open new vistas for the further research in query optimization and will improve performance of object databases.

Experimental results also shows that same queries require more time for executing in SBQL plug-in for java (Table 1). We are looking forward in order to discover reason for same, and working continuously in the same directions.

7 Future Scope

We are working on many optimization methods for improvement of query execution time; here in this paper we have put forward the findings about two optimization methods, Direct navigation and cache-based method; we are working on index based as well as for analysing performance of complex and simple queries. Experimental result can be further extended in caching for distributed environment and data repository and ETL systems as well.

References

1. Jarke, M., Koch, J.: Query optimization in database systems. ACM Comput. Surveys **16**(2), 111–152 (1984)
2. http://www.ipipan.waw.pl/~subieta/SBA_SBQL/overview/#t

3. Pieciukiewicz, T., Stencel, K., Subieta, K.: Recursive query processing in SBQL. *J. Comput. Sci. Polish Ac Sci.* Ed. Elsevier Sci. Publishers, North-Holland, pp. 391–407. ISSN:0138-0648
4. Stencel, B.M.: Optimization of object-oriented queries addressing large and small collections. *IMCSIT 09* ISBN:978-1-4244-5314-6 (2009)
5. Kozañkiewicz, H., Stencel, K., Subieta, K.: Distributed query optimization in the stack-based approach. In: Springer Journal LNCS, **3726**, 904–909. Springer, Berlin (2005)
6. Cybula, P., Subieta, K.: Query optimization through cached queries for object-oriented query language SBQL. *Springer J. Lecture Notes Comput. Sci.* **5901**, 308–320. ISBN:978-3-642-11265-2
7. Cybula, P., Subieta, K.: Decomposition of SBQL queries for optimal result caching, pp. 841–848. *FCCSIS* (2011). ISBN:978-83-60810-22-4
8. Plodezien, J., Subieta, K.: Optimization methods in object query languages
9. Dhande, S.S., Bamnote, G.R.: Query optimization of OODBMS: semantic matching of cached queries using normalization. *ERCICA-2013*, Elsevier Publication DBLP, ISBN:978-93-5107-102-0, Aug 2013
10. Dhande, S.S., Bamnote, G.R.: Query optimization in OODBMS: identifying subquery for complex query management. In: Second International Conference of Database and Data Mining (DBDM 2014) organised by Academy & Industry Research Collaboration Center (AIRCC), Dubai
11. Dhande, S.S., Bamnote, G.R.: Query optimization in object oriented DBMS: direct navigation. In: *ICCUBEIA 2015: First IEEE International Conference on Computing, Communication, Control and Automation*, IEEE Pune section, 26 Feb 2015
12. Dhande, S.S., Bamnote, G.R.: Query-optimization-in-odbms-identifying-subquery-for-complex-query-management. *Int. J. Database Manage. Syst. (IJDMS)* **6**(2) (2014)
13. Satish1, L., Halawani, S.: A fusion algorithm for joins based on collections in odra-object database for rapid application development. *IJCSI Int. J. Comput. Sci.* **8**(4), 2 (2011). ISSN (Online):1694–0814
14. Dhande, S.S., Bamnote, G.R.: Query optimization in object oriented database management system. *IRISS 2015: 9th Inter-Research-Institute Seminar in Computer Science*, ACM India Feb 5, 2015, Goa, Annual event 2015

Linear and Non-linear Buckling Testing on Aluminium Structures

Snigdha Sharma, Shilpi Ghosh, Ankesh Yadav and Shabana Urooj

Abstract In this paper, cylindrical aluminium structures are tested for examination of buckling phenomenon. Testing of the material structures are accomplished by comparison made on the basis of linearity and non-linearity. The computation of various parameters viz. displacement, external work done, energy loss, and total energy consumed are being performed to evaluate the performance and optimal operating conditions of the aluminium structure. The results are visualized with ABAQUS CAE software. It is observed that non-linear buckling is found superior in terms of structural deformations and energy loss as compared to linear buckling. This non-linear buckling has proved to be an eminent technique to reduce the adverse effects of the buckling phenomenon prominent in aluminium structures.

Keywords ABAQUS software · Linear · Non-linear · Buckling · Stress · Deformations

1 Introduction

Buckling phenomenon is a technique that helps determine the critical loading at the stage when the structure becomes unstable. Any structure when subjected to a large compressive stress leads to the condition of sudden failure. This sudden failure

S. Sharma (✉) · S. Ghosh · A. Yadav · S. Urooj
Department of Electrical Engineering, Gautam Buddha University,
Greater Noida 201308, U.P, India
e-mail: sharma.snigdha93@gmail.com

S. Ghosh
e-mail: ghosh.shilpi1991@gmail.com

A. Yadav
e-mail: ankeshyadav.92@gmail.com

S. Urooj
e-mail: shabanabilal@gmail.com

corresponds to the term buckling. Buckling is a form of mathematical instability that leads to structural failure due to the impact of loading. Mathematical analysis of buckling makes use of the axial load which is concentrated at the centroid of the structure. It depicts that the ultimate compressive stress at the point of failure is much larger than the actual compressive stress that the material is able to withstand. When the applied load on the structure increases to a large extent, it reaches a stage when it becomes large enough leading to a state of instability. At this point of instability, the material structure is said to have buckled. On further application of load, buckling of the structure continues if recovery of the structure is possible else it leads to the stage of complete deformation of the structure. This buckled load is uniformly distributed all over the structure.

Buckling analysis can be categorized into two categories: Linear buckling analysis and Non-linear buckling analysis. Aluminium material is chosen as the most appropriate material for testing because of its certain advantages over the other materials. These advantages include excellent thermal and electrical conductivity, good formability, high resistant to corrosion, light weight, good reflector of visible light as well as heat, high ductility, low melting point and density, great impermeability, odourless and high recyclability [1].

A decade ago, engineers recognized Finite Element Analysis (FEA) as a valuable design tool. Then it stopped being regarded only as an analyst's tool and entered the practical world of design engineering. However, until recently, most FEA applications undertaken by the design engineers were limited to the linear analysis [2]. Linear buckling is also known as Eigen value buckling. This analysis predicts the theoretical buckling strength of an ideal elastic structure [3]. The imperfections and non-linearities in the structures prevent most real-world structures from achieving their theoretical elastic buckling strength [4]. Thus, linear buckling analysis often yields quick but non-conservative results [5]. In linear buckling of the structure, the loads are applied uniformly across the whole structure. Linear buckling analysis is generally used to calculate the critical buckling loads of ideal structures. Its response usually involves very high level of deformations prior to the process of buckling in various structures. Historically, engineers were reluctant to use non-linear analysis, because of its complex problem formulation and long solution time [2]. Presently, non-linear FEA software interfaces have become much easier to use [2]. In addition, improved solution algorithms have shortened solution times.

Non-linear buckling analysis is a process used to analyse large extent of deformations in the structures. These deformations are extended to the level at which the structure reaches its minimum or maximum load. Non-linear buckling analysis can be performed with the help of Ryck's algorithm. This analysis helps investigate the post-buckling behaviour of the structure. The yield transforms the unstable post-buckling behaviour into stable behaviour. Unlike in non-linear buckling phenomenon, the increase in the deformation causes a decrease in the corresponding load across the structure. This linear and non-linear buckling analysis of axially compressed shells under impulsive loads helps understand the dynamic buckling mechanism, to work out the influence of important parameters, to

get data for the definition of test shells and to provide the experimental verification [6]. The software executes the detailed analysis of the correlation between structure and mechanical properties of the constituent materials in order to visualize the pre-determined set of properties [7]. This research is highly valuable for the scholars who are performing research on the conditions that may lead to the stage of buckling in different material structures. To make experiment results faster and precise software computation technique is used, thus making analysis of material structures easy [7]. This computational analysis through the software proves to be a better alternative as compared to the hard computing. ABAQUS-CAE supports familiar interactive computer-aided engineering concepts such as feature-based, parametric modelling, interactive and scripted operation and GUI customization [8]. It computes the effects on the structure of a material that relates the visualization of deformities in arrangement of its internal components [9, 10]. In present work, linear as well as non-linear buckling analysis of an aluminium cylindrical shell is performed by Finite Element Analysis method using ABAQUS-CAE 6.10 software. The comparison has been made across linear and non-linear buckling analysis based upon different parameters such as displacement, energy loss, external work done and total energy consumed. The post-buckling adverse effects on the structure of the cylindrical shell are being visualized.

2 Methodology

Aluminium material was used to construct the cylindrical shell for analysing linear as well as non-linear buckling due to its various advantages as discussed above. The chemical composition of the material Al 1100 used to make the cylinder includes 99.8 % Aluminium and 0.2 % Copper. The mechanical properties defined for the cylindrical shell include 70 GPa Modulus of Elasticity and 0.3 Poisson's Ratio.

The cylindrical shell structure when subjected to high level of load leads to buckling after a certain extent. The detailed analysis of the aluminium structure has been performed involving linear as well as non-linear buckling. Further, comparison between the linear and non-linear buckling of the cylinder has been performed. The steps followed during the buckling analysis of the cylindrical structure. First, a three-dimensional aluminium cylindrical shell structure has been created using the software. Depth of the cylinder was defined as 0.5 m. Second, the centroids of the upper and the lower section of the cylinder were selected as the two reference points, respectively. Then the constraints were applied on all the nodes of the upper and lower most section of the cylinder. After applying the constraints, immediately, load was applied on the centroid of the upper most section of the cylinder along the z axis and consequently the lower most section was kept fixed. The movement of the lower most section was restricted in all directions while that of the upper most section was allowed only along the z axis so that the cylinder could deform only

along the z axis due to the applied load. All the boundary conditions to the aluminium structure are defined and simulation is done; the extents of structural deformations are clearly observed with the software.

3 Results and Discussion

The simulation results help make a comparative study between the linear and non-linear buckling of the cylindrical structure. The extent of deformation during the linear buckling of the structure is found much higher than compared to the non-linear buckling. The values evaluated during analysis depict the extent of distortion in the structure. The extent of distortion is visualized in different modes which makes the analysis quite easy.

3.1 Linear Buckling Results

Figure 1 represents the linear buckling of the cylindrical structure due to the applied load at mode 1. It shows the deformation along the z axis due to the applied boundary condition. Uniform distortion of the entire structure including all the nodes and element is visualized. Figure 2 depicts the structural distortion at mode 2. It shows that the whole structure is unevenly distorted when the loading increases. The blue region represents the minimum stress level and it goes on increasing depicted by different ranges of colours and the maximum stress is represented by red colour. Figure 3 shows the structural deformation at mode 3. It shows an increment in the red region depicting an increase in the stress level. Thus, the stress

Fig. 1 Distortion in linear buckling at mode 1

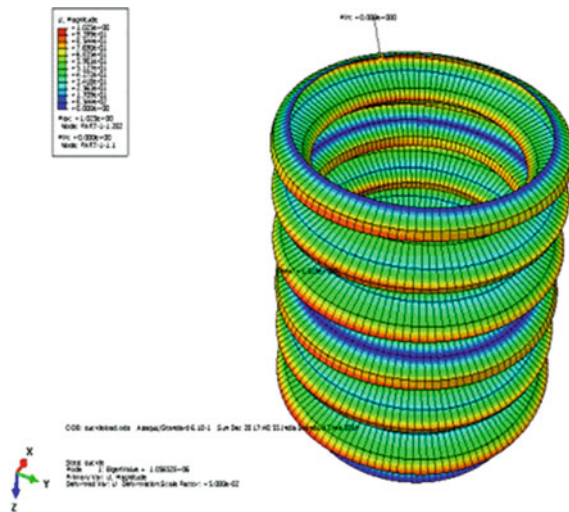


Fig. 2 Distortion in linear buckling at mode 2

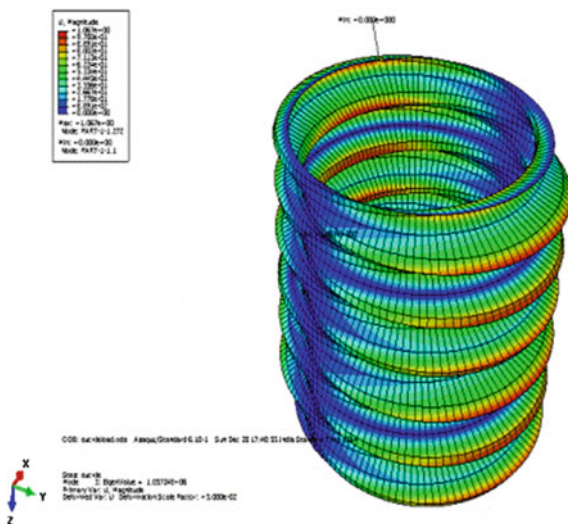
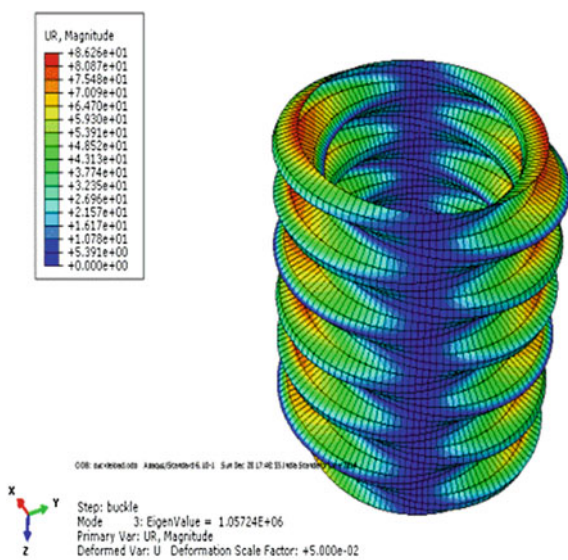


Fig. 3 Distortion due to linear buckling at mode 3



level further increases with the load. Figure 4 depicts the structural distortion at mode 4. At this mode, red region is much larger than the previous modes. It signifies much higher level of stress in this mode. Figure 5 depicts the extended structural distortion at mode 5. It shows a large amount of extension in the deformation level in the structure due to the increase in load. This is this the last mode at which the deformation is maximum.

Fig. 4 Distortion due to linear buckling at mode 4

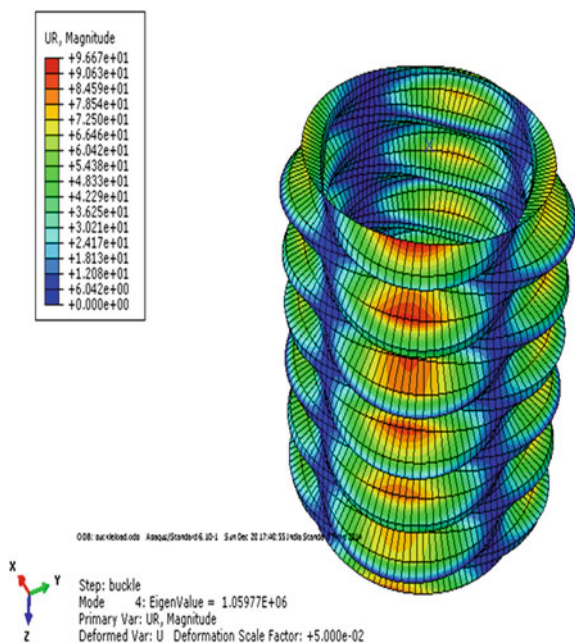


Fig. 5 Distortion due to linear buckling at mode 5

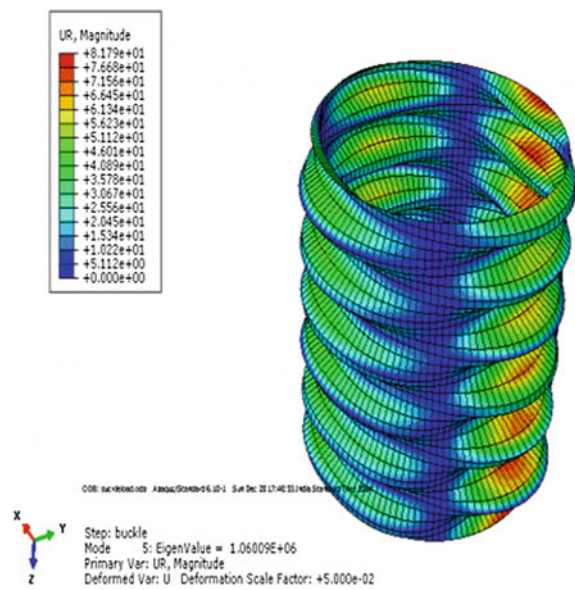
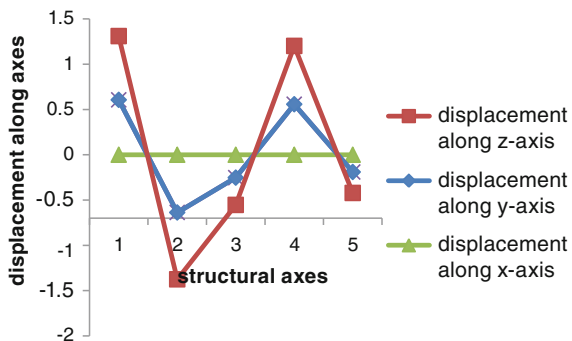


Figure 6 shows the variation of the cylinder displacement across the x , y and z axes with respect to a constant mode. It is clearly notified from Fig. 6 that the displacement across z axis is maximum followed by y axis where the displacement

Fig. 6 Displacement across the x , y and z axis of cylinder

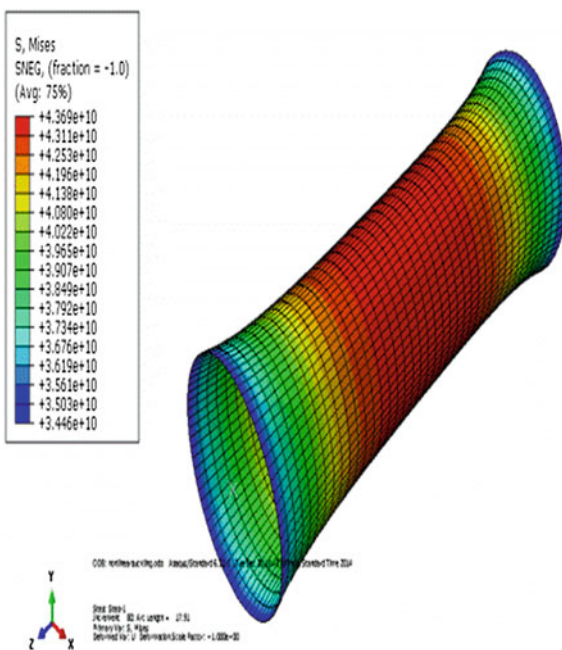


has reduced up to a certain extent preceded by displacement across x axis which is minimum up to the zero value. Thus, the simulated result depicting the displacement across various axes is in accordance with the applied boundary condition across the structure.

3.2 Non-linear Buckling Results

Figure 7 represents the non-linear buckling of the cylindrical structure due to the applied load. It shows an elongation in the structure due to the applied load. The red

Fig. 7 Structural elongation in non-linear buckling



region depicts the maximum stress in the middle region and blue region depicts the minimum stress level at the structural ends. In non-linear buckling, the structure does not get deformed into another shape and is limited to structural elongation only. Figure 8 represents the extent up to which the structure gets elongated. It shows that the elongation takes place in both the ends of the cylinder. The arrows depict the direction of elongation. Figure 9 shows the direction of stress acting along different axis. The blue-, yellow- and red-coloured arrows depict the direction of the stress acting along x , y and z axis, respectively. It helps in evaluation of stress at different nodes along x , y and z axis. Figure 10 shows the structural deformation in the cylinder due to non-linear buckling. It depicts a slight constriction in the middle section of the cylinder. This denotes deformation at a very small level. The red region depicts higher stress value due to deformation in the middle section.

Figure 11 represents the variation of the external work done by the cylinder with respect to arc length. It signifies that the work done is constant with the initial arc length and then starts increasing proportionally with the arc length. Figure 12 shows the energy lost along the arc length of the cylinder. The energy lost is zero which makes the cylinder efficient. Thus, it signifies that the cylindrical system is highly efficient as it restricts wastage of energy. Figure 13 shows the variation of the total energy with respect to arc length of the cylinder. It signifies that as the arc length increases, the energy consumed also increases. Figure 14 represents the variation of the total energy with respect to the load proportionality factor. It signifies that for the initial load, the energy is constant to a maximum magnitude and then consequently, it decreases with the increasing load.

Fig. 8 Structural elongation in non-linear buckling

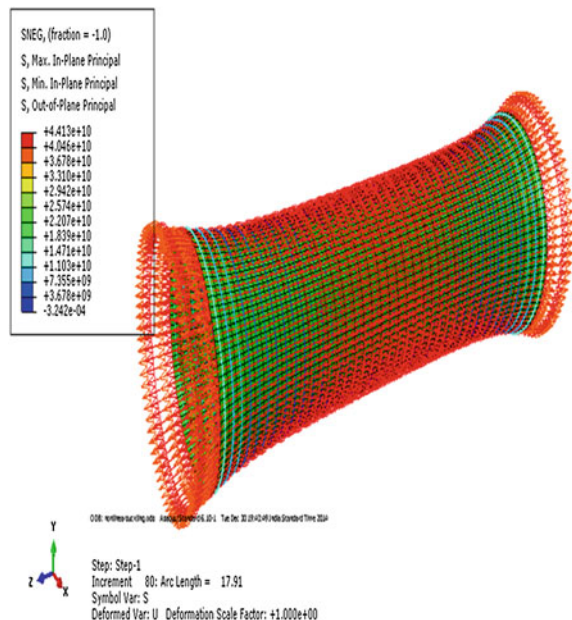


Fig. 9 Stress direction in non-linear buckling

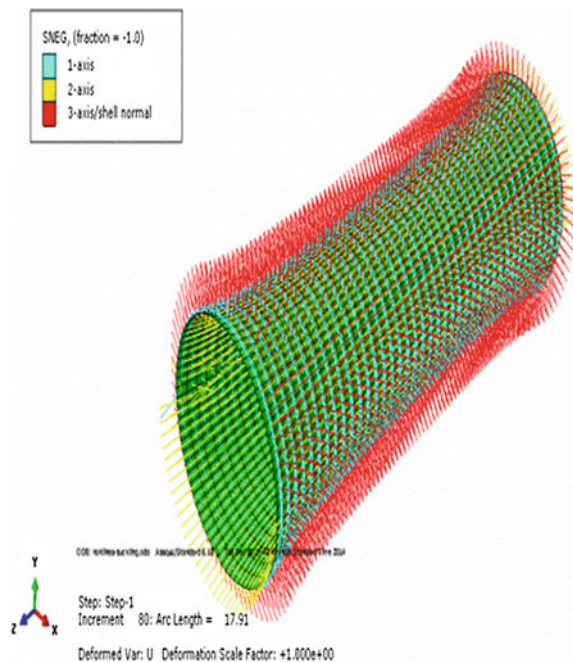


Fig. 10 Structural deformation in non-linear buckling

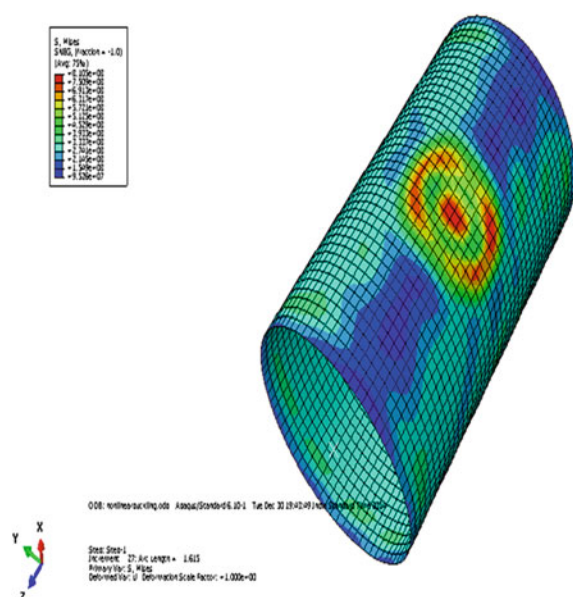


Fig. 11 External work versus arc length of the cylinder

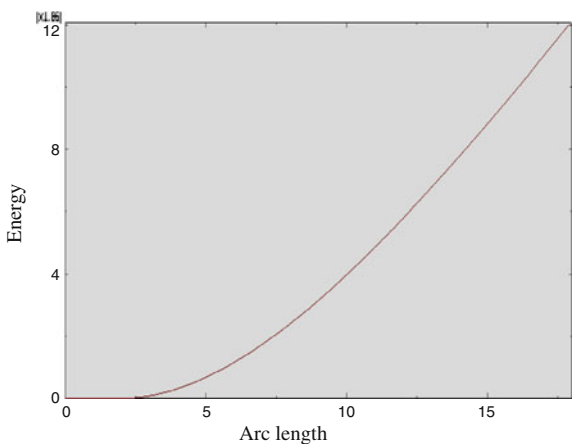


Fig. 12 Energy lost versus arc length of the cylinder

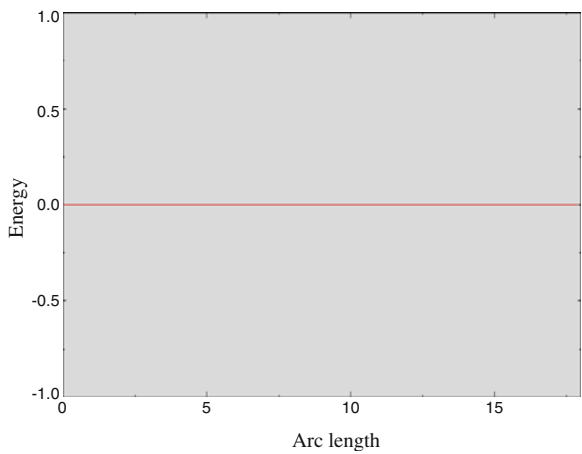


Fig. 13 Total energy versus arc length of the cylinder

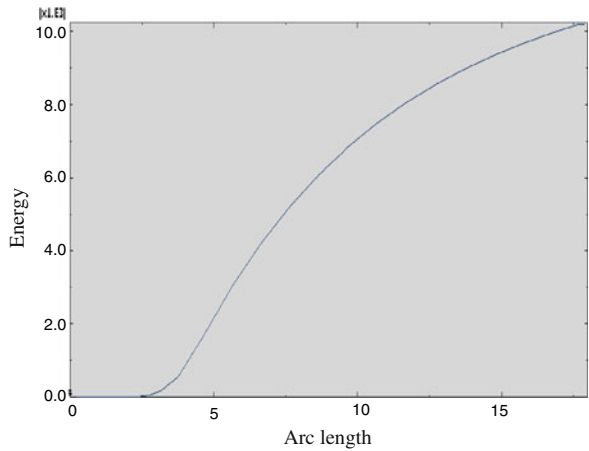
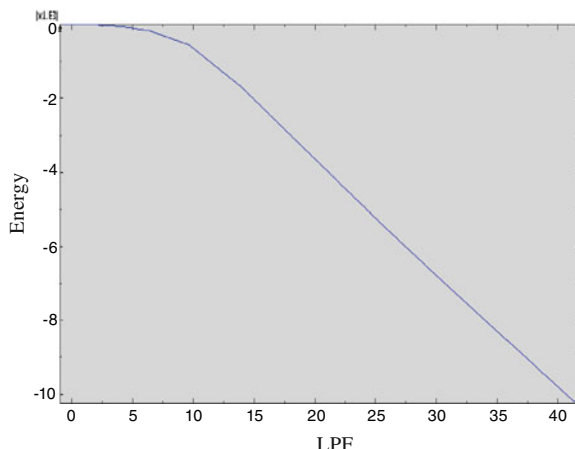


Fig. 14 Total energy versus LPF of the cylinder



4 Conclusion

It is noteworthy that the non-linear buckling of the structures is much more efficient than compared to linear buckling. From the computed results, it can be concluded that the non-linear buckling of any structure due to the uniformly applied load and binary condition produces stress and structural deformation up to very small extent. Linear buckling analysis demonstrates great extent of deformation leading to a highly distorted structure. Therefore, non-linear buckling must be preferred over linear buckling as it provides a cost-effective simulation method, prevents wastage of material during testing and reduces structural distortion up to a large extent. This makes it more applicable in various areas related to material science engineering. This research will enable the future researchers to employ non-linear buckling phenomenon while exploring different material structures under the effect of loading and adverse boundary conditions. This will save a large amount of time and money of the future material science research scholars.

References

1. William, D., Callister, J.: Materials Science and Engineering, 7th edn. Wiley India Pvt. Limited (2010)
2. Report: Understanding Non-linear Analysis, Dassault Solidworks, NPTL, pp. 1–16 (2008)
3. Report: Buckling Analysis, FEMI LABS, vol. 2, pp. 1–6
4. Novoselac, S., Ergic, T., Balicevic, P.: Linear and nonlinear buckling and post buckling analysis of a bar with the influence of imperfection. Tech. Gaz. **19**(3), 695–701 (2012)
5. Motamed, M., Moosavi Madhhadi, M.: Rubber/carbon nanotube nanocomposite with hyperelastic matrix. J. Solid Mach. **2**(1), 43–49 (2010)
6. Degenhardt, R., Klein, H., Kling, A., Temman, H., Zimmermann, R.: Buckling and Post Buckling Analysis of Shells Under Quasi-Static and Dynamic Loads

7. Urooj, S., Yadav, A., Singh, M., Singh, M., Dohare, R., Ghosh, S., Sharma, S.: Computation & analysis of aluminium and steel by using ABAQUS software for engineering applications. In: International Conference on Innovative Applications of Computational Intelligence on Power, Energy and Controls with their Impact on Humanity, pp. 103–108 (2014)
8. Kvocak, V., Tomko, M., Kozlejova, V.: Modelling of encased steel beams in abaqus program. In: IEEE 17th International Conference on Intelligent Engineering Systems (INES), pp. 255–259, 19–21 June (2013)
9. Urooj, S., Sharma, S., Ghosh, S., Singh, M., Yadav, A.: Computation of Vibration of Aluminium Based Structure for Power System Application, India, December 2014
10. Han, J., Li, Z., Song, J.: The application of finite element analysis software (ABAQUS) in structural analysis. In: International Conference on Computational and Information Sciences (ICCIS), Chendu, pp. 68–71, 17–19 Dec 2010

A Performance Analysis of OpenStack Open-Source Solution for IaaS Cloud Computing

**Vo Nhan Van, Le Minh Chi, Nguyen Quoc Long,
Gia Nhu Nguyen and Dac-Nhuong Le**

Abstract Cloud computing is a great design of technology ever made which provides services, applications, and resources through a network. Cloud computing gives the opportunity to use a very large amount of resources on demand. There are many cloud infrastructures as a service (IaaS) frameworks that exist for users, developers, and administrators and they have to make a decision about which environment is best suited for them. In this paper, we focus to analyze and evaluate the performance of the open-source OpenStack for IaaS cloud computing, and give the comparison between OpenStack and VMware. We outline some of our initial findings by providing such a testbed on OpenStack. The experimental results showed the advantages of OpenStack solution in cloud computing where infrastructure is provided as a service.

Keywords Open-source · Cloud computing · OpenStack · IaaS

V.N. Van · N.Q. Long · G.N. Nguyen
Duytan University, DaNang, Vietnam
e-mail: vovannhan@duytan.edu.vn

N.Q. Long
e-mail: nguyenquoclong@duytan.edu.vn

G.N. Nguyen
e-mail: nguyengianhu@duytan.edu.vn

L.M. Chi
Danang ICT Infrastructure Development Center, DaNang, Vietnam
e-mail: chilm@danang.gov.vn

D.-N. Le (✉)
Faculty of Information Technology, Haiphong University, Haiphong, Vietnam
e-mail: Nhuongld@hus.edu.vn

1 Introduction

Cloud Computing is an important topic in information technology in recent years. It can be outlined as dynamically expandable shared resources accessed over a network. The prime feature of cloud computing is that a user needs to pay for what he uses. The shared resources are storage, computing, services, etc. Based on the supported style of resources provided, cloud design can be divided into three kinds of delivery models: *infrastructure as a service* (IaaS), *platform as a service* (PaaS), *software as a service* (SaaS) [1, 2].

The main goal of IaaS computing model is to deliver high performance computing power that satisfies the requests from the user. Virtualization is a technique that could be used to improve computing power. Although cloud computing was the interested topic, cloud computing deployment still has many problems to consider and need to be solved. Beside traditional risks such as security, storage problems, stability, and data loss, the cost for cloud deployment is one of the important problems to any company who has to balance between invested cost and benefits. This means that the choice of solution to deploy a Cloud system is very important commercial cloud or open-source cloud [3]. The growth of Open-source Cloud computing is shown in Table 1.

1.1 Benefits from Open-source Cloud Deployment

The benefits from cloud computing can be referenced from many documents, for example from, Canonical [4] or CSA [5]. This part of article focuses on the benefits of open-source cloud deployment when compared with other commercial clouds. According to Canonical, a big company contributed in lots of famous open-source projects such as Ubuntu platform, OpenStack, and Ubuntu One; main features of open-source cloud deployment are:

Table 1 Open-source cloud computing timeline

Name	Year	Description	Deployment
Eucalyptus	Early 2008	AWS API-compatible platform	Eucalyptus
OpenNebula	Early 2008	RESERVOIR European Commission funded project	Private and hybrid clouds and for the federation of clouds
CloudStack	May-10	Began at cloud.com	Public, private hybrid cloud services
OpenStack	2010	By Rackspace and NASA	Public and private cloud platform

- *Avoiding vendor lock-in:* commercial products usually are total solutions which have manufacture standards such as APIs, image format, and special storage. These features make the cloud not to be highly integrated with other system and make the current IT infrastructure of company may not be reused.
- *Community support:* open-source cloud computing projects are always supported by community all over the world with thousands of programmers, coders in cloud function development and bug fix. This advantage can not be found in any commercial companies or products.
- *Scalability and licensing:* cost is a big problem in scaling cloud system with commercial solution. Licensing cost is calculated based on number of servers, CPUs, or VMs. But in open-source cloud, all of them are free and the problem of license for scaling system is solved.
- *Modules development:* when customer needs a new function in commercial solution, the best way is a new upgrade from vendor. However, with open-source solution, customer can develop the function by themselves, and that function will be better for company's business/purposes.

1.2 IaaS Framework Overview

In the first part of this section, we present the overview of the existing works on IaaS model and open-source cloud deployment; this section introduces some IaaS Frameworks such as, Eucalyptus, Nimbus, OpenNebula, OpenStack, Apache Cloud Stack, and IBM Smart Cloud.

Eucalyptus [6] is a private cloud solution and one of the appropriate choices to build on-premise cloud in company and organization. Eucalyptus supports all the existing IT infrastructures such as types of server, network devices, and no need of a specialized hardware. One of the advantages of Eucalyptus is compatible with Amazon EC2 and Amazon S3. It has five high-level components: Cloud Controller, Cluster Controller, Storage Controller, Elastic Block Storage, and Node Controller.

Nimbus [7] is a solution focused on IaaS from a computer cluster. The nimbus toolkit consists of the following components: workspace service, workspace resource manager, workspace pilot, workspace control tools, IaaS Gateway, Context broker, Workspace client, cloud client, and Nimbus Storage service. Nimbus has two products that are Nimbus platform for cloud resources managing and deploying and Nimbus Infrastructure usually for scientific community.

OpenNebula [8] is an open-source toolkit used for creating private, public, and hybrid infrastructure as a cloud from a heterogeneous-distributed environment. OpenNebula is also used for the management of virtual data centers. It has a core used for maintaining virtual machines, web service, and language-specific bindings. OpenNebula uses a shared file system to run its functions; typically OpenNebula uses a *Network File System* (NFS) for all disk images and files. When a user wants to create a virtual machine, a configuration file from user defines the required

configuration of the virtual machine, and this file is used by virtual machine manager of OpenNebula. One of the disadvantages of OpenNebula is the NFS mentioned above that does not have encryption techniques and can be vulnerable to sniffing attacks.

OpenStack [9] is an Open-Source cloud operating system for building private and public clouds. OpenStack is totally an open source and designed to be a very large IaaS private cloud with large network and virtual machines. The first five main components of OpenStack consist of OpenStack Compute (*Nova*), OpenStack Object Storage (*Swift*), OpenStack Image Service (*Glance*), OpenStack Dashboard (*Horizon*), and OpenStack Identity (*Keystone*). OpenStack development is still in progress. Every 6 month, a new version of OpenStack is released with fixed bug and new features.

Apache Cloud Stack [10] is a top-level project of the Apache Software Foundation. Cloud Stack is an Open-source tool used to manage large networks of virtual machines as an infrastructure as a cloud computing platform. Cloud Stack is designed for both private cloud and public cloud. Same as OpenStack, CloudStack supports multi-hypervisors such as VMWare, KVM, XenServer, and Xen cloud platform. Users can manage cloud through web interface, command line tools, and an API. Virtual machines running on the hypervisors can have features such as snapshots, attach volumes, and ISO images.

IBM Smart Cloud [11] is one of the commercial and enterprise solutions, which is developed based on open-source solution. It is used for building private, public, and hybrid cloud provided by IBM. The cloud system using IBM Smart Cloud has advantages in security and scalability; especially the product IBM Smart Cloud Enterprise + is designed for critical and important workloads.

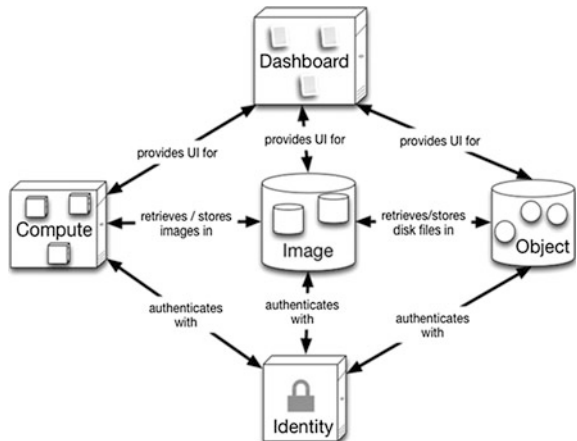
2 Development of OpenStack Cloud Computing Project

The previous part presented cloud computing benefits based on open-source solution; this part of article concentrates on the introduction of an open-source solution—which is OpenStack to build a cloud system providing IaaS.

2.1 *OpenStack*

OpenStack [9, 12, 13] has a 6-month period development, has a new version each 6 months. Each new version usually improves previous function for stability and deploys new functions. OpenStack is free totally and its components are written by Python language. The logical architecture of OpenStack is shown in Fig. 1 below. In which,

Fig. 1 OpenStack architecture



- Compute (*Nova*): provides and manages compute function for instances (*Virtual machines*).
- Image Service (*Glance*): stores image of instance and is used by Nova when an instance is deployed.
- Object Storage (*Swift*): provides storage function.
- Dashboard (*Horizon*): provides web based for administration of OpenStack.
- Identity (*Keystone*): provides authentication and authorization for all services in OpenStack.

2.2 OpenStack Features

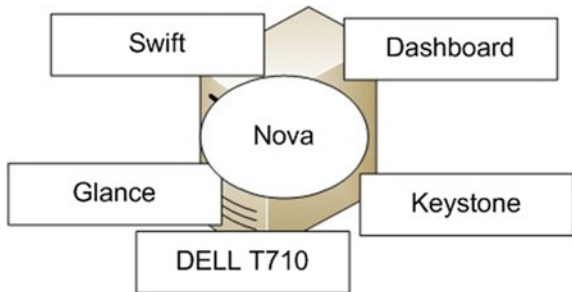
OpenStack has full of cloud computing features that provide IaaS. These features are presented through projects inside OpenStack such as Nova and Swift. This part presents some main features of OpenStack when compared with a famous cloud solution in the world—VMWare [12, 13] (Table 2).

However, when compared with VMware—a leading cloud computing solution in the world—OpenStack has some disadvantages [14, 15, 16, 17, 18]:

- OpenStack currently is developed to provide IaaS; VMware can be deployed in various service models (PaaS, SaaS).
- OpenStack does not have some automatic and intelligent mechanism in setting priority VMs and no support in live migration between physical hosts, while these functions are supported in VMware vMotion.
- OpenStack does not stop/shutdown idle physical hosts and automatic turn on when it needs more resources.
- OpenStack does not support storage cluster. Storage system (*Swift*) is only deployed for volumes in LVM format.

Table 2 Comparison of some features between VMWare and OpenStack

Feature	VMware	OpenStack
Live migration	vMotion	KVM live migration
Networking	vShield	Nova-network
Virtual switch	vDS	Quantum
Storage resource scheduler	SDRS	Nova-scheduler
Storage API	Storage APIs	Nova-volume

Fig. 2 Our cloud testbeds deployment on OpenStack

2.3 Our Cloud Testbeds on OpenStack

All the sub-projects of OpenStack are deployed in one physical server; hardware configuration: DELL T710, CPU 8 cores, and RAM 4 GB (Fig. 2).

3 Our Experiment and Results

This section includes the test results found from our Cloud Testbeds deployment; OpenStack Essex was installed and configured with these services:

- Create and manage virtual machines (instance);
- Manage provisioned resource of instances;
- Operate and manage through web-based Dashboard;
- Authenticate through Keystone; and
- Manage images through Glance.

Disadvantages:

- Our Cloud Testbeds did not deploy Swift storage function.
- Image services are linux based such as Debian, CentOS, Ubuntu, haven't Windows in image service list.

Our Cloud Testbeds uses test cases to estimate OpenStack operation; then testing the stability of instance creation and instance using, write down parameter related to

resource and operated time of instance. All the test cases use different numbers of instances and different types of instance. Estimation is done through four test cases:

- Case study 1: Create 01 Cirros instance. Cirros is an image which is supported by OpenStack with limited features of Linux, same as TTY Linux.
- Case study 2: Create 01 Ubuntu 12.04 64 bits instance.
- Case study 3: Create 05 Cirros instance.
- Case study 4: Create 05 Ubuntu 12.04 64 bits instances.

Note that, all the test cases are done five times. The information was noted and estimated include:

- Instance was created successfully or not.
- Creation time of instance and Deleted time of instance
- Memory Usage (RAM) of physical host before and after creating instances.

Estimated results: In five test cases, all the instances were created and deleted successfully with 100 %. All the created instances work properly. Figures 3 and 4 compare the memory usage before and after creating an instance, create and delete time of an instance in case study 1 and case study 2.

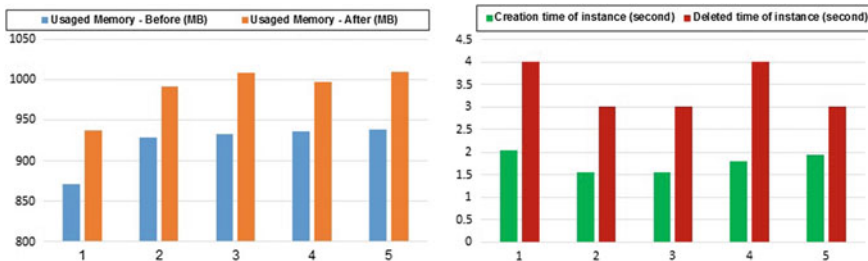


Fig. 3 Memory usage before and after creating an instance, create and delete time of an instance in case study 1

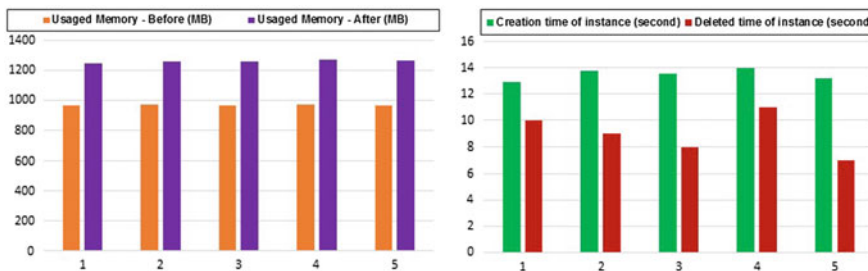


Fig. 4 Memory usage before and after creating an instance, create and delete time of an instance in case study 2

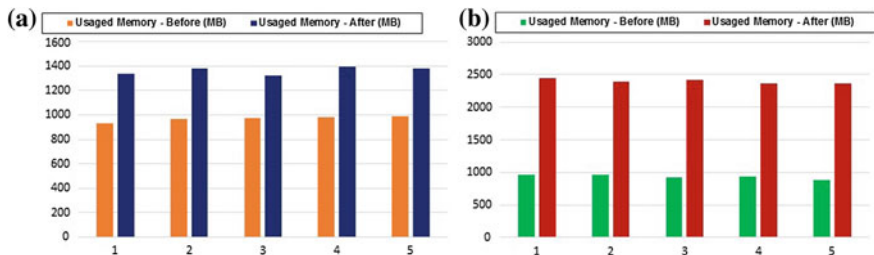


Fig. 5 Memory usage before and after creating an instance in case study 3(a) and case study 4(b)

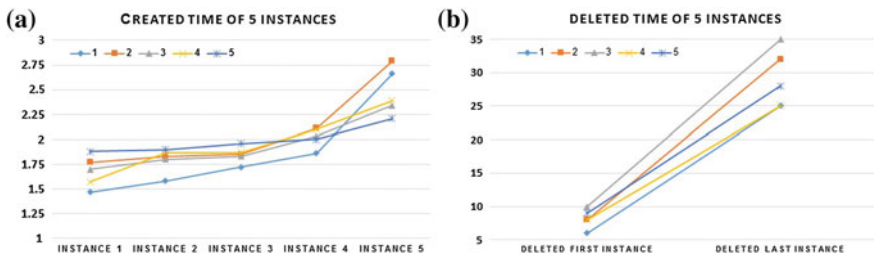


Fig. 6 Comparison of the created and deleted time of 5 instances in case study 3

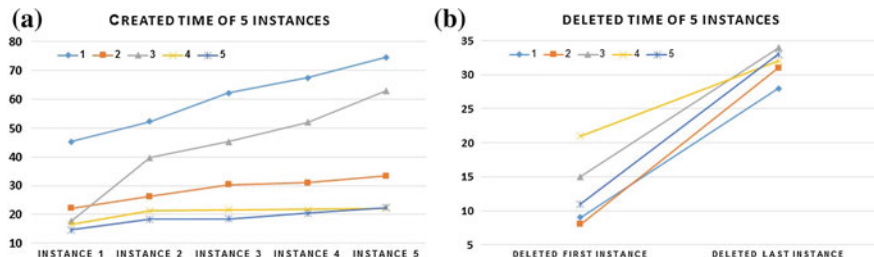


Fig. 7 Comparison of the created and deleted time of 5 instances in case study 4

The memory usage before and after creating an instance in case study 3(a) and case study 4(b) are shown in Fig. 5. Figures 6 and 7 show the comparison of the time between create and delete time of five instances in Case study 3 and Case study 4.

The related resources and time information of test cases are compared in Table 3.

Table 3 Comparison of some features between VMWare and OpenStack

Features	Case study				
	1	2	3	4	5
Memory usage before creating instances (Mb)	921.2	967.4	968.2	934.2	932
Memory usage after creating instances (Mb)	988.4	1261.6	1362.2	2394.6	1854.6
Created time of instances (s)	1.78	13.49	2.478	43.124	10.836
Deleted time of instances (s)	3.4	9	29	31.6	41.4

4 Conclusion and Future Work

Open-source cloud computing deployment is a difficult choice in all companies, especially leading technical company in the world. In this paper, we focus to analyze and evaluate the performance of the open-source OpenStack for IaaS cloud computing, and give the comparison between OpenStack and VMware. We outline some of our initial findings by providing such a testbed on OpenStack. The experimental results showed the advantages of OpenStack solution in cloud computing where infrastructure is provided as a service. Our research investigated the possible IaaS on OpenStack cloud computing environment. However, our testbeds still was in tiny environment and need to be scaled more to get better results and conclusion. In the future works, we would like to focus on a bigger open-source cloud system with more IaaS services such as variety of operating systems and storage services and finally become an OpenStack IaaS production.

References

- Pettey, C., Goasduff, L.: Gartner executive programs worldwide survey of more than 2,000 CIOs identifies cloud computer as top technology priority for CIOs in 2011. Gartner Research, Stamford (2011)
- Mell, P., Grance, T.: The NIST Definition of Cloud Computing (2011)
- Sabahi, F.: Cloud computing security threats and responses. In: 2011 IEEE 3rd International Conference on Communication Software and Networks (ICCSN) (2011)
- Canonical. Ubuntu Cloud: Technologies for future-thinking companies 2012. <http://www.canonical.com/about-canonical/resources/white-papers/ubuntu-cloud-technologies-future-thinking-companies>
- Cloud Security Alliance: About Cloud Security Alliance: <https://cloudsecurityalliance.org/research/security-guidance>
- Eucalyptus: <http://open.eucalyptus.com>
- Nimbus Project: <http://www.nimbusproject.org>
- OpenNebula: <http://www.opennebula.org>
- OpenStack: <http://www.openstack.org>
- Apache CloudStack: <http://cloudstack.apache.org/docs/en-US/index.html>

11. IBM SmartCloud Entry for SystemX: <http://www-03.ibm.com/systems/x/solutions/cloud/starterkit/index.htm>
12. Renski, B.: VMWare, OpenStack: Comparing Technology and Philosophy (2012)
13. How to compare VMware and OpenStack 2012: <http://www.slideshare.net/mirantis/how-to-compare-vmware-and-openstack>
14. OpenStack Compute 2012: <http://openstack.org/projects/compute/>
15. OpenStack Object Storage 2012: <http://openstack.org/projects/storage/>
16. OpenStack Image Service 2012: <http://openstack.org/projects/image-service/>
17. Infrastructure as a Service with Comprehensive Management and Security 2012: <http://www.vmware.com/products/datacenter-virtualization/vcloud-suite/overview.html>
18. Litvinski, O., Gherbi, A.: Openstack scheduler evaluation using design of experiment approach. In: IEEE Proceeding on Object/Component/Service-Oriented Real-Time Distributed Computing (ISORC), pp. 1–7 (2013)

The Application of Sub-Pattern Approach in 2D Shape Recognition and Retrieval

Muzameel Ahmed and V.N. Manjunath Aradhy

Abstract In 2D shape recognition and retrieval approach using shape feature extraction, statistical shape analysis methods such as PCA, ICA and NMF are commonplace, and these methods using subspace approach, have not been adequately investigated for recognition and retrieval of 2D shapes. The main hurdle in achieving higher recognition efficiency seems to be the shape sensitivity. In this paper we suggest, subspace method approach. The main idea is to use modular technique to improve the recognition and retrieval efficiency. Normally in the earlier methods proposed so far, a complete image is considered in training and matching process, in modular method approach partial image is used for training and matching the 2D images. The recognition and retrieval process is carried out in two phase, in the first phase uses the ridgelet transform applied. The second phase PCA is used for dimensionality reduction and to extract the effective features. For recognition and retrieval a study was conducted by using seventeen different distance measure technique. The training and testing process is conducted using leave-one-out strategy. The retrieval process is carried out by considering standard test “bull eyes” score. The proposed method is tested on the standard dataset MPEG-7. The experiment results of Subspace ridgelet PCA are compared with Subspace PCA method.

Keywords 2D object recognition • Retrieval • Subspace PCA • Subspace ridgelet PCA • Modular approach • Principal component analysis • Ridgelet transform • Distance measure techniques

M. Ahmed (✉)

Department of Computer Science and Engineering, Jain University, Bengaluru, India
e-mail: muzchk@yahoo.com

V.N.M. Aradhy

Department of MCA, Sri Jayachamarajendra College of Engineering, Mysore, India
e-mail: aradhyav1980@yahoo.co.in

1 Introduction

In the field of artificial intelligence, machines learning are training process is equipped with all the senses of human being, like smell sense, touch sense, hearing sense, taste sense and vision sense. Machine vision is a area, which depicts the effect of human eye in the case of machine. Computer vision is the ability to make machine view and recognize object in a scene. Over the year computer vision have made enormous progress in this field to achieve high quality visual perception and object recognition. To recognize an object, there are various properties that are used for the purpose of recognition and classification, like object shape, object color, object texture and object brightness. Of all the properties shapes is the most appealing feature used for recognition of objects. Shape representation is done using two major approaches, one the boundary based approach which uses image object contour information and the second approach requires a holistic representation, which gives the general information about the shape [1].

Bribiesca and Wilson [2], presented a method for two dimensional object miss match. The contour of the other object are compared and equated to a represent invariant under translation, rotation and scaling. Bandera et al. [3] proposed a algorithm, where contour are mentioned by curvature function, decayed in the fourier domain as linear combination of a set of demonstrative object and object is recognize by multilevel grouping. Kumar and Rockett [4] proposed a method representing scaling, translation and rotation inspired by invariance properties of angle of the triangle which are used to build signature histogram of local 2D object. Khalil and Bayoumi [5] proposed a method to recognize 2D object under translation, rotation and scaling transformation, by using the technique based on the continuous wavelet transform and neural networks. Mcneill and Vijaykumar [6], present a corresponding-based technique for efficient shape classification and retrieval. Shapes are represented by a large number of points on the contour, the points lie at fixed intervals on the contour or radial angle. Which gives a robust description of shapes. Belongie et al. [7], present a method to measure similarity between shapes, and exploit it for recognition. In this framework it solves for correspondences between points on the two shapes, by using the correspondence to estimate an aligning transforms.

Nagabhushan et al. [8] proposed a technique which is based on 2-directional 2-dimensional fisher's linear discriminate analysis for object face recognition. Sun et al. [9], proposed a method that adopts the eigen values of covariance matrix, resampling and autocorrelation transformation to extract prominent properties, and then use minimum euclidean distance approach and back propagation neural networks for grouping. Nam et al. [10], presented a method for similar leaf image retrieval. The method compares the accurate measurement of leaf matches, by considering leaf shape and venation properties. Arodz [11], proposed a method using the radon transform properties to drive the invariant transformation involving translation compensation, angle representation and 1D fourier transform. Daliri and Torre [1], proposed a algorithm based on dynamic programming to find the object match.

2D shape recognition using biological sequencing alignment tools was proposed by Manuele et al. [12]. The techniques existing for object recognition and shape categorization do not entirely satisfy and produced complete solution. This inspires us to develop and test new techniques for recognition and retrieval of 2D shape objects.

The paper is formatted into following section. In the Sect. 2 we will discuss the proposed method for recognition and retrieval, Sect. 3 presents the experiment results, Sect. 4 we discuss analysis of result and in Sect. 5 we present the discussion and conclusion.

2 Proposed Method

This section, we describe our idea of the proposed approach for object shape recognition and retrieval. The proposed sub modular approach consists of two phases. The first phase consists of applying ridgelet transform. In the ridgelet transform which operates very well with line singularities in 2D shapes object, the main aim is to transform a line singularity into point singularity using the radon transform. By using the wavelet transform to effectively manage the point singularity in the radon domain. Second phase consists of applying PCA to get the dimensionality reduction and to extract the effective features. The suggested approach is to use modular technique to improve the recognition and retrieval efficiency. Normally in the earlier methods proposed so far over the years, a complete image is considered in training and matching process. In modular approach the image is subdivided into many parts, each part is trained and tested separately. Suppose an image is sub divided into four parts, each of the part is trained and tested individually. And if two subdivided parts of the image used for testing match with the original image, then it is considered as 50 % match, if it is three subpart of the image to be tested, matches with the original image, then it is considered as 75 % match and likewise so on.

2.1 Ridgelet Transform Application

In high dimension representation of the image, wavelet are consider to be having weak representation. Candes and Donoho have come with a efficient technique to represent two dimension images called ridgelet transform. The ridgelet transform is a combination of radon transform and one dimensional wavelet transform. The radon transform have received wide range of application in recent years. In two dimensional image feature extraction the ridgelet transform are good, where object with lines can be represented into a domain of line parameters, every line in the image is represented by top position at the appropriate line parameters. These features encourage line detection applications in image processing in a great way [13].

One dimensional wavelet transform are efficient in representing zero-dimensionality or points singularity. Therefore the ridgelet transform is used to transform lines singularity into points singularity precisely. The continuous ridgelet transform (CRT), defined by [14], growing on with the radon transform, it is effective in its application [15].

With two variable integrable function $f(x_1, x_2)$ its radon transform (RDN) is expressed as

$$\text{RDN}_f(\theta, t) = \int_{\mathbb{R}^2} (f(x_1, x_2) \delta(x_1 \cos \theta + x_2 \sin \theta - t)) dx_1 dx_2 \quad (1)$$

In radon transform [15], transform the spatial domain into the projection domain (θ, t) , where every point represent a straight line in the spatial domain. Likewise, every point in the spatial domain becomes a sine curve in the projection domain.

The CRT is the implementation of a single dimensional wavelet $(\psi_{ab}(t)) = a^{-1/2}\psi((t - b)/a)$ to the slice of a radon transform:

$$\text{CRT}(a, b, \theta) = \int_R \psi_{a,b}(t) \text{RDN}_f(\theta, t) dt. = \int_{\mathbb{R}^2} (\psi_{a,b,\theta}(x_1, x_2) f(x_1, x_2)) dx_1 dx_2. \quad (2)$$

where the $\psi_{a,b,\theta}(\bar{x})$ in 2D are expressed by a wavelet-type function $\psi(t)$ as:

$$\psi_{a,b,\theta}(x_1, x_2) = a^{-1/2}\psi((x_1 \cos \theta + x_2 \sin \theta - b)/a). \quad (3)$$

This implies that the ridgelet function will remain stable along the lines where $x_1 \cos \theta + x_2 \sin \theta = \text{constant}$ [15].

Wavelets can very effectively represent shape with discontinues point singularities, while ridgelets transform are very good in representing shape object with lines singularities.

Digital image processing, discrete transform is needed to apply ridgelet transform. With this reason Do and Vetterli [16], have proposed finite ridgelet transform (FRIT). FRIT [15] is part of FRAT, which is expressed as sum of image pixels in a image, on a certain set of lines. These lines are expressed in a finite geometry in a likewise as the lines for the continuous radon transform (CRT) in the euclidean geometry, expressed by $Z_p = 0, 1, \dots, p - 1$, where p is a prime number and Z_p is finite field with modulo p operations.

The FRAT of a discrete function f on the finite grid Z_p^2 is expressed by:

$$\text{FRAT}_f(k, l) = \frac{1}{\sqrt{p}} \sum_{(i,j) \in L_{k,l}} f(i, j). \quad (4)$$

Let $L_{k,l}$ represents a group of pixels that forms a line on the lattice Z_p^2 , i.e.

$$L_{k,l} = \begin{cases} (i,j) : j = (ki+l)(\text{mod} p), i \in Zp & \text{if } 0 \leq k \leq p \\ (l,j) : j \in Zp & \text{if } k = p \end{cases} \quad (5)$$

The FRAT is a summation of radon coefficient of all the lines that pass through a defined point [15]. This encourages the use of ridgelet transform in 2D image processing job in a appealing way as the point singularities are well joined together with counter or edges.

2.2 Principal Component Analysis

Ridgelet transform produces a large dimension feature vector, extracted out of two dimension image. To reduce this large dimension feature vector, we apply PCA [17]. The PCA technique adopts the Karhunen-Loeve transform to effectively represent and recognize 2D images. In our approach we are using PCA technique for effective feature extraction, on the result obtained from ridgelet transform. The PCA technique is explained as follows:

Let M be the number of vectors of size $N (L \times L)$, p_i 's be the pixel values and $i = 1, \dots, M$.

$$x_i = [p_1 \dots p_n]^T \quad (6)$$

The mean of all images is calculated. Let m be the mean image which is $N \times 1$.

$$m = \frac{1}{M} \sum_{i=1}^M x_i \quad (7)$$

Then next the covariance matrix C is calculated using:

$$C = \frac{1}{M} \sum_{i=1}^M w_i w_i^T \quad (8)$$

Then next the eigenvectors e_i and the corresponding eigenvalues λ_i are calculated. From the above M eigenvectors, only k should be chosen corresponding to largest eigenvalues. An eigenvectors of a highest eigenvalues describe more characteristic features of an image. Using the k eigenvectors e_i and $i = 1, \dots, M$ feature extraction computed by PCA is as follows:

$$F_i = e_k^T (x_i - m) \quad (9)$$

For each image there is a feature vector F_i , then identification of a image is done by selecting a random new image into the eigenspace to get its feature vector F_{new} .

Then after computing the distances measure between unknown image and each known image using different distance measure classification techniques for classification purpose.

2.3 Distance Measure Classification Techniques

The features extracted out of the training images, and the image to be tested should be grouped for the purpose of analysis. This is accomplished by a technique called clustering. Clustering is the process of grouping together object or instance of similar type, so their should some means to classify the object based on their similarity or dissimilarity. Distance measure and similarity measure techniques are used for the purpose of object classification. The distance between two instance x_i and y_j is denoted by $d(x_i, y_j)$. Distance measure is also called metric distance measure if it satisfy the properties. (1) Triangle inequality $d(x_i, y_k) \leq d(x_i, y_j) + d(x_j, y_k) \forall x_i, x_j, x_k \in S$. (2) $d(x_i, y_j) = 0 \Rightarrow x_i = x_j \forall x_i, x_j \in S$. A good distance measure is considered to be symmetric and obtain least value (usually zero) in the instance of same vectors.

In this paper we have explored seventeen different distance measure techniques for classification. The distances between feature vector of trained and test images are calculated using the distance measure techniques. The techniques used are Euclidean, Manhattan, Mahalanobis, Minkowski, Modified Manhattan, Modified Squared Euclidean, Squared Euclidean, Weight Angle, Weight Manhattan, Weight Modified Manhattan, Canberra, Modified Normed Distance, Mean Squared Error, Weight Modified SSE, Weight SSE, Angle and Corr. co-efficient [18].

3 Experiment Results and Comparative Study

Here we exhibit and compare the outcome of our methods. We have two methods to compare with each other. One is the subspace PCA technique for recognition and retrieval and the second is the subspace ridgelet PCA for recognition and retrieval. Both the methods are test on standard collected MPEG-7 dataset. The MPEG-7 dataset is a collection of both natural and artificial objects, which has 70 different object, each in a class of 20 samples, for a total of 1400 samples. The dataset is a challenging one as it has samples which are very dissimilar to the other sample in the same class and samples which are very similar to samples in the other class.

The recognition test is carried out using the leave-one-out strategy, where one sub sample is left out in a class and remaining nineteen sub samples are trained. The sub sample left out of training will be tested. The sub sample is considered to be recognized, if it's test matches in the same class. The retrieval process is carried out by considering the standard test ‘bullseye’ score, where each sub sample is tested.

Retrieval is considered to be correct if the test sub sample belongs to the same class as being tested. The amount of right matches in the top 40 result are accounted, including the self match. For every method the retrieval rate is taken as the count of the maximum likely number of correct extraction. That is 28,000 (1400 shapes * 20 right extraction) [1]. The experimental results were extracted using seventeen different distance measure classifiers, namely Euclidean, Manhattan, Mahalanobis, Minkowski, Modified Manhattan, Modified Squared Euclidean, Squared Euclidean, Weight Angle, Weight Manhattan, Weight Modified Manhattan, Canberra and many more. And also the experimental results were extracted by varying the projection vector value between 10 and 50, by increment value in terms of 10 for recognition and retrieval in both subspace PCA and subspace ridgelet PCA. Tables 1 and 2 show the result of subspace PCA and subspace ridgelet PCA, recognition rate respectively. The recognition accuracy of PCA is 89.64 (using modified square eculidean) shown in Table 1, and ridgelet PCA is 91.14 (using weight SSE) shown in Table 2. Retrieval rate of PCA and ridgelet PCA, is shown in Tables 3 and 4 respectively. Retrieval rate for PCA is 65.00 (using weight.angle) shown in Table 4, ridgelet PCA is 66.31 (using weight.angle) shown in Table 4.

Table 1 Recognition rates using subspace PCA with different classifier methods and by varying projection values between 10 and 50

Classifier Methods	10	20	30	40	50
Manhattan	86.43	88.79	88.50	88.50	87.57
Euclidean	86.64	88.93	89.43	88.43	87.86
Mahalanobis	17.86	33.50	45.36	51.64	55.79
M.D between normed distance	71.79	86.07	87.50	88.43	88.43
Minkowski	86.29	88.29	88.57	88.43	88.36
Modified Manhattan	87.29	88.36	89.21	89.21	89.14
Modified Squared Euclidean	87.29	89.14	89.64	89.00	88.57
Mean Squared Error	86.64	88.93	89.43	88.43	87.86
Squared Euclidean	86.64	88.93	89.43	88.43	87.86
Weighted Angle	71.79	86.07	87.50	88.43	88.43
Weighted Manhattan	86.93	88.36	88.50	88.29	87.50
Weighted Modified Manhattan	87.21	88.71	88.93	89.21	88.43
Weighted Modified SSE	87.21	88.50	89.57	88.93	88.64
Weighted SSE	87.00	88.57	89.14	88.21	88.50
Canberra	87.00	88.93	89.21	89.07	88.64
Angle	86.86	89.00	89.21	88.50	88.29
Correlation co-efficient	85.93	88.50	89.29	88.86	88.43

Table 2 Recognition rates using subspace ridgelet PCA with different classifier methods and by varying projection values between 10 and 50

Classifier methods	10	20	30	40	50
Manhattan	88.57	90.50	90.21	90.21	90.50
Euclidean	88.00	89.43	90.07	90.14	89.93
Mahalanobis	04.86	06.50	07.21	06.36	07.57
M.D between normed distance	68.50	83.14	87.36	87.86	88.14
Minkowski	88.00	89.42	90.70	90.14	89.92
Modified Manhattan	88.78	90.57	90.57	90.42	90.50
Modified Squared Euclidean	88.35	89.21	89.64	89.71	89.71
Mean Squared Error	88.00	89.42	90.07	90.14	89.92
Squared Euclidean	88.00	89.42	90.07	90.14	89.92
Weighted Angle	68.50	83.14	87.35	87.85	88.14
Weighted Manhattan	89.42	90.71	90.71	90.21	89.57
Weighted Modified Manhattan	88.42	90.14	89.78	89.50	88.71
Weighted Modified SSE	89.50	90.00	89.92	89.71	89.42
Weighted SSE	89.71	91.14	91.00	90.85	90.85
Canberra	88.92	90.78	91.00	90.85	90.78
Angle	88.78	90.07	90.35	90.57	90.28
Correlation co-efficient	88.57	89.50	90.21	90.28	90.35

Table 3 Retrieval rates using subspace PCA with different classifier methods and by varying projection values between 10 and 50

Classifier Methods	10	20	30	40	50
Manhattan	61	63	63	63	62
Euclidean	61	64	64	64	63
Mahalanobis	23	36	42	45	46
M.D between normed distance	61	65	65	65	65
Minkowski	60	62	61	61	61
Modified Manhattan	61	63	64	64	64
Modified Squared Euclidean	62	64	64	64	64
Mean Squared Error	61	64	64	64	63
Squared Euclidean	61	64	64	64	63
Weighted Angle	61	65	65	65	65
Weighted Manhattan	62	64	64	63	63
Weighted Modified Manhattan	62	64	64	63	63
Weighted Modified SSE	62	64	64	63	63
Weighted SSE	61	64	64	63	63
Canberra	61	64	64	64	64
Angle	61	64	64	63	63
Correlation co-efficient	61	64	64	63	64

Table 4 Retrieval rates using subspace Ridgelet PCA with different classifier methods and by varying projection values between 10 and 50

Classifier Methods	10	20	30	40	50
Manhattan	61.78	64.18	64.43	64.48	64.37
Euclidean	60.37	61.86	62.06	62.19	62.21
Mahalanobis	10.53	12.77	14.16	14.80	15.25
M.D between normed distance	60.78	65.38	66.05	66.31	66.31
Minkowski	60.37	61.86	62.06	62.19	62.21
Modified Manhattan	59.87	62.18	62.64	62.72	62.66
Modified Squared Euclidean	59.53	60.92	61.00	61.00	60.98
Mean Squared Error	60.37	61.86	62.06	62.19	62.21
Squared Euclidean	60.37	61.86	62.06	62.19	62.21
Weighted Angle	60.78	65.58	64.05	66.31	66.31
Weighted Manhattan	63.62	65.58	64.55	63.74	62.75
Weighted Modified Manhattan	61.23	62.22	60.83	59.65	58.41
Weighted Modified SSE	60.90	61.10	60.29	59.58	58.78
Weighted SSE	63.61	65.48	65.62	65.70	65.54
Canberra	61.86	64.38	64.51	64.55	64.55
Angle	62.69	63.67	63.61	63.43	63.29
Correlation co-efficient	62.14	63.51	63.45	63.43	63.31

4 Analysis of Results

Here we analyze the outcomes of subspace PCA and subspace ridgelet PCA for recognition and retrieval accuracy rate. Ridgelet PCA recognition accuracy result with weighted SSE (weighted sum of squared errors) distance measure technique outperforms all the other distance measure techniques mentioned, and also the PCA recognition results using seventeen distance measure techniques. In weighted SSE distance measure the quality of clustering, which is also known as scatter. It calculates the error of each data point that is, its euclidean distance to the closest centroid and then computes the total sum of the squared error. Therefore in the recognition of binary image object there is a lesser squared error rate and it has closest centroid in the cluster. Therefore weighted SSE gives higher recognition rate compared to other distance measure technique. For the retrieval rate, subspace ridgelet PCA with weighted angle distance measure technique outperform all other distance measure techniques, and also the subspace PCA retrieval result using different distance measure techniques. Weighted angle distance measure technique, deals with the issue of length normalization. Because long data will be more the same with each other by virtue of length. The data can be internally normalized by taking angle rather than the similarity between vectors. For the data d_i and query q can be computed as vector product. For binary vector the inner product is a number of matched query terms in the data. For weighted term vector it is a sum of product of the weight of matched term. Inner product favors long data with a large

Fig. 1 MPEG-7 dataset images

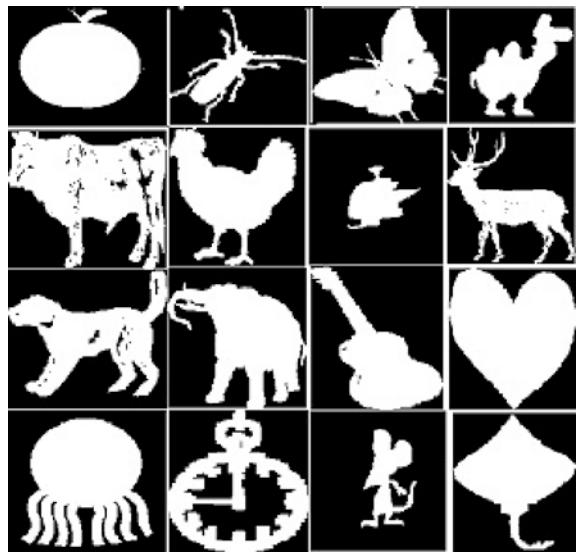
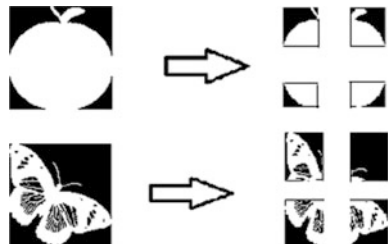


Fig. 2 Subdivision of the image



numbers of unique terms, and measures the matched terms. Distance measure between the vectors d_1 and d_2 is got by the cosine, angle x between them. So the cosine measure is used for the purpose of retrieval (Figs. 1 and 2).

5 Conclusion

In the computer vision application field, the important aspect is the recognition and retrieval rate. Developing an efficient and accurate system for recognition and retrieval is a real challenge as, extracting shape based features in comparison with complex and extraordinary human vision perception this is not a easy job. In this paper, we have made a study and comparison of shape based feature extraction and representation methods. The two methods are subspace PCA and subspace ridgelet PCA, both the methods are tested on MPEG-7 database, which has a collection of 70 different object and 20 samples in each of the class ($70 \times 20 = 1400$).

The recognition process is conducted using leave-one-out strategy. And the retrieval rate are computed by counting the top 40 matches in the test query. Seventeen different distance measure classification techniques are used for categorization. And the experimental results are obtained by varying the projection vector value between 10 and 50, in the increments of 10. The comparative study of both the approaches result is performed, and it is found that the subspace ridgelet PCA has better and encouraging result, to that of subspace PCA in terms of recognition and retrieval.

References

1. Daliri, M.R., Torre, V.: Robust symbolic representation for shape recognition and retrieval. *Pattern Recogn.* **41**, 1782–1798 (2008)
2. Bribiesca, E., Wilson, R.G.: A measure of 2d shape-of-object dissimilarity. *Appl. Math. Lett.* **10**(6), 107–115 (1997)
3. Bandera, F.A., Urdiales, C., Sandoval, F.: 2d Object recognition based on curvature functions obtained from local histograms of the contour chain code. *Pattern Recogn. Lett.* **20**, 49–55 (1999)
4. Rajeev, K., Peter, R.: Triplet geometric representation: a novel scale, translation and rotation invariant feature representation based on geometric constraints for recognition of 2d object features. *Image Vis. Comput.* **15**, 235–249 (1997)
5. Khalil, I.M., Bayoumi, M.M.: Invariant 2d object recognition using the wavelet modulus maxima. *Patten Recog. Lett.* **21**, 863–872 (2000)
6. McNeill, G., Vijayakumar, S.: 2d shape classification and retrieval. In: Proceeding of International Joint Conference on Artificial Intelligence, pp. 1483–1488 (2005)
7. Malik, J., Belongie, S., Puzicha, J.: Shape matching and object recognition using shapes contexts. *IEEE Trans. Pattern Anal. Mach. Intell.* **24**(24), 509–522 (2002)
8. Guru, D.S., Nagabhushan, P., Sheker, B.H.: (2d)2 fld: an efficient approach for appearance based object recognition. *Neurocomputing*, **69**, 934–940 (2006)
9. Sun, T.-H., Liu, C.-S., Tien, F.-C.: Invariant 2d object recognition using eigenvalues of covariance matrices, re-sampling and autocorrelation. *35*, 1966–1977 (2008)
10. Hwang, E., Nam, Y., Kim, D.: A similarity-based leaf image retrieval scheme: Joining shape and venation features. *Comput. Vision Image Underst.* **110**, 245–259 (2008)
11. Tomasz, A.: Invariant object recognition using radon-based transform. *Comput. Inform.* **24**, 183–199 (2005)
12. Manuele, B., Pietro, L.: 2d shape recognition using biological sequencing alignment tools. *Pattern Recogn.* 1359–1362 (2012)
13. Miroslaw, M.: Radon transformation and principal component analysis method applied in postal address recognition task. *Int. J. Comput. Sci. Appl.* **7**(3), 33–44 (2010)
14. Candes, E.J., Donoho, D.L.: Ridgelet: a key to higher dimensional intermittency. *Philoso. Trans. R. Soc.* 2495–2509 (1999)
15. Moschetti, F., Grania, L., Vanderghenst, P.: Ridgelet transform applied to motion compensated images.: In Proceedings of the ICASSP, pp. 381–384 (2003)
16. Do, M.N., Vetterli, M.: Finite ridgelet transform for image representation. *IEEE Trans. Image process.* (2002)
17. Turk, M., Pentland, A.: Eigenfaces for recognition. *J Cogn. Neurosci.* **3**, 71–86 (1991)
18. Perlibakar, Vytautas: Distance measure for pca-based face recognition. *Pattern Recogn. Lett.* **25**, 711–724 (2004)

A Data-Driven Approach for Option Pricing Algorithm

Dipti Ranjan Mohanty and Susanta Kumar Mishra

Abstract There are multiple option pricing methodologies and yet they still occupy an important place in academic research. Pricing an option is regarded as one of the most challenging questions in finance. Though the Black Scholes model is more popular to price an option, the binomial model is also very effective. However, the binomial model for pricing an option is computationally challenging. Therefore, an algorithmic implementation of the binomial option pricing algorithm is inefficient. This paper proposes using the Vector class template of C++ to make the binomial pricing model more efficient.

Keywords Binomial option pricing · Option pricing algorithm

1 About Vector Class Template

The C++ STL offers a class template called Vector. Vector in its implementation is similar to a dynamic array. Vector is a type of the ‘container’ data structure. A Vector like an array allows for random access; however unlike an array it also has the ability to resize itself when adding or removing items.

In order to create a vector, a pointer is created to a dynamically allocated array. There are two terms to define the size; size of the vector and capacity. Size of the vector implies the number of elements and capacity means the size of the internal array.

D.R. Mohanty (✉)
Ciber Inc, Boston, USA
e-mail: ydiprimohanty@gmail.com

D.R. Mohanty
SOA University, Bhubaneshwar, India

S.K. Mishra
Faculty in Finance and Center Head, Koustuv Business School, Bhubaneswar, India
e-mail: susanta65@gmail.com

There is an obvious consideration when new items are added to the vector. It might so happen that when these new items are added, the size of the vector exceeds its capacity. In such an instance there is a reallocation which allows additional memory in a new region. This reallocation helps in efficient usage of storage as when a new region is allocated, the old region is simultaneously freed up. It is important to note here that in vectors storage is automatically allocated.

So far as the characteristics of Vectors are concerned, it allows for random access. In addition, Vectors are not very efficient at adding or deleting items in the middle though it is possible nonetheless. Further, vectors also allow for range checking.

Among the prime advantages of a vector, first it allocates memory out of available storage when additional size is required. Second, vectors can uniquely expand or contract in the run time. In other words, vectors can swiftly allocate additional memory as required. Third, Vectors permits defining the container's initial capacity. Further, in Vectors accessing specific items by their position is more efficient than the other data types.

2 Binomial Option Pricing

Cox et al. [1] proposed a variant of this model in 1979. The underlying assumptions of this model are essentially straightforward and simple to understand. The first assumption is that the stock price (underlying) follows a random walk. A subsequent assumption which is a standard in a host of other valuations is that arbitrage opportunities do not exist. Further, as the name suggests, there are only two possible values for the stock price movement, up by a certain percentage or down by a certain percentage. A précis of the methodology is that it is possible to set up a portfolio consisting of some number of a particular stock and an option so that the value of the portfolio at the end of the time period is fixed (no uncertainty). Since the portfolio carries no uncertainty about its value at the end of the period (no risk), it should earn only the risk free rate. Hence, we can calculate backwards to arrive at the option's price.

In the single period model (Fig. 1), we consider a portfolio with long position in Δ shares. The portfolio also has a short position (sold) one unit of an option in the

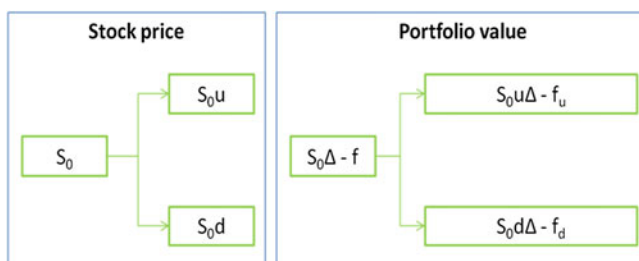


Fig. 1 Representation of uptick and downtick

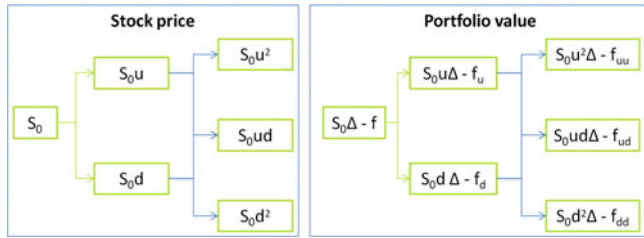


Fig. 2 Representation of uptick and downtick in a two-period model

same stock. S_0 is the current stock price, S_{0u} is the stock price on the uptick and S_{0d} is the stock price on the downtick. Also, ‘ f ’ is the current value of the option. Equating the value at the end of the period for both uptick and downtick and simplifying, we get

$$f = e^{-rT}[pf_u + (1-p)f_d],$$

where the symbols have their usual meanings and

$$p = (e^{-rT} - d)/(u - d)$$

Similar to the single period model, we represent the two-period model (Fig. 2) as below.

In this case, there is the second period which leads to three possibilities in the movement of the stock price as shown in the diagram. Extending similar logic as single period model, we simplify f as

$$f = e^{-2r\Delta t}[p^2f_{uu} + 2p(1-p)f_{ud} + (1-p)^2f_{dd}]$$

Now that we have introduced the single period and two-period binomial models, we can extend the number of steps to make the valuation more realistic. However, the essence of the argument remains the same.

3 Review of Existing Literature

Li and Zhang [2] identified the number of state variables required for options pricing. They discussed the principal component analysis approach and summarily rejected it for its lacuna. The two primary objections the authors have about the principal component analysis are the inconsistency of stopping rules and the nonlinearity in implied volatilities. The authors therefore suggest an alternate technique. They suggest nonparametric regression with nonlinear principal components. These components, they suggest, be extracted from the implied volatilities of various moneyness and maturities as proxies for the transformed state variables. The authors

then apply this new methodology to the S&P 500 index options data between the years 1996–2005 and conclude that the two state variables are sufficient to price the index options.

Su et al. [3] apply their model on Financial Time Stock Exchange (FTSE) 100 index option. The ad hoc Black–Scholes option-pricing model using a separate implied volatility for each option is used as benchmark. The study establishes that the HN GARCH has smaller valuation errors than the ad hoc BS model for the data considered.

Constantinides et al. [4] use American call and put options on the S&P 500 index futures from 1983 to 2006 that violate a certain defined stochastic dominance upper bound. They term these as potentially profitable opportunities. They then put in place a trading policy for an investor who holds only the market index along with the risk free asset. Their core argument is that trading policies that exploit these violations lead to out of sample portfolio returns that dominate portfolio returns that do not exploit them. The research uses quotes of the S&P 500 futures options and the underlying futures for the period between February 1983 and July 2006 from CME. For daily index return, the study uses historical sample of logarithmic returns between January 1928 and January 1983. The test objective is to check whether the portfolio profitability of the index and option traders is statistically different in months in which there is a violation of the bounds. The most significant outcome of their research is obtained by comparing the portfolio return of an option trader following this strategy with the portfolio return of an index trader who does not trade in options over the defined period. In these tests, the result is that the return of the call writer dominates the index trader's return. Further, this is true under a variety of methods for estimating the underlying return distribution. It also holds when the trader is allowed to vary the portfolio position by adding other risky assets beyond the index to the portfolio.

Liu [5] studied the impacts of equity options in Japan. In particular, the study talks about the impact of an option listing on the behavior of underlying stocks' key parameters such as price, trading volume, and volatility. In order to measure the price effects, the market model approach presented in Brown et al. [6] has been leveraged. The author finds that prices continue to rise significantly in the 2 days following option listing for a majority of stocks and then return to normal in the remaining post-event days. However, the study finds no significant change in the long-term trading volume following the listings of options in Japan, relative to the control sample. The author argues that the reason for the absence of a volume increase could be spillover of the volume effect from the sample to the control. Further, the impact of listing on volumes in Japan seems to be in line with the evidence from the United States (Cao [1999, p. 153]). As far as volatility is concerned, the mean volatility ratios suggest stronger volatility rises for the treatment sample. Further, there is a significant difference in volatility effect. In other words, the stocks with options are shown to have significantly higher price volatility than the stocks without options. The author, however, acknowledges that the forward-looking exchange officials might be selecting stocks for option listing in anticipation of higher future volatilities.

4 The Source Code

To summarize this model, we need to first identify the number of periods which gives us the nodes. Next is identifying the values of the option at the terminal nodes. From this terminal node, we then continue ‘driving on reverse gear’ to arrive at the value of the option at the starting point. From a programming perspective, this means building a tree where the value at each node is determined by the value at the succeeding node.

In the C++ source code example given below (Fig. 3), we have considered the valuation for an European Call Option. However, suitable changes can be made to convert it into a program for the European Put option.

A similar (and a little simpler) code can be written using dynamic array for the Call Value and Underlying asset price. This shall involve recursive calculation of the option price and underlying asset price from within the loop. However, in the program above, we have taken a different approach. Here instead of dynamic arrays, we have used a vector class instead.

5 Test Output for Sample Data

In order to test the above model and compare the output to the well-known Black Scholes output some hypothetical data was considered.

For the purpose of simplicity, a European Put with a current stock price (underlying) of \$100 and a strike price of \$101 was considered. It is assumed that the risk-free interest rate is 5 % and the stock paid no dividends. Further, a volatility of 30 % with a time to maturity of 2 years was assumed.

Using this hypothetical data, let us see the behavior of our model vis-à-vis the Black Scholes (Fig. 4). The option price suggested by the Black-Scholes for this data is a single value of \$12.1256. However, as per the definition of Binomial the value changes as per the number of steps that we chose for the iteration. The below chart plots the changing Binomial output for the above data with increasing number of steps. This output is the blue line in the chart. The constant Black-Scholes output (\$12.1256) is also given for reference by the red line.

As can be seen in the chart, the model output *converges* to the Black-Scholes output when the number of steps increases (Table 1).

Also given above is the tabular representation of the output. It shows that when the number of steps is high (Say 200), the difference is only marginal (around 0.01 % in this case).

```

#include
#include <vector>
#include <cmath>
int main()
{
    double spot,strike,rate,up,down,steps,optionVal; //Initialization of the variables
    cout<<"Input Spot,strike,rate,up,down,steps";
    cin>>spot>>strike>>rate>>up>>down>>steps; //Accept the input parameters from the user
    optionVal = OptionValuation_Vector(spot,strike,rate,up,down,steps); //This uses the valuation function
    cout<<"Option Valuation is "<<optionVal;
    return 0;
}

//Following is the main valuation function

double OptionValuation_Vector(const double& Spot, const double& Strike, const double& Rate, const
double& Up, const double& Down, const int& Steps)
{
    double Inv_Rate=exp(-Rate);
    double UpUp=Up*Up;
    double Prob_Up=(exp(Rate)-Down)/(Up-Down);
    double Prob_Down=1-Prob_Up; //Total probability of Up and Down is 1
    vector<double> P_Underlying(Steps+1); //Declaring the vector data structure
    P_Underlying[0]=Spot*pow(Down,Steps);
    for (int i=1;i<=Steps;++i)
    {
        P_Underlying[i]=UpUp* P_Underlying[i-1]; //Price of underlying in case all nodes are moving
        up
    }
    vector<double> Val_Call(Steps+1); //Declaring the call value vector
    for(int i=0;i<=Steps;++i)
    {
        Val_Call[i]=max(0,( P_Underlying[i]-Strike));
    }
    for(int j=Steps-1;j>=0;--j)
    {
        for(int i=0;i<=j;++i)
        {
            Val_Call[i]=(Prob_Up*Val_Call[i+1]+ Prob_Down*Val_Call[i])*Inv_Rate;
        }
    }
    return Val_Call[0];
}

```

Fig. 3 A sample source code demonstrating the approach

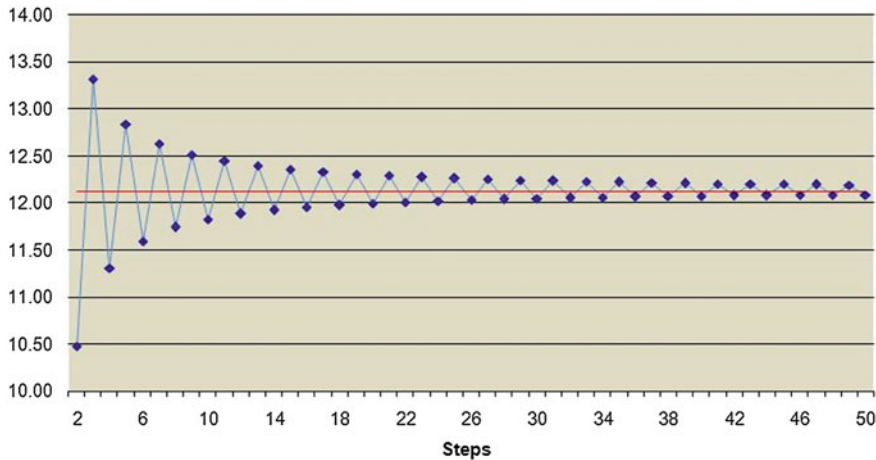


Fig. 4 Price generated (*Model Price*) by number of steps in iteration

Table 1 Convergence to Black-Scholes

Number of steps	Black Scholes output	Model output	Difference (%)
10	12.1256	11.8286	2.45
15	12.1256	12.3597	1.93
20	12.1256	11.9975	1.06
25	12.1256	12.2640	1.14
30	12.1256	12.0507	0.62
35	12.1256	12.2232	0.80
40	12.1256	12.0760	0.41
45	12.1256	12.2005	0.62
50	12.1256	12.0904	0.29
100	12.1256	12.1165	0.08
125	12.1256	12.1498	0.20
150	12.1256	12.1235	0.02
175	12.1256	12.1417	0.13
200	12.1256	12.1264	0.01

6 Conclusion

In sum, this program uses Vector to store the underlying asset prices and the call values at each node. This helps allocate memory out of available storage when additional size is required. It also helps expand or contract in the run time making this program more efficient.

Further, this code can also be easily modified to accommodate valuation of American (Call and Put) options. To do this, the value of the option at each node

can be calculated as the higher of waiting for the option to expire or exercising it at the node. This tweak in the code makes it suitable to calculate the American options valuation. As is well known, the Black Scholes model however cannot be tweaked easily to accommodate the valuation of the American options.

References

1. Cox, J.C., Ross, S.A., Rubinstein, M.: Option pricing: a simplified approach. *J. Financ. Econ.* **7**, 229–263 (1979)
2. Li, G., Zhang, C.: On the number of state variables in options pricing. *Manag. Sci.* **56**(11), 2058–2075 (2010). ISSN:0025-1909
3. Su, Y.C., Chen, M.D., HanChing, H.: An application of closed-form GARCH option-pricing model on FTSE 100 option and volatility. *Appl. Financ. Econ.* **20**, 899–910 (2010)
4. Constantinides, G.M., Czerwonko, M., Carsten Jackwerth, J., Perrakis, S.: Are options on index futures profitable for risk-averse investors? Empirical Evidence. *J. Financ* LXVI(4) (2011)
5. Liu, S.: Equity options and underlying stocks' behavior: further evidence from Japan. *Int. Rev. Financ.* **10**(3), 293–312 (2010)
6. Brown Stephen J., Jerold B. Warner.: Using daily stock returns: the case of event studies. *J. Financ. Econ.* **14**(1), 3–31 (1985)

Moderator Intuitionistic Fuzzy Sets and Application in Medical Diagnosis

Bhagawati Prasad Joshi and Pushpendra Singh Kharayat

Abstract The notion of intuitionistic fuzzy sets (IFSs) helps to an observer to incorporate the hesitancy value in the degree of membership function. The hesitancy factor comes from his basic knowledge, past experience, situation, depth of the standard terminologies, and many more characteristics; so the degree of membership function involved uncertainty under IFSs. Hence, the uncertainty included with an observer in the choice of membership grade under IFSs needs to be further improved by a moderator parameter to make the uncertain behavior more accurate. This can be done by introducing the concept of moderator intuitionistic fuzzy set (MIFS) as a generalization of IFSs. Furthermore, some properties and operators are defined over MIFSs similar to IFSs. Finally, a real-life problem of medical diagnosis is considered to apply the proposed approach effectively.

Keywords Intuitionistic fuzzy sets · Accuracy function · Score function · Medical diagnosis

1 Introduction

Zadeh [1] introduced the concept of fuzzy sets (FSs) as the generalization of traditional classical sets. Atanassov [2] presented the concept of intuitionistic fuzzy sets (IFSs), which is defined by a membership degree, non-membership degree, and a hesitancy degree. So IFSs theory is a more suitable and powerful tool to deal with uncertainty and vagueness in real applications than FSs and achieved much more attention to practitioner since its existence. IFSs theory is widely applicable in

B.P. Joshi (✉) · P.S. Kharayat
Seemant Institute of Technology, Pithoragarh 262501, Uttarakhand, India
e-mail: bpjoshi.13march@gmail.com

P.S. Kharayat
e-mail: kharayatpushpendrasingh@gmail.com

decision-making, medical diagnosis, data analysis, artificial intelligence, etc., due to the handling property of IFSs with uncertainty. In most of the real applications of IFSs theory, the comparability of two intuitionistic fuzzy numbers (IFNs) is widely used to make a proper decision. Thus, Chen and Tan [3], and Hong and Choi [4] proposed score function and accuracy function, respectively, to compare two IFNs, and based on these functions, Xu [5] proposed a procedure to compare two IFNs. In [6], De, Biswas, and Roy studied the Sanchez's approach [7, 8] for medical diagnosis and extended it with the theory of IFSs. In [9], Sanchez's method of medical diagnosis is extended to demonstrate a practical medical application of generalized intuitionistic fuzzy soft set. An application of generalized intuitionistic fuzzy soft set and generalized intuitionistic fuzzy soft relation for medical diagnosis is presented in [10]. Yu [11] considered the confidence level of the information provided by the experts under intuitionistic fuzzy environment. Many researchers proposed different aggregation operators to combine intuitionistic fuzzy information to make reasonable decisions. Here, we do not consider this issue of aggregation of intuitionistic fuzzy information.

Besides these achievements, we focus on the issue of making the uncertain behavior to more accurate and realistic. So it is observed that the notion of IFSs helps to an observer to include the hesitancy value in the degree of membership function. As we know, the hesitancy value comes from his background, basic knowledge, past experience, situation, depth of the standard terminologies, and many more characteristics, so the membership degree involved uncertainty under IFSs. Hence, the uncertainty included with an observer in the choice of membership grade under IFSs needs to be further improved by a moderator parameter to make the uncertain system more accurate and it is a kind of assessment value of the information given by the observer. The moderator parameter (provided by other observer to improve the original information) is incorporated in the original information by introducing the concept of moderator intuitionistic fuzzy set (MIFS) as a generalization of IFSs. Similar to the operations defined by Atanassov [12] for IFSs, we have defined some operations and relations over MIFSs. The proposed notion of MIFSs is applied to a medical diagnosis problem [6], and it is observed that we get the same results as obtained by [6]. The effectiveness of the proposed approach is that the information provided by an observer is further verified by other observer with the help of moderator parameter to make the uncertain behavior more accurate.

2 Preliminaries

In this section, first the definition of IFS is presented and then the notion of the developed study is included.

2.1 *Intuitionistic Fuzzy Set*

Let X be a non-empty set called a universe of discourse. An IFS A in X is defined as an object of the following form: $A = \{\langle x, t_A(x), f_A(x) \rangle : x \in X\}$; here, the functions $t_A : X \rightarrow [0, 1]$ and $f_A : X \rightarrow [0, 1]$ define the “degree of membership” and the “degree of non-membership” of the element $x \in X$, respectively, and for every element x of X , $0 \leq t_A(x) + f_A(x) \leq 1$. The degree of non-determinacy (uncertainty) for each element x of X in the IFS A is defined by $\pi_A(x) = 1 - t_A(x) - f_A(x)$, where $\pi_A(x) \in [0, 1]$. This part remains indeterministic due to the hesitation of the decision-maker.

2.2 *Motivation and Concept of Moderator Intuitionistic Fuzzy Set*

Let us first consider an example to see the validity and need of moderator intuitionistic fuzzy sets (MIFS). Consider “the set of real numbers very close to zero” and suppose one is interested to find the degree of belongingness of any real number to the set, such as the degree of belongingness of real numbers one and two to the set. It is clear that the degree of belongingness of one is greater than that of two. The degree of belongingness of any real number to the set depends on the range of real numbers available to an observer, i.e., here the degree of belongingness purely depends upon the available range to an observer. On the other side, the concept of IFSs is made possible to an observer by incorporating the hesitancy factor in membership degree. The hesitancy value comes from his background, basic knowledge, past experience, situation, dearth of the standard terminologies, and many more characteristics, so the membership degree involved uncertainty under IFSs.

Therefore, the indeterminacy included with an observer in the choice of membership degree under IFSs is required to be further improved by an additional parameter (called moderator parameter) which is a kind of assessment value to the information given by an observer to make the uncertain system more accurate, and this is the main reason to introduce the concept of MIFS. The MIFS improves the degree of membership function by comprising second information with the original information. The possibility of the overall uncertainty can be removed by involving the moderator parameter in the knowledge representation systems having only original information. Hence, the concept of MIFS provides the uncertainty atmosphere of the membership grade much more accurate, which cannot consider in more detail by means of the IFSs theory. The moderator intuitionistic fuzzy information can really improve the existing knowledge-based systems with a higher accuracy in the final decisions. If the moderator parameter is not taken under consideration, then the original performance stay uncertified and uncleared; this leads that the authenticity of the evaluation objects is conflicted.

3 Moderator Intuitionistic Fuzzy Set (MIFS)

Let an observer provide the original information (t, f) , where t is the degree of belongingness and f is the degree of non-belongingness of the evaluation object. If the moderator parameter is considered, then the original performance is improved and enhanced. The moderator parameter (provided by other observer to improve the original information) is of the form of intuitionistic fuzzy numbers (t_M, f_M) , where $t_M \in [0, 1]$ is the truth degree of the correctness (or improvement) in the original information and $f_M \in [0, 1]$ is the falsity degree of the correctness in the original information such that $0 \leq t_M + f_M \leq 1$ comprising in the original information by introducing the concept of MIFS as a generalization of IFSs.

Definition 1 Let X be a non-empty set called a universe of discourse. A MIFS A in X is defined as an object of the following form: $A = \{\langle(x, t_A(x), f_A(x)), (t_M(x), f_M(x))\rangle : x \in X\}$; here, the functions $t_A : X \rightarrow [0, 1]$, $f_A : X \rightarrow [0, 1]$ and $t_M : X \rightarrow [0, 1]$, $f_M : X \rightarrow [0, 1]$ define the “degree of membership,” the “degree of non-membership” and the “truth degree of moderator parameter,” and the “falsity degree of moderator parameter” of the element $x \in X$, respectively. For every element x of X , $0 \leq t_A(x) + f_A(x) \leq 1$ and $0 \leq t_M(x) + f_M(x) \leq 1$. Some operations and relations for MIFSs are studied to deal with the real applications.

3.1 Operations and Relations over MIFSs

Similar to the operations defined by Atanassov [12] for IFSs, here we proposed some operations and relations over MIFSs. For two MIFSs $A = \{\langle(x, t_A(x), f_A(x)), (t_M(x), f_M(x))\rangle : x \in X\}$ and $B = \{\langle(x, t_B(x), f_B(x)), (t_{M'}(x), f_{M'}(x))\rangle : x \in X\}$, the following operations are defined:

(1) *Containment*

$$A \subseteq B = t_A(x) \leq t_B(x), f_A(x) \geq f_B(x), t_M(x) \leq t_{M'}(x) \& f_M(x) \geq f_{M'}(x)$$

(2) *Equality* $A = B = t_A(x) = t_B(x), f_A(x) = f_B(x), t_M(x) = t_{M'}(x)$

$$\& f_M(x) = f_{M'}(x)$$

(3) *Complement* $A^C = \{\langle(x, f_A(x), t_A(x)), (f_M(x), t_M(x))\rangle : x \in X\}$

(4) *Union* $A \cup B = \left\{ \begin{array}{l} \left\langle (x, \max(t_A(x), t_B(x)), \min(f_A(x), f_B(x))), \right. \\ \left. (\max(t_M(x), t_{M'}(x)), \min(f_M(x), f_{M'}(x))) \right\rangle : x \in X \end{array} \right\}$

(5) *Intersection* $A \cap B = \left\{ \begin{array}{l} \left\langle (x, \min(t_A(x), t_B(x)), \max(f_A(x), f_B(x))), \right. \\ \left. (\min(t_M(x), t_{M'}(x)), \max(f_M(x), f_{M'}(x))) \right\rangle : x \in X \end{array} \right\}$

(6) *\oplus -Union*

$$A \oplus B = \left\{ \begin{array}{l} \langle (x, t_A(x) + t_B(x) - t_A(x) \cdot t_B(x), f_A(x) \cdot f_B(x)), \\ \langle (t_M(x) + t_{M'}(x) - t_M(x) \cdot t_{M'}(x), f_M(x) \cdot f_{M'}(x)) \rangle \end{array} : x \in X \right\}$$

(7) \otimes -Intersection

$$A \otimes B = \left\{ \begin{array}{l} \langle (x, t_A(x) \cdot t_B(x), f_A(x) + f_B(x) - f_A(x) \cdot f_B(x)), \\ \langle (t_M(x) \cdot t_{M'}(x), f_M(x) + f_{M'}(x) - f_M(x) \cdot f_{M'}(x)) \rangle \end{array} : x \in X \right\}$$

It is easy to demonstrate the validation of the defined operations.

Example 1 If $X = \{a, b, c, d\}$, let the MIFSs A and B have the form
 $A = \left\{ \begin{array}{l} \langle (a, 0.1, 0.7), (0.3, 0.4) \rangle, \langle (b, 0.5, 0.3), (0.4, 0.4) \rangle, \\ \langle (c, 0.4, 0.5), (0.3, 0.6) \rangle, \langle (d, 0.1, 0.6), (0.5, 0.2) \rangle \end{array} \right\},$

$B = \left\{ \begin{array}{l} \langle (a, 0.7, 0.1), (0.2, 0.4) \rangle, \langle (b, 0.3, 0.2), (0.5, 0.4) \rangle, \\ \langle (c, 0.5, 0.5), (0.3, 0.4) \rangle, \langle (d, 0.2, 0.2), (0.6, 0.2) \rangle \end{array} \right\}$. Then

$$(1) \quad A^c = \left\{ \begin{array}{l} \langle (a, 0.7, 0.1), (0.4, 0.3) \rangle, \langle (b, 0.3, 0.5), (0.4, 0.4) \rangle, \\ \langle (c, 0.5, 0.4), (0.6, 0.3) \rangle, \langle (d, 0.6, 0.1), (0.2, 0.5) \rangle \end{array} \right\}$$

$$(2) \quad A \cup B = \left\{ \begin{array}{l} \langle (a, 0.7, 0.1), (0.3, 0.4) \rangle, \langle (b, 0.5, 0.2), (0.5, 0.4) \rangle, \\ \langle (c, 0.5, 0.5), (0.3, 0.4) \rangle, \langle (d, 0.2, 0.2), (0.6, 0.2) \rangle \end{array} \right\}$$

$$(3) \quad A \cap B = \left\{ \begin{array}{l} \langle (a, 0.1, 0.7), (0.2, 0.4) \rangle, \langle (b, 0.5, 0.2), (0.4, 0.4) \rangle, \\ \langle (c, 0.4, 0.5), (0.3, 0.6) \rangle, \langle (d, 0.1, 0.6), (0.5, 0.2) \rangle \end{array} \right\}.$$

$$(4) \quad A \oplus B = \left\{ \begin{array}{l} \langle (a, 0.73, 0.07), (0.44, 0.16) \rangle, \langle (b, 0.65, 0.06), (0.7, 0.16) \rangle, \\ \langle (c, 0.7, 0.25), (0.51, 0.24) \rangle, \langle (d, 0.28, 0.12), (0.8, 0.04) \rangle \end{array} \right\}.$$

$$(5) \quad A \otimes B = \left\{ \begin{array}{l} \langle (a, 0.07, 0.73), (0.06, 0.64) \rangle, \langle (b, 0.15, 0.44), (0.2, 0.64) \rangle, \\ \langle (c, 0.2, 0.75), (0.09, 0.76) \rangle, \langle (d, 0.02, 0.68), (0.3, 0.36) \rangle \end{array} \right\}.$$

Proposition 1 Let $A = \{(x, t_A(x), f_A(x)), (t_M(x), f_M(x)) : x \in X\}$ and $B = \{(x, t_B(x), f_B(x)), (t_{M'}(x), f_{M'}(x)) : x \in X\}$ be two MIFSs, then the following operators are also MIFSs.

(1) A^c , (2) $A \cup B$, (3) $A \cap B$, (4) $A \oplus B$, (5) $A \otimes B$.

These follow trivially.

Theorem 1 The following relations (equalities) are valid for every three MIFSSs A , B , and C : (1) $A \cup B = B \cup A$, (2) $A \cap B = B \cap A$, (3) $A \oplus B = B \oplus A$, (4) $A \otimes B = B \otimes A$, (5) $(A \cup B) \cup C = A \cup (B \cup C)$, (6) $(A \cap B) \cap C = A \cap (B \cap C)$, (7) $(A \oplus B) \oplus C = A \oplus (B \oplus C)$, (8) $(A \otimes B) \otimes C = A \otimes (B \otimes C)$, (9) $(A \cup B) \cap C = (A \cap C) \cup (B \cap C)$, (10) $(A \cap B) \cup C = (A \cup C) \cap (B \cup C)$, (11) $A \cup A = A$, (12) $A \cap A = A$, (13) $A \oplus A = A$, (14) $A \otimes A = A$, (15) $(A \cup B)^c = A^c \cap B^c$ (16) $(A \cap B)^c = A^c \cup B^c$

The above follows trivially. Throughout this paper, $\alpha = \{(t_\alpha, f_\alpha), (\mu_\alpha, v_\alpha)\}$ is called a moderator intuitionistic fuzzy number (MIFN), where $t_\alpha, f_\alpha, \mu_\alpha, v_\alpha \in [0, 1]$, $0 \leq t_\alpha + f_\alpha \leq 1$ and $0 \leq \mu_\alpha + v_\alpha \leq 1$.

3.2 Score and Accuracy Function for MIFNs

Similar to the accuracy and score functions of intuitionistic fuzzy numbers proposed in [3, 4], here we presented accuracy and score functions over MIFNs. Using the equality and containment property of MIFSSs, the following relations are valid for two MIFNs $a = \{(t_a, f_a), (\mu_a, v_a)\}$ and $b = \{(t_b, f_b), (\mu_b, v_b)\}$:

- (1) $a = b$ if and only if $t_a = t_b, f_a = f_b$ and $\mu_a = \mu_b, v_a = v_b$
- (2) $a \leq b$ if and only if $t_a \leq t_b, f_a \leq f_b$ and $\mu_a \leq \mu_b, v_a \leq v_b$

However, the second condition is not satisfied in most of the situations. This can be illustrated with the following example:

Example 2 For two different MIFNs $a = \{(0.6, 0.3), (0.4, 0.5)\}$, and $b = \{(0.6, 0.2), (0.3, 0.4)\}$, the second condition cannot be used to compare them. Hence, to overcome this situation, score and accuracy function are defined to compare two MIFNs.

Definition 2 Let $a = \{(t_a, f_a), (\mu_a, v_a)\}$ and $b = \{(t_b, f_b), (\mu_b, v_b)\}$ be two moderator intuitionistic fuzzy numbers, then $S(a) = t_a + \mu_a - f_a - v_a$, $S(b) = t_b + \mu_b - f_b - v_b$ are the score functions and $H(a) = t_a + \mu_a + f_a + v_a$, $H(b) = t_b + \mu_b + f_b + v_b$ are the accuracy functions of a and b .

- (1) If $S(a) < S(b)$, then a is smaller than b , denoted by $a < b$.
- (2) If $S(a) = S(b)$, then If $H(a) < H(b)$ then a is smaller than b , denoted by $a < b$ and If $H(a) = H(b)$ then a and b represent the same information, denoted by $a = b$.

4 Medical Diagnosis Approach Based on Moderator Intuitionistic Fuzzy Relations (MIFRs)

In order to apply the concept of MIFSs to real-life problems, a medical diagnosis problem is considered to implement the concept of MIFSs effectively. First, let we consider a set of n patients $P = \{p_i(i = 1, 2, \dots, j)\}$ and for each patient a set of symptoms $S = \{s_i(i = 1, 2, \dots, k)\}$ is provided. Let the patients be diagnosed for the set $D = \{d_i(i = 1, 2, \dots, l)\}$. Then, let a MIFR R_1 is given from P to S . Further, we have taken another MIFR R_2 from S to D . The composition R of the MIFRs R_1 and R_2 gives the physical situation of a patient with respect to the diagnoses set and are evaluated by the following formulae [6]:

$$t_R(p_j, d_l) = \max_{s \in S} \{ \min(t_{R_1}(p_j, s), t_{R_2}(s, d_l)) \}. \quad (1)$$

$$f_R(p_j, d_l) = \min_{s \in S} \{ \max(f_{R_1}(p_j, s), f_{R_2}(s, d_l)) \} \quad (2)$$

$$\mu_R(p_j, d_l) = \max_{s \in S} \{ \min(\mu_{R_1}(p_j, s), \mu_{R_2}(s, d_l)) \} \quad (3)$$

$$v_R(p_j, d_l) = \min_{s \in S} \{ \max(v_{R_1}(p_j, s), v_{R_2}(s, d_l)) \} \quad (4)$$

Then, the score and accuracy functions are utilized to find the solutions.

5 Numerical Illustration

Let us consider a set of four patients $P = \{p_1, p_2, p_3, p_4\}$ and for each patient, a set of symptoms $S = \{\text{Temperature } (s_1), \text{Headache } (s_2), \text{Stomach pain } (s_3), \text{Chest pain } (s_4)\}$ is provided. Let the possible diseases may be the set $D = \{\text{Viral fever } (d_1), \text{Malaria } (d_2), \text{Typhoid } (d_3), \text{Chest problem } (d_4)\}$. The symptoms of patients are presented in the form of a MIFR R_1 which is given in Table 1. Table 2 depicts the knowledge in terms of symptoms of the diseases as a MIFR R_2 . The patients' diagnosis over the possible diseases is obtained using the formulae presented in Sect. 4 and presented in Table 3.

Finally, the score of Table 3 is obtained and presented in Table 4 in which the maximum score in a row indicates the diagnosis for the patient. Here, it is clear that patients p_1, p_3 , and p_4 suffer from Malaria and patient p_2 suffers from Typhoid. The results obtained here are same as obtained if we applied the procedure of [6].

Table 1 The moderator intuitionistic fuzzy assessment relation from P to S

R_1	Temperature (s_1)	Headache (s_2)	Stomach pain (s_3)	Chest pain (s_4)
p_1	$\{(0.8,0.1), (0.6,0.4)\}$	$\{(0.6,0.1), (0.6,0.2)\}$	$\{(0.2,0.8), (0.4,0.4)\}$	$\{(0.1,0.6), (0.2,0.6)\}$
p_2	$\{(0.0,0.8), (0.2,0.7)\}$	$\{(0.4,0.4), (0.5,0.4)\}$	$\{(0.6,0.1), (0.5,0.4)\}$	$\{(0.1,0.8), (0.1,0.7)\}$
p_3	$\{(0.8,0.1), (0.5,0.4)\}$	$\{(0.8,0.1), (0.7,0.2)\}$	$\{(0.0,0.6), (0.3,0.6)\}$	$\{(0.0,0.5), (0.1,0.6)\}$
p_4	$\{(0.6,0.1), (0.5,0.3)\}$	$\{(0.5,0.4), (0.5,0.3)\}$	$\{(0.3,0.4), (0.4,0.4)\}$	$\{(0.3,0.4), (0.4,0.5)\}$

Table 2 The moderator intuitionistic fuzzy assessment relation from S to D

R_2	Viral fever (d_1)	Malaria (d_2)	Typhoid (d_3)	Chest problem (d_4)
s_1	$\{(0.4,0.0), (0.5,0.4)\}$	$\{(0.7,0.0), (0.8,0.2)\}$	$\{(0.3,0.3), (0.4,0.4)\}$	$\{(0.1,0.8), (0.2,0.6)\}$
s_2	$\{(0.3,0.5), (0.2,0.6)\}$	$\{(0.2,0.6), (0.3,0.5)\}$	$\{(0.6,0.1), (0.5,0.4)\}$	$\{(0.0,0.8), (0.1,0.7)\}$
s_3	$\{(0.1,0.7), (0.1,0.6)\}$	$\{(0.0,0.9), (0.1,0.8)\}$	$\{(0.2,0.7), (0.3,0.6)\}$	$\{(0.2,0.8), (0.3,0.6)\}$
s_4	$\{(0.1,0.7), (0.1,0.8)\}$	$\{(0.1,0.8), (0.2,0.6)\}$	$\{(0.1,0.9), (0.2,0.8)\}$	$\{(0.8,0.1), (0.7,0.2)\}$

Table 3 The composition of relations R_1 and R_2

R	d_1	d_2	d_3	d_4
p_1	$\{(0.4,0.1), (0.5,0.4)\}$	$\{(0.7,0.1), (0.6,0.4)\}$	$\{(0.6,0.1), (0.5,0.4)\}$	$\{(0.2,0.6), (0.3,0.6)\}$
p_2	$\{(0.3,0.5), (0.2,0.6)\}$	$\{(0.2,0.6), (0.3,0.5)\}$	$\{(0.4,0.4), (0.5,0.4)\}$	$\{(0.2,0.8), (0.3,0.6)\}$
p_3	$\{(0.4,0.1), (0.5,0.4)\}$	$\{(0.7,0.1), (0.5,0.4)\}$	$\{(0.6,0.1), (0.5,0.4)\}$	$\{(0.1,0.5), (0.3,0.6)\}$
p_4	$\{(0.4,0.1), (0.5,0.4)\}$	$\{(0.6,0.1), (0.5,0.3)\}$	$\{(0.5,0.3), (0.4,0.4)\}$	$\{(0.3,0.4), (0.4,0.5)\}$

Table 4 Scores of the composition of relations

	d_1	d_2	d_3	d_4
p_1	0.4	0.8	0.6	-0.7
p_2	-0.6	-0.6	0.1	-0.9
p_3	0.4	0.7	0.6	-0.7
p_4	0.4	0.7	0.2	-0.2

6 Conclusion and Future Remarks

This study proposed a generalization of IFSs by introducing the moderator parameter of the IFNs. The moderator parameter is a kind of assessment value which certified the original information. This moderator parameter reduces the indeterminacy involved in knowledge representing systems under IFSs. It may be observed that there is always involved some kind of uncertainty in the presentation of information due to the background, knowledge, experience, depth of the standard terminologies, and many more. This type of situation is suitably corrected or improved by comprising the moderator parameter to the original performance and leads to give the idea of defining MIFSSs. Furthermore, some properties and operators are defined over MIFSSs. Finally, a real-life problem of medical diagnosis is considered to apply the proposed approach effectively. The results obtained are

consistent and validated with the help of using the procedure presented in [6] and obtained the same results.

The concept of MIFSs further certified the information under IFSs. In future, we will work on applying the presented concept to other real-life problems such as decision-making, supply selection, etc., and compared the results with that obtained from IFS theory.

Acknowledgments The authors are very thankful to the Director, Seemant Institute of Technology, Pithoragarh, India for his kind support and proper guidance.

References

1. Zadeh, L.A.: Fuzzy set. *Inf. Control* **8**, 338–353 (1965)
2. Atanassov, K.: Intuitionistic fuzzy sets. *Fuzzy Sets Syst.* **20**, 87–96 (1986)
3. Chen, S.M., Tan, J.M.: Handling multi criteria fuzzy decision-making problems based on vague set theory. *Fuzzy Sets Syst.* **67**, 163–172 (1994)
4. Hong, D.J., Choi, C.H.: Multi criteria fuzzy decision-making problems based on vague set theory. *Fuzzy Sets Syst.* **114**, 103–113 (2000)
5. Xu, Z.S.: Intuitionistic fuzzy aggregation operations. *IEEE Trans. Fuzzy Syst.* **15**, 1179–1187 (2007)
6. De, S.K., Biswas, R., Roy, A.R.: An application of intuitionistic fuzzy sets in medical diagnosis. *Fuzzy Sets Syst.* **117**(2), 209–213 (2001)
7. Sanchez, E.: Solutions in composite fuzzy relation equation. Application to medical diagnosis Brouwerian Logic. In: Gupta, M.M., Saridis, G.N., Gaines, B.R. (eds.) *Fuzzy Automata and Decision Process*. Elsevier, North-Holland (1977)
8. Sanchez, E.: Resolution of composition fuzzy relation equations. *Inform. Control.* **30**, 38–48 (1976)
9. Agarwal, M., Hanmandlu, M., Biswas, K.K.: Generalized intuitionistic fuzzy soft set and its application in practical medical diagnosis problem. In: 2011 IEEE International Conference on Fuzzy Systems, Taipei, Taiwan 27–30 June 2011
10. Agarwal, M., Biswas, K.K., Hanmandlu, M.: Generalized intuitionistic fuzzy soft set with application in decision making. *Appl. Soft Comput.* **13**, 3552–3566 (2013)
11. Yu, D.: Intuitionistic fuzzy information aggregation under confidence levels. *Appl. Soft Comput.* **19**, 147–160 (2014)
12. Atanassov, K.: *Intuitionistic fuzzy sets: Theory and Applications*. Springer, Berlin (1999)

An Empirical Comparative Study of Novel Clustering Algorithms for Class Imbalance Learning

Ch. N. Santhosh Kumar, K. Nageswara Rao and A. Govardhan

Abstract Data mining is the process of discovering knowledge from the vast data sources. In Data mining, classification and clustering are the two broad branches of study. In Clustering, k -means algorithm is one of the bench mark algorithms used for numerous applications. The popularity of k -means algorithm is due to its efficient and low usage of memory. One of the short comings of k -means algorithm is degradation of performance, when applied to imbalance distributed data. The results of cluster size generated by k -means are relatively uniform, in spite of the input data with non-uniform cluster sizes, which is defined as “uniform effect” in the literature. This paper proposes several novel algorithms to solve the above said problem. The proposed algorithms are compared with each other. The experiments conducted with the proposed algorithm on eleven UCI datasets with evaluation metrics show that proposed algorithms are effective to solve the problem of “uniform effect.”

Keywords Imbalanced data · K -means clustering algorithms · Oversampling · Uniform effect

1 Introduction

Research community had paid a good interest in analysis performance of k -means algorithm. One of the identified limitations of k -means algorithm towards imbalance datasets is its degradation of its performance. The problem of performance degradation for k -means algorithm towards imbalance dataset is termed as ‘uniform effect’ [1]. The area of class imbalance learning is directly related to many real world

Ch.N. Santhosh Kumar (✉)
Department of CSE, JNTU-Hyderabad, Hyderabad, A.P, India
e-mail: santhosh_ph@yahoo.co.in

K.N. Rao
PSCMR College of Engineering and Technology, Vijayawada, A.P, India

A. Govardhan
CSE & SIT, JNTU Hyderabad, Hyderabad, A.P, India

problems such as remote-sensing [2], pollution detection [3], risk management [4], fraud detection [5], and especially medical diagnosis [6–9]. In cluster analysis, the rare class is the class of interest for knowledge discovery. The information of “natural” clusters with nonspherical shapes using multiple representative points to achieve improved robustness over single-linked algorithm was proposed by Guha et al. [10]. The technique for discovery of the arbitrary shapes and sizes of clusters using multiprototype clustering algorithm was proposed by Liu et al. [11].

2 Related Work

The research in the field of clustering is exponentially increased in the recent years; the problem of class imbalance learning is thoroughly investigated with different oversampling and under-sampling techniques. The details about some of the developments are given below.

Lago-Fernández et al. [12] have proposed a new set of validation techniques based on the clusters’ negentropy and it has been introduced. The compact clusters which are not strongly overlapped can be formed by using clusters’ negentropy. One of the limitations of this approach is visible if the region contains only few data points. The authors have proposed different heuristics to solve this problem. Alejo et al. [13] have proposed a new dynamic method which uses SMOTE and a newly proposed over-sampling technique with sequential back propagation algorithm. The author uses back propagation mean square error (MSE) for identifying the oversampling rate.

Wang [14] has proposed a method for addressing class imbalance problem by using hybrid sampling SVM approach and oversampling. Santhosh Kumar et al. [15] have proposed a novel algorithm using under-sampling and intelligent technique to solve the problem of ‘uniform effect’ in k -means algorithm. Brzezinski et al. [16] have proposed accuracy updated ensemble (AUE2) a data stream classifier for improved performance. Poolsawad et al. [17] have investigated on different methods of sampling, i.e., over-sampling and under-sampling, to assess the performance of classification algorithms on clinical imbalance datasets. Oreški et al. [18] have conducted a research on classification problems in purpose of measuring the quality of classification; the accuracy and area under ROC curve measures are used. Stefanowski et al. [19] have studied several resampling strategies for data pre-processing. Tomašev et al. [20] have used k -nearest neighbor methods for class imbalance learning.

3 The Proposed Methods

This section mainly focuses on the presentation of the proposed algorithms. The four algorithms, which have been published in different journals and conferences, are presented for a comparative study. The details of each and every algorithm are provided below.

3.1 Under-Sampled K-Means (USKM) [21]

The under-sampled K-means (USKM) algorithm is published by the authors in [21]. The proposed framework of USKM can be detailed as below.

The data source to be modeled is taken and divided into majority and minority subsets. The further part of the investigation is to be done on the majority subset. In the next phase, influential attributes are to be identified; this can be done by using a correlation-based feature subset (CFS) filter. In the next stage, the weak and noisy instances from the majority subset are identified and eliminated. The range of weak and noise instances is removed by using expert technique. In the final stage, the stronger majority and minority subsets are combined to form a complete data source. The improved data source is applied to a base algorithm; in this case k -means algorithm is used.

Algorithm 1: USKM

Selection Phase

- Step 1: **begin**
- Step 2: $k \leftarrow 0, j \leftarrow 1$.
- Step 3: **Apply CFS** on subset N ,
- Step 4: Find F_j from N , $k =$ number of features extracted in CFS
- Step 5: **repeat**
- Step 6: $k=k+1$
- Step 7: Select the range for weak or noises instances of F_j .
- Step 8: Remove ranges of weak attributes and form a set of major class examples N_{strong}
- Step 9: **Until** $j = k$
- Step 10: Form a new dataset using P and N_{strong}
- Step 11: **End**

Clustering Phase

- Step 1: Select k random instances from the training data subset as the centroids of the clusters $C_1; C_2; \dots; C_k$.

Step 2: For each training instance X :

- a. Compute the Euclidean distance $D(C_i, X), i = 1 \dots k$
- b. Find cluster C_q that is closest to X .
- c. Assign X to C_q .

Update the centroid of C_q .

(The centroid of a cluster is the arithmetic mean of the instances in the cluster.)

- Step 3: Repeat Step 2 until the centroids of clusters $C_1; C_2; \dots; C_k$ stabilize in terms of mean-squared error criterion.

3.2 Imbalanced K-Means (IKM) [22]

The imbalanced K-means (IKM) algorithm is published by the authors in [22].

The proposed framework of IKM can be detailed as below.

The data source to be modeled is taken and divided into majority and minority subsets. The further part of the investigation is to be done on the minority subset.

The analysis of the minority subset can be done to element noisy and borderline instances. The influential instances in the minority subset are resampled i.e., replica of existing instances, synthetic instances generation, and hybrid of both. The amount of replication of instances depends upon the unique properties of the data sources. In the final stage, the stronger minority and majority subsets are combined to form a complete data source. The improved data source is applied to a base algorithm; in this case k -means algorithm is used.

Suppose that the whole training set is T , the minority class is P and the majority class is N , and

$$P = \{p1, p2, \dots, pnum\}, N = \{n1, n2, \dots, nnum\},$$

where $pnum$ and $nnum$ are the number of minority and majority examples. The detailed procedure of IKM is as follows.

Algorithm 2 : IKM

Input:

A set of minor class examples P , a set of major class examples N , $jPj < jNj$, and F_j , the feature set, $j > 0$.

Output:

Average Measure { AUC, Precision, F-Measure, TP Rate, TN Rate }

External selection Phase

Step 1: For every pi ($i = 1, 2, \dots, pnum$) in the minority class P , we calculate its m nearest neighbors from the whole training set T . The number of majority examples among the m nearest neighbors is denoted by m' ($0 \leq m' \leq m$).

Step 2: If $m/2 \leq m' < m$, namely the number of pi 's majority nearest neighbors is larger than the number of its minority ones, pi is considered to be easily misclassified and put into a set MISCLASS.

MISCLASS = m'

Remove the instances m' from the minority set.

Step 3: For every ni ($i = 1, 2, \dots, nnum$) in the majority class N , we calculate its m nearest neighbors from the whole training set T . The number of majority examples among the m nearest neighbors is denoted by m' ($0 \leq m' \leq m$).

Step 4: If $m/2 \leq m' < m$, namely the number of ni 's minority nearest neighbors is larger than the number of its majority ones, ni is considered to be easily misclassified and put into a set MISCLASS.

MISCLASS = m'

Remove the instances m' from the majority set.

Step 5: For every p_i' ($i = 1, 2, \dots, p_{\text{num}}$) in the minority class P , we calculate its m nearest neighbors from the whole training set T . The number of majority examples among the m nearest neighbors is denoted by m' ($0 \leq m' \leq m$).

If $m' = m$, i.e. all the m nearest neighbors of p_i' are majority examples, p_i' is considered to be noise or outliers or missing values and are to be removed.

Step 6: For every p_i'' ($i = 1, 2, \dots, p_{\text{num}}$) in the minority class P , we calculate its m nearest neighbors from the whole training set T . The number of majority examples among the m nearest neighbors is denoted by m' ($0 \leq m' \leq m$).

If $0 \leq m' < m/2$, p_i'' is a prominent example and need to be kept in minority set for resampling.

Step 7: The examples in minority set are the prominent examples of the minority class P , and we can see that $PR \subseteq P$. We set

$$PR = \{p_1', p_2', \dots, p_{d_{\text{num}}}'\}, 0 \leq d_{\text{num}} \leq p_{\text{num}}$$

Step 8: In this step, we generate $s \times d_{\text{num}}$ synthetic positive examples from the PR examples in minority set, where s is an integer between 1 and k . One percentage of synthetic examples generated are replica of PR examples and other are the hybrid of PR examples.

Clustering Phase

Step 1: Select k random instances from the training data subset as the centroids of the clusters $C_1; C_2; \dots; C_k$.

Step 2: For each training instance X :

- a. Compute the Euclidean distance $D(C_i, X), i = 1 \dots k$
- b. Find cluster C_q that is closest to X .
- c. Assign X to C_q . Update the centroid of C_q .

(The centroid of a cluster is the arithmetic mean of the instances in the cluster.)

Step 3: Repeat Step 2 until the centroids of clusters $C_1; C_2; \dots; C_k$ stabilize in terms of mean-squared error criterion.

3.3 Visual K-Means (VKM)

The visual *K*-means (VKM) algorithm is published by the authors. The different components of our new proposed framework are elaborated below.

- Partitioning majority and minority classes

The unbalanced dataset is partitioned as majority and minority subsets. Since our approach is a under-sampling approach, we need to focus on the majority dataset.

- Applying visualization technique on majority class

In the next phase of the approach, we need to apply a visualization technique on the majority dataset to identify different clusters. Here we have considered OPTICS clustering algorithm to apply on the majority subset for visualization.

- Identification of minor clusters

The result of ordering points to identify clustering structure (OPTICS) algorithms is used for the identification of number of clusters in the majority subset. We need to identify the weak or outlier clusters and delete those from the majority subset. The amount of deletion will depend upon the unique properties of the dataset. After removing weak and outlier clusters, form a new majority subset N_i .

- Forming new balanced dataset

The new majority subset N_i and the minority subset P are combined to form a new likely balanced dataset. This newly formed balanced dataset is applied to a base algorithm; in this case k -means is used to obtain different measures such as AUC, Precision, F-measure, TP Rate, and TN Rate.

Algorithm 3: Visual _K-means:

Selection Phase

Step 1: **begin**

Step 2: {Input: A set of minor class examples P , a set Of major class examples N , $jPj < jNj$ }

Step 3: **Apply** OPTICS on N ,

Step 4: Identify Clusters i from N

Step 5: Delete minority class clusters from i and form N_i .

Step 6: Combine P and N_i to form N_Pi

Step 7: **End**

Clustering Phase

Step 1: Select k random instances from the training data subset as the centroids of the clusters C1; C2; ...Ck.

Step 2: For each training instance X:

- a. Compute the Euclidean distance $D(C_i, X), i = 1...k$
- b. Find cluster C_q that is closest to X.
- c. Assign X to C_q . Update the centroid of C_q .

(The centroid of a cluster is the arithmetic mean of the instances in the cluster.)

Step 3: Repeat Step 2 until the centroids of clusters C1; C2; ...Ck stabilize in terms of mean-squared error criterion.

3.4 K-Subset [23]

The *K*-Subset algorithm is published by the authors in [23]. The entire process is given in the following algorithm 4,

- Dividing Majority and Minority Subset

An easy way to sample a dataset is by selecting instances randomly from all classes. However, sampling in this way can break the dataset in an unequal priority way and more number of instances of the same class may be chosen in sampling. To resolve this problem and maintain uniformity in sample, we propose a sampling strategy called weighted component sampling. Before creating multiple subsets, we will create the number of majority subsets depending upon the number of minority instances.

- Identifying number of Subsets of Majority class

In the next phase of the approach, the ratio of majority and minority instances in the unbalanced dataset is used to decide the number of subset of majority instances (T) to be created.

$$T = \text{no. of majority inst } (N)/\text{no. of minority inst } (P).$$

- Combining the majority Subsets and minority Subsets

The so formed majority subsets are individually combined with the only minority subsets to form multiple balanced sub-datasets of every dataset. The number of balanced sub datasets formed depends upon the imbalance ratio and the unique properties of the dataset.

- Averaging the measures

The subsets of balanced datasets created are used to run multiple times, and the resulted values are averaged to find the overall result. These newly formed multiple subsets are applied to a base algorithm; in this case k -means is used to obtain different measures such as AUC, Precision, F-measure, TP Rate, and TN Rate

Algorithm 4 : K-subset

```

1: {Input: A set of minor class examples  $P$ , a set Of major class examples  $N$ ,  $jPj < jNj$ , and  $T$ ,  
the number of subsets to be sampled from  $N$ .}  

2:  $i \leftarrow 0$ ,  $T=N/P$ .  

3: repeat  

4:  $i = i + 1$   

5: Randomly sample a subset  $Ni$  from  $N$ ,  $jNij = jPj$ .  

6: Combine  $P$  and  $Ni$  to form  $NPi$   

7: Apply filter on a  $NPi$   

8: Train and Learn a Base algorithm (K-means) using  $NPi$ . Obtain the values of AUC,TP,FP,F-  
Measure  

9: until  $i = T$   

10: Output: Average Measure;
```

4 Datasets

In this research, the datasets considered are of only binary nature. We have taken Breast, Breast_w, Colic, Credit-g, Diabetes, Heart-c, Heart-h, Heart-stat, Hepatitis, Ionosphere, Sonar; 11 binary data sets from UCI [24] machine learning repository.

The metrics of evaluation are estimated by using tenfold cross-validation (CV) technique. In tenfold CV, the dataset is divided into 10 equal partitions, and in every run onefold is used for testing and ninefolds are used for training. The process will continue by switching the onefold for testing from training folds. The data partitions are available for interested readers at UCI.

5 Experimental Results

The experimental results of the comparative analysis are given in this section.

Tables 1, 2, 3, 4, and 5 report the results of Accuracy, AUC, Precision, F-measure, and Recall, respectively. The results show that proposed IKM clustering algorithm is at least as effective as and at times more effective than USKM, VKM, and K -subset algorithms. USKM compared with accuracy on other algorithms has performed well. The performance of VKM compared with other proposed algorithms performs better on some of the high dimension datasets showing the applicability of the algorithm. The performance of K -Subset compared with other proposed algorithms presests the unique behavior with sick and sonar datasets.

Finally, we can conclude that the proposed algorithms can be applicable on real world datasets depending upon the context and scenario of the domain.

Table 1 Summary of tenfold cross-validation performance for accuracy on all UCI datasets

Datasets	USKM	IKM	VKM	K -Subset
Breast	51.22 ± 9.58	55.78 ± 11.87	—	—
Breast_w	96.94 ± 2.14	95.36 ± 2.19	94.84 ± 2.76	94.64 ± 3.15
Colic	70.53 ± 9.73	68.07 ± 9.07	59.58 ± 10.37	76.96 ± 10.2
Credit-g	53.26 ± 6.17	57.08 ± 5.99	—	—
Diabetes	72.24 ± 7.05	63.13 ± 5.92	64.20 ± 6.55	63.07 ± 6.22
Hepatitis	71.27 ± 12.96	74.46 ± 11.04	70.85 ± 13.04	76.65 ± 16.03
Ionosphere	72.35 ± 8.00	71.01 ± 8.06	71.80 ± 8.43	69.70 ± 10.3
Labor	64.50 ± 21.07	—	66.00 ± 21.37	64.37 ± 25.06
Sick	66.00 ± 7.62	—	76.90 ± 8.16	79.19 ± 5.16
Sonar	51.92 ± 11.46	52.73 ± 11.13	50.02 ± 11.57	70.10 ± 14.44
Vote	89.52 ± 7.04	—	85.05 ± 5.43	88.19 ± 8.84

Table 2 Summary of tenfold cross-validation performance for AUC on all UCI Datasets

Datasets	USKM	IKM	VKM	K -subset
Breast	0.499 ± 0.092	0.552 ± 0.116	—	—
Breast_w	0.964 ± 0.025	0.953 ± 0.022	0.947 ± 0.028	0.947 ± 0.030
Colic	0.702 ± 0.098	0.689 ± 0.086	0.622 ± 0.100	0.766 ± 0.105
Credit-g	0.518 ± 0.060	0.569 ± 0.059	—	—
Diabetes	0.688 ± 0.071	0.625 ± 0.059	0.614 ± 0.068	0.634 ± 0.062
Hepatitis	0.749 ± 0.134	0.758 ± 0.114	0.744 ± 0.135	0.768 ± 0.160
Ionosphere	0.719 ± 0.091	0.709 ± 0.080	0.714 ± 0.097	0.703 ± 0.102
Labor	0.624 ± 0.221	—	0.644 ± 0.221	0.640 ± 0.254
Sick	0.661 ± 0.118	—	0.556 ± 0.153	0.768 ± 0.054
Sonar	0.519 ± 0.115	0.527 ± 0.111	0.498 ± 0.116	0.719 ± 0.148
Vote	0.886 ± 0.073	—	0.860 ± 0.051	0.877 ± 0.089

Table 3 Summary of tenfold cross-validation performance for precision on all UCI datasets

Datasets	USKM	IKM	VKM	<i>K</i> -subset
Breast	0.671 ± 0.083	0.693 ± 0.105	–	–
Breast_w	0.959 ± 0.030	0.936 ± 0.032	0.936 ± 0.040	0.921 ± 0.048
Colic	0.762 ± 0.138	0.798 ± 0.110	0.787 ± 0.120	0.765 ± 0.130
Credit-g	0.639 ± 0.053	0.667 ± 0.058	–	–
Diabetes	0.721 ± 0.050	0.628 ± 0.048	0.692 ± 0.052	0.592 ± 0.054
Hepatitis	0.493 ± 0.187	0.613 ± 0.153	0.479 ± 0.183	0.787 ± 0.220
Ionosphere	0.615 ± 0.170	0.717 ± 0.112	0.585 ± 0.170	0.821 ± 0.131
Labor	0.497 ± 0.396	–	0.518 ± 0.389	0.631 ± 0.327
Sick	0.954 ± 0.034	–	0.945 ± 0.028	0.845 ± 0.068
Sonar	0.526 ± 0.159	0.530 ± 0.128	0.525 ± 0.128	0.866 ± 0.142
Vote	0.930 ± 0.094	–	0.947 ± 0.054	0.906 ± 0.131

Table 4 Summary of tenfold cross-validation performance for F-measure on all UCI datasets

Datasets	USKM	IKM	VKM	<i>K</i> -subset
Breast	0.587 ± 0.109	0.617 ± 0.129	–	–
Breast_w	0.975 ± 0.017	0.955 ± 0.021	0.952 ± 0.026	0.947 ± 0.030
Colic	0.654 ± 0.129	0.629 ± 0.146	0.597 ± 0.138	0.729 ± 0.143
Credit-g	0.602 ± 0.071	0.613 ± 0.076	–	–
Diabetes	0.786 ± 0.072	0.676 ± 0.078	0.714 ± 0.064	0.668 ± 0.056
Hepatitis	0.597 ± 0.171	0.679 ± 0.141	0.585 ± 0.165	0.755 ± 0.197
Ionosphere	0.650 ± 0.173	0.710 ± 0.130	0.634 ± 0.174	0.661 ± 0.145
Labor	0.476 ± 0.348	–	0.508 ± 0.350	0.640 ± 0.303
Sick	0.775 ± 0.058	–	0.873 ± 0.067	0.804 ± 0.066
Sonar	0.485 ± 0.159	0.512 ± 0.136	0.522 ± 0.132	0.724 ± 0.151
Vote	0.867 ± 0.091	–	0.851 ± 0.059	0.862 ± 0.102

Table 5 Summary of tenfold cross-validation performance for recall on all UCI datasets

Datasets	USKM	IKM	VKM	<i>K</i> -subset
Breast	0.536 ± 0.149	0.573 ± 0.169	–	–
Breast_w	0.991 ± 0.014	0.976 ± 0.021	0.970 ± 0.031	0.977 ± 0.030
Colic	0.601 ± 0.178	0.561 ± 0.221	0.521 ± 0.208	0.735 ± 0.183
Credit-g	0.577 ± 0.105	0.579 ± 0.118	–	–
Diabetes	0.873 ± 0.111	0.742 ± 0.122	0.744 ± 0.094	0.772 ± 0.083
Hepatitis	0.822 ± 0.236	0.799 ± 0.194	0.816 ± 0.229	0.781 ± 0.251
Ionosphere	0.700 ± 0.198	0.732 ± 0.160	0.701 ± 0.200	0.594 ± 0.178
Labor	0.520 ± 0.401	–	0.565 ± 0.406	0.710 ± 0.363
Sick	0.660 ± 0.101	–	0.822 ± 0.129	0.772 ± 0.087
Sonar	0.485 ± 0.202	0.519 ± 0.180	0.539 ± 0.172	0.654 ± 0.190
Vote	0.823 ± 0.121	–	0.779 ± 0.093	0.837 ± 0.133

6 Conclusion

This paper proposes several novel algorithms to solve the above said problem. The proposed algorithms are compared with each other. The experiments conducted with the proposed algorithm on eleven UCI datasets with evaluations metrics show that proposed algorithms are effective to solve the problem of “uniform effect.” In this part of the research, the proposed algorithms are applied to only binary datasets; the future extension of the algorithms can be done for the multi-class and high-dimensional dataset.

References

1. Xiong, H., Wu, J.J., Chen, J.: K-means clustering versus validation measures: A data-distribution perspective. *IEEE Trans. Syst. Man Cybern. B Cybern.* **39**(2), 318–331 (2009)
2. Lu, W.-Z., Wang, D.: Ground-level ozone prediction by support vector machine approach with a cost-sensitive classification scheme. *Sci. Total. Environ.* **395**(2–3), 109–116 (2008)
3. Huang, Y.-M., Hung, C.-M., Jiau, H.C.: Evaluation of neural networks and data mining methods on a credit assessment task for class imbalance problem. *Nonlinear Anal. R. World Appl.* **7**(4), 720–747 (2006)
4. Cieslak, D., Chawla, N., Striegel, A.: Combating imbalance in network intrusion datasets. In: *IEEE International Conference Granular Computing*, pp. 732–737 (2006)
5. Mazurowski, M.A., Habas, P.A., Zurada, J.M., Lo, J.Y., Baker, J.A., Tourassi, G.D.: Training neural network classifiers for medical decision making: The effects of imbalanced datasets on classification performance. *Neural Netw.* **21**(2–3), 427–436 (2008)
6. Freitas, A., Costa-Pereira, A., Brazdil, P.: Cost-sensitive decision trees applied to medical data. In: Song, I., Eder, J., Nguyen, T. (eds.) *Data Warehousing Knowl. Discov. Lecture Notes Series in Computer Science*
7. Kilic, K., Uncu, Ö., Türkmen, I.B.: Comparison of different strategies of utilizing fuzzy clustering in structure identification. *Inf. Sci.* **177**(23), 5153–5162 (2007)
8. Celebi, M.E., Kingravi, H.A., Uddin, B., Iyatomi, H., Aslandogan, Y.A., Stoecker, W.V., Moss, R.H.: A methodological approach to the classification of dermoscopy images. *Comput. Med. Imag. Grap.* **31**(6), 362–373 (2007)
9. Peng, X., King, I.: Robust BMPM training based on second-order cone programming and its application in medical diagnosis. *Neural Netw.* **21**(2–3), 450–457 (2008). Berlin/Heidelberg, Germany: Springer, 2007, vol. 4654, pp. 303–312
10. Guha, S., Rastogi, R., Shim, K.: Cure: an efficient clustering algorithm for large databases. In: *Proceedings International Conference ACM Special Interest Group Manage Data*, pp. 73–84 (1998)
11. Liu, M.H., Jiang, X.D., Kot, A.C.: A multi-prototype clustering algorithm. *Pattern Recognit.* **42**, 689–698 (2009)
12. Lago-Fernández, L.F., Aragón, J., Martínez-Muñoz, G., González, A.M., Sánchez-Montañés, M.: Cluster validation in problems with increasing dimensionality and unbalanced clusters. *Neurocomputing*, Elsevier **123**, 33–39 (2014)
13. Alejo, R., García, V., Pacheco-Sánchez, J.H.: An efficient over-sampling approach based on mean square error back propagation for dealing with the multi-class imbalance problem. *Neural Process Lett.*, Elsivier. doi:[10.1007/s11063-014-9376-3](https://doi.org/10.1007/s11063-014-9376-3)

14. Wang, Q.: A hybrid sampling SVM approach to imbalanced data classification. Hindawi Publishing Corporation Abstract and Applied Analysis, vol. 2014, p. 7. Article ID 972786. <http://dx.doi.org/10.1155/2014/972786>
15. Santhosh Kumar, N., Nageswara Rao, K., Govardhan, A., Sudheer Reddy, K., Ali Mirza, M.: Undersampled K -means approach for handling imbalanced distributed data. *Prog. Artif. Intell.* Springer. doi:[10.1007/s13748-014-0045-6](https://doi.org/10.1007/s13748-014-0045-6)
16. Brzezinski, D., Stefanowski, J.: Reacting to different types of concept drift: the accuracy updated ensemble algorithm. *IEEE Trans. Neural Networks Learn. Syst.* <http://dx.doi.org/10.1109/TNNLS.2013.2251352>
17. Poolsawad, N., Kambhampati, C., Cleland, J.G.F.: Balancing class for performance of classification with a clinical dataset. In: Proceedings of the World Congress on Engineering 2014, vol. I, WCE n, U.K
18. Oreški, G., Oreški, S.: An experimental comparison of classification algorithm performances for highly imbalanced datasets. Presented at CECIIS 2014
19. Stefanowski, J.: Overlapping, rare examples and class decomposition in learning classifiers from imbalanced data. *Emerg. Paradig. Mach. Learn. Smart Innov. Syst. Technol.* **13**, 277–306 (2013)
20. Tomašev, N., Mladenović, D.: Class imbalance and the curse of minority hubs. *Knowledge-Based Syst. J.* (2013). doi:<http://dx.doi.org/10.1016/j.knosys.2013.08.031>
21. Santhosh Kumar, Ch.N., Nageswara Rao, K., Govardhan, A., Sudheer Reddy, K., Mahmood, A.M.: Undersampled K -means approach for handling imbalanced distributed data. *Progress in Artificial Intelligence.* ISSN:2192-6352 *Prog. Artif. Intell.* **3**, 29–38 (2014). doi:[10.1007/s13748-014-0045-6](https://doi.org/10.1007/s13748-014-0045-6). Published in Springer-Verlag Berlin Heidelberg April 2014
22. Santhosh Kumar, Ch.N., Nageswara Rao, K., Govardhan, A., Sudheer Reddy, K.: Imbalanced K -means: An algorithm to cluster imbalanced—distributed data. *Int. J. Eng. Technol. Res. (IJETR).* vol.2, Issue-2, Feb. 2014. ISSN:2321-0869
23. Santhosh Kumar, Ch.N., Nageswara Rao, K., Govardhan, A., Sandhya, N.: Subset K-Means approach for handling imbalanced-distributed data. Springer International Publication Switzerland 2015—Emerging ICT for Bridging the Future—Proceedings of the 49th Annual Convention of the Computer Society of India CSI, vol. 2. Advances in Intelligent Systems and Computing, vol. 338. doi:[10.1007/978-3-319-13731-5_54](https://doi.org/10.1007/978-3-319-13731-5_54), 2015, pp. 497–508. Published in Springer International Publication Switzerland 2015
24. Blake, C., Merz, C.J.: UCI repository of machine learning databases. Machine-readable data repository. Department of Information and Computer Science, University of California at Irvine, Irvine (2000). <http://www.ics.uci.edu/mlearn/MLRepository.html>
25. Witten, I.H., Frank, E.: Data Mining: Practical Machine Learning Tools and Techniques, 2nd edn. Morgan Kaufmann, San Francisco (2005)

Augmenting Women's Safety-in-Numbers in Railway Carriages with Wireless Sensor Networks

Anusha Rahul, Vishnu Narayanan, Alin Devassy
and Anand Ramachandran

Abstract Sexual harassment of women traveling on railway carriages is a widespread problem. The predominant method used to address this problem is for women to travel in groups, utilizing Safety-in-Numbers, to hinder and discourage attacks against them. However, when the number of women in a railway carriage is low, there is no safety system in place to detect the imminent danger and proactively alert security personnel. In this work, we consider a system that keeps track of the number of passengers in a railway carriage using a wireless sensor network and automatically notifies security personnel when the number of passengers goes below a certain threshold. Here, we consider different scenarios and evaluate if our solution approach will work in the different cases considered. We also evaluated different techniques for automatically counting the number of people aboard a railway carriage. Our initial experimental results show that we are able to estimate the number of people in a room (considered in lieu of a railway carriage) with a high degree of accuracy using the background subtraction method. We hope that the proposed architecture in concert with the people counting technique will be able to significantly improve the safety of women traveling in railway carriages.

Keywords Background subtraction · Global system for mobile communications railway (GSM-R) · OpenCV/C++ · People counting · Wireless sensor network (WSN)

A. Rahul (✉) · A. Ramachandran
Amrita Center for Wireless Networks and Applications,
Amrita University, Coimbatore, India
e-mail: anusharahul@gmail.com

A. Ramachandran
e-mail: anandramachandran@am.amrita.edu

V. Narayanan
Department of Electronics and Communication Engineering,
Amrita University, Coimbatore, India
e-mail: vishnunarayananb@gmail.com

A. Devassy
Analog Devices Inc, Coimbatore, India
e-mail: aalinandu@gmail.com

1 Introduction

Today, traveling in trains is unsafe for women. The problem has become so exacerbated that several countries around the world, such as Brazil, Mexico, Egypt, Japan, Malaysia, Israel, Taiwan, and India, have introduced women-only railway carriages [1]. While this approach has stemmed the problem to a degree, numerous incidents of sexual predators targeting women-only railway carriages have been reported [2].

Women are frequently warned about traveling during off-peak hours, i.e., during early or late hours of the day, due to the risk of attacks against them. One way to solve this problem is for women to travel in groups, utilizing Safety-in-Numbers, to hinder and discourage attacks against them. However, when groups disperse, such as when different members of a group get off from a train at different stations, the few passengers left in a railway carriage are vulnerable to attack. Indeed, several incidents of sexual predators boarding a women-only railway carriage and attacking a lone passenger have been reported [3]. As a measure to counter this problem, several solutions have been proposed. Smartphone apps that can identify and report a crime [4], and manually triggered emergency alarms provided on-site (in several locations within a railway carriage) that can alert security personnel [5] are the most common of such solutions.

However, the aforementioned solutions are reactive and are activated only after an attack has taken place. This is primarily the case because victims are often unwilling to raise an alarm proactively, afraid of the embarrassment caused, if a prematurely raised alarm were to turn out to be false. There is thus a need for a system that would automatically detect an unsafe situation and notify authorities to take proactive action.

Proactive actions could be one or more of the following:

- (1) Notify a security guard (called a Railway Police Force Officer in some countries) to immediately board the railway carriage if possible and stand guard.
- (2) Notify a central monitoring authority so that the carriage in question could be monitored remotely, e.g., using live close circuit cameras.

In this paper, we propose one such automated system using wireless sensor networks, which monitors women-only railway carriages and provides a proactive notification in case an unsafe situation arises. Our solution hinges on the Safety-in-Numbers philosophy and assumes that attackers will likely not target women-only railway carriages where there are a significant number of women (see Fig. 1). We thus use wireless sensor networks and image processing techniques to monitor the number of women aboard a women-only carriage and trigger a warning signal when the number is below a certain threshold. As mentioned above, the signal is a proactive warning message and is delivered to a central monitoring authority who then forwards it to security personnel who can board the carriage and stand vigil. The message is further processed by the central monitoring authority



Fig. 1 The figure shows three separate situations of a women-only railway carriage. In case A, there are a large number of women in the carriage (*green dots*), and hence an attacker will be deterred from attacking anyone. In case B, there are only a few women in the carriage (*red dots*), and an attacker might attack or harass a woman. In case C, the wireless sensor network detects the presence of only a few women in the train and send a security officer (*blue triangle*) to stand guard in the carriage, effectively deterring any attack (colour figure online)

who besides monitoring the carriage remotely can also study the frequency, location, time, and other details of such warnings so as to improve the security situation further.

2 Assumptions

When the number of women in the carriage becomes low, the women-only railway carriage, which was a point of safety, now becomes an excluded spot and thus a dangerous place for women. Compartments of the local intra-city trains do not have access (in or out) to other compartments. Because of this isolated situation that they are in, we must design solutions where we expect that they will not get any help from the passengers in the other compartments.

The underlying assumptions that our solution approach hinges on are as follows:

- (1) Consider women-only railway compartments of local, intra-city trains, similar to the ones in different metros in India.
- (2) Compartments of these trains do not have access (in or out) to other compartments when the train is in motion (i.e., no vestibules).
- (3) Compartments have two entrances on each side, for a total of four entrances, two facing a platform, and the other two facing the train tracks.
- (4) Entrances may not have doors.

- (5) Current solutions rely on an alert mechanism that needs to be manually triggered if a miscreant attacks a woman, or even enters the compartment. In contrast, we target a problem where we send an automatic proactive alarm when the number of women in a women-only compartment is low.

3 Solution Approach

The proposed solution consists of a set of cameras that need to be installed in every woman's railway carriage (see Fig. 2). Along with the cameras, the compartment consists of a computational system that processes the images from the camera and estimates the number of people covered by each camera, a local aggregator for aggregating the count of people in the compartment and making a decision on whether to raise an alarm, and finally, a GSM-R transceiver for sending warning messages if the number of passengers in the compartment goes below a certain threshold.

When an unsafe situation is detected, the data is transmitted from the aggregator using wireless technology either to a base station or to Road-Side-Units which in turn transmit the data to a Central Control Room. The Central Control Room, in turn, transmits this message to the Engine Driver as well as to the railway protection force (RPF) officer appointed in the train. The RPF officer is now alerted to a potentially unsafe situation and should make his/her way to the affected carriage as soon as possible. Likewise, the Central Control Room could simultaneously monitor the railway carriage remotely, possibly using the live feed from the cameras. Now that the number of potentially dangerous situations is limited, the number of personnel needed for monitoring the women's carriages will be low.

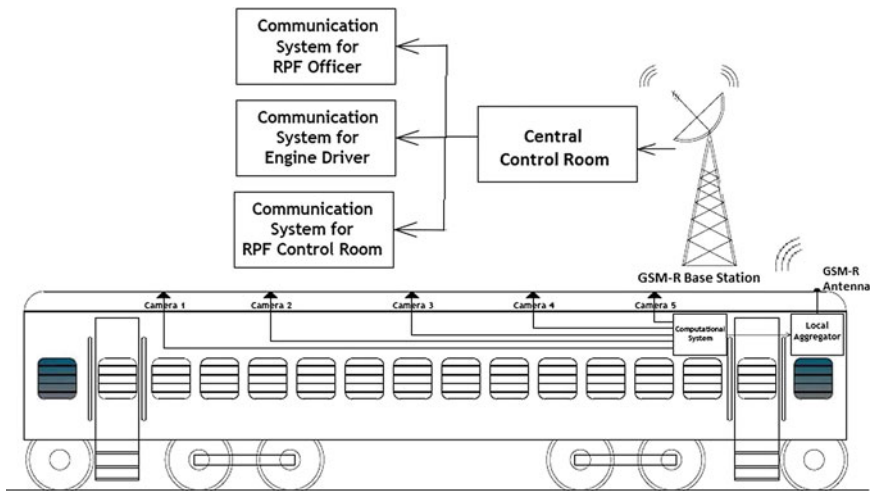


Fig. 2 Solution approach for augmenting women's safety-in-numbers in railway carriages

4 Related Work

The widespread problem with safety in railway carriages has fostered two basic approaches to solve the problem. We highlight these two approaches below.

Sun et al. [6] proposed a distributed surveillance system for monitoring the railway carriages using CCTV camera. Fuentes et al. [7] proposed a video surveillance system for improving personal security in public transport using image processing technique. Although the use of video surveillance technology has gained tremendous popularity in security systems, it is still not an apt deterrent technology. The main purpose of the system is to try to identify a criminal using footage of a crime scene. Although the system indirectly provides some deterrence since it scares the criminal into believing that he could be caught, it can only be a secondary method and not the primary method for preventing attacks. Furthermore, video data at reasonable resolutions requires tremendous bandwidth, which is often infeasible. Last, but not the least, monitoring several hundreds of video feeds manually is a mundane task. As a result, video footage is not monitored effectively in real time, allowing attackers to escape from a crime scene before a timely alarm can be raised.

The other method that has gained popularity in recent times is the use of mobile phones and smart phone apps to record criminal activity and/or seek help during danger. Once again, this method is not a powerful deterrent, as victims tend to ask for help only when attacked and not proactively when they sense a vulnerable situation. Yet another problem that plagues this method is the fact that cellular network coverage is often poor and limited along railway lines. This lack of coverage, if consistent in certain areas could be used effectively by a malicious attacker as a point of attack. After an exhaustive study of related work, we concluded that there exists no effective and proactive system for ensuring safety in women-only railway carriages.

The advantage of our proposed method is that an alert signal is sent proactively when the passengers in a railway carriage are in a vulnerable position. This enables security personnel to direct their attention to a small area and avert the attack in the first place.

Since our solution depends upon estimating the number of people in a railway carriage by analyzing the video images from a camera, we studied several known techniques used for people counting. Merad et al. [8] proposed a Fast People Counting System based on Head Detection from skeleton graphs. They used background subtraction method for head detection and estimated the number of people in a room. This method, though fairly accurate, suffers from the drawback that the result can be easily corrupted when many people are close together.

Our algorithm for people counting uses a variant of background subtraction along with assumptions on the average width and girth of a person. This helps us estimate the number of people accurately in situations when the number of people is low.

In our proposed solution, the alert message can be communicated in railway systems using GSM-R Technology. GSM-R [9] supports voice/data communication between drivers/guards of trains, train controllers, and station masters. This network is extremely reliable and can be used for our communication purposes.

5 Implementation of People Counting

The most critical part of this project was to accurately and quickly determine the number of people in a women-only railway carriage. As a first step, we took an existing video of people entering and exiting a room and as seen from above the door and tried to estimate the number of people in the room using this information.

Barandiaran et al. [10] proposed a real-time people counting technique using multiple lines and optical flow for detecting direction. We developed an algorithm incorporating back ground subtraction, width analysis, direction detection using OpenCV library. We describe the algorithm used in this program below.

Algorithm

- Step 1: Take video as input and store the first image (i.e., image without people) from video as background
- Step 2: Process video frame by frame
- Step 3: Select the area of interest i.e., up line and down line
- Step 4: For knowing the presence of people passing through the line, subtract real-time frame from image without people
- Step 5: From the presence of lines find the maximum occupied width
- Step 6: Draw the lines without flicker when people have crossed it completely
- Step 7: Do width analysis for knowing the no. of people i.e., either 1, 2, or 3
- Step 8: Identify the direction of flow i.e., towards the area of interest or away from the area of interest
- Step 9: Increment the count if the direction of flow is towards the area of interest
- Step 10: Decrement the count if the direction of flow is away from the area of interest
- Step 11: Calculate the number of people in the area of interest
No. of people towards the area of interest-No. of people away from the area of interest
- Step 12: Return this number as people count

6 Experimental Setup

Our experimental setup consists of a room with a single point of entry, i.e., single door. On the top of this door which is mounted a Logitech C270 Webcam [11]. The camera is connected via USB to a core i5 computer having 4 GB RAM which studies the video stream of people entering and exiting the doorway. The computer processes the video feed with two horizontal lines that are used to determine the direction of movement of people, viz., entering or exiting the room. In future, we would like to replace the computer with a Raspberry Pi [12]/Beagle Board [13] or any other single-board processor.

7 Experimental Results

The people counting program was tested using an .mp4 video feed of people entering and exiting a doorway. The video gives a top view of people at a door and can thus be used to determine the number of people who are currently in the room. Our program measured the number of people entering the room using an Up counter, and the number of people exiting the room using a Down counter. When a person crossed the lower horizontal “green” line first and then crossed the upper horizontal “green” line, we assumed that he/she was entering the room and incremented the Up counter. We similarly incremented the Down counter when a person left the room. The difference between the two counters gave us the number of people in the room.

When tested on this input, our program gave perfect results with no errors. Figures 3 and 4 show the two different snapshots of the program in action. In the figure on the left, 6 people are in the room, while in the one on the right; one person has left, leaving behind 5 people in the room.

We have currently succeeded in counting the number of people passing through a doorway and thereby estimating the number of people in a room accurately. Our future work is to come up with an algorithm that would determine the threat level based on the number of women in the railway carriage. Based on initial surveys and brainstorming, we feel that if the number of women in a railway carriage is below 3, then we should raise an alarm and notify the authorities of a potentially unsafe situation. This threshold is currently ad hoc and needs to be studied extensively in order to solidify the algorithm and solution further.

Fig. 3 Result 1



Fig. 4 Result 2



8 Research Challenges

There are a few key scenarios that need to be studied for the system to be appreciated.

These scenarios have been described below:

A. Scenario 1: Train in a tunnel

Consider the situation shown in Fig. 5. The figure shows a potentially dangerous situation that could develop. An attacker might enter the railway carriage when the train is passing slowly through a long tunnel. The system needs to be able to detect the occurrence of a breach and an intrusion and signal an automatic alert. Perhaps more importantly, wireless systems will not function in a tunnel. Furthermore, the system requires infrastructural support in the form of base stations of GSM-R or Road-Side-Units so that the moving train can communicate with security personnel and to the central authority boarded in the station without any loss of information [9].

B. Scenario 2: Miscreants hidden in the carriage

Consider the situation shown in Fig. 6. The figure shows yet another potentially dangerous situation that could develop. A male attacker might enter the railway carriage in disguise (as a woman) and hide in some part of the railway carriage, say

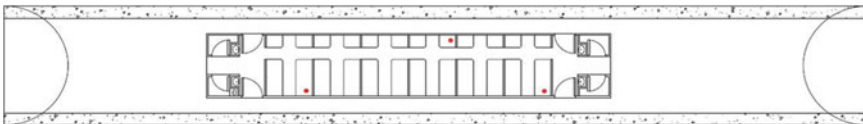


Fig. 5 Train in a tunnel could pose potential communication problems

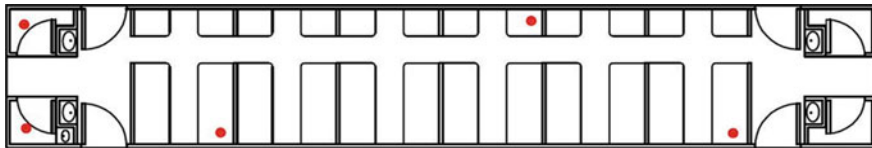


Fig. 6 Miscreants hidden in a railway carriage might evade detection

the restroom. The people counter would have originally picked him up and would therefore include him in the people count and not potentially set-off the alarm. The attacker could then come out of the restroom when the train is on its way and attack the victim. This is not a simple scenario to detect and thwart. One possible solution would be to monitor traffic outside the restroom and set off an alarm if necessary. Counting the people accurately is also a research challenge. When the train departs from a station, people tend to rush into the compartments leading to a miscount.

9 Conclusion

In this paper, we propose a novel solution for ensuring the safety of women passengers traveling in a railway carriage. We depend of the philosophy of Safety-In-Numbers, whereby sexual predators targeting women will be deterred from attacking women who are traveling in large groups, that too in the confines of a women-only railway carriage. However, when the number of women in the carriage becomes low, what was initially a point of safety, now becomes an excluded spot and thus dangerous place for women. We propose a solution to count the number of people in a women-only railway carriage and notify security personnel if the count is below a threshold. We claim that our system is proactive and automatic and is therefore a better deterrent than reactive systems that rely on mobile phones or alarm triggers.

Our solution is as yet simplistic. We need to consider situations and scenarios where an attacker might be hidden in parts of the railway carriage, e.g., the restrooms, and attack a victim. Again, a miscreant might board the train while it is exiting a railway station and thus offset the people counter and push the limit past the threshold, giving the appearance that the carriage is safe while it is actually not the case. We intend to study these outliers and provide a comprehensive solution to the problem. In addition we intend to build prototypes and test the solution in the field.

Acknowledgments We would like to express our sincere gratitude to our respected teachers, friends, and family for their continued love and support. Our sincere thanks are due to the Department of Wireless Networks and Applications, which provided the tools, infrastructure, and equipment as well as the opportunity and impetus to do this research. We would also like to express our gratitude to our beloved Chancellor Sri. Mata Amritanandamayi Devi (AMMA) for the immeasurable motivation and encouragement that she has provided for doing this work.

References

1. http://en.wikipedia.org/wiki/Women-only_passenger_car
2. <http://www.ndtv.com/article/world/thailand-to-re-launch-women-only-train-carriages-564390>
3. <http://www.thehindu.com/news/national/kerala/at-a-glance-soumya-rape-and-murder-case/article2618029.ece>
4. <http://timesofindia.indiatimes.com/city/mumbai/Soon-women-on-WR-locals-can-use-app-to-call-RPF-personnel-for-help/articleshow/39771156.cms>
5. Fracchia, R., Meo, M.: Alert service in VANET: analysis and design. In: Proceedings of the International Symposium on Wireless Vehicular Communications (WiVeC) (2013)
6. Sun, J., Velastin, S.A., Lo, B.: A distributed surveillance system to improve personal security in public transport. In: Proceedings of the European Workshop for the Integration of Knowledge, Semantics and Digital Media Technology (2004)
7. Fuentes, L.M., Velastin, S.A.: Assessment of Image Processing as a means of Improving Personal Security in Public Transport, Book Chapter. Video Based Surveillance Systems (2001)
8. Merad, D., Aziz, K.E., Thome, N.: Fast people counting using head detection from skeleton graph. In: Seventh IEEE International Conference on Advanced Video and Signal Based Surveillance (2010)
9. Rao, P.: Gsm-r global system for mobile communication-railway, CSI Communications (2012)
10. Barandiaran, J., Murguia, B., Boto, F.: Real-time people counting using multiple lines. In: 9th IEEE International Workshop on Image Analysis for Multimedia Interactive Services (2008)
11. Logitech C270 Webcam: <http://www.logitech.com/en-in/product/hd-webcam-c270>
12. Raspberry Pi: <http://www.raspberrypi.org/>
13. Beagle Board: <http://beagleboard.org/BLACK>

Analysis of Student Feedback by Ranking the Polarities

**Thenmozhi Banan, Shangamitra Sekar, Judith Nita Mohan,
Prathima Shanthakumar and Saravanakumar Kandasamy**

Abstract Feedbacks in colleges and universities are often taken by means of online polls, OMR sheets, and so on. These methods require Internet access and are machine dependent. But feedbacks through SMS can be more efficient due to its flexibility and ease of usage. However, reliability of these text messages is a matter of concern in terms of accuracy, so we introduce the concept of text preprocessing techniques which includes tokenization, parts of speech (POS), sentence split, lemmatization, gender identification, true case, named entity recognition (NER), parse, conference graph, regular expression NER, and sentiment analysis to improve more accurate results and giving importance even to insignificant details in the text. Our experimental analysis on sentiment trees and ranking of feedbacks produces exact polarities to an extent. By this way, we can determine better feedback results that can be supplied to the faculty to enhance their teaching process.

Keywords Sentiment analysis · Feedback analysis · Polarity calculation · Ranking

T. Banan (✉) · S. Sekar · J.N. Mohan · P. Shanthakumar · S. Kandasamy
School of Information Technology and Engineering, VIT University,
Vellore, India
e-mail: thenmozhi.b2013@vit.ac.in

S. Sekar
e-mail: s.shangamitra2013@vit.ac.in

J.N. Mohan
e-mail: judithnita.m2013@vit.ac.in

P. Shanthakumar
e-mail: s.prathima2013@vit.ac.in

S. Kandasamy
e-mail: ksaravanakumar@vit.ac.in

1 Introduction

Feedback is considered as one of the best approaches for appraisal everywhere. Professors are very much interested in knowing the feedbacks about their teaching practices which is usually a blend of professional and personal aspects, through which the professors will be able to make improvements on their teaching skills. This kind of motivation helps in investing more time and effort, which is necessary to deliver a good lecture. There are many traditions to obtain feedbacks from students; some are intended to give verbal or written comments in a clear-cut way, while others are like questionnaires, but this may impose some restrictions on the preference of answers due to the amount of choices that are kept fixed [1].

Although these methods were used for a good amount of time assuming that they produce reliable and effective results, they do possess some shortcomings based on the factors like specificity, timeliness, and manner. Due to the evolution of computers, the paper feedbacks were electronically processed to get reliable and accurate results in time, for instance OMR (optical mark recognition) for processing human-marked documents or forms to conclude the results on tests or surveys. In due course of time, many websites and blogs offer polling through which they collect information in the form of feedbacks. These methods remain popular till date, but we have to consider about the people who are inaccessible to any of these things. This leads to the thought of finding a replacement for the above stated approaches, which is available for almost everyone. The mobile phone and its text messaging features are considered as affordable and easy way for offering feedbacks. Online surveys are another way of gathering feedbacks but in [2], they have mentioned that students give less response to give feedbacks, but when it comes to SMS feedback it is easy to type from a place and send it in fraction of seconds without Internet.

SMS has been a buzzword for the younger generation since its launch. Short message service is one of the extensively used data application with an average of 3.5 billion active users which is about 80 % of mobile phone users during 2010 [3]. A standard SMS text uses 140 bytes (octets) per message, which translates to 160 characters (7 bits bytes) of the English alphabet using 7-bit encoding or as few as 70 characters for languages using non-Latin alphabets using UTF-16 encoding [3]. Using the text messages, a feedback mechanism can be a good choice for better and efficient results. Leong et al. processed the text messages that are received as feedbacks, through text mining and sentiment analysis [4]. The uncertainties of the text messages were also handled through different models and the best one out of them was chosen, and the percentages of positive and negative feedbacks were calculated at the end. Since the input in this process is text messages and each text varies based on the meaning and domain, the context plays a major role in retrieving [5]. The process of sentiment mining is mostly used in social networks to value the customer relationship which in turn helps the company or the product to be improved [6].

Information gathering paves a new way for technology improvement, which could be achieved better by a rich opinion resource than the fact-based analysis. Opinion mining with sentiment analysis helps to reveal the subjectivity of the text with seamless opinion and sentiment which directly assists opinion-oriented information-seeking systems [7]. Garcia-Sanchez et al. introduced an innovative approach to resolve the drawbacks faced in their proposed model [8]. They used ontology-based feature selection; vector analysis has been performed in sentiment mining and in addition to SentiWordNet, they had used different methods in polarity identification.

Text categorization [9] is another process involved in mining using the saved corpus. Here, the concept called feature selection plays a major role. In common, feature selection could be made of high-frequency term occurred in the document or corpus, but they have used student's t test which gives distribution range of the term frequency in the corpus for appropriate feature selection [10]. Finally, ranking gives the result of the feedback given for the faculty.

1.1 Literature Survey

Hogenboom et al. have proposed a work where an additional target language has been supported in sentiment lexicon. The reference language is analyzed for the given text, and mapping their sentiment scores to a new target language of sentiment lexicon based on their relations between the lexicons. In this paper, the lexicon-based sentiment analysis method is used for English as a reference language and Dutch as another language. Sentiment of seed words in a semantic lexicon is considered for the target language. They have focused on 600 positive and 600 negative Dutch documents for sentiment classification, and this classification uses regular expressions to divide the words. POS and lemmatization are done for better sentiment accuracy of words [11].

Ortigosa et al. have proposed a method for sentiment analysis in Facebook. It helps to extract the sentiment polarity of the user text and the major emotional changes are detected like smileys. This method has been followed in a Facebook application called SentBuk that retrieves the user messages from Facebook. These messages are classified and polarity is shown through an interface to the users and also supports emotion finding, statistics among the users. This classification method has used the hybrid approach where lexicon-based and machine learning techniques are followed. The phases behind this approach are (i) message classification, (ii) preprocessing, (iii) tokenization, (iv) emotion detection, and (v) interjection detection [12]. This approach has acquired 83.7 % of accuracy. The paper also talks about the E-learning system where the emotional feedbacks about the user can be taken into consideration for better learning systems which are deeply discussed.

Xiaofei et al. have proposed a work to categorize the text based on K-means algorithm which in turn uses centroids for feature selections [14]. Using centroid detection for feature selection helps in avoiding the direct feature search or feature

evaluation. Here, the cluster of centroids which is highly relevant to the class is chosen as a feature for text categorization. In this paper, the authors have used cosine distance and Euclidean distance as the two metrics for collecting features and they have experimented the feature selected with three classifiers, namely, k -NN, NC, and SVM. As a result, NC, k -NN, and SVM methods with k -means feature selection (KMF) outperform original methods without KMF. SVM is better in accuracy but in running time, KMF is faster than all three original methods. In addition to this, they have observed that for similar distance in k -means, the cosine distance is more suitable than Euclidean distance in feature selection. From this paper, it is proven that the text categorization is improved in accuracy using k -means feature selection [13].

Iman et al. have proposed a work to identify the semantic orientations of words in resource-lean languages. This method computes the polarity of foreign nodes based on their semantic relations with two sets of positive and negative English nodes. ‘Morkov random walk model’ used on a semantic network of words to identify the polarity of words. Semantic network construction assumes that there is a correlation between two node senses and lemmaPOS. In a semantic network, mixing different senses of a word in a lemmaPOS decreases the accuracy of relations between nodes, since different senses of a word may have different semantic orientations [15].

Emma et al. have proposed a work to explore text processing in the field of sentiment analysis. In this paper, they have used SVM machine learning classifier instead of linguistic methods and lexicon-based methods in sentiment classification. The text preprocessing is achieved by cleaning up the noises over the text which in turn gives proper dimension. The preprocessing is carried out through many steps like white space removal, online text cleaning, stemming, expanding abbreviation, negation handling, stop words removal, and feature selection based on syntactic position, and at last it is called as transformation. Then filtering is attained through chi-squared statistical analysis. Here, they have experimented different data in testing the importance of feature using methods like feature frequency (FF), term frequency-inverse document frequency (TF-IDF), and feature presence (FP) [16]. The dataset with no preprocessing and preprocessed data with classifiers is tested, where preprocessed data resulted with more accuracy. And the dataset with chi-squared filtering and without filtering is tested, where data with filtering achieved more precision. In both the case, FP attained highest accuracy with processed and filtered data, and thus the text preprocessing has played major role in accurate sentiment analysis.

2 Detailed Description

We have used a model for text processing and sentiment analysis on feedbacks called the “Sentiment tree bank model” by Stanford University [18]. Generally, text processing is not being done in an efficient way. It requires a lot of supervised

training, evaluation of resources, and powerful modules for optimized results. To overcome this shortcoming, the sentiment detection tree bank model is used. This model performs text processing and sentiment analysis using the components of natural language processing systems like tokenization, sentence split, parts of speech (POS), lemmatization, named entity recognition (NER), gender, true case, parse, regular expression NER, conference graph, and sentiment [17, 18].

2.1 Text Processing

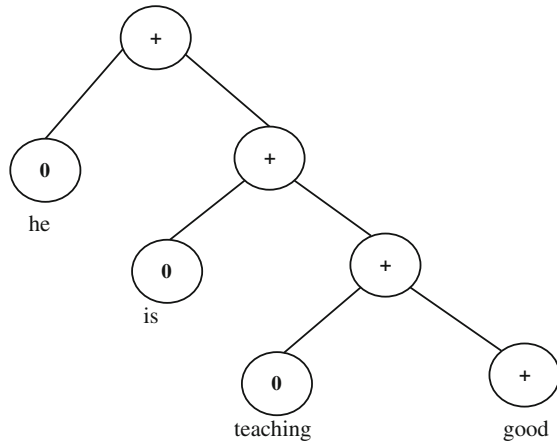
In *Tokenization*, the sentences are broken into words and phrases called tokens. These tokens become the input for the further phases like text mining or parsing. There are different types of tokenizers like PTBTokenizerAnnotator, used to tokenize the text and saves the character offsets of each token in the input feedback. Comparison of tokenizers like Stanford tokenize, OpenNLPTokenizer, customer parser, hypothetical tokenizer, and naive white space parser is been explained in [19]. Out of which naive whitespace parser exhibits the poor part of tokenizing. The hypothetical tokenizer supports better tokenization, the tokens are separated by punctuators or whitespaces which may or may not be in the token list, and this is extended to handle noisy text. This is also known as word segmentation. For instance, consider the input feedback “Your teaching is good.” These words are treated as a single semantic group for further processing. Now the feedback will be tokenized as “your,” “teaching,” “is,” and “good”. Heuristics rules for tokenization are followed to remove the blank spaces, brackets, slashes, and quotation marks [20]. Related forms of words are analyzed in stemming which does not deal about parts of speech (POS). It is said that porter stemmer gives less error rate and produces best output in [21]. The rules of porter stemmer are modified as context-aware stemmer in [21] and it has produced 93.3 % of meaningful words. In *Parts of speech*, each token is tagged with a POS label like verb, noun, adjective, etc. For instance, “he is teaching good” is recognized as he(s) is(p) teaching(v) good (A). In *Sentence split*, a sequence of tokens is split into sentences [19]. In *Lemmatization*, the lemmas for all tokens are generated in the corpus. It is the processes of grouping different inflected forms of a word so that they can be evaluated as a single item. It is used to produce the word lemma for all tokens in the corpus in a dictionary form. It is for full text and separation between words based on the POS which have dissimilar meaning. Lemmatizer is made to run before parsing because stems along with the POS which in turn can be used to find lemma [22]. In *named entity recognition* (NER), the named entities like PERSON, LOCATION ORGANIZATION, and numerical entities like DATE, TIME, MONEY and NUMBER are recognized. Named entities are recognized using CRF sequence taggers trained on various corpora. Numerical entities are recognized using a rule-based system. One of the ways of entity detection is chunking which usually selects a subset of tokens. Chunked grammar indicates how the sentences are chunked. A rule says that chunker has to find an optional determiner, adjectives,

and then a noun. With the same example, chunk parser is created and tested. Result obtained will be a tree [23]. In *true case*, the tokens is recognized in the text where the detail was lost, e.g., all upper case text. The token text is adjusted to match its true case. In Parse, full syntactic analysis is provided using the constituent and the dependency representations. In *Regular Expression NER*, a simple rule-based NER over token sequences using Java regular expressions is implemented. The goal is to provide a simple framework to incorporate named entity labels that are not annotated. For example, the list of regular expressions that is distributed in the file recognizes ideologies as (IDEOLOGY), nationalities as (NATIONALITY), religions as (RELIGION), and titles as (TITLE). In *Coreference graph*, pronominal and nominal coreference resolution algorithms are implemented. The complete coreference graph with head words is mentioned as nodes, which is saved in the corresponding annotation.

2.2 Sentiment

Socher et al's sentiment model is implemented. A binary tree of the sentence is attached to the sentence level CoreMap. The nodes of the tree then contain the predicted scores for this sub-tree. The sentiments are classified into positive (+), and very positive (++) , neutral (0), and very negative (-), negative (-). The sentences get divided by tokenization and other concepts explained before. The root node of the tree will have the final sentiment of the input feedback; child node will have the result of the leaf node; and the leaf node will have the word. For instance a sentiment tree is represented as shown in Fig. 1 [18].

Fig. 1 Sentiment tree



2.3 Ranking

It is the process of identifying the relationship between two and more items [24]. Ranking is considered in many problems from web search engine to produce recommendation, and usually this process will give solution to many problems. The ranking process has been done for recommending the product over the website and here the feedback is taken as implicit, i.e., the number of clicks or views made by the customers [25]. And also they have conducted Bayesian analysis for personalized ranking. In social network, the problem of ranging comes when ranking two profiles by the rating given by others to each of them; here, the ratings depend on each other rate indirectly. The result of this process gives the most popular or rated profile; for this type of ranking, they uses Facemash algorithm in social network [26]. This is one of the processes of ranking individuals rather than products and movies, but the ranking is done among two individuals alone.

3 Proposed Architecture

After text preprocessing and sentiment analysis as mentioned above, next, we perform the ranking process as represented in Fig. 2. We have ranked a set of feedbacks given for a particular faculty for the particular course. This process is taken into account for the purpose of categorizing the faculty in their course, helps faculty to improve their teaching process, and also might be helpful in future for promotion or any awards to the faculty. The input of this process is the output obtained from the sentiment analysis, so that the input will be a set of positive and negative with their percentile in each category. Using the statistics with the percentile obtained in the sentiment analysis, categorization can be done. By applying the algorithm, results can be determined whether the feedback obtained for the faculty is positive or negative, or neutral.

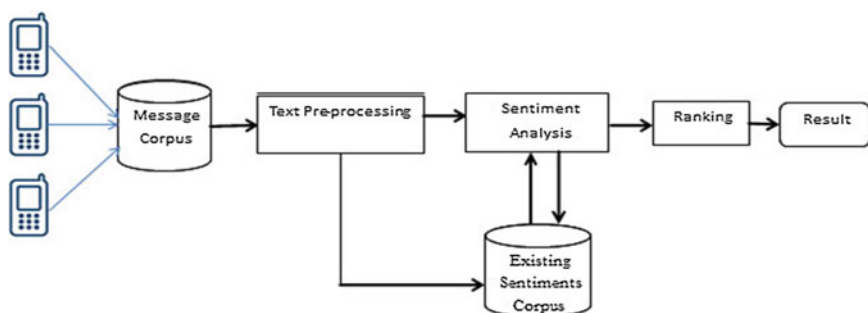


Fig. 2 Feedback processing model

Algorithm 1: In this, let us consider the parameters like very negative as ‘vn,’ negative as ‘n,’ neutral as ‘nu,’ positive as ‘p,’ and very positive as ‘vp.’ And let ‘N’ be the number of feedbacks given for the faculty and ‘i’ be some variable ranging from ‘0’ to ‘N’.

Polarity Determination Algorithm

Input: 1 to N histogram with feedback values {vn, n, nu, g, vg}

Output: Identifies the polarity of the cumulative feedback as positive, neutral, and negative.

For i equal to 1 to N

Repeat

$$\sum \text{vn} + = \text{vn}_i; \quad \sum \text{n} + = \text{n}_i; \quad \sum \text{nu} + = \text{nu}_i; \quad \sum \text{p} + = \text{p}_i; \quad \sum \text{vp} + = \text{vp}_i;$$

End Loop

$$\text{vn} = \sum \text{vn}/N; \quad \text{n} = \sum \text{n}/N; \quad \text{nu} = \sum \text{nu}/N; \quad \text{p} = \sum \text{p}/N; \quad \text{vp} = \sum \text{vp}/n;$$

$$\text{Neg} = \text{vn} + \text{n}/2;$$

$$\text{Pos} = \text{vp} + \text{p}/2;$$

If Neg == Pos then

Res = nu;

Else

Res = Max[Neg, Pos]

End if

Stop

In step 3, the summation of each category is calculated, followed by the mean of each sum. In steps 6 and 7, considering the assumption that twice the negative value is a very negative value and twice the positive value is a very positive value, we calculate the actual positive and negative values using the formula as given in the algorithm. In step 8, we check if the positive and negative values are equal, and if true the neutral value is given as the result. Otherwise, the maximum of negative or positive value is given as the result. This process gives a statistical report of the percentile of each category given, which gives the total prediction about the feedbacks given to the faculty for a particular subject.

4 Experimental Analysis

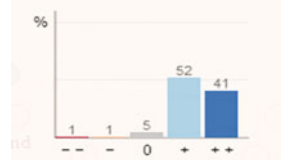
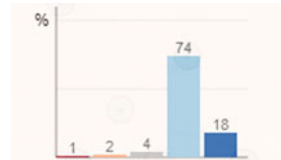
We have used the dataset of the movie reviewing website “rotten tomatoes” [28] available in the “Recursive Deep Models for Semantic Compositionality over a Sentiment Treebank” project of the Stanford Natural Language Processing Group

official website. This dataset has about 2,15,154 phrases in the parse trees of 11,855 sentences [27]. We have analyzed the dataset and found that the model produces convincingly accurate results. Some of the results of the student feedbacks are sent through SMS and the available movie reviews are shown below.

4.1 Polarity Determination

The sample student feedbacks are listed in Table 1 from S. no.1 to 6 which is collected randomly from students of our department. Having got the percentages of the polarity from the above table, we process the results for the final step called “Ranking.” The below Table 2 is obtained by applying the “Polarity Determination” algorithm which depicts the measure of scale indicating the

Table 1 Polarity analysis

S. no.	Sentence	Expected result	Obtained result	Accuracy														
1	I was stunned that we came up with some good ideas and solved some problems right during the class	Positive	Positive	 <table border="1"> <caption>Data for Sentence 1</caption> <thead> <tr> <th>Polarity</th> <th>Percentage (%)</th> </tr> </thead> <tbody> <tr> <td>1</td> <td>1</td> </tr> <tr> <td>1</td> <td>1</td> </tr> <tr> <td>5</td> <td>5</td> </tr> <tr> <td>0</td> <td>0</td> </tr> <tr> <td>+</td> <td>52</td> </tr> <tr> <td>++</td> <td>41</td> </tr> </tbody> </table>	Polarity	Percentage (%)	1	1	1	1	5	5	0	0	+	52	++	41
Polarity	Percentage (%)																	
1	1																	
1	1																	
5	5																	
0	0																	
+	52																	
++	41																	
2	I had been dreading to take this course, but this turned out to be very interesting and enthusiastic because of your teaching	Positive	Positive	 <table border="1"> <caption>Data for Sentence 2</caption> <thead> <tr> <th>Polarity</th> <th>Percentage (%)</th> </tr> </thead> <tbody> <tr> <td>1</td> <td>2</td> </tr> <tr> <td>2</td> <td>4</td> </tr> <tr> <td>4</td> <td>0</td> </tr> <tr> <td>0</td> <td>74</td> </tr> <tr> <td>+</td> <td>18</td> </tr> <tr> <td>++</td> <td>0</td> </tr> </tbody> </table>	Polarity	Percentage (%)	1	2	2	4	4	0	0	74	+	18	++	0
Polarity	Percentage (%)																	
1	2																	
2	4																	
4	0																	
0	74																	
+	18																	
++	0																	
3	I am very satisfied with his teaching	Positive	Positive	 <table border="1"> <caption>Data for Sentence 3</caption> <thead> <tr> <th>Polarity</th> <th>Percentage (%)</th> </tr> </thead> <tbody> <tr> <td>1</td> <td>7</td> </tr> <tr> <td>2</td> <td>28</td> </tr> <tr> <td>4</td> <td>28</td> </tr> <tr> <td>0</td> <td>29</td> </tr> <tr> <td>+</td> <td>8</td> </tr> <tr> <td>++</td> <td>0</td> </tr> </tbody> </table>	Polarity	Percentage (%)	1	7	2	28	4	28	0	29	+	8	++	0
Polarity	Percentage (%)																	
1	7																	
2	28																	
4	28																	
0	29																	
+	8																	
++	0																	
4	I cannot understand what he teaches and the teaching must be little more detailed	Negative	Negative	 <table border="1"> <caption>Data for Sentence 4</caption> <thead> <tr> <th>Polarity</th> <th>Percentage (%)</th> </tr> </thead> <tbody> <tr> <td>1</td> <td>13</td> </tr> <tr> <td>2</td> <td>57</td> </tr> <tr> <td>4</td> <td>24</td> </tr> <tr> <td>0</td> <td>4</td> </tr> <tr> <td>+</td> <td>2</td> </tr> <tr> <td>++</td> <td>0</td> </tr> </tbody> </table>	Polarity	Percentage (%)	1	13	2	57	4	24	0	4	+	2	++	0
Polarity	Percentage (%)																	
1	13																	
2	57																	
4	24																	
0	4																	
+	2																	
++	0																	

(continued)

Table 1 (continued)

S. no.	Sentence	Expected result	Obtained result	Accuracy
5	He used to discourage the students when he was asked a question and also possesses attitude	Negative	Negative	
6	The problem worked in the class does meet our needs. The course is boring and not useful	Negative	Negative	

Table 2 Polarity value table

Scale	F1	F2	F3	F4	F5	F6	Σ	Mean
--	1	1	7	13	7	6	35	5.8
-	1	2	28	57	42	66	196	32.6
0	5	4	28	24	26	27	114	19
+	52	74	29	4	22	2	183	30.5
++	41	18	8	2	4	0	73	12.16

following symbols ‘--’ as very negative, ‘-’ as negative, ‘0’ as neutral, ‘+’ as positive, and ‘++’ as very positive. F1 through F6 shows the student feedback. The summation (Σ) and mean of the same are calculated. From this table values, the actual ‘Neg’ and ‘Pos’ values are calculated:

$$\text{Neg} = 5.8 + 32.6/2 = 22.1$$

$$\text{Pos} = 12.16 + 30.5/2 = 27.41$$

From the two values, it is analyzed that the result for the supplied dataset is positive. Similarly, we can calculate the feedback results for any faculty.

5 Conclusion

Our model incorporates the following phases namely text preprocessing, sentiment analysis, and ranking. In text preprocessing and sentiment analysis, each feedback is split into words and their polarities are identified. On applying polarity determination algorithm, we are able to find overall polarity of the feedbacks for the corresponding faculty. These are further analyzed using text preprocessing,

sentiment mining, and categorization phases where the abstract texts are removed and the polarity is identified by which the faculty is categorized based on the feedbacks. Through this process, the faculty will be able to know their lecture feedback in a reliable manner. We conclude that our idea can give convincing results on the feedbacks that are sent through short message service. Also the students can convey their feedback on the teaching process of the faculty. Thus, the faculty and the students are equally benefitted by improving their lecture delivery that in turn increases the interest of the students toward the course.

References

1. Forster, F., Hounsell, D., Thompson, S.: *Handbook on Tutoring and Demonstrating*. University of Edinburgh, London (1995)
2. Gathering Feedbacks from Students. <http://cft.vanderbilt.edu/guides-sub-pages/student-feedback>
3. Wikipedia Text messaging. http://en.wikipedia.org/wiki/Text_messaging
4. Leong, C.K., Lee, Y.H., Mak, W.K.: Mining sentiments in SMS texts for teaching evaluation. *Expert Syst. Appl.* **39**, 2584–2589 (2012)
5. Zhang, L., Wang, X., Zhang, L., Chen, Y., Shi, Y.: Context-based knowledge discovery and its application. In: DM-IKM'12 Proceedings of the Data Mining and Intelligent Knowledge Management Work. ACM, New York, USA (2000)
6. Mostafa, M.M.: More than words: social networks' text mining for consumer brand sentiments. *Sci. Direct J. Expert Syst. Apps.* **40**, 4241–4251 (2014)
7. Pang, B., Lee, L.: Opinion mining and sentiment analysis. *ACM J. Found. Trends Info. Ret.* **2**, 1–135 (2008)
8. Martinez, I.P., Sanchez, F.G., Garcia, R.V.: Feature-based opinion mining through ontologies. *Sci. Direct J. Expert Syst. Apps.* **41**, 5995–6008 (2014)
9. Crammer, K., Singer, Y.: On the algorithmic implementation of multiclass kernel-based vector machines. *J. Mac. Learn. Res.* **2**, 265–292 (2001)
10. Wang, D., Zhang, H., Liu, R., Wang, W.L.D.: T-test feature selection approach based on term frequency for text categorization. *Sci. Direct J. Pat. Recogn. Lett.* **45**, 1–10 (2014)
11. Hogendoorn, A., Heerschop, B., Frasincar, F., Kaymak, U., Jong, F.D.: Multi-lingual support for lexicon-based sentiment analysis guided by semantics. *Sci. Direct J. Decis. Support Syst.* **61**, 43–53 (2014)
12. Ortigosa, A., Martín, J.M., Carro, R.M.: Sentiment analysis in Facebook and its application to e-learning. *Comp. Human Behav.* **31**, 527–541 (2014)
13. Zhou, X., Hu, Y., Guo, L.: Text categorization based on clustering feature selection. In: 2nd International Conference on Information Technology and Quantitative Management, vol. 31, pp. 398–405 (2014)
14. Amorim, R.C.: Learning feature weights for K-means clustering using the Minkowski metric. Ph. D thesis, University of London, UK (2011)
15. Dehdarbehbahani, I., Shakery, A., Faili, H.: Semi-supervised word polarity identification in resource-lean languages. *Neural Net.* **58**, 50–59 (2014)
16. Haddi, E., Liu, X., Shi, Y.: The role of text pre-processing in sentiment analysis. *Int. Conf. Inf. Technol. Quant. Manage.* **17**, 26–32 (2013)
17. About Sentiment Analysis. <http://nlp.stanford.edu/sentiment/index.html>
18. Sentiment Analysis Tree Bank. <http://nlp.stanford.edu/sentiment/treebank.html>
19. Language Processing-Art of tokenization. <https://www.ibm.com/developerworks/community/blogs/nlp/entry/tokenization?lang=en>

20. Jiang, J., Zhai, C.X.: An empirical study of tokenization strategies for biomedical information retrieval. *J. Info. Ret.* **10**, 341–363 (2012)
21. Rendle, S., Freudenthaler, C., Gantner Z., Thieme, L.S.: BPR: Bayesian personalized ranking from implicit feedback. In: UAI'09 Proceedings of the 25th Conference on Uncertainty in Artificial Intelligence. AUAI Press Arlington, Virginia, US (2009)
22. The Shotgun Approach. <http://shotgunapproach.wordpress.com/2010/10/08/the-algorithm-for-facemash-in-the-social-network>
23. Bird, S., Klein, E., Loper, E.: Natural language processing with python. O'Reilly Media, US (2009)
24. Jivani, A.G.: A comparative study of stemming algorithms. *J. Comp. Tech. Apps.* **6**, 1930–1938 (2013)
25. Ingason, A.K., Helgadottir, S., Rognvaldsson, H.L.E.: A mixed method lemmatization algorithm using a hierarchy of linguistic identities (HOLI). *Adv. NLP.* **5221**, 205–216 (2008)
26. Wikipedia Ranking. <http://en.wikipedia.org/wiki/Ranking>
27. Socher, R., Perelygin, A., Wu, J.Y., Chuang, J., Manning, C.D., Ng, A.Y., Potts, C.: Recursive Deep Models for Semantic Compositionality Over a Sentiment Treebank. Empirical Methods in Natural Language Processing. Stanford University, Stanford (2013)
28. Feedback Data sets. <http://www.rottentomatoes.com>

Seizure Onset Detection by Analyzing Long-Duration EEG Signals

Garima Chandel, Omar Farooq, Yusuf U. Khan
and Mayank Chawla

Abstract Seizures in epileptic patients affect tremendously their daily life in terms of accidents during driving a vehicle, swimming, using stairs, etc. Automatic seizure detectors are used to detect seizure as early as possible so that an alarm can be given to patient or their family for using anti-epileptic drugs (AEDs). In this paper, an algorithm has been proposed for automatic seizure onset detection by analysis of electroencephalogram (EEG) signals. The method is based on few wavelet transform-based features and two statistical features without wavelet decomposition for improving the performance of detector. The mean, energy, and entropy were calculated on different wavelet decomposed subbands, and mean absolute deviation and interquartile range were calculated on raw signal. Classification between seizure and nonseizure types of EEG signals was done successfully by linear classifier. The algorithm was applied to CHB-MIT EEG dataset for seizure onset detection and achieved 100 % sensitivity with mean latency of 1.9 s.

G. Chandel (✉) · O. Farooq

Department of Electronics Engineering, Aligarh Muslim University,

202002 Aligarh, Uttar Pradesh, India

e-mail: chandelgarima5@gmail.com

O. Farooq

e-mail: omar.farooq@amu.ac.in

Y.U. Khan

Department of Electrical Engineering, Aligarh Muslim University, Aligarh

202002, Uttar Pradesh, India

e-mail: yusufkhan1@gmail.com

M. Chawla

S-Labs, 101, 102 Vindhya C5, IIIT-Hyderabad Campus Gachibowli,

Hyderabad 500032, India

e-mail: mayankchawla1@gmail.com

1 Introduction

Seizures are small-duration abnormality indication due to firing of excessive number of neurons in the brain. Epileptic patients mostly suffer with fear of occurrence of next seizure because recurrent seizures affect their daily life in terms of physical damage during daily activities such as driving, swimming, etc. Automatic seizure detectors are used for detecting seizure event and seizure onset to help in giving quick treatment to epileptic patients [1].

Analysis of electroencephalogram (EEG) signal plays very important role in detection of seizures by automatic seizure detectors. The details of different types of EEG analysis techniques can be found in review by Acharya et al. in [1]. Many methods are developed in the past few years to increase the performance of seizure detectors by analyzing EEG signals. Steps including most of the seizure detection algorithms are shown in Fig. 1, and these include preprocessing of EEG signals to remove artifacts, useful features extraction to differentiate seizure, and normal events, and finally training and classification to make decision that event is seizure or not [1]. Shob proposed an algorithm to detect the onset of epileptic seizures using spectral features and support vector machine (SVM) for classification [2]. Another work by Weidong Zhou et al. used features based on wavelet transform [3], and classifications were done by the Bayesian linear discriminant analysis (BLDA). The short-time Fourier transform (STFT), the Wigner distribution (WD), the continuous wavelet transform (CWT), and model-based matched wavelet transform (MOD) are four time-frequency and time scale methods which have been used by Tamara et al. [4] for feature extraction and evaluated results by linear classifier.

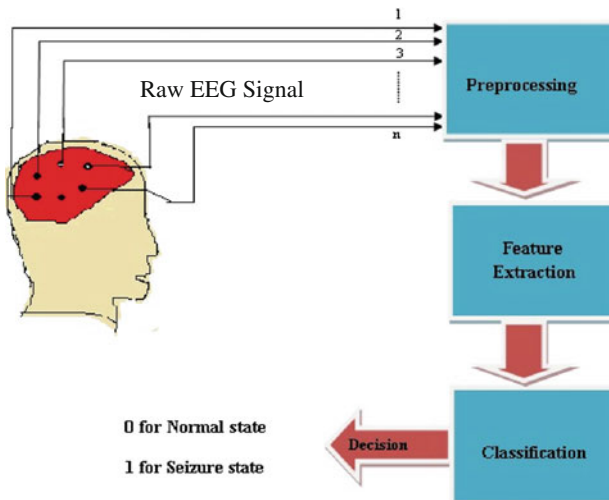


Fig. 1 General block diagram of automatic seizure detector

In this paper, an algorithm is presented using publicly available scalp EEG dataset for detection of seizure event and seizure onset. The two statistical features with raw data and three time–frequency domains, i.e., wavelet transform-based features on different subbands, are extracted from the EEG signal of 23 epileptic patients to discriminate seizure and normal states of long-duration scalp EEG signals. Finally, classification is obtained by linear classification. All seizures under test for each subject were detected with 100 % sensitivity and mean latency of 1.9 s, which is better than mean latency in work by Khan et al. [5].

2 Materials

This work used the free downloadable CHB-MIT EEG database. This data was recorded at Children's Hospital Boston [6] and consisting of EEG recordings from 23 pediatric subjects (17 females, 5 males, 1 unknown) grouped in 24 cases. In majority of the cases, data is divided into records of one hour duration and numbers of these segmented files are different for each case. Sampling frequency used in recording of all EEG signals is 256 Hz with 16-bit resolution. Total data consists of 916 h of continuously recorded EEG and including total 198 seizures. In most of the cases, 23-channel EEG signal recording was done, but in few cases, it is done using 24 or 26 channels. EEG electrode positions were used internationally in 10–20 systems for recording these signals.

The proposed seizure detection algorithm was tested on 23 epileptic patients with long-duration continuous recordings of scalp EEG signals. Age of epileptic patients for recording of these EEG signals was between 1.5 and 22 years. Figure 2

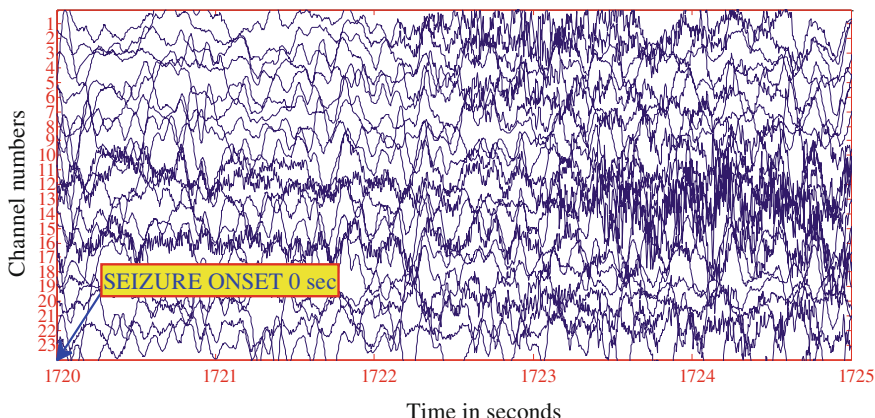


Fig. 2. EEG signal of Patient 1 during first 6 s of seizure under test

shows first 6 s scalp EEG signal of patient 1 (P1) during seizure under test. In P1, seizure actually starts from 1720s as marked by experts in database and it is detected without any delay by the proposed seizure onset detection algorithm. This shows that the proposed algorithm gave good performance on the EEG data used for the study.

3 Methods

The proposed method for seizure onset detection follows general steps as explained earlier in Sect. 1. The long-duration EEG signals consist of huge number of samples. These are reduced to few features to discriminate seizure and normal states of EEG signal. In this paper, some wavelet-based and some time-domain features without wavelet decomposition are extracted and then sent to a linear classifier for seizure onset detection. The algorithm used is explained in brief as follows:

1. The segmentation of EEG signal was done using rectangular window of M points of each channel. This results in X number of epochs per channel.
2. The Daubechies 6 wavelet with level k was used to get various approximate and detailed coefficients of segmented EEG signals. Two statistical features (MAD and IQR) without wavelet decomposition were also used to improve the overall performance.
3. Among k levels of decomposition, only W number of detailed coefficients and last approximate coefficient were used because of the fact that seizures occur between 5 and 40 Hz.
4. Mean, energy, and entropy were calculated over selected wavelet coefficients for every epoch in each channel. These parameters serve as a few representatives of many wavelet coefficients.
5. To reduce the size of feature vector, average of these three wavelet-based parameters and two time-domain features without wavelet decomposition has been used. This also decreases computational complexity.
6. These selected features with and without wavelet decomposition were given to linear classifier to detect seizure with minimum latency.

3.1 Feature Extraction

Features with Wavelet Decomposition The wavelet transform (WT) is used for the analysis of nonstationary signals. Since the EEG is nonstationary in nature, it is a good choice to use wavelet transform in comparison to other transforms [3] such as fast Fourier transform (FFT) or short-time Fourier transform (STFT). The major advantage of WT over FFT and STFT is its good time–frequency resolution for all

frequency ranges. Because of this reason, wavelet transform-based features are used in the proposed work.

The signal $s(t)$ can be analyzed using discrete wavelet transform at different frequency bands with different resolutions through decomposing the signal into a detail information coefficient ($D_{i,j}$) and approximate coefficient ($A_{i,j}$). The wavelet coefficients can be calculated by

$$D_{ij}(t) = \int_{-\infty}^{\infty} s(t) 2^{-i/2} \varphi(2^{-i}t - j) dt \quad (1)$$

$$A_{ij}(t) = \int_{-\infty}^{\infty} s(t) 2^{-i/2} \psi(2^{-i}t - j) dt \quad (2)$$

where functions $\varphi(t)$ and $\psi(t)$ are the basic scaling, i is the scale index, and j is the translation parameter.

In this work, W , number of detail coefficients and last approximate coefficient (total $W + 1$) were used for selecting required subbands to analyze EEG signal. Mean, energy, and entropy of selected wavelet coefficients on per epoch basis for each channel were used as features to discriminate between normal and seizure states of EEG signals. Hence, there are $3 * (W + 1)$ number of wavelet-based features for X number of epochs per channel.

The mean, energy, and entropy values at each wavelet decomposition level were calculated as

$$\text{Mean}_k = \frac{1}{N} \sum_{j=1}^N C_{kj} \quad (3)$$

$$\text{Energy}_k = \sum_{j=1}^N |C_{kj}|^2 \quad (4)$$

$$\text{Entropy}_k = \sum_{j=1}^N C_{kj}^2 \log(C_{kj}^2) \quad (5)$$

where $k = 1, 2, \dots, l$ is the decomposition levels of wavelet transform, N is the number of detail or approximate coefficients, and C is the wavelet coefficient at each level.

Features without Wavelet Decomposition Two statistical features, mean absolute deviation and interquartile range, were also used to improve the overall performance of seizure onset detection method. MAD and IQR values were calculated per epoch basis for each channel on raw EEG signals.

The mean absolute deviation (MAD) is the average distance between each data value and the mean of total number of samples m , and it is the good measure of variability [7].

$$\text{MAD} = \frac{1}{m} (|S_n^x - \text{mean}(S_n^x)|) \quad (6)$$

where n is the channel number, x is the frame number, and S is the sample value.

Interquartile range is also a measure of variability. It is the difference between the first and third quartiles, i.e.,

$$\text{IQR} = Q_3 - Q_1 \quad (7)$$

where Q_1 and Q_3 are the first and third quartile, respectively.

The first and third quartiles are defined as 25 % of the data lie below Q_1 (and 75 % is above Q_1) and 25 % of the data lie above Q_3 (and 75 % is below Q_3), respectively.

3.2 Classification

Total $3 * (W + 1)$ number of wavelet-based features and two statistical features without wavelet decomposition for X number of epochs per channel were extracted from feature extraction stage. As each epoch has n number of channels, therefore for each epoch feature, vector dimension is $n * (3 * (W + 1) + 2)$ and hence for X number of epochs, total feature vector dimension becomes $n * (3 * (W + 1) + 2) * X$. Feature vector with such a large dimension increases the computational complexity, and therefore to reduce the dimension of extracted features, average of these $3 * (W + 1) + 2$ features of n channels was used. Hence, dimensionality of feature vector is reduced from $n * (3 * (W + 1) + 2) * X$ to $(3 * (W + 1) + 2) * X$ for classification of seizure and normal states of EEG signals. This reduction in size of feature vector decreases the computational complexity of seizure onset detector. After feature extraction, all the selected features are applied as input to the last stage of seizure onset detector, i.e., classifier. Classifier is used to make decision that a segmented EEG belongs to seizure state or normal state. Classifier can be linear or nonlinear. Linear classifiers are cheaper and simple to use in comparison to non-linear classifiers such as SVM and ANN [8]. Hence, in the present work, the algorithm is implemented using linear classifier.

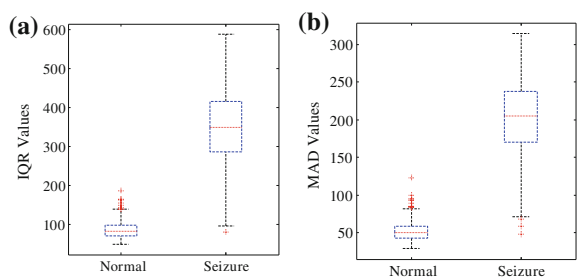
4 Results and Discussion

In this work, long-duration EEG data from 23 epileptic patients of CHB-MIT database is used. The segmentation of the 23-channel (n) scalp EEG signals was done using nonoverlapping rectangular window of 256 points (M) for each channel. This results in 3600 number of epochs (X) per channel for one hour duration files, and hence, the value of X depends on the duration of recorded signals in each patient. The Daubechies-6 wavelet with level 5 (k) was used to get various approximate and detailed coefficients of segmented EEG signals. Among five levels of decomposition, only three (W) number of detailed coefficients (D3, D4, and D5) and last approximate coefficient A5 were used because of the fact that seizures occur between 0 and 40 Hz [7]. Mean, energy, and entropy were calculated over four selected wavelet coefficients (last three details and one approximate coefficients) for every epoch in each channel. These parameters serve as a few representatives of many wavelet coefficients. Hence, there are 12 number of wavelet-based features ($3 * (W + 1) = 12$) for each epoch of 23 channels.

In addition with wavelet-based features, two time-domain features without decomposition were also used to improve the overall performance of seizure onset detection method. Time-domain information related to EEG signal can be achieved using box plots, and therefore box plots of normal and seizure EEG signals were plotted. Figure 3a, b shows box plots of IQR and MAD values for normal and seizure states of EEG signal. The small red cross symbols in the plots are the outlier values indicating the larger deviations in the distribution of data. The presence of these outliers shows that mean absolute deviation can also be used as statistical feature and it is also clear from this figure that there are huge differences in IQR and MAD values for normal and seizure states. Hence, these two become good statistical features for discriminating between normal and seizure activities of EEG signals. Therefore, MAD and IQR values were calculated per epoch on the basis of each channel on raw EEG signals.

It has been observed by experiment that in proposed seizure onset detection method, feature vector formed with the combination of 12 wavelets and two without wavelet-based features gave better performance in comparison to only

Fig. 3 a, b Box plots of IQR and MAD values of normal and seizure states for P1



either wavelet or without wavelet-based features. Due to this, for improvement of detector performance, the combination of wavelet and without wavelet features was used in study. Total dimension of feature vector for classification between normal and seizure activities of EEG signal was 14 for every epoch in each of 23 channels and this form $14 * 23$ size feature vector for every epoch. The dimension of feature vector plays very important role in classification, i.e., feature vector with a large dimension increases the computational complexity of the classifier. Therefore, it is necessary to reduce the dimension of feature vector but it is also necessary to consider that reduction in size of feature vector should not affect the performance of detector. The dimension of extracted feature vector was reduced by taking average of 14 features of 23 channels for every epoch. Hence, dimensionality of feature vector was reduced from $14 * 23$ to 14 for each epoch.

After feature extraction, all the selected features were applied as input to the linear classifier. For training of the classifier, minimum 60 % of seizures were used and remaining seizures were used for testing to identify seizure or normal EEG signals. Classifier was also trained with 1 h duration normal signal. Normal and seizure activities of EEG signal were assigned 0 and 1 label, respectively. The classifier performance was measured using sensitivity and latency [9]. Sensitivity was measured as the percentage of test seizure events marked by experts during which classifier label 1, i.e., seizure at least for one or more epochs. The detector was able to detect all the tested seizures, and hence this refers to 100 % sensitivity of the detector. Latency was measured as the delay between the seizure onset event and the end of the first seizure epoch within this event which was actually marked as a seizure by the expert. Each patient has one or more tested seizures, and hence for latency calculation, average of delay in seconds was considered. Figure 4 shows average latency for each patient. In the cases studied, the overall sensitivity and average latency of the proposed method were 100 % and 1.9 s, respectively. The proposed algorithm used linear classifier available in MATLAB statistics toolbox and evaluated on a computer with CPU 2.20 GHz and RAM 4 GB.

The comparison of the proposed work with other available methods which have used the same CHB-MIT EEG database as test bench is shown in Table 1.

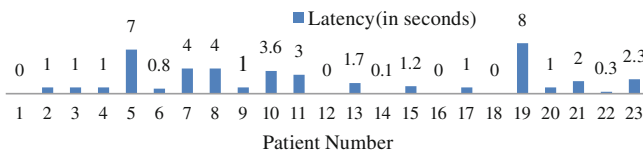


Fig. 4 Average latency for each patient

Table 1 Comparison of present results with other methods

Papers (year)	Mean sensitivity (%)	Mean latency (s)
Shoeb et al. [2], (2010)	96	4.2
Lee et al. [10], (2011)	97.6	4.95
Sukumaran et al. [11], (2012)	100	4.5
Khan et al. [5], (2012)	100	3.2
Kim et al. [12], (2013)	94.1	12.96
This work	100	1.9

5 Conclusion

The conclusion from the present study is that for the ease of epileptic patients and their families, and seizure onset detectors with low latency are required. In this work, an algorithm is proposed for the detection of seizure onset in epileptic patients with mean latency of 1.9 s and sensitivity of 100 %. The present algorithm may be used for real-time medical application of seizure onset detection with some modifications. In future, the proposed algorithm may be implemented by using intracranial EEG signals.

References

1. Acharya, U.R., Sree, S.V., Swapna, G., Martis, R.J., Suri, J.S.: Automated EEG analysis of epilepsy: a review. *Knowl.-Based Syst.* **45**, 147–165 (2013)
2. Shoeb, A.H., Guttag, J.V.: Application of machine learning to epileptic seizure detection. In: Proceedings of the 27th International Conference on Machine Learning (ICML-10), pp. 975–982 (2010)
3. Zhou, W., Liu, Y., Yuan, Q., Li, X.: Epileptic seizure detection using lacunarity and Bayesian linear discriminant analysis in intracranial EEG. *IEEE Trans. Biomed. Eng.* **60**(12), 3375–3381 (2013)
4. Nijssen, T.M., Aarts, R.M., Cluitmans, P.J., Griep, P.A.: Time-frequency analysis of accelerometry data for detection of myoclonic seizures. *IEEE Trans. Inf. Technol. Biomed.* **14**(5), 1197–1203 (2010)
5. Khan, Y.U., Farooq, O., Sharma, P.: Automatic detection of seizure onset in pediatric EEG. *Int. J. Embed. Syst. Appl.* **2**(3), 81–89 (2012)
6. Shoeb, A., Edwards, H., Connolly, J., Bourgeois, B., Treves, S.T., Guttag, J.: Patient-specific seizure onset detection. *Epilepsy Behav.* **5**(4), 483–498 (2004)
7. Rafiuddin, N., Uzzaman Khan, Y., Farooq, O.: Feature extraction and classification of EEG for automatic seizure detection. In: 2011 International Conference on Multimedia, Signal Processing and Communication Technologies (IMPACT), pp. 184–187. IEEE (2011)
8. Liang, S.F., Shaw, F.Z., Young, C.P., Chang, D.W., Liao, Y.C.: A closed-loop brain computer interface for real-time seizure detection and control. In: 2010 Annual International Conference of the IEEE Engineering in Medicine and Biology Society (EMBC), pp. 4950–4953. IEEE (2010)
9. Ahammad, N., Fathima, T., Joseph, P.: detection of epileptic seizure event and onset using EEG. In: BioMed Res. Int. **2014**, 7 (2014)

10. Lee, K.H., Kung, S.Y., Verma, N.: Improving kernel-energy trade-offs for machine learning in implantable and wearable biomedical applications. In: 2011 IEEE International Conference on Acoustics, Speech and Signal Processing (ICASSP), pp. 1597–1600. IEEE (2011)
11. Sukumaran, D., Enyi, Y., Shuo, S., Basu, A., Zhao, D., Dauwels, J.: A low-power, reconfigurable smart sensor system for EEG acquisition and classification. In: IEEE Asia Pacific Conference on Circuits and Systems (APCCAS), pp. 9–12. IEEE (2012)
12. Kim, T., Artan, N. S., Selesnick, I.W., Chao, H.J.: Seizure detection methods using a cascade architecture for real-time implantable devices. In: 2013 35th Annual International Conference of the IEEE Engineering in Medicine and Biology Society (EMBC), pp. 1005–1008. IEEE (2013)

Enhancing the Performance of MapReduce Default Scheduler by Detecting Prolonged TaskTrackers in Heterogeneous Environments

Nenavath Srinivas Naik, Atul Negi and V.N. Sastry

Abstract MapReduce is now a significant parallel processing model for large-scale data-intensive applications using clusters with commodity hardware. Scheduling of jobs and tasks, and identification of TaskTrackers which are slow in Hadoop clusters are the focus research in the recent years. MapReduce performance is currently limited by its default scheduler, which does not adapt well in heterogeneous environments. In this paper, we propose a scheduling method to identify the TaskTrackers which are running slowly in *map* and *reduce* phases of the MapReduce framework in a heterogeneous Hadoop cluster. The proposed method is integrated with the MapReduce default scheduling algorithm. The performance of this method is compared with the unmodified MapReduce default scheduler. We observe that the proposed approach shows improvements in performance to the default scheduler in the heterogeneous environments. Performance improvement was observed as the overall job execution times for different workloads from HiBench benchmark suite were reduced.

Keywords MapReduce · Task scheduler · TaskTrackers · Heterogeneous environment

N.S. Naik (✉) · A. Negi
School of Computer and Information Sciences, University of Hyderabad,
Hyderabad 500046, India
e-mail: srinuphdcs@gmail.com

A. Negi
e-mail: atulcs@uohyd.ernet.in

V.N. Sastry
Institute for Development and Research in Banking Technology,
Hyderabad 500057, India
e-mail: vnsastry@idrbt.ac.in

1 Introduction

A large number of organizations across the world use Apache Hadoop, created by Doug Cutting [1], which is an open source implementation of the MapReduce framework. Improvements in MapReduce scheduling give a better performance for Hadoop users [2]. The basic assumption of Hadoop is that nodes of the cluster are homogeneous [3] but in the current day scenarios, a collective number of computational machines are prepared with heterogeneous computing resources [4]. Fast changing hardware and utilization of legacy hardware with newer hardware are practical reasons needed for heterogeneous clusters to increase [5].

It is well known that the following issues directly affect the performance of MapReduce framework [6]: node heterogeneity, stragglers, data locality, and “slow TaskTrackers” [7, 8]. These issues have been undervalued by researchers in most of the proposed MapReduce scheduling algorithms [9], which leads to the poor performance of Hadoop [10]. Minimizing the execution time of a job by appropriately assigning tasks to the available heterogeneous nodes in the cluster is a common goal of the MapReduce scheduler [11] and it is likewise a significant research topic because it enhances the performance of MapReduce framework.

In this research work, we address the problem of identifying TaskTrackers which are running slowly in each phase of the MapReduce framework by integrating it with the MapReduce default scheduler in the heterogeneous Hadoop cluster. The scheduling of tasks needs to consider heterogeneity of the nodes as speed, capacity, and other hardware characteristics. The proposed approach helps the JobTracker not to schedule any task on these identified “slow TaskTrackers,” instead schedules on the remaining TaskTrackers, which minimizes the job execution time. In this paper, by “slow TaskTracker,” we are referring to a TaskTracker which has some tasks under it that are running slower relative to other tasks by calculating their progress.

The rest of the paper is structured as follows. A background of the MapReduce default scheduler is given in Sect. 2. Procedure for identifying TaskTrackers which are running slowly in each phase of the MapReduce framework in heterogeneous Hadoop cluster is given in Sect. 3, and Sect. 4 conducts a performance evaluation of the proposed work. Finally, we conclude the paper by giving few outlines of our future work in Sect. 5.

2 Background Work

This section provides a brief view of the MapReduce default scheduling algorithm with its limitations.

2.1 MapReduce Default Scheduling Algorithm

FIFO scheduler [12] is the MapReduce default scheduler for all Hadoop applications. The progress score (PS) of a task t is based on how much of a task's (key, value) pairs have been finished and it is in the range of $[0, 1]$ [13]. It is denoted by PS_t , which is calculated using Eq. (1) for *map* tasks and Eq. (2) for *reduce* tasks:

$$PS_t = X/Y \quad (1)$$

$$PS_t = (1/3) (K + X/Y) \quad (2)$$

where X is the number of (key, value) pairs that have been processed successfully, Y is the overall number of (key, value) pairs, and K is the stage (shuffle, sort, and merge) value in a *reduce* phase.

The average progress score of a job PS_{avg} is calculated using Eq. (3), $PS[i]$ is the progress score of a task t_i , and n is the number of executable tasks in a job.

$$PS_{avg} = \sum_{i=1}^n PS[i]/n \quad (3)$$

2.1.1 Limitations of MapReduce Default Scheduler

1. Default scheduler does not work better in heterogeneous environments.
2. Default scheduler cannot identify the TaskTrackers which run slowly in *map* and *reduce* phases in a heterogeneous Hadoop cluster.
3. Default scheduler response time is not efficient for jobs which executes for smaller time period as compared to longer ones.

3 Proposed Method for Identifying Slow TaskTrackers in Heterogeneous Environment

Finding TaskTrackers which are running slowly in terms of task progress present in each of the *map* and *reduce* phases of the MapReduce framework is an interesting and important research problem because an efficient way of finding it can result in significant reduction of overall job execution time in heterogeneous environment. The prolonged TaskTrackers can result in resource wastage and hamper other TaskTrackers in the cluster.

The progress scores of each TaskTracker in the cluster during *map* and *reduce* phases are calculated using Eqs. (4) and (5):

$$\text{PMTT}_i = \sum_{j=1}^M \text{PS}_j / M \quad (4)$$

$$\text{PRTT}_i = \sum_{j=1}^R \text{PS}_j / R \quad (5)$$

Here, the progress scores of i th TaskTracker in *map* and *reduce* phases are PMTT_i and PRTT_i . PS_j is the progress score of a task calculated based on how much of task's (key, value) pairs have been finished per second. M and R are the number of *map* and *reduce* tasks on the i th TaskTracker in the cluster.

The average progress scores of all TaskTrackers in the Hadoop cluster for a given job in *map* and *reduce* phases are calculated using Eqs. (6) and (7):

$$\text{APMTT} = \sum_{i=1}^T \text{PMTT}_i / T \quad (6)$$

$$\text{APRTT} = \sum_{i=1}^T \text{PRTT}_i / T \quad (7)$$

Here, APMTT and APRTT are the average progress scores of all TaskTrackers in the cluster during *map* and *reduce* phases. T is the number of TaskTrackers present in the Hadoop cluster.

We can find the TaskTrackers which are running slowly in each of the *map* and *reduce* phases using Eqs. (8) and (9):

$$\text{PMTT}_i > \text{APMTT}(1 + \text{TTTH}) \quad (8)$$

$$\text{PRTT}_i > \text{APRTT}(1 + \text{TTTH}) \quad (9)$$

For the i th TaskTracker in the cluster, if it satisfies the above Eqs. (8) and (9), then we can say that particular TaskTracker is running slowly compared to other TaskTrackers in the cluster in terms of task progress of *map* and *reduce* tasks in heterogeneous Hadoop cluster. We explained our proposed method in Algorithm 1 step by step.

TaskTracker Threshold (TTTH) is in the range of $[0, 1]$ which is used to categorize the TaskTrackers into slow or fast in terms of their tasks progress. According to Eqs. (8) and (9), if TTTH is too small, then it will categorize some of the fast TaskTrackers to be slow. If TTTH is too large, then it will categorize some “slow TaskTrackers” to be fast in terms of progress of *map* and *reduce* tasks. Thus, we have chosen 0.5 as an appropriate value for TTTH in our experiments.

Input: The set of TaskTrackers present in the heterogeneous Hadoop cluster.

Output: The set of TaskTrackers which are running slowly in each of the *map* and *reduce* phases.

Algorithm 1 Identifying slow TaskTrackers in *map* and *reduce* phases

```

1: set slowMapTaskTrackers
2: set slowReduceTaskTrackers
3: for each TaskTracker i in the cluster do
4:   for each running task j of the job do
5:     if task j is a Map task then
6:        $ProgressScore_j \leftarrow X/Y$ 
7:     else
8:        $ProgressScore_j \leftarrow 1/3 * (K + X/Y)$ 
9:     end if
10:    end for
11:   for each MapTaskTracker in the cluster do
12:      $PSMTT_i = \sum_{j=1}^M PS_j/M$ 
13:   end for
14:   for each ReduceTaskTracker in the cluster do
15:      $PSRTT_i = \sum_{j=1}^R PS_j/R$ 
16:   end for
17:    $APSMTT = \sum_{i=1}^T PSMTT_i/T$ 
18:    $APSRTT = \sum_{i=1}^T PSRTT_i/T$ 
19:   if  $PSMTT_i > APSMTT(1 + TTH)$  then
20:     slowMapTaskTrackers.add(ith TaskTracker)
21:   end if
22:   if  $PSRTT_i > APSRTT(1 + TTH)$  then
23:     slowReduceTaskTrackers.add(ith TaskTracker)
24:   end if
25: end for
26: return slowMapTaskTrackers
27: return slowReduceTaskTrackers

```

4 Evaluation

In this section, we now briefly discuss the experimental environment and workload description, and then explain the performance analysis of the proposed method in a heterogeneous Hadoop cluster.

4.1 Experimental Environment

We followed numerous stages to establish the experimental setup required to conduct our experiments and considered heterogeneous nodes in a Hadoop cluster as presented in Table 1. It has different Hadoop cluster hardware environments and configurations. We used Hadoop cluster of six different heterogeneous nodes in

Table 1 Hadoop evaluation environment

Node type	Hardware configuration	Hadoop configuration
Master node	Intel Xeon(R) CPU E3110 @ 3.00 GHz, 4 GB RAM, 500 GB Disk space	
Slave node 1	Intel core i3-3220 CPU @ 3.30 GHz, 2 GB RAM, 500 GB Disk space	2 map and 1 reduce slots per node
Slave node 2	Intel core 2 duo CPU E7500 @ 2.93 GHz, 2 GB RAM, 320 GB Disk space	2 map and 1 reduce slots per node
Slave node 3	Intel Pentium CPU G640 @ 2.80 GHz, 2 GB RAM, 500 GB Disk space	1 map and 1 reduce slots per node
Slave node 4	Intel core 2 duo Processor P8400 @ 2.26 GHz, 3 GB RAM, 250 GB Disk space	2 map and 1 reduce slots per node
Slave node 5	Intel core i5- 2310 CPU @ 3.10 GHz, 4 GB RAM, 500 GB Disk space	4 map and 1 reduce slots per node

terms of hardware configurations like different processor speeds, RAM, and disk space for evaluation. One of the nodes was chosen as a master node which runs the Hadoop distributed file system (NameNode) with 64 MB as default block size and MapReduce runtime (JobTracker). The remaining five nodes were worker nodes (DataNodes and TaskTrackers). The nodes were interconnected by Ethernet switch. All systems in the cluster use Ubuntu 14.04 operating system, JDK version 8, and Hadoop 1.2.1 version for performance evaluation.

4.2 Workload Description

We evaluate our proposed method using different benchmarks of HiBench benchmark suite [14] like microbenchmarks (sort, wordcount, terasort), web search benchmarks (nutch indexing, pagerank), and machine learning benchmarks (bayesian classification, k-means clustering) because it is a new, realistic, and comprehensive benchmark suite for Hadoop. Input data of all these workloads are default size of HiBench benchmark suite. These different benchmarks show the key characteristics of MapReduce clearly and widely used by the Hadoop research community to evaluate the scheduling algorithms in their experiments.

4.3 Performance Analysis of the Proposed Method

We evaluated the performance of the proposed method and integrated it with the MapReduce default scheduling algorithm to identify the TaskTrackers which are running slowly in *map* and *reduce* phase of the MapReduce framework. We can

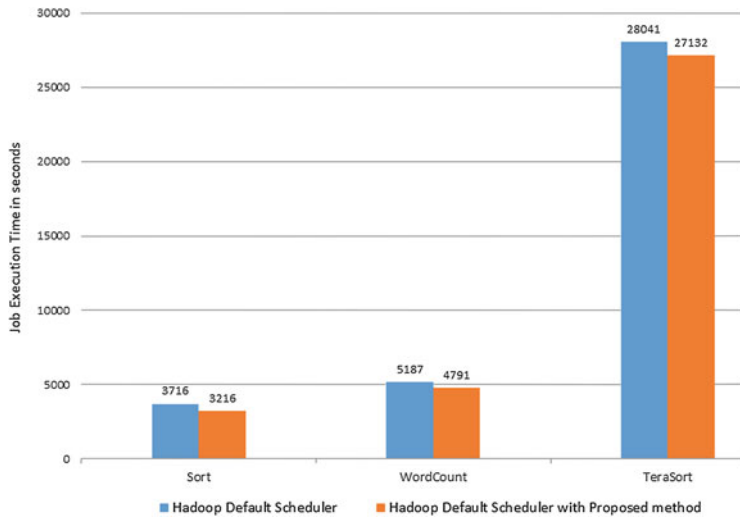


Fig. 1 Comparison of Job execution time for microbenchmarks

predict the JobTracker in such a way that it will not schedule any *map* and *reduce* tasks on these identified “slow TaskTrackers” in heterogeneous Hadoop cluster. We compared our proposed method with the MapReduce default scheduler because it is simple, fast algorithm, and extensively used in recent research. It has no procedure to find the “slow TaskTrackers” in each phase of the MapReduce framework and assumes nodes in the cluster as homogeneous.

In our experiments, we have analyzed how “slow TaskTrackers” in each phase of the MapReduce framework affect the execution time of a job; showed the performance improvement by comparing our proposed method with the existing MapReduce default scheduler; and executed different benchmarks like micro-benchmarks, web search benchmarks, and machine learning benchmarks from the HiBench benchmark suite under heterogeneous environments by considering the job execution time as a metric for evaluation of the system.

The performance comparison of the MapReduce default scheduler and MapReduce default scheduler with our proposed method is as shown in Figs. 1 and 2. In all of these different benchmarks, our proposed method achieved the best and consistent results in terms of minimum job execution time compared to the default scheduling algorithm in heterogeneous environments.

The Job execution time in our proposed method reduced when running different workloads like sort, terasort, wordcount, pagerank, nutch indexing, Bayesian classification, and K-means clustering to 500, 909, 396, 1073, 1049, 281, and 451 s, respectively, compared to the MapReduce default scheduler.

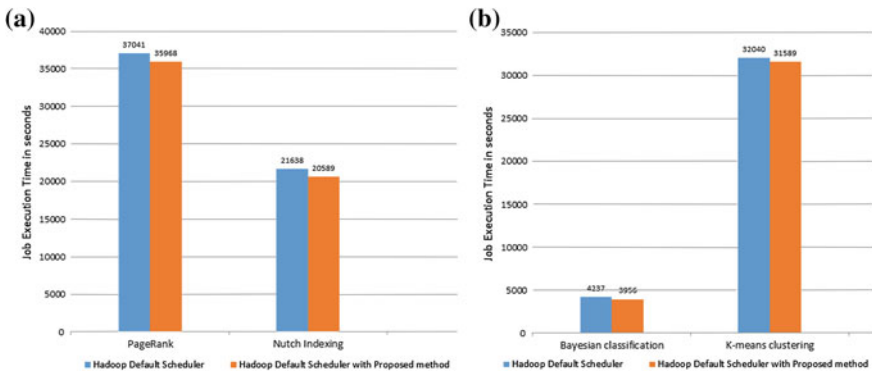


Fig. 2 Comparison of Job execution times for **a** web search benchmarks, **b** machine learning benchmarks

5 Conclusion and Future Work

In this paper, we have proposed a novel scheduling method for MapReduce default scheduler and integrated it with default scheduler. It identifies the TaskTrackers which are running slowly in *map* and *reduce* phases of the MapReduce framework in heterogeneous cluster. In this proposed method, when a JobTracker schedules a *map* or *reduce* task on a TaskTracker, first it identifies the “slow TaskTrackers” in *map* or *reduce* phase depending on the type of task scheduled. The proposed method will not schedule tasks on these particular TaskTrackers instead schedules it on the remaining TaskTrackers in the Hadoop cluster. Our proposed method shows the best performance in terms of job execution time compared to the MapReduce default scheduler when executing the microbenchmarks, web search benchmarks, and machine learning benchmarks of HiBench benchmark suite. Thus, our proposed approach improves the performance of the MapReduce framework in the heterogeneous environments by minimizing the overall execution time of a job.

As part of the future research work, we would like to integrate and implement our proposed approach in other MapReduce schedulers for large clusters like fair and capacity schedulers to further enhance the performance of the MapReduce framework in heterogeneous environments.

Acknowledgments Nenavath Srinivas Naik expresses his gratitude to Prof. P.A. Sastry (Principal), Prof. J. Prasanna Kumar (Head of the CSE Department), and Dr. B. Sandhya, MVSR Engineering College, Hyderabad, India for hosting the experimental test bed.

References

1. Dean, J., Ghemawat, S.: MapReduce: simplified data processing on large clusters. *Commun. ACM* **51**, 107–113 (2008)
2. Dean, J., Ghemawat, S.: MapReduce: a flexible data processing tool. *Commun. ACM* **53**(1), 72–77 (2010)
3. Dawei, J., Beng, C.O., Lei, S., Sai, W.: The performance of MapReduce: an in-depth study. *VLDB* **19**, 1–2 (2010)
4. Tian, C., Zhou, H., He, Y., Zha, L.: A dynamic MapReduce scheduler for heterogeneous workloads. In: Proceedings of the 2009 Eighth International Conference on Grid and Cooperative Computing, pp. 218–224 (2009)
5. Rasooli, A., Down, D.G.: An adaptive scheduling algorithm for dynamic heterogeneous Hadoop systems. In: Proceedings of the 2011 Conference of the Center for Advanced Studies on Collaborative Research, pp. 30–44. Canada (2011)
6. Zaharia, M., Borthakur, D., Sarma, J.S., Elmeleegy, K., Shenker, S., Stoica, I.: Job Scheduling for Multi-user MapReduce clusters. Technical Report, University of California, Berkeley (2009)
7. Chen, Q., Zhang, D., Guo, M., Deng, Q., Guo, S.: SAMR: A self adaptive MapReduce scheduling algorithm in heterogeneous environment. In: Proceedings of the 10th IEEE International Conference on Computer and Information Technology, pp. 2736–2743. Washington, USA (2010)
8. Tan, J., Meng, X., Zhang, L.: Delay tails in MapReduce scheduling. Technical Report, IBM T. J. Watson Research Center, New York (2011)
9. Rasooli, A., Down, D.G.: A hybrid scheduling approach for scalable heterogeneous Hadoop systems. In: Proceeding of the 5th Workshop on Many-Task Computing on Grids and Supercomputers, pp. 1284–1291 (2012)
10. Nanduri, R., Maheshwari, N., Reddyraja, A., Varma, V.: Job aware scheduling algorithm for MapReduce framework. In: Proceedings of the 3rd International Conference on Cloud Computing Technology and Science, pp. 724–729, Washington, USA (2011)
11. Naik, N.S., Negi, A., Sastry, V.N.: A review of adaptive approaches to MapReduce scheduling in heterogeneous environments. In: IEEE International Conference on Advances in Computing, Communications and Informatics, pp. 677–683. Delhi, India (2014)
12. Zhenhua, G., Geo, R.F., Zhou, M., Yang, R.: Improving resource utilization in MapReduce. In: IEEE International Conference on Cluster Computing, pp. 402–410 (2012)
13. Rasooli, A., Down, D.G.: COSHH: a classification and optimization based scheduler for heterogeneous Hadoop systems. *J. Future Gener. Comput. Syst.* **36**, 1–15 (2014)
14. Shengsheng, H., Jie, H., Jinquan, D., Tao, X., Huang, B.: The HiBench benchmark suite: characterization of the MapReduce-based data analysis. In: IEEE 26th International Conference on Data Engineering Workshops, pp. 41–51 (2010)

Prototype of a Coconut Harvesting Robot with Visual Feedback

Alexander J. Cyriac and V. Vidya

Abstract This paper discusses about the design and development of a semi-autonomous robot that is intended for harvesting coconuts. The robot is composed of two parts: the climbing mechanism and the harvesting mechanism. The harvesting mechanism consists of a robotic arm with three degrees of freedom and has a circular saw as the end effector. It also consists of a camera that is fixed on the wrist of the robotic arm, with which the video of the tree top is sent to the ground station in real time. For this a Linux-based ARM board is used. The climbing mechanism consists of a circular chassis. Three wheels that are powered by DC motors with sufficient torque are set at equal distance around the coconut tree. There are another three motors that ensure sufficient tightening of the climbing mechanism to the coconut tree. The climbing part also has a special mechanism to rotate around the coconut tree, so that the robotic arm gets full coverage around the coconut tree. The entire movement of the robot is controlled from the ground station, using a remote controller.

Keywords Coconut harvesting · Tree climbing robot · Video streaming · RF remote control

1 Introduction

Harvesting of coconuts plays a very important role in agriculture. It also plays as a main role in the economy of many developing countries. The traditional way of coconut harvesting involves a lot of risk. It is quite common in these days that many

A.J. Cyriac (✉) · V. Vidya

Department of Electrical and Electronics Engineering, Amrita School of Engineering,
Amrita Vishwa Vidyapeetham, Coimbatore, India
e-mail: cyriacalexander@gmail.com

V. Vidya
e-mail: v_vidya1@cb.amrita.edu

© Springer India 2016

S.C. Satapathy et al. (eds.), *Proceedings of the Second International Conference on Computer and Communication Technologies, Advances in Intelligent Systems and Computing* 380, DOI 10.1007/978-81-322-2523-2_22

people fell off the coconut tree causing severe injuries and even death. Also, as the new generation is becoming more conscious about the social status, only a very few people select coconut harvesting as their career. So coconut harvesting is turned to be a big challenge in the agricultural field.

All these problems attracted the interest of many young engineers who makes coconut harvesting a key area for research. Many engineers came forward with innovative ideas. Rajesh Kannan Megalingam and Tom Charly described about their coconut harvesting robot which is hexagonal in shape, in the paper “CocoBot: A Kinect-based Coconut Tree Climber” [1]. It is a wireless remote controlled fixed ground station model that uses Microsoft Xbox 360 for controlling the robot instead of switches and joystick. But this is not a reliable way of controlling, because the user should be in line-of-sight with the Microsoft kinect Xbox 360, which is in the climbing robot. And it is too dangerous if the user is controlling the robot by standing beneath the coconut tree. Moreover, there will be a lot of obstacles and the output will be affected by the difference in daylight. They also discussed about an adjustable ladder-type robot, which is not suitable in uneven and slop surfaces.

In another model designed by Mani A and Jothilingam A in “Design and Fabrication of Coconut Harvesting Robot” [2], it is an octagon-shaped chassis with four active wheels. But this model is very wide and can get damaged by the coconuts that fall down while harvesting. They make use of a robotic arm with three degrees of freedom which have sufficient reachability. The joints of the robotic arm are controlled by stepper motors. Servomotors would have given better control.

Hariskrishna and Vineet Pandey proposed the “Design of Climbing Mechanism for a Tree Climbing Robot” [3]. They make use of two grippers for climbing instead of wheels. This design is very fast compared to both the previous designs. But it requires very powerful motors, and moreover this motion will become impossible with a robotic arm. And there is no suitable place for fixing the robotic arm for harvesting the coconuts.

Widanagamage, Galge, and Salgado designed a tree climbing mechanism “Treebot: An Autonomous Tree Climbing Robot Utilizing Four Bar Linkage System” [4]. It climbs the tree with a worm motion using worm gear and wheel system. This model is also relatively fast. It is a very rigid model and has provision to place a robotic arm on its top. But a separate mechanism has to be designed to give movement to the robotic arm around the coconut tree. Also it is very rigid and bulky.

As none of these designs are fully reliable, in this paper, I propose another design with much more reliability than the currently existing model. The details of the design are explained in the forthcoming Sects. 2, 3, 4, 5, and 6.

2 Video Streaming

In all semi-autonomous coconut harvesting robots, the robot is controlled from the ground station. But none of the currently existing models give a clear view of the tree top and where the robotic arm is cutting. And the user will not have a clear

view due to sunlight and the view may get obstructed due to coconut leaves. Also it is not comfortable to stand a lot of time looking upward.

In this proposed model, live video streaming is also added. For this a low-cost USB camera is mounted on the wrist of the robotic arm, which captures the video and transmits it to the ground station in real time. This gives the user a visual feedback from the tree top, so that the robot can be easily controlled with the help of the streamed video.

3 Climbing Mechanism

The climbing mechanism of the coconut harvester consists of a circular chassis. The entire circular chassis can be divided into three 120° arcs. The arcs are joined together with hinges. One of the three joints can be opened and fixed around the coconut tree (Fig. 1).

For the demonstration of the prototype, a 4.5^{\parallel} pipe is considered as the coconut tree to climb. The circular chassis is of 7.5^{\parallel} diameter.

In the center of all the three arcs, there is a leg for climbing. Each leg consists of four DC motors and two wheels. They are responsible for climbing, tightening, holding, and rotating around the tree. Among the two wheels, one wheel is vertical to the ground and the other wheel is horizontal to the ground. The vertical wheel helps the robot to climb up and climb down, while the horizontal wheel helps the robot to rotate around the coconut tree (Fig. 2).

Fig. 1 Top view of climbing mechanism

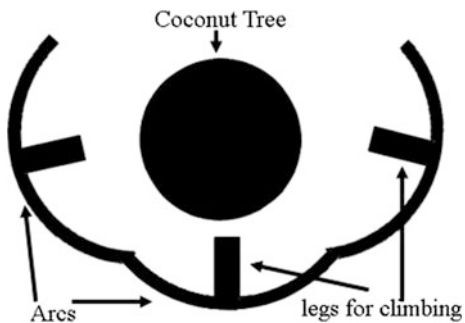


Fig. 2 One leg in an arc

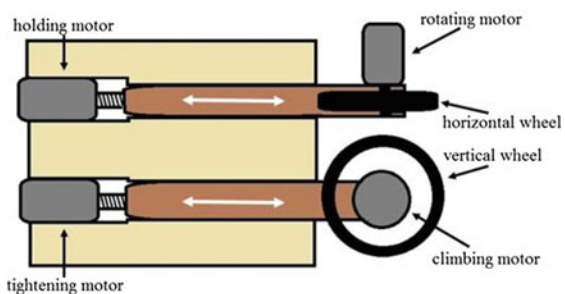
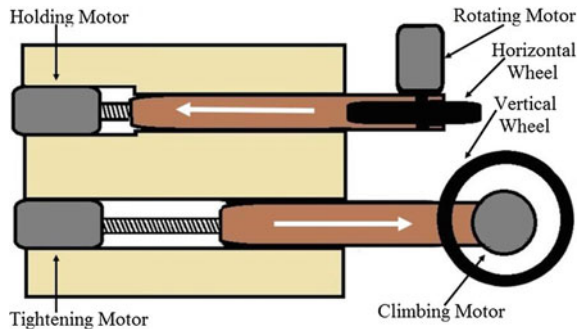


Fig. 3 Tightening motor pushes the vertical climbing wheel

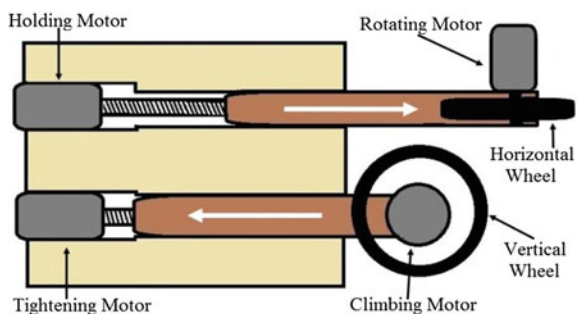


When the climbing motor is powered, the vertical wheels attached to it rotate clockwise or counter clockwise to move the robot up or down. For climbing, the vertical wheels must be attached firmly to the coconut tree. The tightening motor is responsible for it. This motor has threads in its shaft. The vertical wheel is attached to the other end of the threaded shaft. So when the shaft rotates, the rotational motion is converted to linear motion. So the vertical wheel for climbing can be pushed out for tightening or pulled in for loosening (Fig. 3).

The robot has to be held tight and should maintain its position, when it reaches the top of the coconut tree. The holding motor is responsible for it. This motor also has threads in its shaft. The horizontal wheel is attached to the other end of the threaded shaft. So when the shaft rotates, the rotational motion is converted to linear motion. So the horizontal wheel comes in contact with the coconut tree from all the three arcs and the robot will be held tight in its position.

As the bunch of coconuts will be all around the coconut tree, the workspace of the robotic arm must include all the points around the coconut tree. For this the climbing part is made to rotate around the coconut tree, and the vertical climbing wheel is pulled back and the rotating motor is powered. So the horizontal wheel attached to the rotating motor rotates and the robot will also rotate around the coconut tree (Fig. 4).

Fig. 4 Holding motor pushing the horizontal wheel for holding and rotating around the coconut tree



4 Harvesting Mechanism

The robotic arm and camera are the most important parts of the harvesting mechanism. The circular chassis of the climbing part is the base of the robotic arm. The robotic arm can rotate around the coconut tree with the help of the horizontal rotating wheels of the climbing part. The robotic arm has two more links and thereby the degree of freedom is three. Since precise control is needed, all the joints of the robotic arm have been controlled by servomotors. The robotic arm is also equipped with a circular saw as the end effector. This is controlled by a high-speed motor (Fig. 5).

The entire climbing mechanism and harvesting mechanism were controlled by a Linux-supported ARM cortex-A8-based board (Beaglebone Black). It controls all the twelve DC motors in the climbing mechanism and the high-speed DC motor of the circular saw for harvesting coconuts through a driver circuit. It provides pulse width modulated signals to both the servomotors of the robotic arm. The robot also consists of a Wi-Fi transmitter for transmitting the video to the ground station and an RF receiver for receiving the controls from the ground station (Fig. 6).

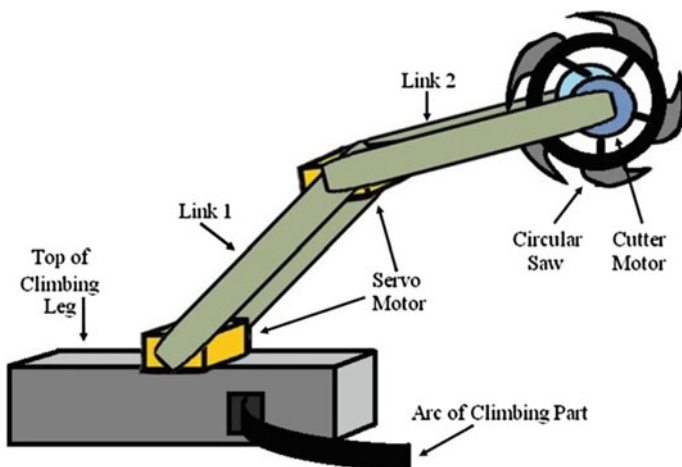
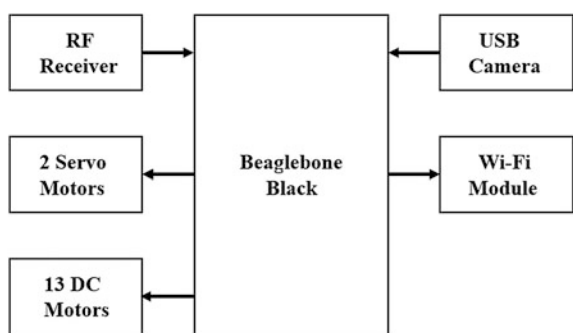


Fig. 5 Harvesting mechanism

Fig. 6 Block diagram of robot



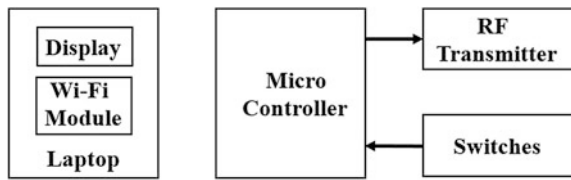


Fig. 7 Block diagram of ground control station

5 Ground Control Station

The ground control station consists of a control unit and a display (laptop) for viewing the streamed video. The control unit consists of switches for controlling the robot and a RF transmitter to transmit these control signals to the robot (Fig. 7).

6 Conclusion

In this work, a method for coconut harvesting is proposed. The hardware setup and the controlling units are designed. A prototype of the robot has been developed. A live video is streamed wirelessly to the ground controlling station successfully. Thus, a semi-autonomous coconut harvesting robot is designed and developed.

As a future scope, the introduction of video processing would help to identify the coconuts to be harvested and the robotic arm can be moved to the correct position using inverse kinematics, and thus making the robot fully autonomous.

References

1. Rajesh Kannan, M., Tom Charly K., Harikrishna Menon, T., Venu Madhav, R.: CocoBot: a Kinect based coconut tree climber. *Int. J. Appl. Eng. Res.* **7**(11), 1335–1339 (2012). ISSN 0973-4562
2. Mani, A., Jothilingam, A.: Design and fabrication of coconut harvesting robot: COCOBOT. *Int. J. Innovative Res. Sci. Eng. Technol.* **3**(3), 8373–8381 (2014)
3. Harikrishna, T.V., Harshavardhan, P.D.P.R., Pandey, V.: Design of climbing mechanism for a tree climbing robot. *Int. J. Current Eng. Technol.* ISSN 2277-4106
4. Widanagamage, B.C., Gallego, T.N., Salgado, S., Wijayakulasooriya, J.: Treebot: an autonomous tree climbing robot utilizing four bar linkage system. In: Research Symposium on Engineering Advancements (2014)

Suppression of Impulse Noise in Digital Images Using Hermite Interpolation

Saumya Satpathy, Figlu Mohanty and Prasant Kumar Pattnaik

Abstract This paper includes a methodical way to suppress impulse noise in digital images using the concept of popular Hermite interpolation. Hermite interpolator is a spline where each piece is a third-degree polynomial specified in Hermite form by its values and first derivatives at the end points of the corresponding domain interval. Our proposed technique is mostly divided into two phases: (a) noise cancellation and (b) edge preservation. The principle of Hermite interpolation has been applied in edge preservation process. Computational outcomes of this approach give out up to 90 % of impulse noise suppression.

Keywords Hermite interpolation · Digital image · Edge preservation · Impulse noise

1 Introduction

Digital images often get corrupted during its acquisition and transmission, due to switching or sensor temperature. Impulse noise is an extensive issue that normally results from improper medium between the recording system and recorded images.

S. Satpathy (✉) · F. Mohanty · P.K. Pattnaik
School of Computer Engineering, KIIT University, Bhubaneswar, India
e-mail: s.satpathy11@gmail.com

F. Mohanty
e-mail: figlu92@gmail.com

P.K. Pattnaik
e-mail: patnaikprasant@gmail.com

It is mandatory to eliminate the noise from digital images for any further image analysis. This elimination process is known as image de-noising.

The medium filter is the most widely used technique to discard impulse noise from digital images. The major drawback of this filter is that it leaves a blurring effect in the edges of the images [1]. In order to improve the medium filter, weighted median filter and centre weighted median filter have been proposed.

In [2], the authors have proposed a decision-based signal adaptive median filtering algorithm to remove a special type of noise called impulsive noise. The concept of homogeneity level is explained for the values of picture elements based on their global and local statistical attributes. It uses a co-occurrence matrix representing the correlation between a pixel and its neighbours in order to determine the upper and lower bound of homogeneity level. Here, noisy pixels are first selected using the homogeneity level and then de-noising process is followed. This technique refines noise up to 30 % density.

In [3], to deal with the edge preserving issues, the authors have proposed a hybrid algorithm combining medium-based filtering along with pattern-matching technique. Therefore, to avoid misclassification of thin line impulses, a directional impulse detection method is used. This technique refines images corrupted with 20 % noise density.

Besdok and Yuksel [4] have proposed a Jarque–Bera test based median filters to remove impulse noise. The pixel values derived from standard median filter replace the affected pixels only. This method recovers images up to 90 % of noise density.

In [5], the authors have proposed a two-stage filtering technique to eliminate impulse noise. The two stages are impulse noise detection and restoration of the corrupted pixels. In the first stage, it determines the location of impulses using adaptive median filter-based impulse detector. In the second stage, it periodically replaces the noisy pixels with the weighted sum of its neighbouring noise-free pixels. The technique restores up to 30 % of noise.

In [6], the authors discussed a directional weighted median filter for the shedding of random-valued impulse noise. The difference between the centre pixel and its neighbouring pixels associated with four main directions is used by the impulse detector instead of substituting the corrupted pixels identified by the outcome of median filter. This technique uses the details of four directions to obtain the pixel values with the intention of preserving the image details. DWM restores the image up to 60 % of noise density.

In [7], the authors have discussed a method, i.e. a perfect combination of adaptive median filter and switching median filter. The flexibility of the filter is reliable on the adaptive median filter configuration so that its size can be varied according to the local noise density. Here, the role of switching median filter is to quicken the process as the corrupted pixels are refined. This method refines up to 95 % of noise density.

In [8], an improved progressive switching median filter technique has been explained. It is a two-step process. The first step includes the prior detection of noisy pixels by comparing the pixel value with the maximum and minimum values of pixels within a window. In the second step, the noise impulses are refined based on the information obtained from above step. Therefore, this mechanism gives results up to 30 % noise density.

In [9], the authors have discussed on impulse noise removal scheme that mainly focuses on few noise-free pixels. This algorithm is continual in nature for a small window size. The average value of the noise-free pixels substitutes the corrupted pixels. The process continues till all the corrupted pixels are refined. Thus, it gives up to 80 % of noise removal.

In [10], pixel correlation-based impulse noise removal has been introduced. In the noise detection step, the corrupted pixel areas are first determined by the help of features of impulse noise along with an analytical process. In the evaluated candidate region, the final corrupted pixels are separated using the maximal values in a mask. In the correction step, the noisy pixels get corrected using the correlation between the noise-free pixels in the mask. Hence, it restores images affected with 90 % of noise density.

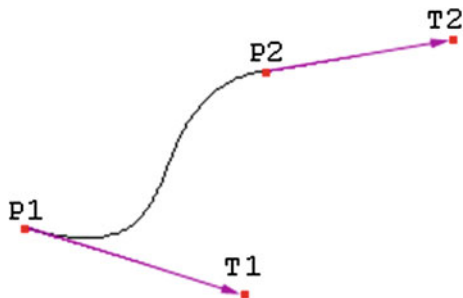
In [11], the authors have explained a mechanism based on two different threshold values (maximum and minimum). The mean of the components in every row and column is determined by considering 3×3 window size. Two different threshold values are obtained from the above mean values and this threshold detects the noisy pixels. Then median of elements of the noise-free group is estimated and this value replaces the noisy pixels. The same process goes on for the entire image and thus recovers up to 90 % of noise density.

In [12], the authors proposed a mechanism, i.e. adaptive median-based lifting filter to remove homogenous salt and pepper noise. However, any composition occupying less than half of the filter's neighbourhood tends to be discarded. Hence, it gives results up to 90 % of noise density.

In [13], the authors introduced a new technique, i.e. B-Spline interpolation, to shed salt and pepper impulse noise in the fingerprint dataset. This is a two-step technique, i.e. noise cancellation and edge preservation. This mechanism refines up to 85 % of noise density.

2 Hermite Interpolation

Hermite curves can be easily determined and are efficient enough to smoothly interpolate between key points. The following vectors are required to draw a Hermite curve:

Fig. 1 Hermite curve

- P1: the starting point of the curve to be drawn.
- T1: the tangent shows the curve leaving the start point.
- P2: end point.
- T2: the tangent shows the curves meeting the endpoint (Fig. 1).

The above four vectors are multiplied with four hermite functions and computed together:

$$h1(x) = 2x^3 - 3x^2 + 1 \quad (1)$$

$$h2(x) = -2x^3 + 3x^2 \quad (2)$$

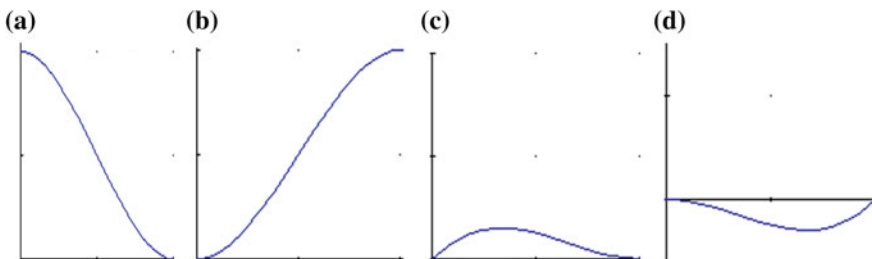
$$h3(x) = x^3 - 2x^2 + x \quad (3)$$

$$h4(x) = x^3 - x^2 \quad (4)$$

The four graphs show the four functions in Fig. 2.

The above facts are described in vector and matrix format:

- s* The interpolation point and its powers up to three
- c* The parameters of our Hermite curve
- h* The matrix form of the four Hermite polynomials

**Fig. 2** **a** Function $h1$, **b** function $h2$, **c** function $h3$, **d** function $h4$

$$s = \begin{pmatrix} x^3 \\ x^2 \\ x^1 \\ 1 \end{pmatrix} \quad c = \begin{pmatrix} P1 \\ P2 \\ T1 \\ T2 \end{pmatrix} \quad h = \begin{pmatrix} 2 & -2 & 1 & 1 \\ -3 & 3 & -2 & -1 \\ 0 & 0 & 1 & 0 \\ 1 & 0 & 0 & 0 \end{pmatrix}$$

To determine P (point) on the curve draw vector s , multiply it with the matrix h and then multiply with vector c :

$$P = s \times h \times c$$

3 Suppression of Impulse Noise in Digital Images Using Hermite Interpolation

In our proposed technique, we have used the mechanism of Hermite interpolation in order to remove the impulse noise from the digital images.

Algorithms:

3.1 Step 1: Removal of Impulse Noise

```

Input: Original image I(i,j)
I(i,j) image with noise n(i,j)
Window w of size (3 × 3), where w ∈ R
As defined in Stage-I, for four pixels in m and k = 0 to 1,
{
U0 ← (2*k^3) - (3*k^2) + 1;
U1 ← (-2*k^3) + (3*k^2);
U2 ← k^3 - 2*k^2 + k;
U3 ← (k^3) - (k^2);
NP = U0*m (1) + U1*m(2) + U2*m(3) + U3*m(4)
r(i,j) ← np (Replacing old value of pixel with the new pixel value)
}
Replace o(i,j) ← r(i,j)
Where, NP = new pixel, r(i,j) = Refined Image
o(i,j) = Output image

```

3.2 Step 2: Preservation of the Edge

```

For all o (i,j) and k = 0 to 1
For i = 1: L4 (Corrupted Pixels)

```

```

m(1) ← Upper variable of o(i,j)
m(2) ← Below variable of o(i,j)
m(3) ← Variable left of o(i,j)
m(4) ← Variable right of o(i,j)
U0 ← (2*k^3) - (3*k^2) + 1;
U1 ← (-2*k^3) + (3*k^2);
U2 ← k^3 - 2*k^2 + k;
U3 ← (k^3) - (k^2);
NP = U0*m (1) + U1*m(2) + U2*m(3) + U3*m(4)
ER(i,j) ← NP (Replacing noisy pixel with the new pixel value np)
Output: ER (Noise-free and edge retained Image)

```

4 Results and Discussion

The grey-scale images of different dimensions are taken into account for the experiment. The simulation process has been done in MATLAB R2013a and the outputs are measured in *peak signal-to-noise ratio (PSNR)* (Figs. 3, 4 and Table 1).



Fig. 3 **a** Original image of lena. **b** Original image of chilly

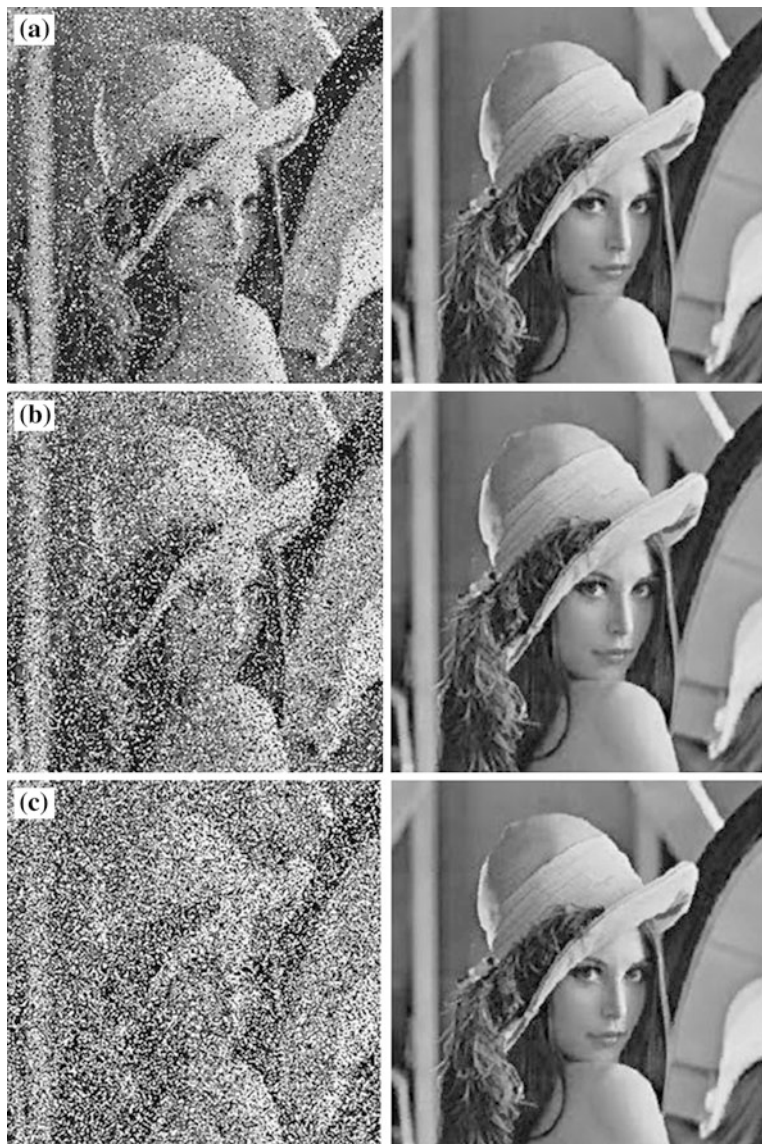


Fig. 4 **a** Noise density of 30 % impulse and restored image of lena. **b** Noise density of 60 % impulse and restored image of lena. **c** Noise density of 90 % impulse and restored image of lena. **d** Noise density of 30 % impulse and restored image of chilly. **e** Noise density of 60 % impulse and restored image of chilly. **f** Noise density of 90 % impulse and restored image of chilly

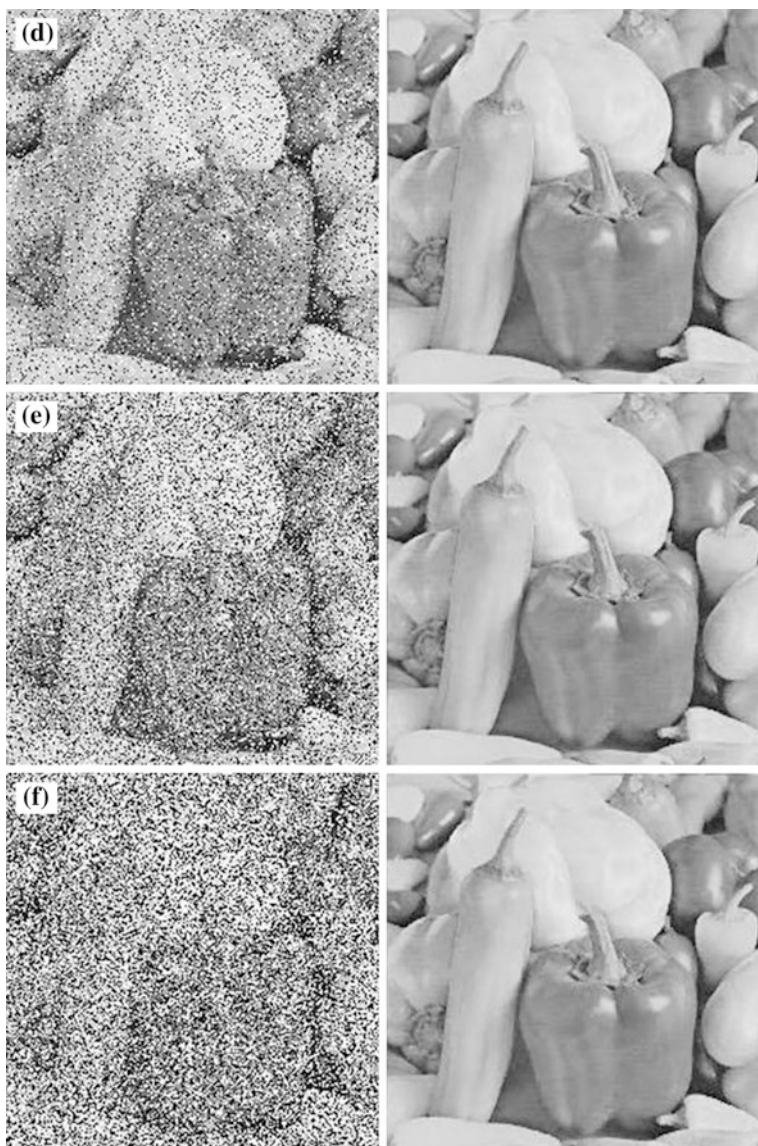


Fig. 4 (continued)

Table 1 PSNR values at different noise densities

Images noise density (%)	Chilly	Lena
	PSNR (in dB)	
10	41.6492	40.9301
20	38.9308	37.9953
30	37.0081	35.9776
40	35.4195	35.1143
50	34.5177	33.8730
60	33.6987	33.1139
70	33.1762	32.5486
80	32.5729	31.8811
90	32.0665	31.4073

5 Conclusion

Image de-noising is required for the post-processing analysis of the corresponding image. Here, a novel technique for the elimination of impulsive noise in digital images using Hermite interpolation has been suggested. The proposed mechanism not only sheds noise from digital images but also performs efficiently for edge preservation. Our algorithm de-noises images up to 90 % noise density.

References

1. Bovik, A.: *Handbook of Image and Video Processing*. Academic, New York (2000)
2. Gouchol, P.; Dept. of Comput. Sci., Yanbian Univ., Yanji, China; Liu, J.-C., Nair, A.S.: Selective removal of impulse noise based on homogeneity level information. *IEEE Transactions*, pp. 85–92 (2003)
3. Xiao, X., Li, S.: Detail-preserving approach for impulse noise removal from images. In: *IEEE Transactions*, pp. 28–32, 14–16 Sect 2004
4. Besdok, E., Yuksel, M.E.: Impulsive noise suppression from images with Jarque-Bera test based median filter. *Int. J. Electron. Commun.* **59**, 105–110 (2005)
5. Mansoor Roomi, S.M., Lakshmi, I.M., Abhai Kumar, V.: A recursive modified Gaussian-filter for impulse noise removal. In: *IEEE Transactions*, pp. 549–552, 26–28 Sep 2006
6. Dong, Y., Xu, S.: A new directional weighted median filter for removal valued impulse noise, pp. 193–196 (2007)
7. Ibrahim, H., Kong, N.S.P., Theam F.N.: Simple adaptive median filter for the removal of impulse noise from highly corrupted images. In: *IEEE Transactions*, pp. 1920–1927, Nov 2008
8. Kuykin, D.K., Khryashchev, V.V., Apalcov, I.V.: An improved switching median filter for impulse noise removal. *IEEE Transactions*, 1314–1319, 18–23 May 2009
9. Majid, A., Mahmood, M.T.: A novel technique for removal of high density impulse noise from digital images. IN; *IEEE Transactions*, pp. 139–143, 18–19 Oct 2010
10. Song, Y., Han, Y., Lee, S.: Pixel correlation-based impulse noise reduction. *IEEE Trans*, pp. 1–4, 9–13 Feb 2011

11. Gupta, V., Shandilya, M.: Image de-noising by dual threshold median filtering for random valued impulse noise. In: IEEE Transactions, pp. 1–5 (2012)
12. Syamala Jaya Sree, P., Pradeep Kumar, Rajesh, S., Ravikant, V.: Salt-and-pepper noise removal by adaptive median-based lifting filter using second-generation wavelets. *SIViP* 7(1), 111–118 (2013)
13. Syamala Jaya Sree, P., Prasant Kumar, P., Ghrera, S.P.: A Novel Algorithm for Suppression of Salt and Pepper Impulse Noise in Fingerprint Images Using B-Spline Interpolation, pp. 521–528. Springer International Publisher, New York (2014)

Wireless Personal Area Network and PSO-Based Home Security System

Anita Gehlot, Rajesh Singh, Piyush Kuchhal, M.S. Yadav,
Mahesh Kr. Sharma, Sushabhan Choudhury and Bhupendra Singh

Abstract For monitoring and controlling unwanted events like intrusion of burglars/thieves at home/locality/city, the security systems are much required. In this paper, an efficient and low-cost wireless security system is proposed with ZigBee and GSM modems. In the proposed system, city is divided into sections and sections into colonies/sectors. The section security system comprises multiple cluster nodes with one cluster head. Cluster nodes and cluster head are linked via ZigBee network. The cluster heads of all sections communicate with central control room (main server) of the city via GSM in order to make its coverage area large. The network optimization for efficient routing of the cluster node and cluster head is done using PSO algorithm. Cluster node is an embedded device connected with ZigBee modem and switches in each room as per user's requirement. If there is an intrusion at home, in any locality of the city, the resident is to press the switch. This information is communicated by cluster node through ZigBee network to the corresponding cluster head which in turn communicates to the central control room

A. Gehlot (✉) · R. Singh · P. Kuchhal · S. Choudhury
University of Petroleum and Energy Studies, Dehradun, India
e-mail: anita@ddn.upes.ac.in

R. Singh
e-mail: rsingh@ddn.upes.ac.in

P. Kuchhal
e-mail: pkuchhal@ddn.upes.ac.in

S. Choudhury
e-mail: schoudhury@ddn.upes.ac.in

M.S. Yadav
Kurukshetra University, Kurukshetra, India
e-mail: msyadav1_kuk@yahoo.com

M.Kr. Sharma
CERRI Pilani, Pilani, India
e-mail: mahesh@ceeri.ernet.in

B. Singh
Schemetics Microelectronics, Dehradun, India
e-mail: itsbhupendrasingh@gmail.com

(main server) via GSM network. Cluster head is equipped with audio alarm system like a hooter and this system is activated as soon as the switch in the cluster node is pressed. The identity of cluster node is conveyed to the cluster head via communication network. For future enhancement, the system in the cluster node may be fitted with other sensors like temperature, smoke, fire, etc., for detection of various hazardous conditions.

Keywords Cluster node • GSM • Security system • Server • ZigBee

1 Introduction

Security is a major issue in developing smart cities. Selection of method is the most important part to control and monitor the security systems. For this purpose, some prior art has been studied and conclusion is made on the basis of liability and feasibility of the proposed system. Qian et al. discussed that ZigBee technology can be used for smart campus monitoring. The system is based on collection and monitoring of energy consumption parameters and environmental status of building like temperature, humidity, and air quality level. Furthermore, the system is integrated with campus GIS [1]. Ranjitha Pragnya et al. presented the ZigBee-based wireless sensor network for monitoring the health of senior citizens who are living alone, through monitoring their daily activities. The system includes MEMS device comprising temperature sensor and force sensor. The system was evaluated on real-time tests with four different senior citizens [2]. Obaid et al. proposed ZigBee-based voice controlled wireless smart home system for senior citizens and disabled people. Household appliances are controlled with voice command recognition and operated the appliances with predefined tasks [3]. Sathya Narayanan et al. introduced an intelligent system for home automation, based on PIC microcontroller, ZigBee, speech recognition, and GSM technology. The proposed technology is used to control home appliances. The system also provides the security system for fire hazards and send message through GSM module [4]. Mudunuru et al. described a wireless sensor network using LPC2148 ARM 7 board. An alarm is set through smoke sensors, when fire is detected and also transmits information to other nodes to set alarm wirelessly to prevent major disaster [5]. Primicanta et al. discussed a GSM-based system for taking readings from LPC's meter automatically without visiting the customer's sites [6]. Chen et al. speak about need of home security and control by deploying sensor nodes and convey the message to user through SMS using GSM. This system provides a user friendly portable monitoring system [7]. Ahmad et al. introduced the intelligent home automation system (IHAM) using PIC microcontroller with the ZigBee, speech recognition, and GSM network to control the home appliances [8]. Kanagamalliga et al. described smart security system. This system comprises ZigBee, GSM, sensors, and

smartphone for security monitoring and control, when the user is out of the home [9]. Shanmugasundaram et al. presented intelligent smart home system using ZigBee, GSM, sensors (smoke, IR motion sensors), and RFID [10]. Liu et al. discussed a real-time acquisition of the parameters of temperature, humidity, infrared, smoke, gas, fire, and theft alarm-based design of the smart home system based on ZigBee technology and GSM/GPRS network [11].

The above literature survey suggests that the home automation and security system is available for individual home but in those systems, the security of locality/city as a whole is not taken care of. In order to secure all the homes in the locality/city using a common security system, this paper proposes an emergency network home security system. ZigBee and GSM combination is a reliable and feasible combination for most of the security-based applications.

2 Hardware Development

The whole system is divided into three parts—cluster node, cluster head, and control room. As shown in Fig. 1, the city is divided into sections including one colony in one section. Every section has cluster nodes with each house having facility of switches in all rooms of the house and a cluster head. When any of the switches gets on, ZigBee sends a message as alert signal to cluster head with house number in which the intruders enter. Hooter attached to cluster head gets on and

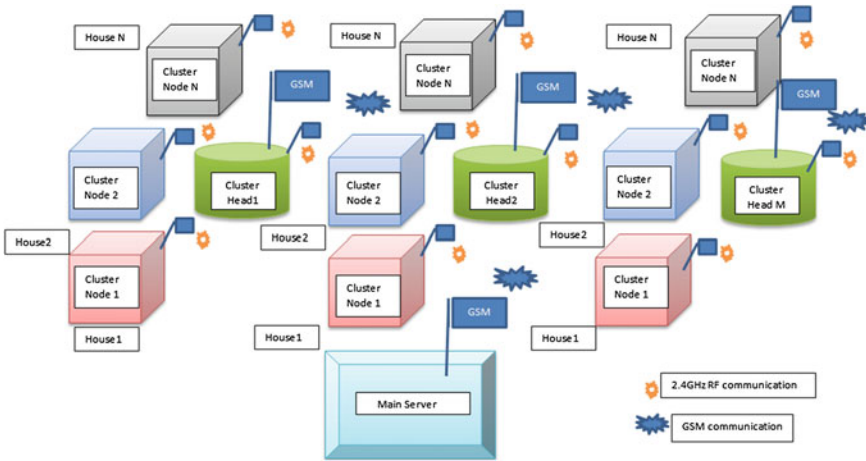


Fig. 1 System block diagram

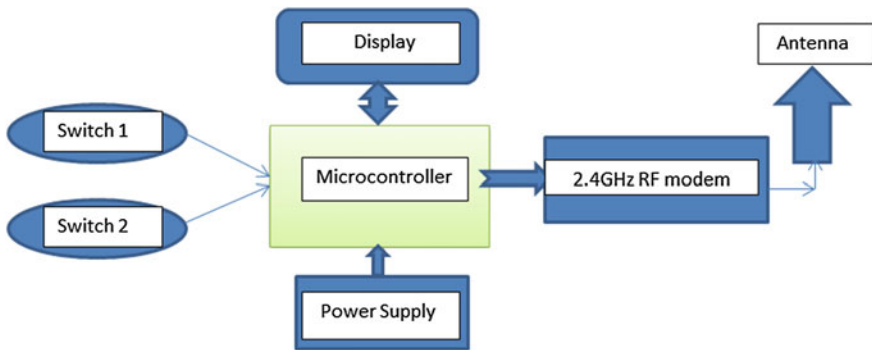


Fig. 2 Cluster node

also sends this warning signal to control room through GSM modem, with cluster head number, and required action command is given through police station.

2.1 Cluster Node

It comprises microcontroller, power supply, switches, and ZigBee modem. As per the proposed system, every house would have a central cluster node with a number of switches placed with boards already used in houses to drive household devices. When any of the switches gets on, signal is generated and ZigBee modem transmits it to cluster head, as shown in Fig. 2. ZigBee modem is in sleep mode if no signals are generated, and this consumes less energy. As at cluster node ZigBee modem is used which is a license free node, it is not needed to recharge it each month or it can be said that maintenance cost is low.

2.2 Cluster Head

Every group of cluster nodes in a section has a cluster head which comprises microcontroller, hooter, ZigBee, and GSM modem, as shown in Fig. 3. If node receives alert signal from cluster node through ZigBee modem, hooter gets switched on and also sends it to main control room via GSM to make its coverage area large. This control room can be in police control rooms where LCD displays the section number and alert message, and instant help can be sent.

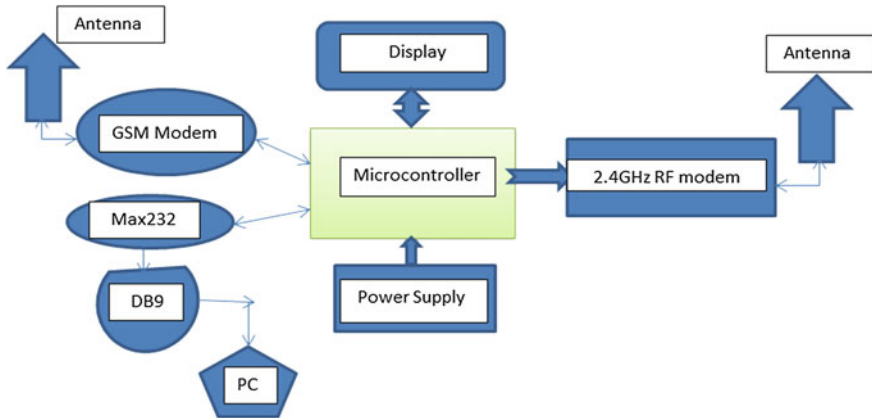
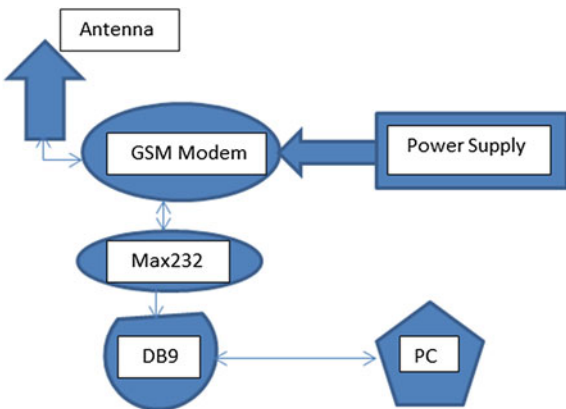


Fig. 3 Cluster head

Fig. 4 Main server



2.3 Main Server

It receives the information from different cluster heads. Main server contains all information regarding all cluster nodes through cluster head (Fig. 4).

2.4 Component Description

Table shows the description of components of cluster node, cluster head, and main server.

S. No.	Device/module	Specifications and working
1.	ATmega16	ATmega16 is used. It is a low-power CMOS 8-bit microcontroller based on the AVR RISC architecture
2.	RF modem	RF data modem working at 2.4 GHz frequency. Receives and Transmits serial data of adjustable baud rate of 9600/4800/2400/19,200 bps at 5 or 3 V level for direct interfacing to microcontrollers
3.	GSM modem	GSM/GPRS Modem-TTL (5 V) is built with Tri-band GSM/GPRS engine, works on frequencies Tri-band GSM/GPRS 900/1800/1900 MHz
4.	2N2222	NPN transistor which is used as switch
5.	Relay	12 V/1A ice cube relay as switch to operate hooter
6.	LCD	16 * 2 LCD to display the information for user and connected in cluster head and cluster node
7.	Crystal	14.7456 MHz frequency to set the baud rate of microcontroller to 9600 and connected in cluster head and cluster node
8.	Switch 1 and 2	DPDT switches are used
9.	Power supply	12 V/500 mA supply to operate the cluster node
10.	Power supply/DC source	12/1A supply to operate the cluster head
11.	AC source	12 V AC source to operate the hooters
12.	MAX232	Level converter IC used in cluster head and main server to link the data in PC
13.	DB9	9 pin serial female port
14.	Capacitor	22pF to connect crystal in microcontroller ATmega16

3 Routing Algorithm

There are number of cluster nodes in a particular section which is controlled by a cluster head. The cluster nodes need to communicate among themselves and also need to communicate to cluster head and main control room. Since the numbers of nodes are large, the communication need to be done using optimized routing algorithm. There are several methods for network optimization. The traditional methods like Kruskal's algorithm, minimum spanning tree, and prim's algorithm have the drawback of limited exploration of search space and insensitivity to scaling. Hence, PSO has been used for network routing. PSO also has the advantage of less memory usage.

3.1 PSO Algorithm

For parameter initialization, every particle is given a random position and velocity.

1. Input all the desired constraints like number of nodes and number of edges
2. Initialize the particle positions and velocities
3. Evaluate the fitness value of system with unit step response
4. Calculate system constraints for each particle and total error
5. Compare the individual fitness value of each particle to its previous value, and if it is better than previous one, replace with new value, i.e., local best position otherwise do not change
6. The position of particle having lowest error is global best value
7. Update position and velocity of particles according to (1)
8. Go back to step (3) and repeat all steps until system constraints are met

Here, for the optimization of parameters, the following equation has been used:
 $n = 40;$ % Size of the swarm “no of birds”
 $bird_setp = 40;$ % Maximum number of “birds steps”
 $dimension = 2;$ % Dimension of the problem
 $c2 = 1.3;$ % PSO parameter C1
 $c1 = 0.14;$ % PSO parameter C2
 $w = 0.9;$ % PSO momentum or inertia
 $fitness = 0 * ones(n, bird_setp);$
 $velocity = w*velocity + c1*(R1.(L_b_position-c_position)) + c2*(R2.(g_b_position-c_position));$ and
 $c_position = c_position + velocity$ [12].

4 Circuit and Simulation

The circuit diagram of cluster node as shown in Fig. 5 has two switches made up of push button which is attached in portB of microcontroller ATmega16. The crystal oscillator of 14.7456 MHz is connected with ATmega16 microcontroller to generate baud rate at 9600. The RF modem has four pins, Rx, Tx, Vcc, and ground, which are connected to Tx(15), Rx(14), 5 V, and ground of microcontroller ATmega16, respectively. The control pins RS, RW, E of 16 * 2 LCD are connected with PD6 (20), PD5(19), and PD7(21) pins of ATmega16 and upper data pins of LCD D4, D5, D6, and D7 are connected to PC0(22), PC1(23), PC2(24), and PC3(25) of ATmega16 microcontroller. The circuit diagram of cluster head has RF modem, crystal oscillator, and LCD which are connected with ATmega16 microcontroller in the same way as that of cluster node. The hooter is also connected with one pin of ATmega16 microcontroller using 2N2222 and relay12 V/1A.

Figure 6 shows proteus simulation model for the system. The simulation is done before hardware implementation to check accuracy and feasibility. The above

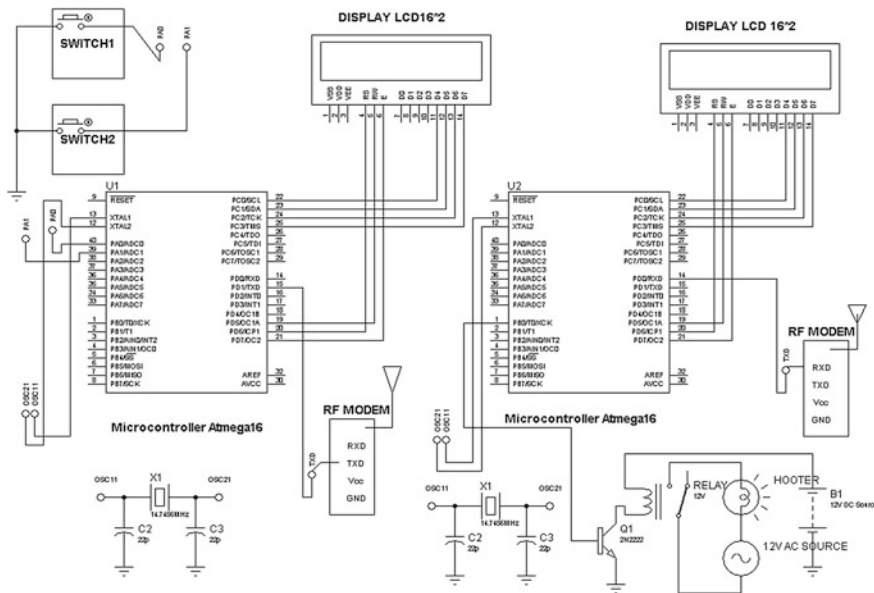


Fig. 5 Circuit diagram of cluster node and cluster head

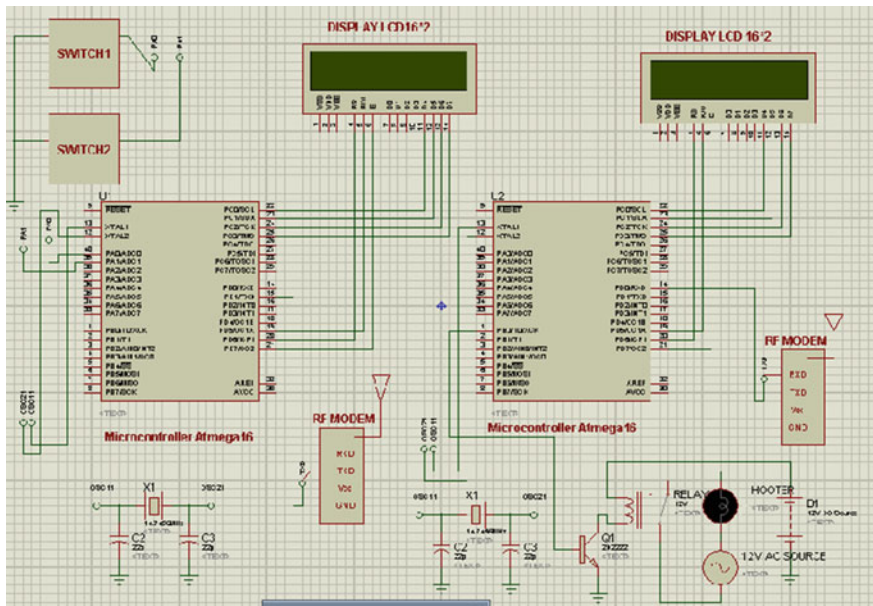


Fig. 6 Proteus simulation of system

circuit diagram is realized using proteus software and tested by writing the code in AVR studio 4. The embedded “C” code is written for cluster node and cluster head separately.

5 Experimental Setup and Results

The hardware implementation is done by integrating CC2500 ZigBee modem and GSM modem with ATmega16 microcontroller, switches in the cluster node, and hooter in the cluster head. The cluster nodes and cluster head and their connectivity are simulated by proteus software. In this paper, the design and development of an emergency home security system has been implemented. The network routing optimization has been implemented using PSO algorithm. Simulation has been done and a prototype is developed to check the feasibility and reliability of the system. The developed system can detect the outsider intrusion at home. It is observed that prototype is working properly. The system is low cost because of the use of license free network for communication. The system is efficient because of the integration of two wireless technologies. The system has real-time application for emergency security system (Fig. 7).

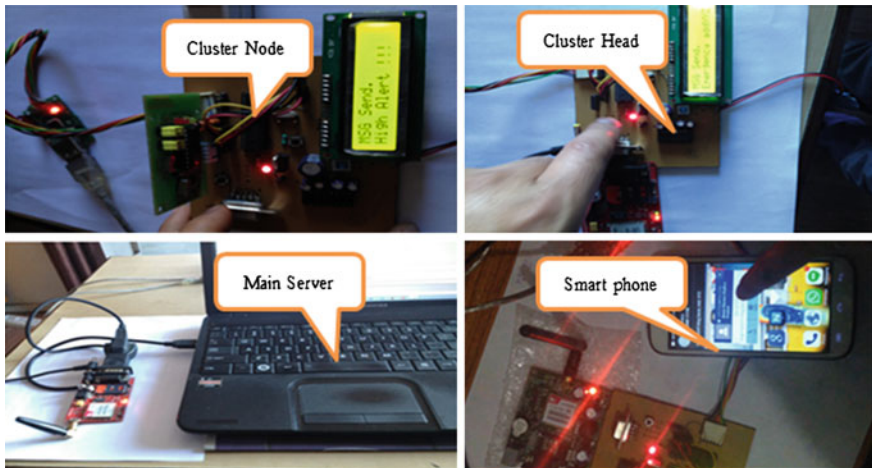


Fig. 7 Developed prototype for the system

6 Conclusion and Future Scope

In this paper, emergency home security system based on ZigBee technology and GSM network has been designed. ZigBee technology is used to achieve a fast rate, low-cost, and low-power wireless network communications. The security agencies can receive SMS messages via cell phone or PC and sound alarm through hooter in case of any emergency. The system can be upgraded to detect other emergency condition like fire, smoke, motion, etc., by integrating the appropriate sensors with the existing hardware with minor modification. The system is low cost as it uses free band to communicate between cluster node and cluster head, and even if no signal is generated, the system remains in sleep mode and consumes less energy.

References

1. Qian, K., Ma, X., Peng, C., Qing, J., Mengyuan, X.: A ZigBee-based building energy and environment monitoring system integrated with campus GIS. *Int. J. Smart Home* **8**(2), 107–114 (2014)
2. Ranjitha Pragnya, K., Sri Harshini, G., Krishna Chaitanya, J.: Wireless home monitoring for senior citizens using ZigBee network. *Adv. Electron. Electr. Eng.* **3**(3) 249–256. Research India Publications, ISSN 2231-1297
3. Obaid, T., Rashed, H., El Nour, A.A., Rehan, M., Saleh, M.M., Tarique, M.: ZigBee based voice controlled wireless smart home system. *Int. J. Wireless Mobile Netw. (IJWMN)* **6**(1) (2014)
4. Sathy Narayanan, V., Gayathri, S.: Design of wireless home automation and security system using PIC Microcontroller. In: International Journal of Computer Applications in Engineering Sciences Special Issue on National Conference on Information and Communication (NCIC'13), vol. III, Special Issue, Aug 2013, ISSN: 2231-4946
5. Suneel Mudunuru, V., Narasimha Nayak, Madhusudhana Rao, G., Sreenivasa Ravi, K.: Real time security control system for smoke and fire detection using ZigBee. *Int. J. Comput. Sci. Inf. Technol.* **2**(6), 2531–2540 (2011)
6. Primicanta, A.H., Nayan, M.Y., Awan, M.: ZigBee-GSM based automatic meter reading system. In: International Conference on Intelligent and Advanced Systems (ICIAS), 2010 15–17 June 2010. Print ISBN: 978-1-4244-6623-8
7. Chen, H.-C., Chang, L.-Y.: Design and implementation of a ZigBee-based wireless automatic meter reading system. *Przeglad Elektrotechniczny (Electrical Review)*, ISSN: 0033-2097 (2012)
8. Ahmad, A.W., Jan, N., Iqbal, S., Lee, C.: Implementation of ZigBee-GSM based home security monitoring and remote control system. In: IEEE 54th International Midwest Symposium on Circuits and Systems (MWSCAS) (2011)
9. Kanagamalliga, S., Vasuki, S., Vishnu Priya, A., Viji, V.: A ZigBee and embedded based security monitoring and control system. *Int. J. Inf. Sci. Tech. (IJIST)* **4**(3) (2014)
10. Shannugusundaram, M., Muthuselvi, G., Sundar, S.: Implementation of PIC16F877A based intelligent smart home system. *Int. J. Eng. Technol. (IJET)* **5**(2) (2013)

11. Liu, Z.: Hardware design of smart home system based on ZigBee wireless sensor network. In: AASRI Conference on Sports Engineering and Computer Science (SECS 2014), AASRI Procedia, vol. 8, pp. 75–81 (2014)
12. Singh, R., Kuchhal, P., Choudhury, S., Anita: Design and experimental evaluation of PSO and PID controller based wireless room heating system. *Int. J. Comput. Appl.* **107**(5), 9–14 (2014). ISSN 0975-8887

A Framework for Ranking Reviews Using Ranked Voting Method

Rakesh Kumar, Aditi Sharan and Chandra Shekhar Yadav

Abstract The reviews of the products are increasing rapidly on the web due to the rapid growth and uses of the Internet. The products review makes very big impact on consumer's interest in buying or not buying a product. However, there are various products, which have thousands of user-generated reviews. Mining this enormous online reviews and finding the important reviews for a user became a challenging task. It is very hard for consumers to find out the true quality of a particular product due to the presence of large number of reviews for a single product. To solve this problem, we are proposing a ranking mechanism which can be efficiently used to rank different reviews in accordance to their aspects rating. Here, the ranking mechanism uses the numerous ratings of the aspect and calculates the aggregate score of the review. This paper demonstrates the ranking of various reviews by means of their aspects rating through ranked voting method. Both the practicability and the benefits of the suggested approach are illustrated through an example.

Keywords Aspect identification · Aspect classification · Review ranking · Ranked voting method

R. Kumar (✉) · A. Sharan · C.S. Yadav
SC&SS, Jawaharlal Nehru University, New Delhi, India
e-mail: rakesh.kmr2509@Gmail.com

A. Sharan
e-mail: aditisharan@Gmail.com

C.S. Yadav
e-mail: chandrtech15@Gmail.com

1 Introduction

Due to expansion of the Internet, web has now become the most popular information source for the consumers. People freely share the reviews of the products on the web site, web forum, BBS, and blog. Lots of consumers decide whether to buy a product or not, on the basis of product reviews. The manufacturers also analyze the product reviews to improve the quality of the particular products and to increase customer satisfaction. It has become a regular process among both online and off-line consumers to keep them self-updated about the reviews of any particular product from online web sites before going to purchase. This leads to useful customer reviews on e-commerce web sites. Because of this, in order to seek confidence in a product, potential customers habitually browse through a large number of online reviews prior to purchasing. Moreover, reviews play an important and vital role to appraise the quality of products online. However, enormously increasing volume of reviews has led to another problem of information overload. It is not easy to extract collective view of useful information from reviews due to the presence of large volume of reviews. These reviews are too much to manage through collection–reading analysis handwork. Thus, automatic search analysis of these reviews becomes very necessary and important.

As a result of above scenario, opinion review mining has recently gained the interest of various researchers working in the field of text analysis and opinion mining. Opinion mining comes into being.

“Sentiment analysis, also called opinion mining, is the field of study that analyzes people’s opinions, sentiments, evaluations, appraisals, attitudes, and emotions toward entities such as products, services, organizations, individuals, issues, events, topics, and their attributes” [1]. It represents a wide problem space. This online word-of-mouth represents new and measurable sources of information with many practical applications.

Opinion mining is a new and challenging area of research. Initial work done in this area pertains to sentiment classification, where a review is classified as positive or negative. However, by nature, most reviews are of mixed type, and while they are positive for one aspect, they may be negative on another aspect. Therefore, an interesting sentiment analysis with respect to product reviews is analyzing the reviews on the basis of aspects. Furthermore, the reviews can be ranked with respect to specific aspects. This can be very helpful in recommending the reviews on the basis of aspects.

To deal with these problems, we have proposed a review ranking approach using aspects rating, which can help customer in choosing best reviews focusing on the aspects of their interest. Proposed framework for ranking reviews is based on ranked voting method, which aims to automatically identify important reviews using consumer aspects rating. Our main contribution in this framework is ranking approach, which takes as input aspects rating and ranks the reviews on the basis of aspects rating.

This paper is organized as follows: Sect. 2 presents the general framework for sentiment classification of reviews. Sect. 3 proposes the framework for ranking reviews based on ranked voting method. In the next section, we illustrate our method with example. Finally, we conclude the paper with a summary and directions for future work in Sect. 5.

2 General Framework for Aspect Classification

This section presents the general framework used for sentiment classification at aspect level as shown below in Fig. 1. This framework is used to classify the aspects of review into different classes on the basis of their strength.

We start with an overview of its pipeline (see Fig. 1) consisting of three main components: (a) consumer reviews; (b) aspect identification; and (c) aspect classification. Given the consumer reviews of a product, we have to first identify the aspects in the reviews and then analyze consumer opinions on the aspects via a sentiment classifier. The various steps used in this framework are discussed below in detail.

2.1 Consumer Reviews

Reviews are general opinion about various products, movies, books, etc., given by the users. These reviews are used to find out the opinion of users about these products. Consumer reviews are composed in different formats on various forum websites. The websites such as CNet.com require consumers to give an overall rating on the product, describe concise positive and negative opinions (i.e., Pros and Cons) on some product aspects, as well as write a paragraph of detailed review in free text. Some websites, e.g., Viewpoints.com, only ask for an overall rating and a paragraph of free-text review. The others such as Reevo.com just require an overall rating and some concise positive and negative opinions on certain aspects. In summary, besides an overall rating, a consumer review consists of pros and cons reviews, free-text review, or both. There are various review datasets available online.

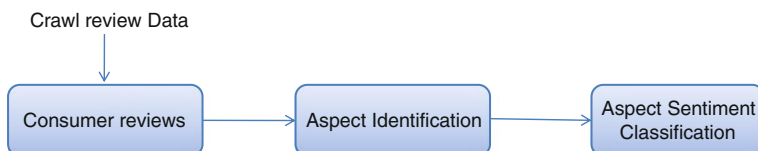


Fig. 1 General framework for system

2.2 Aspect Identification

For the consumer reviews, we can identify the aspects by extracting the frequent noun terms in the reviews. Previous studies have shown that aspects are usually nouns or noun phrases [2], and we can obtain highly accurate aspects by extracting frequent noun terms from the pros and cons reviews [3]. For identifying aspects in the free-text reviews, a straightforward solution is to employ an existing aspect identification approaches. One of the most notable existing approaches is that proposed by Hu and Liu [4]. It first identifies the nouns and noun phrases in the documents. The occurrence frequencies of the nouns and noun phrases are counted, and only the frequent ones are kept as aspects. Although this simple method is effective in some cases, its well-known limitation is that the identified aspects usually contain noises. Recently, Wu et al. [5] used a phrase dependency parser to extract noun phrases, which form candidate aspects. To filter out the noises, they used a language model by an intuition that the more likely a candidate to be an aspect, the more closely it related to the reviews. The language model was built on product reviews and used to predict the related scores of the candidate aspects. The candidates with low scores were then filtered out.

2.3 Aspect Sentiment Classification

The task of analyzing the sentiments expressed on aspects is called aspect-level sentiment classification in literature [4]. Existing techniques include the supervised learning approaches and the lexicon-based approaches, which are typically unsupervised. The lexicon-based methods utilize a sentiment lexicon consisting of a list of sentiment words, phrases, and idioms, to determine the sentiment orientation on each aspect [6]. While these methods are easy to implement, their performance relies heavily on the quality of the sentiment lexicon. On the other hand, the supervised learning methods train a sentiment classifier based on training corpus. The classifier is then used to predict the sentiment on each aspect. Many learning-based classification models are applicable, for example, Support Vector Machine (SVM), Naive Bayes, Maximum Entropy (ME) model, etc. [7]. Supervised learning is dependent on the training data and cannot perform well without sufficient training samples. However, labeling training data is labor-intensive and time-consuming process.

Given the classified output for different aspects of a review data, the information can be utilized to rank the review based on the strength of aspects for the product. Our system captures this idea to extend the functionality of existing system. The details of proposed system are presented in the next section.

3 Framework for Proposed System

The main contribution of this paper is to suggest a review ranking mechanism based on the strength of aspects of the product. The proposed framework is the extension of the general framework of aspect-level sentiment classification as discussed in the previous section. Here, the rating of the aspect corresponds to the score of the aspect. The proposed framework is simple and effective, which ensures good review selection as well as returns top-k efficient review to the customers. The input to our system is the set of aspect and their corresponding rating. Output is top-k efficient reviews based on the efficiency of aspect. To assign a rank to the review through aspects, there are some general steps that have to be followed (Fig. 2).

3.1 Data Preparation for Ranking Algorithm

From the classified aspects, ranked voting dataset is prepared. The format of the dataset is shown below (Table 1). Let m be the number of reviews in review web site and $k(k \leq m)$ be the number of aspect from the numbers 1 to k (here $k = 5$).

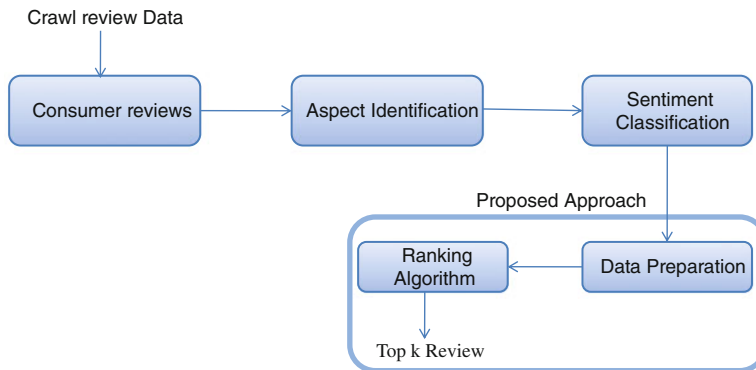


Fig. 2 Proposed framework for review ranking

Table 1 Data representation

Review	Aspect1	Aspect2	Aspect3	.	Aspectk
Review1	r_{11}	r_{12}	r_{13}		r_{1k}
Review2	r_{21}	r_{22}	r_{23}		r_{2k}
Review3	r_{31}	r_{32}	r_{33}		r_{3k}
.					
Reviewm	r_{m1}	r_{m2}	r_{m3}		r_{mk}

Let r_{ij} be the number of j th place aspect rating of the review in i th place where $i = 1 \dots m$ and $j = 1 \dots k$. Now our dataset is prepared for ranked voting algorithm. In the next step, we can apply ranked voting algorithm.

3.2 Ranking of Reviews

After data preparation, the ranked voting algorithm can be applied to rank the reviews. In this work, to find a best review for a user, ranked voting method is used [8]. In ranked voting system, voter ranks alternatives in order of preference. In our case, the aspect rating corresponds to the order of preference. There is a long list of aspects to find an efficient review. Each aspect will act as a voter, and reviews are candidates for them. Thus, a ranked voting dataset is prepared. In research, some methods have been proposed to analyze ranked voting data such as data envelopment analysis (DEA) introduced by Cook and Kress [9]. But DEA often suggests more than one efficient candidate. Some methods are proposed to discriminate these efficient candidates. But order of preference may be changed because of existence of an inefficient candidate. Tsuneshi Obata and Hiroaki Ishii introduced [8] a novel method which does not use information of inefficient candidate to discriminate efficient candidates given by DEA. Proposed work considers the same method to find a best review for a user. The ranked voting method is applied in two steps:

3.2.1 Find Efficient Reviews

Let m be the number of reviews in market (web site) and $k (k \leq m)$ be the number of aspect, i.e., a user has to select one review and assigns a numerical rating to their aspects from the numbers 1 to k . Let r_{ij} be the number of j th place aspect rating of the review i th where $i = 1 \dots m$ and $j = 1 \dots k$. Now preference score z_i should be calculated for each review i as a weighted sum of aspect ratings with certain weight w_i , i.e.,

$$z_i = \sum_{j=1}^k w_j r_{ij} \quad (1)$$

Using data envelopment analysis (DEA), Cook and Kress [9] have proposed a method for estimating preference scores without imposing any fixed weights from outset. Each review score is calculated with their most favorable weights. Their formulation is the following:

$$Z_o^* = \text{maximize} \sum_{j=1}^k w_j r_{ij} \quad (2)$$

$$\text{s.t. } \sum_{j=1}^k w_j r_{ij} \leq 1, \quad i = 1, \dots, m, \quad (3)$$

$$w_{j+1} - w_j \geq d(j, \in), \quad j = 1, \dots, k-1, \quad (4)$$

$$w_k \geq d(k, \in), \quad (5)$$

where $d(\cdot, \in)$, called the discrimination intensity function, is non-negative and non-decreasing in \in , and satisfies $d(\cdot, 0) = 0$. Parameter \in is non-negative.

After applying DEA, value of z_i will be one for all efficient reviews. After the problems are solved for all reviews, several (not only one) reviews often achieve the maximum attainable score one. We call these reviews as efficient reviews. We can judge that the set of efficient reviews is the top group of reviews, but cannot single out only one best among them.

3.2.2 Discriminate Efficient Reviews

Let \hat{z}_o be normalized preference score of efficient reviews ($z_i = 1$) that has to be calculated. Model for ranked voting method with discrimination of efficient reviews is as follows:

$$1/\hat{z}_o = \text{minimizew} \|w\|, \quad (6)$$

$$\text{s.t. } \sum_{j=1}^k w_j r_{oj} = 1, \quad (7)$$

$$\sum_{j=1}^k w_j r_{ij} \leq 1, \quad i \neq 0, \quad (8)$$

$$w_{j+1} - w_j \geq d(j, \in), \quad j = 1, \dots, k-1, \quad (9)$$

$$w_k \geq d(k, \in), \quad (10)$$

where $d(\cdot, \in)$ called discrimination intensity function is non-negative and non-decreasing in $\in \geq 0$ and satisfies $d(\cdot, 0) = 0$. Constraint (7) is for efficient reviews, constraint (8) is for reviews which are not efficient, and constraint (9) means aspect of higher place which may have greater importance than that of the lower place. The normalized preference score \hat{z}_o is obtained as a reciprocal of the optimal value. Review with highest normalized preference score will be the winner, i.e., best review for user.

Our method does not use any information about inefficient reviews and the problem of changing the order of efficient reviews does not occur, because there is no existence of an inefficient review. In the next section, we present our method with an example.

4 Illustration of Our Method with Example

We illustrate our method with an example (Table 2). Preference scores for each review are calculated by Cook and Kresss basic model (2)–(5). Here, we use $d(\cdot, \epsilon) = 0$. Their preference scores are as shown in Table 3.

After the problems are solved for all reviews, several (not only one) reviews often achieve the maximum attainable score one. We call these reviews as efficient reviews. Hence, in the above shown example, the reviews review1, review2, review9, review10, and review6 seem to be efficient. We can judge that the set of efficient reviews is the top group of reviews, but cannot single out only one best among them.

In order to discriminate efficient reviews, we can apply our approach. which does not use information of inefficient review. So we can apply our proposed approach to discriminate efficient review (Table 4) to find a best review for a user. Their scores are as follows:

review1: 34.999913, **review6:** 32.999963, **review2:** 31.999979, **review9:** 29.882341, and **review10:** 28.315784

From the above result, it can be observed that the review **review1: 34.999913** is the best among them.

Table 2 Sample data ($m = 10, k = 5$)

Review	Aspect1	Aspect2	Aspect3	Aspect4	Aspect5
Review1	35	11	9	11	8
Review2	22	42	32	16	9
Review3	28	16	9	10	11
Review4	13	11	14	22	21
Review5	16	9	10	8	6
Review6	34	22	11	14	10
Review7	12	16	20	21	28
Review8	10	10	14	26	30
Review9	32	24	22	16	13
Review10	26	31	32	22	16

Table 3 Review with preference score

S. no.	Review	Preference score	S. no.	Review	Preference score
1	Review1	1	6	Review3	0.822123
2	Review2	1	7	Review7	0.763779
3	Review9	1	8	Review8	0.708661
4	Review10	1	9	Review4	0.637795
5	Review6	1	10	Review5	0.487603

Table 4 Sample data ($m = 5$, $k = 5$)

Review	Aspect1	Aspect2	Aspect3	Aspect4	Aspect5
Review1	35	11	9	11	8
Review2	22	42	32	16	9
Review9	32	24	22	16	13
Review10	26	31	32	22	16
Review6	34	22	11	14	10

5 Conclusions and Future Works

Due to the enormous increase in online reviews, there are various products which have thousands of user-generated reviews. Mining this enormous online reviews and tuning these abundant individual consumers view into collective consumer's choice become a challenging task. To solve this problem, we have proposed a ranking mechanism which can be efficiently used to rank different reviews in accordance to their aspects rating. The ranked voting method has been used to rank the reviews. The effectiveness of our approach has been shown through an example. Ranked voting method does not use inefficient review's information to discriminate efficient reviews; therefore, order of efficient review never changes even if inefficient reviews are added or removed.

In future, this framework may also be applied for recommendation of the top-k reviews on the basis of aspects reviews rating. Furthermore, this approach can be applied in different applications in opinion mining. In this work, our framework is only illustrated through example. Furthermore, we can extend this model on various reviews available in real life.

References

1. Liu, B.: Sentiment analysis and opinion mining. *Synth. Lect. Hum. Lang. Technol.* **5**(1), 1–167 (2012)
2. Liu, B.: Sentiment analysis and subjectivity. In: *Handbook of Natural Language Processing*. Marcel Dekker, Inc., New York (2009)
3. Liu, B., Hu, M., Cheng, J.: Opinion observer: analyzing and comparing opinions on the web. In: *Proceedings of 14th International Conference on WWW*, pp. 342–351. Chiba, Japan (2005)

4. Hu, M., Liu, B.: Mining and summarizing customer reviews. In: Proceedings of SIGKDD, pp. 168–177. Seattle, WA, USA (2004)
5. Wu, Y., Zhang, Q., Huang, X., Wu, L.: Phrase dependency parsing for opinion mining. In: Proceedings of ACL, pp. 1533–1541, Singapore (2009)
6. Ohana, B., Tierney, B.: Sentiment classification of reviews using SentiWordNet. In: Proceedings IT&T Conference, Dublin, Ireland (2009)
7. Pang, B., Lee, L., Vaithyanathan, S.: Thumbs up? Sentiment classification using machine learning techniques. In: Proceedings of EMNLP, pp. 79–86. Philadelphia, PA, USA (2002)
8. Obata, T., Ishii, H.: A method for discriminating efficient candidates with ranked voting. *Eur. J. Oper. Res.* **151**, 233–237 (2003)
9. Cook, W.D., Kress, M.: A data envelopment model for aggregating preference rankings. *Manage. Sci.* **36**(11), 1302–1310 (1990)

Multi-level Thresholding Segmentation Approach Based on Spider Monkey Optimization Algorithm

**Swaraj Singh Pal, Sandeep Kumar, Manish Kashyap,
Yogesh Choudhary and Mahua Bhattacharya**

Abstract Image Segmentation is an open research area in which Multi-level thresholding is a topic of current research. To automatically detect the threshold, histogram-based methods are commonly used. In this paper, histogram-based bi-level and multi-level segmentation are proposed for gray scale image using spider monkey optimization (SMO). In order to maximize Kapur's and Otus's objective functions, SMO algorithm is used. To test the results of SMO algorithm, we use standard test images. The standard images are pre-tested and Benchmarked with Particle Swarm Optimization (PSO) Algorithm. Results confirm that new segmentation method is able to improve upon result obtained by PSO in terms of optimum threshold values and CPU time.

Keywords Image segmentation · Thresholding · Spider monkey optimization algorithm

1 Introduction

Image segmentation is essential and important technique for advance image analysis. In general, image segmentation divides an image into related sections and subsections or regions which consist of pixel/voxel and their relationship among

S.S. Pal (✉) · S. Kumar · M. Kashyap · Y. Choudhary · M. Bhattacharya
ABV-Indian Institute of Information Technology and Management, Gwalior
Madhya Pradesh, India
e-mail: swarajsinghpal@gmail.com

S. Kumar
e-mail: sandeep2006iiitm@gmail.com

M. Kashyap
e-mail: manishkashyap.iiit@gmail.com

Y. Choudhary
e-mail: yogeshchoudhary135@gmail.com

many data features values. There are several application of image segmentation includes: medical imaging application [1, 2], object recognition, machine vision, object detection, and quality inspection [3] of material.

There are many approaches of image segmentation such as segmentation based on edge detection, threshold-based methods, region-based segmentation methods, etc. [4]. Among all approaches of image segmentation, threshold-based segmentation is simple but effective approach. The threshold-based segmentation approach can be classified into two ways: bi-modal and multi-modal approach. In bi-modal, one threshold value is selected for segmentation and generates two classes. But in the real world, segmentation problems image's histograms are always multi-modal type. Therefore, it is a big problem to find the exact Position of different valley in multi-modal histograms. Hence, the problem of multi-modal thresholding is an interesting area of research.

In past decades, most of the thresholding approaches have been proposed [5]. A survey of thresholding techniques [5] presented a variety of thresholding techniques including both global and local thresholding, among which, the global histograms-dependent techniques are broadly used for determine the threshold [6, 7]. The global thresholding method can be classified into point-dependent and region-dependent methods [5]. In point-dependent methods use gray level dispersion of each class has a density that follows a Normal distribution. These techniques are highly computationally complex.

Otsu's methodology [8] chooses the best threshold worth by maximizing variance of gray levels between classes. Kapur's realize the best threshold values by maximizing of entropy of the histogram [9]. Otsu's and Kapur's methodology each ways are extended to multi-level thresholding issues, however, ineffective to work out best threshold values owing to the exponential growth in process time. To improve the performance, many approaches have been developed for solving the multi-level thresholding problem. To reduce the computational time, evolutionary algorithms are applied for selecting the multi-modal thresholds such as particle swarm optimization algorithm [6].

Spider Monkey Optimization (SMO), first introduced by J.C. Bansal et al., is one in all the fashionable heuristic algorithmic program [10] supported foraging dy of spider monkeys. Spider monkeys are categorized as fission–fusion social organization primarily based animals. During this paper, the SMO algorithmic program is employed for choosing the multi-modal threshold values. The SMO technique is checked on varied various test pictures, and results are compared with the PSO in terms of best threshold values and C.P.U. time.

2 Problem Formulation

The best multi-thresholding strategies choose the threshold values such the various classes of the image histogram satisfy the specified properties. This is executed by solving an objective function in terms of maximization or minimization, which uses

the chosen threshold as parameters. During this paper, 2 best thresholding strategies are used: first methodology given by Kapur et al. (thresholding using the entropy of the histogram) and the second methodology is given by Otsu (using gray level histogram).

2.1 Kapur's Method (Entropy of Histogram)

Kapur has developed a new algorithm for bi-modal [9] or bi-level thresholding, and this bi-modal thresholding is described as follows: Let L be the gray level within the given image and these gray level range are $\{0, 1, 2, \dots, (L - 1)\}$. Then, prevalence chance of gray level g is outlined by the below equation:

$$P_g = \frac{h(g)}{N} \quad \text{for } (0 \leq g \leq (L - 1)),$$

where $h(g)$ denotes the number of pixel for the corresponding gray level L , and the total number of pixel is denoted by N in the image which is also denote this way $N = \sum_{g=0}^{L-1} h(g)$. Then the objective is maximizing the fitness function as follows:

$$f(s) = H_0 + H_1, \quad (1)$$

where

$$\begin{aligned} H_0 &= - \sum_{g=0}^{s-1} \frac{P_g}{w_0} \ln \frac{P_g}{w_0}, & w_0 &= \sum_{g=0}^{s-1} P_g \text{ and} \\ H_1 &= - \sum_{g=s}^{L-1} \frac{P_g}{w_1} \ln \frac{P_g}{w_1}, & w_0 &= \sum_{g=s}^{L-1} P_g \end{aligned}.$$

Above Kapur's entropy of histogram methodology also extension to multi-modal thresholding or multi-level thresholding drawback and may be describe as follows: n -dimensional optimisation problem, for choosing n best threshold values for a given image $[s_1, s_2, \dots, s_n]$, wherever the target is to maximization of the objective function:

$$f([s_1, s_2, \dots, s_n]) = H_0 + H_1 + H_2 + \dots + H_n \quad (2)$$

where

$$\begin{aligned} H_0 &= - \sum_{g=0}^{s_1-1} \frac{P_g}{w_0} \ln \frac{P_g}{w_0}, & w_0 &= \sum_{g=0}^{s-1} P_g, \\ H_1 &= - \sum_{g=s_1}^{s_2-1} \frac{P_g}{w_0} \ln \frac{P_g}{w_0}, & w_0 &= \sum_{g=s_1}^{s_2-1} P_g, \\ H_2 &= - \sum_{g=s_2}^{s_3-1} \frac{P_g}{w_0} \ln \frac{P_g}{w_0}, & w_0 &= \sum_{g=s_2}^{s_3-1} P_g, \\ H_n &= - \sum_{g=s_n}^{L-1} \frac{P_g}{w_0} \ln \frac{P_g}{w_0}, & w_0 &= \sum_{g=s_n}^{L-1} P_g. \end{aligned}$$

2.2 Otsu's Method (Gray Level Histogram-Based Method)

The Otsu developed a method, which is based on between class variance [8], is used to determine the threshold values and describe as follows:

Let L be the gray level of the given image and the range of the gray level is $\{1, 2, \dots, L\}$. The number of pixel at the g level is denoted by f_g , and the total number of pixel N is equal to $(f_1 + f_2 + \dots + f_L)$. At the g th level, image occurrence probability is given as follows:

$$p_g = \frac{f_g}{N}, \quad p_g \geq 0, \quad \sum_{g=1}^L p_g = 1.$$

If image is bi-level image then it is divide into two classes, C_0 and C_1 , at threshold level s , class C_0 contains the gray levels from 0 to s and C_1 contain other gray level with $s + 1$ to L , and the gray level probabilities ($w_0(s)$ and $w_1(s)$) distribution for the two classes are describe as follows:

$$C_0 : \frac{p_1}{w_0(s)}, \dots, \frac{p_s}{w_0(s)},$$

and

$$C_1 : \frac{p_{s+1}}{w_1(s)}, \dots, \frac{p_L}{w_1(s)},$$

where $w_0(s) = \sum_{g=1}^s p_g$ and $w_1(s) = \sum_{g=s+1}^L p_g$.

Mean values of C_0 and C_1 classes are μ_0 and μ_1 , respectively, and describe as follows:

$$\mu_0 = \sum_{g=1}^s \frac{gp_g}{w_0(s)},$$

$$\mu_1 = \sum_{g=s+1}^L \frac{gp_g}{w_1(s)}.$$

Let the mean intensity of the whole image is μ_S and it is easy to show that

$$w_0\mu_0 + w_1\mu_1 = \mu_S, \text{ and } w_0 + w_1 = 1.$$

Using analysis, the total variance of the level is:

$$\sigma_{BC}^2 = \sigma_0 + \sigma_1,$$

where $\sigma_0 = w_0(\mu_0 - \mu_S)^2$ and $\sigma_1 = w_1(\mu_1 - \mu_S)^2$.

The objective function can be defined as:

$$\text{Maximize } J(s) = \sigma_{BC}^2 = \sigma_0 + \sigma_1. \quad (3)$$

Above method can also be extended for multi-modal thresholding problems [8] and can be describing as follows: n -dimensional improvement drawback, for determination of n best threshold values for a given image $[s_1, s_2, \dots, s_n]$, which divide the initial image into n -categories such as C_0 for $[0, \dots, s_1 - 1]$, C_1 for $[s_1, \dots, s_2 - 1]$... and C_n for $[s_n, \dots, L - 1]$, and the best threshold values are selected by maximizing the following equation:

$$\text{Maximize } J(s) = \sigma_0 + \sigma_1 + \sigma_2 + \dots + \sigma_n, \quad (4)$$

where

$$\sigma_0 = w_0(\mu_0 - \mu_S)^2,$$

$$\sigma_1 = w_1(\mu_1 - \mu_S)^2,$$

$$\sigma_2 = w_2(\mu_2 - \mu_S)^2,$$

and so on.

$$\sigma_n = w_1(\mu_n - \mu_S)^2.$$

In this paper, the SMO technique is employed to seek out the best threshold values by maximizing the target the objective of Kapur's methodology and also Otsu's methodology for multi-modal thresholding.

3 Overview of Spider Monkey Optimization Algorithm

Spider monkey optimization algorithm is a newest addition in group of swarm intelligence. SMO is motivated by intelligent foraging behavior of fission–fusion social structure creatures [11–13].

3.1 Major Steps or Phases of Spider Monkey Optimization (SMO) Algorithm

The SMO progression consists of 7 major phases. Description of each step or phase as follows:

3.1.1 Phase 1

The first phase is initialization of the population. Initial population size is N here each monkey $\text{SM}_k(k = 1, 2, \dots, N)$ is D -dimensional vector. SM_k -Denotes the k th Spider Monkey (SM) in the population. Each SM_k is initialized as follows:

$$\text{SM}_{kj} = \text{SM}_{\min j} + \gamma * (\text{SM}_{\max j} - \text{SM}_{\min j}) \text{ here } \gamma \in (0, 1).$$

Here $\text{SM}_{\max j}$ and $\text{SM}_{\min j}$ are the boundaries.

3.1.2 Phase 2

The second phase is called Local Leader Phase (LLP). In this phase, the position is update using local leader experience and local group member experience. The position updates equation for k th SM (which is a member of i th local group) is:

$$\text{SM}_{\text{new}kj} = \text{SM}_{kj} + \gamma_1 * (\text{LL}_{ij} - \text{SM}_{kj}) + \gamma_2 * (\text{SM}_{rj} - \text{SM}_{kj}).$$

Here $\gamma_1 \in (0, 1)$ and $\gamma_2 \in (-1, 1)$

Here SM_{kj} is the j th dimension of the k th SM, and LL_{kj} denotes the j th dimension of the i th local group leader position. SM_{rj} Denotes the j th dimension of the r th SM which is selected randomly within i th group and $r \neq k$.

3.1.3 Phase 3

In this phase position of Global Leader is updated hence it is called Global Leader Phase (GLP). Position is updated using Global Leader's experience and local group member's experience and equation as follows:

$$\text{SM}_{\text{new}kj} = \text{SM}_{kj} + \gamma_1 * (\text{GL}_j - \text{SM}_{kj}) + \gamma_2 * (\text{SM}_{rj} - \text{SM}_{kj}),$$

where $\gamma_1 \in (0, 1)$ and $\gamma_2 \in (-1, 1)$

Here GL_j is the j th dimension of global leader position and $j \in \{1, 2, \dots, D\}$.

In GLP phase, the location of SM_k is updated based on probabilities p_i 's which are considered using their fitness value and calculate as follows:

$$p_k = 0.9 * \frac{\text{fit}_k}{\text{max_fit}} + 0.1, \quad (5)$$

Here fit_k is fitness value of the k th SM, and max_fit is the maximum fitness in the group [14].

3.1.4 Phase 4

This phase is Global Leader Learning (GLL) phase. By applying a voracious selection approach in the given population, the position of GL is updated. The updated location of the global leader is selected as the position of SM which has the best fit in the same population. Then it is checked that the position of GL is updating or not; Global limit count is incremented by 1 iff the position of GL is not updated.

3.1.5 Phase 5

This phase is Local Leader Learning (LLL) phase. In this phase, greedy selection algorithm is applied to the group. The algorithm looks for the position of unexcelled fitness in the group. This position of SM is updated position for Local Leader (LM). Local Limit count is incremented by 1 iff LL is not updated.

3.1.6 Phase 6

In the Local Leader Decision (LLD) phase, it may be the case that following the above procedure, any of the LL positions are not updated. In such situation, a random initialization is usually done or the following equation is used in conjunction with mutual information from GL to update the same. If any LL position is

not updated up to a predefined threshold called LL_{limit} , then the above procedure is done.

$$SM_{\text{new}ij} = SM_{ij} + \gamma * (GL_j - SM_{ij}) + \gamma * (SM_{ij} - SM_{kj}),$$

where $\gamma \in (0, 1)$.

3.1.7 Phase 7

This is Global Leader Decision (GLD) phase. In this phase, the different strategies for updating the GL position is followed and it is exceed to predetermined threshold values called GL_{limit} . If GL position is not updated till a GL_{limit} , the entire population is divided into a smaller groups starting from 2, 3, 4... till maximum number of group (MG) is formed. In rarest of rare case when MG is formed but GL is not updated, combining all the groups in a single group required.

3.2 SMO Algorithm for Multi-level Thresholding Problem

- Step 1. Initialize the population, LL_{limit} , GL_{limit} , and perturbation rate (pr).
- Step 2. Calculate the fitness value
- Step 3. Select leader by apply greedy selection approach (both LL and GL)
- Step 4. While (termination condition is not fulfilled) do
- Step 5. Generate a new position for finding the objective and that positions are calculated using self experience, local leader experience, and group member experience.
- Step 6. Based on fitness value, we select the best one between existing position and newly generated position using greedy selection approach.
- Step 7. Using Eq. 5, compute the probability of each individual in a group.
- Step 8. Generate new position for each individual in a group selected by p_k , based on individual's experiences.
- Step 9. Using the greedy selection approach, modernize the position of LL and GL, in all the groups.
- Step 10. Re-direct every individuals in a particular foraging by algorithm iff any local leader is not update her location after a predetermined threshold that is LL_{limit} .
- Step 11. If any Global Group Leader is not updating her location after predetermined threshold that is GL_{limit} that Group Leader divides the group into smaller subgroups.
- Step 12. End While

4 Result and Discussions

The pertinency and viability of above-mentioned approach for multi-level thresholding in the field of image segmentation is tested on five standard test images. Results which are obtained by SMO approach compared with PSO technique. Five images namely Camera man, Lena, Hunter, Butterfly, and Living room are showed with their corresponding histograms in Fig. 1. The parameters of SMO algorithm are given in Table 1.

The proposed approach is applied on entropy of the histogram-based objective function (kapur's extended function) and compared with PSO. Table 2 shows the objective values, optimal thresholds, and CPU time. The proposed approach gives a better result compare to PSO method. In Fig. 2, the quality of the segmentation for all five test images is better when $n = 5$ than other value of n .

The second case includes Otsu's method. When we applied SMO approach on between class variance-based objective function (Otsu's objective function) and compare with PSO method, the objective values, optimal thresholds values, and CPU time are shown in Table 3. Results show that objective values of SMO

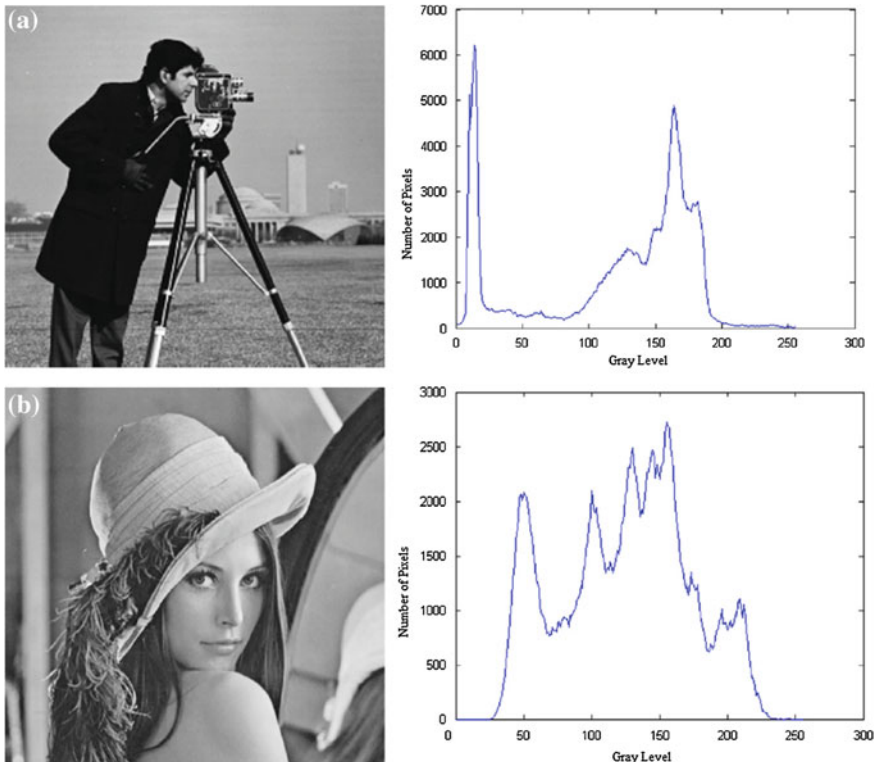
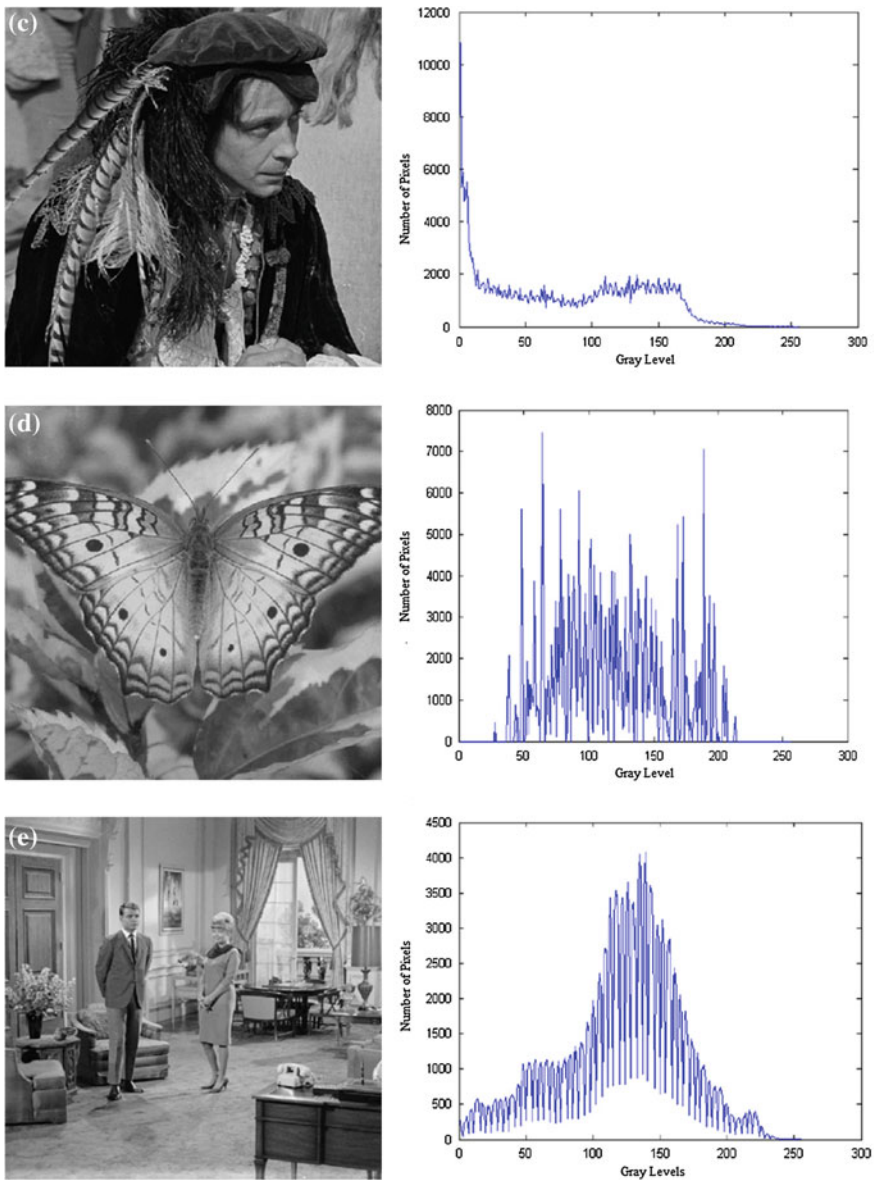


Fig. 1 Standard Images and its corresponding Histograms (a–e)

**Fig. 1** (continued)**Table 1** Parameter used for SMO methods

Parameter	Value
The swarm size N	50
Maximum number of group MG	5
Global leader limit GL_{limit}	50
Local leader limit LL_{limit}	1500
Perturbation rate pr	0.1–0.4

Table 2 Comparison, when Kapur's objective function is used

Test images	<i>n</i>	Objective values			Threshold values			CPU time		
		SMO	PSO	SMO	PSO	SMO	PSO	SMO	PSO	SMO
Cameraman	2	12.3546	12.22596	117,195		116,195		7.8126		8.0525
	3	16.2409	15.22246	95,140,194		96,139,192		8.1267		9.1265
	4	19.1052	18.0007	41,96,140,201		76,116,150,202		8.6269		9.3525
	5	21.5112	19.9252	41,85,115,151,199		70,96,119,155,198		9.1262		10.1084
	Lena	2	12.5470	12.3320	96,165	99,166		7.2064		7.8004
Hunter	3	16.2006	15.9252	88,143,189		86,150,181		7.7334		8.0121
	4	17.9808	17.7388	73,115,153,185		92,130,161,191		8.5656		9.1734
	5	20.6509	20.4452	64,95,139,162,195		74,114,144,170,197		8.8845		9.4024
	2	12.4733	12.3908	84,178		82,178		7.3592		8.0001
	3	15.6622	15.1268	58,105,176		85,127,167		8.1813		8.8055
Butterfly	4	18.3718	18.0402	50,98,138,182		73,132,172,200		8.8354		9.0025
	5	21.6525	20.2559	49,95,138,178,222		90,120,165,191,218		9.7252		10.1521
	2	10.3729	10.0023	96,145		95,142		7.2572		7.7122
	3	12.5746	12.3131	74,108,153		63,126,171		7.9905		8.2562
	4	14.8726	14.2571	71,97,128,157		71,113,163,185		8.2521		9.0000
LivingRoom	5	16.9292	16.1144	74,97,120,144,169		92,116,143,157,182		8.7563		9.5241
	2	12.4058	12.4000	89,171		86,175		7.2572		7.7122
	3	15.6055	15.1250	71,125,174		73,159,188		7.9905		8.2562
	4	18.9195	18.1410	60,105,148,188		58,125,173,203		8.2521		9.0000
	5	21.2298	20.6252	47,94,135,168,202		72,97,118,159,199		8.7563		9.5241



Fig. 2 Segmented Image based on SMO approach when number of threshold 3, 4, and 5 (a'-e')

Table 3 Comparison, when Otsu's objective function is used

Image name	<i>n</i>	Objective values			Threshold values			CPU time		
		SMO	PSO	SMO	PSO	SMO	PSO	CPU time	SMO	PSO
Cameraman	2	3654.5029	3610.4242	71,142	71,143	71,135,167	71,135,167	3.1567	3.5011	4.2113
	3	3684.5623	3678.2006	62,119,156	62,119,156	65,122,148,173	65,122,148,173	4.3245	4.8223	5.2456
	4	3838.1202	3725.2342	49,105,143,171	49,105,143,171	45,79,122,148,173	45,79,122,148,173	4.7678	5.2456	5.6445
Lena	5	3868.2239	3860.2515	39,87,126,152,175	39,87,126,152,175	90,150	93,152	3.5252	3.6445	4.2897
	2	1968.5656	1960.3423	78,125,171	78,125,171	78,113,135,178	78,113,135,178	4.5236	4.7299	5.2543
	3	2129.0786	2128.0007	77,117,159,184	77,117,159,184	66,92,123,159,183	66,92,123,159,183	4.9567	5.2543	5.2543
	4	2190.0567	2181.6734	79,111,141,168,189	79,111,141,168,189	51,118	52,117	3.2012	3.8166	4.4262
	5	2250.6022	2215.6725	36,87,134	36,87,134	35,83,131,158	35,83,131,158	4.2642	4.9671	5.2362
Hunter	2	3164.2244	3164.0034	98,151	98,151	36,84,126,153,178	36,84,126,153,178	4.8023	5.2362	5.6121
	3	3315.2230	3314.8967	78,119,163	78,119,163	80,114,146,178	80,114,146,178	3.8121	4.2045	4.8198
	4	3390.3504	3257.1256	75,106,138,168	75,106,138,168	73,105,128,155,182	73,105,128,155,182	5.1812	5.4234	5.8134
	5	3295.1229	3275.9808	89,146	89,146	80,126,166	80,126,166	3.8281	4.3456	4.7211
	6	1554.5634	1553.2902	68,109,142,179	68,109,142,179	57,99,129,157,191	57,99,129,157,191	4.0132	5.1623	5.8134
Butterfly	2	1668.2189	1665.4564	89,146	89,146	80,126,166	80,126,166	3.9567	3.5234	4.3456
	3	1708.4732	1703.5645	75,106,138,168	75,106,138,168	73,105,128,155,182	73,105,128,155,182	3.8281	4.3456	4.7211
	4	1734.0212	1731.8967	89,146	89,146	80,126,166	80,126,166	3.8281	4.3456	4.7211
	5	1599.8220	1599.0065	68,109,142,179	68,109,142,179	57,99,129,157,191	57,99,129,157,191	4.0132	5.1623	5.8134
	6	1759.8257	1757.2367	89,146	89,146	80,126,166	80,126,166	3.8281	4.3456	4.7211
LivingRoom	2	1836.3242	1822.8743	89,146	89,146	80,126,166	80,126,166	3.8281	4.3456	4.7211
	3	1868.9966	1865.9812	89,146	89,146	80,126,166	80,126,166	3.8281	4.3456	4.7211
	4	1868.9966	1865.9812	89,146	89,146	80,126,166	80,126,166	3.8281	4.3456	4.7211
	5	1868.9966	1865.9812	89,146	89,146	80,126,166	80,126,166	3.8281	4.3456	4.7211
	6	1868.9966	1865.9812	89,146	89,146	80,126,166	80,126,166	3.8281	4.3456	4.7211

algorithm are higher than the PSO methods, and the quality of segmentation is better than the PSO methods in Fig. 2, and it is clearly showed that the segmentation is the best when $n = 5$.

Computational efficiency of both approaches is compared, based on the average CPU time in second taken to converge the solution, which is shown in Tables 2 and 3. The results prove that SMO converges quickly than the PSO approach.

5 Conclusion

In this paper, the Spider Monkey Optimization (SMO) algorithm is proposed for solving multi-level thresholding problems. Verification of efficiency and effectiveness for proposed SMO approach, two studies is examined in which the kapur's method and Otsu's method objective function are considered. The SMO approach tested on the various standard images, and the result is verified by those obtained by PSO approach. The observational results show that the SMO approach outperforms over PSO approach in terms of optimal threshold values and computational time and converge rapidly. Future research is to be carried out to test the feasibleness of proposed approach and comparison to other techniques on various types of image processing applications.

References

1. Saha, S., Bandyopadhyay, S.: Automatic MR brain image segmentation using a multiseed based multiobjective clustering approach. *Appl. Intell.* **35**(3), 411–427 (2011)
2. McInerney, T., Terzopoulos, D.: A dynamic finite element surface model for segmentation and tracking in multidimensional medical images with application to cardiac 4D image analysis. *Comput. Med. Imaging Graph.* **19**(1), 69–83 (1995)
3. Brosnann, T., Sun, D.-W.: Improving quality inspection of food product by computer vision—a review. *J. Food Eng.* **61**(1), 3–16 (2004)
4. Fu, K.-S., Mui, J.K.: A survey on image segmentation. *Pattern Recogn.* **13**(1), 3–16 (1981)
5. Sankur, B., Sezgin, M.: Image thresholding techniques: a survey over categories. *Pattern Recogn.* **34**(2), 1573–1607 (2001)
6. Maitra, M., Chatterjee, A.: A hybrid cooperative–comprehensive learning based PSO algorithm for image segmentation using multilevel thresholding. *Expert Syst. Appl.* **34**(2), 1341–1350 (2008)
7. Bhandari, A.K., et al.: Cuckoo search algorithm and wind driven optimization based study of satellite image segmentation for multilevel thresholding using Kapur's entropy. *Expert Syst. Appl.* **41**(7), 3538–3560 (2014)
8. Otsu, N.: A threshold selection method from gray-level histograms. *Automatica* **11**(285–296), 23–27 (1975)
9. Kapur, J.N., Sahoo, P.K., Wong, A.K.C.: A new method for gray-level picture thresholding using the entropy of the histogram. *Comput. Vision, Graphics, Image Process.* **29**(3), 273–285 (1985)

10. Bansal, J.C., et al.: Spider monkey optimization algorithm for numerical optimization. *Memetic Comput.* **6**(1), 31–47 (2014)
11. Kennedy, J.: Particle swarm optimization. In: *Encyclopedia of Machine Learning*, pp. 760–766. Springer, New York (2010)
12. Ma, M., et al.: SAR image segmentation based on Artificial Bee Colony algorithm. *Appl. Soft Comput.* **11**(8), 5205–5214 (2011)
13. Karaboga, D., et al.: A comprehensive survey: artificial bee colony (ABC) algorithm and applications. *Artif. Intell. Rev.* **42**(1), 21–57 (2014)
14. Maitra, M., Chatterjee, A.: A hybrid cooperative–comprehensive learning based PSO algorithm for image segmentation using multilevel thresholding. *Expert Syst. Appl.* **34**(2), 1341–1350 (2008)

Dynamic Multiuser Scheduling with Interference Mitigation in SC-FDMA-Based Communication Systems

P. Kiran and M.G. Jibukumar

Abstract Virtual multiple input multiple output (V-MIMO) systems employ a variety of scheduling algorithms to group multiple users and allocate the same set of physical resources to improve the spectral efficiency by exploiting the multiplexing capability in cellular uplink (UL) communication. This paper proposes an efficient dynamic scheduling algorithm for SC-FDMA-based UL network. It estimates the possible interference caused due to adding a new user to existing multiuser group and optimally selects users such that the interference level is within the limit for the receiver to perform flawless detection. A threshold for interference level based on the average SINR of the receiver ensures that users can be dynamically added to an existing group provided the total interference after adding new user is under the limit. Our extensive simulation results based on 3GPP LTE UL network shows that the proposed algorithm has much better performance than the existing random dynamic scheduling technique.

Keywords Dynamic scheduling · Virtual MIMO · Multiuser scheduling · SC-FDMA · Uplink scheduling

1 Introduction

Introduction of single carrier—frequency division multiple access (SC-FDMA) technique has improved the efficiency of multiuser transmission technology by reducing the peak to average power ratio (PAPR), thereby making it a part of 3GPP LTE specifications. SC-FDMA with multiuser scheduling is used in LTE cellular uplink (UL) [1]. Multiuser scheduling, which is also known as virtual multiple input

P. Kiran (✉) · M.G. Jibukumar

School of Engineering, Cochin University of Science and Technology, Kochi 22, India
e-mail: kirang37@gmail.com

M.G. Jibukumar
e-mail: jibukumar@cusat.ac.in

multiple output (V-MIMO) is the technique where more than one user is allocated with the same set of physical resources and are allowed to perform simultaneous transmissions by utilizing the spatial multiplexing concept [1, 2]. Small physical size of user equipment (UE) limits the number of antennas that can be mounted on it. Thus, by having multiple antennas (N_r , number of antennas) at the base station, known as eNodeB for LTE, and single antenna at each UE, a V-MIMO system can be formed with a maximum of N_r number of UEs connected to the eNodeB, sharing the same set of resources. Spatial resolution among jointly scheduled users is an important factor to be considered, as it determines the resolvability of multiple received signals. Thus, the users to perform joint scheduling need to be chosen based on some factor such that the multiuser interference (MUI) is at minimum and the signals from different users can be resolved with reliable levels of accuracy.

1.1 Literature Review

Different approaches and implementation algorithms have been proposed for multiuser scheduling in LTE cellular UL. The basic method is Random Pairing and scheduling (RPS) [1]. Here, multiple UEs are selected randomly and are scheduled together to use the same set of physical resource blocks (PRBs). For an eNodeB having N_r receive antennas, N_r UEs can be randomly selected and scheduled together. UEs can also be scheduled dynamically whenever the number goes below N_r . In Determinant Scheduling (DS) scheme, UEs with close to orthogonal channels are chosen [2]. Channel orthogonality ensures least MUI and thus, high signal resolution at the receiver. Identifying orthogonal channels and scheduling the UEs become an exhaustive task as the number of resource requesting UEs increases. And, UEs with least orthogonal channels will suffer from resource starvation. This problem is overcome in Proportional Fair Scheduling (PFS), where average throughput of the resource requesting user is taken as the parameter to be considered for scheduling [3, 4]. Among the resource requesting UEs, the ones with higher average throughput are jointly scheduled. PFS again, will not support dynamic scheduling. Han et al. [5] propose an SINR-based multiuser scheduling technique, which uses average received SINR as the parameter for scheduling. UEs with large SINR at the receiver and relatively small SINR gap among themselves are scheduled together to use the same PRBs. SINR-based scheduling converges to random scheduling if used dynamically. The Group-based scheduling (GS) given in [6] is a suboptimal scheduling method where UEs are divided into two groups—low SNR group and high SNR group based on a defined SNR threshold. UEs from high SNR group alone are considered for scheduling. This method supports dynamic pairing but does not have any interference limiting mechanisms. Correlation-based scheduling given in [7] utilizes the correlation among user channels as the parameter for scheduling. User/UE with highest channel gain among resource requesting UEs is selected as first user. The second UE selected will have the least channel correlation with the first UE. Similarly, the third selected

UE will have the least correlation with both first and second UEs and so on. This also is a complex and exhaustive selection process, which exploits the spatial diversity and multiplexing in terms of channel correlation.

The main factor deciding effectiveness of multiuser V-MIMO communication is the means by which users are selected for scheduling. In this paper, we propose an efficient dynamic scheduling technique where the interference level is estimated each time before a new user is added to a multiuser group. User will be added only if the total interference level (sum of existing and estimated) is below the threshold. This ensures a good quality signal at the eNodeB from all users in the multiuser group along with improving spectral efficiency.

The remainder of the paper is organized as follows. Section 2 gives the system model for SC-FDMA cellular uplink and provides an analysis of interference calculation method for two users, paired to form a 2X2 V-MIMO. Section 3 presents the interference estimation technique which is derived based on Sect. 2. The proposed dynamic pairing algorithm is given in Sect. 4 and the simulation results and analysis in Sect. 5.

2 System Model

A single cell scenario is considered, with base station at the center of the cell and N_a number of UEs uniformly distributed throughout the circular area of the cell. The system uses SC-FDMA technique for UL communication. Let N_u out of N_a users are requesting the eNodeB for resource allocation at a time. If there is N_r number of receive antennas at eNodeB, and then N_r out of N_u users can be selected and scheduled together to use same PRBs for uplink communication. eNodeB uses a minimum mean square error—frequency domain equalizer (MMSE-FDE) receiver.

2.1 Transmitted SC-FDMA Signal

Consider a two-user paired system for SC-FDMA with localized spectrum mapping-based cellular uplink having M_b symbol block transmission and $N_r = 2$. A maximum of two users can be paired. At the transmitter of each UE, $M_{b1} = \{s_1(n); n = 0, 1, 2, \dots, M_{b1} - 1\}$ and $M_{b2} = \{s_2(n); n = 0, 1, 2, \dots, M_{b2} - 1\}$ symbols, respectively, are transformed into frequency domain symbols by taking M_b -point FFT to form $\{S_1(k); k = 0, 1, 2, \dots, M_{b1} - 1\}$ and $\{S_2(k); k = 0, 1, 2, \dots, M_{b2} - 1\}$. DFT output of the users will be:

$$S_1(k) = \sqrt{\frac{1}{M_b}} \sum_{n=0}^{M_b-1} s_1(n) \exp\left(-j2\pi k \frac{n}{M_b}\right) \quad (1)$$

$$S_2(k) = \sqrt{\frac{1}{M_b}} \sum_{n=0}^{M_b-1} s_2(n) \exp\left(-j2\pi k \frac{n}{M_b}\right) \quad (2)$$

These symbols are then mapped to N_{sub} number of subcarriers by localized spectrum mapping—all the symbols are mapped to adjacent subcarriers, to generate $S'_1(k)$ and $S'_2(k)$. Then N_{sub} point IDFT is applied over the frequency mapped signal to obtain the equivalent time domain transmit signals.

$$s_1(n) = \sqrt{\frac{1}{N_{\text{sub}}}} \sum_{k=0}^{N_{\text{sub}}-1} S'_1(k) \exp\left(j2\pi n \frac{k}{N_{\text{sub}}}\right) \quad (3)$$

$$s_2(n) = \sqrt{\frac{1}{N_{\text{sub}}}} \sum_{k=0}^{N_{\text{sub}}-1} S'_2(k) \exp\left(j2\pi n \frac{k}{N_{\text{sub}}}\right) \quad (4)$$

Cyclic prefix is inserted to avoid inter block interference, and the signal is transmitted.

2.2 Received SC-FDMA Signal Analysis

A parametric channel model with frequency selective fading is considered for the analysis. Let the combined received signal of two users at the receiver be given as

$$\{r_{N_r}(n); n = 0, \dots, N_{\text{sub}} - 1\} \quad (5)$$

After taking N_{sub} -point DFT of received signal, the frequency domain signal $\{R_{N_r}(k); k = 0, \dots, N_{\text{sub}} - 1\}$. $R_{N_r}(k)$ is as follows:

$$\begin{aligned} R_{N_r}(k) &= \sqrt{\frac{1}{N_{\text{sub}}}} \sum_{n=0}^{N_{\text{sub}}-1} r_{N_r}(n) \exp\left(-j2\pi k \frac{n}{N_{\text{sub}}}\right) \\ &= \sum_{u=1}^2 \sqrt{P_u} H'_{u,N_r}(k) S'_u(k) + N_{N_r}(k) \end{aligned} \quad (6)$$

where $H'_{u,N_r}(k)$ and $N_{N_r}(k)$ are the channel gain and AWGN respectively. After spectrum de-mapping and frequency domain equalization for each, the time domain estimate of signal is obtained by taking M_b -point IDFT.

$$\begin{aligned} \hat{r}_u(n) &= \frac{1}{M_b} \sum_{k=0}^{M_b-1} \widehat{R}_u(k) \exp\left(j2\pi n \frac{k}{M_b}\right) \\ &= \hat{s}_u(n) + I(n) + \hat{z}(n) \end{aligned} \quad (7)$$

where $u = 1, 2$ and $\hat{R}_u(k)$ is the transformed vector after FDE. This consists of the desired signal, the interference component (ISI and MUI), and the noise component. Each component can be mathematically represented and thus the power levels of each can be calculated.

3 Interference Estimation

For the two-user pairing system, interference experienced by user-1 at the receiver due to user-2 signal is given as

$$I(n) = \frac{1}{M_b} \sum_{k=0}^{M_b-1} \left\{ \sqrt{P_2} \hat{H}_2(k) S_2(k) \right\} \exp\left(j2\pi k \frac{n}{M_b}\right) \quad (8)$$

where $\hat{H}_2(k)$ is the FD equalized channel matrix of user-2. Interference power due to second user is given as

$$E\{I(n)I^*(n)\} = \frac{P_2}{M_b N_0} \sum_{k=0}^{M_b-1} |\hat{H}_2(k)|^2 \quad (9)$$

where N_0 is the noise level. Equation (9) shows the interference level caused due to a user, which can be calculated if the channel matrix and transmit power of the user are known at the receiver. In LTE UL, the sounding reference signal (SRS) transmitted periodically to eNodeB by each UE registered in the cell is used to get the channel state information (CSI). Also, the transmission power of each UE is decided by eNodeB itself and thus, both the information is available at eNodeB. Hence, possible interference power due to a user to an existing group of users using the same PRBs can be estimated as

$$P_{\text{int}} = \frac{P_{\text{transmit}}}{M_b} \sum_{k=0}^{M_b-1} |H(k)|^2 \quad (10)$$

which is derived from (9) considering the channel matrix H without any equalization. Equation (10) provides interference power as a parameter to choose whether a user can join a multiuser group. Whenever a user is requesting eNodeB for resource allocation, eNodeB can automatically estimate possible interference that the user may cause using (10), and decide whether to add that user to an existing multiuser group. Thus, an interference check while dynamically scheduling users can be performed, by which, the signal quality and spectral efficiency can be improved, compared to random dynamic scheduling.

4 Dynamic Scheduling Algorithm

An algorithm for dynamically scheduling users to form multiuser groups is proposed here based on Eq. (10). The idea is to dynamically schedule users based on estimated possible level of multiuser interference that the user is going to introduce into existing scheduled users. The algorithm is split into two parts—the first part is for forming a new multiuser group and the second part for dynamic scheduling UEs to an existing multiuser group. In the first part, eNodeB selects a few users (maximum N_r users) from the set of all resource requesting users (N_u). All N_u users are first arranged in ascending order based on their channel gain. User with the highest channel gain is selected first. Then, user with the next highest channel gain is considered. Possible interference due to this user to existing grouped users (first user alone, in this case) is estimated using (10). If this is below the threshold interference level, this user is added to the multiuser group. This is continued until the total interference crosses the threshold or the number of grouped users reaches N_r . The second part of the algorithm says how a user is dynamically added to an existing group. Here, while a user arrives with resource request, eNodeB checks the existing multiuser group for number of users. If it is less than N_r , the possible interference level of the user is estimated using (10) and this is added to the existing group.

Let N_a users be present in a cell and registered with eNodeB. Let eNodeB have N_r receive antennas and the UEs are equipped with single antenna each. If N_u users are requesting eNodeB for resource allocation at a time, eNodeB can choose N_r out of N_u users to schedule together and allocate the same set of resource blocks.

Part-I: Multiuser Group Formation

- Step 1: Let $N_u = \{1, 2, 3...u\} \in N_a$, each user having $h \in H_u = \{h_1, h_2, h_3,...,h_u\}$ as channel matrix, h is of $[1 \times N_r]$ dimension, be requesting for resource allocation with eNodeB.
- Step 2: Arrange $\{N_u\}$ in ascending order based on estimated interference using (10)
- Step 3: Select first user as: $u_i \in N_u$ with $h_i \in H_u$ such that $|h_i| > |h|$; $\{h, h_i\} \in H_u$; $h_i \neq h$
- Step 4: Let Y_i be the average received SINR of eNodeB. Then an interference threshold for the eNodeB to operate under given average SINR is obtained as:

$$I_{\text{threshold}} = \frac{P_t}{10^{\left(\frac{1}{\gamma_i+10}\right)}} \quad (11)$$

- Step 5: Schedule user u_k with u_i ; for all $u_k \in N_u$; $u_k \neq u_i$ such that estimated interference due to u_k (using (10)) plus existing interference of grouped users (from (9)) is below the threshold interference level.

- Step 6: Add as many as N_r users to the group if the interference (calculated by extending (9) for more than two users) plus estimated interference for each user to be added is below the threshold.

Part-II: Dynamic Scheduling

Whenever the number of scheduled users in a group is less than N_r ;

- Step 1: Find the interference threshold for eNodeB using (11).
 Step 2: If a user ‘U’ request for resource allocation, estimate its interference level using (10).
 Step 3: If sum of estimated interference and existing interference is below the threshold calculated in step 2; add ‘U’ to the existing group.
 Step 4: Add users till total count reaches N_r , by repeating steps 2 and 3.

5 Simulation and Analysis

LTE system level UL simulation was performed to analyze the performance of proposed algorithm using MATLAB. Localized SC-FDMA block transmission with QPSK modulation is used for UL scenario simulation. The wireless channel considered here is a frequency selective Rayleigh fading channel having uniform power delay. Ideal channel estimation is assumed and eNodeB has an MMSE-FDE receiver.

Simulation parameters: Modulation and coding scheme—QPSK; transmit power = 25 dbm (max. value for LTE); noise power = 0 – – 20 dbm; $N_r = 1 – 8$; $U = 1 – 16$; receiver antenna gain = 5 db; type of receiver—MMSE; FFT size = 512; type of SC-FDMA—localized; block size = 16; channel—frequency selective Rayleigh fading channel.

Figure 1 shows a comparison of spectral efficiency for the proposed dynamic multiuser scheduling with interference mitigation technique and the random dynamic scheduling technique. The graph clearly shows the improvement in spectral efficiency of dynamic scheduling with interference mitigation, compared to random dynamic scheduling. At medium and high SNR conditions, the performance of dynamic scheduling with interference mitigation is very high, achieving high spectral efficiencies.

Variation in spectral efficiency with increase in number of users at different receive SNR values is given in Fig. 2a. Here N_r is fixed and only the number of resource requesting users (N_u) is varied. There is a linear increase in spectral efficiency till selected users equal N_r , but after that, it attains saturation. For $N_u > N_r$ cases, eNodeB has more options to choose the best N_r users from, and thus the small increase in spectral efficiency is due to eNodeB selecting the users with least interference from the available lot. Figure 2b gives the N_r versus Spectral Efficiency plot for eNodeB for dynamic scheduling with interference mitigation over different

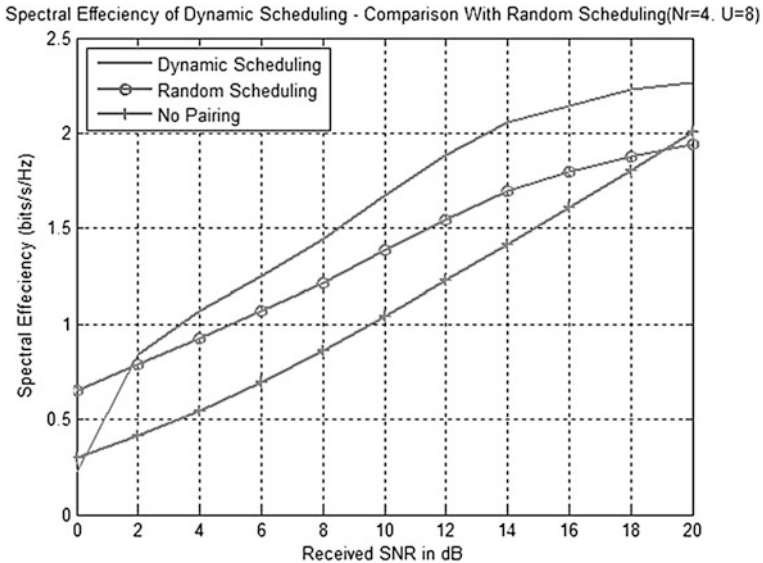


Fig. 1 Spectral efficiency of dynamic pairing—a comparison with random scheduling

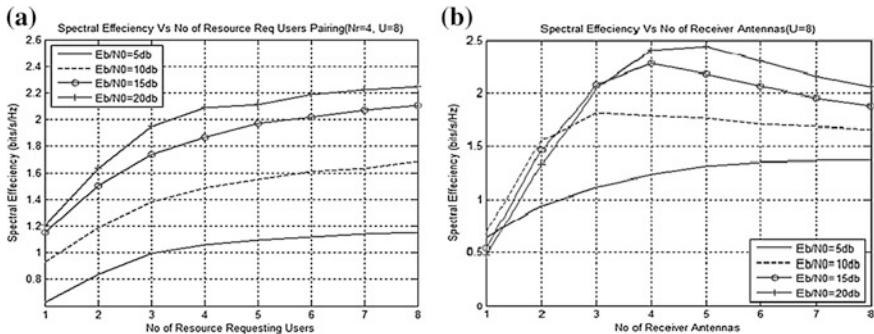


Fig. 2 a) Spectral efficiency versus no of users, b) spectral efficiency versus N_r

values of received SINR levels. The result agrees with the fact that spatial multiplexing gain can be achieved only at high SNR conditions. With increase in N_r , number of users that can be grouped will also increases. The increase in MUI due to increase in users explains the small decrease in spectral efficiency for large N_r values. Thus, for large N_r conditions, scheduling of N_r users to use same set of PRBs for UL transmission is possible with a small trade-off for spectral efficiency. For users requiring high data rates, the number of co-scheduled users need to be limited to around half the number of receive antennas.

6 Conclusion

A new method for dynamic multiuser scheduling with interference mitigation by interference estimation is proposed in this work. The proposed algorithm estimates the possible interference level that can occur due to addition of a new user to an existing multiuser group, based on the user channel conditions and transmit power, and decides whether the user needs to be added or not. The proposed work provides a method where interference level is used as a parameter to consider while performing dynamic multiuser scheduling. Our extensive simulation and analysis shows that the proposed algorithm is far better than random scheduling algorithm.

References

1. Nortel, 3GPP TSG-RAN1 WG1 #42 R1-0501162: UL Virtual MIMO Transmission for E-UTRA. San Diego, USA, 10–14 October 2005
2. Nortel, 3GPP TSG-RAN1 WG1 #43 R1-051422: UL Virtual MIMO System Level Performance Evaluation for EUTRA. Seoul, Korea, 7–11 November 2005
3. GPP TSG-RAN1 #46, R1-062052: UL System Analysis with SDMA. Tallinn, Estonia, August 2006
4. Girici, T., Zhu, C., Agre, J.R., Ephremides, A.: Proportional Fair Scheduling Algorithm in OFDMA-Based Wireless Systems with QoS constraints. *IEEE J. Commun. Netw.* **12**(1), (2010)
5. Han, J., Tao, X., Cui, Q.: Simplified SINR-based user pairing scheduling for virtual MIMO. In: *IEEE 69th Vehicular Technology Conference*, Spring (2009)
6. Song, Y., Su, G., Wang, S., Xie, Y.: Group-based user pairing of virtual MIMO for uplink of LTE system. In: *2nd International Conference on Consumer Electronics, Communications and Networks* (2012)
7. Mehboodiya, A., Peng, W., Adachi, F.: An adaptive multiuser scheduling and chunk allocation algorithm for uplink SIMO SC-FDMA. In: *IEEE International Conference on Communications* (2014)

Design of Proportional-Integral-Derivative Controller Using Stochastic Particle Swarm Optimization Technique for Single-Area AGC Including SMES and RFB Units

K. Jagatheesan, B. Anand, Nilanjan Dey and M.A. Ebrahim

Abstract In this work, electromechanical oscillations in single-area power systems can be effectively reduced by the influence of energy storage unit, and it helps in the load leveling process and performance improvement of the system. This proposed paper describes the application of super magnetic energy storage (SMES) unit and redox flow battery (RFB) in single-area non-reheat, single, and double reheat thermal power system. The commonly used industrial PID controller act as a control strategy and the optimal gain values are obtained using three different cost functions with stochastic particle swarm optimization technique (SPSO). The dynamic performance of the investigated power system is obtained and examined with one percent step load perturbation.

Keywords Automatic generation control (AGC) · Interconnected power system · Energy storage unit · Stochastic particle swarm optimization (SPSO) · Proportional-integral-derivative controller (PID)

K. Jagatheesan (✉)

Department of EEE, Mahendra Institute of Engineering and Technology,

Namakkal, Tamilnadu, India

e-mail: jaga.ksr@gmail.com

B. Anand

Department of EEE, Hindusthan College of Engineering and Technology,

Coimbatore, Tamilnadu, India

e-mail: b_anand_eee@yahoo.co.in

N. Dey

Department of CSE, BCET, Durgapur, India

e-mail: neelanjan.dey@gmail.com

M.A. Ebrahim

Department of Electrical Engineering, Faculty of Engineering at Shoubra,

Benha University, Cairo, Egypt

e-mail: mohamedahmed_en@yahoo.com

1 Introduction

The performance of all electrical apparatus is intensely depends on the quality of power supply. But getting good quality of power from generating unit is more complex, due to continuously variable power surplus, mismatch between power generation and demand and due to occasional system blackouts. Consistency in frequency and power interchange between control areas ensures the quality of power. This objective can be achieved by introducing load frequency control (LFC) or automatic generation control (AGC). The responsibility of LFC is to keep or maintain very close to the system frequency at specified nominal value, to sustain the specified power interchange between control areas and keep generation of each unit at the most economical value [1–3].

To solve this problem, the superior artificial intelligence (AI)-based controller and an energy storage unit is more crucial. From the literature survey, it reveals that many control strategies have been proposed. They are namely: particle swarm optimization (PSO) [4–6], ant colony optimization (ACO) [6–9], firefly algorithm (FA) [10], Imperialist competitive algorithm (ICA) [11], bacterial foraging algorithm (BFA) [12], and artificial bee colony (ABC) [13] have been reported in the literature. An Energy storage unit having the ability to control the active and reactive power, and it has been reported in the literature [1–17]. This paper proposes stochastic particle swarm optimization (SPSO) technique to optimize PID controller gain values of the single-area power system. SMES and RFB energy storage unit have been implemented in this single-area thermal power system to control the frequency of a generating unit.

This paper is ordered as follows. The proposed system is designed in Sect. 2. The PSO and SPSO optimization technique is described in Sects. 3 and 4, respectively. The simulation models of proposed system and the results are explained in Sect. 5. The conclusion is provided at the end of this paper.

2 Proposed System

The general block diagram arrangement of single-area thermal power system, including turbine, governor, and generator and PID controller with energy storage unit is shown in the Fig. 1, and the nominal values are given in the appendix (9).

2.1 Steam Turbine

The nature of the steam turbine is to convert high-pressure and high-temperature steam into useful mechanical energy. This mechanical energy is converted into electrical energy with the help of a generator. The turbine output power is depends

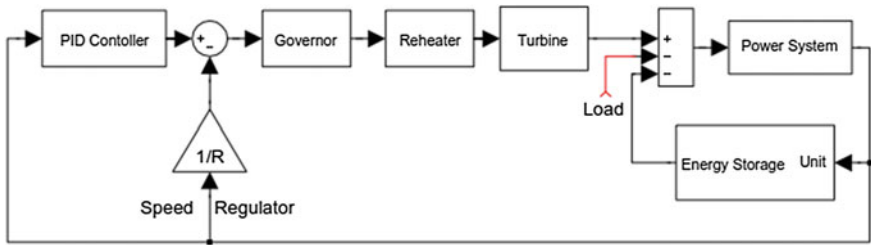


Fig. 1 Block diagram of single-area thermal power system

on flow rate (kg/s) of steam turbine and overall efficiency turbine. These parameters depend on different steam stages (LP, HP, IP, and VHP) available in turbine [1–3]. Based on the pressure stages tandem-compound turbine classified into non-reheat, single-stage reheat, and double-stage reheat turbines.

The transfer function of tandem-compound type non-reheat turbine is given by

$$G_T(S) = \frac{\Delta P_T(S)}{\Delta X_E(S)} = \frac{1}{1 + ST_r}$$

The transfer function of tandem-compound type single-stage reheat turbine is given by

$$G_T(S) = \frac{1}{(1 + ST_t)} \left(\frac{1 + \alpha ST_r}{1 + ST_r} \right)$$

The transfer function of tandem-compound type double-stage reheat turbine is given by

$$G_T(S) = \frac{(S^2 T_{r1} T_{r2} + \beta S T_{r2} + \alpha S (T_{r2} + T_{r1}) + 1)}{(1 + ST_{r1})(1 + ST_{r2})(1 + ST_t)}$$

2.2 Superconducting Magnetic Energy System (SMES)

In this proposed work, SMES energy unit is implemented in single-area thermal power system to stabilize the frequency system stability and frequency oscillations during sudden load demand. Frequency deviation (Δf) is given as input to SMES, and output is changed in the control vector (7). The suitable Simulink model of SMES unit is shown in Fig. 2.

The power output terminal of SMES unit is equipped with limiter at the rate of $-0.01 \leq \Delta P_{SM} \leq 0.01$ pu MW. The control gain value and time constant of energy unit are 0.12 and 0.03 s, respectively.

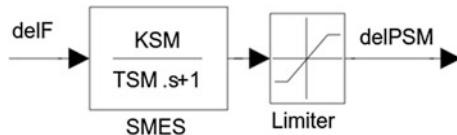
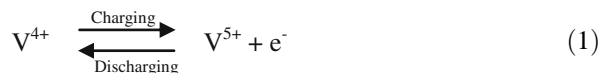


Fig. 2 Simulink model of SMES unit

2.3 Redox Flow Battery (RFB)

The salient features of RFB are simple operating principle, long life, quick response, suitability for higher rating system and ease of maintenance. Based on these features, nowadays RFB is introduced into load frequency control (LFC) application for the improvement of power system operation (8). The transfer function of RFB in LFC application is given in the equation.

Reaction at positive electrode:



Reaction at negative electrode:



3 Stochastic Particle Swarm Optimization Technique ‘SPSO’

The controller parameters in power system are tuned by using conventional method. The conventional tuning method is less accurate and consumes more time. The drawbacks of above said issue in conventional tuning method is over come by introducing evolutionary computation (EC) technique [4, 18]. The EC work's based on the principle of Darwin's theory, and it is “Survival of the fittest” which is proposed in 1859. But evolutionary computation attracted by researchers from 1991s, due their simplicity and effective solution for complex problems. In this work, population-based new stochastic particle swarm optimization (SPSO) is developed and proposed to design proportional-integral-derivative (PID) controller for solving AGC problem in power system operation the SPSO overcome the draw backs of Conventional PID controller tuning process [4, 18].

Keenney and Eberhart first introduce particle swarm optimization (PSO) technique in 1995 [4, 18]. The position of flown i th particle in space t time step t is calculated using:

$$x_i^{k+1} = x_i^k + v_i^{k+1} \quad (3)$$

The velocity updates are obtained using:

$$\begin{aligned} v_i^{k+1} = & wv_i^k + c_1 \text{rand}_1 \times (p\text{best}_i - x_i^k) \\ & + c_2 \text{rand}_2 \times (g\text{best} - x_i^k) \end{aligned} \quad (4)$$

By combining position and velocity updating equation, the draw backs of basic PSO techniques are over come. The result increases local search capability. But it reduces the global search capability [4, 18]. This issue is overcome by swarm best position p_g and p_j obtained using Tabu Search gives the new particle position. The value of $x_j(t + 1)$ is given by:

$$\begin{aligned} x_j(t + 1) = & G_1(x_j(t)), \quad \text{if (random} < P_{\text{select}}) \\ x_j(t + 1) = & G_2(x_j(t)), \quad \text{other wise} \end{aligned} \quad (5)$$

4 Result and Discussion

In this cram, performance of single-area thermal power system is simulated by Matlab/Simulink environment with three different scenarios. In all the three scenarios, gain values of PID controller are optimized using stochastic particle swarm optimization (SPSO) technique considering ISE, IAE, and ITAE cost functions after occurring one percent step load perturbation in the power system.

4.1 Non-Reheat Thermal Power System with Energy Storage Units

In the first scenario, thermal generating unit is equipped with on-reheat turbine, PID controller, and two different energy storage units. The Simulink model of the proposed system is shown in Fig. 3 and performance of corresponding is shown in Figs. 4, 5, 6 and 7.

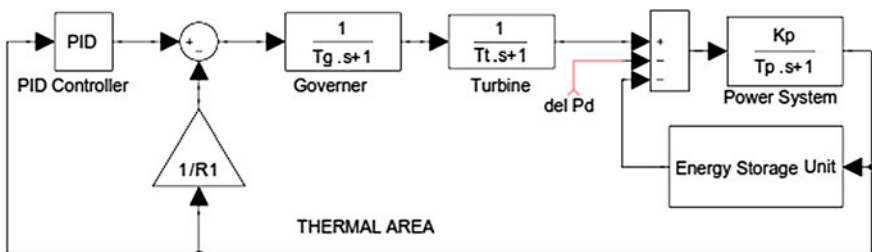


Fig. 3 Simulink model of non-reheat thermal power system with SMES and RFB unit

Fig. 4 Comparison of delf with SMES unit

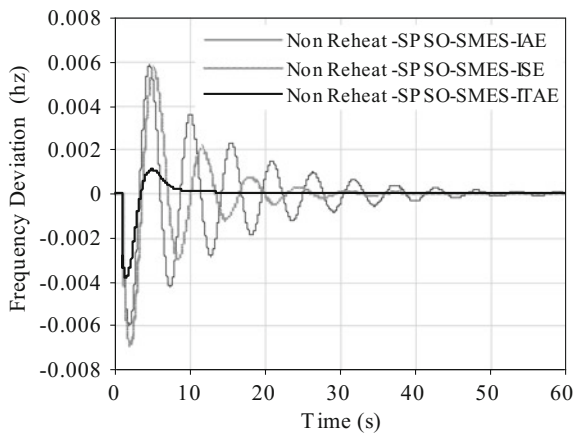


Fig. 5 Comparison of ACE with SMES unit

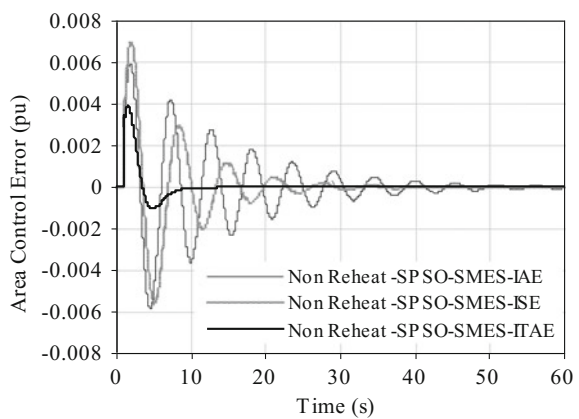


Fig. 6 Comparison of delf with RFB unit

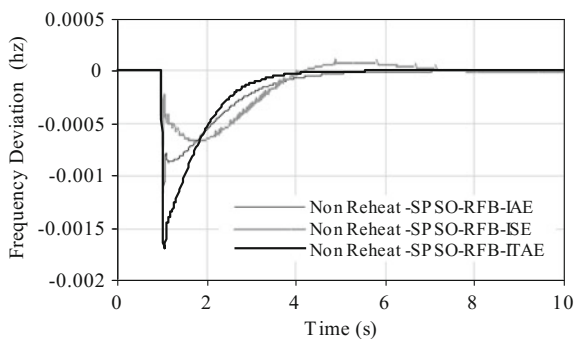
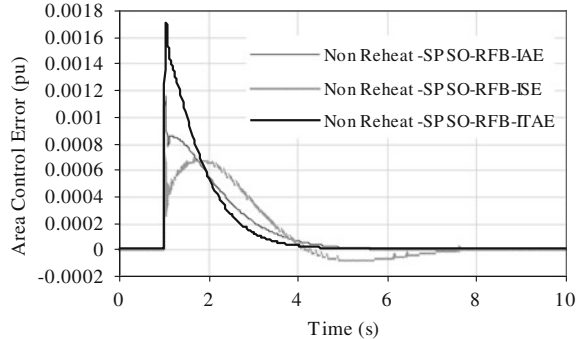


Fig. 7 Comparison of ACE with RFB unit



4.2 Single Reheat Thermal Power System with Energy Storage Units

In the second scenario, investigated system equipped with single-stage reheat turbine, PID controller, and SMES and RFB energy storage units. The transfer function model investigated system is shown in Fig. 8, and controlled frequency deviation and area control error are shown in Figs. 9, 10, 11 and 12, respectively.

4.3 Double Reheat Thermal Power System with Energy Storage Units

In the third scenario, the proposed system is designed with Double-stage reheat turbine, PID controller, and energy storage units. Matlab Simulink model of proposed system is shown in Fig. 13, and responses are given in the Figs. 14, 15, 16, and 17.

The dynamic performance of the system with non-reheat turbine and PID controller with different cost functions and energy storage units is compared and shown in Figs. 4, 5, 6, and 7. The critical observations of the dynamic responses, clearly seen, that system with SMES and ITAE cost-based controller give fast settled

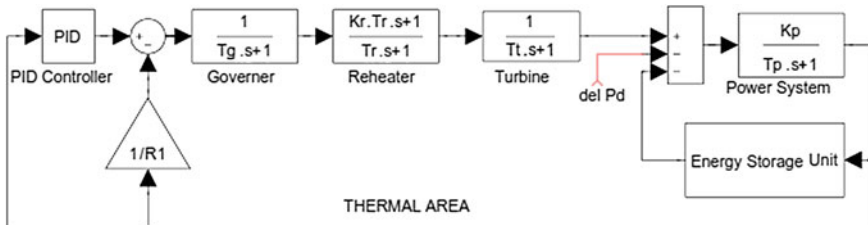


Fig. 8 Simulink model of single reheat thermal power system with SMES and RFB unit

Fig. 9 Comparison of delf with SMES unit

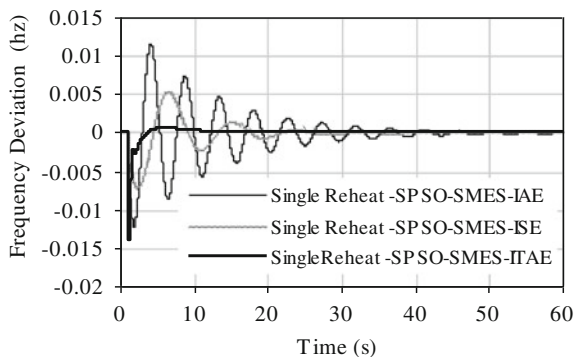


Fig. 10 Comparison of ACE with SMES unit

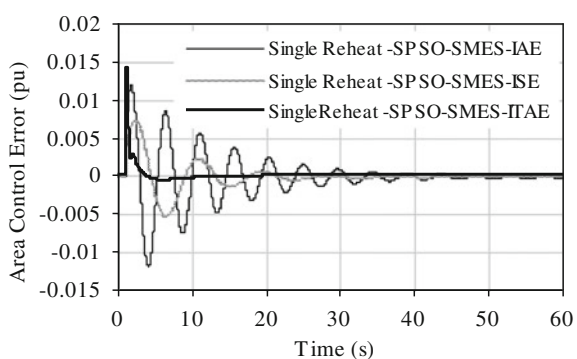


Fig. 11 Comparison of delf with RFB unit

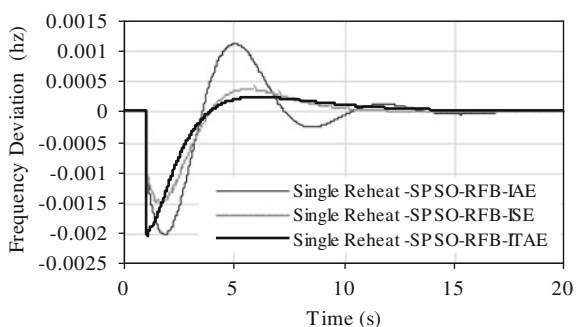
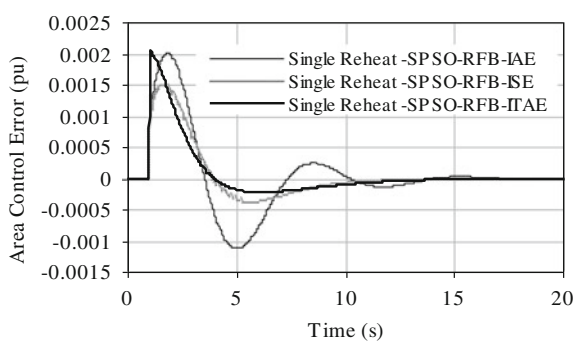


Fig. 12 Comparison of ACE with RFB unit



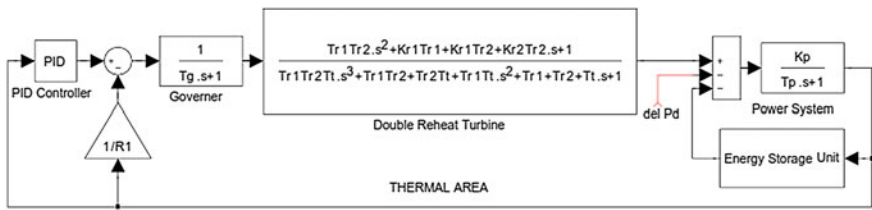


Fig. 13 Simulink model of double reheat thermal power system with SMES and RFB unit

Fig. 14 Comparison of delF with SMES unit

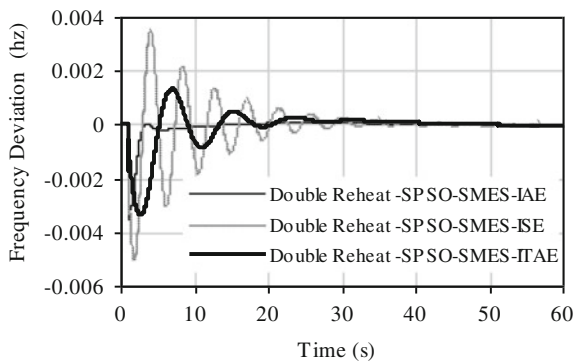


Fig. 15 Comparison of ACE with SMES unit

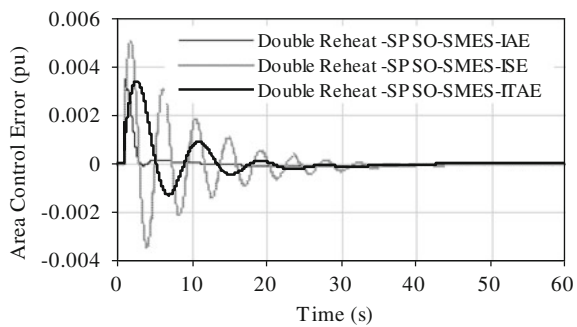


Fig. 16 Comparison of delF with RFB unit

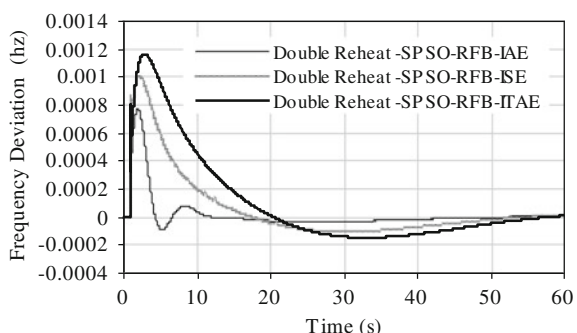
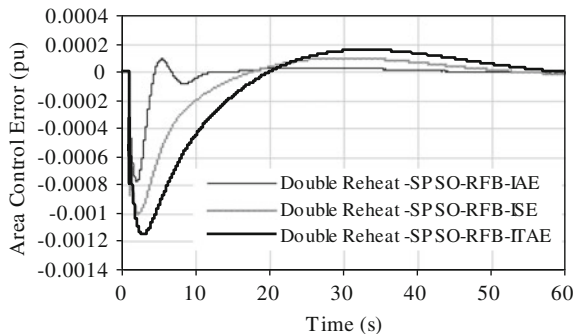


Fig. 17 Comparison of ACE with RFB unit



response with minimum over shoot compared other two cost functions and RFB energy storage unit.

The dynamic performance of single-area reheat thermal power system with SPSO optimizes PID controllers and three different cost functions are obtained, compared and shown in Figs. 9, 10, 11, and 12. From this response comparison, it is clearly seen that the response corresponding to PID controller with ITAE cost function and SMES unit is better than that of other two cost function and RFB energy storage unit.

The controlled performance of double reheat turbine equipped single-area power system is shown in Figs. 14, 15, 16, and 17. Performance comparison reveals that the system equipped with IAE-based PID controller with SMES unit effectively reduces the settling time with lesser damping oscillations compares to other two cost function and Redox Flow Battery energy storage unit.

5 Conclusion

In this paper, the dynamic performance of the single-area power system with a SPSO optimized PID controller with different cost functions and different steam configurations is obtained and compared effectively. Simulation result shows that the performance of system with ITAE cost function-based controller with SMES unit gives superior result, in the case of reheat and non-reheat turbine compared to other cost functions and RFB unit. But in double reheat turbine equipped system gives better result with IAE cost function-based controller and SMES unit compared to other functions and RFB unit.

References

1. Nagrath, J., Kothari, D.P.: Power System Engineering. Tata Mc-Graw Hill Publishing Company Limited, New Delhi (1994)
2. Kundur, P.: Power System Stability and Control. Tata Mc-Graw Hill Publishing Company Limited, New Delhi (1994)
3. Elgerd, O.I.: Electric Energy System Theory: An Introduction, pp. 315–389. Tata Mc-Graw Hill Publishing Company Limited, New York (1970)
4. Ebrahim, M.A., Mostafa, H.E., Gawish, S.A., Bendary, F.M.: Design of decentralized load frequency based-PID controller using stochastic particle swarm optimization technique. Int. Conf. Electr. Power Energy Convers. Syst. 1–6 (2009)
5. Dey, N., Samanta, S., Yang, X.S., Chaudhri, S.S., Das, A.: Optimisation of scaling factors in electrocardiogram signal watermarking using cuckoo search. Int. J. Bio-Inspired Comput. (IJBIC) **5**(5), 315–326
6. Jagatheesan, K., Anand, B., Dey, N.: Automatic generation control of thermal-thermal-hydro power systems with PID controller using ant colony optimization. Int. J. Serv. Sci. Manag. Eng. Technol. Issue (2015) (in press)
7. Omar, M., Solimn, M., Abdel ghany, A.M., Bendary, F.: Optimal tuning of PID controllers for hydrothermal load frequency control using ant colony optimization. Int. J. Electr. Eng. Inf. **5**(3), 348–356 (2013)
8. Samanta, S., Acharjee, S., Mukherjee, A., Das, D., Dey, N.: Ant weight lifting algorithm for image segmentation. IEEE Int. Conf. Comput. Intell. Comput. Res. (ICCIC) 1–5 (2013)
9. Samanta, S., Chakraborty, S., Acharjee, S., Mukherjee, A., Dey, N.: Solving 0/1 knapsack problem using ant weight lifting algorithm. IEEE Int. Conf. Comput. Intell. Comput. Res. (ICCIC) 1–5 (2013)
10. Day, N., Samanta, S., Chakraborty, S., Das, A., Chaudhuri, S.S., Suri, J.S.: Firefly algorithm for optimization of scaling factors during embedding of manifold medical information: an application in ophthalmology imaging. J. Med. Imag. Health Inf. **4**(3), 384–394
11. Abbas Taher, S., Hajikbari Fini, M., Falahati Aliabadi, S.: Fractional order PID controller design for LFC in electric power systems using imperialist competitive algorithm. Ain Shams Eng. J. **5**, 121–135 (2014)
12. Saikia, L.C., Sinha, N., Nanda, L.: Maiden application of bacterial foraging based fuzzy IDD controller in AGC of a multi-area hydrothermal system. Electr. Power Energy Syst. **45**, 98–106 (2013)
13. Balasundaram, P., Akilandam, C.I.: ABC algorithm based load-frequency controller for an interconnected power system considering nonlinearities and coordinated with UPFC and RFB. Int. J. Eng. Innovative Technol. **1**, 1–11 (2012)
14. Anand, B., Ebenezer Jeyakumar, A.: Load frequency control with fuzzy logic controller considering non-linearities and boiler dynamics. ACSE **8**, 15–20 (2009)
15. Tripathy, S.C., Balasubramaniam, E., Chandramohan Nair, P.S.: Adaptive automatic generation control with SMES in power systems. IEEE Trans. Energy Convers. **7**, 434–441 (1992)
16. Chidambaram, I.A., Paramasivam, B.: Genetic algorithm based decentralized controller for load-frequency control of interconnected power systems with RFB considering TCPS in the tie-line. Int. J. Electron. Eng. Res. **1**, 299–312 (2009)
17. Anand, B., Ebenezer Jeyakumar, A.: Load frequency control with fuzzy logic controller considering non-linearities and boiler dynamics. ACSE **8**, 15–20 (2009)
18. Jagatheesan, K., Anand, B., Ebrahim, M.A.: Stochastic particle swarm optimization for tuning of PID controller in load frequency control of single area reheat thermal power system. Int. J. Electr. Power Eng. **8**(2), 33–40. ISSN:1990-7958

An Enhanced Microstrip Antenna Using Metamaterial at 2.4 GHz

Sunita, Gaurav Bharadwaj and Nirma Kumawat

Abstract There has been a tremendous increase in demand for low-cost and compact antennas using techniques to improve their electromagnetic properties. To improve negative permittivity and negative permeability, the design and simulation of left-handed metamaterials (LHM) are used and presented. Our purpose is the betterment of return loss of antenna with the use of new incorporated LHM structure. The incorporated design has dimensions of 32 mm × 32 mm. The design has improved return loss and bandwidth while maintaining the VSWR and gain to the same level required for mobile applications as BLUETOOTH at 2.4 GHz. The proposed design is compared with conventional patch antenna which shows a significant improvement in return loss up to −41.06 dB and bandwidth 29 MHz.

Keywords Gain · Metamaterial · Bluetooth · Omega shape · Return loss

1 Introduction

Recently, microstrip patch antenna have gained much attention because of their many advantages including ease of installation, mechanical reliability with respect to radiation property, versatility in polarization, and resonant frequency.

Sunita (✉) · G. Bharadwaj

Government Women Engineering College, Ajmer, Rajasthan, India
e-mail: Olasunita30@gmail.com

G. Bharadwaj
e-mail: gwecaexam@gmail.com

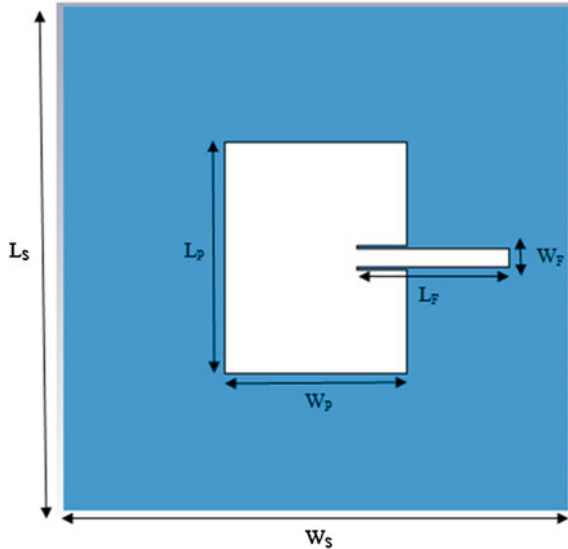
N. Kumawat
Ajmer Institute of Technology, Ajmer, Rajasthan, India
e-mail: kumawatnirma@gmail.com

© Springer India 2016

S.C. Satapathy et al. (eds.), *Proceedings of the Second International Conference on Computer and Communication Technologies, Advances in Intelligent Systems and Computing* 380, DOI 10.1007/978-81-322-2523-2_29

311

Fig. 1 Geometry of the reference antenna

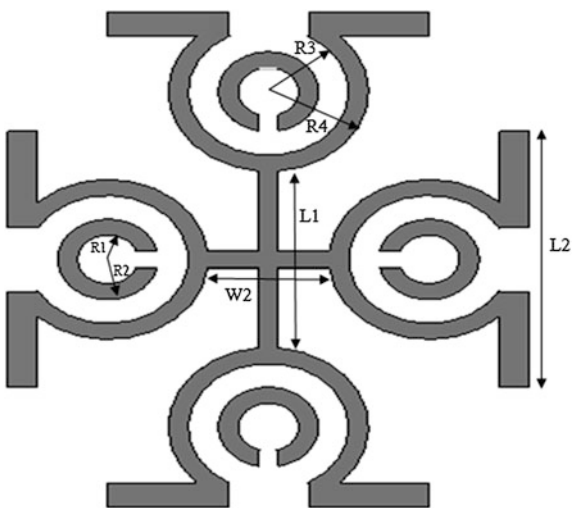


The materials which exhibit the property of negative permeability and negative permittivity at particular frequencies are left-handed metamaterials.

Several multiband antennas using metamaterial have been reported in the literature [1–8]. The examination of LHM becomes interesting due to its unique properties like negative refraction and backward wave [1, 2]. The combination of thin wires (TW) and SRR is usually the basic building block of LHM, though new structures like fishnet, omega shaped, spiral multi-split, and S-Shape also exhibit the property of metamaterials [3, 4]. Since 2001, after the first prototype by Smith, LHM became a topic of interest due to the negative μ and ϵ which improves many antenna properties and the use in microwave circuits, antennas became very extensive [5]. The different shapes are used in designing metamaterial multiband antennas such as spiral and tapered shapes [6, 7]. A novel metamaterial-inspired technique is also used [8] (Fig. 1).

In this paper, we study and analyze the properties of rectangular microstrip patch and compare with the LHM structure of the same. The LHM design consists of circular rings inside of omega-shaped structures connected with rectangular stripes as illustrated in Fig. 2.

Fig. 2 Structure of the metamaterial with dimension



2 Antenna Design

The antenna proposed in this paper is designed on FR4 substrate with dielectric constant 4.3 and loss tangent 0.02. The thickness of the substrate is 1.6 mm. The overall dimension of the antenna is $90 \times 90 \times 1.6$ mm³. A rectangular-shaped patch is formed of dimension 32.908×25.43 mm². A microstrip inset line feed is used to achieve impedance matching having width of 2.9 mm. A slot is cut for inset feed of dimension 4 mm \times 8 mm. To increase the return loss and bandwidth, another substrate with the same property and dimensions is introduced between the metamaterial and the patch. A metamaterial structure is designed using four Ω slot shapes on the substrate. The dimensions of the proposed antenna are listed in Figs. 3, 4, and Table 1.

Fig. 3 Metamaterial between two waveguide ports

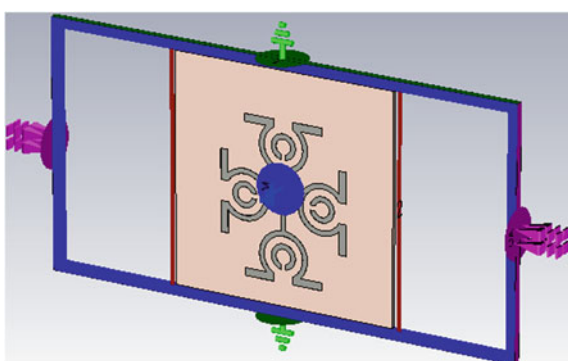


Fig. 4 Structure of the optimized antenna

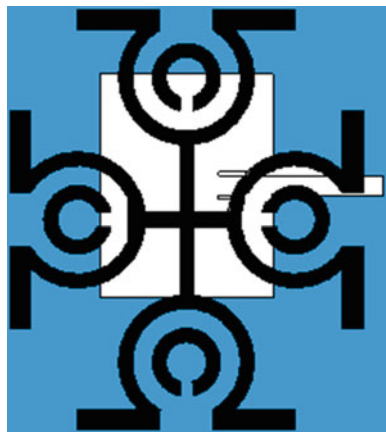


Table 1 Dimension of the proposed antenna

Parameters	Values (mm)
W_S	90.00
L_S	90.00
W_P	25.43
L_P	32.90
W_F	02.90
L_F	24.28
L_1	20.00
L_2	36.00
W_2	12.00
R_1	03.00
R_2	05.00
R_3	08.00
R_4	10.00

3 Result Discussion

This design obtained S-parameters in complex form. For the verification of double-negative metamaterial properties of incorporated structure, the values of S-parameter were exported to MS Excel program and Nicolson, Ross, and Weir approach were used to calculate graph of permeability and permittivity with respect to frequency. Figures 5 and 6 shows the metamaterial property (negative permeability and permittivity). The following equations were used for the MS Excel program.

Fig. 5 Graph between frequency and permeability

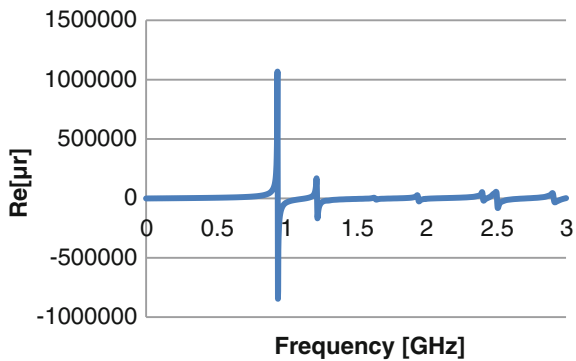
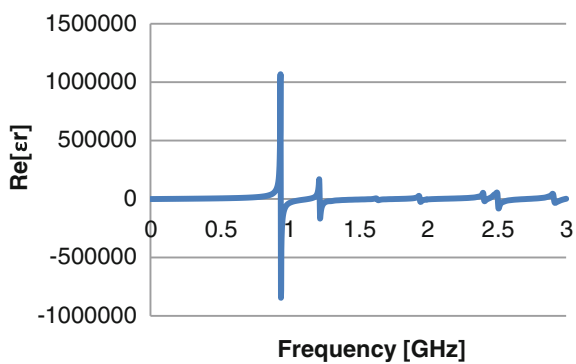


Fig. 6 Graph between frequency and permittivity



$$\mu_r = \frac{2 \cdot c \cdot (1 - v_1)}{w \cdot d \cdot i \cdot (1 + v_2)} \quad (1)$$

$$\epsilon_r = \mu_r + \frac{2 \cdot S_{11} \cdot c \cdot i}{w \cdot d} \quad (2)$$

Figure 7 shows the return loss curve in which a narrow band is observed for the resonant frequency at 2.4689 GHz. We obtain the bandwidth of 29 MHz. Figure 8 shows the simulated radiation pattern of far-field directivity for resonating frequency at 2.46 GHz with 7.1 dBi. It is seen that the radiation pattern is unidirectional in nature.

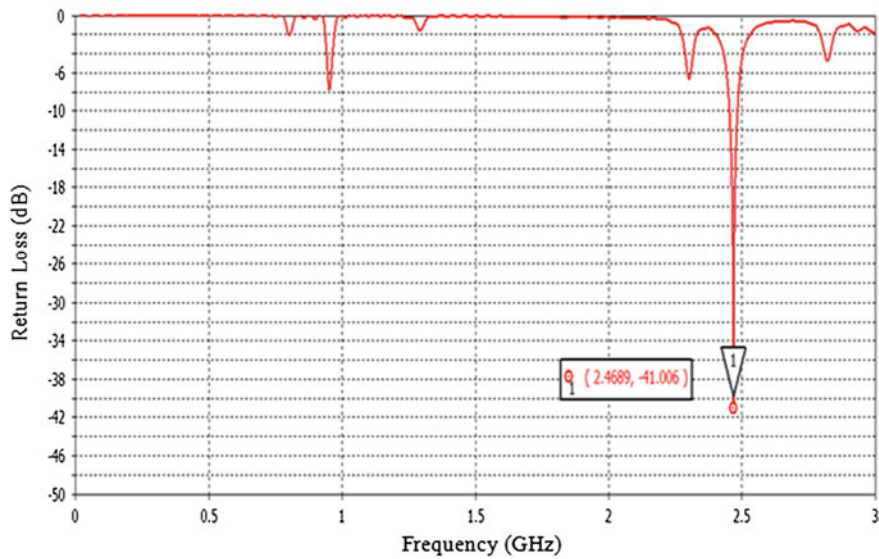
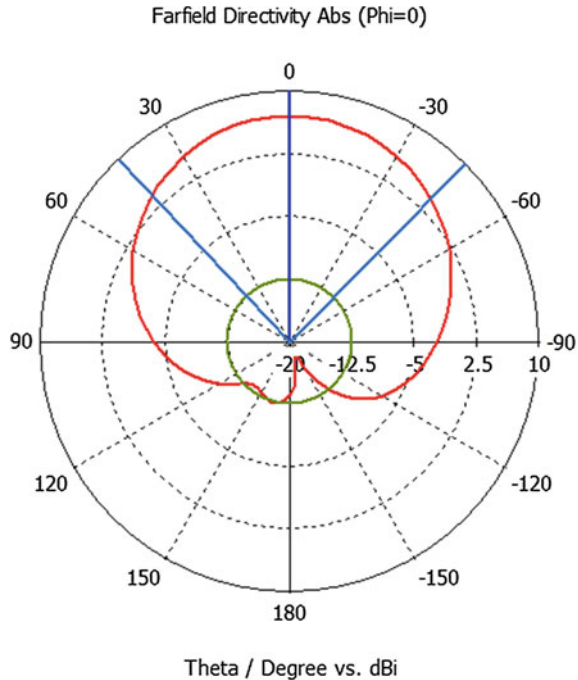


Fig. 7 Simulated return loss curve of the proposed antenna

Fig. 8 Simulated radiation pattern of far-field directivity for resonating frequency 2.46 GHz



4 Conclusion

The article presented here concludes that the incorporation of LHM structure has meliorated the antenna performance. The comparison between microstrip antenna and LHM structure shows improvements in bandwidth and return loss. The final model of LHM structured antenna has return loss of -41.06 dB on 2.4 GHz which shows its adequacy for ISM band, bluetooth, and WLAN applications. The antenna and the meta structure are designed with $\epsilon = 4.3$, $h = 1.6$ mm and $\epsilon = 4.3$, and $h = 3.2$ mm from the ground plane, respectively: the design is simulated on CST software. However, despite the improvements in return loss, a increment in bandwidth was observed. If the side lobe can be reduced, the gain of the antenna with LHM structure can be further improved.

References

1. Aydin, A., Kaan, G., Ekmel, O.: Two-dimensional left-handed metamaterial with a negative refractive index. *J. Phys. Conf. Ser.* **36**, 6–11 (2006)
2. Shelby, R.A., Smith, D.R., Shultz, S.: Experimental verification of a negative index of refraction. *Science* **292**, 77–79 (2001)
3. Wu, B.-I., Wang, W., Pacheco, J., Chen, X., Grzegorczyk, T., Kong, J.A.: A study of using metamaterials as antenna substrate to enhance gain. *Progr. Electromagn. Res.* **51**, 295–328 (2005)
4. Alici, K.B., Ozbay, E.: Characterization and tilted response of a fishnet metamaterial operating at 100 GHz. *J. Phys. D Appl. Phys.* **41**, 135011 (2008)
5. Smith, D.R., Padilla, W.J., Vier, D.C., Nemat-Nasser, S.C., Schultz, S.: Loop-wire medium for investigating plasmons at microwave frequency. *Phys. Rev. Lett.* **84**, 4184 (2000)
6. Rahimi, M., Ameelia Roseline, A., Malathi, K.: Compact dual-band patch antenna using spiral shaped electromagnetic band gap structures for high speed wireless networks. *Int. J. Electron. Commun.* **66**, 963–968 (2012)
7. Sadeghzadeh, R.A., Zarrabi, F.B., Mansouri, Z.: Band-notched UWB monopole antenna design with novel feed for taper rectangular radiating patch. *Progr. Electromagn. Res. C* **47**, 147–155 (2014)
8. Ouedraogo, R.O., Rothwell, E.J., Diaz, A.R., Fuchi, K., Temme, A.: Miniaturization of patch antennas using a metamaterial-inspired technique. *IEEE Trans. Antennas Propag.* **60**(5), 2175–2182 (2012)

Adaptive MAC for Bursty Traffic in Wireless Sensor Networks

Akansha Verma, M.P. Singh, Prabhat Kumar and J.P. Singh

Abstract High throughput, low delay in message delivery, and energy-efficient operation are certain challenges that medium access control (MAC) protocol for wireless sensor network (WSN) has to meet. Traffic patterns and load of network may change during the lifetime of the network and thus the adaptability in duty cycle, wakeup interval, and reliability of transport are mandatory. This paper presents a new adaptive mechanism which is effective in changing traffic conditions, i.e., when a burst of traffic is generated from a particular region. The acknowledgments per packet level guarantees reliability, lowering the cost on retransmissions. Also the adaptive wakeup interval of a node and corresponding adaptations in the preamble length makes it more energy efficient.

Keywords Wireless sensor networks · Medium access control · Duty cycling

1 Introduction

Wireless sensor networks (WSN), owing to their flexible deployment, have become the focus of many applications from various domains. These battery powered nodes are beneficial for many industrial as well as surveillance scenarios. Though they are flexible in terms of deployment, there are several other issues concerning these networks. One such issue is energy efficiency which is required to guarantee a long

A. Verma (✉) · M.P. Singh · P. Kumar · J.P. Singh
CSE Department, NIT, Patna, Bihar, India
e-mail: akineha1991@gmail.com

M.P. Singh
e-mail: mps@nitp.ac.in

P. Kumar
e-mail: prabhat@nitp.ac.in

J.P. Singh
e-mail: jps@nitp.ac.in

network life. Energy conservation in WSNs is required at every layer, but it is much more significant at medium access control (MAC) layer as this layer has a high potential for saving energy. Therefore, this layer implements means for collision and idle listening avoidance, etc., to cut the consumption of energy. The hardware choices particularly radio transceiver also effects the energy requirements. Generally, packet-oriented radios have improved energy per byte ratio compared to the byte or bit-oriented radios. Communication, being the key source of energy depletion, has caught efforts to be focused at optimizing it, especially at MAC layer. Among the various proposals in the past, preamble sampling protocol has emerged to be much efficient. The basis of these protocols is low-power listening (LPL) mechanism. Here the strategy is of sending a preamble in the beginning of every data. In this scenario, every node check the radio on fixed periodic interval to sense the channel this time is called as wakeup interval and is same for every node. If no preamble is detected, nodes go to sleep; otherwise it receives a preamble, and then accepts the data. Preamble in these protocols aims at synchronizing the nodes and makes sure that the node receives the data. Load of traffic in the network typically changes with time, sometimes there is burst of data, sometimes sporadic transmissions with high load, and sometimes very low load. Thus, only adaptive protocols which have the ability to adjust according to these traffic changes are helpful in such applications. Thus, when there is more traffic wakeup interval as well as preamble should be short and when there is no or little traffic it could be long.

In this paper, we have presented a novel technique which is adaptive, energy efficient, and reliable. Adaptive wakeup interval of every node ensures that it does not miss any traffic in case of burst transfer; the receiver's preamble length also varies accordingly thus reducing the energy consumption required in long preambles.

The rest of the paper is organized as follows. Section 2 shows some of the related work on the MAC layer, Sect. 3 states the aim of design, Sect. 4 gives the proposed work, and finally Sect. 5 concludes the paper.

2 Related Work

Most MAC protocols avoid idle listening, a main source of energy wastage by duty cycling the radio of the node. A bunch of such protocols have been proposed in the past based on duty cycling. These protocols can be categorized as synchronous and asynchronous protocols. Some famous synchronous protocols are S-MAC [1], T-MAC [2], R-MAC [3], etc. These protocols make use of a synchronization mechanism to synchronize their duty cycles with the neighboring nodes. On the contrary, asynchronous protocols such as B-MAC [4], X-MAC [5], WiseMAC [6], RI-MAC [7], and MaxMac [8] allow nodes to have their own independent duty cycles. These protocols use preamble sampling mechanism for communication.

S-MAC is the most primitive MAC protocol and is based on IEEE 802.11 which uses RTS/CTS/ACK method for accessing the medium. T-MAC optimizes S-MAC by limiting the listen interval when there are no traffic conditions, whereas they fail to perform optimally when there is bursty nature of traffic which is their major disadvantage.

Like S-MAC, B-MAC is a primitive asynchronous protocol which is based on preamble sampling method of communication between nodes. In this approach, every node performs a channel sampling according to its wakeup interval (duty cycle) to check for any transmission. The sender sends a preamble before the data packet to show its intention of sending the data, but it should last longer than the receiver's sleep interval in order to make sure that the receiver gets it. But this gives rise to overhearing by other unintended receivers. To avoid this problem, X-MAC introduces short preamble with destination address on it, thus nodes not involved in communication can go to sleep. B-MAC and X-MAC are efficient for lighter load of traffic but when the traffic increases, i.e., becomes bursty their efficiency degrades. WiseMAC is somewhat same as B-MAC, but instead of a constant length of preamble it varies the preamble according to the neighbor's schedule which it learns eventually. MaxMac is intended to add to the efficiency in case of high traffic. It switches to CSMA-like nature when traffic crosses a threshold. RI-MAC is receiver oriented protocol which relies on low-power probing (LPP) mechanism, in which every node sends a beacon indicating that it is awake. Cross-layer optimizations of LPL are presented in [9, 10]. In [11–13] a ring-based approach is introduced for sensing the channel in which each and every node has its turn and the network works as if it's a virtual ring. In [14] a multitone-based approach is introduced, whereas in [15] a hybrid MAC is given. Receiver-based protocols have also advanced in recent years, one of which is given in [16], but they are not that efficient as too much overhead packets are involved which increases traffic. Section [17] introduces a novel approach which is a modification of X-MAC.

3 Goals and Issues

The development of this method is encouraged by the nature of traffic in a WSN. The pattern of traffic in WSN could be slow or bursty. A bursty traffic basically has a high traffic pattern at some point of time in the network, after that it is normal. Some examples of such traffic conditions could be found in event detecting applications like surveillance. At any point if an event occurs, a huge load of traffic is generated targeted at the base station. This traffic burst may include any fragments of a large image (from source to sink) or some coding information (from sink to the source) in either case the nodes should be adaptive to such change and should communicate in an energy-efficient manner. Moreover, reliability, scalability, and throughput are certain other aspects which drive the way of this research. Aiming at handling the different traffic patterns, the sampling period as well as the preamble length should be adaptive. This demanded for the usage of asynchronous protocols,

which does not have overhead of managing synchronization as synchronization management also adds extra complexity in the protocol.

There have been many works like X-MAC and WiseMAC in this area; however, they perform well only in light traffic loads and there is no provision for reliability. Our method handles the traffic burst by adapting the sampling schedule as well as preamble length of the nodes to provide energy-efficient communication. Also the data acknowledgment provides reliability for packet delivery.

4 Proposed Work

In a scenario where a large sensor network operates in an event driven manner, on detection of an event node situated in that area starts reporting it to the sink at some constant rate. Irrespective of the routing policy, only certain set of nodes will be involved in relaying data to the sink. In a situation like this, auto adaptability of these nodes is required so as to achieve an energy-efficient communication. When the traffic becomes high the sampling interval or the wakeup interval of the node should decrease so that it does not miss any transmission while sleeping. As, here bursty traffic is considered, there is a possibility of receiving packets at very short interval, and thus a static sampling interval is not that effective. This method decreases the sampling interval as the traffic increases. Figure 1 shows the problem with a static sampling interval.

Thus we see that static sampling interval increases the probability of losing a packet causing sender to resend it whereas if a node's sampling interval decreases as the traffic increases it will not miss those packet. Figure 2 shows this scenario.

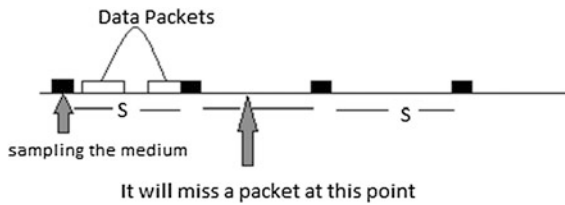
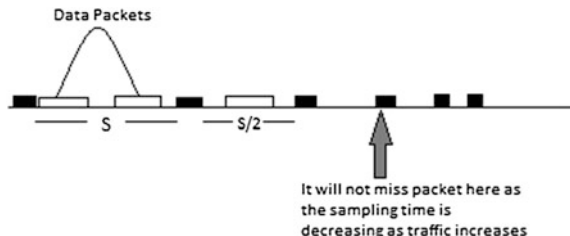


Fig. 1 Static sampling time

Fig. 2 Dynamic Sampling Interval



This type of sampling patterns of a node is helpful in the scenarios of bursty traffic where the probability of traffic for some time period increases, thus nodes should respond to this increase in traffic by listening to channel readily, as the possibility of transmission is more. As a node reduce its sampling time it is important for other nodes (potential senders) to decrease their preamble length as well. Thus this approach helps in coordinating these issues.

4.1 Sender-Side Operations

In the planned approach, the initial span of the preamble is set to MAX which is equal to the initial span of the sampling interval of other nodes. Each node has a table with three entries: sensor id, wakeup_Int, and time out. This entry is updated as soon as the full data transmission is over and it gets an acknowledgment (DAck) packet from the other node, which will have the wakeup interval of that node (This is explained in receiver's section). If a receiver has an entry in the table, sender sends a preamble equals the size of the wakeup interval, else if there is no entry for that particular receiver then it will send a preamble having length MAX. The intended node's id is present at the beginning of the preamble which will make other unintended nodes to go to sleep as soon as they hear it. After receiving the preamble acknowledgment (PAck) packet from the receiver, sender sends the data packet. After successfully transmitting the data it waits for the data acknowledgment (DAck) packet on receiving the DAck packet the transmission stops.

If a node has further data packets to send to a particular node, it has a continue bit which is set one; this allows the receiver to be aware of more incoming packets.

4.2 Receiver Side Operations

Initially, the wakeup interval of the receiver is set to MAX, i.e., the sampling period is set to MAX. As the traffic increases (as we are talking about bursty traffic) receiver will get more than one frame or may find a frame with continue bit set to one, which will make it decrease its wakeup interval. Indication of a continue bit set to one or receiving two frames continuously within same interval is an indication of increase in traffic (as we are here dealing with the bursty traffic), thus it increases the probability of further increase in traffic (as the burst has just started). We have thought of reducing the sampling interval by half, this will increase a chance of receiving any packet which is generated after a short time since last transmission. It is likelihood of receiving a packet as a burst of traffic is generated. This information regarding the change in sampling interval is piggybacked and broadcasted with the new sampling interval of the node in DataAck packet. Other nodes, on hearing this broadcast (intended node and unintended node), will update their table entry

corresponding to this node, and in case of the next transmission for the node this updated sampling time is used to determine the length of the preamble.

4.3 Overview of the Proposed Technique

In Fig. 3 the whole scenario is explained; initially the sender checks its table for the entry of the corresponding receiver, as it is not present it will send preamble length equals to MAX along with the receiver's id in the beginning. The receiver, on receiving the preamble, replies with PAck packet notifies the user for sending the data packets. Here, the user has more than one packet to send to the receiver so it will set the continue bit as one. This bit set one will indicate the receiver of increase in traffic; therefore, it will diminish its sampling time (we considered reducing by half). Now this information is piggybacked in the DAck Packet and sent to the sender. The sender modifies its table after the completion of the transmission. Now for the next transmission, it will check for the table for the sender's entry and will now send the next preamble whose length will be equivalent to the new sampling interval.

This solution is adaptive in case of burst of traffic generates as a result of some event occurred at some portion of the network. The acknowledgement sent after each data packet ensures the reliable deliverance of every data packet thus avoiding the retransmissions. When the traffic is reduced, the node resumes the earlier configuration by setting the sampling time equal to MAX.

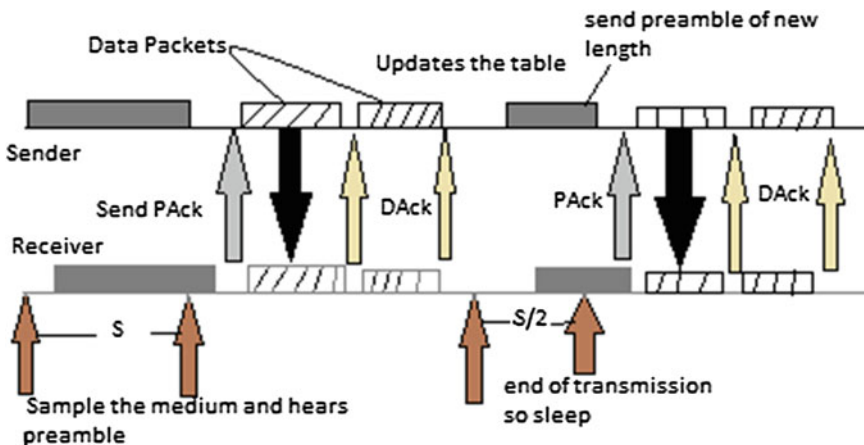


Fig. 3 Overview of the method

5 Conclusion

The planned approach is beneficial for applications generating bursty traffic such as surveillance application where a burst of traffic is generated for certain amount of time interval. This approach is also resilient to loss of packet in the network. In future, we are planning to implement it in the simulation environment using omnet++ simulator and compare it with other similar protocols like B-MAC, X-MAC, and WiseMAC. We are planning to compare three parameters namely energy consumption, delay, and throughput.

References

1. Ye, W., Heidemann, J., Estrin, D.: An energy-efficient MAC protocol for wireless sensor networks. In: Information Science Institute (ISI), University of Southern California (USC), pp. 1–10 (2002)
2. van Dam, T., Langendoen, K.: An adaptive energy efficient MAC protocol for wireless sensor networks. In: SenSys03, pp. 1–6. Los Angeles, California, USA (2003)
3. Yessad, S., Nait-Abdesselam, F., Taleb, T., Bensaou, B.: R-MAC reservation medium access control protocol for wireless sensor networks. In: 159 Conference: Local Computer Networks. University of Bejaia, Algeria (2007)
4. Polastre, J., Hill, J., Culler, D.: Versatile low power media access for wireless sensor networks. In: SenSys’04, pp. 95–107. Baltimore, USA (2004)
5. Buettner, M., Yee, G., Anderson, E., Han, R.: X-MAC a short preamble MAC protocol for duty-cycled wireless sensor networks. In: SenSys’06, pp. 307–320. Boulder, USA (2006)
6. El-Hoiydi, A., Decotignie, J.D.: WiseMAC an ultra low power MAC protocol for multi-hop wireless sensor networks. In: ISCC’04, pp. 244–251. Alexandria, Egypt (2004)
7. Sun, Y., Gurewitz, O., Johnson, D.B.: RI-MAC a receiver initiated asynchronous duty cycle MAC protocol for dynamic traffic load. In: SenSys’OS, pp. 1–14. Raleigh, NC, USA (2008)
8. Hurni, P., Braun, T.: MaxMAC a maximally traffic-adaptive MAC protocol for wireless sensor networks. In: EWSN’10, Coimbra, Portugal (2010)
9. Escobar, S., Chessa, S., Carretero, J.: Cross-layer optimization of low power listening MAC protocols for wireless sensor networks. IEEE (2011). 978-1-4577-0681-3/11/2011
10. Sha, M., Hackmann, G., Lu, C.: Energy-efficient low power listening for wireless sensor networks in noisy environments. In: IPSN13, pp. 1–12. Philadelphia, Pennsylvania, USA (2013)
11. Bernard, T., Fouchal, H.: A low energy consumption MAC protocol for WSN. In: IEEE ICC Ad-hoc and Sensor Networking Symposium, pp. 533–537. France (2012)
12. Bernard, T., Fouchal, H.: Efficient communications over wireless sensor networks. In: IEEE Global Communications Conference (Globecom 2010), pp. 1–5. Miami, December (2010)
13. Swain, A.R., Hansdah R.C., Chouhan, V.K.: An energy aware routing protocol with sleep scheduling for wireless sensor networks. In: 24th IEEE International Conference on Advanced Information Networking and Applications, pp. 993–940 (2010)
14. Dash, S., Swain, A.R., Ajay, A.: Reliable energy aware multi-token based MAC protocol for WSN. In: 26th IEEE International Conference on Advanced Information Networking and Applications, pp. 144–151 (2012)
15. Abdeli, D., Zelit, S.: RTH-MAC a real time hybrid MAC protocol for WSN (2013). doi:978-1-4799-1153-0/13/

16. Tang, L., Sun, Y., Gurewitz, O., Johnson, D.: EM-MAC a dynamic multichannel energy efficient MAC protocol for wireless sensor networks. In: 12th ACM International Symposium on Mobile Ad Hoc Networking and Computing (MobiHoc11), Paris, May 2011
17. Anwander, M., Wagenknecht, G., Braun T., Dolfus, K.: BEAM a burst-aware energy-efficient adaptive MAC protocol for wireless sensor networks. In: 7th International Conference on Networked Sensing Systems (INSS10) Kassel, Germany (2010)

Secured Authentication and Signature Routing Protocol for WMN (SASR)

Geetanjali Rathee, Hemraj Saini and Satya Prakash Ghrera

Abstract Security provisions are a significant influence in the conception of security system for wireless mesh networks (WMNs). It is therefore necessary to guard the identities of individual clients to avoid personal privacy concerns. Numerous susceptibilities exist in different protocols for WMNs (i.e. Overhead, storage, availability of resources). These ambiguities can be discussed by probable attackers to bring down the network performance. In this manuscript, we offer a secure authentication and signature routing protocol (SASR) based on diffie-helman model and threshold signature for reducing response time and improve the security at mesh node. The proposed approach validates the certification of the mesh nodes effectively and paves the path for secure communication. Since the protocol uses Diffie-Helman key mode and threshold signature, very little key is enough for obtaining the needed protection. This thins out the bandwidth allocation for key, so the security constraints will not move the bandwidth by any means, which is an additional advantage over other systems.

Keywords Wireless mesh network · Diffie-Helman · SASR · Authentication · Threshold · Security

G. Rathee (✉) · H. Saini · S.P. Ghrera
Computer Science Department, Jaypee University of Information Technology,
Waknaghat, Solan, Himachal Pradesh, India
e-mail: geetanjali.rathee123@gmail.com

H. Saini
e-mail: hemraj1977@yahoo.co.in

S.P. Ghrera
e-mail: sp.ghrera@gmail.com

1 Introduction

Due to the reason that wireless mesh networks (WMNs) are becoming a progressively prevalent replacement skills for last-mile associativity to the home and public networking, it creates a necessity to design proficient and secure communication protocols for such network setups. Currently, implemented security and confidentiality protocols are dependent on confidence and the repulsion network entity (Sen 2010a, b). Most of them are architects for secreting mobile ad hoc networks (MANETs)[1] which prevents unauthorized access, thus strong authentication is required. Authentication is controlled in any two transmitting arrangements (either a set of MCs or MR) to know the legality. They get the shared common keys which are applied in cryptographic algorithms extracting data unification. The study has already been borne out on public key crypto systems to manage secure communication, but it passes to the performance issues such as cluster heads availability, response time, and overhead of traffic. We have offered a secured authentication and signature routing protocol (SASR) for reducing traffic overhead inside the web and improve the security at mesh client side. The proposed Authentication protocol verifies the certification of the mesh nodes effectively and paves the path for secure communication. Since our protocol uses Elliptic curve cryptography (ECC), even a small sized key is enough for obtaining the needed protection.

2 Related Work

Mishra and Arbaugh [2, 3] proposed a standard technique for customer confirmation and access control to ensure an abnormal state of adaptability and straightforwardness to all clients in a remote system. In order to adapt to the security issue, a key (Proactive) circulation has been proposed by (Prasad and Wang 2005) [4–7]. Prasad et al. [8] proposed a technique in which, a lightweight validation and (AAA) bookkeeping base is utilized for giving constant, on-interest, endways security in heterogeneous systems together with WMNs. The issue of client security in WMNs has additionally pulled in the consideration for examination group. In Wu et al. (2006) [9–11], a lightweight protection, protecting arrangement has been introduced to accomplish decently kept up harmony between system execution and activity protection conservation.

In [12, 13], a limited validation plan has been proposed, in that verification is accomplished generally between the MRs and the MCs in a mixture expansive scale WMN worked with various administrators. Every administrator keeps up its own CA. Every CA is in charge of issuing authentications to its clients. Remote double validation convention (WDAP) (Zheng et al. 2005) [14] has suggested 802.11 WLAN and can be reached out to WMNs.

Table 1 Comparative analysis of previously proposed approaches

Protocol	AIM	Cons
AISA [2, 3]	Provide client authentication	Security problem with real time traffic
FPBPKD [4]	Proactive key distribution	Traffic overhead problem
LHAP [7]	Authenticate mobile clients in dynamic environment	Increases computational overhead
LAAA [8]	Provide continuous end to end security in a heterogeneous network	User privacy concerns

In the initial strategic initiative, we have studied the previous proposed approach, the analysis of which is shown in Table 1, showing their drawbacks and objectives. In the third section, we have proposed a solution which reduces the above cons.

3 Proposed System

A strong base for secure communication in WMNs is the aim of this paper with good access control. In our model we consider the hierarchical WMNs architecture which consists of three layers. For our framed model, the topmost layer is the backbone Internet gateway (IGWs) which supplies the Internet connectivity to a second stratum. The second layer is Wireless mesh routers (MRs) which forwards the traffic to IGWs through multi-hop mode. The third layer comprises of mesh clients (MCs) which are wireless user devices. In our case single MR and its corresponding mesh clients form a Zone. In this network providing security and confidentiality to the user is a major constraint and challenging as well.

3.1 Key Distribution

Each mesh client in MRs agrees on a shared key ‘ks’ with zone MR using group Diffei-Helman key algorithm. Every zone maintains a shared key with its MR. Whenever a new mesh client enters into a zone it needs to agree upon a shared key ‘Ks’ with MR. Each zone MR of any zone needs to harmonize with adjacent zone MR with a cluster shared key ($KC_1, 2, KC_1, 3, KC_2, 3 \dots KC_m, n$) with group Diffie-Helman key algorithm. Zone shared key value changes depending on the number of neighboring zones. The adjacent zone shared key for every zone MR is shared with its neighbor MR where the shared key (KS) ensures the intra zone authentication and shared cluster key (Ksh) provides inter cluster authentication.

As a cluster head selection is based on metric ‘AK’, it can contain more keys and compute the cryptographic operations.

3.2 Inter Zone Communication

If we consider a situation in which a mesh client source ‘Sr’ in a zone wants to communicate with destination mesh client ‘Dn’ in an adjacent zone. Besides, a source mesh client and destination mesh client contains a shared key of respected zones and their zone MR contains shared keys of the zone as well as all the zone shared keys. The following steps are followed during communication:

1. Mesh client Source ‘S’ encrypts the message with shared key ‘ K_{ns} ’ and transmits it to zone MR where ‘ n ’ is cluster number.
2. Zone MR decrypts the message and confirms the authentication of mesh client Source, as it contains shared key of the respective zone.
3. The message is coded with the shared key ‘ KCm, n ’ destination Zone MR which forwards it to neighboring zones.
4. Next, the message is decrypted for authentication purpose after reaching the destination mesh client zone MR.
5. Later, encrypt the message with shared key of respective zone and forward to the destination client. Finally, the destination mesh client decrypts the message with a shared key.

Figure 1 shows the diagrammatic representation of key distribution and inter zone communication.

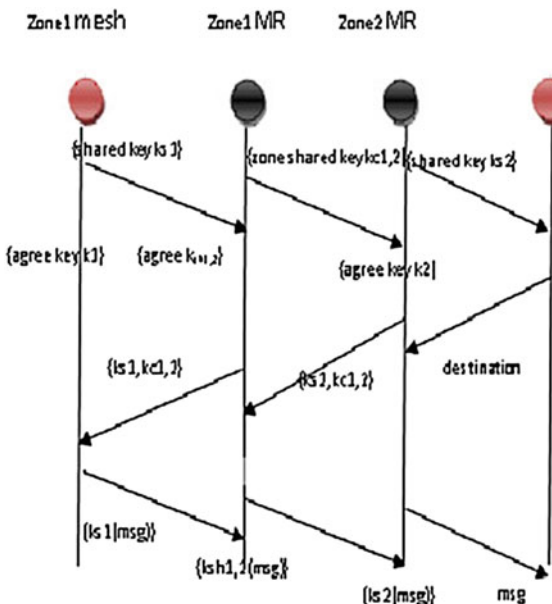
3.3 Authentication Protocol Procedure

In order to access the receiving node, sender ‘sr’ will generate a random number r_1 to calculate the requesting code Rc. The ‘sr’ will pass Rc as a request to the receiver as an authentication verification initiation. While at the receiver side, the receiver will send another generated random number r_2 to the sender. The authentication verification AV will be generated by sender in response. To complete the verification process, AV will be sent at the receiver side. If AV of the sender and receiver are the same, then authentication process will be finished.

3.4 Cluster Formation and Cluster Head Selection

In cluster formation, a fixed radius circle is formed by a node as the midpoint and choosing randomly trivial distance as radius ‘ r ’. The middle node is selected

Fig. 1 Key distribution and intercluster communication



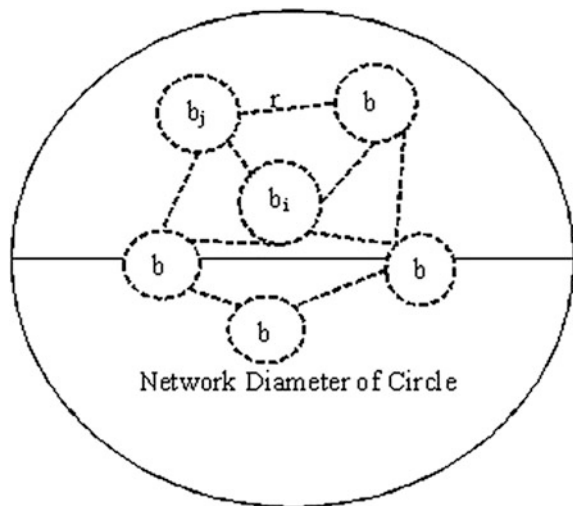
randomly within the range of 1 hop distance. The midpoint of the original circle is designed by calculating the mean of all points and radius r is augmented by the distance two of the successive nodes. The nodes then respond back and in this manner the clusters are formed which is depicted in Fig. 2.

The cluster head selection of cluster head (CH) in a WMN based on the Trust-value and within hop distance. For this purpose, consider that there are n which are within distance d of a CH for given Trust-Value. Also, the lifetime of cluster starts from the time a node is selected as CH until it changes its status to normal node. The cluster lifetime mainly depends on mobility issues and on link stability. It is assumed that the neighboring node is maintained in the table for $3 * \text{counter}$ seconds and is rejected in case there is no more grouping message received. First, Message History (MH) for all nodes is taken as null 0 or ≥ 1 . The TRUST-VALUE (TV) can be further calculated as indicated in Eq. (1):

$$\text{TV}_{i,j} = (\text{TV}_{i,j} + \text{TV}_{i-1,j} + \text{TV}_{i-2,j}, \dots, \text{TV}_{0,j}) / \text{MH} \quad (1)$$

where $i, j \in \text{node}$, $\text{TV}_{i,j}$ represents TRUST_VALUE of node i on node j . When a node forwards a packet, it bears some extent of energy, which depends on packet size and its behavior. Hence the only individual energy power is taken while constructing the path. The CH selection technique can be explained as below:

Step 1: First, initialize the parameters CHcurr , CHprev , TIMEprev , $\text{Curr}()$ to 0 or null.

Fig. 2 Cluster formation

- Step 2: Then, the clustering message sending time will be set as time_out which is calculated as thrice of the return.
- Step 3: After that, calculate the TV of each node from the Eq. (1).
- Step 4: Initialize the MH as 0 or null.
- Step 5: The given condition will be checked by using
 while (Time_{prev-Curr ()} or TRUST_VALUE (CH_{prev}) ≤ 1 =0)
 Do
 CH_{prev} remains as CH
 End while
- Step 6: Compare TV of previous and current Cluster Head using
 If (TV (CH_{prev}) = TV (CH_{cur}) and MH (CH_{prev}) = MH (CH_{cur}))
 Then
 both CH_{prev} and CH_{cur} remains as CH; else
 Select new CH
 End if

4 Authentication Technique Using Threshold Signature

4.1 Generation of Pseudonyms

The generation of pseudonym required for privacy of each node starts with nodes having the desired trust value (TV). The CH generates pseudonyms for the entire node inside the cluster by using corresponding polynomial. Also, each CH calculates $\text{id}_R = H_0(\text{ID}_R)$ and secret sharing $f_m^{\text{CH}_j}(x) : \text{PK}_R = f_m^{\text{CH}_j}(x)(\text{id}_A)$ where $(1 \leq R \leq n_1)$.

4.2 Authentication Techniques

The authentication process starts with the generation of threshold signature. The network consists of the following parameters: (a) cluster head; (b) a set of Member Node $X = \{N_1, \dots, N_{S_2}\}$ where N_{S_2} represents identity of the i th ($1 \leq i \leq S_1$) member; (c) a set of signer $Y = \{K_1, \dots, K_{S_2}\}$ where K is a subset of N and K_{S_2} represents the identity of the j th ($1 \leq j \leq S_2$) member; (d) a verifier v . The technique is explained in the following sections.

4.3 Generation of Threshold Signature

In order to generate a threshold signature for message N , a number of S_2 (b_1, b_2, b_3, b_4, b_5) nodes performs as follows: Initially, all the member node asks for threshold signature. This is started by one of the signers by sending a threshold generation request to selected CH along with a list of signers as (TK_1, \dots, TK_{S_2}) . In the next step they send tokens. For this CH selects a random token $T_R \in Z^*_q$ where $1 \leq R \leq S_2$ and sends them to the corresponding signers securely. After that, each signer creates a signature: $\text{sig}_{PKR} = H_0(N) * K_{PKR}$ and calculates with a corresponding token: $T \cdot \text{sig}_{PKR} = TA \cdot \text{sig}_{PKR}$. Later start sending signature along with the pseudonym public key. Here, the message tuple is sent by each node by verifying V and CH_j .

$$(N, Q_{PKR}, Q_{PK1}, T * \text{sig}_{PKR}, \text{HMAC}_{PKR}(M, Q_{PKV}, T \cdot \text{sig}_{PKA}))$$

5 Performance Calculation

We evaluate the performance of proposed work using NS-2 with the appropriate extension and later we have evaluated the accessibility of the security arrangements with its overhead in view of the random waypoint flexibility model. We have discussed all the parameters in the Table 2 to simulate our work. In the end, source nodes generate constant bit rate (CBR) traffic. Traffic session is generated randomly on selected different source-destinations with a packet size of 512 bytes. Every node in a network has to run our algorithm to become the cluster head. CH broadcasts their beacons over 2 hops every 20 s. The lifetime of key is chosen between 200 and 300 s. As accessibility or availability is a vital constraint of any security infrastructure, we calculate it by distributing the number of member nodes with the entire number of available nodes. Communication overhead is another important parameter as security protocols always make extra overhead. We consider the number of nodes in the network where nodes are randomly interleaving within networks. We validate our system by considering portability and more ever we

Table 2 Simulation parameters

Parameters	Size
No. of nodes	200
Area size	500 × 500
Mac	802.11
Routing protocol	SCATSCA
Simulation time	50 s
Traffic source	CBR
Packet size	512 bytes
Attacker	5, 10, 15, 20 and 25
Antenna	Omni antenna
Speed	5, 10, 15, 20 and 25

Fig. 3 Availability (hop count)

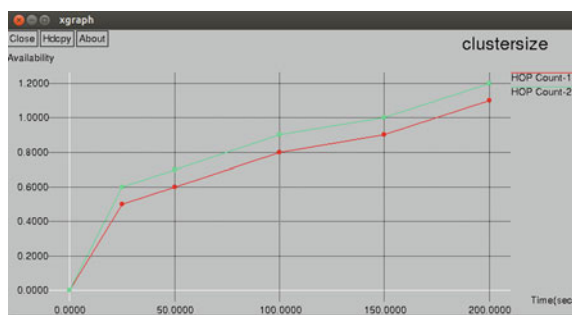
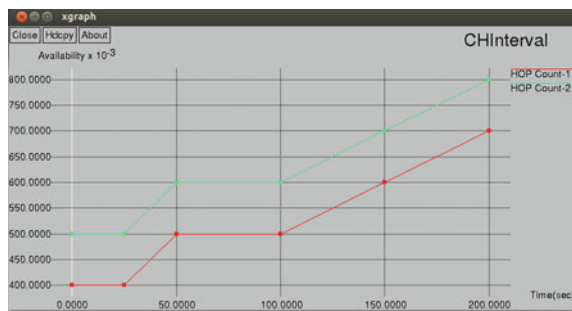


Fig. 4 Availability (CH interval)

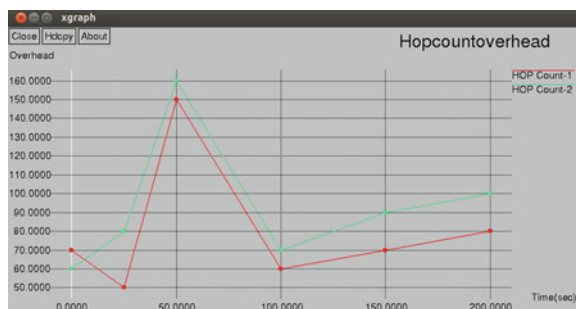


validate the performance of organization by considering authentication time (i.e. Availability time). Later we simulate proposed model to validate node's optimized packet processing capability with respect to the residual battery as well as current traffic status. Figures 3, 4, 5 and 6 depicts that it is likely to organize security infrastructure with an adequate performance and overhead.

Fig. 5 Overhead (CH interval)



Fig. 6 Overhead (hop count)



6 Conclusion

In this paper, we proposed a secured authentication and signature routing protocol (SASR) for WMN with Threshold Signature and certificate Revocation. In this technique, a secure cluster is made based on the trust value. For each node participating in the cluster formation, trust value is calculated. The node with high trust value is considered as the Cluster Head. The selected CH is further verified (using Threshold Signature) for the security improvement. All authenticated nodes in cluster are assigned to certification Authority and based on trust value they are updated in trust list and accused list. After that revocation technique is followed out to block the participation of any attackers in further actions. The advantage of the proposed technique is that it provides a secure and reliable network for secure communication.

References

1. Ferdous, R., Muthukumarasamy, V., Sithirasenam, E.: Trust-based cluster head selection algorithm for mobile ad hoc networks. In: Trust, Security and Privacy in Computing and Communications (TrustCom), IEEE 10th International Conference (2011)
2. Smith, T.F., Waterman, M.S.: Identification of common molecular subsequences. J. Mol. Biol. **147** (1981)

3. Mishra, A., Arbaugh, W.A.: An Initial Security Analysis of the IEEE 802.1X Standard. Computer Science Department Technical Report CS-TR-4328, pp. 5–197, University of Maryland, USA, February 2002
4. Kassab, M., Belghith, A., Bonnin, J.-M., Sassi, S.: Fast pre-authentication based on proactive key distribution for 802.11 infrastructure networks. In: Proceedings of the 1st ACM Workshop on Wireless Multimedia Networking and Performance Modeling (WMuNeP), pp. 46–53. Montreal, Canada, October 2005
5. Ben Salem, N., Hubaux, J.-P.: Securing wireless mesh networks. In: IEEE Wireless Commun. **13**, 50–55 (2006)
6. Cheikhrouhou, O., Maknavicius, M., Chaouchi, H.: Security architecture in a multi-hop mesh network. In: Proceedings of the 5th Conference on Security Architecture Research (SAR), Seignosse-Landes, France, June 2006
7. Zhu, S., et al.: A light-weight hop-by-hop access protocol. In: Distributed Computing Systems Workshops, 2003. Proceedings 23rd International Conference on IEEE, pp. 749–755 (2003)
8. Prasad, N.R., Alam, M., Ruggieri, M.: Light-weight AAA infrastructure for mobility support across heterogeneous networks. Wireless Pers. Commun. **29**, 205–219 (2004)
9. Moustafa, H., Zhang, et al.: Providing authentication, trust, and privacy in wireless mesh networks. In: Security in Wireless Mesh Networks, pp. 261–295. CRC Press, USA (2007)
10. Fantacci, R., Maccari, L., Pecorella, T., Frosali, F.: A secure and performant token-based authentication for infrastructure and mesh 802.1X networks. In: Proceedings of the 25th IEEE International Conference on Computer Communications (INFOCOM'06), Poster Paper, Barcelona, Spain, April 2006
11. Anil Kumar, V., Praveen Kumar Rao, K., Prasad, E., Gowtham Kumar, N.: Clustering based certificate revocation in mobile ad hoc networks. Int. J. Comput. Sci. Manag. Res. **2**, (2013)
12. Park, Y., Park, Y., Moon, S.: Anonymous cluster-based MANETs with threshold signature. Hindawi Publ. Corporation Int. J. Distrib. Sens. Netw. (2013)
13. Liu, W., Nishiyama, H., Ansari, N., Yang, J., Kato, N.: Cluster-based certificate revocation with vindication capability for mobile ad hoc networks. In: IEEE Trans. Parallel Distrib. Syst. (2013)
14. Yu, Y., Zhang, L.: A secure clustering algorithm in mobile ad hoc networks. IPSCSIT **29**, (2012)

A Minimal Subset of Features Using Correlation Feature Selection Model for Intrusion Detection System

Shilpa Bahl and Sudhir Kumar Sharma

Abstract The intrusion detection system (IDS) research field has grown tremendously in the past decade. Current IDS uses all data features to detect intrusions. Some of the features may be irrelevant and redundant to the detection process. The purpose of this study is to identify a minimal subset of relevant features to design effective intrusion detection system. A proposed minimal subset of features is built by selecting common features from six search methods with correlation feature selection method. The paper presents empirical comparison between 7 reduced subsets and the given complete set of features. The simulation results have shown slightly better performance using only 12 proposed features compared to others.

Keywords Correlation feature selection · Intrusion detection system · Machine learning · User to root attack class

1 Introduction

Intrusion detection system (IDS) complement conventional computer network protection techniques, namely user authentication, data encryption, and firewall. IDS has been recognized as an intense research area owing to the rapid increase in sophisticated attacks [1, 2]. The objective of IDS is to detect any anomalous or unusual activity as an attempt to break the security policy mechanism of networks. The design of IDS can be formulated into any one of the following two distinct approaches in the machine learning (ML) problem domain. (1) signature-based misuse system and (2) anomaly-based system. A signature-based system can be

S. Bahl (✉) · S.K. Sharma
KIIT College of Engineering, Gurgaon, India
e-mail: gerashilpa@gmail.com

S.K. Sharma
e-mail: sudhir_sharma99@yahoo.com

treated as a pattern classification problem. In the supervised classification approach, a model is constructed by the training data and network traffic data is classified into different types of attacks during testing phase [3]. An anomaly-based system is a semi-supervised approach where a model is built using normal usage of network traffic data and is a flagged exception to that model during testing phase [4]. Many current studies have used data clustering techniques for gaining insight into traffic data. A clustering-based system is an unsupervised approach in which network traffic data is categorized on the basis of their characteristic [5]. This paper addresses classification approach for building effective and efficient IDS.

The KDD Cup'99 dataset is a publically available benchmark for evaluating IDS techniques [6]. This dataset has a huge number of duplicate instances. In this paper, we used publically available NSL-KDD 99 dataset [7, 8]. This dataset is an improved version of KDD Cup'99 dataset without any duplicate instances. The dataset has 42 features including one class labeled feature. The used training dataset consists of 21 different attacks. These attacks are further categorized into four different types: (1) denial of service attacks (DoS); (2) probing attacks (Probe); (3) remote to local attacks (R2L), and (4) user to root attacks (U2R). The number of examples of U2R and R2L attack classes is very less in the dataset. Many research studies reported low detection rate for U2R and R2L attack classes [9–11]. There is no pattern classification algorithm or ML algorithm that could be trained successfully on KDD dataset to perform acceptable level of misuse detection performance for U2R and R2L attack categories. The testing dataset has substantial new attacks with signatures that are not correlated with similar attacks in the training dataset [12].

The effectiveness and accuracy of an ML classification system depends upon the quality of input dataset or the representative features of the given dataset. The feature selection (FS) is a class of well-known dimensionality reduction techniques in the feature space. An FS algorithm selects a subset of relevant features and discards other irrelevant and redundant features. It is common in ML to select relevant features in the pre-processing step prior to start of actual learning phase due to the adverse effect of irrelevant features on the ML system [13]. FS algorithms have been extensively investigated in the field of pattern recognition and ML for decades [14]. In general, FS algorithms fall into two broad categories, the filter method or the wrapper method. The filter method is independent of the classification algorithm. Filter method produces the most relevant subset of features based on the characteristics of the dataset. A predetermined classifier is used to evaluate the selected subset of features in the wrapper method. The wrapper method is more computationally expensive than the filter method [15–17]. The investigation and research on FS algorithm is still continued due to improving ML performance, decreasing computational complexity, and lowering required storage.

The objective of this paper is to select a minimal subset of the most relevant features of the given NSL-KDD dataset. The six subsets of features are selected using correlation feature selection (CFS) method. A minimal subset of features is proposed in this study to maintain the compactness and better performance of intrusion detection system. A Naïve Bayes algorithm is used for comparing the performance of seven reduced subset of features with all 41 features.

For demonstration, this paper presents only simulation results for U2R attack class. We achieve slightly better performance using only 12 features compared to others.

The rest of this paper is organized as follows: Sect. 2 describes related work. Section 3 describes the experimental setup. Section 4 presents results and discussion. Section 5 presents conclusions.

2 Related Work

The ten standard classification algorithms are used to compare the performance of four different types of attacks. The detection rate of U2R class is reported in the range from 1.2 to 32.8 % [9]. Two classifiers from rule-based family (Decision table and PART) were used with FS algorithms. The detection rate of U2R class is reported in the range from 0.70 to 20.0 % [10]. Nine classification algorithms are used to compare the performance of four different types of attacks. The detection rate for U2R class is reported in the range from 2.2 to 29.8 %. The best results are also compared with three well-known published results including winner of the KDD 99 intrusion detection competition [11]. There are discrepancies in the findings reported in the literature for U2R and R2L attack classes. The detection rate for these classes outlie the acceptance level using standard training and testing dataset [18].

A couple of features selection algorithms have been evaluated to decide a quality subset of features for decision tree family of classifiers [19]. Enhanced support vector and decision function for features selection was proposed in [20]. Mukkamala et al. identified 17 and 12 features using Bayesian network and CART classifier respectively [21]. They concluded by proposing a hybrid architecture involving ensemble and base classifiers. Minimal subsets have been extracted with 6, 5, 6 and 5 features for Probe, DoS, R2L and U2R individual attack classes respectively [22].

3 Experimental Setup

We used a laptop of Intel T2080, 1.73 GHz with 2 GB RAM. WEKA 3.7.11 data mining tool with default parameter setting used in this study [23, 24].

3.1 Proposed Research Methodology

The objective is to select a minimal subset of features to distinguish all attacks available in the training dataset using CFS with six search methods. In each FS algorithm, the selected features are kept in the original training and testing data files

and other features are removed permanently. Therefore, we have six sets of training and testing files. Some of the relevant features were commonly selected by all six FS methods. In the proposed approach, we chose these commonly selected features and built a new subset containing only 12 features.

3.2 KDD Cup 99 Dataset

In this study, we used NSL-KDD Cup 99 dataset [7]. We used KDD Train+ 20 % and KDDTest+ full datasets. The total examples in training and testing dataset are 25,192 and 22,544 respectively. The total examples of U2R class in training and testing dataset are 11 and 67 respectively. The training and testing dataset have different attacks. These attacks are categorized into four distinct types and presented in Tables 1 and 2. The number of different attacks in training and testing dataset is 21 and 37 respectively. The KDDTest+ has some novel attacks that are not available in KDDTrain + dataset. Each dataset has common 41 features. These features are categorized into four groups, namely basic features, content features, traffic features, and same host features. The names of these 41 features are presented in the second column of Table 4.

3.3 Correlation Feature Selection Measure

The correlation feature selection (CFS) is a well-known supervised filter technique used in this study. Features are said to be relevant if they are highly correlated with the predictive of the class and uncorrelated with each other [25]. The CFS is used to evaluate the merit of a subset of features consisting of k features by (1).

$$R_{FC} = \frac{K r_{cf}}{\sqrt{K + k(K - 1)r_{ff}}} \quad (1)$$

Table 1 Different attacks in KDDTrain+

DOS	Probe	R2L	U2R
Neptune	Satan	Guess_Password	Buffer_overflow
Teardrop	Nmap	Warezmaster	Loadmodule
Land	Portsweep	Warezclient	rootkit
Smurf	IPSwEEP	Sendmail	
Pod		Multihop	
		ftppwrite	
		Imap	
		Spy	
		Phf	

Table 2 Different attacks in KDDTest+

DOS	Probe	R2L	U2R
Neptune	Satan	Guess_Password	Buffer_overflow
Teardrop	Nmap	Warezmaster	Loadmodule
Land	PortswEEP	Sendmail	Rootkit
Smurf	IPSweep	Multihop	Sql Attack
Pod	Mscan	ftppwrite	Perl
back	Saint	Imap	Ps
mailbomb		Phf	Xterm
Processtable		Http tunnel	
worm		Xlock	
udpstrom		named	
Apache2		Xsnoop	
		Snmpgetattack	
		snmpguess	

where

R_{FC} = correlation between the class and the features

r_{cf} = average value of all feature-class correlations

r_{ff} = average value of all feature-feature correlations

The merit of a subset is one of the performance metrics to identify the best subset. The degree of correlation should be high between the feature and the class attribute and lowest between the features. As the number of features increases, the degree of correlation between the class and the features increases. As the new added features are less correlated with the already selected features and may have good predominance over a high correlation with the classes. Moreover, R_{FC} should be high for high strength of correlation between features and class [25]. In this paper we have used six search methods (Best first, Greedy stepwise, Genetic Search, Scatter Search, Random Search, and Exhaustive Search) to generate candidate feature subsets iteratively using sequential backward elimination approach. They are presented in the second column of Table 3.

3.4 Naïve Bayes Algorithm

In this paper, we employed Naïve Bayes algorithm for comparing the performance on reduced subsets and given dataset. The Naïve Bayes algorithm is a simple probabilistic classifier that calculates a set of probabilities by counting the frequency and combinations of values in a dataset. The algorithm assumes all attributes to be independent of the given value of the class attribute. It has been observed that the performance of Naïve Bayes algorithm is comparable to decision tree family algorithms and selected neural network classifiers [3].

Table 3 The details of feature subset selection methods

Serial no.	Search method	Selected subset of features	# Features selected	Merit subset	# Subsets formed
1	Best first	[2, 3, 4, 5, 6, 8, 10, 12, 23, 25, 29, 30, 35, 36, 37, 38, 40]	17	0.725	680
2	Greedy stepwise	[2, 3, 4, 5, 6, 8, 10, 12, 23, 26, 29, 30, 35, 36, 37, 38, 40]	17	0.725	684
3	Genetic Search	[2, 3, 4, 5, 6, 8, 12, 13, 22, 23, 25, 26, 27, 29, 30, 31, 32, 33, 36, 37, 38]	21	0.708	400
4	Scatter Search V 1	[2, 3, 4, 5, 6, 8, 11, 12, 14, 23, 25, 29, 30, 35, 36, 37, 38, 40]	18	0.722	17866
5.	Exhaustive search	[2, 3, 4, 5, 6, 8, 10, 12, 14, 23, 25, 29, 30, 31, 35, 36, 37, 38, 40]	19	0.721	860
6.	Random Search	[2, 3, 4, 5, 6, 8, 10, 11, 23, 25, 26, 27, 29, 30, 36, 37, 38]	17	0.726	896

4 Results and Discussion

The second, third, fourth, fifth, and sixth columns of Table 3 show the used search method, selected subset of features, the number of selected features, merit of selected subset, and the number of subsets formed respectively. The details of selected features are presented in Table 4. The features are given in column 2. The assigned labels to features are given in column 1. The search methods are presented in columns 3–8 in Table 4. The total, i.e., how many times a feature is selected using six different search methods is presented in column 9 of Table 4. The random search and exhaustive search methods are more computationally expensive than the best first and greedy-stepwise search methods. A proposed subset of features is chosen from Table 4. This minimal subset contains features labeled as 2, 3, 4, 5, 6, 8, 23, 29, 30, 36, 37, and 38 in Table 4. These 12 features are commonly selected by all six investigated search methods with CFS. This subset contains the most important and reliable features. All these features belong to basic, traffic, and host categories. The 15 features including 7 features of content category are not selected at all by any feature selection method.

These features are unimportant and irrelevant to distinguish all attacks available in the training dataset. The third category of features contains the remaining 14 features. We constructed multiclass—hierarchical classifier during training phase. The constructed model is tested by testing dataset. All simulation results for all attack types available in the training data set were saved. For brevity, we present the summary results of only U2R attack class for demonstrating the performance comparison on reduced dataset and all 41 features. Four additional attacks of U2R class in the KDDTest+ dataset are Perl, Sqlattack, Xterm, and ps. These are not detected and not considered in the summary results of Table 5.

Table 4 The details of selected features

Label	Feature	Best first	Greedy stepwise	Genetic search	Scatter search V1	Exhaustive search	Random search	Total
1	Duration	✓	✓	✓	✓	✓	✓	0
2	Protocol-type	✓	✓	✓	✓	✓	✓	6
3	Service	✓	✓	✓	✓	✓	✓	6
4	Flag	✓	✓	✓	✓	✓	✓	6
5	src_bytes	✓	✓	✓	✓	✓	✓	6
6	dst_bytes	✓	✓	✓	✓	✓	✓	6
7	Land							0
8	wrong_fragment	✓	✓	✓	✓	✓	✓	6
9	Urgent							0
10	Hot	✓	✓		✓	✓	✓	4
11	num_failed_logins				✓	✓	✓	2
12	logged_in	✓	✓	✓	✓	✓	✓	5
13	num_compromised			✓	✓	✓		1
14	root_shell					✓		2
15	su_attempted							0
16	num_root							0
17	num_file_creation							0
18	num_shells							0
19	num_access_files							0
20	num_outbound_cmds							0
21	is_host_login							0
22	is_guest_login				✓		1	1
23	Count	✓	✓	✓	✓	✓	✓	6

(continued)

Table 4 (continued)

Label	Feature	Best first	Greedy stepwise	Genetic search	Scatter search V1	Exhaustive search	Random search	Total
24	srv_count	✓		✓	✓	✓	✓	0
25	seor_rate		✓			✓	✓	5
26	srv_seor_rate		✓	✓			✓	3
27	rror_rate			✓			✓	2
28	rv_rror_rate			✓				0
29	ame_srv_rate	✓	✓	✓	✓	✓	✓	6
30	diff_srv_rate	✓	✓	✓	✓	✓	✓	6
31	rv_diff_host_rate			✓		✓		2
32	dst_host_count			✓				1
33	dst_host_srv_count			✓				1
34	dst_host_same_srv_rate				✓	✓		0
35	dst_host_diff_srv_rate	✓	✓		✓	✓		4
36	dst_host_same_src_port_rate	✓	✓	✓	✓	✓	✓	6
37	dst_host_srv_diff_host_rate	✓	✓	✓	✓	✓	✓	6
38	dst_host_seor_rate	✓	✓	✓	✓	✓	✓	6
39	dst_host_srv_seor_rate							0
40	dst_host_rror_rate	✓	✓		✓			4
41	dst_host_srv_rror_rate							0

Table 5 Average results of performance metrics for U2R class

Search method	Accuracy	RMSE	DR	FPR	F-score	AUC	Time
41 features	33.91	0.240	10.2	0.03	0.03	0.56	3.90
Best first	62.53	0.177	14.0	0.04	0.05	0.60	1.16
Greedy stepwise	62.63	0.178	14.0	0.04	0.05	0.60	1.11
Genetic search	52.42	0.198	13.5	0.04	0.04	0.75	2.29
Scatter search V1	60.52	0.180	10.6	0.05	0.04	0.57	1.69
Exhaustive search	40.90	0.213	13.8	0.06	0.04	0.68	1.95
Random search	63.78	0.172	13.6	0.02	0.04	0.59	1.34
12 features (proposed)	65.43	0.168	14.1	0.01	0.05	0.75	0.95

The detection rate of loadmodule attack is very poor in all experiments. Table 5 presents simulation results for all 41 features and 7 selected subset of features for U2R attack class. Table 5 presents the overall accuracy, root mean squared error (RMSE), time to build a model in columns second, third, and eighth respectively. Table 5 also presents the average of many standard metrics for three different attacks of U2R class. The average of detection rate (DR) in %, false positive rate (FPR) in %, F-score, and area under ROC curve (AUC) are presented in columns fourth, fifth, sixth, and seventh respectively in Table 5.

On the basis of Table 5, the performance of IDS is not worsening using CFS with six search methods. The performance of classifier on the proposed subset is better than other subsets. The proposed subset of features is not only the smallest subset but also contributed to improving the overall accuracy and detection rate of U2R type of attacks. This empirical study helps network administrator in the collection of the most appropriate network traffic data labels and to design online intrusion detection system effectively.

5 Conclusion

In this paper, we investigated correlation feature selection with six search methods. We obtained six subsets of existing features of KDD dataset. We proposed a minimal subset of features that has only 12 features. We evaluated the performance of reduced dataset using Naïve Bayes classifier. We demonstrated performance comparisons between 7 different subsets of features and all existing 41 features. The empirical results revealed that overall accuracy and detection rate of U2R type of attacks had improved significantly by correlation feature selection method. The performance of identified subset is better than the others. This empirical study helps network administrator in the collection of the most appropriate network traffic data and designing online intrusion detection system.

References

1. Van der Geer, J., et al.: Intrusion detection system: a review, the art of writing a scientific article. *J. Sci. Commun.* **163**, 51–59 (2000)
2. Van der Geer, J., et al.: Managing Cyber Threats: Issues, Approaches, and Challenges, vol. 5. Springer (2006)
3. Han, J., Kamber, M., Pei, J.: Data Mining, Concepts and Techniques. Southeast Asia Edition (2006)
4. Tavallaei, M., Stakhanova, N., Ghorbani, A.A.: Toward credible evaluation of anomaly-based intrusion-detection methods. *Syst. Man Cybern. Part C: IEEE Trans. Appl. Rev.* **40**(5), 516–524 (2010)
5. Sánchez, R., Herrero, Á., Corchado, E.: Visualization and clustering for SNMP intrusion detection. *Cybern. Syst.* **44**(6–7), 505–532 (2013)
6. KDD Cup 1999: <http://kdd.ics.uci.edu/databases/kddcup99/kddcup99.html> (2014, Oct)
7. NSL-KDD Data set for Network-Based Intrusion Detection Systems: <http://nsl.cs.unb.ca/KDD/NSL-KDD.html> (March 2014)
8. Revathi, S., Malathi, A.: A detailed analysis of KDD cup99 dataset for IDS. *Int. J. Eng. Res. Technol. (IJERT)* **2**(12), (2013)
9. Nguyen, H., Choi, D.: Application of data mining to network intrusion detection: classifier selection model. In: APNOMS 2008, LNCS 5297, pp. 399–408, 2008. © Springer, Berlin Heidelberg (2008)
10. Bahl, S., Sharma, S.K.: Improving classification accuracy of IDS using feature subset selection. In: Proceedings of International Conference IEEE ACCT 2015, India
11. Sabhnani, M., Serpen, G.: Application of machine learning algorithms to KDD intrusion detection dataset within misuse detection context. In: MLMTA, pp. 209–215 (2003)
12. Sabhnani, M., Serpen, G.: Why machine learning algorithms fail in misuse detection on KDD intrusion detection data set. *Intel. Data Anal.* **8**(4), 403–415 (2004)
13. Chizi, B., Maimon, O.: Dimension reduction and feature selection. In: Data Mining and Knowledge Discovery Handbook, pp. 83–100. Springer (2010)
14. Maaten, V., Laurens, J.P., Postma, E.O., Jaap, H., Herik, V.: Dimensionality reduction: a comparative review. *J. Mach. Learn. Res.* **10**(1–41), 66–71 (2009)
15. Stańczyk, U.: Ranking of characteristic features in combined wrapper approaches to selection. *Neural Comput. Appl.* 1–16 (2015)
16. Jiliang, T., Alelyani, S., Liu, H.: Feature selection for classification: a review. In: Aggarwal, C. (ed.) Data Classification: Algorithms and Applications. CRC Press in Chapman & Hall/CRC Data Mining and Knowledge Discovery Series (2014)
17. Solanki, M., Dhamdhere, V.: Intrusion detection technique using data mining approach: survey. *Int. J. Innovative Res. Comput. Commun. Eng.* **2**(11), (2014)
18. Engen, V., et al.: Exploring discrepancies in findings obtained with the KDD Cup'99 data set. *Intell. Data Anal.* **15**(2), 251–276 (2011)
19. Piramuthu, S.: Evaluating feature selection methods for learning in data mining applications. *Eur. J. Oper. Res.* **156**, 483–494 (2004)
20. Zaman, S., Karay, F.: Features selection for intrusion detection systems based on support vector machines. In: Consumer Communications and Networking Conference, CCNC 2009 IEEE, pp. 1–8
21. Peddabachigari, S., Abraham, A., Grosan, C., Thomas, J.: Modeling intrusion detection system using hybrid intelligent systems. *J. Netw. Comput. Appl.* **30**(1), 114–132 (2007)
22. Staudemeyer, R.C., Omlin, C.W.: Extracting salient features for network intrusion detection using machine learning methods. *S. Afr. Comput. J.* **52**, 82–96 (2014)
23. Weka Data Mining Machine Learning Software: <http://www.cs.waikato.ac.nz/ml/weka>
24. Witten, I.H., Frank, E., Hall, M.A.: Data Mining-Practical Machine Learning Tools and Techniques. Morgan Kaufmann (2011)
25. Hall, M.A.: Correlation-based Feature Selection for Machine Learning, Thesis (1999)

Analysis of Single-Layered Multiple Aperture Shield for Better Shield Effectiveness

N.S. Sai Srinivas, VVSSS. Chakravarthy and T. Sudheer Kumar

Abstract Shield Effectiveness (SE) is a most significant parameter that determines the electromagnetic compatibility (EMC) characteristics of the system. Calculation of this parameter is the prerequisite for understanding the standards of the system. Many techniques are implemented for the betterment of this parameter. In this paper, implementation of various perforated shield materials are proposed and their corresponding frequency responses are evaluated. Distance between the source of electromagnetic interference (EMI) and the system under test (SUT) has a direct impact on SE. Investigations by varying this distance is presented in this paper. The functioning of the material as shield in the presence of such environment is given.

Keywords EMC · EMI · Shield effectiveness · Perforated materials

1 Introduction

In the modern environment, it can be observed that there is a vast utilization of electronic circuitry. These electronics are existing in every civil, commercial, and industrial systems. Due to this, these systems have to work in the close vicinity with each other. Hence there is a possibility of malfunctionality with every electronic gadget due to certain level of interference known as electromagnetic interference (EMI). With the time, the severity of the problem due to EMI is also developing. This is a severe task for the electronic engineers to design the system without characteristics of EMI source and capability to work in an EMI environment.

N.S. Sai Srinivas (✉)
Department of ECE, Andhra University, Visakhapatnam, India
e-mail: satya_srinivasnettmi@live.com

VVSSS. Chakravarthy
Department of ECE, Raghu Institute of Technology, Visakhapatnam, India

T. Sudheer Kumar
Department of ECE, Vishnu Institute of Technology, Bheemavaram, AP, India

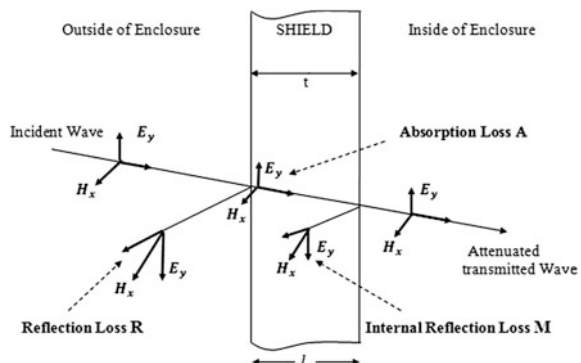
EMI causes degradation in the reception of a signal due to radio frequency (RF) interference. This is an electromagnetic disturbance in the RF range [1–4]. Simply, the EMI interrupts the normal operation of electronic systems. Overwhelming use of electronic gadgets reached an alarming stage due to this EMI effects in many civilian and military applications. To provide an adequate solution for the EMI problem, the shielding or absorbing of the electromagnetic field is considered.

The general practice is to choose good conducting materials as shields to enclose the SUT. Latest research suggested many materials for effective shielding. In this work, such shielding environment composed of different materials is considered. Simulation is carried out with aluminum, copper, and polymer perforated sheets as shields. The corresponding SE is calculated for different number of apertures like $n = 1, 4$, and 9 . Similarly, a comparative analysis is being carried out by varying the distance between the EMI source and SUT as $1, 5$, and 10 m respectively. The remaining part of the paper is divided into four sections. Introduction and significance of SE is mentioned in Sect. 2. The formulation of SE is described in Sect. 3. Results with respect to different shielding materials are given and discussed in Sect. 4. Overall conclusion is given in Sect. 5.

2 Shield Effectiveness

Electromagnetic (EM) shielding is the technique that reduces or prevents coupling of undesired radiated EM energy into equipment [5–10]. EM shielding is effective in varying degrees over a wide range of the EM spectrum from DC to microwave frequencies. Shielding problems are difficult to handle because perfect shielding integrity is not possible because of the presence of intentional discontinuities in shielding walls, such as panel joints, vent-holes or switches [11–14]. Representation of shielding mechanisms for plane waves is shown in the Fig. 1.

Fig. 1 Demonstration of shield effectiveness mechanism



Shielding effectiveness (S) is defined

$$\text{As for Electric fields as } S = 20 \log \frac{E_i}{E_t} \text{ dB} \quad (1)$$

$$\text{Magnetic fields as } S = 20 \log \frac{H_i}{H_t} \text{ dB} \quad (2)$$

where

E_i = incident E-field strength

E_t = transmitted E-field strength

H_i = incident H-field strength

H_t = transmitted H-field strength

Two basic mechanisms, reflection loss (R) and absorption loss (A), are responsible for the shielding. Therefore, shielding theory is based on the transmission behavior through metals and reflection from the surface of the metal. A detailed description of the A and R is given as follows:

Absorption Loss (AL): This factor corresponds to the attenuation observed by the wave as it progresses in the medium.

Reflection Loss (RL): Reflection losses are an interaction between the impedance of an incident wave and the waveguide. It is dependent on the type of field and the wave impedance.

Correction factor (BF): This accounts for multiple reflections in thin shields.

C' , C'' and C''' are three different factors corresponding to area, waveguide depth, and conductor employed between holes, respectively.

Total SE is given by [1]

$$S = A + R + B + C' + C'' + C''' \quad (3)$$

3 Single Perforated Shield-Double Interface

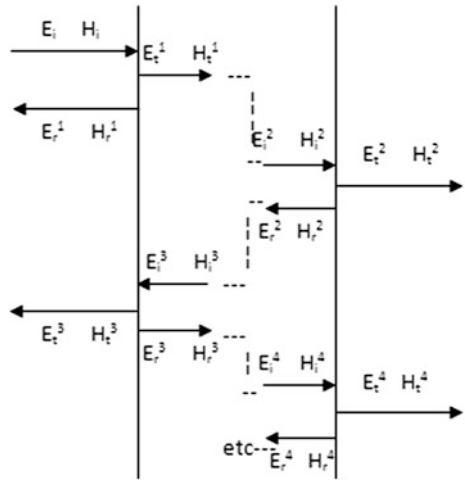
Description of the single perforated shield with double interface is given as shown in Fig. 2. The mathematical formulation of the SE

and the corresponding transmission coefficients are as follows

$$p_E = \gg \frac{E^t}{E^i} = \frac{2\eta_2}{\eta_2 + \eta_1} = \frac{Z(l)}{\eta + Z(l)} = \frac{2K}{1 + K} \quad (4)$$

$$P_H = \gg \frac{H^t}{H^i} = \frac{2\eta_1}{\eta_1 + \eta_2} = \frac{2\eta}{\eta + Z(l)} = \frac{2}{1 + K} \quad (5)$$

Fig. 2 Double Interface showing multiple reflections for single shield



where $K = \frac{\eta_2}{\eta_1}$ or $\frac{Z(l)}{\eta}$

When two mismatches are considered as in a planar sheet, the net transmission coefficients are the product of the transmission coefficients across the two boundaries.

$$p = p_E = p_H = p_E(0) \cdot p_E(l) = p_H(0) \cdot p_H(l) = \frac{4k}{(1+k)^2} \quad (6)$$

By definition, the reflection loss is

$$R = -20 \log_{10} |p| = 20 \log_{10} \frac{|1+k|^2}{4|k|} \quad (7)$$

When k is either small or large

$$\begin{aligned} R &= 20 \log_{10} \frac{1}{4|k|}, |k| \ll 1 \\ R &= 20 \log_{10} \frac{|k|}{4}, |k| \gg 1 \end{aligned} \quad (8)$$

$$C' = -10 \log(a \cdot n) \quad (9)$$

where ‘ a ’ is the hole area and ‘ n ’ is number of holes for exposed area

$$C'' = -20 \log_{10} \left[1 + \frac{35}{(\pi f w^2 \sigma \mu)^{1.15}} \right] \quad (10)$$

where 'w' is the conductor width between holes

$$C''' = 20 \log_{10} \left[\frac{1}{\tanh \left(\frac{A}{8.686} \right)} \right] \quad (11)$$

4 Results

The analysis of shielding effectiveness is carried out for various perforated single shield conducting materials, like aluminum, copper, and polymer by varying the distance between source and shield. The frequency variations of both TE wave and

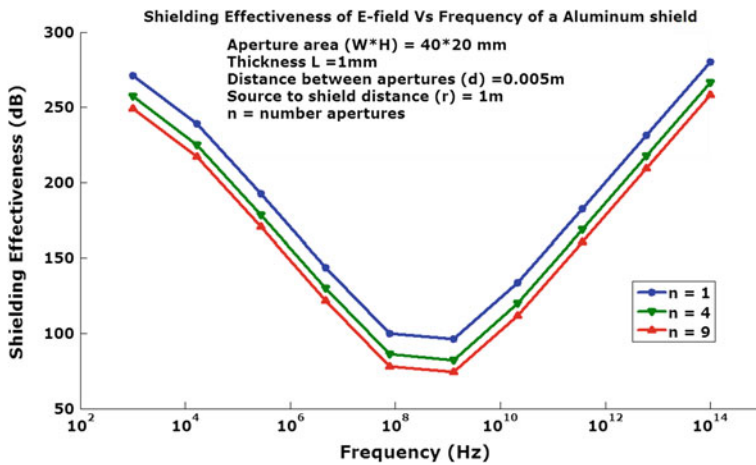


Fig. 3 Frequency versus SE for Al perforated shield at E-field

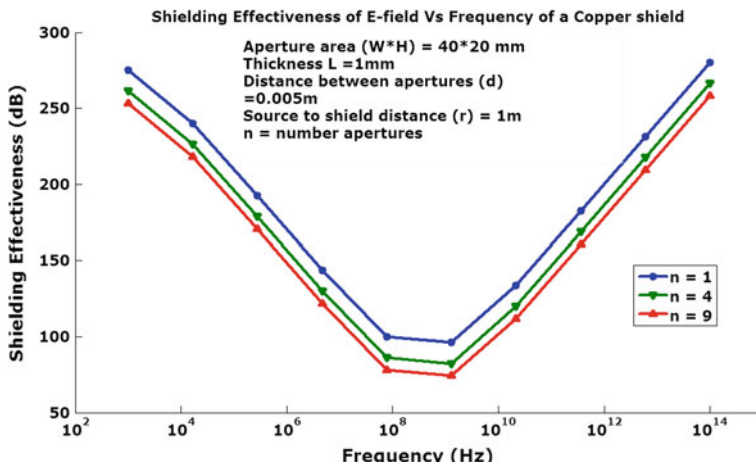


Fig. 4 Frequency versus SE for Cu perforated shield at E-field

TM wave for all three types of shields for vertical and horizontal at single and multiple apertures are considered.

Figures 3, 4, 5, 6, 7, 8, 9, 10, and 11 shows the variation of the SE as a function of frequency for single layer aluminum, copper, and conductive polymer perforated shields at E-field. Let us consider a single perforated shield having horizontal apertures, with aperture area ($W * H$) = 40 * 20 mm, thickness of material L = 1 mm and distance between apertures ‘ d ’ = 0.005 m. We compare the shielding effectiveness according to the frequency. For all the materials, the SE decreases at low frequencies. When it reaches the cutoff frequency f_c = 1.19 GHz, it increases. The SE also varies according to the number of apertures ‘ n ’ and distance between source to shield ‘ r ’.

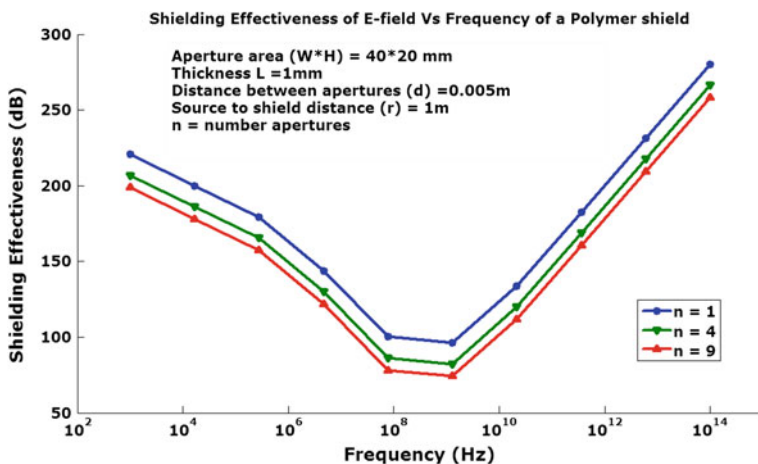


Fig. 5 Frequency versus SE for polymer perforated shield at E-field

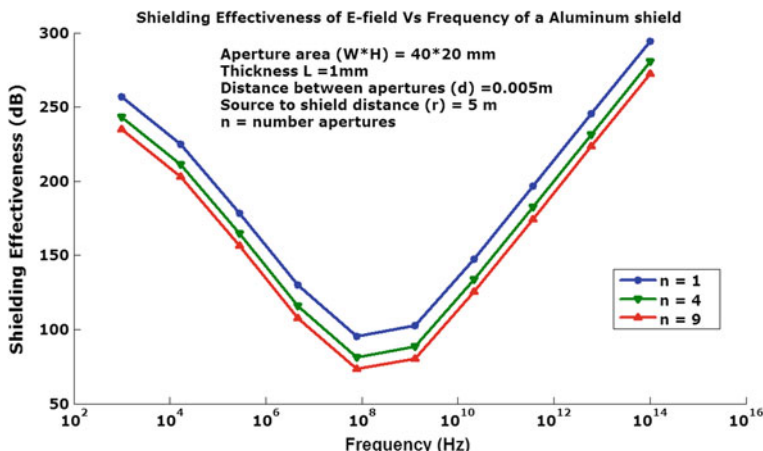


Fig. 6 Frequency versus SE for Al perforated shield at E-field

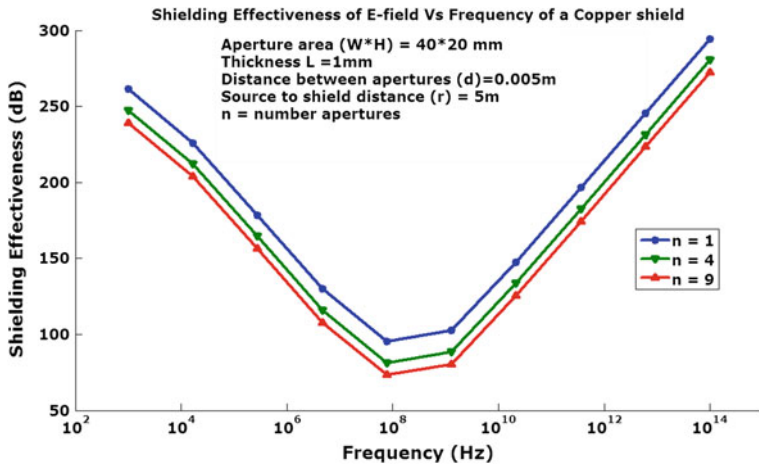


Fig. 7 Frequency versus SE for Cu perforated shield at E-field

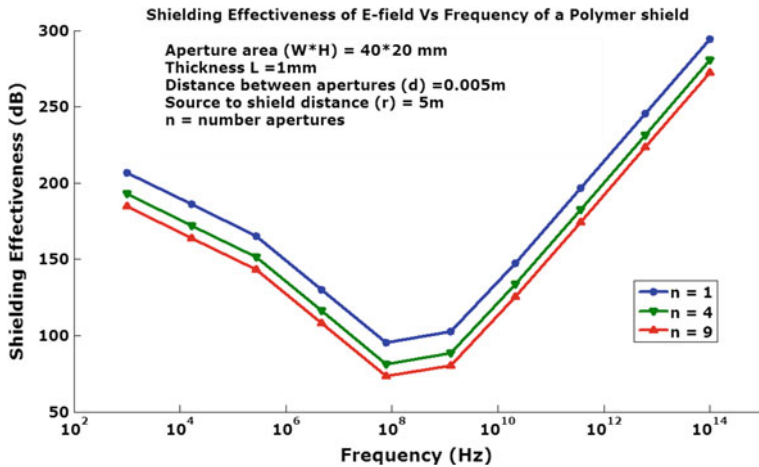


Fig. 8 Frequency versus SE for polymer perforated shield at E-field

Now the source to shield spacing is enhanced to 5 m. Figures 6, 7, and 8 show the variation of the SE with frequency in this case.

Figures 9, 10, and 11 show the frequency response of the SE when the spacing is enhanced to 10 m.

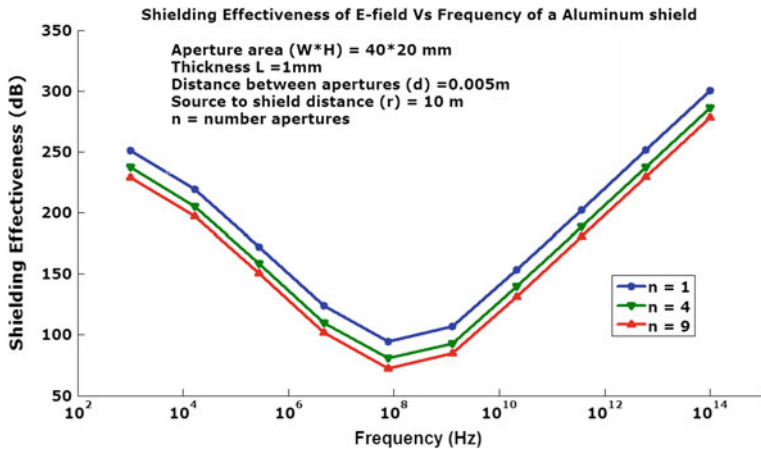


Fig. 9 Frequency versus SE for Al perforated shield at E-field

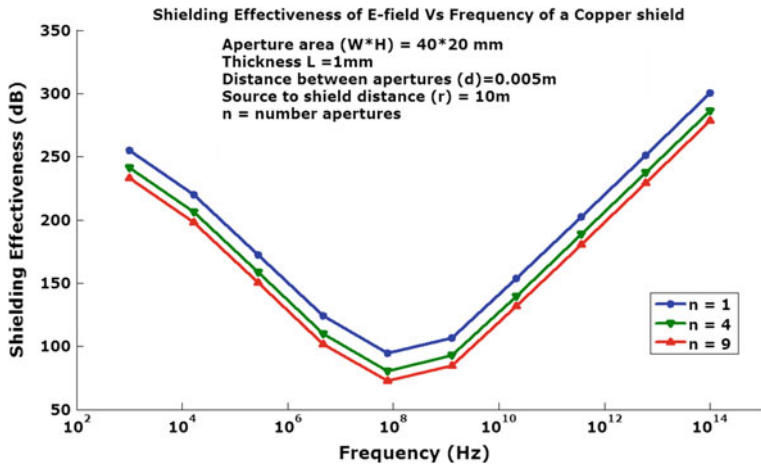


Fig. 10 Frequency versus SE for Cu perforated shield at E-field

5 Conclusion

The SE of single perforated shields constructed with conductive Polymer-E, metals such as copper and aluminum are evaluated. It can be inferred from the results that a conductive polymer has a very high conductivity to weight ratio, and thus it can yield the same SE performance as that of a conductor with less weight at high and low frequency ranges. In the above results, Cu and Al materials exhibit better shielding effectiveness because of their high conductivity. Polymer-E provides

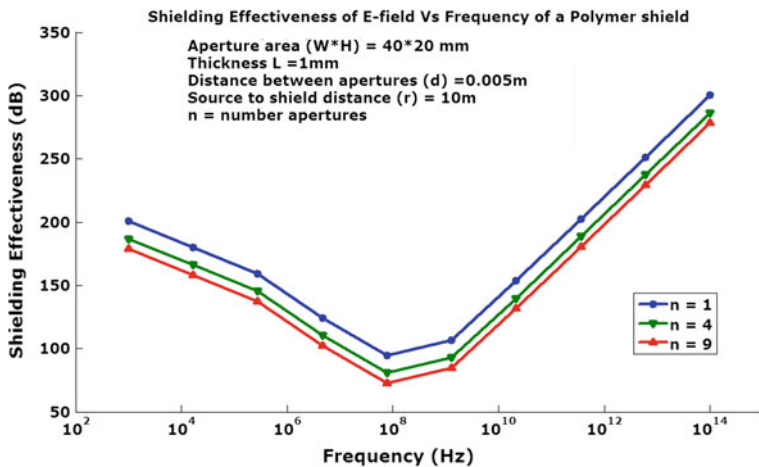


Fig. 11 Frequency versus SE for polymer perforated shield at E-field

good shielding effectiveness with same frequency considerations. From the above analysis, we can compute the electromagnetic shielding effectiveness.

References

1. Kodali, V.P.: Engineering Electromagnetic Compatibility, Principles, Measurements and Technologies. S Chand and Company Ltd (2000)
2. Liao, S.Y.: Microwave Devices and Circuits, 3rd edn. Pearson Edition
3. Paul, R.C.: Introduction to Electromagnetic Compatibility. John Wiley Interscience, New York (1992)
4. Ott, Henry W.: Electromagnetic Compatibility Engineering. Wiley, New Jersey (2009)
5. Jayasree, P.V.Y.: Analysis of Shielding effectiveness of single, double and laminated shields for oblique incidence of EM waves. Progr. Electromagn. Res. B **22**, 187–202 (2010)
6. Robinson, M.P., Benson, T.M., Christopoulos, C., Dawson, J.F., Ganley, M.D., Marvin, A.C., Porter, S.J., Thomas, D.W.P.: Analytical formulation for the shielding effectiveness of enclosures with apertures. IEEE Trans. Electromagn. Compat. **40**(3), 240–248 (1998)
7. Naaman, H.: Synthesis of new conductive electronic polymers. In: Proceedings of International Congress Synthetic Metals, Kyoto, Japan, June 1986
8. Ehinger, K., Summerfield, S., Bauhofer, W., Roth, S.: DC and microwave conductivity of iodine-doped polyacetylene. J. Phys. C: Solid State Phys. **17**, 3753–3762 (1984)
9. Naishadham, K., Kadaba, P.K.: Measurement of the microwave conductivity of a polymeric material with potential applications in absorbers and shielding. IEEE Trans. Microwave Theory Technol. **39**, 1158–1164 (1991)
10. Konefal, T., Dawson, J.F., Marvin, A.C.: Improved aperture model for shielding prediction. IEEE Int. Symp. Electromagn. Compat. 187–192 (2003)
11. Jordan, E.C., Balmain, K.G.: Electromagnetic Waves and Radiating Systems. Eastern Economy Edition
12. Schulz, R.B., Plantz, V.C., Brush, D.R.: Shielding theory and practice. IEEE Trans. Electromagn. Compat. **30**, 187–201 (1988)

13. Cowdell, R.B.: Simplified shielding for perforated shields. *IEEE Trans. Electromagn. Compat.* 308–318 (1963)
14. Chadda, D.: Electromagnetic interference and compatibility—shielding techniques. In: Module 3, IMPACT Learning Material Series Prepared by Indian Institute of Technology, New Delhi (1997)

MRI Classification of Parkinson's Disease Using SVM and Texture Features

S. Pazhanirajan and P. Dhanalakshmi

Abstract A novel method for automatic classification of magnetic resonance image (MRI) under categories of normal and Parkinson's disease (PD) is then classified according to the severity of the medical specialty drawbacks. In recent years, with the advancement in all fields, human suffers from numerous specialty disorders like brain disorder, epilepsy, Alzheimer, Parkinson, etc. Parkinson's involves the malfunction and death of significant nerve cells within the brain, known as neurons. As metal progresses, the quantity of Dopastat made within the brain decreases, defeat someone, and make them unable to manage movements commonly. In the planned system, T_2 (spin-spin relaxation time)—weighted MR images are obtained from the potential PD subjects. For categorizing the MRI knowledge, bar graph options and gray level co-occurrence matrix (GLCM) options are extracted. The options obtained are given as input to the SVM classifier that classifies the information into traditional or PD classes. The system shows a satisfactory performance of quite 87 %.

Keywords Electroencephalogram (EEG) · Parkinson's disease (PD) · Gray-level co-occurrence matrix (GLCM) · Support vector machine (SVM)

1 Introduction

Parkinson's disorder (PD) is the second most typical neurodegenerative illness moving several individuals worldwide. A calculable 7 to 10 million individuals worldwide reside with paralysis agitans. Incidence of Parkinson's will increase with

S. Pazhanirajan (✉) · P. Dhanalakshmi
Department of Computer Science and Engineering,
Annamalai University, Chidambaram, India
e-mail: pazhani.sambandam@yahoo.co.in

P. Dhanalakshmi
e-mail: abidhana01@gmail.com

age, however, associate in nursing calculable 4 % of individuals with palladium square measure diagnosed before the age of fifty. The MR image is used to identify spatial map and properties associated with a specific nuclei or proton present in the region being analyzed. The hydrogen proton is the most common form of nuclei used in MRI. These properties are the spin-lattice relaxation time T_1 , spin-spin relaxation time T_2 , and the spin density p . To detect PD, various signals (EEG, speech, etc.) and images (MRI, C.T, etc.) have been undertaken [1].

In [2], of this paper, the authors have proposed a novel technique for automated segmentation of brain structures that are related to PD from low resolution sonographic images. The authors have performed averaging of adjusted spatially varying TCS image as preprocessing step to avoid noise in the image. The segmentation is performed by a tailored shape-based active contour segmentation algorithm.

A novel region of interest (ROI)-based CAD technique using T_1 -weighted magnetic resonance imaging (MRI) was used to discriminate PD patients from healthy subjects. Features are constructed from gray matter (GM), white matter (WM), and cerebrospinal fluid (CSF) values of voxel from these regions. A decision model is built with the help of support vector machine classifier. The results demonstrate that the proposed method has an accuracy of 86.67 % in identifying PD patients from health subjects [3].

In an expert system proposed in [4], a supervised machine learning approach for identifying sensitive medical image biomarkers which enables automatic diagnosis of individual subjects. Morphological T_1 -weighted magnetic resonance images (MRIs) of PD patients and PSP patients were analyzed using principal component analysis as feature extraction technique and support vector machine is used for classification.

2 Feature Extraction

2.1 Histogram Processing

The histogram of a digital image with intensity levels in the range $[0, L - 1]$ is a discrete function

$$s(r_k) = \frac{n_k}{n}, 0 \leq k \leq L - 1$$

where r_k is the k th gray level, n_k is the number of pixels in the image with that intensity level, n is the number of pixels in the MRI with $k = 0, 1, 2, \dots, L - 1$. In short, $s(r_k)$ gives an estimate of the probability of occurrence of intensity level r_k [5].

2.2 Histogram Feature Extraction

Histogram equalization is an image enhancement method which uses a monotonically increasing transformation function [6]. The original intensity values r_i are transformed using the function $T(r)$ into new intensity values of the output image as follows:

$$s_i = T(r_i) = \sum_{j=0}^i s_r(r_j) \quad (1)$$

$$\sum_{j=0}^i s_r(r_j) = \sum_{j=0}^i \frac{n_j}{n} \quad \text{for } i = 0, 1, \dots, L-1 \quad (2)$$

where $S_r(r_i)$ is the probability-based histogram of the input image that is transformed into the output image with the histogram $S_s(s_i)$. The histogram of the input image is stretched using the transformation function $T(r_1)$ in Eq. (2) in such a way that the intensity values in the output image occurs with equal probability of occurrence.

This method achieves uniform distribution by redistributing the intensity values of an image. This methodology could cause saturation in some regions of the image leading to loss of details and high-frequency data which will be necessary for interpretation.

2.3 Texture Feature

The GLCM is created from a grayscale image and hence the values that are checked for co-occurrence are pixels with gray level (grayscale intensity) [7].

2.3.1 Derivation of Texture Features from a Co-occurrence Matrix

In the simplest form, the GLCM $s(a, b)$ is the distribution of the number of occurrences for a pair of gray values a and b separated by a distance vector $d = [dx; dy]$.

We used 22 textural features in our study. The following equations define these features. Let $s(a, b)$ be the (a, b) th entry in a normalized GLCM [8]. we define also

$$s_x(a) = \sum_{b=1}^N s(a, b) \quad (3)$$

$$s_y(i) = \sum_{a=1}^N s(a, b) \quad (4)$$

Table 1 Haralick texture features (characteristics 1 to characteristics 22)

S. no	Characteristics	S. no (continued)	Characteristics
1	Contrast	12	Maximum probability
2	Correlation	13	Sum of squares
3	Energy/angular second moment	14	Sum average
4	Homogeneity	15	Sum variance
5	Autocorrelation	16	Sum entropy
6	Maximal correlation coefficient	17	Difference variance
7	Cluster prominence	18	Difference entropy
8	Cluster shade	19	Information measure of correlation 1
9	Dissimilarity	20	Information measure of correlation 2
10	Entropy	21	Inverse difference normalized
11	Homogeneity	22	Inverse difference moment normalized

$$s_{x+y}(k) = \sum_{a=1}^N \sum_{b=1}^N s(a,b), \quad k = 1, 2, \dots, 2N \quad (5)$$

$$a + b = k$$

$$s_{x-y}(k) = \sum_{a=1}^N \sum_{b=1}^N s(a,b), \quad k = 0, 1, \dots, N-1 \quad (6)$$

$$|a - b| = k$$

and μ_x , μ_y , σ_x , and σ_y as the means and standard deviations of S_x and S_y , respectively. We used the [9] and [10] Haralick texture features with their equations (1–22) in Table 1.

3 Modeling Technique for SVM

Support vector machine (SVM) relies on the principle of structural risk decrease [11]. SVM learns associate degree best separating hyper plane from a given set of positive and negative examples. SVM are often used for pattern classification. For linearly severable knowledge, SVM finds a separating hyperplane that separates the information with the biggest margin. For linearly indivisible knowledge, it translates the information within the input area into a high-dimension area

$$x \in R^I \rightarrow \Phi(x) \in R^H \quad (7)$$

with kernel operate $\Phi(x)$, to find out the separating hyperplane. SVMs area unit evaluated as well-liked tools for learning from the given knowledge [12, 14]. The explanation is that, SVMs area unit is simpler than the normal pattern recognition approaches that supported the mix of a feature choice procedure and a standard classifier.

SVM is generally applied to linear margins. If a linear boundary is out of place, the SVM will map the input vector into a high dimensional feature area. Nonlinear mapping is selected by the SVM constructs to associate the best separating hyperplace in the higher dimensional area. A kernel function K is defined for generating the inner products to construct machines with different kinds of non-linear decision surfaces within the input area.

$$K(x, x_i) = \Phi(x) \cdot \Phi(x_i) \quad (8)$$

4 Experimental Results

4.1 Dataset

We evaluated the accuracy of our technique by acting experiments on information obtained as a part of the Parkinson's progression markers initiative (PPMI) (https://www.ida.loni.usc.edu/services/Menu/IdaData.jsp?page=DATA&subPage=AVAILABLE_DATA&project=PPMI). An outline of demographic and psychology details of subjects utilized in our study is bestowed in Table 2.

The database consists of 595 different data groups are available, which 32 are normal and 78 are PD.

4.2 Image Acquisition and Preprocessing

The structural T_2 -weighted magnetization ready fast gradient echo images were nonheritable on a 1.5-T Vision scanner during an imaging period. From the original

Table 2 Clinical characteristics of PD patients and control subjects

Total number of data characteristics	Control	With PD
MRI data (n)	32	78
Age	45 ± 59	45 ± 69
Sex (M/F)	32 (17/15)	78 (52/26)
Format	DCM	DCM

image knowledge, the region of interest is fixed to a size of 95×95 . The ROI is fixed such that it provides enough information for feature selection. Image parameters: TR = 9.7 ms, TE = 4.0 ms, Flip angle = 10, TI = 20 ms, TD = 200 unit of time., 128 mesial 1.25 mm slices while not gaps and pixels resolution of 512×512 .

4.3 Feature Extraction

The features are extracted using Histogram and GLCM. Histogram is an image enhancement technique which normalizes gray level in the image. There are 8 histogram features and 22 GLCM features extracted from the image data which are combined to form a 30-dimensional feature vector. The cropped image is of size 95×95 . From the 120 MR images within the dataset, we have used 80 images for training and 40 pictures for testing. The training image set consists of 48 control images and 32 abnormal MR images. Within the training phase, the images are applied to the SVM which creates models numbered zero and one, 0 belong to Normal, 1 belong to PD. In the testing phase, the images are applied to the SVM which extracts the features from the images and creates models, these models are compared with the existing models to classify the image.

4.4 Modeling Using SVM

We use a nonlinear support vector machine modeling that is employed to classify the image. The 30 features that are extracted within the previous section are provided to SVM for model generation. The model generated by the SVM classifies the image information into traditional and Parkinson's sickness. The character of the dataset, total range of dataset used per class, and also the classification are accuracy is bestowed in Table 3 (Figs. 1 and 2).

Table 3 Statistical parameters of classification accuracy

Statistical parameters	Specificity	Sensitivity	Total classification accuracy
Accuracy	True +ve/ (True +ve) + (False -ve)	True -ve/ (False +ve) + (True -ve)	(True +ve) + (True -ve)/(P + N)
(%)	83	89	87

Fig. 1 Control versus parkinson using SVM

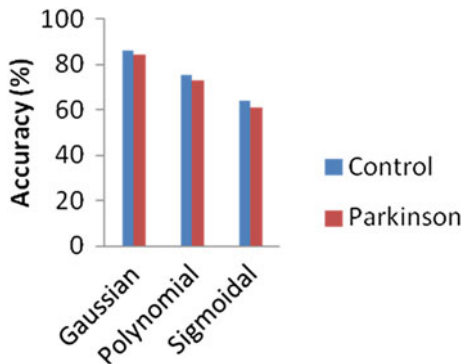
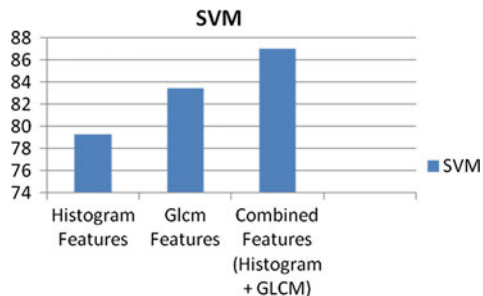


Fig. 2 Performance of classification for different combination of feature



5 Conclusions

In this paper, a system for classifying MRI image is described. ROI is manually calculated by cropping the MRI image. Histogram and GLCM features are extracted from the cropped image. 30 features are extracted from the ROI image. The features are given as input to the SVM for classification as Normal and PD. The experimental results show that the classification by SVM can produce a performance of accuracy, sensitivity, and specificity for the classifier (SVM). Measures could only be viewed on testing multiple images.

References

1. Pezard, L., Jech, R., Ruezlicika, E.: Investigation of non-linear properties of multichannel EEG in the early stages of Parkinson's disease. *Clini Neurophysiol* **122**, 38–45 (2001)
2. Sakalauskas, A., Lukosevicius, A., Lauckaitė, K., Jegelevicius, D., Rutkauskas, S.: Automated segmentation of transcranial sonographic images in the diagnostics of parkinson's disease. Elsevier—Ultasonics, **53**(1), 111–121 (2013)

3. Rana, B., Juneja, A., Saxena, M., Gudwani, S., Senthil Kumaran, S., Agrawal, R.K., Behari, M.: Regions-of-interest based automated diagnosis of Parkinson's disease using T1-weighted MRI. Elsevier—*Expert Syst. Appl.* **42**(9), 4506–4516 (2015)
4. Salvatore, C., Ceresa, A., Castiglioni, I., Gallivanone, F., Augimeri, A., Lopez, M., Arabia, G., Morelli, M., Gilard, M.C., Quattrone, A.: Machine learning on brain MRI data for differential diagnodid of Parkinson's disease and progressive supranuclear palsy. Elsevier—*J. Neurosci. Methods* **222**, 230–237, 30 Jan 2014
5. Gonzalez, R.C., Woods, R.E.: Digital Image Processing, 3rd edn. Prentice Hall, Upper Saddle River (2008)
6. Freeborough, P.A., Fox, N.C.: MR image texture analysis applied to the diagnosis and tracking of Alzheimer's disease. *IEEE Trans. Med. Imaging* **17**(3), June 1998
7. Haralick, R.M., Shanmugam, K.: Textural features for image classification. *IEEE Trans. Syst. Man Cybern. SMC-3*(6), Nov 1973
8. Soh, L.-K., Tsatsoulis, C.: Texture analysis of SAR sea ice imagery using gray level co-occurrence matrices. *IEEE Trans. Geosci. Remote Sens.* **37**(2), March 1999
9. Clausi, D.A.: An analysis of co-occurrence texture statistics using gray level co-occurrence matrices. *Can. J. Remote Sens./J. Can. de Teledetect.* **28**(1), 45–62 (2002)
10. Sarage, G.N., Sagar Jambhorkar, S.: Enhancement of mammography images for breast cancer detection using histogram processing techniques. *IJCST* **2**(4), 2011
11. Dhanalakshmi, P., Palanivel, S., Ramalingam, V.: Classification of audio signals using SVM and RBFNN. Elsevier, pp. 6069–6075 (2009)
12. Jing, H., Bai, J., Zhang, S., Xu, B.: SVM-based audio scene classification. In: Proceeding of IEEE, pp. 131–136 (2005)
13. Yegnanarayana, B., Kishore, S.P.: AANN: an alternative to GMM for pattern recognition. *Neural Netw.* **15**, 459–469 (2002)
14. Dhanalakshmi, P.: Classification of audio for retrieval applications. Ph.D. Thesis, Annamalai University (2010)

Variational Mode Feature-Based Hyperspectral Image Classification

Nikitha Nechikkat, V. Sowmya and K.P. Soman

Abstract Hyperspectral image analysis is considered as a promising technology in the field of remote sensing over the past decade. There are various processing and analysis techniques developed that interpret and extract the maximum information from high-dimensional hyperspectral datasets. The processing techniques significantly improve the performance of standard algorithms. This paper uses variational mode decomposition (VMD) as the processing algorithm for hyperspectral data scenarios followed by classification based on sparse representation. Variational Mode Decomposition decomposes the experimental data set into few different modes of separate spectral bands, which are unknown. These modes are given as raw input to the classifier for performance analysis. Orthogonal matching pursuit (OMP), the sparsity-based algorithm is used for classification. The proposed work is experimented on the standard dataset, namely Indian pines collected by the airborne visible/infrared imaging spectrometer (AVIRIS). The classification accuracy obtained on the hyperspectral data before and after applying Variational Mode Decomposition was analyzed. The experimental result shows that the proposed work leads to an improvement in the overall accuracy from 84.82 to 89.78 %, average accuracy from 85.03 to 89.53 % while using 40 % data pixels for training.

Keywords Hyperspectral imaging · Variational mode decomposition · Classification · Orthogonal matching pursuit

N. Nechikkat (✉) · V. Sowmya · K.P. Soman
Center for Excellence in Computational Engineering and Networking,
Amrita Vishwa Vidyapeetham, Coimbatore, Tamil Nadu, India
e-mail: nikitagireesan@gmail.com

V. Sowmya
e-mail: sowmiamrita@gmail.com

K.P. Soman
e-mail: kp_soman@amrita.edu

1 Introduction

In less than 30 years, imaging spectroscopy has transformed itself from being a sparse research tool to a product available to the user community. In order to study the special properties of the hyperspectral images, standardized data processing techniques are required. The narrowness and the continuous nature of the wavelengths measured define a sensor as hyperspectral. Reflected radiations are measured in a series of narrow and continuous wavelength bands which provide abundant information regarding the subject under observation. Many image analysis algorithms are developed to exploit the extensive information contained in hyperspectral imagery. However, the computational complexity involved in processing is influenced by the high dimension of the hyperspectral image [1].

Many techniques have been proposed for image classification based on sparsity. The applications of sparse representation include hyperspectral unmixing, target detection, etc. These applications rely on the fact that signals of the same class usually lie in a low-dimensional space despite the high dimensionality [2]. All the approaches represent the image pixels as linear combinations of a small number of dictionary samples (known as atoms) chosen from an overcomplete training dictionary. The image pixels can be recovered from minimum number of samples by solving sparse regression problem under the given circumstances.

Another fact about sparse representation for hyperspectral image classification is that, the simultaneous usage of spatial and spectral information causes notable improvement in the performance of classification techniques [3].

The paper uses variational mode decomposition (VMD) method for improved results in classification accuracies of the hyperspectral data. The preprocessing method being used is the Inter Band Block correlation method which removes the noisy bands and the water absorption bands automatically using the average interband blockwise correlation coefficient measure and a thresholding strategy [4]. VMD is used to extract the features of the preprocessed hyperspectral image data. The extracted features are analyzed using sparsity-based classification method. Here, we have used OMP [5] as the classification algorithm. The classification accuracies of the standard hyperspectral dataset before and after performing Variational Mode Decomposition is compared to show the effectiveness of our proposed method.

2 Variational Mode Decomposition (VMD)

The goal of Variational Mode Decomposition is to decompose the input signal into discrete number of modes (sub-signals) that have specific sparsity properties while reproducing the input. The modes are compact around a center pulsation determined along with the decomposition (ω_k). The VMD algorithm can be summarized as

1. Using Hilbert transform, compute the associated analytical signal for each mode to obtain the unilateral frequency spectrum.
2. Mix the mode's frequency spectrum with the exponential tuned to the respective estimated center frequency, to shift the spectrum to the baseband.
3. Through the $H1$ Gaussian smoothness of the demodulated signal, estimate the bandwidth [6].

2.1 Two-Dimensional Variational Mode Decomposition

Two-Dimensional (2D) VMD is a non-recursive 2D model, which concurrently extracts the signal to various modes. [7]. The model aims at decomposing the input image into a number of 2D modes and their respective center frequencies, where the band limited modes can be used to reproduce the input image. The 2D model is analogous to its 1D counterpart, minimizing the constituent subsignals bandwidth while maintaining data fidelity. The analytic signal in 1D is achieved by suppressing the negative frequencies. In 2D, one half-plane of the frequency domain is set to zero. The analytical signal is selected relative to the vector ω_k , the center pulsation. The 2D analytic signal, $u_{AS,k}(\vec{x})$ can be defined as

$$\hat{u}_{AS,k}(\omega) = (1 + \text{sgn}(\omega \cdot \omega_k))\hat{u}_k(\omega) \quad (1)$$

which is further redefined based on the fourier properties as

$$u_{AS,k}(\vec{x}) = u_k(\vec{x}) * (\delta(\langle \vec{x}, \vec{\omega}_k \rangle) + \frac{j}{\pi \langle \vec{x}, \vec{\omega}_k \rangle})\delta(\langle \vec{x}, \vec{\omega}_k \rangle) \quad (2)$$

where $u_k(\vec{x})$ denotes each mode and $*$ denotes convolution. From this definition of 2D analytic signal, the functional to be minimized can be defined as

$$\min_{u_k, \omega_k} \left\{ \sum_k \left\| \nabla [u_{AS,k}(\vec{x}) e^{-j \langle \vec{\omega}_k, \vec{x} \rangle}] \right\|_2^2 \right\} \quad (3)$$

such that, $\sum_k u_k = f$

where f is the original image. We proceed by Alternate Direction Method of Multiplier optimization to address the reconstruction constraint. u_k and ω_k are optimized by considering the 2D analytic signal. The augmented Lagrangian included functional can be written in the fourier domain as (we are dealing with L2-norms),

$$\begin{aligned}\hat{u}_k^{n+1} = \operatorname{argmin}_{\hat{u}_k} \alpha \| j(\vec{\omega} - \vec{\omega}_k) [(1 + \operatorname{sgn}(\vec{\omega} \cdot \vec{\omega}_k)) \hat{u}_k(\vec{\omega})] \|_2^2 \\ + \left\| \hat{f}(\vec{\omega}) - \sum_k \hat{u}_k(\vec{\omega}) + \frac{\hat{\lambda}(\vec{\omega})}{2} \right\|_2^2\end{aligned}\quad (4)$$

which yields the Wiener filter result

$$\begin{aligned}\hat{u}_k^{n+1}(\vec{\omega}) = \left(\hat{f}(\vec{\omega}) - \sum_{i \neq k} \hat{u}_i(\vec{\omega}) + \frac{\hat{\lambda}(\vec{\omega})}{2} \right) \frac{1}{1 + 2\alpha |\vec{\omega} - \vec{\omega}_k|^2} \\ \forall \omega \in \Omega_k : \Omega_k = \{ \omega | \omega \cdot \vec{\omega}_k \geq 0 \}\end{aligned}\quad (5)$$

Optimizing for $\vec{\omega}$ is similar to the one-dimensional VMD case, except that here, the domains are the half-planes and hence, there are two components. The update goal is

$$\hat{\omega}^{n+1} = \operatorname{argmin}_{\vec{\omega}_k} \left\{ \alpha \| j(\vec{\omega} - \vec{\omega}_k) [1 + \operatorname{sgn}(\vec{\omega} \cdot \vec{\omega}_k) \hat{u}_k(\vec{\omega})] \|_2^2 \right\} \quad (6)$$

where α is the bandwidth constraint. The minimization is solved by letting the first variation w.r.t. $\vec{\omega}_k$ vanish. The resulting solutions are the first moments of the mode's power spectrum $|\hat{u}_k(\vec{\omega})|^2$ on the half-plane Ω_k :

$$\omega_k^{n+1} = \frac{\int_{\Omega_k} \omega_k |\hat{u}_k(\omega)|^2 d\omega}{\int_{\Omega_k} |\hat{u}_k(\omega)|^2 d\omega} \quad (7)$$

3 Orthogonal Matching Pursuit

Orthogonal matching pursuit (OMP) is one of the most basic greedy algorithms widely used because of its simplicity to implement and analyze [5]. The method seeks to update the estimate of the signal without taking into account the global structure. It exactly adds one atom to the signal at every iteration. Let b be the observation and A be the measurement matrix, start with $x = 0$, and the residual $r = Ax - b$. The hyperspectral data is D -dimensional. Every step of the algorithm consists of two parts:

1. Select the atom i that is most correlated with the residual r .
2. Update x by solving the least squares problem using only the atoms that have been selected.

3.1 OMP-Based Classification

The two stages of the classification algorithm include the computation of the sparse vector using OMP algorithm and assigning the class labels to the test pixel by finding the residue. The inputs to the classifier include the Dictionary matrix (matrix formed by concatenating randomly selected training samples from each class) A , the test pixel vector b of size $D \times 1$ and Sparsity level k . And, the output of the system is the sparse vector x_k with k non-zero entries.

The implementation steps of the algorithm can be found in the paper [8].

4 Methodology

The method proposed focuses on using VMD as a processing step before classification to improve the overall classification accuracy. The effectiveness of using VMD as a processing algorithm is illustrated using the classification accuracy obtained for the standard hyperspectral dataset before and after applying VMD. The major steps involved in the experiment are: the preprocessing using inter band block correlation (IBBC) method, the processing involving VMD and Classification. Figure 1 shows the flowchart being followed for the proposed work.

4.1 Preprocessing

Any processing performed on raw data to prepare it for another processing procedure can be defined as data preprocessing. Hyperspectral images are high-dimensional datasets which are collected by hyperspectral remote sensors simultaneously in dozens or hundreds of narrow, adjacent spectral bands. The computational complexity in processing the vast amount of data makes preprocessing an inevitable process while experimenting with hyperspectral images [9]. Here, we use inter band block correlation (IBBC) method to remove the noisy

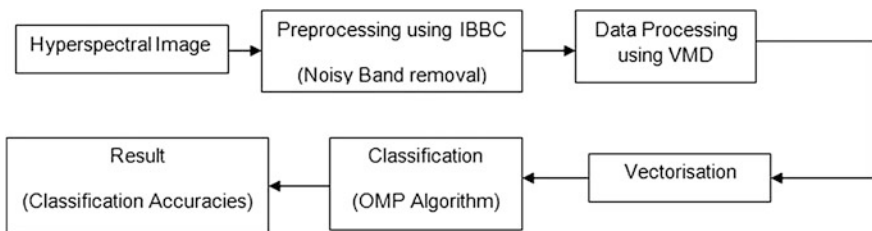


Fig. 1 Flowchart of the proposed method

bands and water bands, where the algorithm is defined based on the average inter band block wise correlation coefficient measure and a thresholding strategy [4]. The process resulted in the removal of noisy bands and water bands. The remaining bands were given as input to the variational mode feature extraction process.

4.2 Processing

The preprocessed data was given as input to the VMD. VMD adaptively decomposes the experimental data set into few different modes of separate spectral bands, which are unknown. The number of modes to which each band has to be decomposed is specified by the number K . The generated modes are concatenated to reproduce a hyperspectral cube of dimension $m \times n \times (K * b)$, where $m \times n$ is the dimension of each band and b refers to the number of bands, $(K * b)$ is the total number of bands obtained as a result of VMD. These $(K * b)$ modes are vectorized. The size of the vectorized data is $(K * b) \times (m * n)$, where $m * n$ is the total number of pixels in each band. This vectorized variational mode decomposed feature data is the input to the OMP classifier.

4.3 Classification

Identifying and classifying the constituent elements of a scene to their respective categories defines the classification process. Here, the scene is classified mainly into c classes. But, including the background pixels make it $c + 1$. OMP is one of the widely used algorithms, as it is one of the simplest algorithms to implement and analyze. Initially, pixels of the hyperspectral data under consideration are separated into training and testing samples. Sparse representation of the test sample with respect to the training sample is obtained from the dictionary matrix generated by random selection of pixels from each class.

5 Experimental Results

The experiments were conducted on the standard hyperspectral dataset acquired by the airborne visible/infrared imaging spectrometer (AVIRIS) sensor operated by the National Aeronautics and Space Administration Jet Propulsion Laboratory.

5.1 Dataset Description

The Indian pines is a scene comprising of 224 spectral bands in the wavelength range of 400–2500 nm with spatial resolution of 20 m per pixel and nominal spectral resolution of 10 nm. The image was collected by the AVIRIS instrument on June 12, 1992 over a 2×2 mile portion of Northwest Tippecanoe, Indiana. The water bands and the noisy bands in the image set are removed prior to processing. The image size is 145×145 pixels per band and the ground truth of the scene provides information about 16 mutually exclusive classes in which one represents building, five represents vegetation types, and ten corresponds to crop types. The background represented as white is also considered during classification.

5.2 Accuracy Assessment Measures

The classification accuracy can be calculated using the statistical measurements obtained from the confusion matrix (classification error matrix). Confusion matrix is generated by comparing the results obtained by classification to a reference data (ground truth data). Confusion matrix is a square matrix with size max (class labels), with the main diagonal giving the correctly classified pixels and the non-diagonal elements giving the misclassified pixels. The analysis is carried out by considering the classification accuracies before and after applying Variational mode decomposition. The statistical parameters considered are overall accuracy (OA), average accuracy (AA) and the class-wise accuracies [1].

5.3 Results and Discussion

The experiments were carried out with the proposed method on the Indian pines dataset. The effectiveness of the method was stated based on the comparison of the classification accuracies obtained before and after applying the VMD technique. To show the effectiveness of the proposed method, the preprocessed bands are feature extracted using VMD and classified by OMP. Figure 2 shows the classification accuracies of the proposed method for Indian pines dataset with 10, 20, 30, 40 % of the data used for training. Table 1 defines the classification accuracies obtained for the proposed method with 10, 20, 30, 40 % of the data used for training. From the table, it can be noted that the OA increased from 77.91 to 79.41 %, 82.15 to 85.81 %, 84.82 to 89.78 % while using the proposed method with 20, 30, 40 % of the data used for training. Also, a significant change in the AA can be observed from 79.95 to 81.71 %, 83.01 to 86.38 % and 85.03 to 89.53 % for 20 to 40 % training data respectively.

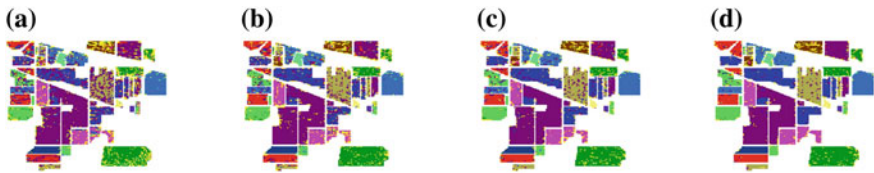


Fig. 2 Classification maps of the proposed method for Indian pines dataset. **a-d** classification results for 10, 20, 30, 40 % data used for training respectively for the proposed method

Table 1 Classification accuracies of the proposed method for Indian pines dataset with 10, 20, 30, 40 % of the data used for training before and after applying VMD

Training Pixel (Percentage)	10		20		30		40	
Class	Without feature extraction	Proposed method						
1	93.48	84.78	91.3	93.48	93.48	95.65	89.13	93.48
2	62.46	51.26	73.53	64.29	79.27	79.2	81.51	85.64
3	68.67	55.78	73.98	73.25	77.71	79.28	83.37	89.4
4	62.03	54.43	66.67	66.67	65.82	73.84	77.22	75.95
5	83.44	72.67	90.68	76.4	90.27	86.54	90.27	88.61
6	82.88	73.01	83.01	75.48	89.18	86.03	86.99	92.88
7	100	100	96.43	92.86	100	92.86	92.86	92.86
8	91.84	95.4	92.89	95.4	94.98	96.86	96.44	98.33
9	100	100	100	100	100	100	100	100
10	72.33	52.98	77.37	72.22	80.56	79.53	84.26	85.6
11	74.38	86.03	81.55	90.96	86.15	93.89	87.41	96.17
12	63.07	61.89	69.14	70.32	75.38	78.41	79.26	89.88
13	99.02	97.07	98.54	98.54	98.54	98.54	100	99.02
14	65.77	70.51	65.61	98.54	68.38	85.69	74.39	90.36
15	29.02	46.11	38.34	62.69	42.49	70.98	51.04	69.43
16	89.25	89.25	80.65	92.47	84.95	84.95	84.95	84.95
17	71.73	71.33	79.46	79.79	83.99	86.28	86.48	89.52
OA	71.39	70.32	77.91	79.41	82.15	85.81	84.82	89.78
AA	77.02	74.27	79.95	81.71	83.01	86.38	85.03	89.53

6 Conclusion

The experimental results state that the Variational Mode Decomposition is an effective method that acts as a good processing technique for hyperspectral images. The variational Mode Decomposition acts as a feature extractor which aids in efficiency of classification.

References

1. Kavitha, B., Sowmya, V., Soman, K.: Spatial preprocessing for improved sparsity based hyperspectral image classification. In: International Journal of Engineering Research and Technology, vol. 1, no. 5. 1em plus 0.5em minus 0.4em, ESRSA Publications (2012)
2. Chen, Y., Nasrabadi, N.M., Tran, T.D.: Hyperspectral image classification using dictionary-based sparse representation. *IEEE Trans. Geosci. Remote Sens.* **49**(10), 3973–3985 (2011)
3. Song, B., Li, J., Dalla Mura, M., Li, P., Plaza, A., Bioucas-Dias, J.M., Atli Benediktsson, J., Chanussot, J.: Remotely sensed image classification using sparse representations of morphological attribute profiles. *IEEE Trans. Geosci. Remote Sens.* **52**(8), 5122–5136 (2014)
4. Bhushan, D.B., Sowmya, V., Manikandan, M.S., Soman, K.: An effective pre-processing algorithm for detecting noisy spectral bands in hyperspectral imagery. In: International Symposium on Ocean Electronics (SYMPOL), pp. 34–39. 1em plus 0.5em minus 0.4em, IEEE, 2011
5. Cai, T.T., Wang, L.: Orthogonal matching pursuit for sparse signal recovery with noise. *IEEE Trans. Inf. Theory* **57**(7), 4680–4688 (2011)
6. Dragomiretskiy, K., Zosso, D.: Variational mode decomposition. *IEEE Trans. Signal Process.* **62**(3), 531–544 (2014)
7. Dragomiretskiy, K., Zosso, D.: Two-dimensional variational mode decomposition. In: Energy Minimization Methods in Computer Vision and Pattern Recognition, pp. 197–208. 1em plus 0.5em minus 0.4em, Springer (2015)
8. Suchithra, M., Sukanya, P., Prabha, P., Sikha, O., Sowmya, V., Soman, K.: An experimental study on application of orthogonal matching pursuit algorithm for image denoising. In: International Multi-Conference on Automation, Computing, Communication, Control and Compressed Sensing (iMac4s), pp. 729–736. 1em plus 0.5em minus 0.4em, IEEE (2013)
9. Vidal, M., Amigo, J.M.: Pre-processing of hyperspectral images essential steps before image analysis. *Chemometr. Intell. Lab. Syst.* **117**, 138–148 (2012)

Implementation of Fuzzy-Based Robotic Path Planning

Divya Davis and P. Supriya

Abstract Path planning is one of the prime robot problems which essentially call for smooth navigation of the robot through an optimal path by avoiding barriers of any kind. In this work, Fuzzy Logic approaches are attempted and compared for obstacle avoidance through an unknown environment. In this approach, it considers inputs from sensors placed on the robot, which include the distance from nearest obstacle towards left, front and right besides the information on the angular variation from the target. The fuzzy rules are employed to control the velocity of left and right wheels of the robot. A defuzzification procedure is applied to the left and right velocity wheels, and results are compared with the defuzzified values obtained from Sugeno-weighted average method. The second approach ignores the four inputs and follows the same fuzzy technique. A comparison of the two approaches indicates that the first method is more precise. Finally path planning using Sugeno-based fuzzy logic controller has implemented in I robot Create (mobile robot) by interfacing with Arduino Uno.

Keywords Fuzzy logic controller · Path planning · Obstacle avoidance · Mobile robot · Fuzzy rule base

1 Introduction

Robotics is a versatile domain with various areas open. Robotic path planning and obstacle avoidance of various techniques have stirred great interest in the research community. The optimal robotic path planning challenge is defined as the design of a collision-free optimal path. Literature has several heuristic-based path planning

D. Davis (✉) · P. Supriya

Amrita Vishwa Vidyapeetham, Amrita School of Engineering, Coimbatore, India
e-mail: martha.divya@gmail.com

P. Supriya

e-mail: p_supriya@cb.amrita.edu

© Springer India 2016

S.C. Satapathy et al. (eds.), *Proceedings of the Second International Conference on Computer and Communication Technologies, Advances in Intelligent Systems and Computing* 380, DOI 10.1007/978-81-322-2523-2_36

375

algorithms which can be classified mainly as Potential Field methods and soft computing methods. The soft computing methods generally considered are neural networks, genetic algorithms and fuzzy logic. In this work, two fuzzy logic approaches and their implication are discussed in detail. The fuzzy-based robotic path planning algorithm is based on the assumption that the location of the target is known in advance and also the obstacles during the traversal are known apriori [1–9].

Fuzzy logic basics are studied [1]. Fuzzy set theory and fuzzy logic are the significant tools for managing ambiguous, ill defined data in rational decision-making systems [1]. A fuzzy logic-based control system when applied to mobile robot it promotes collision-free navigation of mobile robot to be easily modelled using linguistic terminology with ease. Intelligent decisions can be made in real-time, thus allowing for uninterrupted robot motion. This is due to the relative computational simplicity of fuzzy rule-based systems [1]. Fuzzy logic runs for the number of intermediate nodes along the path. In [1] four inputs of fuzzy are discussed to determine the path: one of them is the angle difference to the target θ , and the other three are distance to the left, front and right obstacle. The angle difference to target makes the connection between the current position and the final position by considering the direction towards the target. In each iteration angle difference to the target and distance to the nearest obstacle in three sides is first normalized in the interval [0, 1], and then the fuzzy membership is determined to different fuzzy functions. In this case, in each location of workplace lattice space, whatever the angle difference between the nodes to the target is less, and node has been more distant from the nearest obstacle. In this more fuzzy, possibility for selection as the next node is in the path, it means that node has higher-priority coefficient achieves compared to other nodes [2].

An intelligent choice employed in real-time facilitates uninterrupted motion of robot. In many research papers, this method results in planning the path of mobile robot along with obstacle avoidance at unknown environments in an optimized way. Due to its way of inferring the range as linguistic variables like slow, l_slow (little slow) and reasoning with an uncertainty, this approach which is based on fuzzy has become the best to implement in controllers. Different movements of mobile robot in dynamic environment achieved using fuzzy are through developing certain rules with all combination of input linguistic variables. The number of rules in this rule table increases with number of inputs in fuzzy logic controller (FLC). In literature, many algorithms were proposed based on obstacle avoidance and mobile robot path planning [3].

Behaviour-based architecture was explained in some papers. This framework was based on hierarchical behaviour which was proposed in various systems. The approach helps in systematic designing of FLC and also aid the mobile robot to respond in a well-organized way at dynamic environment. The ultrasonic sensor is used for localizing and measuring the distance to left, front and right obstacle. Angular velocities of both wheels are fuzzified and defuzzified. The technique employed for fuzzification is Singleton and that for defuzzification is Mamdani and Sugeno method [4]. Another method for path planning mobile robot using fuzzy

logic is Distance Transform Method [3]. Based on environmental variations a behaviour-based control system can develop a controlled system for a mobile robot or a robot manipulator. Brooks proposed an appealing method known as the subsumption architecture. The control system constructed using subsumption architecture is distributed concurrently to various elemental behaviours. The results from such behaviours are fused. Section two of the paper describes the fuzzy formulation for path planning. The architecture and modelling parameters of the robot is discussed in section three. The result of the two approaches is studied in section four. Section five brings out the conclusions of the work and future scope of robotic path planning. Initially FLC was designed using the Mamdani. However, implementation of Mamdani-based FLC into an embedded platform was cumbersome and computationally expensive. So FLC implementation was carried by Sugeno-weighted average method in I robot create using arduino uno.

2 Fuzzy Formulation

The traditional fuzzy logic system mainly consists of four steps—fuzzification, knowledge base, fuzzy reasoning and defuzzification. The fuzzification is the first step that transforms the scalar input values into linguistic terms named as fuzzy variables. The next step is the knowledge base which mostly aims at storing applicable data and rules for control. The most significant step is fuzzy reasoning that generates fuzzy results by the combination of the knowledge base and fuzzy rules table. The final step is defuzzification which converts fuzzy-based linguistic terms to scalar output values, thereby controlling the wheel velocity of the robot. The basic block representation of a FLC used for robotic path planning is shown in Fig. 1.

The ultrasonic sensors are placed at left, front and right sides of robot. The inputs for the first FLC are distance of obstacles measured by the respective sensors and the angle between orientation of the robot and destination. In the first FLC, the output variables are velocities of left and right wheels. The inputs from sensors are fuzzified and made all possible rule combinations and defuzzified using weighted average method. This is implemented using Sugeno. Based on the left and right wheel velocity, angle difference to target is calculated and again fed back to FLC. The FLC representation for the problem is portrayed in Fig. 2.

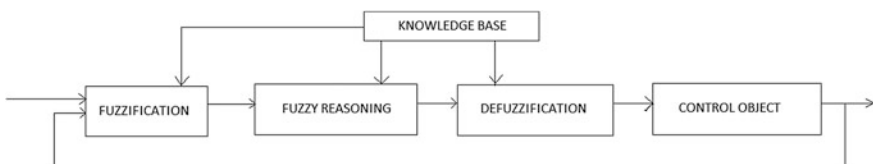


Fig. 1 Fuzzy logic controller



Fig. 2 Fuzzy logic controller

The basic block diagram of FLC comprises of distances to left obstacle, right obstacle, front obstacle and angle difference to target. Fuzzy rules are framed by employing all the possibilities of the problem and expertise of the researcher. The control rules are persuaded by observable knowledge. Rule base is a collection of multiple fuzzy relations between input and output linguistic terms, which are obtained based on observation, experimentation and experience of operator. Moreover, the real number of fuzzy rules should be selected based on various parameters like accuracy and computation speed. The traditional principle is on the completeness of the premises. The second FLC employs first three inputs and has the same output variables. Based on these inputs, FLC will automatically control left and right velocity of wheel.

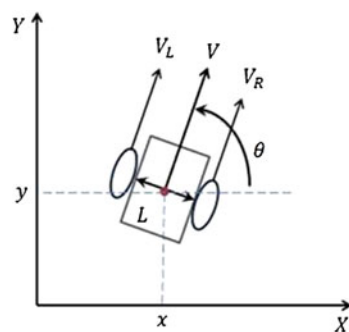
3 Mobile Robotic System

The kinematics model of mobile robot system as same as specified in [2]. The robotic architecture with linear velocities V_L and V_R is shown in Fig. 3.

The left and right wheel angular velocities are chosen as ω_L and ω_R , respectively. Linear velocities for the left and right wheels are V_L and V_R , respectively. The relationship V_L , V_R , ω_L and ω_R is as follows. The relationship between left and right wheels of angular velocity and linear velocity is based on the fundamental relation between the two velocities [2]:

$$V_L = r \omega_L \quad \text{and} \quad V_R = r \omega_R \quad (1)$$

Fig. 3 Mobile robotic architecture



In the two Eq. (1), r is radius of the wheel and the linear velocity of the mobile robot is V :

$$V = (V_R + V_L)/2 \quad (2)$$

$$\omega = (V_R - V_L)/L = (r\omega_L - r\omega_R)/L \quad (3)$$

The dynamic model for the mobile robot relates linear velocity V , angular velocity ω and the orientation θ represented in matrix form as in (4):

$$\begin{bmatrix} x' \\ y' \\ \theta' \end{bmatrix} = \begin{bmatrix} \cos \theta & 0 \\ \sin \theta & 0 \\ 0 & 1 \end{bmatrix} \cdot \begin{bmatrix} v \\ \omega \end{bmatrix} \quad (4)$$

Hence it becomes apparent that specified in Eq. (5):

$$x' = v \cos \theta, y' = v \sin \theta \text{ and } \theta' = \omega \quad (5)$$

4 Result Analysis

4.1 Simulation Results

Path planning of mobile robot system is considered with several fuzzy rules. The fuzzy form for path planning is carried out for path planning is shown in Fig. 4.

(A) Method 1:

Fuzzy rules for the mobile robot are formulated considering 4 inputs and 2 outputs. Inputs and outputs considered in this method are mentioned in Sect. 2 and in Fig. 2. Each input and output is graphically represented in Fuzzy logic tool box to form FLC with membership functions of triangular and trapezoidal in shape as shown in Fig. 4. Each membership functions are classified with different linguistic variables.

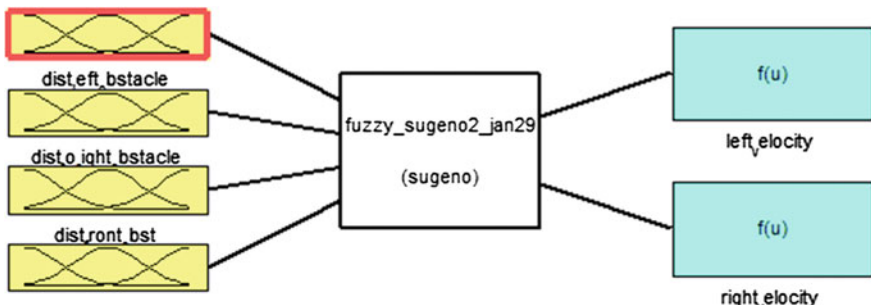


Fig. 4 FLC controller

Linguistic variables chose for distance to left obstacle, distance to right obstacle and distance to front obstacle are near and far. The variable near has maximum membership value (mv) defined between 0:30, between 30:120 the membership value decreases linearly and between 120:150 the mv is 0. Similarly the variable far has maximum membership value (mv) defined between 120:150, between 30:120 the membership value increases linearly and between 0:30 the mv is 0. The values of near and far define the membership function as trapezoidal. The input angle difference to target has three linguistic variable left, front and right. Variable left has maximum membership value between $-90:-30$; membership values are linearly decreasing between $-30:0$ and zero membership value between $0:90$. Similarly right has maximum membership value between $0:90$; membership values are linearly increasing between $-30:0$ and zero membership value between $0:-90$. Linguistic variable front has linearly increasing and decreasing values between $-30:0$ and $0:30$. So left and right membership took as trapezoidal and front as triangular. Output velocities of left and right wheels have five linguistic variables which are slow, l_slow, mid, l_fast, fast. Variable slow, l_slow, mid, l_fast and fast [2] have maximum membership function constant of about 100, 200, 300, 400 and 500, respectively, according to Sugeno-based-weighted average method. Here as per these ranges, slow and fast have trapezoidal membership, and rest all have triangular membership (Fig. 5).

Considering all possible combinations of inputs fuzzy rule base comprises of 24 rules. Estimating the defuzzified output for about 4 rules and comparing the results both manually and in tool box. Basic rules taken here are: (1) If dist_left is near and dist_front is far and dist_right is near and angle_target is front, then right_velocity is l_fast and left_velocity is l_fast. (2) If dist_left is near and dist_front is near and dist_right is near and angle_target is left, then right_velocity is l_slow and left_velocity is slow. (3) If dist_left is far and dist_front is far and dist_right is near and angle_target is front, then right_velocity is mid and left_velocity is l_slow. (4) If dist_left is far and dist_front is far and dist_right is far and angle_target is left, then right_velocity is fast and left_velocity is l_fast. In fuzzy tool box for inputs of

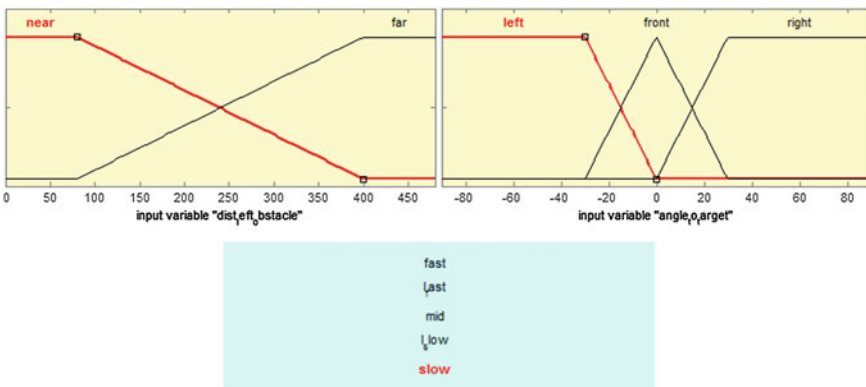


Fig. 5 Fuzzy inputs and outputs

about 100, 100, 100 and 0 outputs obtained are 359 and 344 mm/s. This is compared with mathematical calculated value by weighted average of defuzzification using Sugeno fuzzy inference system.

$$x^* = \frac{\sum_{i=1}^n m^i w_i}{\sum_{i=1}^n m^i} \quad (6)$$

Using the above formula, mathematically calculated the same values for outputs for corresponding inputs which are 350 and 340 mm/s.

(B) Method 2:

This same experimental approach as done in first method is repeated excluding the input angle difference to target then it is fuzzified and defuzzified the output. But in this case for same inputs defuzzified outputs obtained are 336 and 331 mm/s for left and right velocity of wheel, respectively. In path planning of mobile robot first approach give more accurate response than second approach.

4.2 Hardware Results

Particular fuzzy logic is written using arduino 1.5.6 IDE and implemented in arduino uno board. The Arduino Uno is a microcontroller board running on the ATmega328 which operates in 5 V. It comprises of fourteen digital input/output pins of which six can also be configured as PWM outputs, six analogue input pins and a 16 MHz crystal oscillator. It also has a power jack, an ICSP header, USB connection and a reset button. This includes a flash memory of about 32 kB, SRAM of 2 kB and EEPROM of 1 kB. FLC controls the output velocity of left and right wheels based on inputs which are distance to left, front and right obstacle (Fig. 6).



Fig. 6 I robot create performance when obstacle in *left* and *front*

Distance is calculated from ultrasonic sensor of pwm o/p by measuring the duration of pwm pulse multiplied with the scale. This arduino is interfaced with the I robot create. I robot create is a mobile robot developed by MIT university which is mainly controlled using ATmega168. In order to customize movement, I create is interfaced with arduino and it send serially open interface commands to I create using cargo bay connector with a baud rate of 57,600 bps. Three ultrasonic sensors are interfaced with arduino board to calculate distance to front, left and right obstacle. The figure below shows the movement of I robot create when obstacle in left and front.

5 Conclusions and Future Scope

The robotic path planning with known target and known obstacle is articulated using two Sugeno fuzzy-based methods. The various fuzzy stages like suitable identification of input and output parameters along with linking them to the fuzzy-based variables are carried out. The relation between variables is carried out. The relation between the input, output and fuzzy variables is framed using fuzzy rules. The output is finally transformed to output real-time values using defuzzification. The output parameters are compared with weighted average-based defuzzified mathematical expression. The first method is found to be more accurate as it uses more inputs which enable to infer that high number of inputs in fuzzy results in better accuracy. With encouraging results in the first method of fuzzy-based path planning, this has implemented in I Robot create interfaced with three ultrasonic sensors.

References

1. Purian, F.K., Sadeghian, E.: Path Planning Of Mobile Robots Via Fuzzy Logic In Unknown Dynamic Environments With Different Complexities, pp. 528–535. JBASR. Text Road Publication (2013)
2. Li, X., Choi, B.-J.: Design of obstacle avoidance system for mobile robot using fuzzy logic systems. IJSH 7(3), (2013)
3. Tunstel, E., Lippincott, T., Jamshidi, M.: Introduction to fuzzy logic control with application to mobile robotics. In: NASA Center for Autonomous Control Engineering
4. Zoumpinos, G.T., Aspragathos, N.A.: Fuzzy logic path planning for the robotic placement of fabrics on a work table. In: Robotics and Computer-Integrated Manufacturing, pp. 174–186. Elsevier (2008)
5. Gupta, I., Riordan, D.: Distance Transform Path Planning for Mobile Robots Using Fuzzy Logic. Dalhousie University, Halifax, Canada
6. Hung, L.-C., Chung, H.-Y.: Design of Hierarchical Fuzzy Logic Control for Mobile Robot System. Department of Electrical Engineering National Central University
7. Jin, S., Choi, B.-J.: Fuzzy Logic System Based Obstacle Avoidance for a Mobile Robot. FGIT-CA/CES3 (2011)

8. Jin, T., Choi, B.-J.: Obstacle avoidance of mobile robot based on behavior hierarchy by fuzzy logic. *Int. J. Fuzzy Logic Intell. Syst.* **12**(3), 245–249 (2012)
9. Rusu, C.G., Birou, I.T.: Obstacle avoidance fuzzy system for mobile robot with IR sensors. In: 10th International Conference, 27–29 May 2010

Texture Segmentation by a New Variant of Local Binary Pattern

Mosiganti Joseph Prakash and J.M. Kezia

Abstract This paper highlights the local binary pattern (LBP) method in the unsupervised texture segmentation task. It has been made into a really dominant measure of image texture, showing outstanding results in terms of computational complexity and accuracy. The LBP operator is a theoretically simple yet very efficient approach for texture analysis. The LBP concept is slightly modified, i.e., instead of considering the center pixel value for generation of binary values, the present paper utilized average of all the eight neighboring pixels of the center pixel. The binary code generated is separated into “Diamond-LBP Code (DLBPC)” and “Corner LBP code (CLBPC).” The proposed new variant local binary pattern (NVLBP) segmentation approach is simple, rotationally invariant and easy to understand. This method also resulted in good segmentation which is noticed from the entropy, standard deviation, contrast, and discrepancy values.

Keywords LBP · Texture · Segmentation · Rotationally invariant

1 Introduction

One of the most popular structural approaches used to measure the textural information of images is the local binary pattern (LBP). LBP exhibits local properties of textures strongly. The LBP is known for its low sensitivity to changes in illum-

M.J. Prakash (✉)

CSE Department, Stanley College of Engineering and Technology for Women,
Affiliated to Osmania University, Abids Chapel Road, Near L B Stadium,
Hyderabad 500001, Telangana, India
e-mail: mjoseph7@gmail.com

J.M. Kezia

ECE Department, Stanley College of Engineering & Technology for women,
Affiliated to Osmania University, Abids Chapel Road, Near L B Stadium,
Hyderabad 500001, Telangana, India
e-mail: sakakezia1981@gmail.com

nation and computational complexity. LBP can describe local texture properties in an efficient and significant manner. This process can be easily extended to the entire image.

Recently, many research scholars exhaustively applied LBP on various applications and they derived various variants of LBP. Some of them are applied for face detection [1, 2], face recognition [3–6], face authentication [7, 8], facial expression recognition [9], age recognition [10], image retrieval [11], object detection [12], segmentation [13–17], etc. In most of the cases, LBP is evaluated by computing the differences between the gray value of a central pixel ‘ x ’ and the gray values of its ‘ p ’ neighboring pixels on a circle or radius ‘ R ’ around ‘ x ’. Based on this, a binary value one is allocated to the neighboring pixel if the difference is greater than or equal to zero otherwise a zero is allocated.

The present paper derived a “New variant of LBP-based segmentation (NVLBPS)” that generates two strong patterns that influence the LBP. The proposed approach considers two sets of texture elements each with four pixels on a 3×3 LBP grid. These two sets are named as “Corner and Diamond-LBP (C&DLBP).” LBP codes are evaluated separately on these two C&DLBP’s. Based on C&DLBP’s rotationally invariant texture segmentation is evaluated.

2 Proposed NVLBP Segmentation Approach

A 3×3 circular neighborhood consists of a set of nine elements and can be represented as $P = \{p_c, p_0, p_1, \dots, p_7\}$, where p_c represents the gray level value of the central pixel and $P_i (0 \leq i \leq 7)$ represents the gray level values of the peripheral pixels. Each 3×3 circular neighborhood can be characterized by a set of binary values.

The proposed “New variant of LBP (NVLBP)” segmentation approach considered the average value of nine pixels of a 3×3 neighborhood as Δp_i of Eq. (1). This average value is compared with neighboring pixels to convert them into binary values. The present approach considered average value instead of central pixel value because it consists of strong and accurate information of the 3×3 subimage (Fig. 1).

$$b_i = \begin{cases} 0 & \Delta p_i \geq p_i \\ 1 & \Delta p_i < p_i \end{cases} \quad (1)$$

where $\Delta P_i = \frac{(\sum_{i=0}^7 P_i) + P_c}{9}$, $\Delta P_i = 160$

For each 3×3 neighborhood, a unique LBP code is derived from the Eq. (2).

$$\text{LBP}_{P,R} = \sum_{i=0}^7 b_i \times 2^i \quad (2)$$

(a)	(b)
174	254
194	125
124	148
124	122
124	161

Fig. 1 **a** 3×3 Subimage. **b** Formation of LBP using average of 9 pixels

The above LBP code generates a single integer code $LBP \in [0, 255]$.

The proposed NVLBP new variant of LBP, i.e., NVLBP contains the texture information using eight neighboring pixels around the central pixel. The level of this information depends on ordering of the neighboring pixels. In the proposed NVLBP approach, texture segmentation is carried out by separating the neighborhood pixels of 3×3 subimage into diamond and corner pixels. The corner pixels are not connected pixels. The present paper proposed a new method of evaluating LBP code called “Corner LBP code (CLBPC)” and “Diamond-LBP Code (DLBPC)”.

The texture information is obtained by the proposed CLBPC and DLBPC from the mathematical model representing two groups of four-texture elements are shown in Figs. 2 and 3. A 3×3 grid can have four such patterns of DLBPC and CLBPC as shown in Figs. 2 and 3, respectively.

Each texture element in the two groups has one of the two possible values {0, 1} as given in Eqs. (3) and (4):

$$DLBPC = \sum_{d=0}^3 b_d * 2^d \quad (3)$$

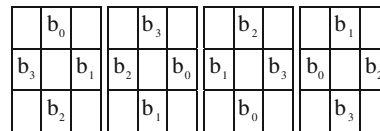


Fig. 2 Representation of four-patterns of DLBPC

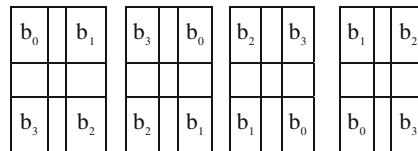


Fig. 3 Representation of four-patterns of CLBPC

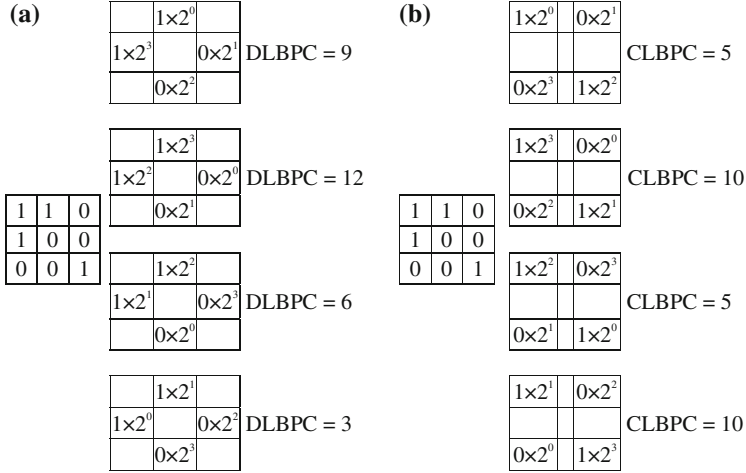


Fig. 4 **a** Four possible values of DLBPC. **b** Four possible values of CLBPC

$$\text{CLBPC} = \sum_{c=0}^3 b_c * 2^c \quad (4)$$

The b_d and b_c are the i th element of DLBPC and CLBPC, respectively. The entire process of transforming an image neighborhood into DLBPC and CLBPC is shown in Fig. 4. The elements in the DLBPC and CLBPC may be ordered differently. The values of DLBPC and CLBPC vary depending on the position of elements which can be labeled using the Eqs. (3) and (4).

For a fine and rotationally invariant segmentation, the proposed NVLBP segmentation evaluated the minimum value from each of the four possible values of DLBPC and CLBPC as shown in Figs. 2 and 3. In the above Figs. 2 and 3, the minimum DLBPC is three and CLBPC is five, respectively. Then the absolute difference between these two minima of DLBPC and CLBPC is evaluated. In the above figure, difference is two. This difference, i.e., value two is substituted for central pixel. This process is repeated on an entire image in a convolution manner. This results a fine and accurate segmentation.

3 Results and Discussions

The proposed NVLBP segmentation approach is experimented on 50 Brodatz texture images [18], 50 Vistex images [19], and smoke images [20]. Some of the results are shown in Fig. 5. The results clearly indicate fine segmentation.

The proposed NVLBP segmentation algorithm is compared with the other well-known methods of segmentation Yu-hua Chai [21], Busireddy [22]. The final

Original Input Images	Output of Existing Methods Corresponding to Input Image		Output of Proposed Methods NVLBP Corresponding to Input Image
	Yu-hua Chai[21]	Busireddy Method[22]	
Bark-07			
Bark-05			
D72			
D69			
Smoke-1041			
Smoke-1037			
(a)	(b)	(c)	(d)

Fig. 5 **a** Original images. **b** Output of Yu [21]. **c** Output of Busireddy [22]. **d** Proposed NVLBP segmentation method output

Table 1 Performance comparison of the proposed NVLBPS algorithm on 150 images

Segmentation metrics	Average values of proposed method	Average values of existing methods	
		Busireddy	Yu-hua
Entropy	1.3288	1.3175	0.4446
Standard deviation	0.4986	1.8336	409.1075
Contrast	0.8437	1.4312	254.9683
Discrepancy	-8.29E+03	-1.27E+05	-3.2E+07

outputs of existing methods [21], [22] and the proposed NVLBP segmentation algorithms are shown in Fig. 5b, c, and d, respectively. The proposed algorithm is able to extract the uniform regions of the image efficiently. Table 1 shows the values of entropy, standard deviation, contrast, and discrepancy of the proposed algorithm and the other existing two segmentation schemes [21, 22]. The segmentation metric values of Table 1 clearly indicate a good segmentation detail of the proposed method over the other two existing methods. The average values of segmentation metrics for the proposed method, Yu et al. [21] and Busireddy [22] are shown in Table 1. The average entropy value of the proposed algorithm is 1.32 which is higher when compared to other two methods. The value 1.32 indicates accurate segmentation without over or under segmentations. The low standard deviation value indicates good segmentation with high uniformity. The low value of internal region contrast indicates high uniformity. The high value of discrepancy indicates fine segmentation. The results of the proposed algorithm indicate fine & accurate segmentation. The comparison segmentation metrics charts for proposed algorithm and existing methods are shown in Figs. 6 and 7.

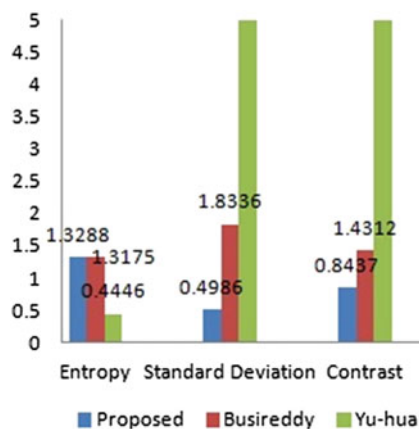
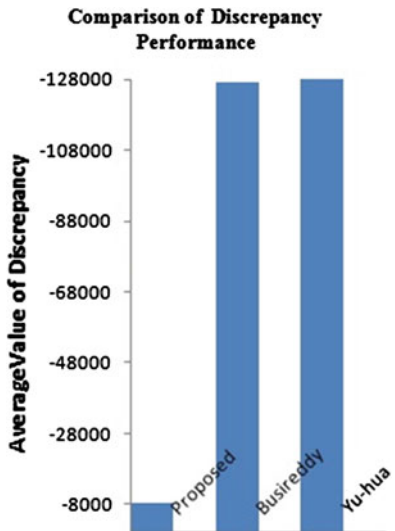
Fig. 6 Entropy, standard deviation, contrast comparison of proposed, and existing methods

Fig. 7 Discrepancy comparison of proposed method and existing methods



4 Conclusion

The present paper addressed the problem of rotational invariant texture segmentation by proposing a NVLBP. This method drastically reduces the LBP code from 256 to 16. This reduction is useful for formation of a GLCM or any type of real-time applications, by which a good classification can be obtained by reducing computational complexity. Further, by dividing the LBP code into two it has shown a new path for segmentation with local properties.

References

1. Jin, H., Liu, Q., Lu, H., Tong, X.: Face detection using improved LBP under Bayesian framework. In: Proceeding of Third International Conference on Image and Graphics, pp. 306–309 (2004)
2. Zhang, L., Chu, R., Xiang, S., Liao, S., Li, S.Z.: Face detection based on multi-block LBP representation. In: The Second International Conference on Biometrics, pp. 11–18 (2007)
3. Ahonen, T., Hadid, A., Pietikainen, M.: Face description with local binary patterns: application to face recognition. *IEEE Trans. Pattern Anal. Mach. Intell.* **28**(12), 2037–2041 (2006)
4. Ahonen, T., Hadid, A., Pietikainen, M.: Face recognition with local binary patterns. In: The Eighth European Conference on Computer Vision, pp. 469–481 (2004)
5. Lahdenoja, O., Laiho, M., Paasio, A.: Reducing the feature vector length in local binary pattern based face recognition. In: IEEE International Conference on Image Processing, pp. 11–14 (2005)

6. Liao, S., Zhu, X., Lei, Z., Zhang, L., Li, S.Z.: Learning multi-scale block local binary patterns for face recognition. In: The Second International Conference on Biometrics, pp. 828–837 (2007)
7. Heusch, G., Rodriguez, Y., Marcel, S.: Local binary patterns as an image preprocessing for face authentication. In: The Seventh International Conference on Automatic Face and Gesture Recognition, pp. 9–14 (2006)
8. Rodriguez, Y., Marcel, S.: Face authentication using adapted local binary pattern histograms. In: The 10th European Conference on Computer Vision, pp. 321–332 (2006)
9. Shan, C., Gong, S., McOwan, P.W.: Facial expression recognition based on local binary patterns: a comprehensive study. *Image Vis. Comput.* **27**(6), 803–816 (2009)
10. Kellokumpu, V., Zhao, G., Li, C., Pietikainen, M.: Dynamic texture based gait recognition, In: Lecture Notes in Computer Science, vol. 5558, pp. 1000–1009. Springer, Berlin (2009)
11. Takala, V., Ahonen, T., Pietikainen, M.: Block-based methods for image retrieval using local binary patterns. In: Proceeding of the 14th Scandinavian Conference on Image Analysis, pp. 882–891 (2005)
12. Heikkil, M., Pietikainen, M., Heikkil, J.: A texture-based method for detecting moving objects. In: Proceeding of the 15th British Machine Vision Conference, 2004, pp. 187–196. Science, pp. 1000–1009 (2009)
13. Joseph, P., Vijaya Kumar, V.: A new texture based segmentation method to extract object from background in global. *J. Comput. Sci. Technol. Graph. Vis.* **12**(15), 47–53 (2012)
14. Joseph, P., Vijaya Kumar, V., VinayaBabu, A.: Morphology based technique for texture enhancement and segmentation. *Int. J. Sig. Image Process.* **4**(1), 49–56 (2013)
15. Joseph, P., Kezia, S., Santi Prabha, I., Vijaya Kumar, V.: IEEE Conference on Innovative Pattern Based Morphological Method for Texture Segmentation, Chennai, June 4–6, pp. 11–15 (2013)
16. Joseph, P., Kezia, S., Santi Prabha, I., Vijaya Kumar, V.: A new approach for texture segmentation using gray level textons. *Int. J. Sig. Image Process.* **6**(3), 81–89 (2013)
17. Joseph, P., Kezia, S., SantiPrabha, I., Vijaya Kumar, V.: A novel approach for texture segmentation based on rotationally invariant patterns. *Int. J. Comput. Eng. Sci.* **2**(2), 1–8 (2013)
18. Brodatz database: <http://www.ux.uis.no/~tranden/brodatz.html>
19. VisTex database: <http://vismod.media.mit.edu/pub/VisTex/VisTex.tar.gz>
20. Smoke database: <http://minus.com/Mqe0ynq33>
21. Yu, C.Y., Zhang, Y.M., Fang, J., Wang, J.J.: Texture analysis of smoke for real time fire detection. In: Second International Workshop on Computer Science and Engineering, pp. 511–515 (2009)
22. Ramana Reddy, B.V., Mani, M.R., Vijaya Kumar, V.: A random set view of texture segmentation. *JSIP* **1**(1), 24–30 (2010)

Integrating Writing Direction and Handwriting Letter Recognition in Touch-Enabled Devices

Akshay Jayakumar, Ganga S. Babu, Raghu Raman
and Prema Nedungadi

Abstract Optical character recognition (OCR) transforms printed text to editable format and digital writing on smart devices. Learning to write programs has made learners trace an alphabet to learn the flow of writing and OCR by itself is less effective as it ignores the directional flow of writing and only focuses on the final image. Our research designed a unique android-based multilingual game-like writing app that enhances the writing experience. A key focus of the research was to compare and identify character recognition algorithms that are effective on low-cost android tablets with limited processing capabilities. We integrate a quadrant-based direction checking system with artificial neural networks and compare it to the existing systems. Our solution has the dual advantage of evaluating the writing direction and significantly increasing the accuracy compared to the existing systems. This program is used as the literacy tool in many villages in rural India.

Keywords Character recognition · Online recognition · Offline recognition · Neural networks · Quadrant-based direction checking · Alphabet rules · Self-organizing map · ANN · OCR

A. Jayakumar (✉) · G.S. Babu · R. Raman · P. Nedungadi
Amrita CREATE, Amrita University, Kollam, Kerala, India
e-mail: akshayjayakumar@am.amrita.edu

G.S. Babu
e-mail: gangasbabu@am.amrita.edu

R. Raman
e-mail: raghu@amrita.edu

P. Nedungadi
e-mail: prema@amrita.edu

1 Introduction

The pressing need of dealing with primary children and adult literacy is to offer new methodologies to effectively learn to read and write. In rural India, with limited access to computers, mobile devices can offer motivation, student engagement, and learning outcomes similar to personal computers [1]. Learning to write an alphabet correctly includes reproducing the correct image and adhering to the direction styles followed by a particular language. In our previous work, we presented a case study that showed the effectiveness of the tablet-based writing program in increasing the motivation and significantly reducing the learning time to master the alphabet. This program is being used at a tribal learning center [2].

The majority of existing programs for learning to write evaluate the alphabet based on specific hidden points. A few others use the OCR algorithm to recognize the alphabet drawn on the screen, though there is a need for additional research in Indian languages [3]. Offline character recognition is a technique used to identify a written character where parameters such as strokes, directions, and so on are no longer available. Online character recognition samples the data and attempts to recognize it as the character is written and the order of strokes is readily available [4]. The complexity associated with the recognition varies based on the language, the number of characters/alphabets, and the differences in the alphabet characteristics that makes up each one unique from the others. For example, an alphabet's image might be a subset of another one or it might share similar features. These can impact the performance of the handwriting recognition.

Character recognition typically uses feature-based or template-based methods [5, 6]. The feature-based methods in character recognition include: hidden Markov models [7], support vector machines [8, 9], and artificial neural networks (ANN) [9, 10].

In this paper, we discuss our proposed solution, which is unique in its ability to consider both the directional flow of writing and the shape of the character irrespective of the area of the screen. Our initial version was a great success in terms of motivating the learners and increasing the accuracy of evaluation.

2 Proposed System

Aksharamala provides an interactive alphabet learning and real-time evaluation environment that is designed to make the language learning experience engaging and effective. This application teaches how to trace and write alphabets and makes it fun by showing attractive animations, audio, and further improves its effectiveness as a learning tool with real-time evaluation.

A learner can write with a stylus or use the finger, and our online character recognition interprets and translates the digital data such as finger-strokes or stylus movements into digital text.

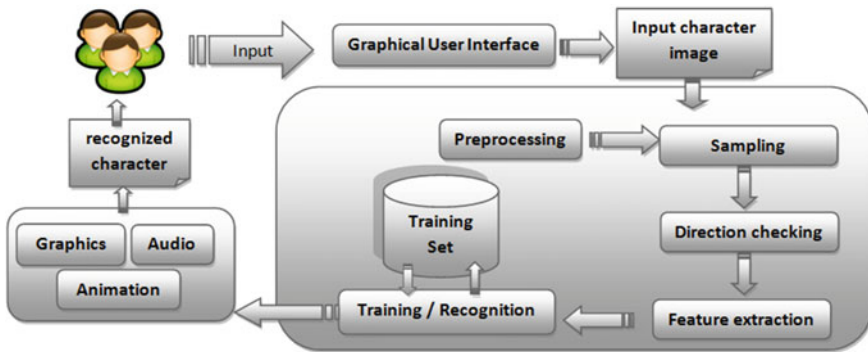


Fig. 1 Architecture of Aksharamala

The proposed system mitigates the weaknesses of other existing writing applications. An existing character recognition algorithm, neural network is used in the proposed system. As direction checking was a primary goal of the proposed system, neural network alone is insufficient as it recognizes alphabets without taking the direction parameters into account. Further research to identify the direction of writing paved the way for the new quadrant-based direction checking system that enabled Aksharamala to facilitate direction checks and significantly improve the recognition accuracy.

The overall functioning of Aksharamala is illustrated in Fig. 1. Prior to writing or tracing the alphabet, a short audio clip and animation aids the learner. Recognition of the drawn alphabet commences when the user has completed the drawing. The letter is extracted as an image and further computational processing such as sampling, preprocessing of the extracted image, direction checking, feature extraction, and recognition is done to identify the alphabet. All these processes are optimized to deliver performance in low processing tablets along with improved accuracy of recognition.

Features of our solution include:

- Traced letter being evaluated in real time to give feedback for the learner.
- Support for multiple languages like Hindi, Malayalam, Tamil, Telugu, Gujarati, and so on.
- Mapping made possible to any of the supported languages with any direction styles, i.e., from left-to-right, right-to-left, top-to-bottom, and so on.

3 Methodology

We discuss our approach for handwritten character recognition, algorithmic inferences, and the working. Our task at hand is to recognize a given unknown alphabet. We first train the system with various handwritings for each alphabet.

The algorithm tries to match the new input to find the most probable candidate so as to uniquely identify the input. Specific features such as direction are also identified in real time, as and when a user draws an alphabet.

3.1 Approach

The major shortcoming of just using ANN is its inability to accurately differentiate between alphabets with similar characteristics and its inability to identify the direction of writing. Integrating quadrant-based direction checking that captures the direction of the writing overcomes the shortcoming associated with ANN.

3.2 Self-organizing Map (Artificial Neural Network)

Several types of analysis, recognition, and interpretation can be associated with handwriting. An algorithm that can recognize a single handwritten character written by any person regardless of its shape, size, and style is required. Here we use Kohonen neural network [11] that is a self-organizing map (SOM). SOM by its property, is able to deduce relationships, and learn and adapt based on the inputs. The approach has been found to be very suitable for handwritten character recognition as it provides fast feature extraction and classification.

The alphabets written on a digital surface using a stylus or finger is cropped out with a fixed ratio, converted, sampled horizontally and vertically, and finally mapped on a 5×7 matrix template [12]. This matrix is then converted into vectors and used as inputs to the two layer self-organizing maps network [12]. The input to a SOM is submitted to the neural network via the input neurons [11]. The input neurons receive floating point numbers that make up the input pattern to the network [11]. Presenting an input pattern to the network will cause a reaction by the output neurons [11]. For a given input, the network is trained using unsupervised learning. On the links between the input layer and output layer a random weight matrix is defined [12]. In the training process of the network, this random weight matrix moves closer and closer to the input [12], when it becomes nearly equal to the input, the training stops. For every input character only one of the output neurons win [12]. In a self-organizing map, the value is produced by only one output neuron which wins and it is either true or false. Therefore, the output from the self-organizing map is usually the index of the neuron that is fired [11].

3.3 Drawbacks of Neural Network

As ANN is highly adaptive, its recognition is tolerant of minor errors and changes in patterns [13]. Figure 2 shows an example of such a case where only the first input is a valid representation of the Malayalam alphabet ‘അ’ (Aa).

As ANN chooses the most similar alphabet from the training set, it selects the letter ‘അ’ (Aa) for all the input images as seen in Fig. 3, thus accepting error inputs.

Another drawback is that using only ANN ignores the writing direction of the alphabet. Alphabets in some languages are ‘left-to-right’ and in some they are ‘right-to-left’ oriented. To evaluate if a student has learnt to write, the correct writing direction needs to be considered.

3.4 Quadrant-Based Direction Checking

Our quadrant-based direction checking for character recognition complements the functioning ANN. Quadrant-based direction checking involves defining a rule for each alphabet, preprocessing, and mapping the image into a matrix format, defining quadrants, identifying the start and end quadrants, and finally determining the direction and then matching with the rules.

Fig. 2 Quadrant marked alphabet

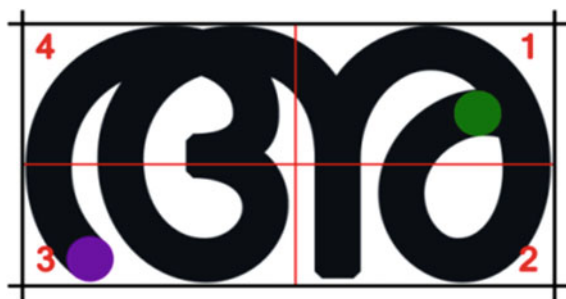
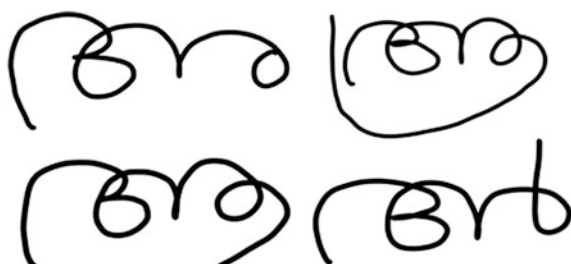


Fig. 3 Input to neural network

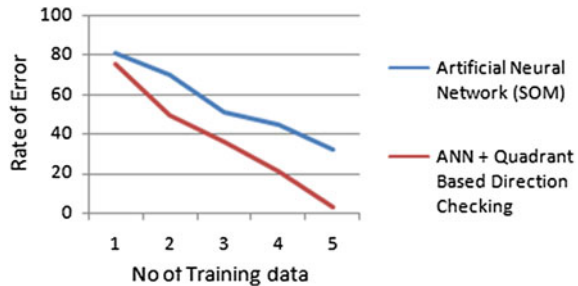


- Step 1. Define a rule for each alphabet.** A specific rule, consisting of the features extracted from the training set is defined for each alphabet in a language. The ‘start’ and ‘end’ tag specifies the quadrant where the alphabet would start and end in a regular writing style. The direction tag contains a code that represents the possible writing directions. In some cases, we use the combination of two or more codes to exactly define the direction.
- Step 2. Image Preprocessing.** We use online character recognition to find the set of coordinates for the alphabet written by the user. The character written on the drawing area is then cropped out, converted, sampled, positioned vertically, and mapped on a matrix template.
- Step 3. Define Quadrant.** The output from the previous step is the input to this step. We determine the boundaries and the quadrants for the scanned alphabet, as seen in Fig. 2.
- Step 4. Identify the quadrant in which the start and end coordinates reside.** After defining the quadrants, we determine the quadrants that represent the starting and ending coordinates of the input alphabet. The starting and ending quadrants would vary for different alphabets. Since the same alphabet can be written in different styles, there is a possibility for an alphabet to have more than one quadrant as its starting or ending points. To illustrate this, consider the case of the alphabet ‘ഓ’. Alphabet ‘ഓ’ can be written in different ways so that the ending coordinates may be in the first or second quadrant, but given any valid instance of the alphabet ‘ഓ’, the starting coordinates ought to fall in the third quadrant. Thus, an alphabet can have these values varying depending on the writing style, shape, and stroke width.
- Step 5. Calculating direction and rule matching.** Once the start and end quadrants are calculated, we need to check the direction of the alphabet scanned. Rules derived from the alphabet are compared with the predefined rule to obtain a match. If the input alphabet obeys the rule, it implies that the alphabet is written in the correct direction and it is recognized as valid.

4 Experimentation

Initial tests were conducted with ANN using training data set for languages, mainly Malayalam. The training data set contained only five instances of every alphabet written in various writing styles. Out of the five instances for every alphabet, one was written correctly and the others were written with random variations and shaky hand strokes, this was done with the intention to introduce some imperfections. The input test data to the ANN was extracted from the user written alphabet on the tablet device and it was seen that the ANN-based recognition had an accuracy of 83 %. Our proposed method of the Quadrant-based direction checking along with ANN

Fig. 4 Error rate produced by the two algorithms



significantly improved the recognition accuracy to 97 %, which was revealed in the test performed on the same input while retaining the previous training set.

The number of training data has a significant effect on the error rate of recognition. For a lower number of training data the error rate was observed to be high and with more training data included, there was a drop in the error rate. For any given case, ANN produced error rates higher than that of ANN combined with direction checking system for the same training data and input (shown in Fig. 4). The results show that the combination of ANN and Quadrant-based direction checking; together with training sets containing more instances of every letter could provide higher accuracy of recognition of alphabets.

5 Conclusion

Technology-enhanced language learning requires an accurate evaluation system with immediate feedback to the learner. A comprehensive evaluation of a learner's writing requires verification and feedback of both the writing direction and the final image. Our proposed integration of ANN and quadrant-based direction checking enhances the previous system in two ways; in its ability to evaluate the writing direction and in improved accuracy of evaluating the final image. Moreover, our method is language independent and has been successfully used in multiple Indian languages such as Malayalam, Tamil, Hindi, Gujarati, and Telugu. While OCR systems typically require numerous samples to learn a character, our method requires fewer training data per character. And most importantly, the system works with the low processing power of android tablets and without the support of higher end servers. The system is deployed in multiple village centers as part of the Amrita rural india tablet-enhanced education (RITE) program.

Acknowledgments This work derives its inspiration and direction from the Chancellor of Amrita University, Sri Mata Amritanandamayi Devi. We are grateful for the support of our colleagues at Amrita CREATE and the staff at Amrita University.

References

1. Nedungadi, P., Raman, R.: A new approach to personalization: integrating e-learning and m-learning. *Education Tech. Research Dev.* **60**(4), 659–678 (2012)
2. Nedungadi, P., Jayakumar, A., Raman, R.: Low cost tablet enhanced pedagogy for early grade reading: Indian context. In: Humanitarian Technology Conference (R10-HTC), 2014 IEEE Region 10, pp. 35–39. IEEE, Aug 2014
3. Ma, H., Doermann, D.: Adaptive Hindi OCR using generalized Hausdorff image comparison. *ACM Trans. Asian Lang. Inf. Process.* **2**(3), 193–218 (2003)
4. Cha, S.H., Srihari, S.N.: Writing speed and writing sequence invariant on-line handwriting recognition. *Pattern Recogn.* **10**, 9789812386533_0020 (2001)
5. Pal, U., Chaudhuri, B.B.: Indian script character recognition: a survey. *Pattern Recogn.* **37**(9), 1887–1899 (2004)
6. Govindan, V.K., Shivaprasad, A.P.: Character recognition—a review. *Pattern Recogn.* **23**(7), 671–683 (1990)
7. Shaw, B., Kumar Parui, S., Shridhar, M.: Offline handwritten devanagari word recognition: A holistic approach based on directional chain code feature and HMM. In: International Conference on Information Technology, ICIT'08, pp. 203–208. IEEE (2008)
8. Pal, U., Wakabayashi, T., Kimura, F.: Comparative study of Devnagari handwritten character recognition using different feature and classifiers. In: 10th International Conference on Document Analysis and Recognition, ICDAR'09, pp. 1111–1115. IEEE (2009)
9. Arora, S., Bhattacharjee, D., Nasipuri, M., Basu, D.K., Kundu, M.: Recognition of non-compound handwritten devnagari characters using a combination of mlp and minimum edit distance. arXiv preprint arXiv:1006.5908 (2010)
10. Kompalli, S., Nayak, S., Setlur, S., Govindaraju, V. Challenges in OCR of Dev anagari Documents. In: ICDAR, pp. 327–333. Aug (2005)
11. Heaton, J.: Introduction to Neural Networks with Java. Heaton Research, Inc (2008)
12. Sharma, K.S., Karwankar, A.R., Bhalchandra, A.S.: Devnagari character recognition using self organizing maps. In: 2010 IEEE International Conference on Communication Control and Computing Technologies (ICCCCT). pp. 687–691. IEEE Oct 2010
13. Araokar, S.: Visual character recognition using artificial neural networks.arXiv preprint cs/050501 (2005)

A New Approach for Single Text Document Summarization

**Chandra Shekhar Yadav, Aditi Sharan, Rakesh Kumar
and Payal Biswas**

Abstract This paper proposes an extraction-based hybrid model for a single text document summarization. The hybrid model is depending on the linear combination of statistical measures like sentence position, TF-IDF, aggregate similarity, centroid, and sentiment analysis. Our idea to include sentiment analysis for salient sentence extraction is derived from the concept that emotion plays an important role in communication to effectively convey any message; hence, it can play vital role in text document summarization. As we know for any sentence, emotions (calling sentiments) may be negative, positive, or neutral. Sentence which has strong sentiment are more important for us which may be either negative or positive.

Keywords Single document summarization • Sentiment analysis • Hybrid model

1 Introduction

Automatic text document summarization is an interdisciplinary research area of computer science that includes AI, data mining, statistics, as well as psychology. We can classify text document summarization in two ways (by techniques), abstractive summarization and extractive summarization. Abstractive summarization is more human like summary. Abstractive summarization needs things as information fusion, sentences compression, and reformation.

C.S. Yadav (✉) · A. Sharan · R. Kumar · P. Biswas
SC & SS, Jawarlal Nehru University, New Delhi, India
e-mail: chandrtech15@gmail.com

A. Sharan
e-mail: aditisharan@gmail.com

R. Kumar
e-mail: rakesh.kmr2509@gmail.com

P. Biswas
e-mail: payal.biswas786@gmail.com

In extractive summarization, the important task is to find informative sentences, subpart of sentence or phrase, and include these extractive elements into the summary. The early work in document summarization started with “Single Document Summarization,” by Luhn in [1], using frequency-based model. Baxendale in [2], suggested sentence position-based model. Edmondson [3] also proposed an effective technique based on four features (1) sentences position, (2) frequency of word, (3) presence of cue words, and (4) the skeleton of document.

Work has also been in field of multidocument summarization [4–6]. The main challenge of multidocument summarization is a diversity of information, coverage, and redundancy. Sarkar [7], Goldstein proposed MMR-based approach in [8], Alguliev et al. in [6] proposed approach for redundancy.

A lot of works have been done in this field, but producing a good quality summary and further judging if a summary is good is still a challenging task. Goldstein in [5] concludes that (1) “human judgment of the quality of a summary varies from person to person”. Hence, it is sometimes difficult to judge the quality of the summary. For evaluation, most researcher use the “Recall Oriented Understudy for Gisting Evaluation” (ROUGE) introduced by Lin [9].

In this paper, we are proposing a hybrid method for single text document summarization, which is linear combination of statistical features as used in [4, 10–13] and new kind of semantic feature, i.e., sentiment analysis. The idea which is used in this paper has been derived from different papers like for statistical features and their collective sum derived from [10, 11], centroid measure are taken from [3, 12]. The idea of sentiment analysis is motivated from the concept that emotion plays an important role in communication to effectively convey any message; hence, it can play vital role in text document summarization.

Outline of the paper is as follows. Section 2 contains our proposed hybrid algorithm, Sect. 3 shows experiments and results. Section 4 deals with conclusion and future work.

2 Summarization Algorithm

Our summarization approach is based on salient sentence extraction. The importance of any sentence is decided by the combined score given by sum of statistical measures and semantic measures. In the next step, we are explaining our approach (algorithm) used in this paper. Basically, work of summarization can be divided into three PASS (1) Sentence Scoring, (2) Redundancy Removal, and (3) Evaluation.

PASS 1: Sentence Scoring**Input:** Document (number of sentences)**Output:** Scored sentences

- Step 1: Score the sentence given with 5 different measures,
 Outcome is $M \times N$ Matrix (M no. of sentences, N no. of measures) (1) Aggregate cosine similarity, (2) Position, (3) Sentiment of sentence, (4) Centroid score of sentence, (5) $TF \times IDF$.
- Step 2: Normalize columns of matrix
- Step 3: Add all the features for every sentence, calling this sum as a score of sentence.
- Step 4: Sort according to ascending order of score.

PASS 2: Algorithm for Redundancy**Input:** Number of sentences in descending according to total score**Output:** Extracted sentencesParameter Initialization: (1) Summary= "" // Empty summary, (2) Similarity Threshold " θ ", (3) L - required length

- Step 1: Summary = (Topmost scored sentence)
- Step 2: For $i=1$ to (number of sentences)
 If (Similarity (Summary, i th sentence) $< \theta$ AND Length (summary) $< L$)
 Then: Summary= Summary + i th sentence
- Step 3: Rearrange Summary sentences, as given in Source Document for maintain cohesiveness.

PASS 3: Evaluation of Summary**Input:** Different summaries as "Gold Summaries" and "Peer summaries"**Output:** Precision, Recall and F-score

- Step 1: Generate different summary, different length using MEAD, MICROSOFT, OPINOSIS, HUMAN (Shuman) and Our-Proposed algorithm.
- Step 2: For experiment 1
 Model summary: MEAD, MICROSOFT, OPINOSIS
 Peer summary: Our-Proposed algorithm
- Step 3: Used Rouge-N ($N=1$ to 10), ROUGE-L, ROUGE-W (we set $W=1.5$), ROUGE S*, ROUGE SU* measure to find Precision, Recall, and F-Measure.

2.1 Detail Approach

PASS 1: Sentence Scoring

We are proposing a hybrid model for salient sentence extraction for "Single Text Document Summarization" based on two techniques statistical methods and semantic method.

A. Statistical Features

- (1) The location feature (Score 1): The model which we used in this implementation is given below, where N is total number of sentences.

$$\text{Score}(S_i) = 1 - \frac{i-1}{N} \quad (1 < i < N) \quad (1)$$

i —is the position of sentence in the text

- (2) The aggregation similarity feature (Score 2): It is given by the following Eqs. (2) and (3), in which W_{ik} is defined as the binary weight of k th word in i th sentence. Similarity measure also plays important role in text summarization. In our implementation, we are using cosine similarity that is widely used,

$$\text{Sim}(S_i, S_j) = \sum_{k=1}^n W_{ik} \cdot W_{jk}, \quad (2)$$

$$\text{Score}(S_i) = \sum_{j=1, j \neq i}^n (\text{Sim}(S_i, S_j)) \quad (3)$$

- (3) Frequency feature (Score 3): In our method, we are using traditional method of “TF-IDF” measure given in equation number four. Here, TF_i , IDF_i is the term frequency and inverse document frequency of i th word in the document, respectively, and ND represents total number of documents. To normalization a column vector, we follow this technique given in Eq. (5),

$$W_i = (\text{TF}_i) \times (\text{IDF}_i) = tf_i \times \log \frac{ND}{df_i} \quad (4)$$

$$X_i = X_i \times \frac{1}{\sqrt{\sum_{i=1}^n X_i^2}} \quad (5)$$

- (4) Centroid feature (Score 4): The centroid score C_i for sentence S_i is computed, as the sum of the centroid scores $C_{w,i}$ of all words appeared in the particular sentence.

$$C_i(\text{si}) = \sum_w C_{w,i} \quad (6)$$

B. Semantic Feature or Sentiment Feature

- (5) Sentiment feature (Score 5): For finding sentiment score for a sentence, first we find all entities present in sentence then find sentiment score of each entities and then do sum of all entity’s sentiment score (i.e., sentiment strength). If sentiment score of an entity is “−0.523” it means sentiment of entity is negative and strength is “0.523”. Here $|A|$ representing mode (A), i.e., $|-A| = |A| = A$.

$$\text{Score}^5 = \sum_{i=1}^n |\text{Sentiment(Entity}_i)| \quad (7)$$

Once sentences are scored, we arrange them in ascending order according to total score (as Eq. 8). Detailed result of individual scores is given in Table 1, and last column is total score of all scores.

$$\text{TotalScore}(S_i) = \sum_{k=1}^5 w_k \times \text{score}_k \quad (8)$$

Table 1 Different features scores and total score for sentences

Sent no.	Position score	TF * IDF	Aggregate cosine sim.	Centroid score	Sentiment score	Sum of all
0	1	0.175146269	0.154823564	0.750856924	0.661311	2.742137758
1	0.98245614	0.127104001	0.156975892	0.307405503	0	1.573941537
2	0.964912281	0.170528144	0.185519412	0.50702023	0.394824	2.222804067
3	0.947368421	0.182701719	0.174777773	0.663083509	0.217356	2.185287422
4	0.929824561	0.119835913	0.144151017	0.440031566	0	1.633843058
5	0.912280702	0.184106205	0.176538454	1	0.389024	2.661949361
6	0.894736842	0.128152365	0.144782619	0.353263066	0	1.520934892
51	0.105263158	0.076719171	0.044899933	0.102930791	0	0.329813053
52	0.087719298	0.126084523	0.149793298	0.206132535	0.327554	0.897283655
53	0.070175439	0.127388217	0.037996007	0.137435141	0.363308	0.736302803
54	0.052631579	0.113474586	0.064967719	0.114433381	0	0.345507265
55	0.035087719	0.100535505	0.066218503	0.247865211	0	0.449706939

PASS 2: Redundancy Removing

To remove redundancy, we used the same model as proposed by Sarkar in [7] which, the top most sentence (according to totalscore defined in Eq. 8) is added in summary, will add the next sentence in the summary; if still summary length is less than L and similarity (new-sentence, summary) $<\theta$. The output of this step is a summary with minimal redundancy and length nearly equal to L but the position of the sentence is zigzag that lost the sequence and cohesiveness. To maintain the sequence, we need to rearrange the sentences according to that given in initial index.

In Table 2 we are representing the result of sentences extracted using MEAD, Microsoft, and ourmodel-generated summary with different length. (Due to the reason that limitation only provides sentence ID). The truth is we do not have details of Microsoft-generated summary. This summarizer is inbuilt inside Microsoft Office package. When we observed it was found that Microsoft summarizer is not reducing redundancy; sentence four and 18 are almost similar sentences. Since OPINOSIS summarizer is abstractive type, below in Fig. 1 we are giving summarization result length as 10 % summary generated by OPINOSIS System.

PASS 3: Evaluation

To generate different model summary, we used three approaches (1) our text dataset was given to five persons to write a summary in about 20–40 % words, (2) we generated summary by MEAD tool; in this approach, we are taking linear combination of position and centroid score, $\text{score(mead)} = (w_1 \times \text{centroid}) + (w_2 \times \text{position})$ with $w_1 = w_2 = 1$, and (3) third model summary is generated by OPINOSIS [14] (4) Microsoft System. To evaluate summary, we are using ROUGE evaluation package. ROUGE finds recall, precision, and F-score for evaluation results. Based on N-gram co-occurrence statistics it (ROUGE) measures how much the peer summary overlaps with the GOLD summary.

Table 2 Extracted sentence ID using different systems

OUR-proposed	Microsoft	MEAD
0	4	0
5	18	1
27	26	2
35	29	3
37	32	4
42	14	5
44		8
52	—	14
—	—	29

"Indian air force has deployed 13 more aircraft for relief and rescue operations. a total of 93 sorties and dropped about 12,000 kgs of relief and equipment , said .Indian air force flew 70 civil administration personnel to the temple premises to the surroundings there . for the past few days on Thursday started with 23 more consigned to flames .people have so far been evacuated from the flood and landslide-hit areas of Uttarakhand so far and so far .gen chait said on Friday that about 8,000 to 9,000 people are still stranded in Badrinath .efforts to help those in distress in different inaccessible parts of the state and the hill state .rs18 crore to support the victims of the massive calamity in the state and the hill state .rescue and police personnel have recovered 48 dead bodies from the river Ganga in Haridwar . Evacuating all the people stranded in the upper reaches of the state and the hill state". "

Fig. 1 OPINOSIS-generated summary-10 % length

3 Experiment and Results

In this section, we are presenting two experiments done on the mentioned dataset. "In 16 June 2013, was a multi-day cloudburst centered on the North Indian state of Uttarakhand caused devastating floods along with landslides and became the country's worst Natural Disaster." Corpus is self-designed, taken from various newspapers, The Hindu, Times of India. This dataset is published in paper [15, 16].

3.1 *Experiment 1*

We created four types of model which summaries: (1) human summary (via we gave dataset to five persons to summarize it, based on their experience with the instruction to summarize it within 20–40 % words length. Due to limitations and user experiences, the generated summary varies from 24 to 52 % words length), (2) MEAD, (3) Microsoft, and (4) OPINOSIS system.

In Experiment 1, we took a summary (generated by algorithm discussed in Sect. 2) as system-generated summary and the other summary as model summary. In the next step, we find different Rouge scores ($N = 1$ to 10, ROUGE-L, ROUGE-W where $W = 1.5$, ROUGE S*, and ROUGE -SU*) as defined.

It measures three things recall, precision, and F-score for any system-generated summary (peer summary) and model summary (or reference summary).

We are comparing our system-generated summary, with other's (as model summary) same length summary. Result of this Experiment 1 is given in Tables 3, 4, and 5, for 10, 20, and 30 % length, respectively, (due to limitation of space, we provide only three tables). Figure 2 shows F-measure with different model summaries of length nearly 30 % and our summary length is nearly 27 %. From Figs. 2,

Fig. 2 Showing different F-Score

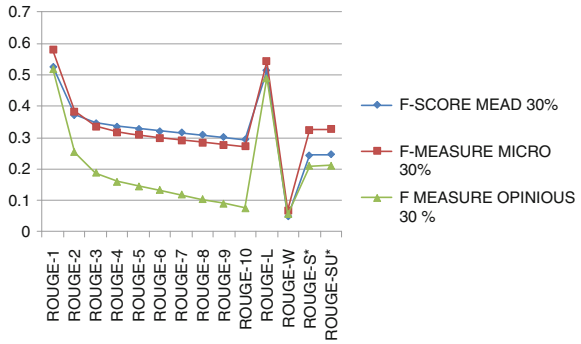


Fig. 3 Different precision score

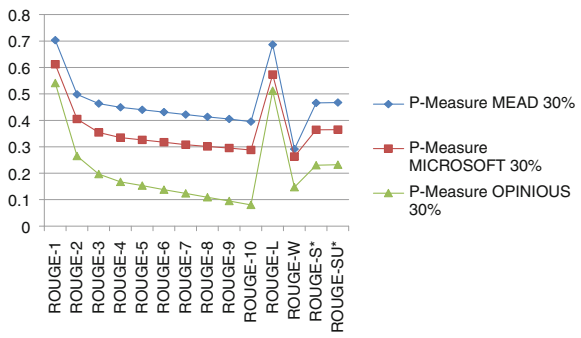


Fig. 4 Different recall scores

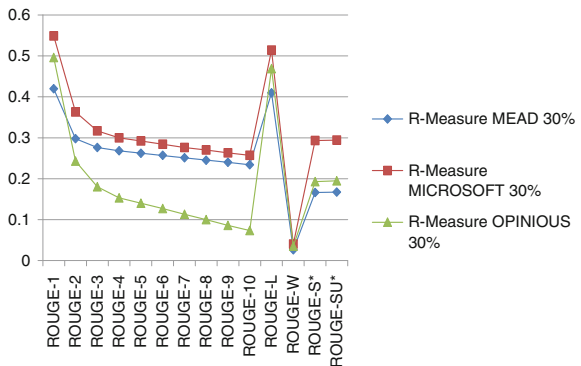


Table 3 Summary generated by our algorithm considered as system summary other summary as model summary

MEASURE	MEAD-10			MICRO SOFT			OPIOSIS		
	R	P	F	R	P	F	R	P	F
ROUGE-1	0.46	0.71	0.56	0.35	0.28	0.31	0.508	0.464	0.485
ROUGE-2	0.35	0.54	0.42	0.03	0.03	0.03	0.258	0.235	0.246
ROUGE-3	0.33	0.51	0.4	0	0	0	0.209	0.19	0.199
ROUGE-4	0.32	0.47	0.39	0	0	0	0.187	0.17	0.178
ROUGE-5	0.32	0.49	0.38	0	0	0	0.171	0.156	0.163
ROUGE-6	0.31	0.48	0.38	0	0	0	0.155	0.141	0.147
ROUGE-7	0.31	0.47	0.37	0	0	0	0.138	0.126	0.132
ROUGE-8	0.3	0.47	0.36	0	0	0	0.122	0.111	0.116
ROUGE-9	0.29	0.46	0.35	0	0	0	0.105	0.095	0.1
ROUGE-10	0.29	0.45	0.35	0	0	0	0.088	0.08	0.084
ROUGE-L	0.45	0.69	0.54	0.31	0.24	0.27	0.474	0.433	0.453
ROUGE-W	0.03	0.35	0.06	0.02	0.08	0.03	0.041	0.154	0.065
ROUGE-S*	0.16	0.37	0.22	0.1	0.06	0.08	0.22	0.183	0.2
ROUGE-SU*	0.16	0.37	0.22	0.1	0.06	0.08	0.223	0.186	0.203

3, and 4 (for 30 % summary length) it is clear that we are getting high precision, F-score w.r.t. MEAD reference summary and high recall w.r.t Microsoft-generated summary.

4 Conclusion and Future Work

In this work, we have taken the dataset designed by us. We presented a hybrid text document summarization algorithm based on linear combination of different statistical measures and semantic measures. To calculate score of a sentence, we just added all the scores for every sentence and picked up a sentence based on the highest score among all. In the next step, we selected next sentence based on next highest score and added it to summary if the similarity between summary and sentence is lower than threshold to maintain redundancy and coverage. We stop our algorithm when the desired length summary is found.

To generate several summaries of various lengths, we used methods like MEAD, Microsoft, OPINOSIS, and HUMAN and for evaluation different ROUGE score is used. In this experiment, we take summary (generated from proposed algorithm) as system summary and all the others as model summary and we observed that we are getting high precision almost every time, that denotes we covered most relevant results.

Limitation of our work is that, in step 2, i.e., salient sentence extraction, we are initializing two parameters: L-desired summary length and θ similarity threshold manually. In future, we will use soft computing technique to learn different weights for different feature scores, and we can extend our approach for multidocument summarization; we will extend this experiment for benchmark dataset.

Acknowledgments Thanks to UGC for funding and special thanks to Iskandar Keskes (Miracle laboratory, ANLP-Research Group, Sfax-Tunisia), Ashish Kumar (SC & SS, LAB-01, JNU).

Appendix

See Tables 3, 4 and 5

Table 4 Summary generated by our algorithm as system summary other summary as model summary

MEASURE	MEAD-10			OPIOSIS		
	R	P	F	R	P	F
21 % summary						
ROUGE-1	0.399	0.619	0.485	0.508	0.521	0.515
ROUGE-2	0.251	0.39	0.306	0.267	0.273	0.27
ROUGE-3	0.222	0.345	0.27	0.207	0.212	0.21
ROUGE-4	0.214	0.334	0.261	0.181	0.185	0.183
ROUGE-5	0.211	0.329	0.257	0.166	0.17	0.168
ROUGE-6	0.207	0.323	0.253	0.151	0.155	0.153
ROUGE-7	0.204	0.318	0.248	0.137	0.14	0.138
ROUGE-8	0.2	0.313	0.244	0.122	0.125	0.123
ROUGE-9	0.196	0.308	0.24	0.107	0.11	0.108
ROUGE-10	0.193	0.302	0.235	0.092	0.094	0.093
ROUGE-L	0.391	0.607	0.475	0.485	0.496	0.49
ROUGE-W	0.027	0.287	0.05	0.04	0.167	0.065
ROUGE-S*	0.151	0.365	0.214	0.201	0.211	0.206
ROUGE-SU*	0.152	0.367	0.215	0.203	0.203	0.208

Table 5 Summary generated by our algorithm as system summary, other summary as model summary

MEASURE	MEAD-25			MEAD-30			MICRO 25			MICRO 30			OPINIOUS		
	27 % summary	R	P	F	R	P	F	R	P	F	R	P	F	R	P
ROUGE-1	0.49	0.69	0.57	0.42	0.70	0.53	0.64	0.57	0.60	0.55	0.61	0.58	0.50	0.54	0.52
ROUGE-2	0.35	0.49	0.41	0.30	0.50	0.37	0.45	0.40	0.42	0.36	0.41	0.38	0.24	0.27	0.25
ROUGE-3	0.33	0.46	0.38	0.28	0.46	0.35	0.39	0.35	0.37	0.32	0.35	0.34	0.18	0.20	0.19
ROUGE-4	0.32	0.45	0.37	0.27	0.45	0.34	0.37	0.34	0.35	0.30	0.34	0.32	0.15	0.17	0.16
ROUGE-5	0.31	0.44	0.36	0.26	0.44	0.33	0.36	0.33	0.34	0.29	0.33	0.31	0.14	0.15	0.15
ROUGE-6	0.30	0.43	0.36	0.26	0.43	0.32	0.35	0.32	0.34	0.28	0.32	0.30	0.13	0.14	0.13
ROUGE-7	0.30	0.42	0.35	0.25	0.42	0.32	0.34	0.31	0.33	0.28	0.31	0.29	0.11	0.12	0.12
ROUGE-8	0.29	0.41	0.34	0.25	0.41	0.31	0.34	0.30	0.30	0.27	0.30	0.29	0.10	0.11	0.10
ROUGE-9	0.28	0.41	0.33	0.24	0.41	0.30	0.33	0.30	0.31	0.26	0.30	0.28	0.09	0.10	0.09
ROUGE-10	0.28	0.40	0.33	0.23	0.40	0.29	0.32	0.29	0.30	0.26	0.29	0.27	0.07	0.08	0.08
ROUGE-L	0.47	0.67	0.56	0.41	0.69	0.51	0.60	0.54	0.57	0.51	0.57	0.54	0.47	0.51	0.49
ROUGE-W	0.03	0.30	0.06	0.03	0.29	0.05	0.05	0.26	0.08	0.04	0.26	0.07	0.04	0.15	0.06
ROUGE-S*	0.22	0.44	0.29	0.17	0.47	0.25	0.39	0.32	0.35	0.29	0.36	0.32	0.19	0.23	0.21
ROUGE-SU*	0.22	0.44	0.29	0.17	0.47	0.25	0.39	0.32	0.35	0.29	0.37	0.33	0.20	0.23	0.21

References

1. Luhn, H.P.: The automatic creation of literature abstracts. *IBM J. Res. Dev.* **2**, 159–165 (1958)
2. Baxendale, P.B.: Machine-made index for technical literature: an experiment. *IBM J. Res. Dev.* **2**, 354–361 (1958)
3. Edmundson, H.P.: New methods in automatic extracting. *J. ACM* **16**, 264–285 (1969)
4. Radev, D.R., Jing, H., Sty, M., Tam, D.: Centroid-based summarization of multiple documents. *Inf. Process. Manage.* **40**, 919–938 (2004)
5. Goldstein, J., Mittal, V., Carbonell, J., Callan, J.: Creating and evaluating multi-document sentence extract summaries. In: Proceedings of the 9th International Conference Information and Knowledge Management, pp. 165–172. ACM (2000)
6. Alguliev, R.M., Aliguliyev, R.M., Hajirahimova, M.S., Mehdiyev, C.A.: MCMR: Maximum coverage and minimum redundant text summarization model. *Expert Syst. Appl.* **38**, 14514–14522 (2011)
7. Sarkar, K.: Syntactic trimming of extracted sentences for improving extractive multi document summarization. *J. Comput.* **2** (2010)
8. Carbonell, J., Goldstein, J.: The use of MMR, diversity-based reranking for reordering documents and producing summaries. In: Proceedings of the 21st International Conference Research and Development in Information Retrieval, pp. 335–336. ACM SIGIR (1998)
9. Lin, C.Y.: Rouge: A package for automatic evaluation of summaries. In: Proceedings of the Text Summarization Branches Out, ACL-04 Workshop, pp. 74–81 (2004)
10. Ko, Y., Seo, J.: An effective sentence-extraction technique using contextual information and statistical approaches for text summarization. *Pattern Recogn. Lett.* **29**, 1366–1371 (2008)
11. Yeh, J.Y., Ke, H.R., Yang, W.P., Meng, I.H.: Text summarization using a trainable summarizer and latent semantic analysis. *Inf. Process. Manage.* **41**, 75–95 (2005)
12. Radev, D.R., Blair-Goldensohn, S., Zhang, Z.: Experiments in single and multi-document summarization using MEAD. In: 1st Conference Document Understanding, New Orleans, LA (2001)
13. Kim, J.H., Kim, J.H., Hwang, D.: Korean text summarization using an aggregate similarity. In: Proceedings of the 5th International Workshop on Information Retrieval with Asian languages, pp. 111–118. ACM (2000)
14. Ganesan, K., Zhai, C., Han, J.: Opinosis: a graph-based approach to abstractive summarization of highly redundant opinions. In: Proceedings of the 23rd International Conference Computational Linguistics, pp. 340–348. ACL (2010)
15. Yadav, C.S., Sharan, A., Joshi, M.L.: Semantic graph based approach for text mining. In: International Conference Challenges in Intelligent Computing Techniques, pp. 596–601. IEEE (2014)
16. Yadav, C.S., Sharan, A.: Hybrid approach for single text document summarization using statistical and sentiment features. *Int. J. Inf. Retr. Res. (IJIRR)*, **5**(4), 46–70 (2015)

Analysis, Classification, and Estimation of Pattern for Land of Aurangabad Region Using High-Resolution Satellite Image

**Amol D. Vibhute, Rajesh K. Dhumal, Ajay D. Nagne,
Yogesh D. Rajendra, K.V. Kale and S.C. Mehrotra**

Abstract Land use land cover (LULC) information extraction is a crucial exercise for agricultural land. The present study highlights the advantages of remote sensing, GIS, and GPS techniques for LULC mapping from high-resolution remote sensing data. High spatial resolution (5.8 m) satellite imagery of IRS-P6 Resourcesat-II LISS-IV having three spectral bands was utilized for LULC classification and for data processing ENVI 4.4 tool and Arc GIS10 software were used. Eight training samples for LULC classes have been selected from the image. Supervised classification using maximum likelihood (ML), Mahalanobis distance (MD), and minimum distance to means (MDM) were applied. The performances of above classifiers were evaluated in terms of the classification accuracy with respect to the collected real-time ground truth information. The evaluation result shows that the overall accuracies of LULC classifications are approximately 84.40, 77.98, and 74.31 % with Kappa coefficients 0.82, 0.74, and 0.70 for the ML, MD, and MDM, respectively. It is noticed that ML has a better accuracy than the MD and MDM classifiers and it is a more effective method for complex and noisy remote sensing data because of its unified approach for estimation of parameters.

A.D. Vibhute (✉) · R.K. Dhumal · A.D. Nagne · Y.D. Rajendra · K.V. Kale · S.C. Mehrotra
Department of Computer Science & IT, Dr. B. A. M. University, Aurangabad, 431004
Maharashtra, India
e-mail: amolvibhute2011@gmail.com

R.K. Dhumal
e-mail: dhumal19@gmail.com

A.D. Nagne
e-mail: ajay.nagne@gmail.com

Y.D. Rajendra
e-mail: yogesh.rajendra@gmail.com

K.V. Kale
e-mail: kvkale91@gmail.com

S.C. Mehrotra
e-mail: mehrotra.suresh15j@gmail.com

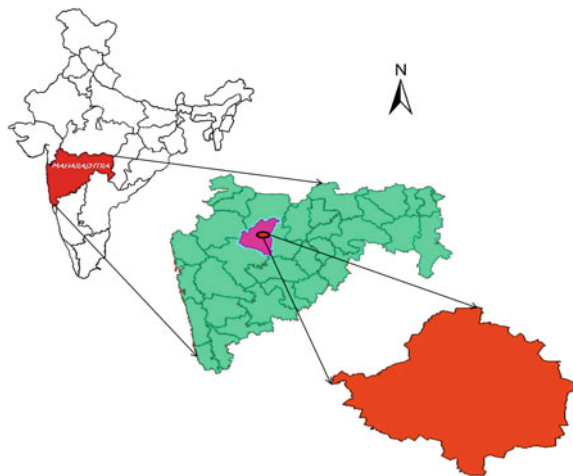
Keywords Maximum likelihood classifier • Land use/land cover • Supervised classification • Remote sensing

1 Introduction

One of the major natural resources is land and in remote sensing study land cover area estimation is the most conspicuous application. In the present era, information technology plays an imperative role in the land use land cover global ecological change detection, which is useful for decision support system. The term land use is an area used by peoples for their requirement, whereas land cover is the physical objects on the terrain exterior which are covered by various parts of the environment also manmade elements such as water, rocks, soils, settlements, etc. [1]. Nowadays, sustainable land use is a crucial problem. Land use land cover pattern mapping is a vital for various recognitions and their monitoring which is helpful in planning and managing the limited land resources for upcoming best profit. Furthermore, the planning of LULC helps to overcome the present evils and observing their future growth which permitting most earth productivity and preserving the natural atmosphere [2, 3]. Land cover land use mapping plays an important role in various fields such as planning and management of earth, hydrological modeling, urban ecoenvironment monitoring, atmosphere sustainable expansion, also different hydrologic processes like soil moisture status and penetration. Due to rapid growth, urbanization, population coupled with increasing burden made on land resources the existing land is decreasing hastily. Hence it is necessary to monitor and manage the available land which is depending on the accessibility of exact land use information. Remote sensing (RS) coupled with geographic information system (GIS) and global positioning system (GPS) technologies are essential for extracting and analyzing the LULC patterns knowledge, preparation of geospatial database, and monitoring the land transformation on time and cost-effective manner [4–7]. Recent days, panchromatic and multispectral remote sensing data as well as aerial photographs have been used in the development of LULC maps from regional, national, and global scales [3, 8]. The USGS devised a land use and land cover classification system for use with remote sensor data in the mid-1970s [9]. In the existing study, we have used level-II of Anderson classification for LULC mapping analysis.

The present study highlights the advantages of remote sensing and geographic information system with global positioning system techniques for analyzing the land use/land cover area estimation for Aurangabad region of Maharashtra, India. This paper covers five parts such as introduction, study area, used satellite data, detailed methodology, and results with discussion.

Fig. 1 Location map of Aurangabad area, Maharashtra, India



2 Study Area

The study area Aurangabad, located on $19^{\circ} 45' - 20^{\circ} 00'$ N latitude and $75^{\circ} 15' - 75^{\circ} 30'$ E longitude which is the central part of Maharashtra, India. Its total land area is 123 km^2 (47 m^2) and the elevation is high 568 m (1,864 ft) [10]. The study area is complex in nature; in this work agricultural area, settlements, bare soil, water bodies, and hilly surrounding area were selected as a region of interest (ROI). Mapping land use/land cover in hilly area of the Aurangabad has always posed big defiance. The Fig. 1 shows the location map of study area.

3 Datasets

To perform this study, different types of data have been gathered. The data was acquired from different sources. Satellite imagery and field data were the primary resources of data. The field data was collected through GPS and digital camera of Sony Experia Smartphone, and ground truth points were matched with Google Earth. Survey of India (SOI) toposheet at 1:50,000 scales were used as a predominant source for base map preparation. The geometrically and radiometrically corrected orthorectified IRS-P6 Resourcesat-II LISS-IV satellite high spatial resolution multispectral image was used for preparation of geomorphology map. This data is received from Linear Imaging and Self Scanning Sensor (LISS-IV) which operates in three spectral bands (B2, B3, B4) with 5.8 meter fine spatial resolution (at Nadir) and a swath of 23.5 km in multispectral mode (Mx) with three bands, while 70 km in mono mode with any one single band. The radiometric resolution of LISS-IV data is 10 bits and the camera can be tilted up to $\pm 26^{\circ}$ in the across track

direction. The data used in this study was rectified to the Universal transverse mercator (UTM) zone 43 North and World Geodetic System (WGS)-84 datum.

4 Methodology

In this study, EVVI 4.4 (Environment for Visualizing Images) image analysis tool and Arc GIS10 software packages were used for data processing, per-pixel classification and analysis of the data. The overall methodology for this study is shown in Fig. 2, and the method is discussed in the following sections.

4.1 Preprocessing

In the preprocessing of satellite images, geometric and radiometric corrections with image enhancement were carried out. The main objectives of these operations were to correct the degraded image data for generating a more realistic illustration of the original view and to improve the satellite imagery for better classification [8]. For this study, we used orthocorrected (geometric as well as radiometric corrected) satellite imagery from NRSC, Hyderabad. Three individual bands were extracted from multispectral satellite data, which was in band-interleaved-by-pixel

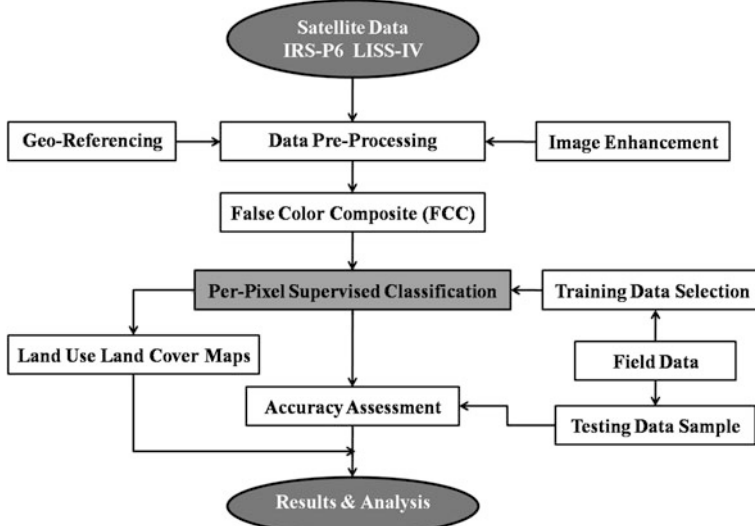


Fig. 2 Workflow diagram for proposed methodology

(BIP) format. Standard false color composite (FCC) were generated of IRS P6 LISS-IV data for better visual interpretation.

4.2 Per-pixel Classification

“Image pixels can be classified either by their multivariable statistical properties, such as the case of multispectral classification (clustering), or by segmentation based on both statistics and spatial relationships with neighboring pixels” [11]. The two major categories of per-pixel image classification methods are unsupervised and supervised classifications. In supervised classification technique, user trains the area through collected various ground control points and his knowledge. This classification method depends on the statistics of training areas. Ground control points are collected and classification is controlled by the user’s knowledge, hence the classification can be misguided by incorrect training area information and/or incomplete user knowledge [11]. So user has the perfect knowledge of the land cover type or spectral reflectance of the interested area in the image which is beneficial for the training dataset [1].

In the present study, supervised parametric or statistical methods were implemented such as minimum distance to means classifier and Mahalanobis distance classifier and maximum likelihood classifier.

4.2.1 Minimum Distance to Mean Classifier

According to the mean or average spectral value in each class signature, the minimum distance to means classifier is used for classification of various unidentified patterns of the image data, while ignoring covariance matrix and standard deviation. The spectral distance between image data and the class in multifeature space is identified as an index of class similarity to classify minimum distance as a maximum similarity [1]. For all class, the mean or average spectral value in each band is considered. Hence this classifier is mathematically simple and computationally able with some drawbacks [8]. The following equation shows the decision rule behind this classifier:

$$\text{Pixel } X \in C_j \quad \text{if } d(C_j) = \min[d(C_1), d(C_2), \dots, d(C_m)] \quad (1)$$

where $\min[d(C_1), d(C_2), \dots, d(C_m)]$ is a function for identifying the smallest distance among all those inside the bracket. For instance, $\min [23.4, 35.2, 47.8, 12.3, 56.7]$ returns a value of 12.3; $d(C_j)$ refers to Euclidean distance between pixel X and the center of information class C_j . It is calculated using the Eq. (2):

$$d(C_j) = \sqrt{\sum_{i=1}^n [\text{DN}(i,j) - C_{ij}]^2} \quad (2)$$

This calculation is repeated m times with all information classes, for each pixel in the input image data [12].

4.2.2 Mahalanobis Distance Classifier

It is also known as Manhattan distance which depends on the correlations between variables to analyze and identify various objects. According to known data, it measures the similarity of an unknown data set [1]. In this classifier, each band is utilized for classification which is the statistical summation of the entire differences between two pixels in the similar band. In deriving the difference, the use of total value reduces the need to worry about which pixel value should be subtracted from which pixel. There are no differences going to negate themselves in the total, because of positive difference. This distance, D_m is calculated using Eq. 3.

$$D_m = \sum_{i=1}^n |\text{DN}_{Ai} - \text{DN}_{Bi}| \quad (3)$$

Hence, Mahalanobis spectral distance is generally used much more for classification due to less complexity and simpler to calculate than the Euclidean spectral distance [12].

4.2.3 Maximum Likelihood Classifier

The maximum likelihood classifier is one of the most popular algorithms of classification based on Bayes theorem with two weighting factors for estimating the probability density functions. First, the user trains the particular signatures or the “a priori probability” of each class in the given scene. Second, the cost of misclassification is weighted for each class as per its probability. Together, these factors result in superior reducing the misclassification. This classifier classifies spectral response patterns of an unknown pixel through estimating both the variance and covariance of the class.

In the remote sensing image classification, maximum likelihood technique is most widely used due to its popularity, in which a pixel belongs to maximum likelihood is categorized into the related class. It is a statistical decision criterion to assist in the classification of overlapping signatures; pixels are assigned to the class of highest probability. We may compute the statistical probability of a given pixel value being a member of a particular land cover class. The probability density functions are used to classify an undefined pixel by computing the probability of the

pixel value belonging to each category. After evaluating the probability in each category, the pixel would be assigned to the most likely class with highest probability value or be labeled “unknown” if the probability values are all below a threshold [1, 8, 13, 14].

This classifier relies on the second-order statistics of the Gaussian probability density function model for each class. The basic discriminant function for pixel s is

$$X \in C_i \text{ if } (C_j/X) = \max[p(C_1/X), p(C_2/X), \dots, p(C_m/X)] \quad (4)$$

where $\max [p(C_1/X), p(C_2/X), \dots, p(C_m/X)]$ is a function that returns the largest probability among those inside the bracket. For instance, $\max [0.45, 0.32, 0.67, 0.83, 0.71]$ returns a value of 0.83. The information class corresponding to this probability is used as the identity for pixel X . $p(C_j/X)$ denotes the conditional probability of pixel X being a member of class C_j . It is solved using the Bayes theorem:

$$P(C_j/X) = p(X/C_j) * p(C_j)/p(X) \quad (5)$$

where $p(X/C_j)$ is the conditional probability or priori probability, $p(C_j)$ is the occurrence probability of class C_j in the input image and $p(X)$ is the probability of pixel X occurring in the input image, which can be written as:

$$p(X) = \sum_{j=1}^m p(X/C_j) * p(C_j) \quad (6)$$

where m is the number of classes, $p(X)$ is supposed as normalization constant to ensure $\sum_{j=1}^m p(C_j/X)$ equals to 1. In the real implementation of maximum likelihood classification, for specifying the probability of each information class, the user gives the opportunity. Hence the class of a posterior probability is defined as

$$p(C_j/X) = \frac{p(X/C_j)p(C_j)}{\sum_{j=1}^m p(X/C_j)p(C_j)} \quad (7)$$

where $p(C_j)$ is the prior probability of class C_j and $p(X/C_j)$ is the conditional probability of observing X from class C_j (probability density function). Thus the computation of $p(C_j/X)$ is reduced to determination of $p(X/C_j)$. The analysis of $p(X/C_j)$ can be expressed as for the satellite multispectral imagery:

$$p(X/C_j) = \frac{1}{(2\pi)^{n/2} |\sum j|^{0.5}} \times \exp \left[-\frac{1}{2} (\text{DN} - \mu_j)^T \sum_j^{-1} (\text{DN} - \mu_j) \right] \quad (8)$$

where $\text{DN} = (\text{DN}_1, \text{DN}_2, \dots, \text{DN}_n)^T$ is the vector of pixel with n number of bands $\mu_j = (\mu_{j1}, \mu_{j2}, \dots, \mu_{jn})^T$ is the mean vector of the class C_j and $\sum j$ is the covariance matrix of class C_j which can be written as [12]:

$$\sum j = \begin{bmatrix} \sigma_{11} & \sigma_{12} & \dots & \sigma_{1n} \\ \sigma_{21} & \sigma_{22} & \dots & \sigma_{2n} \\ \dots & \dots & \dots & \dots \\ \sigma_{n1} & \sigma_{n2} & \dots & \sigma_{nn} \end{bmatrix} \quad (9)$$

4.3 Accuracy Assessment

In the LULC classification of remote sensing, data accuracy assessment is a vital part. For the classification accuracy assessment, ground control points are necessary to generate error or confusion matrix which is in the form of producer's accuracy, user's accuracy, and overall accuracy with Kappa coefficient. A classified label against actual observed ground observation at a specified location can be determined by an error matrix. The nonzero nondiagonal value indicates the error between the classified object from the corresponding observed object [15]. The producer's accuracy, user's accuracy, overall accuracy and Kappa coefficient is calculated though Eqs. 10, 11, 12, and 13, respectively.

$$\text{Producer's accuracy} = \frac{C_{xx}}{\sum r} \times 100 \% \quad (10)$$

where C_{xx} is the element at position x th row and x th column and $\sum r$ is row sums.

$$\text{User's accuracy} = \frac{C_{yy}}{\sum c} \times 100 \% \quad (11)$$

where $\sum c$ is column sums.

$$\text{Overall accuracy} = \frac{\sum_{x=1}^A C_{xx}}{N} \times 100 \% \quad (12)$$

where N and A is the total number of pixels and classes, respectively.

$$k = \frac{\sum_{i=1}^r (X_{ii} - \sum ci \sum ri)}{N^2 - \sum_{i=1}^r (\sum ci \sum ri)} \quad (13)$$

where r = number of rows and columns in the error matrix, X_{ii} = number of observations in row i and column i , $\sum ci$ = masrginal total of column i , $\sum ri$ = marginal total of row i , N = total number of observations [15].

5 Results and Discussion

From the satellite image, minimum 150 pixels were taken as trained samples for each class. Three supervised classifiers were used to extract the different features in the satellite image from the trained samples. This image was classified into eight various classes like Agricultural crop area, agricultural without crops, built-up area, bare soil, hilly area, hill with trees, hill without trees, and water bodies. Figure 3 shows the final classified LULC maps through maximum likelihood, Mahalanobis distance, and minimum distance classifiers, respectively.

The resulted areas derived from classification are listed in Table 1 and Fig. 4 indicate that an average covered area from the total.

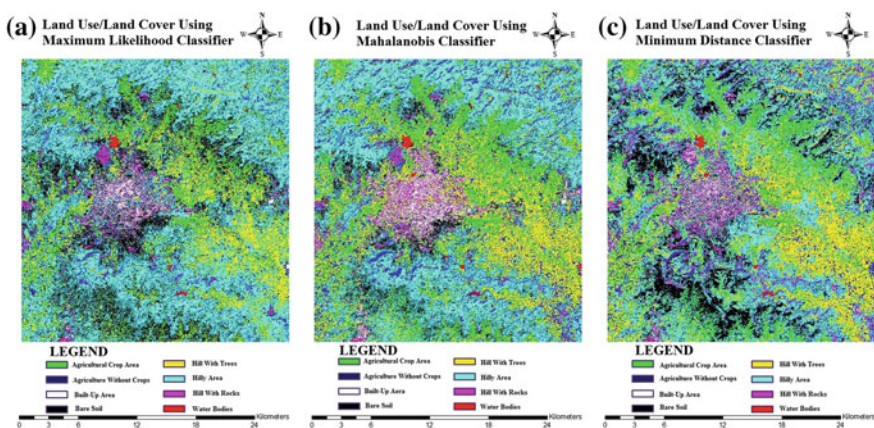


Fig. 3 Land use/land cover map. **a** Maximum likelihood classifier. **b** Mahalanobis classifier. **c** Minimum distance classifier

Table 1 LULC distribution in Aurangabad region using different classifier

Classes	Maximum likelihood classifier		Mahalanobis distance classifier		Minimum distance classifier	
	Area (Km ²)	Area (%)	Area (Km ²)	Area (%)	Area (Km ²)	Area (%)
Agricultural crop area	56.69	7.23	89.53	11.42	82.06	10.47
Agriculture area without crops	36.24	4.62	68.05	8.68	55.73	7.11
Built-up area	16.38	2.09	29.68	3.79	19.56	2.49
Bare soil	164.48	20.99	85.88	10.96	122.59	15.64
Hill with trees	125.86	16.06	183.20	23.38	191.34	24.42
Hilly area	359.48	45.88	287.47	36.69	250.53	31.98
Hill with rocks	21.68	2.76	35.30	4.50	58.42	7.45
Water bodies	2.55	0.32	4.25	0.54	3.13	0.40
Unclassified	0	0.00	0	0.00	0	0.00
Total area	783.40	100.00	783.40	100.00	783.40	100.00

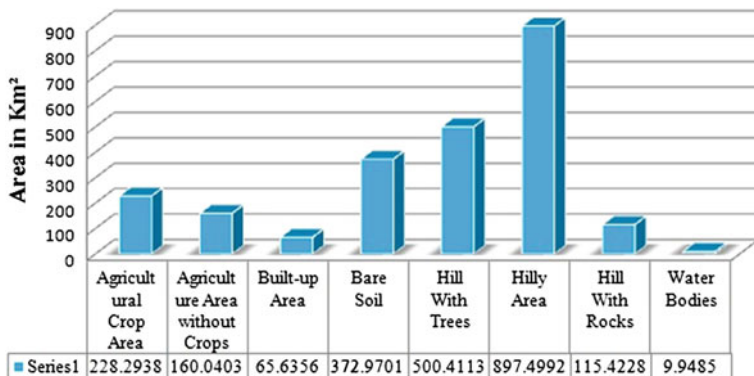


Fig. 4 An average covered regions from the study area

Result of classified area shows that the hilly area and hills with trees are covered the most part in the studied region, whereas bare soil is also the third most covered part. Agriculture crop area and area without crops are less as covered compared to hilly areas. Built-up area and water bodies are very less in the studied region. Only half percent area is under water bodies including dams, reservoir, etc. Finally, when it is calculated average area from the study area, it is found that an average 897.49 km^2 area is under hills which are the highest area and an average 500.41 km^2 area is hill with trees, various vegetations as well as an average 115.42 km^2 area is hilly rocks. Bare soil is covered near about 372.97 km^2 area which is the most useful for agriculture purpose or any other use. Only an average 388.33 km^2 area is under agriculture from that 228.29 km^2 area is various crops. Built-up area is an average 65.63 km^2 . In the studied region, hilly area (with rocks, trees and vegetations) is the highest area, where as the lowest one area is water body which covers only an average 9.94 km^2 from the total.

Lastly, we have computed error matrix with total 109 ground control points from the field visit for accuracy assessment of classification and to estimate the LULC maps of the study region. Google Earth and Google map were frequently utilized for the verification of classification accuracy and verification to remote confusion regarding the decision of land use land cover map. The error matrix resulting from the training set pixels for Maximum likelihood, Mahalanobis and Minimum distance classifiers are given in Tables 2, 3, and 4, respectively. Tables 2, 3, and 4 described that, the major diagonal elements of the error matrix are the training set pixels that were correctly classified into their LULC classes. The statistics in Tables 2, 3, and 4 were used to compute the Producer's and User's accuracy of individual LULC class and also showed the overall accuracy of the classification.

Figure 5 illustrates that, the overall accuracy and Kappa coefficient of maximum likelihood, Mahalanobis, and minimum distance classifier. According to accuracy assessment results, overall classification accuracy for the Maximum likelihood classifier was 84.40 %, for Mahalanobis classifier it was 77.98 %, whereas it was 74.31 % for Minimum distance classification. Moreover, Kappa statistics depicted

Table 2 Error matrix: accuracy assessment of LULC classification for maximum likelihood classifier

Classes	Reference points							Row total	
	Agri crop1	AgriWithoutCrop1	BuiltUpAreal	Bare soil	HillyTrees1	HillyAreal	HillWithRocks1	Water bodies1	
Unclassified	0	0	0	0	0	0	0	0	0
Agricultural crop area	15	0	0	0	0	0	0	0	15
Agriculture area without crops	0	13	0	0	0	0	0	0	13
Built-up area	0	1	6	0	0	0	3	0	10
Bare soil	0	0	2	10	1	0	0	0	13
Hill with trees	0	0	0	0	12	0	0	0	12
Hilly area	0	0	0	2	0	14	0	0	16
Hill with rocks	0	0	5	3	0	0	12	0	20
Water bodies	0	0	0	0	0	0	0	10	10
Column total	15	14	13	15	13	14	15	10	109
<i>Accuracy</i>									
Producer's accuracy (%)	100.00	92.86	46.15	66.67	92.31	100.00	80.00	100.00	
User's accuracy (%)	100.00	100.00	60.00	76.92	100.00	87.50	60.00	100.00	
Overall accuracy (%)	84.4037								
kappa coefficient	0.8213								

Table 3 Error matrix: accuracy assessment of LULC classification for Mahalanobis distance classifier

Classes	Reference points							Row total
	Agri crop 1	AgriWithoutCrop 1	BuiltUpArea1	Bare soil1	HillyTrees1	HillyArea1	HillWithRocks1	
Unclassified	0	0	0	0	0	0	0	0
Agricultural crop area	15	0	0	0	0	0	0	15
Agriculture area without crops	0	14	0	0	0	0	0	14
Built-up area	0	0	7	4	0	0	5	0
Bare soil	0	0	0	6	0	0	0	6
Hill with trees	0	0	0	0	13	0	0	13
Hilly area	0	0	0	3	0	14	4	21
Hill with rocks	0	0	6	2	0	0	6	14
Water bodies	0	0	0	0	0	0	10	10
Column total	15	14	13	15	13	14	15	109
<i>Accuracy</i>								
Producer's accuracy (%)	100.00	100.00	53.85	40.00	100.00	100.00	40.00	100.00
User's accuracy (%)	100.00	100.00	43.75	100.00	100.00	66.67	42.86	100.00
Overall accuracy (%)	77.9817							
Kappa coefficient	0.7482							

Table 4 Error matrix: accuracy assessment of LULC classification for minimum distance classifier

Classes	Reference points								Row total
	Agri crop 1	AgriWithoutCrop 1	BuiltUpArea1	Bare soil1	HillWithTrees1	HillyArea1	HillWithRocks1	Water bodies1	
Unclassified	0	0	0	0	0	0	0	0	0
Agricultural crop area	15	0	0	0	0	0	0	0	15
Agriculture area without crops	0	14	0	0	0	0	0	0	14
Built-up area	0	0	4	0	0	0	9	0	13
Bare soil	0	0	1	10	0	5	0	0	16
Hill with trees	0	0	0	13	0	0	0	0	13
Hilly area	0	0	1	4	0	9	0	0	14
Hill with rocks	0	0	7	1	0	0	6	0	14
Water bodies	0	0	0	0	0	0	10	0	10
Column total	15	14	13	15	13	14	15	10	109
<i>Accuracy</i>									
Producer's accuracy (%)	100.00	100.00	30.77	66.67	100.00	64.29	40.00	100.00	
User's accuracy (%)	100.00	100.00	30.77	62.50	100.00	62.50	42.86	100.00	
Overall accuracy (%)	74.3119								
Kappa coefficient	0.7059								

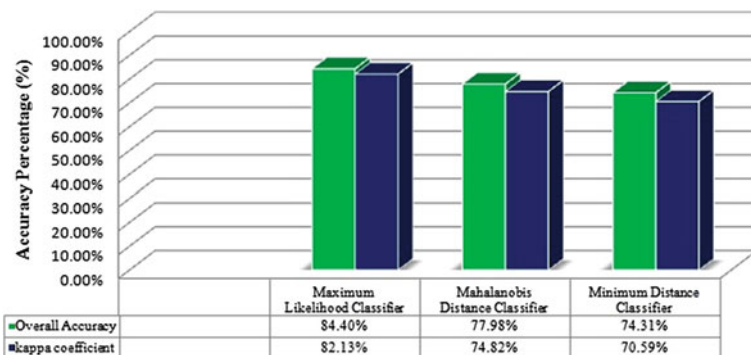


Fig. 5 Overall accuracy with Kappa coefficient

that the overall Kappa value was higher in the maximum likelihood classification than the Mahalanobis distance and Minimum distance classification techniques (Tables 2, 3, and 4) and it was found to be 82.13 % in the Maximum likelihood classification, 74.82 % in the Mahalanobis distance, and 70.59 % in the Minimum distance classification (in percentage).

6 Conclusions

The present study highlights the advantages of RS coupled with GIS and GPS. The LULC mapping was analyzed according to per-pixel-based image classification through IRS-P6 LISS-IV high spatial resolution satellite image. Three supervised classifiers were used for the classification such as maximum likelihood classifier, Mahalanobis distance, and minimum distance classifier. It is observed that, hilly area including trees, vegetation, and rocks are mostly available surroundings of the studied Aurangabad region, whereas bare soil and agricultural area are the second and third priority according to covered area. Very few areas are under water bodies including dams, reservoir, etc. Also it was noticed that, maximum likelihood technique is better for mixed pixels like hills including trees, vegetations, and rocks. According to classification results, it was found that maximum likelihood classifier gives better results than other statistical classifiers such as Mahalanobis distance and Minimum distance. The maximum likelihood method estimate the optimum parameters using unified approach and works well for well defined distribution, whereas Mahalanobis distance and Minimum distance are based on minimizing the distance matrices.

Acknowledgments Authors would like to acknowledge UGC for facility provided under UGC SAP (II) DRS Phase-I F.No.-3-42/2009 to Department of Computer Science & IT, Dr. Babasaheb Ambedkar Marathwada University, Aurangabad. And financial assistance under UGC-BSR research fellowship.

References

1. Vibhute, A.D., Gawali, B.W.: Analysis and modeling of agricultural land use using remote sensing and geographic information system: a review. *Int. J. Eng. Res. Appl. (IJERA)* **3**(3), 081–091 (2013)
2. Sadoun, B., Al Rawashdeh, S.: Applications of GIS and remote sensing techniques to land use management. In: IEEE/ACS International Conference on Computer Systems and Applications, pp. 233–237. IEEE (2009)
3. Zhang, Y., Chen, X., Su, S., Wu, J.: Making the best use of landsat MSS images for land use/cover change analysis. In: International Conference on Environmental Science and Information Application Technology. IEEE (2009)
4. Xiong, Y., Wang, R., Li, Z.: Extracting land use/cover of mountainous area from remote sensing images using artificial neural network and decision tree classifications. In: International Symposium on Intelligence Information Processing and Trusted Computing. IEEE (2010)
5. Kumar, V., Rai, S.R., Rathore, D.S.: Land use mapping of Kandi Belt of Jammu region. *J. Indian Soc. Remote Sens.* **32**(4), 323–328 (2004)
6. Shamsudheen, M., Dasog, G.S., Tejaswini, N.B.: Land use/land cover mapping in the coastal area of North Karnataka using remote sensing data. *J. Indian Soc. of Remote Sens.* **33**(2), 253–257 (2005)
7. Joshi, R.K., Rawat, G.S., Padaliya, H., Roy, P.S.: Land use/land cover identification in an Alpine and Arid region (Nubra Valley, Ladakh) using satellite remote sensing. *J. Indian Soc. Remote Sens.* **33**(3), 371–380 (2005)
8. Lillesand, T.M., Kiefer, R.W., Chipman, J.W.: *Remote Sensing and Image Interpretation*, 6th edn. Wiley India Pvt. Ltd., New Delhi (2008)
9. Anderson, J.R., Hardy, E.E., Roach, J.T., Witmer, R.E.: A land use and land cover classification system for use with remote sensor data. In: Geological Survey Professional Paper, vol. 964 (2001). <http://landcover.usgs.gov/pdf/anderson.pdf>
10. <http://en.wikipedia.org/wiki/Aurangabad>, Maharashtra. Accessed 27 Sept 09 2014 08:03 p.m
11. Liu, J.G., Mason, P.J.: *Essential Image Processing and GIS for Remote Sensing*. Wiley, London (2009)
12. Gao, J.: *Digital Analysis of Remotely Sensed Imagery*. The McGraw-Hill Companies, Inc., New York (2009)
13. Al-Ahmadi, F.S., Hames, A.S.: Comparison of four classification methods to extract land use and land cover from Raw Satellite Images for some remote Arid Areas, Kingdom of Saudi Arabia. *JKAU Earth Sci.* **20**(1), 167–191 (2009 A.D./1430 A.H.)
14. Sharma, S., Pradhan, R.: Classification methods for land use and land cover pattern analysis. *Int. J. Innovative Technol. Explor. Eng. (IJITEE)* **4**(1) (2014). ISSN: 2278-3075
15. Vibhute, A.D., Nagne, A.D., Gawali, B.W., Mehrotra, S.C.: Comparative analysis of different supervised classification techniques for spatial land use/land cover pattern mapping using RS and GIS. *Int. J. Sci. Eng. Res.* **4**(7) (2013). ISSN 2229-5518

A Novel Fuzzy Min-Max Neural Network and Genetic Algorithm-Based Intrusion Detection System

Chandrashekhar Azad and Vijay Kumar Jha

Abstract Today in the era of ICT, security of data and services on the WWW has become the most important issue for web service providers. Loopholes in the security systems of WWW may break the integrity, reliability, and availability of data and services. Today, intrusion detection systems based on data mining is the best security framework for the Internet. In this paper a novel intrusion detection system is proposed which is based on the fuzzy min-max neural network and the genetic algorithm. The proposed model is trained using fuzzy min-max neural network and the learning system is optimized by application of genetic algorithm. The developed system is tested on the KDD Cup dataset. The parameters classification accuracy and classification error were used as a final performance evaluator of the learning process. The experimental results show that the proposed model gives superior performance over other existing frameworks.

Keywords IDS · Anomaly detection · Misuse detection · FMM NN · Genetic algorithm

1 Introduction

Today, we are living in the digital era and the needs and wants of humans are dependent on the World Wide Web like online shopping, property booking, online food booking, etc. [1]. Due to all these interconnections, the World Wide Web increases day-by-day voluminously. That is why today computer network is the most important foundation for governments and web service providers. Data and

C. Azad (✉) · V.K. Jha

Department of Computer Science and Engineering, Birla Institute of Technology,
Mesra 835215, Ranchi, India
e-mail: csazad@bitmesra.ac.in

V.K. Jha
e-mail: vkjha@bitmesra.ac.in

© Springer India 2016

S.C. Satapathy et al. (eds.), *Proceedings of the Second International Conference on Computer and Communication Technologies, Advances in Intelligent Systems and Computing* 380, DOI 10.1007/978-81-322-2523-2_41

429

services hosted on the remote computer require a robust security framework to maintain the integrity, reliability, and availability of the data and services. There are many applications such as firewall, access control, antivirus, anti-spammer, etc., which are availed as security frameworks but they do not provide hundred percent security to the network resources. The reason behind failing of the security services is most of the security equipment are based on the data patterns and they require timely and updated fine-tuning to cope with the recent network attacks. Due to innovations in science and technology, the everyday data access rate through the network has expanded exponentially and the manual analysis of these is almost impossible. So there is need for automatic attack detection system, which can possibly extract useful information from the network data. Intrusion detection system based on the data mining may be the best options for the computer network security infrastructure.

1.1 Intrusion Detection System

An intrusion detection system (IDS) is a hardware or software or both that attempt to detect the malicious activity in the World Wide Web [2]. The intrusion detection system can be categorized into two broad categories, namely anomaly detection and misuse detection systems. Misuse detection system is a system that has ability to detect malicious activity in the computer network against the known malicious activities. In other words, we can say that misuse detection systems are based on the attack pattern and if any upcoming packets fall within the existing results or signatures, the request or the packet is treated as an attack, otherwise they are treated as normal traffic. It is difficult to maintain the rule base for all types of attacks or network vulnerabilities, they require timely updation. In anomaly detection system, the administrator of the system defines various cases of normal pattern. If any of the upcoming packet violates this, the packet is treated as anomaly. It is difficult to maintain a rule-based anomaly detection system for cases where a normal user may use the system resources or network resources in a different way that was not mentioned in the predefined rules or patterns. This results as an anomaly and triggers a false alarm.

2 Related Work

In [3] a novel hybrid RBF/Elman neural network-based IDS is proposed, the system is evaluated on DARPA dataset and the effectiveness of the system is shown with the help of an ROC curve. In [4] FC-ANN-based IDS proposed where fuzzy clustering is used to produce different training subsets. The different ANN models were trained and aggregated using fuzzy aggregation module to produce an enhanced system performance. In [5] two intrusion detection systems, ICLN and

SICLN, are proposed. ICLN is an unsupervised classification method while SICLN is based on supervised classification method. In [6] feedforward neural network and back propagation network-based IDS is proposed to track unusual traffic in the computer network and the system is evaluated using the DARPA dataset. In [7] a multilevel hierachal Kohenan net-based IDS was proposed and the system was trained and evaluated using randomly selected data instances from the KDD CUP dataset. In [8] authors presented neural network-based intrusion detection system where they presented the network data analysis, development of the feature selection method, generation of the learning dataset. The system was trained using the error-back propagation and Levenberg-Marquardt neural network. In [9] authors used the asymmetric cost of the false positive and negative error for performance enhancement of the neural network-based IDS. The proposed method focuses on security as well as the system performance objectives. In [10] NeC4.5 intrusion detection system is proposed, the system uses the ensembles of neural network for the training set generation, and C4.5 classification is used for final classification task. Most of the intrusion detection systems presented in the literature do cope with multiple scanning of the training set, overlapping classes problem, parameter settings, problem of nonlinear separability, etc.

3 Materials and Method

3.1 Fuzzy Min-Max Neural Network

Fuzzy min-max neural network (FMMNN) classification is based on the concept of hyperbox fuzzy sets [11]. In this neural network, learning is performed by the series of expansion and contraction processes and testing of the patterns is carried out by finding the membership value of each input pattern corresponding to each hyperbox fuzzy sets. The membership value lies between 0 and 1.

3.2 Fuzzy Set Hyperbox

A fuzzy set hyperbox represents a region in the n-dimensional pattern space. The hyperbox is defined by its min point, max point, and the membership function. The hyperbox fuzzy set is defined in Eq. (1):

$$B_j = \{A, v_j, w_j, F(A, v_j, w_j)\} \quad \forall A \in I^n \quad (1)$$

Here B_j is the j th hyperbox, A is the n-dimensional input vector, v_j is the min point of the B_j , w_j is the max point of the B_j , and $F(A, v_j, w_j)$ is the membership function.

Suppose $A(a_1, a_2, a_3 \dots a_n)$ is an input pattern, then the min and max points of hyperbox B_j are defined in Eqs. (2) and (3):

$$v_j = (v_{j1}, v_{j2}, v_{j3}, \dots, v_{jn}) \quad (2)$$

$$w_j = (w_{j1}, w_{j2}, w_{j3}, \dots, w_{jn}) \quad (3)$$

3.3 Membership Function

The membership function of the fuzzy hyperbox is used to measure the degree of belongingness of the input pattern to a hyperbox. The value of the membership function of a hyperbox B_j for the input pattern A_j lies between 0 and 1. The membership function is the sum of the two's complement of the average of the min point violation and the average of the max point violation. The membership function is defined in Eq. (4):

$$\begin{aligned} b_j(X_h) = & \frac{1}{2n} \sum_{i=1}^n [\max(0, 1 - \max(0, \gamma \min(1, x_{hi} - w_{ji}))) \\ & + \max(0, 1 - \max(0, \gamma \min(1, v_{ji} - x_{hi})))] \end{aligned} \quad (4)$$

Here $b_j(X_h)$ membership value of the input pattern X_h corresponds to the hyperbox b_j . γ is the sensitivity parameter that regulates the membership value, i.e., when the distance between hyperbox b_j and the input pattern X_h increases, the membership value decrease and vice versa.

4 FMM-Based Learning Methodology for IDS

The hyperbox learning process is the combination of the three subprocesses of expansion, overlap test, and the contraction process. In the intrusion detection learning process, first we select the input pattern along with the class label and then find the appropriate hyperbox for the same class. If the chosen hyperbox can accommodate the selected input pattern, we adjust the min and the max points of the hyperbox, otherwise we create the new hyperbox and assign the corresponding min and max points. Due to expansion of the existing hyperboxes or the new hyperbox creation process, it may create the problem of overlapping with the existing hyperboxes. Overlapping is eliminated with the help of contraction process. The hyperbox expansion, overlap test, and the contraction process are explained in the following subsections.

4.1 Hyperbox Expansion Phase

The goal of the hyperbox expansion process is to assign input pattern to the already existing hyperboxes that have the highest degree of membership value. If the membership function cannot accommodate it, then create a new hyperbox. The size of the hyperbox depends on the parameter θ which represents the size of the hyperbox. Let (x_h, c_h) be an ordered pair of the input pattern, $x_h = (x_{h1}, x_{h2}, \dots, x_{hn})$ be the set of the n input attributes, and c_h be the class label of the input pattern. The input pattern x_h is included in the hyperbox b_j .

$$n\theta \geq \sum_{i=1}^n (\max(w_{ji}, x_{hi}) - \min(v_{ji}, x_{hi})) \quad (5)$$

If Eq. (5) is satisfied then update the min and max points of the fuzzy hyperbox b_j , using Eqs. (6) and (7). Otherwise, create a new hyperbox and assign labels to the hyperbox. Then assign the min and max points to the hyperbox.

$$v_{ji}^{\text{new}} = \min(v_{ji}^{\text{old}}, x_{hi}) \quad \forall i = 1, 2, 3, \dots, n \quad (6)$$

$$w_{ji}^{\text{new}} = \max(w_{ji}^{\text{old}}, x_{hi}) \quad \forall i = 1, 2, 3, \dots, n \quad (7)$$

4.2 Hyperbox Overlap Test Phase

Suppose box B_1 is expanded in the previous step and box B_m is the box in the pattern space representing another class. The testing of possible overlap between the B_1 and the B_m is carried out by dimension-by-dimension comparison. The index of the dimension of the smallest overlap along any dimension is saved for contraction process. If $\delta^{\text{old}} - \delta^{\text{new}} > 0$ then $\Delta = i$ and $\delta^{\text{old}} = \delta^{\text{new}}$. Here Δ is the dimension index where there overlap exists. The overlap test is carried out for all the dimensions. If the overlap does not exist then the minimum overlap is set to indicate that the contraction is not necessary, i.e., $\Delta = -1$, initially $\delta^{\text{old}} = 1$.

Case 1. $v_{ji} < v_{ki} < w_{ji} < w_{ki}$

$$\delta^{\text{new}} = \min(w_{ji} - v_{ki}, \delta^{\text{old}})$$

Case 2. $v_{ki} < v_{ji} < w_{ki} < w_{ji}$

$$\delta^{\text{new}} = \min(w_{ki} - v_{ji}, \delta^{\text{old}})$$

Case 3. $v_{ji} < v_{ki} < w_{ki} < w_{ji}$

$$\delta^{\text{new}} = \min(\min(w_{ki} - v_{ji}, w_{ji} - v_{ki}), \delta^{\text{old}})$$

Case 4. $v_{ki} < v_{ji} < w_{ji} < w_{ki}$

$$\delta^{\text{new}} = \min(\min(w_{ji} - v_{ki}, w_{ki} - v_{ji}), \delta^{\text{old}})$$

4.3 Hyperbox Contraction Phase

The contraction process minimally disturbs the size of the hyperboxes. The contraction process depends on Δ , if $\Delta > 0$ then Δ is adjusted that will minimally disturb the shape of the boxes. The contraction process is covered in the following below-mentioned cases:

Case 1. $v_{j\Delta} < v_{k\Delta} < w_{j\Delta} < w_{k\Delta}$

$$w_{j\Delta}^{\text{new}} = v_{k\Delta}^{\text{new}} = \frac{(w_{j\Delta}^{\text{old}} + v_{k\Delta}^{\text{old}})}{2}$$

Case 2. $v_{k\Delta} < v_{j\Delta} < w_{k\Delta} < w_{j\Delta}$

$$w_{k\Delta}^{\text{new}} = v_{j\Delta}^{\text{new}} = \frac{(w_{k\Delta}^{\text{old}} + v_{j\Delta}^{\text{old}})}{2}$$

Case 3. (a) $v_{j\Delta} < v_{k\Delta} < w_{k\Delta} < w_{j\Delta}$ and $(w_{k\Delta} - v_{j\Delta}) < (w_{j\Delta} - v_{k\Delta})$ $v_{j\Delta}^{\text{new}} = w_{k\Delta}^{\text{old}}$

Case 3. (b) $v_{j\Delta} < v_{k\Delta} < w_{k\Delta} < w_{j\Delta}$ and $(w_{k\Delta} - v_{j\Delta}) > (w_{j\Delta} - v_{k\Delta})$ $w_{j\Delta}^{\text{new}} = v_{k\Delta}^{\text{old}}$

Case 4. (a) $v_{k\Delta} < v_{j\Delta} < w_{j\Delta} < w_{k\Delta}$ and $(w_{k\Delta} - v_{j\Delta}) < (w_{j\Delta} - v_{k\Delta})$ $w_{k\Delta}^{\text{new}} = v_{j\Delta}^{\text{old}}$

Case 4. (b) $v_{k\Delta} < v_{j\Delta} < w_{j\Delta} < w_{k\Delta}$ $(w_{k\Delta} - v_{j\Delta}) > (w_{j\Delta} - v_{k\Delta})$ $v_{k\Delta}^{\text{new}} = w_{j\Delta}^{\text{old}}$

4.4 Genetic Algorithm

Genetic algorithm is a search-based optimization technique and is based on the idea of natural selection. The genetic algorithm is basically used for optimization process. For example, in data clustering it can be used for centroid optimization. The optimization process starts from the selection of the initial population, then the selected individuals are evolved iteratively. The population is generated through crossover and mutation in each iteration is called generation. The fitness of each individual is evaluated in each generation. If the fitness of the newly generated offspring are better than the previous one, then the previous one is replaced by the new generated offspring, otherwise the previous offspring are kept as it is. The optimization process continues up to the n th generation or until some stopping criteria are achieved [12].

- **Crossover:** The crossover operator is used to mate two parents (chromosomes) to produce a new offspring (chromosomes).
- **Mutation:** Mutation operation is used to maintain the genetic diversity from one generation of the population to the next generation. The mutation process depends on the encoding as well as the crossover operation.
- **Fitness function:** The fitness function is used to evaluate the quality of the offspring which are generated through the crossover and mutation operations.
- **Termination:** The termination in GA tells when to stops the process. Common terminating conditions are: (1) A solution is found that satisfies minimum

criteria (ii) after fixed number of generations, (iii) allocated budget (computation time/money) reached, (iv) if system no longer produces better results, and (v) combinations of the above, etc.

5 Proposed FMM GA Algorithm

Input: Training set, testing set, θ (theta), γ and (sensitivity parameter), v_{ij} , w_{ij} , CP (Crossover probability) and MP (Mutation probability)

Output: FMM GA neural network

Process:

Step 1.

Start

Step 2.

Load the dataset

Step 3.

Specify the initial parameters θ , γ , CP, and MP.

Step 4.

If the input pattern is the first input pattern in the learning process, then assign the value of v_{ij} and w_{ij} .

Step 5.

For $i = 2$ to n

Step 5.1.

[Hyperbox expansion] For the j th input pattern identify the same class hyperbox that can accommodate it according to the membership function given in Eq. (4) and the expansion criteria given in Sect. 4.1. If not, create a new hyperbox and assign the min and max (v_{ij} and w_{ij}) of the hyperbox and then assign label of the box.

Step 5.2.

[Overlap Test] Check the overlap between the newly created or expanded hyperbox according to the cases given in Sect. 4.2 with existing. If any overlap goes to Step 5.3, else go to Step 5.4.

Step 5.3.

[Contraction process] Eliminate the overlap by minimally adjusting the dimensions of the hyperboxes according to the cases given in Sect. 4.3.

Step 5.4.

Increment i.

Step 5.5.

Stopping criteria matched, then go to Step 6 else go to Step 5.

Step 6.

Randomly select two parents having the same class by random selection.

Step 7.

Do crossover and mutation based on CP and MP to generate two new offspring. If

there is any overlap due to crossover and mutation, handle this according to Sects. 4.2 and 4.3.

Step 8.

Fitness evaluation and keep the best solutions and increment the generation.

Step 9.

If stopping criteria match, then go to Step 10 else go to Step 6.

Step 10.

Stop.

The FMM method for learning will execute a series of expansion, overlap test, and contraction process to complete the training process. Due to series of expansion, overlap test, and contraction processes, the size of the hyperboxes is affected and due to this the classification accuracy may be compromised. Therefore, in this paper genetic algorithm is used to optimize the hyperboxes. In other words, the genetic algorithm is used to optimize the min and max values of the hyperboxes. The algorithm begins with the fuzzy min-max learning expansion, overlap test, and the contraction process using the KDD CUP dataset. After the FMM learning the genetic algorithm is used to perform optimization task. The genetic algorithm (GA) modules begin with the chromosomes selection from the population; here the two hyperboxes are randomly chosen for crossover and mutation, which have the same class labels. The min and max values of the one selected chromosome is crossover with the min and max values of the other selected hyperbox. After the crossover operation the mutation operation is used to change the gene value(s) of the offspring so that the genetic diversity from one generation of population to the next generation of population can be maintained. Again, after crossover and mutation operations the new offspring are tested for possible overlaps with the other hyperboxes, if any, the contraction process is carried out. Finally, the fitness function is used to evaluate the fitness of the new offspring. The best individuals having high fitness values are updated in the population and the worst individuals are discarded. The genetic operations are repeated up to n generations. In our experimentation we tested the GA for n equal to 100,150,250 generations.

6 Results and Discussion

The developed IDS is evaluated with the KDD CUP 99 dataset. The dataset contains a wide variety of intrusion and normal data collected by the DARPA. The dataset contains a total of 41 attributes and one class attribute or the decision attribute, which describes the category of the traffic pattern, whether it is normal or attack [13]. In this experiment, a total of 11,850 instances were taken for experimentation, 7821 instances for training, and 4029 instances for testing the FMM IDS. The dataset is first preprocessed to remove the duplicate entries and convert the nominal attribute into numeric. Outlier and extreme values are filter based on interquartile ranges concept of Weka [14]. The FMM-based IDS is tested

Table 1 Result of the FMM GA IDS

θ	FMM NN		^a FMM GA	
	Accuracy	Error	Accuracy	Error
0.1	91.4231	8.5769	93.6548	6.3452
0.2	92.5032	7.4968	95.9391	4.0609
0.3	95.1770	4.8230	95.4330	4.5670
0.4	92.5032	7.4968	93.0114	6.9886
0.5	94.4162	5.5838	94.4162	5.5838

^aproposed**Table 2** Comparison of the FMM GA IDS with other systems

Methods	Accuracy	Error
MLP classifier	89.5658	10.4342
Multilayer perceptron	93.5964	06.4036
RBF classifiers	90.3946	09.6054
RBFN classifiers	81.8069	18.1931
SMO	91.6356	08.3644
Naïve bayes	67.3616	32.6384
LibSVM	91.4867	08.5133
KDD cup winner [15]	91.8000	08.2000
KDD cup runner UP [16]	91.5000	08.5000
FMM NN	95.1770	04.8230
Proposed FMMGA IDS	95.9391	04.0609

on sensitivity parameter $\gamma = 1$ and the following θ values 0.1, 0.2, 0.3, 0.4, and 0.5. Here θ is the size of the hyperbox.

Table 1 shows the result of our FMM NN and the FMM GA-based IDS on the different θ values 0.03, values 0.1, 0.2, 0.3, 0.4 and 0.5, FMM GA and FMM NN are implemented in the Windows 8, and 4 GB RAM, Core i5 processor and MATLAB 2014 environment. The FMM GA gives the better result compared to FMM NN. In FMM GA we used random selection, one point crossover with 80 % crossover probability, and mutation probability with 1 %. In the experimental process the method is executed 50 times for each θ values and the best results are recorded. The system gives the best performance at $\theta = 0.2$. At $\theta = 0.2$ FMM GA-based IDS provide the 95.9391 % accuracy and 4.0609 % classification error. The system gives 95.4330 % accuracy and 4.5670 % classification error at $\theta = 0.3$, which is the second best result. Table 2 shows the comparison of the proposed system with the other systems. The proposed FMM GA-based system is compared with the FMM NN, MLP classifiers, multilayer perceptron, and RBF classifier, RBFN Classifiers, SMO, naïve Bayes, LibSVM, KDD Cup Winner and KDD Cup Runner UP. The result of the MLP classifiers, multilayer perceptron, RBF classifier, RBFN Classifiers, SMO, naïve Bayes, LibSVM are evaluated on weka with default values. The proposed FMMGA IDS gives the best result and is adaptive in nature, can distinguish overlapping classes, and takes single scanning of the dataset for learning.

7 Conclusion and Future Work

In this paper an intrusion detection system is proposed which is based on the fuzzy min-max neural network and the genetic algorithm. The proposed system is evaluated using the KDD CUP dataset and the classification accuracy, classification errors are taken as the performance parameter. The dataset is first preprocessed to remove duplicated instances, outlier and extreme values, and then convert nominal attribute to numeric. The fuzzy min-max learning concept is used for the learning process and the genetic algorithm is used for hyperbox optimization. The proposed method is novel and it will have the online adaption capability, nonlinear separability, can distinguish from the overlapping classes, nonparametric classification, and less training time requirement for training compared to the traditional neural networks. The critical experimentation on the proposed system shows that the system performs well.

In the future, the proposed method can be used with the new membership function with different optimization techniques (such as PSO, ABC, etc.) to further improve the classification accuracy over the different datasets.

References

1. Liao, H.J., Lin, C.H.R., Lin, Y.C., Tung, K.Y.: Intrusion detection system: a comprehensive review. *J. Netw. Comput. Appl.* **36**(1), 16–24 (2013)
2. Yang, H., Li, T., Hu, X., Wang, F., Zou, Y.: A survey of artificial immune system based intrusion detection. *Sci. World J.* **11**, 1–5 (2014)
3. Tong, X., Wang, Z., Haining, Y.: A research using hybrid RBF/Elman neural networks for intrusion detection system secure model. *Comput. Phys. Commun.* **180**(10), 1795–1801 (2009)
4. Wang, G., Hao, J., Ma, J., Huang, L.: A new approach to intrusion detection using artificial neural networks and fuzzy clustering. *Expert Syst. Appl.* **37**(9), 6225–6232 (2010)
5. Lei, J.Z., Ghorbani, A.A.: Improved competitive learning neural networks for network intrusion and fraud detection. *Neurocomputing* **75**(1), 135–145 (2012)
6. Shun, J., Malki, H.A.: Network intrusion detection system using neural networks. In: Fourth International Conference on Natural Computation, 2008, ICNC'08, vol. 5, pp. 242–246. IEEE (2008)
7. Sarasamma, S.T., Zhu, Q.A., Huff, J.: Hierarchical Kohonen net for anomaly detection in network security. *IEEE Trans. Syst. Man Cybern. Part B: Cybern.* **35**(2), 302–312 (2005)
8. Linda, O., Vollmer, T., Manic, M.: Neural network based intrusion detection system for critical infrastructures. In: International Joint Conference on Neural Networks, 2009, IJCNN 2009, pp. 1827–1834. IEEE (2009)
9. Joo, D., Hong, T., Han, I.: The neural network models for IDS based on the asymmetric costs of false negative errors and false positive errors. *Expert Syst. Appl.* **25**(1), 69–75 (2003)
10. Zhou, Z.H., Jiang, Y.: NeC4.5: neural ensemble based C4.5. *IEEE Trans. Knowl. Data Eng.* **16**(6), 770–773 (2004)
11. Simpson, P.K.: Fuzzy min-max neural networks. I. Classification. *IEEE Trans. Neural Netw.* **3**(5), 776–786 (1992)
12. Freitas, A.A.: Evolutionary algorithms for data mining. In: Data Mining and Knowledge Discovery Handbook, pp. 435–467. Springer, New York (2005)

13. Cup, K.D.D.: Dataset (2009). <http://kdd.ics.uci.edu/databases/kddcup99/kddcup99.html>
14. Hall, M., Frank, E., Holmes, G., Pfahringer, B., Reutemann, P., Witten, I.H.: The WEKA data mining software: an update. ACM SIGKDD Explor. Newslett. **11**(1), 10–18 (2009)
15. Pfahringer, B.: Winning the KDD99 classification cup: bagged boosting. ACM SIGKDD Explor. Newslett. **1**(2), 65–66 (2000)
16. Levin, I.: KDD-99 classifier learning contest: LLSoft's results overview. SIGKDD Explor. **1**(2), 67–75 (2000)

Real-Time Fault Tolerance Task Scheduling Algorithm with Minimum Energy Consumption

Arvind Kumar and Bashir Alam

Abstract In this paper, we propose a fault tolerance real-time task scheduling algorithm with energy minimization. A fault in a system can be recovered at runtime without participation of external agent. It maintains enough time redundancy so that task can be re-executed in presence of fault. It can be achieved by check-pointing policy which gives reliability in a system. For reliable fault tolerance in a system, optimal number of checkpoints is applied and save the system from complete re-execution. Energy minimization can be achieved by dynamic voltage scaling (DVS). In this paper, existing real-time scheduling algorithm has been modified for fault tolerance and energy minimization. To minimize energy consumption voltage level is adjusted with respect to deadline of the system and check the schedulability of test on each task. The worst-case execution time is associated with voltage level for each task. The result shows that energy consumption is reduced with maximum task scheduling in a system.

Keywords Real-time system • Fault tolerance • DVS • Scheduling

1 Introduction

There are three different types of fault such as: transient, intermittent, and permanent fault which can arrive in a system. A transient fault is caused by some inherent error in the system. Transient faults are mainly considered for fault tolerance because these faults can be removed at runtime by re-execution of task. Transient faults are more frequently occurring in a system than permanent or intermittent

A. Kumar (✉) · B. Alam

Department of Computer Engineering, Faculty of Engineering and Technology,
Jamia Millia Islamia, New Delhi, India
e-mail: arvinddagur@gmail.com

B. Alam

e-mail: babashiralam@gmail.com

© Springer India 2016

S.C. Satapathy et al. (eds.), *Proceedings of the Second International Conference on Computer and Communication Technologies, Advances in Intelligent Systems and Computing* 380, DOI 10.1007/978-81-322-2523-2_42

441

fault. Fault tolerance is used to avoid failure in presence of fault in a system. A fault can not be easily detected in the system. To tolerate transient fault in real-time systems, we should use the most common time redundancy fault tolerance techniques such as re-execution, checkpointing, or rollback [1, 2]. Checkpointing is that approach which saves first necessary state of the system onto CPU [3].

DVFS is commonly used approach to minimize energy consumption in the real-time systems. Dynamic voltage and frequency scaling (DVFS) is assigned a voltage level that is adjusted according to available slack. During execution, each task is assigned a voltage level and adjusted that voltage to minimize energy consumption [4–6]. The energy consumption can be defined for each task such that, if E is the energy required for a system, V is voltage, and f is frequency then $E \propto V^2f$.

By reducing voltage or frequency of a system, the total power consumption is also reduced. In this paper, we proposed a task scheduling algorithm such that a transient fault can recover on run time. Proposed approach is also used to reduce energy consumption in presence of fault.

Rest of the paper is organized as follows. The Related work is presented in Sect. 2. In Sect. 3 basic models have been explained. The proposed algorithm with problem description is presented in Sect. 4. Section 5 shows the results and analysis of this paper. Finally Sect. 6 concludes the paper.

2 Related Work

Most of the systems are depends upon time constraint. The systems which depend upon time are known as real-time systems. These systems can be categorized in hard and soft real-time systems. There are many scheduling algorithm for real-time system [2, 7–9]. There are two basic algorithms for real-time task scheduling. Static scheduling algorithm based on fixed period and dynamic scheduling algorithm based on dynamically arrival of task. Earliest deadline first (EDF) scheduling approach is used to schedule aperiodic tasks in various time critical applications. However, EDF does not provide mechanisms for faults tolerance and energy minimization. The purpose of real-time systems is to provide services on time even there is fault in the system.

Various approaches also have been proposed for fault tolerance in real-time systems [1, 2, 7, 8, 10]. The transient fault in a system is tolerated using checkpointing [7]. Energy minimization approaches in real-time systems also have been proposed by many authors [4, 5]. The commonly used approaches for energy minimization are depending upon voltage and frequency. DVS is basic approach for energy minimization based on dynamic voltage scaling and its corresponding frequency scaling approach without fault tolerance [11]. The researchers are working to combine DVS approach with fault tolerance [12].

3 Models

3.1 Task Model

A set of aperiodic tasks where $T = \{T_1, T_2, \dots, T_n\}$ is considered for scheduling. Each task $T_i = (a_i, c_i, d_i)$ has three variables such as a_i is arrival time, c_i is computation time, and d_i is deadline. Each task T_i is associated with voltage V_i and frequency f_i and released on its arrival time with execution/computation time and deadline [2, 8]. We consider at least one task is arriving at initial time.

3.2 Energy Model

There are two voltage level defined for a system. V_{\max} is maximum voltage level and V_{\min} is minimum voltage level. The energy minimization can be achieved by reducing voltage level from maximum to minimum. A task executes between these two voltage levels. We consider voltage level $V = \{V_{\min} \text{ to } V_{\max}\}$ where each voltage level is associated with its corresponding frequency and speed. The energy consumption can be computed by applying $E \propto V^2 f$.

4 Problem Description and Proposed Approach

We design a non-preemptive task scheduling algorithm for fault tolerance and minimized energy consumption. The tasks are independent, aperiodic, and non-preemptive. The proposed approach is used to tolerate only single transient fault in the system. We are considering various assumptions for each task T_i in a task set T . Each task in the task set has arrival time, execution/computation time, and deadline. There are n number of checkpoints applied for fault tolerance with overhead $r = 1$. We consider at least one task is arriving at time $t = 0$. A task is executed at various voltage level to reduce energy consumption and it lies between $V_{\min} < V < V_{\max}$. We also consider m is number for checkpoints applied on higher priority task. WCET is worst-case execution time required to finish each task.

The proposed algorithm works as follows

Input: Set of tasks $T = \{T_1, T_2, T_3, \dots, T_n\}$, Voltage V and Frequency f.

Output: Tasks Schedulability with fault tolerance and energy minimization

1. Begin
2. At $t = 0$
 - Find the number of task arrived
 - Select the task with minimum deadline
3. While(true), //Checks the schedulability of each task
 - { If $c_i \leq d_i - a_i$
 - Then Task can be scheduled
 - else task is not schedulable
 - check schedulability of another task
 - }
 - go to step 4
4. if (fault = true) then
5. Apply optimal number of checkpoint
6. Find the total worst case execution time for fault recovery.
7. $WCET = c_i + (c_i/n) + n*r + \sum_{j \in T_h}^n c_j + (c_j/m) + m*r$
 - If ($WCET < d_i$)
 - Then Task is schedulable
 - Apply DVS to minimize energy consumption start with minimum voltage level
 - Else task not schedulable with fault tolerance
8. Exit

Let us consider a set of four aperiodic tasks given in Table 1 and calculate the WCET with assuming that no fault is in the system. We apply the schedulability test and check all the tasks are schedulable on maximum voltage level V. We then apply DVS on the task set as shown in Table 2 to minimize the energy consumption. We reduce the voltage level up to 0.5 V on first task and then check the schedulability. First task is schedulable on reducing voltage 0.5 V then again apply DVS on all other tasks with consideration of deadline. Task 2, task 3, and task 4 are also schedulable with 0.5 V. By applying mean, we can say that energy consumption is reduced up to 50 % in the given task set.

Table 1 Task schedulability without fault

a_i	c_i	d_i	m	WCET	Schedulability test
0	2	7	0	2	Yes
2	4	20	0	4	Yes
3	6	25	0	10	Yes
7	4	32	0	14	Yes

Table 2 Task schedulability with DVS without fault

a_i	c_i	d_i	m	Voltage level (V)	WCET	Schedulability test	Energy saving (%)
0	2	7	0	0.5	4	Yes	50
2	4	20	0	0.5	12	Yes	50
3	6	25	0	0.5	24	Yes	50
7	4	32	0	0.5	32	Yes	50

Table 3 Task schedulability with fault

a_i	c_i	d_i	m	WCET	Schedulability test
0	2	7	1	3	Yes
2	4	20	2	9	Yes
3	6	25	3	18	Yes
7	4	32	2	24	Yes

Table 4 Task schedulability with DVS with fault

a_i	c_i	d_i	m	Voltage level (V)	WCET	Schedulability test	Energy saving
0	2	7	2	0.5	6	Yes	50 %
2	4	20	3	0.75	16	Yes	25 %
3	6	25	3	1.0	25	Yes	0
7	4	32	2	1.0	31	Yes	0

We then apply fault tolerance approach and then check schedulability as shown in Table 3. All tasks are schedulable with single transient fault tolerance on maximum power supply. Then we apply DVS to reduce energy consumption as shown in Table 4. We reduce the voltage level by half of actual voltage. First task is schedulable on 0.5 V with 50 % energy saving but the second task is not schedulable on the same. We then apply increased voltage level and second task is schedulable on 0.75 V with 25 % energy saving. Rest of the two tasks are schedulable on maximum voltage level with no energy saving. Here we again apply mean which results approx 18.5 % energy saving. Table 4 shows the various voltage level and task schedulability. The tasks are schedulable with fault tolerance and save energy.

5 Results and Simulation

To simulate the proposed algorithm, we did some simple experiments and analyzed the results. The experiments have been done in C++ and then the results are compared. We check the schedulability and apply DVS on various voltage levels. DVS is suitable approach in reducing energy consumption. We then applied fault

tolerance and checked the schedulability. Most of the tasks are schedulable with single transient fault. After this, we tested the schedulability with DVS and fault tolerance and found that the tasks are schedulable with fault tolerance and energy consumption is reduced. The proposed approach is more suitable to tolerate transient fault with minimum energy consumption. As described in the proposed algorithm, each task scheduled by existing EDF is also schedulable by proposed approach in presence of fault. The task with sufficient deadline will be schedulable if it has been scheduled with proposed approach.

Graph in Fig. 1 shows the task schedulability when there is no fault in the system. This graph is also showing the task schedulability with DVS used for energy minimization. Each task has its own arrival time, execution time, and deadline, respectively. WCET (without fault) shows the schedulability using existing EDF approach. WCET of each task is less than its deadline which shows task schedulability. WCET (without fault, with DVS) shows the task schedulability with energy minimization.

Graph in Fig. 2, shows the task schedulability with fault using proposed approach. This graph is also showing the task schedulability of four tasks when

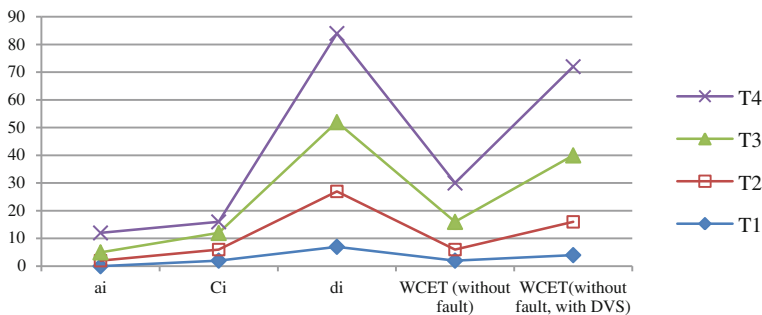


Fig. 1 Task scheduling with existing approach without fault and with DVS

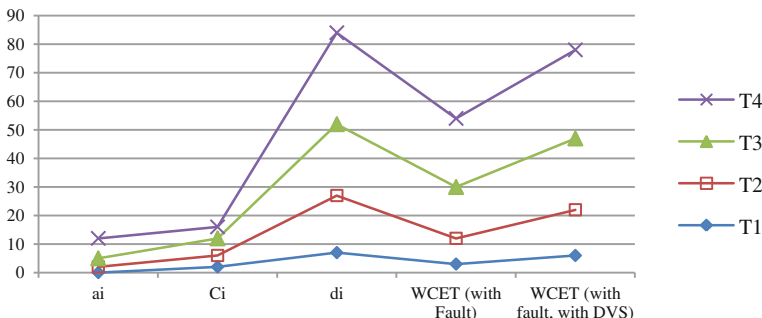


Fig. 2 Task scheduling with proposed approach with fault and with DVS

there is fault in the system with minimum energy consumption. WCET (With fault) and WCET (with fault, with DVS) of each task is less than respective deadline which shows that the tasks are schedulable when there is fault in the system with minimum energy consumption.

6 Conclusion

Fault tolerance in a real time is achieved using checkpointing and energy consumption is achieved using by DVS approaches. The proposed approach is the combination of both existing fault tolerance approach and energy minimization approaches simultaneously. This proposed scheduling algorithm is more suitable for scheduling large number of tasks in presence of fault. It is able to reduce energy consumption by 10–15 % in the presence of fault. As each task is associated with a voltage level as well as frequency, DVS used various voltage and frequency level to minimize energy consumption. The existing algorithm is modified such that feasibility for each task within minimized energy consumption is achieved. An experiment has shown the comparison between existing EDF approach and proposed approach with and without fault, respectively. Existing EDF could find a feasible schedule but proposed approach is better for fault tolerance scheduling with energy minimization.

References

1. Dima, C., Girault, A., Lavarenne, C., Sorel, Y.: Off-line real-time fault-tolerant scheduling. In: Euromicro Workshop on Parallel and Distributed Processing, Mantova, Italy, February 2001
2. Alam, B., Kumar, A.: A real time scheduling algorithm for tolerating single transient fault. Inf. Syst. Comput. Netw. (ISCON). In: 2014 International Conference on, pp. 11–14, 1–2 March 2014
3. Pradhan, D.K.: Fault Tolerance Computing: Theory and Techniques. Prentice Hall (1986)
4. Huang, K., Santinelli, L., Chen, J., Thiele, L., Buttazzo, G.: Adaptive dynamic power management for hard real-time systems. In: Proceedings of the IEEE Real-Time Systems Symposium (2009)
5. Zhang, Y., Chakrabarty, K.: Energy-aware adaptive checkpointing in embedded real-time systems. In: Proceedings of the DATE (2003)
6. Pillai, P., Shin, K.: Real-time dynamic voltage scaling for low-power embedded operating systems. In: Proceedings of the ACM Symposium on Operating Systems Principle (2001)
7. Liu, Y., Liang, H., Wu, K.: Scheduling for Energy Efficiency and Fault Tolerance in Hard Real Time Systems. 978-3-9810801-6-2/DATE10 © 2010 EDAA, pp. 1444–1449
8. Kumar, A., Alam, B.: Real time scheduling algorithm for fault tolerant and energy minimization. Issues Challenges Intell. Comput. Tech. (ICICT). In: 2014 International Conference on, pp. 356–360, 7–8 Feb 2014
9. Kumar, A., Yadav, R.S., Ranvijay, A.J.: Fault tolerance in real time distributed system. Int. J. Comput. Sci. Eng. (IJCSE) 3(2), 933–939 (2011)
10. Izosimov, V., Pop, P., Eles, P., Peng, Z.: Scheduling of fault-tolerant embedded systems with soft and hard timing constraints. In: Proceedings of the DATE (2008)

11. Woonseok, K., Dongkun, S., Han-Saem, Y., Jihong, K., Sang, M.L.: Performance comparison of dynamic voltage scaling algorithms for hard real-time systems. In: Proceedings of the Eighth IEEE Real-Time and Embedded Technology and Applications Symposium (RTAS'02), pp. 219–228 (2002)
12. Melhem, R., Mossé, D., Elnozahy, E.: The interplay of power management and fault recovery in real-time systems. *IEEE Trans. Comput.* **53**(2), 217–231 (2004)

Completely Separable Reversible Data Hiding with Increased Embedding Capacity Using Residue Number System

Geethu Mohan and O.K. Sikha

Abstract Separable reversible data hiding techniques facilitate hiding and extraction of data in the encrypted domain. This paper proposes a novel method to embed binary data in an encrypted cover image that provides complete independence of data extraction and covers image recovery. This allows the content owner to retrieve the host signal without any distortion regardless of the embedded data and the data hider to perform lossless extraction of embedded message. The method also provides a high data-embedding capacity using Residue number system (RNS) technique and ensures that only an authorized person can access the contents of the plain image.

Keywords Separable reversible data hiding · Residue number system (RNS) · Privacy preserving data embedding

1 Introduction

In this internet era, the trend has been shifted from “easy access” of information to “secure access.” Data hiding is SA method where the secret data is embedded into a cover media like images or any other signals and later the data is recovered from the host. Reversible data hiding is the data hiding technique in which stego-media can be restored to the original host signal without distortion [1]. Reversible data hiding techniques are classified into three classes—algorithms for fragile authentication, algorithms to achieve high data-embedding capacity, and algorithms for semi-fragile authentication [2]. Honsinger et al.’s patent in 2001 [3] describes how can we use reversible data hiding mechanism to provide fragile authentication.

G. Mohan (✉) · O.K. Sikha
Amrita School of Engineering, Amrita Vishwa Vidyapeetham (University),
Coimbatore, India
e-mail: m_geethu@cb.amrita.edu

O.K. Sikha
e-mail: ok_sikha@cb.amrita.edu

They have used modulo256 addition for embedding data into cover image. Goljan et al. [4] proposed a reversible data hiding scheme, known as R-S scheme to perform lossless data embedding in images. Xuan et al. came up with three reversible data hiding methods [5–7] based on integer wavelet transform. The three algorithms were developed on the IWT domain and they embed data into the high-frequency subband coefficients.

Application of RDH in encrypted images enables data hiding in the encrypted domain, so that the contents of the plain image are unavailable to the data hider. In applications like remote sensing, law enforcement, military imaging, and medical image systems, it may be required to embed some extra information like source information, authentication information, metadata to be used by the databases or data mining applications, additional data to manage the storage/distribution of images, etc. In such cases, recovery of the host media without any distortions is highly desirable. Also, it should be possible to perform the data embedding and extraction in the encrypted image so that plain image contents are accessible only to the content owner [8, 9]. In [10] Zhang proposes a reversible data hiding algorithm where data is embedded into the encrypted image. To retrieve the data, the image is initially decrypted. Thereafter, the data is extracted based on the features of the decrypted image. Here the data extraction process is done in the plain image which causes privacy concerns. In medical image databases, military images, etc., it should be possible to perform data embedding as well as extraction in the encrypted domain so that the privacy of the image contents is preserved. Zhang [11] presents a separable reversible data hiding method, in which the data embedding and extraction process is independent of the image encryption and decryption. Here, the image is initially encrypted using an encryption key. In the encrypted image, data is hidden by the data hider using a data hiding key. At the receiver side, a data hider with data hiding key can directly extract the data from the encrypted image. A receiver with both encryption and data hiding key can perform image decryption and data extraction. A person with encryption key alone can partially recover the original image. Ma et al. [8] proposed another scheme with better reversibility and higher data-embedding capacity than the methods in [10, 11]. But here also the content owner without the data hiding key cannot perfectly recover the original image. A separable RDH method is proposed in [12] which allows reconstruction of the cover image without performing data extraction but has a limited data-embedding capacity.

Chaos: a state of disorder is a mathematical discipline which deals with the study of behavior of nonlinear dynamical systems. Dynamic systems are assumed to be deterministic but they are highly sensitive towards the initial conditions, i.e., points in the chaotic system are closely approximated by other point with significantly different future trajectories. Edward Lorenz came up with “Lorenz system” which is able to provide a chaotic solution for a certain initial condition and parameter. People have used the dynamic behavior of chaos systems for securing data through encryption. The main advantages of the chaotic encryption approach include: good privacy due to both nonstandard approach and vast number of variants of chaotic systems, high flexibility in the encryption system design, large, complex, and

numerous possible encryption keys and simpler design [13]. In this work we have used a chaos-based procedure to generate permutation key [14].

Residue number system [15] allows an integer N to be represented by a set of k integers (n_1, n_2, \dots, n_k) using a k -tuple (v_1, v_2, \dots, v_k) called moduli. Each residue n_i is obtained as $n_i = N \bmod v_i$. An integer N can be uniquely represented as a k -tuple residue vector (n_1, n_2, \dots, n_k) , provided that every pair (v_i, v_j) of the modulus vector is relatively prime and $\prod_{i=1}^k v_i > N$. Given the residue vector and corresponding modulus vector, integer N can be calculated using Chinese remainder theorem. A method to embed three water mark images in a color image using RNS has been proposed in [16].

This paper proposes a new scheme for separable reversible data hiding in encrypted domain with high data-embedding capacity. The original image is encrypted using an encryption key. The data to be embedded undergoes a chaos-based permutation and is embedded into the encrypted image. At the receiver side, the embedded bits are extracted and the reverse permutation is applied to obtain the original data. The content owner can perfectly reconstruct the cover image from the marked encrypted image without going through the data extraction phase.

2 Proposed System

Figure 1 gives an outline of the proposed system.

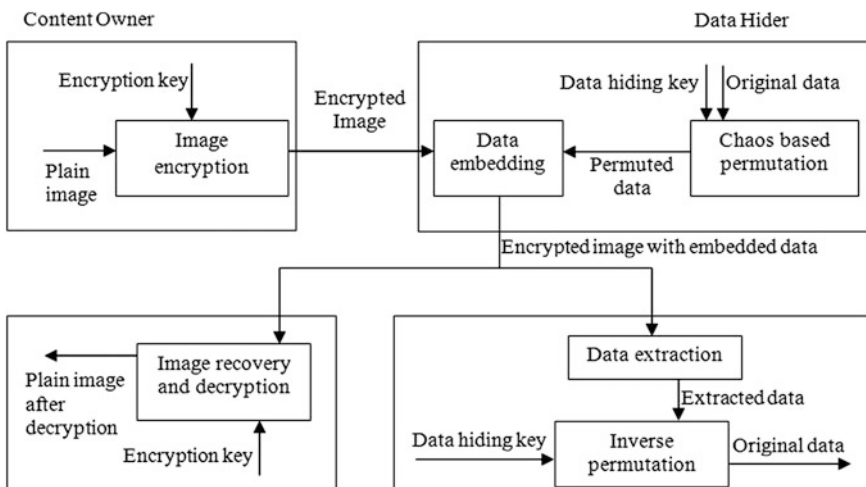


Fig. 1 Block diagram of the proposed system

2.1 Image Encryption

The input is an $N \times N$, 8-bit grayscale image, I with pixel grayscale values falling into the range [0, 255]. The input image I is encrypted using a standard encryption algorithm to form the encrypted image E . This encrypted version is provided as input to the data hiding stage, so that the original contents of the image remains inaccessible to a person without the encryption key.

2.2 Data Hiding

Let the binary data to be embedded into the encrypted image E , is represented as d (1), $d(2)$, ..., $d(L)$, where L denotes the length of the binary data vector d . The binary string is then shuffled using a chaos-based algorithm [14]. Let the binary string after permutation be denoted by D . The main disadvantage of usual permutation procedure is the high demand for memory, i.e., we require a permutation key as long as the message, which will double the memory requirement. Irrespective of the length of data to be embedded, chaos method will allow to randomly permute the bits based on the initial condition. The input image is scanned row wise and the data bits are embedded into each pixel value. Depending on the length of D and size of image E , the data embedding proceeds as follows.

Case 1: $L \leq N * N$

Binary string D is embedded into the encrypted image based on the following rule

- If $D(x) = 0$ and $E(i,j) \bmod 2 = 0$, then $E'(i,j) = E(i,j)$.
 - If $D(x) = 1$ and $E(i,j) \bmod 2 = 0$, then $E'(i,j) = E(i,j) + 1$.
 - If $D(x) = 0$ and $E(i,j) \bmod 2 = 1$, then $E'(i,j) = (E(i,j) + 1) * -1$.
 - If $D(x) = 1$ and $E(i,j) \bmod 2 = 1$, then $E'(i,j) = -E(i,j)$.
- (1)

where $E'(i,j)$ is the value obtained after embedding a bit into encrypted image pixel $E(i,j)$ and $1 \leq x \leq L$.

Case 2: $L > N * N$

A set of residue matrices R_1, R_2, \dots, R_m is generated from E using residue number system where m is calculated as $L/(N * N)$. A modulus vector V , (v_1, \dots, v_m) is chosen such that $\prod_{i=1}^m v_i > 255$ and $\gcd(v_i, v_j) = 1 \forall i, j = 1, 2, \dots, m$ and $i \neq j$.

The element at location (i, j) of the k th residue matrix $R_k(i,j)$ is calculated as $R_k(i,j) = E(i,j) \% v_k$, so that $E(i,j)$ is represented by m residues $R_1(i,j), \dots, R_m(i,j)$ that are distributed across m residue matrices.

Now data bits $D_{x*N*N+1}$ to $D_{N*N*(x+1)}$ for $x = 0$ to $L - 1$ can be embedded in residue matrix R_{x+1} following the rule in Eq. (1).

2.3 Data Extraction

The data embedded into the encrypted image can be extracted and the data hider with the corresponding data hiding key can apply the inverse permutation to get back the original data. The data extraction is done on the encrypted image, which prevents the image content from being viewed by an unauthorized user. The input to the data extraction phase is the encrypted, data-embedded image E' . The pixels of the input image are scanned row wise to extract the embedded bits as follows.

If the absolute value of $E'(i, j)$ is even or equal to 0, then the data bit embedded is 0. If the absolute value of $E'(i, j)$ is odd, then the data bit embedded is 1.

Once the data bits are extracted, the original binary data can be obtained by performing the inverse permutation.

2.4 Image Recovery

The encrypted image E is reconstructed from E' as follows.

If the absolute value of $E'(i, j)$ is even or equal to 0,

$$\begin{aligned} \text{Encrypted pixel value } E(i, j) &= E'(i, j), \text{ if } E'(i, j) \geq 0. \\ &= \text{abs}(E'(i, j)) - 1 \text{ if } E'(i, j) < 0. \end{aligned} \quad (2)$$

If the absolute value of $E'(i, j)$ is odd,

$$\begin{aligned} \text{Encrypted pixel value } E(i, j) &= E'(i, j) - 1 \text{ if } E'(i, j) > 0. \\ &= \text{abs}(E'(i, j)) \text{ if } E'(i, j) < 0. \end{aligned} \quad (3)$$

where $\text{abs}(z)$ denotes the absolute value of z .

If the image consists of only one share, as described in Case 1 of Sect. 2.2, the above steps will recover the pixels of encrypted image E . When the image is divided into multiple shares as in Case 2, the recovery is done as follows.

The rule specified in (2), (3) is applied to each of the data-embedded residue matrices to get back m residue matrices (R_1, \dots, R_m).

The encrypted pixels $E(i, j)$, $1 \leq i, j \leq N$ is obtained by solving the following set of congruences using Chinese remainder theorem.

$$E(i, j) \equiv R_1(i, j) \pmod{v_1}$$

$$E(i, j) \equiv R_2(i, j) \pmod{v_2}$$

$$\vdots$$

$$E(i, j) \equiv R_m(i, j) \pmod{v_m}, \quad \text{where } (v_1, \dots, v_m) \text{ is the modulus vector.}$$

Once the encrypted image E has been reconstructed, the content owner can use the encryption key to get back the plain image. The method ensures that the original image is perfectly recovered.

3 Results and Discussion

The complete separation of data hiding/extraction and cover image recovery is ensured by the proposed method in the following aspects. Data hider can perform data embedding and extraction on the encrypted image. From the extracted bits, the original data can be recovered using the permutation/data hiding key. The content owner can recover the encrypted image from the data-embedded encrypted image without having the knowledge of the data hiding key. The recovered image can be further decrypted with the encryption key to get back the plain image. If the data has been embedded into multiple shares of the image using RNS, then the data hider should recreate the original encrypted image using the modulus vector before the content owner can perform decryption. Otherwise, the modulus vector should be communicated over a secure channel to the content owner so that the encrypted image reconstruction is fully performed by the content owner. Compared to the method in [12], the proposed method provides higher data-embedding capacity and allows complete reconstruction of the cover image from the encrypted stego image using only the encryption key.

The privacy of the content owner is preserved since the data hiding and extraction is performed in the encrypted domain. A person having the data hiding key can correctly recover the embedded message from the extracted data bits. When the data is stored into the residue matrices, an additional layer of security is provided by the fact that the embedded data can be fully extracted only if all the residue matrices are available. Besides, recreation of the cover image is possible only with the knowledge of the modulus vector and availability of all the residue matrices.

In an $N \times N$ grayscale image N^2 bits can be embedded, as per the method specified in Case1. The embedding capacity can be increased as per the method in Case2, at the cost of increase in storage space. In this case, the number of bits that can be embedded is limited by the size of the modulus vector that is chosen to create the residue matrices. With a modulus vector of length m , the method can embed $m * N^2$ bits.

The proposed system was tested using four standard 256×256 -sized images and the obtained results are shown in Table 1. $\text{PSNR} = \infty$ indicates that the original image has been perfectly reconstructed from the encrypted embedded image (Fig. 2).

Table 1 PSNR and similarity index (SSIM) of four standard test images. Number of shares = 1 denotes case 1 of Sect. 2.2. Number of shares = 2, 3 indicates the result corresponding to case 2 with modulus vector length = 2, 3, respectively

Image	Number of shares-1		Number of shares-2		Number of shares-3	
	PSNR	SSIM	PSNR	SSIM	PSNR	SSIM
Lena	∞	1	∞	1	∞	1
Barbara	∞	1	∞	1	∞	1
Boat image	∞	1	∞	1	∞	1
Cameraman	∞	1	∞	1	∞	1

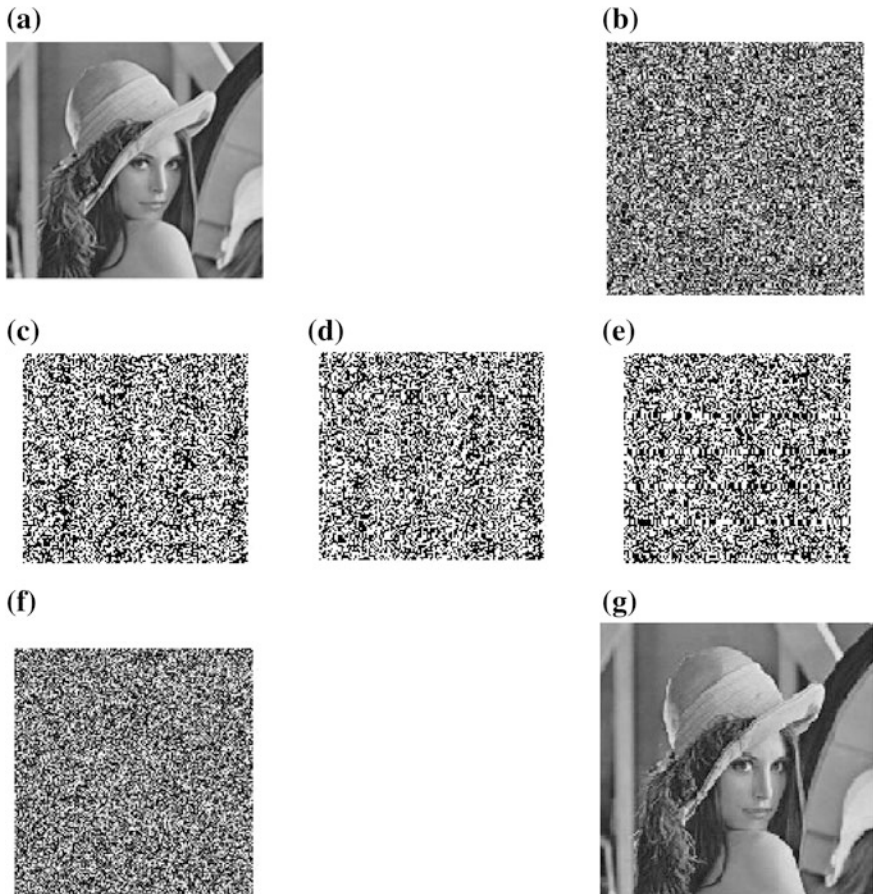


Fig. 2 **a** Original Lena image. **b** Encrypted Lena image. **c–e** Encrypted data-embedded residue matrices. **f** Image after data recovery. **g** Decrypted image

4 Conclusion and Future Work

The proposed algorithm performs separable reversible data hiding on encrypted images allowing complete independence of data embedding/extraction from cover image reconstruction. Performing the data embedding and extraction in encrypted domain ensures that privacy of the content owner is preserved. Also it ensures that the embedded data and original image is available to users with appropriate keys. A drawback of the method is the increased storage requirements when data is embedded into multiple shares of the image created using RNS techniques. The data hiding process can be made more secure by pseudorandomly selecting the pixels positions to embed the data bits. Future work includes making the data hiding more secure and robust, along with reducing the space requirements without sacrificing the data-embedding capacity.

References

- Nosrati, M., Karimi, R., Hariri, M.: Reversible data hiding: principles, techniques, and recent studies. *World Appl. Program.* **2**(5), 349–353 (2012)
- Shi, Y.Q.: Reversible data hiding. Cox, I.J., et al. (eds.): IWDW 2004, LNCS 3304, pp. 1–12 (2005)
- Honsinger, C.W., Jones, P., Rabbani, M., Stoffel, J.C.: Lossless recovery of an original image containing embedded data. US Patent: 6,278,791 (2001)
- Goljan, M., Fridrich, J., Du, R.: Distortion-free data embedding. In: Proceedings of 4th Information Hiding Workshop, pp. 27–41. Pittsburgh, April (2001)
- Xuan, G., Zhu, J., Chen, J., Shi, Y.Q., Ni, Z., Su, W.: Distortionless data hiding based on integer wavelet transform. In: *IEE J. Electron. Lett.* **38**(25), 1646–1648 (2002)
- Xuan, G., Shi, Y.Q., Ni, Z.: Lossless data hiding using integer wavelet transform and spread spectrum. In: IEEE International Workshop on Multimedia Signal Processing, Siena, Sept 2004
- G. Xuan, Shi, Y.Q., Ni, Z.: Reversible data hiding using integer wavelet transform and companding technique. In: Proceedings of IWDW04, Korea, Oct 2004
- Ma, K., Zhang, W., Zhao, X., Yu, N., Li, F.: Reversible data hiding in encrypted images by reserving room before encryption. In: *IEEE Trans. Inf. Forensics Secur.* **8**(3) 553–562 (2013)
- Coatieroux, G., Lecornu, L., Sankur, B., Roux, C.: A review of image watermarking applications in healthcare. In: 28th Annual International Conference of the IEEE Engineering in Medicine and Biology Society, pp. 4691–4694. EMBS '06, 30 Aug–3 Sept 2006
- Zhang, X.: Reversible data hiding in encrypted image. *IEEE Signal Process. Lett.* **18**(4), 255,258 (2011)
- Zhang, X.: Separable reversible data hiding in encrypted image. In: *IEEE Trans. Inf. Forensics Secur.* **7**(2), 826–832 (2012)
- Fujiyoshi, M.: Separable reversible data hiding in encrypted images with histogram permutation. In: IEEE International Conference on Multimedia and Expo Workshops (ICMEW), pp.1–4. 15–19 July (2013)
- Grigoras, V., Grigoras, C.: Chaos encryption method based on large signal modulation in additive nonlinear discrete-time systems. In: Proceedings of the 5th WSEAS International Conference on Non-Linear Analysis, Non-Linear Systems and Chaos, Bucharest, 16–18 Oct 2006

14. Prasad, M., Sudha, K.L.: Chaos Image Encryption using Pixel shuffling. In: Wyld, D.C. et al. (eds) CCSEA 2011, CS & IT 02, pp. 169–179 (2011)
15. Garner, H.L: The residue number system. IRE Trans. Electron. Comput. **EC-8**(2), 140–147 (1959)
16. Banerjee, S., Chakraborty, S., Dey, N., Pal, A.K., Ray, R.: High payload watermarking using residue number system. Int. J. Image Gr. Signal Process. **3**, 1–8 (2015)

A Metric for Ranking the Classifiers for Evaluation of Intrusion Detection System

Preeti Aggarwal and Sudhir Kumar Sharma

Abstract Imbalance in data is quite obvious while studying intrusion detection system (IDS). Classification algorithms are used to identify the attacks in IDS, which has many parameters for its performance evaluation. Due to imbalance in data, the classification results need to be revisited given that IDS generally evaluates detection rate and false alarm rate which belongs to two different classes. This paper validates a new metric NPR used for ranking the classifiers for IDS. The metric is made functional on KDD data set and then the classifiers are ranked and compared with results on another data set.

Keywords Intrusion detection system • Imbalanced data • KDD data set • False alarm rate • Detection rate • NPR

1 Introduction

Internet is an open platform inviting all sorts of users and applications with different intentions and motivations. The exponential growth of internet users has made it apparent to make the use of intrusion detection system (IDS) obligatory. The IDS basically uses the host or the network traffic data to study the pattern of data exchange and hence detect the malicious activity. The techniques of IDS involve misuse and anomaly detection [1].

KDD data set is a very popular data set used in the study of IDS. This data set has evolved from the novel DARPA [2] data set to enhanced KDDCUP'99 data set [3]. The latest improvement of KDD data set is the NSL-KDD [4] data set which

P. Aggarwal (✉) · S.K. Sharma

School of Engineering and Technology, Ansal University, Gurgaon, India
e-mail: preetaggerwal@gmail.com

S.K. Sharma
e-mail: sudhir_sharma99@yahoo.com

overcomes some of the disadvantages of earlier versions [5] like redundancy in the data set.

The imbalance in data [6] is understandable in case of IDS because the chances of attacks happening on the system are not very frequent as compared to the routine data flowing through the network. Therefore, the network traffic data will always carry more normal instances and less attack instances. This realistic imbalance present in data set used for the study of IDS gives rise to biasing of classification results towards the class having comparatively more number of instances. Though there are many techniques available to overcome the problem of imbalance in data set like bagging and boosting [7, 8], very few measures are available which can help interpret the results better. The ensemble approach is also quite useful to tackle the problem of imbalanced data sets [9].

Some of the well-known metrics used for the study IDS are accuracy and F-score. Accuracy is the overall measure of the system's performance in terms of correct 'positive class' predictions. Considering the case of imbalanced data, a high accuracy value may actually mean good accuracy for the class having more number of instances but not for the sparse class [10]. F-score is the combined measure of the detection rate and precision for a classifier which does not present much information about the negative class. The negative class is also required to be studied for IDS because false positive predictions lead to false alarm rates. Receiver operating characteristic (ROC) curve [11] is a graphical measure that looks at the true and false prediction of anomalies in the system at the same time. Though ROC curve does allow comparison of classification algorithms with respect to detection rate and false alarm rate, it does not suggest strictly, the best algorithm. The NPR metric [12] is another measure used to compare the classifiers in view of imbalance data set which not only compares but also ranks the algorithms for suitability in terms of minimum biasing of results and the classifiers with best possible combination of detection and false alarm rate.

1.1 *Objective*

The aim of this work is to extend the research proposing a new metric NPR [12] by validating the results on another version of NSL-KDD [4] data set. NPR metric, the negative-positive ratio of true predicted instances suggests measuring the degree of imbalance in the test data set. The NPR metric is helpful in ranking the classification algorithms for IDS. This paper presents the further simulation of NSL-KDD data set and applies NPR metric to compare and rank the same set of ten algorithms as done in the original work. The purpose of this study is to validate the use of NPR metric and its extensibility on other data sets. The NPR metric presents how the key performance measures like detection rate and false alarm rate can be compared on the same scale which is otherwise not possible because detection rate belongs to the positive class of instances and false alarm rate belongs to negative class of instances (assuming a binary classifier). The rest of the paper is organized as follows: Sect. 2

illustrates the related work with NPR and other performance metrics. Section 3 describes the experimental setup and simulation. Section 4 presents the results and discussion with Sect. 5 conveying the conclusion.

2 Related Work

2.1 Performance Metrics

The simulation results for any classification algorithm are produced in the form of a confusion matrix. Since binary data is considered for study, the classification results will be generated for two classes, one is normal and the other is anomalous. For IDS, the anomalous class instances represent the attacks and hence called the positive class whereas the normal instances are categorized as part of negative class. The elements of confusion matrix are: true negative (TN) defined as the number of instances rightly predicted as negative, true positive (TP) identified as the number of instances accurately predicted as positive, false negative (FN) characterized as the number of instances inaccurately predicted as negative and false positive (FP) defined as the number of instances mistakenly predicted as positive. All the other popular metrics used for the evaluation of IDS are generated from these four basic elements of confusion matrix. Some of these metrics are known as accuracy, detection rate, false alarm rate, precision, and *F*-score [13].

2.2 NPR Metric

The NPR metric [12] is considered for analysis of classification results on test data. It is defined as the ratio of correctly predicted negative instances to the correctly predicted positive instances hence the name NPR. Equation (1) presents [12] NPR mathematically:

$$\text{NPR} = \frac{\text{Number of True Negative Instances (TN)}}{\text{Number of True Positive Instances (TP)}}. \quad (1)$$

For any data set simulated on a classifier, two values of NPR can be calculated. These values of NPR are evaluated keeping in mind the actual distribution of data in positive and negative classes and the predicted distribution of data in the two classes. The analysis of change in the distribution of data instances in the actual and predicted behavior leads to the assessment of performance for any classifier.

Table 1 Study of NPR metric

S. No.	Case	Remarks
1	$NPR_p > NPR_a$	More negative instances predicted than actual
2	$NPR_p < NPR_a$	More positive instances predicted than actual

Equation (2) gives NPR for the actual distribution of data set and the Eq. (3) shows the distribution of same data set for predicted instances after simulation [12].

$$NPR_a = \frac{NI_a}{AI_a} = \frac{TN_a}{TP_a} \quad (2)$$

$$NPR_p = \frac{NI_p}{AI_p} = \frac{TN_p}{TP_p}. \quad (3)$$

The actual NPR metric [12] suggests four possible variations in NPR based on which the classification results can be assessed for detection and false alarm rate. Table 1 presents the central approach to investigate the applicability of NPR metric. Here, only two broad cases for analysis are summarized. Case 1 suggests when the predicted NPR is higher than the actual NPR for a classification algorithm, the predicted number of negative instances is higher leading to the interpretation that the detection rate is comparatively higher whereas the false alarm rate is comparatively lower. Similarly, case 2 presents a scenario when the predicted NPR is less than the actual one meaning that the detection rates are much higher than expected with higher false alarm rates.

The NPR metric puts forward a broad scheme based on which two commonly used metrics can be compared which are detection and false alarm rate. Due to imbalanced data commonly used/available for IDS, detection and false alarm rate are not comparable as they are generated from different instance classes having unequal number of records. Therefore, NPR helps overlook this imbalance in data by considering those algorithms which have predicted NPR nearly equal to actual NPR suggesting accurate interpretation of results for respective classifier.

3 Experimental Setup and Simulation

3.1 Proposed Approach

The approach of this research work is to validate the result [12] of NPR metric by applying it on another data set for the same set of ten algorithms and later compare the ranking of these ten classification algorithms with the original ranking.

Table 2 Data instances

	Normal class instances	Anomalous class instances	Total
KDDTrain+ _20 % (training data)	13,449	11,743	25,192
KDDTest + (Test Data)	9711	12,833	22,544

3.2 Data Set

Binary version of NSL-KDD [4] data set is used for this empirical study having 42 attributes. The last attribute of the data set is ‘class’ attribute signifying the label for data as normal or anomalous. As shown in Table 2, the data set is available in two files, one having the training data used for building the classification model and the other is the test data file used to test the classification model for IDS. The actual value of NPR (NPR_a) for test data is calculated referring Table 2:

$$NPR_a = \frac{9711}{12833} = 0.76. \quad (4)$$

3.3 Used Classifiers

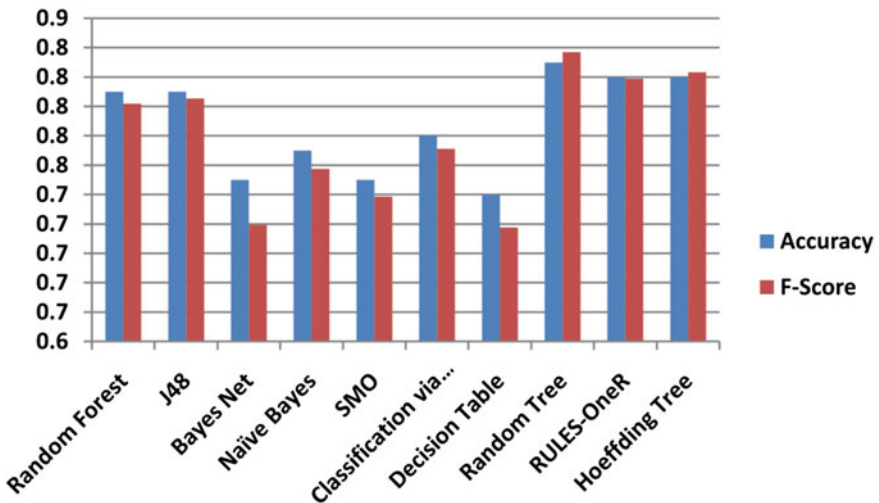
In this study, the same set of classification algorithms are used as used in the original proposal [12] to be able to compare and validate the results. The algorithms are selected such that they cover different classes of machine learning algorithms. Four classifiers are considered from Tree-based category: Random tree, Random Forest, J48 and Hoeffding. Naïve Bayes, Bayes Net are used under Bayesian networks and decision table, OneR are rule-based algorithms. The other algorithms are SMO which is a support vector machine algorithm and classification via regression, a meta class algorithm [14, 15]. The tool used for the simulation of ten algorithms under study is Weka 3.7.11 [16]. The default setting of Weka is used for all the algorithms.

4 Results and Discussion

The ten selected classification algorithms are simulated for KDD data set on Weka tool. Table 3 presents the results for all the ten algorithms. The first column lists the ten algorithms under study which are considered for ranking using NPR. The next four columns display values for TN, FN, FP, TP parameters for each of the algorithms extracted from the confusion matrix after simulation. The other columns follow present values for accuracy, False alarm rate, detection rate, precision and

Table 3 Summary of results

Algorithm	TN	FN	FP	TP	Accuracy	FAR	DR	Precision	F-score	NPR
Random forest	9446	4067	265	8766	0.81	0.03	0.68	0.97	0.80	1.08
J48	9436	3996	275	8837	0.81	0.03	0.69	0.97	0.81	1.07
Bayes Net	9449	5479	262	7354	0.75	0.03	0.57	0.97	0.72	<i>1.28</i>
Naïve Bayes	9010	4582	701	8251	0.77	0.07	0.64	0.92	0.76	1.09
SMO	8984	4893	727	7940	0.75	0.07	0.62	0.92	0.74	1.13
Regression	9426	4602	285	8231	0.78	0.03	0.64	0.97	0.77	1.15
Decision table	9389	5472	322	7361	0.74	0.03	0.57	0.96	0.72	<i>1.28</i>
Random tree	8898	3011	813	9822	0.83	<i>0.08</i>	0.77	0.92	0.84	0.91
OneR	9300	3652	411	9181	0.82	0.04	0.72	0.96	0.82	1.01
Hoeffding tree	8977	3340	734	9493	0.82	<i>0.08</i>	0.74	0.93	0.82	0.95

**Fig. 1** Plot of accuracy and *F*-score for ten classification algorithms

F-score. The last column displays the value for predicted NPR for each algorithm considering the same actual NPR as 0.76. The best results are highlighted bold in print and poor results are *underlined*.

Looking at the observations from Table 3, the significant points are as follows: Random forest recorded minimum false alarm rate with Bayes Net, J48, regression and decision table followed by OneR, and then SMO, Naïve Bayes. The worst false alarm rate is registered for Hoeffding tree and Random tree. Random tree is identified with highest detection rate followed by Hoeffding tree.

The plot of accuracy and *F*-score for the ten classifiers is shown in Fig. 1 putting Random tree algorithm on the top. Similarly Fig. 2 displays the distribution of false

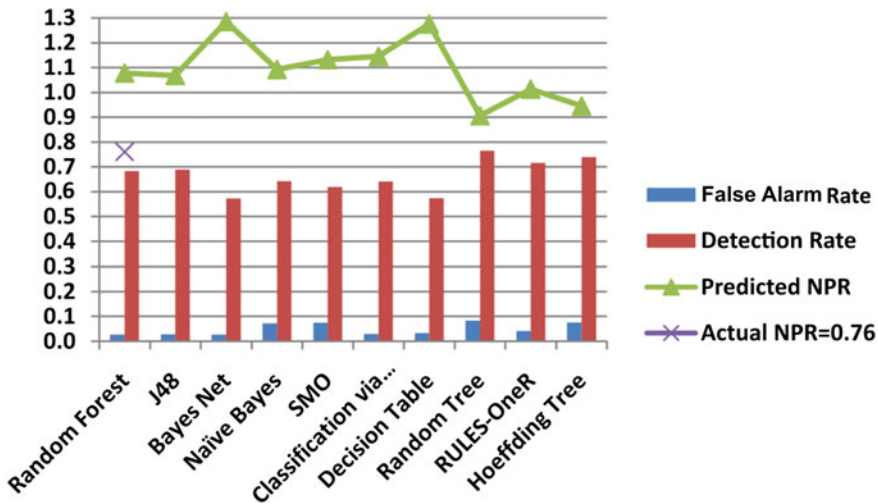


Fig. 2 Plot of false alarm rate, detection rate, and predicted NPR for ten algorithms

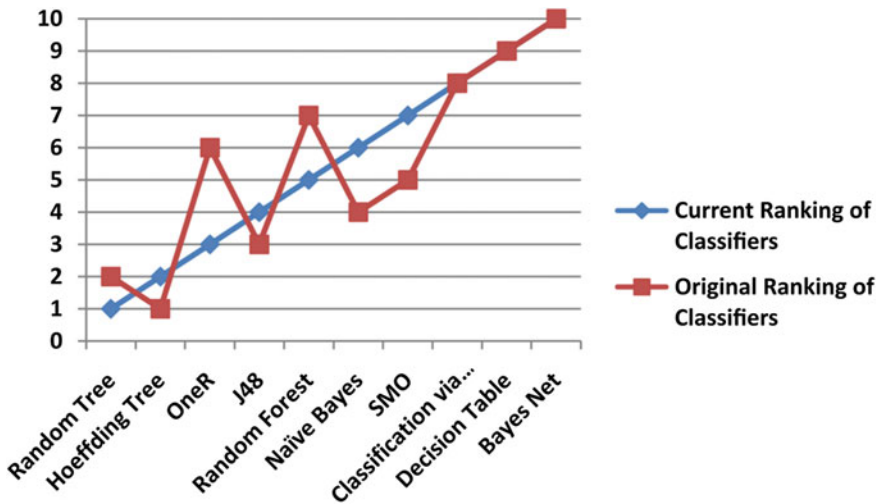


Fig. 3 Plot for ranking of ten classifiers with current and original data set

alarm rate, detection rate, and predicted NPR for the same set of classification algorithms.

The results of this paper are compared in Fig. 3 with the ranking done on same set of ten algorithms for different versions of KDD data sets using NPR. The original ranking of classifiers is taken from the previous research work [12] where NPR was proposed and the KDD data set with more number of instances as

described in Table 1 is taken for current ranking of classifiers. The ranking is done such that the smallest rank value represents the best algorithm.

The aim of this comparison is to validate the ranking of classifiers done through NPR metric. From Fig. 3, it can be observed that the top two algorithms from original ranking only switch their places in the current simulation whereas the last three algorithms hold the same rankings for both the data sets. Though variation is visible in the rankings of algorithms for the two data sets in the middle order, it is not much variant for J48, Random Forest, Naïve Bayes and SMO.

5 Conclusion

Selection of best classifier for IDS is of prime significance to be able to develop efficient IDS. The data imbalance makes it critical to re-interpret the classification results to ensure insignificant biasing towards any one class. NPR is one such metric which tries to identify those algorithms that show minimum or no biasing to a specific class of instances. In this paper ten algorithms were simulated on KDD data set. The results were used to rank the algorithms through NPR and later compared with original ranking of the same algorithms that was done while proposing NPR. The comparison results show association in ranking of algorithms simulated on different versions of KDD data set when ranked using NPR. Hence, it can be concluded that NPR is applicable to ranking of classification algorithms when comparing detection rate and false alarm rate for IDS.

References

1. Tsai, C.-F., et al.: Intrusion detection by machine learning: a review. *Expert Syst. Appl.* **36** (10), 11994–12000 (2009)
2. DARPA Intrusion Detection Evaluation. MIT Lincoln Labs. <http://www.ll.mit.edu/mission/communications/ist/corpora/ideval/index.html>
3. KDD Cup 1999. <http://kdd.ics.uci.edu/databases/kddcup99/>
4. NSL-KDD Data Set for Network-Based Intrusion Detection Systems. <http://nsl.cs.unb.ca/NSL-KDD/>
5. Tavallaei, M., Bagheri, E., Lu, W., Ghorbani, A.A.: A detailed analysis of the KDD CUP 99 data set. In: Proceedings of IEEE Symposium on Computational Intelligence in Security and Defense Applications, pp. 1–6 (2009)
6. Chawla, N.V.: Data Mining for Imbalanced Datasets: an Overview. *Data Mining and Knowledge Discovery Handbook*, pp. 875–886. Springer, New York (2010)
7. Kotsiantis, S., Kanellopoulos, D., Pintelas, P.: Handling imbalanced datasets: a review. *GESTS Int. Trans. Comput. Sci. Eng.* **30**(1), 25–36 (2006)
8. Hulse, V., Jason, Khoshgoftaar, T.M., Napolitano, A.: Experimental perspectives on learning from imbalanced data. In: Proceedings of the 24th International Conference on Machine Learning. ACM (2007)

9. González, S., et al.: Testing Ensembles for Intrusion Detection: On the Identification of Mutated Network Scans. Computational Intelligence in Security for Information Systems, pp. 109–117. Springer, Berlin Heidelberg (2011)
10. Han, J., Kamber, M.: Data Mining: Concepts and Techniques, 3rd edn. Morgan Kaufmann, San Francisco (2012)
11. Ferri, C., Hernández-Orallo, J., Modroiu, R.: An experimental comparison of performance measures for classification. *Pattern Recogn. Lett.* **30**(1), 27–38 (2009)
12. Aggarwal, P., Sharma, S.K.: A new metric for proficient performance evaluation of intrusion detection system. In: Proceedings of 8th International Conference on CISIS, Advances in Intelligent Systems and Computing, Spain, Springer (2015) (Accepted on 27 Feb 2015)
13. Sokolova, M., Lapalme, G.: A systematic analysis of performance measures for classification tasks. *Inf. Process. Manage.* **45**(4), 427–437 (2009)
14. Witten, I.H., Frank, E., Hall, M.A.: Data Mining-Practical Machine Learning Tools and Techniques, Morgan Kaufmann, San Francisco (2011)
15. Aggarwal, P. and Sharma, S. K.: An empirical comparison of classifiers to analyze intrusion detection. In: Proceedings of International Conference on ACCT, India, IEEE Xplore (2015)
16. Waikato Environment for Knowledge Analysis (weka) version 3.7.11. <http://www.cs.waikato.ac.nz/ml/weka/>

Analysis of Different Neural Network Architectures in Face Recognition System

E.V. Sudhanva, V.N. Manjunath Aradhya and C. Naveena

Abstract Face Recognition is considered to be as one of the finest aspects of Computer Vision, also various Feature Extraction and classification techniques including Neural Network Architectures have made it even more interesting. In this paper, an attempt towards developing a model for better feature representation/extraction and cascading it with neural networks classifier is presented. In order to derive better use of face recognition system for faster and better surveillance, analysis is carried out which provides a greater knowledge on the entire process and clarifies on various parameters effecting the system. Most popular Single-Layer Neural Networks such as generalized regression neural network (GRNN) and probabilistic neural network (PNN) are used with different subspace methods to provide a distinguished analysis. The experimental results in this work have revealed that the combination of subspace method with neural networks has increased the robustness and speed of face recognition system. Performance analysis of the proposed model is carried out by conducting the experiments on three benchmarking databases such as ORL, Yale and Feret.

Keywords Face recognition • Eigen values • Eigenfaces • PCA • KPCA • GRNN • PNN • Recognition rate

E.V. Sudhanva (✉)

Department of CS, Jain University, Bangalore, India
e-mail: sudhanva_ev@yahoo.co.in

V.N. Manjunath Aradhya

Department of MCA, Sri Jayachamarajendra College of Engineering,
Mysore, India
e-mail: aradhya.mysore@gmail.com

C. Naveena

Department of CSE, HKBK College of Engineering, Bangalore, India
e-mail: naveena.cse@gmail.com

1 Introduction

A derivative application of Computer Vision, Pattern Recognition and Biometrics is Face Recognition. Face is an essential feature in an individual which presents major trait. Face Recognition brings down these traits which are distinct in the images, forming to recognize a particular individual. It is easier to recognize and track an individual through computers.

In recent years, most of the face recognition approaches have achieved better and faster results. An effort in providing an analysis for better face recognition considering traditional feature extraction techniques such as PCA and KPCA with neural network architecture such as GRNN and PNN and results are obtained in terms of recognition rate [1–3]. The results are discussed and analysed for better combination architecture. In this regard, the literature study states: Subspace methods in face recognition are discussed. Principal Components are obtained from face images so as it can be used for recognition of faces [4, 5]. A non-linear way of deriving principal components with a kernel was best described in [6]. In [7] the class-specific method was introduced and matrix was divided into Within-Class scatter matrix and Between-class scattermatrix to further reduce the Feature Matrix space.

An overview about subspace methods used with neural network for Face Recognition is surveyed. PCA for feature extraction and BPNN for classification were proposed in [8]. A two-level haar wavelet transform is used to decompose frontal face image into sub-bands. With Eigenface feature is extracted and is used as an input to the classification algorithm BPNN, described in [9]. In [1] Gabor filter is used as an input to the Feed Forward Neural Network (FFNN). Use of Back Propagation Neural network (BPNN), the transformation of different inputs and comparison of unknown face with the given face which is in the database is presented in [2]. In [3] curvelet transform and Linear Discriminant Analysis (LDA) are used to extract feature and Radial Basis Function Network (RBFN) is used for the purpose of Classification.

These provide with various kinds of subspace methods with neural network in face recognition. The impact of neural networks on subspace methods is better well not discussed. Considering this an attempt is made to present an analysis of various single-layer neural networks with subspace methods.

The organization of the paper is as follows: In Sect. 2, proposed feature extraction and different classification techniques of face recognition are presented. In Sect. 3, Experimental results are discussed and analysis is briefed. Finally, Conclusions are drawn.

2 Proposed Method

In this section, an overview of different subspace methods used in face recognition with different Neural Network architectures is presented.

2.1 Subspace Methods for Feature Extraction

2.1.1 Principal Component Analysis

The image space of face is represented as $f(a, b)$ which is a two-Dimensional array. PCA as described in [4, 5] represents the training image set of data into singular columns. These singular columns are derived points which are mapped onto a smaller image space represented as subspace.

Let the training set of faces be $A = (A_1, A_2, \dots, A_m)$. The mean face of this training set is calculated by $z = \frac{1}{x} \sum_{y=1}^x a_m$ where each face differs by $\phi_i = a_i - z$.

The image array obtained is a high dimension vector space which is then analysed by Principal Component Analysis. The high dimension vector space A is subjected to obtain eigen value and eigen vector by the following covariance matrix.

$$C = \frac{1}{x} \sum_{y=1}^x \phi_y \phi_y^T = L L^T \quad (1)$$

where the matrix $L = [\phi_1, \phi_2, \dots, \phi_x]$. The covariance matrix expresses vector and scalar values as Eigen vectors and Eigen values. The obtained covariance matrix is subjected as feature matrix. The feature matrix is distinguished into individual face class by using neural networks for classification.

2.1.2 Kernal Principal Component Analysis

The Covariance matrix ‘ C ’ calculated out of the training set image space ‘ A ’ is subjected to kernal idea [6]. Kernal is a non-linear mapping function which is used for estimating the mapping of the covariance matrix. The kernal mapping function is represented as

$$\hat{X} = X - 1_N X - X 1_N + 1_N X 1_N \quad (2)$$

where $(1_N)_{ij} = \frac{1}{N}$.

The kernal matrix ‘ X ’ is a square matrix which is of the same dimension of the covariance matrix ‘ C ’. The non-linear principal components obtained using gaussian method of KPCA on each and every image collectively forms a feature matrix. The obtained Kernal feature matrix is further classified using neural networks.

2.2 Neural Network Architectures for Classification

2.2.1 Single-Layer Neural Network

It commits only single synapse due to single hidden layer. Single-layer neural network pertains to obtain substantial adaptation.

2.2.2 Generalized Regression Neural Network

A GRNN is a variation of the radial basis neural networks, which is based on kernal regression networks [10, 11]. GRNN does not require iterative training procedure as back propagation networks.

GRNN consists of four layers: input layer, pattern layer, summation layer, and output layer. The obtained feature matrix from ‘ C ’ and ‘ X ’, respectively, from PCA and KPCA is fed to GRNN for Classification. The summation layers consist of two summation neurons P and Q . P computes weighted matrix where as Q computes the unweighted outputs of the pattern layer. This Layer merely distinguishes P and Q neuron, predicting towards K'_i to an unknown input vector L as

$$K'_i = \frac{\sum_{i=1}^n a_i \cdot \exp - F(x, x_i)}{\sum_{i=1}^n \exp - F(x, x_i)} \quad (3)$$

$$F(x, x_i) = \sum_{z=1}^y \left(\frac{x_i - x_i c}{\sigma} \right)^2. \quad (4)$$

This neural network results into individual face classes. Network obtained further is simulated with testing feature matrix for recognition rate.

2.2.3 Probabilistic Neural Network

PNN was first proposed in [12]; the architecture contains many interconnected processing units represented by neurons and is stacked in successive layers. The feature matrix obtained by the subspace methods is fed into the input layer. The input layer does not perform any computation; from this layer the values are transported to the pattern layer. The pattern layer computes accordingly its output by

$$\phi_{ij}(x) = \frac{1}{(2\pi)^{\frac{d}{2}} \sigma^d} \exp \left[- \frac{(x - x_{ij})^T (x - x_{ij})}{2\sigma^2} \right]. \quad (5)$$

The successive pattern layer computes to the maximum likelihood of pattern ' x ' which classified and surfaced to ' C_j '. The Bayes's decision rule further presents with

$$\hat{j}(x) = \operatorname{argmax}\{p_i(x)\}, i = 1, 2, \dots, m \quad (6)$$

where $\hat{j}(x)$ denotes the classified output. This classified network is simulated with feature matrix of testing images to obtain recognition result.

3 Experimental Results and Performance Analysis

The proposed work is experimented on three databases. They are ORL, Yale, FERET databases.

3.1 Subspace Methods and Generalized Regression Neural Network (GRNN)

To classify the train images feature matrix obtained from subspace methods such as PCA and KPCA, a GRNN classification algorithm is applied. In order to evaluate the recognition results, the experiment was conducted for different weights by varying 0.2 weights from 0.2 to 1.4 as to find the threshold value. In this section experiment results of subspace methods such as PCA and KPCA with GRNN are discussed [13–19].

3.1.1 PCA and GRNN

The results of PCA and GRNN for ORL, Yale and FERET database are shown in Table 1.

3.1.2 KPCA and GRNN

The recognition results of KPCA and GRNN for ORL, Yale and FERET databases are shown in Table 2.

From Tables 1 and 2 we can clearly distinguish KPCA with GRNN outperforms in all the three databases when compared to PCA with GRNN. The increase in training images results an increase in recognition result. Lesser the weights the Neural network gives better performance.

Table 1 Recognition results for PCA and GRNN

Database	ORL			Yale			FERET		
Training images	120	200	280	60	75	105	45	75	105
Testing images	280	200	120	105	90	60	105	75	45
Weights	<i>Recognition results</i>								
0.2	67.50	77.50	91.66	74.28	78.66	93.33	65.71	68.0	91.11
0.4	67.50	77.50	91.66	74.28	78.66	93.33	65.71	68.0	91.11
0.6	67.50	77.50	91.66	74.28	78.66	93.33	66.66	68.0	91.11
0.8	67.14	77.50	92.50	74.28	76.0	93.33	66.66	68.0	88.88
1.0	66.07	79.0	92.50	74.28	76.0	91.11	66.66	66.66	88.88
1.2	66.07	79.0	92.50	74.28	76.0	91.11	66.66	68.0	86.66
1.4	66.07	77.0	92.50	74.28	76.0	91.11	66.66	66.66	84.44

3.2 Subspace Methods and Probabilistic Neural Network (PNN)

To obtain the better classification of face images, a PNN is applied with the subspace methods. In this section recognition results of subspace methods such as PCA and KPCA with PNN are discussed. Recognition rates were measured by differing 0.2 weight i.e., from 0.2 to 1.4.

3.2.1 PCA and PNN

The recognition results of PCA and PNN for ORL, Yale and FERET databases are shown in Table 3.

3.2.2 KPCA and PNN

The recognition results of KPCA and PNN for ORL, Yale and FERET databases are shown in Table 4.

KPCA with PNN outperform PCA with PNN by considering above Tables 3 and 4. From the above conducted experiments it clearly shows that KPCA as a subspace method with Single-layer neural network outperforms PCA.

3.3 Performance Analysis

By analysing the experimental results, combination of KPCA and GRNN yields better recognition rate 90.83, 93.33 and 93.33 % for ORL, Yale and FERET databases when compared to other subspace methods with GRNN. With the

Table 2 Recognition Results for KPCA and GRNN

Database	ORL			Yale			FERET		
Training images	120	200	280	60	75	105	45	75	105
Testing images	280	200	120	105	90	60	105	75	45
Weights	<i>Recognition results</i>								
0.2	67.14	83.50	90.83	66.66	77.33	93.33	69.52	73.33	93.33
0.4	67.50	82.0	85.83	66.66	78.66	93.33	69.52	73.33	93.33
0.6	68.21	79.0	80.83	66.66	78.66	93.33	69.52	74.66	93.33
0.8	66.42	76.50	78.33	66.66	78.66	86.66	69.52	73.33	84.44
1.0	66.07	74.0	78.33	65.71	74.66	84.44	69.52	70.66	80.0
1.2	65.71	73.50	77.50	65.71	73.33	84.44	69.52	68.0	80.0
1.4	65.0	74.0	77.50	65.71	73.33	82.22	69.52	68.0	80.0

Table 3 Recognition results for PCA and PNN

Database	ORL			Yale			FERET		
Training images	120	200	280	60	75	105	45	75	105
Testing images	280	200	120	105	90	60	105	75	45
Weights	<i>Recognition results</i>								
0.2	67.50	77.50	91.66	74.28	78.66	93.33	65.71	68.0	91.11
0.4	67.50	77.50	91.66	74.28	78.66	93.33	65.71	68.0	91.11
0.6	67.50	77.50	91.66	74.28	78.66	93.33	66.66	68.0	91.11
0.8	67.14	77.50	92.50	74.28	76.0	93.33	66.66	68.0	88.88
1.0	66.07	79.0	92.50	74.28	76.0	91.11	66.66	66.66	88.88
1.2	66.07	79.0	92.50	74.28	76.0	91.11	66.66	68.0	86.66
1.4	66.07	77.0	92.50	74.28	76.0	91.11	66.66	66.66	84.44

combination of subspace methods and PNN, the recognition results were same as subspace methods with GRNN as such the combination of KPCA and PNN exhibits similar performance.

GRNN is a highly parallel structure with one-pass learning algorithm. It approximates and arbitrates the function between input and output vectors which estimates the training data directly. Pattern classification presents with network creation as in PNN. This architecture directly implements the one-pass learning algorithm. The non-linear mapping nature of KPCA and with GRNN which is a function approximation architecture and the PNN a classification network which both network are simple supervised neural network gives an added advantage for better classification and recognition.

Withal, the comparative study proves that the better recognition rates obtained for the combination of KPCA and GRNN and KPCA and PNN. Hence from the analysis for achieving highest recognition rate in face recognition system, KPCA and GRNN and KPCA and PNN are better suitable.

Table 4 Recognition Results for KPCA and PNN

Database	ORL			Yale			FERET		
Training images	120	200	280	60	75	105	45	75	105
Testing images	280	200	120	105	90	60	105	75	45
Weights <i>Recognition results</i>									
0.2	67.14	83.50	90.83	66.66	77.33	93.33	69.52	73.33	93.33
0.4	67.50	82.0	85.83	66.66	78.66	93.33	69.52	73.33	93.33
0.6	68.21	79.0	80.83	66.66	78.66	93.33	69.52	74.66	93.33
0.8	66.42	76.50	78.33	66.66	78.66	86.66	69.52	73.33	84.44
1.0	66.07	74.0	78.33	65.71	74.66	84.44	69.52	70.66	80.0
1.2	65.71	73.50	77.50	65.71	73.33	84.44	69.52	68.0	80.0
1.4	65.0	74.0	77.50	65.71	73.33	82.22	69.52	68.0	80.0

4 Conclusion

A successful face recognition system mainly depends on the feature extraction methods and the pattern classifier. Extraction of a representative feature set increases the efficiency of performance by reducing the space dimension. Neural networks are non-linear processes that perform learning and classification. They also perform well in recognizing the facial expression. In this regard, for an efficient face recognition, we performed an analysis with each of the subspace methods such as PCA and KPCA as a feature extraction methods with neural networks such as GRNN and PNN as a classifier. As a result, KPCA and GRNN and KPCA and PNN exhibit better performance. The main purpose of the proposed analysis work made towards face recognition is to identify the appropriate neural network model with the better feature extraction methods in achieving better recognition rate. So that a system can work reliable with a good learning capacity and insensitivity to small or gradual changes in the face image. With this the applicability and capability of better suitable neural network models with their performance in terms of recognition rates are described.

References

1. Kumar, K.: Artificial neural network based face detection using gabor feature extraction. *Int. J. Adv. Technol. Eng. Res. (IJATER)* **2**, 220–225 (2012)
2. Revathy, N., Guhan, T.: Face recognition system using back propagation artificial neural network. *Int. J. Adv. Eng. Technol. (IJAET)* **3**, 321–324 (2012)
3. Radha, V., Nallammal, N.: Neural network based face recognition using RBFN classifier. In: Proceedings of the World Congress on Engineering and Computer Science (WCECS), vol. 1 (2011)

4. Turk, M.A., Pentland, A.P.: Eigenfaces for recognition. *J. Cognit. Neurosci.* **3**, 71–86 (1991)
5. Turk, M.A., Pentland, A.P.: Face recognition using eigenfaces. In: Proceedings of IEEE Computer Society Conference on Computer Vision and Pattern Recognition (1991)
6. Scholkopf, B., Smola, A., Müller, K.R.: Kernel principal component analysis. *Adv. Kernel Methods Support Vector Learning*, pp 327–352 (1999)
7. Belhumer, P.N., Hespanha, J.P., Kriegman, D.J.: Eigenfaces vs fisherfaces: recognition using class specific linear projection. *IEEE Trans. Pattern Anal. Mach. Intell.* **19**(3), 711–720 (1997)
8. Chaudhary, U., Mubarak, C.M., Rehman, A., Riyaz, A., Mazhar, S.: Face recognition using PCA-BPNN algorithm. *Int. J. Modren Eng. Res. (IJMER)*, **2**, 1366–1370 (2012)
9. Daramola, S.A., Odeghe, O.S.: Efficient face recognition system using artificial neural network. *Int. J. Comput. Appl.* **41**(21), 12–15 (2012)
10. Specht, D.F.: A general regression neural network. *IEEE Trans. Neural Networks* **2**(6), 568–576 (1991)
11. Demuth, H.B., Beale, M.: Neural network toolbox for use with MATLAB Users Guide Version 4. Mathworks (2002)
12. Specht, D.F.: Probabilistic neural networks. *IEEE Int. Conf. Neural Networks*, pp. 525–532 (1990)
13. Beale, H., Hagan, M.T., Demuth, H.B.: Neural network toolbox users guide 2013a, Mathworks (2013)
14. <http://www.cl.cam.ac.uk/research/dtg/attarchive/facedatabase.html>
15. <http://www.nist.gov/itl/iaid/ig/colorferet.cfm>
16. <http://cvc.yale.edu/projects/yalefaces/yalefaces.html>
17. Sahoolizadeh, A.H., Heidari, B.Z., Dehghani, C.H.: A new face recognition method using PCA, LDA and neural network. *Int. J. Electr. Electron. Eng.* **2**(5), 6–12 (2008)
18. Esbati, H., Shirazi, J.: Face recognition with PCA and KPCA using Elman neural network and SVM. *Int. J. Electr. Electron. Eng.* **5**(10), 135–140 (2011)
19. Hoang, L.T.: Applying artificial neural networks for face recognition. In: *Advances in Artificial Neural System*, vol. 2011, Hindawi Publishing Corp

A Novel Approach for Diagnosis of Noisy Component in Rolling Bearing Using Improved Empirical Mode Decomposition

Rahul Dubey and Dheeraj Agrawal

Abstract The Bearing is utilized to give free direct development to the moving part or with the expectation of complimentary revolution around a fixed axis. Bearings are considered a main part in various mechanical systems. Multi component vibration signals are generated when the machine works. Accelerometers are used to capture generated vibration signal. Vibration signal analysis is effectively used to diagnose bearing faults. There are various methods using empirical mode decomposition (EMD) as their fundamental method to diagnose bearing faults. The proposed method consists of analyzing the kurtosis of residue obtained after removing higher frequency components of the original signal. The proposed technique identifies the boisterous frequency segment in the signal through the iterative procedure. The experimental data were collected from Case Western Reserve University, Ohio. The simulation is done over MATLAB 7.8.1.

Keywords Rolling bearing · EMD · IMF · Signal processing

1 Introduction

Life cycle of software and hardware has a most important phase known as repair and maintenance. Industries face the problem of high maintenance cost and interruption in production due to the machine fault problems. Rolling element bearing is given to backings and finds pivoting shafts in the machine. Rolling element bearings are classified into the ball bearing and roller bearing. Rolling action is the main

R. Dubey (✉) · D. Agrawal

Department of Electronics & Communication, Maulana Azad National Institute of Technology, Bhopal, India
e-mail: rahul.dubey0686@gmail.com

D. Agrawal

e-mail: dheerajagrawal@manit.ac.in

© Springer India 2016

S.C. Satapathy et al. (eds.), *Proceedings of the Second International Conference on Computer and Communication Technologies, Advances in Intelligent Systems and Computing* 380, DOI 10.1007/978-81-322-2523-2_46

479

working principle of rolling element bearing, whereas sliding action is the main principle of plain bearing.

Various properties of machine parts like vibration, lubrication, temperature have also been used for bearing fault detection. During the running state of the machine, vibration signal get generated; vibration is known as the oscillation of an object around equilibrium position. Vibration signature analysis is a most prominent and historical method for the detection of faults in machines [1].

The Geometry of the ball bearing is shown in Fig. 1. With reference to Fig. 1, F_{OF} is the outer frequency, F_{CG} is the cage frequency, F_{IN} is the inner frequency. F_{SH} is the shaft rotation frequency, F_B is the ball rotational frequency, F_{IRF} is the ball pass inner raceway frequency, F_{ORF} is the ball pass outer raceway frequency. The Fig. 2 shows the additional geometry of the ball bearing required to calculate the fault frequencies.

The frequencies are to be calculated by following formula:

$$f_{cg} = \frac{n}{2}(1 - \cos\alpha) \quad (1)$$

Fig. 1 A typical bearing structure

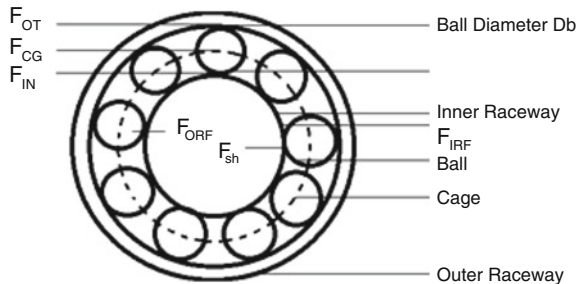
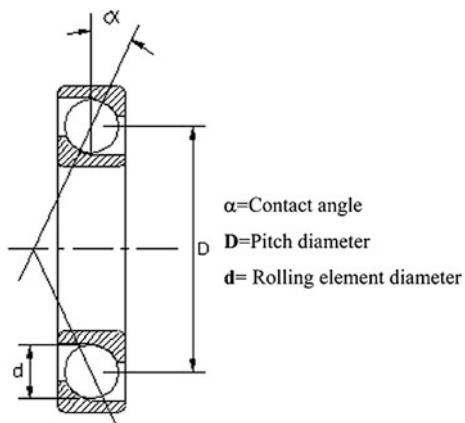


Fig. 2 A rolling bearing structural information



$$f_{\text{irf}} = \frac{n}{2} N_b \left(1 + \frac{d}{D} \cos \alpha \right) \quad (2)$$

$$f_b = \frac{n}{2} \left(\frac{d}{D} \right) \left[1 - \left(\frac{d}{D} \right)^2 \cos^2 \alpha \right] \quad (3)$$

$$f_{\text{bp}} = \frac{n}{2} N_b \left(1 - \frac{d}{D} \cos \alpha \right). \quad (4)$$

In the previous years, it has been proven that the kurtosis analysis provides early stage detection of fault when it is compared with a raw signal, where the presence of faults indicates by the kurtosis value greater than three [2]. Wavelet analysis is the most used method for the detection of fault [3]. The main use of the wavelet is the analysis of non-stationary signal. Static window size was the main problem of wavelet transforms. Since bearing signs have different frequency parts henceforth to break down different frequencies there will be a need of variable size window as per frequency range indicated.

The issues of wavelet transform of fixed window size taken into account Huang et al. [4] to develop new technique for the detection of non-linear and non-stationary time domain signal, their proposed technique known as EMD.

Sawalhi et al. worked on application of spectral analysis for bearing fault diagnosis. Spectral kurtosis gives a fundamentally the same sign of the band to be demodulated without obliging previous data information [5]. Yan and Lu used improved Hilbert-Huang Transform for detecting weak signals in bearing fault diagnosis. Iterative errors had been minimized by using wavelet transform [6].

Sawalhi et al. proposed an algorithm to improve the surveillance capability of spectral kurtosis using minimum entropy deconvolution (MED) technique. The effect of transmission path can be effectively deconvolved from the original signal containing impulses using MED technique [7].

Liu et al., in 2014 proposed a three stage method to detect the bearing faults based on the HHT and SVD. Fault classification has been done by using neural network along with HHT and SVD [8].

2 Signal Decomposition and Analysis

This section will provide the detail about EMD method, intrinsic mode function (IMF) decomposition for the signal. EMD method and proposed steps are explained in this section.

2.1 Empirical Mode Decomposition

Huang et al. presents an algorithm to extract all the frequency component of a vibration signal into a finite set, these finite sets of frequency components known as IMF. The EMD algorithm proposed by Huang et al., is written as follows [4]:

All the extrema of signal $x(t)$ is obtained. Two envelopes $X_{\min}(t)$ and $X_{\max}(t)$ is obtained by the interpolation between minima, and respective maxima. The average $a(t)$ of the envelope is computed, which is further subtracted from the $x(t)$ to obtained detail component $h(t)$. If the obtained $h(t)$ is an IMF, the procedure is repeated to get residual signal $r(t)$, otherwise replace the $x(t)$ with $h(t)$, and repeat the whole steps [4]

$$a(t) = \frac{X_{\min}(t) + X_{\max}(t)}{2} \quad (5)$$

$$h(t) = x(t) - a(t) \quad (6)$$

$$r(t) = x(t) - h(t). \quad (7)$$

The vector of the IMFs consists of various frequency bands of $x(t)$ from high range to lower. The residual of a signal $x(t)$ represents its central tendency. Figure 3 shows the signal, and its IMFs', three IMFs' shown here in this figure.

3 Methodology Adopted

Signal $x(t)$ is an arbitrary bearing signal which includes any kind of fault occurred in bearings. Kurtosis of this signal $x(t)$ is determined. The EMD of the signal $x(t)$ is done to decompose the signal into the IMF. The first IMF is subtracted from the original signal to extract the residue. The kurtosis value of the extracted residue is determined which is compared with the kurtosis value of the original signal to find the noise component in the signal. After subtracting first IMF, if the kurtosis value of the residue found to be less than the original signal, it indicates the presence of fault (noise component) in the signal, and the process is repeated for remaining IMF with considering residue as base signal. In another case, when a kurtosis value of the residue is same as the original signal, the original signal is kept fixed and the process is repeated for remaining IMF until the kurtosis of the residue becomes less than 3.

3.1 Proposed Algorithm (Pseudo Code)

1. Let $r \rightarrow x(t)$, where $x(t)$ is sample consisting of vibrating data.
2. Interpolation between minima (resp maxima) with the help of the cubic spline method is performed to acquire lower envelope and Upper envelope.
3. The mean of upper & lower envelope value is designated by mx_i , the difference between signal $x(t)$, and mx_i is the first component i.e.

$$fc_i = r - mx_i$$

if fc_i is an IMF,

then fc_i is the first component of r

else

fc_i is treated as original signal, and repeat Step (3), and Step (4).

4. Repeat Step (2), (3), (4)

$$r = \sum_{j=1}^n C_j + r_n$$

where,

r_n = Residue of a signal decomposes into n-empirical modes.

$C_1, C_2, C_3, \dots, C_n$ = Various Intrinsic Mode function of r

5. Find Kurtosis value of signal space ‘r’ using

$$K = \frac{\frac{1}{N} \sum r_i^4}{(\frac{1}{N} \sum (r_i^2))^2}$$

6. Find $n = \text{length}(C)$, Initialize $V = []$.

for $i = 1 : n$

$$d_i = r - c_i$$

$$K_i = \frac{\frac{1}{N} \sum d_i^4}{(\frac{1}{N} \sum (d_i^2))^2}$$

If $K_i < K$

$$r = d_i$$

else if

$$V = [V, d_i]$$

end

end

7. $M = \text{length}(V)$;

for $K = 1 : M$

$$X(K) = \sum_{n=0}^{N-1} v(n) e^{\frac{-j2\pi MK}{N}}, \text{ for } K = 0, 1, 2, \dots, N-1$$

8. $K_N = \frac{\frac{1}{N} \sum d_i^4}{(\frac{1}{N} \sum (d_i^2))^2}$

If $K_N \leq 3$

Stop

else

Repeat Step (7), (8), (9).

end

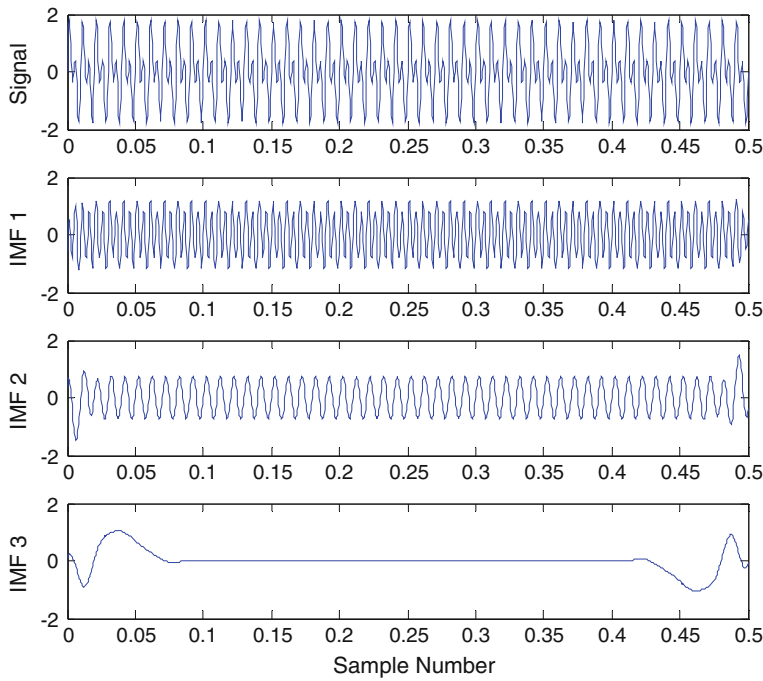


Fig. 3 Signal and IMFs decomposition

4 Experimental Result

The Fig. 4 shows the test stand for bearing fault analysis. The main component of this test stand has one motor of rating 2 hp is shown left in the Fig. 4, a torque transducer/encoder is placed at the centre of the test stand, the dynamometer is shown at a right end of the test stand, and control electronics not shown in open arrangement. Data were collected at both ends drive ends, and fan end. Accelerometers were placed there to collect the oscillating data, which is further processed in a Matlab environment. These signals are available online at the bearing data centre of case western reserve university, Ohio [9].

The different specification frequencies for existing faults are shown in Table 1.

Table 2 shows the kurtosis analysis of the baseline data collected from [9]. The MATLAB signal processing toolbox is used to decompose the signal into its IMFs, and Kurtosis analysis is done over the various samples, and respective values are written in the Table 2. Kurtosis values have been calculated for various sample size, which was randomly chosen amongst the population of vibration samples.

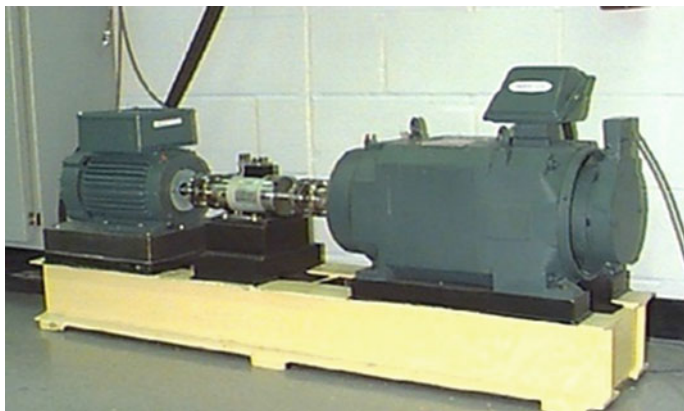


Fig. 4 Test stand for bearing fault system [9]

Table 1 Fault specification

Fault type	Defect frequency (Hz)	
	Drive end bearing	Fan end bearing
Inner ring	5.4152	4.9469
Outer ring	3.5848	3.0530
Cage train	0.3982	0.3817
Rolling element	4.7135	3.9874

Table 2 Kurtosis analysis for raw signal

Sample size	Baseline data	
	Drive end	Fan end
2000	3.0967	2.8314
4000	3.3652	2.9132
8000	3.3244	2.7663
16,000	3.1206	2.6303
32,000	3.1274	2.7336
64,000	3.1154	2.6795

In the proposed algorithm, the original signal is decomposed into an IMF; the kurtosis value of the original faulty signal is calculated. In the first step, the first IMF (highest frequency component) gets subtracted from the original signal, and the kurtosis value of the residue is then observed. If the kurtosis value of the residue decreases to 3, it proves that the frequency component which has been removed is the noisiest component. If decrement in the value of kurtosis for residue is not significant, the procedure is repeated until the kurtosis value of the residue becomes three. The Tables 3 and 4 shows the experimental result of the proposed algorithm over the data collected from Case western reserve university, Ohio, United states. The analysis has been done in two states, in the first state, individual IMFs' have

Table 3 Outcome of the proposed algorithm in first state

a = x130_DE_Time (1:1024,:)	(Outer race fault signal)		
Kurtosis (a) = 7.9988			
b = emd (a)			
b = {1 × 9} vector (IMFs' of a)			
	Associated frequency	Kurtosis	
d1 = a - b{1}	F_1	a	$d(x)$
d2 = a - b{2}	F_2	7.9988	7.7438
d3 = a - b{3}	F_3	7.9988	7.9708
d4 = a - b{4}	F_4	7.9988	7.9791
d5 = a - b{5}	F_5	7.9988	7.9905
d6 = a - b{6}	F_6	7.9988	7.9922
d7 = a - b{7}	F_7	7.9988	7.9628
d8 = a - b{8}	F_8	7.9988	7.958
d9 = a - b{9}	F_9	7.9988	7.989

Table 4 Outcome of the proposed algorithm in second state

	Associated frequency	Kurtosis	
d1 = a - b{1}	F_1	a	$d(x)$
e1 = d1 - b{2}	F_2	7.9988	5.0521
e2 = d1 - b{3}	F_3	7.9988	4.1447
e3 = e2 - b{4}	F_4	7.9988	3.6599
e4 = e3 - b{5}	F_5	7.9988	3.5668
e5 = e3 - b{6}	F_6	7.9988	3.5639
e6 = e3 - b{7}	F_7	7.9988	3.2565
e7 = e3 - b{8}	F_8	7.9988	3.5027

been subtracted from the original signal, while in second state IMFs' were removed from the residue calculated after removing higher IMF from the original signal. Table 3 shows the result of the first state in which outer race fault signal is considered as an original signal, and individual IMFs' has been removed from the original signal and the corresponding kurtosis value has been recorded. Table 4 shows the outcome of the second state in which individual IMFs' has been removed from the residue until kurtosis value of the residue becomes 3. It has been proved in the literature that the kurtosis value of more than 3 indicates the presence of faulty component in the signal.

Let $f_1, f_2, f_3, \dots, f_9$ is the associated frequency with individual IMF components. From the Table 4, It is clearly seen that the frequency component f_1, f_3, f_4, f_7 having noisy component as after their removal from the residue, the kurtosis value decreases to a level where it is considered to be signaled without noise.

5 Conclusion

During this research, diagnosis of bearing fault with the help of empirical mode decomposition has been analyzed, and the problems of empirical mode decomposition detect bearing faults have been considered. A novel approach is proposed which easily identified noisy component in a signal using Empirical Mode Decomposition. Kurtosis values of the signal are taken as a parameter of examination for the proposed algorithm. The proposed algorithm can be used in an industry as a Human-Computer interface to machineries; hence by using the proposed algorithm productivity of the machines can be improved. Further enhancements to this research, neural network techniques can be used to improve the efficiency of the proposed algorithm, and the classification of the bearing fault can also be done using neural network classification.

References

1. Bhende, A.R., Awari, G.K., Untawale, S.P.: Assessment of bearing fault detection using vibration signal analysis. *VSRD-TNTJ* **2**(5), 249–261 (2011)
2. Badaoui, M., Guillet, F., Parey, A., et al.: Dynamic modelling of spur gear pair and application of empirical mode decomposition-based statistical analysis for early detection of localized tooth defect. *J. Sound Vib.* **294**, 547–561 (2006)
3. Li, H., Yin, Y.: Bearing fault diagnosis based on laplace wavelet transform. *Telkomnika* **10**(8), 2139–2150 (2012)
4. Huang, N.E., Long, S.R., Shen, Z., et al.: The empirical mode decomposition and the Hilbert spectrum for nonlinear and non-stationary time series analysis. *Proc. R. Soc. Lond.* **454**, 903–995 (1998)
5. Sawalhi, N., Randall, R.B.: The application of spectral kurtosis to bearing diagnostics. In: Annual Conference of the Australian Acoustical Society Australia, pp. 393–398 (2004)
6. Yan, J., Lu, L.: Improved Hilbert-Huang transform based weak signal detection methodology and its application on incipient fault diagnosis and ECG signal analysis. *Signal Process.* **98**, 74–87. Elsevier (2014)
7. Sawalhi, N., Randall, R.B., Endo, H.: The enhancement of fault detection and diagnosis in rolling element bearings using minimum entropy deconvolution combined with spectral kurtosis. *Mech. Syst. Signal Process.* **21**, 2616–2633. Elsevier (2007)
8. Liu, H., Wang, X., Lu, C.: Rolling bearing fault diagnosis under variable conditions using Hilbert-Huang transform and singular value decomposition. *Math. Probl. Eng.* pp. 1–10. Hindawi Corporation (2014)
9. Case Western Reserve University Bearing Data Center Available at: <http://csegroups.case.edu/bearingdatacenter/pages/welcome-case-western-reserve-university-bearing-data-center-website>

A Novel Solution of Dijkstra's Algorithm for Shortest Path Routing with Polygonal Obstacles in Wireless Networks Using Fuzzy Mathematics

Dhruba Ghosh, Sunil Kumar and Paurush Bhulania

Abstract This paper centralizes the idea of shortest path routing using a new approach to Dijkstra's algorithm. Our new algorithm gives best solution as compared to the previously proposed algorithms using fuzzy mathematics with well-defined explanation in terms of complexity. The algorithm is valid for negative-weight graphs as well as a number of obstacles in the path of routing. It will search out the shortest path for routing and the shortest route which costs minimum. The minimum cost consuming shortest route is valuable routing for Ultra Large Scale Integrated chip.

Keywords Advanced research projects agency network • Fuzzy mathematics • Interior gateway routing protocol • Netchange • Very large-scale integration • Ultra large-scale integration

1 Introduction

Starting from static phase to dynamic phase, shortest path algorithm serves well in all its aspects and prospects. The rising demand of ultra large-scale integrated chips in the market of electronics has proved that shortest path algorithm is necessary for routing technology. The long way journey from single transistor to very large-scale integrated chip has witnessed the enormous growth of electronics industry with innovation of new computer technologies. The main and foremost problem while routing is to find out the shortest path with maximum number of obstacles

D. Ghosh (✉) · S. Kumar · P. Bhulania
Amity University, Noida, Uttar Pradesh, India
e-mail: dhrubaghosh5@gmail.com

S. Kumar
e-mail: skumar34@amity.edu

P. Bhulania
e-mail: pbhulania@amity.edu

considering complexity constraint. Though the high-level mathematical approaches and the fuzzy mathematics have helped a lot to solve a problem for static environment, the dynamicity in electrical circuits requires an environment to support the continuous change in the network topology.

With increasing speed of wireless communication, the traffic problem becomes less predictable and the routing problem becomes much complex as compared to the previous ones. The routing algorithms which are already mentioned in the literature are of two categories: distance-vector algorithm and link-state algorithm [1–4]. The common examples of distance-vector algorithms are advanced research projects agency network (ARPANET) algorithm, Netchange algorithm, and interior gateway routing protocol (IGRP) [5, 6]. A distance-vector routing protocol is hinged on the information of rate of traffic congestion from the router. The term “distance vector” generally designates the array of distances from the source node to each and every destination point [7]. The Bellman Ford algorithm which is nothing but the advancement of Dijkstra’s algorithm is often agonized “Count to Infinity Problem” [8] because of formation of closed loop while approaching to distance-vector algorithm.

The paper is organized as follows: Sect. 1 gives the introduction to the routing technology in wireless network; Sect. 2 points out an example of “Count to Infinity Problem”; Sect. 3 overviews primitive routing algorithms; Sect. 4 measures the stability and responsiveness of routing algorithm in a dynamic environment; Sect. 5 discusses the complexity level of traditional Dijkstra’s algorithm; Sect. 6 focuses on the optimization of Dijkstra’s algorithm in a dynamic environment; Sect. 7 points out a new approach to overcome the disadvantages of Dijkstra’s algorithm; Sect. 8 elaborates the simulation results of our newly proposed algorithm and at last Sect. 9 concludes that our proposed theorems find out strong analogy with the simulation results.

2 Example of Count to Infinity Problem

If we take an example with five routers or nodes, we can see that (Fig. 1).

Table 1 clearly shows that all the nodes or routers are aware of the shortest routing path. Each and every node broadcasts the distance of neighbor nodes to all other nodes. It is concluded from this table that there is a great need of awareness of distance so that count to infinity problem is avoided. The drawback of “count to infinity problem” is its wasting of bandwidth due to unawareness of broadcasting and also wastage of time [9–11].

Due to the increasing demand of wireless data network, the router often faces a problem for excessive overloading of data path [12].

The main contribution of our paper is to propose a novel algorithm to improve Dijkstra’s algorithm to meet the demand of high speed in a ULSI circuit. The advantage of our algorithm is its less complexity with a round trip path. This round

Fig. 1 Routing in a network of 5 nodes

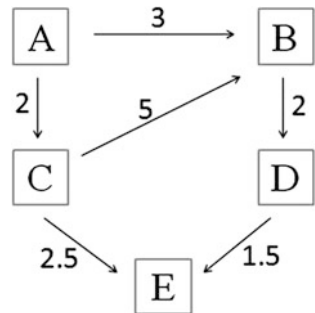


Table 1 Weighted and directed routing path in a 5-node network

	To A	To B	To C	To D	To E
From A	3	2			
From B				2	
From C	5				2.5
From D					1.5
From E					

trip path or the Eulerian circuit specifies the connection of the source point to the source points via interconnecting routers.

3 Overview of Dijkstra's Algorithm

The significance of a new algorithm lies in its adaptability and stability in diverse environments. In spite of being simple, the static algorithms are unable to adapt in dynamic environments. The dynamic algorithms are compatible with the increasing complexity of traffic and eventually become more time consuming as compared to the static and quasi-static algorithms.

From the advent of Dijksta's algorithm to the Ant Colony Optimization algorithm, the complexity of solution generally increases with problem complexity but the main hindrance to optimism is that Dijksta's algorithm is only valid for positive weighted graphs. Bellman Ford algorithm is more versatile in comparison with Dijksta's algorithm for its validity for negative-weight graphs [13]. There are also many other types of algorithms based on real-life problems available in the literature. These are Floyd's Algorithm, Chinese Postman algorithm, Binary Genetic algorithm, Pareto Genetic algorithm, Permutation Genetic algorithm, Delaunay Triangulation Algorithm, Kahng and Robin's Steiner Optimization Algorithm, Hwang's Heuristic Approach Algorithm, Thompson's Algorithm and Ant Colony Optimization Algorithm [14, 15].

Dijksta's algorithm is only valid for single-source node and it gives best result for each and every path connected to the source node. Though it is the most

primitive of shortest path algorithm, it proposed the foremost idea and scope of routing protocols. These protocols generally follow a set of well-defined rules and regulations. Dijkstra's algorithm is generally known as the “best first search” algorithm and in terms of high speed, it is much more useful than the algorithm proposed afterwards.

Dijkstra's algorithm states that: “It makes out the shortest path starting from the source node with comparing the distance from the source node to each and every unvisited neighbor node” [16].

4 Stability and Responsiveness in a Dynamic Environment

The responsiveness of any algorithm is greater for global routing method as compared to graph searching. In case of global routing method, the obstacles of the routing path are already known to the nodes. Global routing method is unable to cope up with the changing traffic condition. Graph searching method is located at the other facet of routing technology where shortest optimized route is searched at each and every node in the network. To overcome inter-signal interference in a high speed serial link, there is often need of congestion control in a routing path of a wireless network. The efficacy of dynamic routing over static routing is its changeability of routing path wherever needed. From micro-fluidic chip to VLSI chip, dynamicity is the exigency in network routing.

Han et al. proposed a novel approach to multipath routing in Internet technology by considering local stability condition, restraining for Eulerian circuit. As the dynamicity is directly proportional to the responsiveness of an algorithm, dynamicity will automatically increase with increasing rate of responsiveness.

5 Traditional Algorithm of Dijkstra

The primitive algorithm of Dijkstra is based on the complexity level of $O|N|^2$ where N is the number of routers or nodes. Further, with increasing of complexity based on the problem of Fibonacci heap, the running time complexity is increased by $O(|E|+N \log |N|)$ where “ E ” is the number of edges. The steps are as follows:

- Assign an initial value to the initial node and infinite to all other nodes.
- The infinite valued nodes are all set as unvisited nodes of the graph.
- Calculate distance from the source node to each and every neighbor node to find out the shortest path.
- Avoid visited graphs in each and every step.

6 Dynamic Perspective of Dijkstra's Algorithm

To meet the demand of highly dynamic environment, Dijkstra's algorithm must follow the Bellman's "Principle of Optimality". According to Bellman [3], to persuade certain objectives such as, minimization of routing time, minimization of cost, maximization of utility, and maximizing profit, dynamic problems are partitioned into various multi-period problems in course of time.

In terms of Bellman's "Principle of Optimality," "Regardless of the decisions taken to enter a particular state in a particular stage, the remaining decisions made for leaving that stage must constitute an optimal policy" [17]. Bellman's "Principle of Optimality" is basically a dynamic decision problem which is not viable for a number of work constraints. In terms of optimal controllability, stochastic evolution problem can be easily defined by Hamiltonian's equation. The analytical solution of Bellman's equation gives rise to infinite horizon solutions for multi-dimensional NP hard problems.

Bellman's equation can be stated as:

$$V(x) = \max\{U(a, x) + \partial F(y)\} \quad (1)$$

where y denotes the state of transition and x denotes the functionality of the optimization problem.

To ameliorate Bellman's equation, Markov's decision for dynamic problem established its solution stochastically. Markov's process is distributed in discrete time region randomly without following any rule. Here, each and every case of state transition is dependent on the chance. It is based on the iteration principle to pick out the best result.

7 Novel Approach to Dijkstra's Algorithm

Theorem 1 *Each node should follow the topological control algorithm to update the dynamicity of the network.*

Theorem 2 *The straight line which connects the nodes always gives the shortest path (Triangle Law of inequality).*

Theorem 3 *If there lays any polygonal obstacle in the path of interconnection, the routing path should make the minimum angle to avoid the hindrance in connection.*

Theorem 4 *To maintain closed loop and to adjust the cost of routing, it is advisable to follow source to source routing.*

Pseudocode of our newly proposed algorithm is as follows:

```

function Dijkstranew_algorithm (G,S,N)
    alt S ==0      //the distance of source to source is
                   // zero
    alt S N==infi //the distance of source to each and
                   // every node is infinite
    if
        vertex ≠ S
        alt S_vertex==infi
    else
        vertex==S
    end
        if t>0
            iteration starts;
    //Routing path is finalized based on a set of
    rules //(Theorem 1, 2, 3 and 4)
    //Update the routers of the changeability of the
    //routing path
Iteration++;

```

The non-fictional application of Dijkstra's algorithm is solely based on unpredictability of the changing environment. As compared to heuristics, meta-heuristics fuzzy mathematics always give out better result in terms of optimality.

Assuming uniformity of the n routers in a network, the constraints $(x_1, x_2 \dots x_n)$ can be utilized for interconnection. Fuzzification is based on the reality of changeability and depends on the constraint level.

$$ax_n < z \quad (2)$$

where a is the cost of unit length of routing path and z is the upper limit of total desired cost level.

Following Eq. (2)

$$F(x) = 1 \quad \text{when } ax_n < z \quad (3)$$

Otherwise

$$F(x) = 0 \quad (4)$$

The degree of optimization is always dependent upon the constraint, that is, maximum time level t_n , assuming $F(x)$ is the continuous function in the time domain.

Each and every router should be traversed once at a time during routing.

$$\sum_{i=0}^N x_i = 1 \quad (5)$$

and

$$\sum_{j=0}^N x_j = 1. \quad (6)$$

The location of each node is described as $x(i, j)$.

8 Results and Discussion

The graph in Fig. 2 for routing simply follows the Dijkstra's algorithm with updating the continuous change of dynamic environment. The interconnecting paths in our simulation result are always following the straight line. Here, the routing protocol is not following the priority of router rather it is following the shortest path in minimum time to cover all of the routers. Our routing approach makes a closed loop and follows the rules of source to source routing. The open loop always fails to control the flow of graph and eventually, congestion will be higher in the network.

Figure 2 proves that, in this example, the graph is based on 40 nodes and the connecting path in each and every node will always be a straight line to cover the whole network in a shortest path.

Table 2 proves that our proposed algorithm proves to be lesser complex. Though the Genetic Algorithm and the Swarm Particle Optimization depend on the stochastic level, their complexity level is more due to the larger amount of constraints. The lesser complexity level also signifies the feasibility of obtaining solution and implies lesser cost of routing. These results are only valid for complex network having number of nodes (N) greater than number of vertices (V) and edges (E). It is

Fig. 2 Simulated graph for 40 nodes with shortest routing path based on the MATLAB program by Kirk [18] and finds similarity with Table 2

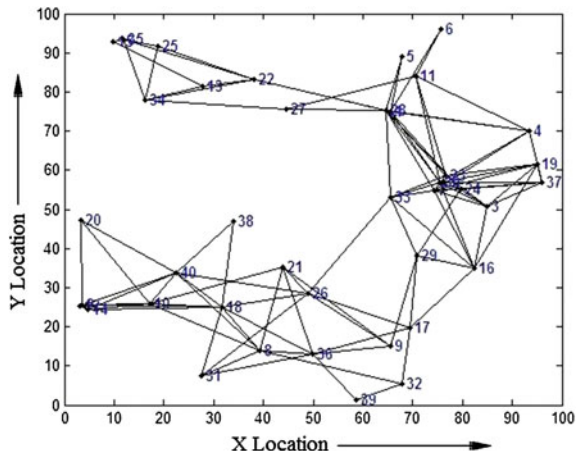


Table 2 Comparisons of complexity level of various routing algorithms

Name of algorithm	Complexity level
Traditional Dijkstra algorithm with Fibonacci heap	$O(V \log V + E)$
Bellman Ford's algorithm	$O(V\log V)$
Floyd's algorithm	$O N ^3$
Chinese Postman algorithm	$O N ^3$
Binary Genetic algorithm	To the extent of 10^6 – 10^9 (based on the diversity level of prokaryotes)
Pareto Genetic algorithm	To the extent of 10^6 – 10^9 (based on the diversity level of prokaryotes)
Permutation Genetic algorithm	To the extent of 10^6 – 10^9 (based on the diversity level of prokaryotes)
Ant Colony Optimization	$O(N^2 + (N\log N)/\rho)$ where ρ defines the pheromone trail
Delaunay triangulation	$O(N\log N)$
Kahng and Robbins Steiner optimization	$O(N^3\log N)$
Hwang's heuristic approach	$O(N\log N)$
Thompson's algorithm	$O(mV^2\log V)$ (for $m*m$ grid)
New approach to Dijkstra algorithm	$O N + (V - N) $

possible when only number of nodes is greater than 3. The proposed algorithm proves out to be less complex as compared to the Dijkstra's algorithm and also others. Table 2 is strictly based on analytical simulation and our 40 nodes graph is obtained from simulation using MATLAB 7.0.

9 Conclusion

The new approach to Dijkstra's algorithm is analyzed comprehensively using fuzzy environment. This novel approach is focused on the dynamic environment. Our algorithm also considers a set of polygonal obstacles in the routing path. We find a strong and supportive algorithm in view of minimal complexity, shortest path, and minimum cost routing. It is concluded that our simulation work strictly follows the proposed theorems. This new approach to Dijkstra's algorithm gives feasible solution often in adverse conditions. The fuzzy environment is supportive in the case of probabilistic case. Our algorithm is not following the conditional priority probability of the nodes rather than it is focused on determining shortest route path in a network. The routing path is not at all fixed for each and every condition but it will check whether the result will be best or not after a number of iterations.

By testing all the existing routing paths, our result simply proves the proposition which is stated in our theorems. The calculation of complexity level is nothing but the complex analysis of any problem based on Mathematics.

References

1. Ahuja, R.K., Magnanti, T.L., Orlin, J.B.: Network Flow Theory, Algorithms, and Applications. Prentice-Hall, Englewood-Cliffs, NJ (1993)
2. Bellman, R.: On the theory of dynamic programming. Proc. Natl. Acad. Sci. **38**, 716–719 (1952)
3. Bellman, R.: Dynamic Programming. Princeton University Press, Princeton, NJ (1957)
4. Bellman, R.: On a routing problem. Q. Appl. Math. **16**(1), 87–90 (1958)
5. Berge, C.: Theorie des Graphes et ses Applications. Dunod, Paris (1958)
6. Berge, C., Ghoulia-Houri, A.: Programming, Games, and Transportation Networks. John Wiley and Sons, NY (1965)
7. Dantzig, G.B., Thapa, N.M.: Linear Programming 2: Theory and Extensions. Springer Verlag, Berlin (2003)
8. SCI.OP-RESEARCH: Changing minimization to maximization, do the following problems change? SCI.OP-RESEARCH Digest **11**(13), Mon 5 April 2004. www.deja.com/group/sci.op-research (2004)
9. Dijkstra, E.W.: A note on two problems in connexion with graphs. Numer. Math. **1**, 269–271 (1959)
10. Dreyfus, S.: An appraisal of some shortest-path algorithms Operations Research **17**, 395–412 (1969)
11. Gass, S.I., Harris, C.M.: Encyclopedia of operations research and management science. Kluwer, Boston, Mass (1996)
12. Microsoft Shortest Path Algorithms Project: research.microsoft.com/research/sv/SPA/ex.html
13. Smith, D.K.: Networks and Graphs: Techniques and Computational Methods. Horwood Publishing Limited, Chichester, UK (2003)
14. Sniedovich, M.: Dynamic Programming. Marcel Dekker, NY (1992)
15. Winston, W.L.: Operations Research Applications and Algorithms, 4th edn. Brooks/Cole, Belmont, CA (2004)
16. Mohammadi, M.B., Hooshmand, R.A., Fesharaki, F.H.: A new approach for optimal placement of PMUs and their required communication infrastructure in order to minimize the cost of the WAMs. IEEE Trans. Smart Grid (99) (2015)
17. Gocheva-Ilieva, S.: Bellman's Optimality Principle. snow@uni-plovdiv.bg
18. Kirk, J.: MATLAB Central. www.mathworks.com

Asymmetric Coplanar Waveguide-Fed Monopole Antenna with SRR in the Ground Plane

S. Nikhila, Poorna Mohandas, P. Durga and Sreedevi K. Menon

Abstract In this paper, a compact Asymmetric Coplanar Waveguide (ACPW)-fed monopole antenna with Split Ring Resonator (SRR) in the ground plane is presented. Inclusion of SRR in the ground plane of ACPW offers a considerable bandwidth enhancement. SRR and Complementary SRR (CSRR) in the ground plane of ACPW are analyzed and bandwidth enhancements of 37.4 and 21.5 % at 2.52 GHz are obtained respectively, in comparison with ACPW-fed monopole antenna. The antennas offer an omni-directional pattern. Peak Gain of the antenna is found to be ~ 2 dBi for all the configurations in the frequency band of interest.

Keywords Asymmetric coplanar waveguide (ACPW) · Monopole antenna · SRR · CSRR

1 Introduction

Planar monopole antennas are very attractive as they exhibit wide bandwidth, omni-directional pattern, low cost, and ease of fabrication. Many designs employing different radiating and ground plane shapes have been studied for monopole designs [1, 2]. Microstrip-fed monopole antennas have also been of research interest offering a wide bandwidth with Omni-directional coverage [3]. Coplanar Waveguide-fed monopole antenna is a suitable choice for Monolithic Microwave Integrated Circuit (MMIC) application since ground plane and radiating patch are in

S. Nikhila (✉) · P. Mohandas · P. Durga · S.K. Menon
Department of Electronics and Communication Engineering,
Amrita Vishwa Vidyapeetham, Clappana P.O, Kollam 690525, India
e-mail: nikhilashaji@gmail.com

S.K. Menon
e-mail: sreedevikmenon@am.amrita.edu

same plane and it offers a good reflection and radiation characteristics [4]. The concept of Coplanar Waveguide (CPW)-fed monopole can be extended to an Asymmetric Coplanar Waveguide (ACPW)-fed monopole antenna which gives appreciable bandwidth with Omni-directional coverage [5].

Defected Ground Structures (DGS) are found to be effective as filters for Asymmetric Coplanar Waveguide (ACPW) [6]. Different types of DGS can be used in the ground plane to enhance the filter characteristics [3]. SRR and Complimentary Split Ring Resonator (CSRR) can form a type of DGS which when implemented in the ground plane of transmission line as it provides filter characteristics [7]. Modifying the ground plane of Coplanar Waveguide (CPW)-fed monopole antenna is found to enhance antenna characteristics considerably [8–11].

In this paper effect of SRR and CSRR in the ground plane of ACPW-fed monopole antenna is analyzed. The performance of these antennas is compared with ACPW antenna, fabricated on same substrate and resonant frequency.

2 Asymmetric Coplanar Waveguide-Fed Monopole Antenna Design

The antenna geometry of ACPW-fed monopole is presented in Fig. 1.

The feed line is designed for 50Ω on a substrate with dielectric constant $\epsilon_r = 4.4$ and thickness $h = 1.6$ mm using standard design equations [9]. For the antenna design with $L_1 = 33.5$ mm, $L_2 = 12$ mm, $W_2 = 26.7$ mm, the antenna resonates at 2.52 GHz offering a 2:1 VSWR bandwidth of 18.35 %. ACPW-fed monopole provides an Omni-directional radiation pattern with a peak gain of 1.18 dBi at the resonant frequency. The ground plane of this antenna is modified with DGS to enhance the bandwidth. The results obtained are presented in the next section.

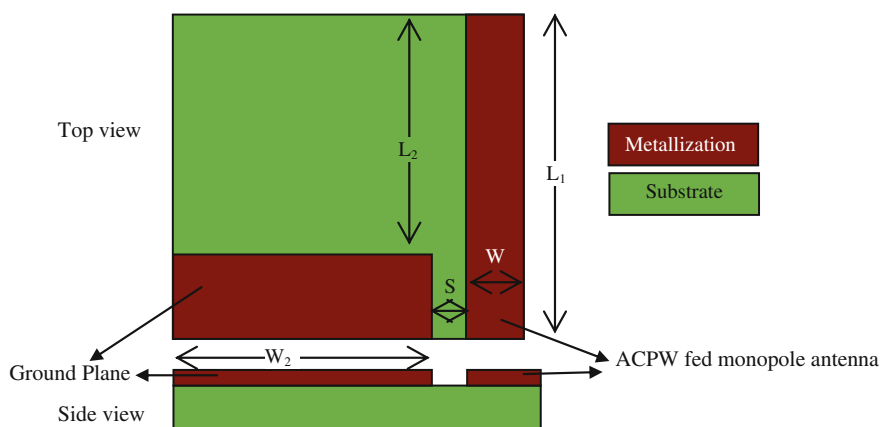


Fig. 1 Geometry of ACPW-fed monopole antenna

3 Bandwidth Enhancement Using Split Ring Resonator and Complimentary Split Ring Resonator

Split Ring resonator and Complimentary Split Ring Resonator are implemented on the ground plane of ACPW-fed monopole antenna. Figure 2a, b shows the geometry of ACPW-fed monopole antenna with SRR and CSRR in the ground plane, respectively.

Fig. 2 **a** Split ring resonator (SRR). **b** Complimentary split ring resonator (CSRR)

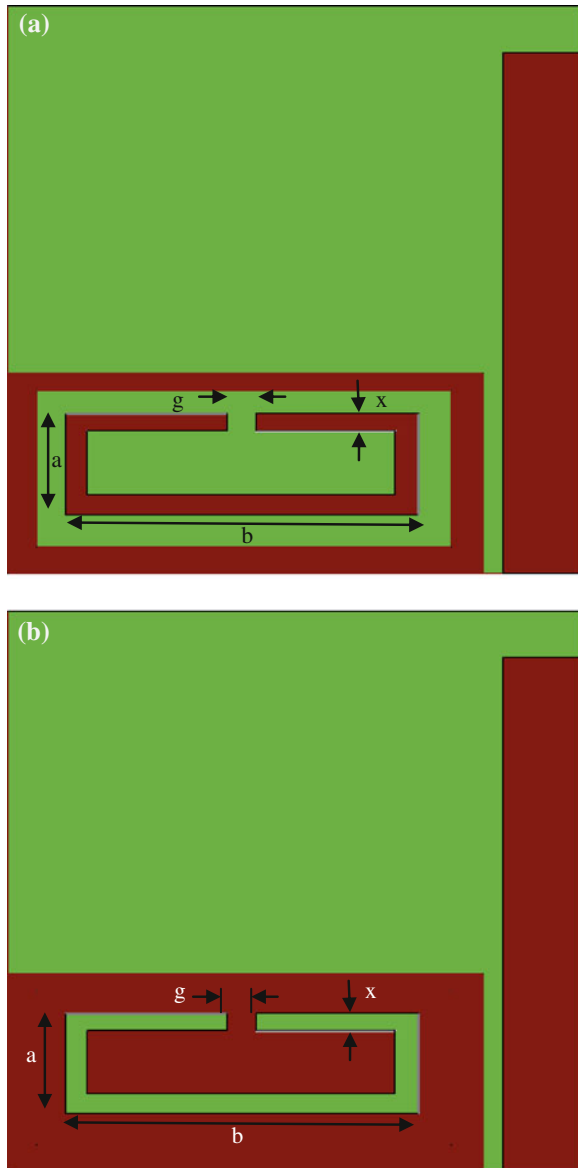
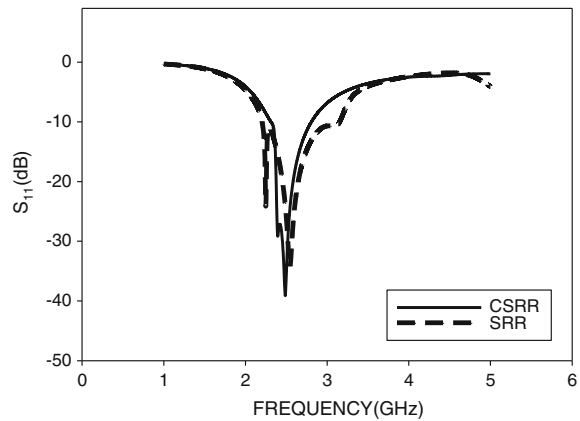


Fig. 3 Return loss

For the antenna resonating at 2.528 GHz SRR and CSRR of dimensions $g = 2$ mm, $x = 2$ mm, $a = 5$ mm, and $b = 20$ mm are implemented in the ground plane. The inclusions are found to enhance the bandwidth of the antenna by 37.4 % for SRR and 21.5 % for CSRR. This bandwidth enhancement is achieved without gain deterioration and a slight frequency shifts towards the lower side encompassing 2.528 GHz. The variation of return loss with frequency is depicted in Fig. 3.

The radiation characteristics of the above-mentioned antennas is analyzed in the frequency band and is plotted in Figs. 4 and 5.

It is found that the radiation pattern of ACPW-fed monopole antenna with SRR in the ground plane and ACPW-fed monopole antenna with CSRR in the ground plane is similar to that of a monopole antenna giving omni-directional characteristics.

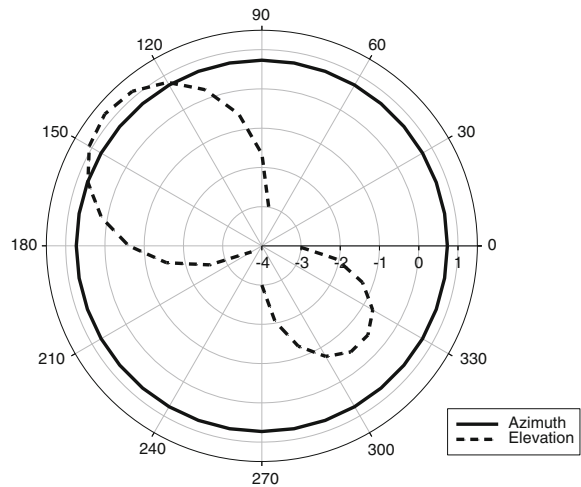
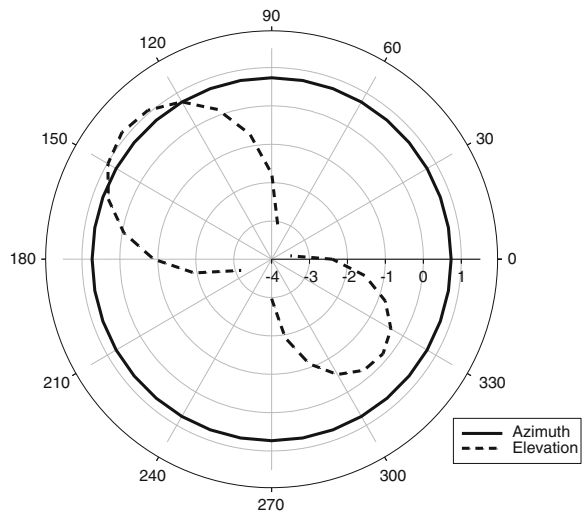
Fig. 4 Radiation pattern of ACPW-fed monopole antenna with SRR in the ground plane

Fig. 5 Radiation pattern of ACPW-fed monopole antenna with CSRR in the ground plane



The pattern is similar to ACPW-fed monopole antenna with a wider bandwidth. The gain of the three antennas is also studied and the bandwidth enhancement is obtained without compromising the gain of the antenna.

4 Result and Analysis

The Asymmetric Coplanar Waveguide-fed monopole antennas with SRR and CSRR are found to be effective radiators. For the three antennas, the characteristics observed at the resonant frequency 2.52 GHz is presented in Table 1. Bandwidth enhancement for the monopoles is achieved without increasing the size or volume of the antenna. Due to its enhanced bandwidth and compact size, these antennas can be used for MMIC applications. It is also suitable for sensor applications due to its omni-directional radiation pattern.

Table 1 Antenna properties

Antenna	Bandwidth (%)	Gain (dBi)
ACPW-fed monopole	18.35	1.18
ACPW-fed monopole with SRR	37.4	1.26
ACPW-fed monopole with CSRR	21.5	1.16

Acknowledgments This project is partly funded by a grant from Information Technology Research Agency (ITRA), Department of Electronics and Information Technology (Deity), Govt. of India.

References

1. Agrawall, N.P., Kumar, G., Ray, K.P.: Wideband planar monopole antennas. *IEEE Trans. Antennas Propag.* **46**(2), 294–295 (1998)
2. Ammann, M.J., Chen, Z.N.: Wideband monopole antennas for multiband wireless systems. *IEEE Antennas Propag. Mag.* **45**(2), 146–150 (2003)
3. Naghshvarian-Jahromi, M.: Novel wideband planar fractal monopole antenna. *IEEE Trans. Antennas Propag.* **56**(12), 3844–3849 (2008)
4. Lin, X.C., Yu, C.C.: A dual-band CPW-fed inductive slot-monopole hybrid antenna. *IEEE Trans. Antennas Propag.* **56**(1), 282–285 (2008)
5. Bhuvana, N.S., Das, A.T., Menon, S.K.: On chip ACPW fed monopole antenna. In: 2nd International Conference on Signal Processing and Integrated Networks, pp. 617–619, Feb 2015
6. Menon, S.K., Vasudevan, K., Anandan, C.K., Mohanan, P.: Compact asymmetric coplanar waveguide filter. *IEEE Electron. Lett.* **41**(11), 26 (2005)
7. Bonache, J., Gil, I., Garcia-Garcia, J., Martin, F.: Novel microstrip bandpass filters based on complementary split-ring resonators. *IEEE Trans. Microwave Theory Tech.* **54**, 265–271 (2006)
8. Antoniades, M.A., Eleftheriades, G.V.: A compact multiband monopole antenna with a defected ground plane. *IEEE Antennas and Wireless Propag. Lett.* **7**, 652–655 (2008)
9. Garg, R., Bhartia, P., Bahl, I.: Microstrip Antenna Design Handbook, 1st edn, pp. 794–795. Artech House, Boston (2001)
10. Lu, J.-H., Loiu, C.-W.: Planar dualband circular polarization monopole antenna for wireless local area networks. *IEEE Antennas Wireless Propag. Lett.* **14**, 478–481 (2015)
11. Saghanezhad, S.A.H., Atashaf, Z.: Miniaturized dualband CPW fed antennas loaded with U-shaped metamaterials. *IEEE Antennas Wireless Propag. Lett.* **14**, 651–658 (2015)

Image Processing of Natural Calamity Images Using Healthy Bacteria Foraging Optimization Algorithm

P. Lakshmi Devi and S. Varadarajan

Abstract The digital Image processing has emerged as an effective tool for analyzing the digital images of various fields and applications of engineering. Threshold technique is the most useful and well known among segmentation methods because of its robustness, simplicity, and high precision. This paper is an attempt to make an efficient segmentation Natural calamity images by Healthy Bacteria Foraging Optimization Algorithm.

Keywords Healthy bacterial foraging optimization • Natural disasters • Image segmentation • Thresholding

1 Introduction

Extraction of very minute details from natural calamity (NC) images is a challenging task for meteorological department of the Government. The current research attempts to investigate the better method for segmentation of NC images and seems that hopeful results have been obtained by Healthy Bacterial Foraging Optimization Algorithm (H-BFOA). For experimentation, we have procured NC Images of the calamity that was took place in Jammu and Kashmir of India in the month of September 2014. Extraction of color segmentation over gray-level segmentation gives very faithful results towards the required information [1, 2]. A unique idea of segmentation of NC images with H-BFOA for the extraction of

P. Lakshmi Devi (✉)

Department of Electronics and Communication Engineering, Annamacharya Institute of Technology and Sciences, Rajampet 516126, India
e-mail: drlakshmi143@gmail.com

S. Varadarajan

Department of Electronics and Communication Engineering,
Sri Venkateswara University College of Engineering, Tirupati 517501, India
e-mail: varadasouri@gmail.com

information is explained in the following sections. In image analysis, image segmentation is the most important prospect and image segmentation which divides the image into distinct and self-similar pixel groups [3, 4].

1.1 Color Image Segmentation

Color Images segmentation process is a different task, and for the past two decades huge research went with the aspirant researches in this field. To extract information from color image means that it has to be decomposed into identifiable items using color image processing techniques plus gray image processing techniques. In the visible electromagnetic spectrum, Color is a perceptual phenomenon related to human response to different wavelengths [5]. Color is the most well-known feature of any image and using vision algorithms information can be extracted from the respective image. The gray scale image has less information compared to color Image [6]. Besides many Image segmentation algorithms with BFOA [7] and researchers with Fuzzy set and Fuzzy Logic [8] also have been used for segmenting color images with a soft computing techniques [9] are used.

2 Bacterial Foraging Optimization Algorithm

In 2002, BFOA was introduced by Passino and it becomes a comprehensive optimization algorithm. It can be used in solving real-world optimization problems in several application domains. The life cycle of BFOA is given below [10]:

1. Chemotaxis,
2. Swarming,
3. Reproduction, and
4. Elimination and Dispersal.

Tumbling or Swimming are the two different exhibited actions by a bacterium during foraging [11]. The orientation of the bacterium can be modified by tumble action. Swimming is just as the chemotaxis step; the bacterium will move in its current direction. The movement of chemotaxis can be sustained until a bacterium goes in the direction of positive-nutrient gradient. The best half of the population can go for reproduction after certain number of complete swims and rest can be eliminated. For escaping local optima, an elimination dispersion event is carried out to liquidate some bacteria at random with a very small probability. Later, new replacements are initialized at random locations of the search space. Considering the foraging behavior of *Escherichia coli*, it has a common type of bacteria with a diameter of 1 μm , length of about 2 μm and under certain circumstances it can reproduce in 20 min. It has the ability to move from a set of up to six rigid 100–200 rps spinning flagella, each driven by a biological motor. The *E. coli* bacterium

alternates between running (at 10–20 $\mu\text{m s}$, but they cannot swim straight) and tumbling (changing the flagella). When the flagella are rotating in clockwise, they operate as propellers and hence an *E. coli* bacteria may be run or tumble. In elimination-dispersal event the gradual or unexpected changes in the local environment where a bacterium population lives it may occur due to the various reasons such as a significant local rise of temperature may kill a group of bacteria that are currently in a region with a high Concentration of nutrient gradients. BFO has various applications like Option Model calibration [12], image processing [13], RFID Network scheduling [14].

3 Proposed Method

Following are the steps for the proposed algorithm:

1. I is an image contains N pixels with gray levels from $0_L - 1$.
2. Input image into RGB planes.
3. Initialize $TR = 0$, $TG = 0$, $TB = 0$.
4. Bacterial search area of a Red component image size into $[m n]$.
5. $Nc = 1$, $Ns = 1$ i.e., Chemotactic and Swim length is one.
6. By using image histogram, calculate the health status $H(i + 1)$ of all image pixels. The health status of $H_i(i + 1)$ is given by $H(i + 1)/(m * n)$.
7. Calculate the Euclidean Distance (ED), between adjacent pixels x and y .
8. If $Ed <$ some threshold, then replace first pixel with adjacent pixel.
9. Calculating the health status of new pixels and varying the health status of Bacteria. A small local rise of temperature which keeps the bacteria in warm condition by varying health status results in quick and potential growth.
10. Calculating the difference of Health status of adjacent pixels. If the value is less than threshold health status then they can be treated as unpopular colors and can be removed to produce a new color.
11. Adding the color value to TR , TG , TB , and move the pixel over the entire image.
12. Do the same for Green and Blue images.
13. Individual thresholds as given by

$$TR = T(1)/(m * n)$$

$$TG = T(2)/(m * n)$$

$$TB = T(3)/(m * n).$$

14. Final Threshold: $TH = (TR + TG + TB)/3$.
15. Compute the performance indices as PSNR, Standard Deviation (SD), Entropy, and Class Variance and compare these values with Otsu method.

4 Performance Measures

To calculate and compare the resultant threshold of an image with the proposed algorithm and OTSU method, following performance measures are considered:

- (a) **PSNR:** Peak Signal to Noise Ratio (PSNR) is calculated by using the Eq. 1.

$$\text{PSNR} = 10 \log_{10} \frac{R^2}{\frac{1}{N \times N} \sum_{i=0}^{N-1} \sum_{j=0}^{N-1} (f(i,j) - f(i-j))^2} \text{dB}, \quad (1)$$

where

$N \times N$ = size of the input image,

$f(i, j)$ = gray-level pixel values of the input, and

$\hat{f}(i, j)$ = gray-level pixel values of the reconstructed images.

In generally PSNR is used to analyze quality of image, sound, and video files in dB (decibels). PSNR calculation of two images, one input and an altered image, describes to which level the two images are equal.

In Eq. 1, R is the maximum fluctuation in the input image. If the input image has a double-precision floating-point data type, then R is 1 that we considered with proposed algorithm H-BFOA for the segmentation of NC images. But in case of Otsu method, R value considered is 255, and hence better PSNR values are expected with H-BFOA, compared to Otsu method.

- (b) **Standard Deviation (SD):** The standard Deviation of an image is given by Eq. 2.

$$\sigma^2 = \frac{1}{n \times n} \sum_{j=1}^n \sum_{i=1}^m (x_{ij} - \hat{\mu})^2. \quad (2)$$

This corresponds to the degree of deviation between the gray levels and its mean value, for the overall image.

- (c) **Entropy E:** The information entropy expression of an image is given by Eq. 3.

$$E = - \sum_{i=0}^{L-1} P_i \ln P_i, \quad (3)$$

where

L = Number of gray level and

P_i = Ratio between the number of pixels whose gray value equals i (0 to $L - 1$) and the total pixel number contained in an image. The richness of information in an image is measured by information entropy. If the value of

P_i is constant for arbitrary gray level then it can be observed as the entropy will reach its maximum.

- (d) **Class Variance:** Class variance of the segmented image is computed by the following computation method: If the histogram is divided into two classes by the gray-level intensity t (threshold), then the probabilities of the respective classes can be expressed by the following Eqs. 4a and 4b.

$$P_1(t) = \sum_{i=0}^t P(i) \quad (4a)$$

$$P_2(t) = \sum_{i=t+1}^{N-1} P(i). \quad (4b)$$

Also, the class means $m1$ and $m2$ are given by Eqs. 5a and 5b.

$$m1(t) = \sum_{i=0}^t \frac{i_p(i)}{P_1(t)} \quad (5a)$$

$$m2(t) = \sum_{i=0}^t \frac{i_p(i)}{P_2(t)}. \quad (5b)$$

The two class variances are given by the Eqs. 6a and 6b.

$$\sigma_1^2(t) = \sum_{i=0}^t (i - m1)(i - m1) \frac{P_i}{P_1(t)} \quad (6a)$$

$$\sigma_2^2(t) = \sum_{i=t+1}^{N-1} (i - m2)(i - m2) \frac{P_i}{P_2(t)} \quad (6b)$$

The total class variance (σT) is given by Eq. 7:

$$\sigma T^2 = \sigma B^2 + \sigma W^2, \quad (7)$$

where

σB^2 = between class variance and

σW^2 = within class variance.

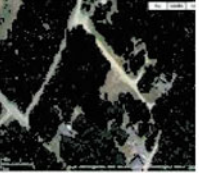
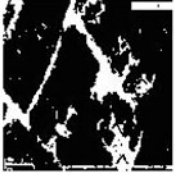
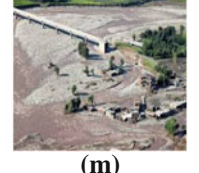
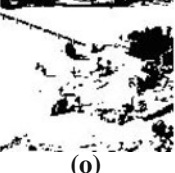
Input NC IMAGES	H-BFOA Output	OTSU Output
		
		
		
		
		
		

Fig. 1 Input and output result images

Equations for class variance and within class variance are given by the following Eqs. 8a and 8b.

$$\sigma W^2(t) = P_1(t) \sigma_1^2(t) + P_2(t) \sigma_2^2(t) \quad (8a)$$

$$\sigma B^2(t) = P_1(t) \cdot P_2(t) \{ m_1(t) - m_2(t) \}^2. \quad (8b)$$

5 Experimental Results

The proposed algorithm H-BFOA is used to segment NC images. The input images Fig. 1a, d, g, j, m are taken from *Googleimages.com* and are shown in Fig. 1. The health status of adjacent pixels is equal to 0.005 on H-BFOA then, Fig. 1b, e, h, k, n are the H-BFOA outputs. Figure 1c, f, i, l, o is the OTSU output images. The result images infer clearly that the color images have more information than gray-level images. More specifically, with H-BFOA for NC images we could distinguish color shades over water. The proposed H-BFOA is compared with OTSU method and results are tabulated. Tables 1, 2, 3, and 4 depict the performance indices for all the images. Peak Signal Noise Ratio (PSNR), Entropy, Standard Deviation (SD), and Class Variance (CV) are compared with the OTSU method and tabulated.

Table 1 Entropy comparison:: H-BFOA and OTSU

S. no.	Performance measures		
	Entropy	H-BFOA	OTSU
1	Image 1	0.9954	0.9219
2	Image 2	0.8839	0.7220
3	Image 3	0.9961	0.9934
4	Image 4	0.9492	0.7447
5	Image 5	0.9912	0.8845

Table 2 SD comparison:: H-BFOA and OTSU

S. no.	Performance measures		
	SD	H-BFOA	OTSU
1	Image 1	0.4984	0.4727
2	Image 2	0.4592	0.4000
3	Image 3	0.4987	0.4977
4	Image 4	0.4823	0.4085
5	Image 5	0.4970	0.4594

Table 3 CV comparison:: H-BFOA and OTSU

S. no.	Performance measures		
	CV	H-BFOA	OTSU
1	Image 1	0.0025	0.0022
2	Image 2	0.0021	0.0016
3	Image 3	0.0025	0.0025
4	Image 4	0.0023	0.0017
5	Image 5	0.0025	0.0021

Table 4 PSNR comparison::
H-BFOA and OTSU

S. no.	Performance measures		
	PSNR	H-BFOA	OTSU
1	Image 1	60.4397	53.2975
2	Image 2	55.9701	49.4018
3	Image 3	57.0629	51.0116
4	Image 4	57.9642	31.8375
5	Image 5	60.5905	51.8821

6 Conclusion

H-BFOA method is proved to be an efficient particularly when segmentation is done for NC images and very firm information could be extracted through a proper thresholding process. The performance indicator values PSNR, Entropy, SD, and CV are significant with the proposed algorithm and the same is proved to be efficient. In future the work can be extended with a scale area depth of location for a specific type of NC images.

References

1. Hu, X., Shen, J., Shan, J., Pan, L.: Local edge distributions for detection of salient structure textures and objects. *IEEE Geosci. Remote Sens. Lett.* **10**(3), 446–450 (2013)
2. Zhang, L., Yang, K.: Region-of-interest extraction based on frequency domain analysis and silent region detection for remote sensing image. *IEEE Geosci. Remote Sens. Lett.* **11**(5), 916–920 (2014)
3. Lang, F., Yang, J., Li, D., Zhao, L., Shi, L.: Polari metric SAR image segmentation using statistical region merging. *IEEE Geosci. Remote Sens. Lett.* **11**(2), 509–513 (2014)
4. Zhang, L., Li, H., Wang, P., Yu, X.: Detection of regions of interest in a high-spatial-resolution remote sensing image based on an adaptive spatial sub sampling visual attention model. *GIsci. Remote Sens.* **50**(1), 112–132 (2013)
5. Rosenfeld, A., Kak, A.: *Digital Picture Processing*, vol. 2. Academic Press, New York (1982)
6. Cheng, H.D., Jiang, X.H., Sun, Y., Wang, J.L.: Color image segmentation: advances and prospects. *Pattern Recogn.* **34**(12), 2259–2281 (2011)
7. Beenu, S.K.: Image segmentation using improved bacterial foraging algorithm. *Int. J. Sci. Res. (IJSR)* (2013)
8. Borji, A., Hamidi, M., Moghadam, A.M.E.: CLPSO-based fuzzy color image segmentation. In: *Proceedings of the North American Fuzzy Information Processing Society*, pp. 508–513 (2007)
9. Sowmya, B., Sheelarani, B.: Color image segmentation using soft computing techniques. *Int. J. Soft Comput. Appl.* **4**, 69–80 (2009)
10. Dasgupta, S., Das, S.: Bacterial foraging optimization algorithm: theoretical foundations, analysis, and applications. *Stud. Comput. Intell.* **203**, 23–55 (2009)
11. Zareh, S., Seyedjavadi, H.H., Erfani, H.: Grid scheduling using cooperative BFO algorithm. *Am. J. Sci. Res.* (62), 78–87 (2012). ISSN:1450-223X
12. Passino, K.M.: *Biomimicry for Optimization, Control, Automation*. Springer, London (2005)

13. Bakwad, K.M, Pattnaik, S.S., Sohi, B.S., Devi, S., Panigrahi, B.K., Sastri, G.S.V.R.: Bacterial foraging optimization technique cascaded with adaptive filter to enhance peak signal to noise ratio from single image. IETE J. Res. **55**(4), (2009)
14. Liu, W., Chen, H., Chen, H., Chen, M.: RFID network scheduling using an adaptive bacteria foraging algorithm. J. Comput. Inf. Syst. (JCIS) **7**(4), 1238–1245 (2011)

Necessitate Green Environment for Sustainable Computing

Bhubaneswari Bisoyi and Biswajit Das

Abstract The concept of green computing is eminently applied in the field of technology in order to reduce carbon dioxide emission and to have minimal impact on environment. Practice of green computing is used in designing, manufacturing, and discarding of computers, servers, monitors, printers, other storage devices, etc. Delve into this field of technology is abiding into key areas such as energy efficient use of computers and scheming algorithms that can be implemented for efficient management of computer technologies. It has been observed that energy consumed by IT section in an organization is around 60 % of the total energy consumed. It is expected that using green computing organization will be able to create value for both customer as well as in business. This paper focuses on review of the literature on sustainable Information technology and key area of focus is realization of green computing for a safe environment.

Keywords Green computing · Energy management · Reduction of carbon foot print

1 Introduction

Human green computing alternative can be also called as “Green IT” is now under surveillance by researchers, business process, organizations for running an energy efficient system. Initially the main focus of computing was to resolve complex issues in a shorter period with superior accuracy. But in the recent past, green computing has been gaining a vital position in organization in order to achieve energy efficiency, reduce power consumption of devices. The main focus of green

B. Bisoyi (✉) · B. Das
KIIT University, Bhubaneswar, India
e-mail: bhubaneswari.bisoyi@gmail.com

B. Das
e-mail: biswajit@ksom.ac.in

computing is to analyze and practice computation of resources in efficient manner and environment friendly. Many workstations are being made from unsafe resources such as cadmium, mercury, and other material. When we dispose these computers, it shall lead to contamination of atmosphere and affect the environment to a great extent. In order to reduce the impact of computer and other electronic devices used in our day to day activities, many programs have been introduced such as in 1991 the Environmental Protection Agency has introduced green lights program for efficient lighting. Thereafter in year 1992, Energy Star program was introduced for energy efficient designing of work stations. On the other hand during last decade green computing has gained grip. With fastest development in internet-based business process, frequently allegorically referred as cloud computing and the expense to sprint IT infrastructure are few major drivers of green computing. The overall expenditure of energy has risen drastically due to rapid expansion of data center and this is resulting in ejection of CO₂ to the atmosphere. When we study the energy bill of a company approximately 50 % of energy is consumed by data center.

Among various practices of green computing, it includes switching off the monitor while unused or using power saving screens like LED, LCD as a substitute of conventional CRT screen, folder giving out practices, virtualization of servers, using more energy efficient, and fewer raucous cooling methods [1, 2].

Green computing deals with several concerns [3, 4]. To be in specific, the aspirations are as follows:

- (a) To minimize energy utilization of the products in order to achieve energy efficiency.
- (b) To lessen the detrimental effects to the atmosphere during the application of perilous equipment.
- (c) To amplify the living instant of the product.
- (d) To capitalize on energy competence throughout the product's life span.
- (e) To encourage recyclability of obsolete artifacts and industrial unit desecrates.

2 Cause Motivating the Implementation of Green Computing

The following factors that are affecting huge data hub, desktop screen, and other devices are leading to the espousal of implementing green computing practices [5, 6].

2.1 The Express Development of Internet

With the rapid expansion of electronic data due to growth in business leads to setting up of huge data hubs. This expansion is outcome from the speedy implementation of internet communications and media, the automation of industry progression and functions, lawful prerequisites for maintenance of traces, and debacle revival. The present usage of Internet has grown further by 10 % per annum that leads to increase in demand of data hub at a rate of 20 % CAGR. With globalization there is a huge expansion in business process such as banks, investments, real estate, medical process, and manufacturing transport services; all are utilizing information technology for running their business. The introduction of the Sarbanes-Oxley Act with its prerequisite to maintain electronic reports has amplified storage insisting in few businesses at 50 % CAGR.

2.2 Escalating Cooling Necessities

With rise in data hub, internet usage and dependency on information technology server power density has also increased that led to a simultaneous increase in data hub heat density. The cooling requirement for each watt of server is approximately ranging between 1 and 1.5 W. The proportion of cooling power to server power prerequisites shall persist to augment with rise in density of data center server.

2.3 Rises in Expense of Power Consumption

The expense of power consumed for running data center and for cooling of the devices is about 50 % of the electricity expense. For a server rated 0.5 KWh costing \$4,000, one observation it was anticipated that it would use roughly about \$4,000 of electricity for operation and cooling over three years, at \$0.08 per KWh and twice that in Japan. With rise in demand for power globally maintenance and operation cost of data hub is mounting. Therefore, implementation of green computing for utilizing energy in an efficient approach is obligatory.

2.4 Limitations on Power Delivered and Admittance

When we consider top companies such as Google, Microsoft, and Yahoo, there is a huge need for large data hubs and for setting up data centers requirement of power may not be available at any considerable price in major American cities.

Therefore, they have constructed new data hubs in the Pacific Northwest where there are using power generated from hydro-electric resources at a cheaper price.

2.5 Low Server Deployment Rates

The major issue of Data center competency is in terms of consumption of energy. For bigger data centers, utilization rate of server ranges between 5 and 10 %. Minimal use of server means companies are paying excess amount for energy. Low server utilization means companies are overpaying for energy, protection, functional support, while only using a diminutive proportion of computing ability.

2.6 Budding Consciousness of Its Impact on the Atmosphere

Carbon emissions are proportional to power utilized. In the year 2007 near about 0.5 % of total electricity was consumed for operating near about 44 million servers worldwide. In U.S the total power used for operating the data center is more than 1 % of total electricity. It is anticipated that the rate of carbon emission from operations would grow by 11 % annually to 340 metric megatons by 2020. With increase in dependency on information technology the manufacturing of IT product would rise and this shall add to carbon.

3 Strategy for Putting Green Computing in Practice

Implementing the green computing practices has become a challenge in the present business process. Strategies are being planned to optimize the efficiency of data hub for better operation with lower cost and to lessen impact on environment [5, 6]. Few steps for implementing green computing in an efficient manner are mentioned below:

- (a) Developing a green computing plan after conversation with strategic team that shall comprise factors such as recycling policies, commendation for dumping of used devices and proposal for buying of green computer devices. The best practices of green computing and strategy should include utilization of energy, diminution of consuming paper, re-use of old machines in an efficient way by reducing its impact on environment.
- (b) Disposing worn or unused electronic devices in an environment friendly manner. Recycling of such systems through programs: planet partners recycling service.

- (c) Procurement of products through electronic product environmental assessment tool registered products (EPEAT).
- (d) Reprocessing of used paper: several ways of reducing use of paper by using e-mail, electronic documentation. Minimal usage of paper by printing both side and recycling of paper at regular interval.

4 Execution of Green Computing Stratagem

4.1 *Build in Infrastructure of Data Hub*

With increase in business world the requirement for data centers are also increasing to a greater extent. This development has put pressure on data center that are decade older and devices in such data centers require more power to drive as it has already reached their useful period and its efficiency level has already reduced. This type of data centers uses double power for operating and also for cooling system. In this case, preeminent strategy is to build up new data center with a design which is more energy saving or to retrofit existing centers.

4.2 *Execution of Cooling Devices*

There is an increase power requirement and this also requires appropriate dissipation of heat density in an efficient manner. The load or energy used for cooling and ventilation of devices is at par with that of requirement for running servers. The various techniques used for management of cooling devices used in data center are airflow mechanism, designing of data centers to make certain superior flow of air, installing efficient air conditioning, fluid heat amputation structures, temperature recuperation systems, and elegant thermostats.

4.3 *Product Blueprint*

When we consider an example of performance of microprocessor, it has increased with a cumulative annual growth rate of 50 % from the year 1981 to 2003. At present several core microchips are used that operate at slower regulator rapidity and lesser voltages than distinct-core mainframes and be able to influence memory and other architectural machinery to operate in energy efficient way. Therefore, the main focus is to design servers that consume energy in proportion to the work executed.

4.4 Virtualization

In order to meet the primary need of rowing business virtualization plays a vital role. It is primarily concerning IT most advantageous in terms of energy competency and expenditure diminution. It perks up the deployment of accessible IT possessions while reducing power utilized, investments, and man power costs. The virtualization of data hub influences four areas: server hardware and operating systems, storage, networks, and functional infrastructure. This technique is particularly helpful for lengthening the existence of older data hubs where there is no chance of extension. The energy requirement of virtual server is less than stand-alone servers [3].

This technology initially build up IBM as CP/CMS during the period 1960 to augment the operational competency of mainframes. At present this concept is applied in $\times 86$ servers in data hubs. Virtualization emphasizes the initiative of “green computing” by strengthening servers and takes full advantage of CPU dispensation control on additional servers.

4.5 Cloud Computing and Cloud Services

The need of internet-based computing is to consolidate all data hubs, software know-how so that it can be readily available whenever necessary. The term “cloud computing” refers to a computing form that endeavors to create high-performance computing obtainable through internet. Cloud computing facilitates developers to create, deploy, and run easily scalable services that are high performance, reliable, and free the user from position and infrastructure apprehensions. As cloud computing prolong to grow it has progressively taken on service attributes. These services include efficacy computing, software as a service, platform as a service, and infrastructure as a service [7, 8].

5 Contribution of Green Computing for Good Environment

In this era of globalization, using of computer and the requirement of electricity rise in each step therefore we cannot stop using these, but we need to put on to practice few actions to keep our environment healthy. The following actions should be taken by us.

5.1 Reducing Release of Carbon Foot Print

The main use of green computing is to reduce emission of carbon dioxide to environment. There is a huge impact of green house gases such as carbon dioxide, methane, chlorofluorocarbon that produced from several sources. The rise or fall in concentration of these gases influences the atmosphere by increasing temperature. This would lead to ruthless natural calamities distressing both life and the world's economy (Table 1).

5.2 Solar Computing

Accompanied by the development in alternative-energy sources, solar computing initiative is a noteworthy division of green computing assignments. Solar cells energy-proficient silicon, platform, and structure knowledge and facilitates to build up effusive solar-power-driven apparatus that are environment friendly, soundless, and exceedingly dependable. Solar cells need especially modest safeguarding throughout their life span, and once initial setting up expense are enclosed, they supply energy at almost no cost. Worldwide there is a rapid increase in manufacturing of solar cell over the last few years; and as more governments begin to recognize the benefits of solar power, and the development of photovoltaic technologies goes on, costs are expected to continue to decline [8, 9].

5.3 Turn Off Your Computer

The power consumption by personal computer and its secondary devices results in emission of carbon dioxide. We need to put in practice to shut down our systems when not in use; this shall save energy and reduce emission of carbon dioxide to a major extent (Table 2).

Table 1 Power consumption of different devices over the life cycle

	Desktop	Laptop	Plasma	LED-LCD
Power consumptions (W)	150	40	203 W/m ² + 0 W	172 W/m ² + 20 W
Embodied energy (MJ/unit)	2100	1362	5096 MJ/m ²	3218 MJ/m ²
Carbon emission (kgCO ₂ e)	350	227	849 kgCO ₂ e/m ²	536 kgCO ₂ e/m ²

Table 2 Power Consumed by Various Systems

Sl no.	Types of Devices	Functional units				Total power required
		Output device	Tangential devices	Central processing		
1	CRT	High	Low	Same for all	High	
2	LCD	Medium	Low	Same for all	Medium	
3	LED	Low	Low	Same for all	Low	

5.4 Make Use of Energy Star Tagged Products

The devices that are fabricated with energy star conserve use of power during its lifecycle. The concept behind energy star is to apply features of Green Computing. These devices are assembled with a design to conserve energy. These gadgets are designed to enter into energy saving mode while unused. Therefore, we use “Energy Star” tagged desktops, monitors, laptops, printers, scanners, and other computing devices [10].

5.5 Slumber Approach and Lay Quiescent Mode

The Slumber approach of our system sets the processor in a low power state so that we can promptly recommence operation. This approach saves power. It saves 60–70 % of energy. The lay quiescent mode permits us to close up all processes. When we are not using our computer for a squat phase of time we have to lie it in dormant. It saves the power when computer is not in use.

5.6 Planning for Power Management

The operation time period of computer shall be planned in advance so that the allocated work shall be completed within the stipulated time frame and effective power management can be carried out. This shall reduce ejection of carbon dioxide to atmosphere.

5.7 Avoid Use of Screen Saver

The consumption of electricity continues to occur even when the systems is not in use. This is due to running of screen savers. Screen saver can be a realistic,

manuscript or a figure that demonstrates on workstation monitor when it is not used for predetermined occasion. The best method is to remove screen savers.

5.8 Turn-Down Monitor Brightness

The heat generated due to utilization of energy by devices leads to emission of carbon dioxide. When we increase the brightness of our systems energy requirement also increases, thus built of heat.

5.9 Impede Unofficial Disposal

The dumping of computer and its constituents employ noxious substances while manufacturing, and when we exercise unofficial discarding they have destructive force on our surroundings. So to minimize the detrimental impact we shall implement formal disposing [11].

6 Conclusion

This paper highlights the significance of green computing practices. It also defines the obligatory steps that can be followed by organizations, business process for building up of healthy atmosphere. With increase in pollution from various sources this concept helps in reducing the carbon foot print around the atmosphere. So with a modest wisdom of appreciative and necessitate of green computing, we have to take the action at present or even from now. Green computing symbolizes a conscientious way to deal with the concern of global warming. By implementing green computing practices business leaders can contribute optimistically to ecological stewardship and safe guard the atmosphere.

References

1. Ong, D., Moors, T., Sivaraman, V.: Complete life-cycle assessment of the energy/CO₂ costs of videoconferencing vs. face-to-face meetings, Piscataway. In: Online Conference on Green Communications (GreenCom), pp. 50–55. IEEE, (2012)
2. Maria Kazandjieva, M., Brandon Heller, B., Omprakash Gnawali, O., Philip Levis, P., Christos Kozyrakis, C.: Green enterprise computing data: assumptions and realities, In: International Green Computing Conference (IGCC), pp. 1–10, IEEE (June 2012)
3. Mala, A., Uma Rani, C., Ganesan, L.: Green computing: issues on the monitor of personal computers. Int. J. Eng. Sci. 3(2), Issn(e): 2278–4721, Issn(p): 2319–6483, pp. 31–36, (May 2013)

4. Mala, A., Umarani, C., Ganesan, L.: Green computing: issues on the primary memory of personal computers. In: IOSR J. Comput. Eng. (IOSR-JCE) **12**(1), 56–60, (May–Jun 2013), e-ISSN: 2278–0661, ISSN: 2278–8727
5. Harmon, R.R., Auseklis, N.: Sustainable IT services: assessing the impact of green computing practices. In: Proceedings of PICMET, pp. 1707–1717, IEEE, Portland, (Aug 2–6 2009)
6. Sharmila Shinde, S., Simantini Nalawade, S., Ajay Nalawade, A.: Green computing: go green and save energy. In: Int. J. Adv. Res. Comput. Sci. Softw. Eng. **3**(7), 1033–1037 (July 2013)
7. Patra, C., Nath, A.: Green computing—New Paradigm of energy efficiency and e-Waste minimization—a pilot study on current trends. Int. J. Adv. Res. Comput. Sci. Manag. Stud. **2**(11), 542–553 (2014)
8. Kumar, S., Green computing. Int. J. Sci. Res. **4**(2), 67–69, (2015), ISSN: 2277–8179
9. Jindal, G., Gupta, M.: Green computing “future of computers”. Int. J. Emerg. Res. Manag. Technol. **1**(2), pp. 14–18, (2012), ISSN: 2278–9359
10. Pardeep Mittal, P., Navdeep Kaur, N.: Green computing—need and implementation. Int. J. Adv. Res. Comput. Eng. Technol. (IJARCET) **2**(3), 1200–1203 (2013)
11. Patil, M.G., Kumbhar, R.D.: Green computing: somewhat solution to drought. Int. J. Adv. Res. Comput. Sci. Softw. Eng. **3**(6), 1062–1065 (2013)

Determinantal Approach to Hermite-Sheffer Polynomials

Subuhi Khan and Mumtaz Riyasat

Abstract In this article, the determinantal definition for the Hermite-Sheffer polynomials is established using linear algebra tools. Further, the Hermite-Sheffer matrix polynomials are introduced by means of their generating function.

Keywords Hermite polynomials · Sheffer polynomials · Determinantal definition

1 Introduction

The Hermite polynomials are frequently used in many branches of pure and applied mathematics, engineering, and physics. The 2-variable Hermite Kampé de Feriet polynomials (2VHKdFP) $H_n(x, y)$ are defined as [2]:

$$H_n(x, y) = n! \sum_{k=0}^{\lfloor \frac{n}{2} \rfloor} \frac{y^k x^{n-2k}}{k!(n-2k)!} \quad (1)$$

and specified by the generating function

$$\exp(xt + yt^2) = \sum_{n=0}^{\infty} H_n(x, y) \frac{t^n}{n!}. \quad (2)$$

S. Khan (✉) · M. Riyasat
Department of Mathematics, Aligarh Muslim University, Aligarh, India
e-mail: subuhi2006@gmail.com

M. Riyasat
e-mail: mumtazrst@gmail.com

These polynomials are the solutions of the heat equation

$$\frac{\partial}{\partial y} H_n(x, y) = \frac{\partial^2}{\partial x^2} H_n(x, y), \quad (3)$$

$$H_n(x, 0) = x^n. \quad (4)$$

A polynomial sequence $\{s_n(x)\}_{n=0}^{\infty}$ ($s_n(x)$ being a polynomial of degree n) is called Sheffer A -type [10, p. 17], if $S_n(x)$ possesses the exponential generating function of the form:

$$A(t) \exp(xH(t)) = \sum_{n=0}^{\infty} s_n(x) \frac{t^n}{n!}, \quad (5)$$

where $A(t)$ and $H(t)$ have (at least the formal) expansions:

$$A(t) = \sum_{n=0}^{\infty} \alpha_n \frac{t^n}{n!}, \alpha_0 \neq 0 \quad (6)$$

and

$$H(t) = \sum_{n=1}^{\infty} b_n \frac{t^n}{n!}, b_1 \neq 0, \quad (7)$$

respectively.

The Sheffer sequence for $(1, H(t))$ is called the associated Sheffer sequence for $H(t)$ and the Sheffer sequence for $(A(t), t)$ becomes the Appell sequence [1] for $A(t)$.

Thus, the associated Sheffer sequence $p_n(x)$ is defined by the generating function

$$\exp(xH(t)) = \sum_{n=0}^{\infty} p_n(x) \frac{t^n}{n!} \quad (8)$$

and the Appell sequence $A_n(x)$ is defined by the generating function

$$A(t) \exp(xt) = \sum_{n=0}^{\infty} A_n(x) \frac{t^n}{n!}. \quad (9)$$

The Appell and Sheffer sequences arise in numerous problems of applied mathematics, theoretical physics, approximation theory and several other

mathematical branches, which appear in even the most basic problems of quantum mechanics.

In the past few decades, there has been a renewed interest in Sheffer polynomials. Properties of Sheffer polynomials are naturally handled within the framework of modern classical umbral calculus by Roman [10]. Another aspect of such study is to find the differential equation and recursive formula for Sheffer polynomial sequences. The mathematical concept of a Sheffer polynomial set has been used as a tool for determining how a signal changes when its complex cepstrum is scaled by a constant, see for example [11].

The Hermite-based Sheffer polynomials (HSP) ${}_{HS} s_n(x, y)$ are introduced in [8] by combining the 2VHKdFP $H_n(x, y)$ and Sheffer polynomials $s_n(x)$. The HSP are defined by the generating function of the form:

$$A(t) \exp(xH(t) + y(H(t))^2) = \sum_{n=0}^{\infty} {}_{HS} s_n(x, y) \frac{t^n}{n!}. \quad (10)$$

Since, for $A(t) = 1$, the Sheffer polynomials $s_n(x)$ reduce to the associated Sheffer polynomials $p_n(x)$. Therefore, by taking $A(t) = 1$ on the l.h.s. of Eq. (10), we obtain the generating function of the Hermite-associated Sheffer polynomials (HASP) ${}_{HP} p_n(x, y)$ as:

$$\exp(xH(t) + y(H(t))^2) = \sum_{n=0}^{\infty} {}_{HP} p_n(x, y) \frac{t^n}{n!}. \quad (11)$$

The determinantal forms of the Appell and Sheffer sequences are studied by Costabile and Longo in [4, 5] respectively. The determinantal approach considered in [4, 5] provides motivation to consider the determinantal forms of the mixed special polynomials.

In this article, the determinantal definition of the HSP ${}_{HS} s_n(x, y)$ is established using the generating functions of the HSP ${}_{HS} s_n(x, y)$ and HASP ${}_{HP} p_n(x, y)$. Further, the Hermite-Sheffer matrix polynomials are introduced by means of the generating function.

2 Determinantal Approach

The determinantal definition of the HSP ${}_{HS} s_n(x, y)$ is established using certain linear algebraic tools. In order to derive the determinantal definition of the HSP ${}_{HS} s_n(x, y)$, we prove the following result:

Theorem 1 The HSP $_{HS_n}(x, y)$ of degree n are defined by

$$_{HS_0}(x, y) = \frac{1}{\beta_0}, \quad (12)$$

$$_{HS_n}(x, y) = \frac{(-1)^n}{(\beta_0)^{n+1}} \times \begin{vmatrix} 1 & _{HP_1}(x, y) & _{HP_2}(x, y) & \cdots & _{HP_{n-1}}(x, y) & _{HP_n}(x, y) \\ \beta_0 & \beta_1 & \beta_2 & \cdots & \beta_{n-1} & \beta_n \\ 0 & \beta_0 & \binom{2}{1}\beta_1 & \cdots & \binom{n-1}{1}\beta_{n-2} & \binom{n}{1}\beta_{n-1} \\ \times & 0 & 0 & \beta_0 & \cdots & \binom{n-1}{2}\beta_{n-3} & \binom{n}{2}\beta_{n-2} \\ \cdot & \cdot & \cdot & \cdots & \cdot & \cdot & \cdot \\ \cdot & \cdot & \cdot & \cdots & \cdot & \cdot & \cdot \\ 0 & 0 & 0 & \cdots & \beta_0 & \binom{n}{n-1}\beta_1 \end{vmatrix},$$

$n = 1, 2, \dots,$

(13)

where

$$\begin{aligned} \beta_0 &= \frac{1}{\alpha_0}, \\ \beta_n &= -\frac{1}{\alpha_0} \left(\sum_{k=1}^n \binom{n}{k} \alpha_k \beta_{n-k} \right), \quad n = 1, 2, \dots \end{aligned}$$

Proof Let $_{HS_n}(x, y)$ be a sequence of polynomials with generating function given in Eq. (10) and α_n, β_n , be two numerical sequences such that

$$A(t) = \alpha_0 + \frac{t}{1!} \alpha_1 + \frac{t^2}{2!} \alpha_2 + \cdots + \frac{t^n}{n!} \alpha_n + \cdots, \quad n = 0, 1, \dots; \quad \alpha_0 \neq 0, \quad (14)$$

$$\widehat{A}(t) = \beta_0 + \frac{t}{1!} \beta_1 + \frac{t^2}{2!} \beta_2 + \cdots + \frac{t^n}{n!} \beta_n + \cdots, \quad n = 0, 1, \dots; \quad \beta_0 \neq 0, \quad (15)$$

satisfying

$$A(t)\widehat{A}(t) = 1. \quad (16)$$

Then, according to the Cauchy-product rules, we find

$$A(t)\widehat{A}(t) = \sum_{n=0}^{\infty} \sum_{k=0}^n \binom{n}{k} \alpha_k \beta_{n-k} \frac{t^n}{n!},$$

by which, we have

$$\sum_{k=0}^n \binom{n}{k} \alpha_k \beta_{n-k} = \begin{cases} 1 & \text{for } n = 0, \\ 0 & \text{for } n > 0. \end{cases} \quad (17)$$

Hence,

$$\begin{cases} \beta_0 = \frac{1}{\alpha_0}, \\ \beta_n = -\frac{1}{\alpha_0} \left(\sum_{k=1}^n \binom{n}{k} \alpha_k \beta_{n-k} \right), \quad n = 1, 2, \dots. \end{cases} \quad (18)$$

Let us multiply both sides of Eq. (10) by $\widehat{A}(t)$, so that we have

$$A(t)\widehat{A}(t) \exp(xH(t) + y(H(t))^2) = \widehat{A}(t) \sum_{n=0}^{\infty} {}_H s_n(x, y) \frac{t^n}{n!}. \quad (19)$$

In view of Eqs. (11), (15) and (16), we find

$$\sum_{n=0}^{\infty} {}_H p_n(x, y) \frac{t^n}{n!} = \sum_{n=0}^{\infty} {}_H s_n(x, y) \frac{t^n}{n!} \sum_{k=0}^{\infty} \beta_k \frac{t^k}{k!}. \quad (20)$$

By multiplying the series on the r.h.s. of Eq. (20) according to Cauchy-product rules, the previous equality leads to the following system of infinite equations in the unknown ${}_H s_n(x, y)$, $n = 0, 1, \dots$,

$$\begin{cases} {}_H s_0(x, y) \beta_0 = 1, \\ {}_H s_0(x, y) \beta_1 + {}_H s_1(x, y) \beta_0 = {}_H p_1(x, y), \\ {}_H s_0(x, y) \beta_2 + \binom{2}{1} {}_H s_1(x, y) \beta_1 + {}_H s_2(x, y) \beta_0 = {}_H p_2(x, y), \\ \vdots {}_H s_0(x, y) \beta_n + \binom{n}{1} {}_H s_1(x, y) \beta_{n-1} + \cdots + {}_H s_n(x, y) \beta_0 = {}_H p_n(x, y). \end{cases} \quad (21)$$

From the first equation of system (21), we get assertion (12). Also, the special form of system (21) (lower triangular) allows us to work out the unknown ${}_H s_n(x, y)$. Operating with the first $n + 1$ equations simply by applying the Cramer's rule, we find

$$\begin{aligned}
 & {}_H s_n(x, y) \\
 &= \frac{\left| \begin{array}{cccccc} \beta_0 & 0 & 0 & \cdots & 0 & 1 \\ \beta_1 & \beta_0 & 0 & \cdots & 0 & {}_H p_1(x, y) \\ \beta_2 & \binom{2}{1}\beta_1 & \beta_0 & \cdots & 0 & {}_H p_2(x, y) \\ \vdots & \ddots & \ddots & \ddots & \ddots & \ddots \\ \beta_{n-1} & \binom{n-1}{1}\beta_{n-2} & \binom{n-1}{2}\beta_{n-3} & \cdots & \beta_0 & {}_H p_{n-1}(x, y) \\ \beta_n & \binom{n}{1}\beta_{n-1} & \binom{n}{2}\beta_{n-2} & \cdots & \binom{n}{n-1}\beta_1 & {}_H p_n(x, y) \end{array} \right|}{\left| \begin{array}{cccccc} \beta_0 & 0 & 0 & \cdots & 0 & 0 \\ \beta_1 & \beta_0 & 0 & \cdots & 0 & 0 \\ \beta_2 & \binom{2}{1}\beta_1 & \beta_0 & \cdots & 0 & 0 \\ \vdots & \ddots & \ddots & \ddots & \ddots & \ddots \\ \beta_{n-1} & \binom{n-1}{1}\beta_{n-2} & \binom{n-1}{2}\beta_{n-3} & \cdots & \beta_0 & 0 \\ \beta_n & \binom{n}{1}\beta_{n-1} & \binom{n}{2}\beta_{n-2} & \cdots & \binom{n}{n-1}\beta_1 & \beta_0 \end{array} \right|}, \quad (22) \\
 & n = 1, 2, \dots
 \end{aligned}$$

Now, expanding the determinant in the denominator of Eq. (22) and transposing the determinant in the numerator, we find

$$\begin{aligned}
 & {}_H s_n(x, y) \\
 &= \frac{1}{(\beta_0)^{n+1}} \begin{vmatrix} \beta_0 & \beta_1 & \beta_2 & \cdots & \beta_{n-1} & \beta_n \\ 0 & \beta_0 & \binom{2}{1}\beta_1 & \cdots & \binom{n-1}{2}\beta_{n-2} & \binom{n}{1}\beta_{n-1} \\ 0 & 0 & \beta_0 & \cdots & \binom{n-1}{2}\beta_{n-3} & \binom{n}{1}\beta_{n-2} \\ \cdot & \cdot & \cdot & \cdots & \cdot & \cdot \\ 0 & 0 & 0 & \cdots & \beta_0 & \binom{n}{n-1}\beta_1 \\ 1 & {}_H p_1(x, y) & {}_H p_2(x, y) & \cdots & {}_H p_{n-1}(x, y) & {}_H p_n(x, y) \end{vmatrix}, \tag{23}
 \end{aligned}$$

where $n = 1, 2, \dots$ which after n circular row exchanges, that is, after moving the i th row to the $(i + 1)$ th position for $i = 1, 2, \dots, n - 1$, yields assertion (13).

Several important polynomials belong to the Sheffer family. By considering the suitable values of the coefficients in the determinantal definition of the Hermite-Sheffer polynomials, the determinantal definitions of the corresponding members can be obtained.

3 Concluding Remarks

Special matrix functions appear in statistics, Lie group theory and number theory [3]. Hermite matrix polynomials have been introduced and studied in [7] for matrices in $\mathbb{C}^{n \times n}$ whose eigenvalues are all situated in the right open half-plane.

We recall that the Hermite matrix polynomials $H_n(x; A)$ are defined by [7]:

$$H_n(x; A) = n! \sum_{k=0}^{\lfloor n/2 \rfloor} \frac{(-1)^k}{(n-2k)!k!} (x\sqrt{2A})^{n-2k}, n \geq 0 \tag{24}$$

and are specified by the generating function of the form [7]:

$$\exp\left(xt\sqrt{2A} - t^2I\right) = \sum_{n=0}^{\infty} H_n(x; A) \frac{t^n}{n!}, \tag{25}$$

where A is a matrix in $\mathbb{C}^{n \times n}$ such that

$$\operatorname{Re}(\mu) \not\leq 0, \quad \mu \in \sigma(A). \tag{26}$$

Recently, Khan and Raza [9] introduced the 2-variable Hermite matrix polynomials (2VHMaP) $H_n(x, y; A)$. The 2VHMaP $H_n(x, y; A)$ are defined by the generating function of the form:

$$\exp\left(xt\sqrt{\frac{A}{2} + yt^2 I}\right) = \sum_{n=0}^{\infty} H_n(x, y; A) \frac{t^n}{n!} \quad (27)$$

It is also shown in [9] that the 2VHMaP $H_n(x, y; A)$ are quasi-monomial with respect to the following multiplicative and derivative operators:

$$\widehat{M}_H = \left(x\sqrt{\frac{A}{2}} + 2y \left(\sqrt{\frac{A}{2}} \right)^{-1} \frac{\partial}{\partial x} \right) \quad (28)$$

and

$$\widehat{P}_H = \left(\sqrt{\frac{A}{2}} \right)^{-1} \frac{\partial}{\partial x}, \quad (29)$$

respectively.

Here, we combine the 2-variable Hermite matrix polynomials (2VHMaP) $H_n(x, y; A)$ with Sheffer polynomials $s_n(x)$ to introduce a mixed family.

In order to introduce the Hermite-Sheffer matrix polynomials (HSMaP) denoted by ${}_{HS} s_n(x, y; A)$ by means of generating function, we prove the following result:

Theorem 2 *The HSMaP ${}_{HS} s_n(x, y; A)$ are defined by the following generating equation:*

$$\exp\left(x\sqrt{\frac{A}{2}}H(t) + y(H(t))^2 I\right) = \sum_{n=0}^{\infty} {}_{HS} s_n(x, y; A) \frac{t^n}{n!}, \quad (30)$$

where A is a matrix in $\mathbb{C}^{n \times n}$ and satisfies condition (26).

Proof Replacing x by the multiplicative operator \widehat{M}_H of 2VHMaP $H_n(x, y; A)$ in the generating function (5) of the Sheffer polynomials $s_n(x)$, we find

$$A(t) \exp(\widehat{M}_H H(t)) = \sum_{n=0}^{\infty} s_n(\widehat{M}_H) \frac{t^n}{n!}. \quad (31)$$

Using the expression of \hat{M}_H given in Eq. (28) in the above equation, we have

$$\begin{aligned} A(t) \exp\left(\left(x\sqrt{\frac{A}{2}} + 2y\left(\sqrt{\frac{A}{2}}\right)^{-1}\frac{\partial}{\partial x}\right)H(t)\right) \\ = \sum_{n=0}^{\infty} s_n \left(x\sqrt{\frac{A}{2}} + 2y\left(\sqrt{\frac{A}{2}}\right)^{-1}\frac{\partial}{\partial x}\right) \frac{t^n}{n!}. \end{aligned} \quad (32)$$

Using the notations $X := x\sqrt{\frac{A}{2}}$, so that $\frac{\partial}{\partial X} := \left(\sqrt{\frac{A}{2}}\right)^{-1}\frac{\partial}{\partial x}$ and then decoupling the exponential operator on the l.h.s. of Eq. (32) using the Crofton-type identity [6]:

$$f\left(X + 2\lambda\frac{\partial}{\partial X}\right)\{1\} = \exp\left(\lambda\frac{\partial}{\partial X}\right)\{f(X)\} \quad (33)$$

and denoting the resultant Hermite-Sheffer matrix polynomials (HSMaP) on the r.h.s. by ${}_{HS} s_n(x, y; A)$, that is,

$${}_{HS} s_n(x, y; A) = s_n(\hat{M}_H) = s_n\left(x\sqrt{\frac{A}{2}} + 2y\left(\sqrt{\frac{A}{2}}\right)^{-1}\frac{\partial}{\partial x}\right), \quad (34)$$

we get assertion (30) after simplification.

Certain properties such as the series definition, operational representation, recurrence relations, differential equations, determinantal definition, etc., for the HSMaP ${}_{HS} s_n(x, y; A)$ are yet to be explored. This aspect will be taken up in the next investigation.

Acknowledgments The authors are thankful to the reviewer for useful suggestions toward the improvement of the paper.

References

1. Appell, P.: Sur Une Classe de Polynômes. Ann. Sci. École. Norm. Sup. **9**(2), 119–144 (1880)
2. Appell, P., Kampé de Fériet, J.: Fonctions Hypergéométriques et Hypersphériques: Polynômes d’ Hermite. Gauthier-Villars, Paris (1926)
3. Constantine, A.G., Muirhead, R.J.: Partial differential equations for hypergeometric functions of two argument matrix. J. Multivariate Anal. **3**, 332–338 (1972)
4. Costabile, F.A., Longo, E.: A determinantal approach to Appell polynomials. J. Comput. Appl. Math. **234**(5), 1528–1542(2010)
5. Costabile, F.A., Longo, E.: An algebraic approach to Sheffer polynomial sequences. Integral Transforms Spec. Funct. **25**(4), 295–311 (2013)

6. Dattoli, G., Ottaviani, P.L., Torre, A., Vázquez, L.: Evolution operator equations: integration with algebraic and finite difference methods, applications to physical problems in classical and quantum mechanics and quantum field theory. *Riv. Nuovo Cimento Soc. Ital. Fis. (4)* **20**(2), 1–133 (1997)
7. Jódar, L., Company, R.: Hermite matrix polynomials and second order matrix differential equations. *Approx. Theory Appl. (N.S.)* **12**(2), 20–30 (1996)
8. Khan, S., Al-Saad, M.W.M., Yasmin, G.: Some properties of Hermite-based Sheffer polynomials. *Appl. Math. Comput.* **217**(5), 2169–2183 (2010)
9. Khan, S., Raza, N.: 2-variable generalized Hermite matrix polynomials and Lie Algebra representation. *Rep. Math. Phys.* **66**(2), 159–174 (2010)
10. Roman, S.: *The Umbral Calculus*. Academic Press, New York (1984)
11. Schmidlin, D.J.: The bond between causal complex Cepstra and Sheffer polynomials. *IEEE Trans. Circuits Syst. II: Express Briefs* **52**(2), pp. 99–103 (2005)

Intelligent Traffic Monitoring System

**Satya Priya Biswas, Paromita Roy, Nivedita Patra,
Amartya Mukherjee and Nilanjan Dey**

Abstract Traffic congestion in cities is a major problem mainly in developing countries; to encounter this, many models of traffic system have been proposed by different scholars. Different ways have been proposed to make the traffic system smarter, reliable, and robust. This paper presents the various approaches made to enhance the traffic system across the globe. A comparative study has been made of different potential researches in which intelligent traffic system (ITS) emerges as an important application area. Important key points of each research are highlighted and judged on the basis of implementing them in developing countries like India. A model is also proposed which uses infrared proximity sensors and a centrally placed microcontroller and uses vehicular length along a length to implement intelligent traffic monitoring system.

Keywords Infrared proximity sensors • RF module • Bluetooth module • ITS

S.P. Biswas (✉) · P. Roy · N. Patra · N. Dey
Department of CSE, Bengal College of Engineering and Technology,
Durgapur, India
e-mail: thesatya01@gmail.com

P. Roy
e-mail: paromitaroy646@gmail.com

N. Patra
e-mail: niveditapatra111@gmail.com

N. Dey
e-mail: neelanjandey@gmail.com

A. Mukherjee
Department of CSE, Institute of Engineering and Management,
Salt Lake, Kolkata, India
e-mail: mamartyacse1@gmail.com

1 Introduction

The traffic jam is a daily-life problem in any metropolitan city. With the rise of standard of living, the number of vehicles is increasing at an exponential rate. In response to this, many researches are done in developing an intelligent traffic system (ITS), i.e., a traffic system which is involved in a much closer interaction with all the components of a traffic including vehicles, drivers, and even pedestrian. It not only provides safety at intersections and prevents traffic jam, but manages the traffic as a whole. Developed countries like America, Japan, and U.K. have already implemented ITS on their roads and still many researches are going on to make traffic systems more advanced and suitable for developing countries also. Apart from surveying various research works on ITS, this paper proposes a model which follows a simple algorithm based on the length of traffic on each lane. The length of traffic on the other lanes affects the time allotted to the current lane. Proximity sensors instead of WAN are to be used to determine the length of the traffic. The proposed idea can reduce the traffic in all lanes proportionately reducing the chances of congestion without the use of WANs. Besides, it also manages the occurrence of any emergency vehicles such as ambulance, fire brigade, etc. in any lane and also provides the mechanism to detect the route of a vehicle. Once implemented, it does not require any human assistance for its working.

2 Classification of ITS

ITS is being researched and implemented through various means such as the use of wireless sensor networks, RFID, applying various concepts of graph theory to find the minimized path and many other. Here, the concept of ITS has been classified into two broad domains, namely, (I) real-time system and (II) data analysis system.

Real-time systems have been further diversified into two fields:

- I. Path optimization and II. Traffic density. The data analysis systems are also divided into two parts:
 - i. Green light optimization, ii. Information chaining systems.

2.1 *Real-Time Systems*

Real-time systems in case of traffic managing system take the input of the current situation through video surveillance or WSNs and deal with the situation. The traffic signals are controlled according to the presence of vehicles and are operated

automatically in real time. A real-time optimization model was used by Dotolie et al. [1] that investigated the issue of traffic control in urban areas. The model took into considerations the traffic scenarios which also include pedestrians. This technique was applied for analyzing real case studies. Wenjie et al. [2] concentrate on calculating the time that a vehicle requires to reach the intersection from a particular point, dynamically, by the use of sensors. By this, data performs various calculations to find the green light length. Albers et al. [3] used real-time data to monitor current traffic flows in a junction so that the traffic could be controlled in a convenient way. Reliable short-term forecasting video captured in a recorder plays an important role in monitoring the traffic management system. The data required can be easily provided by the CCTV cameras that can be beside the roads as per requirement. Van Daniker [4] visualized the use of transportation incident management explorer (TIME) for calculating real-time data. Challal et al. [5] proposed a distributed wireless network of vehicular sensors to get a view of the actual scenario and used its various sectors to lower the congestion but not taking decisions in real time. The use of two types of sensor network was proposed, vehicular sensor network and wireless sensor network, and the combination of these two permits the monitoring as well as managing of the traffic. Chandak et al. [6] used video surveillance for realizing the real-time scenario. It deals with decreasing response time of the emergency cars by establishing communication between emergency cars and traffic lights. The data collected in real time can be used to determine the traffic density and also based on the traffic present. Several path optimization techniques can be used, which are discussed in the next two sections.

2.1.1 Traffic Density

Realization of the traffic density at a particular intersection for a given time can also help in reducing traffic congestion at that point. This data can be analyzed to determine several factors like green light length, traffic at the particular time, etc. Zhou et al. [7] used the concept of adaptive traffic light control algorithm which manipulates both the sequence and length of traffic lights in accordance with the detected traffic. The algorithm uses real-time data like the waiting time of vehicles, volume of traffic in each lane, etc. to determine traffic light sequence and optimal length of green light. The algorithm produces lower vehicle's average waiting time, thus providing much higher throughput. The system proposed by Sinhmar [8] used IR sensors to determine the density of traffic based on which the traffic signals were updated to provide a smooth flow of vehicles. Hussain et al. [9] proposed a system that uses a central microcontroller at every junction which receives data wireless sensor placed along the road that determines the traffic density. The microcontroller uses this data to control the traffic using the programmed algorithm to manage the traffic in an efficient manner. Srivastava et al. [10] suggested ways to determine the

number of vehicles using weight sensors, then with the use of a programmable logic controller to analyze the data, and then park in automated parking or has diverge them accordingly.

2.1.2 Path Optimization Technique

Finding the best and shortest path to destination can be used as a tool to minimize the traffic along a path. The traffic along the road can be sent to the incoming vehicle proving them the idea about the traffic and thus they can take an alternative path to the destination. Gambardella [11] and Bertelle et al. [12] proposed to find an optimized path for transportation using the concept of ant colony optimization. Once an optimized path is found, we can add several other features to make it more convenient and avoid traffic jams. Ozkurt et al. [13] have proposed the use of video surveillance and neural network to reduce the traffic stress across the network. Xia [14] researched to find an optimal road network and analyze the traffic dynamics by the movement of each car and the statistical property of the whole network. Kale et al. [15] designed a system that uses the traffic information and sends it to the incoming ambulance by allowing it take way according to the situation. The various performance evaluation criteria are used such as average waiting time, the average distance traveled by vehicles, and switching frequency of green light at a junction.

2.2 Data Analysis Systems

Data analytical systems are those systems that take the present or statistical data, process them in the processor, and then act according to predefined algorithm. Like real-time systems, it may collect data in real time, but is unable to take any decision in real time, i.e., it must follow the instructions that are provided to it. Yousef et al. [16] suggested a scheme of solving traffic congestion in terms of the average waiting time and length of the queue at the isolated intersection and provide efficient flow in global traffic control on multiple intersections with the accordance of real-time data. Thus, the data collected can be used in various ways depending on the perspective of the user. The next two sections define such ways of using the data.

2.2.1 Information Chaining System

The data collected at one junction can be sent to the other junction informing it about the situation and allowing it to take measures. The same can be used in case of cars, ambulance, and other vehicles. This is quite similar to the path optimization technique, but here the path that would be taken by the user is not suggested by the

system, and it just warns the others in case of any unwanted situation. Malik et al. [17] described the traffic control on a real-time basis using the traffic lights. Wireless sensors are deployed on each of the lanes that are able to detect number of vehicles passing and also the awaited vehicles and convey the information to the nearest control station. Blessy et al. [18] proposed a system that uses other vehicles to deliver messages about any congested path. They used an adjustable field radar-based system, vehicle controller sensor, which senses the count of the vehicles, rejecting the humans for certain distances. GSM service is used to send information about the congested junction to the server located in a remote location which in turn will inform its adjacent signal junction and also to other drivers about the congestion, forming a chain-like structure informing one another and suggesting them to change route if necessary.

2.2.2 Green Light Optimization

One of the main causes of traffic congestion is large red light delays, so controlling traffic signals and optimizing the length of the green light will become helpful. Chen et al. [19] have given the solution for minimizing waiting time of vehicles by testing the setting problems of traffic light. Here, the graph model is used to represent the traffic network. In order to achieve optimal solution [20–24], the paper has used particle swarm optimization [25, 26], ant colony optimization [27] and genetic algorithms which have greater importance. Soh et al. [28] presented a MATLAB simulation of fuzzy traffic controller for controlling traffic flow in the multilane isolated signalized intersection. The controller controls the traffic light timings and phase sequence to ensure smooth flow of traffic with minimal waiting time, queue length, and delay time. Jantan et al. [29] proposed monitoring system in addition to the traffic light system to determine different street cases (e.g., empty, normal, crowded) with different weather conditions using small associative memory depending on the stream of images, which are extracted from the streets' video recorders. It also gives a high flexibility to learn different street cases using different training images. Placzek [30] described a method which is designed to be implemented in an online simulation environment that enables optimization of adaptive traffic control strategies. Performance measures are computed using a fuzzy cellular traffic model, formulated as a hybrid system combining both cellular automata and fuzzy calculus. Dakhole et al. [31] used ARM7-based traffic control system that proposes a multiple traffic light control and monitoring system that reduce the possibilities of traffic jams, caused by traffic lights. This system uses ATmega16 and ARM7 for its processing. Jaiswal et al. [32] described the optimization of traffic signals by focusing on three areas—Ambulance, priority vehicles (like VIP cars, police jeeps), and Traffic density control—thus providing a stoppage free path for ambulances, preventing traffic congestion, and also managing traffic density by increasing duration of green light of the lane where density is high (Table 1).

Table 1 Summarization of classification of ITS

		Name	Summarization	Remarks
Intelligent traffic system	Real-time system	Traffic density	Finding the density of vehicles along a road and follow a certain algorithm to direct the vehicles	On spot detection and handling of traffic. Requires good financial investment
		Path optimization	Deciding an optimal path, for an incoming vehicle based on the traffic present at the approaching junction	Real-time analysis of data to find an easy path, but not applicable for all situations where alternative path is not present
	Data analysis system	Information chaining system	To inform the vehicles about the traffic along any lane and directing them to change to another route if necessary	Useful in routing of vehicles in an optimized path, but highly developed and error-free system is required else ambiguous situation may arise
		Green light optimization	Use of different logics like fuzzy logic and other simulation techniques to determine the green light length so that every lane is provided with some appropriate time slot	Highly efficient system. Requires large capital for implementation

3 Proposed Method

The proposed model mainly concentrates on the following factors:

- (i) Unnecessary consumption of the time slice in a certain lane, when there are fewer vehicles.
- (ii) If any lane has any emergency vehicle such as ambulance, it also has to wait for its turn.
- (iii) A lane with less or more traffic has to wait for the same time span.

Normally, the green signal in the traffic light remains on for a fixed interval for each road. In the existing system, congestion of vehicles may happen if lots of vehicles are waiting in a particular lane and the other lane which has fewer numbers of vehicles is made free.

3.1 Hardware Implementation of the Method

In the proposed model, infrared proximity sensor, AT Mega 2560, and RF modules have been used to design the system. The infrared sensors will be used to collect data from the lane and fetch the collected data to the microcontroller. In each road, there will be four infrared sensors which will be placed at a certain distance from the intersection, placed on either side of the roads in pair dividing the considered length of the road from the intersection into two zones—a high density zone and low density zone. The presence of vehicles in each region is sensed by two proximity infrared sensors placed at either side of the road in the opposite direction. The sensors are placed by keeping a certain distance so that they do not have an intersection point. The use of two sensors eliminates the factor if “vehicles are present along one side only,” i.e., it gives us the real view in what manner the vehicles are aligned along the road. The sensors are connected to the analog pins of the microprocessor and the traffic lights to the digital pins. While placing the sensors, it is to be kept in mind that the range of the sensors does not intersect, which will result in erroneous data read (Fig. 1).

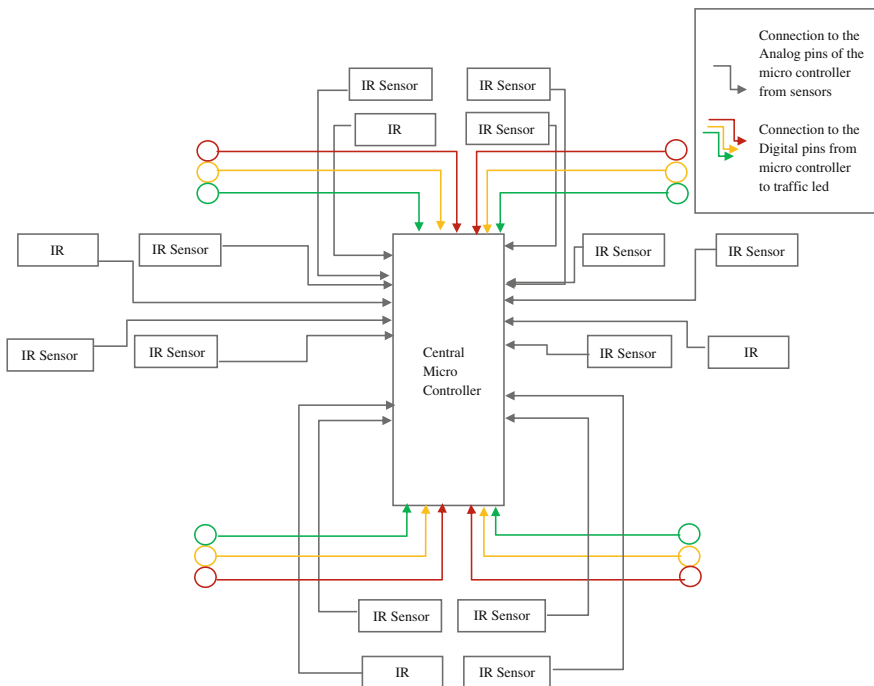


Fig. 1 Schematic circuit diagram of the proposed model

3.2 Prioritizing the Lanes

Moreover, it gives us the option to classify the density into multiple values. Like, if all the four sensors of one lane sense the value low, then there will be no traffic and the priority assigned is zero in this case. When both the two sensors in low intensity zone sense the value as low, but both the sensors in high intensity zone sense the value as high, then this case will not be considered, and it is not possible. Suppose one of the two sensors in low intensity zones gives the value as high, but the two sensors in high intensity zone sense the value as low, which will indicate that the traffic is very less in this lane and the priority assigned is one. If two sensors from the same side one from low and the other from the high intensity zone sense the value as high, then it will indicate that one side of both zones is full and the other side is free from traffic and the priority assigned is two. Then if both the sensors in low intensity zone sense the value as high, but the sensors in high intensity zone sense the value as low, then the low intensity zone is full but no vehicle in the high intensity zone and the priority assigned is three. When both the sensors in low intensity zone sense the value as high and one of the sensors in high intensity zone senses the value as high, then it will indicate that low intensity zone is full but no vehicle in one side of the high intensity zone and the priority assigned is four. If all the four sensors provide the value as high, then it will indicate that there is vehicle in both the zones, i.e., both is full which gives high alert and priority assigned to this case is five (Fig. 2).

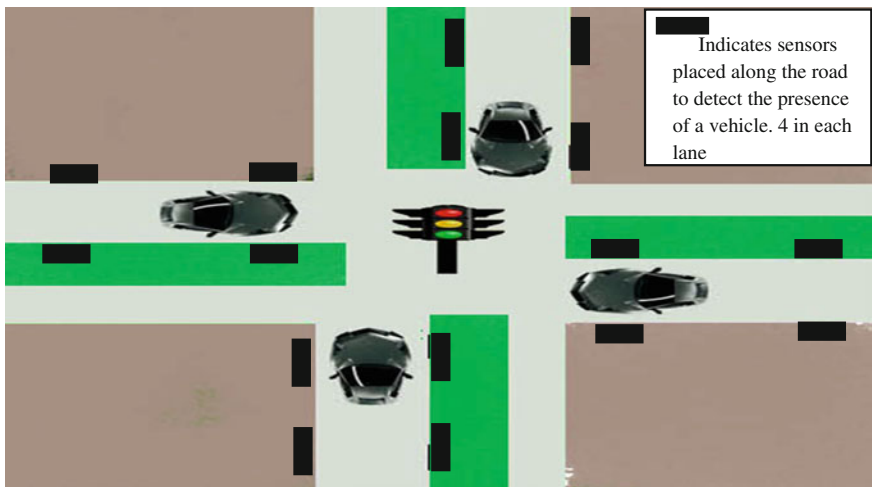


Fig. 2 Conceptual view of the proposed model

3.3 Algorithm for the Control of Traffic Lights

The proposed algorithm initially senses the vehicular length of each lane and sets its priority and pushes it into the stack.

The sequence in which the lanes are pushed will be executed in this sequence only. Sense_and_Set check the length of the vehicles and set their time accordingly, also keeps a check that the lane with lower priority initially may have acquired a higher priority than its preceding lane; in such case, the green light duration T_i , to be provided to the present lane, is decreased. The stack is popped after execution of each lane. Once the stack is empty, the lanes are once again pushed into the stack according to priority and executed accordingly.

Control_Algo

P_STACK [4]: Stack to store the lane according to priority.

Ti: Green Time assigned to the lane.

P_i, P_{i-1}: Priority assigned to the top two lanes.

While (true) repeat

Sense_and_Push () for setting the P_STACK

While (Length.P_STACK not equal to 0) repeat

Sense_and_Set (P_STACK): sense the priority for the lane at the top of the P_STACK and setting the green light time of the lane at the top of the P_STACK.

Execute (P_STACK, T_i): Execute the green Light of the lane at the top of the P_STACK.

End.

Sense_and_Push ()

Sense each lane and prioritize them.

Push the lane according to their priority into P_STACK, the lane at the top of the P_STACK has maximum priority.

End.

Sense_and_Set (P_STACK)

If there is an emergency vehicle across any lane

Bring it to the top of the P_STACK, Set T_i

Return.

Else

Sense the priority of the top two elements of the stack.

P_i= Priority of the lane at the top of the stack.

If (i=0)

P_{i-1} =0.

Else

P_{i-1} = Priority of the lane next to the top of the stack.

Set T_i according to P_i

If (P_i < P_{i-1})

Indicating that the vehicle length has increased after setting the P_STACK.

Update T_i

End.

Execute (P_STACK, T_i)

Set the green light for the lane at the top of P_STACK for time T_i

Set the yellow light for the lane next to the top of the P_STACK for time T_i indicating that it will be executed next and red to the other two lanes..

Pop P_STACK

End.

4 Conclusion

The work presents review of the existing research done in field and tries to develop a system suitable for developing countries. The project has two objectives, which are, first, calculating the length of the vehicles on the road for the flow of the traffic smoothly without congestion and, second, developing priority-based signaling which will help to give the priority to the emergency vehicles such as ambulance. The microcontroller can be programmed easily which gives scope for deployment better algorithms in future. The sensors are to be fitted on the side of the roads and connected to the controller at the intersection. These are some hectic jobs which are to be dealt before implementing the system, but once implemented, it will make our traffic system more convenient and cities smarter.

References

1. Mariagrazia, D., Pia, F.M., Carlo, M.: Real time traffic signal control: application to coordinated intersections. In: IEEE International Conference, vol. 4, pp. 3288, 3295. 5–8 Oct 2003
2. Wenjie, C., Lifeng, C., Zhanglong, C., Shiliang, T.: A realtime dynamic traffic control system based on wireless sensor network, parallel processing, 2005. In: International Conference on ICPP Workshops, pp. 258–264. 14–17 June 2005, ISSN: 1530-2016, Print ISBN: 0-7695-2381-1
3. Queen, C.M., Albers, C.J., Forecasting traffic flows in road networks: a graphical dynamic model approach, 29 July 2008
4. VanDaniker M.: Visualizing real time and archived traffic incident data. In: Proceedings of the 10th IEEE International Conference on Information Reuse and Integration, pp. 206–211. IEEE Press Piscataway, ©2009, ISBN: 978-1-4244-4114-3
5. Sharma, A., Chaki, R., Bhattacharya, U.: Wireless sensor networks. In: 3rd International Conference on ICECT, Jan 2011. doi:[10.1109/ICECTECH.2011.5941955](https://doi.org/10.1109/ICECTECH.2011.5941955)
6. Amine Kafi, M., Challal, Y., Djenouri, D., Bouabdallah, A., Khelladi, L., Badache, N.: A study of wireless sensor network architectures and projects for traffic light monitoring. In: International Conference on Ambient Systems, Networks and Technologies, pp. 543–552, 28 Aug 2012
7. Zhou, B., Cao, J., Zeng, X., Wu, H.: Adaptive traffic light control in wireless sensor network-based intelligent transportation MATLAB. In: Vehicular Technology Conference Fall, IEEE 72nd, pp. 1–5, 6 Sept 2010
8. Promila Sinhmar, A.: Intelligent traffic light and density control using ir sensors and microcontroller. Int. J. Adv. Technol. Eng. Res. **2**(2), 30–35 (2012)
9. Hussian, R., Sharma, S., Sharma, V., Sharma, S.: WSN applications: automated intelligent traffic control system using sensors. Int. J. Soft Comput. Eng. **3**(3), 77–81 (2013)
10. Srivastava, M.D., Prerna, Sachin, S., Sharma, S., Tyagi, U.: Smart traffic control system using PLC and SCADA. Int. J. Innov. Sci. Eng. Technol. **1**(2), Dec 2012
11. Gambardella Luca M.: Ant colony optimization for ad-hoc networks. In: The first MICS workshop on routing for Mobile Ad-Hoc Networks, Zurich, 13 Feb 2003
12. Cyrille, B., Antoine, D., Sylvain, L., Damien, O.: Road traffic management based on ant system and regulation method (2006)
13. Ozkurt, C., Camci, F.: Automatic traffic density estimation and vehicle classification for traffic surveillance systems using neural network. Math. Comput. Appl. **14**(3), 187–196 (2009)

14. Yongxiang, X., Traffic control and optimization in road networks, 4 Sept 2009
15. Kale, S.B., Dhok, G.P.: Design of intelligent ambulance and traffic control. *Int. J. Comput. Electron. Res.* **2**(2) 2013
16. Yousef, K.M., Al-Karaki, J.N., Shatnawi, A.M.: Intelligent traffic light flow control system using wireless sensors networks (2010)
17. Malik, T., Yi, S., Hongchi, S.: Adaptive traffic light control with wireless sensor networks. In: *Proceedings of IEEE Consumer Communications and Networking Conference*, pp. 187–191, 2007/1
18. Blessy, A., Devi, Reeona: An automatic traffic light management using vehicle sensor and GSM model. *Int. J. Sci. Eng. Res.* **4**(6), 2354–2358 (2013)
19. Shiuan-Wen, C., Chang-Biau, Y., Yung-Hsing, P.: Algorithms for the traffic light setting problem on the graph model (1996)
20. Dey, N., Samanta, S., Yang, X.-S., Chaudhri, S.S., Das, A.: Optimisation of scaling factors in electrocardiogram signal watermarking using cuckoo search. *Int. J. Bio-Inspired Comput. (IJBIC)* **5**(5), 315–326 (2013). (Impact Factor: 1.681) (Science Citation Index, Scopus)
21. Day, N., Samanta, S., Chakraborty, S., Das, A., Chaudhuri, S.S., Suri, J.S.: Firefly algorithm for optimization of scaling factors during embedding of manifold medical information: an application in ophthalmology imaging. *J. Med. Imaging Health Inform.* (Impact Factor: 0.623) (Science Citation Index Expanded (SciSearch), Scopus)
22. Samanta, S., Acharjee, S., Mukherjee, A., Das, D., Dey, D.: Ant Weight Lifting Algorithm for Image Segmentation, 2013 IEEE International Conference on Computational Intelligence and Computing Research(ICCIC), Madurai, Dec 26–28 2013 [IEEE Xplore]
23. Samanta, S., Chakraborty, S., Acharjee, S., Mukherjee, A., Dey, N.: Solving 0/1 Knapsack Problem using Ant Weight Lifting Algorithm. In: 2013 IEEE International Conference on Computational Intelligence and Computing Research(ICCIC), Madurai, Dec 26–28 2013 [IEEE Xplore]
24. Chakraborty, S., Pal, A.K., Dey, N., Das, D., Acharjee, S.: Foliage Area Computation using Monarch Butterfly Algorithm. In: 2014 International Conference on Non Conventional Energy (ICONCE 2014), JIS college of Engineering, Kalyani, January 16–17, 2014. [IEEE Xplore]
25. Dey, N., Chakraborty, S., Samanta, S.: Optimization of watermarking in biomedical signal. Lambert Publication, Heinrich-Böcking-Straße 6, 66121 Saarbrücken, ISBN-13: 978-3-659-46460-7
26. Chakraborty, S., Samanta, S., Mukherjee, A., Dey, N., Chaudhuri, S.S.: Particle Swarm Optimization Based Parameter Optimization Technique in Medical Information Hiding. In: 2013 IEEE International Conference on Computational Intelligence and Computing Research (ICCIC), Madurai, Dec 26–28 2013 [IEEE Xplore]
27. Jagatheesan, K., Anand, B., Dey, N.: Automatic Generation Control of Thermal-Thermal-Hydro power systems with PID controller using Ant Colony Optimization, *International Journal of Service Science, Management, Engineering, and Technology (IJSSMET)*, Vol 6, Issue 2
28. Azura Che Soh/Lai Guan Rhung: MATLAB simulation of fuzzy traffic controller for multilane isolated intersection. *Int. J. Comput. Sci. Eng.* **02**(04), 924–933 (2010)
29. Emad, I., Kareem, A., Jantan, A.: An intelligent traffic light monitor system using an adaptive associative memory. *Int. J. Inf. Process. Manag.* **2**, 2(2.4), 23–39 (2011)
30. Placzek, B.: Performance evaluation of road traffic control using a fuzzy cellular model. In: 6th International Conference on HAIS, Wroclaw, pp. 59–66. Proceedings, Part II, 23–25 May 2011
31. Dakhole, A.Y., Moon, M.P.: Design of intelligent traffic control system based on ARM. *J. VLSI Signal Proc.* **4**(4), 37–40 (2014). Ver. I
32. Jaiswal, S., Agarwal, T., Singh, A., Lakshita, : Intelligent traffic control unit. *Int. J. Electr. Electron. (ISSN NO. (Online): 27-2626 and Computer Engineering* **2**(2), 6–72 (2013)

Analysis of Mining, Visual Analytics Tools and Techniques in Space and Time

K. Nandhini and I. Elizabeth Shanthi

Abstract All living things are connected to the space and time, which really shows a necessity to improve their sophistication for leading a better life. Exploration and prediction in space and time has been the tough chore to the researchers and developers. Development in the technology helps to elevate the persevering difficulties. Two interdisciplinary approaches in the computer science that has become pre-eminent in the effective analysis of space and time are data mining and visual analytics. Visual analytics is one interactive user interface where we can explore and visualize the data using visual analytic tools. So, visual analytics with the complex data requires a competent approach for accuracy which is nevertheless a data mining process. But the real scenario is, techniques and tools are more developed but may not nail in terms of accuracy and speed for handling complex-and time-oriented data. The main cause of the dearth may be more new tools and techniques developed by more researchers are not deliberated. The mission of the research paper is to study the techniques and tools of data mining and visual analytic in space and time.

Keywords Data mining · No-SQL databases · Space and time · Spatial data · Spatio-temporal · Temporal data · Visual analytics · Geographical analysis

1 Introduction

Dealing with the huge multifaceted data has become more often in day-to-day operations in any domain. There are lots and lots of data may store in databases, data warehouses, cloud or secondary discs. These data collection may have noise,

K. Nandhini (✉) · I. Elizabeth Shanthi

Department of Computer Science, Avinashilingam Institute for Home Science and Higher Education for Women, Deemed University, Coimbatore, Tamil Nadu, India
e-mail: nandhinik2@gmail.com

I. Elizabeth Shanthi
e-mail: shanthianto@gmail.com

missing values or wrong entry while acquire in a data operations such as modify, update, insert or delete operations. Perceiving the information from these technical hitches is really a frantic situation to the data scientist.

The necessity of the data mining arose from the natural evolution of information and database technology [1]. Identifying the information from the massive multi-dimensional data stored in databases or data warehouses are really beyond the human ability. It comprises large set of numerical and categorical value of data. Mostly these data mining techniques help broadly to comprehend the text, web, or spatial techniques [2]. Visualization helps the human to understand and able to make quick decision even if it is enormous complex data. It supports the user to interact with the data by querying, and also different views are enabled to identify the structure, pattern and behaviour of the data. Space and time is one of the visual analytic application categories which deal with spatial analysis [3]. In daily life, people face problems mostly related to space and time. For example, tourists who are entirely new to a place with language barrier also, can collect the information through local people. However, there may be a chance of miscommunication which will lead to wrong place. In this innovative world there are other options also like GIS or Maps which helps the tourists in a better way.

2 Motivation

There is always some interestingness to find undiscovered neighbourhood of earth which were tracked conventionally by using maps. These maps are imperfect for decision-making and poor models to solve the problems. The expectation and interestingness rise to develop an advance technology deals with geo-visual analysis. There are many scenario shows that the unfortunate risk happens to the living things which are really challenging for survival on that precise condition. Consider, a few examples, such as natural disaster, traffic management, global market crash, etc., which are really needed to distillate by making decisions. The combined strength of visual analytics and data mining provides an informative edge. Space and time is one of the fundamental visual analytic applications.

In India, September 2014 Jammu and Kashmir faced many deaths, loss of assets, and health issues due to heavy flood. The major reason behind this was poor decision making due to lack of analyzing tools in the system. The issues may be major or minor but the people are in a haste to take decisions in a short period. Space and time data are pigeonholed by space related, change in state and if the data related to space and changes in state are called geospatial data, temporal data and spatio-temporal, respectively [3]. These kinds of data are collected through WiMAX, LiDAR, RFID or GPS [4].

3 Mining and Visual Analytic Approaches

3.1 Geospatial Data

Geospatial analyses are classified into four types where the different techniques fall into that classification. They are data reduction techniques, exploratory data analysis, statistical models (quantitative information) and mathematical modelling [4]. An exploratory data analysis technique permits to explore first-or second-order variation of the spatial data. First-and second-order variations describes spatially distributed data and dependence between observations. Global and local autocorrelation, Hot spots and density are collectively used to measure the similarity, overall behaviour and unsupervised learning procedure [4, 5]. Statistical foundation characterized the spatial problem as pointing process, lattice and geostatistics.

The geospatial data can be represented into two forms which are *vector* data and *raster* data [6]. Vector data are discrete and signified in lines, polygons and points. These data mostly used to make boundaries, rivers, etc. Raster data are continuous and signified in grid cells which help to identify the pattern of a geospatial data.

Spatial association mining is one of the techniques to identifying the spatial pattern relationship [7, 8]. Spatial clustering, regionalization and point pattern analysis are commonly used to find the geospatial data patterns similarity, dissimilarity and hot spot analysis respectively [8]. In meteorological applications like climate change, urban, hydrometeorology and energy is compared with different clustering algorithms. In these applications commonly used algorithms in all applications are k-Means and Hierarchical. DBSCAN, EM, wave clusters has been used to study the characteristics, outliers or predictions which are basically to analyze the atmospheric circulation, air quality or weather forecasting [9]. Multilevel association rules and hierarchical clustering for multi-directed graphs are applied to spatial data analysis [10].

The above data mining techniques enhanced by adding visualization with human intervention affords the quick decision and accuracy in emergency scenario which is nonetheless visual analytics. Exploration of geospatial data can view in bar chart, tree maps, parallel co-ordinate plots and glyphs are widely used [3].

3.2 Temporal Data

At present, temporal data analysis has become the fascinated area in the visual analytic field. Sequence of continuous, real-valued elements are called time seer. Mining techniques applied to diverse approaches of the temporal data such as time-domain continuous representation, discretization, transformation, generative models and transactional databases with timing information [11]. In health application, to investigate Charcot foot (diabetes) association analysis mining applied

and uses node graph and network visualization approach [12]. To scale the columnar databases association with apriori algorithm has been used [13].

There are different visualization techniques for analyzing the temporal data which exhibits vibrant view. Figure 1a shows matrix visualization [14] with colour scale, Fig. 1b shows interactive stream graph [15] (Twitter topic explorer), Fig. 1c shows dynamic graph clustering [16] (change of cluster almost every step), Fig. 1d shows heat map [17] and Fig. 1e shows parallel coordinates.

3.3 Spatio-Temporal Data

In this section, information related to both spatial and temporal called spatio-temporal data is considered. Moving bike, tornado, flood, hurricane are the few examples for spatio-temporal data. These data are very complex and growing size in daily manner. Data mining helps in a better way to achieve efficiency and

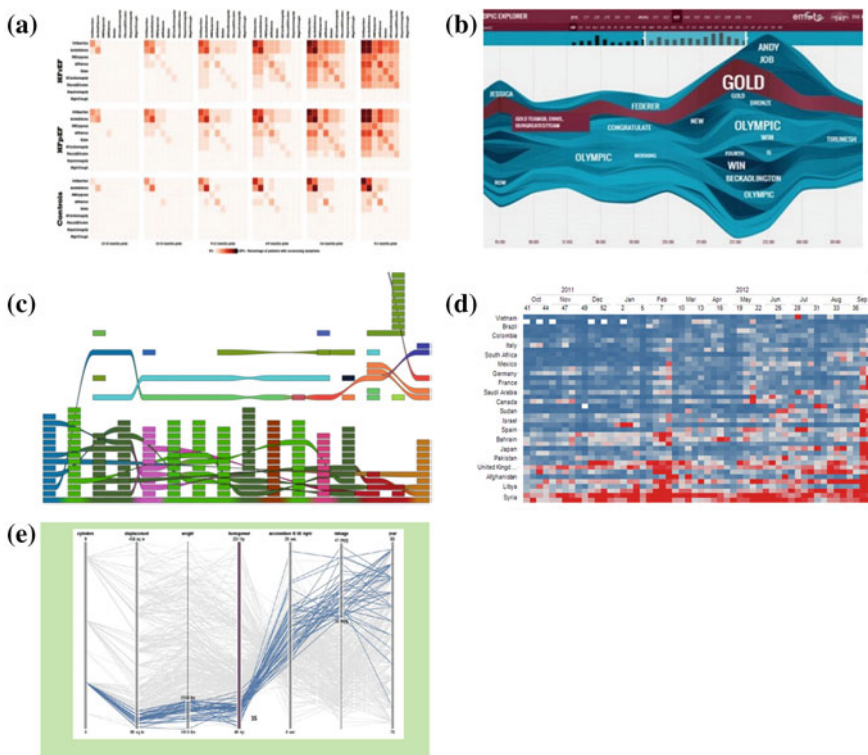


Fig. 1 Visualization techniques for temporal data. **a** Matrix visualization. **b** Stream graph. **c** Dynamic graph clustering. **d** Heat map. **e** Parallel coordinates

accuracy for prediction or understanding the characteristics of the data. Here most frequent data mining functionalities are involved to categorize the recent research in spatio-temporal. This study focus on the following categories,

- *Association analysis:* Analyzing the marine environmental elements using aprio algorithm with two-dimensional association analysis [18]. Semantic Traffic Analysis and Reasoning CITY (STAR CITY) generates the association rules between snapshots in traffic and it uses apriori algorithm [19]. To identify the association between the marine attributes in Western pacific data association rule with apriori applied [20].
- *Clustering:* To investigate the burglary crime data TKNN-clustering algorithm (TKNN-Triangular Kernel Nearest Neighbour) applied [21, 22]. For effective analysis of winter road management using weather data k-means nearest algorithm applied based on Euclidean distance [23]. Passing analysis in a football, clustering helps to identify the temporal correlations between the players [24].
- *Regression:* An appropriate method for rainfall forecasting in mining method is regression model. Support vector regression (SVR) model affords best performing techniques such as kernel method [25]. Intelligent large-scale traffic prediction for traffic analysis uses the SVR is applied [26]. SVR combined with PCA method applied to automated controller of north palette river reservoir system for speeding p the process and speed [27].
- *Outlier analysis:* Road accident black spots, kernel density estimation based on kNN and LOF are adapted [28]. To identify the anomalous behaviour of the user (SPAM detection) PCA-based technique proposed in a Facebook [29]. To detect the unusual behaviour such as walking with high speed or any unusual change in the crowd scenes, Gaussian mixture model (GMM) and markov random field (MRF) combined and adapted [30].

Figure 2a shows multivariate hypercube [31] is to analyze the multi-dimensional spatio-temporal patterns, Fig. 2b shows bar charts and spatial maps [32], Fig. 2c shows video visual analytics [33], Fig. 2d shows trajectory network [34] and Fig. 2e shows flow map [35], taxi trip clusters.

4 Databases and Software Tools

4.1 Databases (*NoSQL*)

In recent years, NoSQL databases are growing rapidly due to non-relational data stored by the organization for future use. These data have variety and huge volume such as spatio-temporal data. NoSQL databases are categorized as key-value stores, column-oriented database, document-based stores, graph databases, multimodel

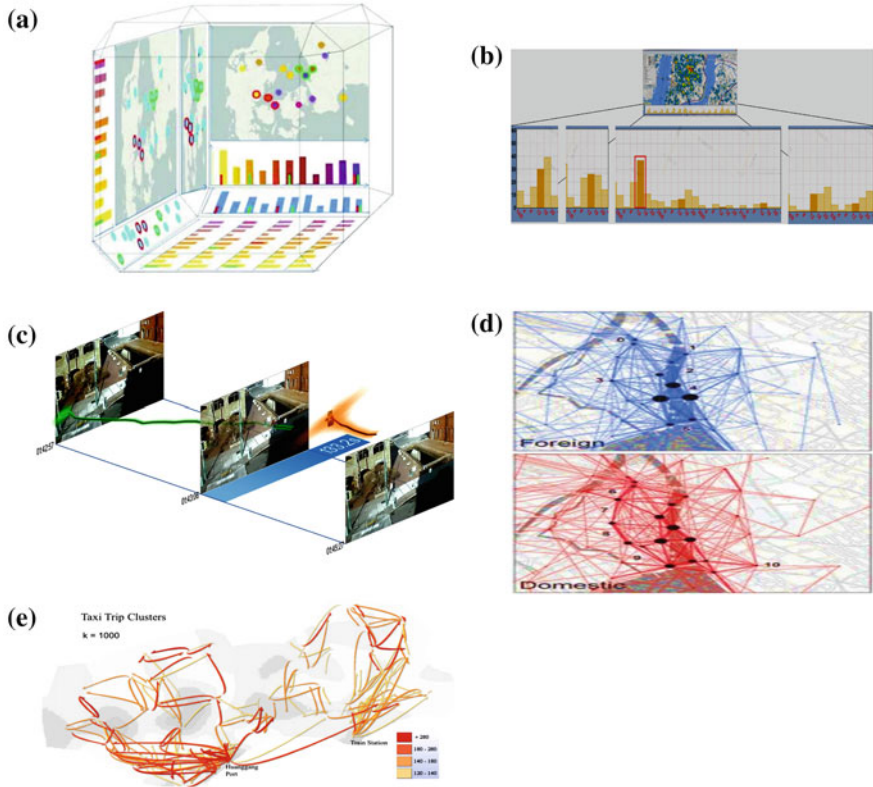


Fig. 2 Techniques for visualizing spatio-temporal data. **a** Multivariate data cube. **b** Spatial map, bar charts. **c** Video visual analytics. **d** Flow map. **e** Trajectory network

databases, XML databases and few other databases which are not categorized [36, 37]. These databases are characterized by CAP theorem which is consistency, availability and partition tolerance. Accessibility in their databases [37, 38] is given in Table 1.

4.2 Software Tools

The software tools commonly used for analyzing spatio-temporal data are listed in Table 2.

Table 1 Databases with convenience in CAP

Sl. No	Databases	Consistency	Availability	Partition tolerance	Data model/stores
1	Amazon dynamo	N	Y	Y	Key-value stores
2	Voldemort	N	Y	Y	
3	TokyoCabinet	N	Y	Y	
4	Redis	Y	N	Y	
5	Cassandra	N	Y	Y	Column-oriented
6	HBase	Y	N	Y	
7	Vertica	Y	Y	N	
8	SimpleDB	N	Y	Y	Document-oriented
9	CouchDB	N	Y	Y	
10	MongoDB	Y	N	Y	

Table 2 Open source geo spatial analysis tool

Sl. No.	Software tools	Features
1	ArcGIS	It contains spatial data exploration tool, surface generation, spatial modelling, geoweighted regression [39][40]
2	GeoDA	Data input/output, spatial data manipulation, visualization and queries, mapping and EDA [39]
3	CrimeSTAT III	Crime event analysis, vector (N Levine), spatial distribution analysis, hot spot analysis, kernel density analysis and trip distribution-based modelling [39]
4	GeoVISTASTudio	Data exploration, knowledge discovery, geo-computation and visualization [39]
5	geoR	R Language offers many packages for geospatial analysis, geostatsp, ggplot2, etc. [39]
6	GRASS	It supports both raster and vector, image processing, graphics, maps production [39]
7	pySAL	Spatial regression analysis, spatial data analytic functions based on python programming [39]
8	GWR	Geographical weighted regression analysis [39]
9	STARS	Analysis of areal data measured overtime [39]
10	SAM	It is user friendly, menu driven and graphical interface [39]

5 Challenges and Opportunities

Space and time is a broad area for research and development with more number of challenges and opportunities. The following topics are to be tugged:

- *Data science:* A long-term desire and provocative in data science is in need of proactive insight discovery of knowledge from the huge accumulated data. As it is an evolving field there are more opportunities for the researchers and developers. Companies and research development hunting for the talents with more analytical skills and broad knowledge in data science tools and techniques.
- *Databases in CAP and software tools:* Nearly 150 NoSQL databases [37] are available globally. It is highly challenging to choose the appropriate one because there are databases which covers only two properties of CAP i.e. (Consistency +Availability, Availability+Partition tolerance, Partition tolerance+Consistency) There will be trade-off between any one properties of CAP in every database. Most of the databases are open source where developers and researcher finds more chances to work on it. Open-source geospatial analysis tools have more interactive visualization techniques and datasets. As per the need of the application the datasets and tools may vary with the performance. However, these tools enhance more opportunity to the young researchers by practicing and gaining knowledge.

6 Conclusions

There are many interdisciplinary approaches in a computer science technology that hook for a hidden prospect to uncover the complexity in a real-time circumstances. With no apprehension visual analytics and mining will be the future front running approach in space and time. There are many mining techniques involved to achieve efficacy and accuracy in geospatial analysis. Mostly clustering techniques govern the grouping data and finding outliers in spatial data, but still several techniques evolved in data mining as per need of the application. At present, visual Analytics is one of the best ways to explore a data which easily fascinates the users and help them to unearth the confounding state. Different visualization techniques and statistical methods comfort the data scientists for dealing the large multifaceted data and to make verdict. Geographical analysis helps to motivate the different applications in a way to identify the problems based on location. These headway technologies knobs the recent buzz word ‘Big Data’ which embraces huge volume, variety, velocity, veracity, and value. The above key factors provide fast decision making, diverse knowledge, efficiency, and accuracy with human intervention. Undoubtedly, this scenario will rule the research world in the near future.

References

1. Han, J., Kamber, M.: Data Mining: Concepts and Techniques. Morgan Kauffman, San Francisco (2006)
2. Mohammed, A., et al.: A unified approach for spatial data query. *Int. J. Data Mining Knowl. Manag. Process* **3**(6), 55–71 (2013)
3. Sun, G.D., Wu, Y.C., Liang, R.H., et al.: A survey of visual analytics techniques and applications: state-of-the-art research and future challenges. *J. Comput. Sci. Technol.* **28**(5), 852–867 (2013)
4. Fotheringham, S.A., Rogerson, P.A.: The SAGE Handbook of Spatial Analysis. SAGE Publications, London (2008)
5. Spatial Data Mining. www.iasri.res.in/ebook/win_school_aa/notes/spatial_data_mining.pdf
6. Gennady, A., et al.: Space, time and visual analytics. *Int. J. Geogr. Inf. Sci.* **24**(10), 1577–1600 (2010)
7. Angela, L., Schmidt, A., Tischendorf, L.: Data mining and linked open data—new perspectives for data analysis in environmental research. *Ecol. Model.* **295**, 5–17 (2015)
8. Yoo, J.S., Boulware, D., Kimmey, D.: Incremental and parallel association mining for evolving spatial data: a less iterative approach on map reduce (2015)
9. Jeremy, M., Guo, D.: Spatial data mining and geographic knowledge discovery—an introduction. *Comput. Environ. Urban Syst.* **33**(6), 403–408 (2009)
10. Yuzuru, Tanaka, et al.: Geospatial visual analytics of traffic and weather data for better winter road management. *Data mining for geoinformatics*, pp. 105–126. Springer, New York (2014)
11. Petelin, B., et al.: Multi-level association rules and directed graphs for spatial data analysis. *Expert Syst. Appl.* **40**(12), 4957–4970 (2013)
12. Xie, Y., et.al.: Silverback: Scalable association mining for temporal data in columnar probabilistic databases. *Data Engineering (ICDE)*, IEEE, pp. 1072–1083 (2014)
13. Wei, Tian, et al.: A survey on clustering based meteorological data mining. *Int. J. Grid Distrib. Comput.* **7**(6), 229–240 (2014)
14. Antunes, C.M., Oliveira, A.L.: Temporal data mining: an overview. *KDD workshop on temporal data mining*, pp. 1–13 (2001)
15. Twitter topic explorer, www.datainterfaces.org
16. Perer, A., Sun, J.: MatrixFlow: temporal network visual analytics to track symptom evolution during disease progression. In: *AMIA Annual Symposium Proceedings*, vol. 2012, pp. 716–725 (2012)
17. Quantifying protests around the world, www.recordedfuture.com
18. Xue, C. J., Q. Dong., W. X. Ma.: Object-oriented spatial-temporal association rules mining on ocean remote sensing imagery. In: *IOP Conference Series: Earth and Environmental Science*, vol. 17, no. 1, IOP Publishing, (2014)
19. Freddy, L., et al.: Smart traffic analytics in the semantic web with STAR-CITY: scenarios, system and lessons learned in Dublin City. *Web Semantics: Science, Services and Agents on the World Wide Web* **27**, 26–33 (2014)
20. Ma, W., Xue, C., Zhou, J.: Mining time-series association rules from Western Pacific spatial-temporal data. In: *IOP Conference Series: Earth and Environmental Science*. vol. 17. no. 1. IOP Publishing (2014)
21. Musdholifah, A., Hashim, S.Z.M.: Triangular kernel nearest neighbor based clustering for pattern extraction in spatio-temporal database. In: *Intelligent Systems Design and Applications (ISDA)*, pp. 67–73. IEEE (2010)
22. Musdholifah, A., Hashim, S.Z.M.: Scatter-PCA for visual clustering of spatio-temporal data. *IJCSNS* **14**(1), 72–76 (2014)
23. Munson, Michael E., et al.: Data mining for identifying novel associations and temporal relationships with Charcot foot. *Journal of diabetes research*, Vol. 2014 (2014)
24. Guðmundsson, J., Wolle, T.: Football analysis using spatio-temporal tools. *Comput. Environ. Urban Syst.* **47**, 16–27 (2014)

25. Reddy, P.: Sequential spatio-temporal pattern mining with time lag. Dissertation. University of Illinois, Chicago (2014)
26. Tayyab Asif, M., et al.: Spatiotemporal patterns in large-scale traffic speed prediction. IEEE Trans. Intell. Transp. Syst. **15**(2), 794–804 (2014)
27. Mohan, A.: A new spatio-temporal data mining method and its application to reservoir system operation. Dissertation. University of Nebraska, Nebraska (2014)
28. Schubert, E., Zimek, A., Kriegel, H.P.: Generalized outlier detection with flexible kernel density estimates. In: Proceedings of the 14th SIAM International Conference on Data Mining (SDM), Philadelphia (2014)
29. Viswanath, B., et al. : Towards detecting anomalous user behavior in online social networks. In: Proceedings of the 23rd USENIX Security Symposium (USENIX Security), pp. 223–238. San Deigo (2014)
30. Lu, T., Wu, L., Ma, X., Shivakumara, P., Tan, C.L.: Anomaly detection through spatio-temporal context modeling in crowded scenes. In: 22nd International Conference Pattern Recognition (ICPR), pp. 2203–2208. IEEE (2014)
31. Olsilagers, F., Worring, M.: The spatiotemporal multivariate hypercube for discovery of patterns in event data. In: IEEE Conference Visual Analytics Science and Technology (VAST), pp. 235–236. IEEE (2012)
32. Junghoon, C., et al.: Public behavior response analysis in disaster events utilizing visual analytics of microblog data. Comput. Graphics **38**, 51–60 (2014)
33. Markus, H., et al.: Uncertainty-aware video visual analytics of tracked moving objects. J. Spat. Inform. Sci. **2**, 87–117 (2015)
34. Straumann, R.K., Çöltekin, A., Andrienko, G.: Towards (Re) constructing narratives from georeferenced photographs through visual analytics. Cartogr. J. **51**(2), 152–165 (2014)
35. Zhu, X., Guo, D.: Mapping large spatial flow data with hierarchical clustering. Trans. GIS **18** (3), 421–435 (2014)
36. Leavitt, N.: Will NoSQL databases live up to their promise? Computer **43**(2), 12–14 (2010)
37. List of NoSQL databases. <http://nosql-database.org/>
38. Visual Guide to NoSQL Systems. <http://blog.nahurst.com/visual-guide-to-nosql-systems>
39. Opensource GIS Products. <http://www.spatialanalysisonline.com/SoftwareFree.pdf>
40. ArcGIS. <http://www.csiss.org/gispopsci/research/tools/ArcGIS.php>

Dimensionality Reduced Recursive Filter Features for Hyperspectral Image Classification

S. Lekshmi Kiran, V. Sowmya and K.P. Soman

Abstract Dimensionality reduction techniques have been immensely used in hyperspectral image classification tasks and is still a topic of great interest. Feature extraction based on image fusion and recursive filtering (IFRF) is a recent work which provides a framework for classification and produces good classification accuracy. In this paper, we propose an alternative approach to this technique by employing an efficient preprocessing technique based on average interband blockwise correlation coefficient followed by a stage of dimensionality reduction. The final stages involve recursive filtering and support vector machine (SVM) classifier. Our method highlights the utilization of an automated procedure for the removal of noisy and water absorption bands. Results obtained using experimentation of the proposed method on Aviris Indian Pines database indicate that a very low number of feature dimensions provide overall accuracy around 98 %. Four different dimensionality reduction techniques (LDA, PCA, SVD, wavelet) have been employed and notable results have been obtained, especially in the case of SVD (OA = 98.81) and wavelet-based approaches (OA = 98.87).

Keywords Preprocessing · Feature extraction · Band selection · Recursive filtering · Wavelet · IFRF · SVM · PCA · LDA · SVD

S. Lekshmi Kiran (✉) · V. Sowmya · K.P. Soman

Centre for Excellance in Computational Engineering and Networking (CEN),
Amrita Vishwa Vidyapeetham, Amritanagar, Coimbatore 641112, Tamil Nadu, India
e-mail: lekshmikiran5@gmail.com

V. Sowmya
e-mail: sowmiamrita@gmail.com

K.P. Soman
e-mail: kp_soman@amrita.edu

1 Introduction

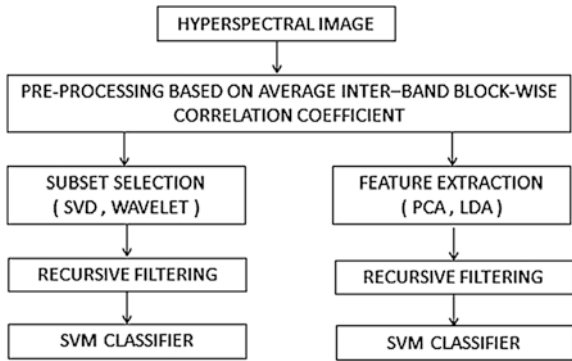
Hyperspectral image processing has been an area of active research owing to the large number of applications associated with it and large datasets which urge the development of less-complex and more accurate processing mechanisms to deal with the high-dimensional data. Dimensionality reduction techniques like feature extraction and subset selection are frequently used methods to tackle the same. As the name suggests, dimensionality reduction techniques help to reduce the dimensions associated with a dataset which finds significance in various fields like data mining, pattern classification, etc. by solving the so-called curse of dimensionality issue. This is done by removing the less-important and redundant information. Depending on the application, it may be categorized into feature extraction and feature selection. While feature selection carries out a subset selection process of the actual features, the former method extracts new features from the actual ones using a linear or nonlinear mapping. Various articles highlight the significance of these techniques [1, 2].

The vast area of hyperspectral data analysis is being improved day by day since large amount of spectral information is available from the sensors and is effectively being utilized by researchers. This is evident from the innumerable number of techniques that have been formulated over time. The integration of spatial and spectral content in hyperspectral images has paved a way for varied approaches like composite kernel framework, extended morphological profiles, attribute profiles, etc. Spectral–spatial classification methodology based on edge-preserving filtering (EPF) has already been formulated [3]. Different types of edge-preserving filters are available such as joint bilateral filter, guided filter, domain transform filter, etc.

In recent days, filtering approaches are being greatly utilized in hyperspectral image classification. Feature extraction based on image fusion and recursive filtering (IFRF) is a recent method proposed by Kang et al. [4]. The pros and cons of feature selection methods over feature extraction have been discussed in this paper. In addition to this, the authors also highlight the fact that, the selection of best subset of features is not an easy task.

In this paper, we formulate an alternative technique to the proposed IFRF method. Here, we highlight the presence of an effective preprocessing step prior to dimensionality reduction. This helps in an automated procedure for the removal of noisy and water absorption bands which promotes in both complexity reduction and at the same time, increment in efficiency of classification. Preprocessing technique based on average interband blockwise correlation coefficient is a recent work and has been utilized in our methodology [5]. The preprocessed data is then subjected to dimensionality reduction, recursive filtering, and classification. Dimensionality reduction has been carried out using feature extraction techniques like PCA and LDA and also using band subset selection procedures like SVD and wavelet-based band selection. The proposed method is tested on standard Indiana Pines dataset and has resulted in notable classification accuracy.

Fig. 1 Flow chart for the proposed approach



2 Proposed Method

Flowchart for the proposed method is shown in Fig. 1. The preprocessing stage based on average interband blockwise correlation coefficient holds the key for this approach since, it helps in boosting the computational efficiency and classification accuracy. This is highly significant in the case of feature selection methods like SVD where computational cost increases largely as the number of dimensions increase. Dimensionality reduction has been carried out using four different techniques (SVD, PCA, LDA, wavelet) and a discussion regarding the analysis of classification results has been included. The last two stages, recursive filtering and classification using SVM, are similar to [4].

2.1 Preprocessing Based on Average Interband Blockwise Correlation Coefficient

Many hyperspectral datasets contain noisy and water absorption bands. Noise is produced by miscellaneous factors including thermal effects, atmospheric scattering, sensor noise, quantization errors, and transmission errors. The preprocessing algorithm utilized in our work helps in the removal of high grade noise and low signal-to-noise ratio (SNR) bands in hyperspectral imagery (HSI) and thereby improves the effectiveness of dimensionality reduction in terms of complexity and efficiency.

Preprocessing algorithm can be summarized as follows. Each band of HSI is divided into blocks of equal size, say $m \times m$, which is ensured by zero padding. Block size m has been chosen by us as 8, 16, and 32 and the best results obtained among these have been reported. Spatial correlation among two successive bands is then measured using interband cross-correlation coefficient which is calculated between each block of the two bands. A correlation matrix is formed and is denoted as $\rho = [\rho_{1i}, \rho_{2i}, \rho_{3i}, \dots, \rho_{(k-1)i}]$ where ρ_{li} denotes the correlation coefficient between

the blocks of first and second band, and so on. Here, i varies from 1 to the total number of blocks.

The noisy bands are then detected and removed based on a threshold condition. A detailed explanation of the above can be found in the [5]. The method claims a chance of falsely detecting noisy bands only up to 3.18 % and thus has been utilized here.

2.2 Feature Extraction

In feature extraction, the original set of D features is transformed using a linear/nonlinear mapping to produce a new set of features from which, a small set ' d ' is extracted ($d \ll D$) using a threshold condition. We have utilized two such methods—principal component analysis (PCA) and linear discriminant analysis (LDA) [1, 6]. The former does not make use of class information while the latter does. In PCA, ' d ' features are extracted by choosing ' d ' eigenvectors of the covariance matrix with maximum eigenvalues. The same procedure is repeated in the case of LDA, proposed by Fisher, except for the fact that the matrix chosen is different [1, 6]. Fisher discriminant can be explained as a classification function:

$$f(x) = \text{sgn}(\langle w, \phi(x) \rangle + b)$$

where the aim is to find the direction w which maximizes the class separability. It can be extended to nonlinear case by employing kernel Fisher discriminant analysis (KFD) [7].

2.3 Band Subset Selection

As discussed, the objective of dimensionality reduction is to summarize maximum information in a few bands. Dimensionality reduction using band subset selection refers to algorithms based on singular value decomposition (SVD), wavelets, support vector machines, etc. where independent bands are extracted from the hyperspectral imagery due to the existence of high correlation among the bands. Compared to techniques like PCA, the aim here is to find the most significant features from the original set having maximum eigenvalues. An attractive element of this process is that, it preserves the physical meaning of the data. In terms of efficiency, SVD-based method is known to outperform these methods though it involves high computational complexity. In this paper, this high complexity issue has been initially dealt with by using the preprocessing technique. SVD and wavelet-based methods have been utilized in our work as band selection techniques and their performances have been evaluated.

Subset selection analysis using SVD is a method formulated by Velez-Reyes and Jimenez [8]. Let the transformation matrix to reduce the data from ' n ' dimensions to a lower dimension ' p ' ($p \ll n$) be denoted as A . This matrix should be such that, it will minimize the loss of information. For this purpose, an optimization problem is defined by introducing a gauge function which is often a unitary invariant norm.

As we know, the main problem to deal with is, subset selection. The aim is to find a permutation matrix P which will reorder the columns of the original matrix of HSI such that the desired bands occur in the first few columns of the permuted matrix.

Wavelet has been accepted as a good choice for feature extraction since wavelet decomposition results in detail and approximation coefficients, where the major attraction is that all information (fine scale and large scale) will be included in the decomposition coefficients [9–11]. In wavelet-based band selection method, discrete wavelet transform (DWT) is performed which involves signal decomposition employing a scaling function and a wavelet function whose shape is decided by the high-pass and low-pass filter coefficients designed according to the application [12]. This is analogous to the theory of sub-band coding described in [13]. Image reconstruction using wavelets call for the need of a symmetrical wavelet system (to achieve linear phase) which is satisfied by the two commonly used wavelets, namely Haar and biorthogonal wavelets. While Haar is both symmetric and orthogonal, it may not be often suitable for practical purposes and has motivated the development of a biorthogonal wavelet. Biorthogonal, unlike Haar, has two scaling and two wavelet functions referred to as the primal and dual. Let the primal basis set be denoted as $\{p_1, p_2, \dots, p_n\}$. It represents an n -tuple of vectors which are independent but not orthogonal. Inverse of the matrix formed by taking these vectors as its rows is calculated and the columns of the inverse matrix become the members of the dual set, denoted as $\{d_1, d_2, \dots, d_n\}$.

In our experiments, we have performed 2-level discrete biorthogonal wavelet transform (DBWT) of each band of every window resulting in six sub-bands for every band. The average energy of resulting sub-bands is calculated and the maximum, median, and minimum wavelet energy bands are then chosen as the subsets in each window.

2.4 Recursive Filtering and SVM Classifier

Domain Transform for Edge-Aware Image and Video Processing [14] discusses three realizations for 1D (one-dimensional) EPF's (edge-preserving filters) based on a domain transform approach. This has been formulated for image and video processing applications where common filtering approaches like bilateral filter or anisotropic diffusion may not be practical. Edge-preserving smoothing is often done using a filter kernel in 5D. A transformation satisfying the property of isometry (distance preserving transformation) can be used to produce an EPF in a lower dimensional space [14].

Transform domain recursive filtering approach has been utilized in this work. Two parameters involved in this stage are the spatial and range parameters of the EPF, denoted as δ_s and δ_r . The influence of these parameters in classification has been clearly mentioned in [4].

The final stage of classification is done using SVM classifier. It is a widely adopted supervised learning model applied in regression analysis and linear/nonlinear classification. Learning an SVM can be formulated as an optimization problem. A library for SVM namely LIBSVM is available and has been utilized in our work [15].

3 Experimental Setup

We know that hyperspectral image provides information about objects in hundreds of narrow spectral bands. AVIRIS (Airborne Visible Infrared Imaging Spectrometer) is a widely known sensor in the field of remote sensing and aids in the study of global environment. One of the most popular and standard hyperspectral image datasets provided by AVIRIS is the Indian Pines dataset captured over NW Indiana's Indian Pine test site in June 1992 involving classification task of 16 types of crops. This dataset is freely available and has been utilized for our experimental studies. Using AVIRIS sensor, scanning is done in 224 spectral bands (wavelength range 400–2500 nm) but, four of them contain only zeroes and have been removed. The 20 noisy and water absorption bands are usually removed manually, but here, we have automated the process by using the preprocessing technique. Preprocessing is done with block sizes varying as 8, 16, and 32. Two different threshold conditions, namely standard deviation and $2 * \text{mean}$, have also been utilized in the preprocessing step. The number of bands effectively utilized for classification is initially reduced through this preprocessing stage and is further reduced greatly by using dimensionality reduction procedures. In our experiments, we have chosen the resulting image, after dimensionality reduction to have only a very few number (10 dimensions). The third stage of recursive filtering involves two parameters in which we have fixed $\delta_s = 200$ throughout the experimental process and seven different values of δ_r (0.3, 0.4, 0.5, 0.6, 0.7, 0.8, 0.9) have been utilized each time to find out the best results. The three most popular quality indices used in hyperspectral image analysis, namely overall accuracy (percentage of correctly classified pixels) denoted as OA, average accuracy (percentage of correctly classified pixels for each class) denoted as AA, and kappa coefficient have been employed. Kappa coefficient is a well-made measure and is usually developed with the help of a confusion matrix. It compares the observed accuracy with a random chance and indicates the measure of agreement between the ground truth information (actual values) and the values obtained using a classifier.

4 Results and Discussion

As discussed above, the experiment has been conducted using AVIRIS database. Background pixels have been excluded and then 1024 samples have been randomly selected for training purpose. The best classification results obtained by using the proposed technique have been tabulated in Tables 1 and 2. It indicates good classification accuracy especially in the case of SVD and wavelet-based band selection methods. The highest overall accuracy obtained in the case of SVD is 98.81 ($\delta_s = 200$, $\delta_r = 0.7$) and that in the case of wavelet-based approach is 98.87 ($\delta_s = 200$, $\delta_r = 0.3$) and is quite comparable to the results obtained in [4]. In our case, block size (of the preprocessing stage) corresponding to the highest values of classification is 16 for all the four dimensionality reduction methods. Standard deviation when chosen as the threshold condition for the preprocessing stage produces better results than $2 * \text{mean}$ condition except in the case of SVD. Our method emphasizes the fact that even though the number of dimensions has been greatly reduced using stages of preprocessing and dimensionality reduction, it has resulted in improvement of classification results.

Table 1 Class-wise accuracy for Indian Pines obtained by the proposed method

Class	PCA	LDA	SVD	Wavelet
Alfalfa	74.19	23.71	95.83	95.83
Corn-notill	86.97	90.57	99.01	98.50
Corn-mintill	85.24	95.40	99.59	99.46
Corn	79.07	82.04	95.00	91.94
Grass-pasture	93.17	92.79	99.25	99.51
Grass-trees	92.37	90.11	100	100
Grass-pasture-mowed	100	48.00	61.90	92.86
Hay-windrowed	94.95	100	100	100
Oats	58.82	50.00	62.50	100
Soybean-notill	91.83	90.11	98.44	97.90
Soybean-mintill	94.96	94.88	98.07	99.23
Soybean-clean	86.23	87.55	99.42	99.80
Wheat	87.58	98.59	98.60	98.60
Woods	99.49	99.48	99.92	100
Buildings-grass-trees-drives	90.88	94.70	100	98.14
Stone-steel-towers	80.70	90.20	97.87	75.41

Table 2 Accuracy measures for Indian Pines obtained by the proposed methods—OA: overall accuracy, AA: average accuracy and kappa

Method	OA	AA	Kappa
PCA	91.6	87.28	90.36
LDA	92.56	83.01	91.46
SVD	98.81	94.09	98.63
Wavelet-based	98.87	96.70	98.70

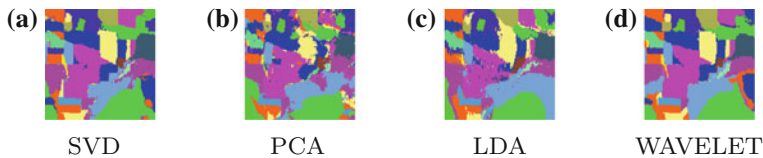


Fig. 2 Classification map obtained on experimentation of the proposed method in Aviris Indian Pines dataset (excluding background pixels)

Table 1 presents the classwise accuracy of Indian Pines dataset obtained by the proposed method. Classification map of the concerned area, obtained after classification, indicating the 16 classes is shown in Fig. 2. The number of features chosen in this work is 10 which reflects the fact that, information contained in hyperspectral data is redundant.

5 Conclusion

The proposed method can be used as an alternative for the feature extraction method based on IFRF since it deals with the issue of computational complexity without compromising with the classification accuracy. The stages of recursive filtering and SVM classifier which are common to both the approaches can be further modified by using varied methodologies that are available. We intend to extend our work in future by using different filtering approaches like Gabor filter, Savitzky Golay (SG) filter, etc. and analyzing their performance characteristics for hyperspectral imagery. Further, the final stage of SVM classification can also be modified by making use of algorithms such as Random Kitchen Sink.

References

1. Dash, M., Liu, H.: Dimensionality Reduction: Wiley Encyclopedia of Computer Science and Engineering. Wiley (2008)
2. Bharath Bhushan, D., Nidamanuri, R.R.: Assessment of the impact of dimensionality reduction methods on information classes and classifiers for hyperspectral image classification by multiple classifier system. *Adv. Space Res.* **53**(12), 1720–1734 (2014)
3. Kang, X., Li, S., Benediktsson, J.A.: Spectral-spatial hyperspectral image classification with edge-preserving filtering. *IEEE Trans. Geosci. Remote Sens.* **52**(5), 2666–2677 (2014)
4. Kang, X., Li, S., Benediktsson, J.A.: Feature extraction of hyperspectral images with image fusion and recursive filtering. *IEEE Trans. Geosci. Remote Sens.* **52**(6), 3742–3752 (2014)
5. Bharath Bhushan, D., Sowmya, V., Sabarimalai Manikandan, M., Soman, K.P.: An effective pre-processing algorithm for detecting noisy spectral bands in hyperspectral imagery. In: Ocean Electronics (SYMPOL), 2011 International Symposium, IEEE, pp. 34–39 (2011)
6. John, S.-T., Cristianini, N.: Kernel Methods for Pattern Analysis. Cambridge University Press (2004)

7. Bo, L., Wang, L., Jiao, L.: Feature scaling for kernel fisher discriminant analysis using leave-one-out cross validation. *Neural Comput.* **18**(4), 961–978 (2006)
8. Velez-Reyes, M., Jimenez, L.O.: Subset selection analysis for the reduction of hyperspectral imagery. *IEEE Int. Geosci. Remote Sens. Symp. Proc.* **3**, (1998)
9. Bruce, L.M., Koger, C.H., Li, J.: Dimensionality reduction of hyperspectral data using discrete wavelet transform feature extraction. *IEEE Trans. Geosci. Remote Sens.* **40**(10), 2331–2338 (2002)
10. Kaewpijit, S., Le Moigne, J., El-Ghazawi, T.: Automatic reduction of hyperspectral imagery using wavelet spectral analysis. *IEEE Trans. Geosci. Remote Sens.* **41**(4), 863–871 (2002)
11. Burnase, S.R., Swamy, S.: Hyperspectral image reduction using discrete wavelet transform. *IOSR J. Electr. Electron. Eng.* 13–16 (2014)
12. Soman, K.P., Ramachandran, K.I.: *Insight Into Wavelets From Theory to Practice*. Prentice-Hall, New Delhi (2005)
13. Vaidyanathan, Parishwad, P.: *Multirate Systems and Filter Banks*. Pearson Education, India (1993)
14. Gastal, E.S.L., Oliveira, M.M.: Domain transform for edge-aware image and video processing. *ACM Trans. Graphics (TOG)* **30**(4), (2011). ACM
15. Chang, C.C., Lin, C.J.: LIBSVM: a library for support vector machines. *ACMTrans. Intell. Syst. Technol.* **2**(3), 27–127 (2011)

Customized Web User Interface for Hadoop Distributed File System

**T. Lakshmi Siva Rama Krishna, T. Ragunathan
and Sudheer Kumar Battula**

Abstract Distributed file system (DFS) is one of the main components of a cloud computing system used to provide scalable storage solutions for Big Data applications. hadoop distributed file system (HDFS) is one of the core components of Apache Hadoop project and many IT companies are using HDFS to store and manage Big Data. HDFS provides both command line and web-based interface to the users for storing and accessing data. The web-based user interface (WBUI) is used only for browsing the file system whereas the command line interface (CLI) is used for creating a file and performing read or write operations on the file. The CLI provides many more facilities and note that CLI is not user friendly as the user has to remember and type the commands to access the HDFS. In this paper, we propose a new customized web user interface (CWBUI) for the HDFS. We have developed CWBUI using servlets and java server pages (JSP) and deployed the same in a Hadoop cluster. The CWBUI is found to be very helpful in using the HDFS in an interactive manner without the need of typing commands in the user interface.

Keywords Hadoop distributed file system · Web user interface · Hadoop · Distributed file system

T. Lakshmi Siva Rama Krishna (✉)
Jawaharlal Nehru Institute of Advanced Studies (JNIAS), Hyderabad, India
e-mail: sivamca.mtech@gmail.com

T. Ragunathan · S.K. Battula
Department of CSE, ACE Engineering College, Hyderabad, India
e-mail: ragu_savi@yahoo.com

S.K. Battula
e-mail: sudheer.itdict@gmail.com

1 Introduction

Distributed file system (DFS) is one of the main components of a cloud computing system used to provide scalable storage solutions for Big Data applications. In [1], authors show that hadoop distributed file system (HDFS) [2] performance was good for the file sizes greater than default block size of HDFS and performance was poor for the file size which was less than the default block size. HDFS is the storage system developed by Apache Hadoop a popular open-source project. HDFS was modeled after google file system (GFS) [3]. Hadoop runs an internal web server to provide the status of the cluster [4] and to browse the file system. Let us call this interface supported in the HDFS as WBUI. In the existing HDFS to perform file system operations such as read, write, copy, and create files/directories HDFS shell commands are used. We use these commands in command line interface (CLI) or in an application program to access the data from HDFS. Both of these methods require the user to remember the commands to use the same in the CLI or in the application program.

In this paper, we propose a new customized web-based user interface (CWBUI) for HDFS. The advantage of the proposed CWBUI is that by clicking function buttons displayed on the screen, users can perform file system operations such as read, write, copy, create files/directories in the HDFS. Another advantage of the proposed approach is that users can easily upload the files from the CWBUI by clicking the upload button which is not available in the existing WBUI of HDFS. Cloudera distribution of Hadoop consists of Hue [5] which is a graphical user interface to operate and develop applications for Apache Hadoop. Hue applications are collected into a desktop style environment and delivered as a web application, requiring no additional installation for individual users [5]. There are similarities between Hue and our proposed approach. However, there are some differences between Hue and our proposed CWBUI: (i) In Hue there is no facility to view the replication factor and other disk utilities where as in our proposed CWBUI a facility is available to view the replication factor of HDFS files and other disk utilities.

Rest of the paper is organized as follows. In Sect. 2, we describe HDFS. In Sect. 3, we explain how to access HDFS and difficulty that a new HDFS user will face with the shell commands. In Sect. 4, we explain our proposed CWBUI. Section 5 covers the experimental results. The last section concludes the paper.

2 Hadoop Distributed File System

In the year 2003, Google proposed a highly scalable, fault tolerant, dynamic distributed file system called as GFS. Later Google introduced Map-Reduce [6] programming model. Map Reduce is a mechanism to achieve parallelism. Map-Reduce

frame work was also implemented by open-source Hadoop [7] and Microsoft Dryad [8]. Since the GFS is a proprietary DFS, the research team of Yahoo decided to develop an open-source implementation of GFS and Map-Reduce. Then the open-source project was named as Apache Hadoop. HDFS is the file system component of Hadoop. HDFS was built to support high throughput, fault-tolerant, streaming reads and writes of extremely large files. The HDFS is the primary storage system developed by Hadoop which is a popular open-source project. HDFS was modeled after GFS. HDFS was designed to deploy on low-cost hardware with fault-tolerant feature. HDFS provides high throughput while accessing application data and is suitable for applications that have large data sets. HDFS relaxes few POSIX [9] requirements to enable streaming access to file system data. HDFS stores file system metadata and application data separately. The dedicated server which stores meta data is called namenode and other servers stores application data are known as data nodes. All servers are connected and communicated with each other by means of TCP/IP based protocols. Hadoop is used for storing and processing large amount of data sets in a cloud environment [10].

3 Interaction with HDFS

In this section, we describe how to interact with HDFS through shell commands. The HDFS shell includes various commands that directly interact with the HDFS. The name of the shell script is *hadoop*.

Figure 1 displays the list of various HDFS commands. The HDFS commands are like unix shell commands. The users can access the HDFS by using these shell commands. Accessing HDFS through CLI requires the users to remember the Hadoop shell commands. To simplify the actions performed by the users of Hadoop, we have designed and implemented an efficient GUI for HDFS called as CWBUI.

4 Proposed CWBUI for HDFS

We can browse HDFS itself with a basic file browser interface. To simplify the actions done by the users of the Hadoop while accessing HDFS, we have designed and implemented CWBUI. The advantage of the proposed CWBUI is that, by clicking function buttons displayed on the screen, users can perform file system operations such as read, write, copy, create files/directories to and from HDFS easily. Another advantage of the proposed approach is that users can easily upload the files from the CWBUI by clicking the upload button a feature which is not available in the existing web user interface of HDFS.

```

Usage: hadoop fs [generic options]
      [-cat [-ignoreCrc] <src> ...]
      [-chgrp [-R] GROUP PATH...]
      [-chmod [-R] <MODE[,MODE]... | OCTALMODE> PATH...]
      [-chown [-R] [OWNER] [:[:GROUP]] PATH...]
      [-copyFromLocal <localsrc> ... <dst>]
      [-copyToLocal [-ignoreCrc] [-crc] <src> ... <localdst>]
      [-count [-q] <path> ...]
      [-cp <src> ... <dst>]
      [-df [-h] [<path> ...]]
      [-du [-s] [-h] <path> ...]
      [-expunge]
      [-get [-ignoreCrc] [-crc] <src> ... <localdst>]
      [-getmerge [-nl] <src> <localdst>]
      [-help [cmd ...]]
      [-ls [-d] [-h] [-R] [<path> ...]]
      [-mkdir [-p] <path> ...]
      [-moveFromLocal <localsrc> ... <dst>]
      [-moveToLocal <src> <localdst>]
      [-mv <src> ... <dst>]
      [-put <localsrc> ... <dst>]
      [-rm [-f] [-r|-R] [-skipTrash] <src> ...)
      [-rmdir [--ignore-fail-on-non-empty] <dir> ...)
      [-setrep [-R] [-w] <rep> <path/file> ...)
      [-stat [format] <path> ...)
      [-tail [-f] <file>]
      [-test -[ezd] <path>]
      [-text [-ignoreCrc] <src> ...)
      [-touchz <path> ...)
      [-usage [cmd ...]]
```

Fig. 1 HDFS shell commands

Figure 2 describes the architectural overview of proposed CWBUI. The proposed CWBUI is a HTML-based application. Clients can access the proposed CWBUI from a remote location by specifying the IP address of the data node where the web browser is running. The proposed CWBUI supports a simplified interaction model that consists most of the operations that we can perform through CLI of the existing HDFS. We have implemented the proposed CWBUI using JAVA Servlets and Java Server Page (JSP) programs using which we can perform the basic file system operations on the HDFS. The proposed CWBUI for HDFS overcome the difficulty of remembering the commands, specifying the arguments and giving options by designing text boxes in HTML pages to pass or specify the arguments. The CWBUI also consists of a drop down list to select or specify the options of to perform specific task.

The following are the file system shell application program interfaces (APIs) to upload and download files to/from local file system to HDFS.

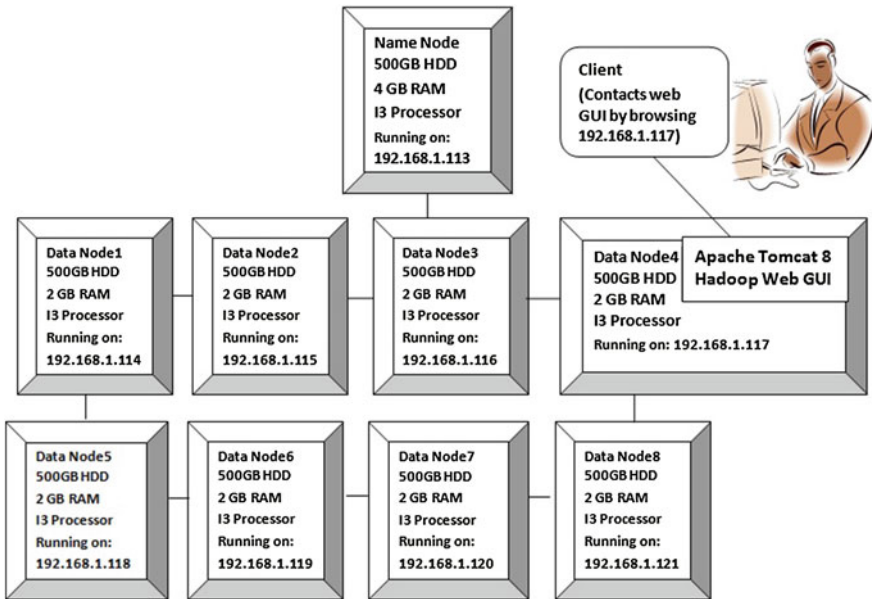


Fig. 2 Architecture for proposed CWBUI

4.1 Upload Files to HDFS

void copyFromLocalFile(boolean delSrc, boolean overwrite, Path src, Path dst)

The above-mentioned method is used to upload file from the local disk (from the specified source path) to HDFS (to specified destination path). The parameter value *boolean delSrc* in the above method indicates that if the *delSrc* value is false the specified file will be copied to the destination location and the file will be available at both source and destination locations after copying. Otherwise, the file will be moved from the source location and the file is available only at the destination location after copying. Next, parameter value *boolean overwrite* indicates that, if the *overwrite* variable value is true then the if any content is exists in the file that will be overwritten. Otherwise, it will display an error message. The parameter *Path src* is used to specify the source path and the parameter *Path dst* is used to provide the destination path.

4.2 Download Files from HDFS

copyToLocalFile(Path src, Path dst) The *copyToLocalFile()* method is used to download a file which is already available in the HDFS to a specified location in the

local file system by specifying the source path from HDFS to the destination path in the local file system. In the above method *Path src* is the source path of HDFS and *Path dst* is the destination path at the local file system. We have implemented Hadoop file system shell commands using JAVA Servlets and JSP programs.

5 Experimental Results

5.1 Experiment Environment

Our test platform is built on a Hadoop cluster with ten nodes. Out of these, nine nodes are used as data nodes and one node is dedicated as name node. Each data node has an I3 Processor, 2 GB of RAM, 500 GB SATA HDD and name node has an I3 processor, 4 GB of RAM, and 500 GB SATA HDD. We have installed Ubuntu-12.04 with kernel 3.2.1 in these ten nodes and on top of Ubuntu the Hadoop version 0.20.0 and open JDK 6 are installed. In one data node, we have also installed Apache Tomcat server to deploy our proposed CWBUI code. We have deployed the all the HTML pages, Servlet and JSP programs in one of the data nodes where Apache Tomcat server is available. The proposed CWBUI for HDFS does not require any special client to be installed instead a simple web browser is sufficient to access and manage the HDFS cluster. Clients are able to access proposed CWBUI for HDFS from any remote location by specifying the IP address, since it is deployed in the web server.

5.2 CWBUI for HDFS

In this section, we present the proposed CWBUI for HDFS and its functionality.

Figure 3 depicts the home page of the proposed CWBUI for HDFS which is having various menu options like File operations of HDFS, Directory operations, File permissions and Disk utilities. Figure 4 displays the various file operations in HDFS. Figure 5 displays the various implemented options under directory operations menu item. Figure 6 shows the available options under file permissions menu item and Fig. 7 exposes various options available under disk utilities menu item.



Fig. 3 Home page of CWBUI for HDFS



Fig. 4 Various file operations in HDFS



Fig. 5 Various directory operations in HDFS

Hadoop users can click on any of these options under menu items to explore desired functionality.

Figure 8 shows the file upload functionality by specifying the required path in the space provided in the interface screen then users need to click on the upload button available on the page to upload the contents from the local file system to HDFS. Figure 9 displays the contents of the directory after uploading the file into HDFS and we can observe that the uploaded file in Fig. 9 is highlighted with an



Fig. 6 Various file permissions in HDFS



Fig. 7 Various disk utilities in HDFS

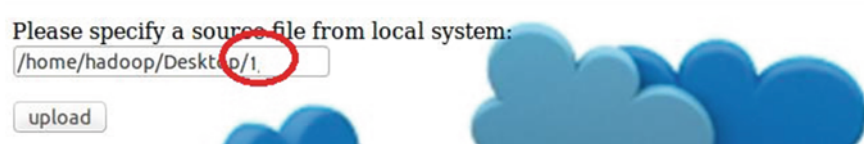
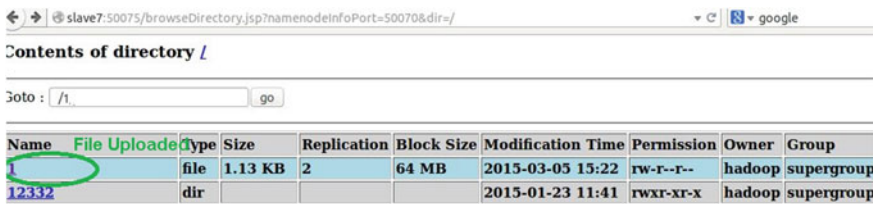


Fig. 8 Upload file from local file system to HDFS



Name	File Uploaded	Type	Size	Replication	Block Size	Modification Time	Permission	Owner	Group
1		file	1.13 KB	2	64 MB	2015-03-05 15:22	rw-r--r--	hadoop	supergroup
12332		dir				2015-01-23 11:41	rwxr-xr-x	hadoop	supergroup

Fig. 9 Display file in HDFS after upload

oval symbol. Due to space constraint we have not explained all the implemented options. The advantage of proposed CWBUI for HDFS is that, the users can access the HDFS without any difficulty.

6 Conclusion

Performing file system operations such as read, write, copy, create files/directories to and from existing Hadoop distributed file system (HDFS) is difficult for new Hadoop users. The new Hadoop users either have to use HDFS shell commands or to write programs to perform a specific task. To overcome the difficulty faced by new Hadoop users, we have proposed a new customized web user interface (CWBUI) for HDFS. The advantage of the proposed CWBUI is that, by clicking the function buttons displayed on the screen, users can perform file system operations such as read, write, copy, create files/directories to and from HDFS easily. Another advantage of the proposed approach is that users can easily upload the files from the Web UI of HDFS by clicking the upload button the feature which is not available in the existing WBUI of HDFS. For implementation of the proposed CWBUI for HDFS, we have setup a Hadoop cluster with ten nodes and modified the existing web user interface of HDFS. The Hadoop users can easily access the HDFS through the proposed CWBUI for HDFS. As a part of future work, we wish to list the files based on type of the file (such as .doc, .pdf, .txt) which is useful to identify the files presented in the HDFS based on file type and we are also planning to list the files present in HDFS based on file creation time.

References

1. Krishna, T.L.S.R., Ragunathan, T., Battula, S.K.: Performance evaluation of read and write operations in hadoop distributed file system. In: Parallel Architectures, Algorithms and Programming (PAAP), 2014 Sixth International Symposium on, pp. 110–113. IEEE, July 2014
2. Shvachko, K., Kuang, H., Radia, S., Chansler, R.: The hadoop distributed file system. In: Mass Storage Systems and Technologies (MSST), 2010 IEEE 26th Symposium on, pp. 1–10. IEEE, May 2010

3. Ghemawat, S., Gobioff, H., Leung, S.T.: The Google file system. ACM SIGOPS Oper. Syst. Rev. **37**(5), 29–43 (2003). ACM
4. HDFS User Guide: <https://hadoop.apache.org/docs/stable/hadoop-project-dist/hadoop-hdfs/HdfsUserGuide.html>
5. Hue manual: http://cloudera.github.io/hue/docs-3.5.0/manual.html#_introduction
6. Dean, J., Ghemawat, S.: MapReduce: simplified data processing on large clusters. Commun. ACM **51**(1), 107–113 (2008)
7. Hadoop-website: <http://hadoop.apache.org/>
8. Dryad Project Website: <http://research.microsoft.com/enus/projects/dryad/>
9. Josey, A.: The Single UNIX Specification Version 3. Open Group (2004)
10. Daci, G., Gjermen, F.: Review of limitations on namespace distribution for cloud filesystems. In: ICT Innovations 2012, Web Proceedings, p. 419 (2012). ISSN:1857-7288

Reinforcing Web Accessibility for Enhanced Browsers and Functionalities According to W3C Guidelines

Eye for All—An Essence for Internet Technology

Nehal Joshi and Manisha Tijare

Abstract In today's democratic society, the notion that all citizens have equal opportunity to express their views and opinions and right to information irrespective of any disability are elementary principles. The Web is becoming the centerpiece of this new information age. However, web sites are prone to accessibility issues and in some way or the other are inaccessible to people with disabilities. This paper provides a useful touchstone for those developers who have been standing at the shores of designing accessible web sites and even for those who have taken a deep dive in web designing in making Web accessible to all. This paper presents development of a validating and analysis tool to rate a web site on accessibility checkpoints by W3C (WCAG 2.0). Efforts are made in attaining web accessibility using web scrapping as a technology. Paper also contains tightly bound relations between various HTML attributes and tags using Bayesian Network.

Keywords Web accessibility · Human information processing · Disabled people · Human computer interaction and usability · Web scrapping · Context providing · Natural language processing · HTML · Bayesian network

N. Joshi (✉) · M. Tijare
Symbiosis International University, Lavale, Pune, India
e-mail: nehal.joshi@sitpune.edu.in

M. Tijare
e-mail: manishat@sitpune.edu.in

1 Introduction

In past days, information gathering and sharing was limited to library, physical media, or print media, which faced physical disabilities like broken leg, arm, etc. But advancement in information technology has brought an oceanic change in this information retrieval with the buzz word as web sites. There has been a substantial growth in digital data or e-media. In the current scenario of the world, now the communication and information sharing has become very easy with the help of World Wide Web. But even this media faced accessibility issue in form of cognitive disabilities, learning disabilities, sensory disabilities, and many more. People with disabilities may use assistive technologies such as screen readers, Braille printers, and alternative pointing devices, however, this is only effective if the web site is designed to be flexible and accessible. One of the most crucial challenges for the business companies be it e-commerce, health, education, or entertainment from past many years is to promote their business which still remains the same due to competition in market. Hence, web site hit and time for which user stays on the web site is of great significance. Failure to which is a failure to keep business afloat. For instance, one estimate, as many as 300,000 disabled people use screen reader software to browse the Web [1]. So, this counts to 300,000 potential customers, who cannot access a web site unless it is built for accessibility.

Time on the web site(Positive Aging) \propto Ease of web site surfing(Good Web page)

Time off the web site(Negative Aging) \propto Bad Web page

On a bird's-eye view, web sites are only for visually aided people but in contrast even visually impaired people access them. This research is into development of an efficient tool which checks for most common violated and important checkpoints for web accessibility given by WCAG 2.0. This tool will assess electronic resources used by people of all abilities or disabilities and is concerned for minimizing exclusion from access to digital information which can too easily occur when individuals are disabled in any form. Dive in technology has facilitated users to access resources in multiplicity to suit their needs and requirements. Also author has found tightly bound relations between various HTML attributes and tags using Bayesian Network.

Roadmap: The remaining paper consists of understanding web accessibility and its importance and areas of study in Sect. 2, followed by implementation strategy and details in Sect. 3. Section 4 provides critical evaluation in the form of research results. Lastly, Sect. 5 concludes the research paper.

2 Methodological Stance

In general terms, web accessibility means that any person using any web browsing technology must be able to visit any site and get all the information available at the web site in same way.

2.1 Disabilities

Blindness, partially sighted, color blindness, epilepsy, learning disability, old age people, limited bandwidth are few of the disabilities which may restrict web accessibility. So, this research caters to most of the disabilities mentioned above. If any disabled person is unable to access web site in any form to any extent can sue the respective owner or company legally [2, 3].

2.2 Accessibility Today

2.2.1 Laws

Every country has different law for disabled people and the web usage though extent of those laws is fundamentally variable. The idea of disability protection laws is to create equal access for individuals with disabilities. The Equality Act came into force in October 2010, replacing the disability discrimination act (DDA) in England, Scotland, and Wales.

2.2.2 Technology

Various problems are faced by users especially those who use assistive technologies for web browsing, when developers neglect grammar or syntax of web development. Few among them are discussed below:

1. In Fig. 1a a simple login page is displayed. Here, negligence in closing a div tag led to password text box to appear for username field, which can create a huge misunderstanding when text to speech readers convey the message to disabled people and even to a fit person rushing to login.
2. Similarly, in Fig. 1b a table describing certain edibles is designed. Here carelessness in proper opening and closing of `<td>` `<tr>` tags of a table led vegetables heading out of context. So, whenever a text to speech reader would read this table it will read vegetables first and then edibles and following text giving a wrong insight into the information to the user.

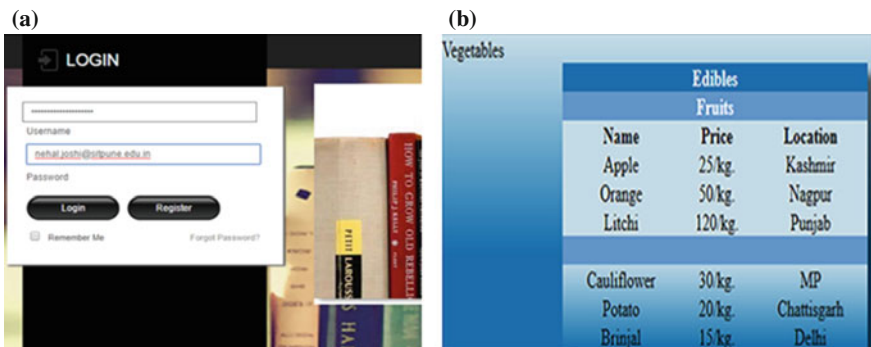


Fig. 1 Web page design samples. **a** Poor web page design sample, **b** wrong table design

As a solution to above problems, the tool presented “Eye for all” here validates web pages for such or similar problems and reports to the developer.

2.3 Focused Areas of Study

With guidelines laid down by W3C still web masters do not consider them while designing web pages. For a web site to be accessible it must be correctly designed. The problem areas in the current scenario which are catered by the tool are as follows:

- Blind people use talking browsers or text-to-speech conversion plug-ins for accessing Web. But for maximum times no text is provided to read which is a huge hindrance for blind to access Web. Media elements like image, having no alternate text are unattended in such scenarios.
- Developers while designing often choose colors of their choice irrespective of contrast ratio given by W3C which is problematic for color blind people.
- Content of web sites are having either too easy content or way too tough, this is inaccessibility issue for learning disabled people. This could further affect search engine optimization in turn because search engines look for content of web sites to display in their search results. And with growing competition every business organization prefers to be in top 10 search result.
- Using CSS is certainly a good designing practice but excessive dependency on CSS can lead to accessibility issues for the people having low bandwidth where style sheets may be delayed or at times not at all rendered.
- Tables these days are more commonly used for styling instead of content. But what if those blocks are not having proper start and closing tags. So, they must be used very carefully for styling.
- Enhanced browsers and the functionalities provided by various tools according to W3C are incompatible, to rectify it the solution would be creating web

services. For the browser to be capable of producing text for screen readers to read, a totally different approach would be to have a web service that provides a subset of the functionality for every guideline by W3C.

3 Implementation

3.1 *Formulated Strategy*

URL of the web site or HTML code is extracted and scrapping of the code is done to analyze and validate web page based on various guidelines for web accessibility. Finally, a web mashup is used to culminate the report contents which rates web site on grounds of web loss. All the implementations are done using windows communication foundation (WCF) services which is an improvised solution to a problem mentioned. It enhances implementation by building service-oriented architecture as well supports interoperability. .Net platform with C# language, HTML5, CSS3, JQuery, JavaScript is used to implement the same.

One of the techniques for web harvesting known as web content harvesting is used in implementation which exploits what is already known about the general structure of documents and then extracts information from the Web and mechanize the reading, copying, and storing necessary to collect information for analysis to be done against several guidelines of WCAG 2.0, and web mashup has proved to be useful for pulling together information to display report.

3.2 *Modules Implemented*

Modules implemented are mentioned in Fig. 2. Details of few of them are given in following sections. *Eye For All—the tool implemented is an online app and thus operable across operating systems and irrespective of configuration of systems.*

3.2.1 Language Check

This module is implemented with intent to help users in checking readability of content on their web site and enhance search engine optimization. Content of web sites are either too easy or way too tough, this is inaccessibility issue for learning disabled people. This could further degrade web site's lookup in search results. Readability depends on several factors, here emphasis is laid on count of hard words that is syllable count on a page. Linguistics was studied in depth by author and came up with following readability formulas to rate the content of web site:



Fig. 2 Modules implemented

Formula 1 Gunning Fog Index [4]

$$\text{GradeLevel} = 0.4(\text{ASL} + \text{PHW}) \quad (1)$$

where

ASL: Average Sentence Length, PHW: Percent Hard Words

Fog index of 7 or 8 is considered as best. A score beyond 12 is considered to be difficult.

Formula 2 The Flesch Reading Ease [4]

$$\text{ReadabilityEase} = 206.835 - (1.015 \times \text{ASL}) - (84.6 \times \text{ASW}) \quad (2)$$

where

ASL = Average Sentence Length, ASW = Average number of syllables per word.

For Flesch Reading Ease output is vice versa of Fog Index, i.e., higher the number easier the content is.

Formula 3 The Flesch-Kincaid Grade Level [4]

$$\text{GradeLevel} = (0.39 \times \text{ASL}) + (11.8 \times \text{ASW}) - 15.59 \quad (3)$$

To implement above-mentioned formulae natural language processing fields like sentence boundary disambiguation, segmentation, automated content rating, syllable discovery, and web scrapping a data extraction technology for Web, are used by the researcher. Abstract algorithm is given in algorithm 1.

Algorithm 1 Language check abstract algorithm

```

1: procedure LANGUAGE CHECK
2:   URL  $\leftarrow$  URL Of Required Web page
3:   HTMLCode  $\leftarrow$  HTML Code of the page
4:   Body Content  $\leftarrow$  Get body content from HTMLCode
5:   para  $\leftarrow$  Get paragraph of 100 words
6:   sc  $\leftarrow$  number of Syllables in para based on occurrence of vowels and silent characters
7:   stc  $\leftarrow$  number of Sentences in para based on full stop occurrence
8:   for each sentence do
9:     Remove special characters
10:    Remove numbers
11:    Next
12:    wc  $\leftarrow$  Get Word Count in Para
13:    ASL  $\leftarrow$  wc/stc
14:    PHW  $\leftarrow$   $100 * sc/wc$ 
15:    ASW  $\leftarrow$  wc/stc
16:   RS  $\leftarrow$  Readability score

```

3.2.2 Context Probing and Preview for Images

Disabled people say blind uses text-to-speech converters to browse Web. Audio browsers read text for them and help to decide on navigation and information retrieval. A roadblock is met in the absence of text for the hypermedia elements.

One of the democracy while surfing the Web is freedom to move among pages or web sites. It is equally important among developers and users. Studies have shown that this freedom is further tangled, when the user does not have context or preview information which are prime factors in mobility decisions.

So, this module scraps for the image elements on the web page and extracts information regarding presence or absence of alternate text. In absence of alternate text link segmentation an application of natural language processing is used for context probing and preview for the image. Abstract algorithm is given in algorithm 2.

Algorithm 2 Image check abstract algorithm

```

1: procedure IMAGE CHECK
2:   URL  $\leftarrow$  URL Of Required Web page
3:   HtmlCode  $\leftarrow$  Extract HtmlCode from the URL
4:   while HtmlCode has Imagetag do
5:     Check for various image extensions
6:     link  $\leftarrow$  Fetch only link in src tag
7:     imgname  $\leftarrow$  Fetch suggestion by link segmentation
8:     Check image code for alt tag
9:     IF imgcode contains alt text
10:    alttext  $\leftarrow$  Fetch alttext and display
11:    ELSE IF (imgcode contains empty alt text)
12:      Report imgname and empty text
13:    ELSE imgcode does not contains alt text
14:      Report as invalid and imgname
15:   END WHILE

```

3.2.3 Frames Check

Frames or iframes help reduce bandwidth and server load because the same content does not need to be loaded every time a new page is called or visited. This helps people with low bandwidth inaccessibility. The title attribute of the frame or iframe element is essential to describe the summary of contents residing on each frame. This will in turn help users to make mobility decisions if the title attribute provides sufficient information to let user determine which frame to enter and explore in detail, thus saving surfing time too and increasing positive aging of the web site. Flow chart is provided in Fig. 3a.

3.2.4 Bayesian Network Approach for Web Accessibility

The Bayesian model used here for web accessibility is based on two types of Bayesian Network which is commonly known as the Naive Bayes Classifier [5] and simple Bayes Classifier. Naive Network is based on the Naive assumption that every attribute (every leaf in the Network) is independent from the rest of the attributes and vice versa for simple Bayes. Equations used are:

$$P(X_i = x_i | X_j = x_j) := P(x_i | x_j) := \frac{P(x_i, x_j)}{P(x_j)} \quad (4)$$

In Short

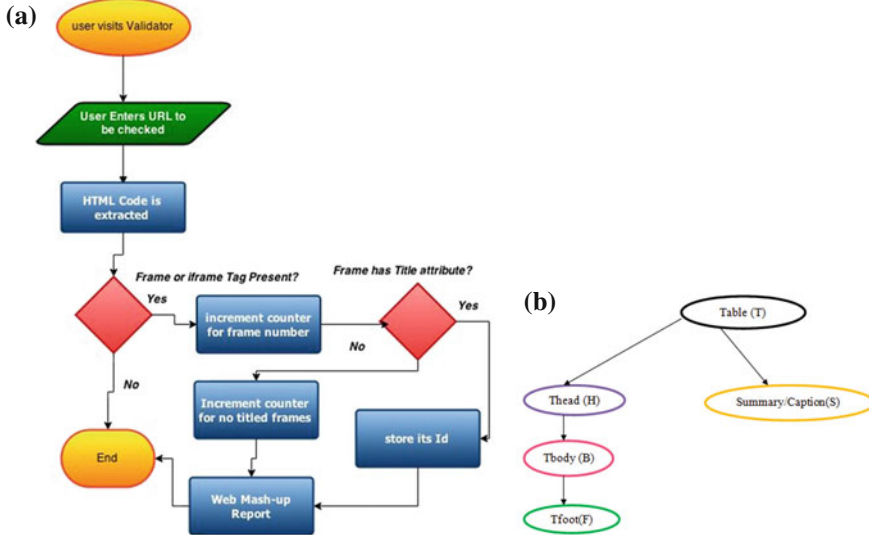


Fig. 3 Frame check flow and Bayes net. **a** Frame check flowchart, **b** table tag Bayesian Network

$$P(X_1, X_2, \dots, X_n) = \prod_{i=1}^n P(X_i | \text{Parents}(X_i)) \quad (5)$$

Three Bayesian Networks for three HTML tags namely heading, table, and image tag are drawn, to determine the extent of dependence or independence between HTML tags and their respective attributes, which in turn will lay emphasis on their presence while designing a web page for enhanced web accessibility. For Heading Tag (H) as parent node, font type (T), font size (S), font weight (W), and color (C) attributes are used as leaf nodes (V) in Naive Bayesian Network.

$$P(T, C, S, W/H) = P(H) \prod_{j=1}^4 P(V_j/H) \quad (6)$$

The prime probability $P(H)$ is calculated by counting the occurrences of tag it determines be table tag, image tag, or heading tag in the most popular web sites from entertainment, education, health, government, and other informative genre and dividing it by the total number of testing web sites considered, call it as a sample and not population data. Calculating average in mathematics so as to proceed with this calculation is a base for the remaining calculations.

The other probabilities mentioned in equation are also calculated based on sample web sites considered for test and by applying Boolean algebra and conditional probability on tag considered and its leaf attribute or child node in combination. Similar calculations are done for all the Bayesian Networks. For Table Tag

(T) as parent node and attributes mentioned in Fig. 3b as leaf nodes a simple Bayesian Network is drawn.

$$P(F/B, H, T) = P(C_i) \prod_{J=i}^3 P(V_i/C_i) = P(F) * [P(B/F) * P(H/F) * P(T/F)] \quad (7)$$

$$P(B/H, T) = P(C_i) \prod_{J=i}^2 P(V_i/C_i) = P(B) * [P(H/B) * P(T/B)] \quad (8)$$

4 Research Result

4.1 Statistics Obtained Using Tool

A real study was made on few web sites to evaluate based on the approach discussed in the work. Efficient and optimized tool developed during the research was used to validate several most popular, highly rated, and clicked web pages against checkpoints considered during study. All the web pages validated were bifurcated on industry they cater to be education, health, entertainment, and many more. Study was performed on bunch of these web pages to get statistics like average violations per industry and further these were categorized for being fully accessible or significantly inaccessible. For each web page, it was observed that which accessibility checkpoint (WCAG 2.0), is violated.

Table 1 shows the overall accessibility rating of all test sites evaluated. It states the number of violations for WCAG and the number of web pages that fall into the categories segregated in study: Fig. 4b displays an average, number of accessibility violations for various categories of web pages bifurcated on industry they cater to for the WCAG 2.0 guidelines.

4.2 Bayesian Results

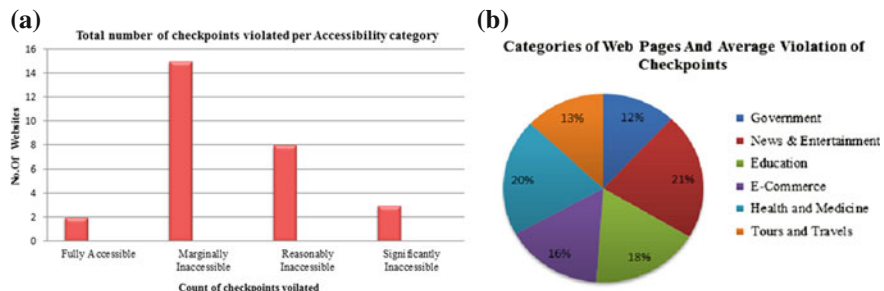
- For heading tag conditional dependence value of 0.934 indicates that inference is true that they are closely bound to each other. Mentioned attributes must be present when heading tag occurs for better web accessibility.

Heading tag is evidence (E) variable and attributes are query variables (Q). Inference is that query variables should appear with evidence variable for improved web accessibility.

Hypothesis Testing (Table 2):

Table 1 Total number of checkpoints violated per accessibility category

Accessibility categories	No. of violations	No. of web pages
Fully accessible	0	2
M marginally accessible	1–2	15
R easonably inaccessible	3–4	8
S ignificantly inaccessible	5+	3

**Fig. 4** Tool results. **a** Total number of checkpoints violated per accessibility category, **b** categories of web pages and average violation of checkpoints**Table 2** Hypothesis testing data

Sample Standard Deviations	4.16025
Sample standard variance, s^2	17.30769
Population standard deviation, σ	3.99704
Population standard variance, σ^2	15.97633
Sample mean, population mean	19.8
Population size	13
Significance level	0.05

Null Hypothesis: Font size is greater than 14px.

Result:

T-Score Test Value: -0.03987

P-Value: 0.4841

Conclusion: Since the *P*-value 0.4841 is greater than the significance level 0.05, we cannot reject the null hypothesis and thus for headings font size must be greater than 14px to avoid any digital divide.

- For Table tag

$$P(F/B, H, T) = 1.296 \times 10^{-5}$$

$$P(B/H, T) = 0.015$$

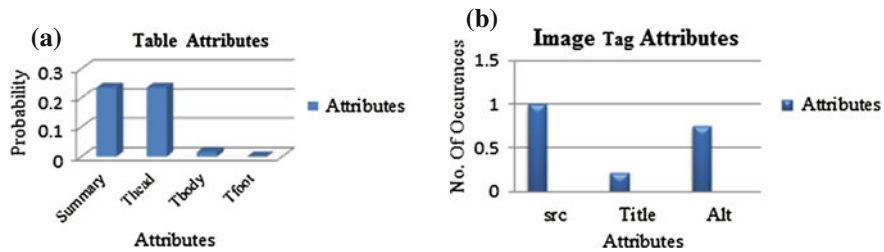


Fig. 5 Bayesian results. **a** Table results, **b** image results

Conclusion: Very small figure in output shows that there is negligible independence among tfoot, thead, tbody attributes and hence should be used in conjunction with each other for improved web accessibility (Fig. 5).

- For Image Tag

For image tag probability value of 0.982 indicates that occurrence of *S*, *T*, *A* attributes when Image tag present is high which means these attributes must be present along with the image tag, which can enhance web accessibility.

5 Conclusion

Study concludes that a lot of strategic planning has to be done for achieving web accessibility for all. This study evaluated web loss for several web sites, and unfortunately more than 60 % sites were found to be inaccessible; according to the WCAG 2.0. Tool was used to validate most of the popular web sites, those web sites failed in passing web accessibility criteria as many of them had no title tags for frames, color contrast ratio was not satisfying 4.5:1 ratio, readability score turned out to be high, and excessive dependency on CSS was found. Thus acute care must be taken while designing web sites to change the belief that disabled people are offline.

Also industries which cater the field violates the most required checkpoint for that particular field. For example, News industry violates language check which is a must for its readers. Similarly, image check is most violated in tour's and travels industry.

Results from Bayesian Network analysis yields negligible independence among html tags which states that they must be used altogether for enhanced web accessibility. The result clearly states that table tag must have thead, tfoot, tbody element altogether for improved web accessibility. Similarly, Image tag must have alternate text for text-to-speech tools to read content for the user to enhance understandability of the context. So, accessibility testing tools should be made easier to use and more effective and efficient, this can help bridge the gap between developers and accessibility guidelines.

Acknowledgments The author would like to thank college, department, HOD Prof. Shraddha Phansalkar, guide Prof. Manisha Tijare, and Project manager Dr. Preeti Mulay for providing an opportunity to work in this direction as a contribution towards both technology and society.

References

1. Tedeschi, B.: Advocates of people with disabilities take online stores to task. *The New York Times*, (Jan. 2001)
2. Moss, T.: Disability Discrimination Act (DDA) web accessibility. 2005. url: <http://www.webcredible.co.uk/user-friendly-resources/web-accessibility/uk-website-legal-requirements.shtml> (visited on 10/02/2014)
3. Moss, T.: Web Accessibility and UK Law: Telling It Like It Is. 2004. url: <http://www.alistapart.com/articles/accessuk/> (visited on 10/02/2014)
4. Crossley, S.A., Allen, D.B., McNamara, Danielle S.: Text readability and intuitive simplification: a comparison of readability formulas. *Reading Foreign Lang.* **23**(1), 84–101 (2011)
5. Langley, P., Sage, S.: Induction of selective Bayesian Classifiers. In Proceedings of the 10th International Conference on Uncertainty in Artificial Intelligence, UAI'94. Seattle, WA: Morgan Kaufmann Publishers Inc. pp. 399–406 (1994) isbn: 1-55860-332-8. url: <http://dl.acm.org/citation.cfm?id=2074394.2074445>

Feature and Search Space Reduction for Label-Dependent Multi-label Classification

Prema Nedungadi and H. Haripriya

Abstract The problem of high dimensionality in multi-label domain is an emerging research area to explore. A strategy is proposed to combine both multiple regression and hybrid k-Nearest Neighbor algorithm in an efficient way for high-dimensional multi-label classification. The hybrid kNN performs the dimensionality reduction in the feature space of multi-labeled data in order to reduce the search space as well as the feature space for kNN, and multiple regression is used to extract label-dependent information from the label space. Our multi-label classifier incorporates label dependency in the label space and feature similarity in the reduced feature space for prediction. It has various applications in different domains such as in information retrieval, query categorization, medical diagnosis, and marketing.

Keywords Multi-label · Multiple regression · Hybrid kNN · PCA

1 Introduction

In today's world, we most often deal with multi-label data, that is, data assigned to more than label at the same time. Defining this formally, in single-label classification, an object x_i is assigned to one class c_i , but in multi-label classification an object x_i is assigned to a set of classes, $c_1, c_2 \dots c_l \subseteq C$ simultaneously, where C is the total number of labels.

P. Nedungadi (✉) · H. Haripriya
Amrita CREATE, Amrita University, Kollam, Kerala, India
e-mail: prema@amrita.edu

H. Haripriya
e-mail: haripriya@am.amrita.edu

There are many real world examples for multi-label data and we can quote a few. A movie can belong to the categories of action, crime, thriller, or drama simultaneously. A newspaper article may belong to a person, a country, some local, national, or international category.

High dimensionality is a curse for almost all machine-learning problems. Linear as well as non-linear dimensionality reduction methods are proposed for linear as well as non-linear datasets. Techniques for dimensionality reduction such as PCA [1], CCA [2], kernel PCA [3], Sammon's non-linear mapping [4], and SVD handle high dimensional data.

Like all existing classification techniques, the multi-label domain also has complexity problems when dealing data with high dimensions. Thus, our objective is to effectively reduce the dimensions of data residing in the high-dimensional space. A new version of PCA and kNN that is a hybrid kNN is proposed in one of our works [5] to reduce the search as well as the feature space of traditional kNN. A new approach for multi-label classification based on multiple regression is proposed in another work [6] of ours. In this paper, we propose a strategy for dimensionality reduction, and multi-label prediction by a hybrid approach using our works [5, 6].

We combined multiple regression with hybrid kNN for label set prediction of high-dimensional data. Multiple regression is used for generating models for label sets. Traditional kNN are computationally intensive since its search space is the entire training data. So applying kNN only for neighboring vectors in the principal components reduces the inputs for the kNN classifier as well as the feature space. Our proposed hybrid feature space reduced multi-label classifier has various applications in high-dimensional domains such as information retrieval, query categorization, medical diagnosis, marketing, and text categorization.

The remaining sections of the paper are the following; Sect. 2 explains the existing techniques for multi-label classification. Section 3 explains briefly the basics of our paper. Section 4 discusses our proposed approach in detail; Sect. 5 details the experimentations and result analysis and Sect. 6 concludes our work briefly.

2 Related Work

Most of the existing classifiers in machine-learning [3] deals with single-label classification. Methods to extend existing classifiers in order to deal with multi-labeled data are discussed in [7–12, 26]. Some methods that are also under research [4, 13, 14] convert multi-label dataset into a set of single-label dataset to fit with the existing classifiers. Dimensionality reduction in high-dimensional space for multi-label is discussed in [15–18].

ML-kNN [7] used the concept of traditional k-Nearest Neighbor algorithm and the maximum a posteriori principle for label set prediction. A Ranking-based kNN Multi-Label Classification [8, 13] also used k-nearest-neighbor-based ranking approach for the multi-label classification. Ranking SVM and kNN concepts are used for multi-label prediction. An approach to analyze features for specific label is discussed in [12]. But these approaches have not considered interdependencies between the label sets and thus ignored the possibility of co-occurrence of labels.

This problem can be eliminated by the mapping of each label in the feature space as a robust subspace, MSE [6], and formulating the prediction as finding the group sparse representation of a given instance on the subspace ensemble.

A Naive Bayesian Multi-label Classification Algorithm [19] is a problem transformation approach. Naive Baye's ignores feature dependency and so in real world application it will result in a decrease in prediction accuracy.

In [13, 14, 20], Ranking SVM is used for document retrieval. Ranking SVM belongs to the category of multi-label dataset in which a single query matches with multiple documents. For non-linear data sets when between the number of samples and the number of features is very low, the possibility of lower accuracy will be high.

A decision tree algorithm C4.5 [21] that is used for the analysis of phenotype data is discussed in [9]. It is simple and easy to learn. More informative attributes are used for tree splitting. But attempts for generalization results in decrease in performance. BPMLL [22] is an extension of traditional back-propagation algorithm proposed an error function that adapt according to the characteristics of multi-label data and thus can be used for multi-label learning. But the neural network complexity becomes high in the training phase.

A probabilistic kNN and logistic regression-based approach for label set prediction is discussed in [23]. The distance between neighboring instances and their labels are used for prediction. Random k-Labelsets (Rakel) [24] divide the label set and considers the label correlation ship. But both these approaches consume more time in applications with large number of training samples and labels.

AdaBoost [10, 25] creates an accurate hypothesis by utilizing a set of weak hypotheses. It uses information from misclassified data. This algorithm is extended to handle multi-labeled data, but it is sensitive to both noisy data and outliers. A method to reduce dimensionality reduction in the label space with association rule is discussed in [11]. But this approach does not guarantee reduction without information loss.

To solve this problem, a joint learning framework [18] is used, in which we perform dimensionality reduction and multi-label classification simultaneously. This is a novel joint learning framework [3] which performs reduction in dimensions and multi-label inference in semi-supervised setting. A multi-label dimensionality reduction method, MDDM [4], attempts to project the original data into a lower dimensional feature space by maximizing the dependence between the

original feature space and its class labels. But these methods cannot provide an explicit modeling of the label dependency and thus their performance improvements due to exploring label structure are of less significance.

In our proposed approach, we combined the advantages of kNN and multiple regression for multi-label classification. We not only combined feature as well as a label correlation in our approach, but we have also done some dimensionality reduction in the feature space of our multi-label data, thereby reducing the search space as well as the feature space for prediction.

3 Multiple Regression and Traditional kNN

Multiple regression is an extension of simple linear regression for incorporating the dependencies of more than one variable. In our approach we considered the dependence property of labels in the label space.

The equation for multiple regression is

$$Y_{\text{pred}} = \alpha + \beta_1 X_1 + \beta_2 X_2 + \beta_3 X_3 + \cdots + \beta_n X_n \quad (1)$$

where Y_{pred} is the variable to be predicted, the X 's are the dependent variables of the response variable or the predictors, and the β 's are the weights or coefficients associated with the predictors.

If we want to predict the class of a newly arrived data, traditional kNN will perform a similarity computation in the entire input space. The most similar k neighbors from the training data will be used for testing. Among various measures, we used cosine similarity for similarity computation. Considering two feature vectors x and y , cosine similarity is computed using [3];

$$\cos(\Theta) = \text{similarity}(x, y) = \frac{x \cdot y}{\|x\| * \|y\|}. \quad (2)$$

The similarity values range from 0 to 1. When the value is 1 they are equal or most similar and when it is 0 they are less similar. Cosine similarity will generate a metric that says how two vectors are related by looking at the angle instead of the magnitude.

4 System Architecture

Our objective is to classify a data into more than one class instead of a single class. We combined hybrid kNN and multiple regression for prediction label set of a data. When a test data is given hybrid kNN it will reduce the feature space as well as the search space.

Multiple Regression and kNN is the main algorithm of our proposed multi-label classifier. The input to our algorithm is the training data with its associated label set and the test data.

Algorithm 1 - Multiple Regression and Hybrid kNN

```

Input: { Train data with Label set, Test data }
Output: { Label set of test data }
1: Generate models using multiple regression on the label set of training data.
2: Compute Principle components of train data.
3: Select some eigen vectors with largest eigen value.
4: Project entire training data and the test data along each selected PC.
5: Perform binary search over each projected space to find  $L$  nearest neighbors .
6: Select the most similar  $k$  neighbors.
7: for  $i : 1$  to  $k$ 
    Each Label value prediction using generated model
8: end
9: Average predicted value along each label
10: for  $i : 1$  to  $C$ 
    if (average < threshold) then
        Test data has no label named  $i$ 
    else
        Test data has label named  $i$ 
11: end
12: Predict the Label set

```

Multiple regression is used to obtain the information from the dependent labels, i.e., from the label space. We assume that for the occurrence of one label, all other labels will contribute. A weight is associated with the labels that give the information about its dependency. A linear model is generated for each label by using the labels from the training set.

We used hybrid kNN for finding the most similar k neighbors from our training set. We limit the kNN search space by finding the L nearest neighbors along each principal component in the dimensionally reduced feature space. The data that are clustered in the original space will also be closer in the projected space and along each of the principal components. A threshold value is used for predicting the label.

The architecture of the training phase of multi-label classifier is shown in Fig. 1. It is composed of two phases, model generation and reduced search space generation phase.

The architecture of the testing phase of multi-label classifier is shown in the Fig. 2. When a new data arrives, we project the newly arrived data along the principal components. In order to reduce the classification time and increase the efficiency of kNN, project the vector along each component and select the L nearest neighbors. These neighbors are the input dataset for kNN. Prediction is based on the most similar k neighbors from the nearest neighbors.

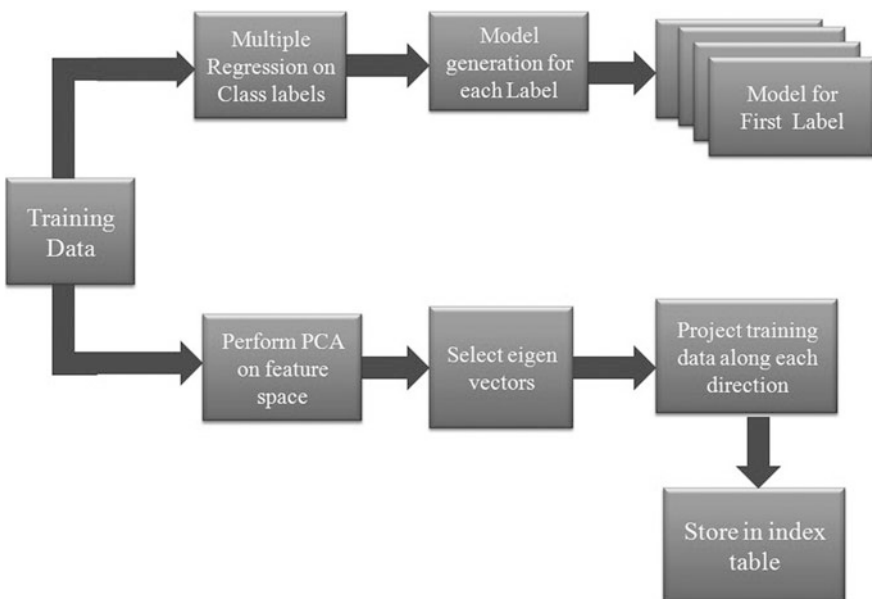


Fig. 1 Training phase of multi-label classifier

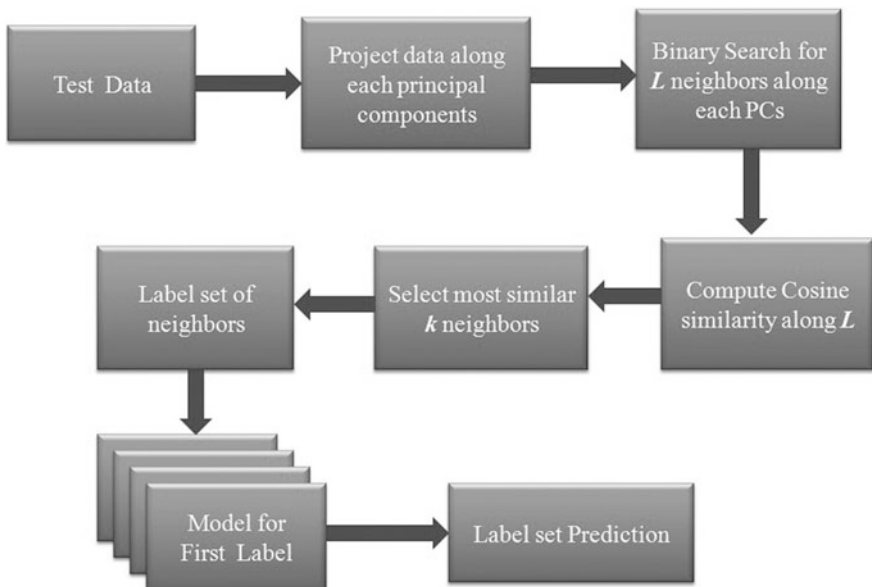


Fig. 2 Testing phase of multi-label classifier

5 Experimental Evaluation

We cannot evaluate a multi-label learning system with the common measures such as precision, recall, etc., since they are used for evaluating the performance of single-label learning system.

Hamming loss: It evaluates how many times an instance-label pair is misclassified [1, 2], which means a label not belonging to the instance is predicted or a label belonging to the instance is not predicted. The smaller the value of hamming loss, the better the performance and ranges between 0 and 1 and Δ is the symmetric difference between two sets.

$$\text{hloss}_s(h) = \frac{1}{p} \sum_{i=1}^p \frac{1}{Q} |h(x_i) \Delta Y_i|. \quad (3)$$

We have used a multi-label dataset from Knowledge Extraction based on the Evolutionary Learning (KEEL Dataset) data repository. The L value chosen is 80 for both the datasets.

The hamming loss computed for our proposed method is one regression-based method and ML-kNN on the Yeast dataset with 103 attributes and 14 labels that are shown in Table 1.

Table 1 shows our approach outperforms Regression and ML-kNN at $k = 15$ and $k = 45$. At $k = 6$ hamming loss of our approach is equal to ML-kNN and outperform Regression. Table 2 shows the hamming loss computed for the Emotions dataset that are 72 attributes and 6 labels. At $k = 5$ to $k = 7$ and for $k = 10$ our approach

Table 1 Hamming loss on yeast data set compared with ML-kNN, regression, hybrid multi-label

Yeast	Hamming loss					
	$k = 5$	$k = 6$	$k = 14$	$k = 15$	$k = 40$	$k = 45$
ML-kNN	0.2042	0.2126	0.2074	0.2063	0.2144	0.2123
Regression	0.2154	0.214	0.2108	0.2077	0.2097	0.2134
Combined	0.2169	0.2126	0.2088	0.2057	0.2103	0.2111

Table 2 Hamming loss on emotions data set compared with ML-kNN, regression, hybrid multi-label

Emotions	Hamming loss					
	$k = 5$	$k = 6$	$k = 7$	$k = 8$	$k = 9$	$k = 10$
ML-kNN	0.294	0.3081	0.2959	0.2978	0.2828	0.2846
Regression	0.2912	0.2846	0.2781	0.279	0.279	0.2856
Combined	0.2753	0.2781	0.2753	0.2809	0.2884	0.2846

(Combined) outperforms ML-kNN and Regression. Since both data sets have high-dimensional feature space, we can guarantee that our method will give high accuracy in the high-dimensional feature space.

6 Conclusion

Multi-label data classification in high-dimensional space is a new area to explore. In our paper, we proposed a new method for high-dimensional multi-label prediction. A model generation phase fits well in our method to gather label-dependent information from the label space and hybrid kNN is used to compute neighbors from the projected feature space. A hybrid kNN algorithm based on PCA is proposed, to reduce the dimension and efficiently find neighbors along each principal component so as to restrict the kNN search space. This combination is good enough to capture useful information from the label, as well as from the reduced feature space.

Acknowledgments This work derives inspiration and direction from the Chancellor of Amrita University, Sri Mata Amritanandamayi Devi.

References

1. Smith, L.I.: A tutorial on principal components analysis. Cornell Univ. USA **51**, 52 (2002)
2. Hotelling, H. Relations between two sets of variates. Biometrika, 321–377 (1936).
3. De Leeuw, J. (2011). History of nonlinear principal component analysis
4. Sammon, J.W.: A nonlinear mapping for data structure analysis. IEEE Trans. Comput. **18**(5), 401–409 (1969)
5. Nedungadi, P., Harikumar, H., Ramesh, M.: A high performance hybrid algorithm for text classification. In 5th International Conference on the Applications of Digital Information and Web Technologies (ICADIWT), IEEE, pp. 118–123 (2014)
6. Nedungadi, P., Haripriya, H.: Exploiting label dependency and feature similarity for multi-label classification. In: International Conference on Advances in Computing, Communications and Informatics (ICACCI) IEEE, pp. 2196–2200 (2014)
7. Zhang, M.L., Zhou, Z.H.: ML-KNN: A lazy learning approach to multi-label learning. Pattern Recogn. **40**(7), 2038–2048 (2007)
8. Chiang, T.H., Lo, H.Y., Lin, S.D.: A Ranking-based KNN Approach for Multi-Label Classification. In: ACML. pp. 81–96 (2012)
9. Clare, A., King, R. D.: Knowledge discovery in multi-label phenotype data. In: Principles of data mining and knowledge discovery, pp. 42–53, Springer Berlin Heidelberg (2001)
10. Schapire, R.E., Singer, Y.: BoosTexer: a boosting-based system for text categorization. Mach. Learn. **39**(2–3), 135–168 (2000)
11. Charte, F., Rivera, A., del Jesus, M.J., Herrera, F.: Improving multi-label classifiers via label reduction with association rules. In: Hybrid Artificial Intelligent Systems, pp. 188–199, Springer Berlin Heidelberg (2012)
12. Zhang, M. L., Wu, L. (2011). LIFT: Multi-label learning with label-specific features

13. Hang, L.I.: A short introduction to learning to rank. *IEICE Trans. Inform. Syst.* **94**(10), 1854–1862 (2011)
14. Joachims, T.: Optimizing search engines using clickthrough data. In: *Proceedings of the 8th ACM SIGKDD International Conference on Knowledge Discovery and Data Mining*, ACM. pp. 133–142 (2002)
15. Ji, S., Ye, J.: Linear Dimensionality Reduction for Multi-label Classification. In: *IJCAI* **9**, pp. 1077–1082 (2009)
16. Qian, B., Davidson, I.: Semi-Supervised Dimension Reduction for Multi-Label Classification. In *AAAI*. **10**, pp. 569–574 (2010)
17. Zhang, Y., Zhou, Z.H.: Multilabel dimensionality reduction via dependence maximization. *ACM Trans. Knowl. Disc. Data (TKDD)* **4**(3), 14 (2010)
18. Zhou, T., Tao, D.: Multi-label subspace ensemble. In *International Conference on Artificial Intelligence and Statistics*. pp. 1444–1452 (2012)
19. Wei, Z., Zhang, H., Zhang, Z., Li, W., Miao, D.: A naive Bayesian multi-label classification algorithm with application to visualize text search results. *Int. J. Adv. Intell.* **3**(2), 173–188 (2011)
20. Cao, Y., Xu, J., Liu, T.Y., Li, H., Huang, Y., Hon, H.W.: Adapting ranking SVM to document retrieval. In: *Proceedings of the 29th annual international ACM SIGIR conference on Research and development in information retrieval*, ACM pp. 186–193 (2006)
21. Quinlan, J.R.: Induction of decision trees. *Mach. Learn.* **1**(1), 81–106 (1986)
22. Prajapati, P., Thakkar, A., Ganatra, A.: A survey and current research challenges in multi-label classification methods. *Int. J. Soft Comput.* **2** (2012)
23. Cheng, W., Hüllermeier, E.: Combining instance-based learning and logistic regression for multilabel classification. *Mach. Learn.* **76**(2–3), 211–225 (2009)
24. Tsoumakas, G., Katakis, I., Vlahavas, I.: Random k-labelsets for multilabel classification. *IEEE Trans. Knowl. Data Eng.* **23**(7), 1079–1089 (2011)
25. Rätsch, G., Onoda, T., Müller, K.R.: Soft margins for AdaBoost. *Mach. Learn.* **42**(3), 287–320 (2001)
26. Aggarwal, C.C., Zhai, C.: A survey of text classification algorithms. In: *Mining text data*. pp. 163–222, Springer US

Link Expiration-Based Routing in Wireless Ad Hoc Networks

Shweta R. Malwe, B. Thrilok Chand and G.P. Biswas

Abstract Wireless ad hoc networks are dynamic and infrastructureless networks. The dynamicity of the network and ignorance of the link availability are the basic reason for inefficient routing and hence causes unsuccessful data transmission between the peers. The prediction of link expiration can overcome the problem of link failure during routing. In this paper, we modified the routing mechanism by considering the network dynamicity in terms of Link Expiration Time (LET). The proposed routing technique is reactive in nature and performs route discovery based on LET with minimized control overhead. The simulation results show that the proposed scheme outperforms the existing Dynamic Source Routing (DSR) in terms of control overhead, hop count, etc., and provides better link duration time than the existing protocol.

Keywords Wireless ad hoc network · Link expiation time (LET) · Routing · Control overhead · Link duration time

1 Introduction

Wireless ad hoc networks have been a prime focus of research due to its features like dynamicity, quick deployment, multi-hop data transfer, light weight devices, and its decentralized nature make them suitable for emergency conditions like natural disasters, military conflicts, etc. The network nodes lying within the transmission range of one another, forms logical connection referred as link.

S.R. Malwe (✉) · B. Thrilok Chand · G.P. Biswas
Department of Computer Science and Engineering, Indian School
of Mines, Dhanbad, India
e-mail: shweta.malve26@gmail.com

B. Thrilok Chand
e-mail: thrilokchand@gmail.com

G.P. Biswas
e-mail: gpbiswas@gmail.com

The frequently changing topology is the main restriction in such networks and hence it is difficult to design a protocol that guarantees Quality of Service (QoS) issues in the network [1].

Many areas of networking have been explored in the literature. Media Access Control (MAC) layer mainly focuses on the spectrum access and its utilization. Link control is another important issue as it deals with the stability of the connection which depends on the mobility of nodes in the network [1]. Routing of data packets in ad hoc networks is governed by different protocols to route a data packet effectively from one node to another. A successful route setup depends on the stability of the connecting links in the active route. If a route is established without the knowledge of link availability, frequent retransmission may lead to broadcast storm in the network which will degrade end-to-end network performance. In order to increase bandwidth consumption and reduce the information loss, routing must be molded to use the link availability status before data transmission arrives.

In this paper, we proposed a reactive routing technique based on DSR that utilizes the information of link availability status during route discovery phase. The obtainability of link is termed as LET which refers to the time left for the link to be available for communication. Routing will be performed on the basis of the link expiration at each node in the network. The proposed technique will not only reduce the information loss but will also increase the network performance with minimized control overhead. Simulation is performed to compare the proposed protocol with the existing reactive routing protocols in terms of successful transmission rate, hop count, control overhead, etc.

The organization of the paper is as follows. Section 2 includes the background works. Section 3 presents the link expiration estimation technique and the proposed Link Expiration-based Routing (LER) protocol. Section 4 includes the simulation results. Section 5 concludes the paper.

2 Related Works

It is a very challenging issue in highly mobile network to find a stable route between source and destination nodes. Several routing schemes are proposed in the literature but only some of them deal with the node's mobility and underlying connecting link's information. Routing in wireless ad hoc networks can be categorized as proactive (based on routing table), reactive (source initiated), and hybrid techniques [2]. Several routing protocols like DSDV [3], AODV [4], DSR [5], etc., are explained in the literature. Other routing techniques include multipath, location aware, hierarchical, etc. [2]. Some of the proposals are made for routing and topology control by considering link duration. In [6], improvements for different routing protocols are presented by using the prediction of mobility features and location information of the nodes in the wireless networks. In [7], authors provided a mobility model that measures the availability of path or routes in the network based on mobility of nodes. To provide constant path, the probabilities of link and

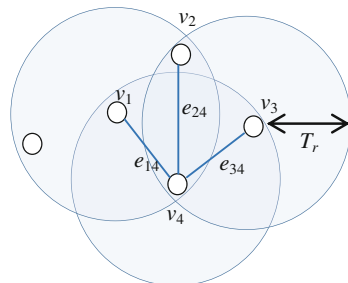
path availability is derived in [8], where the nodes move randomly and an optimal path is selected. In [9], prediction-based link accessibility is devised to estimate the link reliability by considering the dynamic nature of the channel which improves routing in the network. In [10, 11], authors developed different methods to identify the reliable links in wireless network environment based on the analysis of route durations in various mobility scenarios and by using GPS receivers to find the node positions for identifying link status. In [12], a novel packet receiving time is considered to predict the link state information in the network to improve the stability of links. In [13], authors used Particle Swarm Optimization (PSO) based lifetime prediction algorithm for route recovery in mobile ad hoc networks. A prediction-based model for topology control and routing has been proposed in [14] which is a cross-layer between cognitive radio unit and routing. The model predicts link availability by considering link interference and dynamic network topology, aiming in the reduction in route re-estimation in the network.

3 Proposed Link Expiration-Based Routing (LER) Protocol

A wireless ad hoc network can be molded as a network topology by using a graph, $G = \{V, E\}$, where the set of vertices, V represents the nodes in the network, enabled with Global Positioning System (GPS) and the connecting links between the nodes are presented by the set of edges, E which are assumed bidirectional.

To model the wireless transmission between the nodes, a radio link model is assumed in which each node has a certain transmission range, refer Fig. 1. Each node with fixed transceiver power and omnidirectional antenna can periodically discover neighbors by sending/responding *hello*-like short messages and records in a table. In our algorithm, we consider the nodes to have slow and constant mobility to have consistent network graph at any time. In such networks, one of the major issues is the link failure due to mobility of the nodes. To improve the same, reliable or stable route selection is required during routing process.

Fig. 1 Network topology



3.1 Terminologies

We use the following terminologies in the proposed routing protocol:

- (1) The set of nodes in the network is denoted by $V = \{v_1, v_2, \dots, v_N\}$, where N is the total number of nodes.
- (2) T_r represents the fixed transmission range of the node.
- (3) (x_i, y_i) : The position coordinates of node v_i .
- (4) Link in the network is the logical connection between two nodes with overlapping transmission range. The set of links in the network is denoted by $E = \{e_{ij} \mid v_i \text{ and } v_j \text{ are reachable}\}$.
- (5) V^e : the velocity of each node in the network (assumed as constant).
- (6) LET_{ij} : LET between the nodes v_i and v_j .

3.2 Link Expiration Estimation

We define LET as the time left for a link to be available for data transmission. Following algorithm depicts the estimation of link expiration between two neighboring nodes v_i and v_j presented in Fig. 2.

Algorithm LET_estimation
<pre> Step 1. Node v_i and v_j receive neighbouring information at periodic time intervals. Step 2. At node v_i, calculate the effective distance, D between v_i and v_j as, $D = \sqrt{(x_i - x_j)^2 + (y_i - y_j)^2}$ Step 3. Since $D < T_r$, we calculate the remaining distance, d for the link to be available between the nodes as, $d = T_r - D$ Step 4. If (v_i and v_j are moving apart from each other) then calculate, (i) $D_1 = d/2$ (ii) $\text{LET}_{ij} = D_1 / V^e$ EndIf If (v_i and v_j are moving towards each other) then calculate, (i) $D_2 = D + (d/2)$ (ii) $\text{LET}_{ij} = D_2 / V^e$ EndIf </pre>

```

Step 1. Node  $v_i$  and  $v_j$  receive neighbouring information at periodic time
       intervals.
Step 2. At node  $v_i$ , calculate the effective distance,  $D$  between  $v_i$  and  $v_j$  as,
       
$$D = \sqrt{(x_i - x_j)^2 + (y_i - y_j)^2}$$

Step 3. Since  $D < T_r$ , we calculate the remaining distance,  $d$  for the link to be
       available between the nodes as,
       
$$d = T_r - D$$

Step 4. If ( $v_i$  and  $v_j$  are moving apart from each other) then calculate,
       (i)  $D_1 = d/2$ 
       (ii)  $\text{LET}_{ij} = D_1 / V^e$ 
     EndIf
     If ( $v_i$  and  $v_j$  are moving towards each other) then calculate,
       (i)  $D_2 = D + (d/2)$ 
       (ii)  $\text{LET}_{ij} = D_2 / V^e$ 
     EndIf

```

According to LET, we categorize the links as:

1. *Epiring*: A link with LET lesser than the threshold value. Such links must not be involved during route setup.

Fig. 2 Link expiration condition for two reachable nodes

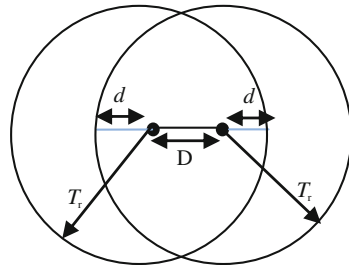
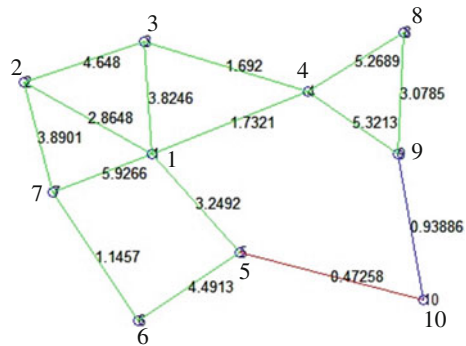


Fig. 3 Network with links based on LETs



2. *Avoidable*: Such links are having lower LET but can be used for a short period of time.
3. *Active*: They are available for data transmission having large LET.

Figure 3 shows a network of 10 nodes with their LETs (in seconds) between the neighbors. A constant threshold value is considered for link categorization. Links with $\text{LET} > 1$ are the active links (indicated as green), links with $\text{LET} < 0.5$ are the expiring links (indicated as red), and blue links are the avoidable one if LET lies between 0.5 and 1.

3.3 Proposed Link Expiration-Based Routing (LER) Protocol

The proposed routing protocol is reactive in nature and works on the principle of DSR. Two control packets, route request (RREQ) and route reply (RREP) are used for route estimation. The salient feature of link expiration-based routing is limited flooding of the control packets and LETs of the connecting links. The following algorithm explains the RREQ generation and forwarding. Once RREQ reaches destination, RREP will be generated and passed on the reverse active route.

3.3.1 Algorithm

RREQ_forward (v_m)	RREQ_receive (v_m)
<pre> // Let v_i is the source that finds a route to the destination v_j. Each RREQ forwarding node, v_m (including v_i), calls RREQ_forward (). For k = 1 to N_{g_m} do, If (v_k is an active neighbor and $LET_{mk} >$ threshold) then, If ($v_k == v_j$) Call RREP_forward (v_j) else Include v_m's id in the active route. Send RREQ packet to v_k. Call RREQ_forward (v_k) EndIf EndIf Done </pre>	<pre> Each node receiving RREQ, v_m (including v_i), calls RREQ_receive (). For k=1 to N_{g_m} do, Call LET_estimation. //using the recent received information. If (e_{km} is an active link) Call RREQ_forward (v_k) //avoidable links are considered for short interval data transmission. EndIf Done </pre>

To illustrate the proposed LER protocol, let us assume that node 5 tries to communicate with node 9. If DSR is applied, the active route selected will be {5-10-9} which includes the expiring link also. However, LER protocol will select the path {5-1-4-9} as an active route. In this scenario, packet drop probability with DSR has increased in comparison with the LER protocol.

3.3.2 Algorithm Analysis

Lemma 1 *LER protocol ensures successful data transmission over DSR.*

Proof For a source node v_s and destination v_d , DSR protocol works on the shortest path between the source and destination without predicting the link status and may include expiring links. However, LER protocol provides a path with the consideration of link expiration with a threshold value t , which can be mathematically presented as follows:

$$(LET_{sd})_{DSR} = LET_{si} + LET_{ij} \dots + LET_{zd} \quad (1)$$

$$(LET_{sd})_{LER} = LET_{sk} + LET_{km} \dots + LET_{rd} \text{ provided } LET > t \quad (2)$$

Since only active (or avoidable) links are considered by LER protocol, it signifies that $(LET_{sd})_{LER} > (LET_{sd})_{DSR}$ and hence will allow a stable route for data transmission.

4 Simulation Results

We performed extensive experiments on the proposed and existing algorithms on the randomly generated networks using MATLAB R2013a. We compared the proposed LER protocol with the existing DSR protocol and the existing PCTC protocol. The simulation scenario is presented in Fig. 4.

The route discovery in LER involves limited flooding of control packets in the network using LET estimation, whereas DSR involves pure flooding. Figure 5a presents the comparison between proposed LER and existing DSR protocol in terms control overhead. Control overhead refers to the summation of the emitted control packets in the network during the setup of the maximum active routes.

In order to present the effectiveness of routing performance of the proposed LER protocol, we compared it with DSR in terms of successful transmission rate as the percentage of successful transmission over total transmission in Fig. 5b. The proposed LER protocol also depends on the existing topology as DSR but involves only the active and sometimes avoidable links for route discovery. Hence, there exists a slight increment in the hop count between a specific source and destination as shown in Fig. 6a. However, the route longevity is increased and shows

Parameter	Value
Simulation Area, A	$500 \times 500 \text{ m}^2$
Number of nodes, N	20 to 100
Transmission range (T_s)	80 m
Number of simulation iterations	25
Δ	3-6
V^e	5 m/sec

Fig. 4 Simulation scenario

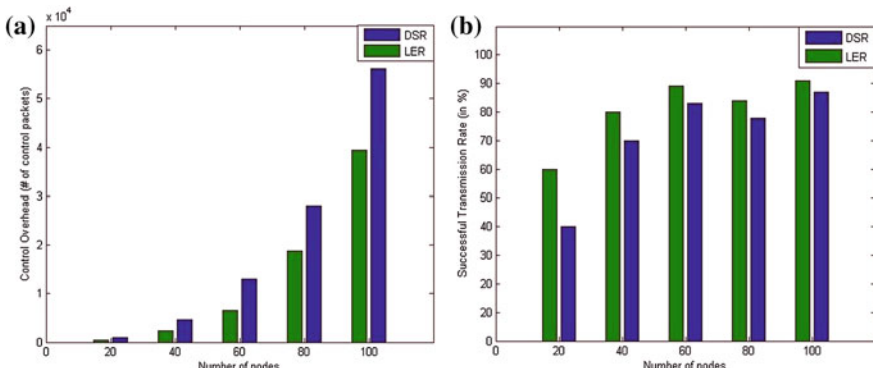


Fig. 5 Control overhead and successful transmission rate comparison between proposed LER and DSR

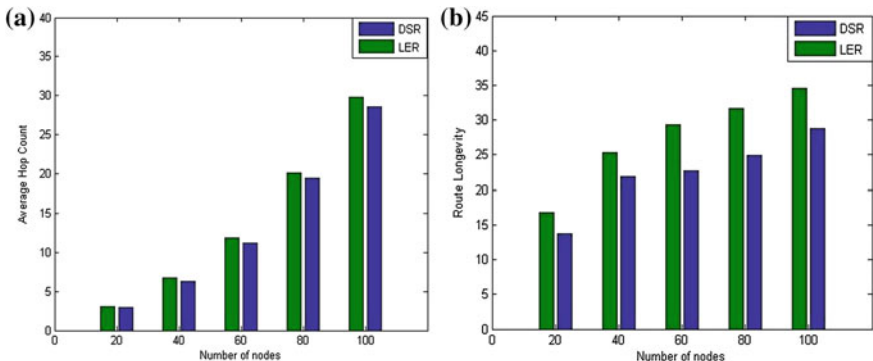
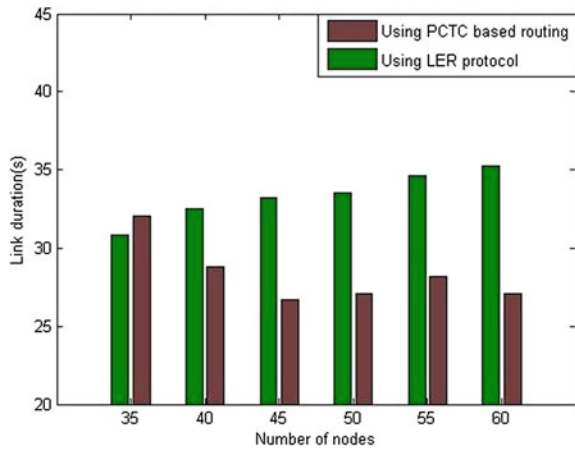


Fig. 6 Comparison of average hop count and route longevity

Fig. 7 Comparison of link duration



improvement over DSR, as shown in Fig. 6b, avoiding the problem of unsuccessful transmission due to link breakage.

In [14], routing based on prediction-based cognitive topology control (PCTC) was presented. The proposed LER protocol, over the same simulation scenario [14], shows improvement over PCTC-based routing in terms of link duration(s) is shown in Fig. 7. In LER, the link expiration calculation depends on GPS provided information, there may some variations in LETs but will not hamper the overall performance of the network.

5 Conclusion

To improve routing in wireless ad hoc networks, we proposed a link Expiration-Based Routing (LER) protocol for optimized route estimation with minimized control overhead. The protocol initializes with LET calculation during neighbor discover at periodic intervals. LET of a link is the time for which the link is available to communicate based on the parameters like mobility, distance, etc. Using LET, we limit the flooding of control packets during route estimation, resulting in the stable active route generation. Simulation results shows that an average of 42.2 % of control overhead is reduced by LER over DSR and a maximum of 20 % increment in successful transmission in the network. Due to selective route estimation, there is a slight increase in average hop count, however, a longer link/route longevity is achieved. The LER protocol acquires the knowledge of link status, thereby improves the routing and overall network performance in the network.

References

1. Breed, G.: Wireless ad hoc networks: basic concepts. *High Freq. Electron.* **1**, 44–47 (2007)
2. Royer, E., Toh, C.-K.: A Review of current outing Protocols for Ad hoc Mobile Wireless Networks. *IEEE Personal Communications*, April (1999)
3. Perkins Charles, E., Bhagwat, P.: Highly dynamic destination-sequenced distance-vector routing (DSDV) for mobile computers. *ACM SIGCOMM Comput. Commun. Rev.* **24**(4), 234–244 (1994)
4. Perkins, C.E., Royer, E.M.: Ad-hoc on-demand distance vector routing. In: *Proceedings of Mobile Computing Systems and Applications*, IEEE, pp. 90–100, (1999)
5. Johnson, D.B.: The dynamic source routing protocol for mobile ad hoc networks. *draft-ietf-manet-dsr-09. txt* (2003)
6. Su, W., Lee, S.-J., Gerla, M.: Mobility prediction in wireless networks. In: *Proceedings of MILCOM 2000, 21st Century Military Communications Conference Proceedings*. vol. 1. IEEE, (2000)
7. McDonald, A.B., Znati, T. A path availability model for wireless ad-hoc networks. In: *Proceedings of Wireless Communications and Networking Conference*, IEEE, (1999)
8. Carofiglio, G., Chiasserini, C.F., Garetto, M., Leonardi, E.: Route stability in MANETs under the random direction mobility model. *IEEE Trans. Mob. Comput.* **8**(9), 1167–1179 (2009)
9. Jiang, S., He, D., Rao, J.: A prediction-based link availability estimation for routing metrics in MANETs. *IEEE/ACM Trans. Netw.* **13**(6), 1302–1312 (2005)
10. Agarwal, S., Ahuja, A., Singh, J.P., Shorey, R.: Route-lifetime assessment based routing (RABR) protocol for mobile ad-hoc networks. In: *IEEE International Conference on Communications*, 2000, vol. 3, pp. 1697–1701. IEEE, (2000)
11. Gerharz, M., de Waal, C., Frank, M., Martini, P.: Link stability in mobile wireless ad hoc networks. In: *Proceedings of 27th Annual IEEE Conference on Local Computer Networks, LCN 2002*, pp. 30–39, IEEE, (2002)
12. Alsharabi, N., Y ping Lin, Rajeh, W.: Avoid link breakage in on-demand ad-hoc network using packet's received time prediction. In: *Proceedings of the 19th European Conference on Modelling and Simulation* (2005)

13. Han, Q., Bai, Y., Gong, L., Wu, W.: Link availability prediction-based reliable routing for mobile ad hoc networks. *IET Commun.* **5**(16), 2291–2300 (2011)
14. Guan Quansheng, F., Richard, Y., Jiang, S., Wei, G.: Prediction-based topology control and routing in cognitive radio mobile ad hoc networks. *IEEE Trans. Veh. Technol.* **59**(9), 4443–4452 (2010)

Analysis of Dual Beam Pentagonal Patch Antenna

R. Anand, Jesmi Alphonsa Jose, Anju M. Kaimal
and Sreedevi Menon

Abstract In this paper, we present a high gain, dual beam pentagonal patch antenna. The pentagonal geometry is inspired from a rectangle patch antenna and a triangle patch antenna. The architecture of the antenna resembles an irregular pentagon comprised a triangle placed on top of a rectangle. FEM is used for the analysis of the antenna design. The pentagonal antenna gave good reflection and radiation characteristics with a 2:1 VSWR bandwidth of 8.1 % at resonant frequency. As we combined the geometry of a rectangle and a triangle for the pentagonal design, the single pentagon patch antenna radiated two directional beams with a peak gain of 6.1 dBi at resonant frequency. Even though the pentagon patch had slightly less gain than the rectangular patch, it had an additional advantage since it radiated in two directions. The proposed pentagonal antenna architecture can be used in applications where there is a need to produce a dual beam without the need of any additional circuits for switching.

Keywords Pentagonal patch • Dual beam • Rectangular patch antenna • Triangular patch antenna

R. Anand (✉) · J.A. Jose · A.M. Kaimal
Amrita Center for Wireless Networks and Applications,
Amrita Vishwa Vidyapeetham, Kollam, Kerala, India
e-mail: anandr@am.amrita.edu

J.A. Jose
e-mail: jesmiao@gmail.com

A.M. Kaimal
e-mail: anjumk@am.amrita.edu

S. Menon
Department of Electronics and Communication,
Amrita Vishwa Vidyapeetham, Kollam, Kerala, India
e-mail: sreedevikmenon@am.amrita.edu

1 Introduction

Patch antenna is gaining much attention due to its low cost and ease in fabrication. The geometry of the radiating element controls the characteristics of the patch antenna. Various geometries of the radiating element such as rectangle, circle, and triangle, are considered in previous studies [1–3]. The patch antenna designed for any one of such geometry produces a single directional beam. As there is a huge demand for dual band operation, patch antenna with dual beam is highly desired. Works related to dual beam in patch antenna make use of dual feed. Hexagonal-shaped patch antenna with dual feed is proposed in [4]. Even though the hexagonal patch antenna produces dual beam, the procedure adopted is complex. To the best of our knowledge, a simple geometry for the patch antenna with dual beam using single feed has not yet proposed.

The pentagonal-shaped radiating element for patch antenna design is not explored by many works. In [5, 6], authors have used pentagonal shape for the radiating patch and ground plane in the design of coplanar antennas. In this work, we aim to design a dual beam pentagonal patch antenna. The geometry of the radiating element considered is pentagonal shape, which resembles triangle placed on top of a rectangle. The shape of the proposed pentagonal patch antenna is motivated from a rectangular patch antenna and a triangular patch antenna. The characteristics of the pentagonal patch antenna are analyzed. The proposed geometry is simple and it does not involve a complex design and it can produce dual beam without any additional feed.

2 Antenna Design

The pentagonal shape of the patch antenna is motivated from a rectangular patch antenna and a triangular patch antenna. So, we used the characteristics of an inset feed rectangular patch antenna and an inset feed triangular patch antenna, with resonant frequency at 2.45 GHz, as a reference. The dimensions of the two reference antennas are taken according to design equations [1]. The dimensions are based on design requirement like resonant frequency, operation bandwidth, and radiation pattern.

The transmission line model is used for calculation of the dimension of the rectangular patch antenna [1]. For the given resonant frequency f_r , the width of the rectangular patch W is given as

$$W = \frac{C}{2f_r \sqrt{\frac{\epsilon_r + 1}{2}}}, \quad (1)$$

where C is the velocity of light and ε_r is the relative permittivity of the substrate. The effective dielectric constant of the substrate ε_{eff} is expressed as

$$\varepsilon_{\text{eff}} = \left(\frac{\varepsilon_r + 1}{2} \right) + \frac{\varepsilon_r - 1}{2} \left(1 + \frac{12h}{W} \right)^{-0.5}. \quad (2)$$

The equation for effective length of the patch L_{eff} is

$$L_{\text{eff}} = \frac{C}{2f_r \sqrt{\varepsilon_{\text{eff}}}}. \quad (3)$$

The normalized extension of the patch (ΔL) is

$$\Delta L = 0.412 h \left[\frac{(\varepsilon_{\text{eff}} + 0.3)}{(\varepsilon_{\text{eff}} + 0.258)} \frac{\left(\frac{W}{h} + 0.264 \right)}{\left(\frac{W}{h} + 0.8 \right)} \right]. \quad (4)$$

The actual length of the rectangular patch antenna (L) is given as

$$L = L_{\text{eff}} - 2\Delta L. \quad (5)$$

The length of the rectangular patch controls the resonant frequency. The width of the rectangular patch controls the input impedance and radiation pattern [7]. The input impedance at the corner of the patch R_r is given by

$$R_r = 90 \left(\frac{\varepsilon_r^2}{\varepsilon_r - 1} \right) \left(\frac{L}{W} \right)^2. \quad (6)$$

The input impedance at any point y_0 of the rectangular patch R_{in} is given as

$$R_{\text{in}}(y = y_0) = R_r \cos^2 \left(\frac{\pi y_0}{L} \right). \quad (7)$$

The side view of the patch antenna is shown in Fig. 1a. The rectangular patch antenna was designed for the resonant frequency of 2.45 GHz. The substrate used for the rectangular patch antenna design is Teconic TLC with relative permittivity $\varepsilon_r = 3.2$ and a low dielectric loss tangent of 0.003, having a thickness of 1.6 mm. Using the above design equations, the width and length of the rectangular patch were obtained as $W = 42.42$ mm and $L = 32.37$ mm and the geometry of the patch was as shown in Fig. 1b. The rectangular patch antenna was fed by a 100Ω inset fed micro-strip transmission line. Using impedance equation, the antenna is fed at $(L/3, W/2)$ in order to achieve perfect impedance match.

The triangular geometry was constructed having width of the rectangular patch antenna (W) as the base of the triangle ($W1$) and the height of the triangle (H).

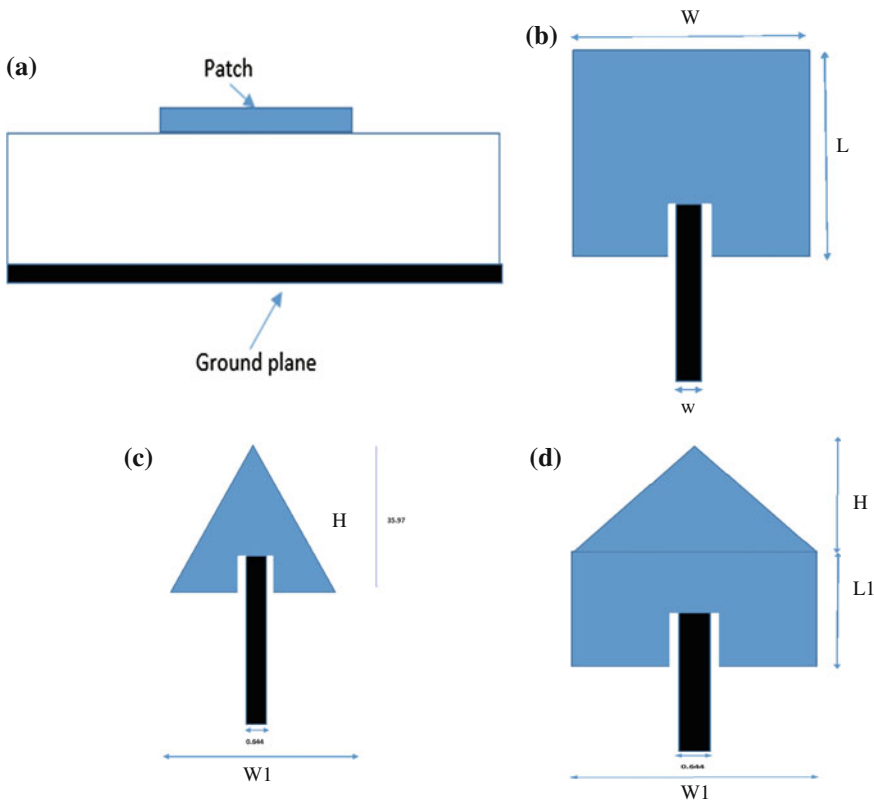


Fig. 1 **a** Side view of the patch antenna. **b** Dimensions of the reference patch antenna. **c** Dimensions of the reference triangle antenna. **d** Dimensions of the pentagonal patch antenna

The triangular patch antenna was fed by a $100\ \Omega$ transmission line. Using trial and error method, the antenna was fed at $(0.29 \times L, W/2)$ to achieve perfect impedance match. With the aid of several simulation results, the length of the base (W_1) and height of the triangle (H) were increased from 32.37 to 35.97 mm to make the triangular patch resonate at 2.45 GHz. The geometry of the triangular patch is shown in Fig. 1c.

For the construction of the pentagonal geometry, a rectangle with equal length (L) and width (W) of 35.97 mm and a triangle with equal base (W) and height (H) of 35.97 mm are considered. The pentagonal patch antenna is created using the rectangle and triangle geometry as shown in Fig. 1d. The pentagonal patch antenna was inset fed by a $100\ \Omega$ micro-strip transmission line at $(0.29 \times L, W/2)$ for perfect impedance match. In Table 1, the dimensions used in the paper are summarized.

Table 1 Dimensions used for the study

Variable	Dimensions (mm)
W	42.42
L	32.37
H	35.97
W_1	35.97
L_1	35.97
W	0.644

3 Reflections and Radiation Characteristics

In this session, we discuss the characteristics of the rectangular patch antenna, the triangular patch antenna, and the pentagonal patch antenna. The characteristics of the antennas include Return Loss (RL), Voltage Standing Wave Ratio (VSWR), input impedance, gain, and radiation pattern.

The RL and VSWR of the rectangular patch antenna, the triangular patch antenna, and the pentagonal patch antenna are plotted in Figs. 2 and 3, respectively. For the rectangular patch antenna, the resonant frequency occurs at 2.45 GHz with 2:1 VSWR bandwidth of 12.3 % of resonant frequency. In the triangular patch antenna, the resonant frequency is found to be 2.41 GHz with 2:1 VSWR bandwidth of 4.6 % of resonant frequency. For the pentagonal patch antenna, the resonant frequency is 2.49 GHz with 2:1 VSWR bandwidth of 8.1 % of resonant frequency in operational bandwidth (between 2.48 and 2.5 GHz).

Figure 4 shows the gain of the rectangular patch antenna, the triangular patch antenna, and the pentagonal patch antenna. Both the rectangular patch antenna and

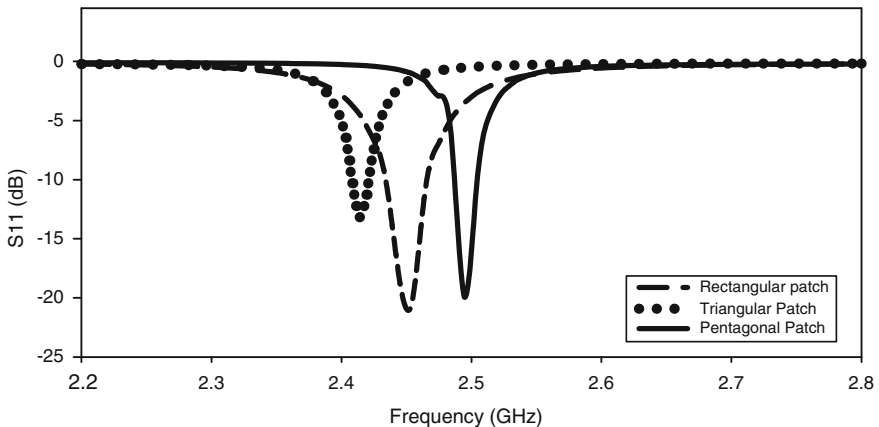


Fig. 2 Return loss characteristics of the antennas. The return loss of the rectangular patch antenna, the triangular patch antenna, and the pentagonal patch antenna are plotted in *dashed line*, *dotted line* and *continuous line*, respectively

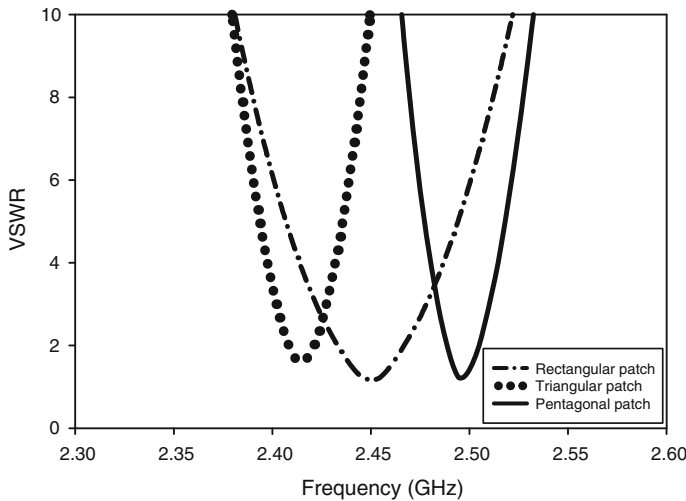


Fig. 3 VSWR of the three antennas. The VSWR of the rectangular patch antenna, the triangular patch antenna and the pentagonal patch antenna are plotted in *dashed line*, *dotted line* and *continuous line*, respectively

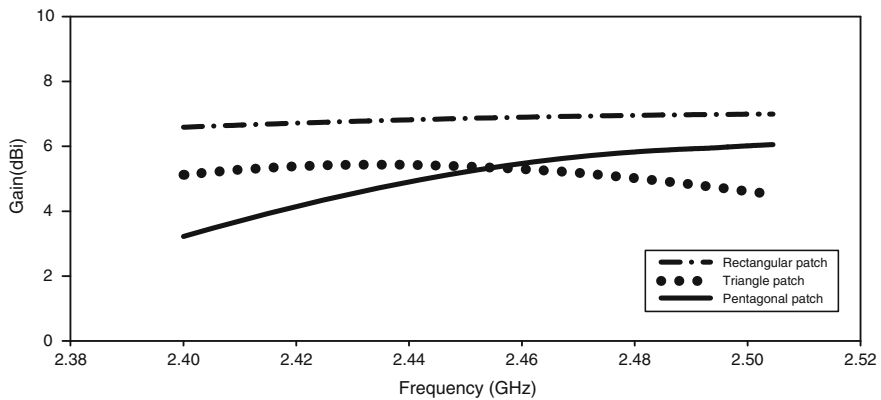


Fig. 4 Variation of gain with frequency plot of the three antennas. The gain of the rectangular patch antenna, the triangular patch antenna, and the pentagonal patch antenna are plotted in *dashed line*, *dotted line*, and *continuous line*, respectively

the triangular patch antenna produce a single beam, with peak gain of 5.8 and 5.3 dBi, respectively. For the pentagonal patch antenna, the peak gain is found to be 6.1 dBi. In the entire operating bandwidth, the gain is better than 5.8 dBi.

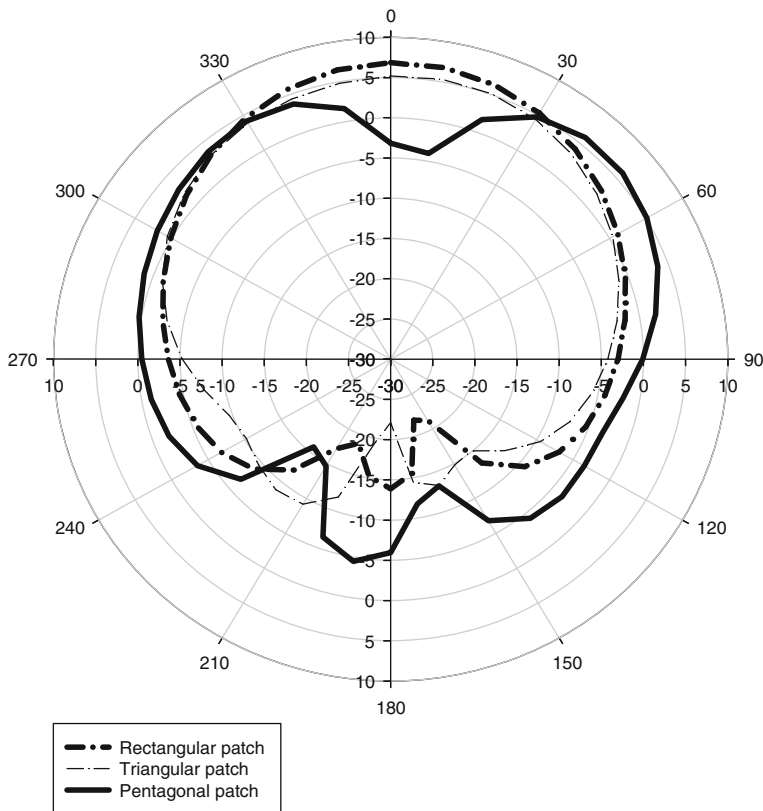


Fig. 5 Azimuth plot of the three antennas. The radiation plot of the rectangular patch antenna, the triangular patch antenna, and the pentagonal patch antenna are plotted in *dashed line*, *dotted line*, and *continuous line*, respectively

The radiation characteristics of all the three patch antenna are studied in Figs. 5 and 6 using two-dimensional azimuth plane plot(x-y plane) and elevation plane plot (y-z plane), respectively. For the rectangular patch antenna, the Half Power Beam Width (HPBW) is found to be 80° in azimuth plane and 70° in elevation plane. For the triangular patch antenna, the HPBW is found to be 90° in azimuth plane and 70° in elevation plane. From the radiation plots of the two antennas, it can be seen that the pattern of the rectangular and the triangular patch antenna is directional with single beam pointing towards the z axis. On the other hand, radiation plots for a pentagonal patch antenna shows dual beam radiation. The HPBW is found to be $40^\circ/20^\circ$ (for the two directional beams) in azimuth plane and 80° in elevation plane.

The reflection and radiation characteristics of the rectangular patch antenna, the triangular patch antenna, and the pentagonal patch antenna are summarized in

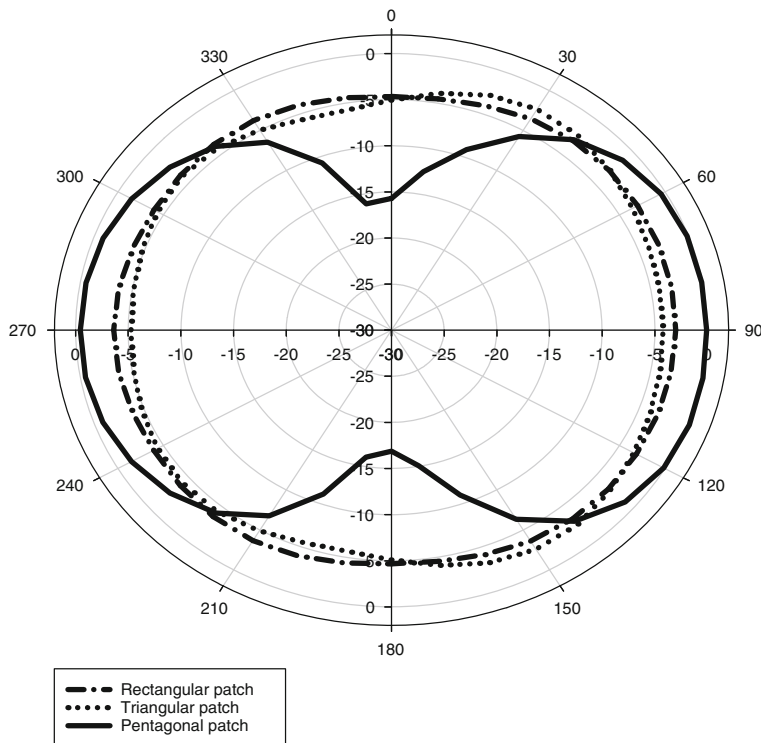


Fig. 6 Elevation plot of the three antennas. The radiation plot of the rectangular patch antenna, the triangular patch antenna, and the pentagonal patch antenna are plotted in *dashed line*, *dotted line*, and *continuous line*, respectively

Table 2 Comparison between rectangular, triangular, and pentagonal patch antenna

S. no.	Patch antenna type	Resonant frequency (GHz)	Bandwidth (MHz)	Peak gain (dBi)	HPBW	No. of beams
1	Rectangle	2.45	30	6.9	80°	1
2	Triangle	2.41	20	5.3	90°	1
3	Pentagon	2.49	20	6.1	40°/20°	2

Table 2. Even though the pentagon patch has slightly less gain than the rectangular patch, it had an additional advantage since it radiated in two directions. The proposed pentagonal antenna architecture can be used in applications where there is a need to produce a dual beam without the need of any additional circuits for switching.

4 Conclusion

In this work, pentagonal patch antenna with good reflection and radiation characteristics is proposed. In comparison with the rectangle and the triangle patch antennas, the pentagonal patch antenna produces dual beam with a single feed. The proposed dual beam pentagonal antennas can be applied in areas such as object detection, RF ablation, MIMO, among others. Future work involves gain enhancement in pentagonal patch antenna using antenna array [8].

Acknowledgments We would like to express our immense gratitude to our beloved Chancellor Sri. Mata Amritanandamayi Devi (AMMA) for providing the motivation and inspiration to do this research work. This project is partly funded by a grant from Information Technology Research Academy (ITRA), Department of Electronics and Information technology (DeitY), Govt. of India. The authors would like to thank Dr. Maneesha V. Ramesh, Director, Amrita Center for Wireless Networks and Applications (Amrita WNA) and Mr. Sethuraman Rao, Professor, Amrita WNA and colleagues who have willingly helped me with their abilities

References

1. Balanis, C.A.: *Antenna Theory: Analysis and Design*. Wiley, New York (1997)
2. Garg, R., Bhartia, P., Bahl, I., Ittipiboon, A.: *Microstrip Antenna Design Handbook*. Artech House, Boston (2001)
3. Banerjee, S., Saha, S., Sanyal, S.: Dual band and tri band pentagonal microstrip antenna for wireless communication systems. *IJESE* **1**(5), (2013)
4. Basu, S., Srivastava, A., Goswamy, A.: Dual frequency hexagonal microstrip patch antenna. *IJSRP* **3**(11), (2013)
5. Jesmi, J., Anand, R., Sreedevi, K.: Study of coplanar pentagonal antenna. In: 10th International Conference on Microwave, Antenna, Propagation and Remote Sensing, pp. 303–306, ICMARS Proceedings (2014)
6. Jesmi, J., Anand, R., Sreedevi, K.: A coplanar pentagonal antenna for wireless applications. In: 2nd International Conference on Signal Processing and Integrated Networks (SPIN-2015), pp. 303–306, IEEE Proceedings (2015)
7. Antenna Theory Website: <http://www.antenna-theory.com>
8. Dharsandiya, F., Parmar, I.: Optimization of antenna design for gain enhancement using array. *IJARCSSE* **4**(1), (2014)

Combination of CDLEP and Gabor Features for CBIR

L. Koteswara Rao, D. Venkata Rao and Pinapatruni Rohini

Abstract The retrieval of an image can be done by extracting the local texture information. The procedure involves the calculation of patterns of texture present in an image. Local binary patterns became the first of its kind in which the gray value of a pixel in the middle position is compared with all of its surrounding pixels. The patterns of the texture obtained are converted into a histogram and the same becomes a feature vector in the process of comparison and subsequent retrieval process. One among several modifications to LBP was directional extrema patterns, which employs a technique of deriving the data by comparison of the pixel at the middle with two immediate pixels in four possible directions. To increase the performance further, an integrated approach is proposed for a CBIR system in which CDLEP is integrated with Gabor filters. The precision and recall values are found to decide the performance of the proposed framework.

Keywords Color · Gabor filters · LBP · DLEP · Histogram · Image retrieval · Precision · Recall

1 Introduction

Nowadays as a result of substantial growth in the Internet and other digital technologies, large number of images are produced and shared across the world. However, it is difficult to utilize the image data without a proper management

L. Koteswara Rao (✉)

Research Scholar of JNTUH, Asst.Prof. at FST, IFHE, Hyderabad, India
e-mail: kots.lkr@gmail.com

D. Venkata Rao

Narasarao Pet Institute of Technology, Narasaraopet, Guntur, India
e-mail: dv2002in@yahoo.co.in

P. Rohini

Department of CSE, Faculty of Science and Technology, IFHE, Hyderabad, India
e-mail: rohini10@gmail.com

system to index and retrieve the same. Earlier, the images used to be named as per the interpretation of the person. This method became inefficient and complex for large databases. To address these issues, a method called content-based image retrieval was introduced. It is based on the extraction of inherent content present in an image. A comparison is made between the image from the dataset and the query image to find the level of similarity based on which a ranking is done. The performance is measured in terms of precision and recall. In general, the performance of any CBIR system depends on the efficient extraction of features like color, texture, shape, etc., in order to retrieve the images [1–3].

Texture is one among the other features that gives more information about the content of any image. It refers to the innate properties of the surface in an object and the relationship to the surrounding environment. Researchers have proposed various approaches that are based on structural and statistical methods. In [4], use of texture feature for classification of images was discussed. Arivazhagan et al. [5] proposed texture classification using wavelet transform. In [6] texture classification and segmentation was proposed using wavelet packet frames and Gaussian mixture model. Use of Gabor wavelets in texture classification for rotation invariant features was given by [7].

Gabor filters have been popular in the field of image processing and texture analysis [8] for many years. It is a linear band-pass filter that is similar and close to the human visual system. It provides the spatial frequency information.

1.1 Contribution

The existing directional local extrema pattern (DLEP) obtains the edge information based on local extrema in 0° , 45° , 90° , and 135° directions of an image. In this paper, we propose a combination of features such as color DLEP and Gabor filters to improve the performance when compared to the directional local extrema pattern. The organization of this paper is as follows. Section 2 gives a review of various types of local patterns. Section 3 explains Gabor feature. Section 4 covers the proposed work for retrieval system. Section 5 contains the results. The conclusions are given in Sect. 6.

1.2 Related Work

A method based on local binary pattern was introduced by Ojala et al. [9], the idea of LBP was extended to face recognition and other applications in [10]. However, LBP has the drawback of rotational invariance in classifying the texture in an image. Local derivative pattern by considering the nth order of local binary Pattern was proposed by Zhang et al. [11]. Murala et al. [12] proposed directional local extrema pattern as a feature vector for texture analysis of an image. An improvement to DLEP was proposed by Rao et al. [13, 14]. The DLEP is different from

existing local binary patterns and other variations mainly in terms of directional edge information present in an image.

2 Local Patterns and Variations

2.1 Local Binary Pattern (LBP)

Local binary pattern was introduced by Ojala [9]. In this method, the gray value of the center pixel is taken as threshold and the difference between center pixel and its neighbors is taken into account based on which either a binary 1 or 0 is assigned. The process is followed until all the pixels surrounding the center pixel are covered.

$$\text{LBP}_{P,R} = \sum_{p=0}^{P-1} y(z_p - z_c) 2^p, y(x) = \begin{cases} 1, & x > 0 \\ 0, & x \leq 0 \end{cases}$$

, where z_c represents the gray value of centre pixel and z_p represents the gray value of P equally spaced pixels on circumference of the circle with radius R .

2.2 Local Directional Pattern (LDP)

The concept of local directional pattern [13] is based on LBP, which uses the edge response of neighborhood pixels to encode the texture content of an image. It assigns an eight-bit binary code to each pixel of an input image.

A binary value of 1 or 0 is assigned based on the occurrence of an edge.

$$\text{LDP}_n = \sum_{i=1}^8 f_i(m_i - m_k) * 2^i, f_i(x) = \begin{cases} 1, & x \geq 0 \\ 0, & x < 0 \end{cases}$$

2.3 Directional Local Extrema Patterns (DLEP)

The idea of local binary pattern was used by Subrahmanyam et al. [12] to create a new feature vector called DLEP for content-based image retrieval. In this method, the values of two immediate pixels in a particular direction are compared with the center pixel to assign either 0 or 1. In other words, it derives the spatial information of the texture using the local extrema of center gray pixel g_c . The extrema values in four directions are computed by taking the difference in intensity values of the centre pixel and all of its neighbors using the equations specified below.

The calculation is as shown below.

$$P'(n_i) = P(n_c) - P(n_i); \quad i = 1, 2, \dots, 8$$

The local extremes are based on the equations given below.

$$P_\alpha(nc) = S_3(P'(n_i) * P'(n_{j+4})); j = (1 + \alpha/45) \\ \forall \alpha = 0^\circ, 45^\circ, 90^\circ, 135^\circ$$

$$S_3(P'(n_j), P'(n_{j+4})) = \begin{cases} 1 & P'(n_j) * P'(n_{j+4}) \geq 0 \\ 0 & \text{else} \end{cases}$$

The DLEP is computed as ($\alpha^\circ = 0^\circ, 45^\circ, 90^\circ$ and 135°) follows:

$$\text{DLEP}(P(n_c)) = \{\hat{P}_\alpha(n_c); \hat{P}_\alpha(n_i); P_\alpha(n_z); \dots; \hat{P}_\alpha(n_8)\}$$

The details of DLEP can be seen in Fig. 1. In the next stage, the image to be searched is converted into DLEP patterns containing the values starting from 0 to 511.

After calculation of DLEP, the image is represented by constructing a histogram based on the equation specified below.

$$H_{\text{DLEP}\alpha}(i) = \sum_{j=1}^{A_1} \sum_{k=1}^{A_2} f_2(\text{DLEP}(j, k) | \alpha, \ell); \\ \ell \in [0, 511]$$

, where the size of input image is $A_1 \cdot A_2$. The procedure for calculation of DLEP for center pixel marked in violet color is presented in Fig. 1. The directions are evaluated using the difference between the center pixel and its neighbors.

As an example, the DLEP in 90° direction for the pixel at the middle position marked in violet color is shown in Fig. 2. For the center pixel value 25, it can be noticed that two neighboring pixels are less in intensity values. Therefore, this pattern is represented as 1. In the same way the rest of the bits of DLEP pattern are calculated and the result is 111110110. Similarly, the DLEP's are computed for $0^\circ, 45^\circ$, and 135° directions. The improved DLEP is given in [15].

28	13	93	11	50
31	41	24	38	51
43	22	25	83	61
55	14	18	16	72
32	28	63	78	33

	$0_{(25)}$	$1_{(83)}$	$2_{(16)}$	$3_{(18)}$	$4_{(14)}$	$5_{(22)}$	$6_{(41)}$	$7_{(24)}$	$8_{(38)}$	DLEP
P(0°)	0	1	0	1	0	1	1	1	0	174
Q(45°)	0	0	1	1	1	1	1	1	0	126
R(90°)	1	1	1	1	1	0	1	1	0	502
S(135°)	0	1	1	1	1	0	1	0	1	245

Fig. 1 Illustration of DLEP for 3×3 pattern

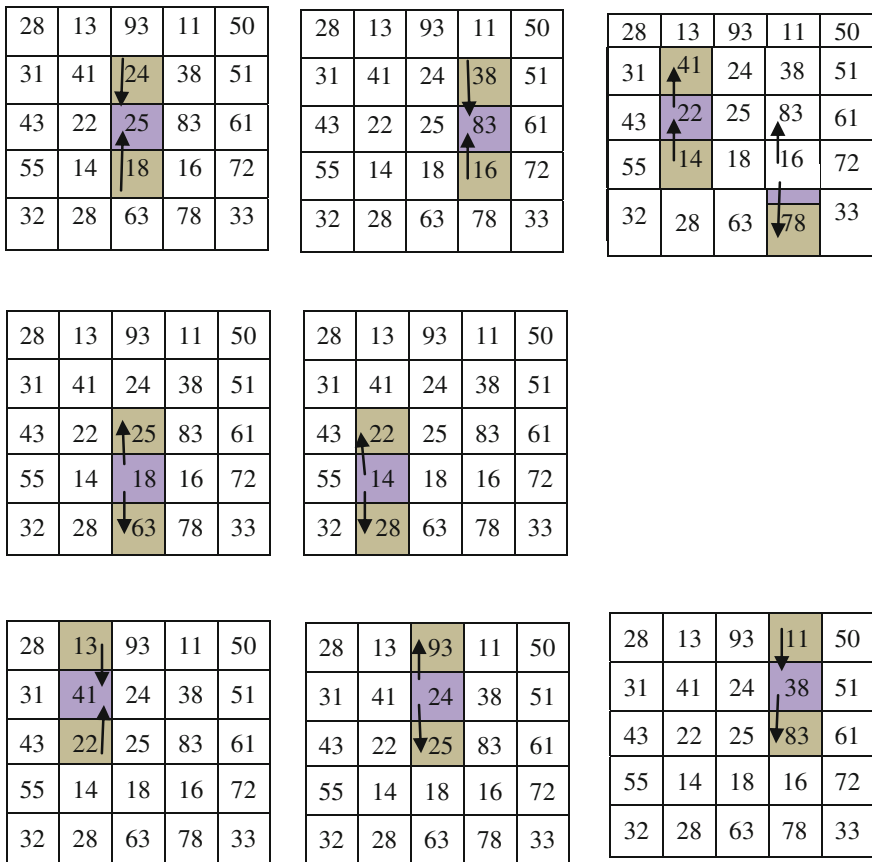


Fig. 2 Example to compute DLEP in 90° direction (110011110)

3 Gabor Feature

The Gabor filter is found to be efficient for texture representation and discrimination. The representation of 2-D Gabor filter is as specified below.

$$\psi_{f,\theta}(x, y) = \exp \left[-\frac{1}{2} \left\{ \frac{x^2 \theta_n}{\sigma_x^2} + \frac{y^2 \theta_n}{\sigma_y^2} \right\} \right] \exp(2\pi f x \theta_n)$$

Here, f is the central frequency of sinusoidal plane and θ is the orientation of x y plane.

$$\begin{bmatrix} x\theta_n \\ y\theta_n \end{bmatrix} = \begin{bmatrix} \sin \theta_n & \cos \theta_n \\ -\cos \theta_n & \sin \theta_n \end{bmatrix} \begin{bmatrix} x \\ y \end{bmatrix} (n-1)$$

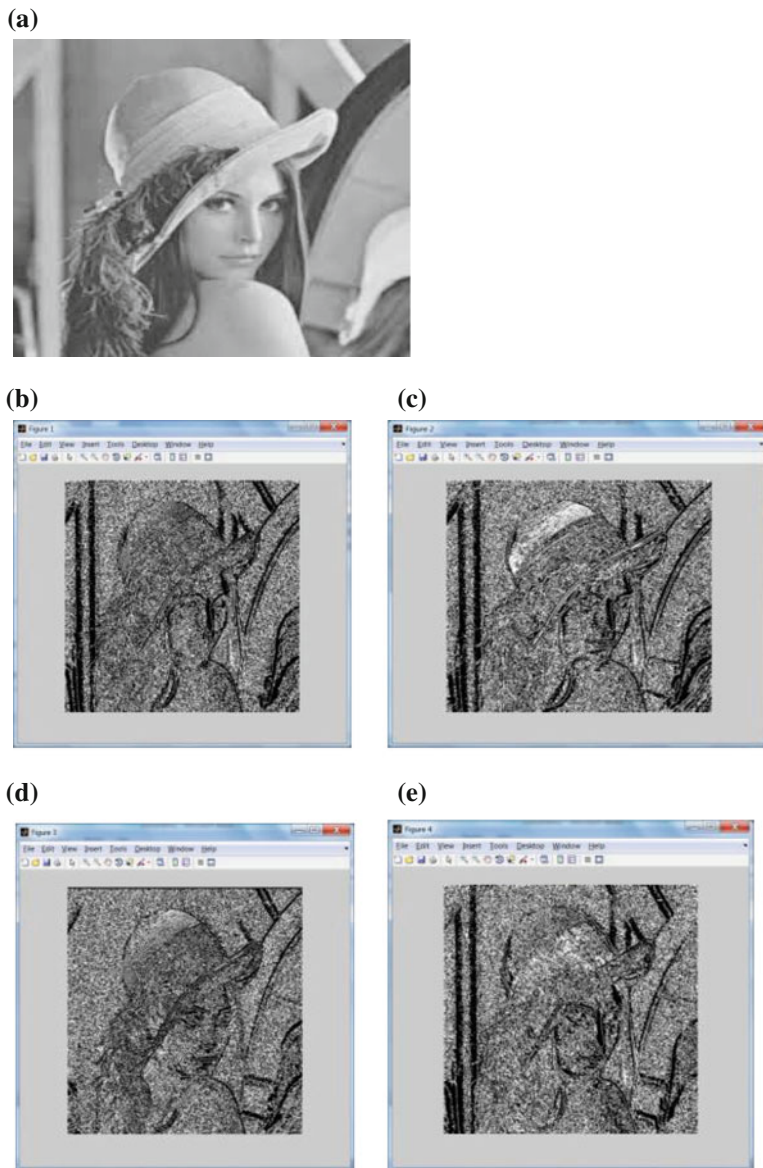


Fig. 3 Example of DLEP maps; **a** Sample image **b** 0° **c** 45° **d** 90° **e** 135°

θ_n is the rotation of xy plane by θ_n angle results Gabor filter at the orientation θ_n .

$$\text{angle}\theta_n = \frac{\pi}{p}$$

, where $n = 1, 2, \dots, p$, $p \in \mathbb{N}$ and p is the orientation.

4 Proposed Gabor CDLEP System

See Fig. 4.

4.1 Proposed Algorithm

1. Compute the color moments for the given image and then convert RGB image into grayscale image.
2. Use Gabor filter to get the spatial information about the image .
3. Obtain the local extrema in 0° , 45° , 90° , and 135° directions.
4. Compute the CDLEP patterns in four directions mentioned in step 2.
5. Get a histogram for the CDLEP patterns obtained in step 4 and concatenate to get the texture feature vector.
6. Combine these two features to get a feature vector that can be used in image retrieval.

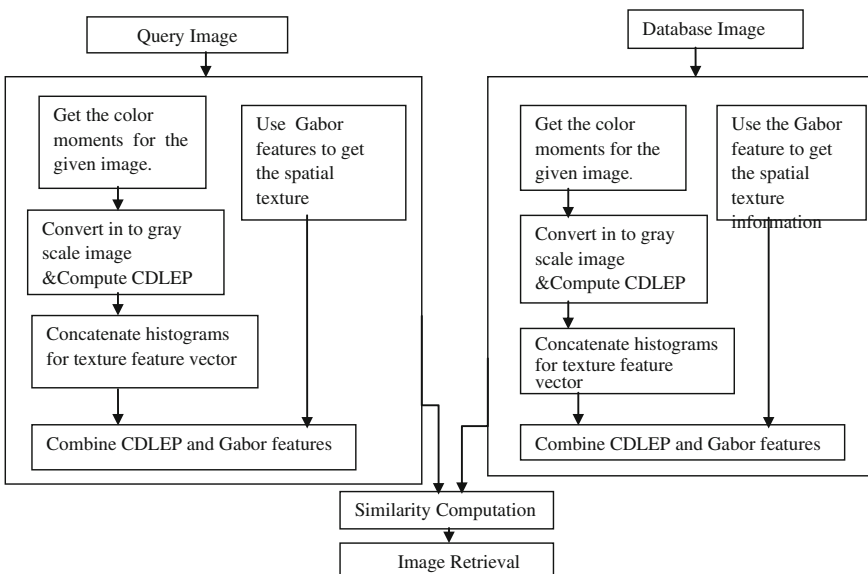


Fig. 4 Proposed CDLEP+Gabor for content-based image retrieval

4.2 Query Matching

Once the texture feature is extracted, the feature vector for query image is done. In the same manner, feature vectors for all images in the database are computed. To select the similar image to the query image, the distance between query image and database images is calculated using standard distance measuring metrics.

5 Experimental Results

Performance of the Gabor CDLEP is evaluated on standard corel-1 k database [16]. The precision (P) and recall (R) values are computed as per the relationship mentioned here under.

$$P = \frac{\text{No. of relevant images retrieved from the data base}}{\text{No. of images retrieved}}$$

$$R = \frac{\text{No. of relevant images retrieved from the data base}}{\text{No. of relevant images in the database}}$$

The top ten results for different categories of the database are shown in Table 1. (The comparisons in terms of average precision and average recall are given in Figs. 5 and 6) respectively.

Table 1 Comparison of precision and recall values for DLEP and CDLEP

Category	Existing DLEP	CDLEP +Gabor feature	Category	DLEP	CDLEP +Gabor feature
Africans	69.3	80	Africans	39.7	41
Beach	60.5	80	Beach	37.3	39
Building	72.0	100	Building	34.9	41
Buses	97.9	90	Buses	74.1	67
Dinosaur	98.5	100	Dinosaur	88.0	85
Elephant	55.9	80	Elephant	29.0	34
Flower	91.9	100	Flower	70.8	83
Horse	76.9	100	Horse	41.7	42
Mountain	42.7	60	Mountain	29.0	30
Food	82.0	90	Food	47.0	43
Average precision (%)	74.8	88.0	Average recall (%)	49.16	50.5

Fig. 5 Category-wise performance in terms of precision

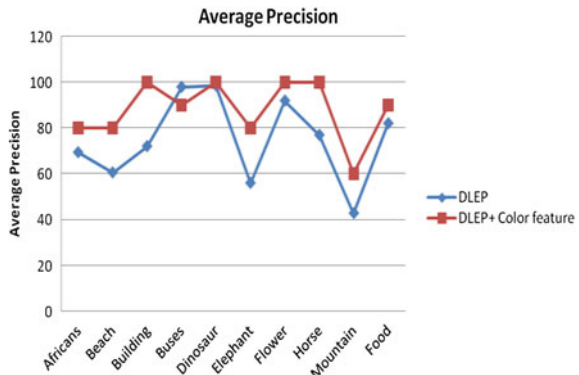
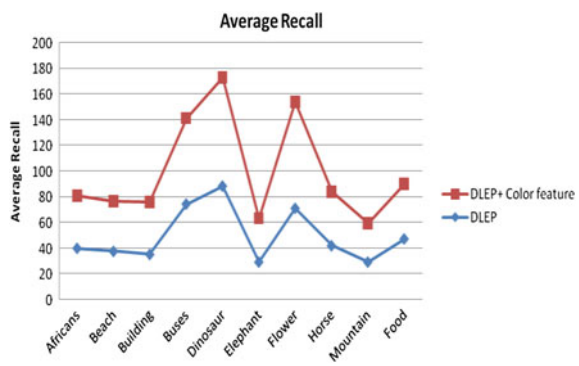


Fig. 6 Category-wise performance in terms of recall



6 Conclusion

It is proved that the proposed method outperforms the existing DLEP or CDLEP both in terms of precision and recall. The integrated approach involving Gabor filters and CDLEP extracts more spatial data present in the image when compared to LBP or any other related local pattern operators. This work can be further enhanced by calculating the magnitudes of the pixels in each direction.

References

1. Datta, R., Joshi, D., Li, J., Wang, J.: Image retrieval-ideas, influences and trends of the new age. *ACM Comput. Surv.* **40**(2), 1–60 (2008)
2. smulders, A.M., Worring, M., Santini, S., Gupta, A., Jain, R.: Content based image retrieval at the end of early years. *IEEE Trans. PAMI* **22**(12), 1349–1380 (2000)
3. Rui, Y., Huang, T.S., Chang, S.F.: Image retrieval: current techniques, promising directions & open issues. *J. Vis. Commun. Image Represent.* **10**(4), 39–62 (1999)

4. Haralick, R.M., Shanmugam, K., Dinstein, I.: Texture features for image classification. *IEEE Trans. Syst. Man Cybern.* **8**, 610–621 (1973)
5. Arivazhagan, S., Ganesan, L.: Texture classification using wavelet transform. *24(9)10*, 1513–1521 June 2003
6. Kim, Soo chang, Kang, Tae Jin: Texture classification and segmentation using wavelet packet frame and Gaussian mixture model **40**(4), 1207–1221 (2007). elsevier
7. Arivazhagan, S., Ganesan, L.: Texture classification using Gabor wavelets based rotation invariant features **27**(16), 1976–1982 (2006)
8. Yegnanarayana, Raghu P.: Segmentation of Gabor filtered textures using deterministic relaxation. *IEEE Trans. Image Process.* **5**(12), 1625–1636 (1996)
9. Ojala, T., Pietikainen, M., Harwood, D.: A comparative study of texture measures with classification based on feature distributions. *J Pattern Recogn.* **29**(1), 51–59 (1996)
10. Hadid, A., Ahonen, T., Pietikainen, M, Face analysis using local binary patterns. In: handbook of texture analysis, Imperial college press London, pp. 347–373 (2008)
11. Zhang, B., Gao, Y., Zhao, S., Liu, J.: Local derivative pattern versus local binary pattern: face recognition with higher-order local pattern descriptor. *IEEE Trans. Image Process.* **19**(2), 533–544 (2010)
12. Murala, S., Maheswari, R.P., Balasubramanian, R.: Directional local extrema pattern: a new descriptor for content based image retrieval (2012)
13. Kabir, J., Chae Kyung, H.: Local Directional Pattern for face recognition. IEEE Conference (2010)
14. Rao, L.K., Venkatrao, D.: A feature vector for cbir based on dlep and gabor feature *IJETT* **12** (2014)
15. Rao, L.K., Venkatrao, D., Rohini, P.: Improved DLEP as a feature vector for CBIR. IEEE Conference (2013)
16. <http://wang.ist.psu.edu/docs/related/>

Scheduling Real-Time Transactions Using Deferred Preemptive Technique

Sohel A. Bhura and A.S. Alvi

Abstract Preemptions are necessary to obtain feasible schedule for real-time processing. A nonpreemptive scheduler can block higher priority transactions affecting schedulability of the system. This paper presents deferred preemptive technique scheduling algorithm using EDF to overcome the drawbacks of fully preemptive scheduler that substantially reduces number of preemptions in comparison with fully preemptive scheduling.

Keywords EDF · Preemption · Real-time · Scheduling

1 Introduction

For uniprocessor scheduling, a preemptive earliest deadline first is a proven optimal scheduling algorithm, i.e., if a task set can be scheduled with a given algorithm then it can also be preemptively scheduled with EDF [1]. Nonpreemptive regions of low priority tasks due to blocking in nonpreemptive scheduler is a key disadvantage that significantly degrades schedulability for systems that have a wide range of task execution times and periods [2]. Blocking or priority inversion is undesirable

S.A. Bhura (✉)
Babasaheb Naik College of Engineering, Pusad, India
e-mail: sabhura@rediffmail.com

A.S. Alvi
Department of Computer Science & Engineering, Prof. Ram Meghe Institute of Technology & Research, Badnera, India
e-mail: abrar_alvi@rediffmail.com

in application domain requiring high throughput and faster responses. Thus considering the scenario for particular application, an appropriate scheduler that reduces number of context switches due preemptions is required.

Thus preemptions can induce a significant runtime overhead, increasing the total execution time of the preempted tasks due to cache and other pipeline-related costs. As EDF alone cannot reduce the number of preemptions, it cannot be considered as an optimal algorithm in such cases, as concluded in Sects. 5 and 6.

In addition, to know about how long a task is blocked and is a cause of priority inversion, we also need to focus on the resources these task hold as these may cause serious problems for safety—critical tasks requiring short interactive responses thereby affecting the schedulability of the system.

In this paper, we thus focus to resolve some of these issues to limit the number of preemptions caused and compute how far a transaction can be blocked by any lower priority transaction, thus requiring limited preemptive scheduling technique, i.e., deferred preemption is presented to reduce the preemption overhead.

2 Mathematical Model

The mathematical model considers following parameters for scheduling “ n ” (number of) tasks on a single processor [3–6].

The parameters R_i and D_i are used to identify the timing behavior, whether the tasks meet their deadline and B_i , q_i are used to identify the blocking of higher priority task because of lower priority and the possible largest nonpreemptive time interval experienced by each task.

3 Related Work

Many preemptive and nonpreemptive algorithms for scheduling real-time transactions exist. For nonpreemptive technique, any transactions once started, execution will complete even if higher priority transactions enter the system. In contrast, in preemptive scheduling if higher priority transaction arrives, currently executing transaction is suspended and later resumed if no higher priority transaction exists. Preemptive and nonpreemptive scheduling technique is widely studied in many of the existing literature [3, 4, 7, 8], for scheduling of sporadic tasks systems.

For preemptive scheduling, any sporadic task system is feasible if it satisfies the condition.

$$\sum_{i=1}^n \frac{C_i}{P_i} \leq 1. \quad (1)$$

Using (1) it seems that any scheduling algorithm is optimal if the above condition is satisfied as suggested in [1, 4], preemptive EDF is an optimal scheduling algorithm. Martel et al. in [7], in their work proved that EDF is not an optimal scheduling algorithm when considering nonpreemptive scheduling of sporadic task having deadlines same as their periods. Bartonga and Wu [9] in their work suggested limited Preemptive EDF in which, they suggest that if a task is divided into nonpreemptive chunks it can improve the performance without affecting the schedulability of the system. A recurring task model for uniprocessor was suggested by Baruah and Chakraborty [10] that shows how fully preemptive algorithms had large runtime overhead. As a result, although there is sufficient research work on real-time fixed priority based on limited preemptive techniques [11–18], further possibility to minimize number of preemptions needs to be addressed. Very recently, Lee and Shin [19] suggested mixed preemptive and nonpreemptive approach that denies preemption of transactions under certain assumptions.

4 EDF Using Deferred Preemptive Technique

In 1973 Liu and Layland [1] suggested the most popular real-time disk scheduling algorithm—earliest deadline first (EDF). EDF serves the transactions in the ascending order of their deadlines. Lower deadline transaction will be served first.

Real-time systems are characterized by their strict timing constraints, in our approach we analyzed that a nonpreemptive system can degrade the schedulability of the system due to priority inversion, while a preemptive scheduler introduces many unwanted preemptions causing high runtime overhead. In our approach, we considered deferred preemptive technique that identifies maximum blocking that a task can incur without violating the schedulability of the system. The algorithm proposed is given as below.

4.1 Algorithm

Step 1. Arrange the transactions in an increasing order of their deadlines.

[Set parameters tid, arrivaltime, aet, deadline, blocking tolerances (β) & largest non-preemptive time intervals(q) of each transaction]

Step 2. Select the transaction (TID current) with minimum release time and deadline.

Find the completion time (ct) of the selected transaction.

Step 3. [Repeat Steps 3 & 4 until there are no more transactions]

Select the transaction (TID next) with minimum release time and deadline.

Step 4. if(traversenext==0)

```
{
    if(arrivaltimenext<ct+qi)
        {
            if(deadlinenext>=deadline)
                {
                    i.e. no preemption
                    go to step 3
                }
            if(deadlinenext<deadline)
                {
                    i.e. preempt current TID
                    preempt=preempt+1;
                    isthereTID=1;
                }
        }
}
```

for preempted task

compute remaining time for preempted task

insert the preempted transaction again

go to step 3

```

    }
if(isthereTID==0)
{
```

i.e no preempting transaction

Serve the current transaction completely, set traverse=1

If (completiontime> deadline)

Set successful = false

Else Set successful = true} } }

4.2 Largest Nonpreemptive Time Interval

When higher priority task enters the system to avoid blocking due to priority inversion, we need to identify the largest nonpreemptive interval Q_i for high priority task T_i without affecting schedulability of the system.

That is the schedulability of any task set can be preserved if it satisfies (1), for avoiding can be maintained by computing the largest nonpreemptive time interval Q_i for every task T_i that, it can continue execution without being preempted.

This was proposed for fixed priorities by Buttazzo et al. [20], Sanjay and Marko [21], had suggested for EDF. The main basis is to avoid blocking and identify how far any task can be blocked. Accordingly blocking tolerance, for a task, can be calculated as:

$$\beta_i = \left\lfloor T_i \left(U(i) - \sum_{h:P_h \geq P_i} \frac{C_h}{T_h} \right) \right\rfloor. \quad (2)$$

Using (2), we compute maximum amount of blocking β_i for any task T_i where

U = Total utilization

T = Deadline of transaction,

P = Priority,

C = Average execution time of transaction

In order to obtain feasible solution, we compute largest nonpreemptive time interval Q_i for every transaction T_i is given by

$$Q_i = \min_{k:P_k > P_i} \{\beta_k + 1\}. \quad (3)$$

To obtain better results of Q_i , we proceed stating with highest priority transactions following the transactions with lower priority, as per the theorem stated below.

Lemma (using [22]) *The largest interval in Q_i preserving feasibility of transactions in T_i can be computed as*

$$Q_i = \min\{Q_{i-1}, \beta_{i-1} + 1\}. \quad (4)$$

where Q_1 is initially set to ∞ and β_1 is computed as deadline—execution time required for that task.

Consider the following task set (Table 2).

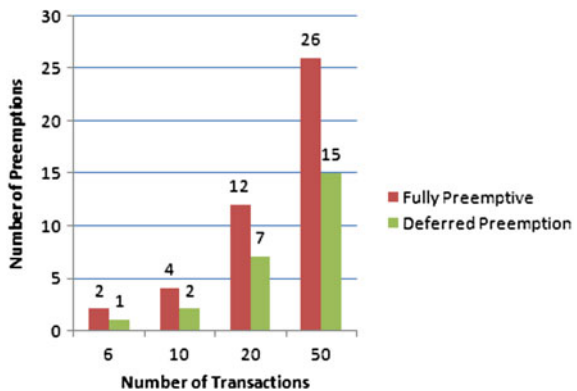
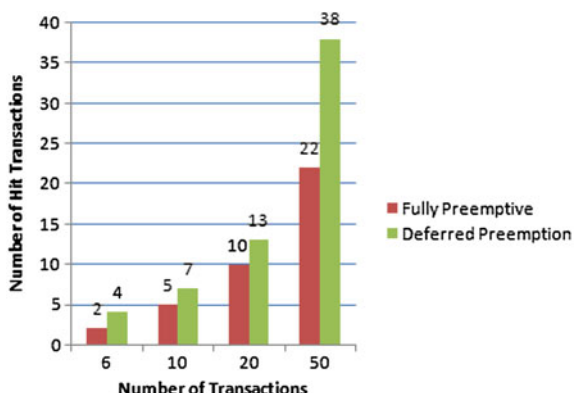
Using (2), (3), and (4), the values for β_i and Q_i are computed, results are shown in next section.

Table 1 Parameter calculation

Parameter	Description
T	A set of request $T = \{T_0, T_1, \dots\}$
N	Number of input requests
T_{id}	A real-time request
R_i	Release time of T_i
D_i	Deadline of T_i
AET	Average execution time of T_i
B_i	Blocking tolerance
Q_i	Longest nonpreemptive interval

Table 2 Sample transaction set

T_i	R_i	E_i	D_i
T_1	0	2	6
T_2	6	40	18
T_3	10	30	16
T_4	12	80	30
T_5	18	16	42
T_6	30	12	36

Fig. 1 Number of preemptions for different set of transactions**Fig. 2** Number of hit transactions

5 Performance Evaluation

In this section, we compared fully preemptive and deferred preemptive approach. Using values as indicated in Table 1 for random release time, execution time and deadline, the simulation results in Figs. 1 and 2 shows that our approach performs better than fully preemptive approach. We used number of preemptions and number of hit transactions as performance measures to evaluate the performance. The limited preemptive approach (deferred preemption) is more efficient as compared to fully preemptive approach yielding higher number of hit transactions as well as less number of preemptions. Following graphs shows this performance evaluation.

6 Conclusion

As discussed in the previous sections, preemptive scheduler can affect the schedulability of the system by blocking higher priority transactions while preemptive scheduling has unwanted preemptions as it is apparent from Fig. 1. We have evaluated the performance of fully preemptive and limited preemptive approach (deferred preemptive) and used number of preemptions and number of hit transactions as performance measures to evaluate the performance. From the scheduling results, it is concluded that limited preemptive approach gives better performance as compared to fully preemptive approaches yielding higher number of hit transactions as well as less number of preemptions.

References

1. Liu, C.L., Layland, J.W.: Scheduling algorithms for multiprogramming in a hard-real-time environment. *J. Assoc. Comput. Mach.* **20**(1), 46–61 (1973)
2. Baker, T.P.: Stack-based scheduling of real-time processes. *Real-Time Syst.: Int. J. Time-Crit. Comput.* **3** (1991)
3. Mok, A.K.: Fundamental design problems of distributed systems for the hard-real-time environment. Ph.D. thesis, Laboratory for Computer Science, Massachusetts Institute of Technology. Available as Technical Report No. MIT/LCS/TR-297 (1983)
4. Baruah, S., Mok, A.K., Rosier, L.E.: Preemptively scheduling hard-real-time sporadic tasks on one processor. In: Proceedings of the 11th Real-Time Systems Symposium. IEEE Computer Society Press, Orlando (1990)
5. Amdani, S.Y., Ali, M.S., Mundada, S.M.: Mathematical model for real time disk scheduling problem. in: Proceedings published in International Journal of Computer Applications® (IJCA) (2012)
6. Amdani, S.Y., Ali, M.S.: An overview of real-time disk scheduling algorithms. *Int. J. Emerg. Technol.* **2**(1), 126–130 (2011)
7. Jeffay, K., Stamat, D., Martel, C.: On non-preemptive scheduling of periodic and sporadic tasks. In: Proceedings of the 12th Real-Time Systems Symposium, IEEE Computer Society Press, San Antonio, Dec 1991

8. George, L., Rivierre, N., Spuri, M.: Preemptive and nonpreemptive real-time uniprocessor scheduling. Tech. Rep. RR—2966, INRIA: Institut National de Recherche en Informatique et en Automatique (1996)
9. Marinho, J., et al.: Limited pre-emptive global fixed task priority. In: IEEE 34th Real-Time Systems Symposium, pp. 182–191, Dec 2013
10. Baruah, S., Chakraborty, S.: Schedulability analysis of non-preemptive recurring real-time tasks. In: International Workshop on Parallel and Distributed Real-Time Systems (IPDPS), Rhodes, April 2006
11. Baruah, S.: The limited-preemption uniprocessor scheduling of sporadic task systems. In: Proceedings of the EuroMicro Conference on Real-Time Systems, IEEE Computer Society Press, Palma de Mallorca, July 2005
12. Wang, Y., Saksena, M.: Scheduling fixed-priority tasks with preemption threshold. In: Proceedings of the International Conference on Real-time Computing Systems and Applications, IEEE Computer Society (1999)
13. Regehr, J.: Scheduling tasks with mixed preemption relations for robustness to timing faults. In: Proceedings of the 23rd IEEE Real-Time Systems Symposium, pp. 315–326. IEEE Computer Society, Cancun, Dec 2002
14. Burns, A.: Preemptive priority based scheduling: An appropriate engineering approach. In: Son, S. (ed.) Advances in Real-Time Systems, pp. 225–248 (1994)
15. Gopalakrishnan, R., Parulkar, G.: Bringing real-time scheduling theory and practice closer for multimedia computing. In: Proceedings of ACM Sigmetrics Conference on Measurement and Modeling of Computer Systems, pp. 1–12, May, 1996
16. Bril, R., Lukkien, J., Verhaegh, W.: Worst-case response time analysis of real-time tasks under fixed-priority scheduling with deferred preemption revisited. In: ECRTS ’07: Proceedings of the 19th Euromicro Conference on Real-Time Systems, pp. 269–279. Pisa (2007)
17. Simonson, J., Patel, J.: Use of preferred preemption points in cache-based real-time systems. In: Proceedings of IEEE International Computer Performance and Dependability Symposium (IPDS), pp. 316–325, April 1995
18. Wu, Y., Bertogna, M.: Improving task responsiveness with limited preemptions. In: Proceedings of the 14th IEEE International Conference on Emerging Technologies and Factory Automation, ETFA’09. IEEE Press
19. Yao, G., Buttazzo, G., Bertogna, M.: Bounding the maximum length of non-preemptive regions under fixed priority scheduling. In: Proceedings of IEEE International Conference on Embedded and Real-Time Computing Systems and Applications (RTCSA), IEEE Computer Society Press, Beijing, May–June 2009
20. Buttazzo, G., Yao, G., Bertogna, M.: Bounding the maximum length of non-preemptive regions under fixed priority scheduling. In: Proceedings of 15th IEEE International Conference Embedded Real-Time Computer System Applications (RTCSA’09), pp. 351–360. Beijing, 24–26 Aug 2009
21. Baruah, S., Bertogna, M.: Limited preemption EDF scheduling of sporadic task systems. IEEE Trans. Ind. Inform. **6**(4), (2010)
22. Zhu, Y.: Evaluation of scheduling algorithms for real-time disk I/O (2002)

An Intelligent Packet Filtering Based on Bi-layer Particle Swarm Optimization with Reduced Search Space

B. Selva Rani and S. Vairamuthu

Abstract In this proliferation world, quantity of information available is increasing in a rapid speed. Due to enormous increase in availability of data, many researches are trying to fetch the most relevant information from the available sources. Many organizations and institutions rely heavily on internet for their sources and solutions, chances for intrusion grow significantly. So, there arise a need for a mechanism that protects their network and data from other external forces. The threat for organization's network and data can be minimized by deploying firewalls. In this paper, an intelligent packet filtering mechanism in a firewall based on Bi-Layer Particle Swarm Optimization has been proposed which minimizes the search space. With the reduced search space, finding a match between the field values of the incoming packet and the rules in the rule set can be done in an effective manner.

Keywords Firewall · Packet filtering · Rule set · Collective intelligence · Particle swarm optimization

1 Introduction

A swarm is a large number of homogeneous, simple agents interacting locally among themselves, and their environment, with no central control to allow global interesting behavior to emerge. A population-based or swarm-based algorithm can produce optimal and robust solutions with least cost. Because of this behavior, these

B. Selva Rani (✉)

School of Information Technology and Engineering, VIT University,
Vellore 632014, India
e-mail: bselvarani@vit.ac.in

S. Vairamuthu

School of Computing Science and Engineering, VIT University,
Vellore 632014, India
e-mail: svairamuthu@vit.ac.in

kinds of algorithm started getting focused by many researchers to find solutions for many complex problems [1]. These techniques also termed as *Collective Intelligence algorithms (CI)* attempt to design or refine distributed problem-solving agents inspired by the collective behavior of social insect colonies and other animal societies.

Properties of such algorithms include as follows: (i) Nature of complexity (ii) Adaptive in any kinds of environments and (iii) Autonomous behaviors [2]. In this paper, we propose an approach for an efficient packet filtering firewall based on Bi-layer particle swarm optimization (BL-PSO).

Particle Swarm Optimization is a kind of such nature-inspired computing, pioneered by Eberhart and Kennedy, which was inspired by the cooperative behavior of a flock of birds. Initially, PSO algorithms were only employed for continuous problems as studied by Qin et al. [3]. In Particle Swarm Optimization, each swarm will be initialized randomly with the solutions available from the search space [4]. Then, the particles move through the solution space to arrive at the best solution. Using a utility measure called as a *cost function* or *fitness function* the solution would be evaluated.

2 Background

2.1 Packet Filtering Firewalls

By employing various safety postures, the configurable devices or programs which control the traffic in and out of a network can be considered as a firewall [5]. Embedded with the rules in firewalls, the direction of a packet is considered to be playing a vital role in protecting spoofing in source address, filtering packets in the exit gateways [6]. Stallings categorized firewalls as (i) Circuit level (ii) Application level and (iii) Packet filters [7]. A Packet Filtering Firewall scrutinizes the incoming and outgoing packets of the organization's network based on their rules. The rules are designed according to the security policy of the trusted network and arranged in a table, known as *rule set*. Each rule contains information about the packets like *Source IP address*, *Source Port*, *Destination IP address*, *Destination Port* etc. as separate fields. For each set of such information there is an action field which indicates whether to forward or block the packet. The following table shows some sample rules in a rule set (Table 1).

The first rule says that the packets coming from the source address 192.168.145.* to any destination address to port number 51 have to be accepted. The second rule says that the packets coming from the source address 192.168.145.* and source port 80 to the destination address 10.10.1.* have to be dropped. Similarly the third rule says that the packets from any source address to the destination address 10.3.0.200

Table 1 Sample rules in a rule set

Source IP address	Source port	Destination IP address	Destination port	Action
192.168.145.*	–	–	51	Accept
192.168.145.*	80	10.10.1.*	–	Drop
..*.*	Any	10.3.0.200	Any	Drop

have to be dropped. The original packet filter was designed to perform a sequential search in the rule set in order to find a match between the parameters of the incoming or outgoing packets with the corresponding parameters in the rule set. Sreelaja et al. concluded that firewalls employing Neural Networks for filtering of packets possess major drawback like permitting packets from unknown address (addresses that are not part of firewalls' rules) [8].

2.2 Particle Swarm Optimization

Particle swarm optimization shortly PSO is one of the promising collective intelligence models. It was inspired from the supportive behavior of birds, fly in group without any clash even for long distances. They can suddenly change their direction without any collision, avoid the predators, scatter or group again very quickly because of the interaction between them. Based on this behavior of birds with common objective and collective behavior, Kennedy and Eberhart introduced PSO in 1995 as a heuristic optimization technique. Each swarm in PSO evaluates the objective function at its current location in solution space so as to arrive at the best solution [9]. In the solution space of dimension ‘n,’ the particles will be assigned random positions initially. They move in the solution space according to its velocity. Every particle keeps track of its best position known as *personal best* or *pBest*, so far and computes the fitness value until the objective is met. Also the best position among all the particle is updated which is known as *global best* or *gBest*.

The novel PSO algorithm comprises the following two computations along with the fitness evaluation:

$$v_i(t + 1) = \omega v_i(t) + c_1 R_1(pBest_i(t) - x_i(t)) + c_2 R_2(gBest(t) - x_i(t)) \quad (1)$$

$$x_i(t + 1) = x_i(t) + v_i(t + 1), \quad (2)$$

where

- $v_i(t + 1)$ is the change in velocity of i th particle at time moment $t + 1$,
- $x_i(t + 1)$ is the change in the position of i th particle at time moment $t + 1$,
- $pBest_i$ is the personal best position of i th particle so far,
- $gBest$ is the global best position of the group of swarms,
- ω is the inertia weight,

c_1 is the cognitive parameter, a positive constant,
 c_2 is the social parameter, a positive constant, and
 R_1 and R_2 are the random numbers

This phenomenon can be applied to solve various optimization problems with the careful mapping of the solution to a fitness function.

3 Bi-layer PSO Based Packet Filtering

3.1 BL-PSO Model for Packet Filtering

Packet Filtering Firewall filters the data flow inside any network based on the rules defined by the administrator in the *rule set*. The rules in the rule set are sorted always in ascending order based on *Source IP Address*. In an n-dimensional search space, solutions for some problems may be represented as a set of points. We can employ PSO technique to solve these kinds of problem as proposed by Ahmed and Glasgow [1]. Here the rules in the *rule set* are defined in a two-dimensional space in which the particles fly with dynamic velocity depending on their own performance, compared with the others in the group of swarms.

A packet filtering firewall filters packets based on the result of mapping the fields in the incoming packets between the respective fields in the rules of a *rule set*. The packet filter compares all the field values to be considered for making a decision and extract the value from the *action* field if a match is found and report whether to forward or deny the packets. If the match is not found then the packet will be logged. Particle Swarm Optimization helps the searching for filtering rules in the *rule set* in an efficient manner. The *rule set* is considered as the solution or search space for the particles. Randomly generated positions of the *rule set* are assigned as the initial positions of the swarms in the search space. Initially, by taking the *network address* of the incoming packet the particles compare the corresponding field value in their respective positions. Now for each particle the fitness value is calculated based on a match or a mismatch. If a match is found we can say that the particle is *fit* to proceed further in the search space. If not, the position and velocity of a particle have to be updated towards the solution in the search space. That is towards the rules in the *rule set* where exactly the match is found in the first field. Once there are equal number of particles and rules with matching in *network address* field, the other field values of the incoming packet are obtained. All the particles look for equality between those values and the field values in the rules indicated by their updated positions. If all the field values are equal with the values in the incoming packet, that particle is said to be *fit* and the corresponding *action*

field value is fetched. There is a possibility of detecting conflict in the rules also using the particles as below:

- Case 1 If no particle is having the required fitness value after comparing all the field values then it can be concluded that no rule is defined for such a combination and hence the packet may be logged.
- Case 2 If more than one particle find the exact match between the incoming packet and the rules then it can be concluded that there is a conflict among the rules and hence it may be brought to the notice of the administrator.

Thus, using the particles the required task of filtering can be done in an effective manner.

3.2 Structures Used in BL-PSO for Packet Filtering

Initially ‘ n ’ number of particles will be generated. The position and velocity of a particle ‘ P_i ’ at a moment ‘ t ’ are given by $x_i(t)$, and the $v_i(t)$. ‘ $pBest_i$ ’ is the best position achieved so far by the i th particle and ‘ $gBest$ ’ is the overall best position of any particle in the entire population. In order to reduce the search space ‘ $gBest$ ’ is considered as three components ‘ $gBest_min$,’ ‘ $gBest_eql$,’ and ‘ $gBest_max$.’

3.3 Construction of BL-PSO for Packet Filtering

In this model, a population consists of ‘ n ’ particles. Each particle is having two components position and velocity. Initially, all the ‘ n ’ particles are in a single layer until the initial search is completed. Initial velocity of the ‘ n ’ particles is assigned with the constant value –2. Let ‘ r ’ be the total number of rules in the *rule set*. ‘ n ’ random numbers between 1 and ‘ r ’ have been generated and they are assigned as the initial positions of ‘ n ’ particles. ‘ c_1 ’ and ‘ c_2 ’ are used to control the progress of particles in the direction of their personal and global finest position, in the range [0, 4] such that $c_1 + c_2 = 4$. ‘ R_1 ’ and ‘ R_2 ’ are used to introduce randomness in searching the solution space, usually in the range [0.0, 1.0].

When a packet arrives, the *Source IP Address* field value is obtained. The ‘ n ’ particles compare this value with the source address values given in the *rule set* indicated by their respective positions. Now the Fitness of each particle is assigned as either +1 or –1 if a match is found or not found by the particles, respectively. If SIP_{inpkt} is equal to SIP_{rset} then $Fitness_i = +1$ otherwise $Fitness_i = -1$, where $Fitness_i$ is the fitness value of the i th particle, SIP_{inpkt} is the value in the *Source IP Address* field of the incoming packet and SIP_{rset} is the value in the *Source IP Address* field of the *rule set*.

'gBest' is considered as a structure with three components *min*, *max*, and *equal* to store the positions of the particles with the *Source IP Address* field value less than, greater than, and equal to the incoming packet's *Source IP Address* filed value, respectively.

Next, the particles segregate themselves into two layers, outer layer with ' $n - 2$ ' particles and inner layer with 2 particles. Among ' n ' particles in the population, two particles whose initial positions are too far from the solution space will be chosen to form the inner layer and the remaining ' $n - 2$ ' particles will form the outer layer. The inner layer particles ' P_{i1} ' and ' P_{i2} ' are assigned the values *gBest.eql_min* and *gBest.eql_max* as their new positions. From these new positions the two particles ' P_{i1} ' and ' P_{i2} ' will start parallel searching in both directions (upward and downward) in the solution space. The objective of these inner layer particles is to shrink the search space precisely lies on the solution space until then the outer layer particles will be idle. Both the particles in the inner layer move with constantly increasing velocity so that their positions are updated exactly one step ahead in opposite directions. i.e.,

$$x_{pi1} = x_{pi1} - 1 \quad (3)$$

and

$$x_{pi2} = x_{pi2} + 1. \quad (4)$$

If there is a mismatch between the *Source IP Address* value of the incoming packet and the value in the rule set then the inner layer particles stop their search and have the previous positions as their current positions. The fitness value of both the particles is +1. These positions will give the lower and upper bound of the solution space, which is to be considered for the further search and the values are stored in the variables r_{lower} and r_{upper} . Now the number of rules in the *rule set* with a match found in the field of *Source IP Address* can be obtained as

$$s = r_{upper} - r_{lower}. \quad (5)$$

After finding the above the inner layer particles join the outer layer particles. The velocity and positions of the particles with the fitness value +1 will not be changed in the next iteration but with -1 will be updated according to Eqs. (1) and (2). While updating the position, a particle refers the position of ' P_{i1} ' as *gBest*, if its current position falls in the range with value less than the lower bound of the solution space. Similarly, a particle refers the position of ' P_{i2} ' as *gBest*, if its current position falls in the range with value greater than the upper bound of the solution space.

By this process the particles promise the faster convergence towards the solution. This continues until the number of particles (let m) with Fitness value +1 is equal to the number of rules in the rule set ‘ s ’ with the match between the *Source IP Address* values, where $m < n$ and $s < r$.

Once there are particles equal to the number of the rules with *Source IP Address* value as same as the incoming packet’s *Source IP Address* value then, the other field values (*Source Port*, *Destination IP Address* and *Destination Port*) of the incoming packet are extracted. These extracted values of the incoming packet are compared with the related field values of the rules in the *rule set* by the particles in their respective positions. Now, the Fitness of the particles is computed based on all the three field values. The Fitness value of the particle is +1 if the *Cost* of that particle is *zero* and -1 if the *Cost* is *non-zero*.

Thus,

$$\text{Cost}_i = (\text{SPort}_{\text{inpkt}} - \text{Sport}_{\text{rset}}) + (\text{DIP}_{\text{inpkt}} - \text{DIP}_{\text{rset}}) + (\text{DPort}_{\text{inpkt}} - \text{Dport}_{\text{rset}}), \quad (6)$$

where

- Cost_i is the cost of the i th particle,
- $\text{SPort}_{\text{inpkt}}$ is the value of *Source Port* number in the incoming packet,
- $\text{SPort}_{\text{rset}}$ is the value of *Source Port* number in the *rule set*,
- $\text{DIP}_{\text{inpkt}}$ is the value of *Destination IP Address* in the incoming packet,
- DIP_{rset} is the value of *Destination IP Address* in the *rule set*,
- $\text{DPort}_{\text{inpkt}}$ is the value of *Destination Port* number in the incoming packet,
- $\text{DPort}_{\text{rset}}$ is the value of *Destination Port* number in the *rule set*,

and

$$\begin{aligned} \text{Fitness}_i = +1 &\quad \text{if } \text{Cost}_i = 0 \\ &\quad - 1 \quad \text{if } \text{Cost}_i \neq 0 \end{aligned} \quad (7)$$

After computing the fitness values of the particles, the action field value (accept or deny) from the corresponding rule from the rule set whose index is given by the particle’s position (with $\text{Fitness} = +1$) is fetched. If more than one particle has Fitness as +1 or no particle has Fitness as +1, it implies that there is a conflict in the rule set or there is no rule in the rule set with the matching values for the incoming packet. In such cases it should be reported to log the packet for auditing. The proposed PSO model for packet filtering is illustrated in Fig. 1.

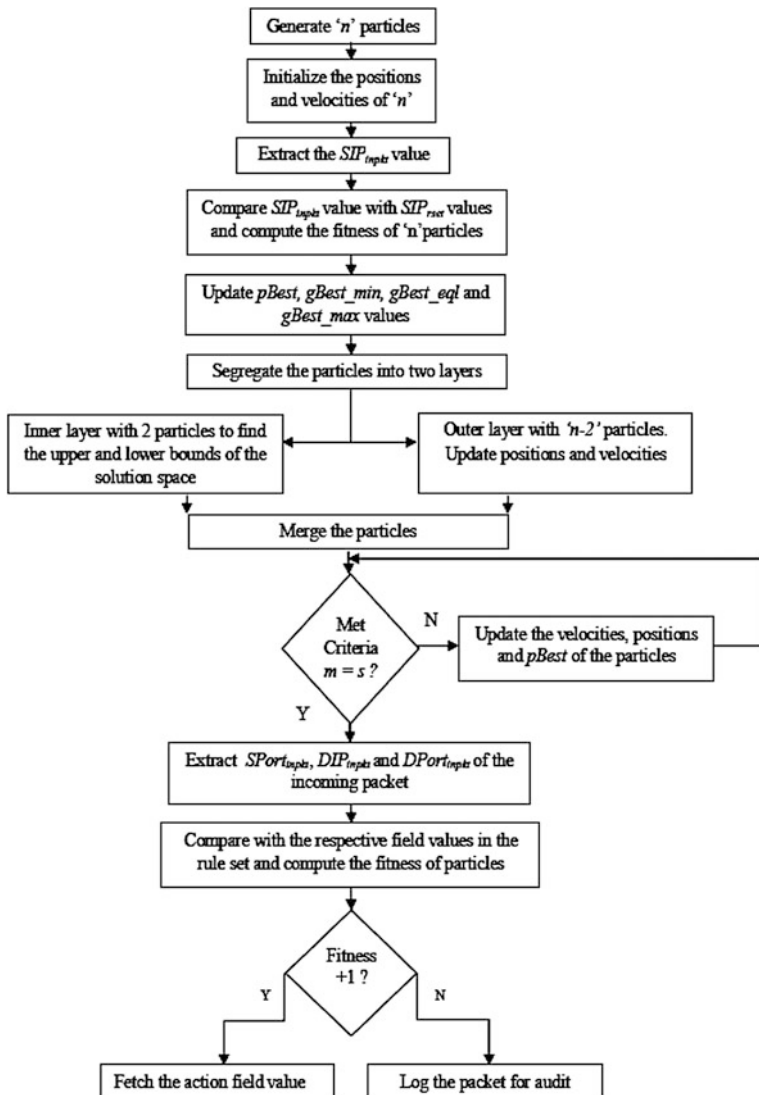


Fig. 1 Proposed BL-PSO-based packet filtering

4 Advantages of BL-PSO in Packet Filtering

Linear search in the rule set of a packet filter is reasonable in case of a limited number of *rules*. When the number of rules increases the time to search the *rule set* also increases. While using Particle Swarm Optimization in a packet filter, the *rule set* is considered as a two-dimensional search space and the initial search is done by

the particles randomly in the solution space. The cost of computation is reduced by dividing the particles into two layers and keeping the outer layer idle (until the *lower* and *upper* bounds are found). Once the ‘*gBest*’ position among the population is identified other particles converge towards that ‘*gBest*’ very quickly which is independent of the total number of rules in the rule set. Hence this optimization algorithm is scalable and fast when compared with the conventional linear search algorithm. Also by computing the fitness values of the particles, the match between the incoming packet’s field values and the values in the rule set is carried out in an efficient manner. So this algorithm proves accuracy in reporting the value in the *action* field to the packet filter.

5 Conclusion and Future Work

This paper proposes an efficient packet filtering mechanism based on Particle Swarm Optimization. The BL-PSO approach proves its strength by converging quickly in the solution space when compared with conventional linear search in which scalability of the rule set is very poor. Using multiple particles in a group, searching in a larger rule set could be carried out in an efficient manner than the linear search both in terms of time and memory. Since the cost and fitness of a particle are computed in accurate manner, the action to be taken for an incoming packet is extracted precisely from the *rule set*. We have several types of Collective Intelligence techniques inspired by nature. In future, it has been planned to apply other such methods for a packet filter, to have an improved performance.

References

1. Ahmed, H., Glasgow, J.: Swarm Intelligence: Concepts, Models and Applications. Technical Report, Queen’s University (2012)
2. Schut, M.C.: On model design for simulation of collective intelligence. Inf. Sci. **180**, 132–155 (2010)
3. Qin, J., Li, X., Yin, Y.: An algorithmic framework of discrete particle swarm optimization. Appl. Soft Comput. **12**, 1125–1130 (2012)
4. Abraham, A., et al.: Swarm intelligence: foundations, perspectives and applications. Stud. Computat. Intell. (SCI) **26**, 3–25 (2006)
5. Scarfone, K., Hoffman, P.: Guidelines on Firewalls and Firewall Policy, National Institute of Standards and Technology, U.S. Department of Commerce
6. Wool, A.: The use and usability of direction-based filtering in firewalls. Comput. Secur. **23**, 459–468 (2004)
7. Stallings, W.: Cryptography and Network Security Principles and Practices, 5/e
8. Sreelaja, N.K., Vijayalakshmi Pai, G.A.: Ant colony optimization based approach for efficient packet filtering in firewall. Appl. Soft Comput. 1222–1236 (2010)
9. Poli, R., Kennedy, J., Blackwell, T.: Particle swarm optimization: an overview. Swarm Intell. **1**, 33–57 (2007)

Storage Optimization of Cloud Using Disjunctive Property of π

Umar Ahmad, Vipul Nayyar and Bashir Alam

Abstract The process of storing data with the help of digits obtained from constant expansion is an interesting one, which stores your data in the digits of a constant, instead of consuming hard drive space. The pattern for a file is looked up in the constant and identified by the index of this pattern into it along with its length. Hence, instead of storing actual data, only the meta-data, i.e., the index and length of a file are stored in the disk. The reverse process takes place while retrieving a file for reading with the help of file location stored in the meta-data. This is achieved by performing preprocessing of digits of the constant and doing pattern recognition in it.

Keywords Storage · Distributed systems · Pi · HPC

1 Introduction

1.1 Characteristics of π

π (or pi) is revered as one of the most significant constants in mathematics due to its variety of interesting properties. It is presumed that π is normal [1], i.e., all the digits present in its expansion are distributed evenly [2]. This implies the presence of a disjunctive sequence in the value of π , meaning that all possible finite sequences of numerical digits will be present somewhere in it.

U. Ahmad (✉) · V. Nayyar · B. Alam

Computer Engineering Department, Jamia Millia Islamia, New Delhi 110025, India
e-mail: ahmad.umar2008@yahoo.in

V. Nayyar
e-mail: nayyar_vipul@yahoo.com

B. Alam
e-mail: babashiralam@gmail.com

1.2 *The Problem*

Retaining data in π is potentially a powerful option for storing large amounts of data into smaller storage disks, but according to a test done with the trivial method, it takes about 5 min to store a 400 line text file. Even considering Moore's Law, a filesystem with this kind design which has greater focus on computation of data rather than storage is not going to be a feasible option for desktop systems or laptops even in the next decade.

With the advent of Cloud, it is being extensively used to provide file storage service for customers and as a backend for hosting multiple applications. But the amount of data that is being stored daily gets accumulated over time and hence, the hosting company needs to expand its storage fleet by adding more racks. Also, implementing RAID on your cluster overwhelms the situation as you now need more space for replication and parity information.

1.3 *The Solution*

Leverage the power of this storage technique on Cloud, where the available computation capacity far exceeds that already existing in a daily use personal computer. We propose to deploy a storage methodology on a large-scale system, which would store and retrieve the data from π and use the accelerators for computationally intensive tasks. The primary use case of this system would be to act as a file storage service. Pattern matching of a file's contents in π for reading and writing purposes would be done in a distributed manner depending on the number of nodes present in the current cluster.

2 Design

2.1 *Representation of Compressed File*

The representation of the compressed file as seen above is done in the form of indexes written in the file. In order to distinguish the indexes for each block, a separator needs to be used. Again in the compressed file, we may leave some blocks uncompressed, as the size of the index calculated may become higher than the actual block size. For this to happen we shall need a second separator which distinguishes the next block as the original block of file. Since the current storage methodology formulated during the course of this project focuses only on compressing printable text characters in files, therefore a suitable choice for selecting separators is the extended ASCII set. Thus, suppose the original pattern is π bytes.

The amount of overhead bytes that are required to get a proper representation while keeping in mind the index length constraint are described below:

- One byte for separator (typically above ASCII code 127)
- Including one byte for separator indicating uncompressed data
- Removing one byte more from pattern in order to obtain compression

$$\text{Size of index} < (\text{Size of pattern}) - 2 \quad (1)$$

The representation for such type of pattern would accommodate both the separators: a separator to signify the original block and a second separator for the index and the constant variable used in the schema. The pattern in the compressed file would look something like this.

```
<s1> <in> <s2> <bl> <s1> <in> <eof>
s1 Separator for indexes
s2 Separator for original data
in Index number
bl Original data from input file
eof End of file
```

2.2 Preprocessing

Calculating the values of π at runtime requires a tremendous amount of computing power. A solution to this problem can be precomputing some π expansion digits at some values in a database and retrieving it via a simple query. This precomputation would be done during the setup of the program. The limit of the number of records stored directly depends on the memory capacity of the system and the chosen size of the pattern. A second problem occurs while searching an index in the database, if the entries are very high in number. Doing a linear search on large number of entries may take significant time. To speed up the lookup process in the database, its optimization procedures are applied. If the data are not found in the limited set of the data stored in the DB, run-time calculation needs to be done. For preprocessing purposes, a mysql database was populated with patterns found in the expansion of pi. First, 100 million decimal digits were downloaded from academic sites [3] which provide digits expansions of many constants in the range of billions and trillions. In order to convert decimal digits into characters, the first 100 million digits were partitioned into groups of two digits. Since a number of two digits can lie in the range of 0–99 only, the Range Scaling formula was applied to these numbers so as to convert them into the range 32–126. This range, as you might know depicts all the printable characters in the standard ASCII set, i.e., 0–127

$$f(x) = \frac{(b - a)(x - \min)}{\max - \min} + a \quad (2)$$

Due to the above process, the number of characters available now, i.e., the index became half (50 million) but they now represent the printable ASCII character set. Next, a sliding window mechanism was used to extract patterns from the newly generated pi expansion file. The size of the pattern that can be looked up or substituted was fixed to length 10. The table in the database stores the ASCII character pattern of length 10, the constant from which this pattern was extracted and the index where it was found in each tuple.

2.3 Calculation of π

There are various methods present to calculate the value of pi. In our case, the formula used is BBP. It is a spigot algorithm which computes π by calculating the n th binary digit, by applying base 16 math. Any required digit of π can be calculated directly with this formula, without the need to calculate any preceding digit. Simon Plouffe discovered the summation style formula in 1995, named BBP after the authors of the paper [4, 5] in which the formula was published, Bailey, Borwein, and Plouffe. The formula is

$$\pi = \sum_{k=0}^{\infty} \left[\frac{1}{16^k} \left(\frac{4}{8k+1} - \frac{2}{8k+4} - \frac{1}{8k+5} - \frac{1}{8k+6} \right) \right] \quad (3)$$

The general form for the calculation of n th digit of any irrational constant is given as

$$\alpha = \sum_{k=0}^{\infty} \left[\frac{1}{b^k} \frac{p(k)}{q(k)} \right] \quad (4)$$

α = constant

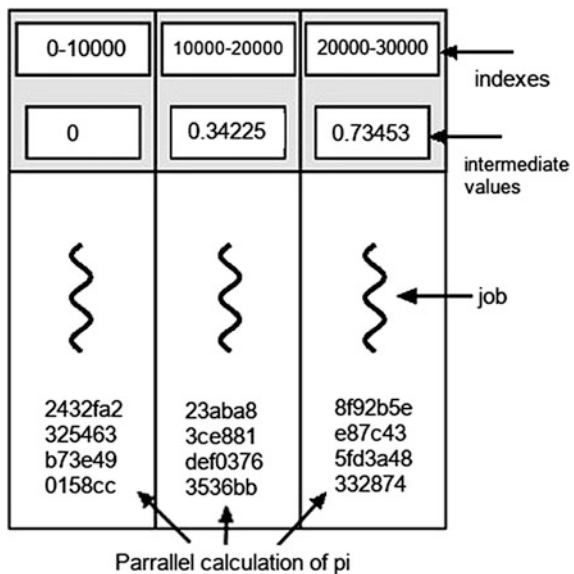
p, q = integer coefficients

$b \geq 2$ is an integer numerical base

Formulas in this form are known as BBP-type formulas [6].

The actual data can be regenerated using this formula and using the values already stored in the index lookup table. For the purpose of linear computation we used a modified version of BBP formula. It is given in the form of equation below:

Fig. 1 Depiction of parallel calculation of π



$$x_n = \left\{ 16x_{n-1} + \frac{120n^2 - 89n + 16}{512n^4 - 1024n^3 + 712n^2 - 206n + 21} \right\} \quad (5)$$

which generates consecutive hex digits. These hexadecimal digits can be obtained via $\lfloor 16x_n \rfloor$

Since the target file to be compressed is in the form of ASCII characters, these hexadecimal pi digits so obtained are again transformed to the form of ASCII so that it might be directly searched. This scheme can be extended further than limiting it to a few characters in ASCII. It can include the full length of 256 ASCII characters or even unicode characters (Fig. 1).

Distributing In order to calculate digits of π expansion or as a matter of fact, any other constant expansion, the above-mentioned BBP-type formulas are used. Although for a digit present at index n , we do not need $n - 1$ digits to calculate it, we do need the intermediate summation value in the formula at $n - 1$. Due to these constraints, skipping indexes in a BBP-type formula to distribute calculation of digits is fairly complex. The solution to this problem is to execute the BBP formula repeatedly till a large index and maintain a list of intermediate values at regular intervals with or without storing the patterns. While searching for an index of a pattern, these intermediate values stored at multiple intervals can trigger the process of skipping the digit computation process and execute it parallelly without running the formula from the start. Based on the infrastructure present in the hands of the user, this algorithm can be deployed in different ways as suitable. For a single node, these intermediate values can be stored in a file and multi-threading can be used to parallelize the process of computing digits in the index range between two stored

intermediate values. For a small cluster, using MPI programming is a better option to leverage the power of multiple nodes. For a large cluster, such as in a data center, using specialized and sophisticated frameworks like Hadoop would be beneficial. The map reduce API present in Hadoop would be ideal to parallelize the standard BBP formula without the need to store intermediate values. This parallelizing technique would also comfort any size limitations that a preprocessing lookup DB might have in a deployment since storing intermediate values allows you to skip π indexes and calculate patterns in run-time without increasing the size of the lookup database.

2.4 Algorithm

Storage The Storage algorithm reads the file to be compressed as input. This algorithm uses a sliding window technique to extract every adjacent pattern of the data block and searches it in the database. On a successful find, the index is returned and is stored in the file.

```

data = read_file('input.txt')
while match != EOF :
    i = i+1
    match = data[i to i+block_size]
    index = find_in_DB(match)
    if found:
        write_to_file('out.txt',index)
    if not found:
        index = search_with_bbp(match)
        if index < sizeOf(data):
            write_to_file('out.txt',index)
        else:
            write_to_file('out.txt',match)

```

If the file is not found the above-mentioned BBP formula calculates the proper index position for the file. The BBP formula runs until either the limit of computation is reached or the index so found is larger in size than the size of the block. The BBP returns either the error or the index. If the error is received, the block is stored as it is without compression.

Retrieval The Retrieval algorithm uses the compressed file as the input. Each block is extracted from the file by splitting its contents using separators. These blocks so extracted contain the index at which the original text has to be created. The database is searched for the index to get the proper ASCII text. If the index is out of bounds, the BBP formula is used to calculate the value at the proper index.

```

data = read_file('input.txt')
while match != EOF :
    i = i+1
    match = data[i]
    if match == 's1':
        index = data[i to i+block_size]
        text = find_in_DB(index)
        if not found:
            text = search_with_BBP(index)
    else if match == 's2':
        text = data[i to i+block_size]
    write_to_file('out.txt',text)

```

These values, so obtained, are replaced by their values, thus obtaining the original file. In the case where the separator found signifies the original block, all the content till the next separator is pasted as it is.

3 Optimization Methods

Even after properly implementing the above methodology, there can be potentially multiple sources of pitfalls that a deployed system can encounter. Therefore, extra optimization steps need to be taken in order to deploy and run a stable and efficient system. Some of these potential pitfalls are:

- The amount of entries or patterns stored in a lookup database can increase linearly when the size of a pattern is increased because of the sliding window process being used while populating the database. This increased size of database can be very difficult and expensive to maintain. Also, a traditional linear search of database tuples while lookup can be very slow.
- Despite the disjunctive property of π , there is no surety that commonly used patterns will be found at lower indexes for a better degree of compression.

3.1 Database Sharding

Sharding is a type of database partitioning technique that separates very large databases into smaller, faster, and more easily managed parts called data shards. As the size and transaction volume of the database tier incurs linear growth, response times tend to grow logarithmically. Sharding is entirely transparent to the application which is able to connect to any node in the cluster and have queries automatically access the correct shards. With its active/active, multi-master architecture,

updates can be handled by any node, and are instantly available to all of the other clients accessing the cluster.

3.2 Using More Constants

Since the type of block in a compressed file is identified by its preceding separator, this storage methodology can be used to store data in different constants having the same properties as π . Therefore, the type of separator (its ASCII code) will determine what separator has been used to compress a pattern or whether the uncompresssed data has been pasted itself. Using more constants similar to π will increase the probability of common patterns being found at lower indexes which would ultimately lead to a better rate of compression.

3.3 Removing Unused Patterns

As the calculation of π is a CPU-intensive process, the lookup table is used. This lookup table can be optimized to contain the entries that occur most frequently in the files and in the overall usage of the compression algorithm. Thus, a separate attribute storing *score* can be added to the DB which stores the frequency of any pattern. Another parameter, namely the *threshold* parameter is maintained, signifying the minimum score required for a pattern to stay in the DB. Once in a while the database is scanned to remove the patterns with score lower than the threshold.

4 Area of Application

This method provides a high compression rate on the cost of high computation power. Thus, the major areas of application are confined to the places having low memory space but high processing power. Some of these places are:

- **Geo-replication:** A process where large amounts of data is regularly exchanged between multiple data centers located in far-off locations or separate continents. Since each node, i.e., the sender and the receiver holds within itself, a very high computing capability and storage capacity, therefore this is a very appropriate use-case for this kind of storage subsystem.
- **Cold Storage:** Data which cannot be deleted but also may not be accessed for many years is the ideal target for storing it in expansion of pi digits as potentially large computing durations can be handled in this case.

5 Conclusion

The idea of storing data in digit expansion of constants like π is prevalent among the online folklore for more than two decades. This project represents the preliminary research work done in this fairly uncharted domain of storage.

The design of a storage system was formulated that enables storing of data in the digit expansion of π and other similar constants, thus achieving compression. A similar storage and retrieval algorithm was devised and tested for multiple samples under controlled conditions. Although this idea is perceived by many to fail under real conditions, based on our work and design, we think that more research and benchmarking using supercomputers can surely be used to find a more efficient method.

6 Future Work

Study the properties present in digit expansion of π and other constants so as to better predict that in which constant expansion, a certain data pattern will lie. Also, since this methodology requires large amounts of processing, therefore it lies in the domain of High Performance Computing applications. Benchmarking this storage process for common data patterns with the help of a supercomputer would be a very big forward step in Storage research.

References

1. Wagon, S.: Is π normal?, *The Mathematical Intelligencer*, vol. 7 (1985)
2. Arndt, J., Haenel, C.: Are the Digits of Pi Random? Lab Researcher May Hold the Key, pp. 22–23. Preuss, Paul (23 July 2001) (2006)
3. Yee, A.J., Kondo, S.: 10 Trillion Digits of Pi. <http://www.numberworld.org>
4. Bailey, D.H., Borwein, P.B., Plouffe, S.: On the rapid computation of various polylogarithmic constants. *Math. Comput.* **66**(218), 903–913 (1997)
5. Bailey, D.H., Borwein, P.B., Plouffe, S.: The Quest for Pi. *Math. Intell.* **19**(1), 50–57 (1997)
6. Bailey, D.H.: The BBP Algorithm for Pi (8 Sept 2006). <http://www.experimentalmath.info/bbp-codes/bbp-alg.pdf>

Co-training with Clustering for the Semi-supervised Classification of Remote Sensing Images

Prem Shankar Singh Aydav and Sonjharia Minz

Abstract The collection of labeled data to train a classifier is very difficult, time-consuming, and expensive in the area of remote sensing. To solve the classification problem with few labeled data, many semi-supervised techniques have been developed and explored for the classification of remote sensing images. Self-learning and co-training techniques are widely explored for the semi-supervised classification of remote sensing images. In this paper, a co-training model with clustering is proposed for the classification of remote sensing images. To show effectiveness of the proposed technique, experiments have been performed on two different spectral views of hyperspectral remote sensing images using support vector machine as supervised classifier and semi-supervised fuzzy c-means as clustering technique. The experimental results show that co-training with clustering technique performs better than the traditional co-training algorithm and self-learning semi-supervised technique for the classification of remotely sensed images.

Keywords Co-training · Remote sensing image classification · Self-learning · Semi-supervised fuzzy c-means · Semi-supervised learning · Support vector machine

1 Introduction

Classification of remote sensing data faces many challenges due to the large data size, high dimensionality, spatial relationship, overlapping nature of classes, spatial relationship, noisy data, limited amount of labeled data, etc. Many supervised classification techniques have been attempted for the classification of remote

P.S.S. Aydav (✉) · S. Minz

School of Computer and Systems Sciences, JNU, New Delhi 110067, India
e-mail: premit2007@gmail.com

S. Minz
e-mail: sona.minz@gmail.com

© Springer India 2016

S.C. Satapathy et al. (eds.), *Proceedings of the Second International Conference on Computer and Communication Technologies, Advances in Intelligent Systems and Computing* 380, DOI 10.1007/978-81-322-2523-2_64

659

sensing images. One of the major problems with supervised classification techniques is that they require large number of training samples. It is very time-consuming and expensive to get labeled samples. To solve problems of limited labeled data, many semi-supervised techniques have been proposed and explored for the classification of remote sensing images. These techniques utilize both labeled and unlabeled data to learn classifier. Self-learning [1], co-training [2], support vector machine [3, 4], generative models [5], graph-based technique [6], and neural network [7] have been applied successfully for the semi-supervised classification of remote sensing images. Persello et al. [8] presented a good survey on semi-supervised technique for classification of remote sensing images.

Co-training is a semi-supervised technique in which two learners are trained independently. In this paper a modified version of co-training is proposed in which each learner takes help of clustering technique to train itself. It is assumed that supervised techniques are not able to extract the underlying distribution with few labeled samples. Clustering techniques extract the underlying distribution from the unlabeled data pool which helps to train the supervised classifier in semi-supervised framework. Remote sensing images contain more than 100 bands, especially hyperspectral images from which it is possible to obtain two independent set of features for co-training. This model can be also applied on multispectral remote sensing images where spectral feature can be treated as one view and spatial features as another view. The main objective of this paper is:

1. To explore co-training technique with two views of spectral bands for the semi-supervised classification of remotely sensed images.
2. To use clustering algorithm to improve the accuracy of traditional co-training algorithm for the classification of remotely sensed images.

The remainder of the paper organized as follows: Sect. 2 describes the semi-supervised concepts, co-training and proposed co-training technique. The experimental results and its analysis are presented in Sect. 3. Section 4 describes the conclusion of the work.

2 Semi-supervised Learning

In many applications, it is difficult to get training samples for the supervised classifier, in those applications unlabeled data are used with limited labeled data for effective training of the classifiers. The main idea in semi-supervised classification is to take advantage of both labeled and unlabeled data. Many semi-supervised techniques have been developed in the literature like self-learning, co-training, graph-based techniques semi-supervised support vector machine, semi-supervised neural network, semi-supervised technique based on generative methods, etc. A good study and survey on semi-supervised techniques is presented by Schwenker et al. [9]. Self-leaning and co-training are widely explored semi-supervised techniques. Self-leaning is an incremental semi-supervised learning technique in which

a classifier is trained with small set of labeled data and that trained classifier is used to select most confident samples from unlabeled data pool which are again added to labeled data pool for training of classifier in the next iteration. In this paper, a co-training technique is proposed for semi-supervised classification, which is an extension of the self-learning technique proposed by Gan et al. [10].

2.1 Co-training

In the co-training framework two different learners are trained in an iterative manner. It is an extension of the self-learning framework in which an ensemble of two supervised classifiers are used to help each other to learn most confident samples for semi-supervised learning. In each iterative step the unlabeled samples classified with high confidence by both learners are added to labeled data pool. It is assumed that most confidently classified unlabelled samples by one classifier may be informative for other classifiers. The classifier may be different or the same classifier on different feature set. Multiview co-training is a semi-supervised learning technique in which the same classifier is used for training on two different set of features. The feature sets are independently sufficient to learn the discriminative function or probability mass function. The whole procedure is summarized in Algorithm 1.

Algorithm-1 Co-Training

Input: A supervised classifier c , labeled data L , Unlabeled data pool U , Two view of features (f_1, f_2), Max Iteration i , Number of classes' k

Output: An ensemble two classifier

Method:

1. Train the supervised classifier C_1, C_2 with initial labeled data L with view f_1 and f_2

Repeat

2. Classify unlabeled data pool U with trained classifier C_1 on view f_1 .
3. Measure the confidence of classified unlabelled data and select t most confident samples from each class (L).
4. Add $(k*t=|T|)$ most confident samples in labeled pool ($L = L \cup T$) and remove those samples from unlabeled pool ($U = U - T$).
5. Classify unlabeled data pool U with trained classifier C_2 on view f_2 .
6. Measure the confidence of classified unlabelled data and select t most confident samples from each class (L).
7. Add $(k*t=|T|)$ most confident samples in labeled pool ($L = L \cup T$) and remove those samples from unlabeled pool ($U = U - T$).
8. Train the supervised classifier C_1, C_2 with labeled data L with view f_1 and f_2 .

Until Max Iteration i or $U==0$

9. Return the trained classifier C_1, C_2 .

2.2 Proposed Co-training with Clustering

The co-training algorithm starts with few labeled data which are not sufficient to learn underlying distribution present in data. The supervised classifier use only labeled data to learn underlying distribution or discrimination function. Clustering techniques are widely used to extract useful information from unlabeled samples. In multiview co-training semi-supervised framework, clustering techniques can be used to cluster the data in each view to extract useful information. The clustering algorithm is used here to cluster the data to determine the samples which are classified with high confidence in each view. The most confident samples can be obtained in each view in the following way:

$$\text{confidence } (x_i(c)) = p_{i,c} * \mu_{i,c} \quad (1)$$

where x_i denotes i th unlabeled sample which is classified into c th class with probability $p_{i,c}$ and membership value for this sample to the c th class is $\mu_{i,c}$, determined by clustering. The whole procedure is summarized in Algorithm 2.

Algorithm-2 Co-Training with Clustering

Input: A supervised classifier c , labeled data L , Unlabeled data pool U , Two view of features $(f1, f2)$,

Max Iteration i , Number of classes' k ,

Output: An ensemble of two classifiers

Method:

Repeat

1. Train the supervised classifier $C1, C2$ with labeled data L on both view $f1$ and $f2$.
2. Learn the clustering phenomena with unlabeled data U and labeled data on both view $f1, f2$.
3. Classify unlabeled data pool U with trained classifier $C1$ on view $f1$.
4. Get the membership value of unlabeled data pool U on view $f1$.
5. Measure the confidence of classified unlabeled data using equation (1) and select t most confident samples from each class (L).
6. Add $(k*t=|T|)$ most confident samples in labeled pool ($L = L \cup T$) and remove those samples from unlabeled pool ($U = U - T$).
7. Classify unlabeled data pool U with trained classifier $C2$ on view $f2$.
8. Get the membership value of unlabeled data pool U on view $f2$.
9. Measure the confidence of unlabeled data U using equation (1) and select t most confident samples from each class.
10. Add $(k*t=|T|)$ most confident samples in labeled pool ($L = L \cup T$) and remove those samples from unlabeled pool ($U = U - T$).
11. Train the supervised classifier $C1, C2$ with labeled data L with view $f1$ and $f2$.
12. Return the trained classifier $C1, C2$.

3 Experimental Results and Analysis

To show the effectiveness of technique proposed above, the experiments are performed with two remote sensing data sets, Botswana and Salinas. The data sets are publically available for the research purposes [11]. Two views of the remotely sensed images have been created by two different methods to perform co-training techniques. The first method is vertical portioning of the data from the middle. In the second method the views have been created by arranging even spectral bands in one view and odd band number in other view. The linear probabilistic support vector machine [12] is used as supervised classifier (SVM) and semi-supervised fuzzy c-means (SFCM) [13] is used for the clustering of the data. In experiment, the co-training with vertical partitions is denoted as COSVM_VP, the co-training with even and odd view is denoted as COSVM_EO, the proposed method co-training with clustering on homogenous view is denoted as COSVM_VP+SFCM, co-training with clustering on even and odd view is denoted as COSVM_EO+SFCM, self-learning denoted as (SSVM) and finally self with clustering have been denoted as SSVM+SFCM.

3.1 Salinas Data Set

This hyperspectral data set was acquired over Salinas Valley, California, USA with AVIRIS sensor. It has 224 spectral bands with 3.7 m of spatial resolution. The data set has 16 land cover classes. In this experiment 10 randomly set label (20 from each class) and unlabeled data set (100 from each class) have been taken from original data set. For each technique the experiments have been performed till ten iterations. The experimental results are shown in Table 1 which includes 10th

Table 1 Salinas data overall classification accuracy

Data sets	SVM	SSVM	SSVM +SFCM	COSVM_VP	COSVM_EO	COSVM_VP +SFCM	COSVM_EO +SFCM
1	0.7520	0.8398	0.8501	0.8355	0.8592	0.8437	0.8723
2	0.7719	0.8107	0.8322	0.8160	0.8644	0.8371	0.8745
3	0.7495	0.8039	0.8199	0.8262	0.8540	0.8354	0.8663
4	0.7381	0.8014	0.8309	0.8139	0.8490	0.8377	0.8688
5	0.7278	0.7941	0.8174	0.8024	0.8595	0.8186	0.8699
6	0.7390	0.7987	0.8190	0.8081	0.8487	0.8448	0.8731
7	0.7570	0.8004	0.8175	0.8175	0.8446	0.8440	0.8723
8	0.7687	0.8055	0.8206	0.8111	0.8450	0.8241	0.8554
9	0.7441	0.7809	0.8288	0.7962	0.8224	0.8303	0.8506
10	0.7635	0.8164	0.8354	0.8049	0.8664	0.8453	0.8808
Mean	0.7511	0.8051	0.8271	0.8131	0.8513	0.83609	0.8684

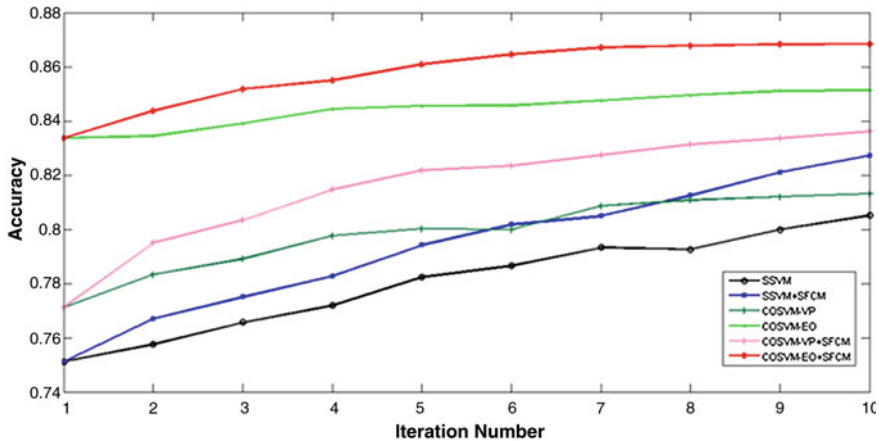


Fig. 1 Mean accuracy (Y-axis) versus iteration number (X-axis) for Salinas data

iteration accuracy of each technique with mean accuracy and standard deviation. The average accuracy trend of each technique is shown in Fig. 1 with different graphs.

The graph of SSVM shown in figure indicates that the accuracy is increasing with increment of iteration number. The SSVM technique has been able to achieve 80.52 % accuracy in its 10th iteration. The trends of SSVM+SFCM show that the technique has always increasing accuracy with iteration number. The final accuracy of SSVM+SFCM is 82.72 % which is better than SSVM. The graph of SSVM+SFCM shows higher accuracy than SSVM in each iteration. The experiment performed with COSVM_VP show that the accuracy is better than SSVM+SFCM in its initial iterations but not able to achieve better accuracy than SSVM+SFCM. The 10th iteration accuracy of COSVM_VP is 81.32 % which is less than SSVM+SFCM. The graph of proposed method COSVM_VP+SFCM show that it has better accuracy than COSVM_VP as well as SSVM+SFCM and SSVM in each iteration. Finally COSVM_VP+SFCM have managed to achieve 83.61 % average accuracy. The accuracy of COSVM_VP+SFCM is always increasing with each iteration.

Co-training experiment performed with even odd feature view has been achieved better accuracy from other techniques. The graph shows that COSVM_EO and COSVM_EO+SFCM have achieved better accuracy than other methods (SSVM, SSVM+SFCM, COSVM_VP, COSVM_VP+SFCM). The proposed method performed on even odd feature set (COSVM_EO+SFCM) have achieved better accuracy than COSVM_EO in each iteration. In the 10th iteration COSVM_EO+SFCM has achieved **86.64 %** accuracy which better than COSVM_E (85.13 %).

3.2 Botswana Data Set

This is a hyperspectral remote sensing image, which contains 145 bands with spatial resolution 30 m per pixel and acquired by NASA earth observing satellite sensor over the Okavango Delta, Botswana. The data set is freely available for the research purposes. The experiment has been performed on first 13 classes of data sets. To show effectiveness of proposed method 10 randomly selected labeled and unlabeled samples have been selected from the original Botswana data set. Each randomly selected sample contains 195 labeled (15 samples from each class) and 1040 samples from unlabeled data pool (80 from each class). Each experiment has been performed till 10 iterations. The experimental results are shown in Table 2 which includes 10th iteration accuracy of each technique with mean accuracy. The average accuracy acquired in iterations with 10 randomly selected data sets has been shown in Fig. 2 with different graphs.

Table 2 Botswana data overall classification accuracy

Data sets	SVM	SSVM	SSVM +SFCM	COSVM_VP	COSVM_EO	COSVM_VP +SFCM	COSVM_EO +SFCM
1	0.7647	0.7809	0.8367	0.8039	0.8188	0.8367	0.8374
2	0.7904	0.7880	0.8066	0.7833	0.8117	0.8185	0.8533
3	0.7965	0.7833	0.8212	0.8235	0.8198	0.8573	0.8563
4	0.7576	0.7302	0.7823	0.8036	0.7975	0.8350	0.8431
5	0.8130	0.7630	0.8208	0.7857	0.8049	0.8333	0.8469
6	0.7968	0.7363	0.7989	0.8080	0.7982	0.8300	0.8428
7	0.7634	0.7664	0.8087	0.7989	0.8151	0.8337	0.8384
8	0.7606	0.7681	0.8218	0.7853	0.8381	0.8293	0.8435
9	0.7765	0.7799	0.8154	0.8076	0.8087	0.8300	0.8675
10	0.8107	0.7911	0.8154	0.7843	0.8134	0.8452	0.8401
Mean	0.7830	0.7687	0.8127	0.7984	0.8126	0.8348	0.8469

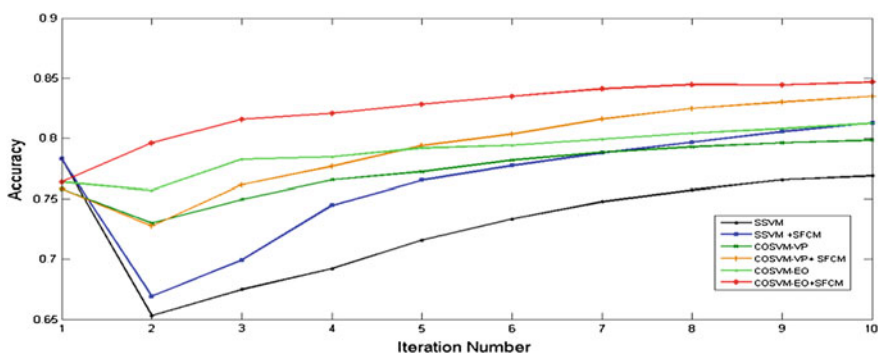


Fig. 2 Mean accuracy (Y-axis) versus iteration number (X-axis) for Botswana data

The graph indicates that average accuracy of SSVM drops in second iteration and after that the accuracy is increased till 76.87 %. The SSVM+SFCM trend indicate that the accuracy has also decreased in second iteration but till tenth iteration, it has managed to achieve 81.28 % accuracy which is better than SSVM. The graph shown in figure of COSVM_VP initially shows better accuracy trend than SSVM+SFCM but finally it has achieved accuracy 79.84 % which is lesser than SSVM+SFCM. The trend of COSVM_EO show initially better accuracy trend than COSVM_VP and SSVM+SFCM. COSVM_EO and finally able to manage 81.26 accuracy which is better than COSVM_VP and almost equals to SSVM+SFCM. The accuracy trend of proposed methods (COSVM_VP+SFCM and COSVM_EO+SFCM) are better than all other methods and finally able to achieve **83.49** and **84.69** respectively. The graph shown is the Fig. 2 indicates that COSVM_EO+SFCM have always increasing accuracy trend and accuracy is greater than other methods in each iteration.

4 Conclusion

In this study a co-training algorithm with clustering has been proposed. The experimental results show that the model is able to achieve good accuracy in comparison to traditional co-training algorithm and self-learning semi-supervised technique for classification of remote sensing images. The proposed framework is wrapper model in which any classifier and clustering technique can be used although, SVM and SFCM have been used in our experiment. In experiment only spectral bands are considered for view creation but to include spatial information the frame work can be extended as co-training semi-supervised technique with spectral and spatial view. In this study only most confident samples are used for training but these samples may not be informative, so for future work the active learning concepts can be integrated with co-training to select the most informative samples.

References

1. Li, J., Dias, J.M.B., Plaza, A.: Semi supervised self-learning for hyperspectral image classification. *IEEE Trans. Geosci. Remote Sens.* **51**(7), 318–322 (2013)
2. Song, X.Q., Liu, R., Aang, W., Jiao, L.: Modified co training with spectral and spatial views for semi supervised hyperspectral image classification. *IEEE J. Sel. Top. Appl. Earth Obs. Remote Sens.* **7**(6), 2044–2055 (2014)
3. Bruzzone, L., Chi, M., Marconcini, M.: A novel transductive SVM for semisupervised classification of remote-sensing images. *IEEE Trans. Geosci. Remote Sens.* **44**(11), 3363–3373 (2006)
4. Chi, M., Bruzzone, L.: Semisupervised classification of hyperspectral images by SVMs optimized in the primal. *IEEE Trans. Geosci. Remote Sens.* **45**(6), 1870–1880 (2007)
5. Jackson, Q., Landgrebe, D.A.: An adaptive classifier design for high-dimensional data analysis with a limited training data set. *IEEE Trans. Geosci. Remote Sens.* **39**(12), 2664–2679 (2001)

6. Valls, G.C., Marsheva, T.V.B., Zhou, D.: Semi-supervised graph-based hyperspectral image classification. *IEEE Trans. Geosci. Remote Sens.* **45**(10), 3044–3054 (2007)
7. Ratle, F., Camps-Valls, G., Weston, J.: Semi supervised neural networks for efficient hyperspectral image classification. *IEEE Trans. Geosci. Remote Sens.* **48**(5), 2271–2282 (2010)
8. Persello, C., Bruzzone, L.: Active and semisupervised learning for the classification of remote sensing images. *IEEE Trans. Geosci. Remote Sens.* **52**(11), 6937–6956 (2014)
9. Schwenker, F., Trentin, E.: Pattern classification and clustering: a review of partially supervised learning approaches. *Pattern Recogn. Lett.* **37**, 4–14 (2014)
10. Gan, H., Sang, N., Huang, R., Tong, X., Dan, Z.: Using clustering analysis to improve semi-supervised classification. *Neurocomputing* **101**, 290–298 (2013)
11. http://www.ehu.es/ccwintco/index.php/Hyperspectral_Remote_Sensing_Scenes
12. Lin, T.W.C., Weng, R.C.: Probability estimates for multi class classification by pair wise coupling. *J. Mach. Learn. Res.* **4**, 975–1005 (2004)
13. Bensaid, A.M., Hall, L.O., Bezdek, J.C., Clarke, L.P.: Partially supervised clustering for image segmentation. *Pattern Recogn.* **29**, 370–379 (1996)

An Integrated Secure Architecture for IPv4/IPv6 Address Translation Between IPv4 and IPv6 Networks

J. Amutha, S. Albert Rabara and R. Meenakshi Sundaram

Abstract An All-IP network is probably getting highly feasible since all applications and services in the telecommunication are already getting IP enabled. Internet Protocol version 6 or IPv6 is a later version of IP suite as it is designed to handle the increasing number of Internet applications. Security has become a major concern for the IP next generation network architecture and is considered as one of the most fundamental requirements for business continuity and service delivery. Several initiatives have been made by researchers to integrate secure IPv4/IPv6 address translation between IPv4 and IPv6 networks. But, not much progress has been reported in the recent past. Hence, in this research, an Integrated Secure Architecture for IPv4/IPv6 Address Translation between IPv4 and IPv6 Networks, with an IPv4/IPv6-Enabled Gateway Translator (IP46EGT), has been proposed to achieve MAC-level, VPN-IPSec, and Certificate level security. Network performance is evaluated and the generated results are tabulated and graphically presented.

Keywords IPv4 · IPv6 · Address translation · Security · IPSec

1 Introduction

The next generation Internet Protocol, IPv6 is intended to replace IPv4, which is gaining popularity now-a-days and exists sparsely in today's world. Although IPv6 contains built-in IPSec security protocol, the initiation of IPv6 makes changes in the

J. Amutha (✉) · S. Albert Rabara · R. Meenakshi Sundaram
St. Joseph's College, Tiruchirappalli 620002, TamilNadu, India
e-mail: roniamutha@gmail.com

S. Albert Rabara
e-mail: a_rabara@yahoo.com

R. Meenakshi Sundaram
e-mail: itsramesh@msn.com

security field and transition from IPv4 creates new risks and weakens the security strategies of an organization. IPv6 is enmeshed with various issues: its global interoperability is limited due to the weakness of the encryption algorithm; IPSec has not yet been fully standardized; there is no protection against Denial of Service/Flooding attacks [1]. One of the core issues with IP security existing today is that it is an “add-on” and not a built-in facility from the start, in which the core functionality is developed first and then satisfies the needs of security requirements. It tends to create problem because IP is becoming an ubiquitous form of communication that affects the entire enterprise [2].

IPSec protocol suite, as an extension to the basic IP Protocol, provides confidentiality and authentication service. It overcomes the security problems caused by the mobility between the node and the home agent [3]. IPSec is compatible with current Internet standards in IPv4. But in IPv6, IPSec is defined as mandatory feature and the objective of improved security is to create routing changes that provide both mobility in the network and safety against various security threats [4].

To prevent the attacker from establishing false connections and to ensure the integrity of the mobile node and its peers, security in the proposed architecture guarantees data origin authentication of IP packets through Cryptographically Generated Address (CGA), while securing binding update message between the mobile node, home agent, and the correspondent node [5]. Hence, in this research, an Integrated Secure Architecture for IPv4/IPv6 Address Translation between IPv4 and IPv6 Networks, with an IPv4/IPv6-Enabled Gateway Translator (IP46EGT), has been proposed to achieve various levels of security, namely MAC-Level Security, VPN-IPSec Security, and Certificate level security. Network performance is evaluated, and the generated results are tabulated and graphically presented.

2 Review of Literature

Frederic et al. [6] proposed various algorithms and tools for ensuring the security configuration of the firewalls, for the generation of the IPv6 addressing scheme, and for an IPv4 enterprise network, in which the firewalls deployed are stateful. A new model was suggested by Nazrul et al. [7] in the form of a new Internet Key Exchange (IKE) authentication in order to ensure end-to-end IPSec interoperability across translation gateway. This model uses Address-Based Keys (ABK) with certificate less signature for securing the communication channel between end nodes using their end IP addresses as public/secret keys for authentication, which eliminates the notification of the revoked keys. Seewald [8] proposed an architecture for NGN which provided flexibility, interoperability, and built-in security technologies (IPSec). Serap et al. [9] proposed an autonomic and self-adaptive

system which integrates the NGN architecture with the ITU-T security model for assuring the security of NGNs and new additional features, enabling it to dynamically detect vulnerabilities, threats, and risk analyses. Mahdi et al. [10] presented a security open architecture model for NGN, based on the concepts of an Integrated Security Module (ISM), to protect data and Targeted Security Models (TSMs) for protecting entities, users, servers, and resources. Faisal et al. [11] proposed the use of Identity-based schemes which enhance the security of the Return Routability Procedure without compromising the performance of mobile nodes. Pekka et al. [12] discussed an internetworking architecture for NGN which consists of cryptographic identifiers between the Internet Protocol layer and the transport protocols. Abdur et al. [13] presented a model named Policy-Based Security Management (PBSM) for the security of the host-based systems which are well supported in IPv6 networks.

3 Proposed Architecture

The proposed unique architecture is designed to integrate the two independent IP versions IPv4 and IPv6, by mutually permitting one version of IP mobile nodes to communicate with another version of IP networks. Therefore IPv4 networks communicate with IPv6 mobile nodes, and IPv6 networks communicate with IPv4 mobile nodes. This is achieved by designing a novel translator namely an IP46EGT which is simulated in the form of a PC-Emulator. The IP46EGT translates IPv4 address into IPv6 address and IPv6 address into IPv4 address. When an IPv6 node communicates with an IPv4 host in the IPv4 network, the translated IPv6 source prefix is configured in the IP46EGT which detects the destination address of the IPv6 packet. If this prefix is the same as the configured prefix, the address mapping takes place and converts the IPv6 address to IPv4 address. Figure 1 represents the proposed Secure IPv4/IPv6 Address Translation architecture between IPv4 and IPv6 Networks.

Three various levels of security namely MAC-level security (level 1), VPN-IPSec security (level 2), and Certificate Level (level 3) security are incorporated in the proposed architecture which provides data integrity, data confidentiality, data origin authentication, and replay attacks. Virtual Private Network (VPN) is incorporated in the proposed architecture to provide secure data transmission between the VPN mobile node and the network. The PC-Emulator in the architecture generates a New Secret Key (NSKG) which is the Cryptographically Generated Address (CGA) for every communication in which the MAC-level security is first established and the secret keys are distributed through a secured VPN-IPSEC tunnel and passed to the certificate server, and a secured connection is established between the end-users. Load balancer balances traffic over multiple

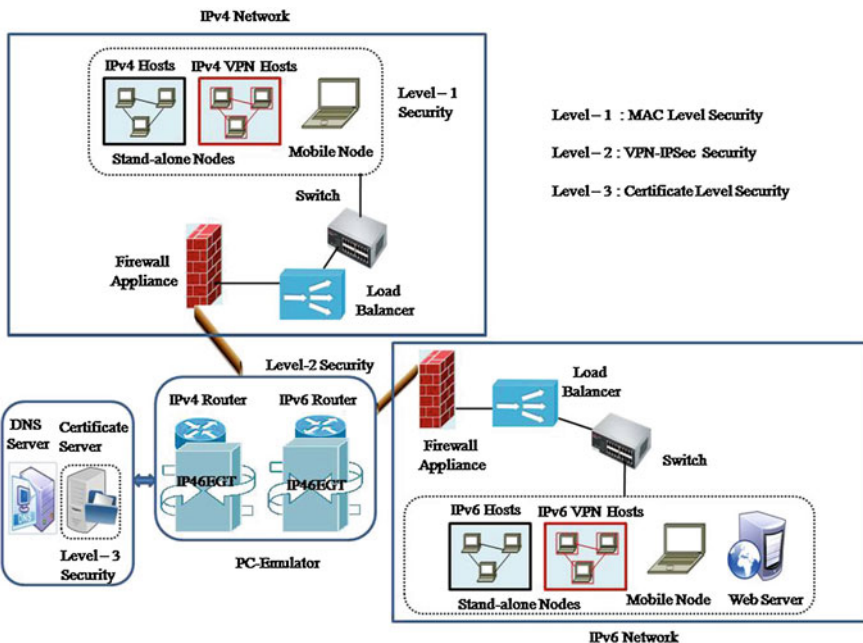


Fig. 1 Proposed secure IPv4/IPv6 address translation architecture

connections which ensure the availability of the network and improves the overall performance of the availability of the services.

Level 1: MAC-Level Security

Media Access Control (MAC) level security is used in the proposed architecture because of its unique identifier assigned to a network interface for communications on the physical network. The source node used for communication consists of a MAC address as the Source Public Key (SPuk), which generates a New Secret Private Key (NSKG) as the Cryptographically Generated Private Address (CGPra) for every communication. The NSKG is a combination of the four-digit random number (SKG) and the last two bit positions of the source client node MAC address (MSKG) that is, $NSKG = SKG + MSKG$. The NSKG is sent to the source and destination to establish an authentication and provides end-to-end security.

Level 2: VPN-IPSec Security

Virtual Private Network (VPN) is incorporated in the proposed architecture to provide secure data transmission between the VPN mobile node and the network. These systems ensure that the data cannot be intercepted. VPN-IPSec permits highly secure site-to-site connectivity and protects IPv4 and IPv6 traffic as it

communicates between end hosts or security gateways. Since the point to point tunnel is established, packets cannot be intercepted by an attacker which provides integrity and authentication between the VPN-IPSec-enabled hosts.

Level 3: Certificate Level Security

To obtain a certificate, a Private Secret Key (NSKG) based on the Public Key (SPuK) is generated from the Level-1 security. A certificate is generated by binding the public and private key and is passed to the certificate server to verify that the information is valid or not. If valid, a secured connection is established between the end-users and the translation between the source and the destination happens. If not, the connection will not be established and the translation process fails.

3.1 Proposed Addressing Concept

IPv4 addresses use 32-bit, and IPv6 addresses use 128-bit identifiers. The type of an IPv6 address is identified by the high-order bits of the address. IPv4-compatible IPv6 address and IPv4-mapped IPv6 addressing concept are used in the proposed architecture to represent the IPv6 address and IPv4 address, respectively, and in order to promote IPv4 and IPv6 translation, the IPv6 global unicast address is modified and used. For the IPv4-mapped IPv6 address, the most significant 16 bits, from 1st to 16th bit are assigned with the format prefix 2001. The address format for IPv6 in IPv4 visited network represents the IPv4-mapped IPv6 address in which the 17th to 32nd bits are assigned FFFF. The next 32 bits, from 33rd to 64th represent the 32-bit IPv4 router address. The least significant 64 bits from 65th to 128th are assigned with Interface Identifier (ID) by the CGA and are depicted in Fig. 2.

For the IPv4-compatible IPv6 address, the IP46EGT extracts the 32-bits from the 33rd to 64th bit position of the network part of the IPv6 address and converts them to its corresponding IPv4 address. The remaining bit positions are assigned with zeroes representing IPv4-compatible IPv6 address.

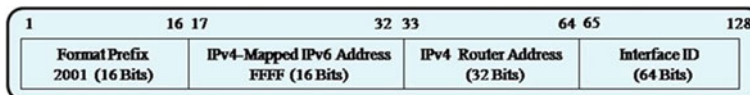


Fig. 2 Proposed addressing format

3.2 Proposed Interface Design

```

Procedure PCEmulator
Begin
{
If
Request_from_MNv6_IPv4RouterAddr_Solicitation_(Rv4_Add)
then
{
Response_Request_from_MNv6_IPv4RouterAddr_Solicitation_
(Rv4_Add);
}// End of If
{ //Key Generation
Secret_Key_Gen()
{ SKG=Random_No_Gen(); //Random Number Generation
MSKG=Get_MAC_ID(PE_MAC,15,17) //Getting MAC_ID
NSKG = SKG +MSKG; // Generation of key
Key_Exchange()
{ Key_Exchange(SRC, DST, NSKG)
{ PE=NSKG;
NSKG-> Send_to_SRC;
NSKG-> Send_to_DST;
}
{ V6BAdd(1-16) ← FP(2001);
V6BAdd(17-32) ← MA(FFFF) ;
V6BAdd(33-64) ← Decimal_to_Hexadecimal(46);
V6BAdd(65-128) ← MAC address;
V6CGABdd = V6BAdd+ NSKG;
IPv6AP ← V6CGABdd + HAv6 //Stores in the address pool
}
If Request_from_MNv4_IPv6RouterAddr_Solicitation_
(Rv6_Add) then
{
Response_Request_from_MNv4_IPv6RouterAdd_Solicitation_
(Rv6_Add);
}// End of If
{ V4BAdd(1-32) ← CA(0000);
V4BAdd(33-64) ← Hexadecimal_to_Decimal(64);
V4CGABAdd = V4BAdd;
IPv4AP ← V4CGABdd + HAv4
} If (Successful(DAD) then
{// Performs Registration and communication happens
} // End of If
End; // End of Begin
}

```

The call flow sequence diagram for the secure address translation from IPv6 to IPv4 and IPv4 to IPv6 is depicted in Figs. 3 and 4, respectively.

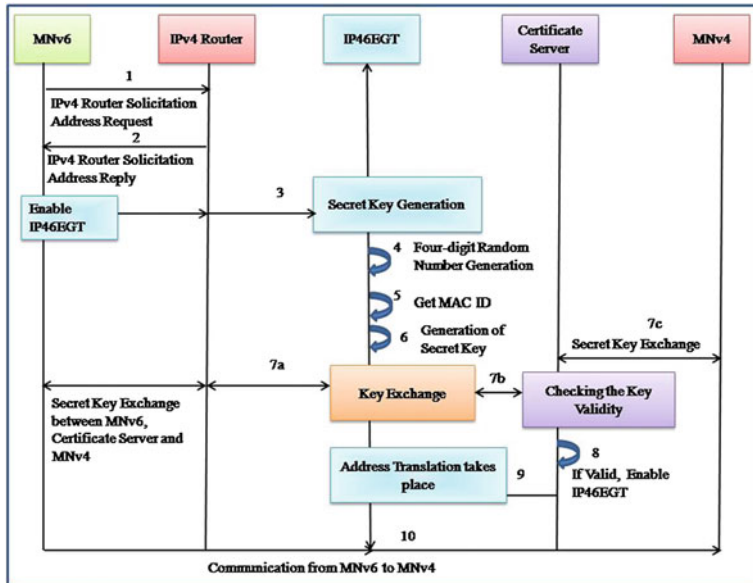


Fig. 3 Call flow sequence diagram from IPv6 to IPv4

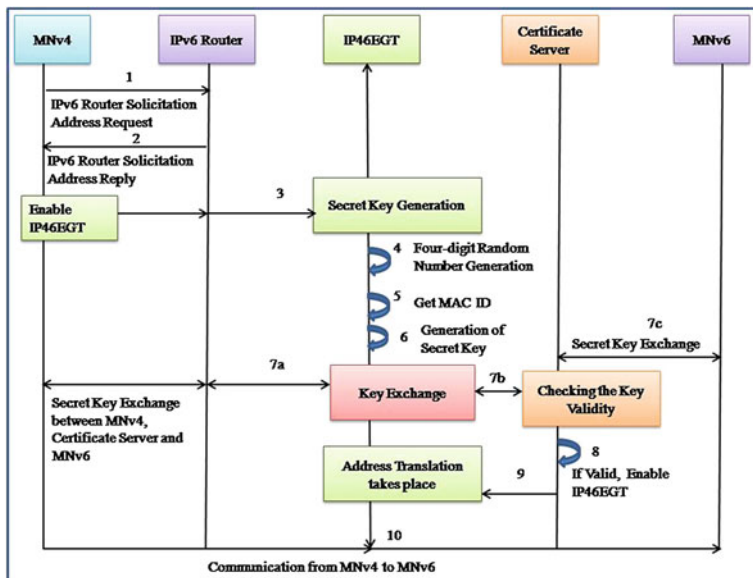


Fig. 4 Call flow sequence diagram from IPv4 to IPv6

4 Experimental Study

The main focus of the experimental study is to test the functionality of the IPv4/IPv6 address translation architecture and to measure the performance on a network. The experimental set-up consists of an IPv4 and IPv6-enabled network which are connected to a private Ethernet segment. The IPv6EGT acts as a gateway between IPv4 and IPv6 Ethernet segments. Ixia Traffic generators are used for generating the required bandwidth. The designed novel translator, an (IP46EGT), is simulated in the form of a PC-Emulator in which IPv4 nodes communicate with IPv6 mobile nodes, and IPv6 nodes communicate with IPv4 mobile nodes. The results of the study are tabulated and presented graphically.

5 Performance Analysis

5.1 Packet Reachability of Ping Packets

Packet Reachability of ping packets is calculated varying in size from 64 bytes to 1440 bytes. Table 1 shows the packet reachability of ping packets. The columns labeled PR-T and PR-TS show the packet reachability using the translator and the security-enabled translator, respectively. The packet reachability of ping packets is depicted in Fig. 5 in which X-axis in the graph represents the packet size in bytes and the Y-axis represents the time interval in microseconds. From the graph, it is observed that the reachability of ping packets using the security-enabled translator (PR-TS) is a little high, when compared to the reachability of packets without security.

5.2 Round-Trip Latency Using Security-Enabled Translator

The round-trip latency between IPv4 and IPv6 with security-enabled translator is tabulated in Table 2. The columns labeled IPv4-IPv6 and IPv6-IPv4 show the

Table 1 Packet reachability of ping packets

Packet size (bytes)	PR-TS (μ s)	PR-T (μ s)
64	27	20
128	30	23
256	32	25
512	32	25
1024	37	30
1440	47	37

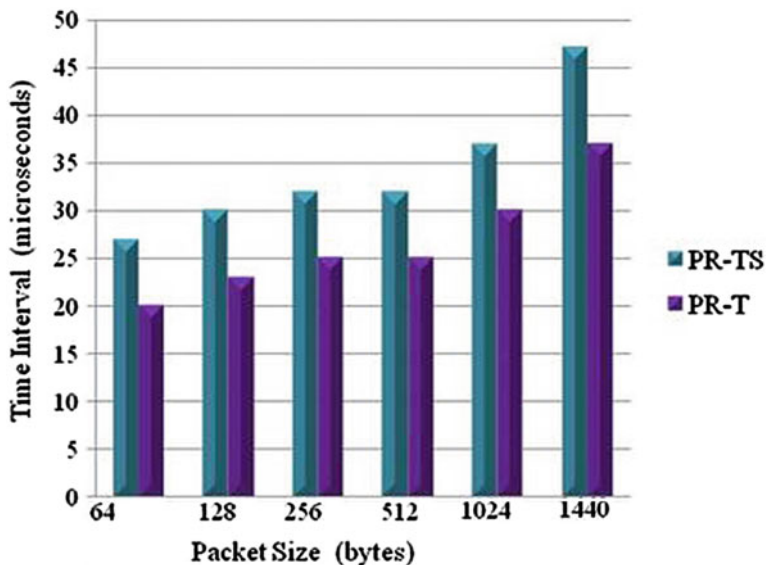


Fig. 5 Packet reachability of ping packets

Table 2 Round-trip latency using security-enabled translator

Packet size (bytes)	IPv4–IPv6 (μs)	IPv6–IPv4 (μs)	IPv4–IPv6 (RTL-S) (μs)	IPv6–IPv4 (RTL-S) (μs)
64	266	244	306	281
128	282	261	334	308
256	327	295	394	347
512	374	360	451	426
1024	587	572	676	651
1440	708	676	808	768

latency between two machines communicating directly observed to be normal as expected. The columns labeled RTL-S show the round-trip latency with security-enabled translator. The communication between the IPv4 and IPv6 nodes with security-enabled translator is depicted in Fig. 6, in which the X-axis in the graph represents the packet size in bytes and Y-axis represents the time interval in microseconds. It is observed that the communication from IPv6 to IPv4 is faster than IPv4 to IPv6 communication with the security-enabled translator.

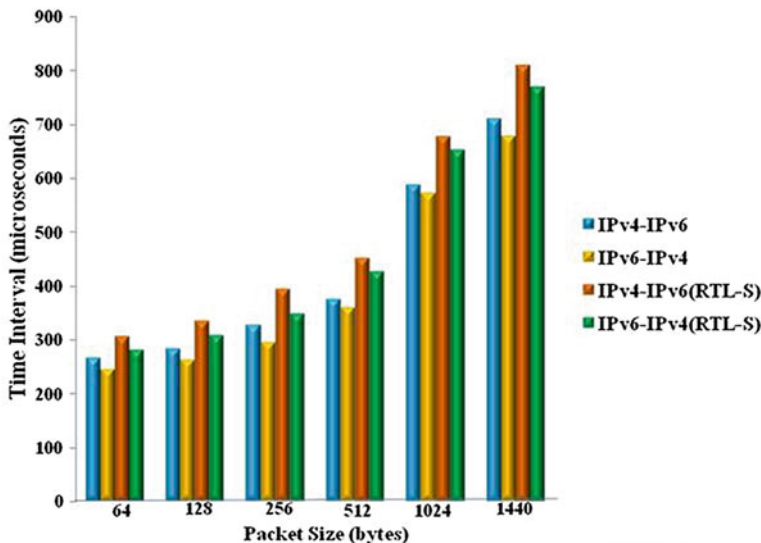


Fig. 6 Round-trip latency using security-enabled translator

6 Conclusion

Security has become a very important issue for the communication between IPv4 and IPv6 networks. Hence, three various levels of security namely MAC-level security, VPN-IPSec security and Certificate Level security are incorporated in the proposed architecture which provides data integrity, availability, authentication, and thereby provides end-to-end secure communication between the source and the destination. Packets which are intercepted by an attacker are dropped by VPN-IPSec-enabled hosts which provide connectionless integrity and authentication. The proposed architecture is tested, and the results are tabulated and graphically presented. Future work focuses on development of the same test bed in the form of security hardware emulation mechanism, combining tunneling and certificate binding to check the capacity handling of the proposed model, with respect to the security performance versus the number of requests.

Glossary

CGA	Cryptographically Generated Address—an address generated by replacing the 64-bit interface identifier of an IPv6 address with the cryptographic hash of the address owner's public key.
IP46EGT	IPv4/IPv6-Enabled Gateway Translator which translates IPv4 address into IPv6 address and IPv6 address into IPv4 address.

Load Balancer	A load balancer is a device which distributes network traffic or application traffic across a number of servers.
MAC	Media Access Control address is a hardware address that uniquely identifies each node of a network.
Round-Trip Latency	It is the time required for a packet to travel from a source node to a destination node and the time taken for an acknowledgment to be received.
VPN-IPSEC	It is used to secure site-to-site connectivity and protects IPv4 and IPv6 traffic as it communicates between end hosts or security gateways.

References

1. Abu, T.Z., Taha, Z., Syed, Z.: Deploying IPv6: Security and Future. International Journal of advanced studies in Computer Science and Engineering(IJASCSE), vol. 3 (2014)
2. Juniper Networks: An IPv6 Security Guide for U.S. Government Agencies. The IPv6 World Report Series, vol. 4 (2008)
3. Huiping, S., Junde, S., Zhong, C.: Survey of Authentication in Mobile IPv6 Network. In: IEEE CCNC Proceedings (2010)
4. Hero, M., Amirhossein, M., Hassan, K., Rosli, S.: Protection of Binding Update Message in Mobile IPv6. In: IEEE UKSim-AMSS 6th European Modelling Symposium (2012)
5. Yvette, E.G., Ronnie, D.C., Byungjoo, P.: A robust secured Mobile IPv6 mechanism for multimedia convergence services. Int. J. Multimedia Ubiquitous Eng. 6(4) (2011)
6. Frederic, B., Olivier, F., Isabelle, C., Ralph, D.: Automated and secure IPv6 configuration in enterprise networks. In: IEEE International Conference on Network and Service Management CNSM (2010)
7. Nazrul, M.A., Asrul, H.Y.: End to End IPsec Support across IPv4/IPv6 Translation Gateway. In: IEEE Second International Conference on Network Applications, Protocols and Services (2010)
8. Seewald, M.G.: Benefits of end-to-end IP for cyber and physical security. IEEE (2012)
9. Serap, A., Marcelo, M.: Challenges for the security analysis of next generation networks. Elsevier (2010)
10. Mahdi, A., Glenford, M., Aboubaker Raphael, P.: Providing Security in 4G Systems: Unveiling the Challenges. IEEE (2010)
11. Faisal, A.H., Chan, Y.Y., Khaled, S.: Secure framework for the return routability procedure in MIPv6. In: IEEE International Conference on Green Computing and Communications and IEEE Internet of Things and IEEE Cyber, Physical and Social Computing (2013)
12. Pekka, N., Andrei, G., Thomas, R.H.: Host Identity Protocol (HIP):Connectivity Mobility, Multi-Homing, Security, and Privacy over IPv4 and IPv6 Networks. IEEE(2010)
13. Abdur, R.C., Alan, S.: Securing IPv6 Network Infrastructure: A New Security Model. IEEE (2010)

Logistic Regression Learning Model for Handling Concept Drift with Unbalanced Data in Credit Card Fraud Detection System

Pallavi Kulkarni and Roshani Ade

Abstract Credit card is the well-accepted manner of remission in financial field. With the rising number of users across the globe, risks on usage of credit card have also been increased, where there is danger of stealing credit card details and committing frauds. Traditionally, machine learning area has been developing algorithms that have certain assumptions on underlying distribution of data, such as data should have predetermined and fixed distribution. Real-word situations are different than this constrained model; rather applications often face problems such as unbalanced data distribution. Additionally, data picked from non-stationary environments are also frequent that results in the sudden drifts in the concepts. These issues have been separately addressed by the researchers. This paper aims to propose a universal framework using logistic regression model that intelligently tackles issues in the incremental learning for the assessment of credit risks.

Keywords Logistic regression learning · Concept drift · Class imbalance · Credit card fraud detection

1 Introduction

The credit card fraud detection has long been appraised as a basic issue in the educational and commercial society. It has become an important point for enterprise communities to assess threats in credit, improve cash flow, cut down frauds, and perform important decision management activities. To earn profit in case of economic organizations, correct results must be obtained and that is critical in

P. Kulkarni (✉) · R. Ade
Dr. D.Y. Patil School of Engineering and Technology,
Savitribai Phule Pune University, Pune, India
e-mail: kulkarnipallavi4@gmail.com

R. Ade
e-mail: rosh513@gmail.com

commercial credit card fraud detection. There are various data mining techniques that can be applied to real-world problems like this mentioned earlier to get accurate analysis and scientific solution of that problem [1].

If learning from enormous data which proceeds into iterations is required, then incremental learning algorithms are preferred. Stream data mining requires a learner that can be incrementally modified to achieve the full advantage of novelty of data, while simultaneously maintaining performance of a learner on older data. Multiple classifier systems, also known as ensemble techniques of machine learning area are pretty popular to learn from non-stationary environment and incremental learning. Non-stationary environment is kind of an environment where sudden concept drift/change can occur. Credit card frauds are considered as rare since their occurrence is less as compared to normal transactions. So the corresponding data are unbalanced because it consists of fraudulent events and regular transactions. Over the time period, attackers are inventing various ideas to commit frauds in financial systems. In case of credit card transactions intruders may steal credentials related to credit cards, they may hack the confidential web sites of banks, the plunder credit card itself. Hence the idea is to develop an algorithmic framework that tackles the problem of credit card risk assessment in non-stationary environment while considering the unbalanced nature of input data in incremental fashion while maintaining efficiency and improvement over existing techniques [2, 3].

2 Related Work

The following section illustrates existing work done in this research field.

2.1 *Credit Card Threat Assessment*

The technique to detect credit card frauds usually applies some classification mechanism on similar data of previous consumer to look for a relation between the characteristics and probable points of failure. One important ingredient needed to achieve this goal is to find an accurate classifier that is able to categorize new applicants or existing consumers as loyal or fraudulent. Many statistical techniques and optimization models, like linear discriminant analysis logit analysis, probit analysis, linear programming, integer programming, k-nearest neighbor (KNN) came into picture. These methods are capable to evaluate threats in credit card system, but they have some drawbacks. There is still room to improve the capability to distinguish between faithful and delinquent customers [1, 4].

Researchers noticed the fact that transpiring artificial intelligence approaches like artificial neural networks, support vector machines are beneficial over statistical models and optimization methods to assess credit card faults. Since ensemble techniques combine two or more distinct learners, have proven higher accuracy to

predict risks than any specific methods. There is no doubt that credit card fault evaluation and modeling is one of the most critical themes in the area of economic risk assessment. In recent years, due to intense difficulties in commercial field, financial crises occurred, so more attention should be paid to credit threat assessment in banking and monetary service [5–10].

2.2 *Concept Drift*

In simpler terms, concept drift is change in class definition over the time. In such cases, it has been assumed that at time instance t , the algorithm A is stipulated with a group of labeled samples $\{X_0, \dots, X_t\}$, where X_i is considered as a v-dimensional vector and every sample has matching class label y_j . If an unclassified sample arrives at time $t + 1$ as X_{t+1} , then the algorithm is anticipated to supply a class label for X_{t+1} . One of the class labels is predicted for newly arrived instance, the actual label Y_{t+1} and a new testing sample X_{t+2} arrive so that one can continue with its testing. There is a data generating function which is responsible for creation of samples at a particular time instance and hence determining nature and distribution of data. In non-stationary environment, underlying and hidden distribution function (f_h) changes over time. Change in distribution function can be described using several methods [11–16].

2.3 *Combined Problem of Concept Drift with Unbalanced Data*

In real world, tremendous applications in non-stationary environments suffer from class imbalance. This is challenging situation in many real-world applications which lead to inaccurate results. Examples include climate monitoring, network intrusion detection system, spam e-mail identification, and finally credit card fraud detection. However, it has been observed that the joint problem of concept drift and unbalanced data has drawn little attention from researchers worldwide. Ensemble techniques are intelligent methods that are able to handle concept drift along with class imbalance. Learn++ family of algorithms has been progressed over the time and has been addressing various issues associated with incremental learning in each new version of Learn++. Among them, Learn++.CDS (Concept Drift with SMOTE) and Learn++.NIE (Non-stationary and Imbalanced Environments) are truly incremental i.e., one pass approaches that do not access previous data and also handle class imbalance problem well. Learn++.CDS applies SMOTE algorithm to balance the classes and its samples. It is integration of two algorithms, Learn++.NSE (Non-stationary Environment) and Synthetic Minority Oversampling TTechnique (SMOTE), which are existing approaches for handling concept drift and class

imbalance, respectively. Learn++.NIE is more efficient framework, which will be discussed in detail in next sections. Both the approaches are able to obtain new knowledge and preserve former knowledge about the environment, which is useful for recurring concepts (e.g., spiral dataset) [5, 6, 11, 15, 16]. A complete survey of concept drift, class imbalance and other incremental learning issues can be found in the review paper [13].

3 Methodology

This section describes a framework that addresses both the issues of stream data mining, i.e., concept drift and class imbalance for credit card threat assessment. For balancing the data, the proposed framework implements sub-ensembles with bagging along with alternate error measures. Bagging variation is a function that smartly tackles class imbalance, it neither generates synthetic samples nor faces under-sampling problem and hence is efficient in terms of performance.

Note that this framework is designed for handling unbalanced data. So obviously it works well when there is concept drift in majority and minority classes of unbalanced data. Figure 1 represents the basic architecture of the proposed framework.

This paper proposes an improved algorithmic system which smartly handles unbalanced data in non-stationary environment with enhanced accuracy in results. Instead of using f-measure as in earlier systems for weight modification, proposed framework uses mapping function which in turn is to be implemented by training Multi-Layer Perceptron neural network (MLP) with backpropagation algorithm. Figure 2 depicts the basic organization of mapping function. As proved in the experiments in next sections, use of MLP in a mapping function leads to knowledge transformation and improved accuracy in the results. This system can also be used for different applications which require handling of concept drift with unbalanced data like spam e-mail identification, student performance prediction, and weather forecast.

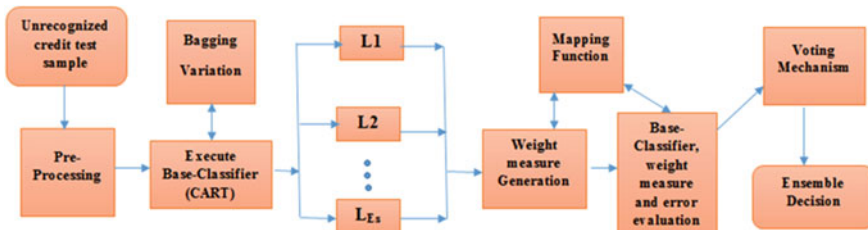


Fig. 1 Architecture of the proposed framework using logistic regression model



Fig. 2 Organization of mapping function

3.1 Proposed Framework Pseudocode

Assumptions of the system:

D: Dataset = { $D_1, D_{t+1}, \dots, D_t, \Phi$ }
T: Time required to process dataset = { T_0, T_1, \dots, t, Φ }
W: voting Weight of data set instances = { $W_1, W_{t+1}, \dots, W_{t+j}, \Phi$ }
H: Final Hypothesis generated :{ $H_1, H_{t+1}, \dots, H_t, \Phi$ }
E: Error values calculated after processing data instance = { $E_1, E_{t+1}, \dots, E_t, \Phi$ }
I= bagging variation for Class imbalance handling (D,C, H)
where D= dataset, C = classifier, H= hypothesis

Step 1: The bagging variation procedure pseudocode

```

for each classifier ( $L_1, L_2, \dots, L_E$ ) do
{
    1. Split data into majority and minority samples
    2. Randomly draw N/T patterns from chunk of majority samples
    3. Call base learner with minority data and part of majority data selected in
       previous phase
    4. Generate a Hypothesis
}
5. Calculate composite hypothesis

```

Step 2: Mapping Function pseudo code:

Update weight measures using MLP neural network for training and testing the algorithmic system

$$Q = (D_1, D_{t+1})$$

Where, Initial weight, $y = f(x)$

Where $f(x) = \langle s, x \rangle + b$

s and x slope and intercept of linear estimation

Step 3: Drift Handling procedure pseudo code:

1. Calculate standard error, epsilon
2. Calculate normalized error, beta
3. Compute weighted sum of errors using sigmoidal parameters 'a' and 'b'.

Output:

After performing these steps in incremental manner, the framework returns eventual hypothesis $H(x)$.

4 Results and Experiments

This section illustrates the experiments held and corresponding output. In the first experiment, data is partitioned into 11 approximately equal slices. In each phase, one chunk is chosen for testing on ad hoc basis, and remaining 9 splits are stipulated sequentially to the proposed framework. Depending on the size of data piece, system produces 4–5 standard error values. Here, these error values are averaged across all executions for simplicity. Table 1 summarizes standard and normalized error values obtained across executions of 11 data bags. The bag size is calculated using standard formula. It is as follows: bag size = no. of instances * m_bagsize-percent/100. Base classifier employed here is CART. PCA is another option. Ensemble size (Es) is another parameter which can change the performance of the system. Here, it is calculated at runtime depending on the data and its seed values. Table 2 summarizes overall performance of the algorithm in terms of accuracy and error. It has been observed that out of bag error for each iteration resulted as 0. This is absolutely good if we consider the nature of the data and system. While determining the performance prediction of any algorithm, the nature and size of the data plays an important role. This system uses German Credit dataset to solve credit risk evaluation problem.

This is the standard dataset downloaded from UCI repository having numerical instances suitable for incremental learning. It consists of 2 classes: good and bad which describe that the threat is present if the resulting sample is found to be bad. Statistical nature of this data has been tested and it is found that data is discrete.

Table 1 Averaged error values computed in executions of the framework

Data bag no.	Standard error (epsilon)	Normalized error (beta)
1	0.2594	0.9782
2	0.2452	1.0427
3	0.2224	1.1335
4	0.2657	0.9652
5	0.2837	0.9905
6	0.2169	1.1668
7	0.2744	0.9448
8	0.2743	0.9544
9	0.2020	1.0165
10	0.2436	1.0611
11	0.2031	1.0148

Table 2 Performance of the system

Mean absolute error	Relative absolute error	Accuracy	Kappa statistics
74.83 %	0.406	96.6243 %	0.2847

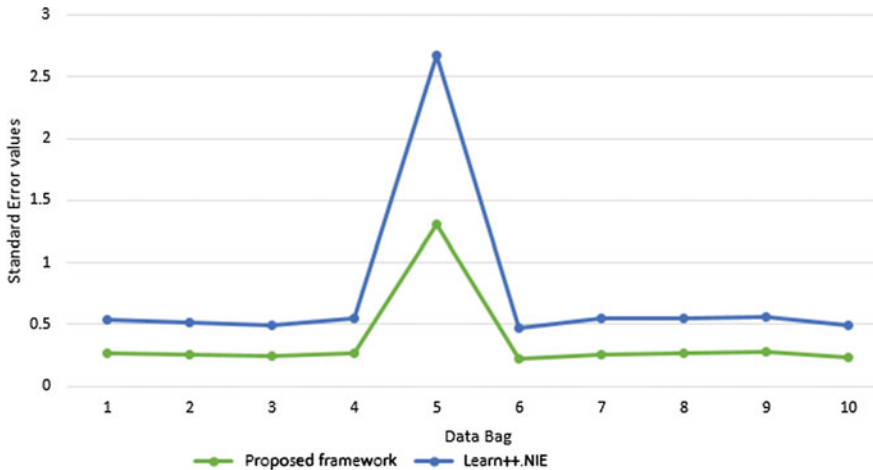


Fig. 3 Comparing performance of Learn+++.NIE with proposed framework

Note that data bag is the part of entire dataset used for rebalancing the dataset. Databags get generated while processing of the algorithm with the provided dataset. The major comparison of this proposed framework with existing technique (i.e., Learn+++.NIE) is depicted in Fig. 3 which shown below. It compares the averaged standard error values of Learn+++.NIE and proposed framework with respect to credit card fraud detection problem.

As the graph illustrates, the error is less if one looks at performance of proposed credit risk assessment framework. In other words, it performs better and overcomes limitations of existing techniques. As said earlier, it has major benefit of knowledge transformation since MLP is applied in proposed framework.

Pseudocode can be mapped to results in the sense that the error values represents drift in the system and data bag is used for rebalancing the data after applying it to Bagging variation procedure.

Since this framework uses base classifier as CART, the results can be represented in the form of decision tree whereby leaf nodes will show the classes and intermediate nodes and path toward leaf node is modeled as complete conditions for the risk assessment. Consider an example, attribute values obtained as: checking status is ≤ 0 , duration is ≤ 11 , foreign_worker = yes, existing credits ≤ 1 , property magnitude = real estate, then class = good. It means that if the fields are having these particular conditions as true, then the corresponding customer is good and there is no fraud in credit. Drawbacks of the proposed system is it becomes complex and takes more time to train and test the system as it uses neural network approach. Since this system addresses wide range of issues, this complexity is affordable for large scale applications (Fig. 4).

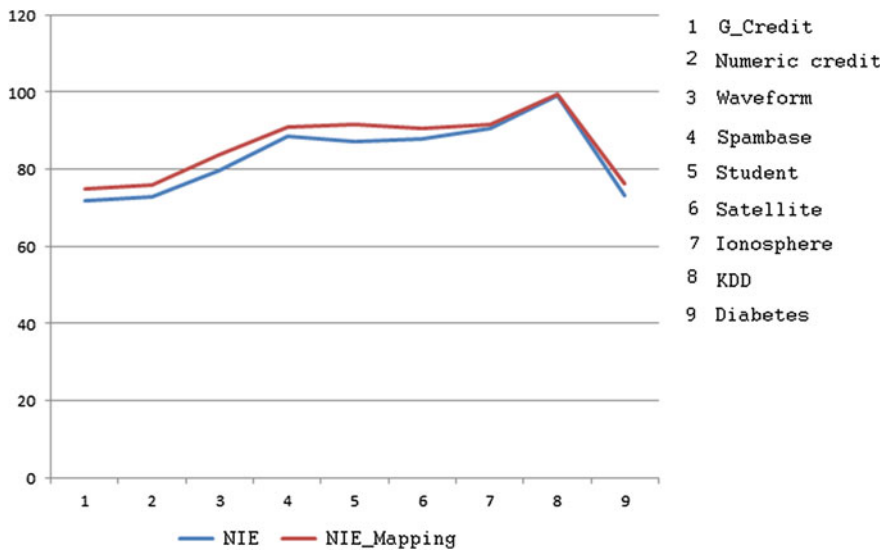


Fig. 4 Comparing performance of proposed framework on different real-time datasets

5 Conclusion and Future Enhancement

If the final objective of clever machine learning techniques is to be able to address a broad spectrum of real-world applications, then the necessity for a universal framework for learning from and adapting to environment where drift in concepts may occur and unbalanced data distribution is present can be exaggerated using the proposed algorithmic system. This system intelligently tackles challenges in incremental learning using logistic learning model of deep learning which in turn leads to knowledge transformation and preservation.

Scope of future work is leading toward a smart technique that will optimally discard drawbacks of the existing research and additionally assessment of these approaches on large scale, real-world applications consisting of formal statistical analyses of these systems, on certain non-stationary environments like Gaussian distribution drifts.

References

1. Wang, G., Ma, J.: A hybrid ensemble approach for enterprise credit risk assessment based on support vector machine. *Expert Syst. Appl.* **39**(5), 5325–5331 (2012)
2. Ditzler, G., Polikar, R.: Incremental learning of concept drift from streaming imbalanced data. *IEEE Trans. Knowled. Data Eng.* **25**(10), 2283–2301 (2013)
3. He, H., Chen, S., Li, K., Xin, X.: Incremental learning from stream data. *IEEE Trans. Neural Networks* **22**(12), 1901–1914 (2011)

4. Razavi-Far, R., Baraldi, P., Zio, E.: Dynamic weighting ensembles for incremental learning and diagnosing new concept class faults in nuclear power systems. *IEEE Trans. Nucl. Sci.* **59** (5), 2520–2530 (2012)
5. Littlestone, N., Warmuth, M.K.: The weighted majority algorithm. *Inf. Comput.* **108**(2), 212–261 (1994)
6. Kulkarni, P., Ade, R.: Prediction of student's performance based on incremental learning. *Int. J. Comput. Appl.* **99**(14), 10–16 (2014)
7. Yu, L., Wang, S., Keung Lai, K.: Credit risk assessment with a multistage neural network ensemble learning approach. *Expert Syst. Appl.* **34**(2), 1434–1444 (2008)
8. Denison, D.G.T., Mallick, B.K., Smith, A.F.M.: A bayesian CART algorithm. *Biometrika* **85** (2), 363–377 (1998)
9. Ade, R., Prashant D.: Efficient knowledge transformation for incremental learning and detection of new concept class in students classification system. In: *Information Systems Design and Intelligent Applications*, pp. 757–766. Springer, India (2015)
10. Ade, R., Deshmukh, P.R.: Classification of students using psychometric tests with the help of incremental Naïve Bayes algorithm. *Int. J. Comput. Appl.* **89**(14), 26–31 (2014)
11. Elwell, R., Polikar, R.: Incremental learning of concept drift in nonstationary environments. *IEEE Trans. Neural Networks* **22**(10), 1517–1531 (2011)
12. Ade, M.R., Pune, G., Deshmukh, P.R., Amravati, S.T.: Methods for incremental learning: a survey. *Int. J. Data Mining Knowled. Manage. Process* **3**(4), 119–125 (2013)
13. Pallavi, K., Ade, R.: Incremental learning from unbalanced data with concept class, concept drift and missing features: a review. *Int. J. Data Mining Knowled. Manage. Process* **4**(6) (2014)
14. Polikar, R., Upda, L., Upda, S.S., Honavar, V.: Learn++: An incremental learning algorithm for supervised neural networks. *IEEE Trans. Syst. Man Cybern. Part C: Appl. Rev.* **31**(4), 497–508 (2001)
15. Freund, Y., Schapire, R.E.: A decision-theoretic generalization of on-line learning and an application to boosting. In: *Computational learning theory*. Springer, Heidelberg, pp. 23–37 (1995)
16. Muhlbaier, M.D., Apostolos T., Polikar, R.: Learn. NC: combining ensemble of classifiers with dynamically weighted consult-and-vote for efficient incremental learning of new classes. *IEEE Trans. Neural Networks* **20**(1), 152–168 (2009)

Music Revolution Through Genetic Evolution Theory

Hemant Kumbhar, Suresh Limkar and Raj Kulkarni

Abstract “Sa_Re_Ga_Ma_Pa_Da_Ni_Sa” is the soul of Indian Music. As we play these 7 nodes at different frequency, different length, and at different reparations on one or more nodes, we will listen n number of feelings, expressions, and emotions. As musician can create such number of tones manually and get famous, all world remember such tone forever. As frequency, node duration, node energy are the parameters for creating different tones for 7 nodes, we can use genetic evolutionary theory for revolutionary musical tones evolution. In this paper, we are proposing novel method for musical tone generation using machine learning algorithm with the help of Narmour Structure Analysis.

Keywords Narmour structure • Genetic algorithm • Music evolution

1 Introduction

Fundamental elements of music are Rhythm, Dynamics, Melody, Harmony, Tone color, Texture, and Form. Rhythm we can say as beat, meter, tempo, and syncopation. Dynamics means forte, piano, crescendo, and decrescendo. Melody we may treat as pitch, theme, conjunct, and disjunct. Harmony can be related as chord, progression, consonance, dissonance, key, tonality, and atonality. Tone color is nothing but register, range, and instrumentation. While talk comes to Texture of music it may be listed as monophonic, homophonic, polyphonic, imitation, and counterpoint. Form of music we can play may be binary, ternary, or strophic. Basic musical concepts such as

H. Kumbhar (✉)

Department of Computer Engineering, SVPM's COE, Baramati, India
e-mail: hemant.kumbhar@gmail.com

S. Limkar

Department of Computer Engineering, AISSMS IOIT, Pune, India
e-mail: sureshlimkar@gmail.com

R. Kulkarni

Department of Computer Science Engineering, WIT, Solapur, India
e-mail: raj_joy@yahoo.com

semitones, note names, intervals, and enharmonic equivalence are on the assumption that the octave is divided into exactly twelve equal parts.

But what is the origin of music are seven swara's. Kharaj—SA represents Agni Deva), Rishabha—RE represents Brahamma Devta, Gandhar—GA represents Sarasvati, Madhyam—MA is God Mahadev, Panchama—PA is Goddess Laxmi, Dhaivata—DHA is Lord Ganesha, and Nishad—NI is Sun God are the seven basic swara in music. Music or song can be composed using these 7 swara, doing frequency changes to high, low or soft.

So musician has to do changes in frequency and length of nodes to compose different tones manually. Musician has to sit for long time to work on particular tone by applying all possible combinations of swara's with all probabilities of sequence, frequency changes and many more. So there is need of machine learning algorithm which will try such thousand of combinations on single click and in very short time to get good tone evolved.

A transformative way to one of the most difficult issues in computer evolved music demonstrating how gifted musical performers control sound properties like loudness of sound i.e., amplitude and time, for example, timing also hard so as to express their perspective of the passionate substance of musical pieces. Beginning with a gathering of sound recordings of genuine exhibitions, they are consecutive covering hereditary calculation so as to get computational models for distinctive parts of expressive execution. These models are utilized to naturally combine exhibitions with the timing and vitality expressiveness that portrays the music created by an expert performer. In particular, developmental calculation gives various potential focal points over other regulated learning calculations, for example, a technique for non-deterministically acquiring models catching diverse conceivable understandings of a musical piece [1].

In this paper, we are proposing a machine learning tool which will help us to evolve new tones from 7 basic swara described above with the help of Narmour structures [1] and Genetic evolutional theory [2–7].

2 Related Work

Since early 1980s, evolutionary algorithms have been used in a number of musical applications like sound synthesis and composition to computational musicology. A Life model for evolutionary algorithms studied for the development of musical knowledge, rooted on the problem of beat synchronization, knowledge evolution, and emotional systems [7]. Machine Learning algorithms are available which can be used for evolution [8, 9]. In [10], an artificial life system for music composition is used as evolving ecology of sonic entities populate a virtual world and their genetic representation permits the creatures to make and listen to sounds. In [11], voice-based rhythm game for training speech motor skills of children with speech disorders are also suggested.

A heuristic-based generic approach for extracting automatically high-level music descriptors from acoustic signals suggested in [12] which uses genetic approach for optimized search. By making use of sound to assist in survival [13], virtual agents evolve implicitly to try to maintain the interest of the human audience. Some work also done in the era of identifying performers from their playing styles by finding out parameters such as pitch, timing, amplitude at an inter-note level, and at an intra-note level [14].

Very promising work found in this area is a computational model which predicts how a particular note in a particular context should be played as per the duration like longer or shorter than its nominal duration [1]; they found out a set of acoustic features from the recordings resulting in a symbolic representation of the performed pieces. These features are low-level descriptors like energy and fundamental frequencies. In [15], two way mismatch method is used for fundamental frequency estimation of musical signals. In [16], onset detection algorithm for pitched material which uses the stability of a pitch percept as the defining property of a sound event is suggested. For marking of structural units, musical punctuation for the marking of melodic structure by commas inserted at the boundaries that separate small structural units is found [17]. Converting a piece of music into an appropriate arrangement for guitar by the purpose of effectively differentiate between candidate arrangements on the basis of both faithfulness to the original piece and on playability is achieved in [5].

Expressive performance model using sequential covering genetic algorithms is suggested in [1, 18–21]. This works on generating rule for predicting next note duration or other features mentioned above to make music more expressive. GenJam short for Genetic Jammer is an evolutionary computation-based, real-time interactive jazz improvisation agent which improvises spontaneous autonomous solos and performs interactive and collective improvisation with a human performer [4]. A musical computer system for generating synthesizer sounds and musical melodies by means of the multi-agent and interacts with human piano players in real-time is suggested in [22].

Genetic algorithms are used as supervised concept learning for a symbolic learning task [2]. Also use of genetic algorithms as a key element in the design and implementation of robust concept learning systems is done [3]. A simple genetic algorithm for music generation by means of algorithmic information theory proposes the use of this distance as a fitness function which may be used by genetic algorithms [6]. In [23] proposed a method to generate emotional music using interactive Genetic Algorithm in which users can get their satisfied emotional, although they have no profound knowledge for composition. In [24] proposed a Genetic Programming method for musical sound analysis which develops a classifier to distinguish between five musical instruments using only simple arithmetic and Boolean operators with 95 features as terminals.

In this paper, we proposed an abstract level music tone generation using seven rhythms introduces in beginning and using Narmour structures, by applying Narmour rules generation using genetic algorithm. Here we are generating tone using jFuge library [25], which gives easiest and very simple way to generate and play tones made up of seven swara with different duration.

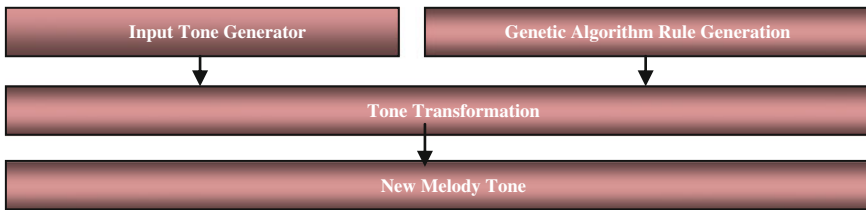


Fig. 1 Proposed system

3 Proposed System

The proposed work shown in Fig. 1 defines a process and generates a random tone with the help of seven swara. This tone is such that each swara applying random duration of playing that swara. This generated tone is treated as input tone to the proposed system. Proposed system applies genetic algorithm and with produces the best rule to apply on input tone. This rule will be applied for each consecutive pair of swara from input tone and suggest the change in duration of that tone like lengthen or shorten the duration by half or one forth etc.

4 Implementation Details

Tone Description We followed the tone description of Narmour structure as it is [1]. Description is as follows. Figure 2 shows how rhythms can be shown on story board and duration, frequency of each node. Detail description is as given in Table 1.

Explanation of above hypothesis is as given in below Fig. 3 [1]. Bit encoding of hypothesis is the base input for our proposed system. Rafael Ramirez [1] proposed the above Narmour structure and hypothesis as “If previous duration is this and pitch is this, then what to do with next rhythm.” They are doing the estimation of duration, frequency, strength, and pitch as a low-level descriptor [1]. Here we are suggesting the different way to find the above value of descriptor. Jfuge is the java library [25] which allows us to treat these rhythms as simple English words like C as Sa, D as Re, E as Ga, F as Ma, G as Pa, A as Da, and B as Ni. And if we write Cq

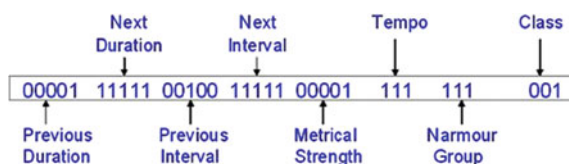


Fig. 2 Hypothesis of tone [1]

Table 1 Parameter setting for genetic algorithm

Parameter name	Value
Number of generations	10
Population size	10
Crossover rate	0.6
Mutation rate	0.05

Fig. 3 Hypothesis bit encoding [1]

Attribute	Bit Meaning
Previous duration	<i>Bit 1</i> : much shorter than current note <i>Bit 2</i> : shorter than current note <i>Bit 3</i> : same than current note <i>Bit 4</i> : longer than current note <i>Bit 5</i> : much longer than current note
Next duration	<i>Bit 1</i> : much shorter than current note <i>Bit 2</i> : shorter than current note <i>Bit 3</i> : same than current note <i>Bit 4</i> : longer than current note <i>Bit 5</i> : much longer than current note
Previous interval	<i>Bit 1</i> : much lower than current note <i>Bit 2</i> : lower than current note <i>Bit 3</i> : same than current note <i>Bit 4</i> : higher than current note <i>Bit 5</i> : much higher than current note
Next interval	<i>Bit 1</i> : much lower than current note <i>Bit 2</i> : lower than current note <i>Bit 3</i> : same than current note <i>Bit 4</i> : higher than current note <i>Bit 5</i> : much higher than current note
Metrical strength	<i>Bit 1</i> : very weak <i>Bit 2</i> : weak <i>Bit 3</i> : medium <i>Bit 4</i> : strong <i>Bit 5</i> : very strong
Tempo	<i>Bit 1</i> : slow <i>Bit 2</i> : nominal <i>Bit 3</i> : fast
Narmour group	000 = "P" group 001 = "D" group 010 = "ID" group 011 = "IP" group 100 = "VP" group 101 = "R" group 110 = "IR" group 111 = "VR" group
Class	<i>Bit 1</i> : shorten/delay/soft/ornamentation <i>Bit 2</i> : same-duration/same-onset/medium/none <i>Bit 3</i> : lengthen/advance/loud/none

it means Sa with Quarter duration. So we used the duration changing factor only as change in music performance as per the genetic algorithms optimized rule as explained in next section.

Tone Generator For Tone generation, random function is used to generate each swara's bit encoding as per the hypothesis bit encoding mentioned in Fig. 3.

$$F(x) = \text{Rand}(n) \quad (1)$$

where $F(x)$ is the function which will generate n number of bits with random values 1 or 0 in Eq. (1) as per the guided in Fig. 3.

Genetic Evolution algorithms for rule generation

```
RuleCreator(generation, populationSize, crossoverRate, mutatePercent)
{
```

1. Generate in Initial Population populationSize number of rules
2. Calculate fitness as

fit = $tp^{1.15}/(tp + fp)$ where tp = true positive and fp = false positive.

3. Sort Initial population in descending of fitness value of each rule.
4. Generate next product with following steps.

Tournament selection method,

Single point crossover,

Single point mutation

5. Display Best Rules.

Tone Transformation For tone transformation create input tone randomly. Then apply best rule generated by genetic algorithm as per the Narmour class given in Fig. 3. Rule Evolved in genetic algorithm will direct about what should be the next swara's duration i.e., shorten or lengthen or keep same.

New Melody Construction As per the modification in input tone and genetic rule save the modified tone as a new Melody composition.

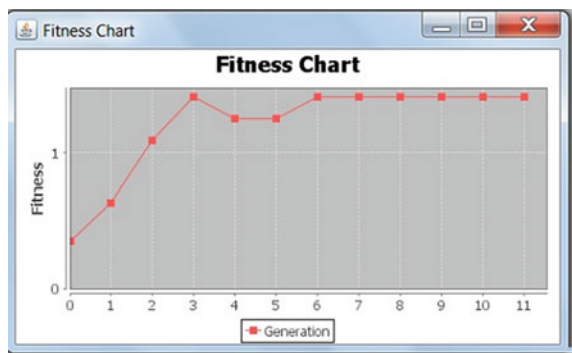
5 Results

- (a) Fitness chart
- (b) Rule generation and tone modification

Table 1 shows parameter setting for genetic algorithm. In Table 2, rule is presented as decimal values like 31 represent decimal value of five bit duration representation as per Fig. 3. Figure 4 shows results of how genetic algorithm improves fitness of rule after every new generation and some level it remains steady stating that this is the best rule for given parameter settings.

Table 2 Tone modification

Original tone	Cn Dw Fi Es Gi Ax Bh Ct
Best rule evolved	31 31 2 8 2 2 2 2
Modified tone	Cw Dw Fi Es Gi Ax Bh Ct

Fig. 4 Fitness chart

6 Conclusions

The results of the conducted experiments were satisfactory and encouraging. It is first step toward melody construction through genetic evolution to modify duration of rhythms only. This modification is done at software abstraction level only using jfuge library. As a future work, we may extend this work for modifying other low-level descriptors and putting music experts intelligence in musical revolution through genetic evolution theory.

References

1. Rafael, R., Esteban, M., Xavier, S.: A rule-based evolutionary approach to music. *IEEE Trans. Evol. Comput.* **16**(1) (2012)
2. Spears, W.M., De Jong, K.A.: Using genetic algorithms for supervised concept learning
3. De Jong, K.A., Spears, W.M., Gordon, D.F.: Using genetic algorithms for concept learning
4. Biles, J.A.: GenJam: Evolutionary Computation Gets a Gig. In: Proceedings of the 2002 Conference for Information Technology Curriculum. Rochester, New York
5. Tuohy, D.R., Potter, W.D.: GA-based Music Arranging for Guitar
6. Alfonseca, M., Univ. Autonoma de Madrid, Madrid, Cebrian, M., Ortega, A.A.: Simple genetic algorithm for music generation by means of algorithmic information theory. In: IEEE Congress on Evolutionary Computation, CEC 2007
7. Suresh, L. et al.: Genetic Algorithm: Paradigm Shift Over a Traditional Approach of Timetable Scheduling. In: Proceedings of the 3rd International Conference on Frontiers of Intelligent Computing: Theory and Applications (FICTA) 2014, Advances in Intelligent Systems and Computing, Vol. 327, pp. 771–780 (2015)
8. Eduardo, C., Marcelo, G., Martins, J.M., Miranda, E.R.: Computational musicology: an artificial life approach. Future Music Lab
9. Goldberg, D.E.: *Genetic Algorithms in Search, Optimization, and Machine Learning*. Addison-Wesley, Reading, MA (1989)
10. Hue, X.: *Genetic algorithms for optimization: Background and applications*. Edinburgh Parallel Comput. Centre, Univ. Edinburgh, Edinburgh, U.K., Ver 1.0, Feb. 1997
11. Eden: *An evolutionary sonic ecosystem*. Springer-verlag, Berlin (2001)

12. Umanski, D., Kogovšek, D., Ozbič, M., Schiller, N.O.: Development of a voice-based rhythm game for training speech motor skills of children with speech disorders. In: Proceedings 8th International Conference Disability, Virtual Reality and Associated Technologies, Sept. 2010 ICDVRAT. ISBN:978 07049 15022
13. François, P., Aymeric, Z.: Evolving automatically high-level music descriptors from acoustic signals. In: International Symposium on Computer Music Modeling and Retrieval (CMMR2003). Springer Verlag, L NCS, 2771 (2003)
14. McCormack, J.: Evolving Sonic Ecosystems. In: Evolving Sonic Ecosystems, Kybernetes (2003)
15. Rafael, R., Esteban, M., Antonio P., Emilia, G., Xavier, S.: Performance-based interpreter identification in saxophone audio recordings. IEEE Trans. Circuits Systems Video Technol **17** (3) (2007)
16. Maher, R.C., Beauchamp, J.W.: Fundamental frequency estimation of musical signals using a two-way mismatch procedure. J. Acoust. Soc. Am. **95**(4) (1994)
17. Nick, C.: Using a pitch detector for onset detection. University of Cambridge, Queen Mary, University of London (2005)
18. Anders, F., Roberto, B., Lars, F., Johan, S.: Musical punctuation on the microlevel: automatic identification and performance of small melodic units. J. New Music Research, Sweden
19. Rafael, R., Emilia, G., Veronica, V., Montserrat, P., Amaury, H., Esteban, M.: Modeling expressive music performance in bassoon audio recordings. ICIC 2006, LNCIS 345, pp. 951–957. Springer-Verlag, Berlin Heidelberg (2006)
20. Rafael, R., Amaury, H.: Inducing a generative expressive performance model using a sequential-covering genetic Algorithm. GECCO'07July 7–11, 2007. ACM 978-1-59593-697-4/07/0007
21. Rafael, R., Amaury, H.: Understanding Expressive Music Performance Using Genetic Algorithms
22. Róisín, L., Jacqueline, W., Michael, O., McDermott, J.: Genetic Programming for Musical Sound Analysis
23. Daichi, A., Hitoshi, I.: Real-time musical interaction between musician and multi-agent system. PhD. 8th Generative Art Conference GA2005
24. Hua, Z., Hefei Shangfei, W., Zhen W.: Emotional Music Generation Using Interactive Genetic Algorithm, Computer Aided Systems Theory. In: EUROCAST 2011, Department of Computer Science Univ. of Sci. & Technol. of China. Springer
25. Loughran, R., Jacqueline, W., O'Neill, M., Mc Dermott, J.: Genetic Programming for Musical Sound Analysis”
26. Java Music Library: <http://www.jfugue.org/>

Low-Cost Supply Chain Management and Value Chain Management with Real-Time Advance Inexpensive Network Computing

K. Rajasekhar and Niraj Upadhyaya

Abstract For increased profitability and sustainability, the E-commerce systems should be backed by efficient and effective Supply Chain Management and Value Chain Management Systems. However, it is very difficult to build such systems as the functions are complex and systems are CAPEX and OPEX intensive. To overcome these problems, an inexpensive supply chain management system was designed and developed successfully with Real-time Advance Inexpensive Network Computing. The results of the research work are presented in this article.

Keywords Computing intelligence • Mobile computing • E-commerce • Value chain management • Supply chain management • RAIN computing

1 Introduction

E-commerce provides significant scope for economic development [1]. For success and sustainability in the present competitive world, the E-commerce systems should be backed by robust, efficient, and effective Supply Chain Management (SCM) and Value Chain Management Systems (VCM). At present, these systems are highly complex, and CAPEX intensive as they depended heavily on solutions which consume heavily the Datacenter server resources. Timely flow of information from each of the node in the supply chain and value chain is very vital for success of any SCM and VCM. Due to last-mile problems, authentic information may not flow

K. Rajasekhar (✉)

NIC, Department of Electronics and Information Technology, MCIT, Government of India,
APSC, Hyderabad 500063, Andhra Pradesh, India
e-mail: sekhar@nic.in

N. Upadhyaya

J.B. Institute of Engineering & Technology, Yenkapally, Moinabad Mandal, R.R. District,
Hyderabad, India
e-mail: nirajup@ieee.org

in-time from the remote nodes to the key stakeholders. Even if flows, solution method is most of the times expensive.

1.1 Article Content

The article has eight parts. Section 1 is introduction, Sect. 2 is research objective and the survey of related work done in the field, Sect. 3 is need for Intelligence computing emphasized and intelligent computing framework defined for a typical SCM and VCM systems. In Sect. 4, the cluster Architecture described, in Sect. 5, the research project practical implementation details were documented, in Sect. 6, the results of research were discussed. The last section is acknowledgement and references.

2 Research Objective

Objective is to develop a low-cost Value chain and Supply chain management to improve the efficiency of E-commerce enterprise systems with device-based computing. Solution should be reliable and sustainable with low OPEX and no CAPEX.

2.1 Study of Related Work Done

For solving SCM and VCM problems, little research has been done so far in the context of device-based computing. Hwang et al., proposed a network-based collaborative intelligent SCM [2]. Lee et al., have adopted a project management approach for building VCM system [3]. Value Chain Network was proposed in the networked economy by Yang et al. [4]. All these systems proposed by earlier researchers have merits but their CAPEX and associated OPEX are more due to system overheads. Even the NFC-based transactions also depended on Cloud or hybrid cloud or mobile cum cloud computing architectures so far.

3 Importance of Low-Cost Supply Chain and Value Chains

In the information era, the entire business processes have become complex, and capital intensive and oriented toward centralized mass production systems. However, production by masses is the need of the hour in countries like India to manage un-employment problems. However, production by masses should ensure

quality and cost effectiveness, so as to compete with organizations that have become virtual and rapidly expanding [5]. The mass production items are usually leveraged on economy of scale. Wherever customized goods or services are required, the production by masses is preferable. However, most of the man-made products are highly expensive. So low-cost value chain and supply chain solutions are very much preferable to ensure sustainability of systems of production by masses. For this, we have devised a standard framework for defining the stages and processes of supply chain and value chain systems.

3.1 Standard Framework

The devised supply chain and value framework has around 12 stages for a typical value addition process at a location. If there are more than one value addition processes or functions and if there are more than one supply chain node, which will typically be the case, if the number of products and ingredients are more than what are indicated in Table 1, then the number of stages shall increase correspondingly. So the rows can be added or deleted depending on the exact processes in value chain and the intermediaries in the supply chain.

3.2 Constraints

For standardization, we have considered seven basic constraints at each stage. These are labeled as C1, C2, C3, C4, C5, C6, and C7.

C1. The Quality Q_i of the process or the function f_i should be maximum while producing or processing material m_i at location l_i . i.e., $OQ_i(m_i, f_i, l_i) = \text{Maximum}$.

C2. The Cost C_i of value addition process or function f_i should be minimum while processing, or for performing function f_i with respect to material m_i , at location l_i . i.e., $OC_i(m_i, f_i, l_i) = \text{Minimum}$.

C3. The Duration D_i of execution of function or value addition process f_i should be minimum or optimum while processing, servicing product or material m_i at location l_i . i.e., $OD_i(m_i, f_i, l_i) = \text{Minimum}$.

C4. The processes and functions should get performed as per the fixed schedule, timeliness is important to avoid delays of entire supply chain or value chain, so the exact Start Time T_i of execution of function f_i on material m_i at location l_i should be at predetermined time t_i .

i.e., $OT_i(m_i, f_i, l_i) = t_i$.

C5. At each stage there should be proper reconciliation of input and the output, so that errors can be easily detected. The Reconciliation factor R_i can be defined as the outcome of stage i divided by the input at stage i . The Reconciliation factor R_i at

Table 1 Standard framework for SCM and VCM

Sl. no	Function/process	Parameters ^a	Optimization condition
1	Raw material indenting	$Li, Fi, Si, m_i, Ci, Di = (ti-ti+1), f_j, l_j$	$OQi(mi,fi,li)=max; OCi(mi,fi,li) =min; ODi(mi,fi,li)=min; OTi(mi,fi,li)=ti; ORi(mi,fi,li)>0;$ Preceding Process sequence no < si Succeeding Process Sequence No > or = to si
2	Raw material procurement	$Li+1, Fi+1, Si+1, Mi+1, Ci+1, Di+1, Fj+1, Lj+1$	$OQi+1=max; OCi+1=min; ODi+1(min); OTi=Ti+1; ORi+1>0$
3	Raw material quality control	$Li+2, fi+2, si+2, mi+2, ci+2, Di+2, f_j+2, l_j+2$	$OQi+2=max; OCi+2=min; ODi+2(min); OTi+2=Ti+2; ORi+2>0$
4	Production scheduling	$Li+3, Fi+3, Si+3, Mi+3, Ci+3, Di+3, f_j+3, l_j+3$	$OQi+3=max; OCi+3=min; ODi+3(min); OTi+3=Ti+3; ORi+3>0$
5	Value addition-1, 2, 3 to n processes	$Li+4, fi+4, si+4, mi+4, ci+4, Di+4, f_j+4, l_j+4$	$OQi+4=max; OCi+4=min; ODi+4(min); OTi+5=Ti+4; ORi+4>0$
6	Value addition last process	$Li+5, fi+5, si+5, mi+5, ci+5, Di+5, f_j+5, l_j+5$	$OQi+5=max; OCi+5=min; ODi+5(min); OTi=Ti+5; ORi+5>0$
7	External quality control of value addition end process	$Li+6, fi+6, si+6, mi+6, ci+6, Di+6, f_j+6, l_j+6$	$OQi+6=max; OCi+6=min; ODi+6(min); OTi=Ti+6; ORi+6>0$
8	Storage	$Li+7, fi+7, si+7, mi+7, ci+7, Di+7, f_j+7, l_j+7$	$OQi+7=max; OCi+7=min; ODi+7(min); OTi-Ti+7; ORi+7>0$
9	Transport documentation	$Li+8, fi+8, si+8, mi+8, ci+8, Di+8, f_j+8, l_j+8$	$OQi+8=max; OCi+8=min; ODi+8(min); OTi=Ti+8; ORi+8>0$
10	Transport	$Li+9, fi+9, si+9, mi+9, ci+9, Di+9, f_j+9, l_j+9$	$OQi+9=max; OCi+9=min; ODi+9(min); OTi=Ti+9; ORi+9>0$
11	Receiving material at node 1, 2, 3, n of supply chain	$Li+10, fi+10, si+10, Mi+10, Ci+10, Di+10, f_j+10, l_j+0$	$OQi+10=max; OCi+10=min; ODi+10(min); OTi=Ti+10; ORi+10>0$
12	Acknowledgement and reconciliation	$Li+11, fi+11, si+11, Mi+11, Ci+11, Di+11, f_j+11, Lj+11$	$OQi+11=max; OCi+11=min; ODi+11(min); OTi=Ti+11; ORi+11>0$

^aParameters for a given process i are: Location id = li; Process or Function Id = fi; Sequence Number = si; Product /Material Id = mi; Cost = Ci; Duration = Di; Start time = ti

location li for manufacture or service material mi by process or function fi should be more than 0. So that at every stage some positive outcome comes, losses, shortages, faults etc., get detected. i.e., $ORi(mi,fi,li) > 0$.

C6. Successful execution of each function at each location in isolation alone is not sufficient, each process should be executed in synchronization with other-related processes i.e., preceding, succeeding, and also other simultaneous processes. So process fi should be executed only after execution of all preceding processes. i.e., Preceding Process(es) sequence nos < si.

C7. The processes slated for execution, later than process f_i , should not be executed before process f_i . So all the Succeeding Process Sequence Number related to manufacturing of material m_i at location l_i , at a particular sequence $S_i + 1 > or = to S_i$.

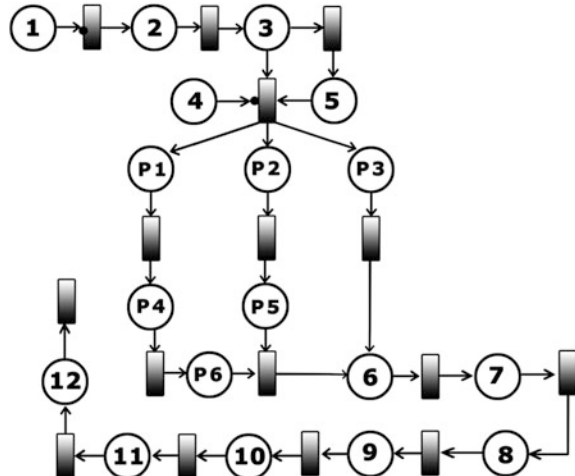
3.3 Intelligent RAIN Droplet Model

To eliminate or minimize CAPEX and OPEX by eliminating the usage of Datacenter and Desktop and Laptops and maximize the utilization of mobile devices, we have devised Real-time Advanced Inexpensive Network (RAIN) Computing [6]. Computation takes place exclusively with intelligently linked mobile devices, called droplets in RAIN computing.

The performance of real-time systems can be modeled with a Reflective and Time Petri Net (TPN), Wang et al., [7] Similarly, the Intelligence and Smartness of RAIN computing can be modeled with appropriate TPN. For example, RAIN droplet can be treated as places cum transition, the network connecting them can be treated as Arcs connecting them as transitions. The Standard functionality embedded in each droplet controls the firing and the logical workflow in the Petrinet. We have identified twelve stages in a typical SCM and VCM. In Fig. 1, the Petrinet model of such a SCM and VCM has been depicted. As shown in figure, some of the processes can happen in parallel.

In Fig. 1, the petrinet modeled 12 stages of a typical intelligent, SCM and VCM
 1. Raw Material Indenting; 2. Raw Material Procurement; 3. Raw Material Quality Control; 4. Production Scheduling; 5. Value Addition Processes (P1, P2, P3, P4, P5 and P6); 6. Value Addition last process; 7. External Quality Control of Value

Fig. 1 Petrinet model of an intelligent SCM and VCM



Addition End process; 8. Storage; 9. Transport documentation; 10. Transport; 11. Receiving Material at Node 1, 2, 3, n of Supply Chain; 12. Acknowledgement and Reconciliation.

4 Cluster Architecture

In the legacy enterprise Value Chain and Supply Chain Management Solutions, the value chain or supply chain framework gets embedded centrally. Such centralized architecture though easy to implement requires overheads. Therefore, for implementing the low-cost SCM and VCM, RAIN computation-based system has been devised.

In the centralized architecture, all the nodes communicate with the centralized unit. Best suited to the datacenter infrastructure-based legacy VCM and SCM. However, their CAPEX and OPEX are high. So RAIN computing-based SCM and VCM has been devised. With RAIN computing, there is no need to centralize the intelligence. So intelligence is smartly distributed into clusters. So with a cluster-based architecture, an Intelligent, and Smart, RAIN computing-based SCM and VCM are devised.

4.1 *Working of RAIN SCM and VCM*

In this, all the related functions and facilities are grouped into a cluster. In each cluster, the RAIN nodes accomplish, distinct, and well-defined tasks. The tasks are defined based on the nearest functions of the nearest facility.

For example, RAIN node $R_i(l,m,f)$ is dedicated to capture the information generated at a facility located at L_i , performing function or process f_i -related material m_i . RAIN node $R(i,l,m,f)$ shall also have the basic intelligence to verify the effectiveness and efficiency of the information captured as shown in Fig. 2. i.e., Node $R(i,l,m,f)$ acts intelligently by verifying all the constraints C_i are true besides efficiency and cost effectiveness.

So this Rain computing system ensures that all constraints at a Node are satisfied before proceeding to subsequent stage(s) in the Supply Chain or Value Chain. i.e., after verification of all constraints at a node, it shall send the information to facilitate reconciliation and trigger subsequent processes to the corresponding RAIN nodes within the cluster.



Fig. 2 Typical RAIN computing node for SCM and VCM

4.2 *Linkages Among Clusters*

When all the functions at a cluster are complete, then one of the nodes, associated with the last process, shall trigger alert to the RAIN node associated with the first process of the next logically linked cluster. Thus without overheads, the intelligence built into the RAIN nodes for efficient and effective SCM and VCM.

5 Research Project Implementation

A typical supply chain management system for a group of around 300 users has been devised for the purpose of indenting and supply of foods to the Child Development Project Offices (CDPOs) in Andhra Pradesh, India, with a Cloud Computing System located at the Data Center with three virtual Servers. In this legacy web-based system, one of the server was used as application server, another as RDBMS server and the third as Messaging Server connected to the SMS Gateway. The setup was

installed behind typical firewalls as per the data center standards. The system was implemented successfully using Cloud cum Mobile Hybrid architecture as it is difficult to install desktop systems at the remote locations. As all 300 group members have mobile phones, with the help of these 300 phones, RAIN computing-based SCM and VCM solution was devised, which has the same functionality as the earlier legacy system. Now, this group has become the test bed to compare the performance of SCM and VCM solutions based on 1. Mobile Cloud Computing and 2. RAIN computing systems. The results based on the feedback from the end users documented and analyzed.

5.1 Research Results

JVM and Android-based pilot Real-time Advanced Inexpensive Networks were created with a small number of mobiles taking into consideration the local regulations of Telecom Regulatory Authority of India TRAI (Tables 2, 3, and 4, Fig. 3).

Table 2 performance metrics—mobile cloud computing system and RAIN computing system

Sl. no.	Operational parameters	Cloud computing system—score in seconds	RAIN computing system—in seconds
1	Indenting	70	65
2	Editing/correcting	30	25
3	Transport alert	30	30
4	Acknowledgment (ACK)	5	8
5	Filtering wrong information	75	79

Table 3 Financial parameters

Sl. no.	Financial parameters	Cloud computing system	RAIN computing system
1	CAPEX	Rs. 2,00,000/Anum	Rs. 12,000/Anum
2	OPEX	Rs. 3,00,000/Anum	Rs. 3000/anum

Table 4 Security features

Sl. no.	Security parameters	Cloud computing system	RAIN computing system
1	Role base authentication	Possible	Possible
2	Operator alerts (SMS gateway, RDBMS)	Required	Not required
3	DOS, DDOS attacks	More	Less

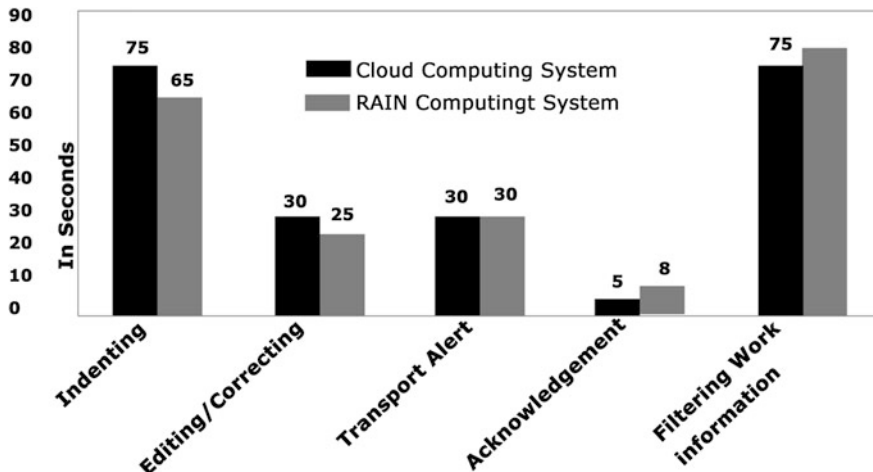


Fig. 3 Performance metrics—mobile cloud computing system and RAIN computing system

5.2 Analysis of the Results

The series 2 corresponds to the system metrics of SCM and VCM with RAIN computing with 300 nodes. The Series 1 is the results of the metrics of the same SCM and VCM with legacy mobile Cloud computing System (Fig. 4).

6 Discussion

RAIN computing-based SCM and VCM plays a vital and important role especially in applications where resources and last-mile problems are major. SCM and VCM are vital for success of E-commerce Solutions. So this generic supply chain and value chain management framework take into consideration all the standard value chain and supply chain functions and processes. It also ensures timeliness of execution under the constraints of quality and costs. The system devised is also scalable so more supply chain nodes or value chain processes or products or materials can be easily added or subtracted as per requirements. The framework also ensures synchronization of the processes and ensures their correct sequence of execution. In case of errors, the alternative paths for supply chain and processes for value chain are also defined to ensure reliability, so that expired items can be rejected, and incase of accidents or sudden escalation of prices in a particular mode of transport, then alternative modes can be adopted by choosing alternative nodes, or when material goes down re-order level, at a value chain, indents get raised. Thus the framework facilitates intelligently linking the processes/functions/facilities/services of one location to those of others and defines priorities and alternative paths.

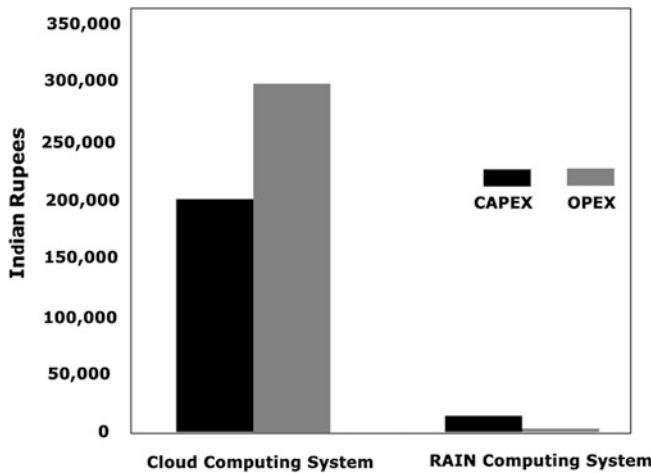


Fig. 4 Financial parameters

The cost of material and services vary with time and location, the performance of processes at different units also may vary. The frame work facilitates comparison of key parameters at each stage, during the process life cycle of each product, to optimize supply chain or value chain solution.

6.1 Conclusions

At low cost, no capex-based low opex-based supply chain management system was successfully designed developed and tested. To prove the cost effectiveness of this RAIN computing-based system, its deliverables and the CAPEX and OPEX were compared with those of the legacy systems. So it is possible to design and develop dynamic low-cost RAIN computing-based supply chain and value chain solutions especially to solve complex supply chains and value chain problems in a sustainable manner.

Acknowledgments The authors acknowledge the services of all the officials of AP Foods Ltd., other officials of Women and Child Welfare Department for successfully implementing the pilot. Authors also acknowledge NIC, DietY for the datacenter infrastructure being provided for hosting and implementing e-Governance projects.

References

1. Wu, X., Tian, H.: Discussion on E-commerce key technology. In: 2010 2nd International Conference on Computer Engineering and Technology (ICCET), vol. 7, pp. V7-88–V7-91. IEEE Press New York (2000)
2. Hwang, H.J., Seruga, J.: An intelligent supply chain management system to enhance collaboration in textile industry. www.sersc.org/journals/IJUNESST/vol4_no4/4.pdf 4, No. 4, Dec 2011
3. Heindel, L.E., Kasten, V.A., Schlieber, K.J.V.: Value chain management: a project management approach. In: Conference Proceedings of the 1995 IEEE Fourteenth Annual International Phoenix Conference on, Computers and Communications, 1995, pp. 297–301. IEEE Press, New York (1995)
4. Yonglin, Y., Qiusheng, Z., Tao, Z.: 2010 International Conference on the Innovation of Value Chain Management in Network Economy Information Management, Innovation Management and Industrial Engineering (ICIII), vol. 1, pp. 341–343. IEEE Press, New York (2010)
5. Lazovic, V., Kovacevic, D.: Changes in the understanding and management of value chain in the information era. In: MIPRO, 2011 Proceedings of the 34th International Convention, pp. 1382–1386. IEEE Press, New York (2011)
6. Rajsekhar, K., Upadhyaya, N.: Modified real-time advanced inexpensive networks for critical infrastructure security and resilience. In: Proceedings of CSI 2013: Springer—Advances in Intelligent and Soft Computing, vol. 248, 249, pp. 777–784. Springer International Publishing, Switzerland (2014)
7. Wang, J., Deng, Y., Xu, G.: Reachability analysis of real-time systems using time Petri nets. In: IEEE Transactions on Systems, Man, and Cybernetics, Part B: Cybernetics, vol. 30, Issue 5, pp. 725–736, IEEE Press, New York (2000)

Opinion Classification Based on Product Reviews from an Indian E-Commerce Website

Debaditya Barman, Anil Tudu and Nirmalya Chowdhury

Abstract Over the past decade, Indian e-commerce sector witnessed a huge growth. Currently this industry has approximately 40 million customers and it is expanding. These people express their experiences with various products, services in several websites, blogs, and social networking sites. To identify and extract any subjective knowledge from these huge unstructured user data, we need to develop a method that can collect, analyze, and classify user opinions. Two popular learning techniques (Supervised and Unsupervised) can be used to classify an opinion into two classes—“Positive” or “Negative.” In this paper, we propose an integrated framework for product review collection and unsupervised classification. The categorization of reviews is generated by the average semantic orientation of the phrases of suggestions or opinions in the review that holds adjectives as well as adverbs. A review can be categorized as an “*Endorsed*” one when the average semantic orientation is “Positive” otherwise it is an “*Opposed*” (“Negative”) one. Our proposed method has been tested on some real-life datasets collected from an Indian e-commerce website. The experimental results obtained show the efficiency of our proposed method for classification of product reviews.

Keywords Opinion mining · E-commerce · Product review · Web mining

D. Barman (✉)

Department of Computer Science, University of Gour Banga, Malda, India
e-mail: debadityabarmar@gmail.com

A. Tudu · N. Chowdhury

Department of Computer Science and Engineering, Jadavpur University,
Kolkata, India
e-mail: anil.cst@gmail.com

N. Chowdhury

e-mail: nirmalya_chowdhury@yahoo.com

1 Introduction

A joint study conducted by PricewaterhouseCoopers (PwC) and Associated Chambers of Commerce and Industry of India (ASSOCHAM) [1] has predicted that Indian e-commerce industry would grow from 3.8 billion USD (approximately) in 2009 to 23 billion USD (approximately) in 2015 due to a Compounded Annual Growth Rate (CAGR) of 35 % approximately. The study predicted that around 65 million Indian consumer will buy online in 2015. Most of these customers share their opinions and experiences about the purchased product in various places like-merchant's website, blogs, social networking sites, etc. These opinions or experiences can be very helpful to the prospective customers, manufacturer companies, and online advertisers. Unfortunately manual analysis of all these reviews is very time-consuming and involves a lot of money to be invested for manpower, particularly for popular items, for which the number of reviews can be up to thousands or even lakhs. Suppose someone wants to buy a specific Mobile phone (say Moto G 2nd edition), normally he or she uses a search engine and search the results of the query "Moto G 2nd edition review." In this case, Google shows the reports about 224,000 (approximate) matches. It is practically impossible to go through all these reviews. In this scenario, the person may target the product reviews in an established online merchant's website. But for a popular product, the number of reviews can be up to hundreds or even thousands (for instance, in "Flipkart" there are approximate 6,980 reviews for the product "Moto G 2nd Edition").

It is a common practice among merchant's to ask their customers to rate their product. So, a person can look for these ratings before making a decision on whether to purchase the product. But these product ratings can be misleading due to the act of spammers. In this paper, we aim to design a system that is capable of extracting, cleaning, and classifying product reviews automatically from a collection of product reviews by "Certified Buyers" (users who purchased this product).

Our opinion classification system takes a review as input and produces a class as output. In first step, a part-of-speech (POS) tagger is used to extract the phrases that hold adjectives or adverbs [2]. The semantic orientation (SO) of each extracted phrase is estimated in the second step. A phrase has a positive semantic orientation when it has good associations (e.g., "Excellent photography") and a negative semantic orientation when it has bad associations (e.g., "Poor Battery") [3]. In the third and final step, the system assigns a given review to a class, "*Endorsed*" or "*Opposed*" based on the average SO of the extracted phrases. If the average is less than zero, the prediction is that the reviewer "*Opposed*" product otherwise, the product is "*Endorsed*" by the reviewer.

Our system is evaluated on a dataset consisting of 250 reviews from a popular Indian e-commerce site named Flipkart.¹ These reviews are randomly selected from five different electronic product domains such as reviews of mobile phone, digital

¹<http://www.flipkart.com/>.

camera, printer, pen drive, and TV. These reviews are written by certified buyers. The system achieves an average success rate of 66.28 %, ranging from 62.7 % for digital camera reviews to 70.6 % for printer reviews.

The rest of this paper is organized as follows: Sect. 2 which discusses the related work on this topic. Section 3 states the formulation of the problem. Section 4 describes in detail the system framework and each system component. We report, in Sect. 5, our experimental results and we provide our conclusions on this work in Sect. 6.

2 Related Work

The semantic orientation (SO) of words or phrases is the foundation of mining sentiment from text. In classic SO algorithm, each word or phrase gets orientation value based on its inclination toward positive or negative word. Positive evaluation (i.e., praise) of a word or phrase can be indicated by a positive SO and a negative evaluation (i.e., criticism) can be indicated by a negative SO of a word or phrase. Detailed discussion on SO can be found in Sect. 3.

In 1997, Hatzivassiloglou and McKeown [4] extracted all conjunctions of adjectives (like and, or, but, either-or, or neither-nor) from the “21 million word 1987 Wall Street Journal” corpus. They used a linear regression model to predict whether each two conjoined adjectives are of same or different orientation by combining information from different conjunctions. The result was a graph where “terms” are nodes and edges are “equal-orientation” or “opposite-orientation.” A clustering algorithm was applied on this graph to create two groups of adjectives. These two groups are connected by different-orientation links, and there are same-orientation connections inside each group. Cluster with higher average frequency was labeled as positive SO and the other one as negative SO based on the hypothesis-positive adjective is used more frequently than negative adjectives.

In 2002, Turney [3] predicted a document’s polarity depending on the average SO of the phrases extracted from the document. Point wise mutual information (PMI) was used to calculate the SO. In fact using PMI, the author computes the dependence between extracted phrases and the positive reference word “*excellent*” and negative reference word “*poor*” using web search hit counts. In this experiment, Turney concluded that this technique requires a very large corpus although this technique is easy to implement, unsupervised, and not restricted to adjectives. PMI method requires too much time for sending queries to Web search engines but it is very efficient and widely used technique. In this experiment, Turney did not consider the case of “*Spam Review*” which often misleads consumers.

In 2003, Turney and Littman [5] developed a method to predict SO of a word by measuring its statistical association with positive or negative set of words. Two statistical measurement were used (PMI and latent semantic analysis (LSA)) to compute the statistical association.

Orientation of many opinion words can change depending on the context. To address this issue in 2007, Ding and Liu [6] proposed several linguistic rules. They tried to determine the orientation of opinions which are used to describe product features using context.

In 2005, Takamura et al. [7] proposed a method to generate a list of positive and negative polarity words from the glosses (i.e., definition or explanation sentences) in a dictionary. They used an electron spin model, where they considered words as a set of electron and the direction of spin as the positive or negative polarity of each word. Average polarity of each word is computed by applying mean field approximation.

In 2001, Tong [8] used a learning algorithm as an alternative of a hand-built lexicon to detect and track opinion in online discussions. In 2002, Pang et al. [9] applied machine learning techniques (such as Naive Bayes, maximum entropy classification, and support vector machines) on the movie review data to perform sentiment classification. However, these techniques did not perform satisfactorily. In 2004, Kamps et al. [10] developed a method to determine SO of adjectives using WordNet-based measurement. In 2004, Hu and Liu [11] applied synonym set and antonym set of adjective in WordNet to determine the SO of adjectives.

In our work, we used the methodologies suggested in the Turney's Experiment [3] although implementation wise it is different. We also handled the "*Spam Review*" issue.

3 Statement of the Problem

This paper presents a method that can collect, analyze, and classify user opinions. An Unsupervised learning technique is used to classify a given opinion into two classes namely "positive" or "negative." The experimental data for implementation of this proposed method have been collected from of reviews given in an Indian e-commerce website namely Flipkart. To illustrate how the proposed method works, let us consider the following review on a mobile phone (we associate id numbers to refer the sentences):

- (1) It is really a nice phone. (2) Speaker is loud enough with super sound quality. (3) I like the 4-inch decent display size. (4) The camera is good enough. (5) I have some excellent photography with this 8MP camera phone. (6) But 1300 MHz poor battery does not last even a day, it really disappointed me. (7) The dual core processor is really amazing, it always works very fast. (8) Almost all kind of games are supported. (9) Although the phone is little costly, but it deserves the cost with these excellent features.

Now, what kind of information we want to mine from this review? Notice that there are several opinions in this review. Sentences (1), (2), (3), (4), (5), (7), and (8) represent positive opinions. Sentence (6) represents negative opinion. Sentence (9) represents both positive and negative opinion. Notice that there are some targets

associated with every opinions. In sentence (1), the target is whole phone. In (2), (3), (4), (5), (6), (7), and (8) sentences the targets are “*Speaker*,” “*Display size*,” “*Camera*,” “*Camera*,” “*Battery*,” “*Processor*,” and “*Games*,” respectively. Sentence (9) has two targets—“*Cost*” and “*Features*”. In this review, there is a holder of the opinions or *opinion holder*—the author of the review (“*I*”).

Generally we express our opinions about the opinion target. Target can be a product, a place, a service, a recipe, an organization, a topic, etc. Let’s call this target object an *entity*. We used the formal definitions given by Bing and Zhang in [12].

3.1 Definition (*Entity*)

An Entity e can be represented by a pair, $e: (T, W)$, where T is a hierarchical representation of components (or parts) or sub-components and W is a set of attributes of e . Each component or subcomponent can also have its own set of attributes.

3.2 Example

A specific brand of mobile phone can be an *entity*, e.g., Moto-X. The *set of components* can be its Display, Processor, RAM, etc., and *set of attributes* can be its price, weight, dimensions, etc. Some *components* can also have their own *set of attributes*. *Attributes* of Display can be resolution (QHD, HD, Full HD, etc.) and touchscreen quality (Capacitive, AMOLED, etc.).

According to the definition of entity, *entity* can be represented as a tree structure. Name of the entity will be the root of the tree and *component* or *subcomponent* will be a non-root node. A set of attributes will be associated with each node. An *opinion holder* can express his or her opinions on any node or any attribute of the node. To simplify this hierarchical representation of the tree, we flat this tree to only two levels. In first level there is root node-*entity*, in second level, there is different *aspects* of the entity, where *aspects* denote both components and attributes.

Generally, an *opinion holder* expresses his or her positive, negative and neutral sentiment, emotion, experience, and attitude about an *entity* or *aspects* of the *entity* in an opinion. These positive and negative sentiments are called *opinion orientations*. We used the formal definition of *Opinion* given by Bing and Zhang in [12].

3.3 Definition (*Opinion*)

An *Opinion* can be represented by a quintuple, $(e_i, a_{ij}, oo_{ijkl}, h_k, t_l)$, where e_i is the name of an *entity*, a_{ij} is an aspect of e_i , oo_{ijkl} is the orientation of the opinion about aspect a_{ij} of entity e_i , h_k is the opinion holder, and t_l is the time when the opinion is expressed by h_k . The opinion orientation oo_{ijkl} can be positive, negative or neutral. It can also be expressed with different strength or intensity levels.

Now, we discuss our main objective of our experiment: *Opinion Classification*, which is a well-studied and well-practiced area in Opinion mining.

3.4 Definition (*Opinion Classification*)

Given an opinionated document d evaluating an *entity* e , assign a class level (positive or negative) to d based on the *opinion orientation* oo of e . *Opinion Orientation* (oo) is determined based on the *opinion* on the *aspect* of the *entity* e . *Entity* e , *opinion holder* h , and the time when the opinion is expressed t are assumed known or irrelevant.

We made following assumptions for our experimentation on *opinion classification*:

1. *Opinion document* d (product review) states opinions on a distinct *entity* e
2. To aggregate *Opinion Orientation* (oo) of multiple *opinion document*, we assume that *opinions* are from a single *opinion holder* h .
3. The time (t) when the opinion is expressed is irrelevant.
4. Reviews from non-certified buyers are considered as spam review.

3.5 *Opinion Classification Based on Unsupervised Learning*

Opinion words or phrases in an *opinion document*, are the dominant indicators to determine the *opinion orientation* of the whole document. In [3], Turney proposed an unsupervised algorithm based on the *Opinion Orientation* (oo) or *Semantic Orientation* (SO) of the phrases. This algorithm consists of three steps. Below, we present a short description of all three steps.

Step 1 Phrase Extraction The algorithm extracts two-word phrases in such a way that one word of the group is an adjective or adverb and the other word is a context word. These phrases are extracted when their part-of-speech (POS) tags conform to the patterns listed in Table 1. For example, the pattern in line 1 in Table 1 [3] indicates that the two-word phrases are executed if the first word is an adjective, and the second word is singular common noun (NN) or plural common noun (NNS).

Table 1 Patterns of POS tags for extracting two-word phrases

	First word	Second word	Third word (Not extracted)
1	JJ	NN or NNS	Anything
2	RB, RBR, or RBS	JJ	Not NN nor NNS
3	JJ	JJ	Not NN nor NNS
4	NN or NNS	JJ	Not NN nor NNS
5	RB, RBR, or RBS	VB, VBD, VBN, or VBG	Anything

3.6 Example

From the sentence “*It’s really a nice phone*” above explained method will extract the phrase “*nice phone*” as it follows the first pattern.

Step 2 (Computation of the SO of extracted phrase) In this step, point wise mutual information (PMI) is used to calculate the SO of extracted phrases:

$$\text{PMI}(\text{term}_1, \text{term}_2) = \log_2 \left(\frac{\Pr(\text{term}_1 \wedge \text{term}_2)}{\Pr(\text{term}_1) \times \Pr(\text{term}_2)} \right) \quad (1)$$

PMI represents the extent of information that we can acquire about the presence of one of the words when we observe the other [12]. The SO of a phrase can be calculated by measuring its association with positive and negative reference word like “*excellent*” and “*poor*.”

$$\text{SO}(\text{phrase}) = \text{PMI}(\text{phrase}, " \text{excellent} ") - \text{PMI}(\text{phrase}, " \text{poor} ") \quad (2)$$

When we search a query in a search engine it usually returns the number of documents where it finds a match. This number is also known as the *hits*. The probability terms at Eq. (1) are calculated by accumulating the hits. In this way, we can compute the probabilities of individual terms and two terms together by searching the individual terms and two terms together, respectively.

To implement this method, Turney [3] used a special operator “NEAR” available with AltaVista search engine. This operator limits the search process to only those documents that holds “the words with in ten words of one another in either word” [12]. Unfortunately AltaVista search engine is not exists any more. In our experiment, we use “AROUND” operator of Google search engine [13]. This operator “AROUND” lets user specify the word distance that separate two terms. If we search for “[“Apple” AROUND (5) “Samsung”] then the search engine only get the web pages that hold the two terms “Apple” and “Samsung” separated by less than five words. To avoid division by zero, a small number 0.01 is added to the hits. So we can rewrite the Eq. (2) as follows:

$$\text{SO(phrase)} = \log_2 \left(\frac{\text{hits}(\text{phrase AROUND}(10)"excellent") \times \text{hits}("poor")}{\text{hits}(\text{phrase AROUND}(10)"poor") \times \text{hits}("excellent") } \right) \quad (3)$$

Step 3 Aggregating SO We assign a given review about a product to a class, “*Endorsed*” or “*Opposed*” based on the average SO of the extracted phrases. If the average is greater than zero, then the prediction is that the *review holder* “*Endorsed*” the product that he or she discussed. Otherwise, the item is “*Opposed*” by the *review holder*.

4 System Framework and Its Components

Motivated by Turney's experiment [3] which implemented PMI technique-based unsupervised algorithm to classify a review as “*recommended*” or “*not-recommended*” using “NEAR” operator of AltaVista search engine, in this paper, we propose a PMI technique-based unsupervised approach to predict whether an *opinion holder* or the reviewer is *endorsing* or *opposing* a product using “AROUND”

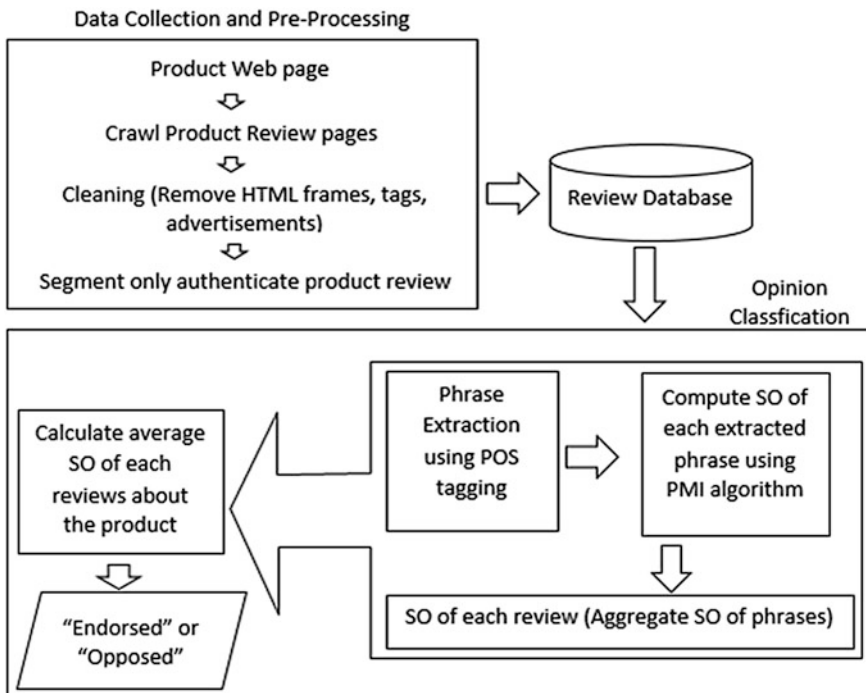


Fig. 1 The system framework

operator of Google search engine based on authentic product review. Figure 1 presents the architectural overview of our opinion classification system and afterward we give overview of the components.

4.1 Data Collection and Pre-processing

Our system accepts a product web-page as an input (e.g., product page for “Hp-deskjet-1510-multifunction-inkjet-printer” in Flipkart: <http://www.flipkart.com/hp-deskjet-1510-multifunction-inkjet-printer-low-cartridge-cost/p/itmldzsmbxmdb2daz>). It automatically locates the product review pages and crawl through them. Note that, there are multiple reviews (depending on the review size) in any product review page. We developed a HTML parser which can extract product reviews along with review author, date of the review, certified buyer tag, and ratings (in scale of five) given by the reviewer, from these webpages by removing various types of HTML frames, tags, advertisements, product description, etc. Only those reviews which are from certified buyers (users who purchased this product) are considered for our experimentation to avoid spam reviews. We stored the reviews in a database so that we can process them offline.

4.2 Opinion Classification

Our opinion classification system works in four steps. In first step, it extracts the phrases which matched the patterns given in Table 1 using POS tagging. SO of each extracted phrase is computed according to equation no. 3 in second step. In third step, it aggregates SO of all the extracted phrases to calculate SO of a review. If the SO of a review is greater than zero, then the prediction is that—the reviewer “*Endorsed*” the product that he or she discussed. Otherwise, the item is “*Opposed*” by the reviewer. Consider the review given in Sect. 3. As you can see at Table 2, the author of this review “*endorsed*” the product. In fourth and final step, we take average of all available authenticate review (reviews by certified buyers) to decide whether the reviewers “*endorsed*” or “*opposed*” the product.

5 Experimental Result

We have used a dataset consisting of 250 certified buyer’s review from a popular Indian e-commerce site named Flipkart for experimentation. In fact, these reviews are randomly selected from five different electronic product domains such as reviews of mobile phone, digital camera, printer, pen drive, and TV. Initially we employed our proposed method to classify whether a particular review is of

Table 2 An example of review processing

Extracted phrase	POS tag	SO
Nice phone	JJ NN	0.1477
Loud enough	JJ JJ	0.9891
Super sound	JJ NN	0.7563
Decent display	JJ NN	1.0673
Good enough	JJ JJ	1.2546
Excellent photography	JJ NN	1.5615
Poor battery	JJ NN	-1.0807
Really disappointed	RB VBD	-0.1348
Really amazing	JJ JJ	0.6781
Very fast	RB JJ	0.6003
Little costly	JJ JJ	-0.9195
Excellent features	JJ NN	0.0748
Average semantic orientation		0.4162

“endorsed” type or “opposed” type. Then we have completed the overall impression of the reviewers on the specific product in the form of “endorsed” and “opposed.” It may be noted that we have considered a product to be is “opposed” by a reviewer, if he or she provides a rating of below *three stars*, otherwise the product is assume to be “endorsed.” The overall impression of the reviewers about a product is considered to be negative if the aggregate product rating is below *three stars* otherwise it is positive.

The experimental results for the evaluation of the individual product review and overall product review for a particular product are provided in Tables 3 and 4, respectively.

It can be observe from Table 3 that our proposed method is able has provided an average *accuracy* value of 0.6627, average *sensitivity* value of 0.6583, and average *specificity* value of 0.7928. The *type I* error rate (false positive) is low for our system because of the high *specificity* and *type II* error rate (false negative) little bit high because of the low *sensitivity*. The probability of a negative review being classified as positive review (false positive) is low compared to a positive review being classified as negative review (false negative), since *type II* error rate is higher than *type I* error rate.

As one can see in Table 4, we predicted the correct classes of four out of five products successfully. Our proposed method could not classify the class of “Moto-x-16-gb” based on the all the review of the product, possibly for the following reason.

We considered only 50 certified buyers’ review to predict whether “Moto-x-16-gb” is “endorsed” or “opposed” by the reviewers. Note that, during review selection, the reviews were selected randomly, from available certified reviewers. Let’s take the following review as an example.

What I like most is ‘OK Google Now’ feature, it works on your voice command. Battery is good, even if the WiFi is on it will work for a day. This phone is fast like a rocket; however,

Table 3 Prediction on individual product review level

Product name	Correct prediction on individual product review level				Accuracy
	Percentage (%)	Sensitivity	Specificity	Precision	
Moto-x-16-gb mobile phone	66.70	0.6333	0.7500	0.7917	0.6667
Canon-eos-600d-dslr-camera	62.70	0.6041	1.0000	1.0000	0.6274
Micromax-32gb200hd-32-inches-led-tv	64.70	0.6364	0.8333	0.9655	0.6470
Sandisk-cruzer-blade-16-gb-pen-drive	66.70	0.6904	0.7142	0.9354	0.6667
Hp-deskjet-1510-multifunction-inkjet-printer	70.60	0.7272	0.6667	0.9412	0.7059
Average performance	66.28	0.6583	0.7928	0.9268	0.6627

Table 4 Prediction on entire product level

Product name	Actual class given by the reviewers	Average SO	Predicted class
Moto-x-16-gb mobile phone	Endorsed	-1.0989	Opposed
Canon-eos-600d-dslr-camera	Endorsed	0.3689	Endorsed
Micromax-32b200hd-32-inches-led-tv	Endorsed	0.6074	Endorsed
Sandisk-cruzer-blade-16-gb-pen-drive	Endorsed	3.0044	Endorsed
Hp-deskjet-1510-multifunction-inkjet-printer	Endorsed	1.3188	Endorsed

the camera is not so cool. My older phone (Motorola Defy) which is just 5 Megapixel Camera clicks better pics than this phone. Other issues - No FM radio and external memory card. Overall it is a great value for money.

The author of this review “*endorsed*” the product by giving it four stars but the author expressed negative opinions on various features of this mobile phone such as its *camera*, *FM Radio*, and *external memory card*. Our method classifies it as “*opposed*” (*SO* of the review = -11.7432) being largely influenced by these negative opinions although the author expressed few positive opinions. In an appropriate review, the rating provided by the reviewer should be based on the number of positive and negative comments about the various features of the product. The review stated above drastically violates this condition. Thus this type of inconsistent review leads to misclassification of the product.

6 Conclusion

In this paper, we propose an integrated framework for product reviews collection followed by unsupervised classification of those reviews. The categorization of review is based on the average semantic orientation of the phrases used to express opinions in the review that contains adjectives as well as adverbs. In order to calculate the SO, we use “AROUND” operator of Google Search engine. A review results in “*Endorsed*” class when the average semantic orientation is “Positive” otherwise it belongs to “*Opposed*” class. Performance of our system is evaluated on a real-life dataset consisting of 250 *certified buyers*’ review collected from an Indian e-commerce website.

The experimental results show that the average classification success rate on distinct product review level is 66.28 %.

There are several ways in which further research can be conducted in this area. For instance, one can use some other operator which is similar but more effective than that of “AROUND” operator of Google search engine. More over Google cannot always be an appropriate search engine for this purpose since in 2006, Taboada et al. [14] observed some inconsistency in the results obtained for the same

word on multiple runs through Google. Thus one may use other search engine such as Yahoo,² Bing³ for implementing such kind of unsupervised review classification method. One may also consider a large static corpus instead of Google, which indexes a dynamic corpus to solve this kind problem.

Acknowledgments This paper is an outcome of the work carried out for the project titled “In search of suitable methods for Clustering and Data mining” under “Mobile Computing and Innovative Applications programme” under the UGC funded—University with potential for Excellence—Phase II scheme of Jadavpur University.

References

1. PWC, ASSOCHAM: Evolution of e-commerce in India Creating the bricks behind the clicks (2014)
2. Brill, E.: Some advances in transformation-based part of speech tagging. In: Proceedings of the Twelfth National Conference on Artificial Intelligence, pp. 722–727. AAAI Press (1994)
3. Turney, P.D.: Thumbs up or thumbs down? semantic orientation applied to unsupervised classification of reviews. In: Proceedings of the 40th annual meeting on association for computational linguistics, pp. 417–424. Association for Computational Linguistics (2002)
4. Hatzivassiloglou, V., McKeown, K.R.: Predicting the semantic orientation of adjectives. In: Proceedings of the 35th Annual Meeting of the ACL and the 8th Conference of the European Chapter of the ACL, pp. 174–181. Association for Computational Linguistics (1997)
5. Turney, P.D., Littman, M.L.: Measuring praise and criticism: inference of semantic orientation from association. ACM Trans. Inform. Syst. (TOIS) **21**(4), 315–346 (2003)
6. Ding, X., Liu, B.: The utility of linguistic rules in opinion mining. In: Proceedings of the 30th annual international ACM SIGIR conference on Research and development in information retrieval, pp. 811–812. ACM (2007)
7. Takamura, H., Inui, T., Okumura, M.: Extracting semantic orientations of words using spin model. In: Proceedings of the 43rd Annual Meeting on Association for Computational Linguistics, pp. 133–140. Association for Computational Linguistics (2005)
8. Tong, R.M.: An operational system for detecting and tracking opinions in on-line discussion. In: Working Notes of the ACM SIGIR 2001 Workshop on Operational Text Classification, vol. 1, p. 6 (2001)
9. Pang, B., Lee, L., Vaithyanathan, S.: Thumbs up?: sentiment classification using machine learning techniques. In: Proceedings of the ACL-02 conference on Empirical methods in natural language processing-Volume 10, pp. 79–86. Association for Computational Linguistics (2002)
10. Kamps, J., Marx, M.J., Mokken, R.J., De Rijke, M.: Using wordnet to measure semantic orientations of adjectives (2004)
11. Hu, M., Liu, B.: Mining and summarizing customer reviews. In: Proceedings of the tenth ACM SIGKDD international conference on Knowledge discovery and data mining, pp. 168–177. ACM (2004)
12. Liu, B., Zhang, L.: A survey of opinion mining and sentiment analysis. In: Mining text data, pp. 415–463. Springer, US (2012)

²<http://search.yahoo.com/>.

³<http://www.bing.com/>.

13. Russell, D.: AROUND has always been around. <http://searchresearch1.blogspot.in/2010/10/around-has-always-been-around.html>. Accessed Mar 5 2015. 8.00 PM IST
14. Taboada, M., Anthony, C., Voll, K.: Methods for creating semantic orientation dictionaries. In: Proceedings of the 5th International Conference on Language Resources and Evaluation (LREC), pp. 427–432 (2006)

Mitigation of Fog and Rain Effects in Free-Space Optical Transmission Using Combined Diversity

Dhaval Shah and Dilipkumar Kothari

Abstract Free-Space Optics (FSO) have been emerging communication field because of several advantages like cost-effective, higher bandwidth, and license free. It is basically line of sight communication and more suitable for last mile connectivity. Signal degradation occurs mostly due to atmospheric interference like rain, fog, etc. Diversity is an efficient solution to overcome these effects. In this paper, we have applied the concept of combined diversity (spatial and wavelength) with help of two receiver antenna to mitigate effects of fog and rain attenuation over transmission. An Equal Gain Combining for array gain enhancement applied at the receiver side. Results also demonstrated improvement in BER performance under strong turbulence.

Keywords Diversity · Fog attenuation · Rain attenuation

1 Introduction

Free-Space Optics (FSO) technology use visible or infrared light for communication. It includes wide range of advantages in modern life's introduces high bandwidth which can accommodate more number of channels to enhance communication throughput. There are more number of advantages over radio frequency communication like unlicensed frequency spectrum, secure communication, etc. [1]. By implementing proper techniques and using efficient transceivers, communication can be made for long distance. As FSO communicates through light, atmospheric condition makes it vulnerable to stand with it. It is well affected by rain, fog, smoke, dust, snow, cloud, etc.

D. Shah (✉) · D. Kothari

Institute of Technology, Nirma University, S. G. Highway, Ahmedabad, Gujarat, India
e-mail: dhaval.shah@nirmauni.ac.in

D. Kothari

e-mail: dilip.kothari@nirmauni.ac.in

© Springer India 2016

S.C. Satapathy et al. (eds.), *Proceedings of the Second International Conference on Computer and Communication Technologies, Advances in Intelligent Systems and Computing* 380, DOI 10.1007/978-81-322-2523-2_70

725

To mitigate atmospheric effects numerous channel models have been introduced according to atmospheric behavior weak to strong [2, 3]. Rain and fog are the main contributor in strong turbulence, and they affect the channel exponentially so, Negative Exponential (NE) model is best fit [4]. Fog is also categorized in two parts according their particle size. (1) Advection fog, which has particle diameter close to 20 μm . (2) Radiation fog, which is mostly find in night and has particle diameter near to 4 μm [5, 6]. Rain attenuation also depends on rain drop size and rain rate [7, 8]. Error control coding with interleaving is one of the solutions to overcome turbulence effects, but it requires large size inter-leavers [9]. Turbulence induced fading can also be mitigated using Maximum Likelihood Sequence detector (MLSD) technique [10]. However, it requires the computing an n-dimensional integral for each of 2^n bit. It will also increase complexity.

Another technique to mitigate effect of atmospheric fluctuation is diversity. There are three ways to apply diversity over signal, namely: Time, Wavelength, and Spatial. In time diversity, signal will be sent multiple times to overcome signal degradation [11]. Second is wavelength diversity, which sends one signal using different wavelengths because at different frequency the effect of channel will be different, and it will help to reduce fog attenuation. Third one is spatial diversity which sends signal in multiple paths. It can be applied where small space multiple channels are present like; situation occurred in rain [12].

In this paper, authors have investigated effect of combined diversity (wavelength and spatial diversity) over rain and fog on negative exponential model. At the receiver side, Equal Gain Combining (EGC) diversity is applied which enhances array gain by addition of receiver's output and increase SNR value over specific BER. Paper finally compares the output of proposed diversity technique over single-input single-output (SISO) under strong turbulence. Authors [13] assume intensity modulation/direct detection (IM/DD) with on-off keying for this work.

This paper is organized as follows: negative exponential channel model is discussed in Sect. 2. Sections 3 and 4 discussed fog and rain attenuation, respectively. Concept of combined (wavelength and spatial) diversity with result is given in Sect. 5. Finally, useful concluding remarks are provided in Sect. 6.

2 Negative Exponential Model

In case of strong irradiance fluctuations where link length spans several kilometers, number of independent scatter become large. In that case, signal amplitude follows a Rayleigh distribution which in turn leads to a negative exponential statistics for the signal intensity (square of field amplitude). This is given by [2].

$$P(I) = \frac{1}{I_0} \exp\left(-\frac{1}{I_0}\right), I \geq 0 \quad (1)$$

where, I_0 is the mean radiance (average photon count per slot). Here $\sigma_{\text{SI}}^2 = 1$ (or in the vicinity of 1). The equations used for finding out the BER and SNR are given below [4]:

$$\text{Spontaneous SNR } \gamma = \frac{S}{N} = \frac{(\eta I)^2}{N_0} \quad (2)$$

$$\text{Average SNR } \mu = \frac{S_{\text{avg}}}{N} = \frac{(\eta \langle I \rangle)^2}{N_0} \quad (3)$$

$$\text{Avg. BER } P_{\text{av}} = \frac{1}{2} \int_0^{+\infty} \operatorname{erfc}\left(\frac{\lambda}{2\sqrt{N_0}}\right) f(I) dI \quad (4)$$

Using Eqs. (1), (2), and (3), the plot of BER versus SNR curve was plotted in Fig. 1. The input is assumed binary and the noise and the input sequence are generated randomly in the code. The noise ‘n’ added in the channel is AWGN with zero mean and variance $N_0/2$. Figure 1 demonstrated BER versus SNR comparison for NE channel model. It is clearly depicted that increasing intensity of transmitting signal will increase SNR which in turn reduces the BER.

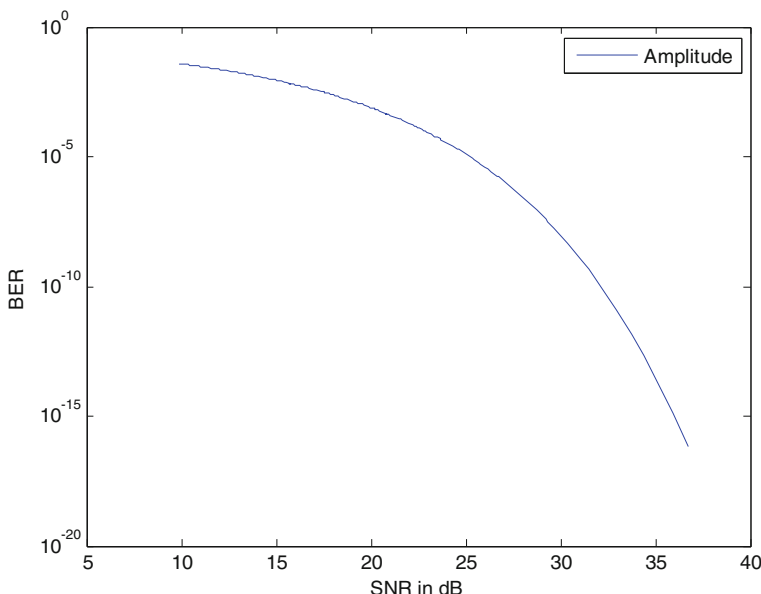


Fig. 1 BER versus SNR curve of negative exponential channel model

3 Fog Attenuation

Generally attenuation due to fog is divided into two main parameters. First one is due to scattering and second is absorption due to water particles. Scattering occurs when light passing through air consisting of particles which are capable of divert path of light propagation either through reflection or refraction. Scattering is mostly depending upon radius of particle and incidence wavelength. Fog particle sizes are mostly same as the incidence wavelength. In this case, scattering co-efficient is computed by Kruse formula [14]. This model represents the relation between visibility (V) and incident wavelength (λ). Kruse's original formula is represented in Eq. (5):

$$\alpha = \frac{3.91}{V} \left(\frac{\lambda}{550 \text{ nm}} \right)^{-q} \quad (5)$$

where, α represent scattering coefficient, V stands for visibility in km, λ for incident wavelength in km, and $q = 0.585(V)^{1/3}$ for $V < 6$ km.

The absorption coefficient (β) value depends upon incident wavelength. Certain molecules absorb specific wavelengths. In fog absorption, coefficient absorption is done by water vapor. There is predefined absorption window of water vapor [15]. Total attenuation find out by summation of scattering and absorption co-efficient as following Eq. (6) (Fig. 2):

$$\theta = \alpha + \beta \quad (6)$$

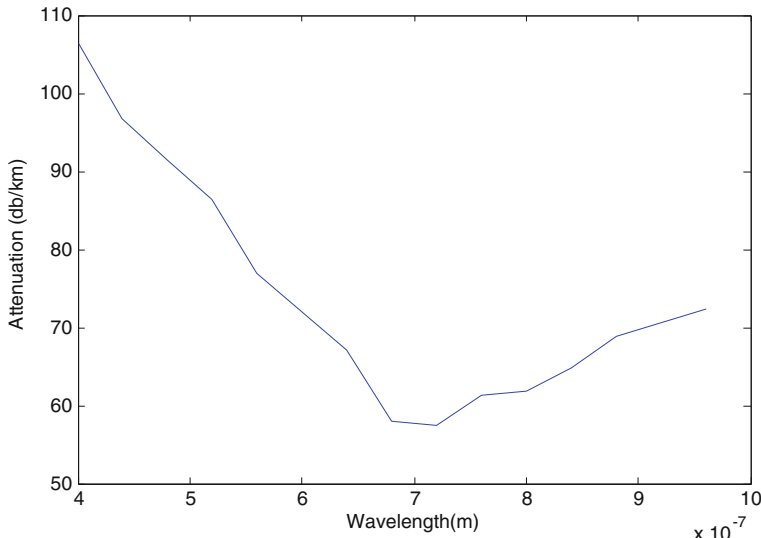


Fig. 2 Fog attenuation for distance over 1 km

Fog can be categorized into two parts. First is advection fog and another is radiation fog based on their particle size. 850 nm give best performance in advection fog and 1500 nm for another. By this point of view, there is space to apply wavelength diversity to overcome fog attenuation because it is difficult to predict type of fog present in atmosphere. Figure 1 illustrated total attenuation over 1 km from source to destination. It is clearly depicted that window 700–850 nm have very less attenuation compare to other. But drawback it cannot be apply more power after certain level because it is harmful to human eye so choose second frequency out of infrared band as 1500 nm, though it has high attenuation than first case.

4 Rain Attenuation

Raindrops are larger than incidence wavelength. This situation is well handle under geometric modal for predicting total attenuation due to rain [16]. Rain attenuation caused by rain rate (R) which is function of distance (d) and it can be expressed by following equation:

$$A = kR(d)^\alpha \quad (7)$$

In Eq. (7), k and α represent polarization, link elevation, and frequency-dependent coefficients. Figure 3 demonstrates the attenuation (dB/km) in optical frequency

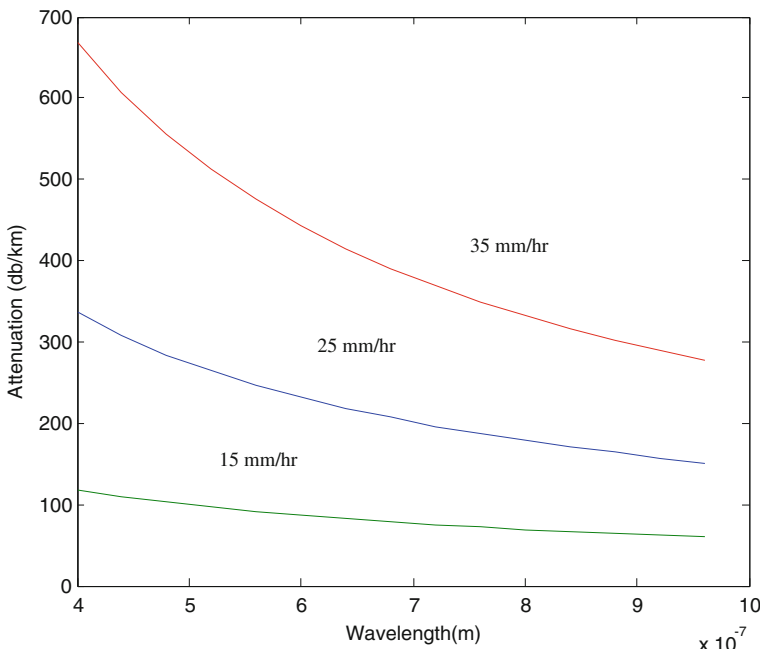


Fig. 3 Rain attenuation at various frequency with $R = 15, 25, 35 \text{ mm/h}$

range in various rain rates. From Fig. 3, it is cleared that as rain rate increases, the attenuation in channel will also increase. It is also depicted that rain attenuation at lower rain rate hardly dependent on wavelength so, applying wavelength diversity in this scenario will not be helpful to degrade rain attenuation. The rain drop rate will be different at every different place, so more than one channel exists in rainy atmosphere. Spatial diversity is more suitable in the scenario where more than one channel is present. Hence, spatial diversity can be used to mitigate rain attenuation.

5 Combined Diversity

Combined diversity means to apply both, wavelength and spatial diversity together to overcome the attenuation due to fog and rain in the channel. Figure 4 shows the diagram of proposed method. At transmitter side, two best frequencies have been selected to apply wavelength diversity which will mitigate fog attenuation. Selection combining is applied to select best result among two wavelengths because particular type of fog gives their best result to specific frequency. To mitigate rain attenuation, transmitting signal will apply through two different paths Single-Input Multiple-Output (SIMO). At the same time, Equal Gain Combining (EGC) is applied at receiver that can add some array gain and enhance the SNR value [17]. Ultimately, proposed method will be compatible in either different types of fog or rain conditions. Figure 5 shows the result of proposed method.

FSO communication with (IM/DD) light propagates with additive white Gaussian noise (AWGN). Statistically any channel is given as following equation:

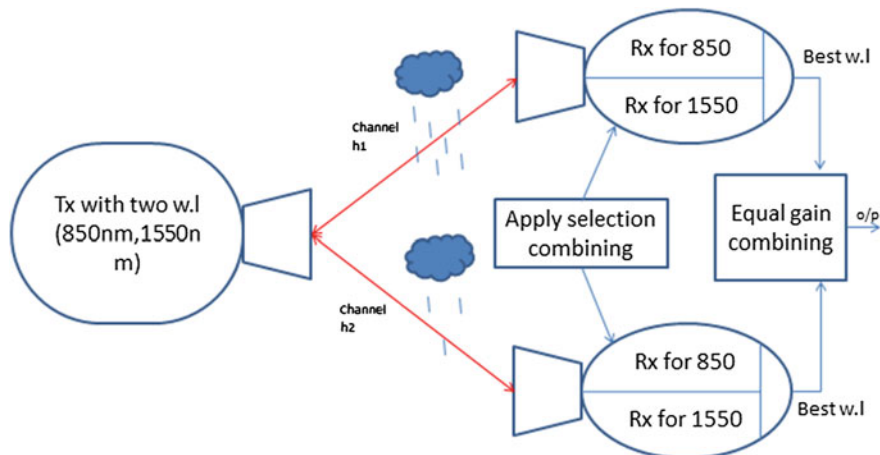


Fig. 4 Combined diversity over attenuated channel with receiver diversity

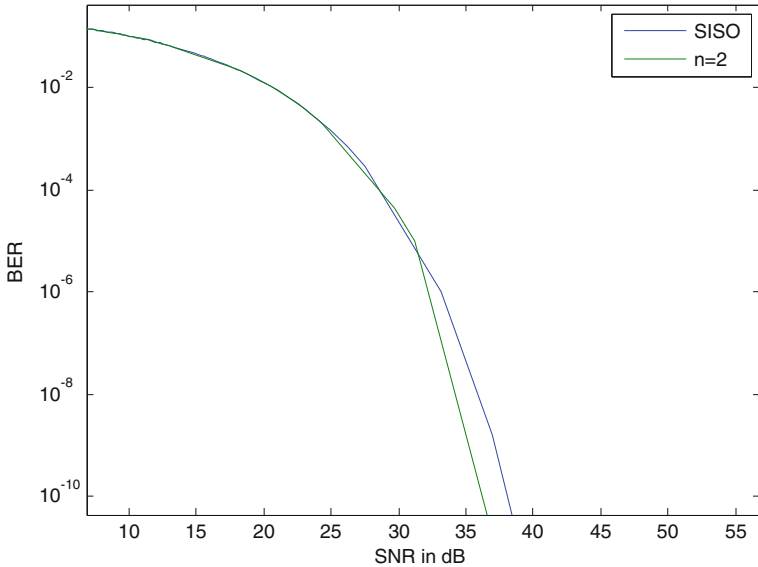


Fig. 5 BER versus SNR for $n = 2$ using combined diversity

$$s = \mu t \sum_{m=1}^M I_m + w_n \quad (8)$$

where s represent received signal, μ represent photo-current conversion ratio, I is for normalized intensity at receiver, t for binary signal, and w_n is for AWGN with zero mean, and variance $\sigma^2 = N_0/2$, and m represent number of link or receiver which is $M = 2$ in our case. Signal will follow negative exponential channel model has been considered for this work as given in Sect. 2.

At receiver side, selection combining and equal gain combining are applied. Selection combining is least complicated because it is only detect maximum irradiance within one aperture in two wavelengths. Therefore selection is made according to:

$$I_{SC} = \max(I_1 + I_2) \quad (9)$$

where, I_1 and I_2 are the irradiance received for wavelength 850 and 1550 nm, respectively. For same channel model, SNR is given for MIMO link as for Equal gain Combining $S = (n \sum I_n)^2 / N_0$ and BER given as function of I as:

$$P(I) = \frac{1}{2} \operatorname{erfc} \left(\frac{\mu \sum_{m=1}^M I_m}{2\sqrt{N_0}} \right) \quad (10)$$

,

where, I_n is normalized irradiance of nth receiver $n = 1, 2$. With the help of this statics, Fig. 5 illustrates the relation between SNR and BER for SISO and SIMO ($n = 2$) channel. It is clearly depicted that SIMO channel performs well over Single-input and single-output (SISO). After selecting best wavelength according to selection combining diversity, route spatial diversity is applied with help of equal gain combining diversity at receiver. It is clearly shown assist of two links array gain will secure and with more links definitely more array gain help to improve the shown graph. As number of link increases, BER will also improve with additional cost. In this paper, authors only concentrate to two simple links with one origin and two receivers SIMO.

6 Conclusion

In this paper, we have investigated the BER performance of FSO links over negative exponential turbulence channels. We have also demonstrated the effect of rain and fog at different wavelength. We applied combined diversity (wavelength and Spatial) to mitigate effects of rain and fog. Our results also demonstrated improvement in BER performance under strong turbulence. In route diversity, if angle between two links is greater than 120° then result will be more enhanced.

References

1. Henniger, H., Wilfert, O.: An introduction to free space optical communication. *Radio Eng.* **19**(2), 203–213 (2010)
2. Parikh, J.: Study on stastical models of atmospheric channel for FSO communication. In: International Conference on Current Trends in Technology. Nuicone (2011)
3. Zhu, X., Kahn, J.M.: Free-space optical communication through atmospheric turbulence channels. *IEEE Trans. Commun.* **50**(8) (2002)
4. Nistazakis, H.E., Assimakopoulos, V.D., Tombras, G.S.: Performance estimation of free space optical links over negative exponential atmospheric turbulence channels. *Optic* **122**, 2191–2194 (2011)
5. Peseck, J., Fise, O., Svoboda, J., Schejbal, V.: Modeling of 830 nm FSO link attenuation in fog or wind turbulence. *Radio Eng.* **19**(2), 237–241 (2010)
6. Naboulsi, S., de Fournel, F.: Fog attenuation prediction for optical and infrared waves. *Optical Eng.* **43**(2), 319–329 (2004)
7. Zvanovec, S.: Diversity statistics of free space optical links affected by rain. *PIERS ONLINE* **7**(7) (2011)
8. Suriza, A.Z., Islam md. rafiqul, Wajdi al-khateeb, Naji, A.W.: Analysis of rain effects on terrestrial FSO based on data measured in tropical climate. *IIMU Eng. J* **12**(5) (2011)
9. Uysal, M., Navidpour, S.M., Li, J.T.: Error rate performance of coded free-space optical links over strong turbulence channels. *IEEE Commun. Lett.* **8**, 635–637 (2004)
10. Zhu, X., Kahn, J.M.: Markov Chain model in maximum- likelihood sequence detection for free-space optical communication through atmospheric turbulence channels. *IEEE Trans. Commun.* **51**(3), 509–516 (2003)

11. Stassinakis, A.N., Hanias, M.P., Nistazakis, H.E., Tombras, G.S.: Evaluation of outage probability for time diversity schemes in free space optical systems over I-K atmospheric turbulence channels. In: 2nd Pan-Hellenic Conference on Electronics and Telecommunications —PACET'12 (2012)
12. Tsiftsis, T.A., Sandalidis, H.G., Karagiannidis, G.K., Uysal, M.: Optical wireless links with spatial diversity over strong atmospheric turbulence channels. *IEEE Trans. Wirel. Commun.* **8**(2), 951–958 (2009)
13. Choi, C., Shoji, Y., Ogawa, H.: Analysis of receiver space diversity gain for millimeter-wave self-heterodyne transmission techniques under two-path channel environments”, TU4A-3
14. Wainright, E., Hazem, H.R., Sluss, J.J.: Wavelength diversity in free-space optics to alleviate fog effects in free-space communication technologies. In: XVII, Proceedings of SPIE, vol. 5712, pp. 110–119
15. Zuev, V.E.: Spectroscopy of atmospheric gases (spectral databases). Institute of Atmospheric Optics SB RAS. Retrieved August 8, (2012)
16. Specific attenuation model for rain for use in prediction methods. Recommendation ITU-R P. 838-1, 2005
17. Anguita, J.A., Cisternas, J.E.: Experimental evaluation of transmitter and receiver diversity in a terrestrial FSO link. IEEE Globecom 2010 Workshop on Optical Wireless Communications (2010)

Technology Involved in Bridging Physical, Cyber, and Hyper World

Suresh Limkar and Rakesh Kumar Jha

Abstract Hyper connectivity is what the world's reality is today. The day is not far away where clients, consumers, and suppliers “go online” to work, play, or consume; no we live in a realm where one and all is just interconnected to each other and with Internet. This new age carries with it an acceleration of formulation and disruption. It is a domain occupied with huge opportunity for folks eager to welcome this and capable to cope with it. Everything around us, transversely each business, firms are ascertaining novel clients, making new income generation method, constructing novel environments, and formulating new business prototypes on a connected stage at an extraordinary place. This paper discusses the technologies responsible for uniting the physical, cyber, and hyper world, i.e., the Internet of things, the Internet of everything along with its high-level representation to realize IoT, WoT, SWoT, W2oT, IoE.

Keywords Physical world · Cyber world · Hyper world · Internet of things · Cloud computing · Web of things · Cloud of things · Web server

1 Introduction

In current scenario, wireless signals at present shields more of the world's inhabitants than the electrical grid [1], and exponential growth of linked devices everywhere is foreseen to hit anywhere from around 50 billion to somewhere

S. Limkar (✉) · R.K. Jha
School of Electronics and Communication Engineering, SMVDU,
Katra, J&K, India
e-mail: sureshlimkar@gmail.com

R.K. Jha
e-mail: jharakesh.45@gmail.com

around one trillion, in the forthcoming 5–6 years [2]. The density of digital data that now connects us is amazing. Cisco evaluated that by the end of year 2015, the quantity of data pass through the Internet for each 5 min equals to the whole magnitude of altogether cinemas ever build [3].

For industries, hyper connected world carries determined increased growth in the novelty. Just take the example of Web evolution it is evolved from static Web to dynamic and tailored as per the client's requirements, affluent application directed via real-time data merged with social networking sites. With rapid application developed on mobile expanded the Web evolution more. As handling of these mobile devices are increasing more day by day and more number of mobile devices to stay associated with laptop to tablet, tablet to phone, and phone to television set, this itself shows that we are adopting a new style of our working, playing, and interacting with others.

This accelerated growth of cyberspace is driven by the amalgamation of computing and telecommunication technology and on the same line with the reputation of omnipresent computing technology; cyberspace has become a part of our daily lives from all corners of the world. Hence, there is extremely more space for human activities here onwards. This leads a significant impact on the intellectual structure of persons and is changing the way we think about ourselves, other persons, and computing things [4].

The introduction of digital spaces has carried revolution in cyber world, which can be regarded as extra realm to us. With quick advancements in numerous technologies, real world, and the emergent cyber world are integrating to design a new world, called the hyper world [5]. The union of real world and cyber world has brought drastic revolutionary changes, because of various digital detonations, including information, connection, service, and intelligence outbreak.

2 Different Types of Worlds

2.1 Physical Versus Cyber World

The physical-first domain comprises of objects and processes that do not generate or communicate digital data unless augmented or manipulated, whereas the ones belonging to the digital-first domain are capable of generating data, and communicating the same on for further use, inherently and by design. For example, a book's hardcopy is an example of a physical world object, whereas its e-book version would be a cyber world object. Similarly, visiting a grocery store is a physical world process, whereas browsing an ecommerce site is a cyber world process.

2.2 *Cyber World*

The Cyber World [5] is just a digital elongation of our real world in a virtual environment. It is true that one cannot build virtual elongation on Web pages. With the help of digital elongation the ordinary users get extraordinary capabilities in comparison to today's standards. The Cyber World will convert the Internet to a more enhanced level of online computing. The Internet links all scattered computers into a unified system. Internet delivers a universal stage for storage of huge data, sharing of resources, publishing services, and computing on the go.

In these years, new information technologies formulate the construction of cyber world [6, 7]. By considering huge technology development in the field of current Internet and Web, like grid computing [8, 9], semantic Web [10–12], service-oriented architecture computing [13], cloud computing [14, 15] cause the cyber world to become either research platform or service platform. If we consider its other side, like development in the field of embedded system, wireless communication, universal computing technologies actuate the progress of the Internet of Things (IoT) [16, 17]. It is predicted that computer will be sole part of cyber world, humans will be the sole part of social world and things will be the sole part of physical world. Difference associated in cyber and real world is discussed in Table 1.

2.3 *Hyper World*

Hyper world is a combination of physical and cyber world and mainly uses information as a medium to link individuals, computers, and physical objects that found in physical world. The presence of hyper world will be on the last layer of Internet of things and Web of things [19, 20].

Table 1 Difference between real and cyber world [18]

Real world	Cyber world
Real activity	Electronics-activity
Real thing: brain, organs, food, air, house, car, Internet, game Real u-Thing: real things with some kind of Attachment, Embedment, Blending, i.e., AEB. AEB of computers, sensors, tags, networks, and/or other devices	E-thing or cyber thing is always made up of real + cyber things
The ownership of a real thing is private may be joint, public, shared	The ownership of a cyber thing may be joint, public, shared, private, or even dynamically changed
UC, ID, Context, Emb. Sys., etc	WbS, SmW, Grid, P2P, Cloud, SaaS
Sensor/M/NEMS, Comps and Per. Nets	Computers and networks/internet

3 Mapping Things to Cyber World

Following ways can be used to map physical objects to the Cyber and Hyper world.

3.1 Internet of Things (*IoT*)

Internet of things is defined as in [21–23]: “universal appearance of a diverse either physical things or physical objects, which can be addressed by unique addressing mechanism, can talk with each other, collectively work with fellow to achieve predefined objectives.” The object/things involved in IoT transmit information associated with it, i.e., like its position, its surrounding temperature, etc. and transfer real-time sensor data about their useful functionalities associated with it. RFID [24] technology is said to be main drivers for the development of IoT because, it possesses distinct capability to track number of unique things.

The notions ubiquitous and pervasive computing is associated with IoT the Internet of things. Expanding a thing with an Internet connection (i.e., an IP address) guarantees its approachability over the Internet and results in an Internet-enabled thing. A high-level representation to realize an Internet-enabled thing is illustrated in Fig. 1.

3.2 Web of Things (*WoT*)

The Internet of Things (IoT) is an active research area, focusing on connecting real-world things over TCP/IP. This trend has recently triggered the research community to adopt the interoperability of the Web (HTTP) as an application

Fig. 1 Internet-enabled things [25]

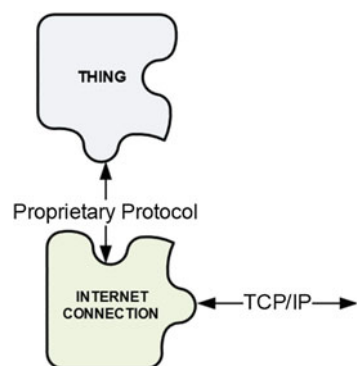
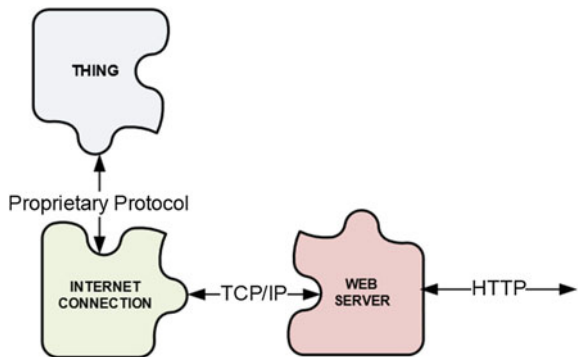


Fig. 2 Web-enabled things
[25]



platform for integrating ‘things’ on the Internet. Harnessing physical things into the virtual world using Web standards is also enriching the arena of conventional Web services to unleash data and functions of real-world things as service providers and consumers on the Internet. This evolution of the Web as a highly interoperable application platform for connecting real world to the fast growing research area called the Web of Things (WoT). Current research on WoT is a catalyst for the realization of IoT, where people and things seamlessly communicate over the Web.

When a thing is Internet-enabled and is also connected to the Web server, it becomes Web enabled. A high-level representation to realize a Web-enabled thing is illustrated in Fig. 2.

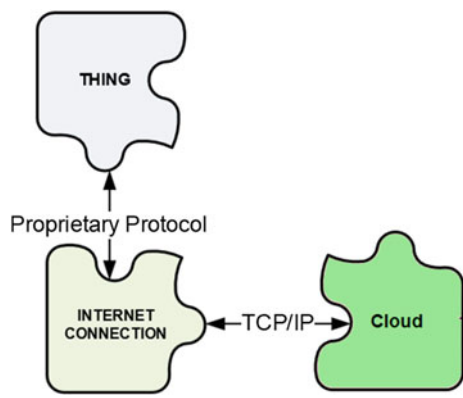
3.3 Cloud of Things (CoT)

The two worlds of Cloud computing and Internet of Things have seen as self-determining evolution rather than parallel development. Still, numerous common benefits originating by combining both have been found in various existing work and same are prophesied in upcoming couple of years. On one side IoT can get the advantage from the cloud, like its virtually infinite capabilities of computation and virtually infinite resources accessible from anywhere with Web services compensate IoT limitations like processing, storage, power. On the other side of it, cloud can benefit from IoT by encompassing its possibility to communicate/interact with physical world things in new disseminated and interactive way. Cloud computing and IoT, analogous features are discussed in Table 2.

When a thing is Internet-enabled and is, also connected to a cloud, it becomes cloud enabled thing [27,28]. A high-level representation to realize a cloud enabled thing is illustrated in Fig. 3.

Table 2 Analogous features of cloud and IoT [26]

IoT	Cloud
Pervasive (objects placed universally)	Ubiquitous (virtual resources usable from universally)
Real-world objects	Virtual resources
Inadequate storage and computational capabilities	Virtually infinite storage and computational capabilities
Internet as a point of coming together all objects	Internet required for delivery of services
It is the source of big data	It is the way to manage big data

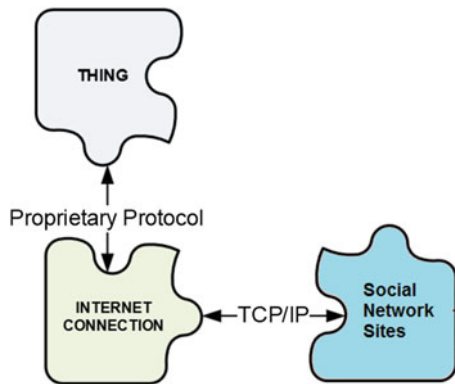
Fig. 3 Cloud-enabled things

3.4 Social Web of Things (SWoT)

The Social Web of things [29] paradigm facilitates users to accomplish and use Web-enabled things and empowers the user an ability to share these devices with other users [30]. Social Network Sites (SNS) increase the popularity of Web 2.0 technology. It permits users to communicate and exchange contents between each other. In recent years, SNS has been extended by an interactive and open Web services. These Web services can extend the social relation between people to relation between them and their Web-enabled devices [31].

When a thing is Internet-enabled and connected to a social network site, it becomes social Web-enabled thing. A high-level representation to realize a social Web-enabled thing is illustrated in Fig. 4.

Fig. 4 Social Web-enabled things



3.5 *Wisdom Web of Things (W2T)*

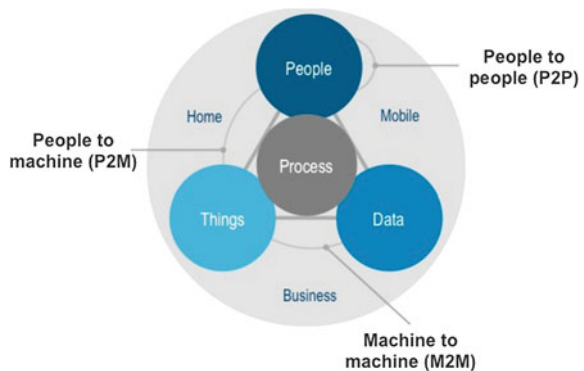
The Wisdom Web of Things it is also referred as W2T, is an extension of the Wisdom Web in the IoT age. Meaning of “Wisdom” is that each object in the WoT can be known itself and others for offering correct service for correct object at a correct time and at the correct situation. W2T emphasizes on the data cycle, namely ‘from things to data, from data to information, from information to knowledge, from knowledge to wisdom, from wisdom to services, from service to humans, and then back to things’ [32].

3.6 *Internet of Everything (IoE)*

The Internet of Everything is the ultimate evolutionary stage of the connected world, in which the foregoing unconnected, physical-first objects and processes, as well as humans, converge with those that are digital-first by their nature. Data and the way the collected data assets are used to create value are the heart of the IoE. The IoE merges and mashes up data assets that are generated from humans, things, and the digital-first domain, and turns them into advanced, data-driven applications, and services. This is often done by applying pertinent analytics to the data.

The Internet of Everything (IoE) is constructed on the networks of persons, processes, data, and objects. IoE is not all about these four elements in isolation. Each of these elements involved in IoE magnifies the capabilities of the other three. It is in the juncture of all of these elements that the real power of IoE is recognized [33] (Fig. 5).

Fig. 5 Internet of everything
[Cisco IBSG 2013]



4 Conclusion

The introduction of digital world has carried revolution in cyber world, which is treated as another realm to us. Speedy advancements in numerous technologies, real and cyber world are merged to formulate a new world and it is called as hyper world. With advances in technology, physical things can be assimilated not only with Internet but also with Web, cloud, and social networking sites. This paper has outlined the expansion of Internet connectivity to the physical things. In order to do so, we first discussed about the various worlds, i.e., the physical world, the cyber world, and the hyper world and summarized various ways through which we can map the physical thing to the cyber and the hyper world.

References

1. <http://www.kpcb.com/insights/internet-trends-2011>
2. <http://blogs.flexerasoftware.com/ecm/2011/07/anyone-for-1-quadrillion-intelligent-connect-devices-on-the-internet.html>
3. http://www.cisco.com/en/US/solutions/collateral/ns341/ns525/ns537/ns705/ns827/VNI_Hyper_connectivity_WP.html
4. Kilger, M.: The digital individual. *Inf. Soc.* **10**, 93 (1994)
5. Ma, J., Wen, J., Huang, R., Huang, B.: Cyber-individual meets brain informatics. *Intell. Syst. IEEE* **26**(5), 30, 37 (2011)
6. Zhong, N., et al.: Web intelligence meets brain informatics. In: Proceedings of the 1st WICI International Workshop Web Intelligence Meets Brain Informatics, LNAI 4845, pp. 1–31. Springer (2007)
7. Ma, J.H.: Smart u-Things-challenging real world complexity. *IPSJ Symp. Ser.* **19**, 146–150 (2005)
8. Fensel, D., et al.: Towards LarKC: a platform for web-scale reasoning. In: Proceedings of the 2008 IEEE International Conference on Semantic Computing, pp. 524–529 (2008)
9. Foster, I., Kesselman, C.: The Grid: Blueprint for a New Computing Infrastructure. Morgan Kaufmann, San Mateo 14 11 (1999)

10. Ma, J.H., Yang, L.T., Apduhan, B.O., Huang, R.H., Barolli, L., Takizawa, M.: Towards a smart world and ubiquitous intelligence: a walkthrough from smart things to smart hyperspaces and UbicKids. *Int. J. Pervasive Comput. Commun.* **1**(1), 53–68 (2005)
11. Berners-Lee, T., Hendler, J., Lassila, O.: The semantic web. *Sci. Am.* **284**(5), 34–43 (2001)
12. Fensel, D., van Harmelen, F.: Unifying reasoning and search to web scale. *IEEE Internet Comput.* **11**(2), 94–96 (2007)
13. Foster, I., Kesselman, C.: *The Grid 2: Blueprint for a New Computing Infrastructure*. Morgan Kaufmann, San Mateo (2003)
14. Singh, M.P., Huhns, M.N.: *Service-Oriented Computing*. Wiley, New York (2005)
15. Armburst, M., et al.: Above the clouds: a Berkeley view of cloud computing. Technical report, EECS Department, University of California, Berkeley
16. Hayes, B.: Cloud computing. *Commun. ACM* **51**(7), 9–11 (2008)
17. Chaouchi, H.: *The Internet of things-connecting objects to the web*. ISTE Ltd.Wiley, New York (2010)
18. Ma, J.: Robots and spacelog in smart spaces for novel ubiquitous services: <http://cis.k.hosei.ac.jp/~jianhua/>
19. Kunii, T.L., Ma, J.H., Huang, R.H.: Hyperworld modeling. In: Proceedings of the International Conference on Visual Information Systems (VIS'96), pp. 1–8 (1996)
20. Ma, J.H., Huang, R.H.: Improving human interaction with a Hyperworld. In: Proceedings of the Pacific Workshop on Distributed Multimedia Systems (DMS'96), pp. 46–50 (1996)
21. Giusto, D., Iera, A., Morabito, G., Atzori, L. (eds.): *The Internet of Things*, Springer (2010)
22. Atzori, L., Iera, A., Morabito, G.: The internet of things: a survey. *Comput. Netw.* **54**(16), 2787–2805 (2010)
23. Ashton, K.: That ‘Internet of Things’ Thing. In: *RFID Journal*, 22 July (2009)
24. Bornhovd, C., Lin, T., Haller, S., Schaper, J.: Integrating automatic data acquisition with business processes experiences with SAP’s auto-id infrastructure. In: VLDB Conference (2004)
25. Sujith, S.M.: Classifying and clustering web of things. PhD Thesis. <https://digital.library.adelaide.edu.au/dspace/bitstream/2440/83366/4/01front.pdf>
26. Botta, A., et al.: On the integration of cloud computing and internet of things. In: Proceedings of the 2nd International Conference on Future Internet of Things and Cloud (FiCloud-2014). Barcelona, Spain, 27–29 Aug 2014
27. Zhou, J., Leppanen, T., Harjula, E., Ylianttila, M., Ojala, T., Yu, C., Jin, H.: Cloud things: a common architecture for integrating the internet of things with cloud computing. In: CSCWD, IEEE (2013)
28. Chao, H.-C.: Internet of things and cloud computing for future internet. In: *Ubiquitous Intelligence and Computing, Lecture Notes in Computer Science* (2011)
29. Chung, T.-Y., et al.: Social web of things: a survey. In: International Conference on Parallel and Distributed Systems (2013)
30. Ciortea, A., et al.: Reconsidering the social web of things, position paper. In: Proceedings of the 2013 ACM Conference on Pervasive and Ubiquitous Computing Adjunct Publication (UbiComp’13 Adjunct) (2013)
31. Kamarlis, A., Papadiomidous, D., Pitsillides, A.: Lessons learned from online social networking of physical things. In: 2011 International Conference on Broadband and Wireless Computing, Communication and Applications (BWCCA), pp. 128, 135. 26–28 Oct (2011)
32. Zhong, N., et al.: Research challenges and perspectives on wisdom web of things (W2T). *J. Supercomput.* **64**(3), 862–882 (2013)
33. Evans, D.: Beyond things: the internet of everything, explained in four dimensions: http://www.huffingtonpost.com/dave-evans/cisco-beyond-things-the-interne_b_3976104.html?ir=India

Cloud Load Balancing and Resource Allocation

An Advancement in Cloud Technology

Himanshu Mathur, Satya Narayan Tazi and R.K. Bayal

Abstract In Last one decade researchers are focus on cloud computing presenting many novel approach for improving storage spaces in digital world. In this paper, we introduce architecture and algorithms that can be implemented to facilitate well-equipped infrastructure within cloud environment for load balancing and resource allocation. This architecture is specially developed for virtual storage drive over cloud. This architecture supports a number of end users, which are authenticating to send requests to the server. This request may demand some resources for its processing, thus, here comes the concept of resource allocation where it is required to allocate and schedule the available resources to process the request of the client. A numerous algorithms have been introduced here for easy configuration for the proposed architecture. The conclusion of this research paper is to provide such a cloud framework which can be implemented for efficient resource allocation and load balancing for multiple clouds.

Keywords Virtual · Cloud · Resource allocation · Load balancing · SaaS · Dynamic · Sharing · Storage · Client · Server · Remote

H. Mathur (✉) · S.N. Tazi
Government Engineering College, Ajmer, India
e-mail: himanshu.cool25@gmail.com

S.N. Tazi
e-mail: satya.tazi@gmail.com

R.K. Bayal
University College of Engineering, RTU, Kota, India
e-mail: rkbayal@gmail.com

1 Introduction

Cloud computing is a viral technology these days; a common trend includes storing of data over the virtual drives. Virtual drives are basically remote storage devices, where an end user can store, save, manipulate, and delete data. Cloud is a technology, where one can remotely manage their own data. Resources such as memory, processor, bandwidth, etc. are required to process the client requests. On server side management of these resources is a tidy task, it's requires proper resource management and resource scheduling for the overall system efficiency. Virtual storage involves a concept of Software as a service (SaaS), this service provides the virtual editor application which allows clients to create and modify data online without installing that application and independent of the platform. Several layers of technology are required to interact with different system elements [1, 2].

2 Related Work

The technologies-based cloud computing is very popular among the people. There are several esteem I.T. organizations who contributed in virtual drive technologies, like Google Drive is a very widely used an appreciated platform provided by the Google. This technology allows a user to store its data on remote server of Google, and can fetch from anywhere using internet. Popular technology is Drop Box provided by Microsoft Corporation. It also allows its users to store their data remotely and share it over the internet. Here is a new technology that enhances the searching performance and results in overall performance growth. Also it contributes in performance by minimizing the idle time for the networking system. Pervasive computing has generally focused more on improving functionality and reliability, we see a transition to using a cloud computing backbone in pervasive systems as an opportunity to bring stronger security to pervasive systems.

Research has been done over Generalized Priority algorithm for efficient execution of task and comparison with FCFS and Round Robin Scheduling. Such algorithms are being tested in cloud Sim toolkit and result shows that it gives better performance compared to other traditional scheduling algorithm. Algorithms are developed for a new generalized priority-based algorithm with limited task, in future we will take more task and try to reduce the execution time as presented and we develop this algorithm to grid environment and will observe the difference of time in cloud a grid. Vast amount of research has been conducted on resource allocation or job placement, especially in the Grid/high-performance computing community. Systems such as Condor and Globus Toolkit have been used to share computing resources across organizations.

Resource allocation model for cloud computing environments and has recently proposed the optimal joint multiple resource allocation method. Several architecture and concepts are being developed providing the detailed comparison on the Grid

computing and Cloud computing. The cloud infrastructures enables the fair resource allocation among multiple users without a large decline in resource efficiency, compared with the conventional method which does not consider the fair allocation. One of the achievements of these models and concepts are successfully able to reduce the request loss probability and as a result, reduce the total amount of resource, compared with the conventional allocation method [3–8].

3 Proposed Layered Architecture

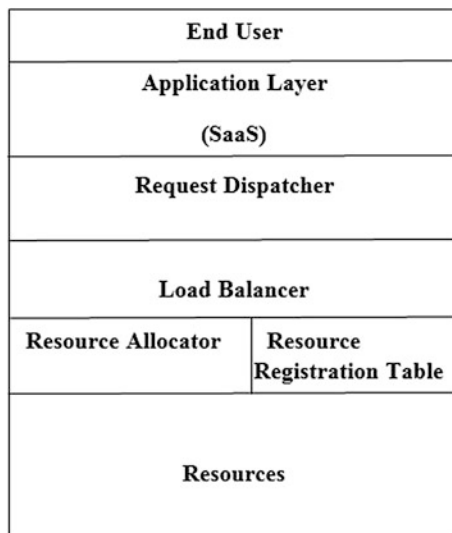
The proposed layered architecture consists of six layers. Figure 1 shows the six layered architecture which represents different elements of the overall system which are strictly bonded via dynamic networking concepts [9].

The Layers of this proposed architecture are discussed as follows.

3.1 End Users

These are the clients of this cloud infrastructure. These are authorized to make request over the server for remote storage and sharing. This is the major source of Load (data for storage) over the network as well as to the virtual space over the server. There could be ‘ n ’(integer) number of end users which are active over the network.

Fig. 1 Layered architecture



3.2 Application Layer

This layer provides the end user interface. It is based on the concept of SaaS. It provides user with all the data operations like file creation, manipulation, removal, and many more. All these user activities are temporarily stored and bind up as a whole request. This request is forwarded to the request dispatcher.

3.3 Request Dispatcher

This component receives a set of activities in form of a request. The request dispatcher checks for the validity and timeliness of the request. Also the request dispatcher is responsible for the session management for the user. The major task of request dispatcher is to filter out the request which requires resources for its processing. These filtered requests are forwarded to the next layer, i.e., load balancer.

3.4 Load Balancer

This is the master server which have access to all the requests from the user and all the resources available at server side. The major function of load balancer is to analyze the end user request and to calculate the total load out of it. Load balancer communicates directly with the resource registration table and gets the current status of the load over the required resources types. Thus it selects the ultimate resource destination for the request. Thus load balancer has two major tasks first is load calculation and second is decision making regarding the resource selection.

3.5 Resource Allocator

This component gets the result of decision making of load balancer, i.e., the resource id and resource type, to which the current requests has to be processed. The major task of resource allocator is to schedule the current request over the resource decided by the load balancer. Thus resource allocator schedules the job over the resource.

3.6 Resource Registration Table

It is type of database which holds the details of all the resources available in the cloud network. This table provides a resource Id for each resource registered to it. Also it maintains the current status of its load. It also defines the type of resource like storage, printer, processor, etc.

3.7 Resources

These are the physical devices which are requested by the clients to process their request.

4 Proposed Algorithms for Configuration

We can monitor the overall resource allocation for virtual drive and cloud computing concepts by using various algorithms for different components performing specific tasks and those collectively gives relevant output. Our research considered the following algorithms.

4.1 Resource Registration Algorithm

This algorithm is required whenever a new resource is introduced in the cloud network. This algorithm makes an entry of resource details within the resource registration database.

```
Begin:  
    Generate Resource Id and store as Rid  
    Allocate network IP to the resource, Rip  
    Get Resource Type, Rtype  
    Get Maximum Capacity, Rmax  
End
```

4.2 Load Balancing Algorithm

```

Begin
Get capacity of each m secondary storage from ArrayRmax[m].
Get size of Client request, d.
Get the current load status of m drives, ArrayLoad[m].
Calculate min(ArrayLoad[m]) and get its index, say i.
If ArraySize[i]>= d then:
Send details of i resource to Request Dispatcher.
Else
Display Error Message.
End

```

4.3 Scheduling Algorithm

The request dispatcher performs the task of scheduling of the job at the i resource. A modified version of multiple queues scheduling an algorithm can be used for scheduling of the jobs. Each layer of queue has its own scheduling algorithm. The queues itself are scheduled in round robin fashion to avoid starvation problem.

```

Begin:
Set quantum time, tq
while(true)
{
If: Job is available
Then: enter the Job Jk in Qd queue.
set timer, t=0
//let there are total d number of queues.
for (q=0;q<d;q++)
{
for (t=0; t<= tq ; t++)
{
process Qq
}
}
}

```

5 Implementation and Analysis

To implement this new algorithmic concept shows in Fig. 2. We require some tools that support this technology. We can use many coding languages like java, php, python, C#, etc. We have implemented this project over php. Further, we need an editor tool; it can be Netbeans, Eclipse, Dreamweaver, etc. Also if we need any backend support for database we can use Xampp, Wamp, Sql Server, MS Access, etc. Wired or wireless connectivity can be performed for internetworking of cloud users [10–12].

The basic concept behind the connectivity is getting the IP addresses of the cloud nodes. To begin with this application, it will ask for request from the client which can be processed over any of the resources available. When the client request has been provided by the client, the request passes to the master server for load balancing. This process runs in background for the client. Now load balancing server forwards the request to various layers of the system and finally to the destination resource.

Fig. 2 Flow chart for load balancing in cloud computing

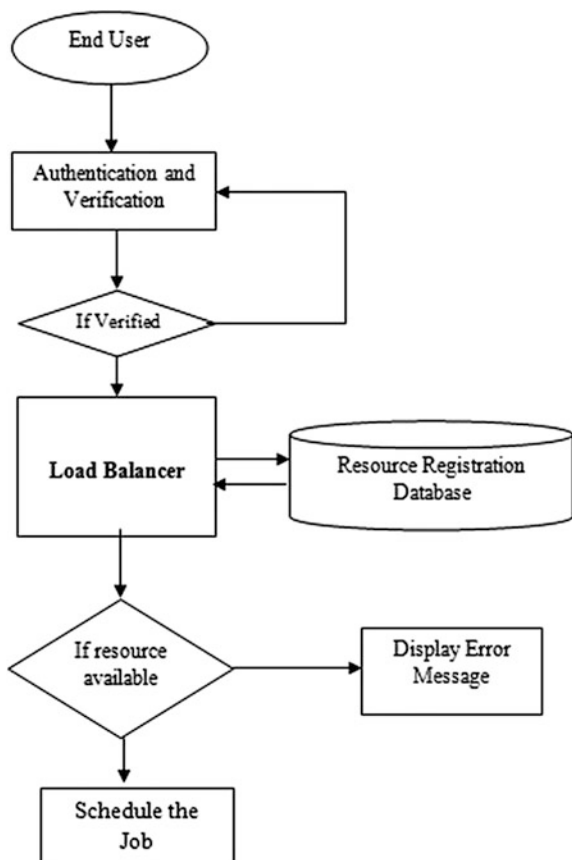


Table 1 Quick sort algorithm complexity

Worst case performance	Best case performance
$O(n^2)$	$O(n \log n)$ (simple partition) or $O(n)$ (three-way partition and equal keys)

The load balancer performs the quick sort on the `ArrayLoad[m]` to find the resource which has minimum utilization in a particular category. Thus, we get the resources which have the maximum current capacity to process the request, and the client request has been fulfilled by allocating the resource to the client request. Here, we used quick sort algorithm whose complexity is as following Table 1.

6 Conclusion and Future Work

Our research works over the cloud technology which solves the load balancing problems faced during virtual drive implementation as well as resource allocation. Centralized client-server model has been used, which consists of client, master server, and secondary storage server. This project prove beneficial for large-scale area where large amount of data is stored on virtual machines as we provide the algorithms to store the data in easiest way without creating any network traffic. This concept can be implemented by any small/big organization for their private virtual network (VPN) over which they can create their separate cloud over which its network users can store and share their data. This implementation will be completely personal for that particular organization. Hence, a VPN can be designed for any organization for easy storage of data and its sharing over the same VPN. As day by day many organizations collects data according to their requirements and store it over the network storage devices which require a good mechanism between client and server for sharing the data. So this problem is also solved by our work. In future, this technology can be implemented over complete wireless networking and for long distances. We can also launch this technology to the smart phones, so that the mobile users can also use this application. To work for mobile users a concept of dynamic IP have to be used and another algorithm regarding the IP configuration have to be proposed. This new technology of cloud computing is also implemented through grid technology over which resource sharing can be a major point of concern. So by using this concept with grid technology, not only data is shared or accessed between client and server but also data is secure by various network protocols.

References

1. Mehta, H., Kanungo, P., Chandwani, M.: Decentralized content aware load balancing algorithm for distributed computing environments. In: ICWET'11. ACM, Mumbai, Maharashtra, India, 978-1-4503-0449-8, 25–26 Feb 2011
2. Eason, G., Noble, B., Sneddon, I.N.: On certain integrals of Lipschitz-Hankel type involving products of Bessel functions. *Phil. Trans. Roy. Soc. London A247*, 529–551 (1955)
3. Toyoshima, S., Yamaguchi, S., Oguchi, M.: Middleware for load distribution among cloud computing resource and local cluster used in the execution of data-intensive application. *J. Database Soc. Japan* **10**(1), 31–36 (2011)
4. Tazi, S.N., Mathur, H., Mishra, V.: Cloud virtual drive load balancing and dynamic networking. In: ACE'14. Kochi, Kerela, India. 27 Dec 2014
5. Uppal, H., Brajkovic, V., Brandon, D., Anderson, T., Krishnamurthy, A.: ETTM: a scalable fault tolerant network manager. In: NSDI (2011)
6. Verma, A., Ahuja, P., Neogi, A.: pMapper: power and migration cost aware application placement in virtualized systems. In: Proceedings of the 9th ACM/IFIP/USENIX International Conference on Middleware, pp. 243–264. Springer (2008)
7. Koseoglu, M., Karasan, E.: Joint resource and network scheduling with adaptive offset determination for optical burst switched grids. *Future Gener. Comput. Syst.* **26**(4), 576–589 (2010)
8. Cardosa, M., Korupolu, M., Singh, A.: Shares and utilities based power consolidation in virtualized server environments. In: Proceedings of the 11th IFIP/IEEE Integrated Network Management. IM 2009, Long Island, NY, USA (2009)
9. Srikanthiah, S., Kansal, A., Zhao, F.: Energy aware consolidation for cloud computing. *Cluster Comput.* **12**, 1–15 (2009)
10. Kusic, D., Kephart, J.O., Hanson, J.E., Kandasamy, N., Jiang, G.: Power and performance management of virtualized computing environments via lookahead control. *Cluster Comput.* **12**(1), 1–15 (2009)
11. Pinheiro, E., Bianchini, R., Carrera, E.V., Heath, T.: Load balancing and unbalancing for power and performance in cluster-based systems. In: Proceedings of the Workshop on Compilers and Operating Systems for Low Power, pp. 182–195 (2001)
12. Yu, M., Yi, Y., Rexford, J., Chiang, M.: Rethinking virtual network embedding: substrate support for path splitting and migration (2008)

A Novel Methodology to Filter Out Unwanted Messages from OSN User's Wall Using Trust Value Calculation

Renushree Bodkhe, Tushar Ghorpade and Vimla Jethani

Abstract Basic challenge in current Online Social Networks (OSNs) is to grant total control and access to its millions of customers (users) over the data and/or messages shared or highlighted on their personal accounts or private spaces. This control would allow users to have a check on its content and in turn would help in building a strong system facilitating OSN users to directly control the data/content. We need to update our training data on regular basis else it will misclassify any unwanted message which is not in our training data resulting into a negative impact on the accuracy of system. Hence to overcome this limitation we are proposing a new approach where-in an adjustable defined system that allows users to apply text filtering algorithms at preprocessing stage so as to categorize the message and trust value calculation. In this technique it will calculate the trust value for each message and give the trustworthiness of users. If that trust value is less than predefined threshold then it will block that user.

Keywords Online social networks • Information filtering • Short text classification

1 Introduction

With every passing decade the means of communication are changing rapidly. In current scenario most effective, speedy, and cost effective means of communication are the Online Social Networks (OSNs), there by, becoming the integral part of human lives.

R. Bodkhe (✉) · T. Ghorpade · V. Jethani

Department of Computer Engineering, Ramrao Adik Institute of Technology Nerul,
Navi Mumbai, India

e-mail: renushreebodkhe@gmail.com

T. Ghorpade

e-mail: tushar.ghorpade@gmail.com

V. Jethani

e-mail: vimlajethani@gmail.com

An OSN is a web-based service that allows individuals to:

1. Create an account with Private or Public features within the service.
2. Prepare their own groups with different people of same interest.
3. View and traverse People in their contact list or other peoples contact list within the service [1].

Information and communication technology (ICT) plays a vital role in today's world. Like never before online security and privacy matters have become burning issues and point of concern for users. "Necessity is the mother of invention" hence, security mechanism is the need of the hour for different ICT [2]. Thus text filtering can thus be used to enable users to have greater control on the content posted on their walls. In current scenario, OSNs grant minimum support to its user from security and privacy point of view. For example, Facebook allows users to state who is allowed to insert messages in their walls (i.e., friends, friends of friends, or defined groups of friends). In OSN content data checking does not happen every time and hence it is highly likely that politically or socially offensive messages gets posted without any check or filter irrespective of the users.

The main goal of the system is to evaluate an automated system, called Filtered Wall (FW), thereby, eliminating undesired data or messages from OSN user walls. The basic concept behind the system is the support for content-based user preferences. It became possible with the use of Machine Learning (ML) text categorization procedure which is capable of automatically assigning with each message a set of categories based on its content. We are of the opinion that strategy is the main factor for social networks as users have minimum control on the content displayed on their private space. As against this with the help of mechanism the user can decide and control the data displayed on his/her private space by defining set of filtering rules. Filtering rules are very flexible in terms of the filtering requirements they can support, in that they allow to specify filtering conditions based on user profiles, user relationships as well as the output of the ML categorization process.

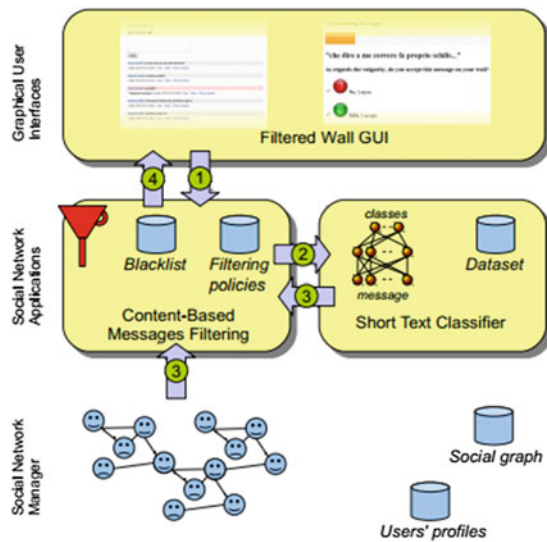
1.1 Filtering Wall Conceptual Architecture

The above figure depicts the three-tier architecture structure in support of OSN services. In Fig. 1 Layer-1, called Social Network Manager (SNM), focuses on providing basic OSN functions, Layer-2 supports external Social Network Applications (SNAs) [3].

The supported SNAs may in turn require an additional layer for their needed Graphical User Interfaces (GUIs). In accordance with this architecture, the proposed system is placed in the second and third layers. Users interact with the system by means of a GUI to set up and manage their FRs/BLs.

As graphically depicted in Fig. 1, the path followed by a message, from its writing to the possible final publication can be summarized as follows:

Fig. 1 Conceptual filtering architecture [3]



1. IF the user tries to post a message on private wall of his or her contacts the message gets intercepted by FW.
2. Metadata gets extracted from the message by an ML-oriented text classifier.
3. This classifier provides metadata which in turn is used by FW along with data extracted from social group and user's profile.
4. Based on the output of Step-3 the message gets published or filtered by FW.

1.2 Filtering Rules

OSNs one message can have varied meaning based on who writes it and in what context just like our direct communication. FRs should facilitate users to have control on the message creators. There are n number of criteria based on which FR are applied on creators. Likewise it is possible to define rules that are applicable based on users age or political or religious views. Under specific social network scenario, based on the information on their social graph creators may also be identified. This implies to state conditions on type, depth, and trust values of the relationship(s) creators should be involved in order to apply them the specified rules. Filtering Rules are customizable by the user. User can have authority to decide what contents should be blocked or displayed on his wall by using Filtering rules. For specifying Filtering rules user profile as well as user social relationship will be considered.

1.3 Radial Basis Function Network (RBFN) Algorithm

```

1: d ← input message
2: for all d ∈ D do
3: perform text categorization
4: if d! = null then
   Filter text for unwanted symbols
5: apply stemming and mark stop-words in d;
6: end for

```

A. Text Filtering

In the text filtering step, all terms that are useless or would introduce in filtering process are removed from the input message. Among such terms are:

- HTML tags (e.g., <table>) and entities (e.g., & ;) if any.
- Non-letter characters, such as “\$”, “%”, or “#” (except white spaces and sentence markers such as ‘.’, ‘?’, or ‘!’).

Note that at this stage the stop-words are not removed from the input.

B. Stemming

The main function of Stemming algorithms is having the words in text form transformed into their grammatical root form which serves mainly to improve system’s information retrieval efficiency. To stem a word means reducing it to more simplistic form. For Example, if we stem the word demanding it would produce term demand. Our main aim is to have all words that have same stem to have same root.

C. Elimination of Stop Words

Once through with stemming next task is to remove unwanted words. These stop words are approximately 400–500 types that includes “is”, “of”, “the”, etc. which provides no relevant information about the message. Process of removing these words is called as Stop-word removal. Of the entire document on an average stop words account for about 20 % of all words. Such techniques help in reducing size of searching and matching each word in message. Size of index is reduced by almost 40 % by Stemming algorithm alone.

2 Literature Review

Below papers form the basis of our study. The techniques, algorithms, and discussions in these papers would be used for our knowledge.

- Vanetti et al. [3] has proposed main service for OSNs in the form of content-based message filtering. This system facilitates OSN users complete

control on the data /content posted on their private spaces. This is achieved via flexible rule-based system, which facilitates user to personalize filtering criteria which is to be applied to their private spaces along with ML-based soft classifier automatically producing membership labels in support of content-based filtering.

- Adomavicius and Tuzhilin [4] give an overview of the field of recommender systems and describe the current generation of recommendation methods that are usually classified into the following four main categories: content-based, collaborative, policy-based personalization, and hybrid recommendation approaches.
- Sriram et al. [5] states, the classification of short text messages. As short texts do not provide sufficient word occurrences, traditional classification methods, such as “Bag-Of-Words” have limitations. The proposed approach effectively classifies the text to a predefined set of generic classes, such as News, Events, Opinions, Deals, and Private Messages.
- Beye et al. [6] discussed a lack of experience and awareness in users, as well as proper tools and design of the OSNs, perpetuate the situation. This paper aims to provide insight into such privacy issues and looks at OSNs, their associated privacy risks, and existing research into solutions.
- Hidalgo et al. [7] discussed, a model for text-based intelligent Web content filtering, in order to demonstrate how this model can be realized, they have developed a lexical Named Entity Recognition system, and used it to improve the effectiveness of statistical Automated Text Categorization methods.

3 Proposed Work

3.1 *Proposed Algorithm*

FR = {Trustier, SOUs, Rule, TuV}.

FR is dependent on following factors.

FR denote filtering rule.

Trustier is a person who defines the rules.

SOUs denote the set of OSN user.

Rule is a Boolean expression defined on content.

Following is the process of implementing Filtering:

FM = {SOUs, Rule == category (Violence, Vulgar, offensive, Hate, Sexual), TuV}

Here,

FM Block Messages at basic level.

SOUs Denotes set of users.

Rule Category of specified contents in message.

TuV is the trust value of sender.

In this process, after giving input message, the system will compare the text with the different categories which are prevented. If the message found in that is prevented type of category then message will display to the user that “can’t send this type of messages”, and still the user wants to send the message he/she can continue with sending the message. The trustier, who gets the message, but the words which are defended in the rule are sent in **** format. After getting the message the trustier will give the Feedback (FB) to the sender and the sender will gain the TuV accordingly.

Process denotes the action to be performed by the system on the messages matching Rule and created by users identified by SOUs.

E.g., FM== {Friends, Rule==category (Vulgar, Sexual), TuV>50}

That is, Trustier will accept the message from friends but message should not contain vulgar or sexual words. Message containing such words will affect the TuV of sender.

Now the question arises, calculation of TuV.

3.2 Trust Value Calculations

The trust value of any user in OSN is dependent on the feedback they gain by the user to whom they sent a message. Feedback from the user must also be trustworthy. That is why the FB can be categorized into following:

1. *Positive with content (PC)*—Good FB, message is acceptable with objectionable content. This will increase the TuV of sender.
2. *Positive without content (PWC)*—Good FB, message is acceptable as this message does not contain objectionable content. This will increase the TuV of sender.
3. *Negative with content (NC)*—Bad FB, such messages must not be sent again, which are against the Rule. This will decrease the TuV of sender.
4. *Negative without content (NWC)*—Bad FB, message does not contain any objectionable content but the trustier is giving negative FB. Such type of FB from trustier will affect the TuV of its own, and the TuV of sender will remain same.

So, based on the above categories the TuV will be calculated as follows:

$$\text{FB as 1 and 2 TuV} = \text{TuV} + \text{abs}[(\text{PC} + \text{PWC}) / (\text{NC} + \text{NWC})] \quad (1)$$

$$\begin{aligned} \text{FB as 3 TuV} &= \text{TuV} - [1 + (\text{NC} + \text{NWC}) / (\text{PC} + \text{PWC})] \\ &\text{for } [(\text{NC} + \text{NWC}) / (\text{PC} + \text{PWC})] < 1 \end{aligned} \quad (2)$$

Otherwise, sends system generated message to sender, FB Negative with content exceeds limit of Threshold Value (ThV) and deduct five points from TuV, so ThV = TuV - 5.

$$\begin{aligned} \text{FB as 4 TuV} &= \text{TuV of sender, but TuV} \\ &= \text{TuV} - [1 + (\text{NC} + \text{NWC}) / (\text{PC} + \text{PWC})] \text{ for Trustier.} \end{aligned} \quad (3)$$

3.3 Trust Value Calculations with an Example

Suppose: user is Priya.

Assume, PC = 5 PWC = 2 NC = 6 NWC = 1 for Priya. & TuV = 30

Message: Acid is chemical so it is used to destroy face.

As we know this message will go into the non-neutral category. Then, trustier will give the feedback to this message.

Hence, we will calculate the trust value using following formula.

$$\text{TuV} = \text{TuV} - [1 + (\text{NC} + \text{NWC}) / (\text{PC} + \text{PWC})]$$

$$\text{TuV} = 30 - [1 + (6 + 1) / (5 + 2)]$$

$$\text{TuV} = 28.85.$$

Here, we can see that the trust value is reduced here for Priya.

As we calculated here value of $(\text{NC} + \text{NWC}) / (\text{PC} + \text{PWC}) = 1.1428 > 1$

So it exceeds the limit and system generated message will be sent to the user. Means this message will be filter out using TuV method. This increases its true positive rate.

Here we will assume that TP = 3 FP = 2 TN = 1 FN = 1

Now our TP = 4 FP = 2 TN = 1 FN = 1

RBFN: Now we will filter out the same message using RBFN but our algorithm failed to filter this message because as per training rules system consider this message as neutral message. Means **acid is chemical** is neutral sentence. Our training data does not contain dangerous as filter word. So this message will not be filter out. Hence it will increase its false negative rate.

So, TP = 3 FP = 2 TN = 1 FN = 2

Performance Parameters: The performances of our proposal are evaluated by various parameters described below:

1. Accuracy: It shows accuracy of sending message between RBFN algorithm and trust value calculation.

$$\text{Accuracy} = (\text{No. of True Positives} + \text{No. of False positives}) / (\text{No. of True Positives} + \text{No. of False positives} + \text{No. of True Negative} + \text{No. of False Negative})$$

2. Precision: It defines refinement in a measurement of the result.

$$\text{Precision} = (\text{No. of True Positives}) / (\text{No. of True positives} + \text{No. of False positives})$$

3. Recall: It is used to find out total recall of true values from the result.

$$\text{Recall} = (\text{No. of True Negatives}) / (\text{No. of True Negative} + \text{No. of False positive})$$

4. F1-measure: It is measurement that combines precision and recall is the harmonic mean of precision and recall, the traditional F1-measure or balanced F1-measure (Table 1).

$$\text{F1 - measure} = (2 * (\text{Precision} * \text{Recall})) / (\text{Precision} + \text{Recall})$$

3.4 Result of Practical Work: Graphical Analysis

Accuracy Figure 2 accuracy graph will show and give the comparative accuracy result between RBFN algorithm and trust value calculation according to the filtering of message counting.

Trust value performance Figure 3 show that the trust value variations according to the message type sent. If trust value goes less than threshold value then that message will be filtered out.

Table 1 Comparison on RBFN and trust value calculation (proposed)

Performance parameters	RBFN (%)	Proposed (%)
Accuracy	62	75
Precision	60	66
Recall	33	50
F-measure	42.58	56.89

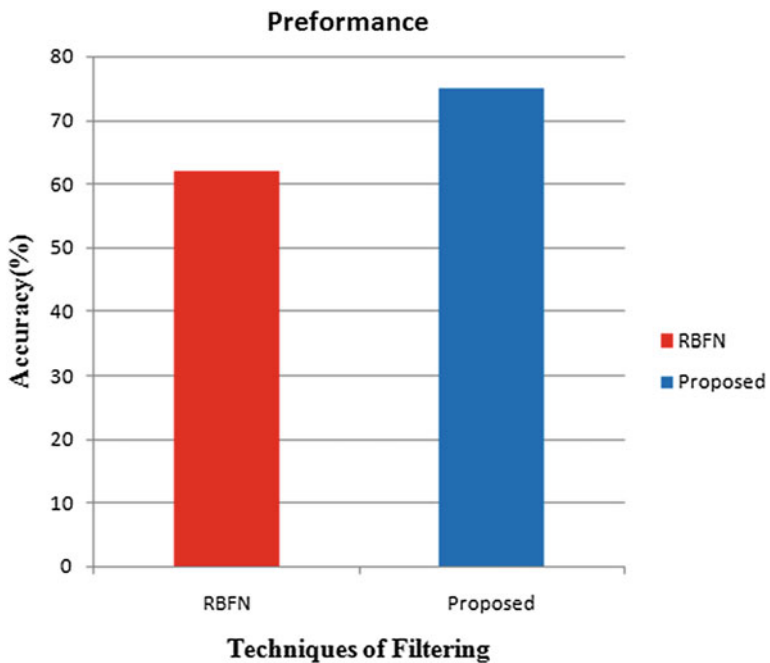


Fig. 2 Accuracy graph

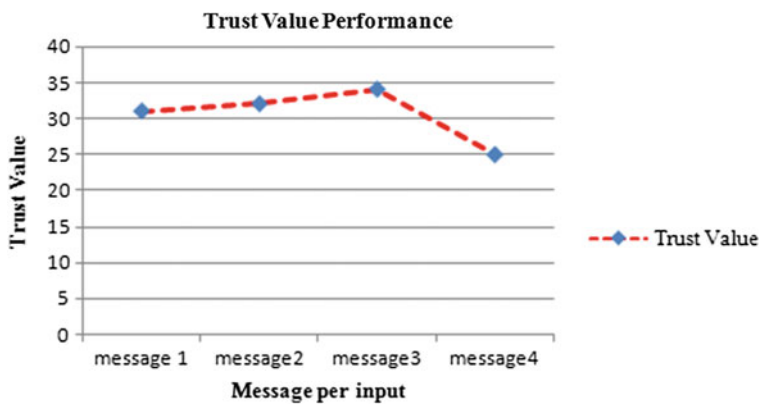


Fig. 3 Graph shows the trust value variations

4 Conclusion

We are developing a system to filter undesired messages from OSN walls. This wall then intern restricts the unwanted messages hence called as the Filtered Wall (FW). We have discussed the idea about filtering system. In addition to that, we have studied strategies and techniques limiting the inferences that an user can do on the enforced filtering rules with the aim of bypassing the filtering system and the flexible rule-based system. We have applied text filtering algorithms at pre-processing stage so as to categorize the messages (like political, violence, etc.) and trust value calculation for these messages. In our proposal, we will calculate trust value for each message and it will give the trustworthiness of user. If that trust value is less than predefined threshold then it will block that user.

In future work, in multi-language work we plan to update and strengthen the training data so as to increase its accuracy on a regular basis. Scope of this work can also be extended to video and images.

References

1. Chau, M., Chen, H.: A machine learning approach to web page filtering using content and structure analysis. *J. Decis. Support Syst.* **44**(2), 482–494 (2008)
2. Adomavicius, A., Tuzhilin, G.: Toward the next generation of recommender systems: a survey of the state-of-the-art and possible extensions. *IEEE Trans. Knowl. Data Eng.* **17**(6), 734–749 (2005)
3. Vanetti, M., Binaghi, E., Ferrari, E., Carminati, B., Carullo, M.: A system to filter unwanted messages from OSN user walls. *IEEE Trans. Knowl. Data Eng.* **25**, 1–14 (2013)
4. Adomavicius, G., Tuzhilin, A.: Toward the next generation of recommender systems: a survey of the state-of-the-art and possible extensions. *IEEE Trans. Knowl. Data Eng.* **17**(6), 734–749 (2005)
5. Sriram, B., Fuhr, D., Demir, E., Ferhatosmanoglu, H., Demirbas, M.: Short text classification in twitter to improve information filtering. In: Proceedings of the 33rd International ACM SIGIR Conference on Research and Development in Information Retrieval, pp. 841–842 (2010)
6. Beye, M., Jeckmans, A., Erkin, Z., Hartel, P., Lagendijk, R., Tang, Q.: Literature overview-privacy in online social networks. In: Distributed and Embedded System (DIES), pp. 1–19 (2010)
7. Hidalgo, J.M.G., Garcia, F.C., Sanz, E.P.: Named entity recognition for web content filtering. In: 10th International Conference on Applications of Natural Language to Information Systems, pp. 1–12 (2005)

Resource Prioritization Technique in Computational Grid Environment

Sukalyan Goswami and Ajanta Das

Abstract A computational grid environment consists of several loosely coupled pool of virtualized heterogeneous resources. The resources are geographically dispersed and their interactions with other components in the grid are independent of location. The grid architecture follows a Client-Broker-Resource system. The broker is as an intermediary between the clients and the resources. The broker allocates the resources to the clients based on the response received by each resource. In this scenario, prioritization of client's request rather to prioritize the resource, which may fulfill clients' request, is a major issue. Eventually, prioritization of resources balances workload in grid. Thus, the objective of this paper is to prioritize the resources, in order to allocate jobs in computational grid, using analytic hierarchy process (AHP) methodology. This technique plays major role in our proposed nearest deadline first scheduled (NDFS) algorithm. This paper also demarks the resources with proper ranking in Unicore grid environment.

Keywords Grid computing · Load balancing · Resource prioritization · Analytic hierarchy process (AHP)

1 Introduction

Grids [6] were originally built to ensure resource and knowledge sharing within scientific community. A lot of progress has been made till now from the inception of grid infrastructure. The grid is a system which is capable to cater to large number of jobs. The properties of heterogeneity and loose coupling differentiate grids from typical high-performance computing. Moreover, participating resources of com-

S. Goswami (✉)

Institute of Engineering & Management, Salt Lake, Kolkata, India

e-mail: sukalyan.goswami@gmail.com

A. Das

Birla Institute of Technology, Mesra, Kolkata Campus, Kolkata, India

e-mail: ajantadas@bitmesra.ac.in

putational grid are generally geographically dispersed. So, the computational grid [6], consists of large number of distributed heterogeneous resources to solve different types of large-scale problems in engineering and science. These problems also deal with enormous amount of data. Hence, the conventional approaches used in distributed systems are incapable of solving problems in computational grid [2].

One of the urgent requirements in grid is designing of an efficient framework to balance load effectively across all participating nodes. Because of irregular task receiving patterns and uneven computational powers, different nodes in different grid sites will generally have unequal load patterns; some nodes may be underutilized whereas some other may be highly overloaded. So, to exploit the full power of such grid systems, scheduling of jobs, allocation, and management of resources are essential functions in grid to be dealt with. The objective of this paper is to prioritize the resources, in order to allocate jobs in computational grid, using AHP [17] methodology. Moreover, the ranking system of resources has been redefined using AHP. In reality, ranking of resources play major role in our proposed NDFS algorithm.

Section 2 presents the related works in this sphere and Sect. 3 proposes prioritization of resources using AHP. Section 4 presents the results with specified ranking of the resources in Unicore grid environment and discussion giving an insight toward future scope of the work. Section 5 concludes this paper.

2 Related Works

There are a few approaches available in computational grid for task scheduling. Stal [18] proposed a solution related with client/server systems. When two independent components—a client and a server—need to interoperate, they have to communicate with each other, which create several dependencies and limitations.

Adebayo et al. [1] proposed two different broker architectures, namely, forwarding broker, and handle-driven broker. Forwarding broker acts as the mediator between clients and servers for any possible transactions. It communicates with proper resource application as per the specific requirement of a client. After computation is over, the forwarding broker sends the result, after retrieving from resource, to the client. The handle-driven broker works in the same line as of a name server. Resource's name, network address, and working request format are sent as a service handle by this type of broker back to the client.

In [19] it is found that multi-criteria decision-making (MCDM) model solves many critical issues related to practical applications. While solving decision and planning problems, which involve multiple criteria, MCDM model helps decision makers. AHP is an effective tool for MCDM. AHP meets the objective of decision making by ranking the choices according to their merits. Initially, subjective judgements are made about attributes' relative importance. Better the initial judgements, more effective are the logical consequence coming out of the AHP calculations.

The load balancing mechanism in computational grid tries to achieve equal distribution of workload among the participating resources, as scheduling of jobs in

computational grid varies based on load factors of the resources. So, resource ranking will play a crucial role in scheduling of jobs, as well as proper utilization of resources. A number of load balancing approaches have been studied earlier in [3, 5, 11–15] and based on this study, a ‘service-oriented load balancing framework’ is and a load balancing algorithm, NDFS, in grid environment are proposed in [9, 10]. The GridSim [4] based simulation results, were compared with existing load balancing algorithms in [7, 9]. These results portrays simulation performance of NDFS was found to be better than many other existing algorithms. This research work currently concentrates on redefining the resource ranking procedure as part of the proposed load balancing algorithm, NDFS [7]. In NDFS, the resource broker is empowered to take consistent decision for scheduling jobs. This paper proposes a novel resource prioritization technique based on AHP.

3 Prioritization of Resources Using Analytic Hierarchy Process

Load balancing in computational grid is more difficult compared to general distributed systems because of few inherent properties of grid, namely, adaptability and scalability, autonomy, resource selection, heterogeneity, and computation-data separation. In spite of these obstacles, prioritizations of resources for allocating the suitable jobs are most important task in order to balance load. Hence, the proposed algorithm NDFS works on the notion of ‘priority scheduling’ based on the deadlines of the tasks submitted.

To deal with critical decision-making processes, Saaty (1980) developed the AHP [17] model. AHP helps the analyst by setting priorities and reaching to final decision by computing a series of pair-wise comparisons. So, in this process the results are synthesized by considering both objective and subjective aspects of a judgement. Moreover, AHP ensures non-biased decision making by calculating consistency of the evaluations made. Next subsection presents the detailed methodology of AHP.

3.1 AHP Methodology

The AHP facilitates in making the best decision by considering alternative options and evaluation criteria. In AHP, the best result will achieve the most suitable trade-off among the different criteria, because some of the criteria could be drastically contrasting. Each evaluation criterion in AHP is weighted according to the decision maker’s pair-wise comparisons of the criteria. Higher the value, the more dominant the corresponding factor. Then, for a particular criterion, options are assigned scores by AHP, again according to the decision maker’s pair-wise comparisons. Figure 1 presents the common rating scale given by Saaty [16].

Intensity of importance	Definition	Explanation
1	Equal importance	Two factors contribute equally to the objective.
2	Weak or slight Moderate importance	Experience and judgment slightly favour one activity over another.
3	Moderate plus Strong importance	Experience and judgment strongly favour one activity over another.
4	Strong plus Very strong or demonstrated importance	An activity is favoured very strongly over another; its dominance demonstrated in practice.
5	Very, very strong Extreme importance	The evidence favouring one activity over another is of the highest possible order of affirmation.
6		
7		
8		
9		
Reciprocals of above	If activity i has one of the above non-zero numbers assigned to it when compared with activity j, then j has the reciprocal value when compared with i	A reasonable assumption.

Fig. 1 The Saaty rating scale [16]

3.2 Dynamic Load Computation Based Resource Ranking

The load of the resources greatly varies in computational grid environment. NDFS schedules jobs in grid based upon the dynamic load computation of the participating resources. Several properties of the processors of the resources were considered, like the number of cores, current CPU utilization, the clock frequency of the CPU, network utilization as well as the available RAM in order to rank the resources in NDFS. Hence, dynamic load computation involves all the properties (or factors) mentioned above. Whenever the resource broker receives any request from the client, it requests for the current status of each of the resources. Then in response, each resource sends its calculated CPU weightage value and RAM availability to the broker.

This paper proposes a novel resource prioritization technique using the AHP methodology, in order to optimize resource ranking procedure. CPU weightage has been optimized by assigning proper weights to different factors, namely,

- x_1 Number of cores of the processor
- x_2 Free CPU usage = $(1 - \text{CPU utilization}/100)$
- x_3 Clock frequency in GHz
- x_4 Free Network usage = $(1 - \text{Network utilization}/100)$

In AHP, a matrix is constructed with the comparative values of the selected factors. For NDFS, the relative importance of CPU usage as opposed to number of cores in a processor while finding ranks of resources to allocate them to submitted jobs in computational grid. According to Saaty rating scale [16] shown in Fig. 1, if factor m is entirely more dominant compared to factor n and is valued at 9, then n is entirely less dominant compared to m and is rated at 1/9.

Hence, the CPU weightage can be defined as:

$$f(\text{CPU weightage}) = \sum w_i x_i \quad \text{where, } \sum w_i = 1, \quad i \in (1, 2, 3, 4) \quad (1)$$

Among the four factors, number of cores is assigned highest priority followed by free CPU usage. In computational grid environment, faster computation of jobs is achievable with higher number of processor cores. Moreover, higher core processor will be able to complete job earlier than others even if those processors are initially equally utilized. On the other hand, grid being a networked environment, network utilization parameter, and clock frequency also play vital roles being equally least prioritized in comparison to the other two factors. Hence, intensity of importance values for each factor is assigned accordingly. A decision matrix for resource ranking along with the eigenvector values, using AHP is proposed and presented in Table 1.

From Table 1, we get the vector of four elements (2.268, 1.012, 0.387, 0.387). This equals the product $A\omega$. According to Saaty [16], $A\omega = \lambda_{\max}\omega$. Now we find four estimates of λ_{\max} by dividing each component of (2.268, 1.012, 0.387, 0.387) by the corresponding eigenvector element. This gives 4.064, 4.048, 4.03125 and 4.03125. Mean of these values, $\lambda_{\max} = 4.0435$.

The Consistency Index is represented as, $CI = (\lambda_{\max} - n)/(n - 1)$ [16]. For NDFS, $n = 4$. So, CI is 0.0145. Finally, the consistency ratio (CR) is found by comparing CI and the corresponding value from a table given by Saaty [16]. So, $CR = 0.0161$, which satisfies the consistency condition of $CR < 0.1$ [16].

Hence, Eq. (1) is redefined as,

$$f(\text{CPU weightage}) = 0.558x_1 + 0.250x_2 + 0.096x_3 + 0.096x_4 \quad (2)$$

Higher the CPU weightage value (from Eq. (2)), higher will be the ranking of that particular resource at the broker site for job scheduling. CPU weightage is calculated at the resource site to decrease the overhead of the resource broker. The

Table 1 AHP decision matrix for resource ranking

	x_1	x_2	x_3	x_4	n th root of product of values	Eigenvector
x_1	1	3	5	5	2.943	0.558
x_2	1/3	1	3	3	1.316	0.250
x_3	1/5	1/3	1	1	0.508	0.096
x_4	1/5	1/3	1	1	0.508	0.096

resource also sends the amount of its available RAM to the broker. The resource broker takes into account the two parameters of all the available resources and makes a decision to assign the job to the resource based on its CPU weightage value as well as its RAM, giving preference to the former.

This research also handles resource failure [8] during load balancing in grid environment. Next section puts the evidence of the above proposed technique.

4 Results and Discussion

This section presents the experimental setup. The computational grid environment is set up with two grid sites, each site having two resources. In all the nodes Unicore [20] is installed as the grid middleware. The resources consist of Intel i3, i5, and AMD Athlon processors with varying clock speeds, and primary memory ranging from 1 to 2 GB communicate through Unicore grid environment, whenever they become an active resource.

The clients submit their desired jobs to resource broker. Then the broker requests for CPU weightage and RAM availability from each of the resources through Unicore.

Table 2 shows the status of all the resources received by the broker in Unicore grid environment. The CPU weightage for each of the resources has been calculated by Eq. (2). Different rank is assigned to each of the available resources. As it can be seen from Table 2, the first rank is assigned to the least utilized resource and the last rank is assigned to the most utilized resource. From the two values returned by the resource, preference is given to the CPU weightage, so the available RAM comes into play only when the earlier value is same for two or more resources. In this research work, it can be clearly understood that the rank 1 is to be assigned to resource 3, since it is least utilized having the maximum value for CPU weightage. Similarly, resource 2 is assigned the rank of 4, since it is most utilized having the minimum value for CPU weightage. The resource 1 is assigned the rank of 2 and resource 4 is assigned rank 3 according to the submitted values. The resource broker assigns the job to the least loaded (or least utilized) resource, i.e., resource 3, so that all the resources in the grid remain in a balanced condition. This experimental result only emphasizes resource ranking of NDFS.

Table 2 Resource status information at grid site1 and grid site2

Resource	Resource information		
	CPU weightage	Available RAM	Rank
Resource 1 (grid site1)	1.5845	698	2
Resource 2 (grid site1)	1.4402	151	4
Resource 3 (grid site2)	1.6455	762	1
Resource 4 (grid site2)	1.5426	574	3

5 Conclusion

The load balancing is very crucial and challenging task for the optimal performance of the grid. Scheduling of jobs in computational grid varies based on load factors of the resources. The load balancing mechanism in computational grid tries to achieve equal distribution of workload among the participating resources. So, resource ranking will play a crucial role in scheduling, for which prioritization of resources is necessary. Hence, dynamic load computation is necessary as well as challenging in grid. This paper presents the redefined and prioritized resource ranking procedure in NDFS using AHP. This paper also determines the ranks of the various resources in Unicore grid environment.

Resource ranking system based on dynamic load computation is modified in this paper with the help of AHP model for making the scheduling of jobs more efficient. Moreover in this approach, the clients do not need to know the addresses of all the resources in the grid. It needs to only remember the address of the resource broker. This research work will be carried forward by implementing in Globus, considering many possible combinations. Moreover, resource failure will be handled in future.

References

1. Adebayo, O., Neilson, J., Petriu, D.: A performance study of client broker server systems. In: Proceedings of CASCON'97, pp. 116–130
2. Balasangameshwara, J., Raju, N.: A hybrid policy for fault tolerant load balancing in grid computing environments. *J. Netw. Comput. Appl.* **35**, 412–422 (2012)
3. Balasangameshwara, J., Raju, N.: Performance-driven load balancing with primary-backup approach for computational grids with low communication cost and replication cost. *IEEE Trans. Comput.* Digital Object Identifier (2012). doi:[10.1109/TC.2012.44](https://doi.org/10.1109/TC.2012.44)
4. Buyya, R., Murshed, M.: GridSim: a toolkit for the modeling and simulation of distributed management and scheduling for grid computing. *J. Concurrency Comput.: Pract. Experience* **14**, 13–15 (2002)
5. Erdil, D., Lewis, M.: Dynamic grid load sharing with adaptive dissemination protocols. *J. Supercomputing*, 1–28 (2010)
6. Foster, I., Kesselman, C., Tuccke, S.: The anatomy of the grid. *Int. J. Supercomputer Appl.* (2001)
7. Goswami, S., Das, A.: Deadline stringency based job scheduling in computational grid environment. In: Proceedings of the 9th INDIACOM, INDIACOM-2015. 11–13 March, 2015
8. Goswami, S., Das, A.: Handling resource failure towards load balancing in computational grid environment. In: Fourth International Conference on Emerging Applications of Information Technology (EAIT 2014) at Indian Statistical Institute, Kolkata, 19–21 Dec, 2014
9. Goswami, S., De Sarkar, A.: A comparative study of load balancing algorithms in computational grid environment. In: Fifth International Conference on Computational Intelligence, Modelling and Simulation, pp. 99–104 (2013)
10. Goswami, S., De Sarkar, A.: Service oriented load balancing framework in computational grid environment. *Int. J. Comput. Technol.* **9**(3), 1091–1098 (2013)
11. Kant Soni, V., Sharma, R., Kumar Mishra, M.: An analysis of various job scheduling strategies in grid computing. In: 2nd International Conference on Signal Processing Systems (ICSPS), 2010

12. Ludwig, S., Moallem, A.: Swarm intelligence approaches for grid load balancing. *J. Grid Comput.* 1–23 (2011)
13. Qureshi, K., Rehman, A., Manuel, P.: Enhanced GridSim architecture with load balancing. *J. Supercomputing*, 1–11 (2010)
14. Rajavel, R.: De-centralized load balancing for the computational grid environment. In: International Conference on Communication and Computational Intelligence, Tamil Nadu, India, 2010
15. Ray, S., De Sarkar, A.: Resource allocation scheme in cloud infrastructure. In: International Conference on Cloud & Ubiquitous Computing & Emerging Technologies, 2013
16. Saaty, T.L.: Decision making with the analytic hierarchy process. *Int. J. Serv. Sci.* **1**(1), 83–98 (2008)
17. Saaty, T.L.: The Analytic Hierarchy Process (AHP) (1980)
18. Stal, M.: The Broker Architectural Framework
19. Triantaphyllou, E., Mann, S.H.: Using the analytic hierarchy process for decision making in engineering applications: some challenges. *Int. J. Ind. Eng.: Appl. Pract.* **2**(1), 35–44 (1995)
20. Unicore. <http://www.unicore.eu>

Fuzzy-Based M-AODV Routing Protocol in MANETs

Vivek Sharma, Bashir Alam and M.N. Doja

Abstract The Mobile ad hoc wireless network is infrastructure less mobile network that allows communication among several mobile devices. The energy and delay of each mobile node affect the network performance in higher load. So, it becomes important to take into account these factors during the path selection. Here, we propose a method to incorporate the concept of fuzzy logic system to existing AODV routing protocol, and to select the optimal path by considering the remaining energy and delay of each node along with hop count. The experiment result shows that the proposed fuzzy-based modify-AODV (M-AODV) routing protocol outperforms the existing AODV in terms of average end-to-end delay and packet delivery ratio.

Keywords Mobile ad hoc routing · Wireless networks · Fuzzy logic system

1 Introduction

In recent years due to technologies advancement in real-time application like communication in battlefield, disaster management, civil, open construction, and urgent meeting at open place, etc. attracted more attention from academia and industry. The ad hoc network is classified into twofold: infrastructure and infrastructure less. Infrastructure less wireless network consists of base stations which are linked with each other. Communication among mobile nodes takes place via those base stations. An infrastructureless ad hoc is also called as Mobile ad hoc

V. Sharma (✉) · B. Alam · M.N. Doja

Department of Computer Engineering, Jamia Millia Islamia, New Delhi, India

e-mail: Vivek2015@gmail.com

B. Alam

e-mail: balam2@jmi.ac.in

M.N. Doja

e-mail: mdoja@jmi.ac.in

© Springer India 2016

S.C. Satapathy et al. (eds.), *Proceedings of the Second International Conference on Computer and Communication Technologies, Advances in Intelligent Systems and Computing* 380, DOI 10.1007/978-81-322-2523-2_75

773

network and applicable in above said areas. Mobile ad hoc network comprises of number of mobile nodes that do not use infrastructure and dynamically form temporal wireless network among them. Each node acts as a router and is capable of dynamic discovery of routes, recover link automatically and movement of nodes [1–3]. The mobile nodes can perform the basic network functions such as routing, forwarding, and service discovery. Communication among nodes in MANETS has constraints of energy, bandwidth and link stability, etc. Therefore, all these constraints should be considered for efficient design of the routing protocols for ad hoc networks. In different environment applications, the ad hoc networks possess different network topology and characteristics. Strength of traffic, network topology, energy consumption, and delay are highly dependent on application environments, and hence, these become important parameters from the routing protocols performance view point. Therefore, the protocol parameters should be configured dynamically in different network environments. To improve the protocol performance, these dynamical configurations should be adapted in the varying of the network topology. Earlier, the MANET's AODV routing protocol only considered hop count as metric and thus not provide optimal solution in some application. The process of each node in MANET depends on available energy. Due to limited size and battery capacity, the energy of each node is limited and thus, it becomes important metric for designing an energy-efficient routing protocol. Communication among mobile nodes is also affected by Delay. In high mobility model end-to-end delay also affects the routing decision. In real-time Scenario, these two factors affect the routing decision. We propose a fuzzy logic-based algorithm for mobile ad hoc networks, which not only considers hop count but also consider remaining energy of each node and delay between the nodes while taking routing decision. The simulation results confirm the merit of our proposed method as compare to traditional AODV.

The remainder of this paper is organized as follows: Existing related research work is described in Sect. 2. The description of the proposed method is depicted in Sect. 3. Section 4 presents the performance of the proposed method, while conclusions are drawn in Sect. 5.

2 Related Work

Due to node movement in dynamic nature of MANETs, there are chances of route breakage. Therefore, the nodes those are more stable in nature to be considered while selecting the route path. Zing et al. [4] proposed a novel FL-DSR protocol which considered inputs metric hop count together with the route life time for choosing the route which has highest route stability. The performance of FL-DSR was better than traditional DSR, because it had lesser number of route break events, improved network throughput, while minimizing control load of the network. During high load, some of nodes are lighter as compare to other nodes in the network and thus it affects the system performance. To balance the network, the load to be evenly

distributed. Song [5] integrated the fuzzy logic system to conventional DSR called MQRFT that selecting the optimal route by considers the network status information like link bandwidth available (LBA), link signal strength (LSS), and buffer occupancy ratio (BaR) as input metric to fuzzy logic system. Michele et al. [6] proposed a fuzzy logic-based method to select improved paths and increased lifetime of the network. Nie et al. [7] proposed the security-level (FLSL) routing protocol based on fuzzy logic that selects the routes with highest security.

3 Fuzzy Systems

The working of Fuzzy inference system [8, 9] consists of following steps: (1) selection of input and output linguistic variable, (2) Fuzzification, (3) inference engine, (4) system rule base, and (5) defuzzification. The process of fuzzification transforms crisp input values into membership values of the fuzzy set. Then, inference engine calculates the fuzzy output using the rule base and finally, the fuzzy output is converted into crisp values by the defuzzification process. The summary of fuzzy system is described in Fig. 1.

3.1 *Modify-AODV (M-AODV)*

In AODV, when a node wants to communicate with other node, in order to find a path, it broadcasts a RREQ packet to the network.

Here, we propose a routing decision method to decide whether a node will appear in the path to continue or not. Route metrics that make the routing decision are available remaining energy at participating node, hop count and end-to-end delay between nodes. Three linguistic variables for inputs are: low, medium, and high. Five linguistic variables for outputs are very low, low, medium, high, and very high, where each one is assigned a value between {0,1}. Triangle membership's function

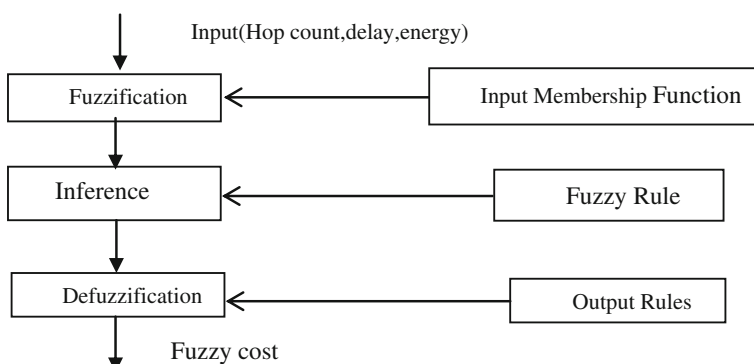


Fig. 1 Fuzzy logic inference system

Table 1 Rule base for M-AODV

Hop count (low)	Energy	Delay		
		Low	Medium	High
Low	Very high	Very high	Very high	Very high
Medium	Very low	Low	Medium	Medium
High	Low	Medium	High	High
Hop count (medium)	Energy	Delay		
		Low	Medium	High
	Low	Very high	Very high	Very high
	Medium	Low	Medium	High
	High	Medium	High	Very high
Hop count (high)	Energy	Delay		
		Low	Medium	High
	Low	Very high	Very high	Very high
	Medium	Medium	High	Very high
	High	Medium	High	Very high

is used to represent the output and input. Fuzzy inference engine applies a set of fuzzy rules on theses evaluations to obtain the desired behavior of the system as shown in Table 1.

Because the route discovery process of AODV is broadcast in nature, the RREQ packet of AODV carries the fuzzy input parameter: hop count, delay, energy. Each node embedded a fuzzy logic system that dynamically evaluates the fuzzy cost each time when RREQ packet arrives. If it finds path with lesser fuzzy cost then it is chosen and update reverse route entry. This process is continued until the packet arrives at the destination. Unsuitable paths are removed from the route discovery process and performance of the routing protocol is optimized. Paths which have a large associated signal loss, higher hop count, and nodes which contain lesser amount of energy are classified as unstable paths.

The proposed algorithm is described as follows:

1. For each node N_i , fetch following parameters:
hop count h_i ,
delay d_i , and
energy factor e_i on arrival of RREQ packet.
2. Next, we calculate the fuzzy cost fc_i for each node N_i .
3. If New fc_i is < stored fc_i of that node,
then update the reverse route entry table.
end of if loop.
4. If the node is Destination, forward the RREQ packet to source from current route.
5. Otherwise go to step 1.

4 Simulation Result

4.1 Simulation Parameters

In this section, we evaluate the performance of the proposed M-AODV protocol and compare with traditional AODV. We consider packet delivery ratio and delay as performance metrics. Packet delivery ratio is defined as the ratio of data packets reaching the destination node to the total data packets generated at the source node, while delay metric is defined as the average of the difference in time between the destination node and the source node. This difference includes the processing time and queuing time. The simulation parameter for M-AODV is considered as described in Table 2. In this simulation, nodes in the networks are set to 30 and are placed within a $700 \text{ m} \times 700 \text{ m}$ area. The transmission range of the nodes is 250 m. We used random waypoint model with node speed ranges from 0 to 10 mps. The traffic pattern consisted of CBR traffic type which generates UDP packets from available nodes. The UDP packet size is 512 bytes. The network simulator NS2.35 is used for simulating the proposed M-AODV. In addition, the MATLAB is used to simulate fuzzy cost using fuzzy logic toolbox. Next, the MATLAB receives the input parameter from the NS2 and processes to produce the results which are feedback to NS2 to help NS2 in making routing decision.

Figure 2 Compares the packet delivery ratio of M-AODV routing protocol and traditional AODV routing protocol for 30 nodes. We varied simulation time from 50 to 250 s. From the Fig. 2, we can observe that M-AODV can achieve higher packet delivery ratio as compared with traditional AODV due to stable path selection.

In Fig. 3, we compare the average end-to-end delay of the M-AODV with traditional AODV routing protocol. It can be observed that the average end-to-end delay of M-AODV reduces to a level that is slightly lower than that of original AODV.

Table 2 Simulation parameters

Environment variable	Values
Routing protocol	AODV
Simulation area	$700 * 700$
Number of nodes	30
Packet size	512
Mobility model	Random way point
Simulation time	50, 100, 150, 200, 250 s
Node speed	10 mbps
Traffic type	CBR

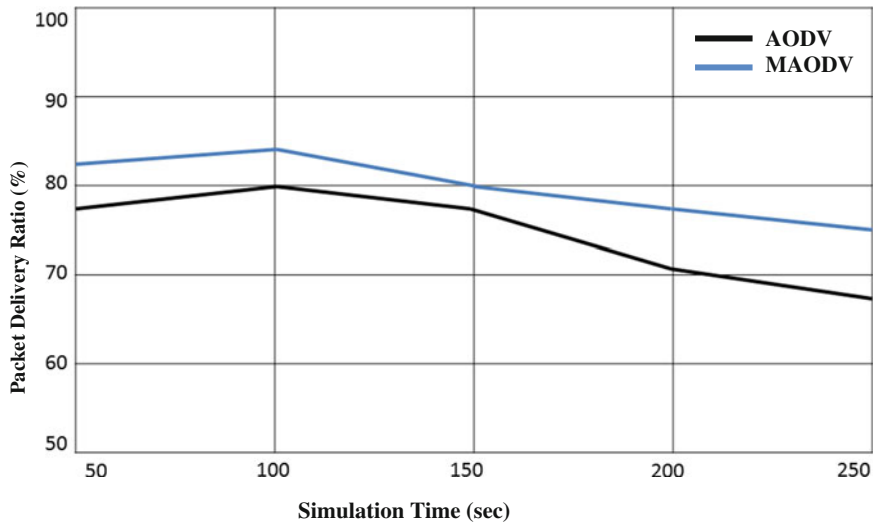


Fig. 2 Packet delivery ratio versus simulation time

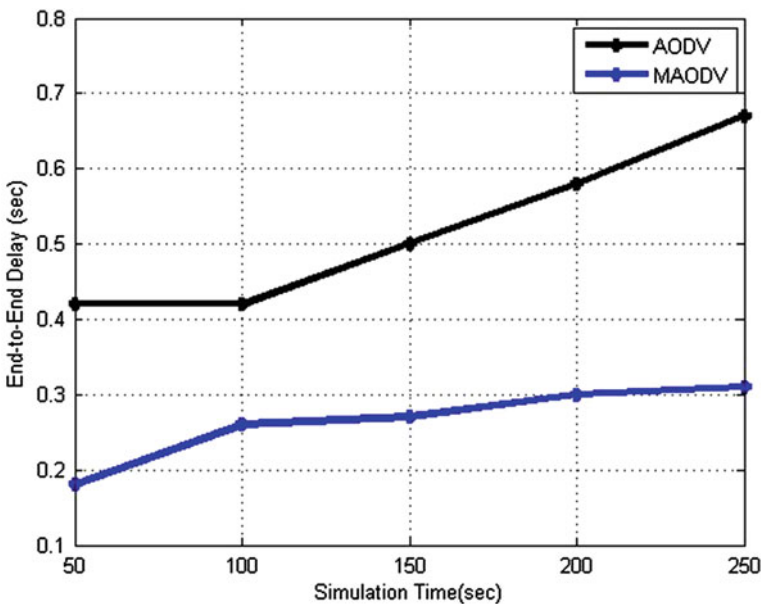


Fig. 3 Delay versus simulation time

5 Conclusion

In this paper, we proposed the existing AODV routing protocol and proposed M-AODV which are available to find more stable path for communication. Further, we compared this protocol's performance with well-known AODV. Our simulation was carried out using NS2.35 simulator and dynamically fuzzy cost is calculated based on metrics hope count, delay and remaining energy using MATLAB Fuzzy logic toolbox. The simulation results show that M-AODV performed better than existing AODV routing protocol in terms of packet delivery ratio and delay.

References

1. Murthy, C.S.R., Manoj, B.S.: Ad Hoc Wireless Networks: Architecture and Protocols. Pearson Ltd (2004)
2. Sharma, V., Alam, B.: Unicast routing protocols in mobile ad hoc networks: a survey. *Int. J. Comput. Appl. USA* **51**, 148–153 (2012)
3. Leo Manickam, J.M., Shanmugavel, S.: Fuzzy based trusted ad hoc on-demand distance vector routing protocol for MANET. In: 3rd International Conference on Wireless and Mobile Computing, Networking and Communications (2007)
4. Zuo, J., Xin Ng, S., Hanzo, L.: Fuzzy logic aided dynamic source routing in cross-layer operation assisted ad hoc networks. In: 72nd IEEE Conference on Vehicular Technology, pp. 1–5 (2010)
5. Song, W., Fang, X.: Multi-metric QoS routing based on fuzzy theory in wireless mesh network. In: IET International Conference on Wireless, Mobile and Multimedia Networks, pp. 1–4 (2006)
6. Lima, M.N., da Silva, H.W., Dos Santos, A.L., Pujolle, G.: Survival multipath routing for MANETs. In: IEEE Conference on Network Operation and Management Symposium, pp. 425–432 (2008)
7. Nie, J., Wen, J., Luo, J., He, X., Zhou, Z.: An adaptive fuzzy logic based secure routing protocol in mobile ad hoc networks. *Fuzzy Sets Syst.* **157**(12), 1704–1712 (2006)
8. Torshiz, M.N., Amintoosi, H., Movaghfar, A.: A fuzzy energy-based extension to AODV routing. International Symposium on Telecommunications, pp. 371–375 (2008)
9. Ross, T.J.: Fuzzy logic with Engineering Application. McGraw Hills Inc., New York, (1995)

Cuckoo Search in Test Case Generation and Conforming Optimality Using Firefly Algorithm

Kavita Choudhary, Yogita Gigras, Shilpa and Payal Rani

Abstract To accomplish the effectual software testing there is a requirement for optimization of test cases. The most challenging task in software testing is the generation of optimal test cases. There are various methods that are being used for generation of test cases and the test case optimization. The paper manifests the two different algorithms for test case generation and optimization of those test cases. The algorithms discussed are based on multi-objective optimization technique and successfully shows the desired results. The Cuckoo search algorithm based on the breeding behavior of Cuckoo bird is used here for the generation of test cases for a discussed problem and another algorithm based on the flashing phenomenon of fireflies is used for the optimization of the generated test cases. The second algorithm used verifies if every node in the given control flow graph is covered by given test cases.

Keywords Brightness value · Code coverage · Cuckoo search · Firefly · Optimal solutions · Target node · Test-case generation

1 Introduction

To perform effective testing of software, it is required to generate good test cases. Those test cases that show the maximum code coverage of program under test on execution are described as good test cases. This generation of such test cases in software testing phase can be defined as the most challenging task. The generation

K. Choudhary (✉) · Y. Gigras · Shilpa
ITM University, Gurgoan, Haryana, India
e-mail: kavitapunia@gmail.com

P. Rani
Banasthali University, Jaipur, India

of test cases can be done manually or through automated tools. Several optimization techniques are introduced to optimize and generate a set of optimal set of solutions to a given problem. In this paper, we have used two algorithms for generation and optimization of the test cases. These algorithms are Cuckoo search algorithm and firefly algorithm. Cuckoo search is an optimization algorithm which is inspired from the breeding behavior of the Cuckoo bird. The algorithm Cuckoo search implies and effects on a wide variety of areas including testing. In order to get high code coverage and optimized results, Cuckoo search algorithm is one of the most effective algorithms used. The name given to the algorithm is captivating and applicable as the basis of this search is the actual breeding behavior of Cuckoo bird. The algorithm adapts this technique and is, therefore, used as optimization technique for many problems. The various Cuckoo species have some specialization in their different breeding patterns so as to reduce the chances of eggs to get discarded among all eggs which increases their productivity. In real time applications Cuckoo search has proved to be highly efficient in various engineering optimization problems and structural optimization problems. The boundary value problems can be solved by the use of cuckoo search algorithm.

One more algorithm is described which is a member of Swarm Intelligence algorithm family. The algorithm is Firefly algorithm which is based on the flashing behavior of fireflies to attract their mate. In this algorithm, the flashing of firefly is used to send information. The scattering of firefly is done at different locations and each firefly is assigned a value based on the objective function. The function is calculated and intensity of light is set as the inverse evaluation. The evaluation is used to get lower function which is further evaluated in a higher intensity light. After this initialization each and every firefly is compared and moves toward the firefly which is brighter. After this moving of fireflies to all brighter fireflies, this brightness is updated by again the evaluation of objective function in a new position. If the position acquired is better then, it becomes best else the process continues till the better position is acquired. The algorithm is checked for its completeness after every generation. Firefly algorithm has been applied for the scheduling task and for the structural designing. Firefly algorithm can be used to solve the optimization problems for the dynamic environment. This algorithm is used here to check whether the given set of solutions which were generated by Cuckoo Search is optimal or not.

2 Literature Review

Tuba et al. [1] put forward a new improved version of cuckoo search that contains the size of step which can be calculated from the sorted fitness matrix not only by permuted. The test results show positive results in most of the cases. Valian et al. [2] put forward an improved cuckoo search algorithm with higher accuracy and convergence rate. Generally, the parameters are kept constant, which might result in lesser efficiency. To overcome this drawback a new and improved cuckoo search is

presented. The improvements in cuckoo search can be applied and used to solve a wide range of problems. Simulation results show that the new strategy of tuning parameters performs better in terms of accuracy of the solutions. Srivastava et al. [3] put forward a new prioritization technique for version specific regression testing. The prioritization of test cases consists of scheduling and proper organization of the test cases in a particular sequence. Regression testing is one important issue during software maintenance process but due to the limited availability of resources, the re-execution of all test cases is not feasible during regression testing. Hence during revision specific regression testing it is important to do those tests that are more advantageous. The technique uses lines of code where the code has been modified for prioritizing the test cases. Zhao et al. [4] proposed a new novel cuckoo search which is established with the help of algorithm of opposition which tries to get the optimum results by enlarging the efficiency of research. The new modification focuses the output establishment stage of algorithm of cuckoo search. During the development OCS showed more powerful exploitation capabilities. The paper puts forward a new effective, efficient, and simple OCS algorithm. The OCS algorithm yields better results than the conventional CS algorithm. Zhang et al. [5] investigated the drawbacks of cuckoo search algorithm and proposed the improved version of cuckoo search by rectifying ability and improvement in the convergence rate. The results of simulation of various test functions show that the faster speed and higher precision of ICS algorithm. As well as the algorithm manifest the greater performance of ICS when different test functions are applied. Yang et al. [6] proposed new approach that combines cuckoo search with non-dominated sorting and archiving techniques. The multi-objective cuckoo search is extended to get high quality pareto fronts. The performance of this new approach is validated by using several test problems. The results show that the newly proposed approach can find pareto fronts with better uniformity and quick convergence. We extended the cuckoo search to solve multi-objective optimization problems and designed a multi-objective cuckoo search (MOCS). We enhance the performance of MOCS by adding non-dominating sorting and niche techniques which leads to better quality of pareto fronts. Then these solutions are selected and archived by adding the diversity and uniformity properties. By using the seven bi-objective test functions the MOCS has been tested and validated and it was found to perform better than the non-dominated sorting genetic algorithm NSGA-II. The test results have been positive but still detailed study is needed to see how this approach can be scaled up to solve large scale problems. Hashmi et al. [7] discusses the implementation of the newly developed firefly algorithm. The test results show that firefly algorithm performed really well and gave accurate results when the population size was increased, while the convergence speed decreased in the same situation. The firefly algorithm has various advantages like being robust, precise, and easiness of implementation but it also suffers from problems like convergence speed. Marichelvam et al. [8] extended a newly developed discrete firefly algorithm to solve hybrid flow shop scheduling problems. In this method two objectives are considered which are Makespan and mean flow time. Then various tests are done which show that the newly proposed method performs better than many other

algorithms. Arora et al. [9] proved the recommendation of selecting the parameter on premises of rate of success and the performance by applying some functions. Analysis on convergence and the dynamic behavior of the firefly algorithm is done. The analysis is done by the use of some tools and produces some worthy suggestion for the selection of the parameter. Then some investigation is performed on the set of parameters and on functions. This shows that results were better when there were small values used for providing the input. Goel et al. [10] proposed a new modified and enhanced version of the conventional firefly algorithm and has been compared with SFA and its two other variants on performance basis. Recent advancements in meta-heuristics have made it necessary for researchers to enhance the current generation of algorithms so that these can be applied to a large set of complex problems. The firefly algorithm, a new nature-inspired is widely used to solve optimization problems. Our test results show that that the newly developed NMFA performs better than the rest of the algorithms. NMFA outperforms the other algorithms with higher accuracy and faster convergence. This new method can be applied to a large number of real-time applications. Liu et al. [11] proposed a path planning method based on firefly algorithm. After the detailed study of the algorithm some random parameters and absorption parameters were designed. These were designed to be adaptive so that it could improve the quality of the solution and convergence speed also. The newly designed Firefly algorithm has many characteristics like simplicity, efficiency that have made more and more people use it for solving complex problems.

3 Test Case Generation and Optimization

Here the *quadratic equation problem* is demonstrated. The Cuckoo Search algorithm which is based on the actual breeding behavior of Cuckoo birds is being used for the generation of the set of solutions where as next algorithm—the firefly algorithm is used to prove that the set of solutions obtained by Cuckoo Search are optimal set of solutions, i.e., the solutions shows the maximum code coverage. The solution for the problem constructs a control flow graph (Fig. 1) which helps to identify some parameters in algorithm.

3.1 Cuckoo Search in Quadratic Equation Problem

The target nodes of the considered problem are node 5, node 7, node 4, node 8, and node 2. Maximum iterations equal to the number of target nodes is 5 and Pop_size is equal to Ceil of $(5/2)$ is 3. Initially, the randomly generated test case solution in cuckoo nest is equal to Pop_size – 1 (i.e., equal to 2) i.e., $\langle 0, 50, 50 \rangle, \langle 15, 25, 90 \rangle$. The fitness value is equal to the number of common branches between the predicate

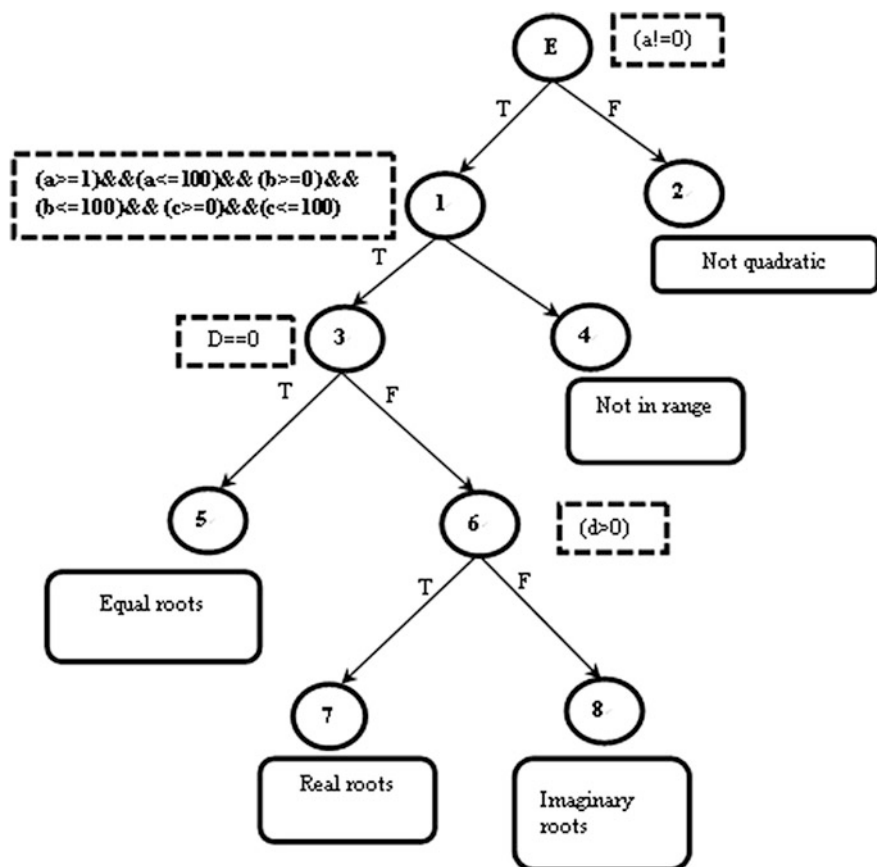


Fig. 1 Control flow graph

of the solution and full path of the target node from the root. Initially OS_{T1} and WS_{T1} equal to NULL.

Iteration-1 ($i = 1$)

The target node selected is node 2. A new random solution $<6, 17, 24>$ is generated. The fitness value for this triplet $<0, 50, 50>$ is equal to 1 and for $<15, 25, 90>$ is equal to 0 and $<6, 17, 24>$ is equal to 0. Now the solution with highest fitness value will be moved to OS_{T1} and rest of the solutions will be moved to WS_{T1} .

Iteration 2

Current Cuckoo Nest is $WS_{T1}(<15, 25, 90>, <6, 17, 24>)$ +New test case generated $(<55, 121, 25>)$. The next target node is node 4. The fitness value for this triplet $<15, 121, 25>$ is equal to 2 and for $<15, 25, 90>$ is equal to 1 and $<6, 17, 24>$ is equal to 1. Now, $OS_{T2} = \{<55, 121, 25>\}$ and $WS_{T2} = \{<15, 25, 90>, <6, 17, 24>\}$

Iteration-3

Current Cuckoo Nest is WS_{T2} + New test case generated ($<50, 100, 50>$). The next target node is node 5. The fitness value for this triplet $<15, 25, 90>$ is equal to 2 and for $<50, 100, 50>$ is equal to 3, and $<6, 17, 24>$ is equal to 2. Now, $OS_{T3} = \{<50, 100, 50>\}$ and $WS_{T3} = \{<15, 25, 90>, <6, 17, 24>\}$

Iteration-4

Current Cuckoo Nest is WS_{T3} + New test case generated ($<50, 50, 1>$). The next target node is node 7. The fitness value for this triplet $<50, 50, 1>$ is equal to 4 and for $<15, 25, 90>$ is equal to 3 and $<6, 17, 24>$ is equal to 3. Now, $OS_{T4} = \{<50, 50, 1>\}$ and $WS_{T4} = \{<15, 25, 90>, <6, 17, 24>\}$

Iteration-5

Current Cuckoo Nest is WS_{T4} + New test case generated ($<50, 50, 100>$). The next target node is node 8. The fitness value for this triplet $<15, 25, 90>$ is equal to 4 and for $<50, 50, 100>$ is equal to 4 and $<6, 17, 24>$ is equal to 4. Fitness value are same for these test cases. So, randomly select any triplet and store the other triplet in WS_{T5} . Therefore, $OSR = \{<0, 50, 50>, <55, 121, 25>, <50, 100, 50>, <50, 50, 1>, <50, 50, 100>\}$

$$WSR = \{WS_{T5}\} = \{<70, 70, 70>, <3, 4, 5>\}$$

Now these set of solutions obtained will undergo Firefly optimization technique to check the optimality, i.e., maximum code coverage.

3.2 *Firefly Algorithm in Optimizing Solution Set*

The target node considered in our problem, i.e., node 5, node 7, node 4, node 8, and node 2 will be having a brightness function ().The Brightness value of the target node will be incremented by 1 after every migration of a firefly corresponding to the node. Initial Brightness value of each target node set to zero. Her, the predicate node will be E, 1, 3, 6.

$$\text{Fitness_value (E)} = 1 \quad \text{Fitness_value (1)} = 6 \quad \text{Fitness_value (3)} = 1 \quad \text{Fitness_value (6)} = 1$$

$$\text{Initial fireflies}\{<0, 50, 50>, <55, 121, 25>, <50, 100, 50>, <50, 50, 1>, <50, 50, 100>\}$$

Iteration 1

First firefly is selected from the initial fireflies, i.e., $<0, 50, 50>$. Firefly started from node E. Then fitness value of firefly is calculated is equal to the no. of condition satisfied by the firefly. Fitness_value of $ff_1 = 0$ and Fitness value of node E = 1. Fitness value of firefly is not equal to the fitness value of node E so, firefly will

move toward right side in the graph, i.e., toward node 2. Node 2 is a target node therefore, brightness value is incremented by 1 and fireflies achieve its destination.

Iteration 2

In iteration 2, we choose the second firefly, i.e., $\langle 55, 121, 25 \rangle$. Firefly started from node E. Then value of fitness of firefly (ff_2) calculated. Fitness_value of $ff_2 = 1$ and Fitness value of node E = 1. Fitness value of firefly is equal to the fitness value of node E so, Firefly will proceed to the left side of graph ,i.e., node 1 and Brightness value incremented by 1 of the corresponding target node. Node 1 is a predicate node. Now we calculate the Fitness_value of firefly (ff_2) corresponding to node 1. Fitness_value of $ff_2 = 4$ and Fitness value of node1 = 6. Fitness value of firefly is not equal to the fitness value of node 1 hence, Firefly will move toward right side of the graph, i.e., node 4 and Brightness value will become 2. Node 4 is a target node therefore, brightness value is incremented to 3 and fireflies achieve its destination.

Iteration 3

In iteration 3, the third firefly is selected, i.e., $\langle 50, 100, 50 \rangle$. Then value of fitness of firefly (ff_3) calculated. Fitness_value of $ff_3 = 1$ and Fitness value of node E = 1. Fitness value of firefly is equal to the fitness value of node E so, Firefly will proceed to the left side of graph, i.e., node 1 and Brightness value incremented by 1. Now we calculate the Fitness_value of firefly (ff_3) corresponding to node 1. Fitness_value of $ff_3 = 6$ and Fitness value of node 1 = 6. Fitness value of firefly is equal to the fitness value of node 1 so, Firefly will move toward left side of the graph, i.e., node 3 and Brightness value will become 2. We calculate the Fitness_value of firefly (ff_3) corresponding to node 3. Fitness_value of $ff_3 = 1$ and Fitness value of node 3 = 1. Fitness value of firefly is equal to the fitness value of node 3 hence, Firefly will move toward left side of the graph, i.e., node 5. Now, Node 5 is a target node therefore, brightness value is incremented to 4 and fireflies achieve its destination.

Iteration 4

In iteration 4, the fourth firefly is selected, i.e., $\langle 50, 50, 1 \rangle$. Then value of fitness of firefly (ff_4) calculated. Fitness_value of $ff_4 = 1$ and Fitness value of node E = 1. Fitness value of firefly is equal to the fitness value of node E so, Firefly will proceed to the left side of graph, i.e., node 1 and Brightness value incremented by 1 of the corresponding target node. Now, we calculate the Fitness_value of firefly (ff_4) corresponding to node 1. Fitness_value of $ff_4 = 6$ and Fitness value of node1 = 6. Fitness value of firefly is equal to the fitness value of node 1 so, Firefly will move toward left side of the graph, i.e., node 3 and Brightness value will become 2. We calculate the Fitness_value of firefly (ff_4) corresponding to node 3. Fitness_value of $ff_4 = 0$ and Fitness value of node 3 = 1. Fitness value of firefly is not equal to the fitness value of node 3 so, Firefly will proceed to right side of graph, i.e., node 6 and brightness value will be 3. Node 6 is a predicate node. Now, we calculate the Fitness_value of firefly (ff_4) corresponding to node 6. Fitness_value of $ff_4 = 1$ and Fitness value of node 6 = 1. Fitness value of firefly is equal to the fitness value of

node 6 hence, Firefly will proceed to left side of graph and brightness value will be 4. Now Node 7 is a target node therefore, brightness value is incremented to 5 and fireflies achieve its destination.

Iteration 5

In iteration 5, the fifth firefly is selected, i.e., $\langle 50, 50, 100 \rangle$. Then value of fitness of firefly (ff_5) calculated. Fitness_value of $ff_5 = 1$ and Fitness value of node E = 1. Fitness value of firefly is equal to the fitness value of node E so, Firefly will proceed to the left side of graph, i.e., node 1 and Brightness value incremented by 1 of the corresponding target node. Now, we calculate the Fitness_value of firefly (ff_5) corresponding to node 1. Fitness_value of $ff_5 = 6$ and Fitness value of node 1 = 6. Fitness value of firefly is equal to the fitness value of node 1 so, Firefly will move toward left side of the graph, i.e., node 3 and Brightness value will become 2. We calculate the Fitness_value of firefly (ff_5) corresponding to node 3. Fitness_value of $ff_5 = 0$ and Fitness value of node 3 = 1. Fitness value of firefly is not equal to the fitness value of node 3 so, Firefly will proceed to right side of graph, i.e., node 6 and brightness value will be 3. Now, we calculate the Fitness_value of firefly (ff_5) corresponding to node 6. Fitness_value of $ff_5 = 0$ and Fitness value of node 6 = 1. Fitness value of firefly is not equal to the fitness value of node 6 hence, Firefly will proceed to right side of graph, i.e., node 8 and brightness value will be 4. Now Node 8 is a target node therefore, brightness value is incremented to 5 and fireflies achieve its destination.

Therefore, the initial set of solutions is the optimal set of solutions which is covering every node in the flow graph.

4 Simulation Results

Earlier the techniques used to generate Test Cases were based on the input/output domain of the problem. But here the work is done by applying multi-objective optimization technique to generate test cases [12, 13]. The technique used shows the successful generation of test cases and shows the comparison of the algorithm with the previous technique used for test case generation. The results depict the reduction in number of test cases generated (Tables 1 and 2).

Table 1 Solutions generated using earlier technique

Test cases	a	b	c	Expected output
1	0	50	50	Not a quadratic equation
2	-1	50	50	Invalid input
3	1	50	50	Real roots
4	50	100	50	Equal roots
5	50	50	50	Imaginary roots
6	50	90	40	Valid input
7	50	101	50	Invalid input

Table 2 Optimal solution and worst solution using Cuckoo search

Iteration (<i>i</i>)	Target node	Path (root to target)	Random solution	Current Cuckoo nest	Path (Cuckoo nest elements)	Fitness value	OS-	WS-
<i>i</i> = 1	Node 2	(EF)	<6,17,24>	<0,50,50> <15,25,90>	(EF) (ET,1T,3F,6F)	1 0	<0,50,50> <6,17,24>	<15,25,90> <6,17,24>
<i>i</i> = 2	Node 4	(ET,1F)	<5,121,25>	<6,17,24> <55,121,25> <15,25,90>	(ET,1F) (ET,1T,3F,6F) (ET,1T,3F,6F)	2	<55,121,25>	<15,25,90> <6,17,24>}
<i>i</i> = 3	Node 5	(ET,1T,3T)	<50,100,50>	<6,17,24> <15,25,90> <6,17,24>	(ET,1T,3F,6F) (ET,1T,3F,6F) (ET,1T,3F,6F)	1 2 2	<50,100,50>	<15,25,90> <6,17,24>
<i>i</i> = 4	Node 7	(ET,1T,3F,6T)	<50,50,1>	<15,25,90> <6,17,24> <50,50,1>	(ET,1T,3F,6F) (ET,1T,3F,6F) (ET,1T,3T,6T)	3 3 4	<50,50,1>	<15,25,90> <6,17,24>
<i>i</i> = 5	Node 8	(ET,1T,3F,6F)	<50,50,100>	<15,25,90> <6,17,24> <50,100,50>}	(ET,1T,3F,6F) (ET,1T,3F,6F) (ET,1T,3F,6F)	4 4 4	<50,50,100>	<15,25,90> <6,17,24>

Table 3 Target node using firefly algorithm

Iteration	Target node	Firefly	Predicate nodes in path	Brightness value of target node	Target node achieved
1	2	<0, 50, 50>	E	2	Yes
2	4	<55, 121, 25>	E-1	3	Yes
3	5	<50, 100, 50>	E-1-3	4	Yes
4	7	<50, 50, 1>	E-1-3-6	5	Yes
5	8	<50, 50, 100>	E-1-3-6	5	Yes

5 Conclusion

Cuckoo search and firefly algorithm can outperform other metaheuristic algorithms in applications. It seems that the approach uses new and better solutions to replace an ordinary or a less effective solution. For imposing the good code coverage and best results of testing cuckoo search and firefly algorithm are used. For corresponding input value, the resultant output covers all the necessary condition and target nodes are achieved. OS data structure covers optimal results. Table 3 represents that target node is achieved by the set of solutions generated by Cuckoo Search. Hence it concludes that the proposed work is an impressive and highly efficient searching algorithm.

References

1. Tuba, M., Subotic, M., Stanarevic, N.: Performance of a modified cuckoo search algorithm for unconstrained optimization problems. *WSEAS Trans. Syst.* **11**(2) (2012). E-ISSN: 2224-2678
2. Valian, E., Mohanna, S., Tavakoli, S.: Improved cuckoo search algorithm for global optimization. *Int. J. Commun. Inf. Technol. IJCIT-2011* **1**(1) (2011)
3. Srivastava, P.R., Reddy, D.V., Reddy, M.S., Ramaraju, C.V.B., Nath, I.C.M.: Test Case Prioritization using Cuckoo Search. doi:[10.4018/978-1-4666-0089-8.ch006](https://doi.org/10.4018/978-1-4666-0089-8.ch006)
4. Zhao, P., Li, H.: Opposition-Based Cuckoo Search Algorithm for Optimization Problems IEEE. doi:[10.1109/ISCID.2012.93](https://doi.org/10.1109/ISCID.2012.93)
5. Zhang, Z., Chen, Y.: An Improved Cuckoo Search Algorithm with Adaptive Method IEEE. doi:[10.1109/CSO.2014.45](https://doi.org/10.1109/CSO.2014.45)
6. He, X., Yang, X.: Non-dominated Sorting Cuckoo Search for Multiobjective Optimization. IEEE (2014). 978-1-4799-4458-3/14/\$31.00
7. Hashmi, A., Goel, N., Goel, S., Gupta, D.: Firefly algorithm for unconstrained optimization. *IOSR J. Comput. Eng. (IOSR-JCE)* **11**(1), 75–78 (2013). e-ISSN: 2278-0661, p-ISSN: 2278-8727
8. Marichelvam, P., Yang X.: A discrete firefly algorithm for the multi-objective hybrid flowshop scheduling problems. *IEEE Trans. Evol. Comput.* **18**(2) (2014)
9. Arora, S., Singh, S.: The Firefly optimization algorithm: convergence analysis and parameter selection. *Int. J. Comput. Appl.* **69**(3), 0975–8887 (2013)
10. Goel, S., Panchal, V.K.: Performance Evaluation of a New Modified Firefly Algorithm, IEEE (2014). 978-1-4799-6896-1/14/\$31.00

11. Liu, C., Gao, Z., Zhao, W.: A New Path Planning Method Based on Firefly Algorithm, IEEE. doi:[10.1109/CSO.2012.174](https://doi.org/10.1109/CSO.2012.174)
12. Srivastava, P.R.: Software Analysis Using Cuckoo Search. Springer International Publishing Switzerland 2015. Advances in Intelligent Informatics. Advances in Intelligent Systems and Computing 320. doi:[10.1007/978-3-319-11218-3_23](https://doi.org/10.1007/978-3-319-11218-3_23)
13. Kirner, R., Haas, W.: Optimizing Compilation with Preservation of Structural Code Coverage Metrics to Support Software Testing. http://uhra.herts.ac.uk/bitstream/handle/2299/13515/paper_Kirner_STVR_2014_preprint.pdf?sequence=4

Time Domain Analysis of EEG to Classify Imagined Speech

Sadaf Iqbal, P.P. Muhammed Shanir, Yusuf Uzzaman Khan and Omar Farooq

Abstract Electroencephalography (EEG) finds variety of uses in the fields ranging from medicine to research. EEG has long been used to study the different responses of the brain. In this paper, EEG has been applied to study the imagined vowel sounds. An algorithm is developed to differentiate three classes of imagined vowel sounds namely /a/, /u/, and ‘rest or no action’ in pairwise manner. The algorithm is tested on three subjects S1, S2, and S3 and high performance is achieved. With classification accuracy ranging from 85 to 100 %, the algorithm shows the potential to be used in Brain Computer Interfaces (BCIs) and synthetic telepathy systems. High classification performance is obtained. Sensitivity ranges from 90 to 100 %. Specificity ranges from 80 to 100 %. Positive predictive value ranges from 81.82 to 100 %. Negative predictive value ranges from 88.89 to 100 %.

Keywords Electroencephalography (EEG) · Imagined · Vowel · Classification · Performance

S. Iqbal (✉) · P.P. Muhammed Shanir (✉) · Y.U. Khan (✉)
Department of Electrical Engineering, Aligarh Muslim University (A.M.U.),
Aligarh 202002, U.P., India
e-mail: sadafiqbal256@gmail.com

P.P. Muhammed Shanir
e-mail: shanirpp@gmail.com

Y.U. Khan
e-mail: yusufkhan1@gmail.com

O. Farooq (✉)
Department of Electronics Engineering, Aligarh Muslim University (A.M.U.),
Aligarh 202002, U.P., India
e-mail: omarfarooq70@gmail.com

1 Introduction

Human beings communicate among themselves by speaking usually. However in certain ailments like advanced amyotrophic lateral sclerosis (ALS) [1], laryngectomy, paralysis, locked-in syndrome (LIS), etc. or in cases where the patient is affected by motor neuron disability [1] the affected people lose their ability to speak thereby adversely affecting their lives. Worldwide the number of ALS patients is estimated to be around 4,50,000 so there is a need to develop some form of communication system for these patients. Also silent speech communication can be utilized to develop synthetic telepathy systems [2].

Several methods have already been used for the speech-paralyzed patients. However noninvasive brain computer interfaces (BCIs) provide the safest and most reliable option to develop speech prostheses for the affected patients. In 1999, researchers successfully developed a BCI in which the first verbal message was communicated using EEG collected from ALS patients [3].

Some BCIs are available in which a person can select words or letters on a screen. Now research is being carried out to improve the existing techniques, by using advanced BCIs to directly predict words and speech rather than to control a spelling device. Then building upon this technique, the final aim would be to develop speech prostheses which can finally replace the entire vocal apparatus of the affected user.

Kim [4] conducted research regarding the phoneme representation in the brain and to find out whether EEG responses for each speech sound could be discriminated. In this work [4] the features were extracted using common spatial pattern and multivariate empirical mode decomposition (MEMD). The study was conducted on the vowels /a/, /i/, and /u/. The results in their study showed that vowel stimuli can be classified from the brain waves.

DaSalla et al. [5] performed experiments on vowel sound imagery. The authors in [5] recorded data on three subjects who had imagined mouth opening and vocalization of sounds /a/, /u/, and ‘rest or no action’ and then extracted features from the data by using common spatial patterns method. Classification was done between /a/ and control state, /u/ and control state and between /a/ and /u/ with a nonlinear support vector machine (SVM) with overall classification accuracies ranging from 68 to 78 %.

1.1 *Introduction of the Current Work Done*

In this paper, the data set used is the one made publicly available by DaSalla et al. Data is downloaded from www.brainliner.jp [6]. The data consists of EEG recording of imagined mouth opening and vocalization of vowel sounds /a/, /u/ and

'rest or no action' as control state. 50 trials of each class are selected for analysis. The algorithm is tested on three subjects S1, S2, and S3. Data is first filtered in the range of 1–45 Hz to remove all physiological and non-physiological artifacts like electronic noise, baseline shift, electromyographic (EMG) artifacts, power line frequency (60 or 50 Hz), and electrocardiographic (ECG) artifacts (60–72 Hz). Time domain analysis is done to extract statistical features from the data. Then features per trial per subject are extracted. The features extracted in this work are mean and standard deviation. A linear classifier is used to classify the data into 'a' versus 'rest' classes, 'u' versus 'rest' classes, and 'a' versus 'u' classes for all the three subjects. High classification performance is obtained using this proposed algorithm. Correct rate ranges from 85 to 100 %. Sensitivity ranges from 90 to 100 %. Specificity ranges from 80 to 100 %. Positive Predictive Value ranges from 81.82 to 100 %. Negative predictive value ranges from 88.89 to 100 %.

2 Data Acquisition

2.1 Subjects

The data is downloaded from www.brainliner.jp from the data base made publicly available by DaSalla et al. [5].

The authors in [5] recorded the EEG of three healthy subjects S1, S2, and S3 out of whom 2 were male and 1 was a female. Since english language vowels had to be analyzed so the participants selected were fluent in english language. The experiment was conducted in accordance with the Declaration of Helsinki with the prior consent obtained from the participants.

2.2 Details of EEG Recording

The subjects were comfortably seated in a chair. A visual cue appeared on the screen which meant that the participant was asked to perform one of the following tasks.

- Imagine mouth opening and imagine vocalization of vowel /a/.
- Imagine lip rounding and imagine vocalization of vowel /u/.
- Control or rest-alert, no action.

The vowel /a/ pronunciation is controlled by digastricus muscle and by mouth opening while vowel /u/ is pronounced by lip rounding and by orbicularis oris muscle so the EEG data obtained in both these cases will be different.

After instructing the subjects to imagine the particular vowel, a visual cue appeared and the data was collected in the following manner. An audible beep was

sounded and a fixation cross remained on the screen for 2–3 s. Then a visual cue appeared and remained on screen for 2 s which implied that the subject should imagine speaking the shown vowel for 2 s. /a/ was shown by mouth opening, /u/ by lip rounding and no action by a fixation cross.

2.3 Apparatus Used

Continuous EEG was recorded first and then sampled at sampling frequency of 2048 Hz, using 64 + 8 active Ag–AgCl electrodes with the help of a BioSemi head cap according to international 10–20 system. The data was stored in software by down sampling at 256 Hz to reduce file size. Visual inspection of the subjects was done during the trials to reject those trials which showed movement.

3 Data Preprocessing

Out of the many available electrodes, properly selecting the electrode which contains neuronal information about speech is important [7]. DaSalla has made available electrode data of only four electrodes positioned in the motor cortex region. This is justified because the speech musculature is innervated in the motor cortex. The sampled data from these four channels was processed using MATLAB. Since EEG data is very sensitive to various physiological and non-physiological artifacts hence its removal is a must. One of the many methods of removing artifacts is by the use of properly selected filter [8]. So in this algorithm a bandpass filter of second order which utilizes butterworth technique is used. Data of all channels for all subjects was bandpass filtered in range of 1–45 Hz. This removed electronic noise and any low frequency baseline shift. The higher cut off frequency 45 Hz is also justified as it will remove any electromyographic (EMG) artifacts and power line frequency (60 or 50 Hz).

4 Feature Extraction

Each trial consists of 128 samples and there are four channels in each file. There are 50 trials for each task /a/, /u/, and ‘rest’ for each subject, thus resulting in a total of 150 trials for a subject and there are three subjects in this experiment. Features are extracted for each trial.

Features are the distinct characteristics that distinguish one dataset from the other. The features extracted in this algorithm are statistical features namely mean and standard deviation per trial.

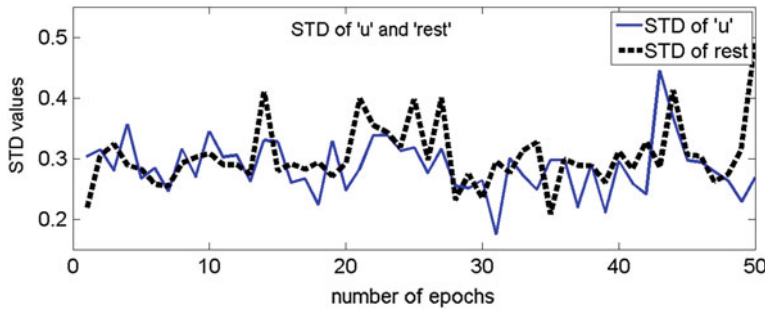


Fig. 1 Solid curve shows STD of ‘u’ and dashed curve shows STD of ‘rest’ class. These two curves are different thereby making STD a good feature

Standard deviation (STD) is defined by Eq. (1)

$$\left(\frac{\sum_1^N (x_i - \text{mean})^2}{N} \right)^{1/2} \quad (1)$$

STD per trial is extracted for all the channels, for all classes and all the subjects. It is distinct for all the classes. Figure 1 shows the STD of classes ‘u’ and ‘rest’ which clearly shows that STD is a good feature.

Mean value is defined by Eq. (2)

$$\frac{\sum_1^n x_i}{N}. \quad (2)$$

where x_i the i th observation and N is the total number of observations per trial.

Mean per trial is extracted for all the channels, for all classes and all the subjects. It is distinct for all the classes. Figure 2 shows the mean of classes ‘u’ and ‘rest’ classes which clearly shows that mean is a good feature.

Taking STD of four channels and mean value of four channels constitutes total eight features. This feature matrix is given as input to classifier.

5 Classification

To classify the data 60 % of the trials were used for training and 40 % of the trials were used for testing. The data was given to a linear classifier. Using a linear classifier makes the complexity of the algorithm lesser and its implementation in practical problems easier.

The aim of classification is to distinguish ‘a’ from ‘rest’ class, ‘u’ from ‘rest’ class, and ‘a’ from ‘u’.

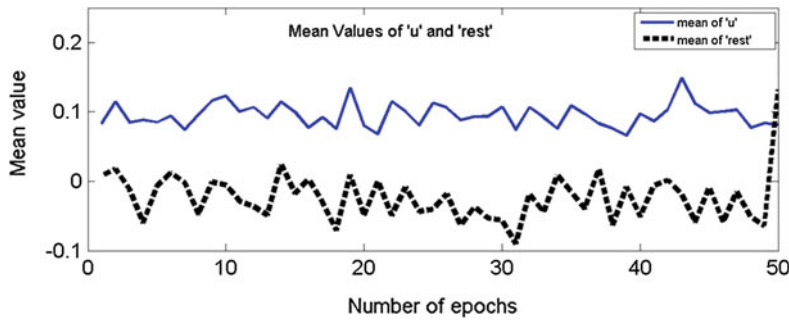


Fig. 2 Solid curve shows mean of ‘*u*’ and Dashed curve shows mean of ‘rest’ class. These two curves are different thereby making mean a good feature

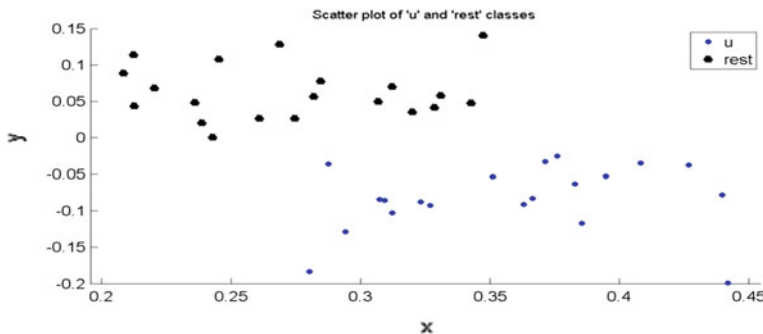


Fig. 3 Scatter plot of ‘*u*’ (lower cluster) and ‘rest’ (upper cluster) classes. This plot shows that the two clusters are linearly separable

Figure 3 shows the scatter plot of ‘*u*’ versus ‘rest’ class. The two classes form separate clusters and hence are clearly distinguishable from each other. Also from Fig. 3 it is clear that the classes are linearly separable, hence use of a linear classifier is justified.

6 Results

The performance of the classifier is evaluated on the basis of five parameters namely accuracy, sensitivity, specificity, positive predictive value (PPV) and negative predictive value (NPV). Accuracy is defined as the ratio of number of correctly classified samples in a group to the total number of events classified. Sensitivity is defined as the ratio of number of correctly classified positive samples in a group to the number of true positive samples. Specificity is defined as the ratio of number of

Table 1 Performance of the proposed algorithm in percentage (%)

Parameter	S1			S2			S3		
	'a'/'rest'	'u'/'rest'	'a'/'u'	'a'/'rest'	'u'/'rest'	'a'/'u'	'a'/'rest'	'u'/'rest'	'a'/'u'
Accuracy	85	100	92.5	97.5	100	92.5	100	100	100
Sensitivity	90	100	90	95	100	90	100	100	100
Specificity	80	100	95	100	100	95	100	100	100
PPV	81.82	100	94.74	100	100	94.74	100	100	100
NPV	88.89	100	90.48	95.24	100	90.48	100	100	100

Table 2 Shows the comparison of this work with the work done by DaSalla et al. [5] (results are in percentage)

Subject	'a'/'re'		'u'/'re'		'a'/'u'	
	DaSalla	This work	DaSalla	This work	DaSalla	This work
S1	79 ± 3	85	82 ± 4	100	72 ± 3	92.5
S2	71 ± 5	97.5	72 ± 4	100	60 ± 5	92.5
S3	67 ± 4	100	80 ± 3	100	56 ± 4	100

correctly classified negative samples in a group to the number of true negative samples. PPV is defined as the ratio of number of correctly classified positive samples in a group to the number of classified positive samples.

Negative predictive value is defined as the ratio of number of correctly classified negative samples in a group to the number of classified negative samples.

The result obtained by using the proposed algorithm is tabulated in Table 1 in percentage (Table 2).

7 Discussion

The high accuracy of 85–100 % shows that the algorithm works well to distinguish between the different classes.

Two different statistical features namely mean and standard deviation are used as features. These two are time domain-based features so the need to use any domain transformation is eliminated in this algorithm. This makes the algorithm faster and simpler.

A linear classifier is used to differentiate between the classes and it is giving high performance which again makes the algorithm simpler and efficient.

Since the performance of this algorithm shows an improvement over the earlier reported algorithm in the literature by DaSalla [5] hence it can be further developed to be implemented in advanced BCIs for the speech impaired patients and synthetic telepathy systems.

8 Conclusion

The proposed algorithm works well on all the three subjects on which it was tested. The use of time domain-based features and a linear classifier makes the algorithm fast, efficient while maintaining computational simplicity. High classification performance is obtained using this proposed algorithm. Also, the algorithm is giving better results than the work reported in the literature by DaSalla [5]. In this work, the Accuracy ranges from 85 to 100 %. Sensitivity ranges from 90 to 100 %. Specificity ranges from 80 to 100 %. Positive predictive Value ranges from 81.82 to 100 %. Negative predictive value ranges from 88.89 to 100 %.

Acknowledgments The authors would like to thank DaSalla et al. for making the data of imagined speech publicly available.

References

1. Barrett, K.E., Susan, M.B., Boitano, S., Heddwen, L.B.: Ganong's Review of Medical Physiology, 23rd edn. Tata McGraw Hill
2. D'Zmura, M., Deng, S., Lappas, T., Thorpe, S., Srinivasanay, R.: Toward EEG sensing of imagined speech. In: Human-Computer Interaction. New Trends, pp. 40–48. Springer Berlin Heidelberg (2009)
3. Birbaumer, N., Ghanayim, N., Hinterberger, T., Iversen, I., Kotchoubey, B., Kübler, A., et al.: A spelling device for the paralysed. *Nature* **398**, 297–298 (1999)
4. Kim, J., Lee, S.-K., Lee, B.: EEG classification in a single-trial basis for vowel speech perception using multivariate empirical mode decomposition. *J. Neural Eng.* **11**(3), 036010 (2014)
5. DaSalla, C.S., Kambara, H., Sato, M., Koike, Y.: Single-trial classification of vowel speech imagery using common spatial patterns. *Neural Netw.* **22**(9), 1334–1339 (2009)
6. [www.brainliner.jp](http://brainliner.jp) (http://brainliner.jp/data/brainlineradmin/Speech_Imagery_Dataset) (2014). Accessed 24 July 2014
7. Pie, X., Barbour, D., Leuthardt, E.C., Schalk, G.: Decoding vowels and consonants in spoken and imagined words using electrocorticographic signals in humans. *J. Neural Eng.* **8**(4), 046028 (2011)
8. Fergus, P., Hignett, D., Hussain, A., Al-Jumeily, D., Abdel-Aziz, K.: Automatic epileptic seizure detection using scalp EEG and advanced artificial intelligence techniques. Hindawi Publ. Corporation BioMed Res. Int. Volume, Article ID 986736, 17 p (2015)

Accurate Frequency Estimation Method Based on Basis Approach and Empirical Wavelet Transform

Lakshmi Prakash, Neethu Mohan, S. Sachin Kumar and K.P. Soman

Abstract Due to proliferating harmonic pollution in the power system, analysis and monitoring of harmonic variation in real-time have become important. In this paper, a novel approach for estimation of fundamental frequency in power system is discussed. In this method, the fundamental frequency component of the signal is extracted using Empirical Wavelet Transform. The extracted component is then projected onto Fourier basis, where the frequency is estimated to a resolution of 0.001 Hz. The proposed approach gives an accurate frequency estimate compared with some existing methods.

Keywords Frequency estimation · Empirical wavelet transform (EWT) · Fourier basis

1 Introduction

The real-time measurement of frequency is now important for many applications in the power system. Several methods have been proposed and adopted to compute frequency for the power system applications. The Fast Fourier Transform is the most widely used method for frequency estimation. Due to leakage effect, picket fence effect, and aliasing effect, it cannot produce a better result [1]. Further extensions and enhancements are done on this method by utilizing the original FFT with different windowing and interpolation to produce an accurate estimate [2]. For zero crossing technique, the signal is considered to be pure sinusoidal and the signal

L. Prakash (✉) · N. Mohan · S. Sachin Kumar · K.P. Soman
Centre for Excellence in Computational Engineering and Networking,
Amrita Vishwavidyapeetham, Coimbatore Campus, Coimbatore 641112,
Tamilnadu, India
e-mail: lakshmiprakash24@gmail.com

N. Mohan
e-mail: neethumohan.ndkm@gmail.com

frequency is estimated from the time between two zero crossing. However, in reality the measured signals are available in distorted form. The paper [3] explains about the estimation of harmonic amplitudes and phases using several variants of recursive least square (RLS) algorithms. When extended complex kalman filter is used for estimation, the accuracy is reached around the nominal frequency due to the shrinkage of Taylor series expansion of nonlinear terms [4]. In prony method [5], using fourier technique algorithm, the distorted voltage signal is filtered and filter coefficients are calculated assuming constant frequency. However, these filter coefficients are not exact due to frequency deviation. Then a complex prony analysis was proposed where the frequency is estimated by approximating the cosine-filtered and sine-filtered signals simultaneously [6]. In the paper [7], using an optimization method, frequency is estimated by comparing the filtered voltage with a mathematical approach. Other approaches to compute frequency are by using recursive DFT and phasor rotating method [8]. Artificial neural networks are also one of the methods adopted for real-time frequency and harmonic evaluation [9]. Harmonics were also estimated using linear least squares method and by singular value decomposition (SVD) [10].

In this paper, a new approach for frequency estimation is discussed. The paper is divided into five sections including the introduction. Section 2 discusses the Empirical Wavelet Transform and linear algebra concept of basis approach used for the proposed method and Sect. 3 explains the proposed algorithm. Section 4 discusses the results and inferences obtained from the proposed method and the conclusions are given in Sect. 5.

2 Background

2.1 Empirical Wavelet Transform

In Empirical Wavelet Transform [11], a bank of N wavelet filters, one low pass and $N - 1$ bandpass filters are made by adapting from the processed signal. A similar approach is used in the fourier method, by building bandpass filters. For the adaption process, the location of information in the spectrum is identified with frequency, $\omega \in [0, \Pi]$. This is used as filter support.

First, the fourier transformed signal is partitioned into N segments. The boundary limits for each segment is denoted using ω_n . Each partition is denoted as $\wedge_n = [\omega_{n-1}, \omega_n]$, $\bigcup_{n=1}^N \wedge_n$. Around each ω_n , a small area of width $2\tau_n$ is defined. The empirical wavelets are defined on each of the \wedge_n . It is a bandpass filter constructed using Littlewood-Paley and Mayer's wavelets. The subbands are extracted using this filtering operations.

Each partition in the spectrum is considered as modes which contain a central frequency with certain support. Since 0 and Π are used as the limits to the spectrum, the number of boundary limits required will be $N - 1$. Therefore the partition

boundaries, ω_n , comprise of 0, selected maxima, and Π . The expression for scaling function $\hat{\phi}_n(\omega)$ is defined as

$$\hat{\phi}_n(\omega) = \begin{cases} 1 & \text{if } |\omega| \leq \omega_n - \tau_n \\ \cos\left[\frac{\pi}{2}\beta(|\omega| - \omega_n + \tau_n)\right] & \text{if } \omega_n - \tau_n \leq |\omega| \leq \omega_n + \tau_n \\ 0 & \text{otherwise} \end{cases} \quad (1)$$

The expression for empirical wavelet function $\hat{\psi}_n(\omega)$ is defined as

$$\hat{\psi}_n(\omega) = \begin{cases} 1 & \text{if } \omega_n + \tau_n \leq |\omega| \leq \omega_{n+1} - \tau_{n+1} \\ \cos\left[\frac{\pi}{2}\beta\left(\frac{1}{2\tau_{n+1}}(|\omega| - \omega_{n+1} + \tau_{n+1})\right)\right] & \text{if } \omega_{n+1} - \tau_{n+1} \leq |\omega| \leq \omega_{n+1} + \tau_{n+1} \\ \sin\left[\frac{\pi}{2}\beta\left(\frac{1}{2\tau_n}(|\omega| - \omega_n + \tau_n)\right)\right] & \text{if } \omega_n - \tau_n \leq |\omega| \leq \omega_n + \tau_n \\ 0 & \text{otherwise} \end{cases} \quad (2)$$

The function $\beta(x)$ is an arbitrary function, the expressions can be referred in [11]. The width around each ω_n is decided using τ_n and it is defined as $\omega_n : \tau_n = \gamma\omega_n$, $0 < \gamma < 1$, $\forall n > 0$. Now for function f , the detail coefficients is obtained by taking the inverse of convolution operation between f and ψ_n (wavelet function).

$$W_f^e(n, t) = ((\hat{f}(\omega))\overline{\hat{\psi}_n(\omega)})^{-1}$$

The approximate coefficients are obtained by taking the inverse of convolution operation between f and ϕ_n (scaling function).

$$W_f^e(0, t) = ((\hat{f}(\omega))\overline{\hat{\phi}_1(\omega)})^{-1} \quad (3)$$

The empirical mode function, denoted by f_k , is given as

$$f_0(t) = W_f^e(0, t) * \phi_1(t) \quad (4)$$

$$f_k(t) = W_f^e(k, t) * \phi_k(t) \quad (5)$$

2.2 Concept of Basis

Any N point signal can be considered as a point in C^N (C denotes the complex space) and the operation of taking its FFT can be considered as a mapping from $C^N \rightarrow C^N$. There are infinite number of choices for a probable basis set in C^N space [12]. Construction of fourier basis in C^N space requires N orthogonal

$$\begin{array}{ccc}
 k=0 & k=1 & k=(N-1) \\
 \left[\begin{array}{ccc}
 \frac{j2\pi 0\times 0}{N} & \frac{j2\pi 1\times 0}{N} & \frac{j2\pi(N-1)\times 0}{N} \\
 e & e & e \\
 \frac{j2\pi 0\times 1}{N} & \frac{j2\pi 1\times 1}{N} & \frac{j2\pi(N-1)\times 1}{N} \\
 e & e & e \\
 \vdots & \vdots & \vdots \\
 \frac{j2\pi 0\times (N-1)}{N} & \frac{j2\pi 1\times (N-1)}{N} & \frac{j2\pi(N-1)\times (N-1)}{N} \\
 e & e & e
 \end{array} \right] & \begin{array}{c} n=0 \\ n=1 \\ \vdots \\ n=(N-1) \end{array} \\
 \boxed{\text{Complex conjugates}}
 \end{array}$$

vectors of the form $e^{\frac{j2\pi kn}{N}}$, $k \in \mathbb{Z}$. Consider the signal $e^{j\theta}$, $\theta = \frac{2\pi nk}{N}$, and $n = \{0, 1, \dots, N-1\}$, we can observe that, irrespective of value of k , θ is varied from $[0, 2\pi)$. We need to take only the samples from the signal corresponding to one period which will constitute the N tuple in C^N space, and n is such that it covers one period. The matrix shown (the Twiddle Matrix) has N Fourier basis arranged column wise.

3 Signal Model and Proposed Method

Consider a continuous-time signal, $x(t)$ with amplitude, frequency, and phase denoted as A , f , and θ , respectively. The signal $x(t) = A \cdot \cos(2\pi f t + \theta)$ can be discretized as

$$x[n] = A \cdot \cos\left(2\pi \frac{f}{f_0 N_0} n + \theta\right) = A \cdot \cos(2\pi f \cdot n \Delta t + \theta) \quad (6)$$

where f_0 is the nominal fundamental frequency, N_0 is the number of samples per cycle at f_0 , and Δt is the sampling period. In the proposed method, a synthetic signal is created and then discretized. Using EWT, the signal is decomposed into various modes. From these modes, fundamental frequency component is extracted. To get the frequency with high resolution, the extracted fundamental frequency component is projected on to a basis matrix. Figure 1 gives the flowchart of the proposed method.

4 Results and Discussions

In this section, the performance of the proposed algorithm is discussed. To demonstrate the effectiveness of this method an input signal is synthesized with fundamental frequency of 50.218 Hz. It contains 20 % third harmonic component and

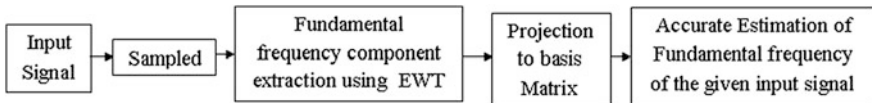
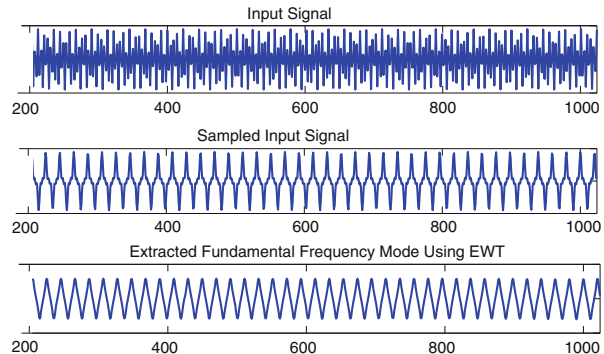


Fig. 1 Flowchart of proposed method of frequency estimation

Fig. 2 Processing stages of signal



10 % fifth harmonic component. The synthesized signal was sampled at the rate of 1024 samples/cycle. As a prefiltering process, the harmonic contents present in the signal are removed or fundamental frequency component is extracted by using EWT. The Fig. 2 gives the processing stages of signal. Generally in a power system, the third and fifth harmonic components causes the main impact. When signal is decomposed using EWT, the first mode always gives a decaying DC component. The second mode gives the fundamental frequency component and rest of the other modes gives the harmonics.

When FFT of this second component is computed, it estimates the frequency as 51 Hz. Since the given input signal is generated at 50.218 Hz the difference in estimated frequency arose due to spectral leakage phenomena. The Fig. 3 gives the frequency spectrum of the extracted component and the effect of spectral leakage is visible.

Now to estimate it most accurately the method proposed in Sect. 2.2 is used. The power system signal has to be maintained within a permissible range of 48–52 Hz. Otherwise, it could result in the grid collapsing. So the extracted fundamental frequency component is projected on to a basis matrix, created for a resolution of 0.001 between the range of 48–52 Hz. By using this approach, estimated frequency is 50.218, which is same as the given input frequency. Figure 4 gives the EWT decomposition of three modes.

From Fig. 5, we can infer that when the number of mode increases, the fundamental frequency component and harmonics get splitted into several modes. By the split of these components, information about fundamental frequency will be less.

Fig. 3 FFT of the extracted fundamental frequency component

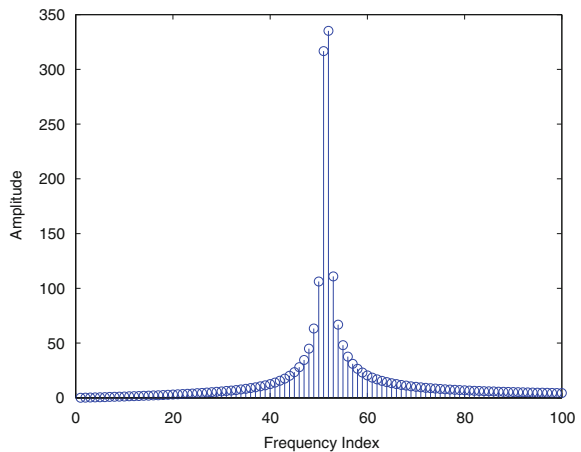


Fig. 4 Signal decomposition using EWT when the mode given is 3

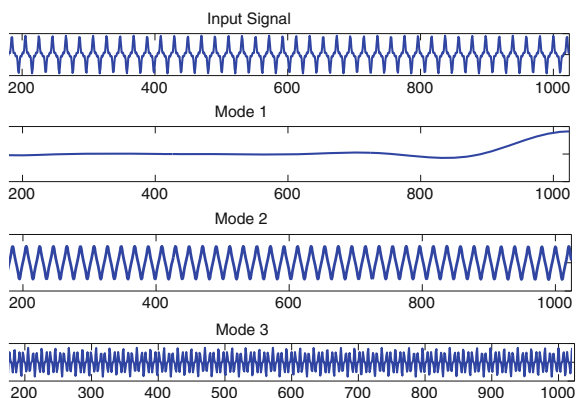
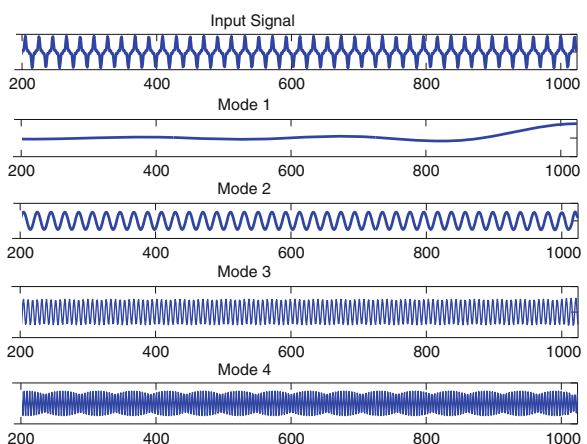


Fig. 5 Signal decomposition using EWT when the mode given is 4



The basis approach is applied for different frequencies and modes, the results are shown in Table 1. From Table 1, we infer that mainly the second mode of the input signal after decomposing gives the accurate frequency estimate the same as the given input frequency of the synthesized signal. The other splitted component also estimates the frequency near to the given input frequency, but it does not give the resolution of 0.001 Hz as expected. Therefore, for accurate estimation, the number of modes in EWT can be fixed as three or four.

Also, the proposed method is compared with many conventional frequency estimation algorithms such as FFT, zero crossing technique, prony method, recursive DFT, and phasor rotation method. Table 2 shows the estimated frequencies obtained from these methods.

Table 1 Frequency estimation using basis approach for different frequencies and modes

S. no.	Input frequency (Hz)	Total number of modes taken in EWT	Mode considered for proposed algorithm	Estimated frequency using proposed algorithm (Hz)
1	50.2180	3	2	50.2180
		4	2	50.2180
		5	2	50.2180
			3	50.2750
		6	2	50.2180
			3	50.2530
		7	2	50.2140
			3	50.2830
			4	50.2530
2	50.149	3	2	50.1490
		4	2	50.1490
		5	2	50.1440
			3	50.1490
		6	2	50.1550
			3	50.1330
		7	2	50.1550
			3	50.1330
			4	50.7750
3	50.6730	3	2	50.6730
		4	2	50.6730
		5	2	50.6670
			3	50.6730
		6	2	50.6580
			3	50.6760
		7	2	50.7480
			3	50.6570
			4	50.7760

Table 2 Comparison with other frequency estimation methods

S. no.	Methods for frequency estimation (Input Frequency = 50.218 Hz)	Estimated frequency (Hz)
1	Fast fourier transform	51
2	Zero crossing technique	50.5
3	Prony method	49.3281
4	Recursive DFT And phasor rotation method	48.4751
5	Method proposed By Micheletti (Ref. [7])	51.3718
6	SW-DFT with dyadic downsampling + Basis approach	50.2300
7	EWT + basis approach	50.218

When sliding window recursive DFT with dyadic downsampling is applied for mode decomposition to find out the fundamental frequency component. The basis approach estimation gives frequency estimate of 50.2300 Hz. From this, it can be inferred that EWT decomposition gives more information about fundamental frequency component when compared to sliding window recursive DFT with dyadic downsampling decomposition method.

5 Conclusion

The paper proposes a new fundamental frequency estimation approach using the concept of basis. The proposed method use EWT to find the fundamental frequency component present in the signal. The frequency is estimated to a resolution of 0.001 Hz by projecting the fundamental frequency component to a basis matrix. This method is compared with many other conventional methods.

References

1. Rajesh, I.: Harmonic analysis using FFT and STFT. In: International Journal of Signal Processing, Image Processing and Pattern Recognition (2014), pp. 345–362
2. Zhang, F., Geng, Z., Yuan, W.: The algorithm of interpolating windowed FFT for harmonic analysis of electric power system. IEEE Trans. Power Delivery **16**, 160–164 (2001)
3. Li, L., Xia, W., Shi, D., Li, J.: Frequency estimation on power system using recursive-least-squares approach. In: Proceedings of the 2012 International Conference on Information Technology and Software Engineering Lecture Notes in Electrical Engineering (2013), pp. 11–18
4. Dash, P.K., Pradhan, A.K., Panda G.: Frequency estimation of distorted power system signals using extended complex kalman filter. IEEE Trans. Power Delivery **14**, 761–766 (1999)
5. Lobos, T., Rezmer, T.: Real-time determination of power system frequency. IEEE Trans. Instrum. Meas. **46**, 877–881 (1997)

6. Nam, S.-R., Lee, D.-G., Kang, S.-H., Ahn, S.-J., Choi, J.-H.: Fundamental frequency estimation in power systems using complex prony analysis. *J. Electr. Eng. Technol.* **154–160** (2011)
7. Micheletti, R.: Real-time measurement of power system frequency. In: *Proceedings of IMEKO XVI World Congress* (2000), pp. 425–430
8. Ribeiro, P.F., Duque, C.A., Ribeiro, P.M., Cerqueira, A.S.: *Power Systems Signal Processing for Smart Grids*. Wiley, New York (2013)
9. Lai, L.L., Chan, W.L., SO, A.T.P., Tse, C.T.: Real-time frequency and harmonic evaluation using artificial neural networks. *IEEE Trans. Power Delivery* **14**, 52–59 (1999)
10. Lobos, T., Kozina, T., Koglin, H.-J.: Power system harmonics estimation using linear least squares method and SVD. In: *IEE Proceedings of the Generation, Transmission and Distribution* (2001) pp. 567–572
11. Gilles, J.: Empirical wavelet transform. *IEEE Trans. Signal Process.* **61**, 3999–4010 (2013)
12. Soman, K.P., Ramanathan, R.: *Digital Signal and Image Processing-The sparse way*. Isa Publication (2012)

Hybrid Recommender System with Conceptualization and Temporal Preferences

M. Venu Gopalachari and P. Sammulal

Abstract From the last couple of decades, the web services on the Internet changed the perspectives of the usage of a normal user as well as the vendor. Recommender systems are the intelligent agents that provide suggestions regarding the navigation in the web site for a user, based on preferences mentioned by the user in the past usage. Although there were several hybrid recommenders available with content-based and collaborative strategies, they were unable to process semantics about temporal and conceptual aspects. This paper incorporates the domain knowledge of the web site and the semantics for the temporal constructs into the hybrid recommender system. The proposed recommender parses the personalized ontology constructed for a user based on temporal navigation patterns and suggests the pages. The effectiveness of this approach is demonstrated by the experiments varying the scale of the data set and analyzed with the user's satisfaction toward the quality of recommendations.

Keywords Hybrid recommender system · Ontology · Usage patterns · Temporal concepts

1 Introduction

Nowadays, every service provider in World Wide Web is trying to assist the customers to avoid the problem of information overload. Personalization [1, 2] is a variant of information system that makes the navigations easier according to the

M. Venu Gopalachari (✉)
Chaitanya Bharathi Institute of Technology, Hyderabad, India
e-mail: venugopal.m07@gmail.com

P. Sammulal
Jawaharlal Nehru Technological University Hyderabad College
of Engineering, Karimnagar, India
e-mail: sam@jntuh.ac.in

preferences of the user, which paves a path to solve the information overload problem. User profiling [3] is the first step to provide personalization around the web site, which finds the pattern of navigation in the web site by processing the log. The major role of user profiling exhibited in recommender systems [4] which analyze the information available and suggests the next page, item, or product that has more likelihood of the user.

Typically, there are two recommenders named content-based recommenders [5] and collaborative filtering recommenders [6], where the first one analyzes the past history and the second one identifies and analyzes other users or items with similar patterns and suggests accordingly. After that the evolution of hybrid recommender [7] integrated the content-based strategy and collaborative filtering which were limited to use only historic patterns without domain knowledge. Many web usage mining algorithms targets on the user preferences by considering the time consumption on each page by the user, but these approaches could not able to find the associations among temporal and conceptual constructs.

This paper proposes a hybrid recommender model that resolves all the above-mentioned problems to get useful suggestions. The temporal conceptual associations could be generated by the proposed approach using sequential association pattern mining. For instance, the example of the association is “user X used to spent more time on news page in the evening time,” where evening is the temporal construct and news is the conceptual construct. The proposed model also clusters the users with similar access sequences of the web pages according to the concept of the page. Finally, the recommender strategy simply parses the ontology and processes the web usage patterns to suggest a web page or an item. In order to track the quality of this approach, user’s ratings were recorded about the recommendations. This proposed approach shows better results when compared to the traditional approaches in terms of quality of recommendations.

The rest of the paper is organized as follows. In Sect. 2, related work is presented. In Sect. 3, the architecture and design details of the proposed recommender strategy are described. Section 4 analyzes the implementation and experimentation part. Finally, Sect. 5 gives conclusion followed by references.

2 Related Work

Nowadays, many of the organizations are depending on the personalized applications such as target marketing, recommenders, etc. There are several query-based methods which uses the keyword matching techniques for the text in the web pages. In [8], Tuzhilin described a recommendation strategy which is based on the frequency of keywords in the previous queries of the user, but did not consider any semantic information. Baumann [9], proposed a method that processes the metadata information of the web pages in recommendations but were unable to extract the semantic relations among complex concepts.

Ontology-based recommenders incorporate the knowledge into history-based or query-based recommenders [10] which improve quality of the recommendations. Thakur [11] proposed a semantic web personalization system that integrates both usage data with content semantics, expressed in ontology that effectively generates useful recommendations. Fong [12], proposed an approach for constructing a user behavior knowledge base with the access history, which uses a fuzzy logic to represent temporal concepts for the web access activities. A collaborative filtering method generally works on identifying the preferences of the active users with similar navigation profiles.

In Tang et al. [13], proposed topic model-based clustering technique, so that it could frame groups of items in active academic social networks, which is a collaborative filtering task. However, hybrid systems such as [7] proposed a recommendation system that combines the content-based and collaborative filtering methods, which tries to overcome the drawbacks of the traditional recommendation systems. But these recommenders were failed to consider the semantics and temporal concepts and solely depend on the usage patterns.

3 Semantic Hybrid Recommender with Temporal Concepts

The proposed hybrid recommender model, as shown in Fig. 1, is designed in three phases: the first phase populates the domain ontology to define conceptual constructs, in the second phase the usage patterns of the user with temporal concepts

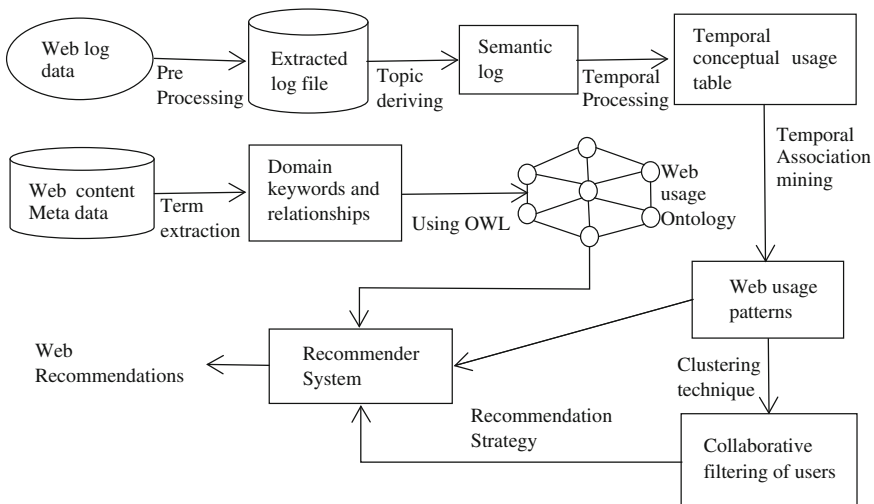


Fig. 1 Architecture of the hybrid recommender system that finally outputs set of recommendations

have to be generated, and the third phase will apply the clustering technique on users with similar patterns. Finally, the recommendation strategy will process the current access pattern of the user and parse the ontology to suggest the user like-lihood web pages.

3.1 Domain Ontology Constructions

Generally, the semantics of the web site are represented as domain knowledge through ontology. Ontology is a conceptual hierarchical model that contains large set of key terms in the domain and the relationships among these terms. The ontologies of a domain can be effectively constructed by web ontology language [14] (OWL), of course, there are many tools available for OWL write-ups. A domain can be defined as a group of web pages that exactly resembles the information of the same field such as medical, bioinformatics, telecommunications, e-governance, etc. Alternatively, domain can be the set of web pages belonging to a web site such as e-commerce and e-retail web sites. In case of e-commerce web site, the set of terms used to tag web pages while developing can be the key terms and the relationships among these key terms can be found by conceptualizing the terms [15].

3.2 Temporal and Conceptual-Based Usage Patterns

The conceptual constructs can be extracted from the log by topic deriving on the title of the web page in the log. This kind of semantic deriving can make concept of the web page clear to further processing. The temporal attributes are constructed from web usage log with some predefined time period values. The usage log constitutes a set of sessions $S = \{S_1, S_2 \dots S_m\}$, where each session contains set records $R = \{r_1, r_2 \dots r_k\}$, which contains URL, title, time stamp, concept of the page, IP address, etc.

Temporal conceptual context table of a user can be generated as follows:

- Step 1: Process the web log to extract the duration of usage of each page in a session S_i of a particular user U_i . The duration can be found by the difference between the time stamps of the current page and the subsequent page.
- Step 2: Calculate the aggregate sum of the duration values for the predefined time periods $\{T_1, T_2 \dots T_i\}$ and for the predefined concepts $\{C_1, C_2 \dots C_j\}$.
- Step 3: Calculate the participation of a user in a particular time period T_1 by dividing with total number of sessions and transforming the result value into $[0, 1]$.
- Step 4: Calculate the participation of a user in a particular concept C_1 by dividing with total number of sessions and transforming the result value into $[0, 1]$.

Table 1 Temporal and conceptual constructs of a particular user

Session Id	T_1	T_2	T_3	C_1	C_2	C_3
SD1SL8FF	0	0	1	0	0.57	0
SD9SL6FF	0	1	0.34	0	0.42	1
SD2SL1FF	1	0	0	0	0.43	1
SD10SL10	0.72	0.31	0	0	0.76	0.94
SD1SL4FF	0	0	1	0	0	1

Table 2 Usage patterns of a particular user

IP Address	Pattern	Support	Confidence
87.194.216.51	[T_1, C_1]	0.026	0.053
87.194.216.51	[T_1, C_2]	0.253	0.253
87.194.216.51	[T_1, C_3]	0.218	0.145
87.194.216.51	[T_2, C_2]	0.233	0.102
87.194.216.51	[T_2, C_3]	0.215	0.08
87.194.216.51	[T_3, C_2]	0.561	0.12

Table 1 shows an instance of a user temporal constructs, which describes the user's interest toward the web page in terms of temporal aspects. The conceptual aggregate values of a user (C_1, C_2, C_3) are also shown in the table for different access sessions participated by the user, which resembles the user's preference toward a concept. For instance, by observing the table, it can be easily declared that the user is not interested in the concept C_1 .

The usage patterns are generated by means of association mining. The minor difference from the traditional mining algorithms is to find the associations among temporal constructs and conceptual constructs. In literature, there were many association algorithms that were proposed, but TITANIC algorithm [16] exhibits a better performance among them. To generate the association patterns, the proposed recommender uses this algorithm and generates the association patterns by using predefined support and confidence measures.

For instance, [T_1, C_2], as shown in table 2, describes that the user is interested to navigate the concept C_2 in the time period T_1 . These association patterns can be stored as ontology by using OWL, where each pattern is a class and its support and confidence becomes the properties of that class.

3.3 Clustering Users with Similar Patterns

In general, collaborative filtering clusters user profiles with similar web access sequence patterns and predicts next web page in the access sequence. Typically, the users in the same cluster will have the same access pattern, predicting near future with the traditional usage recommender system simply suggests the pages in the access sequence. This way of suggesting can limit the quality of recommendations

because of lack of domain knowledge. In order to overcome the mentioned drawback, proposed model uses a novel technique that clusters the users based on the concept of the access sequence rather than a web page alone.

Let U is set of n users $\{u_1, u_2 \dots u_n\}$ with their access sequences

Step 1: The web pages in the domain mapped to the tags using ontology.

For each user u_i where i is 0 to n users

For each access sequence A_j of the user u_i

For each title t_k in the access sequence A_j

Map domain ontology for the web page and assign a tag to the title.

Step 2: Apply clustering technique on users with semantic access tags.

K-means technique can be applied for clustering, whereas the similarity measure that has to be used varies for the current process. Similarity between two users: u_i and u_j depends on their access sequences match ratio (MR_{ij}) which is defined as

$$MR_{ij} = \frac{|Aik \cap Ajk|}{\min_{ij}\{|Aik|, |Ajk|\}} \quad (1)$$

These user's clusters will act as an input for recommenders so that these cluster concepts will participate in the recommendation algorithm.

3.4 Recommendation Strategy

The proposed recommender strategy considers the domain knowledge in addition with the usage knowledge. That means the recommender strategy should take the part of parsing ontology to output quality recommendations. The main objective of the proposed recommender is to identify the current session access sequence and to identify most appropriate past web access sequence of the user, and finally it has to suggest the next page in the access sequence identified. The process of identifying the similar patterns in the user's previous access sequences is one kind of recommendation and identifying clusters that exactly resembles the current access sequence is the collaborative filtering recommendation strategy. This strategy finally outputs a set of pages as recommendations from which the user can get benefited.

4 Experimentation Results

The performance of the system is analyzed by comparing the recommender with usage patterns alone. For this a synthesized data set was collected from the Internet, which contains about 25,000 records on 65 web pages. To identify the accuracy and quality of the recommendations a measure called satisfaction value is recorded from the user, which ranges from 1 to 5, where 5 is high quality and decreases to 1. There are two measures defined to analyze, they are:

$$\text{Hit Ratio} = \frac{A_r}{R_e} \quad (2)$$

$$\text{True Hits} = \frac{S_r}{A_r} \quad (3)$$

where ' S_r ' is the total number of correct recommendations, ' A_r ' is the total number of recommendations accessed by the user, and ' R_e ' is the total number of recommendations.

However, the correct recommendations are those which cross the rating from a predefined threshold value. There are three test cases defined varying the number of records in the data set. Test set 1 contains 1/3 rd of the instances, test set 2 contains 2/3rd of the instances, and test set 3 contains all instances in the data set. The *hit ratio* and *true hits* values for the three recommenders were shown in Table 3 for the three test cases. With this table, it can be a clear illustration of performance improvement in the quality of the recommendations. Figure 2 shows the comparison for all three test cases.

True hits value for the proposed recommender is higher than others which declare that the quality of recommendations is better than the existing approaches. It is clear that when number of samples increases, then definitely proposed recommender with ontology outperform than the traditional approach.

Table 3 Experimentation values for the three kinds of recommenders

Technique/Measure	Hit ratio			True hits		
	Test Case1	Test Case2	Test Case3	Test Case1	Test Case2	Test Case3
Traditional recommender	0.639	0.748	0.753	0.524	0.533	0.587
Content recommender with ontology	0.832	0.881	0.921	0.662	0.723	0.815
Proposed hybrid recommender	0.887	0.930	0.923	0.703	0.783	0.934

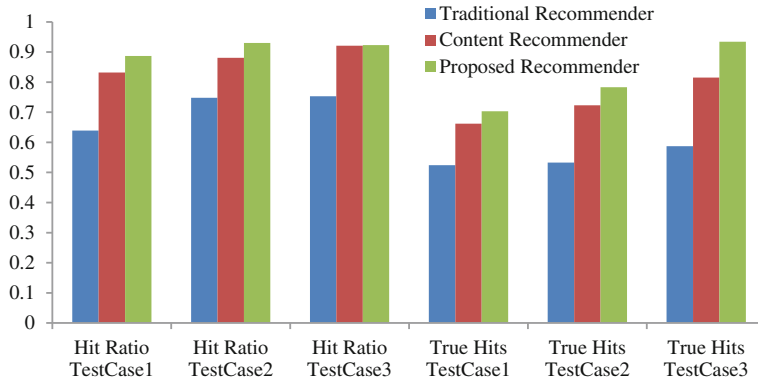


Fig. 2 Comparison among three recommenders for hit ratio and true hits measures

5 Conclusion

In this paper, a hybrid recommender system is proposed that combines the content-based and collaborative filtering techniques using semantics about temporal and conceptual constructs. The proposed system constructed ontology and combined in the process of recommendations to the user. The experiments were observed using a synthesized data set, where the results shown significant performance in terms of quality of recommendations using two measures hit ratio and true hits. In future work, the proposed framework should consider the diversity of the recommendations as well the cold start problem of the recommender system.

References

- Baldonado, M., Chang, C.-C.K., Gravano, L., Paepcke, A.: The Stanford digital library metadata architecture. *Int. J. Digit. Libr.* **1**, 108–1211 (1997)
- Mobasher, B., Cooley, R., Srivastava, J.: Automatic personalization based on web usage mining. *Comm. ACM* **43**(8), 142–151 (2000)
- Schiaffino, S., Amaldi, A.: Intelligent user profiling. *Artificial Intelligence*, pp. 193–216. Springer, Berlin (2009)
- Miao, C., Yang, Q., Fang, H., Goh, A.: A cognitive approach for agent-based personalized recommendation. *Knowl. Based Syst.* **20**, 397–405 (2007)
- Mooney, R.J., Roy, L.: Content-based book recommending using learning for text categorization. In: Proceedings of the 5th ACM Conference Digital Libraries (DL 2000), pp. 195–204 (2000)
- Umyarov, A., Tuzhilin, A.: Improving collaborative filtering recommendations using external data. In: Proceedings of the IEEE 8th International Conference Data Mining (ICDM 2008), pp. 618–627 (2008)
- Melville, P., Mooney, R.J.: Content-boosted collaborative filtering for improved recommendations. In: Proceedings of the 18th National Conference Artificial Intelligence, pp. 187–192 (2002)

8. Tuzhilin, A., Adomavicius, G.: Integrating user behavior and collaborative methods in recommender systems. In: Proceedings of the CHI 1999 Workshop “Interacting with recommender systems”, Pittsburgh, PA (1999)
9. Baumann, S., Hummel, O.: Using cultural metadata for artist recommendations. In: Proceedings of the Third International Conference on WEB Delivering of Music (WEDELMUSIC03). Los Alamitos, CA, USA, pp. 138–141: IEEE Computer Society (2003)
10. Liang, T.P., Lai, H.-J.: Discovering user interests from web browsing behavior: an application to internet news services. In: Proceedings of the 35th Annual Hawaii International Conference on System Sciences (HICSS 2002). Washington, DC, USA, pp. 2718–2727: IEEE Computer Society (2002)
11. Thakur, M., Jain, Y.K., Silakari, G.: Query based personalization in semantic web mining. In: IJACSA, vol. 2, no. 2 (2011)
12. Fong, A.C.M., Zhou, B., Hui, S.C., Hong, G.Y., Do, A.: Web content recommender system based on consumer behavior modeling. *IEEE Trans. Consum. Electron.* **57**(2), 542–550 (2011)
13. Tang, J., Zhang, J., Yao, L., Li, J., Zhang, L., Su, Z.: Arnetminer: extraction and mining of academic social networks. In: Proceedings of the 14th ACM SIGKDD International Conference Knowledge Discovery and Data Mining (KDD 2008), pp. 990–998 (2008)
14. McGuinness, D.L., Van Harmelen, F.: OWL Web ontology language overview. W3C Recommendation. <http://www.w3.org/TR/owl-features/>. Accessed Feb 2004
15. Venu Gopalachari, M., Sammulal, P.: Personalized web page recommender system using integrated usage and content knowledge. In: the Proceedings of 2014 IEEE ICACCCT, pp. 1066–1071 (2014)
16. Gerd Stumme, R., Taouil, Y., Bastide, N., Pasquier, Lakhal, L.: Computing iceberg concept lattices with TITANIC. *Data Knowl. Eng.* **42**(2), 189–222 (2002)

An Approach to Detect Intruder in Energy-Aware Routing for Wireless Mesh Networks

P.H. Annappa, Udaya Kumar K. Shenoy and S.P. Shiva Prakash

Abstract Wireless mesh networks (WMN) possess characteristics such as self-healing, self-configuring and self-discovery. Due to this nature WMN has emerged as the most widely used popular network. Since these devices are operated using battery resources, several works have been carried out for minimizing energy consumption during routing process, thereby increasing network lifetime. WMNs are more vulnerable for attackers due to its wide usage. Many works can be found to detect the intruder during routing without considering energy as a metric. There exist possibilities of intruder to attack the battery resource thereby reducing network efficiency in energy-aware routing. Hence in this work we propose a novel approach to detect an intruder by self-monitoring mechanism of node considering metrics such as packet size, data rate, remaining energy and draining rate of a energy resources of a node. The proposed model consists of three modules, namely self-intrusion detector, monitor and evaluator. It detects and helps in making decisions to participate in the network transmission. The working of the model is analyzed and shows that the proposed model detects intruder effectively, thereby resulting in increase of WMN efficiency.

Keywords Energy-aware routing • Wireless mesh network • Intrusion detection

P.H. Annappa (✉) · U.K.K. Shenoy
Nitte Mahalinga Adyanthaya Memorial Institute of Technology, Nitte
Karnataka, India
e-mail: annappaph2@gmail.com

U.K.K. Shenoy
e-mail: ukshenoy@gmail.com

S.P. Shiva Prakash
Sri Jayachamarajendra College of Engineering, Mysore, Karnataka, India
e-mail: shivasp26@gmail.com

1 Introduction

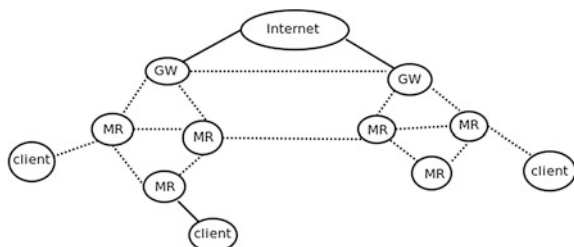
A wireless mesh network (WMN) is a type of communication network where nodes are arranged in mesh topology. To have cost-effective and high bandwidth networks, WMN is a better solution as it maintains good coverage area. The architecture of WMN is as shown in Fig. 1. WMN is formed by mesh clients (MC), mesh routers (MR), and gateways (GW). MR is responsible for forwarding traffic to GW. The data traffic is carried from source to destination using hopping mechanism. The MR acts as relay node that receives and forwards the data from one node to another node during hopping. Relaying not only increases the signal strength but also makes sure that data reaches the destination successfully. The decision of identifying the relay node in order to forward the data is defined by the routing protocol in the network. Routing is a process of transferring packet from source to destination through the best available paths. Recent trends focus on energy-based routing in order to conserve energy which may lead to be attacked by intruder. In energy-based routing, energy resource is used as a metric for making decision in routing. Energy resource of a node plays an important role in path selection at routing level, which increases the network lifetime. There are more possibilities of battery resources being attacked by the intruder so as to reduce network efficiency. Intrusion detection algorithms identifies illegal use and alerts the system. Hence, detection of intruder and alerting the system is very important in energy-based routing.

The next sections in the paper is organized as follows: Sect. 2 unfolds the related work carried out, Sect. 3 presents the design of proposed model and the mathematical model, Sect. 4 discusses about the algorithm for proposed model, Sect. 5 shows the energy-based routing mechanism and analysis of the proposed model. The Sect. 6 contains conclusion.

2 Related Works

In order to detect the intruder, Bradley [1] introduced a model called Watcher, which is installed and executed concurrently in router. The model identifies the amount of data going through neighboring router. It successfully identifies the

Fig. 1 Mesh architecture

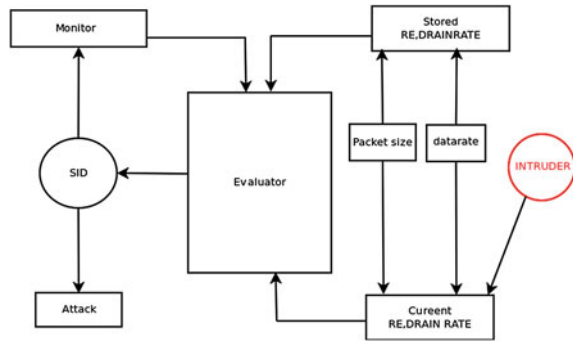


misbehaving router. Further, Zhang and Lee [2] presented a cooperative anomaly detection model. In this model each node observes the neighboring node which is in its radio range by applying cooperative strategy between the nodes. Marti et al. [3] introduced the models called Watchdogs and Path raters in order to detect an intruder. Watchdog process is used to determine the behavior of neighboring nodes and path raters are used to find the misbehaving nodes. TIARA model was introduced by the Ramanujan et al. [4] to detect the intruder in which source node sends flow status message, which contains information about the number of packets to destination nodes. It encrypts the data using digital signature and assigns numbers to the message sequentially to avoid interference. Bhargava and Agrawal [5] introduced the model Malcount, where each node maintains a malcount counter for neighboring nodes, which is the number of observed occurrences of misbehavior nodes. They fix malcount threshold value which is used to define the intruder attack. When a malcount for a node exceeds a specific threshold value an alert message is sent to other nodes. Karygiannis et al. [6] proposed a RESANE model in which the reputation of a nodes is decided based on the node behavior. The node will be eliminated from the network when it continuously misbehaves because of which its reputation might suffer. Further, an efficient model proposed by do Carmo et al. [7] called PRIDE, TRAM and TRAIN. These models suggest methods to overcome resource constraint issues to security administrator. It considers knowledge about WMN traffic and distributes intrusion detection systems functionality. Hassanzadeh et al. [8] introduced traffic and resource-aware intrusion detection model which concentrates on traffic load and path selection for sending a packet.

Battery resource of a node plays an important role in detecting efficiency of network. From the noted works we found that no work has been carried out till date that suggests any model to detect intruder in energy-based routing. Hence, there is need to define a model that detects intruder by self-monitoring mechanism.

3 Proposed Model

The proposed model as shown in Fig. 2 consists of three important modules, namely evaluator, self-intrusion detector (SID) and monitor. It maintains two kinds of information called stored and current status of nodes having metrics remaining energy, draining rate, packet size and data rate of a node. The evaluator module compares these two information to determine whether the node has been attacked. The result is given as input to the next module SID. The SID module will make decision about the attack based on the evaluators. Monitor module is used to monitor the node for further detection of attacks.

Fig. 2 Proposed model

3.1 Mathematical Model

Consider a network of N nodes where N is a set of positive numbers. During routing source node broadcasts RREQ messages to find the destination node. The RREQ message contains $n_{\text{req}}(P_s, d_r, n_d)$, where P_s is packet size, d_r is data rate and n_d is destination id. Let n_0 represent own id of a node and nnT represent next nodes transmission mode. The nodes within communication range of a source node will fetch the destination id n_d from the RREQ packet and compare it with its own id. To calculate the energy consumption there is a need to identify the transmission mode of the next node. Let next node transmission mode be $(\text{nnT}) \in (R_x, T_x)$. It is defined by Eq. 1

$$\text{nnT} = \begin{cases} R_x, & n_d = n_0 \\ T_x, & n_d \neq n_0 \end{cases} \quad (1)$$

The energy value for nnT is decided using the following equations:

$$E_c = \frac{I * V * T * P_s}{d_r} \quad (2)$$

where $I = 220$ mA while receiving packet for $E_c^{R_x}$, $I = 330$ mA while transmitting packet for $E_c^{T_x}$. Hence E_c^{rel} can be calculated using equation

$$E_c^{\text{rel}} = E_c^{R_x} + E_c^{T_x} \quad (3)$$

Further, the remaining energy (RE) of a node is calculated using equation

$$\text{RE} = \text{IE} - E_c(T_x, R_x, \text{rel}) \quad (4)$$

using Eqs. 1 and 4, the decision to participate in routing is made by defining the value for route reply (RREP). The node reply (n_{rep}) is calculated using the following equations:

$$n_{\text{rep}} = \begin{cases} 1, & \text{RE} \geq E_c^T \\ 0, & \text{RE} < E_c^T \end{cases} \quad (5)$$

From Eq. 5 we can defined the condition for establishing communication link.

$$C_L = \begin{cases} 1, & n_{\text{req}} = n_{\text{rep}} \\ 0, & \text{otherwise} \end{cases} \quad (6)$$

The communication link is used to define the status of communication between two nodes. Further, the draining rate of a node R_D is calculated using Eq. 7

$$R_D = \frac{\text{PE} - \text{CE}}{\text{CT} - \text{PT}} \quad (7)$$

Where PE = previous energy, CE = current energy, PT = previous time, CT = current time

$$A_{\text{attack}} = \begin{cases} 0, & (\text{SDR} = \text{CDR} \wedge \text{SRE} = \text{CRE}) \\ 1, & (\text{SDR} \neq \text{CDR} \vee \text{SRE} \neq \text{CRE}) \end{cases} \quad (8)$$

Equation 8 defines the status of a node whether it is attacked or not by comparing the current draining rate and the remaining energy of a node with stored remaining energy and drain rate of a node.

Where SDR = stored drain rate, CDR = current drain rate, SRE = stored remaining energy, CRE = current remaining energy.

4 Algorithms for Proposed Model

In this section we present the algorithms for the proposed model.

Algorithm 1 Energy based routing algorithm

Input : $IE, T_x, R_x, R_{el}, idle, T_h$
 Output : Packet forward decision

```

for  $i := 1$  to  $n$  do
   $RE_i \leftarrow IE - E_c(T_x, R_x, R_{el}, idle)$ 
   $DR_i \leftarrow \frac{RE_{i+1} - RE_i}{T_{i+1} - T_i}$ 
   $s[i] \leftarrow RE_i$ 
   $c[i] \leftarrow RE_i$ 
   $b[i] \leftarrow DR_i$ 
   $d[i] \leftarrow DR_i()$ 
  call Attacker();
  if ( $flag == 1$ ) then
    if ( $c[i].RE_i > T_h$ )||(  $d[i].DR_i > T_h$ ) then
       $FW \leftarrow 1$ 
      call Attacker();
    else
       $FW \leftarrow 0$ 
    end if
  end if
  if ( $flag == 0$ ) then
    Reinitialize
    if ( $c[i].RE_i > T_h$ )||(  $d[i].DR_i > T_h$ ) then
       $FW \leftarrow 1$ 
      call Attacker();
    else
       $FW \leftarrow 0$ 
    end if
  end if
end for
```

In Algorithm 1 remaining energy and draining rate are calculated using Eqs. 4 and 7 respectively. Based on node activity, two copies of remaining energy and drain rate are maintained. These two copies are known as stored copy and current copy. In the case of node being attacked by the intruder, the node will alert the system and it reinitializes routing table value of the corresponding node using the stored copy of the same node at the same instant of time. The decision of participation of node in forwarding packet is made by comparing current remaining energy and drain rate values with its threshold. In case of no attack, current remaining energy and drain rate are compared with its threshold value. If current remaining energy and drain rate are greater than that threshold, node continuously forwards the packet. Attacker is called to check the efficiency of proposed system at different time intervals.

In Algorithm 2 node compares current remaining energy, drain rate, and stored remaining energy drain rate. If intruder attacks the current copy of a node, node detects the attacker based on stored copy of that node.

Algorithm 2 Attacker

```

Input : RE, DR
Output : To decide whether its attacked aren't
for  $i := 1$  to  $n$  do
    if  $(s[i].RE_i == c[i].RE_i) || (b[i].DR_i == d[i].DR_i)$  then
         $attack \leftarrow 0$ 
         $flag \leftarrow 1$ 
    else
         $attack \leftarrow 1$ 
         $flag \leftarrow 0$ 
    return ( $flag$ )
    end if
end for

```

5 Working of Energy-Based Routing Mechanism

Consider a network installed with energy-based routing of WMN. Source node broadcasts RREQ message to neighboring nodes, RREQ message contains packet size, data rate and destination id. The threshold value is fixed based on packet size and data rate. If remaining energy value is greater than that threshold value, it can participate in routing. We fix the value for network parameters as shown in Table 1. Consider an example of energy-based routing in WMN as shown in Fig. 3. Let us consider traffic from node-1 to node-5 where node-1 is source and node-5 is destination to identify the relay node. In our example to transmit a packet from node-1 to node-5, there are several paths available. Consider there exist one shortest path from node-1 → node-9 → node-11 → node-5. So node-9 and node-11 act as relay nodes.

Table 1 Network parameters and values

Parameter	Values
No. of nodes	12
Packet size	256
Data rate	2 Mbps
No. of packets	20
Initial energy	10 J
Transmission power	330 mA
Reception power	220 mA
Energy threshold T_x	0.21 J
Energy reception R_x	0.14 J
Energy relay R_{el}	0.35 J

Fig. 3 WMN

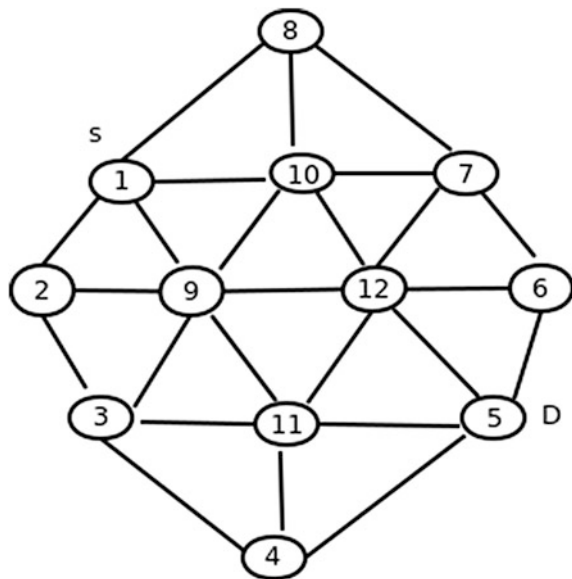


Table 2 shows the node-1, node-11 and node-5 status after transmission, relaying and reception of a packet and it also shows the node-9 status after attack.

5.1 Analysis of Proposed Intrusion Detection System

Source node broadcasts RREQ message to neighboring nodes, RREQ message contains packet size, data rate and destination id. The threshold value is fixed based

Table 2 Relay node-9 status after attack

Node	Transmission mode			E_c^{tot}	R_E	IE	p_s	d_r
	R_X	T_X	R_{el}					
1	×	✓	✗	0.21	9.79	10	256	2
2	×	✗	✗	0	10	10	256	2
4	✗	✗	✗	0	10	10	256	2
5	✓	✗	✗	0.14	9.86	10	256	2
6	✗	✗	✗	0	10	10	256	2
7	✗	✗	✗	0	10	10	256	2
8	✗	✗	✗	0	10	10	256	2
9	✗	✗	✓	9.78	0.22	10	512	3
10	✗	✗	✗	0	10	10	256	2
11	✗	✗	✓	0.35	9.65	10	256	2
12	✗	✗	✗	0	10	10	256	2

Table 3 At 10 s node's status after attack

Node	Transmission mode			E_c^{tot}	Current copy		IE	Stored copy	
	R_X	T_X	R_{el}		CRE	CDR		SRE	SDR
1	✗	✓	✗	3.1	6.9	1	10	6.9	1
2	✗	✗	✗	0	10	0	10	10	0
3	✗	✗	✗	0	10	0	10	10	0
4	✗	✗	✗	0	10	0	10	10	0
5	✓	✗	✗	2.4	7.6	1	10	7.6	1
6	✗	✗	✗	0	10	0	10	10	0
7	✗	✗	✗	0	10	0	10	10	0
8	✗	✗	✗	0	10	0	10	10	0
9	✗	✗	✓	4.5	3	2	10	5.5	1
10	✗	✗	✗	0	10	0	10	10	0
11	✗	✗	✓	4.5	5.5	1	10	5.5	1
12	✗	✗	✗	0	10	0	10	10	0

on packet size and data rate. If the remaining energy value is greater than the threshold that node can participate in routing. Before replying route request it checks by self-monitoring mechanism whether it is attacked or not. Let us consider an example of energy-based routing in WMN as shown in Fig. 3. Table 3 shows relay node-9 status after attack. Relay node-9 detects attacker by self-monitoring mechanism.

6 Conclusion

In this paper we have proposed a novel approach to detect an intruder by self-monitoring mechanism of a node by considering remaining energy of a node as a metric. The analysis shows that the proposed model works efficiently in detecting intruder under static nature of nodes, thereby increasing network performance. Further, the model will be implemented and tested using NS3 simulation.

References

1. Bradley, K.: Detecting disruptive routers: a distributed network monitoring approach. *IEEE Netw.* **12**, 50–60 (1998)
2. Zhang, Y., Lee, W.: Intrusion detection in wireless ad-hoc networks. In: 6th Annual ACM International Conference on Mobile Computing and Networking, pp. 275–283. Boston (2000)
3. Marti, S., Giuli, T., Lai, K., Baker, M.: Mitigating routing misbehavior in mobile ad hoc networks. In: 6th Annual ACM International Conference on Mobile Computing and Networking, pp. 255–265. Boston (2000)

4. Ramanujan, R., Ahamad, A., Bonney, J., Hagelstrom, R., Thurber, K.: Techniques for intrusion-resistant ad hoc routing algorithms (tiara), pp. 660–664 (2000)
5. Bhargava, S., Agrawal, D.: Security enhancements in aodv protocol for wireless ad hoc networks. In: 2001 IEEE Vehicular Technology Conference, pp. 2143–2147 (2001)
6. Karygiannis, E.A.A., Apostolopoulos, A.: Detecting critical nodes for manet intrusion detection. In: 2nd International Workshop on Security, Privacy and Trust in Pervasive and Ubiquitous Computing (SecPerU 2006), pp. 7–15 (2006)
7. do Carmo, R., Hollick, M.: Ids: mobile and active intrusion detection system for ieee 802.11s wireless mesh networks. In: Proceedings of the 2nd ACM workshop on Hot Topics on Wireless Network Security and Privacy (HotWiSec) pp. 10–15 (2013)
8. Hassanzadeh, A.A., Stoleru, R.: Traffic-and-resource-aware intrusion detection in wireless mesh networks. L Technical Report. Texas AM University pp. 1–20 (2014)

Author Index

A

- Ade, Roshani, 681
Aggarwal, Preeti, 459
Agrawal, Dheeraj, 479
Agrawal, Pratik K., 99
Ahmad, Umar, 649
Ahmed, Muzameel, 151
Alam, Bashir, 441, 649, 773
Albert Rabara, S., 669
Alvi, A.S., 99, 631
Amutha, J., 669
Anand, B., 299
Anand, R., 611
Annappa, P.H., 821
Arora, Parul, 1
Aydav, Prem Shankar Singh, 659
Azad, Chandrashekhar, 429

B

- Babu, Ganga S., 393
Bahl, Shilpa, 337
Bamnote, G.R., 99, 119
Banan, Thenmozhi, 203
Barman, Debaditya, 711
Battula, Sudheer Kumar, 567
Bayal, R.K., 745
Bharadwaj, Gaurav, 311
Bhattacharya, Mahua, 273
Bhulania, Paurush, 489
Bhura, Sohel A., 631
Bisoyi, Bhubaneswari, 515
Biswas, G.P., 601
Biswas, Payal, 401
Biswas, Satya Priya, 535
Bodkhe, Renushree, 755

C

- Chakravarthy, VVSSS., 347
Chandel, Garima, 215
Chawla, Mayank, 215
Chi, Le Minh, 141
Choudhary, Kavita, 781
Choudhary, Yogesh, 273
Choudhury, Sushabhan, 251
Chowdhury, Nirmalya, 711
Cyriac, Alexander J., 235

D

- Das, Ajanta, 765
Das, Biswajit, 515
Davis, Divya, 375
Devassy, Alin, 193
Dey, Nilanjan, 299, 535
Dhanalakshmi, P., 357
Dhande, Sheetal, 119
Dhumal, Rajesh K., 413
Divya, P., 11
Doja, M.N., 773
Dubey, Rahul, 479
Durga, P., 499

E

- Ebrahim, M.A., 299
Elizabeth Shanthi, I., 547

F

- Farooq, Omar, 215, 793

G

- Gehlot, Anita, 251
Ghorpade, Tushar, 755

Ghosh, Dhruba, [489](#)

Ghosh, Shilpi, [129](#)

Ghrera, Satya Prakash, [327](#)

Gigras, Yogita, [781](#)

Gondakar, S.N., [83](#)

Gopan, Dhanya, [11](#)

Goswami, Sukalyan, [765](#)

Govardhan, A., [181](#)

H

Hariharan, Balaji, [37](#)

Haripriya, H., [591](#)

I

Iqbal, Sadaf, [793](#)

J

Jagatheesan, K., [299](#)

Jayakumar, Akshay, [393](#)

Jethani, Vimla, [755](#)

Jha, Rakesh Kumar, [735](#)

Jha, Vijay Kumar, [429](#)

Jibukumar, M.G., [289](#)

Jose, Jesmi Alphonsa, [611](#)

Joshi, Bhagawati Prasad, [171](#)

Joshi, Nehal, [577](#)

K

Kaimal, Anju M., [611](#)

Kale, K.V., [413](#)

Kandasamy, Saravanakumar, [203](#)

Kashyap, Manish, [273](#)

Kaur, Jaspreet, [109](#)

Kezia, J.M., [385](#)

Khan, Subuhi, [525](#)

Khan, Yusuf U., [215](#), [793](#)

Kharayat, Pushpendra Singh, [171](#)

Kiran, P., [289](#)

Koteswara Rao, L., [621](#)

Kothari, D.K., [47](#)

Kothari, Dilipkumar, [725](#)

Kuchhal, Piyush, [251](#)

Kulkarni, Pallavi, [681](#)

Kulkarni, Raj, [691](#)

Kumar, Arvind, [441](#)

Kumar, Prabhat, [319](#)

Kumar, Rakesh, [263](#), [401](#)

Kumar, Ram, [37](#)

Kumar, Sandeep, [273](#)

Kumar, Sunil, [489](#)

Kumawat, Nirma, [311](#)

Kumbhar, Hemant, [691](#)

Kuthadi, Venu Madhav, [61](#), [73](#)

L

Lakshmi Devi, P., [505](#)

Lakshmi Siva Rama Krishna, T., [567](#)

Le, Dac-Nhuong, [141](#)

Lekshmi Kiran, S., [557](#)

Limkar, Suresh, [691](#), [735](#)

Long, Nguyen Quoc, [141](#)

M

Malwe, Shweta R., [601](#)

Manjunath Aradhy, V.N., [151](#), [469](#)

Marwala, Tshilidzi, [61](#), [73](#)

Mathur, Himanshu, [745](#)

Meenakshi Sundaram, R., [669](#)

Mehrotra, S.C., [413](#)

Menon, Sreedevi, [611](#)

Menon, Sreedevi K., [499](#)

Menon, Vrindha N., [21](#)

Minz, Sonjharia, [659](#)

Mishra, Susanta Kumar, [163](#)

Mohan, Geethu, [449](#)

Mohan, Judith Nita, [203](#)

Mohan, Neethu, [801](#)

Mohandas, Poorna, [499](#)

Mohanty, Dipti Ranjan, [163](#)

Mohanty, Figlu, [241](#)

Muhammed Shanir, P.P., [793](#)

Mukherjee, Amartya, [535](#)

N

Nageswara Rao, K., [181](#)

Nagne, Ajay D., [413](#)

Naik, Nenavath Srinivas, [225](#)

Nandhini, K., [547](#)

Narayanan, Vishnu, [193](#)

Naveena, C., [469](#)

Nayyar, Vipul, [649](#)

Nechikkat, Nikitha, [365](#)

Nedungadi, Prema, [393](#), [591](#)

Negi, Atul, [225](#)

Nguyen, Gia Nhu, [141](#)

Nikhila, S., [499](#)

P

Pal, Swaraj Singh, [273](#)

Patra, Nivedita, [535](#)

Pattnaik, Prasant Kumar, [241](#)

Pazhanirajan, S., [357](#)

Prakash, Lakshmi, 801
Prakash, Mosiganti Joseph, 385

R

Ragunathan, T., 567
Rahul, Anusha, 193
Rajasekhar, K., 699
Rajendra, Yogesh D., 413
Ramachandran, Anand, 193
Raman, Raghu, 393
Ramesh, Maneesha Vinodini, 11, 21
Rani, Payal, 781
Rathee, Geetanjali, 327
Riyasat, Mumtaz, 525
Rohini, Pinapatruni, 621
Roy, Paromita, 535

S

Sachin Kumar, S., 801
Sai Srinivas, N.S., 347
Saini, Hemraj, 327
Sammulal, P., 811
Santhosh Kumar, Ch. N., 181
Sastry, V.N., 225
Satpathy, Saumya, 241
Sekar, Shangamitra, 203
Selva Rani, B., 639
Selvaraj, Rajalakshmi, 61, 73
Shah, Dhaval, 725
Shaji, Shereena, 21
Shanthakumar, Prathima, 203
Sharan, Aditi, 263, 401
Sharma, Mahesh Kr., 251
Sharma, Snigdha, 129
Sharma, Sudhir Kumar, 337, 459
Sharma, Vivek, 773
Shenoy, Udaya Kumar K., 821
Shilpa, 781
Shivank, 1
Shiva Prakash, S.P., 821
Sikha, O.K., 449
Singh, Amandeep, 109

Singh, Bhupendra, 251
Singh, J.P., 319
Singh, M.P., 319
Singh, Manoj Kumar, 83
Singh, Rajesh, 251
Singh, Ranjit, 109
Soman, K.P., 365, 557, 801
Sowmya, V., 365, 557
Srivastava, Smriti, 1
Sudhanva, E.V., 469
Sudheer Kumar, T., 347
Sunita, 311
Supriya, P., 375

T

Tazi, Satya Narayan, 745
Thrilek Chand, B., 601
Tijare, Manisha, 577
Tudu, Anil, 711

U

Uma, G., 37
Upadhyay, Manisha A., 47
Upadhyaya, Niraj, 699
Urooj, Shabana, 129

V

Vairamuthu, S., 639
Van, Vo Nhan, 141
Varadarajan, S., 505
Varghese, Jobina Mary, 37
Vasan, S.T., 83
Venu Gopalachari, M., 811
Verma, Akansha, 319
Vibhute, Amol D., 413
Vidya, V., 235

Y

Yadav, Ankesh, 129
Yadav, Chandra Shekhar, 263, 401
Yadav, M.S., 251